

Tree Physiology

Rolf T. W. Siegwolf  
J. Renée Brooks  
John Roden  
Matthias Saurer *Editors*

# Stable Isotopes in Tree Rings

Inferring Physiological, Climatic and  
Environmental Responses

OPEN ACCESS

 Springer

# **Tree Physiology**

Volume 8

## **Series Editors**

Frederick C. Meinzer, Corvallis, OR, USA

Ülo Niinemets, Tartu, Estonia

Our perceptions of forests has dramatically changed in the past decades, and forests are now considered central in mitigating climate change, providing vital ecosystem services, and maintaining human health.

Fundamental to understanding our global forest reserves, and managing them according to our current needs, is the need to understand and predict the physiological responses of trees to their abiotic and biotic environment.

Springer's Tree Physiology series takes a broad approach to address this need drawing together expertise from around the world to address issues and present findings, spanning molecular biology, biochemistry, biophysics, ecophysiology and atmospheric sciences, ranging from the cellular to the landscape scale. Providing state-of-the-art analyses on key topics, the volumes constitute an invaluable resource for researchers and advanced students involved in both pure and applied fields – including forestry, ecology, conservation, biodiversity and pest and disease management.

More information about this series at <https://link.springer.com/bookseries/6644>

Rolf T. W. Siegwolf · J. Renée Brooks ·  
John Roden · Matthias Saurer  
Editors

# Stable Isotopes in Tree Rings

Inferring Physiological, Climatic  
and Environmental Responses

 Springer

### *Editors*

Rolf T. W. Siegwolf  
Research Unit Forest Dynamics  
Swiss Federal Institute for Forest  
Snow and Landscape Research WSL  
Birmensdorf, Zürich, Switzerland  
  
Laboratory of Atmospheric Chemistry  
Paul Scherrer Institute  
Villigen, Switzerland

John Roden  
Department of Biology  
Southern Oregon University  
Ashland, OR, USA

J. Renée Brooks  
Pacific Ecological Systems Division  
Center for Public Health and Environmental  
Assessment  
Office of Research and Development  
United States Environmental Protection  
Agency  
Corvallis, OR, USA

Matthias Saurer  
Research Unit Forest Dynamics  
Swiss Federal Institute for Forest  
Snow and Landscape Research WSL  
Birmensdorf, Zürich, Switzerland



ISSN 1568-2544

Tree Physiology

ISBN 978-3-030-92697-7

ISBN 978-3-030-92698-4 (eBook)

<https://doi.org/10.1007/978-3-030-92698-4>

This is a U.S. government work and not under copyright protection in the U.S.; foreign copyright protection may apply 2021.

© The Editor(s) (if applicable) and The Author(s) 2022. This book is an open access publication.

**Open Access** This book is licensed under the terms of the Creative Commons Attribution 4.0 International License (<http://creativecommons.org/licenses/by/4.0/>), which permits use, sharing, adaptation, distribution and reproduction in any medium or format, as long as you give appropriate credit to the original author(s) and the source, provide a link to the Creative Commons license and indicate if changes were made.

The images or other third party material in this book are included in the book's Creative Commons license, unless indicated otherwise in a credit line to the material. If material is not included in the book's Creative Commons license and your intended use is not permitted by statutory regulation or exceeds the permitted use, you will need to obtain permission directly from the copyright holder.

The use of general descriptive names, registered names, trademarks, service marks, etc. in this publication does not imply, even in the absence of a specific statement, that such names are exempt from the relevant protective laws and regulations and therefore free for general use.

The publisher, the authors, and the editors are safe to assume that the advice and information in this book are believed to be true and accurate at the date of publication. Neither the publisher nor the authors or the editors give a warranty, expressed or implied, with respect to the material contained herein or for any errors or omissions that may have been made. The publisher remains neutral with regard to jurisdictional claims in published maps and institutional affiliations.

This Springer imprint is published by the registered company Springer Nature Switzerland AG  
The registered company address is: Gewerbestrasse 11, 6330 Cham, Switzerland

# Preface

The annual increments of tree-ring growth are a useful archive, reflecting tree environment interactions that can be precisely dated, quantified and even subdivided into seasonal time periods. This yearly datable wood material contains information about fundamental physiological mechanisms and processes (e.g. stomatal conductance, photosynthetic assimilation rates) occurring during ring formation. The analysis of the classical tree-ring width and density combined with stable C, O and H isotopes represent a reliable set of climate-sensitive proxies that reflect the impact of environmental variation on tree physiological responses. The strong link between physiology and isotope ratios is described by the well-established biophysical principles of CO<sub>2</sub> and H<sub>2</sub>O gas exchange and isotopic fractionation. This multiproxy approach (classical tree-ring analysis combined with stable isotopes) strengthens the interpretation and provides a more reliable data set for retrospective climate reconstructions and the analysis of environmental changes. In contrast to non-living chronologies (ice cores, stalagmites, etc.), trees modify base physical inputs in response to local microclimates through their physiological response to light, temperature, humidity, water availability, CO<sub>2</sub> and nutrients. These physiological responses to moisture availability, like variation in stomatal conductance, result in subtle changes of the isotope ratios in plants. Although these changes can make interpreting isotopic variation in organic matter more complicated, it also means that these proxies can provide a wealth of additional information, if those signals can be parsed from tree-ring stable isotope chronologies. Thus, a comprehensive understanding of the combined physical, chemical and biological drivers of isotope fractionation in tree rings is crucial for retrospective interpretation. In addition, tree rings and the stable isotopes contained therein integrate dynamic environmental, phenological and developmental variation that can be used to study and present organism function and recent anthropogenic influences apart from their use as proxies for conditions in the distant past. The last few decades have seen tremendous progress in isotopic analytical methods. These advances have significantly improved our understanding of the mechanisms by which tree physiology modifies stable isotope fractionation in organic matter and tree rings.

This textbook is the first to comprehensively cover the field of tree-ring stable isotopes. Our objective was to highlight how tree-ring stable isotopes have been

used to address a range of environmental issues, from paleoclimatology to forest management and anthropogenic impacts on forest growth. This compilation also provides valuable information on fundamental principles, like isotope fractionation, xylogensis and crossdating, as well as methodological topics like sampling, analysis and standardization. The chapters evaluate the weaknesses and strengths of isotope applications in tree rings. In contrast to older tree-ring studies, which predominantly applied a pure statistical approach, this book focuses on physiological mechanisms that influence isotopic signals, which reflect environmental impacts. Focusing on mechanisms that link physiological responses to environmental drivers of isotope variation also clarifies why environmental impacts are not linearly reflected in isotope ratios and tree-ring widths, or why these drivers and responses are not the same on all sites. We believe this volume will be of interest to any researcher and educator who uses tree rings (and other organic matter proxies) to reconstruct paleoclimate, as well as to understand contemporary functional processes and anthropogenic influences on native ecosystems. The use of stable isotopes in biogeochemical studies has expanded greatly in recent years, making this volume a valuable resource to a growing and vibrant community of researchers.

The book is divided into five sections. The first section introduces the history of isotope dendrochronology and how it fits into more traditional dendrochronology (Chaps. 1–3). The second section covers isotope dendrochronological methods, from sampling and dating tree ring cores, chemical treatments with their pros and cons, and determining the accuracy and precision of isotopic measurements, to describing the newest techniques in use (Chaps. 4–7). A core aspect of this book is to describe relevant isotopic fractionation processes for each of the bioelements commonly used in tree-ring studies (Chap. 8–12) and the physiological mechanisms that influence isotopic signals and their interaction with environmental drivers (Chaps. 13–17). In addition, this volume highlights how tree-ring stable isotopes have been successfully applied to reconstruct environmental information. They have also been used to address a range of environmental issues, from paleoclimatology to forest management, pathogens and anthropogenic impacts on forest growth (Chaps. 18–25). Finally, Chap. 26 overviews the most common physiological models simulating or using tree-ring stable isotopic records. Each of the 26 chapters has been authored by leading experts, who provide the most recent developments in their area.

We hope that this volume on the current state of knowledge on tree-ring stable isotope chronologies will provide researchers with a foundation, on which to develop new and unique ways to use them in the future. With continued challenges of climate change, and anthropogenic influences on our environment, we need to understand how ecosystems are responding. Since forests dominate large portions of the planet, and trees are long-lived organisms within forests, isotope dendrochronology can help with this understanding. They sensitively record changes in their environment, as well as their physiological responses to those changes over their entire lifespan, which can be centuries long. Newer techniques for exploring isotopic variation within

annual rings open possibilities for examining growth and physiological responses to individual extreme events. The direction for future research using tree-ring stable isotope chronologies holds great promise and is only limited by our imagination.

## Volume Summary

Part I, Introduction, covers historical and essential background information on dendrochronology, wood formation and the history of isotope dendrochronology. In Chap. 1, Leavitt and Roden (2022) provide a historical overview of isotope dendrochronology starting with the earliest measurements of tree-ring stable isotopes approximately 70 years ago (Craig 1953, 1954) to more recent advancements in the field. Dendrochronology is the time series analysis of the annual growth rings within trees and traditionally focuses on the width of the annual increment, whereas isotope dendrochronology specifically examines the time series of stable isotope ratios contained within tree rings. Chapter 2 focuses on the methodological and scientific foundations of traditional dendrochronology and emphasizes the importance of accurate cross-dating for all dendrochronological work, including isotope dendrochronology (Frank et al. 2022). In Chap. 3, Rathgeber et al. (2022) review the current knowledge of xylogenesis—the formation of wood—and its dynamics over the growing season. Knowing when and how wood is formed is essential to understanding the isotopic ratios contained within the wood and their accurate interpretation.

Part II, Methods, comprises four chapters covering sampling, chemical treatments, quality assurance and quality control of isotopic measurements, and newer methodologies being developed within the field. Chapter 4 summarizes the key aspects of fieldwork and laboratory sampling strategies for tree-ring stable isotopic studies, including requirements and processing that need to be taken into consideration to achieve high-quality results (Belmecheri et al. 2022). In Chap. 5, Helle et al. (2022) evaluate the differences between wood and cellulose isotope ratios, with an overview of three methods for cellulose extraction and where they are best applied. Chapter 6 explains how to evaluate the quality of the isotopic measurements themselves, including how to estimate the accuracy and precision of isotopic data, and the process of calibrating isotope ratios to the international standard scales (Brooks et al. 2022). Chapter 7 describes new methodological developments for stable isotope analysis on both non-structural carbohydrates and tree rings (Rinne-Garmston et al. 2022). They review compound-specific isotope analysis of sugars and cyclitols, UV-laser aided sampling and isotopic analysis of tree rings, and position-specific isotope analysis of cellulose.

Part III provides the details on isotopic fractionation from source to wood for carbon, oxygen, hydrogen and nitrogen and includes a chapter on basic isotopic terminology and one on post-photosynthetic fractionation. Chapter 8 provides the basic terminology, properties and peculiarities of the stable isotopes of the bioelements along with general information on equilibrium and kinetic isotope effects (Werner and Cormier 2022). In Chap. 9, Cernusak and Ubierna (2022) cover carbon



isotope ratios ( $\delta^{13}\text{C}$ ), which were the first isotope ratios to be measured in wood. This chapter covers the basics of how  $\delta^{13}\text{C}$  represents a tree's response to changes in water availability, air humidity, temperature and light through their connection to net photosynthesis ( $A_N$ ) and stomatal conductance ( $g_s$ ) via the ratio of  $\text{CO}_2$  concentrations inside to outside the leaf ( $c_i/c_a$ ). Chapter 10 provides an overview of the current knowledge concerning fractionation mechanisms related to  $\delta^{18}\text{O}_{\text{cell}}$  (Song et al. 2021). The chapter focuses on three main determinants of  $\delta^{18}\text{O}_{\text{cell}}$ : source water isotope ratio ( $\delta^{18}\text{O}_{\text{sw}}$ , also see Chap. 18), leaf water isotope enrichment ( $\Delta^{18}\text{O}_{\text{lw}}$ ) and biochemical fractionations downstream of  $\Delta^{18}\text{O}_{\text{lw}}$ . Chapter 11 addresses stable hydrogen isotope ( $\delta\text{D}$  or  $\delta^2\text{H}$ ) fractionation, which follows the same principles as oxygen isotopes in the water phase (Lehmann et al. 2022). However, during the incorporation of hydrogen into organic molecules,  $\delta^2\text{H}$  is strongly determined by metabolic pathways and the use of different carbohydrate sources. This makes it more difficult to use  $\delta^2\text{H}$  signals to distinguish different water sources or as a climate proxy. Chapter 12 reviews nitrogen isotope ratios ( $\delta^{15}\text{N}$ ) in tree rings along with the fundamentals of forest N cycling, describing trees as an interface between the atmosphere and pedosphere (Savard and Siegwolf 2022). Although the amount of nitrogen in wood is very small, making it experimentally challenging to determine  $\delta^{15}\text{N}$  in tree rings, nitrogen isotope ratios have been applied to air pollution studies that track the sources of N-containing emissions (NOx) and their changes in the atmosphere. Chapter 13 focuses mainly on the downstream path of carbon, as well as post-photosynthetic changes in  $\delta^{13}\text{C}$  from leaf photosynthate production to wood formation, discussing the important link between leaf and tree-ring levels that can significantly alter and dampen the environmental information (Gessler and Ferrio 2022).

Part IV is devoted to physiological interpretation and includes chapters on how and when physiological fractionations might be reflected in tree rings, the potential temporal offset with an annual ring between isotopic environmental signals and when bioelements are preserved in wood. In Chap. 14, Andreu-Hayles et al. (2022) consider how physiological influence on isotopic tree-ring records might change when trees are growing at the edges of their geographical distributions under growth-limiting conditions as compared to the same species growing in more optimum environments. They also consider important caveats where physiological responses to climate may mask or interact with climatological signals complicating interpretation. While the ability to section and analyze isotopic ratios within annual rings into smaller and smaller subsections has increased (see Chap. 7), the time series contained within a single ring is complicated by internal processes as introduced in Chap. 13. In Chap. 15, Kagawa and Battipaglia (2022) discuss post-photosynthetic processes that affect intra-annual variation in the stable isotopes in tree rings, such as timing of cell formations and turnover of stored carbohydrates. One way to constrain the physiological interpretations of tree ring isotopic ratios is to measure multiple isotopes on the same sample. This approach can be useful if one isotope provides independent information about important fractionation events that cause variation in another isotope. In Chap. 16, Roden et al. (2022) describe one such “dual-isotope approach” where  $\delta^{18}\text{O}$  is used to probe the effects of stomatal conductance on  $\delta^{13}\text{C}$  variation for

the same sample. In Chap. 17, the final chapter in this physiological interpretation section, Saurer and Voelker (2022) address the theory behind using  $\delta^{13}\text{C}$  to estimate intrinsic water-use efficiency (iWUE), one of the most widely applied interpretations of plant  $\delta^{13}\text{C}$  values. They show some limitations of the method, give examples of the combined application of iWUE and tree-ring width, discuss photosynthetic limitations of iWUE and show how the method has been applied in large-scale tree-ring networks.

Finally, Part V covers environmental factors impacting isotopic fractionation, important applications like climate reconstruction, and wraps up with a chapter on the current state of models that integrate the principles put forward in the other chapters. In Chap. 18, Allen et al. (2022) address the challenges of determining the  $\delta^{18}\text{O}$  and  $\delta^2\text{H}$  values of source water, a critical environmental parameter for interpreting  $\delta^{18}\text{O}$  and  $\delta^2\text{H}$  values in tree rings. They provide an overview of the terrestrial water cycle and the associated transport and fractionation processes that influence the stable isotope ratios of water used by trees. The authors also highlight obstacles and opportunities that must be considered in order to more accurately interpret the records of O and H isotope ratios in tree cellulose. Chapter 19 introduces isotope dendroclimatology, where tree-ring stable isotope chronologies are used to infer past climate conditions (Gagen et al. 2022). Because of the many interactions between physiology and the environment, as discussed in this book, tree-ring stable isotope chronologies are often used in conjunction with other proxies to tease apart past climate signals. As much of the research on tree-ring stable isotopes has occurred in temperate regions of the world, Chaps. 19 focuses on the dendroclimatology of these regions. To highlight other climate regions, Chap. 20 specifically address research on tree-ring stable isotopes from three different climate zones: 20 boreal (Churakova et al. 2021), Chap. 21 Mediterranean (Battipaglia and Cherubini 2022) and Chap. 22 tropical (van der Sleen et al. 2021) climate zones. The authors focus on the distinct climatological aspects of these regions and how they affect growth and physiology differently than other regions. They discuss how tree-ring stable isotope values are affected by each climate zone and highlight methodological, as well as interpretational issues. Human activities can also impact environmental conditions and growth of forests, which can show up in tree-ring stable isotope chronologies. In Chap. 23, Marshall et al. (2022) review how tree-ring stable isotopes have been used to understand forest responses to management practices. Many controlled experiments have been conducted to examine practices such as thinning and fertilization, some lasting several decades. The length and controlled nature of these experiments allow for the separation of some of the confounding influences on tree-ring stable isotopes. In Chap. 24, Siegwolf et al. (2022) review the impacts of rising  $\text{CO}_2$  and air pollutants on isotope chronologies.  $\text{CO}_2$  and other gaseous compounds affect plant metabolism in individually specific ways and to differing degrees. These differences impact the isotope fractionation, leaving specific fingerprints in the C, O, (H) and N isotope ratios of organic matter. Other organisms can also impact tree-ring stable isotopes but are often overlooked when interpreting isotope chronologies. In Chap. 25, Ulrich et al. (2022) explore how insects and pathogens impact the host tree physiology and how that signal can be manifested within tree-ring isotopic records. In Chap. 26, finally, Wei et al. (2022) review the status of several tree-ring  $\delta^{13}\text{C}$  and  $\delta^{18}\text{O}$

models that simulate physiological processes for trees and stands within ecosystems and/or across catchments. Their review highlights the structural differences among models with varied objectives and the valuable insights that can come from combining process modeling with tree-ring stable isotope data.

Birmensdorf, Switzerland  
Corvallis, USA  
Ashland, USA  
Birmensdorf, Switzerland

Rolf T. W. Siegwolf  
J. Renée Brooks  
John Roden  
Matthias Saurer

## References

- Craig H (1953) The geochemistry of the stable carbon isotopes. *Geochimica et Cosmochimica Acta* 3:53–92
- Craig H (1954) Carbon-13 variations in sequoia rings and the atmosphere. *Science* 119:141–143

# Acknowledgements

We, the editors of this tree physiology textbook would like to acknowledge key people who inspired us with their enthusiasm and profound knowledge. Dr. Fredrick Meinzer was instrumental in creating this volume, as he first approached the editors with the idea. Dr. Meinzer's work in tree physiology has established many physiological foundations central to interpreting stable isotopic variation within plants. Of the many excellent scientists, who have promoted the use of stable isotopes in tree-ring research, we would like to acknowledge especially our mentors and teachers. Dr. James Ehleringer opened our eyes to the world of stable isotope ratios in plant organic matter. Jim was instrumental in creating an international community of plant stable isotope researchers, where the editors and many of the contributing authors met and established fruitful collaborations. Under Jim's inspiration, this community has always aimed at discovering the big picture within the wide field of the ecosystem. We acknowledge his dedication to educating researchers from all over the world about stable isotope ecology. Dr. Fritz Schweingruber, one of the pioneers of dendroecology, has enthusiastically supported the use of stable isotopes in tree-ring analysis to enhance the breadth of dendrochronological interpretations. His openness paved the way to collaborate with the two physicists, Dr. Ueli Siegenthaler and Dr. Hans Oeschger, outstanding climatologists, who made use of stable isotopes in ice core research and helped applying cutting-edge isotope methods to pioneering tree-ring studies. The exemplarily fruitful and close collaboration between Dr. Walter Larcher and Dr. Alexander Cernusca in the fields of ecological plant physiology and physics created an ideal framework within which, it was possible to acquire a versatile and comprehensive basis in experimental ecology. Three other important mentors were Dr. Robert Pearcy and Dr. Thomas M. Hinckley, both leaders in the field of physiological ecology especially related to forest canopies and ecosystems, and Dr. Todd Dawson whose work in stable isotope variation of the hydrologic cycle directly impacted much of our understanding of the source of hydrogen and oxygen isotopes in tree rings. Exploring the interaction between plant productivity and the environmental drivers of carbon, water and nutrient relations in forests is a most fascinating and challenging field of research. The enthusiasm and passion of these teachers and mentors sparked a fascination for environmental research in their students, which

opened our eyes to the field of experimental ecology and enduringly impacted our lives.

We also want to express our thanks to the numerous reviewers for providing their most valuable input, and whose comments contributed significantly to the quality of this volume. Finally, our gratitude goes also to our partners for their patience and support during the production of this book.

The Swiss National Science Foundation provided the funding for Open Access, making this book available for a broad audience, which we gratefully acknowledge.

# Contents

## Part I Introduction

- 1 **Isotope Dendrochronology: Historical Perspective** ..... 3  
Steven W. Leavitt and John Roden
- 2 **Dendrochronology: Fundamentals and Innovations** ..... 21  
David Frank, Keyan Fang, and Patrick Fonti
- 3 **Anatomical, Developmental and Physiological Bases of Tree-Ring Formation in Relation to Environmental Factors** ..... 61  
Cyrille B. K. Rathgeber, Gonzalo Pérez-de-Lis, Laura Fernández-de-Uña, Patrick Fonti, Sergio Rossi, Kerstin Treydte, Arthur Gessler, Annie Deslauriers, Marina V. Fonti, and Stéphane Ponton

## Part II Methods

- 4 **Sample Collection and Preparation for Annual and Intra-annual Tree-Ring Isotope Chronologies** ..... 103  
Soumaya Belmecheri, William E. Wright, and Paul Szejner
- 5 **Stable Isotope Signatures of Wood, its Constituents and Methods of Cellulose Extraction** ..... 135  
Gerhard Helle, Maren Pauly, Ingo Heinrich, Karina Schollän, Daniel Balanzategui, and Lucas Schürheck
- 6 **Tree-Ring Stable Isotope Measurements: The Role of Quality Assurance and Quality Control to Ensure High Quality Data** ..... 191  
J. Renée Brooks, William D. Rugh, and Roland A. Werner
- 7 **Newer Developments in Tree-Ring Stable Isotope Methods** ..... 215  
Katja T. Rinne-Garmston, Gerhard Helle, Marco M. Lehmann, Elina Sahlstedt, Jürgen Schleucher, and John S. Waterhouse

**Part III Isotopic Fractionations from Source to Wood**

**8 Isotopes—Terminology, Definitions and Properties** ..... 253  
 Roland A. Werner and Marc-André Cormier

**9 Carbon Isotope Effects in Relation to CO<sub>2</sub> Assimilation by Tree Canopies** ..... 291  
 Lucas A. Cernusak and Nerea Ubierna

**10 Environmental, Physiological and Biochemical Processes Determining the Oxygen Isotope Ratio of Tree-Ring Cellulose** ..... 311  
 Xin Song, Andrew Lorrey, and Margaret M. Barbour

**11 The Stable Hydrogen Isotopic Signature: From Source Water to Tree Rings** ..... 331  
 Marco M. Lehmann, Philipp Schuler, Marc-André Cormier, Scott T. Allen, Markus Leuenberger, and Steve Voelker

**12 Nitrogen Isotopes in Tree Rings—Challenges and Prospects** ..... 361  
 Martine M. Savard and Rolf T. W. Siegwolf

**13 Postphotosynthetic Fractionation in Leaves, Phloem and Stem** ..... 381  
 Arthur Gessler and Juan Pedro Ferrio

**Part IV Physiological Interpretations**

**14 Limits and Strengths of Tree-Ring Stable Isotopes** ..... 399  
 Laia Andreu-Hayles, Mathieu Lévesque, Rossella Guerrieri, Rolf T. W. Siegwolf, and Christian Körner

**15 Post-photosynthetic Carbon, Oxygen and Hydrogen Isotope Signal Transfer to Tree Rings—How Timing of Cell Formations and Turnover of Stored Carbohydrates Affect Intra-annual Isotope Variations** ..... 429  
 Akira Kagawa and Giovanna Battipaglia

**16 Probing Tree Physiology Using the Dual-Isotope Approach** ..... 463  
 John Roden, Matthias Saurer, and Rolf T. W. Siegwolf

**17 Intrinsic Water-Use Efficiency Derived from Stable Carbon Isotopes of Tree-Rings** ..... 481  
 Matthias Saurer and Steve Voelker

**Part V Environmental Factors Impacting the Isotopic Fractionation**

**18 Spatial and Temporal Variations in Plant Source Water: O and H Isotope Ratios from Precipitation to Xylem Water** ..... 501  
 Scott T. Allen, Matthias Sprenger, Gabriel J. Bowen, and J. Renée Brooks

**19 Climate Signals in Stable Isotope Tree-Ring Records** ..... 537  
 Mary Gagen, Giovanna Battipaglia, Valerie Daux,  
 Josie Duffy, Isabel Dorado-Liñán, Laia Andreu Hayles,  
 Elisabet Martínez-Sancho, Danny McCarroll,  
 Tatiana A. Shestakova, and Kerstin Treydte

**20 Stable Isotopes in Tree Rings of Boreal Forests** ..... 581  
 Olga V. Churakova, Trevor J. Porter, Alexander V. Kirilyanov,  
 Vladimir S. Myglan, Marina V. Fonti, and Eugene A. Vaganov

**21 Stable Isotopes in Tree Rings of Mediterranean Forests** ..... 605  
 Giovanna Battipaglia and Paolo Cherubini

**22 Stable Isotopes in Tree Rings of Tropical Forests** ..... 631  
 Peter van der Sleen, Pieter A. Zuidema, and Thijs L. Pons

**23 Forest Management and Tree-Ring Isotopes** ..... 651  
 John D. Marshall, J. Renée Brooks, and Alan F. Talhelm

**24 Impact of Increasing CO<sub>2</sub>, and Air Pollutants (NO<sub>x</sub>, SO<sub>2</sub>, O<sub>3</sub>)  
 on the Stable Isotope Ratios in Tree Rings** ..... 675  
 Rolf T. W. Siegwolf, Martine M. Savard, Thorsten E. E. Grams,  
 and Steve Veelker

**25 Insect and Pathogen Influences on Tree-Ring Stable Isotopes** ..... 711  
 Danielle E. M. Ulrich, Steve Veelker, J. Renée Brooks,  
 and Frederick C. Meinzer

**26 Process-Based Ecophysiological Models of Tree-Ring Stable  
 Isotopes** ..... 737  
 Liang Wei, John D. Marshall, and J. Renée Brooks

**Index** ..... 757



# Contributors

**Scott T. Allen** Department of Natural Resources and Environmental Sciences, University of Nevada, Reno, NV, USA

**Laia Andreu-Hayles** Lamont-Doherty Earth Observatory of Columbia University, Palisades, NY, USA;  
CREAF, Barcelona, Spain;  
ICREA, Barcelona, Spain

**Margaret M. Barbour** The University of Sydney, School of Life and Environmental Sciences, Sydney, Australia

**Giovanna Battipaglia** Department of Environmental, Biological and Pharmaceutical Sciences and Technologies, University of Campania “L. Vanvitelli”, Caserta, Italy

**Soumaya Belmecheri** Laboratory of Tree-Ring Research, University of Arizona, Tucson, USA

**Gabriel J. Bowen** Geology and Geophysics, University of Utah, Salt Lake City, UT, USA

**J. Renée Brooks** Pacific Ecological Systems Division, Center for Public Health and Environmental Assessment, Office of Research and Development, U. S. Environmental Protection Agency, Corvallis, OR, USA

**Lucas A. Cernusak** College of Science and Engineering, James Cook University, Cairns, QLD, Australia

**Paolo Cherubini** Swiss Federal Institute for Forest, Snow and Landscape Research WSL, Birmensdorf, Switzerland;  
Department of Forest and Conservation Sciences, The University of British Columbia, Main Mall, Vancouver, BC, Canada

**Olga V. Churakova** Institute of Ecology and Geography, Siberian Federal University, Krasnoyarsk, Russian Federation;  
Research Unit Forest Dynamics, Swiss Federal Institute for Forest, Snow and Landscape Research WSL, Birmensdorf, Switzerland

**Marc-André Cormier** Department of Earth Sciences, University of Oxford, Oxford, UK

**Valerie Daux** Laboratoire des Sciences du Climate et de l'Environnement, Université Paris-Saclay, CNRS, CEA, UVSQ, Gif-sur-Yvette, France

**Annie Deslauriers** Département Des Sciences Fondamentales, Université du Québec À Chicoutimi, Chicoutimi, Canada

**Isabel Dorado-Liñán** Forest Genetics and Ecophysiology Research Group, E.T.S. Forestry Engineering, Universidad Politécnica de Madrid, Madrid, Spain

**Josie Duffy** Department of Geography, Swansea University, Swansea, UK

**Keyan Fang** Fujian Normal University, Fuzhou, People's Republic of China

**Laura Fernández-de-Uña** Université de Lorraine, AgroParisTech, INRAE, SILVA, Nancy, France

**Juan Pedro Ferrio** Centro de Investigación Y Tecnología Agroalimentaria de Aragón (CITA), Unidad de Recursos Forestales, Zaragoza, Spain

**Marina V. Fonti** Research Unit Forest Dynamics, Swiss Federal Institute for Forest, Snow and Landscape Research WSL, Birmensdorf, Switzerland;  
Laboratory of Ecosystems Biogeochemistry, Institute of Ecology and Geography, Siberian Federal University, Krasnoyarsk, Russia

**Patrick Fonti** Research Unit Forest Dynamics, Swiss Federal Institute for Forest, Snow and Landscape Research WSL, Birmensdorf, Switzerland

**David Frank** Laboratory of Tree-Ring Research, University of Arizona, Tucson, USA

**Mary Gagen** Department of Geography, Swansea University, Swansea, UK

**Arthur Gessler** Research Unit Forest Dynamics, Swiss Federal Institute for Forest, Snow and Landscape Research WSL, Birmensdorf, Switzerland;  
Institute of Terrestrial Ecosystems, ETH Zurich, Zurich, Switzerland

**Thorsten E. E. Grams** Ecophysiology of Plants, Technical University of Munich, Freising, Germany

**Rossella Guerrieri** ICREA, Barcelona, Spain;  
Forest Ecology Lab, Department of Agricultural and Food Sciences, University of Bologna, Bologna, Italy

**Ingo Heinrich** GFZ German Research Centre for Geosciences, Telegrafenberg, Potsdam, Germany;  
German Archaeological Institute DAI, Berlin, Germany

**Gerhard Helle** Helmholtz-Centre Potsdam, GFZ German Centre for GeoSciences Section 4.3 Climate Dynamics and Landscape Evolution, Potsdam, Germany

**Akira Kagawa** Wood Anatomy and Quality Laboratory, Forestry and Forest Products Research Institute, Tsukuba, Ibaraki, Japan

**Alexander V. Kirilyanov** Institute of Ecology and Geography, Siberian Federal University, Krasnoyarsk, Russian Federation;  
V. N. Sukachev Institute of Forest SB RAS, Federal Research Center “Krasnoyarsk Science Center SB RAS”, Krasnoyarsk, Russian Federation

**Christian Körner** Department of Environmental Sciences, University of Basel, Basel, Switzerland

**Steven W. Leavitt** Laboratory of Tree-Ring Research, University of Arizona, Tucson, AZ, USA

**Marco M. Lehmann** Research Unit Forest Dynamics, Swiss Federal Institute for Forest, Snow and Landscape Research WSL, Birmensdorf, Switzerland

**Markus Leuenberger** Climate and Environmental Physics, Physics Institute and Oeschger Centre for Climate Change Research, University of Bern, Bern, Switzerland

**Andrew Lorrey** National Institute of Water and Atmospheric Research Ltd., Auckland, New Zealand

**Mathieu Lévesque** Forest Ecology, Institute of Terrestrial Ecosystems, Department of Environmental Systems Science, ETH Zurich, Zurich, Switzerland

**John D. Marshall** Department of Forest Ecology and Management, Swedish University of Agricultural Sciences, Umeå, Sweden

**Elisabet Martínez-Sancho** Swiss Federal Institute for Forest, Snow and Landscape Research WSL, Research Unit Forest Dynamics, Birmensdorf, Switzerland

**Danny McCarroll** Department of Geography, Swansea University, Swansea, UK

**Frederick C. Meinzer** USDA Forest Service, Pacific Northwest Research Station, Corvallis, OR, USA

**Vladimir S. Myglan** Siberian Dendrochronological Laboratory, Siberian Federal University, Krasnoyarsk, Russian Federation

**Maren Pauly** GFZ German Research Centre for Geosciences, Telegrafenberg, Potsdam, Germany;  
School of Science, Bath Spa University, Bath, UK

**Thijs L. Pons** Plant Ecophysiology, Institute of Environmental Biology, Utrecht University, Utrecht, The Netherlands

**Stéphane Ponton** Université de Lorraine, AgroParisTech, INRAE, SILVA, Nancy, France

**Trevor J. Porter** Department of Geography, Geomatics and Environment, University of Toronto Mississauga, Mississauga, Canada

**Gonzalo Pérez-de-Lis** Université de Lorraine, AgroParisTech, INRAE, SILVA, Nancy, France

**Cyrille B. K. Rathgeber** Université de Lorraine, AgroParisTech, INRAE, SILVA, Nancy, France

**Katja T. Rinne-Garmston** Natural Resources Institute Finland (Luke), Helsinki, Finland

**John Roden** Biology Department, Southern Oregon University, Ashland, OR, USA

**Sergio Rossi** Département Des Sciences Fondamentales, Université du Québec À Chicoutimi, Chicoutimi, Canada;

Key Laboratory of Vegetation Restoration and Management of Degraded Ecosystems, Guangdong Provincial Key Laboratory of Applied Botany, South China Botanical Garden, Chinese Academy of Sciences, Guangzhou, China

**William D. Rugh** Pacific Ecological Systems Division, Center for Public Health and Environmental Assessment, Office of Research and Development, U. S. Environmental Protection Agency, Corvallis, OR, USA

**Elina Sahlstedt** Natural Resources Institute Finland (Luke), Helsinki, Finland

**Matthias Saurer** Swiss Federal Institute for Forest, Snow and Landscape Research WSL, Birmensdorf, Switzerland

**Martine M. Savard** Geological Survey of Canada (Natural Resources Canada), Québec, QC, Canada

**Jürgen Schleucher** Department of Medical Biochemistry and Biophysics, Umeå University, Umeå, Sweden

**Karina Schollän** GFZ German Research Centre for Geosciences, Telegrafenberg, Potsdam, Germany

**Philipp Schuler** Research Unit Forest Dynamics, Swiss Federal Institute for Forest, Snow and Landscape Research WSL, Birmensdorf (Zürich), Switzerland

**Tatiana A. Shestakova** Woodwell Climate Research Center, Falmouth, MA, USA

**Rolf T. W. Siegwolf** Swiss Federal Institute for Forest, Snow and Landscape Research, WSL, Birmensdorf, Switzerland;

Lab of Atmospheric Chemistry, Paul Scherrer Institute (PSI), Villigen, Switzerland

**Xin Song** College of Life and Marine Sciences, Shenzhen University, Shenzhen, Guangdong Province, China;  
Shenzhen Key Laboratory of Marine Biological Resources and Ecological Environment, Shenzhen University, Shenzhen, Guangdong Province, China

**Matthias Sprenger** College of Natural Resources, North Carolina State University, Raleigh, NC, USA;  
Lawrence Berkeley National Laboratory, Berkeley, CA, USA

**Paul Szejner** Laboratory of Tree-Ring Research, University of Arizona, Tucson, USA;  
Instituto de Geología, Universidad Nacional Autónoma de México, Ciudad de Mexico, Mexico

**Alan F. Talhelm** Department of Forest, Rangeland, and Fire Sciences, University of Idaho, Moscow, ID, USA

**Kerstin Treydte** Swiss Federal Institute for Forest, Snow and Landscape Research WSL, Research Unit Forest Dynamics, Birmensdorf, Switzerland

**Nerea Ubierna** The Australian National University, Canberra, ACT, Australia

**Danielle E. M. Ulrich** Department of Ecology, Montana State University, Bozeman, MT, USA

**Eugene A. Vaganov** Institute of Ecology and Geography, Siberian Federal University, Krasnoyarsk, Russian Federation;  
V. N. Sukachev Institute of Forest SB RAS, Federal Research Center “Krasnoyarsk Science Center SB RAS”, Krasnoyarsk, Russian Federation

**Peter van der Sleen** Forest Ecology and Forest Management Group, Wageningen University and Research, Wageningen, The Netherlands;  
Wildlife Ecology and Conservation Group, Wageningen University and Research, Wageningen, The Netherlands

**Steve Voelker** College of Forest Resources and Environmental Science, Michigan Technological University, Houghton, USA

**John S. Waterhouse** School of Life Sciences, Anglia Ruskin University, Cambridge, UK

**Liang Wei** MOE Key Laboratory of Western China's Environmental System, College of Earth and Environmental Sciences, Lanzhou University, Lanzhou, Gansu, China

**Roland A. Werner** Department of Environmental Systems Science, Institute of Agricultural Sciences, ETH Zürich, Zürich, Switzerland

**William E. Wright** Laboratory of Tree-Ring Research, University of Arizona, Tucson, USA

**Pieter A. Zuidema** Forest Ecology and Forest Management Group, Wageningen University and Research, Wageningen, The Netherlands

**Part I**  
**Introduction**

# Chapter 1

## Isotope Dendrochronology: Historical Perspective



Steven W. Leavitt and John Roden

**Abstract** Although the fields of dendrochronology and light stable-isotope mass spectrometry emerged at different times in the first half of the 20th Century, their convergence with the earliest measurements of isotope composition of tree rings is now *ca.* 70 years old. Much of the early stable isotope analysis (including on wood) explored natural variation of isotopes in the environment, but those researchers making the measurements were already contemplating the role of the isotope composition of the source substrates (e.g., water and CO<sub>2</sub>), biochemical fractionation, and environment as contributors to final tree-ring isotope values. Growing interest in tree-ring isotopes was heavily motivated by paleoclimate or paleoatmosphere reconstruction, but this new field rapidly developed to generate greatly improved mechanistic understanding along with expanded applications to physiology, ecology, pollution, and more. This chapter primarily charts the historical progression in tree-ring C-H-O isotope studies over those seven decades, but it also identifies potential productive emerging and future directions.

### 1.1 Introduction

The roots of stable-isotope dendrochronology extend back to the middle of the 20th Century during the convergence of the maturing discipline dendrochronology with development of powerful isotope analytical tools. By that time, methods and principles of tree-ring studies (see Chap. 2) had already been developed and refined for about 50 years, largely based on the year-to-year variability in size of rings, but to which an arsenal of other tree-ring measurements has progressively been added over the next 50 years (e.g., wood density, cell size, and dendrochemistry including isotopes). Additionally, measurement of isotope ratios by mass spectrometers became

---

S. W. Leavitt (✉)

Laboratory of Tree-Ring Research, University of Arizona, Tucson, AZ 85721, USA

e-mail: [sleavitt@arizona.edu](mailto:sleavitt@arizona.edu)

J. Roden

Biology Department, Southern Oregon University, Ashland, OR 97520, USA

© The Author(s) 2022

R. T. W. Siegwolf et al. (eds.), *Stable Isotopes in Tree Rings*, Tree Physiology 8,  
[https://doi.org/10.1007/978-3-030-92698-4\\_1](https://doi.org/10.1007/978-3-030-92698-4_1)

established by the middle of the century, providing a new tool for quantitative research. A large (and rapidly growing) number of stable-isotope dendrochronology investigations have been conducted since the commingling of the two scientific fields, as related to reconstruction and understanding of weather/climate, ecology, and physiology. We can view any stable-isotope series derived from tree rings as a rich and layered story that has been transcribed by physiological, physicochemical and biochemical processes in response to a wide range of influences from climate to atmospheric chemistry and pollution to ecology (Fig. 1.1).

The dramatic growth of this field from the 1980s into the 2000s is illustrated in the burgeoning number of papers presented at international tree-ring conferences (Fig. 1.2). Several useful overviews are available in the literature related to tree-ring isotope methodology, theory, and applications, such as McCarroll and Loader (2004), Robertson et al. (2008) and Managave and Ramesh (2012). This chapter describes the historical trajectory of studies and their findings from measurements of stable-isotope composition of tree rings. It is not exhaustive, but fortunately further details and more recent advancements and applications are covered in many of the other chapters in this volume.

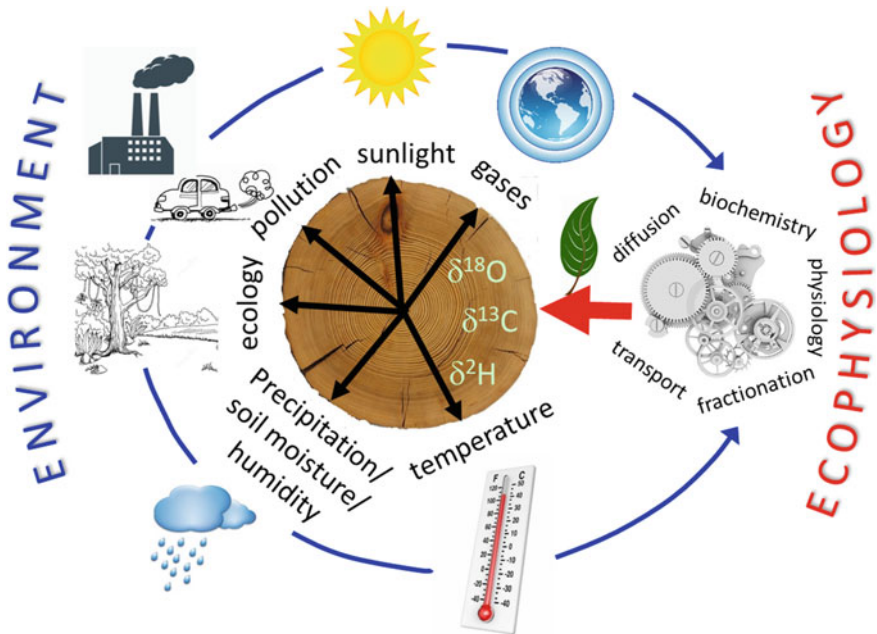


**Fig. 1.1** Schematic representation of interplay between environmental factors and ecophysiology that produces tree-ring C-H-O isotope composition. Environment can influence the ecophysiological, biochemical, and physicochemical mechanisms responsible for producing the isotope composition and consequently isotope dendrochronology can be used to infer environment and ecological events affecting ecophysiology (e.g., insect outbreaks). Tree rings allow identification of changes through time, but if a network of sites is sampled, the tree-ring isotope results can also reveal changes in space (isoscapes)





**Fig. 1.2** Growth in numbers of light-stable-isotope tree-ring papers (oral and poster) presented at major international tree-ring conferences. Other major meetings, such as AGU, EGU, INQUA, AAG, and regional tree-ring meetings in Asia, Europe and the Americas often also feature tree-ring isotope papers in various sessions

## 1.2 Origins

The development of the isotope-ratio mass spectrometer (IRMS) opened the door to isotope measurements on tree rings (and many other materials). Key to the development of IRMS technology was Alfred O.C. Nier at the University of Minnesota, who in the late 1940s–early 1950s produced the “double-focusing” mass spectrometer, which used both electrostatic and magnetic focusing of ion beams containing the isotopes of interest, an advance that is the basis of most modern instrumentation (Prohaska 2015). Harold C. Urey at the University of Chicago then added a dual inlet system into the design for alternately admitting aliquots of reference gas and unknown gas into the mass spectrometer (Brand et al. 2015). His newly configured mass spectrometer was applied to measurement of stable isotope composition of various materials, in collaboration with renowned geochemists in the early stages of their careers, such as Samuel Epstein and Harmon Craig. Urey was able to discern the importance of temperature effects on isotope fractionation in carbonate-water equilibria, which established the potential of isotope “thermometers” as a novel tool in paleoclimatology (Epstein et al. 1951; Fairbridge and Gornitz 2009).

Craig’s Ph.D. research sought to characterize natural carbon isotope variability in the carbon system (Craig 1953) through extensive  $\delta^{13}\text{C}$  analyses of hot-spring gases, carbon in sedimentary, igneous and metamorphic rocks, terrestrial and marine organic carbon, and a variety of freshwater and marine carbonate rocks. Among the organic carbon samples, he analyzed 22 “modern” wood samples (AD 1892–1950) from four continents and 16 “fossil” wood samples primarily from N. America (15 of which were radiocarbon-dated by Willard Libby of the University of Chicago at 2300 to >25,000 years old). In the modern wood, no patterns in isotope composition related to species, age, geographical location or elevation were detected. The  $\delta^{13}\text{C}$  of the fossil wood fell within the range of modern wood,  $-22.5$  to  $-27.3\%$ . Overall, Craig was cognizant that changes in  $\delta^{13}\text{C}$  of  $\text{CO}_2$  could influence the isotope composition of wood but thought any such changes were being “randomly masked” by other factors, probably local environment effects. He was also aware of interannual variability in isotopic composition among rings within individual trees.

In his Science paper the following year, Craig (1954) interpreted the  $\delta^{13}\text{C}$  data in Craig (1953) as indicating that  $\delta^{13}\text{C}$  of atmospheric  $\text{CO}_2$  has not varied by more than 2‰ over the last 25,000 years and may have actually been fairly constant over millions of years. However, the real novelty of the new paper was that it communicated the first-ever  $\delta^{13}\text{C}$  analyses of annual growth rings of a calendar-dated giant sequoia from the Sierra Nevada mountains of California. One or two tree rings in each century were analyzed from the period from 1072 B.C. to A.D. 1649. The  $\delta^{13}\text{C}$  values steadily increased *ca.* 2‰ in the first 150 years of the record, with various upward and downward deviations thereafter. Coincidentally, in long-lived kauri trees in New Zealand, Jansen (1962) found a similar increase in tree-ring  $\delta^{13}\text{C}$  over the first 200 years of the tree’s 800-year life. The sequoia isotope variability did not seem to be related to precipitation (although the tree may have been growing in

a landscape position unlikely to be limited by moisture), and variability of atmospheric  $\delta^{13}\text{C}$  of  $\text{CO}_2$  was discounted. Presaging advancements to come later in the 20th Century, Craig concluded that effects of environmental conditions (e.g., light, temperature, precipitation) on fractionation during photosynthesis and respiration were the primary contributors to the isotope variation observed.

This pioneering tree-ring isotope work in the 1950s exclusively involved stable-carbon isotopes, presumably because the C isotope composition could be readily measured on  $\text{CO}_2$  gas after the wood samples were combusted. Analysis of H and O isotopes in tree-ring cellulose would have to wait until the 1970s when pretreatment and off-line vacuum methodologies were developed for analyzing only non-exchangeable H (by nitration of cellulose) and procedures for analyzing O isotopes in organic matter (by mercury chloride or nickel pyrolysis) were applied to tree rings (see Epstein et al. 1977).

## 1.3 Advances

### 1.3.1 20th Century Spin Up

Over the next several decades of isotope dendrochronology, efforts were largely focused on the use of isotopes in tree rings as paleothermometers, along the line of the great success with isotopic composition of marine forams to understand glacial-interglacial temperature history over the last few million years (e.g., Emiliani 1955; Emiliani and Geiss 1959). These tree-ring isotope efforts began in earnest in the 1970s with a surge of papers attempting to quantify temperature coefficients. For carbon isotopes, the early studies by Libby and Pandolfi (1974), Pearman et al. (1976), Wilson and Grinsted (1977), Tans (1978), Farmer (1979), and Harkness and Miller (1980) found both positive and negative temperature coefficients with tree-ring  $\delta^{13}\text{C}$ . Additionally, the 1970s saw attempts to use tree-ring  $\delta^{13}\text{C}$  as a measure of changes in  $\delta^{13}\text{C}$  of atmospheric  $\text{CO}_2$  (Freyer and Wiesberg 1973; Stuiver 1978; Freyer 1979a, 1981), in an effort to extend the record of regular direct measurements at Mauna Loa and the South Pole, which had just begun at Mauna Loa in the late 1950s (Keeling et al. 1979). Such records are critical to understanding alteration of the global carbon cycle by anthropogenic inputs to the atmosphere of carbon from fossil fuels and land-use change. The above studies did not analyze a common standard wood component nor did they establish a minimum number of trees to be sampled to ensure the  $\delta^{13}\text{C}$  records were representative, which probably also contributes to some of the variability among published results. Variability of isotopes within and between trees and among species was later addressed by Ramesh et al. (1985), Leavitt and Long (1986), and Leavitt (2010). The impetus for developing tree-ring  $\delta^{13}\text{C}$  records as a proxy for long-term changes in  $\delta^{13}\text{C}$  of atmospheric  $\text{CO}_2$  faded by the late 1980s as reliable isotopic measurements on atmospheric gas trapped in ice cores became established (e.g., Friedli et al. 1986) and the role of environmental

influences complicating interpretation of tree-ring  $\delta^{13}\text{C}$  relative to atmospheric  $\delta^{13}\text{C}$  was more fully appreciated.

The development of a plant carbon-isotope fractionation model in the early 1980s (Vogel 1980; Farquhar 1982; see also Chap. 9) provided both the theoretical background with which to better explore the potential of isotope dendrochronology and new insights into the source of the isotope-environment relationships (Francey and Farquhar 1982). Consequently, the next wave of tree-ring  $\delta^{13}\text{C}$  papers usually refined their analysis and interpretations with respect to this model and the reality that a multitude of environmental parameters could actually influence plant  $\delta^{13}\text{C}$  (i.e.,  $\delta^{13}\text{C}$  of atmospheric  $\text{CO}_2$ , temperature, light, moisture, humidity) (e.g., Freyer and Belacy 1983; Peng et al. 1983; Stuiver et al. 1984; Stuiver and Braziunas 1987; Leavitt and Long 1988, 1989). The model provides a basis for understanding differences between  $\delta^{13}\text{C}$  records as well as for selection of tree locations to best capture variability of an environmental parameter of interest.

Meanwhile, H and O isotopes of water in tree rings were also being explored in greater depth in the 1970s. For example, Schiegl (1974) was the first to identify a positive correlation between temperature and  $\delta^2\text{H}$  in tree rings (of spruce), which was predicted based on the established positive relationship between temperature and  $\delta^2\text{H}$  and  $\delta^{18}\text{O}$  of precipitation (Dansgaard 1964), i.e., source water for photosynthates formed in leaves. The whole-wood analysis of Schiegl (1974) left some room for uncertainty because of the suite of compounds in whole wood as well as the fact that analysis of whole wood would include both non-exchangeable and exchangeable hydrogen, the latter unlikely to represent the original composition when the wood was formed. Epstein and Yapp (1976) and Epstein et al. (1976) circumvented these problems by analyzing the cellulose component of wood and removing the exchangeable H atoms by replacing them with nitrate. Tree-ring  $\delta^{18}\text{O}$  studies in these early decades also found positive correlations of  $\delta^{18}\text{O}$  with temperature, but again no specific wood constituent was being analyzed by all studies (e.g., Gray and Thompson 1976; Libby and Pandolfi 1979; Burk and Stuiver 1981). These various early studies identified climate relationships by either spatial gradient analysis of isotope composition of tree rings and mean climate of different sites, or by isotope analysis of tree-ring series compared to inter-annual climate variation, and the results were not always the same. For both  $\delta^2\text{H}$  and  $\delta^{18}\text{O}$ , some studies were also identifying significant correlations with direct water-related parameters such as precipitation and humidity (e.g., Burk and Stuiver 1981; Edwards et al. 1985; Krishnamurthy and Epstein 1985; Ramesh et al. 1986).

With expanded awareness of likely environmental and physiological influences on the isotopic composition of meteoric water and water being fixed in plants, including temperature, evaporation, humidity, and biochemical fractionation by enzymes, increasingly sophisticated models for plant  $\delta^2\text{H}$  and  $\delta^{18}\text{O}$  slowly began to emerge in the 1980s (e.g., Burk and Stuiver 1981; Edwards et al. 1985; Edwards and Fritz 1986; Saurer et al. 1997). A critical advance in model refinement was supported by the experimental work of Roden and Ehleringer (1999a, b, 2000) in the 1990s examining the acquisition of leaf and tree-ring isotope values under controlled environmental conditions including source water isotope composition and humidity. This

culminated in the advanced mechanistic model for tree-ring  $\delta^2\text{H}$  and  $\delta^{18}\text{O}$  developed by Roden et al. (2000) (see also Chaps. 10 and 11). This work exposed the primary contributions of both isotopic composition of source water (taken up by the roots) and evaporation in the leaves (along with the biochemical fractionation) toward influencing the composition of the rings. This supported results of previous empirical  $\delta^2\text{H}$  and  $\delta^{18}\text{O}$  tree-ring studies, which depending on dominant influence, could be alternately reflecting (a) source water isotope composition (and thus temperature related to atmospheric condensation processes) or (b) moisture variables such as evaporation, relative humidity, vapor pressure deficit, rainfall. Further refinements have been made to account for the Péclet effect, the consequence of net convective and diffusive water movement in the leaf (Barbour et al. 2004), and to improve understanding of post-photosynthetic processes influencing isotopes (Gessler et al. 2014).

### 1.3.2 21st Century Expansion

With these models established for stable C, H and O isotopes in tree rings, climate–tree-ring isotope studies in the 2000s could now be planned and interpreted based on refined understanding of the environmental controls on fractionation processes. The wave of these studies was fortuitously aided by the timely development of continuous flow-through technology for gases produced by elemental analyzers and streamed with He carrier gas into the isotope-ratio mass spectrometers (Brenna et al. 1997; see also Chaps. 6 and 7), which resulted in faster analysis. The elemental analyzers contributed to this reduction in analysis time by producing the gases needed for analysis in minutes compared to the previous need for lengthy production and purification of the gases on separate (“off-line”) vacuum-line systems. This new instrumentation also allowed analysis on samples of as little as tens of micrograms instead of several milligrams commonly needed with the previous generation of mass spectrometers.

In the last two decades, tree-ring isotopes (particularly of oxygen and carbon) have been used to explore, identify and reconstruct various elements of temporal climate variability. For example, variability and impact of large-scale climate modes, such as ENSO (El Niño-Southern Oscillation) have been studied with  $\delta^{18}\text{O}$  in the Amazon basin, N. America, and Asia, (e.g., Li et al. 2011; Brienen et al. 2012; Sano et al. 2012; Xu et al. 2013a, b; Labotka et al. 2015; Liu et al. 2017). Many of these studies were based on precipitation/evaporation links to  $\delta^{18}\text{O}$ , but others utilized  $\delta^{18}\text{O}$  in tree rings as related to rainfall and drought (e.g., Treyde et al. 2006; Rinne et al. 2013; Young et al. 2015), humidity (e.g., Wright and Leavitt 2006; An et al. 2013; Labuhn et al. 2016), monsoon variability (e.g., Griebinger et al. 2011; Szejner et al. 2016), and even tropical cyclones (e.g., Miller et al. 2006). Tree-ring  $\delta^{18}\text{O}$  itself has likewise been used to better explore ecophysiological aspects of the models (e.g., Gessler et al. 2013).

Stable-carbon isotopes have likewise been an important component of a sweeping range of tree-ring projects. Some of these studies have sought climatological information, inferring temperature and precipitation (e.g., Barber et al. 2004; Liu et al. 2008, 2014) and even sunlight/sunshine (e.g., Ogle et al. 2005; Young et al. 2010; Gagen et al. 2011; Loader et al. 2013; Hafner et al. 2014) because according to the plant carbon isotope fractionation models, the amount of sunlight can influence rate of photosynthesis, which in turn would affect the ratio of intercellular to ambient CO<sub>2</sub> ( $c_i/c_a$ ) and thus  $\delta^{13}\text{C}$ . Tree-ring carbon isotopes have been used in ecological studies related to destructive insect outbreaks (e.g., Haavik et al. 2008; Hultine et al. 2013), some of which also use  $\delta^{18}\text{O}$  (Kress et al. 2009; Weidner et al. 2010). Many other studies are more ecophysiological in nature, inferring water-use efficiency and stomatal response (e.g., Hietz et al. 2005; Peñuelas et al. 2008; Rowell et al. 2009; Wang et al. 2012; Xu et al. 2013a, b, 2018; Saurer et al. 2014; Frank et al. 2015; van der Sleen et al. 2015) and productivity (Belmecheri et al. 2014). Also, McDowell et al. (2010) identified trees most susceptible to mortality in drought with carbon isotopes that showed their reduced ability to regulate the difference between atmospheric and intercellular leaf CO<sub>2</sub> during drought. Tree-ring  $\delta^{13}\text{C}$  has been used to infer past atmospheric CO<sub>2</sub> concentration (Zhao et al. 2006), and atmospheric CO<sub>2</sub> concentration itself has been considered as a subtle influence in accurately modeling tree-ring  $\delta^{13}\text{C}$  (McCarroll et al. 2009). Wang et al. (2019) found evidence from tree-ring isotopes that rising atmospheric CO<sub>2</sub> is improving water-use efficiency and thereby decreasing strength of relationships of ring width with moisture on the Tibetan Plateau.

Some studies are more focused on plant physiology and biochemistry related to assimilation and translocation processes (e.g., Kagawa et al. 2005; Eglin et al. 2008; Eilmann et al. 2010; Bryukhanova et al. 2011; Rinne et al. 2015). Tree-ring  $\delta^{13}\text{C}$  and  $\delta^{18}\text{O}$  have also helped to identify growth rings in tropical trees where they may not be clearly visible (e.g., Evans and Schrag 2004; Anchukaitis et al. 2008; Ohashi et al. 2009), and tree-ring  $\delta^{13}\text{C}$  studies have even reconstructed snow (Liu et al. 2011) and sea level (Yu et al. 2004). Finally, other applications not involving environment or ecophysiology include assessing tree-ring isotopes as a means of crossdating (e.g., Leavitt et al. 1985; Roden 2008) and as an aid in determining provenience of wood (Kagawa and Leavitt 2010).

Tree-ring  $\delta^{13}\text{C}$  has also been used to investigate aspects of plant nutrition (e.g., Bukata and Kyser 2008; Walia et al. 2010; Silva et al. 2015) and particularly pollution (e.g., Battipaglia et al. 2010; Rinne et al. 2010), which has been a fertile and growing application of tree-ring isotopes. Pollutants may impact processes such as stomatal conductance or photosynthesis, and the C-H-O isotopic composition may reflect that alteration, often accompanied by tree-ring width decline (see also Chap. 24). One of the earliest investigations was of SO<sub>2</sub> pollution from a coal-fired foundry by Freyer (1979b), who found altered tree-ring  $\delta^{13}\text{C}$ . Reduced ring size and less negative  $\delta^{13}\text{C}$  were also found in tree rings in the vicinity of a SO<sub>2</sub>-emitting copper smelter in Utah (Martin and Sutherland 1990). Likewise,  $\delta^{13}\text{C}$  in tree rings was elevated up to ca. 100 km downwind from a copper smelter, and the anomaly originated at the time the smelter opened and was presumed to be a consequence of activation of stomatal

closure (Savard et al. 2004); tree-ring  $\delta^2\text{H}$  also seem to be altered by this pollution (Savard et al. 2005).  $\delta^{15}\text{N}$  in tree rings has been found shifted as a consequence of automobile  $\text{NO}_x$  pollution (Doucet et al. 2012) and  $\delta^{15}\text{N}$  shifts along with  $\delta^{18}\text{O}$  and  $\delta^{13}\text{C}$  in tree rings, which indicate increased iWUE near an oil refinery, are consistent with  $\text{NO}_x$  pollution (Guerrieri et al. 2010). Choi et al. (2005) also found such an increase in iWUE in an area of elevated  $\text{NO}_x$  in S. Korea. Tree-ring isotope evidence for ozone pollution has also been found (Novak et al. 2007), and pollution effects have been identified as reducing climate sensitivity of tree-ring isotopes (e.g., Leonelli et al. 2012; Boettger et al. 2014).

## 1.4 Emerging Directions

Several directions in tree-ring isotopes have seen growing interest over the last couple of decades and are promising for future investigations. For example, **seasonal variations** of isotope composition in tree rings (e.g., Helle and Schleser 2004; Monson et al. 2018; see also Chaps. 7, 14 and 15) can be related to both environmental conditions during the growing season as well as late in the previous season when photosynthates may be stored. The resolution of analysis may vary from 2 to 3 earlywood-latewood subdivisions (e.g., Szejner et al. 2016) to numerous microtomed subdivisions a few tens of microns wide (e.g., Evans and Schrag 2004; Helle and Schleser 2004). Computer-controlled milling (Dodd et al. 2008) and laser dissection have been used to separate small subdivisions *in lieu* of microtoming (e.g., Schollaen et al. 2014) for isotope analysis, and laser ablation holds hope for more rapid analysis of these seasonal isotope variations (e.g., Vaganov et al. 2009; Loader et al. 2017) with the products of ablation admitted to a combustion interface connected to the mass spectrometer.

Other analytical advances applied to tree rings include compound-specific isotope analysis and simultaneous analysis of C and O isotopes (dual-isotope analysis, see Chap. 7). Additionally, interpreting different aspects of the environment with **multiple isotopes** has been suggested and applied. For example, Scheidegger et al. (2000) described how under some circumstances  $\delta^{18}\text{O}$  and  $\delta^{13}\text{C}$  from the same tree ring may separately reflect humidity and rates of carbon fixation, respectively, although complete independence is not likely (Roden and Siegwolf 2012; see also Chap. 16). **Isotopomers** (isotope abundance in different intramolecular positions of the glucose repeat units in cellulose, see also Chap. 7) are also regarded as carrying different environmental signals. Sternberg et al. (2006) concluded that different biosynthetic pathways contribute to heterogeneous distribution of isotope composition, and identified O bonded to the carbon-2 position as carrying the isotopic composition of the original source water. O on other positions then carry cumulative influence of source water composition and humidity, from which source water composition could then be subtracted to attain a more accurate proxy of humidity (Sternberg 2009). Augusti and Schleucher (2007) similarly found H isotope differences depending on position in repeating glucose molecule in cellulose so that physiology

and climate could be independently inferred from position-specific isotope analysis. Large, position-specific differences in C-isotope composition were recently identified in cellulose, interpreted as post-photosynthetic shifts in metabolic branching, which may be influenced by environment (Wieloch et al. 2018).

It may be possible to fold the plant isotope fractionation models (Farquhar et al. 1982; Roden et al. 2000) into mechanistic computer models of tree-ring formation, which use physiological processes and environmental conditions during the growing season (e.g., moisture, temperature, and sunlight) to produce photosynthates, activate cambium, and then divide, expand and mature cells in order to replicate observed growth rings (see Chap. 26). Some models operate at the cell level with short time steps and dozens of tunable input parameters, such as the 'TREERING' model (Fritts et al. 1999) and the 'Vaganov-Shashkin' (VS) model (Vaganov et al. 2011). The model of Hölttä et al. (2010) also operates on very short time steps to simulate whole-tree growth. The simpler 'VS-Lite' model (Tolwinski-Ward et al. 2011) has fewer tunable input parameters and operates on monthly climate data to produce wood increments rather than cell growth, and it has gained greater traction for routine applications. An early effort to add isotope algorithms into such models was made by Hemming et al. (2001), who inserted carbon isotope fractionation (of Farquhar et al. 1982) into the TREERING model. Gessler et al. (2014) reviews the extensive catalog of processes (e.g., physicochemical, metabolic, fractionation, transport, storage) within tree tissues, which can contribute to the final carbon and oxygen isotope composition in tree rings and must be considered in interpretation and modeling of tree-ring isotopes. Babst et al. (2018) describe the state of mechanistic tree-ring growth models, including scaling from tree-ring series to whole tree, and potential integration with dynamic global vegetation models (DGVMs) (see also Chap. 26). Because DGVMs are an important tool for improved understanding of current and future global ecology, carbon and water cycles, forest productivity, carbon sequestration, etc., implementation of accurate tree-ring isotope subroutines would provide another layer of control and validation of many aspects of the Earth system.

Finally, spatial mapping of isotope composition in what are known as "**isoscapes**" is of growing interest as related to fields of ecology, hydrology, climate, geology, forensics, etc. (Bowen 2010). Tree-ring isotopes can play a particularly important role in developing these isoscapes because tree rings can add the temporal component to identify changes in isoscapes through time. A number of tree-ring isoscapes related to climate have been developed in the southwestern USA, Europe, Siberia, and particularly notable in China where a rapid expansion of tree-ring isotope chronologies has been ongoing (Saurer et al. 2002; Leavitt et al. 2010; del Castillo et al. 2013). Gori et al. (2018) have recently explored  $\delta^{18}\text{O}$  and  $\delta^2\text{H}$  isoscapes as a tool for provenancing wood cut during logging operations.



## 1.5 Conclusions

Isotope dendrochronology has been around for *ca.* 70 years, but the explosion in the number and diversity of studies over the last 30 years has been breathtaking. This has been driven by advancements in analytical equipment as well as growing recognition of problems for which isotope composition of tree rings may provide resolution, particularly when knowing changes through time is also important. Tree-ring isotopes provide insights into physiological and biochemical processes from leaves to site of wood formation, and changes in isotope values can be used to infer changes in environmental conditions, such as climate parameters.

The history, advances and findings presented here are intended to provide a solid and useful chronology of events, but this summary is not exhaustive. The contents of this book can fill in more of those gaps.

## References

- An W, Liu X, Leavitt SW, Ren J, Xu G, Zeng X, Wang W, Qin D, Ren J (2013) Relative humidity history on the Batang-Litang Plateau of western China since 1755 reconstructed from tree-ring  $\delta^{18}\text{O}$  and  $\delta\text{D}$ . *Clim Dyn* 42:2639–2654. <https://doi.org/10.1007/s00382-013-1937-z>
- Anchukaitis KJ, Evans MN, Wheelwright NT, Schrag DP (2008) Stable isotope chronology and climate signal calibration in neotropical cloud forest trees. *J Geophys Res* 113:G03030. <https://doi.org/10.1029/2007JG000613>
- Augusti A, Schleucher J (2007) The ins and outs of stable isotopes in plants. *New Phytol* 174:473–475
- Babst F, Bodesheim P, Charney N, Friend AD, Girardin MP, Klesse S, Moore DJP, Seftigen K, Björklund J, Bouriaud O, Dawson A, DeRose RJ, Dietze MC, Eckes AH, Enquist B, Frank DC, Mahecha MD, Poulter B, Evans MEK (2018) When tree-rings go global: challenges and opportunities of retro- and prospective insight. *Quat Sci Rev* 197:1–20
- Barber VA, Juday GP, Finney BP, Wilmking M (2004) Reconstruction of summer temperatures in interior Alaska from tree-ring proxies: evidence for changing synoptic climate regimes. *Clim Change* 63:91–120
- Barbour MM, Roden JS, Farquhar GD, Ehleringer JR (2004) Expressing leaf water and cellulose oxygen isotope ratios as enrichment above source water reveals evidence of a Péclet effect. *Oecologia* 138:426–435
- Battipaglia G, Marzaioli F, Lubritto C, Altieri S, Strumia S, Cherubini P, Cotrufo MF (2010) Traffic pollution affects tree-ring width and isotopic composition of *Pinus pinea*. *Sci Total Environ* 408(3):586–593
- Belmecheri S, Maxwell RS, Taylor AH, Davis KJ, Freeman KH, Munger WJ (2014) Tree-ring  $\delta^{13}\text{C}$  tracks flux tower ecosystem productivity estimates in a NE temperate forest. *Environ Res Lett* 9. <https://doi.org/10.1088/1748-9326/9/7/074011>
- Boettger T, Haupt M, Friedrich M, Waterhouse JS (2014) Reduced climate sensitivity of carbon, oxygen and hydrogen stable isotope ratios in tree-ring cellulose of silver fir (*Abies alba* Mill.) influenced by background  $\text{SO}_2$  in Franconia (Germany, Central Europe). *Environ Pollut* 185:281–294
- Bowen GJ (2010) Isoscapes: spatial pattern in isotopic biogeochemistry. *Ann Rev Earth Planet Sci* 38:161–187. <https://doi.org/10.1146/annurev-earth-040809-152429>
- Brand WA, Douthitt CB, Fourel F, Maia R, Rodrigues C, Maguas C, Prohaska T (2015) Gas source isotope ratio mass spectrometry (IRMS). In: Prohaska T, Irrgeher J, Zitek A, Jakubowski N (eds)

- Sector field mass spectrometry for elemental and isotopic analysis [New developments in mass spectrometry, no 3], Chap 16. The Royal Society of Chemistry, Cambridge, UK, pp 500–549
- Brenna JT, Corso TN, Tobias HJ, Caimi RJ (1997) High-precision continuous-flow isotope ratio mass spectrometry. *Mass Spectrom Rev* 16(5):227–258
- Brienen RJW, Helle G, Pons TL, Guyot JL, Gloor M (2012) Oxygen isotopes in tree rings are a good proxy for Amazon precipitation and El Niño-Southern Oscillation variability. *Proc Nat Acad Sci USA* 109(42):16957–16962
- Bryukhanova MV, Vaganov EA, Wirth C (2011) Influence of climatic factors and reserve assimilates on the radial growth and carbon isotope composition in tree rings of deciduous and coniferous species. *Contemp Probl Ecol* 4(2):126–132. <https://doi.org/10.1134/S1995425511020020>
- Bukata AR, Kyser TK (2008) Tree-ring elemental concentrations in oak do not necessarily passively record changes in bioavailability. *Sci Total Environ* 390(1):275–286
- Burk RL, Stuiver M (1981) Oxygen isotope ratios in trees reflect mean annual temperature and humidity. *Science* 211:1417–1419
- Choi WJ, Lee S-M, Chang SX, Ro H-M (2005) Variations of  $\delta^{13}\text{C}$  and  $\delta^{15}\text{N}$  in *Pinus densiflora* tree-rings and their relationship to environmental changes in eastern Korea. *Water Air Soil Pollut* 164:173–187
- Craig H (1953) The geochemistry of the stable carbon isotopes. *Geochim Cosmochim Acta* 3:53–92
- Craig H (1954) Carbon-13 variations in sequoia rings and the atmosphere. *Science* 119:141–143
- Dansgaard W (1964) Stable isotopes in precipitation. *Tellus* 16:436–468
- del Castillo J, Aguilera M, Voltas J, Ferrio JP (2013) Isoscapes of tree-ring carbon-13 perform like meteorological networks in predicting regional precipitation patterns. *J Geophys Res Biogeosci* 118(1):352–360
- Dodd JP, Patterson WP, Holmden C, Brasseur JM (2008) Robotic micromilling of tree-rings: a new tool for obtaining subseasonal environmental isotope records. *Chem Geol* 252:21–30
- Doucet A, Savard MM, Bégin C, Smirnov A (2012) Tree-ring  $\delta^{15}\text{N}$  values to infer air quality changes at regional scale. *Chem Geol* 320(321):9–16
- Edwards TWD, Aravena R, Fritz P, Morgan AV (1985) Interpreting paleoclimate from  $^{18}\text{O}$  and  $^2\text{H}$  in plant cellulose: comparison with evidence from fossil insects and relict permafrost in southwestern Ontario. *Can J Earth Sci* 22:1720–1726
- Edwards TWD, Fritz P (1986) Assessing meteoric water composition and relative humidity from  $^{18}\text{O}$  and  $^2\text{H}$  in wood cellulose: paleoclimatic implications for southern Ontario, Canada. *Appl Geochem* 1:715–723
- Eglin T, Maunoury-Danger F, Fresneau C, Lelarge C, Pollet B, Lapierre C, Francois C, Damesin C (2008) Biochemical composition is not the main factor influencing variability in carbon isotope composition of tree rings. *Tree Physiol* 28(11):1619–1628
- Eilmann B, Buchmann N, Siegwolf R, Saurer M, Cherubini P, Rigling A (2010) Fast response of Scots pine to improved water availability reflected in tree-ring width and  $\delta^{13}\text{C}$ . *Plant Cell Environ* 33:1351–1360
- Emiliani C (1955) Pleistocene temperatures. *J Geol* 63:538–578
- Emiliani C, Geiss J (1959) On glaciations and their causes. *Int J Earth Sci* 46:576–601
- Epstein S, Buchsbaum R, Lowenstam HA, Urey HC (1951) Carbon-water isotopic temperature scale. *Bull Geol Soc Am* 62:417–426
- Epstein S, Thompson P, Yapp CJ (1977) Oxygen and hydrogen isotopic ratios in plant cellulose. *Science* 198:1209–1215
- Epstein S, Yapp CJ (1976) Climatic implications of the D/H ratio of hydrogen in C-H groups in tree cellulose. *Earth Planet Sci Lett* 30:252–261
- Epstein S, Yapp CJ, Hall JH (1976) The determination of the D/H ratio of non-exchangeable hydrogen in cellulose extracted from aquatic and land plants. *Earth Planet Sci Lett* 30:241–251
- Evans MN, Schrag DP (2004) A stable isotope-based approach to tropical dendroclimatology. *Geochim Cosmochim Acta* 68(16):3295–3305. <https://doi.org/10.1016/j.gca.2004.01.006>
- Fairbridge R, Gornitz V (2009) History of paleoclimatology—biographies. In: Gornitz V (ed) *Encyclopedia of paleoclimatology and ancient environments*. Springer, New York, pp 428–437

- Farmer JG (1979) Problems in interpreting tree-ring  $\delta^{13}\text{C}$  records. *Nature* 279:229–231
- Farquhar GD, O'Leary MH, Berry JA (1982) On the relationship between carbon isotope discrimination and the intercellular carbon dioxide concentration in leaves. *Aust J Plant Physiol* 9:121–137
- Francey RJ, Farquhar GD (1982) An explanation of  $^{13}\text{C}/^{12}\text{C}$  variations in tree rings. *Nature* 297:28–31
- Frank DC, Poulter B, Saurer M, Esper J, Huntingford C, Helle G, Treydte K, Zimmerman NE, Schleser GH, Ahlstrom A, Ciais P (2015) Water-use efficiency and transpiration across European forests during the Anthropocene. *Nat Clim Chang* 5:579–583
- Freyer HD (1979a) On the  $^{13}\text{C}$  record in tree rings. Part 1.  $^{13}\text{C}$  variations in northern hemispheric trees during the last 150 years. *Tellus* 31:124–137
- Freyer HD (1979b) On the  $^{13}\text{C}$  record in tree rings. Part 2. Registration of microenvironmental  $\text{CO}_2$  and anomalous pollution effect. *Tellus* 31:308–312
- Freyer HD (1981) Recent  $^{13}\text{C}/^{12}\text{C}$  trends in atmospheric  $\text{CO}_2$  and tree rings. *Nature* 293:679–680
- Freyer HD, Belacy N (1983)  $^{13}\text{C}/^{12}\text{C}$  records in Northern Hemispheric trees during the past 500 years- anthropogenic impact and climate superpositions. *J Geophys Res* 88:6844–6852
- Freyer HD, Wiesberg L (1973)  $^{13}\text{C}$ -decrease in modern wood due to the large-scale combustion of fossil fuels. *Naturwissenschaften* 60:517–518
- Friedli H, Lotscher H, Oeschger H, Siegenthaler U, Stauffer B (1986) Ice core record of the  $^{13}\text{C}/^{12}\text{C}$  ratio of atmospheric carbon dioxide in the past two centuries. *Nature* 324:237–238
- Fritts HC, Shashkin AV, Downes G (1999) A simulation model of conifer ring growth and cell structure. In: Wimmer R, Vetter RE (eds) *Tree-ring analysis*. Cambridge University Press, Cambridge, UK, pp 3–32
- Gagen MH, Zorita E, McCarroll D, Young GHF, Grudd H, Jalkanen R, Loader NJ, Robertson I, Kirchhefer AJ (2011) Cloud response to summer temperatures in Fennoscandia over the last thousand years. *Geophys Res Lett* 38. <https://doi.org/10.1029/2010GL046216>
- Gessler A, Brandes E, Keitel C, Boda S, Kayler ZE, Granier A, Barbour M, Farquhar GD, Treydte K (2013) The oxygen isotope enrichment of leaf-exported assimilates-Does it always reflect lamina leaf water enrichment? *New Phytol* 200:144–157
- Gessler A, Ferrio JP, Hommel R, Treydte K, Werner RA, Monson RK (2014) Stable isotopes in tree rings: towards a mechanistic understanding of isotope fractionation and mixing processes from the leaves to the wood. *Tree Physiol* 34:796–818
- Gori Y, Stradiotti A, Camin F (2018) Timber isoscapes. A case study in a mountain area in the Italian Alps. *PLoS One* 13(2):e0192970. <https://doi.org/10.1371/journal.pone.0192970>
- Gray J, Thompson P (1976) Climatic information from  $^{18}\text{O}/^{16}\text{O}$  ratios of cellulose in tree rings. *Nature* 262:481–482
- Grieffinger J, Bräuning A, Helle G, Thomas A, Schleser G (2011) Late Holocene Asian summer monsoon variability reflected by  $\delta^{18}\text{O}$  in tree-rings from Tibetan junipers. *Geophys Res Lett* 38:L03701. <https://doi.org/10.1029/2010GL045988>
- Guerrieri R, Siegwolf RTW, Saurer M, Ripullone F, Mencuccini M, Borghetti M (2010) Anthropogenic  $\text{NO}_x$  emissions alter the intrinsic water-use efficiency (WUEi) for *Quercus cerris* stands under Mediterranean climate conditions. *Environ Pollut* 158:2841–2847
- Haavik L, Stephen F, Fierke M, Salisbury V, Leavitt SW, Billings S (2008) Tree-ring  $\delta^{13}\text{C}$  and historic growth patterns as indicators of northern red oak (*Quercus rubra* Fagaceae) susceptibility to red oak borer (*Enapholodes rufulus* (Haldeman) (Coleoptera: Cerambycidae)). *For Ecol Manage* 255:1501–1509
- Hafner P, McCarroll D, Robertson I, Loader N, Gagen M, Young G, Bale R, Sonninen E, Levanič T (2014) A 520 year record of summer sunshine for the eastern European Alps based on stable carbon isotopes in larch tree rings. *Clim Dyn* 43:971–980. <https://doi.org/10.1007/s00382-013-1864-z>
- Harkness DD, Miller BF (1980) Possibility of climatically induced variations in the  $^{14}\text{C}$  and  $^{13}\text{C}$  enrichment patterns as recorded by a 300-year-old Norwegian pine. *Radiocarbon* 22:291–298

- Helle G, Schleser GH (2004) Beyond CO<sub>2</sub>-fixation by Rubisco—an interpretation of <sup>13</sup>C/<sup>12</sup>C variations in tree rings from novel intra-seasonal studies on broad-leaf trees. *Plant Cell Environ* 27:367–380
- Hemming D, Fritts H, Leavitt SW, Wright W, Long A, Shashkin A (2001) Modelling tree-ring δ<sup>13</sup>C. *Dendrochronologia* 19(1):23–38
- Hietz P, Wanek W, Dünisch O (2005) Long-term trends in cellulose δ<sup>13</sup>C and water-use efficiency of tropical *Cedrela* and *Swietenia* from Brazil. *Tree Physiol* 25:745–752
- Hölttä T, Mäkinen H, Nöjd P, Mäkelä A, Nikinmaa E (2010) A physiological model of softwood cambial growth. *Tree Physiol* 30:1235e1252
- Hultine KR, Dudley TL, Leavitt SW (2013) Herbivory-induced mortality increases with radial growth in an invasive riparian phreatophyte. *Ann Bot* 11(6):1197–1206. <https://doi.org/10.1093/aob/mct077>
- Jansen HS (1962) Depletion of carbon-13 in young kauri trees. *Nature* 196:84–85
- Kagawa A, Leavitt SW (2010) Stable carbon isotopes of tree rings as a tool to pinpoint timber geographic origin. *J Wood Sci.* <https://doi.org/10.1007/s10086-009-1085-6>. Special Issue “Wood Science and Technology for Mitigation of Global Warming”
- Kagawa A, Sugimoto A, Yamashita K, Abe H (2005) Temporal photosynthetic carbon isotope signatures revealed in a tree ring through <sup>13</sup>CO<sub>2</sub> pulse-labelling. *Plant, Cell Environ* 28:906–915
- Keeling CD, Mook WG, Tans PP (1979) Recent trends in the <sup>13</sup>C/<sup>12</sup>C ratio of atmospheric carbon dioxide. *Nature* 277:121–123
- Kress A, Saurer M, Buntgen U, Treydte KS, Bugmann H, Siegwolf RTW (2009) Summer temperature dependency of larch budmoth outbreaks revealed by Alpine tree-ring isotope chronologies. *Oecologia* 160(2):353–365
- Krishnamurthy RV, Epstein S (1985) Tree ring D/H ratio from Kenya, East Africa and its palaeoclimatic significance. *Nature* 317:160–162
- Labotka DM, Grissino-Mayer HD, Mora CI, Johnson EJ (2015) Patterns of moisture source variability and climate oscillations in the Southeastern United States: a four century seasonally resolved tree-ring oxygen isotope record. *Clim Dyn* 46:2145–2154. <https://doi.org/10.1007/s00382-015-2694-y>
- Labuhn I, Daux V, Girardclos O, Stievenard M, Pierre M, Masson-Delmotte V (2016) French summer droughts since 1326 CE: a reconstruction based on tree ring cellulose δ<sup>18</sup>O. *Climate of the past* 12:1101–1117. <https://doi.org/10.5194/cp-12-1101-2016>
- Leavitt SW (2010) Tree-ring C-H-O isotope variability and sampling. *Sci Total Environ* 408:5244–5253
- Leavitt SW, Long A (1986) Stable-carbon isotope variability in tree foliage and wood. *Ecology* 67:1002–1010
- Leavitt SW, Long A (1988) Stable carbon isotope chronologies from trees in the southwestern United States. *Global Biogeochem Cycles* 2:189–198
- Leavitt SW, Long A (1989) Drought indicated in carbon-13/carbon-12 ratios of southwestern tree rings. *Water Resour Bull* 25:341–347
- Leavitt SW, Long A, Dean JS (1985) Tree-ring dating through pattern-matching of stable-carbon isotope time series. *Tree-Ring Bulletin* 45:1–9
- Leavitt SW, Treydte K, Liu Y (2010) Environment in time and space: opportunities from tree-ring isotope networks. In: West JB, Bowen GJ, Dawson TE, Tu KP (eds) *Understanding movement, pattern, and processes on Earth through isotope mapping*, Chap 6. Springer, Dordrecht, pp 113–135
- Leonelli G, Battipaglia G, Siegwolf RTW, Saurer M, Morra di Cella U, Cherubini P, Pelfini M (2012) Climatic isotope signals in tree rings masked by air pollution: a case study conducted along the Mont Blanc Tunnel access road (Western Alps, Italy). *Atmos Environ* 61:169–179
- Li Q, Nakatsuka T, Kawamura K, Liu Y, Song HM (2011) Hydroclimate variability in the North China Plain and its link with El Niño-Southern Oscillation since 1784 AD: Insights from tree-ring cellulose δ<sup>18</sup>O. *J Geophys Res* 116(D22):D22106

- Libby LM, Pandolfi LJ (1974) Temperature dependence of isotope ratios in tree-rings. *Proc Nat Acad Sci USA* 71:2482–2486
- Libby LM, Pandolfi LJ (1979) Tree thermometers and commodities: historic climate indicators. *Environ Int* 2:317–333
- Liu X, Shao X, Wang L, Liang E, Qin D, Ren J (2008) Response and dendroclimatic implications of  $\delta^{13}\text{C}$  in tree rings to increasing drought on the northeastern Tibetan Plateau. *J Geophys Res* 113:G03015. <https://doi.org/10.1029/2007JG000610>
- Liu X, Zhao L, Chen T, Shao X, Liu Q, Hou S, Qin D, An W (2011) Combined tree-ring width and  $\delta^{13}\text{C}$  to reconstruct snowpack depth: a pilot study in the Gongga Mountain, west China. *Theoret Appl Climatol* 103:133–144
- Liu Y, Cobb KM, Song H, Li Q, Li CY, Nakatsuka T, An Z, Zhou W, Cai Q, Li J, Leavitt SW, Sun C, Mei R, Shen C-C, Chan M-H, Sun J, Yan L, Lei Y, Ma Y, Li X, Chen D, Linderholm HW (2017) Recent enhancement of central pacific El Niño variability relative to last eight centuries. *Nat Commun* 8. <https://doi.org/10.1038/ncomms15386>
- Liu Y, Wang Y, Li Q, Song H, Linderholm HW, Leavitt SW, Wang R, An Z (2014) Tree-ring stable carbon isotope-based May–July temperature reconstruction over Nanwutai, China, for the past century and its record of 20th century warming. *Quat Sci Rev* 93:67–76. <https://doi.org/10.1016/j.quascirev.2014.03.023>
- Loader NJ, McCarroll D, Barker S, Jalkanen R, Grudd H (2017) Inter-annual carbon isotope analysis of tree-rings by laser ablation. *Chem Geol* 466:323–326
- Loader NJ, Young GHF, Grudd H, McCarroll D (2013) Stable carbon isotopes from Torneträsk, northern Sweden provide a millennial length reconstruction of summer sunshine and its relationship to Arctic circulation. *Quat Sci Rev* 62:97–113
- Managave SR, Ramesh R (2012) Isotope dendroclimatology: a review with a special emphasis on tropics. In: Baskaran M (ed) *Handbook of environmental isotope geochemistry*. Springer, The Netherlands, pp 811–834
- Martin B, Sutherland EK (1990) Air pollution in the past recorded in width and composition of stable carbon isotopes of annual growth rings of Douglas-fir. *Plant Cell Environ* 13:839–844
- McCarroll D, Gagen M, Loader NJ, Robertson I, Anchukaitis KJ, Los S, Young GHF, Jalkanen R, Kirchhefer A, Waterhouse JS (2009) Correction of tree ring stable carbon isotope chronologies for changes in the carbon dioxide content of the atmosphere. *Geochim Cosmochim Acta* 73:1539–1547
- McCarroll D, Loader NJ (2004) Stable isotopes in tree rings. *Quat Sci Rev* 23:771–801
- McDowell NG, Allen CD, Marshall L (2010) Growth, carbon-isotope discrimination, and drought drought-associated mortality across a *Pinus ponderosa* elevational transect. *Glob Change Biol* 16(1):399–415. <https://doi.org/43110.1111/j.1365-2486.2009.01994.x>
- Miller DL, Mora CI, Grissino-Mayer HD, Mock CJ, Uhle ME, Sharp Z (2006) Tree ring isotope record of tropical cyclone activity. *Proc Nat Acad Sci USA* 103:14294–14297
- Monson RK, Szejner P, Belmecheri S, Morino KA, Wright WE (2018) Finding the seasons in tree ring stable isotope ratios. *Am J Bot* 105(5):819–821
- Novak K, Cherubini P, Saurer M, Fuhrer J, Skelly JM, Kräuchi N, Schaub M (2007) Ozone air pollution effects on tree-ring growth,  $\delta^{13}\text{C}$ , visible foliar injury and leaf gas exchange in three ozone-sensitive woody plant species. *Tree Physiol* 27(7):941–949
- Ogle N, Turney C, Kalin R, O'Donnell L, Butler C (2005) Palaeovolcanic forcing of short-term dendroisotopic depletion: the effect of decreased solar intensity on Irish oak. *Geophys Res Lett* 32(4). <https://doi.org/10.1029/2004GL021623>
- Ohashi S, Okada N, Nobuchi T, Siripatanadilok S, Veenin T (2009) Detecting invisible growth rings of trees in seasonally dry forests in Thailand: isotopic and wood anatomical approaches. *Trees-Struct Funct* 23:813–822
- Pearman GI, Francey RJ, Fraser PJ (1976) Climatic implications of stable carbon isotopes in tree rings. *Nature* 260:771–773
- Peng TH, Broecker WS, Freyer HD, Trumbore S (1983) A deconvolution of the tree-ring based  $\delta^{13}\text{C}$  record. *J Geophys Res* 88:3609–3620

- Peñuelas J, Hunt JM, Ogaya R, Jump AS (2008) Twentieth century changes of tree-ring  $\delta^{13}\text{C}$  at the southern range-edge of *Fagus sylvatica*: increasing water-use efficiency does not avoid the growth decline induced by warming at low altitudes. *Glob Change Biol* 14:1076–1088
- Prohaska T (2015) History. In: Prohaska T, Irrgeher J, Zitek A, Jakubowski N (eds) Sector field mass spectrometry for elemental and isotopic analysis [New developments in mass spectrometry No. 3], Chap 2. The Royal Society of Chemistry, Cambridge, UK, pp 10–25
- Ramesh R, Bhattacharya SK, Gopalan K (1985) Dendrochronological implications of isotope coherence in trees from Kashmir Valley, India. *Nature* 317(6040):802–804
- Ramesh R, Bhattacharya SK, Gopalan K (1986) Climatic correlations in the stable isotope records of silver fir (*Abies pindrow*) trees from Kashmir, India. *Earth Planet Sci Lett* 79:66–74
- Rinne KT, Loader NJ, Switsur VR, Treydte KS, Waterhouse JS (2010) Investigating the influence of sulphur dioxide ( $\text{SO}_2$ ) on the stable isotope ratios ( $\delta^{13}\text{C}$  and  $\delta^{18}\text{O}$ ) of tree rings. *Geochim Cosmochim Acta* 74:2327–2339
- Rinne KT, Loader NJ, Switsur VR, Waterhouse JS (2013) 400-year May–August precipitation reconstruction for Southern England using oxygen isotopes in tree rings. *Quat Sci Rev* 60:13–25. <https://doi.org/10.1016/j.quascirev.2012.10.048>
- Rinne KT, Saurer M, Kirdyanov AV, Loader NJ, Bryukhanova MV, Werner RA, Siegwolf RT (2015) The relationship between needle sugar carbon isotope ratios and tree rings of larch in Siberia. *Tree Physiol* 35(11):1192–1205
- Robertson I, Leavitt SW, Loader NJ, Buhay B (2008) Progress in isotope dendroclimatology. *Chem Geol* 252:EX1–EX4
- Roden J (2008) Cross-dating of tree ring  $\delta^{18}\text{O}$  and  $\delta^{13}\text{C}$  time series. *Chem Geol* 252:72–79
- Roden JS, Ehleringer JR (1999a) Hydrogen and oxygen isotope ratios of tree-ring cellulose for riparian trees grown long-term under hydroponic, controlled environmental environments. *Oecologia* 121:467–477
- Roden JS, Ehleringer JR (1999b) Observations of hydrogen and oxygen isotopes in leaf water confirm the Craig-Gordon model under wide-ranging environmental conditions. *Plant Physiol* 120:1165–1173
- Roden JS, Ehleringer JR (2000) Hydrogen and oxygen isotope ratios of tree ring cellulose for field-grown riparian trees. *Oecologia* 123:481–489
- Roden JS, Lin G, Ehleringer JR (2000) A mechanistic model for interpretation of hydrogen and oxygen isotope ratios in tree-ring cellulose. *Geochim Cosmochim Acta* 64(1):21–35
- Roden J, Siegwolf R (2012) Is the dual-isotope conceptual model fully operational? *Tree Physiol* 32:1179–1182
- Rowell DM, Ades PK, Tausz M, Arndt SK, Adams MA (2009) Lack of genetic variation in tree ring  $\delta^{13}\text{C}$  suggests a uniform, stomatally-driven response to drought stress across *Pinus radiata* genotypes. *Tree Physiol* 29:191–198
- Sano M, Xu C, Nakatsuka T (2012) A 300-year Vietnam hydroclimate and ENSO variability record reconstructed from tree ring  $\delta^{18}\text{O}$ . *J Geophys Res* 117(D12). <https://doi.org/10.1029/2012JD017749>
- Saurer M, Aellen K, Siegwolf R (1997) Correlating  $\delta^{13}\text{C}$  and  $\delta^{18}\text{O}$  in cellulose of trees. *Plant Cell Environ* 20:1543–1550
- Saurer M, Schweingruber F, Vaganov EA, Shiyatov SG, Siegwolf R (2002) Spatial and temporal oxygen isotope trends at the northern tree-line in Eurasia. *Geophys Res Lett* 29. <https://doi.org/10.1029/2001GL013739>
- Saurer M, Spahni R, Frank DC, Joos F, Leuenberger M, Loader NJ, McCarroll D, Gagen M, Poulter B, Siegwolf RTW, Andreu-Vailes L, Boettger T, Dorado Liñán I, Fairchild IJ, Friedrich M, Gutierrez E, Haupt M, Hiltunen E, Heinrich I, Helle G, Grudd H, Jalkanen R, Levanić T, Linderholm HW, Robertson I, Sonninen E, Treydte K, Waterhouse JS, Woodley EJ, Wynn PM, Young GHF (2014) Spatial variability and temporal trends in water-use efficiency of European forests. *Glob Change Biol* 20:3700–3712. <https://doi.org/10.1111/gcb.12717>

- Savard MM, Bégin C, Parent M, Smirnoff A, Marion J (2004) Effects of smelter sulfur dioxide emissions: a spatiotemporal perspective using carbon isotopes in tree rings. *J Environ Qual* 33:13–25
- Savard MM, Bégin C, Smirnoff A, Marion J, Sharp Z, Parent M (2005) Fractionation change of hydrogen isotopes in trees due to atmospheric pollutants. *Geochim Cosmochim Acta* 69:3723–3731
- Scheidegger Y, Saurer M, Bahn M, Siegwolf R (2000) Linking stable oxygen and carbon isotopes with stomatal conductance and photosynthetic capacity: a conceptual model. *Oecologia* 125:350–357
- Schiegl WE (1974) Climatic significance of deuterium abundance in growth rings of *Picea*. *Nature* 251:582–584
- Schollaen K, Heinrich I, Helle G (2014) UV-laser-based microscopic dissection of tree rings—a novel sampling tool for  $\delta^{13}\text{C}$  and  $\delta^{18}\text{O}$  studies. *New Phytol* 201(3):1045–1055
- Silva LCR, Gómez-Guerrero A, Doane TA, Horwath WR (2015) Isotopic and nutritional evidence for species- and site-specific responses to N deposition and elevated  $\text{CO}_2$  in temperate forests. *J Geophys Res Biogeosci* 120:1110–1123. <https://doi.org/10.1002/2014JG002865>
- Sternberg LSL (2009) Oxygen stable isotope ratios of tree-ring cellulose: the next phase of understanding. *New Phytol* 181:553–562
- Sternberg L, Pinzon MC, Anderson WT, Jahren H (2006) Variation in oxygen isotope fractionation during cellulose synthesis: intramolecular and biosynthetic effects. *Plant Cell Environ* 29:1881–1889
- Stuiver M (1978) Atmospheric carbon dioxide and carbon reservoir changes. *Science* 129:253–258
- Stuiver M, Burk RL, Quay PD (1984)  $^{13}\text{C}/^{12}\text{C}$  ratios and the transfer of biospheric carbon to the atmosphere. *J Geophys Res* 89:11731–11748
- Stuiver M, Braziunas TF (1987) Tree cellulose  $^{13}\text{C}/^{12}\text{C}$  isotope ratios and climate change. *Nature* 328:58–60
- Szejner P, Wright WE, Babst F, Belmecheri S, Trouet V, Leavitt SW, Ehleringer JR, Monson RK (2016) Latitudinal gradients in tree-ring stable carbon and oxygen isotopes reveal differential climate influences of the North American Monsoon System. *J Geophys Res Biogeosci* 121(7):1978–1991. <https://doi.org/10.1002/2016JG003460>
- Tans PP (1978) Carbon-13 and carbon-14 in trees and the atmospheric  $\text{CO}_2$  increase. Ph.D. Dissertation, State University of Groningen, The Netherlands
- Tolwinski-Ward SE, Evans MN, Hughes MK, Anchukaitis KJ (2011) An efficient forward model of the climate controls on interannual variation in tree-ring width. *Clim Dyn* 36(11–12):2419–2439. <https://doi.org/10.1007/s00382-010-0945-5>
- Treydte KS, Schleser GH, Helle G, Frank DC, Winiger M, Haug GH, Esper J (2006) The twentieth century was the wettest period in northern Pakistan over the past millennium. *Nature* 440:1179–1182
- Vaganov EA, Anchukaitis KJ, Evans MN (2011) How well understood are the processes that create dendroclimatic records? A mechanistic model of the climatic control on conifer tree-ring growth dynamics. In: Hughes M, Swetnam T, Diaz H (eds) *Dendroclimatology. Developments in paleoenvironmental research*, vol 11. Springer, Dordrecht, pp 37–75
- Vaganov EA, Schulze E-D, Skomarkova MV, Knohl A, Brand WA, Roscher C (2009) Intra-annual variability of anatomical structure and  $\delta^{13}\text{C}$  values within tree rings of spruce and pine in alpine, temperate and boreal Europe. *Oecologia* 161:729–745
- van der Sleen P, Groenendijk P, Vlam M, Anten NPR, Boom A, Bongers F, Pons TL, Terburg G, Zuidema PA (2015) No growth stimulation of tropical trees by 150 years of  $\text{CO}_2$  fertilization but water-use efficiency increased. *Nat Geosci* 8:24–28
- Vogel JC (1980) Fractionation of the carbon isotopes during photosynthesis. In: *Sitzungsberichte der Heidelberger Akademie der Wissenschaften (Mathematisch-Naturwissenschaftliche Klasse) Jahrgang 1980*. Springer, Berlin, Heidelberg, pp 111–135
- Walia A, Guy RD, White B (2010) Carbon isotope discrimination in western hemlock and its relationship to mineral nutrition and growth. *Tree Physiol* 30:728–740

- Wang W, Liu X, An W, Xu G, Zeng X (2012) Increased intrinsic water-use efficiency during a period with persistent decreased tree radial growth in northwestern China: causes and implications. *For Ecol Manage* 275:14–22
- Wang W, Liu X, Xu G, Treydte K, Shao X, Qin D, Wang G, McDowell NG (2019) CO<sub>2</sub> fertilization confounds tree-ring records of regional hydroclimate at northeastern Qinghai-Tibetan Plateau. *Earth Space Sci* 6:730–740. <https://doi.org/10.1029/2018EA000529>
- Weidner K, Heinrich I, Helle G, Löffler J, Neuwirth B, Schleser GH, Vos H (2010) Consequences of larch budmoth outbreaks on the climatic significance of ring width and stable isotopes of larch. *Trees-Struct Funct* 24:399–409
- Wieloch T, Ehlers I, Yu J, Frank D, Grabner M, Gessler A, Schleucher J (2018) Intramolecular <sup>13</sup>C analysis of tree rings provides multiple plant ecophysiology signals covering decades. *Sci Rep* 8:5048. <https://doi.org/10.1038/s41598-018-23422-2>
- Wilson AT, Grinsted MJ (1977) <sup>12</sup>C/<sup>13</sup>C in cellulose and lignin as paleothermometers. *Nature* 265:133–135
- Wright WE, Leavitt SW (2006) Boundary layer humidity reconstruction for a semiarid location from tree ring cellulose  $\delta^{18}\text{O}$ . *J Geophys Res* 111:D18105. <https://doi.org/10.1029/2005JD006806>
- Xu G, Liu X, Belmecheri S, Chen T, Wu G, Wang B, Zeng X, Wang W (2018) Disentangling contributions of CO<sub>2</sub> concentration and climate to changes in intrinsic water-use efficiency in the arid boreal forest in China's Altay mountains. *Forests* 9(10):642. <https://doi.org/10.3390/f9100642>
- Xu C, Sano M, Nakatsuka T (2013a) A 400-year record of hydroclimate variability and local ENSO history in northern Southeast Asia inferred from tree-ring  $\delta^{18}\text{O}$ . *Palaeogeogr Palaeoclimatol Palaeoecol* 386:588–598
- Xu G, Liu X, Qin D, Chen T, An W, Wang W, Wu G, Zeng X (2013b) Climate warming and increasing atmospheric CO<sub>2</sub> have contributed to increased intrinsic water-use efficiency on the northeastern Tibetan Plateau since 1850. *Trees-Struct Funct* 27:465–475
- Young GHF, Loader NJ, McCarroll D, Bale RJ, Demmler JC, Miles D, Nayling NT, Rinne KT, Robertson I, Watts C, Whitney M (2015) Oxygen stable isotope ratios from British oak tree-rings provide a strong and consistent record of past changes in summer rainfall. *Clim Dyn* 45:3609–3622. <https://doi.org/10.1007/s00382-015-2559-4>
- Young GHF, McCarroll D, Loader NJ, Kirchhefer AJ (2010) A 500-year record of summer near-ground solar radiation from tree-ring stable carbon isotopes. *Holocene* 20:315–324
- Yu KF, Zhao JX, Liu TS, Wang PX, Qian JL, Chen TG (2004) Alpha-cellulose  $\delta^{13}\text{C}$  variation in mangrove tree rings correlates well with annual sea level trend between 1982 and 1999. *Geophys Res Lett* 31:L11203. <https://doi.org/10.1029/2004GL019450>
- Zhao X-Y, Qian J-L, Wang J, He Q-Y, Wang Z-L, Chen C-Z (2006) Using a tree ring  $\delta^{13}\text{C}$  annual series to reconstruct atmospheric CO<sub>2</sub> concentration over the past 300 years. *Pedosphere* 16:371–379

**Open Access** This chapter is licensed under the terms of the Creative Commons Attribution 4.0 International License (<http://creativecommons.org/licenses/by/4.0/>), which permits use, sharing, adaptation, distribution and reproduction in any medium or format, as long as you give appropriate credit to the original author(s) and the source, provide a link to the Creative Commons license and indicate if changes were made.

The images or other third party material in this chapter are included in the chapter's Creative Commons license, unless indicated otherwise in a credit line to the material. If material is not included in the chapter's Creative Commons license and your intended use is not permitted by statutory regulation or exceeds the permitted use, you will need to obtain permission directly from the copyright holder.





# Chapter 2

## Dendrochronology: Fundamentals and Innovations



David Frank, Keyan Fang, and Patrick Fonti

**Abstract** This chapter overviews long-standing foundations, methods, and concepts of dendrochronology, yet also pays attention to a few related paradigm shifts driven by isotope measurements in tree-rings. The basics of annual ring formation are first reviewed, followed by structural descriptions of tree-rings at the macroscopic-to-microscopic scale including earlywood and latewood in conifers (gymnosperms) and hardwoods (angiosperms), as well as wood anatomical features. Numerous examples of inter-disciplinary applications connected to various tree-ring parameters are provided. With the foundation of tree-rings established, this chapter then describes the process and necessity for crossdating—the process by which each and every ring is assigned to a specific year. Methods and terminology related to field sampling also briefly described. The long-standing paradigm of site selection criteria—well shown to maximize common signals in tree-ring width datasets—is challenged in a brief discussion of newer tree-ring isotope literature demonstrating that robust chronologies with high signal-to-noise ratios can be obtained at non-ecotonal locations. Opportunities for isotope measurements to enable crossdating in otherwise challenging contexts are likewise highlighted. The chapter reviews a conceptual framework to disaggregate tree-ring time-series, with special attention to detrending and standardization methods used to mitigate tree-age/size related noise common to many applications such as dendroclimatic reconstruction. Some of the drivers of long-term trends in tree-ring isotope data such as the increase in the atmospheric concentration of CO<sub>2</sub>, age/size/height trends, and climate variation are presented along with related debates/uncertainties evident in literature in order to establish priorities for future investigations. The development of tree-ring chronologies and related quality control metrics used to assess the common signal and the variance of tree-ring data are described, along with the limitations in correlation based statistics

---

D. Frank (✉)

Laboratory of Tree-Ring Research, University of Arizona, Tucson, USA

e-mail: [davidcfrank@arizona.edu](mailto:davidcfrank@arizona.edu)

K. Fang

Fujian Normal University, Fuzhou, People's Republic of China

P. Fonti

Swiss Federal Institute for Forest, Snow and Landscape Research WSL, Birmensdorf, Switzerland

© The Author(s) 2022

R. T. W. Siegwolf et al. (eds.), *Stable Isotopes in Tree Rings*, Tree Physiology 8,  
[https://doi.org/10.1007/978-3-030-92698-4\\_2](https://doi.org/10.1007/978-3-030-92698-4_2)

21

to determine the robustness of tree-ring datasets particularly in the low frequency domain. These statistical methods will gain relevance as tree-ring isotope datasets increasingly approach sample replications and dataset structures typical for tree-ring width measurements.

## 2.1 The Annual Ring—The Keeper of Time in Dendrochronology

In most parts of the world, the predictable and consistent march of the seasons, as our tilted planet Earth orbits around our sun, is strong enough to induce an annually-rhythmic time interval when environmental conditions are conducive to radial plant growth. Similarly, an annual rhythmic season when conditions are not conducive to growth also occurs, and plants for most dendrochronological purposes undergo a dormant season. This annual alteration of growing and non-growing seasons – perhaps one of the most regular features of the planet Earth on evolutionary time-scales—are often associated with changes in the types, and characteristics, of new wood cells developed over the course of a year (Fig. 2.1). These changes are associated with observable, often both macroscopically and microscopically, delineations in annual rings (e.g., Schweingruber 2001). In conifers (gymnosperms), the tracheid cells produced towards the beginning of the growing season tend to grow to larger sizes, yet have thin cell walls. As the growing season progresses and comes to a close, conifer tracheid cells tend to be smaller, particularly in the radial direction, and have thicker cell walls. In hardwoods (angiosperms), the number of wood cells

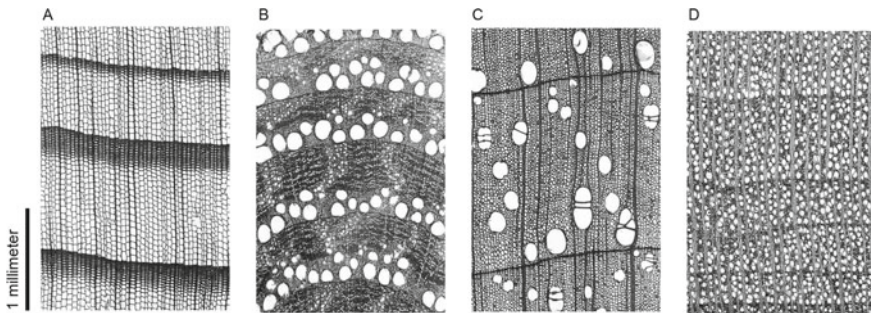


**Fig. 2.1** Examples of wood anatomical and tree-ring structures for **a** gymnosperm (*Abies alba*), **b** a ring porous angiosperm (*Quercus pubescens*) **c** a diffuse to semi-ring porous angiosperm (*Juglans regia*), and **d** a diffuse to semi-ring porous angiosperm (*Malus domestica*). In all cases the outermost rings are towards the top of the images. The xylem of gymnosperms is composed primarily of tracheid cells, with a simpler and more uniform structure amongst species. Angiosperm xylem is composed of a several different types of cells whose characteristics and distributions within annual rings are highly variable amongst species resulting in a diverse range of visual appearances. A very well-prepared surface is necessary to differentiate annual tree-rings. Images from [www.woodanatomy.ch](http://www.woodanatomy.ch) (Schoch et al. 2004)

and the associated structures tends to be more complex and variable, yet annual ring boundaries are also able to be differentiated based upon the characteristics of vessels (often larger and preferentially distributed towards the first part of a ring), and more dense fibers at the end of the growing season. Apart from annual temperature cycles, the monsoon that influences over half of the world's population can also influence the formation of rings due to the prominent hydroclimate seasonality (e.g., Brienen et al. 2016). Especially in tropical regions, elemental composition and/or both stable (especially oxygen) and non-stable (especially carbon, i.e.,  $^{14}\text{C}$ ) isotopes have been used to quantify and confirm annual growth increments (Poussart et al. 2004, 2006; Anchukaitis et al. 2008; Xu et al. 2014). It is these annual growth increments, and our ability to distinguish them and ultimately identify and assign them to an exact year, that is the basis for dendrochronology.

### ***2.1.1 Inter-Annual Variations in Tree-Rings and Tree-Ring Parameters***

The annual rhythm of growing and dormant seasons is the driving factor for annual ring formation. Yet it is the variations in external environmental forcing, predominantly inter-annual variations in weather and climate, that result in different ring traits and properties from one year to the next. Characteristic sequences of wider and narrower rings reflect changes in environmental conditions, and notably also results in a common signal or a unique fingerprint of this environmental variation amongst trees growing in proximal regions and ecological settings (Fritts 1976; Cook and Kairiukstis 1990; Speer 2010). Favorable climatic conditions for tree growth typically results in wider rings. Examples of favorable climatic conditions includes ample moisture for trees growing in more arid ecological settings, or sufficiently high temperatures conducive to photosynthetic activity and cellular growth for high elevation and high latitude trees. Whereas increased ecophysiological stress is typically associated with less radial growth. Although weather/climate variations play a crucial role for assigning the precise year to every ring (see Sect. 2.2), it should be noted that environmental conditions can and do include anything and everything that influences the molecular/isotopic composition, structure, ecophysiological functioning, and growth of trees. Tree-ring width is generally the most easily observable and measurable tree-ring parameter, yet many other tree-ring properties and parameters including wood density, (quantitative) wood anatomical assessments, and of course, stable isotopes, are influenced, often in unique ways, by environmental conditions. The plethora of tree-ring parameters thus expands the range of inter-disciplinary investigations possible with dendrochronology (Fig. 2.2). The rest of this section reviews various (non-stable isotope) tree-ring parameters, and provides an extensive listing of example research applications that have relied upon each of these parameters.

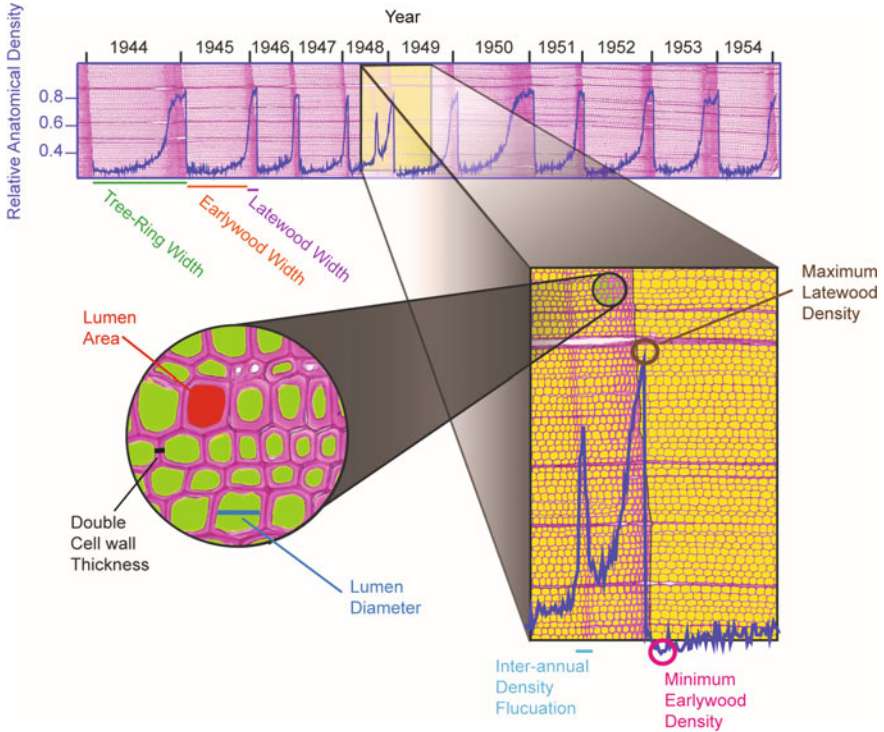


**Fig. 2.2** Illustration of tree-ring and wood anatomical parameters from a sample of Douglas Fir (*Pseudotsuga menziesii*) collected near Tucson, Arizona. Upper panel shows 11 complete annual rings with variability in the total tree-ring width as well as the earlywood and latewood widths. Also shown is a wood density profile based upon anatomical measurements of cell wall thickness using the program ROXAS (von Arx and Carrer 2014). Common ring-width parameters include tree-ring width, earlywood width, and latewood width (top). Important intra-ring density parameters include maximum latewood density and minimum latewood densities, as well as an intra-annual density fluctuation. Average ring density or average earlywood density (not shown in this figure) are also used in research applications (e.g., Babst et al. 2014b). Quantitative wood anatomical parameters include measures of lumen area, lumen diameter and cell wall thickness of the tracheids (bottom left). The lumen diameter and double wall thickness are shown in the radial direction—these can of course be measured in the tangential direction as well

### 2.1.1.1 Tree-Ring Width

A predominance of dendrochronological investigations performed to date have utilized assessments of the total tree-ring width. The ring-width has been long regarded as the basic unit of annual radial tree growth. Tree-ring width measurements are typically performed under a stereomicroscope connected to a linear encoder stage. In cases where rings can be sufficiently resolved with flatbed scanners, digital cameras, or imaged from thin sections, various software packages (e.g., Rydval et al. 2014; von Arx and Carrer 2014; Shi et al. 2019) can facilitate ring detection and

measurement. Investigations relying upon tree-ring width span across the full range of inter-disciplinary applications including archaeological, climatological, ecological, and geological sciences. Examples include: timber trade and resource utilization (Guiterman et al. 2016; Domínguez-Delmás 2020); reconstructions of temperature primarily in higher latitude and/or altitude environments where cooler conditions limit radial tree-growth (Jacoby and D'Arrigo 1989; Esper et al. 2002; Salzer et al. 2014); assessments of past insect activity / outbreaks (Swetnam and Lynch 1989; Speer et al. 2001; Esper et al. 2007); reconstructions of drought (Cook et al. 2004; Fang et al. 2010), precipitation (Büntgen et al. 2011; Griffin and Anchukaitis 2014), streamflow (Woodhouse et al. 2006), and snowpack (Pederson et al. 2011; Belmecheri et al. 2016) variability primarily from locations where moisture limitations, potentially exacerbated by high thermal stress, limits radial growth; quantifying soil erosion rates (Gärtner et al. 2001; Rubiales et al. 2008); dating debris flows and avalanches (Stoffel and Bollschweiler 2008) as well as the construction of ancient (Douglass 1929) and historical structures (Boswijk et al. 2016); quantifying phenotypic traits, variability, and associations with genetic lineage/provenance (Housset et al. 2018); assessments of large-scale ecological disturbances (Pederson et al. 2014), and the resilience of ecosystems to climatic stressors (Chamagne et al. 2017; Kannenberg et al. 2019); understanding and predicting tree mortality (Cailleret et al. 2017); quantifying the climate sensitivity and drivers of forest growth in the past (Babst et al. 2013; St. George and Ault 2014), and making projections about tree growth in the future (Williams et al. 2013; Klesse et al. 2020); reconstructing larger-scale pressure and oceanic and atmospheric circulation indices (Trouet et al. 2009; Villalba et al. 2012; Li et al. 2013); quantifying forest carbon stocks and fluxes (Babst et al. 2014b); and integrating tree-ring and remotely sensed metrics of forest productivity (Coulthard et al. 2017; Seftigen et al. 2018).

Notably, tree-ring width is often divided into the earlywood and latewood widths (Fig. 2.2), sub-annual ring structures that have been demonstrated to carry distinct environmental signals in both angiosperms (Kern et al. 2013) and gymnosperms (Griffin et al. 2011). Measurement and analysis of these sub-annual ring components has allowed skillful reconstructions of the winter precipitation and summer precipitation to be developed from the earlywood and latewood width, respectively (Griffin et al. 2013). The distinct information carried in the intra-annual latewood and earlywood parameters is indicative of the relevance of finer-scale tree-ring parameters.

### 2.1.1.2 Tree-Ring Density

Zooming into a further level of magnification, a second overarching category of measurement parameters involves intra-annual variations in wood density (Fig. 2.2). Over 40 years ago, it was shown that high-resolution intra-annual wood density based upon x-ray measurements of conifer trees offered significant new opportunities for dendrochronology (Parker and Hensch 1971; Schweingruber et al. 1979). In particular the maximum latewood density carries extremely strong common signals

among trees and sites (Schweingruber et al. 1979, Briffa et al. 2002a, Frank and Esper 2005). The maximum latewood density parameter has subsequently taken on a prominent role within the field of dendroclimatology for its skill in reconstructing warm-season temperatures (e.g., Hughes et al. 1984; Briffa et al. 2002b; Fan et al. 2009; Esper et al. 2012; Stoffel et al. 2015; Wilson et al. 2016; Anchukaitis et al. 2017). Meaningful and systematic environmental and ecophysiological signals in the early-wood density, that are notably distinct from tree-ring width and maximum latewood density, have gained increased attention recently (Camarero et al. 2014; Björklund et al. 2017; Buckley et al. 2018; Seftigen et al. 2020). Moreover, inter-annual density fluctuations or so-called false rings are connected to the ecophysiological responses to high aridity during the growing season, as well as to tree age and growth rates (Babst et al. 2016; Battipaglia et al. 2016; De Micco et al. 2016; Zalloni et al. 2016).

Yet, the specialized equipment, labor intensiveness, and relative complexity of x-ray densitometry measurements has dampened the prevalence of density parameters. Regular flat-bed scanners, particularly utilizing blue channel intensity, offer the possibility to measure an optical density (McCarroll et al. 2002). Although there are potential challenges related to potential discoloration, surface preparation, heartwood/sapwood boundaries, and calibration with surface images, the climatic signals in the high frequency domain are comparable to those derived from x-ray-based techniques (e.g., Björklund et al. 2014, 2019; Wilson et al. 2019). However, it should also be noted that recent investigations and reviews (Jacquin et al. 2017; Björklund et al. 2019) have emphasized the equipment specific and resolution dependence on absolute values of the minimum and maximum density. Also crucial is the resolution and ring-width dependence on long-term (or apparent age/size related) trends in density measurements. These factors have potential implications for the divergence phenomena (Björklund et al. 2019; see also Wilmking et al. 2020 and references therein) and clearly merit further research.

At the other end of the technological spectrum, and related to classical x-ray densitometry, are newer applications that employ advanced 3d x-ray tomography (van den Bulcke et al. 2019). Such systems offers labor, analytical, and calibration advantages (Björklund et al. 2019). Other types of x-ray based measurements include measurements of the angle of microfibril in the cell wall via x-ray diffractometry. These microfibril measurements carry strong environmental signatures not reflected in tree-ring width or intra-annual density measurements (Drew et al. 2012). Also, x-ray micro fluorescence allows elemental mapping (see Sect. 2.1.1.4) within annual rings at high resolution (Pearson et al. 2009; Sánchez-Salguero et al. 2019).

### 2.1.1.3 Quantitative Wood Anatomy

Tree-ring width and density parameters are, in fact, relatively simple functions of the number, sizes, distribution, and characteristics (e.g., cell wall thickness) of the wood cells (Vaganov et al. 2006; Fonti et al. 2010). For example, measurements of total tree-ring width in a given tree core are very highly correlated with the corresponding

numbers of cells per ring. Thus, the types of investigations performed using quantitative wood anatomical approaches parallels, and in many respects expands upon, those performed using the tree-ring width and density parameters. Quantitative wood anatomical investigations similarly include climate reconstructions (Panyushkina et al. 2003; Ziaco et al. 2016), assessments of the environmental impacts on tree growth (Carrer et al. 2016; Lange et al. 2020; Puchi et al. 2020), and notably the seasonal progression of environmental influence from the beginning to the end of the annual growth flush (Castagneri et al. 2017; Popkova et al. 2018). The development measurement and analysis techniques for quantitative wood anatomy is contributing to paradigm shifts in tree-ring research that in many respects complements the overall subject of this book on isotopes and tree-rings. Specifically, these high-resolution investigations are contributing to viewing and quantifying the wood cell, and not the annual ring, as the fundamental building block of radial tree growth.

Moreover, wood anatomical studies are yielding deeper mechanistic insights into the growth processes and environmental responses of trees. For example, variations in inter-annual wood density can be well described and modeled as a consequence of competing cell enlargement and cell-wall thickening processes (Cuny et al. 2014; Björklund et al. 2017). Moreover, wood anatomy offers insights into ecophysiological processes related to drought stress and the turgor pressure required to develop and enlarge new wood cells (Friend et al. 2019; Cabon et al. 2020; Peters et al. 2021). Combining tree-ring, wood anatomical, and stable isotope data with complementary measurements from dendrometers (Deslauriers et al. 2007; King et al. 2013a), xylogenesis observations (Belmecheri et al. 2018; Delpierre et al. 2019), sapflow and sapwood area (Peters et al. 2019), offers more holistic assessments of ecosystem functioning, and opportunities to support terrestrial ecosystem and climate modeling approaches with in-situ and long-term data (Zuidema et al. 2018). Notably, it has been recently advocated to include the basic wood formation processes themselves into global vegetation models given the fundamental nature of these processes and the important role forest have on the global carbon balance (Friend et al. 2019).

Some quantitative wood anatomical measurements, for example of the larger vessels in some angiosperms (see Fig. 2.1), can be successfully performed using specifically prepared (e.g., with staining and/or filling vessels) core surfaces and flatbed scanning equipment (Fonti et al. 2009). However, more typically histological thin-sections and transmission microscopy (e.g., von Arx et al. 2016) complemented with specialized imaging and processing software (e.g., von Arx and Carrer 2014) are routinely applied. More specialized techniques such as confocal microscopy have been successfully employed (Ziaco et al. 2016), and there appears to be significant potential for high resolution 3D imaging methods with advancements in physical measurement technology as well as analytical and computation tools (van den Bulcke et al. 2019). Many wood anatomical investigations rely upon new analytical methods such as dividing annual rings into equal-width sectors (Castagneri et al. 2017), or into sequentially ordered and often standardized cell numbers (Popkova et al. 2018) via so-called tracheidograms (Vaganov et al. 2006; Peters et al. 2018). An emergent challenge appears to be to understand if and how the sub-annual timing associated with wood cells (e.g., Ziaco 2020) can be retrospectively inferred. If overcome, this

will open up additional opportunities for multi-seasonal environmental reconstructions. At present, project-specific determinations on whether the added information from quantitative wood anatomical approaches outweighs the additional effort are warranted. However, with continued advancements in quantitative wood anatomy processing and analyses, it is likely that future dendrochronological studies will increasingly be based upon the cellular building blocks.

#### 2.1.1.4 Isotopes and Wood Chemistry

For both brevity here, and completeness, the reader is referred to the rest of the book for a full overview on stable isotopes in tree-rings, as well as other sections in this chapter regarding specific implications to, and methods of, tree-ring research related to stable isotopes.

In terms of non-stable isotopes, dendrochronology has had (e.g., Leavitt and Bannister 2009), and continues to have (Pearson et al. 2018; Reimer et al. 2020) a crucial role in substantially improving the accuracy and precision of radiocarbon dating. Continued technological advancements (e.g., Svalb et al. 2007) are permitting  $^{14}\text{C}$  measurements on long annual tree-ring sequences (Pearson et al. 2020), and continuing to reveal considerable inter-annual to decadal scale variability that is coherent at global-scales (Miyake et al. 2012; Jull et al. 2014; Büntgen et al. 2018). In addition to improving the radiocarbon calibration curve (Reimer et al. 2020), combined dendrochronological and radiocarbon investigations are yielding more, and often annually, precise dates that could not be achieved, at present, by either dendrochronology or radiocarbon studies alone (Oppenheimer et al. 2017; Kuitens et al. 2020; Pearson et al. 2020). Moreover, such coherent signatures in  $^{14}\text{C}$  amongst geographically distant sites, and without common climatic signals, represents a paradigm shift for tree-ring research (Dee and Pope 2016). In essence, this begins to create opportunities for “crossdating” at global scales (see Sect. 2.2 below), and amongst different proxy records (Sigl et al. 2015).

Although wood is primarily composed of carbon, oxygen, and hydrogen, an expansive range of trace elements are incorporated into the annual rings of trees. Subsequent elemental analysis may reflect influences from natural processes such as relatively recent (Sheppard et al. 2008) and ancient (Pearson et al. 2020) volcanic eruptions, be linked to anthropogenic influences such as heavy metals associated with industry (Muñoz et al. 2019), or depend upon year-to-year environmental variations and offer complementary information to the tree-ring width and density parameters (Sánchez-Salguero et al. 2019). Moreover, such measurements can serve as indicators of the annual cycle and help to define annual rings in tropical ecosystems (Poussart et al. 2006), and also provide indications of long-term trends that may be related to tree-age (Scharnweber et al. 2016), or combined climatic and anthropogenic variability (Panyushkina et al. 2016). At present it appears that the more specialized equipment, methods, and time consuming approaches contribute to rather modest sample replications for studies investigating trace elements in tree-rings. This seemingly makes combining such approaches with other independent data the most robust



research pathway. Yet, it appears likely that with ever increased technological capacities, further methodological advancements, and consequently more highly replicated datasets a better understanding of the bioavailability and translocation/immobility will be achieved. This knowledge will presumably open up additional low risk and high reward research avenues.

#### 2.1.1.5 Episodic Ring Features

Superimposed upon the normal progression of tree-ring formation (& analysis), episodic events can impact and leave distinct fingerprints within the annual rings. Such features can in turn be used to understand the nature of these, generally more sporadic, phenomena back in time. Inter-annual density fluctuations have already been discussed as evidence for mid-growing season drought that occurs almost every year in some ecological and climatic settings and very infrequently in others (Zalloni et al. 2016). Other types of episodic markers in tree-rings include so-called frost-rings, whereby freezing temperatures and the formation of ice crystals in the inter-cellular spaces damage developing wood cells (Barbosa et al. 2019 and references therein). Major cold snaps during the growing season that result in frost rings are often connected to major circulation and radiative forcing anomalies from large volcanic eruptions that eject aerosols into the stratosphere (LaMarche and Hirschboeck 1984; D'Arrigo et al. 2001; Salzer and Hughes 2007; Sigl et al. 2015). Tree-rings or especially latewood with anomalously light color (Tardif et al. 2011), or so-called “blue rings” (the term is derived from a common wood anatomical staining that presents incomplete lignification in a blue hue; Piermattei et al. 2015), similarly appear to be an indicator for especially cold conditions late in the growing season. Low-to-medium severity fires can create so-called fire scars that are evidence of localized cambial cell mortality and the subsequent healing over of these wounds. Individual trees often record many dozens of individual fires over their lifespans with composite records successfully used to reconstruct fire history, regimes and return intervals over the past millennia (Swetnam et al. 2009; Taylor et al. 2016). Similarly, traumatic resin ducts and/or compression and tension wood, can be indicative for localized injury or disturbances such as caused by past geomorphic/geological events (Jacoby et al. 1997; Stoffel and Bollschweiler 2008). Moreover, sudden transitions in tree roots, including wood anatomical properties, can be used to reconstruct erosion rates (Gärtner et al. 2001).

## 2.2 Crossdating

Annual ring formation, together with the characteristic coherent year-to-year variability in measurements of tree-ring sequences, gives rise to crossdating. Crossdating is easily the most fundamental concept and important method of dendrochronology, and can be broadly defined as the process by which the exact year is assigned to

each and every ring (Stokes and Smiley 1968; Fritts 1976; Black et al. 2016). It is necessary to crossdate to ensure that all tree-rings, and all subsequent analyses, are properly aligned in time. Most typically crossdating results in the assignment of the exact calendar year to each and every ring. Exceptions to calendric dating exist with more ancient sites where a continuous tree-ring record to modern times has not yet been developed, or is not possible (Roig et al. 2001). While annual ring formation is determined by annually-cyclic growing and dormant seasons, crossdating is rooted upon intra-annual environmental variations, and especially years where strong growth reactions occur in response to more extreme environmental conditions.

Crossdating is necessary to: (1) distinguish inter-annual density fluctuations from annual ring termination (2) identify “locally absent” or so-called “missing rings” resulting from the lack of radial growth over the entire circumference and along the entire stem (and thus not present on the tree-ring sample/radius under investigation), (3) to identify extremely narrow rings e.g., those are only 1–2 cells wide that may have been initially overlooked, (4) to catch any possibilities for error in the assignment or measurement of rings, and (5) in the case of tree-ring materials spanning multiple generations (e.g., from historical or archaeological structures, dead relict wood preserved on the land surface, buried or submerged wood) to align these overlapping segments exactly in time. Only tree-ring sequences with a high degree of certainty in crossdating should be used for dendrochronological applications.

A variety of methods including skeleton plotting, graphical analyses, and statistical assessments of measurement series can be used to perform and assess the crossdating (Stokes and Smiley 1968; Fritts 1976; Holmes 1983; Cook and Kairiukstis 1990; Bunn 2010; Speer 2010). In practice, the development of tree-ring records typically proceeds in a hierarchical order—first working to ensure correct alignment among multiple cores from a given tree, and then amongst trees within a given site. The program COFECHA (Holmes 1983), as well as similar functionality within dPLR package within the R programming environment (Bunn 2008; Bunn et al. 2020), are helpful to verify, or alternatively point to potential errors in, the crossdating for a given sample collection. Such programs allow rapid assessment of synchrony amongst tree-ring series in the hypothesized, as well as temporally lagged positions. The common signal, at least for tree-ring width and maximum latewood density, is typically most evident in stressful years that are associated with narrow rings (or low maximum latewood density) relative to the local mean of approximately one decade to either side of the ring in question. This has given rise to the practice to high-pass filter (i.e., remove multi-decadal to secular variability by detrending), remove autocorrelation, and logarithmically transform tree-ring measurement series prior to crossdating (Holmes 1983; Wigley et al. 1987).

Important considerations in confidently crossdating wood are the length (i.e., number of tree-rings) of records being examined, and the strength of the common signal. Accordingly, measures of synchrony such as the correlation coefficient, combined with information about the series length, can be used to statistically assess the confidence in a crossdated position (Wigley et al. 1987; Loader et al. 2019). The reader is specifically referred to Loader et al. 2019 for both an excellent discussion on the statistical tests for such assessments, and also the importance of tree-ring isotopes

in crossdating (see also below). Any potential or hypothesized dating errors can often be conclusively identified by careful reexamination of the tree-ring samples. Pristine surface preparation is of critical importance. Proper use of successively finer grit sanding and polishing papers or alternatively razor blades / microtomes should allow the individual wood cells to be clearly observed under a microscope (Speer 2010).

Knowledge about the sample context, as well as auxiliary information such as the occurrence and temporal alignment of episodic features such as the presence of intra-annual density variations, frost rings, wide latewood, or traumatic resin canals can offer further confidence to the crossdated position determined from e.g., tree-ring width. Notably, continuous measurement series of wood density or stable isotopes, owing to their high-interseries correlation, can add greatly to the confidence in the assigned dates based upon ring-width (Frank and Esper 2005; Roden 2008; Hartl-Meier et al. 2014; Loader et al. 2019), and in fact open up opportunities to assign the correct dates to samples that could not be crossdated using tree-ring width along (Loader et al. 2019). Once site level crossdating has been achieved, additional independent tests of the crossdating can be garnered by comparison with other regional tree-ring chronologies, or even inferences based upon the expected patterns of tree growth from instrumental records or models of tree growth.

When working with particularly challenging sets of tree-ring samples such as from tropical regions, or on more ancient samples, radiocarbon dating can be performed to either refute (Herrera-Ramirez et al. 2017) or help verify annual ring formation and dating (Andreu-Hayles et al. 2015; Poussart et al. 2006). This represents an iterative advancement in the partnership between dendrochronology and  $^{14}\text{C}$  dating in which tree ring records, and increasingly annually-resolved measurements (Pearson et al. 2018), have long-been crucial to calibrate  $^{14}\text{C}$  dating. The potential to use multi-parameter approaches, including the high inter-series correlation that is becoming increasingly evident in  $^{18}\text{O}$  measurements (Roden 2008; Hartl-Meier et al. 2014; Klesse et al. 2018c; Loader et al. 2019), appear to be a further promising direction for dendrochronological advancement.

## 2.3 Sampling and Site Selection

With the incredible multi-disciplinary range of dendrochronology (see Sect. 2.1.1 above), it is perhaps expected that the protocols and sampling designs to collect tree-ring data exhibit a wide range of variability amongst, and even within, sub-disciplines such as dendroclimatology, dendroecology, and dendroarchaeology (Fritts and Swetnam 1989; Cook and Kairiukstis 1990; Nehrbass-Ahles et al. 2014; Speer 2010). Ignoring the vast range in individual protocols, a typical sampling strategy would, for a location of interest, involve the collection of samples from e.g., two dozen trees. Such a collection of tree-ring samples is usually obtained from a geographically constrained area (e.g., within a few hundred meters), and where the trees are hypothesized to be in the same ecological setting, influenced by the same environmental

factors, and usually of the same species. Such collections are typically crossdated and analyzed together, and referred to as a tree-ring site.

Increment borers are used to extract cores usually approximately 5 mm in diameter. For isotope measurements sometimes larger diameter (e.g., 1 cm) cores are collected to ensure enough sample material for subsequent analysis. Depending upon the research objectives and setting, cross-sections may be obtained and can be preferable especially in situations where samples are taken from trees that are no longer living. Even when the investigation may only involve isotope measurements for the most recent years, it is highly preferable for the collected tree core to span the full bark to pith radius. A full core allows estimates of tree age, and offers the greatest number of rings to facilitate crossdating. Collecting multiple cores per tree facilitates crossdating as well. Two cores per tree is routine. It is recommended to take even more cores per tree when investigating genera (e.g., *Juniperus* spp.) or locations (tropics) that are known to exhibit high within tree variability in the wood anatomical structures and/or ring characteristics. Specific investigations have not found a link between tree coring and increased mortality within multi-decadal time frames (van Mantgem and Stephenson 2004; Wunder et al. 2011).

Generally samples are collected at, or near, 1.37 m above the base of the tree. This corresponds to a routinely applied silvicultural measurement—the tree diameter at breast height (DBH)—and notably allows tree-ring width measurements to be more readily compared, and integrated, with periodic surveys of tree size (Evans et al. 2017). Moreover, collecting cores at this height: (i) mitigates growth irregularities/buttrressing pronounced near the root collar, (ii) allows for the collection of most tree rings (rings produced when the tree was shorter than coring height will be missed), and (iii) is reasonably convenient for the physical collection of the sample (Cook and Kairiukstis 1990; Speer 2010). It is recommended to collect as many auxiliary data when sampling (e.g., tree diameter, height, location, canopy coverage), in order to assist with analysis and interpretation (see below on age/size/height trends), as well as integration into databases and subsequent multi-investigator compilations (Babst et al. 2014a; Brewer and Guiterman 2016).

Recent overviews of the International Tree-Ring Data Bank (ITRDB; Babst et al. 2017; Klesse et al. 2018b; Zhao et al. 2019; Pearl et al. 2020)—a compilation of thousands of tree-ring sites and datasets that have been graciously provided by hundreds of data contributors over the years in spirit of open exchange of scientific data—demonstrate that this collection is not representative of the global forested areas. Data in the ITRDB favor (i) gymnosperms over angiosperms, (ii) higher latitudes over tropical latitudes, (iii) older over younger trees, and (iv) are dominated by the tree-ring width parameter. In terms of tree-ring stable isotope measurements, at present only very few datasets have been submitted to the ITRDB. This presumably reflects the still expanding status of measurement efforts, the greater effort and expense in tree-ring isotope data, and far “younger” efforts to systematically share tree-ring isotope data (Csank 2009).

Sampling of tree-ring sites has been regularly coupled to the specific research question and objective. Recognizing the multiple influences on tree growth (see

Sect. 2.4.1), there is a practice to select trees that are minimally influenced by environmental factors not under primary consideration (Fritts and Swetnam 1989; Cook and Kairiukstis 1990; Speer 2010). For example, when sampling trees for climate reconstruction, individual trees or forest stands whose growth is significantly influenced by factors such as geomorphic activity or obvious disturbance from insect outbreaks would tend to be avoided. For climate reconstruction, this would typically also involve the preferential sampling of trees where growth is most limited by the environmental parameter of interest. And for investigations of fire scars, sampling would focus on trees showing evidence of fire scars. Some, but not all, of the patterns of data collection in the International Tree-Ring Databank are driven by long-standing evidence that the common signal, crossdating, and also climatic information in tree ring sites, are strongest for trees growing near the distributional limits (Fritts 1976). This has been referred to as “The Principle of Tree and Site Selection”. So as described above, sampling for temperature reconstruction tends to take place near the upper or latitudinal treeline, whereas precipitation reconstructions tend to be developed from trees growing near the dry /lower treeline locations. This principle or paradigm of tree and site selection is abundantly supported by investigations utilizing tree-ring width, and amply supported by maximum latewood density. This paradigm, however, seems to be cast in doubt by tree-ring isotopes. There are an increasing number of studies that, in comparison to tree-ring width, show extremely strong common signals amongst proximal tree and sites for stable carbon and especially oxygen isotopes (e.g., Hartl-Meier et al. 2014; Klesse et al. 2018c) questioning the application of this principle to tree-ring sampling without consideration of the tree-ring parameters under investigation. It is plausible that a site selected to maximize the common signal in tree-ring width might not maximize the common signal for oxygen isotopes, and vice-versa. More thought, and empirical assessments, likely are warranted to revisit this topic with stable isotope data. It seems, however, that this should no longer be considered a universal principle for dendrochronology that aims to be inclusive for all tree-ring parameters.

## 2.4 Deconstructing Variability in Tree-Ring Data

### 2.4.1 *The Linear Aggregate Model*

A series of tree-ring measurements can be viewed as a composite of multiple underlying signals—namely all of the factors that influence the tree-ring parameters—whose individual contributions “sum-up” in the observed time-series (Fig. 2.3). The well-known linear aggregate model of tree growth (Cook 1987) formulates this perspective as an elegant conceptual framework that describes an observed tree-ring time series as the sum of the following five factors:

**1) Biological age/size trend.** Many measurements of tree growth change with the age and size of the tree. Some effects, for example, in tree-ring width measurements are

geometric related to distributing a given amount of biomass around an ever-increasing circumference (Biondi & Qeadan 2008). Other age/size related trends may be due to the changing “social status” of trees within the stand and be related to relative access to light (Cook 1985; Klesse et al. 2018c), or perhaps roots to increasing soil depth with time. Many dendrochronology applications attempt to understand, and remove, the influence of age/size related trends in a process called “detrending” (see below).

**2) Climate Signals.** Inter-annual variability in climatic conditions such as temperature, precipitation, soil moisture, and vapor pressure deficit is at the heart of dendrochronology. It is the unique fingerprints of these variations in tree-ring parameters that enable crossdating. While crossdating usually focuses on the year-to-year variability, it should be noted that longer term (e.g., multi-decadal to centennial-scale and beyond) is also imprinted in tree-ring data. Such long-term variability is, however, more challenging to partition from age/size trends as we will see below. The climate signals tend to be common amongst trees at a site, as well as sites within broader regions (on the scale of hundreds of kilometers) provided similarities in the underlying ecological and climatic conditions (Fritts 1976; Schweingruber et al. 1979).

**3) Endogenous Disturbance.** Periodic disturbances to *some* trees at a given site due to tree or stand internal factors are also observed in tree-ring data. A classic example of an endogenous disturbance is related to gap phase dynamics in closed canopy forests. Here, growth pulses can be often observed in remaining trees following the removal (natural or anthropogenic) of nearby tree(s), especially if the tree(s) removed had a dominant canopy position and/or competed for moisture (Giuggiola et al. 2016). Provided the sampling covers a sufficiently large spatial scale relative to the size of the local disturbances, only some trees in a site will show responses to such disturbances. Endogenous disturbances may be the primary subject of dendroecological investigations (Pederson et al. 2014). Whereas for investigations where such disturbances are “noise”, their impact on tree-ring time series can be mitigated by a sufficiently large sample size collected from trees distributed over sufficiently large spatial areas, as well as statistical techniques (e.g., Principal Component Analyses or robust means) that can serve to extract signals common to all trees in a stand (Peters et al. 1981).

**4) Exogenous Disturbance.** Period disturbances affecting, most if not all trees in a stand, such as large-scale insect infestations, massive windthrow events, or fires are also evident in tree-ring data. Again, exogenous disturbances may be the primary topic of dendrochronological investigations. Both for applications aiming to retain or mitigate exogenous disturbance impacts, assessment of multiple sites across broader regions, different species (e.g., host versus non-host for reconstruction) as well as analytical techniques for disturbance detection and/or signal extraction are of value (Swetnam and Lynch 1989).

**5) Error/Noise.** The noise term of this model can be thought to include any variability not accounted for by the first four factors and is presumed to be uncorrelated amongst trees in a stand. Yet, clearly given the conceptual nature of the linear aggregate

model, the “error” term in the originally conceived model may inherently including meaningful and scientifically understandable and interesting components such as genetic variation (King et al. 2013b; Housset et al. 2018). Mixed effects models build on the basic principles of the linear aggregate model. Yet importantly also allow for interactions and a non-independence of the factors (Klesse et al. 2020) with examples including a differential effect of climate on younger versus older trees, or compounded effects of drought induced stress and disturbance from insects on tree-ring width.

### 2.4.2 *Detrending and Standardization*

While each of the terms in the linear aggregate model could receive its own chapter, and the reader is also referred to Cook (1987), a few additional paragraphs will be spent on the process of detrending and standardization. This is due to the importance of differentiating long-term age/size related trends from long-term environmental and ecological signals of interest for many dendrochronological investigations, and because active research focus is warranted as there does not appear to be a universal or best solution to detrend tree-ring data. However, it should be noted from the onset that potential advantages of stable isotope and some quantitative wood anatomical parameters are more moderate age/size related trends (i.e., noise for many applications) in comparison to tree-ring width. This topic is addressed in Sect. 2.4.3.

When aggregating multiple trees into a tree-ring chronology, it is often scientifically favorable to eliminate (to the maximum extent possible) the variation due to the age/size of a tree AND simultaneously retain all (to the maximum extent possible) variation from other factors of interest, say, climate. Moreover, differences in the absolute values of tree-ring measurements, say from a faster versus slower growing tree, or from one with lower versus higher  $^{13}\text{C}$  values, when developing a tree-ring chronology, also must be considered. Tree-ring detrending and standardization is the process by which time-series are handled, often sensu the linear aggregate model, to estimate and remove the age/size related trends and standardize tree-ring data into dimensionless indices (Fritts 1976; Jacoby and D’Arrigo 1989; Cook and Kairiukstis 1990; Cook and Krusic 2005; Melvin and Briffa 2008; Briffa et al. 2013).

There are two major categories of techniques to perform tree ring detrending, namely, those in which detrending curve is based upon (i) the individual tree-ring time series, or alternatively, (ii) a sample/population estimate of the age/size function. Most, if not all, of the earlier studies in dendrochronology relied on estimating the age/size trend on an individual, series-by-series, basis using deterministic (e.g., linear regression or negative exponential) curves that can be expressed as a simple equation, or alternatively, stochastic methods (e.g., moving averages, cubic smoothing splines, etc.) that are adapted to the data. Removal of the age/size trend is then typically achieved by dividing the observed (i.e., the tree-ring measurements) by the estimated (i.e., either the deterministically or stochastically fit curve) resulting in dimensionless tree-ring indices. Individual detrending may be performed with

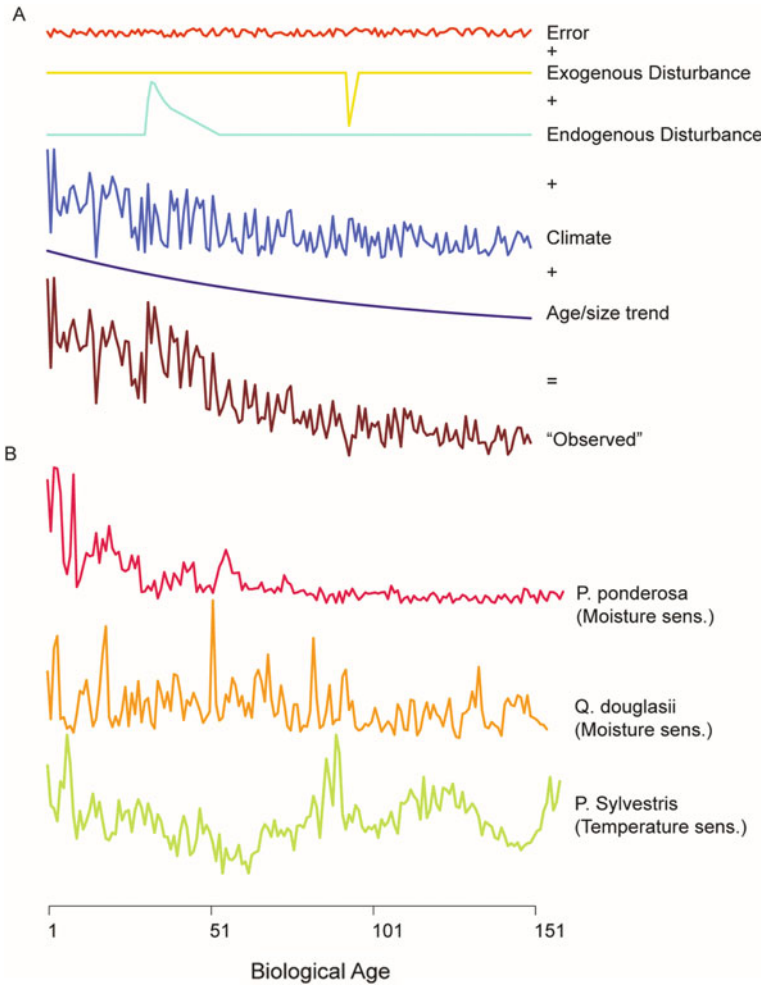


**Fig. 2.3** Illustration of the linear aggregate model. **a** Schematic example using fictitious data showing how an observed time-series can be decomposed as the sum of the age/size trend, climate induced variation, endogenous and exogenous disturbances, and some error term. The interannual variance of the climate term was decreased with increasing tree-age to represent the often observed decreased inter-annual variation in ring-widths as trees grow and distribute biomass around an ever increasing circumference. Note that the long-term trend in the climate term would be difficult to empirically partition from the age/size trend in a single observational time-series. **b** Examples of three time-series of tree-ring measurements scaled to have the same vertical range and aligned by innermost measurement which is assumed to represent a biological/cambial age (years since pith) of 1. The series are a *Pinus ponderosa* from New Mexico, USA (pink; Dean and Robinson 1986), *Quercus douglasii* from California, USA (orange; Stahle et al. 2012, 2013); USA, and *Pinus sylvestris* from higher latitudes in Sweden (green; Esper et al. 2012). The stronger multi-decadal variability evident in the high latitude site from Sweden is consistent with the temperature variations in this region. The *Pinus ponderosa* is a classic example for a negative exponential age/size trend as well as heteroscedasticity



“conservative” methods (e.g., linear regression or negative exponential curves) that attempt to retain longer-term climate information (e.g., Jacoby and D’Arrigo 1989) or alternatively flexible curves that primarily retain inter-annual to decadal-scale variability as is desirable for crossdating (e.g., Holmes 1983). In addition to removing age/size related trends, detrending by division (i.e., ratios) has the benefit of mitigating the commonly occurring heteroscedastic relationships in tree-ring width data namely the often observed relationship between the local variance and mean (or spread versus level). Dividing the tree-ring measurements by the growth curve results in a local normalization of variance structure along the tree-ring series (see Fig. 2.4). For maximum latewood density data (e.g., Helama et al. 2008), and likely also stable isotope data (Büntgen et al. 2020), where such heteroscedasticity is clearly weaker, detrending can be performed by subtracting the modeled aged trend from the tree-ring measurements (e.g., Cook and Peters 1997). Importantly, this detrending, also standardizes tree-ring series to eliminate influences from difference in absolute growth rates (or isotope discrimination) in a tree-ring chronology as all tree-ring data are now in dimensionless indices with a mean of approximately unity.

Three well-recognized pitfalls exist with individual detrending. Firstly, it is not possible to confidently differentiate age/size related trends from other signals of interest such as climate (but see “signal free” detrending discussion below). Secondly, variability on time-scales longer than the individual tree-ring measurement series cannot be retained—the so-called “Segment Length Curse” (Cook et al. 1995)—which is especially problematic for investigations that build multi-centennial or millennial length records from shorter, overlapping, crossdated series. Lastly, biases in the tree-ring indices might be created when the estimated curve approaches values close to zero (Cook et al. 1997). The recognition of these pitfalls, and especially the first two, challenges has driven continued innovations in detrending methods—particularly when long-term (e.g., centennial-scale and beyond) information is sought (e.g., Briffa et al. 2013).

The second category of established methods to remove the age/size related trends, and one in a manner that can preserve low-frequency variability and break the “Segment Length Curse”, is the so-called “Regional Curve Standardization” method (RCS; Briffa et al. 1992; Cook et al. 1995; Esper et al. 2003; D’Arrigo et al. 2006; Helama et al. 2017). The RCS method allows retention of low-frequency signals by detrending all series with the same regional growth curve. Detrended series are thus not constrained to a mean of unity. Rather, they can “float above” or “sink below” the regional mean to capture periods of above or below average growth on time-scales longer than individual trees’ lifespans. In RCS, a population estimate, the so-called regional curve, for the age-related trend is estimated based upon all tree-ring data at a site. Operationally, the regional curve is estimated by aligning all tree-ring series by their cambial age (i.e., first ring after the pith is a cambial age of 1) and averaging the age-aligned data together. In cases where the tree-core (or cross-section) does not include the pith, the number of years to the pith can (and should) be estimated (see Pirie et al. 2015 for a review). Methods for RCS employed in the ARSTAN (Cook and Krusic 2005) and dplR (Bunn 2008; Bunn et al. 2020) frameworks both allow the inclusion of pith-offset information. The detrended tree-ring data are then

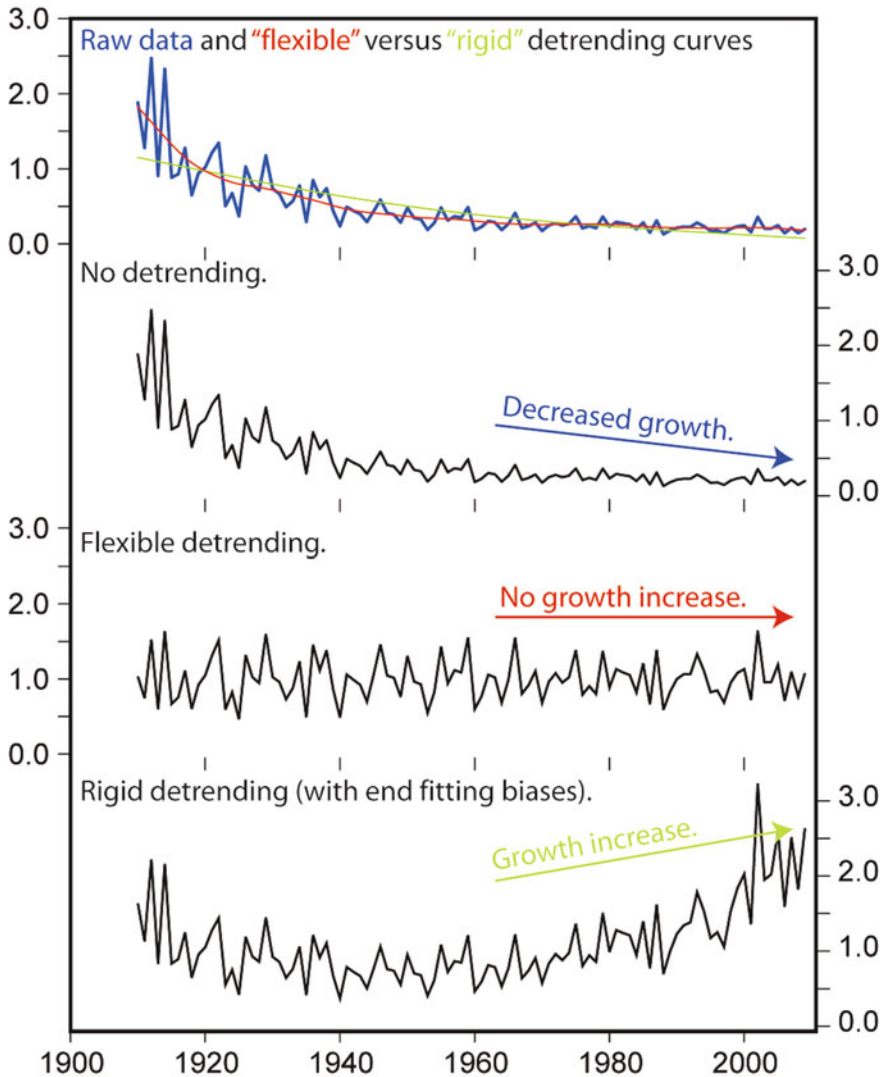


**Fig. 2.4** Schematic illustration of potential challenges in identification of growth trends in tree-ring data with e.g., implications for assessment of CO<sub>2</sub> fertilization effects. The top panel shows a fictitious example of tree-ring width data (blue) with an age/size related trend. Examples of methods applied in the literature to assess growth changes including (i) no detrending (note this method appears useful for the last millennia of multi-millennial tree-ring series where strong conclusions are able to be drawn if an increase in tree-ring width is observed; Salzer et al. 2009), (ii) flexible detrending, (iii) conservative detrending (see also Peters et al. 2015) also with some degree of end-fitting artifacts (see Cook and Peters 1997) are shown. The manner in which these illustrative tree-ring data have been handled impacts potential conclusions on growth trends. This example aims to illustrate the relevance of careful assessments of potential age/size related trends in analysis, interpretation, and dissemination. Note, dividing the tree-ring data with fit curves results in a homoscedastic tree-ring indices in the lower two panels

derived by removing (usually by ratios for tree-ring width data) the regional curve from all measured tree-ring series.

RCS application ideally is performed on tree-ring records (1) with a diverse range of start (pith) and end dates (outermost ring), (2) that are very highly replicated with many individual samples, and (3) from a homogeneous well defined ecological setting where all trees are expected to have similar growth rates and ontogenetic trends (e.g., Esper et al. 2012; Briffa et al. 2013). The first point is important because this helps mitigate the impact of temporally aligned events (such as climatic fluctuations or ecological disturbances) in the calendrically dated tree-ring data from impacting the shape of the regional curve. Secondly, composite datasets comprised of overlapping crossdated sequences for the past millennia from a single, well constrained ecological setting appear ideal for the application of RCS as a single regional curve could theoretically be used (Briffa et al. 2013). Well-replicated datasets are especially critical as the tree-ring indices are not constrained to a mean of one. On one hand, the differences in growth rates that are standardized in individual detrending add noise and greater uncertainty about the mean (e.g., D'Arrigo et al. 2006; Melvin and Briffa 2014b). But on the other hand, the subtle differences in mean growth rates of cohorts of trees that lived at different times is precisely the low-frequency signal that can be retained with RCS (D'Arrigo et al. 2006). And lastly, a homogenous ecological setting is crucial to ensure both uniformity in the underlying climate signal as well as growth rates. This criterion is difficult to ensure, but assessments of the growth rates of different cohorts over time might suggest homogeneity. In cases where there is reason to doubt the homogeneity of a dataset, it is feasible to develop and apply regional curves for distinct dataset subsets, e.g., the modern and ancient portions of a tree-ring chronology. Detrending via multiple RCS cohorts should be performed in situations where sampling differences, site difference, or anthropogenic disturbances (e.g., forest management regimes, responses to elevated CO<sub>2</sub> or nitrogen concentrations) may significantly compromise the homogeneity of the dataset over time. Such approaches have the advantage of reducing potential biases in the final chronology, but at the same time make it more difficult to retain long-term variability of interest (Briffa et al. 2013).

A third approach for detrending that continues to gain traction in tree-ring research is the so-called "Signal Free" method (Melvin and Briffa 2008; Melvin and Briffa 2014a, b). This approach is based upon the recognition that the curves used to detrend tree-ring data, particularly for individual detrending, do not (readily) distinguish between the age/size trends and long-term climatic variability (Melvin and Briffa 2008). Conceptually, the "signal free" approach is similar to the RCS. Yet, instead of developing a population estimate of the regional curve, a population estimate of the common non-age/size related variability (i.e., generally the climate signal) has the central role. Specifically, the signal free method iteratively removes a population estimate of the tree-ring chronology from the tree-ring measurements prior to the next detrending iteration. Multiple iterations are performed until (in most cases) a stable estimate for the tree-ring data and chronology is achieved. The "signal free" method can be applied at the individual series level, or alternatively can be employed to derive a signal-free estimate of the regional curve in RCS. Investigations that

have employed the signal-free detrending have shown a superior retention of lower-frequency climate related signals in the final tree-ring chronology (e.g., Fang et al. 2012; Melvin and Briffa 2014a; Wilson et al. 2019).

Awareness of the potential age/size related trends is crucial for all tree-ring and subsequent detrending/standardization approaches. Moreover, awareness of how such long-term trends, and/or methodological approaches applied to remove them (Fig. 2.4), potentially impacts scientific investigations is also required, as is communicating such information in publications. Continued research on both methodological detrending/standardization methods, and also emphasizing the importance of highly replicated tree-ring records, are both necessary.

### 2.4.3 Long-Term Trends in Tree-Ring Data

Tree-ring data are of great value for the centennial to multi-millennial scale perspectives on changing ecosystems, climate, and societies, including rare, extreme, and long-term variations. A recurring theme in the dendrochronology literature is the faithful decomposition—sensu the linear aggregate model—of the variable of interest while mitigating noise from other factors. As described in Sect. 2.4.3 much of the focus in dendrochronology literature has been on removing age/size related trends, while retaining all long-term climate related trends. This endeavor is particularly challenging due to i) multiple environmental and biological factors and processes that could result in long-term trends in tree-ring data, ii) reduced degrees of freedom to statistically assess and verify lower-frequency changes (e.g., Briffa et al. 2002a; Melvin and Briffa 2014b) and iii) limited opportunities to make direct comparisons with independent long-term records of the same exact phenomena (Emile-Geay et al. 2017) recognizing further differences in seasonality, resolution, and geographic proximity. As dendrochronology continually expands by covering longer periods of time, over more regions, into newer disciplines such as terrestrial carbon cycling and ecophysiology, and with greater reliance on parameters from wood anatomy and stable isotopes, new challenges and opportunities are arising. There are a perhaps a couple of points of note related to these developments, and with a focus on stable isotopes.

Firstly, there is not a consensus on the existence or absence of age/size related trends in stable isotopes (e.g., Klesse et al. 2018c and references therein; Büntgen et al. 2020 and references therein; McCarroll et al. 2020 and references therein), and thus also not for the potential mechanisms of such age/size trends nor how they may differ for carbon and oxygen isotopes. Given the evidence and disparities in the literature, it seems that the following working conclusions can be drawn:

- (1) Investigators should consider the possible existence of age/size related trends in their data, how such potential trends are best quantified, and attempt to identify if and how such methodological approaches related to removing (or not) potential age/size trends, may impact the subsequent analysis and conclusions.

- (2) Age/size/height related noise in most tree-ring stable isotope data appear to be a smaller fraction of the variance in comparison to most tree-ring width data. On one hand, this suggests less than perfect removal, if needed, has less severe consequences on the study. Yet this also suggests, it is more difficult to identify, consider and remove age/size/height related trends.
- (3) Even in the absence of age/size/height trends in tree-ring stable isotope data for a given location and species, the substantial offset in absolute values both within a single tree and amongst different trees at a site (e.g., Leavitt and Long 1986; Klesse et al. 2018c; Esper et al. 2020), indicate standardization and/or thoughtful compositing is required to minimize signals that might be artifacts as individual time-series enter or exit from a tree-ring chronology (e.g., Hangartner et al. 2012; Melvin and Briffa 2014b)

Secondly, the use of  $^{13}\text{C}$  measurements as indicators for both direct climate effects on trees such as, temperature, precipitation and sunshine variation (e.g., Hafner et al. 2014), and to also infer changes in water use efficiency (e.g., Saurer et al 2004), appears to require more efforts to robustly separate  $\text{CO}_2$  and meteorological driven changes in carbon isotope discrimination. Existing approaches include constrained stochastic detrending (McCarroll et al. 2009) and the use of climate variability (Treydte et al. 2009; Frank et al. 2015, but see Lavergne et al. 2019). Further development of well-replicated tree-ring  $^{13}\text{C}$ ,  $^{18}\text{O}$  and tree-ring width / wood anatomy datasets and complemented by detailed ecological / forest biometric data (e.g., Klesse et al. 2018a), as well as integrated empirical-modelling approaches, as facilitated by this book, will offer needed insights and opportunities to disaggregate and understand the drivers of isotope discrimination and forest ecosystem functioning.

## 2.5 Chronology Development, Confidence, Sample Replication, Coherence, and Variance

### 2.5.1 *Tree-Ring Chronologies*

In comparison to other earth and environmental science related fields, the relative ease with which tree-ring samples are collected and measured has greatly facilitated well-developed statistical frameworks for signal and noise assessment in dendrochronology (e.g., Wigley et al. 1984; Cook and Kairiukstis 1990). Multiple cores per tree, multiple trees per site, and multiple sites per region, can be regarded as hierarchical view on drawing samples from a population, and using such samples to estimate population characteristics. Within dendrochronology it is typical, after crossdating, to take the multiple individual measurement time-series and average (or use another statistical measure of central tendency such as the robust mean, median or other percentiles) their values into a single time-series—a tree-ring chronology. A tree-ring chronology enjoys the characteristic that the common signal from the

sampled population of individual trees is enhanced by averaging out “noise” variance specific to individual time-series.

The most basic type of tree-ring chronology consists of the average of all individual tree-ring time-series from a given site. This chronology (e.g., referred to in ARSTAN (Cook and Krusic 2005) as the “Raw” chronology) incorporates all of the underlying signals in the tree-ring data including possible age-size related trends, variance changes due to the heteroscedastic nature of tree-ring data, potentially artifacts from changes in sample replication (see below), and so on. Yet, many investigations derive chronologies after performing data processing and analytical steps (*sensu* the linear aggregate model) to remove such unwanted noise. Thus, typically the tree-ring data are detrended & standardized (see above) prior to averaging together into most tree-ring chronologies. It is broadly recognized there is no objective or perfect way to detrend the tree-ring data, and thus an emphasis on both understanding and communicating in publications how the detrending impacts the retained signals in the final chronology is necessary. When emphasis is on year-to-year variations, as for crossdating, more flexible detrending curves can be used to remove most variability on say time-scales longer than 30-years whilst retaining essentially all year-to-year variations. Similarly, when the preservation of long-term trends is important, as is the case for many global change related investigations, more conservative approaches to retain longer time-scale variability are required (e.g., Jacoby and D’Arrigo 1989; Briffa et al. 1992; Cook et al. 1995; Esper et al. 2002; Melvin and Briffa 2008, 2014a, 2014b; Helama et al. 2017). Serial autocorrelation, or the statistical non-independence of successive years of tree growth due to e.g., biological factors such as carbohydrate reserves (or depletion) and changes in needle/foiar length and capacity, is sometime also removed from tree-ring measurements in a step often referred to as “pre-whitening” via auto-regressive moving average modeling (Meko 1981). It is also standard practice to make a mean chronology with a bi-weight robust mean to mitigate the influence of statistical outliers (Cook 1985). Some recent work has also suggested that other estimates of central tendency and/or dispersion such as percentile chronologies may offer distinct advantages to mitigate noise that is not uniform to all trees in all years (Stine and Huybers 2017).

Within dendrochronology the program ARSTAN (Cook and Holmes 1986; Cook and Krusic 2005) is extremely well established for performing all of the steps related to chronology development and statistical assessments of chronology quality (see below). The *dplR* package (Bunn 2008; Bunn et al. 2020) in the R programming environment has replicated many of the steps in ARSTAN versions, and offers the advantage of ease of integration with other user-defined analytical or graphical procedures. Signal-free detrending can be performed using CRUST (Melvin and Briffa 2014a, 2014b) or ARSTAN variants. Many of the basic procedures can also be performed in user developed algorithms, including potential mixed-effect models which offer innovation potential for the discipline. However, such user-specific approaches may be less well understood by the broader scientific community, and would require elaborate development to meet robust best practices for both chronology development and assessment (see below).

### 2.5.2 Assessment of Chronology Confidence

It is desirable to understand how well the tree-ring data and chronology represents the site, or the theoretical population, that they purportedly sample. In this regard, two important quantities are: (i) an assessment of the correlation or common signal of the tree-ring measurements and (ii) the sample size. In the simplest case where one core is collected per tree, the average correlation coefficient,  $\bar{r}$ , among all possible time-series pairs is a good estimate for the common signal. Understanding what components of the tree-ring data (e.g., age-related trends, autocorrelation, pre-whitened time-series) are included or not in correlation computations is however needed. Similarly, the number of trees (= the number of tree-ring time series) at any given time would be an assessment of the sample size. Yet, the common practice to collect multiple cores per tree somewhat complicates the assessment of the signal and noise (Fritts 1976; Wigley et al. 1984; Briffa and Jones 1990), and thus requires a bit more consideration. In this regard, the first term which may be defined is the effective average number of cores per tree,  $c_{eff}$ , at any given time:

$$\frac{1}{c_{eff}} = \frac{1}{n} \sum_{i=1}^n \frac{1}{c_i}$$

where  $c_i$  is the number of cores from tree  $i$ , for all  $n$  trees at a site.  $c_{eff}$  typically will change over-time as e.g., tree cores that do not come close to the pith no longer contribute data in earlier years. More interesting is, however, the assessment of the correlation (usually either via Pearson's  $r$  or Spearman  $\rho$ ). Notably, the correlation amongst all possible pairs of time-series includes those computed from within the same tree, and those computed among different trees. Typically, measurement series from a single tree will tend to be more highly correlated with each other than measurements series from different trees. Counter-intuitively higher within tree correlations are due to tree-specific noise that, if not accounted for, could lead to inflated confidence in a tree-ring chronology particularly with (i) greater numbers of cores per tree and ii) fewer number of trees per site. An accurate assessment of common signal thus requires computing separately: the average correlation ( $\bar{r}_{tot}$ ) amongst all pairs of time series ( $P_{tot}$ ); the average correlation ( $\bar{r}_{wt}$ ) for the  $P_{wt}$  pairs of times series computed within the same tree; and the average correlation ( $\bar{r}_{bt}$ ) for the  $P_{bt}$  pairs of times series computed between different trees. Typically  $\bar{r}_{bt}$  is calculated as:

$$\bar{r}_{bt} = \frac{1}{P_{bt}} (\bar{r}_{tot} P_{tot} - \bar{r}_{wt} P_{wt})$$

The difference between  $\bar{r}_{wt}$  and  $\bar{r}_{bt}$  is an assessment of the tree-specific noise. Finally, the effective average inter-series correlation,  $\bar{r}_{eff}$ , can be computed as:

$$\bar{r}_{eff} = \frac{\bar{r}_{bt}}{\bar{r}_{wt} + \frac{1-\bar{r}_{wt}}{c_{eff}}}$$

When  $c_{eff} = 1$ ,  $\bar{r}_{eff} = \bar{r}_{bt}$ ; and similarly as  $c_{eff}$  becomes very large,  $\bar{r}_{eff}$  approaches the  $\bar{r}_{bt}/\bar{r}_{wt}$  ratio. For anecdotally reasonable values of  $c_{eff} = 1.9$ ,  $\bar{r}_{wt} = 0.7$ , and  $\bar{r}_{bt} = 0.5$  the above equation yields an  $\bar{r}_{eff}$  of 0.583 reflecting the added value of the multiple cores per tree on top of the  $\bar{r}_{bt} = 0.5$ . With the above terms at hand, it is now possible to estimate how well the particular sample of tree cores represents the theoretical population chronology from which it is drawn. Following Wigley et al. (1984) and Briffa and Jones (1990) the Expressed Population Signal (EPS) can be defined as:

$$EPS \approx \frac{N\bar{r}_{eff}}{(1 + (N - 1)\bar{r}_{eff})}$$

where  $N$  is the number of trees (not cores) that are included in the dataset. EPS values approaching unity approach the theoretical population signal. These same two works also derived and discussed the related statistic, the Subsample Signal Strength (SSS). The SSS defines how well a subset of trees represents the full tree sample. The SSS is relevant as the number of trees varies typically with fewer and fewer trees further back in time. The SSS is defined as:

$$SSS \approx \frac{n(1 + (N - 1)\bar{r}_{eff})}{N(1 + (n - 1)\bar{r}_{eff})}$$

where  $n$  is the subset of trees in a chronology at any given point in time. The SSS can also be expressed and calculated as:

$$SSS = \frac{EPS(n)}{EPS(N)}$$

Notably, the EPS and SSS statistics are a simple function of the two terms—sample size and common signal—that are fundamental to assessing chronology quality. With increases in sample size, a greater proportion of tree and core specific noise is averaged out of the mean chronology, resulting in better and better estimates of the population mean. Similarly, higher correlations between trees are indicative of a strong common signal and lower amounts of noise, with fewer trees generally required (but see below discussion on lower-frequency variation) to achieve a certain robustness. The connections between the theoretical approach of Wigley et al. (1984) and earlier more empirically-based analysis of variance approaches (Fritts 1976) to assess chronology signals, noise, and confidence, have been shown to be essentially identical if the data are normalized (Wigley et al. 1984; Briffa and Jones 1990). It remains outstanding, to the best of our knowledge, to demonstrate the potential equivalence or differences between these statistical frameworks and mixed



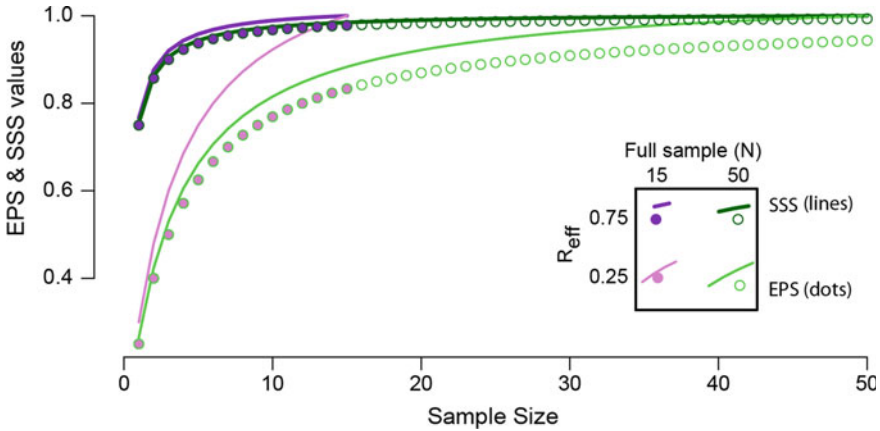


**Fig. 2.5** This figure displays calculations of the Expressed Population Signal (EPS, dots) and Subsample Signal Strength (SSS, lines) statistics for two different levels (0.75 and 0.25; dark and light shades respectively) of effective interseries correlation from illustrative total sample sizes of 15 (purple tones) or 50 (green tones) trees

effects modeling approaches that have gained traction in many environmental and ecological fields in recent years.

The Wigley et al. (1984) paper that introduced the EPS and SSS statistics provided illustrative examples of how such statistics can be used to assess chronology confidence using an illustrative value of  $SSS = 0.85$ . This example was subsequently expanded upon by Briffa and Jones (1990). Within the broader community there has been widespread use of this illustrative threshold 0.85 for EPS and SSS (see Buras 2017) as a criteria to demonstrate chronology robustness. While recognized as arbitrary threshold for the SSS (Wigley et al. 1984) and EPS (Briffa and Jones 1990), this value is also arguably an objective criteria that allows comparisons of chronology confidence among studies (Briffa and Jones 1990). Figure 2.5 illustrates how EPS and SSS change as a function of sample size and correlation. Some notable aspects are: (1) both EPS and SSS rapidly achieve relatively high values at low numbers of series, particularly for higher  $\bar{r}_{eff}$  values; (2) “returns” on additional samples diminish at higher samples sizes (but again see below discussion on lower-frequency variation); (3) the EPS is a more conservative estimate (i.e., more series are required to achieve a given threshold) of absolute chronology robustness; (4) the SSS and EPS are quite similar when the underlying tree-ring data are highly correlated.

Perhaps less widely appreciated, is that these statistics, due to their correlation-based nature, do not assess chronology confidence (or error) that results from absolute differences in the scale or variance of the underlying time-series (Briffa and Jones 1990; Melvin and Briffa 2014b). Furthermore, these statistics are only moderately sensitive to low-frequency (in)coherence, particularly when computed in moving (e.g., 50-year) windows (Melvin and Briffa 2014b). For many highly correlating tree-ring parameters such as tree-ring width from semi-arid or high latitude/altitude

sites (e.g., Breitenmoser et al. 2014; St. George and Ault 2014), maximum late-wood density from high latitude/altitude sites (Briffa et al. 2002a, b; Björklund et al. 2017), and notably stable isotopes across a wide range of ecological and climatic environments (Hartl-Meier et al. 2014), achieving illustrative EPS and SSS benchmarks of e.g., 0.85 may require only 4–5 measurement time-series. Yet, more emphasis appears warranted to address and communicate these estimates of chronology confidence are for (primarily) high-frequency assessments. Similarly, more work (and more samples) are required for any dendrochronological investigations benchmarking longer-term variability. For example, Melvin and Briffa (2014b) describe an approach to estimate lower-frequency coherence by looking at variance ratios of the data before and after high-pass filtering. They suggest that for lower-frequency assessment several times more trees might be actually necessary than inferred from the EPS and SSS calculations. Anecdotally, trend discrepancies amongst investigations of tree-ring isotopes support the notion that many more series will be scientifically important. Thus, two major research agendas are: (1) to better quantify the skill and error especially towards lower-frequency domains, and (2) to develop ever larger tree-ring datasets to increase confidence (and more realistically assess noise) in lower-frequency domains. The former has been a challenge to the paleoclimatic community for decades (e.g., Esper et al. 2004), and becoming a clearly recognized need for assessments of stable isotopes in narrowing the wide range of water use efficiency responses to the anthropogenic increase in CO<sub>2</sub> (e.g., Saurer et al. 2004). Yet, with continued advances in technology and processing efficiency, and decreases in expenses (e.g., Andreu-Hayles et al. 2019), it is foreseeable that we will soon have many more tree-ring isotope datasets with 10's of trees at any given point in time (with less or no pooling across trees) and thus steady progress towards realizing the latter research agenda.

### 2.5.3 Variance Changes in Composite Time-Series

The same fundamental quantities, the sample size and coherence amongst series, also determine the variance,  $S^2$ , of the resulting dataset average—the tree-ring chronology (Wigley et al. 1984; Osborn et al. 1997; and see also Shiyatov et al. 1990). Following Wigley et al. (1984) and Osborn et al. (1997) this relationship can be expressed as:

$$S^2 = \overline{s^2} \left[ \frac{1 + (n - 1)\bar{r}_{eff}}{n} \right]$$

where  $\overline{s^2}$  is the mean variance of the individual tree-ring time-series, and  $n$  is the number of trees (at any given time) and  $\bar{r}_{eff}$  is defined above. Notably, changes in sample replication and/or series coherence over time will cause the variance of the mean chronology to also vary. While series coherence may vary due to a number of reasons (including those that should be retained in the tree-ring chronology), any

variance structure that depends upon sample size must be regarded as an artifact of the sampling and should thus be removed from the final tree-ring chronology (Osborn et al. 1997; Frank et al. 2007). As tree-ring time-series are generally significantly correlated with each other—a general outcome of the common signal and the basis for crossdating—the effective sample size,  $n_{eff}$ , can be defined as:

$$n_{eff} = \frac{n}{1 + (n - 1)\bar{r}_{eff}}$$

which is simply the reciprocal of the bracketed part of the above equation. In this way  $n_{eff}$  serves as the factor by which a mean chronology can be multiplied to yield a chronology corrected for variance artifacts resulting from changes in sample depth. And specifically, multiplication of the mean chronology (after centering about a mean of zero) by  $\sqrt{\bar{r} * n_{eff}}$  yields a mean chronology whose variance is adjusted and the scaling/units are preserved to the variance that would result from the theoretical population chronology (Osborn et al. 1997; Frank et al. 2007). While handling the variance artifacts from changes in sample size are relatively straightforward, variance changes resulting from variable coherence of the individual time-series are more complex to understand and thus address. Variable coherence among tree-ring series could be due to changes in the underlying climate system, and if so should presumably be preserved in the underlying dataset. However, inhomogeneities in tree-ring datasets that might occur e.g., in chronologies composed of samples from living trees linked together with relict / historical samples from more dissimilar (and/or unknown) environments should presumably be corrected. Similarly, changes in climate signal and coherence with tree age could result in variance artifacts in resulting chronologies. In such cases time-dependent estimates of  $\bar{r}_{eff}$  say computed in moving window (e.g., Frank et al. 2007) can be employed as included in more recent versions of ARSTAN (Cook and Krusic 2005).

It can be demonstrated that the variance structure of a tree-ring chronology is less dependent upon changes in sample size when  $\bar{r}_{eff}$  is high. And similarly, changes in sample size are more impactful to the variance at lower sample sizes. With specific reference to tree-ring stable isotope time-series, the general high correlation amongst series (Hartl-Meier et al. 2014) mitigates sample size variance artifacts. Conversely, the generally modest sample sizes for most tree-ring isotope studies to date are conducive to variance artifacts. Such variance artifacts can be mitigated by selecting for measurement a constant number of samples, or employing theoretically-based (see above) or empirically-based (Shiyatov et al. 1990) methods to correct for variance artifacts. Such considerations will be increasingly important to producers and analysts of tree-ring isotope datasets as the prevalence of variable sample replications increases as measurements are performed on all available tree-ring samples rather than small subsets. Most broadly, potential variance artifacts should be kept in mind in all scientific disciplines, including dendrochronology, where data quantities and qualities potentially change over time and space.

## 2.6 Conclusions

This chapter has reviewed foundations of dendrochronology with perhaps greatest relevance for an audience interested in the intersection of stable isotopes and tree-rings. The chapter began with a fairly broad overview of some of the fundamentals of tree-ring formation and wood anatomy, and then comprehensively outlined the diversity of research topics that have been addressed with a broad range of tree-ring parameters. The role of crossdating is highlighted as the key foundation for dendrochronology—namely to ensure that each and every ring is confidently assigned to a correct (and often calendar) year. For readers with a background in tree-ring width measurements, some of the long-standing paradigms that are being challenged with isotope data are perhaps of particular interest. This includes a discussion of the long-standing practices in selecting tree-ring sites towards ecologically extreme sites to obtain a strong common signal. There is now abundant evidence that the stable isotope parameters in tree-rings carry an exceptionally strong signal where tree-ring width data do not. Such findings are opening up new possibilities in all domains of tree-ring research from crossdating and dendroarchaeology to dendroecology and climatology. Moreover, the role of stable isotope data, as well as quantitative wood anatomical data, in mechanistic / ecophysiological applications is highlighted as a research direction with excellent past work as well as substantial potential for further research. For readers that are more familiar with stable isotope measurements, and are part of the forefront in developing well-replicated tree-ring isotope datasets, the sections on chronology development, dendrochronological statistics, and characteristics of times-series may be most useful. Crosscutting issues in this chapter include discussions of age-size related trends in tree-ring data, and recommendations on how such age-size related trends might be characterized and handled for stable isotope datasets. The importance of producing robust well replicated tree-ring datasets is highlighted, and for which the signal and noise, variance, and chronology confidence are well understood and characterized across all time scales. Happy tree-ringing.

**Acknowledgements** We thank Rolf Siegwolf, J. Renée Brooks, John Roden and Matthias Saurer for their leadership and persistence on this entire project and guidance and input on this chapter, Brendan Buckley and an additional anonymous reviewer for constructive suggestions and corrections that greatly improved this chapter, and the US Forest Service (project 16-JV-11221633-182) and Swiss National Science Foundation (182398) for funding.

## References

- Anchukaitis KJ, Wilson R, Briffa KR, Büntgen U, Cook ER, D'Arrigo R, Davi N, Esper J, Frank D, Gunnarson BE et al (2017) Last millennium Northern Hemisphere summer temperatures from tree rings: Part II, spatially resolved reconstructions. *Quatern Sci Rev* 163:1–22
- Anchukaitis KJ, Evans MN, Wheelwright NT, Schrag DP (2008) Stable isotope chronology and climate signal calibration in neotropical montane cloud forest trees. *J Geophys Res Biogeosci* 113

- Andreu-Hayles L, Levesque M, Martin-Benito D, Huang W, Harris R, Oelkers R, Leland C, Martin-Fernández J, Anchukaitis KJ, Helle G (2019) A high yield cellulose extraction system for small whole wood samples and dual measurement of carbon and oxygen stable isotopes. *Chem Geol* 504:53–65
- Andreu-Hayles L, Santos G, Herrera-Ramírez D, Martin-Fernández J, Ruiz-Carrascal D, Boza-Espinoza T, Fuentes A, Jørgensen P (2015) Matching dendrochronological dates with the Southern Hemisphere <sup>14</sup>C bomb curve to confirm annual tree rings in *pseudotsuga rigida* from Bolivia. *Radiocarbon* 57:1–13
- Babst F, Bouriaud O, Alexander R, Trouet V, Frank D (2014) Toward consistent measurements of carbon accumulation: a multi-site assessment of biomass and basal area increment across Europe. *Dendrochronologia* 32:153–161
- Babst F, Bouriaud O, Papale D, Gielen B, Janssens IA, Nikinmaa E, Ibrom A, Wu J, Bernhofer C, Köstner B et al (2014) Above-ground woody carbon sequestration measured from tree rings is coherent with net ecosystem productivity at five eddy-covariance sites. *New Phytol* 201:1289–1303
- Babst F, Poulter B, Bodesheim P, Mahecha MD, Frank DC (2017) Improved tree-ring archives will support earth-system science. *Nat Ecol Evol* 1:0008
- Babst F, Poulter B, Trouet V, Tan K, Neuwirth B, Wilson R, Carrer M, Grabner M, Tegel W, Levanic T et al (2013) Site- and species-specific responses of forest growth to climate across the European continent. *Glob Ecol Biogeogr* 22:706–717
- Babst F, Wright W, Szejner P, Wells L, Belmecheri S, Monson R (2016) Blue intensity parameters derived from *Ponderosa* pine tree rings characterize intra-annual density fluctuations and reveal seasonally divergent water limitations. *Trees* 30
- Barbosa AC, Stahle DW, Burnette DJ, Torbenson MCA, Cook ER, Bunkers MJ, Garfin G, Villalba R (2019) Meteorological factors associated with frost rings in Rocky Mountain Bristlecone Pine at Mt. Goliath, Colorado. *Tree-Ring Res* 75:101–115
- Battipaglia G, Campelo F, Vieira J, Grabner M, De Micco V, Nabais C, Cherubini P, Carrer M, Bräuning A, Čufar K et al (2016) Structure and function of intra-annual density fluctuations: mind the gaps. *Front Plant Sci* 7:595–595
- Belmecheri S, Babst F, Wahl ER, Stahle DW, Trouet V (2016) Multi-century evaluation of Sierra Nevada snowpack. *Nat Clim Chang* 6:2–3
- Belmecheri S, Wright WE, Szejner P, Morino KA, Monson RK (2018) Carbon and oxygen isotope fractionations in tree rings reveal interactions between cambial phenology and seasonal climate. *Plant, Cell Environ* 41:2758–2772
- Biondi F, Qeadan F (2008) A theory-driven approach to tree-ring standardization: defining the biological trend from expected basal area increment. *Tree-Ring Res* 64:81–96
- Björklund JA, Gunnarson BE, Seftigen K, Esper J, Linderholm HW (2014) Blue intensity and density from northern Fennoscandian tree rings, exploring the potential to improve summer temperature reconstructions with earlywood information. *Climate of the past* 10:877–885
- Björklund J, Seftigen K, Schweingruber F, Fonti P, Arx G, Bryukhanova MV, Cuny HE, Carrer M, Castagneri D, Frank DC (2017) Cell size and wall dimensions drive distinct variability of earlywood and latewood density in Northern Hemisphere conifers. *New Phytol* 216:728–740
- Björklund J, von Arx G, Nievergelt D, Wilson R, Van den Bulcke J, Günther B, Loader NJ, Rydval M, Fonti P, Scharnweber T et al (2019) Scientific merits and analytical challenges of tree-ring densitometry. *Rev Geophys* 57:1224–1264
- Black BA, Griffin D, van der Sleen P, Wanamaker AD Jr, Speer JH, Frank DC, Stahle DW, Pederson N, Copenheaver CA, Trouet V et al (2016) The value of crossdating to retain high-frequency variability, climate signals, and extreme events in environmental proxies. *Glob Change Biol* 22:2582–2595
- Boswijk G, Brassey R, Bader H-D, Adamson J, Jones M (2016) Dendrochronological dating of kauri timbers from Browne's spar station (1832–1836), Mahurangi, Auckland, New Zealand. *J Archaeol Sci Rep* 7:129–137

- Breitenmoser PD, Brönnimann S, Frank D (2014) Forward modelling of tree-ring width and comparison with a global network of tree-ring chronologies. *Climate of the past* 10(2):437–449
- Brewer PW, Guiterman CH (2016) A new digital field data collection system for dendrochronology. *Dendrochronologia* 38:131–135
- Brienen RJW, Schöngart J, Zuidema PA (2016) Tree rings in the tropics: insights into the ecology and climate sensitivity of tropical trees. In: Goldstein G, Santiago LS (eds) *Tropical tree physiology: adaptations and responses in a changing environment*. Springer International Publishing, Cham, pp 439–461
- Briffa KR, Jones PD (1990) Basic chronology statistics and assessment. In: *Methods of dendrochronology: applications in the environmental sciences*. Kluwer Academic Publishers, pp 137–152. ISBN 978-0-7923-0586-6
- Briffa KR, Melvin TM, Osborn TJ, Hantemirov RM, Kirilyanov AV, Mazepa VS, Shiyatov SG, Esper J (2013) Reassessing the evidence for tree-growth and inferred temperature change during the Common Era in Yamalia, northwest Siberia. *Quatern Sci Rev* 72:83–107
- Briffa KR, Osborn TJ, Schweingruber FH, Jones PD, Shiyatov SG, Vaganov EA (2002) Tree-ring width and density data around the Northern Hemisphere: Part 1, local and regional climate signals. *The Holocene* 12:737–757
- Briffa KR, Osborn TJ, Schweingruber FH, Jones PD, Shiyatov SG, Vaganov EA (2002) Tree-ring width and density data around the Northern Hemisphere: Part 2, spatio-temporal variability and associated climate patterns. *The Holocene* 12:759–789
- Buckley BM, Hansen KG, Griffin KL, Schmiege S, Oelkers R, D'Arrigo RD, Stahle DK, Davi N, Nguyen TQT, Le CN et al (2018) Blue intensity from a tropical conifer's annual rings for climate reconstruction: an ecophysiological perspective. *Dendrochronologia* 50:10–22
- Büntgen U, Kolář T, Rybníček M, Koňasová E, Trnka M, Ač A, Krusic PJ, Esper J, Treydte K, Reinig F et al (2020) No age trends in oak stable isotopes. *Paleoceanogr Paleoclimatol* 35:e2019PA003831
- Büntgen U, Tegel W, Nicolussi K, McCormick M, Frank D, Trouet V, Kaplan JO, Herzig F, Heussner K-U, Wanner H et al (2011) 2500 years of European climate variability and human susceptibility. *Science* 331:578
- Büntgen U, Wacker L, Galván JD, Arnold S, Arseneault D, Baillie M, Beer J, Bernabei M, Bleicher N, Boswijk G et al (2018) Tree rings reveal globally coherent signature of cosmogenic radiocarbon events in 774 and 993 CE. *Nat Commun* 9:3605
- Bunn AG (2008) A dendrochronology program library in R (dplR). *Dendrochronologia* 26(2):115–124
- Bunn AG (2010) Statistical and visual crossdating in R using the dplR library. *Dendrochronologia* 28:251–258
- Bunn A, Korpela M, Biondi F, Campelo F, Mérian P, Qeadan F, Zang C, Buras A, Cecile J, Mudelsee M, Schulz M (2020) Package 'dplR'
- Buras A (2017) A comment on the expressed population signal. *Dendrochronologia* 44:130–132
- Cabon A, Fernández-de-Niña L, Gea-Izquierdo G, Meinzer FC, Woodruff DR, Martínez-Vilalta J, De Cáceres M (2020) Water potential control of turgor-driven tracheid enlargement in Scots pine at its xeric distribution edge. *New Phytol* 225:209–221
- Caillieret M, Jansen S, Robert EMR, Desoto L, Aakala T, Antos JA, Beikircher B, Bigler C, Bugmann H, Caccianiga M et al (2017) A synthesis of radial growth patterns preceding tree mortality. *Glob Change Biol* 23:1675–1690
- Camarero JJ, Rozas V, Olano JM (2014) Minimum wood density of *Juniperus thurifera* is a robust proxy of spring water availability in a continental Mediterranean climate. *J Biogeogr* 41:1105–1114
- Carrer M, Brunetti M, Castagneri D (2016) The imprint of extreme climate events in century-long time series of wood anatomical traits in high-elevation conifers. *Front Plant Sci* 7:683
- Castagneri D, Fonti P, von Arx G, Carrer M (2017) How does climate influence xylem morphogenesis over the growing season? Insights from long-term intra-ring anatomy in *Picea abies*. *Ann Bot* 119:1011–1020

- Chamagne J, Tanadini M, Frank D, Matula R, Paine C, Philipson CD, Svatek M, Turnbull LA, Volařík D, Hector A (2017) Forest diversity promotes individual tree growth in central European forest stands. *J Appl Ecol* 54:71–79
- Cook ER (1985) A time series analysis approach to tree ring standardization. Doctoral dissertation, University of Arizona
- Cook ER (1987) The decomposition of tree-ring series for environmental studies. *Tree-Ring Bull* 47:37–59
- Cook ER, Briffa KR, Meko DM, Graybill DA, Funkhouser G (1995) The “segment length curse” in long tree-ring chronology development for palaeoclimatic studies. *The Holocene* 5(2):229–237
- Cook ER, Holmes RL (1986) Users manual for ARSTAN. University of Arizona, Tucson, Laboratory of Tree-ring Research
- Cook ER, Kairiukstis LA (eds) (1990) *Methods of dendrochronology: applications in the environmental sciences*. Kluwer Academic Publishers
- Cook ER, Krusic PJ (2005) Program ARSTAN: a tree-ring standardization program based on detrending and autoregressive time series modeling, with interactive graphics. Columbia University, Palisades, NY, Lamont-Doherty Earth Observatory
- Cook ER, Peters K (1997) Calculating unbiased tree-ring indices for the study of climatic and environmental change. *The Holocene* 7:361–370
- Cook ER, Woodhouse CA, Eakin CM, Meko DM, Stahle DW (2004) Long-term aridity changes in the Western United States. *Science* 306:1015
- Coulthard BL, Touchan R, Anchukaitis KJ, Meko DM, Sivrikaya F (2017) Tree growth and vegetation activity at the ecosystem-scale in the eastern Mediterranean. *Environ Res Lett* 12:084008
- Csank AZ (2009) An international tree-ring isotope data bank—a proposed repository for tree-ring isotopic data. *Tree-Ring Res* 65:163–164
- Cuny HE, Rathgeber CBK, Frank D, Fonti P, Fournier M (2014) Kinetics of tracheid development explain conifer tree-ring structure. *New Phytol* 203:1231–1241
- D’Arrigo R, Frank D, Jacoby G, Pederson N (2001) Spatial response to major volcanic events in or about AD 536, 934 and 1258: frost rings and other dendrochronological evidence from Mongolia and northern Siberia: comment on R. B. Stothers, ‘Volcanic Dry Fogs, Climate Cooling, and Plague Pandemics in Europe and the Middle East’ (*Climatic Change*, 42, 1999). *Clim Change* 49:239–246
- D’Arrigo R, Wilson R, Jacoby G (2006) On the long-term context for late twentieth century warming. *J Geophys Res: Atmos* 111:D03103. <https://doi.org/10.1029/2005JD006352>
- Dean JS, Robinson WJ (1996) NOAA/WDS Paleoclimatology—Dean—Rito de los Frijoles—PIPO—I TRDB NM501. NOAA National Centers for Environmental Information. <https://doi.org/10.25921/f6qq-ck73>
- Dee MW, Pope BJS (2016) Anchoring historical sequences using a new source of astrochronological tie-points. *Proc Math Phys Eng Sci* 472:20160263–20160263
- Delpierre N, Lireux S, Hartig F, Camarero JJ, Cheaib A, Čufar K, Cuny H, Deslauriers A, Fonti P, Gričar J et al (2019) Chilling and forcing temperatures interact to predict the onset of wood formation in Northern Hemisphere conifers. *Glob Change Biol* 25:1089–1105
- De Micco V, Campelo F, Luis MD, Bräuning A, Grabner M, Battipaglia G, Cherubini P (2016) Intra-annual density fluctuations in tree rings: how, when, where, and why? *IAWA J* 37:232–259
- Deslauriers A, Rossi S, Anfodillo T (2007) Dendrometer and intra-annual tree growth: what kind of information can be inferred? *Dendrochronologia* 25:113–124
- Domínguez-Delmás M (2020) Seeing the forest for the trees: new approaches and challenges for dendroarchaeology in the 21st century. *Dendrochronologia* 62:125731
- Douglas AE (1929) The secret of the Southwest solved by talkative tree rings. *Natl Geogr Mag* 56(6):736–770
- Drew DM, Allen K, Downes GM, Evans R, Battaglia M, Baker P (2012) Wood properties in a long-lived conifer reveal strong climate signals where ring-width series do not. *Tree Physiol* 33:37–47

- Emile-Geay J, McKay NP, Kaufman DS, von Gunten L, Wang J, Anchukaitis KJ, Abram NJ, Addison JA, Curran MAJ, Evans MN et al (2017) A global multiproxy database for temperature reconstructions of the Common Era. *Sci Data* 4:170088
- Esper J, Büntgen U, Frank DC, Nievergelt D, Liebhold A (2007) 1200 years of regular outbreaks in alpine insects. *Proc Roy Soc b: Biol Sci* 274:671–679
- Esper J, Cook ER, Schweingruber FH (2002) Low-Frequency signals in long tree-ring chronologies for reconstructing past temperature variability. *Science* 295:2250. <https://doi.org/10.1126/science.1066208>
- Esper J, Cook ER, Krusic PJ, Peters K, Schweingruber FH (2003) Tests of the RCS method for preserving low-frequency variability in long tree-ring chronologies
- Esper J, Frank DC, Timonen M, Zorita E, Wilson RJS, Luterbacher J, Holzkämper S, Fischer N, Wagner S, Nievergelt D et al (2012) Orbital forcing of tree-ring data. *Nat Clim Chang* 2:862–866
- Esper J, Frank DC, Wilson RJ (2004) Climate reconstructions: low-frequency ambition and high-frequency ratification. *EOS Trans Am Geophys Union* 85(12):113–120
- Esper J, Riechelmann DF, Holzkämper S (2020) Circumferential and longitudinal  $\delta^{13}\text{C}$  variability in a *Larix decidua* trunk from the Swiss Alps. *Forests* 11:117
- Evans MEK, Falk DA, Arizpe A, Swetnam TL, Babst F, Holsinger KE (2017) Fusing tree-ring and forest inventory data to infer influences on tree growth. *Ecosphere* 8(7):e01889
- Fan Z-X, Bräuning A, Yang B, Cao K-F (2009) Tree ring density-based summer temperature reconstruction for the central Hengduan Mountains in southern China. *Glob Planet Change* 65:1–11
- Fang K, Gou X, Chen F, Li J, D'Arrigo R, Cook E, Yang T, Davi N (2010) Reconstructed droughts for the southeastern Tibetan Plateau over the past 568 years and its linkages to the Pacific and Atlantic Ocean climate variability. *Clim Dyn* 35:577–585
- Fang K, Gou X, Chen F, Liu C, Davi N, Li J, Zhao Z, Li Y (2012) Tree-ring based reconstruction of drought variability (1615–2009) in the Kongtong Mountain area, northern China. *Glob Planet Change* 80–81:190–197
- Fonti P, von Arx G, García-González I, Eilmann B, Sass-Klaassen U, Gärtner H, Eckstein D (2010) Studying global change through investigation of the plastic responses of xylem anatomy in tree rings. *New Phytol* 185:42–53
- Frank DC, Poulter B, Saurer M, Esper J, Huntingford C, Helle G, Treydte K, Zimmermann NE, Schleser GH, Ahlström A et al (2015) Water-use efficiency and transpiration across European forests during the Anthropocene. *Nat Clim Chang* 5:579–583
- Frank D, Esper J (2005) Characterization and climate response patterns of a high-elevation, multi-species tree-ring network in the European Alps. *Dendrochronologia* 22:107–121
- Frank D, Esper J, Cook ER (2007) Adjustment for proxy number and coherence in a large-scale temperature reconstruction. *Geophys Res Lett* 34. <https://doi.org/10.1029/2007GL030571>
- Friend AD, Eckes-Shephard AH, Fonti P, Rademacher TT, Rathgeber CBK, Richardson AD, Turton RH (2019) On the need to consider wood formation processes in global vegetation models and a suggested approach. *Ann Forest Sci* 76:49
- Fritts H (1976) *Tree rings and climate*. Academic Press
- Fritts HC, Swetnam TW (1989) Dendroecology: a tool for evaluating variations in past and present forest environments. In: Begon M, Fitter AH, Ford ED, MacFadyen A (eds) *Academic Press*, pp 111–188
- Gärtner H, Schweingruber F, Dikau R (2001) Determination of erosion rates by analyzing structural changes in the growth pattern of exposed roots. *Dendrochronologia* 19:81–91
- Giuggiola A, Ogée J, Rigling A, Gessler A, Bugmann H, Treydte K (2016) Improvement of water and light availability after thinning at a xeric site: which matters more? A dual isotope approach. *New Phytol* 210:108–121
- Griffin D, Anchukaitis KJ (2014) How unusual is the 2012–2014 California drought? *Geophys Res Lett* 41:9017–9023
- Griffin D, Meko DM, Touchan R, Leavitt SW, Woodhouse CA (2011) Latewood chronology development for summer-moisture reconstruction In the US Southwest. *Tree-Ring Res* 67:87–101



- Griffin D, Woodhouse CA, Meko DM, Stahle DW, Faulstich HL, Carrillo C, Touchan R, Castro CL, Leavitt SW (2013) North American monsoon precipitation reconstructed from tree-ring latewood. *Geophys Res Lett* 40:954–958
- Guterman CH, Swetnam TW, Dean JS (2016) Eleventh-century shift in timber procurement areas for the great houses of Chaco Canyon. *Proc Natl Acad Sci USA* 113:1186
- Hafner P, McCarroll D, Robertson I, Loader NJ, Gagen M, Young GH, Bale RJ, Sonninen E, Levanič T (2014) A 520 year record of summer sunshine for the eastern European Alps based on stable carbon isotopes in larch tree rings. *Clim Dyn* 43:971–980
- Hangartner S, Kress A, Saurer M, Frank D, Leuenberger M (2012) Methods to merge overlapping tree-ring isotope series to generate multi-centennial chronologies. *Chem Geol* 294–295:127–134
- Hartl-Meier C, Zang C, Büntgen U, Esper J, Rothe A, Göttele A, Dirnböck T, Treydte K (2014) Uniform climate sensitivity in tree-ring stable isotopes across species and sites in a mid-latitude temperate forest. *Tree Physiol* 35:4–15
- Helama S, Melvin TM, Briffa KR (2017) Regional curve standardization: state of the art. *The Holocene* 27(1):172–177
- Helama S, Vartiainen M, Kolström T, Peltola H, Meriläinen J (2008) X-ray microdensitometry applied to subfossil tree-rings: growth characteristics of ancient pines from the southern boreal forest zone in Finland at intra-annual to centennial time-scales. *Veg Hist Archaeobotany* 17:675–686
- Herrera-Ramirez D, Andreu-Hayles L, Del Valle JI, Santos GM, Gonzalez PLM (2017) Nonannual tree rings in a climate-sensitive *Prioria copaifera* chronology in the Atrato River, Colombia. *Ecol Evol* 7:6334–6345
- Holmes RL (1983) Computer-assisted quality control in tree-ring dating and measurement. *Tree-Ring Bull* 44:69–75
- Housset JM, Nadeau S, Isabel N, Depardieu C, Duchesne I, Lenz P, Girardin MP (2018) Tree rings provide a new class of phenotypes for genetic associations that foster insights into adaptation of conifers to climate change. *New Phytol* 218:630–645
- Hughes MK, Schweingruber FH, Cartwright D, Kelly PM (1984) July–August temperature at Edinburgh between 1721 and 1975 from tree-ring density and width data. *Nature* 308(5957):341–344
- Jacoby GC, Bunker DE, Benson BE (1997) Tree-ring evidence for an A.D. 1700 Cascadia earthquake in Washington and northern Oregon. *Geology* 25:999–1002
- Jacoby GC, D'Arrigo R (1989) Reconstructed Northern Hemisphere annual temperature since 1671 based on high-latitude tree-ring data from North America. *Clim Change* 14:39–59. <https://doi.org/10.1007/BF00140174>
- Jacquin P, Longuetaud F, Leban J-M, Mothe F (2017) X-ray microdensitometry of wood: a review of existing principles and devices. *Dendrochronologia* 42:42–50
- Jull AJT, Panyushkina IP, Lange TE, Kukarskih VV, Myglan VS, Clark KJ, Salzer MW, Burr GS, Leavitt SW (2014) Excursions in the 14C record at A.D. 774–775 in tree rings from Russia and America. *Geophys Res Lett* 41:3004–3010
- Kannenber SA, Novick KA, Alexander MR, Maxwell JT, Moore DJP, Phillips RP, Anderegg WRL (2019) Linking drought legacy effects across scales: from leaves to tree rings to ecosystems. *Glob Change Biol* 25:2978–2992
- Kern Z, Patkó M, Kázmér M, Fekete J, Kele S, Pályi Z (2013) Multiple tree-ring proxies (earlywood width, latewood width and  $\delta^{13}C$ ) from pedunculate oak (*Quercus robur* L.), Hungary. *Quatern Int* 293:257–267
- Klesse S, Babst F, Lienert S, Spahni R, Joos F, Bouriaud O, Carrer M, Di Filippo A, Poulter B, Trotsiuk V et al (2018) A combined tree ring and vegetation model assessment of European forest growth sensitivity to interannual climate variability. *Glob Biogeochem Cycles* 32:1226–1240
- Klesse S, DeRose RJ, Guterman CH, Lynch AM, O'Connor CD, Shaw JD, Evans MEK (2018) Sampling bias overestimates climate change impacts on forest growth in the southwestern United States. *Nat Commun* 9:5336
- Klesse S, DeRose RJ, Babst F, Black BA, Anderegg LDL, Axelson J, Ettinger A, Griesbauer H, Guterman CH, Harley G et al (2020) Continental-scale tree-ring-based projection of Douglas-fir

- growth: testing the limits of space-for-time substitution. *Glob Change Biol.* <https://doi.org/10.1111/gcb.15170>
- Klesse S, Weigt R, Treydte K, Saurer M, Schmid L, Siegwolf RTW, Frank DC (2018) Oxygen isotopes in tree rings are less sensitive to changes in tree size and relative canopy position than carbon isotopes. *Plant, Cell Environ* 41:2899–2914
- King G, Fonti P, Nievergelt D, Büntgen U, Frank D (2013) Climatic drivers of hourly to yearly tree radius variations along a 6°C natural warming gradient. *Agric for Meteorol* 168:36–46
- King GM, Gugerli F, Fonti P, Frank DC (2013) Tree growth response along an elevational gradient: climate or genetics? *Oecologia* 173:1587–1600
- Kuitemans M, Panin A, Scifo A, Arzhantseva I, Kononov Y, Doeve P, Neocleous A, Dee M (2020) Radiocarbon-based approach capable of subannual precision resolves the origins of the site of Por-Bajin. *Proc Natl Acad Sci* 117:14038–14041
- LaMarche VC, Hirschboeck KK (1984) Frost rings in trees as records of major volcanic eruptions. *Nature* 307:121–126
- Lange J, Carrer M, Pisaric MFJ, Porter TJ, Seo J-W, Trouillier M, Wilmking M (2020) Moisture-driven shift in the climate sensitivity of white spruce xylem anatomical traits is coupled to large-scale oscillation patterns across northern treeline in northwest North America. *Glob Change Biol* 26:1842–1856
- Lavergne A, Graven H, De Kauwe MG, Keenan TF, Medlyn BE, Prentice IC (2019) Observed and modelled historical trends in the water-use efficiency of plants and ecosystems. *Glob Change Biol* 25:2242–2257
- Leavitt SW, Bannister B (2009) Dendrochronology and radiocarbon dating: the laboratory of tree-ring research connection. *Radiocarbon* 51:373–384
- Leavitt SW, Long A (1986) Stable-carbon isotope variability in tree foliage and wood. *Ecology* 67:1002–1010
- Li J, Xie S-P, Cook ER, Morales MS, Christie DA, Johnson NC, Chen F, D'Arrigo R, Fowler AM, Gou X et al (2013) El Niño modulations over the past seven centuries. *Nat Clim Chang* 3:822–826
- Loader NJ, McCarroll D, Miles D, Young GHF, Davies D, Ramsey CB (2019) Tree ring dating using oxygen isotopes: a master chronology for central England. *J Quatern Sci* 34:475–490
- McCarroll D, Duffy JE, Loader NJ, Young GH, Davies D, Miles D, Bronk Ramsey C (2020) Are there enormous age-trends in stable carbon isotope ratios of oak tree rings? The Holocene 0959683620941073
- McCarroll D, Gagen MH, Loader NJ, Robertson I, Anchukaitis KJ, Los S, Young GHF, Jalkanen R, Kirchhefer A, Waterhouse JS (2009) Correction of tree ring stable carbon isotope chronologies for changes in the carbon dioxide content of the atmosphere. *Geochim Cosmochim Acta* 73:1539–1547
- McCarroll D, Pettigrew E, Luckman A, Guibal F, Edouard J-L (2002) Blue reflectance provides a surrogate for latewood density of high-latitude pine tree rings. *Arct Antarct Alp Res* 34:450–453
- Meko DM (1981) Applications of Box-Jenkins methods of timeseries analysis to the reconstruction of drought from tree rings. Doctoral Dissertation, University of Arizona
- Melvin TM, Briffa KR (2008) A “signal-free” approach to dendroclimatic standardisation. *Dendrochronologia* 26(2):71–86
- Melvin TM, Briffa KR (2014) CRUST: software for the implementation of regional chronology standardisation: part 1. Signal-free RCS. *Dendrochronologia* 32(1):7–20
- Melvin TM, Briffa KR (2014) CRUST: software for the implementation of regional chronology standardisation: part 2. Further RCS options and recommendations. *Dendrochronologia* 32(4):343–356
- Miyake F, Nagaya K, Masuda K, Nakamura T (2012) A signature of cosmic-ray increase in ad 774–775 from tree rings in Japan. *Nature* 486:240–242
- Muñoz AA, Klock-Barría K, Sheppard PR, Aguilera-Betti I, Toledo-Guerrero I, Christie DA, Gorena T, Gallardo L, González-Reyes Á, Lara A et al (2019) Multidecadal environmental pollution in a mega-industrial area in central Chile registered by tree rings. *Sci Total Environ* 696:133915

- Nehrbass-Ahles C, Babst F, Klesse S, Nötzli M, Bouriaud O, Neukom R, Dobbertin M, Frank D (2014) The influence of sampling design on tree-ring-based quantification of forest growth. *Glob Change Biol* 20:2867–2885
- Oppenheimer C, Wacker L, Xu J, Galván JD, Stoffel M, Guillet S, Corona C, Sigl M, Cosmo ND, Hajdas I et al (2017) Multi-proxy dating the ‘Millennium Eruption’ of Changbaishan to late 946 CE. *Quatern Sci Rev* 158:164–171
- Osborn TJ, Biffa KR, Jones PD (1997) Adjusting variance for sample-size in tree-ring chronologies and other regional-mean timeseries. *Dendrochronologia* 15:89–99
- Panyushkina IP, Hughes MK, Vaganov EA, Munro MA (2003) Summer temperature in northeastern Siberia since 1642 reconstructed from tracheid dimensions and cell numbers of *Larix cajanderi*. *Can J for Res* 33:1905–1914
- Panyushkina IP, Shishov VV, Grachev AM, Knorre AA, Kirilyanov AV, Leavitt SW, Vaganov EA, Chebykin EP, Zhuchenko NA, Hughes MK (2016) Trends in elemental concentrations of tree rings from the Siberian arctic. *Tree-Ring Res* 72:67–77
- Parker ML, Henschel WES (1971) The use of Engelmann spruce latewood density for dendrochronological purposes. *Can J for Res* 1(2):90–98
- Pearl JK, Keck JR, Tintor W, Siekacz L, Herrick HM, Meko MD, Pearson CL (2020) New frontiers in tree-ring research. *The Holocene* 30:923–941
- Pearson CL, Brewer PW, Brown D, Heaton TJ, Hodgins GWL, Jull AJT, Lange T, Salzer MW (2018) Annual radiocarbon record indicates 16th century BCE date for the Thera eruption. *Sci Adv* 4 <https://doi.org/10.1126/sciadv.aar8241>
- Pearson CL, Dale DS, Brewer PW, Salzer MW, Lipton J, Manning SW (2009) Dendrochemistry of white mountain bristlecone pines: an investigation via synchrotron radiation scanning X-ray fluorescence microscopy. *J Geophys Res* 114:G01023. <https://doi.org/10.1029/2008JG000830>
- Pearson C, Salzer M, Wacker L, Brewer P, Sookdeo A, Kuniholm P (2020) Securing timelines in the ancient Mediterranean using multiproxy annual tree-ring data. *Proc Natl Acad Sci USA* 117:8410
- Pederson N, Dyer JM, McEwan RW, Hessl AE, Mock CJ, Orwig DA, Rieder HE, Cook BI (2014) The legacy of episodic climatic events in shaping temperate, broadleaf forests. *Ecol Monogr* 84:599–620
- Pederson GT, Gray ST, Woodhouse CA, Betancourt JL, Fagre DB, Littell JS, Watson E, Luckman BH, Graumlich LJ (2011) The unusual nature of recent snowpack declines in the north American cordillera. *Science* 333:332–335
- Peters K, Jacoby GC, Cook ER (1981) Principal components analysis of tree-ring sites. *Tree-Ring Bull* 41:1–19
- Peters RL, Balanzategui D, Hurley AG, von Arx G, Prendin AL, Cuny HE, Björklund J, Frank DC, Fonti P (2018) RAPTOR: row and position tracheid organizer in R. *Dendrochronologia* 47:10–16
- Peters RL, Groenendijk P, Vlam M, Zuidema PA (2015) Detecting long-term growth trends using tree rings: a critical evaluation of methods. *Glob Change Biol* 21:2040–2054
- Peters RL, Speich M, Pappas C, Kahmen A, von Arx G, Graf Pannatier E, Steppe K, Treydte K, Strieth A, Fonti P (2019) Contrasting stomatal sensitivity to temperature and soil drought in mature alpine conifers. *Plant, Cell Environ* 42:1674–1689
- Peters RL, Steppe K, Cuny H, De Pauw D, Frank D, Schaub M, Rathgeber C, Cabon A, Fonti P (2021) Turgor—a limiting factor for radial growth in mature conifers along an elevational gradient. *New Phytol*. 229:213–229. <https://doi.org/10.1111/nph.16872>
- Piermattei A, Crivellaro A, Carrer M, Urbinati C (2015) The “blue ring”: anatomy and formation hypothesis of a new tree-ring anomaly in conifers. *Trees* 29:613–620
- Pirie MR, Fowler AM, Triggs CM (2015) Assessing the accuracy of three commonly used pith offset methods applied to *Agathis australis* (Kauri) incremental cores. *Dendrochronologia* 36:60–68
- Poussart PF, Evans MN, Schrag DP (2004) Resolving seasonality in tropical trees: multi-decade, high-resolution oxygen and carbon isotope records from Indonesia and Thailand. *Earth Planet Sci Lett* 218:301–316

- Poussart PM, Myneni SCB, Lanzirrotti A (2006) Tropical dendrochemistry: a novel approach to estimate age and growth from ringless trees. *Geophys Res Lett* 33. <https://doi.org/10.1029/2006GL026929>
- Popkova MI, Vaganov EA, Shishov VV, Babushkina EA, Rossi S, Fonti MV, Fonti P (2018) Modeled tracheidograms disclose drought influence on *Pinus sylvestris* tree-rings structure from Siberian forest-steppe. *Front Plant Sci* 9:1144. <https://doi.org/10.3389/fpls.2018.01144>
- Puchi PF, Castagneri D, Rossi S, Carrer M (2020) Wood anatomical traits in black spruce reveal latent water constraints on the boreal forest. *Glob Change Biol* 26:1767–1777
- Reimer PJ, Austin WEN, Bard E, Bayliss A, Blackwell PG, Ramsey CB, Butzin M et al (2020) The IntCal20 Northern Hemisphere radiocarbon calibration curve (0–55 cal ka BP). *Radiocarbon* 62:725–757. <https://doi.org/10.1017/RDC.2020.41>
- Roden J (2008) Cross-dating of tree ring  $\delta^{18}\text{O}$  and  $\delta^{13}\text{C}$  time series. *Chem Geol* 252:72–79
- Roig FA, Le-Quesne C, Boninsegna JA, Briffa KR, Lara A, Grudd H, Jones PD, Villagrán C (2001) Climate variability 50,000 years ago in mid-latitude Chile as reconstructed from tree rings. *Nature* 410:567–570
- Rubiales JM, Bodoque JM, Ballesteros JA, Diez-Herrero A (2008) Response of *Pinus sylvestris* roots to sheet-erosion exposure: an anatomical approach. *Nat Hazards Earth Syst Sci* 8:223–231
- Rydval M, Larsson LÅ, McGlynn L, Gunnarson BE, Loader NJ, Young GH, Wilson R (2014) Blue intensity for dendroclimatology: should we have the blues? Experiments from Scotland. *Dendrochronologia* 32:191–204
- Salzer MW, Bunn AG, Graham NE, Hughes MK (2014) Five millennia of paleotemperature from tree-rings in the Great Basin, USA. *Clim Dyn* 42:1517–1526
- Salzer MW, Hughes MK (2007) Bristlecone pine tree rings and volcanic eruptions over the last 5000 yr. *Quatern Res* 67:57–68
- Salzer MW, Hughes MK, Bunn AG, Kipfmüller KF (2009) Recent unprecedented tree-ring growth in bristlecone pine at the highest elevations and possible causes. *Proc Natl Acad Sci USA* 106:20348
- Sánchez-Salguero R, Camarero JJ, Hevia A, Sangüesa-Barreda G, Galván JD, Gutiérrez E (2019) Testing annual tree-ring chemistry by X-ray fluorescence for dendroclimatic studies in high-elevation forests from the Spanish Pyrenees. *Quatern Int* 514:130–140
- Saurer M, Siegwolf R, Schweingruber F (2004) Carbon isotope discrimination indicates improving water-use efficiency of trees in northern Eurasia over the last. *Glob Change Biol* 10:2109–2120
- Scharnweber T, Hevia A, Buras A, van der Maaten E, Wilmking M (2016) Common trends in elements? Within- and between-tree variations of wood-chemistry measured by X-ray fluorescence—a dendrochemical study. *Sci Total Environ* 566–567:1245–1253
- Schweingruber FH (2001) *Dendroökologische Holzanatomie*. Haupt
- Schweingruber FH, Bräker OU, Schär E (1979) Dendroclimatic studies on conifers from central Europe and Great Britain. *Boreas* 8:427–452
- Schoch W, Heller I., Schweingruber FH, Kienast F (2004) Wood anatomy of central European species. [www.woodanatomy.ch](http://www.woodanatomy.ch)
- Seftigen K, Frank DC, Björklund J, Babst F, Poulter B (2018) The climatic drivers of normalized difference vegetation index and tree-ring-based estimates of forest productivity are spatially coherent but temporally decoupled in Northern Hemispheric forests. *Glob Ecol Biogeogr* 27:1352–1365
- Seftigen K, Fuentes M, Ljungqvist FC, Björklund J (2020) Using blue intensity from drought-sensitive *Pinus sylvestris* in Fennoscandia to improve reconstruction of past hydroclimate variability. *Clim Dyn* 55:579–594
- Sheppard PR, Ort MH, Anderson KC, Elson MD, Vázquez-selem L, Clemens AW, Little NC, Speakman RJ (2008) Multiple dendrochronological signals indicate the eruption of ParíCutin volcano, Michoacán, Mexico. *Tree-Ring Res* 64:97–108
- Shi J, Xiang W, Liu Q, Shah S (2019) MtreeRing: an R package with graphical user interface for automatic measurement of tree ring widths using image processing techniques. *Dendrochronologia* 58:125644

- Shiyatov SG, Mazepa VS, Cook E (1990) 3.5. Correcting for trend in variance due to changing sample size. In: *Methods of dendrochronology: applications in the environmental sciences*, pp 133–137
- Sigl M, Winstrup M, McConnell JR, Welten KC, Plunkett G, Ludlow F, Büntgen U, Caffee M, Chellman N, Dahl-Jensen D et al (2015) Timing and climate forcing of volcanic eruptions for the past 2,500 years. *Nature* 523:543–549
- Speer J (2010) *The fundamentals of tree-ring research*. University of Arizona Press
- Speer JH, Swetnam TW, Wickman BE, Youngblood A (2001) Changes in Pandora moth outbreak dynamics during the past 622 years. *Ecology* 82:679–697
- Stine AR, Huybers P (2017) Implications of Liebig's law of the minimum for tree-ring reconstructions of climate. *Environ Res Lett* 12:114018. <https://doi.org/10.1088/1748-9326/aa8cd6>
- Stahle DW, Griffin RD, Meko DM, Therrell MD, Edmondson JR, Cleaveland MK, Stahle LN, Burnette DJ, Abatzoglou JT, Redmond KT et al (2013) The ancient blue oak woodlands of California: longevity and hydroclimatic history. *Earth Interact* 17:1–23
- Stahle DW, Griffin RD, Edmondson JR (2012) NOAA/WDS Paleoclimatology—Stahle—Palo Prieto Canyon—QUDG—ITRDB CA662. NOAA National Centers for Environmental Information. <https://doi.org/10.25921/ms97-p403>
- Stoffel M, Bollschweiler M (2008) Tree-ring analysis in natural hazards research—an overview. *Nat Hazard* 8:187–202
- Stoffel M, Khodri M, Corona C, Guillet S, Poulain V, Bekki S, Guiot J, Luckman BH, Oppenheimer C, Lebas N et al (2015) Estimates of volcanic-induced cooling in the Northern Hemisphere over the past 1,500 years. *Nat Geosci* 8:784–788
- Stokes MA, Smiley TL (1968) *An introduction to tree-ring dating*. University of Chicago, Chicago
- St. George S, Ault TR (2014) The imprint of climate within Northern Hemisphere trees. *Quatern Sci Rev* 89:1–4
- Swetnam TW, Baisan CH, Caprio AC, Brown PM, Touchan R, Anderson RS, Hallett DJ (2009) Multi-millennial fire history of the Giant Forest, Sequoia National Park, California, USA. *Fire Ecol* 5:120–150
- Swetnam TW, Lynch AM (1989) A tree-ring reconstruction of western spruce budworm history in the southern Rocky Mountains. *Forest Sci* 35:962–986
- Synal H-A, Stocker M, Suter M (2007) MICADAS: a new compact radiocarbon AMS system. *Nucl Instrum Methods Phys Res, Sect B* 259:7–13
- Taylor AH, Trouet V, Skinner CN, Stephens S (2016) Socioecological transitions trigger fire regime shifts and modulate fire–climate interactions in the Sierra Nevada, USA, 1600–2015 CE. *Proc Natl Acad Sci* 113:13684–13689
- Tardif JC, Girardin MP, Conciatori F (2011) Light rings as bioindicators of climate change in Interior North America. *Glob Planet Change* 79:134–144
- Treydte KS, Frank DC, Saurer M, Helle G, Schleser GH, Esper J (2009) Impact of climate and CO<sub>2</sub> on a millennium-long tree-ring carbon isotope record. *Geochimica et Cosmochimica Acta* 73:4635–4647
- Trouet V, Esper J, Graham NE, Baker A, Scourse JD, Frank DC (2009) Persistent positive north Atlantic oscillation mode dominated the medieval climate anomaly. *Science* 324:78–80
- Vaganov EA, Hughes MK, Shashkin A (2006) *Growth dynamics of tree rings: an image of past and future environments*. Springer
- Van den Bulcke J, Boone MA, Dhaene J, Van Loo D, Van Hoorebeke L, Boone MN, Wyffels F, Beeckman H, Van Acker J, De Mil T (2019) Advanced X-ray CT scanning can boost tree ring research for earth system sciences. *Ann Bot* 124:837–847
- Villalba R, Lara A, Masiokas MH, Urrutia R, Luckman BH, Marshall GJ, Mundo IA, Christie DA, Cook ER, Neukom R et al (2012) Unusual southern hemisphere tree growth patterns induced by changes in the southern annular mode. *Nat Geosci* 5:793–798
- von Arx G, Carrer M (2014) ROXAS—a new tool to build centuries-long tracheid-lumen chronologies in conifers. *Dendrochronologia* 32:290–293

- von Arx G, Crivellaro A, Prendin AL, Čufar K, Carrer M (2016) Quantitative wood anatomy-practical guidelines. *Front Plant Sci* 7:781–781
- van Mantgem PJ, Stephenson NL (2004) Does coring contribute to tree mortality? *Can J for Res* 34:2394–2398
- Wilmking M, van der Maaten-Theunissen M, van der Maaten E, Scharnweber T, Buras A, Biermann C, Gurskaya M, Hallinger M, Lange J, Shetti R et al (2020) Global assessment of relationships between climate and tree growth. *Glob Change Biol* 26:3212–3220
- Williams AP, Allen CD, Macalady AK, Griffin D, Woodhouse CA, Meko DM, Swetnam TW, Rauscher SA, Seager R, Grissino-Mayer HD et al (2013) Temperature as a potent driver of regional forest drought stress and tree mortality. *Nat Clim Change* 3:292–297
- Wilson R, Anchukaitis K, Andreu-Hayles L, Cook E, D'Arrigo R, Davi N, Haberbauer L, Krusic P, Luckman B, Morimoto D et al (2019) Improved dendroclimatic calibration using blue intensity in the southern Yukon. *The Holocene* 29:1817–1830
- Wilson R, Anchukaitis K, Briffa KR, Büntgen U, Cook E, D'Arrigo R, Davi N, Esper J, Frank D, Gunnarson B et al (2016) Last millennium northern hemisphere summer temperatures from tree rings: Part I: the long term context. *Quatern Sci Rev* 134:1–18
- Wigley TML, Briffa KR, Jones PD (1984) On the average value of correlated time series, with applications in dendroclimatology and hydrometeorology. *J Clim Appl Meteorol* 23:201–213
- Wigley TML, Jones PD, Briffa KR (1987) Cross-dating methods in dendrochronology. *J Archaeol Sci* 14:51–64
- Woodhouse CA, Gray ST, Meko DM (2006) Updated streamflow reconstructions for the Upper Colorado River Basin. *Water Resour Res* 42:W05415. <https://doi.org/10.1029/2005WR004455>
- Wunder J, Reineking B, Hillgarter F-W, Bigler C, Bugmann H (2011) Long-term effects of increment coring on Norway spruce mortality. *Can J for Res* 41:2326–2336
- Xu C, Sano M, Yoshimura K, Nakatsuka T (2014) Oxygen isotopes as a valuable tool for measuring annual growth in tropical trees that lack distinct annual rings. *Geochem J* 48:371–378
- Zalloni E, de Luis M, Campelo F, Novak K, De Micco V, Di Filippo A, Vieira J, Nabais C, Rozas V, Battipaglia G (2016) Climatic signals from intra-annual density fluctuation frequency in Mediterranean pines at a regional scale. *Front Plant Sci* 7:579
- Zhao S, Pederson N, D'Orangeville L, HilleRisLambers J, Boose E, Penone C, Bauer B, Jiang Y, Manzanedo RD (2019) The international tree-ring data bank (ITRDB) revisited: data availability and global ecological representativity. *J Biogeogr* 46:355–368
- Ziaco E, Biondi F, Heinrich I (2016) Wood cellular dendroclimatology: testing new proxies in great basin bristlecone pine. *Front Plant Sci* 7:1602
- Ziaco E (2020) A phenology-based approach to the analysis of conifers intra-annual xylem anatomy in water-limited environments. *Dendrochronologia* 59:125662. <https://doi.org/10.1016/j.dendro.2019.125662>
- Zuidema PA, Poulter B, Frank DC (2018) A wood biology agenda to support global vegetation modelling. *Trends Plant Sci* 23(11):1006–1015

**Open Access** This chapter is licensed under the terms of the Creative Commons Attribution 4.0 International License (<http://creativecommons.org/licenses/by/4.0/>), which permits use, sharing, adaptation, distribution and reproduction in any medium or format, as long as you give appropriate credit to the original author(s) and the source, provide a link to the Creative Commons license and indicate if changes were made.

The images or other third party material in this chapter are included in the chapter's Creative Commons license, unless indicated otherwise in a credit line to the material. If material is not included in the chapter's Creative Commons license and your intended use is not permitted by statutory regulation or exceeds the permitted use, you will need to obtain permission directly from the copyright holder.



# Chapter 3

## Anatomical, Developmental and Physiological Bases of Tree-Ring Formation in Relation to Environmental Factors



**Cyrille B. K. Rathgeber, Gonzalo Pérez-de-Lis, Laura Fernández-de-Uña, Patrick Fonti, Sergio Rossi, Kerstin Treydte, Arthur Gessler, Annie Deslauriers, Marina V. Fonti, and Stéphane Ponton**

**Abstract** Understanding the process of wood formation and its dynamics over the growing season is fundamental to interpret the isotopic signature of tree rings. Indeed, the isotopic signal recorded in wood does not only depend on the conditions influencing carbon, water, and nitrogen uptake in the leaves and roots, but also on how these elements are translocated to the stem and incorporated into the developing xylem. Depending on environmental conditions, tree developmental stage, and physiological status, wood formation dynamics can vary greatly and produce tree-ring structures carrying specific isotopic signatures. In this chapter, we present the physiological processes involved in wood formation, along with their relationships with anatomical, developmental, and environmental factors, to understand when and how photosynthetic assimilates are progressively incorporated into the forming xylem, creating the final isotopic signature of a tree ring. First, we review current knowledge

---

C. B. K. Rathgeber (✉) · G. Pérez-de-Lis · L. Fernández-de-Uña · S. Ponton  
Université de Lorraine, AgroParisTech, INRAE, SILVA, 54000 Nancy, France  
e-mail: [cyrille.rathgeber@inrae.fr](mailto:cyrille.rathgeber@inrae.fr)

P. Fonti · K. Treydte · A. Gessler  
Research Unit Forest Dynamics, Swiss Federal Institute for Forest, Snow and Landscape Research  
WSL, Birmensdorf, Switzerland

S. Rossi · A. Deslauriers  
Département Des Sciences Fondamentales, Université du Québec À Chicoutimi, Chicoutimi  
G72B1, Canada

S. Rossi  
Key Laboratory of Vegetation Restoration and Management of Degraded Ecosystems, Guangdong  
Provincial Key Laboratory of Applied Botany, South China Botanical Garden, Chinese Academy  
of Sciences, Guangzhou 510650, China

A. Gessler  
Institute of Terrestrial Ecosystems, ETH Zurich, Zurich, Switzerland

M. V. Fonti  
Laboratory of Ecosystems Biogeochemistry, Institute of Ecology and Geography, Siberian  
Federal University, Svobodny 79, 660041 Krasnoyarsk, Russia

© The Author(s) 2022

R. T. W. Siegwolf et al. (eds.), *Stable Isotopes in Tree Rings*, Tree Physiology 8,  
[https://doi.org/10.1007/978-3-030-92698-4\\_3](https://doi.org/10.1007/978-3-030-92698-4_3)



on the structure and functions of wood. Then we describe the xylogenesis process (how and when the new xylem cells produced by the cambium develop through successive differentiation phases), and its relationships with physiological, developmental, and environmental factors. Finally, we explain the kinetics of xylem cell differentiation and show why the knowledge recently acquired in this field allows us to better understand the isotopic signals in tree rings.

### 3.1 Introduction

Stable isotopes in tree rings represent an important source of information on past environmental conditions and tree functioning (McCarroll and Loader 2004). In a time of global changes, it is crucial to further exploit this valuable natural archive by acquiring a more detailed mechanistic understanding of the processes generating and transferring the isotopic signal into tree rings (Fig. 3.1). Questions regarding the acquisition, transfer, and fixation of the isotopic signal within the ring, in relation with the concurrent environmental factors and tree physiological status, are fundamental to link the source of the isotopic signal to its final destination in wood. Addressing

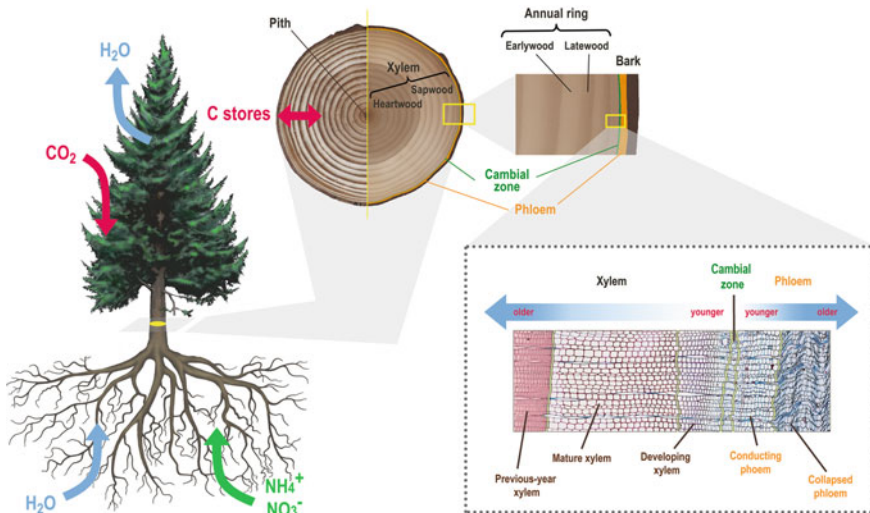


**Fig. 3.1** Basic organization of the tree stem and main fluxes affecting stable isotope composition in tree rings. Water absorption by roots and leaf water transpiration (blue arrows) are related to H and O isotope signals; atmospheric C uptake by leaves and reserve storage-mobilization (red arrows) are related to C and O isotope signals; nitrate and ammonium absorption by roots (green arrow) is related to N isotope signal. The transverse micro-section (bottom right) shows the relative position and age (double blue arrow) of developing and mature zones of xylem (left, inwards) and phloem (right, outwards) that are originated from periclinal divisions in the cambial zone (*i.e.* the cambium and surrounding non-differentiated derivatives)

such questions requires a detailed understanding of how tree rings are formed, which and how internal and external factors influence these processes (Fritts 1976; Schweingruber 1996), and how they eventually determine the intra-ring anatomical (Fonti et al. 2010) and isotopic profile (Gessler et al. 2014).

These issues have been of concern to the scientific community for more than 50 years (Wilson 1970; Denne and Dodd 1981). However, it is only in the last two decades that the number of studies monitoring tree radial growth under both natural or experimental conditions has rapidly increased (De Micco et al. 2019). The approaches developed for the observations of wood growth included the monitoring of stem radial dimension using dendrometers (Kozłowski and Winget 1964; Zweifel 2016), the repeated marking of the cambium via the pinning technique (Gričar et al. 2007b, Yoshimura et al. 1981), and the repeated coring of the stem using a puncher (Rossi et al. 2006a). All these approaches have their strengths and weaknesses, and improvements are still needed. However, thanks to the possibility to assess the developmental stages of xylem cells, only microcoring currently allows to associate the dynamics of xylem cell formation with its anatomical structure and eventually with the tree-ring properties (Rathgeber et al. 2016).

The objective of this chapter is to review the current knowledge on the process of wood formation (*i.e.* xylogenesis) to better interpret the isotopic signature of tree rings. After reminding the structure and functions of the xylem (Sect. 3.2), we describe the mechanisms and pathways of xylem cell differentiation (Sect. 3.3). Finally, we review the current knowledge on the influence of the internal and environmental factors on the dynamics of tree-ring formation (Sect. 3.4), and the kinetics of xylem cell differentiation (Sect. 3.5), before to conclude on how this knowledge can help to better understand tree-ring isotopic signal (Sect. 3.6).

## 3.2 Wood Structure and Functions

Xylem performs three essential functions: (1) conduction of raw sap (*i.e.* soil water containing diluted phytohormones, mineral elements, and other nutrients) from roots to leaves (Sperry et al. 2008); (2) mechanical support (Fournier et al. 2006); and (3) transport and storage of non-structural carbohydrate and defence compounds (Kozłowski and Pallardy 1996). Xylem mainly consists of tracheids (in gymnosperms), and fibres and vessels (in angiosperms), which are elongated cells that die off at the end of their development to fulfil their functions. In mature xylem, these cells are characterized by a thick, rigid and impermeable wall, which delimits an empty lumen through which water can be transported or stored (Domec and Gartner 2002). Additionally, xylem is also composed of parenchyma cells, which are responsible for the storage and radial transport of reserve and defence compounds. They constitute the living part of mature xylem, displaying an active metabolism in their dense cytoplasm surrounded by a thin wall.

### 3.2.1 Xylem Anatomy

#### 3.2.1.1 The Vascular Cambium

The cambium is composed of a thin layer of meristematic cells located between the xylem (*i.e.* the wood) and the phloem (*i.e.* the living bark) (Fig. 3.1), forming a continuous envelope surrounding the stems, branches, and roots of woody plants (Larson 1994; Lachaud et al. 1999; Evert 2006). The cambium produces xylem cells inwards (*i.e.* towards the pith), and phloem cells outwards (*i.e.* towards the bark). Cambial initials are surrounded by a thin primary wall (about 0.1–1.0  $\mu\text{m}$  thick) and have a narrow diameter. They contain many small vacuoles (during the dormant period) or a large central vacuole (during the active period) (Prislan et al. 2013a). Two types of cambial initials can be found in the cambium: (1) the radial initials, which are short and isodiametric cells (about 40  $\mu\text{m}$  in length and 5  $\mu\text{m}$  in tangential and radial diameter); and (2) the fusiform initials, which are long, spindle-shaped cells (about 0.4–4.0 mm in length, 30  $\mu\text{m}$  in tangential diameter, and 5  $\mu\text{m}$  in radial diameter). Radial initials produce the radial elements of xylem and phloem (*i.e.* the elements that are arranged perpendicular to the stem axis in the direction of their length, such as the cells of the ray parenchyma). The fusiform initials are the most numerous (60–90%) and produce the longitudinal elements of xylem and phloem (*i.e.* the elements that are arranged parallel to the stem axis, *e.g.* tracheids, fibres, vessels and sieve tube elements; Larson 1994; Evert 2006).

#### 3.2.1.2 Gymnosperm Xylem Cells

In gymnosperms (*i.e.* conifers or softwood species), xylem is relatively simple and homogeneous, mainly composed of two types of cells: (1) tracheids, which represent more than 90% of the total number of cells and fulfil both mechanical and water conduction functions; and (2) parenchyma cells, which are in charge of the storage and radial transport of various metabolic and defence compounds. Tracheids are elongated, spindle-shaped cells of 3–6 mm in length and 6–60  $\mu\text{m}$  in diameter (Sperry et al. 2006). Tracheids are interconnected through pits, which facilitate water flow both vertically between overlapping tracheids and horizontally between contiguous tracheids. According to tracheid size, tree rings can be divided into earlywood—composed of large, thin-walled tracheids produced at the beginning of the growing season; and latewood—composed of narrow, thick-walled tracheids produced at the end of the season. In numerous species, resin ducts surrounded by living epithelial cells can appear scattered or arranged in radial or tangential bands. Wider tracheids are more efficient in transporting water but disputably more prone to cavitation (Pratt et al. 2007); whereas narrower thick-walled tracheids provide most of the mechanical support but are less conductive (Chave et al. 2009; Cochard et al. 2004; Sperry et al. 2006; Tyree and Dixon 1986).

### 3.2.1.3 Angiosperm Xylem Cells

The more complex and heterogeneous xylem of angiosperms (*i.e.* hardwood species) is typically composed of vessels, fibres and parenchyma. Water conduction is mainly carried out by vessels, while fibres provide mechanical support. Parenchyma cells provide transport of metabolites and storage. Vessels are multicellular tubes up to 500  $\mu\text{m}$  in width formed by dead vessel elements connected through perforation plates and assembled to form pipes (Zimmermann 1983; Brodribb et al. 2012). Depending on the arrangement of vessels along the ring, angiosperm wood may be classified as diffuse- or ring-porous. In diffuse-porous wood, all vessels are of similar size and are uniformly distributed along the ring. The ring-porous structure is characterized by large, highly-efficient vessels in the earlywood and smaller late-wood vessels. In diffuse-porous trees, vessels range from 1 to 30 cm in length, and from 15 to 150  $\mu\text{m}$  in diameter; in ring-porous trees, vessels range from 1 to 10 m in length, and from 15 to 300  $\mu\text{m}$  in diameter (Zimmermann 1982). On the other hand, fibres are long and narrow tracheid-like cells with scarce pits. Some species can also present epithelial cells and secretory canals. Due to their size, ring-porous early-wood vessels are assumed to be functional for only one year because they are highly vulnerable to freezing- and drought-induced embolism (Cochard and Tyree 1990). On the other hand, small vessels are more resistant to cavitation and can potentially be refilled, and thus can be functional for several years (Sperry and Sullivan 1992). Similarly, diffuse-porous xylem usually remains functional for several years.

## 3.2.2 Xylem Cell Wall Structure and Composition

### 3.2.2.1 Xylem Cell Wall Composition

The wall of xylem cells consists of three main chemical components: cellulose, hemicelluloses and lignins. Overall, these components represent more than 90% of wood dry matter (Keegstra 2010). Pectins and a wide variety of proteins can also be found as minor components of xylem cell walls. Cellulose is the world's most abundant organic compound and the key structural component of the cell wall (Mutwil et al. 2008). Cellulose is a long molecule, consisting of a chain of D-glucose units, which presents high tensile strength (Brett 2000). In the cell wall, cellulose is assembled to form long and strong macromolecules, the microfibrils. Hemicelluloses are small and more diverse branched molecules, which interconnect the cell wall components into a coherent whole (Scheller and Ulvskov 2010). Lignins are macromolecules resulting from a complex and heterogeneous assemblage of monolignol units (Freudenberg 1959).

### 3.2.2.2 Middle Lamella and Primary Cell Wall Structure and Composition

The first layer to be developed after cell division is called the middle lamella (ML). The ML is found between the wood cells and ensures the adhesion of a cell with its neighbours. The ML is only 0.5 to 1.5  $\mu\text{m}$  thick and is principally made up of pectins (Fromm 2013).

Plant cells are surrounded by a primary wall (P), which regulates cell volume and content, defines and maintains the shape of the cell, stores nutrients and provides a protective barrier (Fagerstedt and Karkonen 2015). The primary cell wall is thin (approximately 1  $\mu\text{m}$ ), well-hydrated, flexible and extensible. In the early stages of xylem cell differentiation, P is principally composed of cellulose microfibrils (15–40% of the dry mass) linked via hemicellulosic tethers (20–30% of the dry mass) to form cellulose–hemicellulose networks, which are embedded in a pectin matrix (30–50% of the dry mass) and associated with structural proteins (1–10% of the dry mass) (O’Neill and York 2009).

In contrast, during xylem cell maturation, P and ML become highly lignified and combine to constitute what is conveniently termed the compound middle lamella (CML) (Dickson et al. 2017; Koch and Schmitt 2013). After the completion of secondary cell wall formation, the CML has generally a high lignin concentration, reaching for example 67% in poplar (Fromm 2013).

### 3.2.2.3 Secondary Cell Wall Structure and Composition

Unlike the primary wall, the secondary wall (S), which is located between the primary wall and the plasma membrane (PM), only surrounds specific cells, mainly those of woody plants (Evert 2006). Secondary cell walls represent the major constituent of wood and the largest biomass stock in terrestrial plants (Zhong and Ye 2009).

Secondary walls are thick (2–10  $\mu\text{m}$ ), poorly hydrated (approximately 30%), rigid and multi-layered structures. They are composed of cellulose (40–60% of dry mass), hemicellulose (10–40%), and lignin (15–35%) (Cosgrove and Jarvis 2012). Cellulose microfibrils, together with hemicellulose, form the main load-bearing network, in which lignin is impregnated to form another cross-linked matrix ensuring hydrophobicity, rigidity and durability (Zhong and Ye 2009). Hence, with its greater thickness, the lignified secondary wall provides sufficient mechanical support for trees to grow vertically above the ground and cope with the pressures generated in the xylem due to water transport (Speck and Burgert 2011).

Secondary cell walls are commonly composed of three layers: S1 (external), S2 (medium), and S3 (internal). These three layers present similar compositions, but differ in their thickness and orientation of their cellulose microfibrils. Indeed, the thin S1 and S3 layers present transversally oriented microfibril angles (from 60° to 80° concerning the cell axis), while the thick S2 layer presents longitudinally oriented microfibril (5° to 30° concerning the cell axis) (Chaffey 2002; Fromm 2013; Plomion et al. 2001).

### 3.2.2.4 Consideration for Isotope Measurements

Isotope measurements of bulk wood could reflect proportional changes (over the growing season, or between years) of the three main components of the wood cell wall (cellulose, hemi-cellulose and lignin), which can carry different isotopic signatures. Because of different metabolic pathways, wood cellulose and lignin, for instance, differ by ca 3–4‰ in their carbon isotopes composition (Bowling et al. 2008; Wilson and Grinstead 1977). Differences in oxygen isotopes composition between cellulose and lignin are also expected. Indeed, a large proportion of the oxygen atoms present in lignin, for example, comes directly from molecular oxygen available at the site of synthesis, while the rest comes from the exchange with stem water (Barbour et al. 2002). In contrast, all oxygen atoms in cellulose molecules come from water—either from unenriched source water or from evaporation-enriched leaf water (Treydte et al. 2014).

Moreover, the lignin content of the bulk wood integrates the lignin concentration of the different layers of the cell wall and is therefore affected by the anatomical differences exhibited by tree rings, and in particular, by the thickness of the S2 layer. Knowing that the ratio between the thickness of layer S2 (which has a relatively low lignin content) and that of the middle lamella (which has a relatively high lignin content) varies according to the density of the wood (depending on the proportion of early- to late-wood in the ring, for example), tree rings of different densities will therefore exhibit different lignin contents, even if the lignin concentrations of the different cell wall layers are the same (Siddiqui 1976).

To avoid degrading the environmental signal with changing contributions of the different compounds over time, the use of a single component (generally cellulose) is often preferred for C, O and H isotope measurements (McCarroll and Loader 2004).

## 3.3 The Biological Basis of Wood Formation in Relation to Tree Development

Xylogenesis designates the process of xylem formation. During differentiation, the new xylem cells develop into mature and functional wood cells, by undergoing specific morphological and physiological transformations according to their final functions (Wilson 1970). This sequence of processes is common to both angiosperms and gymnosperms, but variations in duration and intensity of the differentiation phases, as well as molecular components, finally result in different cell types and tree-ring structures. Xylogenesis is represented by five successive stages of cell production and differentiation: (1) the division of a cambial cell that creates a new xylem daughter cell; (2) the enlargement of the newly formed xylem cell; (3) the deposition of cellulose and hemicellulose to build the secondary cell wall; (4) the impregnation of the primary and secondary cell walls with lignin; and (5) the programmed cell death (Wilson et al. 1966). Since secondary wall formation and lignification processes

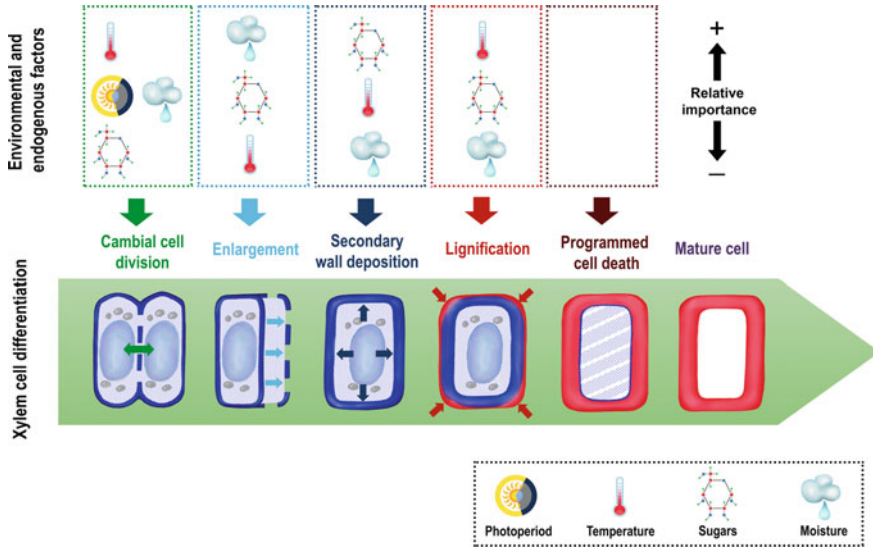


**Fig. 3.2** The sequence of tracheid differentiation from cambial division to maturation and related internal and external drivers. Each stage represents a differentiating tracheid in the cross-section, indicating cambial division (green arrow), enlargement (pale blue arrows), secondary wall thickening (dark blue arrows), lignification (red arrows), and cell death (hydrolysis of the cell content). Cell wall thickening, wall lignification, and programmed cell death stages are frequently regrouped in one unique phase named wall thickening or cell maturation. The main environmental factors affecting tracheid differentiation (photoperiod, temperature, sugar availability, and water content) are ordered according to their relative importance. This general scheme is also valid for angiosperm vessels and fibres

occur almost simultaneously, they are frequently grouped in one phase called cell wall thickening or cell maturation (Fig. 3.2). Parenchyma cells also follow this differentiation sequence but remain alive at maturity. After several years, parenchyma cells also die, while in the same area the last functional tracheids and vessels definitively lose their ability to conduct raw sap. This process is called heartwood formation (or duraminisation) and marks the transition from the sapwood—which is composed of alive, functional wood at the periphery of the tree; to the heartwood—which is composed of dead, non-functional wood at the core of the tree (Hillis 1987; Taylor et al. 2002).

### 3.3.1 The Successive Stages of Xylem Cell Differentiation

#### 3.3.1.1 Cambial Cell Division

Cambial initials can divide in several directions responding to different needs. Anticlinal divisions occur along the tangential direction and allow the cambium to

increase in circumference as the stem grows. Periclinal divisions occur along the radial direction and produce xylem and phloem mother cells (Lachaud et al. 1999). These cells are able to divide again to produce daughter cells that will either retain the characteristics and function of the mother cell (and thus continue to divide) or differentiate into xylem or phloem cells. In general, xylem mother cells divide more often than phloem ones, resulting in a much higher wood than bark production (Evert 2006; Gričar et al. 2009; Grillos and Smith 1959).

Cell division follows a highly ordered sequence of events called the cell cycle (Taiz and Zeiger 2010). A cell generally divides in the direction of its smallest dimension. However, during periclinal division, a cambial cell divides along its length. To facilitate division, fusiform cambial initials contain a large central vacuole filled with water and solutes that reduces the amount of material and energy required for cytoplasm biosynthesis in each mitosis (Lachaud et al. 1999; Cosgrove, 2000a). Nonetheless, the process of cell division is slow in the cambium, with a maximum of one cell being formed per day (Skene 1969; Larson 1994; Mellerowicz and Sundberg 2008; Cuny et al. 2012). To achieve high cell production rates, trees must therefore increase the number of cambial cell layers, which explains the close relationship between the number of cambial cells and xylem production (Cuny et al. 2012; Pérez-de-Lis et al. 2017).

### 3.3.1.2 Cell Enlargement

Cell enlargement is the first stage of wood cell differentiation and consists of an irreversible increase in cell volume. For xylem and phloem cells, cell enlargement only occurs radially. Yet, the radial diameter of xylem tracheary elements can be multiplied by 10 (for gymnosperms) to 100 (for angiosperms). As in cell division, this is achieved by filling the cell vacuoles with water and solutes (Cosgrove 2000a).

The solution inside a plant cell is more concentrated than the one outside. Water is hence attracted into the cell and exerts pressure (the osmotic pressure) on the outside of the cell membrane and primary wall. In equilibrium, the primary wall withstands this osmotic pressure, exerting pressure in the opposite direction (the turgor pressure or turgidity) (Schopfer 2006). However, during cell enlargement, the primary cell wall relaxes under the coordinated action of several enzymes, which break the bonds between its compounds, and of the osmotic pressure which exceeds its yield threshold (Cosgrove 2000b). Cell enlargement, as well as cell division, is regulated by phytohormones, primarily auxins but also cytokinins and gibberellins (Taiz and Zeiger, 2010). These hormones would all act by increasing the extensibility of the primary cell wall, but using many different control pathways.

The loosening of the wall leads to a relaxation of the cell wall stress, which in turn causes a decrease in turgor pressure, allowing water to enter the cell by osmosis, restoring the initial equilibrium between osmotic pressure and turgidity. However, the incoming flow of water causes a dilution of solutes and a reduction of the osmotic potential of the cell, which reduces its water absorption capacity and should thus lead to a rapid cessation of its enlargement. To overcome this problem, enlarging cells



maintain a constant osmotic pressure by actively transporting and breaking down sucrose in glucose and fructose (Koch 2004). Regular cellular enlargement can thus be maintained for several hours or days (Schopfer 2006). However, this could not be possible without the unique combination of elasticity and rigidity of the primary wall, which can withstand distension while resisting the high mechanical forces imposed by turgor pressure (Cosgrove and Jarvis 2012). The thinning of the primary cell wall due to stretching is prevented by the concomitant deposition of newly synthesized wall material (Cosgrove 2000a). The cessation of wall expansion is generally irreversible and is typically accompanied by a reduction in wall extensibility as a result of the deposition of secondary wall layers (Cosgrove and Jarvis 2012).

### 3.3.1.3 Secondary Wall Deposition

The formation of the secondary wall begins with the deposition against the primary wall of a dense matrix of cellulose microfibrils associated with hemicelluloses, forming the S1 layer (Barnett 1981). The synthesis and transport of cellulose and hemicelluloses follow the same processes as in the formation of the primary wall. In the S1 layer, the microfibrils are almost perpendicular to the cell axis (*i.e.* parallel to the cross section); while in the S2 layer, they are deposited almost parallel to the cell axis (*i.e.* perpendicular to the cross section). The S3 layer is formed against S2 with a sudden reorientation of the microfibrils along a transverse helix (Fromm 2013). These sequential changes in the orientation of the microfibrils go hand in hand with the reorientation of the cytoskeleton microtubules (Chaffey 2002). This supports the hypothesis that microtubules control the orientation of cellulose microfibrils in the cell wall, which is responsible for secondary wall birefringence under polarized light, used to detect the wall-thickening process under the microscope (Chaffey 2002).

The secondary wall is not deposited along the whole cell wall surface but is absent around the pits. Pits thus form microscopic openings in the secondary wall, where the modified primary wall (the pit membrane) allows the passage of water and solutes from one cell to the next, making possible the upward flow of sap from the roots to the leaves and the lateral exchange of water and solutes between cells (Siau 1984; Zimmermann 1983; Zwieniecki and Holbrook 2000).

### 3.3.1.4 Lignification

Cell wall lignification is a complex process occurring exclusively in higher plants to strengthen the plant vascular body. Because of the timing of the lignification process and the composition and structure of the cell walls, the proportion of lignin decreases from the outermost (*i.e.* the middle lamella and the primary wall) to the innermost (*i.e.* the secondary wall) layers of the cell wall (Donaldson 1985; Donaldson and Baas 2019). The heavier impregnation of the middle lamella and primary wall allows xylem tracheary elements to stick together and form with fibres (if present) a strong, rigid, and self-supporting network of waterproof “pipes”. Inside the secondary cell

wall, lignin proportions also vary greatly. The S2 layer is less lignified (at least in softwood tracheids; Donaldson 1985), whereas the S3 layer is highly lignified, providing tracheids and vessels a more hydrophobic surface lining, which is thought to facilitate water conduction (Donaldson 1987). Cell wall lignification starts at the cell corners, in the ML and the P, at about the same time as the deposition of the S1 layer, and extends along the ML and the P, before progressing inwards into the S following its deposition (Donaldson 2001). Recently, some authors have suggested that living, parenchymatic xylem cells can contribute to tracheary element lignification in a non-cell-autonomous manner, thus enabling the post-mortem lignification of these elements (Pesquet et al. 2013; Smith et al. 2013).

### 3.3.1.5 Programmed Cell Death

Programmed cell death, or apoptosis, marks the end of xylem cell differentiation and the advent of mature fully functional wood elements (*e.g.* vessels, tracheids). In the xylem, only parenchyma cells and, in some species, fibres possess living protoplasts at maturity (Evert 2006). The apoptosis process involves a highly controlled sequence (hence the term “programmed”) of events that induces a cell to kill itself. In xylem elements, the main trigger for programmed cell death is a regulated entry of calcium ions ( $\text{Ca}^{2+}$ ) into the cell, probably through the channels of the plasma membrane (Groover and Jones 1999; Jones 2001). Death then occurs rapidly (in a few minutes) with the cessation of the cytoplasmic streaming, the sudden rupture of the cell vacuole, and the release of hydrolases that degrade the cell organelles and clean up the cell content (Groover and Jones 1999; Bollhöner et al. 2012). After a few days, the cell consists of an empty space (the lumen) surrounded by a thick wall pierced with pits and, in the case of vessel elements, end openings (*i.e.* perforation plates).

### 3.3.2 Heartwood Formation

Wood conductive and storage functions are lost during heartwood formation, which involves the death of living parenchyma cells, the occlusion of the last remaining conductive elements by gums and tyloses, and the impregnation with secondary metabolites commonly referred as extractives (Evert 2006). These transformations increase the durability of heartwood by making it less attractive to decomposing organisms. The formation of heartwood also reduces the energy expenditure related to living cell maintenance by optimizing the volume of sapwood and thus minimizing its metabolic cost (Taylor et al. 2002).

Non-structural biochemical compounds (including polyphenols, tannins, oils, gums and resins) are responsible for heartwood formation. These extractives are synthesized by the living parenchyma cells at the sapwood edge from compounds available locally or brought from the outer sapwood or phloem, then transferred to

the heartwood by passing from cell to cell through the pits. The extractives impregnate the cell walls in a way that resembles lignification, *i.e.* starting with the middle lamella and then continuing with the primary and secondary walls, and block the pits that connect adjacent cells, rendering them non-conductive (Kuroda et al. 2009).

Tyloses (bubble-shaped parenchyma protrusions entering the lumen of the vessels) are also produced during heartwood formation (De Micco et al. 2016a). Tyloses occlude the vessel lumens and prevent pathogens to spread through the vessel network. When the tylosis completes its expansion, wall materials, including cellulose, hemicelluloses, pectins, suberins and lignins, are deposited in the primary wall, rendering it impermeable and providing further defence against pathogens (Bamber 1976; Bamber and Fukazawa 1985).

The strong heterogeneity between heartwood and sapwood, regarding particularly organic compounds of different isotopic signatures, argues against creating any tree-ring stable isotope records based on whole wood when both sapwood and heartwood tree-rings are present. In such cases, cellulose extraction remains necessary (Weigt et al. 2015). Moreover, whereas radial movements of ions and light molecules are observed within sapwood, they are expected to be minimal in the heartwood, due to the absence of living cells (Ohashi et al. 2017). This may be particularly important to consider when studying N stable isotopes, since most of the N compounds in the sapwood are mobile molecules, seasonally fluctuating and eventually withdrawn from the parenchyma cells before their death (see Chap. 12 for more details).

### 3.3.3 *Influence of Environmental Factors on Wood Formation Processes*

Environmental factors affect wood formation processes (Fig. 3.2), either directly or indirectly through their effect on carbohydrate availability or hormone concentration and sensitivity (Buttò et al. 2019a). The role of environment on cambium division and cell enlargement has been the focus of many studies (Denne and Dodd 1981; Deslauriers et al. 2016, Rossi et al. 2016, 2008). However, the influence of environmental factors on the deposition and lignification of the secondary cell wall remains largely unexplored (Balducci et al. 2016; Cuny and Rathgeber 2016; Cuny et al. 2019; Denne and Dodd 1981).

Temperature exerts direct control on cambial cell division, most probably via the polymerization-depolymerization of the cytoskeleton microtubules, which play important roles in cell division and differentiation (Chaffey 2002). Microtubules are sensitive to temperature: while favourable temperatures allow their polymerization, chilling temperatures tend to disassemble them (Begum et al. 2012b, 2013). The increase of spring temperatures also promotes the enzymatic conversion of starch to soluble sugars, which can then supply the energy for the biosynthesis of the new cell walls (Begum et al. 2010, 2013). Besides, temperature plays a role in the expression of genes related to active auxin transport (Schrader et al. 2003) and influences the

sensitivity and concentration of division- and enlargement-regulating hormones such as auxins, cytokinins, and gibberellins (Ursache et al. 2013). It also modulates wall extensibility and/or yield threshold, possibly controlling the final radial diameter of xylem cells. The lignification process has also been described as sensitive to temperature (Donaldson 2001), which is coherent with the observation of low lignin content in latewood cell walls formed under cold autumn conditions (Gindl et al. 2000; Piermattei et al. 2015).

Of course, water is needed to sustain cambial cell division and enlargement. Indeed, the cambium has been found to stop dividing under water deficit (most likely through the mediation of abscisic acid), probably to limit the number of cells remaining in differentiation without an adequate amount of water (Deslauriers et al. 2016). Moreover, since osmotic pressure is the ‘engine’ of cell wall expansion, water availability must undoubtedly influence cell growth. When a drought occurs, cell enlargement is physically and physiologically inhibited (Nonami and Boyer 2008), resulting in a rapid reduction of the diameter of the cells produced (Rossi et al. 2009b; Balducci et al. 2016). Cell enlargement is thus often depicted as the plant process the most sensitive to water stress (Hsiao 1973). Hence, decreasing water availability in summer has also been considered as one of the main triggers of the transition from the wide earlywood cells to the narrow latewood cells (Kramer 1964), while transient changes in water availability trigger the formation of intra-annual density fluctuations (Balzano et al. 2018). However, wall deposition and lignification appear to be less sensitive to water stress, so that carbon deposition may continue in forming wood even though radial increment stagnates (Carvalho et al. 2015).

Environmental factors can also trigger anatomical changes in mature wood. For instance, tyloses and gums can be formed in sapwood vessels as early as the second part of the growing season, after they become non-functional due to either frost- or drought-induced cavitation (De Micco et al. 2016a, Pérez-de-Lis et al. 2018).

### **3.4 Seasonal Dynamics of Wood Formation in Relation to Tree Phenology**

Tree phenology concerns the particular sequence of developmental events occurring in each organ during the tree life span (Fig. 3.3). Since the canopy is easily observable, leaf phenology has been broadly studied, and it has been proved to be crucial in controlling the acquisition of carbon, the loss of water, and the nutrient cycling in trees (Delpierre et al. 2016). In contrast, the phenology of other organs, such as wood or fine roots, has received less attention, even though it also influences overall plant functioning and biochemical cycles. Phenology is a key determinant of tree fitness and species distribution that integrates the effects of genotype and environmental conditions (Chuine 2010; 2016). Over the last decades, plant phenology and its variation have gained particular importance because environmental changes have produced shifts in phenological events (Anderson et al. 2013) or mismatched

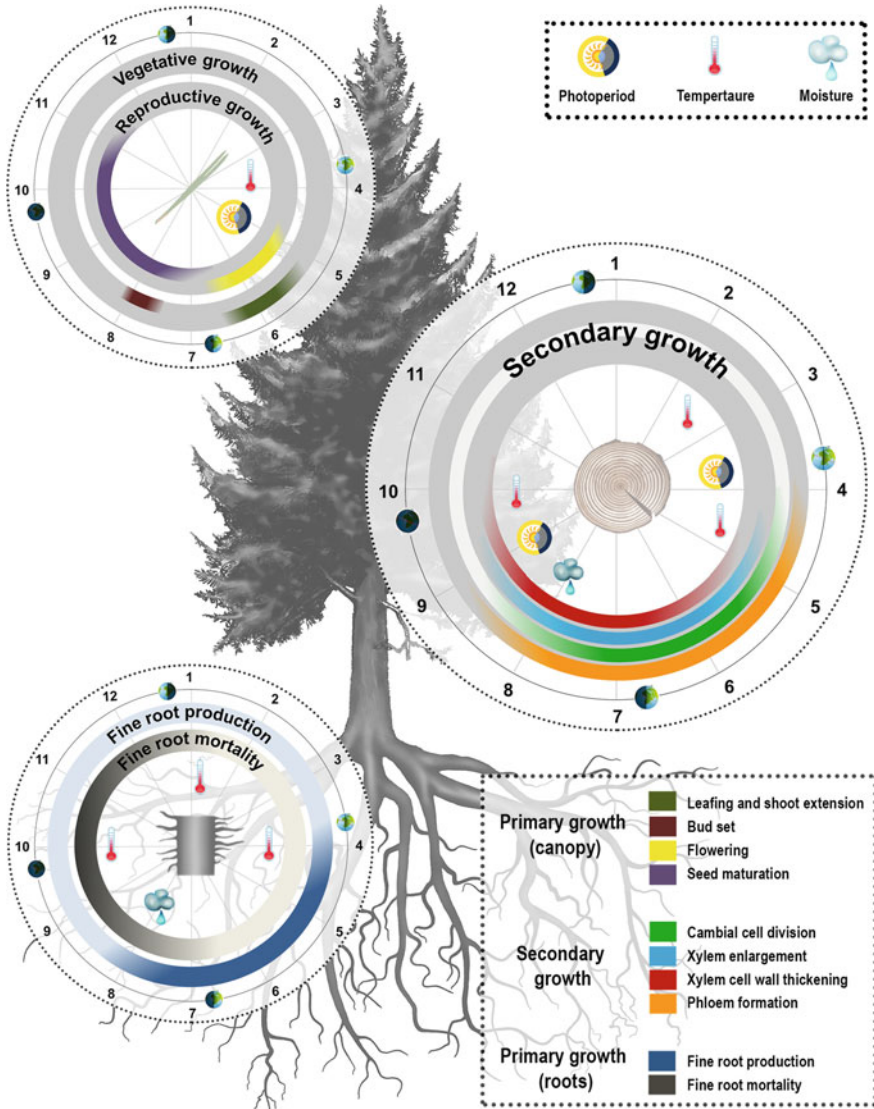


**Fig. 3.3** Representation of tree phenology in northern-hemisphere temperate evergreen conifers and their main environmental cues. The annual course of primary growth in the canopy (upper left) includes both vegetative (flowering and seed maturation) and reproductive events (leaf development and bud set). The annual course of secondary growth in the stem (centre right) includes the main periods of xylem enlargement and maturation, cambial activity, and phloem enlargement. Primary growth in the root system (lower left) includes main periods of fine root production and mortality. Circles are divided into twelve sectors indicating the months of the year, while some relevant environmental cues affecting activity-dormancy cycles are located accordingly

synchronisms among species (Johnson et al. 2010). Whereas most of the studies concerning leaf phenology deal with deciduous angiosperms, the majority of research efforts on the phenology of wood formation have been conducted in conifers, mainly at high elevations and latitudes of the Northern Hemisphere. There are fewer data on deciduous angiosperms in the recent literature, and among them, the majority relate to diffuse-porous species.

Meristem activity underlies several biochemical processes inducing phases of development or maturation of the plant tissues to be renewed. These phases vary according to the organ, ranging from a few days in the primary meristems to several weeks in the secondary meristems (Delpierre et al. 2016; Wilson, 1970). Outside the tropics, the meristems for primary and secondary growth and reproduction follow alternating periods of activity and rest, according to the annual cycle of seasons. This is because most plant physiological processes occur when environmental factors (*e.g.* temperature, water availability, solar radiation) are favourable for growth and reproduction. The growing season, bounded by the phenological phases of growth and dormancy, represents a trade-off between environmental constraints and resource availability. In ecosystems with cold winters, the period of growth results from an optimization between frost risk and carbon gain (Chuine 2010). All overwintering tree tissues, which include leaves in evergreen species, undergo a process of cold acclimation to cope with winter freezing (Cavender-Bares et al. 2005). Cold acclimation implies several biochemical changes, such as intracellular accumulation of sugars and specialized proteins, allowing cells to prevent ice crystal formation, stabilize membranes, and maintain respiration (Cavender-Bares et al. 2005). The primary and secondary meristems further enter dormancy, a resting state under which no growth or tissue maturation is observed (Arora et al. 2003). Three main phases of cambium and bud dormancy have been identified: para-dormancy, endo-dormancy, and eco-dormancy. During paradormancy (late summer and autumn), growth is repressed by the influence of distant organs via the action of hormones (Horvath et al. 2003). During endodormancy (autumn to mid-winter), growth is inhibited by meristem internal factors, which are suppressed at the end of the period by environmental factors such as low temperatures (hereafter called chilling temperatures) and/or long days (photoperiod) (Little and Bonga 1974). During eco-dormancy (mid-winter to mid-spring), growth is only inhibited by environmental factors, ready to restart as soon as favourable conditions arise (Oribe and Kubo 1997).

### ***3.4.1 The Phenology of Cambium and Xylem***

Cambial activity follows the cycle of the seasons (Denne and Dodd 1981; Ladefoged 1952). In extra-tropical regions, the cambium is dormant during winter and active during summer (Delpierre et al. 2016; Wilson 1970), while in tropical regions it may rest during the dry season and be active during the wet season (Bosio et al. 2016). Annual growth rings and typical tree-ring structures, both result from these periodical changes in cambial activity (Evert 2006). In Mediterranean regions and

other seasonally dry areas, one or several pauses in cambial activity can also occur during the growing season, causing intra-annual density fluctuations (IADF), also known as false rings (Balzano et al. 2018).

The key phenological events in the process of wood tissue formation are the beginning and cessation of cell division in the cambial zone (bD and cD, respectively), xylem cell enlargement (bE and cE, respectively), and cell-wall thickening (Rathgeber et al. 2011a). Cell-wall thickening starts with deposition of cellulose in the S1 layer (bT) and ends with the lignification of the S3 layer (cT). While bE and cE are proxies commonly used to compute the duration of cambial activity, bE and cT are commonly used to compute the duration of tree-ring formation (Rathgeber et al. 2016). This sequence of phenological events is structurally fixed, and the delays in the beginning and the end of successive wood formation phenophases are highly conserved among temperate and boreal tree species (Lupi et al. 2010; Rossi et al. 2012, 2013). Considering that the xylem cells produced by cambial division must undergo long differentiation processes, an earlier onset or a higher rate of cambial activity, both presumably associated with a higher number of cells produced along the growing season, would result in a later cessation of wood formation (Rathgeber et al. 2011b; Rossi et al. 2012).

#### 3.4.1.1 Resting Cambium Versus Active Cambium

The inactive cambium is composed of a few layers of dormant cells (ca. 3–6) (Fig. 3.4a), while the active cambium is composed of numerous dividing cells (ca. 6–18) (Fig. 3.4b; Prislan et al. 2013a). During the growing season, new xylem cells, resulting from cambial cell division, are disposed along radial files, and successively undergo the differentiation program related to their identity and their place in the

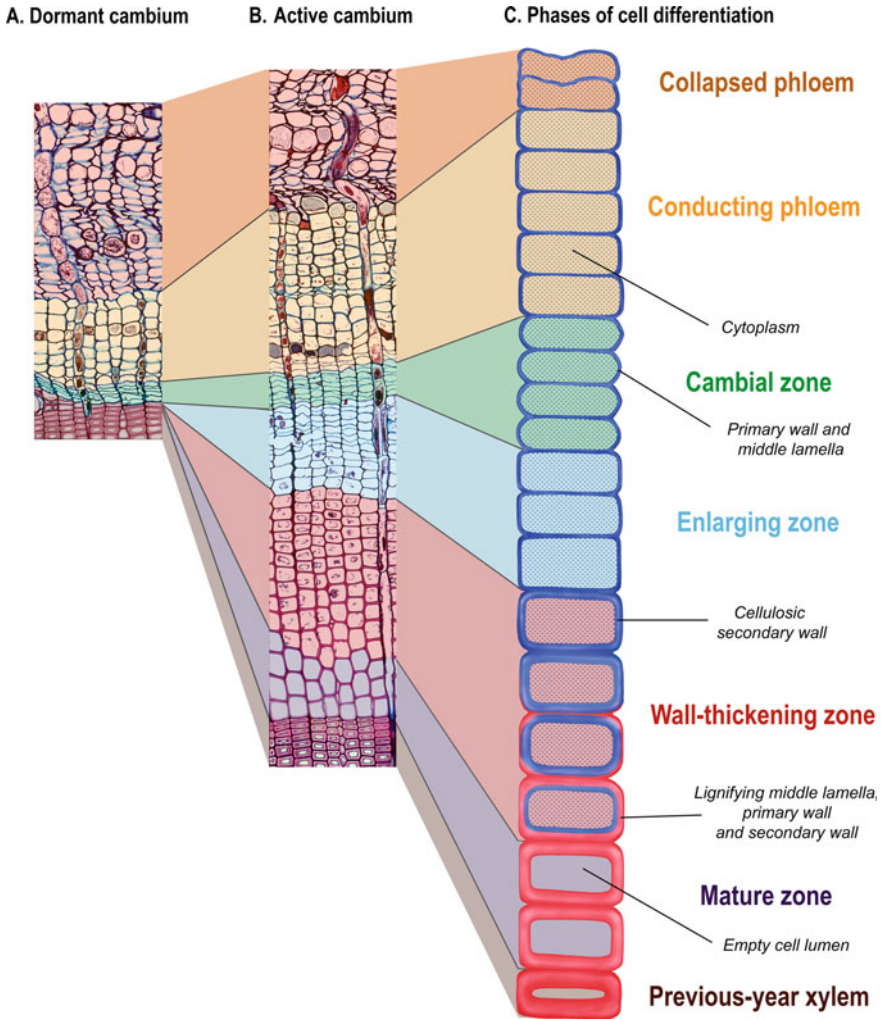


**Fig. 3.4** Cross-sections of dormant **a** and active **b** cambial zones and the adjacent xylem and phloem tissues in Silver fir (*Abies alba* Mill.). **c** Schematic representation of developing xylem and phloem radial files in conifers, indicating the different zones of cell differentiation. Background colours delimit the different zones of xylem and phloem differentiation zones

radial file (Fig. 3.4c). At the tissue level, the different stages of differentiation are well coordinated among all the radial files, creating a characteristic spatial pattern composed of strip-like developmental zones that remains rather stable throughout the growing season (Rathgeber et al. 2016).



### 3.4.1.2 Reactivation of Xylem Formation

At the beginning of the growing season, cambium reactivates and then begins to produce new phloem and xylem cells. Generally, a few over-wintering phloem cells also start to enlarge at about the same time, marking the beginning of stem radial growth and phloem formation (Prislan et al. 2013b). Some weeks after the start of cambial cell division, the derivatives begin radial enlargement, marking the onset of xylem radial growth and wood formation (Wilson 1970; Prislan et al. 2013a). At the end of enlargement, these first xylem cells enter the wall thickening phases (also called maturation phase). In ring-porous species, wall thickening finishes earlier in vessels and surrounding cells, while the neighbouring tissue matures later (Čufar et al. 2011). Because secondary walls hold most of the biomass, the appearance of the first thickening cells can be seen as the effective beginning of carbon sequestration into wood (Cuny et al. 2015). Finally, the first-formed xylem cells undergo programmed cell death and reach their final mature and functional state.

### 3.4.1.3 Cessation of Xylem Formation

In temperate and boreal forests, cambial activity and xylem radial growth rate generally peak around the summer solstice, when the photoperiod is maximal (Rossi et al. 2006b). This period generally marks the transition between early- and late-wood in both conifer and broadleaf species (Cuny et al. 2014; Pérez-de-Lis et al. 2017; Prislan et al. 2018). Cambial activity then starts to slow down until cessation, being soon followed by the end of cell enlargement (flagging the end of stem radial growth). However, the completion of wood formation (marking the end of carbon sequestration) occurs several weeks or months later, ranging from less than one month in diffuse-porous species as European beech (Prislan et al. 2013b, 2018), to more than two months in ring-porous species as white oaks (Lavrič et al. 2017; Pérez-de-Lis et al. 2017), and even more in some conifer species (Cuny et al. 2014; Rossi et al. 2016). Indeed, lignification is a slow process, so the last xylem cells need up to a couple of months to complete cell wall maturation and reach maturity (Cuny and Rathgeber 2016). In some species, cambial activity and cell differentiation can continue in winter if environmental conditions are favourable enough (Dickson et al. 2017; Vieira et al. 2014).

## 3.4.2 *The Phenology of Leaves, Roots and Reserves*

### 3.4.2.1 The Phenology of Leaves

In temperate and boreal regions, the vegetation period manifests strongly in spring with budburst (also called bud break), when leaves or needles emerge from the bud scales and is completed in autumn when deciduous trees avoid winter freezing via

the senescence process that leads to leaf abscission (Fig. 3.3). New buds (either vegetative, reproductive, or compound) are formed after the cessation of primary shoot growth, from late summer to early autumn, depending on the species and the prevailing climate (Gyllenstrand et al. 2007; Rohde et al. 2011). Once formed, buds undergo dormancy from late summer to the following spring. While temperatures and photoperiod are the main cues of leaf phenophases (Basler and Körner 2014), drought may delay bud formation and leaf emergence and advance leaf senescence, although this effect seems to be species-specific (Ogaya and Penuelas 2004). Indeed, in regions with dry–wet seasonality, some tree species partially or completely shed their leaves during the dry season to limit canopy transpiration under increased water stress and vapour pressure deficits (Wright and Cornejo 1990).

### 3.4.2.2 The Phenology of Roots

The secondary growth of coarse roots has seldom been studied, but it follows the same formation processes as aboveground wood (Fig. 3.3). The timing, however, generally follows a shifted calendar, with later onsets and cessations resulting in shorter durations of the differentiation period compared to stem wood (Thibeault-Martel et al. 2008; Lemay et al. 2017). The phenological cycles of production and mortality of rootlets, the finest and apical parts of the root system, are generally studied for ensembles of root branching orders rather than individually. Although growth and mortality may occur simultaneously, the burst of rootlet growth mostly takes place in spring and early summer while mortality occurs in late summer and autumn (McCormack et al. 2014).

### 3.4.2.3 The Seasonal Cycles of Carbon and Nitrogen Reserves

Carbon (C) and nitrogen (N) reserves are key actors of the seasonal variability of tree functioning. In evergreen tree species, starch concentration peaks before budburst, with only slight variations in carbon storage throughout the rest of the growing season (Hoch et al. 2003). On the other hand, the growth of new organs induces a massive, short-distance mobilization of reserves in deciduous trees (Bazot et al. 2013), which typically results in a decrease in carbon reserve concentrations in the majority of tree organs (Barbaroux et al. 2003). However, photosynthesis by the new leaves causes a rapid increase in carbon reserves, which culminates at leaf senescence (El Zein et al. 2011). Leaf senescence and shedding have been observed to be concurrent with a major starch-to-sugar conversion in carbon pools in deciduous oaks, which is probably related to the acquisition of frost resistance before winter (Pérez-de-Lis et al. 2017). The amount of carbon reserves in deciduous species typically decreases during winter as a result of maintenance processes in perennial organs (Barbaroux and Bréda 2002).

In evergreen species, remobilization of nitrogen from older shoots and needles provides the necessary amount for the growth of newly formed tissues (Millard and

Proe 1992). Fluctuations of nitrogen reserves for the rest of the year appear to be less variable than those of carbon reserves (Millard and Grelet 2010). In deciduous trees, nitrogen reserves are mobilised in spring to grow leaves, they remain then at low levels throughout the leafy season, until they increase due to the reabsorption of nutrients occurring during the leaf senescence processes in autumn (Millard and Grelet 2010; El Zein et al. 2011; Bazot et al. 2013). During winter, the level of variation in nitrogen reserves seems to be reduced compared to the level of variation in carbon reserves (El Zein et al. 2011).

### **3.4.3 Seasonal Dynamics of Wood Formation in Relation to Organ Phenology**

The relationships between wood formation and other developmental processes can have a significant effect on tree functioning, including carbon and water fluxes and the allocation of resources (Fig. 3.3). Fine root elongation typically starts before budburst, both in angiosperms and conifers (Lyr and Hoffmann 1967; Konôpka et al. 2005). However, the sequence of wood and leaf phenology differs among tree functional types, affecting their resource-use strategies. For diffuse-porous tree-ring species (e.g. *Fagus sylvatica*) growth is known to begin just after budburst, while maximal growth rate occurs when the leaves are mature, so non-structural carbohydrate (NSC) content variations are low over the year. Thus, diffuse-porous species radial growth is directly related to leaf photosynthesis. On the other hand, for ring-porous species (e.g. *Quercus petraea*), earlywood quickly develops before budburst, depleting carbon reserves from April to June (Barbaroux and Bréda 2002). For conifers (e.g. *Pinus sylvestris*) growth often begins before new needles unfold, but the lack of NSC depletion during the growing season suggests that the substrates for radial growth are provided by previous-year needles (Michelot et al. 2012). Despite being species-specific, the timing of this wood-leaf phenology sequence is not fixed, and delays in the spring phenophases between wood and leaf development are observed from year to year (Takahashi and Koike 2014) and among individuals within species (Perrin et al. 2017).

#### **3.4.3.1 Relationship Between Wood Formation and Tree Phenology in Gymnosperms**

During winter, in temperate regions, xylem and phloem cells can be frozen because of low temperatures. However, xylem cells generally remain functional for several years, while phloem cells are functional for only one or two years maximum. While deciduous conifers overwinter without needles, evergreen conifers still carry several cohorts of needles from previous years, which can photosynthesize when the air temperature is above about  $-3^{\circ}\text{C}$  (Lundmark et al. 1998).

In spring, evergreen conifers start cambial activity early, generally producing new phloem cells first and new xylem cells afterwards. Budburst and new needle unfolding occur a couple of weeks later, at about the same time as shoot elongation (Rossi et al. 2009a; Cuny et al. 2012). Therefore, active cambium and sprouting buds are supplied principally with carbon originating from old needle cohorts. On the other hand, deciduous conifers have been reported to start cambial activity later than cohabiting evergreen conifers (Swidrak et al. 2014). In deciduous conifers, needle unfolding occurs rapidly after the onset of cambial activity, while shoot elongation starts approximately two weeks later, indicating that cambial reactivation relies on carbon reserves stored during the previous year (Rossi et al. 2009a).

At the beginning of the summer, the cambium of conifers produces phloem and xylem cells at a high pace using mainly new assimilates. The transition between the production of early- and late-wood cells occurs at about the same time as the termination of the needle and shoot lengthening (Rossi et al. 2009a; Cuny et al. 2012). Indeed, leaf maturation has long been suggested to be linked to the transition from early- to latewood (Larson 1994).

Cambial activity stops in late-summer or early-autumn, while xylem formation ceases about two months later when latewood is mature (Rossi et al. 2016). Needle abscission in deciduous conifers generally occurs after the end of wood maturation (Swidrak et al. 2014).

### 3.4.3.2 Relationships Between Wood Formation and Tree Phenology in Angiosperms

Because their large vulnerable vessels generally become non-functional within one-year, deciduous ring-porous species have to rebuild their earlywood vessel network each spring to supply raw sap to developing leaves (Cochard and Tyree 1990). Therefore, ring-porous angiosperms generally resume cambial activity before budburst (Pérez-De-Lis et al. 2016; Gričar et al. 2017; Lavrič et al. 2017), which appears to be synchronous with the onset of secondary wall deposition in developing vessels (Pérez-De-Lis et al. 2016; Fernández-de-Uña et al. 2018).

In contrast, the more resistant vessel network of diffuse-porous species can be functional for several years. This may explain why species belonging to this functional group resume cambial activity concurrently or shortly after budburst (Michelot et al. 2012; Prislán et al. 2013b, 2018). Therefore, while the earlywood of ring-porous species is formed using principally carbon reserves, diffuse-porous species earlywood is made of a mixture of carbon coming from previous-year reserves and more recent assimilates (Helle and Schleser 2004). A recent study shows that evergreen angiosperms rely nearly exclusively on recent assimilates to form their rings (Vincent-Barbaroux et al. 2019).

In summer, the cambium produces phloem and xylem cells using recent carbon assimilates from fully mature leaves, which are also used to refill the carbon storage pools (Michelot et al. 2012; Prislán et al. 2013b; Pérez-de-Lis et al. 2017). In ring-porous angiosperms, leaf maturation is followed by the onset of latewood formation,

which is associated with an increase in wood formation rates (Pérez-de-Lis et al. 2017). A high carbon availability, already evoked for conifers, could account for the early-to-latewood transition, although it could be also attributed to a greater production of gibberellins by mature leaves, which are thought to promote the differentiation of latewood fibres (Buttò et al. 2019a).

In early-autumn, the cambium frequently stops producing new cells, while cessation of wood maturation occurs a few weeks later. Senescent leaves can already be seen in the canopy at that time, although most of the leaves will be shed in late autumn (Gričar et al. 2017; Lavrič et al. 2017).

In areas that experience a dry season, a cessation of cambial activity and yellowing of the leaves can be observed as early as early summer. However, in most of the Mediterranean species, the cambium can then resume activity in the autumn when the environmental conditions are more favourable, producing a false ring (Camarero et al. 2010; Pérez-de-Lis et al. 2017).

#### ***3.4.4 Influence of Environment on Seasonal Dynamics of Wood Formation and Tree Phenology***

As described in Sect. 3.3.3, both external and internal factors control xylogenesis and are likely involved in the regulation of its timing. There is strong evidence that temperature has a primary role as an environmental driver for xylogenesis. In natural stands, the onset of cambial activity occurs within a relatively narrow range of daily minimum air temperature (from 2 to 7 °C) (Rossi et al. 2007, 2008, 2013, 2016), resulting in elevation gradients of cambium resumption (Moser et al. 2009; Prislán et al. 2013b; Saderi et al. 2019). Cambial activity can be reactivated during late winter by artificial heating of tree stems (Oribe et al. 2003; Begum et al. 2010). This artificial resumption of cambial activity can nevertheless only be triggered during the ecodormancy phase after the chilling requirement has been fulfilled during endodormancy (Begum et al. 2013). On the other hand, cessation of cambial activity in early autumn occurs at milder temperatures than those for spring resumption (between 5 to 13 °C for conifers) (Rossi et al. 2007, 2008, 2013, 2016), although it can be hastened by artificial cooling (Gričar et al. 2007a; Begum et al. 2012a). This equivocal role of temperature results in the absence of a clear elevation trend in the timing of the cessation of cambial activity (Moser et al. 2009; Prislán et al. 2013b; Saderi et al. 2019). These results demonstrate that cambial division is also driven by other cues such as photoperiod and water stress (Rathgeber et al. 2016). For instance, photoperiod is thought to modulate cambial division rates (Rossi et al. 2006b) and may act as a cue for the onset and cessation of cambial activity (Delpierre et al. 2019; Fernández-de-Uña et al. 2018; Saderi et al. 2019). Likewise, water stress hastens the cessation of cambial activity (Gričar and Čufar 2008; Gruber et al. 2010; Fernández-de-Uña et al. 2017; Saderi et al. 2019).

The close coordination between the phenology of the different organs of a tree suggests that environmental effects on cambial activity could also be indirect via the influence exerted by the environment on other organs, such as buds, leaves and roots. For instance, bud and leaf phenology is mainly under the control of temperature and photoperiod, to prevent frost damage (Chuine 2010). Several stresses, such as drought and mineral deficiencies, can also hasten primary growth cessation and leaf senescence (Delpierre et al. 2016). On the other hand, soil temperature regulates rootlet elongation. A few studies have suggested that rootlet growth can continue at a minimal rate during winter in evergreen trees, although it would not occur below a threshold of 2 to 4 °C (Schenker et al. 2014). Fine root growth may also be reduced or interrupted under drought conditions (Konôpka et al. 2005).

Phenological responses in distant tree organs are coordinated thanks to long-distance signalling mechanisms, which involve the vascular system (Notaguchi and Okamoto 2015). The phytohormones produced in a given organ can regulate the phenology of distant organs, raising the question of the autonomy of an organ phenology. For instance, auxins produced in expanding buds influence the rate of cambial divisions in the stem (Lachaud et al. 1999). However, the presence of auxins in overwintering tissues may decouple the onset of cambial division from the timing of bud elongation, as observed from stem heating experiments (Oribe et al. 2003; Begum et al. 2010). Nonetheless, the auxins produced in elongating buds are likely necessary for sustaining a high division rate in the newly activated cambium. Anyway, temperature remains a major cue for tree phenology because it controls both the break from ecodormancy in buds (hence, the production of auxins), the sensitivity of cambium to auxins, and the level of activity of the enzymes involved in all these different processes.

### 3.5 Kinetics of Tracheid Differentiation in Relation with Tree Physiology

A remarkable aspect of xylogenesis is its capacity to generate various wood forms in response to developmental or environmental constraints (Rowe and Speck 2005). Contrasting wood anatomy can thus be observed between different phylogenetic groups, but also between different individuals of the same group, between different organs inside the same individual, or during the ontogenic trajectory of the tree (Lachenbruch et al. 2011). Besides, wood anatomy is also known to change with environmental conditions either in space or in time (Jansen et al. 2004). Variations in wood anatomy may occur within a single tree ring, such as the transition from early- to late-wood in conifers and ring-porous species. Tracheid diameter, for example, is commonly divided by a factor of five from the beginning to the end of a tree ring in conifer species (Schweingruber 2007; Vaganov et al. 2006). This tree-ring structure reflects structural and physiological trade-offs that are important for tree functioning and performance, as seen in Sect. 3.3.1. These changes in tracheid and

vessel morphology also drive many fundamental wood properties, including the ratio between early- and late-wood and the tree-ring density profile (Fig. 3.5; Rathgeber et al. 2006). Xylogenesis is the key process during which trees balance the afore-said functional and structural trade-offs and fix them permanently in the wood tissue (Rathgeber et al. 2016). However, which and how climatic factors, in interaction with tree physiological state, and developmental control, influence xylem cell differentiation and the resulting tree-ring structure have still not been fully unravelled yet.

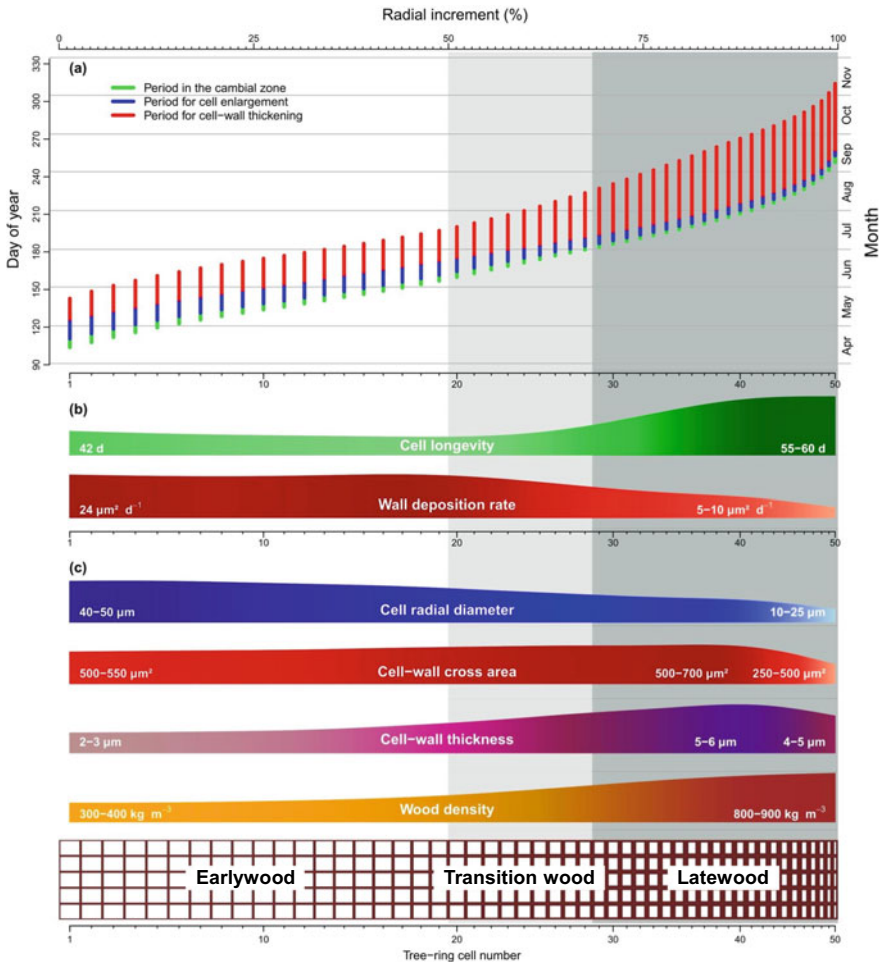


**Fig. 3.5** Kinetics of tracheid differentiation and resulting tree-ring structure in conifers. **a** Timing of cell differentiation phases (division, radial enlargement, and cell-wall thickening) in each successive tracheid along a tree-ring radial file. **b** Cell longevity and cell wall deposition rate. **c** Resulting tree-ring structure, with the evolution of the main anatomical parameters along with a scheme of the corresponding mature tree ring Courtesy of Henri Cuny

### ***3.5.1 From Wood Formation Dynamics to the Kinetics of Tracheid Differentiation***

The kinetics of wood formation have been predominantly studied in conifer species because of their simpler wood structure, formed by tracheids sequentially arranged in rows perpendicular to the ring boundaries. During xylogenesis, cell enlargement and wall thickening are the two fundamental subprocesses that shape xylem cell dimensions and create the resulting tree-ring structure (Cuny et al. 2014). In his pioneering work, Skene (1969) set the framework for studying the kinetics of conifer tracheid differentiation: the final radial diameter of tracheids is the product of the duration and the rate of cell enlargement; whereas the final amount of secondary cell-wall is the product of the duration and the rate of wall material deposition. Cell wall thickness is thus the result of the total amount of wall material deposited for one cell, relative to its final size. Subsequent studies, however, focused mainly on the duration of the processes (cell enlargement and wall deposition) to explain the observed changes in cell features (cell diameter and wall thickness) along the ring, discounting the rates without assessing their importance (Wodzicki 1971; Skene 1972).

The complex inter-plays between the durations and the rates of xylogenesis subprocesses determine the changes in cell features (*e.g.* cell and lumen diameter, lumen area, and wall thickness) that, in turn, create the anatomical structure driving tree-ring density profile (Cuny et al. 2014). There is a positive relationship between the cell radial diameter and the duration of the enlargement phase in conifer tracheids (Cuny et al. 2014; Buttò et al. 2019b) and, to a lesser extent, also in angiosperm vessels (Pérez-de-Lis et al. 2016). Indeed, most of the changes in cell radial diameter are attributable to shifts in the duration of cell enlargement along the ring (Cuny et al. 2014; Buttò et al. 2019b). Cell radial diameter itself accounts for most of the changes in wall thickness, thus making the duration of cell enlargement also responsible for a great proportion of the variations in wood density along the ring, together with the variations in the duration and rates of cell-wall deposition, which contribute equally to cell-wall thickness (Cuny et al. 2014).

#### **3.5.1.1 Relationship between Conifer Tree-Ring Structure and the Kinetics of Tracheid Differentiation**

Wood formation monitoring studies reveal that a strong negative relationship links the duration and rate of cell-wall deposition for the majority of the cells of a ring, except for the very last latewood cells (Fig. 3.5; Cuny et al. 2014, 2019; Balducci et al. 2016; Cuny and Rathgeber 2016).

The duration of enlargement decreases progressively across a conifer ring by about two-thirds from the first to the last cells (Wodzicki 1971; Skene 1972; Cuny et al. 2014). This decrease is particularly abrupt in transition wood of species exhibiting contrasted tree-ring structures (*e.g.* *Larix* spp., *Pinus sylvestris*). Enlarging tracheids



can take between one to four weeks to reach their final size at the beginning of the growing season, while final latewood cells may only take one week (Wodzicki 1971; Skene 1972; Rathgeber et al. 2011a; Cuny et al. 2014). In comparison, the rate of enlargement shows little variations along tree rings (Wodzicki 1971; Skene 1972; Cuny et al. 2014).

On the other hand, wall-thickening duration tends to increase along tree rings, although some species may show a decrease for the last tracheids (Cuny et al. 2014; Buttò et al. 2019b). Secondary wall formation may take two to three weeks for earlywood cells, and three to seven weeks for latewood cells. Conversely, cell-wall deposition rates tend to decrease in transition- and late-wood cells (Cuny et al. 2014).

### 3.5.1.2 Carbon Allocation Along the Ring and the Growing Season

Wall thickness changes have been related to the kinetics of wall deposition (Skene 1969; Wodzicki 1971), and the idea that wall thickness is mainly driven by the duration of wall-thickening is deeply anchored in the scientific literature. However, in opposition to this common belief, the results obtained by Cuny et al. (2014) revealed that the amount of material deposited per cell was almost constant along most of the ring, but decreased dramatically in the last 25% of the ring, reaching minimal values for the last latewood cells, where wood density was maximal. Because of this, changes in the amount of wall material per cell, and the kinetics of wall deposition, only explained 33% of the changes in wall thickness and 25% of the changes in wood density. In other words, more or less constant amounts of wall material are placed into smaller and smaller cell volumes, resulting in increasing wall thickness and wood density. Therefore, increasing cell wall thickness and wood density along tree rings do not reflect higher carbon allocation to woody biomass, but rather a downturn of secondary growth. Thus, the main driver of density changes along the ring is the cell enlargement process.

The same kinetic approach was also used to describe the dynamics of carbon allocation to the xylem (Cuny et al. 2015), showing that woody biomass production lags behind stem-girth increase by over one month in conifers from boreal, temperate, subalpine and Mediterranean regions (Fig. 3.6). In angiosperms, preliminary results show that there is also a time lag between growth in size and in biomass, but it is estimated to be only about two weeks in ring-porous species and probably even less in diffuse-porous species (Andrianantenaina et al. 2019). These time lags question the extension of the equivalence between stem size increase and woody biomass production at intra-annual time scales. They also suggest that these two growth processes exhibit differential sensitivities to local environmental conditions. Indeed, in well-watered sites, the seasonal dynamics of stem-girth increase matched the photoperiod cycle, whereas those of woody biomass production closely followed the seasonal course of temperature (Cuny et al. 2015).

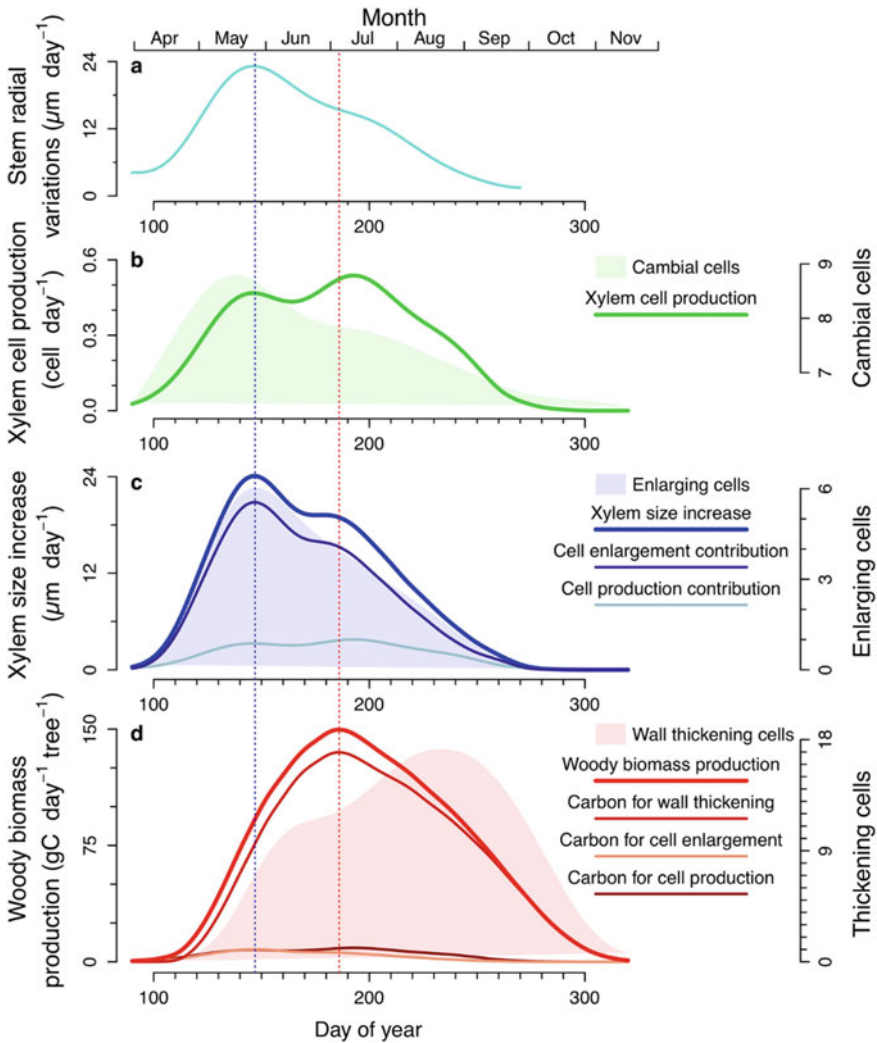


**Fig. 3.6** Seasonal dynamics of stem-girth increase, xylem size increase and woody biomass production. **a** Stem-external radial variations. **b** Rate of xylem cell production through cambial cell divisions and the number of cambial cells (shading). **c** Rate of xylem size increase, with isolated contributions of cell production and cell enlargement, together with the number of enlarging cells (shading). **d** Rate of woody biomass production, which sums the carbon sequestered by wall thickening plus that from cell enlargement and cell production. Shading shows the number of wall thickening cells. Vertical blue and red dashed lines indicate time of maximal rates of xylem size increase and woody biomass production. The curves represent the average data for three sites in Vosges mountains (Northeast of France), including three species (*Abies alba*, *Picea abies* and *Pinus silvestris*) monitored during three years (2007–2009). Figure from Cuny et al. (2015)

### 3.5.2 *Influence of Environmental Factors on the Kinetics of Wood Formation*

In temperate forests, earlywood cells generally develop from mid-April to mid-July; transition-wood, from mid-June to mid-August; and latewood, from the beginning of July to mid-November (Cuny et al. 2014). Each cell in a tree ring experiences particular environmental conditions, potentially uniquely shaping its final dimensions, since each of its differentiation phases occurs within a specific time window. However, the links between tracheid or vessel size and environmental conditions during their formation are still largely unknown.

In conifers, for the majority of the cells along the ring, as the rate of cell wall deposition decreases, the duration of wall deposition increases in the same proportion (Balducci et al. 2016; Cuny and Rathgeber 2016; Cuny et al. 2019). Because of this ‘compensation effect’, the amount of wall material incorporated by the tracheids exhibits little change along a large part of tree rings (Cuny et al. 2014). Only in the second part of the latewood, the compensation effect decreases to become minimal for the very last tracheids (Cuny and Rathgeber 2016). In these last tracheids, variations in the rate of wall deposition result in equivalent variations in the wall cross-area. Because of the compensation effect, the influence of climate on the rate of wall deposition may not be translated into shifts in the amounts of deposited wall material during most of the growing season and thus, could not be recorded in the tree-ring structure, and probably only partially in wood isotopic composition. Indeed, Cuny and Rathgeber (2016) found that for cells presenting a strong compensation, influences of temperature on wall deposition rate were not traced in the wall cross area. Conversely, for cells presenting a weak compensation, highly significant, positive relationships were found between the wall cross area, the daily rate of wall deposition, and the temperature during the period of secondary wall formation (Cuny and Rathgeber 2016; Cuny et al. 2019). Such contrasting sensitivities of early- and late-wood cells to temperature confirm results from dendroclimatology showing that latewood conveys a much stronger climatic signal than earlywood (Wimmer and Grabner 2000). Thus, the lack of compensation for the last latewood cells appears as a clue to explain the supremacy of maximum latewood density as a proxy for past climatic conditions in general, and temperature in particular (Briffa et al. 2002a, b).

On the other hand, Cuny & Rathgeber (2016) observed a strong effect of day-length, but only on the duration of latewood cell enlargement. This absence of a clear climatic determinism of the decreasing tracheid diameter along the ring, a crucial determinant of the whole tree-ring structure, argues for a close control of the kinetics of wood cell differentiation. However, in Mediterranean regions, features such as intra-annual density fluctuations (IADF), show that strong variations of the water regime during the growing season can also break the ‘compensation effect’, and modify tracheid size and tree-ring structure (De Micco et al. 2016b; Zalloni et al. 2016). Indeed, in the first half of the growing season, the enlargement rate of xylem cell can drop to zero during a severe drought, creating a band of latewood-like cells

in earlywood (Balducci et al. 2016). Conversely, in the second half of the growing season, when the cambium encounters exceptionally good water conditions, it may produce a band of earlywood-like cells in the latewood (Balzano et al. 2018).

### 3.6 How Wood Formation Monitoring Can Help to Better Understand Tree-Ring Isotopic Signal

The isotopic composition of tree rings integrates the specific isotopic signatures of the various compounds used to build xylem cell structures (*e.g.* cellulose, hemicelluloses, lignins). The isotopic signature of these compounds is modulated by the physiological processes occurring during the synthesis and delivery of the substrates to the growing xylem (Gessler et al. 2014). We know that the isotopic signature of these substrates is well related to the environmental conditions occurring during their production by photosynthesis (Brandes et al. 2006). However, the relationships between the environmental conditions occurring during carbon assimilation, assimilate transport, xylem formation and the final isotopic signature of a tree ring is rather complex and not completely unravelled yet. For instance, at the beginning of the growing season, the utilization of carbohydrate reserves to build new xylem cells causes a mismatch between the time at which wood is formed and the time at which its carbon was assimilated. Therefore, the isotopic signal recorded in the earlywood could reflect previous-year environmental conditions rather than current spring conditions (Kagawa et al. 2006). Moreover, in this example, the isotopic signal would also be affected by the effect of post-photosynthetic fractionations (see Chap.13). The same considerations apply for the oxygen isotope signal. However, starch remobilization can lead in this case to extended exchange with the reaction water, potentially further diluting the original isotopic signal (Gessler et al. 2014).

High-resolution studies dividing tree rings into a variable number of sectors either manually (Treydte et al. 2014; Zeng et al. 2017) or with automated laser-based systems (Schulze et al. 2004; Schollaen et al. 2014) to provide intra-annual isotopic composition profiles of tree rings are becoming more and more frequent. Such studies not only help to more precisely identify external and endogenous factors driving the isotopic signature of bulk wood or cellulose along the growing season, but can also provide additional insight into the carbohydrate dynamics sustaining xylem cell growth (Helle and Schleser 2004; Ogée et al. 2009; Rinne et al. 2015; Belmecheri et al. 2018).

Intra-ring sectoring in isotope studies is conventionally done by assuming that each ring sector can be somehow attributed to a definite time window according to its position within the ring. This is the case of studies applying both regular (all the sectors exhibit the same width) and irregular (all the sectors do not have the same width, *e.g.* earlywood and latewood) sectoring. In this chapter, we showed that tree-ring formation is the result of a complex succession of developmental processes, which rates and durations vary along the growing season. Therefore, despite their

relatively simple structure, not even conifer tree rings can be seen as a succession of cell rows formed during separate regular time intervals. Rather, the successive cell rows of a tree ring are formed in highly overlapping time intervals of variable durations (Fonti et al. 2018). We showed that, as we move from early- to late-wood, cells spend progressively more time in the wall thickening phase and less in the enlargement phase. A longer period of differentiation, along with higher rates of cell division, increase the amount of forming tissue that can be observed at a given day. Therefore, the amount of tissue in wall thickening is generally higher than that in enlargement zone, increasing along the growing season and with maximum values in summer. This scheme is even more complicated in angiosperms, due to their heterogeneous tree-ring structure and greater variety of cell types with contrasting maturation rates and lifespans. As a result, the association between intra-ring isotopic measurements (taken along several ring sectors) and the time window of formation cannot be accurately inferred by simply using their relative position along the tree ring. The accurate dating of intra-ring sectors requires a good understanding of wood formation processes, which can only be obtained through repeated observation of the developing xylem along the growing season. Therefore, monitoring wood formation is essential for disentangling high-resolution isotope signals stored in the cellulose and bulk wood of tree rings, as well as to assess the extent to which wood formation processes affect the recording of the isotopic signature.

**Acknowledgements** The authors would like to thank Henri Cuny for preparing Fig. 3.5 and Daniel Epron for his comments on the final version of the manuscript. Some of the ideas and materials presented in this chapter were developed with the support from the French National Research Agency (through ANR-11-LABX-0002-01, Lab of Excellence ARBRE), the Swiss National Science Foundation (projects INTEGRAL-121859, CLIMWOOD-160077, and LOTFOR-150205), the Canada Foundation for Innovation, the ‘Consortium de Recherche sur la Forêt Boréale Commerciale’, the ‘Fonds de Recherche sur la Nature et les Technologies du Québec’, and the ‘Forêt d’Enseignement et de Recherche de Simoncouche’.

## References

- Anderson DM, Mauk EM, Wahl ER, Morrill C, Wagner AJ, Easterling D, Rutishauser T (2013) Global warming in an independent record of the past 130 years. *Geophys Res Lett* 40(1):189–193
- Andrianantenaina AN, Rathgeber CBK, Pérez-de-Lis G, Cuny H, Ruelle J (2019) Quantifying intra-annual dynamics of carbon sequestration in the forming wood: a novel histologic approach. *Ann for Sci* 76:1–12
- Arora R, Rowland LJ, Tanino K (2003) Induction and release of bud dormancy in woody perennials: a science comes of age. *HortScience* 38:911–921
- Balducci L, Cuny HE, Rathgeber CBK, Deslauriers A, Giovannelli A, Rossi S (2016) Compensatory mechanisms mitigate the effect of warming and drought on wood formation. *Plant, Cell Environ* 39:1338–1352
- Balzano A, Čufar K, Battipaglia G, Merela M, Prislan P, Aronne G, De Micco V (2018) Xylogenesis reveals the genesis and ecological signal of IADFs in *Pinus pinea* L. And *Arbutus unedo* L. And. *Annals of Botany* 121:1231–1242
- Bamber RK (1976) Heartwood, its function and formation. *Wood Sci Technol* 10:1–8

- Bamber RK, Fukazawa K (1985) Sapwood and heartwood: a review. *Forestry Abstracts* 46:567–580
- Barbaroux C, Bréda N (2002) Contrasting distribution and seasonal dynamics of carbohydrate reserves in stem wood of adult ring-porous sessile oak and diffuse-porous beech trees. *Tree Physiol* 22:1201–1210
- Barbaroux C, Bréda N, Dufrêne E (2003) Distribution of above-ground and below-ground carbohydrate reserves in adult trees of two contrasting broad-leaved species (*Quercus petraea* and *Fagus sylvatica*). *New Phytol* 157:605–615
- Barbour MM, Walcroft AS, Farquhar GD (2002) Seasonal variation in  $\delta^{13}\text{C}$  and  $\delta^{18}\text{O}$  of cellulose from growth rings of *Pinus radiata*. *Plant, Cell Environ* 25:1483–1499
- Barnett JR (1981) Secondary xylem cell development. In: Barnett JR (ed) Xylem cell development. Castle House Publications LTD, Tunbridge wells, pp 47–95
- Basler D, Körner C (2014) Photoperiod and temperature responses of bud swelling and bud burst in four temperate forest tree species. *Tree Physiol* 34:377–388
- Bazot S, Barthes L, Blanot D, Fresneau C (2013) Distribution of non-structural nitrogen and carbohydrate compounds in mature oak trees in a temperate forest at four key phenological stages. *Trees-Struct Funct* 27:1023–1034
- Begum S, Nakaba S, Oribe Y, Kubo T, Funada R (2010) Changes in the localization and levels of starch and lipids in cambium and phloem during cambial reactivation by artificial heating of main stems of *Cryptomeria japonica* trees. *Ann Bot* 106:885–895
- Begum S, Nakaba S, Yamagishi Y, Oribe Y, Funada R (2013) Regulation of cambial activity in relation to environmental conditions: understanding the role of temperature in wood formation of trees. *Physiol Plant* 147:46–54
- Begum S, Nakaba S, Yamagishi Y, Yamane K, Islam MA, Oribe Y, Ko JH, Jin HO, Funada R (2012) A rapid decrease in temperature induces latewood formation in artificially reactivated cambium of conifer stems. *Ann Bot* 110:875–885
- Begum S, Shibagaki M, Furusawa O, Nakaba S, Yamagishi Y, Yoshimoto J, Jin HO, Sano Y, Funada R (2012) Cold stability of microtubules in wood-forming tissues of conifers during seasons of active and dormant cambium. *Planta* 235:165–179
- Belmecheri S, Wright WE, Szejner P, Morino KA, Monson RK (2018) Carbon and oxygen isotope fractionations in tree rings reveal interactions between cambial phenology and seasonal climate. *Plant, Cell Environ* 41:2758–2772
- Bollhöner B, Prestele J, Tuominen H (2012) Xylem cell death: emerging understanding of regulation and function. *J Exp Bot* 63:1081–1094
- Bosio F, Rossi S, Marcati CR (2016) Periodicity and environmental drivers of apical and lateral growth in a Cerrado woody species. *Trees-Struct Funct* 30:1495–1505
- Bowling DR, Pataki DE, Randerson JT (2008) Carbon isotopes in terrestrial ecosystem pools and  $\text{CO}_2$  fluxes. *New Phytol* 178(1):24–40
- Brandes E, Kodama N, Whittaker K, Weston C, Rennenberg H, Keitel C, Adams MA, Gessler A (2006) Short-term variation in the isotopic composition of organic matter allocated from the leaves to the stem of *Pinus sylvestris*: effects of photosynthetic and postphotosynthetic carbon isotope fractionation. *Glob Change Biol* 12:1922–1939
- Brett CT (2000) Cellulose microfibrils in plants: Biosynthesis, deposition, and integration into the cell wall. *Int Rev Cytol* 199:161–199
- Briffa KR, Osborn TJ, Schweingruber FH, Jones PD, Shiyatov SG, Vaganov EA (2002) Tree-ring width and density data around the Northern Hemisphere: Part 1, local and regional climate signals. *Holocene* 12:737–757
- Briffa KR, Osborn TJ, Schweingruber FH, Jones PD, Shiyatov SG, Vaganov EA (2002) Tree-ring width and density data around the Northern Hemisphere: part 2, spatio-temporal variability and associated climate patterns. *Holocene* 12:759–789
- Brodribb TJ, Pittermann J, Coomes DA (2012) Elegance versus speed: examining the competition between conifer and angiosperm trees. *Int J Plant Sci* 173:673–694
- Buttò V, Deslauriers A, Rossi S, Rozenberg P, Shishov V, Morin H (2019a) The role of plant hormones in tree-ring formation. *Trees-Struct Funct*

- Buttò V, Rossi S, Deslauriers A, Morin H (2019) Is size an issue of time? Relationship between the duration of xylem development and cell traits. *Ann Bot* 123:1257–1265
- Camarero JJ, Olano JM, Parras A (2010) Plastic bimodal xylogenesis in conifers from continental Mediterranean climates. *New Phytol* 185:471–480
- Carvalho A, Nabais C, Vieira J, Rossi S, Campelo F (2015) Plastic response of tracheids in *Pinus pinaster* in a water-limited environment: adjusting lumen size instead of wall thickness. *PLoS ONE* 10:1–14
- Cavender-Bares J, Cortes P, Rambal S, Joffre R, Miles B, Rocheteau A (2005) Summer and winter sensitivity of leaves and xylem to minimum freezing temperatures: a comparison of co-occurring Mediterranean oaks that differ in leaf lifespan. *New Phytol* 168:597–612
- Chaffey NJ (ed) (2002) Wood formation in trees—cell and molecular biology techniques. Taylor and Francis, London, New York, pp 364
- Chave J, Coomes D, Jansen S, Lewis SL, Swenson NG, Zanne AE (2009) Towards a worldwide wood economics spectrum. *Ecol Lett* 12:351–366
- Chuine I (2010) Why does phenology drive species distribution? *Philos Trans R Soc B: Biol Sci* 365:3149–3160
- Cochard H, Froux F, Mayr S, Coutand C (2004) Xylem wall collapse in water-stressed pine needles. *Plant Physiol* 134:401–408
- Cochard H, Tyree MT (1990) Xylem dysfunction in *Quercus*: vessel sizes, tyloses, cavitation and seasonal changes in embolism. *Tree Physiol* 6:393–407
- Cosgrove DJ (2000) Expansive growth of plant cell walls. *Plant Physiol Biochem* 38:109–124
- Cosgrove DJ (2000) Loosening of plant cell walls by expansins. *Nature* 407:321–326
- Cosgrove DJ, Jarvis MC (2012) Comparative structure and biomechanics of plant primary and secondary cell walls. *Front Plant Sci* 3(204):201–206
- Čufar K, Cherubini M, Gričar J, Prislan P, Spina S, Romagnoli M (2011) Xylem and phloem formation in chestnut (*Castanea sativa* Mill.) during the 2008 growing season. *Dendrochronologia* 29:127–134
- Cuny HE, Fonti P, Rathgeber CBK, von Arx G, Peters RL, Frank DC (2019) Couplings in cell differentiation kinetics mitigate air temperature influence on conifer wood anatomy. *Plant, Cell Environ* 42:1222–1232
- Cuny HE, Rathgeber CBK (2016) Xylogenesis: coniferous trees of temperate forests are listening to the climate tale during the growing season but only remember the last words! *Plant Physiol* 171:306–317
- Cuny HE, Rathgeber CBK, Frank D, Fonti P, Fournier M (2014) Kinetics of tracheid development explain conifer tree-ring structure. *New Phytol* 203:1231–1241
- Cuny HE, Rathgeber CBK, Frank D, Fonti P, Makinen H, Prislan P, Rossi S, Del Castillo EMEM, Campelo F, Vavrčik H et al (2015) Woody biomass production lags stem-girth increase by over one month in coniferous forests. *Nature Plants* 1:1–6
- Cuny HE, Rathgeber CBK, Lebourgeois F, Fortin M, Fournier M (2012) Life strategies in intra-annual dynamics of wood formation: example of three conifer species in a temperate forest in north-east France. *Tree Physiol* 32:612–625
- De Micco V, Balzano A, Wheeler EA, Baas P (2016) Tyloses and gums: a review of structure, function and occurrence of vessel occlusions. *IAWA J* 37:186–205
- De Micco V, Campelo F, De Luis M, Bräuning A, Grabner M, Battipaglia G, Cherubini P (2016) Intra-annual density fluctuations in tree rings: how, when, where, and why? *IAWA J* 37:232–259
- De Micco V, Carrer M, Rathgeber CBK, Julio Camarero J, Voltas J, Cherubini P, Battipaglia G (2019) From xylogenesis to tree rings: wood traits to investigate tree response to environmental changes. *IAWA J* 40:155–182
- Delpierre N, Lireux S, Hartig F, Camarero JJ, Cheaib A, Čufar K, Cuny H, Deslauriers A, Fonti P, Gričar J et al (2019) Chilling and forcing temperatures interact to predict the onset of wood formation in Northern Hemisphere conifers. *Glob Change Biol* 25:1089–1105

- Delpierre N, Vitasse Y, Chuine I, Guillemot J, Bazot S, Rutishauser T, Rathgeber CBK (2016) Temperate and boreal forest tree phenology: from organ-scale processes to terrestrial ecosystem models. *Ann for Sci* 73:5–25
- Denne MP, Dodd RS (1981) The environmental control of xylem differentiation. In: Barnett JR (ed) Xylem cell development. Castle House Publications, Tunbridge Wells, pp 236–255
- Deslauriers A, Huang JG, Balducci L, Beaulieu M, Rossi S (2016) The contribution of carbon and water in modulating wood formation in black spruce saplings. *Plant Physiol* 170:2072–2084
- Dickson A, Nanayakkara B, Sellier D, Meason D, Donaldson L, Brownlie R (2017) Fluorescence imaging of cambial zones to study wood formation in *Pinus radiata* D. Don. *Trees-Struct Funct* 31:479–490
- Domec JC, Gartner BL (2002) How do water transport and water storage differ in coniferous earlywood and latewood? *J Exp Bot* 53(379):2369–2379
- Donaldson LA (1985) Within- and between-tree variation in lignin concentration in the tracheid cell wall of *Pinus radiata*. *NZ J Forest Sci* 15:361–369
- Donaldson LA (1987) S3 lignin concentration in radiata pine tracheids. *Wood Sci Technol* 21:227–234
- Donaldson LA (2001) Lignification and lignin topochemistry—an ultrastructural view. *Phytochem* 859–873
- Donaldson LA, Baas P (2019) Wood cell wall ultrastructure the key to understanding wood properties and behaviour. *IAWA J* 40(4):645–672
- El Zein R, Maillard P, Bréda N, Marchand J, Montpied P, Gérant D (2011) Seasonal changes of C and N non-structural compounds in the stem sapwood of adult sessile oak and beech trees. *Tree Physiol* 31:843–854
- Evert RF (2006) Esau's plant anatomy: meristems, cells, and tissues of the plant body: their structure, function, and development. John Wiley and Sons, pp 601
- Fagerstedt K, Karkonen A (2015) The plant cell wall. *J Integr Plant Biol* 57(4):328–329
- Fernández-de-Uña L, Aranda I, Rossi S, Fonti P, Cañellas I, Gea-Izquierdo G (2018) Divergent phenological and leaf gas exchange strategies of two competing tree species drive contrasting responses to drought at their altitudinal boundary. *Tree Physiol* 38(8):1152–1165
- Fernández-de-Uña L, Rossi S, Aranda I, Fonti P, González-González BD, Cañellas I, Gea-Izquierdo G (2017) Xylem and leaf functional adjustments to drought in *Pinus sylvestris* and *Quercus pyrenaica* at their elevational boundary. *Front Plant Sci* 8(1200):1201–1212
- Fonti MV, Vaganov EA, Wirth C, Shashkin AV, Astrakhantseva NV, Schulze E-D (2018) Age-effect on intra-annual  $\delta^{13}\text{C}$ -variability within Scots Pine tree-rings from Central Siberia. *For* 9(364):1–14
- Fonti P, Von Arx G, García-González I, Eilmann B, Sass-Klaassen U, Gärtner H, Eckstein D (2010) Studying global change through investigation of the plastic responses of xylem anatomy in tree rings. *New Phytol* 185:42–53
- Fournier M, Moulia B, Stokes A, Coutand C, Fourcaud T (2006) Tree biomechanics and growth strategies in the context of forest functional ecology. In: Speck T, Rowe NP (eds) Herrel A. CRC Press, Ecology and biomechanics. a mechanical approach to the ecology of animals and plants. Boca Raton, pp 1–33
- Freudenberg K (1959) Biosynthesis and constitution of lignin. *Nature* 183:1152–1155
- Fritts HC (1976) Tree rings and climate. Academic Press, London, pp 582
- Fromm J (2013) Xylem development in trees: from cambial division to mature wood cells. In: Fromm J (ed) Cellular aspect of wood formation. Springer-Verlag, Berlin, Heidelberg, New York, Dordrecht, London, pp 3–39
- Gessler A, Ferrio JP, Hommel R, Treydte K, Werner RA, Monson RK (2014) Stable isotopes in tree rings: towards a mechanistic understanding of isotope fractionation and mixing processes from the leaves to the wood. *Tree Physiol* 34:796–818
- Gindl W, Grabner M, Wimmer R (2000) The influence of temperature on latewood lignin content in treeline Norway spruce compared with maximum density and ring width. *Trees-Struct Funct* 14:409–414



- Gričar J, Čufar K (2008) Seasonal dynamics of phloem and xylem formation in silver fir and Norway spruce as affected by drought. *Russ J Plant Physiol* 55:538–543
- Gričar J, Krže L, Čufar K (2009) Number of cells in xylem, phloem and dormant cambium in silver fir (*Abies alba*), in trees of different vitality. *IAWA J* 30:121–133
- Gričar J, Lavrič M, Ferlan M, Vodnik D, Eler K (2017) Intra-annual leaf phenology, radial growth and structure of xylem and phloem in different tree parts of *Quercus pubescens*. *Eur J Forest Res* 136:625–637
- Gričar J, Zupančič M, Čufar K, Oven P (2007) Regular cambial activity and xylem and phloem formation in locally heated and cooled stem portions of Norway spruce. *Wood Sci Technol* 41:463–475
- Gričar J, Zupančič M, Čufar K, Oven P (2007) Wood formation in Norway Spruce (*Picea abies*) studied by pinning and intact tissue sampling method. *Wood Res* 52:1–10
- Grillo SJ, Smith FH (1959) The secondary phloem of Douglas-fir. *For Sci* 5(4):377–388
- Groover A, Jones AM (1999) Tracheary element differentiation uses a novel mechanism coordinating programmed cell death and secondary cell wall synthesis. *Plant Physiol* 119:375–384
- Gruber A, Strobl S, Veit B, Oberhuber W (2010) Impact of drought on the temporal dynamics of wood formation in *Pinus sylvestris*. *Tree Physiol* 30:490–501
- Gyllenstrand N, Clapham D, Källman T, Lagercrantz U (2007) A Norway spruce FLOWERING LOCUS T homolog is implicated in control of growth rhythm in conifers. *Plant Physiol* 144:248–257
- Helle G, Schleser GH (2004) Beyond CO<sub>2</sub>-fixation by Rubisco—an interpretation of <sup>13</sup>C/<sup>12</sup>C variations in tree rings from novel intra-seasonal studies on broad-leaf trees. *Plant, Cell Environ* 27:367–380
- Hillis WE (1987) Heartwood and tree exudates. Springer-Verlag, Berlin, Heidelberg, pp 268
- Hoch G, Richter A, Körner C (2003) Non-structural carbon compounds in temperate forest trees. *Plant, Cell Environ* 26:1067–1081
- Horvath DP, Anderson JV, Chao WS, Foley ME (2003) Knowing when to grow: signals regulating bud dormancy. *Trends Plant Sci* 8:534–540
- Hsiao TC (1973) Plant responses to water stress. *Annu Rev Plant Physiol* 24:519–570
- Jansen S, Baas P, Gasson P, Lens F, Smets E (2004) Variation in xylem structure from tropics to tundra: evidence from vested pits. *Proc Natl Acad Sci USA* 101:8833–8837
- Johnson DM, Büntgen U, Frank DC, Kausrud K, Haynes KJ, Liebhold AM, Esper J, Stenseth NC (2010) Climatic warming disrupts recurrent Alpine insect outbreaks. *Proc Natl Acad Sci USA* 107:20576–20581
- Jones AM (2001) Programmed cell death in development and defense. *Plant Physiol* 125:94–97
- Kagawa A, Sugimoto A, Maximov TC (2006) <sup>13</sup>CO<sub>2</sub> pulse-labelling of photoassimilates reveals carbon allocation within and between tree rings. *Plant, Cell Environ* 29:1571–1584
- Keegstra K (2010) Plant cell walls. *Plant Physiol* 154:483–486
- Koch G, Schmitt U (2013) Topochemical and electron microscopic analyses on the lignification of individual cell wall layers during wood formation and secondary changes. In: Fromm J (ed) Cellular aspect of wood formation. Springer-Verlag, Berlin, Heidelberg, New York, Dordrecht, London, pp 41–69
- Koch K (2004) Sucrose metabolism: regulatory mechanisms and pivotal roles in sugar sensing and plant development. *Curr Opin Plant Biol* 7:235–246
- Konôpka B, Yuste JC, Janssens IA, Ceulemans R (2005) Comparison of fine root dynamics in Scots pine and Pedunculate oak in sandy soil. *Plant Soil* 276:33–45
- Kozlowski TT, Pallardy SG (1996) The physiological ecology of woody plants. Academic Press, San Diego, London, Boston, New York, Sydney, Tokyo, Toronto, pp 411
- Kozlowski TT, Winget CH (1964) Diurnal and seasonal variation in radii of tree stems. *Ecol* 45(1):149–155
- Kramer PJ (1964) The role of water in wood formation. In: Zimmermann MH (ed) The formation of wood in forest trees. Academic Press, New York, London, pp 519–532

- Kuroda K, Yamashita K, Fujiwara T (2009) Cellular level observation of water loss and the refilling of tracheids in the xylem of *Cryptomeria japonica* during heartwood formation. *Trees-Struct Funct* 23:1163–1172
- Lachaud S, Catesson AM, Bonnemain JL (1999) Structure and functions of the vascular cambium. *Comptes Rendus de l'Academie des Sciences—Serie III*, vol 322, pp 633–650
- Lachenbruch B, Moore JR, Evans R (2011) Radial variation in wood structure and function in woody plants, and hypotheses for its occurrence. In: Meinzer FC, Lachenbruch B, Dawson TE (eds) *Size- and age-related changes in tree structure and function*. Springer, Dordrecht, pp 121–164
- Ladefoged K (1952) *The periodicity of wood formation*. Kobenhavn: Det Kongelige danske videnskaberne selskab, pp 98
- Larson PR (1994) *The vascular cambium. Development and structure*. Springer-Verlag, Berlin, Heidelberg, New York, London, Paris, Tokyo, Hong Kong, Barcelona, Budapest, pp 725
- Lavrič M, Eler K, Ferlan M, Vodnik D, Gričar J (2017) Chronological sequence of leaf phenology, xylem and phloem formation and sap flow of *Quercus pubescens* from abandoned karst grasslands. *Front Plant Sci* 8:1–11
- Lemay A, Krause C, Rossi S, Achim A (2017) Xylogenesis in stems and roots after thinning in the boreal forest of Quebec. Canada. *Tree Physiol* 37(11):1554–1563
- Little CHA, Bonga JM (1974) Rest in cambium of *Abies balsamea*. *Can J Bot* 52(7):1723–1730
- Lundmark T, Bergh J, Strand M, Koppel A (1998) Seasonal variation of maximum photochemical efficiency in boreal Norway spruce stands. *Trees-Struct Funct* 13:63–67
- Lupi C, Morin H, Deslauriers A, Rossi S (2010) Xylem phenology and wood production: resolving the chicken-or-egg dilemma. *Plant, Cell Environ* 33:1721–1730
- Lyr H, Hoffmann G (1967) Growth rates and growth periodicity of tree roots. *Int Rev For Res* 181–236
- McCarroll D, Loader NJ (2004) Stable isotopes in tree rings. *Quatern Sci Rev* 23:771–801
- McCormack LM, Adams TS, Smithwick EAH, Eissenstat DM (2014) Variability in root production, phenology, and turnover rate among 12 temperate tree species. *Ecol* 95:2224–2235
- Mellerowicz EJ, Sundberg B (2008) Wood cell walls: biosynthesis, developmental dynamics and their implications for wood properties. *Curr Opin Plant Biol* 11:293–300
- Michelot A, Simard S, Rathgeber C, Dufrière E, Damesin C (2012) Comparing the intra-annual wood formation of three European species (*Fagus sylvatica*, *Quercus petraea* and *Pinus sylvestris*) as related to leaf phenology and non-structural carbohydrate dynamics. *Tree Physiol* 32:1033–1045
- Millard P, Grelet GA (2010) Nitrogen storage and remobilization by trees: ecophysiological relevance in a changing world. *Tree Physiol* 30:1083–1095
- Millard P, Proe MF (1992) Storage and internal cycling of nitrogen in relation to seasonal growth of Sitka spruce. *Tree Physiol* 10:45–48
- Moser L, Fonti P, Büntgen U, Esper J, Luterbacher J, Franzen J, Frank D (2009) Timing and duration of European larch growing season along altitudinal gradients in the Swiss Alps. *Tree Physiol* 30:225–233
- Mutwil M, Debolt S, Persson S (2008) Cellulose synthesis: a complex complex. *Curr Opin Plant Biol* 11:252–257
- Nonami H, Boyer JS (2008) Turgor and growth at low water potentials. *Plant Physiol* 89:798–804
- Notaguchi M, Okamoto S (2015) Dynamics of long-distance signaling via plant vascular tissues. *Front Plant Sci* 6:161
- O'Neill MA, York WS (2009) The plant cell wall. *Annu Plant Rev* 1–44
- Ogaya R, Penuelas J (2004) Phenological patterns of *Quercus ilex*, *Phillyrea latifolia*, and *Arbutus unedo* growing under a field experimental drought. *Ecoscience* 11:263–270
- Ogée J, Barbour MM, Wingate L, Bert D, Bosc A, Stievenard M, Lambrot C, Pierre M, Bariac T, Loustau D et al (2009) A single-substrate model to interpret intra-annual stable isotope signals in tree-ring cellulose. *Plant, Cell Environ* 32:1071–1090
- Ohashi S, Kuroda K, Takano T, Suzuki Y, Fujiwara T, Abe H, Kagawa A, Sugiyama M, Kubojima Y, Zhang C et al (2017) Temporal trends in <sup>13</sup>C concentrations in the bark, sapwood, heartwood,

- and whole wood of four tree species in Japanese forests from 2011 to 2016. *J Environ Radioact* 178–179:335–342
- Oribe Y, Funada R, Kubo T (2003) Relationships between cambial activity, cell differentiation and the localization of starch in storage tissues around the cambium in locally heated stems of *Abies sachalinensis* (Schmidt) Masters. *Trees* 17:185–192
- Oribe Y, Kubo T (1997) Effect of heat on cambial reactivation during winter dormancy in evergreen and deciduous conifers. *Tree Physiol* 17(2):81–87
- Pérez-de-Lis G, Olano JM, Rozas V, Rossi S, Vázquez-Ruiz RA, García-González I (2017) Environmental conditions and vascular cambium regulate carbon allocation to xylem growth in deciduous oaks. *Funct Ecol* 31:592–603
- Pérez-de-Lis G, Rossi S, Vázquez-Ruiz RA, Rozas V, García-González I (2016) Do changes in spring phenology affect earlywood vessels? Perspective from the xylogenesis monitoring of two sympatric ring-porous oaks. *New Phytol* 209:521–530
- Pérez-de-Lis G, Rozas V, Vázquez-Ruiz RA, García-González I (2018) Do ring-porous oaks prioritize earlywood vessel efficiency over safety? Environmental effects on vessel diameter and tyloses formation. *Agric for Meteorol* 248:205–214
- Perrin M, Rossi S, Isabel N (2017) Synchronisms between bud and cambium phenology in black spruce: Early-flushing provenances exhibit early xylem formation. *Tree Physiol* 37:593–603
- Pequet E, Zhang B, Gorzsas A, Puhakainen T, Serk H, Escamez S, Barbier O, Gerber L, Courtois-Moreau C, Alatalo E et al (2013) Non-cell-autonomous postmortem lignification of tracheary elements in *Zinnia elegans*. *Plant Cell* 25(4):1314–1328
- Piermattei A, Crivellaro A, Carrer M, Urbinati C (2015) The “blue ring”: anatomy and formation hypothesis of a new tree-ring anomaly in conifers. *Trees-Struct Funct* 29:613–620
- Plomion C, Leprovost G, Stokes A (2001) Wood formation in trees. *Plant Physiol* 127(4):1513–1523
- Pratt RB, Jacobsen AL, Ewers FW, Davis SD (2007) Relationships among xylem transport, biomechanics and storage in stems and roots of nine *Rhamnaceae* species of the California chaparral. *New Phytol* 174:787–798
- Prislan P, Čufar K, Koch G, Schmitt U, Gričar J (2013) Review of cellular and subcellular changes in the cambium. *IAWA J* 34:391–407
- Prislan P, Gričar J, de Luis M, Smith KT, Čufar K (2013) Phenological variation in xylem and phloem formation in *Fagus sylvatica* from two contrasting sites. *Agric for Meteorol* 180:142–151
- Prislan P, Mrak P, Žnidaršič N, Štrus J, Humar M, Thaler N, Mrak T, Gričar J (2018) Intra-annual dynamics of phloem formation and ultrastructural changes in sieve tubes in *Fagus sylvatica*. *Tree Physiol* 39:262–274
- Rathgeber CBK, Cuny HE, Fonti P (2016) Biological basis of tree-ring formation: a crash course. *Front Plant Sci* 7:734
- Rathgeber CBK, Decoux V, Leban JM (2006) Linking intra-tree-ring wood density variations and tracheid anatomical characteristics in Douglas fir (*Pseudotsuga menziesii* (Mirb.) Franco). *Ann for Sci* 63:699–706
- Rathgeber CBK, Longuetaud F, Mothe F, Cuny H, Le Moguédec G (2011) Phenology of wood formation: Data processing, analysis and visualisation using R (package CAVIAR). *Dendrochronologia* 29:139–149
- Rathgeber CBK, Rossi S, Bontemps JD (2011) Cambial activity related to tree size in a mature silver-fir plantation. *Ann Bot* 108:429–438
- Rinne KT, Saurer M, Kiryanov AV, Loader NJ, Bryukhanova MV, Werner RA, Siegwolf RTW (2015) The relationship between needle sugar carbon isotope ratios and tree rings of larch in Siberia. *Tree Physiol* 35:1192–1205
- Rohde A, Bastien C, Boerjan W (2011) Temperature signals contribute to the timing of photoperiodic growth cessation and bud set in poplar. *Tree Physiol* 31:472–482
- Rossi S, Anfodillo T, Čufar K, Cuny HE, Deslauriers A, Fonti P, Frank D, Gričar J, Gruber A, Huang JG et al (2016) Pattern of xylem phenology in conifers of cold ecosystems at the Northern Hemisphere. *Glob Change Biol* 22:3804–3813

- Rossi S, Anfodillo T, Cufar K, Cuny HE, Deslauriers A, Fonti P, Frank D, Gricar J, Gruber A, King GM et al (2013) A meta-analysis of cambium phenology and growth: linear and non-linear patterns in conifers of the northern hemisphere. *Ann Bot* 112:1911–1920
- Rossi S, Deslauriers A, Anfodillo T (2006) Assessment of cambial activity and xylogenesis by microsampling tree species: an example at the Alpine timberline. *IAWA J* 27:383–394
- Rossi S, Deslauriers A, Anfodillo T, Carraro V (2007) Evidence of threshold temperatures for xylogenesis in conifers at high altitudes. *Oecologia* 152:1–12
- Rossi S, Deslauriers A, Anfodillo T, Morin H, Saracino A, Motta R, Borghetti M (2006) Conifers in cold environments synchronize maximum growth rate of tree-ring formation with day length. *New Phytol* 170:301–310
- Rossi S, Deslauriers A, Griçar J, Seo JW, Rathgeber CBK, Anfodillo T, Morin H, Levanic T, Oven P, Jalkanen R (2008) Critical temperatures for xylogenesis in conifers of cold climates. *Glob Ecol Biogeogr* 17:696–707
- Rossi S, Morin H, Deslauriers A (2012) Causes and correlations in cambium phenology: towards an integrated framework of xylogenesis. *J Exp Bot* 63:2117–2126
- Rossi S, Rathgeber CBK, Deslauriers A (2009) Comparing needle and shoot phenology with xylem development on three conifer species in Italy. *Ann for Sci* 66:206
- Rossi S, Simard S, Rathgeber CBK, Deslauriers A, De Zan C (2009b) Effects of a 20-day-long dry period on cambial and apical meristem growth in *Abies balsamea* seedlings. *Trees-Struct Funct* 23:85–93
- Rowe N, Speck T (2005) Plant growth forms: an ecological and evolutionary perspective. *New Phytol* 166:61–72
- Saderi S, Rathgeber CBK, Rozenberg P, Fournier M (2019) Phenology of wood formation in larch (*Larix decidua* Mill.) trees growing along a 1000-m elevation gradient in the French Southern Alps. *Ann for Sci* 76:1–17
- Scheller HV, Ulvskov P (2010) Hemicelluloses. *Annu Rev Plant Biol* 61:263–289
- Schenker G, Lenz A, Körner C, Hoch G (2014) Physiological minimum temperatures for root growth in seven common European broad-leaved tree species. *Tree Physiol* 34:302–313
- Schollae K, Heinrich I, Helle G (2014) UV-laser-based microscopic dissection of tree rings—a novel sampling tool for  $\delta^{13}\text{C}$  and  $\delta^{18}\text{O}$  studies. *New Phytol* 201:1045–1055
- Schopfer P (2006) Biomechanics of plant growth. *Am J Bot* 93:1415–1425
- Schrader J, Baba K, May ST, Palme K, Bennett M, Bhalerao RP, Sandberg G (2003) Polar auxin transport in the wood-forming tissues of hybrid aspen is under simultaneous control of developmental and environmental signals. *Proc Natl Acad Sci USA* 100:10096–10101
- Schulze B, Wirth C, Linke P, Brand WA, Kuhlmann I, Horna V, Schulze ED (2004) Laser ablation-combustion-GC-IRMS—a new method for online analysis of intra-annual variation of  $\delta^{13}\text{C}$  in tree rings. *Tree Physiol* 24:1193–1201
- Schweingruber FH (1996) Tree rings and environment. *Dendroecology*. Berne, Stuttgart, Vienna: Haupt Paul, Swiss federal institute for forest, snow and landscape research, WSL/FNP, Birmensdorf, pp 609
- Schweingruber FH (2007) Wood structure and environment. Springer-Verlag, Berlin, Heidelberg
- Siau JF (1984) Transport processes in wood. Springer, Berlin, Heidelberg, New York, Tokyo, pp 245
- Siddiqui KM (1976) Relationship between cell wall morphology and chemical composition of earlywood and latewood in two coniferous species. *Pak J For* 26:21–34
- Skene DS (1969) The period of time taken by cambial derivatives to grow and differentiate into Tracheids in *Pinus radiata*. *Ann Bot* 33:253–262
- Skene DS (1972) The kinetics of tracheid development in *Tsuga canadensis* Carr. and its relation to tree vigour. *Ann Bot* 36:179–187
- Smith RA, Schuetz M, Roach M, Mansfield SD, Ellis B, Samuels L (2013) Neighboring parenchyma cells contribute to *Arabidopsis* xylem lignification, while lignification of interfascicular fibers is cell autonomous. *Plant Cell* 25:3988–3999

- Speck T, Burgert I (2011) Plant stems: functional design and mechanics. *Annu Rev Mater Res* 41:169–193
- Sperry JS, Hacke UG, Pittermann J (2006) Size and function in conifer tracheids and angiosperm vessels. *Am J Bot* 93:1490–1500
- Sperry JS, Meinzer FC, McCulloh KA (2008) Safety and efficiency conflicts in hydraulic architecture: scaling from tissues to trees. *Plant, Cell Environ* 31:632–645
- Sperry JS, Sullivan JEM (1992) Xylem embolism in response to freeze-thaw cycles and water-stress in ring-porous, diffuse-porous, and conifer species. *Plant Physiol* 100(2):605–613
- Swidrak I, Gruber A, Oberhuber W (2014) Xylem and phloem phenology in co-occurring conifers exposed to drought. *Trees-Struct Funct* 28:1161–1171
- Taiz L, Zeiger E (2010) *Plant Physiology*. Sinauer Associates Inc., Sunderland, pp 782
- Takahashi K, Koike S (2014) Altitudinal differences in bud burst and onset and cessation of cambial activity of four subalpine tree species. *Landsc Ecol Eng* 10:349–354
- Taylor AM, Gartner BL, Morrell JJ (2002) Heartwood formation and natural durability—a review. *Wood Fiber Sci* 34:587–611
- Thibeault-Martel M, Krause C, Morin H, Rossi S (2008) Cambial activity and intra-annual xylem formation in roots and stems of *Abies balsamea* and *Picea mariana*. *Ann Bot* 102:667–674
- Treydte K, Boda S, Graf Pannatier E, Fonti P, Frank D, Ullrich B, Saurer M, Siegwolf R, Battipaglia G, Werner W et al (2014) Seasonal transfer of oxygen isotopes from precipitation and soil to the tree ring: source water versus needle water enrichment. *New Phytol* 202:772–783
- Tyree MT, Dixon MA (1986) Water-stress induced cavitation and embolism in some woody-plants. *Physiol Plant* 66(3):397–405
- Ursache R, Nieminen K, Helariutta Y (2013) Genetic and hormonal regulation of cambial development. *Physiol Plant* 147:36–45
- Vaganov EA, Hughes MK, Shashkin AV (2006) Growth dynamics of conifer tree rings: images of past and future environments. Springer-Verlag, Berlin, Heidelberg, pp 351
- Vieira J, Rossi S, Campelo F, Freitas H, Nabais C (2014) Xylogenesis of *Pinus pinaster* under a Mediterranean climate. *Ann for Sci* 71(1):71–80
- Vincent-Barbaroux C, Berveiller D, Lelarge-Trouverie C, Maia R, Máguas C, Pereira J, Chaves MM, Damesin C (2019) Carbon-use strategies in stem radial growth of two oak species, one Temperate deciduous and one Mediterranean evergreen: what can be inferred from seasonal variations in the  $\delta^{13}\text{C}$  of the current year ring? *Tree Physiol* 39:1329–1341
- Weigt RB, Bräunlich S, Zimmermann L, Saurer M, Grams TEE, Dietrich HP, Siegwolf RTW, Nikolova PS (2015) Comparison of  $\delta^{18}\text{O}$  and  $\delta^{13}\text{C}$  values between tree-ring whole wood and cellulose in five species growing under two different site conditions. *Rapid Commun Mass Spectrom* 29:2233–2244
- Wilson AT, Grinsted MJ (1977)  $^{12}\text{C}/^{13}\text{C}$  in cellulose and lignin as palaeothermometers. *Nature* 265(5590):133–135
- Wilson JW (1970) *The growing tree*. The University of Massachusetts Press, Amherst, pp 152
- Wilson JW, Wodzicki T, Zahner R (1966) Differentiation of cambial derivatives: proposed terminology. *For Sci* 12:438–440
- Wimmer R, Grabner M (2000) A comparison of tree-ring features in *Picea abies* as correlated with climate. *IAWA J* 21:403–416
- Wodzicki TJ (1971) Mechanism of xylem differentiation in *Pinus silvestris* L. *J Exp Bot* 22:670–687
- Wright SJ, Cornejo FH (1990) Seasonal drought and leaf fall in a tropical forest. *Ecol* 71:1165–1175
- Yoshimura K, Hayashi S, Takao I, Shimaji K (1981) Studies on the improvement of the pinning method for marking xylem growth I. Minute examination of pin marks in Taeda Pine and other species. *Wood Res* 67:1–16
- Zalloni E, de Luis M, Campelo F, Novak K, De Micco V, Di Filippo A, Vieira J, Nabais C, Rozas V, Battipaglia G (2016) Climatic signals from intra-annual density fluctuation frequency in Mediterranean pines at a regional scale. *Front Plant Sci* 7:1–11

- Zeng X, Liu X, Treydte K, Evans MN, Wang W, An W, Sun W, Xu G, Wu G, Zhang X (2017) Climate signals in tree-ring  $\delta^{18}\text{O}$  and  $\delta^{13}\text{C}$  from southeastern Tibet: insights from observations and forward modelling of intra- to interdecadal variability. *New Phytol* 216:1104–1118
- Zhong R, Ye Z-H (2009) Secondary cell walls. *Encycl Life Sci* 1–9
- Zimmermann MH (1982) Functional xylem anatomy of angiosperm trees. Baas, P. Springer, New perspectives in wood anatomy. Forestry sciences. Dordrecht, pp 59–70
- Zimmermann MH (1983) Xylem structure and the ascent of sap. Springer, Berlin, Heidelberg, New York, Tokyo, pp 146
- Zweifel R (2016) Radial stem variations—a source of tree physiological information not fully exploited yet. *Plant Cell & Environ* 39(2):231–232
- Zwieniecki MA, Holbrook NM (2000) Bordered pit structure and vessel wall surface properties. Implications for embolism repair. *Plant Physiol* 123 (3):1015–1020

**Open Access** This chapter is licensed under the terms of the Creative Commons Attribution 4.0 International License (<http://creativecommons.org/licenses/by/4.0/>), which permits use, sharing, adaptation, distribution and reproduction in any medium or format, as long as you give appropriate credit to the original author(s) and the source, provide a link to the Creative Commons license and indicate if changes were made.

The images or other third party material in this chapter are included in the chapter's Creative Commons license, unless indicated otherwise in a credit line to the material. If material is not included in the chapter's Creative Commons license and your intended use is not permitted by statutory regulation or exceeds the permitted use, you will need to obtain permission directly from the copyright holder.



# **Part II**

## **Methods**

# Chapter 4

## Sample Collection and Preparation for Annual and Intra-annual Tree-Ring Isotope Chronologies



Soumaya Belmecheri, William E. Wright, and Paul Szejner

**Abstract** This chapter provides guidance for conducting studies based on stable isotope measurements in tree rings to infer past and present climate variability and ecophysiology. Balancing theoretical perspectives of stable isotope variations recorded in tree rings, intended research applications (paleoclimate or ecophysiology) and resource limitations, this chapter describes key aspects of field sampling strategies and laboratory sample processing. It presents an overview of factors influencing variations and thus interpretations of carbon and oxygen isotopes, including juvenile/age effects, canopy status and stand characteristics to inform sampling strategies that optimize a robust paleoenvironmental and physiological signal with statistically defined confidence limits. Fieldwork considerations include the selection of a study site and trees, field equipment, and sample requirements to recover sufficient material for isotopic measurements, and the desired environmental signal. Aspects of laboratory sample processing include choosing a sampling resolution (e.g. whole ring, earlywood/latewood, thin section, etc.), sample pooling within and between trees, and particle size requirements for chemical extraction and analytical repeatability. Finally, this chapter provides a case study highlighting the potential benefits and limitations of high-resolution sub-seasonal sampling.

### 4.1 Introduction

Stable isotope ratios of carbon ( $\delta^{13}\text{C}$ ) and oxygen ( $\delta^{18}\text{O}$ ) as measured in tree rings (cellulose or wood) are commonly used to understand eco-physiological processes and environmental conditions governing tree-growth (McCarroll and Loader 2004; Gessler et al. 2014). Because of the relationship between photosynthetic carbon

---

S. Belmecheri (✉) · W. E. Wright · P. Szejner  
Laboratory of Tree-Ring Research, University of Arizona, Tucson, USA  
e-mail: [sbelmecheri@email.arizona.edu](mailto:sbelmecheri@email.arizona.edu)

P. Szejner  
Instituto de Geología, Universidad Nacional Autónoma de México, Ciudad de México, Mexico



isotopic fractionation ( $\Delta^{13}\text{C}$ ) and the ratio of leaf internal and ambient  $\text{CO}_2$  concentrations ( $c_i/c_a$ ),  $\delta^{13}\text{C}$  in tree rings has been used to characterize the relationship between the physiology involved in photosynthesis and the environment (Farquhar et al. 1989). This tool further provides a retrospective annual to intra-annual record of photosynthesis activity under varying atmospheric  $\text{CO}_2$  via  $\delta^{13}\text{C}$ -derived estimates of intrinsic water use efficiency (*iWUE*), the ratio of carbon gain to water loss (Saurer et al. 2014, see Chap. 17). The  $\delta^{18}\text{O}$  in tree rings is related to the  $\delta^{18}\text{O}$  of soil water, which reflects the  $\delta^{18}\text{O}$  of precipitation (see Chap. 18), and leaf water evaporative enrichment (Roden and Ehleringer 2000; Barbour et al. 2004; Treydte et al. 2014). Thus  $\delta^{18}\text{O}$  in tree rings has been used to reconstruct past eco-hydrological processes and atmospheric circulation patterns (Sidorova et al. 2010; Ballantyne et al. 2011; Brienen et al. 2012; Zhu et al. 2012; Xu et al. 2019, 2020; Nagavciuc et al. 2019), and provided a tool to evaluate the effects of relative humidity and air temperature on photosynthesis (Wright and Leavitt 2006b).

Sampling living trees for stable isotope analyses of tree rings involves many choices. Typically, the tree species and general locations selected are determined by the research questions. For example, in temperate or water limited environments,  $\delta^{13}\text{C}$  has been used to reconstruct drought and its impact on tree physiology (Lévesque et al. 2014). In boreal or temperature limited environment,  $\delta^{13}\text{C}$  has been used to reconstruct cloudiness (Young et al. 2010). Optimizing field sampling to have the best chance of addressing the research hypothesis and recovering the desired 'signal' requires choices regarding the site microenvironment, individual tree characteristics, and appropriate sampling equipment. Some of these choices can affect the stable isotope ratio(s) recorded in the wood (tree rings). However, other decisions related to practicalities of getting adequate sample mass and the methods employed during the subsequent processing must also be taken into consideration.

After choosing the research question and the tree species, the most important field consideration is site selection. The most common site selection criteria include proximity to compatible instrumented weather data, extra-site conditions, and stand characteristics (e.g., monoculture/mixed species, natural/planted, density, substrate, aspect, slope, and age). Ideally, instrumented weather data have been recorded close to the site of interest, at a similar elevation and aspect. Extra-site conditions refer to the surrounding topography and land use. For example, a hydrologic connection (with respect to lateral flow through soils) of the tree site with higher elevations likely indicates that the available water in deeper soils will have a mixture of local stable oxygen isotope values and values characteristic of higher elevations (see Chap. 18 for source water considerations in site selection). Subsurface flow and runoff can also cause differences across the area chosen for sampling, by providing water with different stable oxygen isotope values to some trees (Dawson and Ehleringer 1991). Stable carbon isotope values can also be affected through differences in water status driven by differences in microsite conditions, i.e., if some of the trees have access to the subsurface flow or runoff while others do not. In addition, major changes in land use can alter the timing of moisture input, e.g., from snowpack, and can even affect the local climate (Salati and Nobre 1991; D'Almeida et al. 2007; Perugini et al. 2017). Selecting sites where environmental data and historical land-use data is available

maybe critical to the success of a project, and researchers should consider carefully what information they need for their specific research questions when selecting sites.

Stand characteristics can affect the growth rate of the trees and their sensitivity to changes in the local climate. For example, competition for light and water can reduce the ability of a tree to respond optimally to favorable environmental conditions (Moreno-Gutiérrez et al. 2012; Voelker et al. 2019). Mature trees within a closed canopy stand will be buffered to some extent from the direct effects of drought and heat by lower vapor pressure deficit caused by the transpiration of the neighboring trees (Talbot et al. 2003). Subcanopy trees within a closed-canopy forest may incorporate a larger proportion of respired CO<sub>2</sub> during photosynthesis than canopy-dominant trees (see Chaps. 19 and 24) and may have lower carbon assimilation rates due to lower light input (e.g., Cerling et al. 2004). Stable isotopes contained within subcanopy trees may reflect more information on stand dynamics and competition than canopy-dominant trees, particularly if a tree has changed competitive status over time. The isotopic composition within canopy dominant trees is more likely to reflect climate variation over time (Barnard et al. 2012).

Achieving the desired temporal resolution from the sampled wood requires knowledge about the length of the growing season and the growth rate of the species at the chosen site. Obtaining an adequate amount of material (e.g., whole wood, cellulose) for the desired temporal resolution may require careful consideration of the diameter of the increment borer used for sampling and the number of samples taken from each tree. Many studies involving subannual sampling use the relatively time-stable earlywood/latewood boundary as a time marker to designate the subannual divisions, but subannual sampling can also be executed using successive equal segments within a ring (Xu et al. 2020). These two options have a technical but fundamental difference. On the one hand, utilization of the earlywood/latewood technique yields a predetermined number of slices per year, whereas the successive equal-segment cut technique yields a variable number of samples per year and among trees because it will depend on the ring width of individual trees and specific years. Independent of the sectioning method used, variable tree growth rates should play an important role in how the samples are prepared. It is necessary to avoid unbalanced mass among trees if the samples are combined. For example, if the trees are combined (pooled), it is preferable to select the same mass of material per tree to avoid biased isotopic signals from the trees that have more mass on the same section (Leavitt 2010; Dorado Liñán et al. 2011).

For tree-ring stable isotope analyses, several components can be analyzed: whole wood, holocellulose,  $\alpha$ -cellulose, or lignin. The  $\alpha$ -cellulose molecule is often the preferred material because it is more resistant to environmental degradation than all major wood-constituents except lignin. Additionally,  $\alpha$ -cellulose is a single molecule formed by a specific series of biochemical steps and it does not undergo isotopic exchange after deposition, in contrast to hemicellulose, for example, which can exchange at the carbonyl bonds. Several methods can be used to extract  $\alpha$ -cellulose from whole wood material (see Chap. 5 for cellulose extraction details). While there is a prevalence of  $\alpha$ -cellulose analyses in tree-ring isotope studies based on the advantages described above, whole wood remains another component of choice because it

requires less analytical time and cost. A number of studies have assessed the coherence of the climate signal recorded in both whole wood and  $\alpha$ -cellulose (Borella et al. 1998; Barbour et al. 2001; Loader et al. 2003; Ferrio and Voltas 2005; Cullen and Grierson 2006; Sidorova et al. 2008; Szymczak et al. 2011; Bégin et al. 2015; Weigt et al. 2015), but there is no consensus as to whether both components record similar climate signals (i.e., strength and timing) for both  $\delta^{13}\text{C}$  and  $\delta^{18}\text{O}$ . Ultimately, the choice of  $\alpha$ -cellulose versus whole wood can be informed by a preliminary analysis of the studied site and species (Guerrieri et al. 2017), particularly when aiming to conduct large-scale (e.g. network) or long-term (e.g. millennial scale) paleoclimate and physiology reconstructions (Leavitt et al. 2010).

This chapter provides guidelines for field sampling and sample processing in the context of the current major areas of research using stable isotope ratios from stem wood, i.e., tree physiology and climatology. Specifically, it provides an overview of how to account for various factors influencing the isotopic signal recorded in tree rings when designing and conducting a tree-ring stable isotope study for either paleoclimate or ecophysiology investigations. The overview will cover theoretical and practical aspects of site and tree selection, sample collection and tree ring sample preparation. Finally, an emphasis on high-resolution tree ring isotope analyses will be presented in order to highlight the potential ecophysiological and paleoclimatological insights that may be gained from highly resolved intra-annual measurements of stable isotopes in tree rings.

## 4.2 Sample Collection

### 4.2.1 Site and Tree Selection

Site selection should minimize the influence of any local micro-environment effects on the isotopic signal recorded by individual selected trees. A common approach is to select canopy-dominant trees with no direct competition (McCarroll and Loader 2004; Leavitt 2010). Usually, dominant trees will also be older than subdominant or subcanopy trees, and when trees of the same age are compared, the dominant trees are likely to have wider ring widths for the same years. The choice of older trees is primarily motivated by the goal of developing long multi-centennial paleoclimate and paleophysiological reconstructions or to avoid isotopic trends observed in early growth years, the so-called "juvenile or canopy effect" for  $\delta^{13}\text{C}$  (Monserud and Marshall 2001) or "age-related-effect" for  $\delta^{18}\text{O}$  (Treydte et al. 2006). Age-related isotope trends appear to be more consistent for  $\delta^{13}\text{C}$  than  $\delta^{18}\text{O}$  (Young et al. 2011; Xu et al. 2011; Labuhn et al. 2016; Lavergne et al. 2017; Friedman et al. 2019; Duffy et al. 2019). Overall, fewer studies have addressed these trends and their causes for  $\delta^{18}\text{O}$  compared to  $\delta^{13}\text{C}$ . Age-related trends are avoided by only including rings formed after the first (or inner) 20–50 years from the pith. The number of years included within the juvenile period is not constant, so a preliminary test on a single core may

be advisable prior to expending money and time on unusable samples. An alternative to omitting the juvenile tree growth is to mathematically remove the juvenile isotopic trend using different detrending methods such as the regional curve standardization “RCS” detrending method (Gagen et al. 2008; Esper et al. 2010, 2015; Helama et al. 2015).

The majority of paleoclimate tree-ring isotope-based studies use an approach similar to classic dendrochronology studies where old, dominant and sensitive trees (“big trees”) are selected (Gagen et al. 2011; Loader et al. 2013a). Minimizing micro-environment effects is addressed ad hoc during field collection (through tree selection), while isotopic trends related to developmental stages are addressed post hoc during sample preparation by excluding the inner rings or by detrending. The “classic” dendroclimatology sampling approach can, however, be biased when estimating past and projected responses of forest growth (based on tree-ring width) to climate variability and trends (Klesse et al. 2018a). This bias in targeting climatically sensitive and dominant trees for  $\delta^{13}\text{C}$  chronologies has been investigated with respect to their use to infer physiological responses of trees to rising atmospheric  $\text{CO}_2$  concentrations, i.e., *iWUE* (Brienen et al. 2017). In this recent analysis of *iWUE* derived from tree-ring  $\delta^{13}\text{C}$ , Brienen et al. (2017) used a size-stratified sampling approach to infer how developmental effects, particularly the interaction between tree height and age, affect the derived trend of  $^{13}\text{C}$  discrimination and the corresponding *iWUE* magnitude over the twentieth century. Within a given site, the size-stratified approach involves sampling trees from all size classes at similar  $\text{CO}_2$  levels. Such stratification enables comparison of age or height effects independent of  $\text{CO}_2$  trends (Klesse et al. 2018b). This sampling approach has shown that when accounting for tree height, the magnitude of *iWUE* trends derived prior to height correction was significantly diminished or nonexistent in conifers (Monserud and Marshall 2001). There are several mechanisms, physical and physiological, by which tree-height can affect variations and trends in tree-ring  $\delta^{13}\text{C}$ . These include gradients of light, VPD and  $\delta^{13}\text{C}$  of atmospheric  $\text{CO}_2$  between canopy and subcanopy trees. These mechanisms are indirect because they result from tree status in the canopy (canopy position) and therefore are mediated by stand structure, particularly in closed canopy forests (e.g. shade tolerant tree species) (Vadeboncoeur et al. 2020).

In contrast, direct mechanisms of height effect result from hydraulic resistance linked to either reduced water potential or turgor when trees get taller. This leads to reduced stomatal conductance (McDowell et al. 2011), reduced  $\text{CO}_2$  concentration inside the leaves and consequently less isotopic discrimination, which explains artefactual increases in *iWUE* as being related to height rather than a physiological response of stomatal conductance and photosynthesis to higher atmospheric  $\text{CO}_2$ . An important caveat when considering the height effect is the underlying assumption that the height of average photosynthetic carbon gain impacting stem growth at ~130 cm (height at which tree rings are commonly sampled) is linearly related to height growth. This in turn depends on species, light compensation points, stand density and relative dominance of the sampled individuals. Brienen et al. (2017) found that at constant atmospheric  $\text{CO}_2$ , *iWUE* in young understory trees increased by a factor of two or three throughout a tree’s life span in several species. These developmental

trends were attributed to an increase in tree height and were not restricted to the early part of tree growth as previously thought (Treydte et al. 2006; Esper et al. 2010, 2015; Helama et al. 2015).

Despite potential biases of height effects discussed above, the magnitude of *iWUE* increases over the twentieth century, as derived from tree-ring  $\delta^{13}\text{C}$  measurements from several tree species in temperate, boreal and tropical forests is, however, remarkably consistent amongst tree species and forest ecosystems (Saurer et al. 2004, 2014; van der Sleen et al. 2014; Frank et al. 2015). Further, it is consistent with estimates derived from  $\delta^{13}\text{C}$  measurements of atmospheric  $\text{CO}_2$  (Keeling et al. 2017). The *iWUE* estimates derived from tree rings using the “classic” sampling strategy are therefore robust and are further supported by results of process-based biogeochemical (Keller et al. 2017) and vegetation models (Frank et al. 2015). Recent findings corroborate that using  $\delta^{13}\text{C}$  for climate and physiological inferences is reliable for years when trees are in canopy dominant positions, particularly for shade-tolerant species (Klesse et al. 2018a) with the underlying assumption that stand density and therefore competition remained unchanged over time (Voelker et al. 2019).

The application of tree-ring isotope studies to constrain the carbon cycle and atmosphere-biosphere interactions at the ecosystem level offer exciting opportunities (Belmecheri et al. 2014; Babst et al. 2014; Guerrieri et al. 2019; Lavergne et al. 2019, 2020; Szejner et al. 2020a). However, the commonly used sampling strategies ignore spatial scaling issues (e.g., stem, to leaf, to stand, to forest, to region, to global) (Medlyn et al. 2017; Yi et al. 2019). One example illustrating this challenge is the divergence in *iWUE* magnitude and other physiological metrics between tree-ring isotopes, leaf-gas exchange measurements, and estimates from direct measurements of carbon and water exchange using Eddy Covariance flux towers (Medlyn et al. 2017; Keen 2019; Yi et al. 2019; Lavergne et al. 2019). These discrepancies persist at site level, with trees sampled in the vicinity (and footprint) of a flux tower (Belmecheri et al. 2014; Medlyn et al. 2017; Guerrieri et al. 2019). Methodological assessments to identify sampling strategies when reconstructing forest productivity from tree-ring widths have demonstrated the influence of sampling design on estimates of forest growth and productivity (Nehrbass-Ahles et al. 2014). Future research in tree-ring isotopes when applied as records of carbon–water dynamics may benefit from conducting similar sampling design assessments.

Ultimately, site choice and sampling design will depend on the scientific application (paleoclimate, ecophysiology), but also require prior knowledge of environmental and micro-climate conditions at the site(s), either through site reconnaissance, monitoring (Wright 2001; Wright and Leavitt 2006a; Treydte et al. 2014; Belmecheri et al. 2018), or preliminary and published studies.

#### 4.2.2 *Sample Replication*

Typically, in a homogenous site, between four and six trees are sufficient to achieve a representative common variability at the site level. This is similar to the strong

common signal measured by “Expressed Population Signal” when using tree-ring widths (Wigley et al. 1984; McCarroll and Loader 2004). However, the number of trees required to build a representative isotopic chronology that captures a significant proportion of the site variance depends on the tree species, site conditions and the isotope considered (C, O or H). One approach would be to assess the between-tree variability (or inter-tree differences) on a subset of years-rings (10–30 years) or on only every 5th or 10th ring over the time period of interest before analyzing all of the samples (Leavitt 2010). This exploratory step is particularly relevant when considering pooled versus individual measurements of tree-ring isotopes (see Sect. 4.3.2 of this chapter).

While the majority of isotopic studies report between 4–6 trees as a sufficient sample size to achieve a representative signal (McCarroll and Loader 2004; Leavitt 2010), this number should be considered a minimum to be informed by preliminary isotopic analyses as described above. The number of trees required can be influenced by attributes of individual trees, such as circumferential variability in tree vigor, stand status (e.g. dominant, subdominant, subcanopy), micro-climate and local hydrology, and strongly depends on the environmental signal recorded in the tree-ring isotopes. These factors contribute to circumferential isotope variability within a ring (intra-tree) and between trees within a site (inter-tree). The typical inter-tree isotopic variability is 1–3‰ for  $\delta^{13}\text{C}$  and 1–4‰ for  $\delta^{18}\text{O}$ , whilst the approximate intra-tree variability is 0.5–1.5‰ for  $\delta^{13}\text{C}$  and 0.5–2‰ for  $\delta^{18}\text{O}$ , though this aspect has not been widely studied. Because the goal for paleoclimate reconstructions is to estimate the site mean value, not individual tree values, and because inter-tree isotopic variability is considerably greater than intra-tree variability, sampling a higher number of trees in a given site has been prioritized in order to capture a representative isotopic record with high precision of the sample mean for paleoclimate reconstructions.

The strength of the environmental signal recorded in the tree-ring isotopes can be assessed through (1) inter-series correlations of tree-ring isotopic series and (2) correlations between tree-ring isotopes and environmental signals (e.g. climate data). It is therefore not unusual to use up to 8–10 trees per site (Daux et al. 2011). When the aim is to build robust paleoclimate and physiological reconstructions, the number of trees is determined by the confidence interval represented by the absolute difference between individual tree-ring isotopic time-series (Loader et al. 2013b). In this context, increasing the number of trees will enhance the dominant environmental signal and reduce uncertainties in reconstructions. The absolute difference in the stable isotope values between trees can vary through time, and consequently, the theoretical number of trees required for a representative isotopic chronology may vary, too. Changes in the strength of the common signal through time cannot be determined beforehand, so the number of trees included in developing the isotopic chronology should be if possible.

### 4.2.3 Choosing Field Sampling Equipment

Sampling wood from living trees is usually done with an increment borer. Standard diameters of the borer bit include 4.3, 5.15, 10 and 12 mm. The larger borer sizes are often chosen to ensure that an adequate amount of wood is recovered for stable isotope analyses, but these borers are relatively expensive and smaller diameter borers may already be available. It is worthwhile to consider the total mass of  $\alpha$ -cellulose that can be recovered from wood based on the average ring width (or the minimum ring width of the sample), or the average width of the desired tree-ring subdivision.

Analytical masses used for isotopic analysis and reported in publications from 2009 to 2019 ( $n = 285$ ) range from 0.04 to over 1 mg for carbon isotope analysis (median = 0.3 mg;  $n = 145$ ) and from 0.05 to over 1 mg for oxygen isotope analysis (median = 0.2 mg,  $n = 140$ ). The exact amount required depends on the analytical method and machine sensitivity. Therefore, determining the sample mass required for isotopic analyses should be confirmed with the analytical laboratory of interest.

Table 4.1 indicates the mass of  $\alpha$ -cellulose recoverable from wood samples when using 4.3 mm diameter and 5.15 mm diameter increment borers, assuming 40%  $\alpha$ -cellulose. The values in Table 4.1 assume that 10% of the volume is removed during surfacing (e.g., sanding, microtome). The cross-diameter distance equivalent to 10% of the volume, to account for surfacing, is 0.81 mm and 0.68 mm for the 5.15 mm and 4.3 mm borers, respectively. This table can be used to determine the amount of  $\alpha$ -cellulose that can be recovered from a specific subdivision increment for the two standard diameters of increment borer. A better estimate for individual tree species can be calculated if the percentage of  $\alpha$ -cellulose in the wood is known.

The following example describes the procedure to use Table 4.1 for a given tree species and the width of a ring or a ring-subdivision: *Pseudotsuga menziesii* (Douglas-fir) is reported to contain about 45%  $\alpha$ -cellulose. The specific gravity of this species is  $\sim 0.47$  (though the specific gravity of wood varies with moisture content, ring width, and with the part of the ring considered e.g. earlywood versus latewood). Let's assume that the trees were sampled using a 5.15 mm borer, and that the cores are sampled at 0.5 mm wide subdivisions. According to Table 4.1, a core from a 5.15 mm borer, for a tree with a wood density of 0.47 and a subdivision width of 0.5 mm will yield  $\sim 1.8$  mg of  $\alpha$ -cellulose. These values are calculated assuming 40%  $\alpha$ -cellulose. To convert the  $\alpha$ -cellulose to the specific yield for Douglas-fir of 45%  $\alpha$ -cellulose, simply multiply the yield from Table 4.1 by the ratio of the actual  $\alpha$ -cellulose % to the % of  $\alpha$ -cellulose used to make Table 4.1 ( $1.8 \text{ mg} * 45\%/40\% = 2.0 \text{ mg } \alpha\text{-cellulose}$ ).

Material losses during processing, other than during surfacing and chemical extraction, are not included in these calculations, so the table values should be considered the maximum recoverable amount of  $\alpha$ -cellulose for a species with 40%  $\alpha$ -cellulose. The values presented in the Table 4.1 can be applied to any desired linear distance to be subsampled (e.g., whole ring, earlywood, latewood, etc.), but when considering the density of the wood to be sampled, researchers should be aware that

the density of latewood is somewhat greater than both the density of earlywood and the reported average wood density for the tree species.

Consider *Pinus ponderosa* as another example of the use of the information summarized in Table 4.1. Wood density within a single species can vary greatly depending on the tree age, the rate of growth, seasonal changes in climate, and other factors determining the wood composition. A typical value for the specific gravity (unitless; approximately equal to the density measured in  $\text{g cm}^{-3}$ ) of oven-dried *Pinus ponderosa* is 0.40 (Miles and Smith 2009), i.e., equal to ca.  $0.40 \text{ g cm}^{-3}$ . Based on Table 4.1, recovery of 2.0 mg of  $\alpha$ -cellulose using a 4.3 mm increment borer, requires a ring width or ring subdivision of at least 0.95 mm. For a 5.15 mm increment borer, the ring width or ring subdivision required to recover 2.0 mg of cellulose is at least 0.67 mm (Table 4.1). For a 12 mm increment borer (not shown),

**Table 4.1** Alpha-cellulose recovery: Theoretical amount of  $\alpha$ -cellulose (mg) recoverable from wood cores using 5.15 and 4.3 mm increment borers and containing 40%  $\alpha$ -cellulose. The value of 40%  $\alpha$ -cellulose was chosen because it is less than the percentage present in most tree species (N = 83, Table 3, (Pettersen 1984)). These values assume that 10% of the wood was removed during surfacing. For the 5.15 and 4.3 mm borers this means removing wood to a depth of ~0.8 and ~0.7 mm, respectively. The “ring or subdivision width” indicates the width in mm of the whole ring or of a ring subdivision (e.g. earlywood, latewood, thin sections). If the percentage of  $\alpha$ -cellulose in the wood of a chosen tree species is known, then a more accurate estimate of the maximum recoverable  $\alpha$ -cellulose can be estimated (see text)

		Wood density ( $\text{mg/mm}^3$ )										
<b>5.15 mm</b>		<b>0.3</b>	<b>0.35</b>	<b>0.4</b>	<b>0.45</b>	<b>0.5</b>	<b>0.55</b>	<b>0.6</b>	<b>0.65</b>	<b>0.7</b>	<b>0.75</b>	<b>0.8</b>
Ring or subdivision width (mm)	3.0	6.7	7.9	9	10.1	11.2	12.4	13.5	14.6	15.7	16.9	18
	2.5	5.6	6.6	7.5	8.4	9.4	10.3	11.2	12.2	13.1	14.1	15
	2.0	4.5	5.2	6	6.7	7.5	8.2	9	9.7	10.5	11.2	12
	1.5	3.4	3.9	4.5	5.1	5.6	6.2	6.7	7.3	7.9	8.4	9
	1.0	2.2	2.6	3	3.4	3.7	4.1	4.5	4.9	5.2	5.6	6
	0.9	2	2.4	2.7	3	3.4	3.7	4	4.4	4.7	5.1	5.4
	0.8	1.8	2.1	2.4	2.7	3	3.3	3.6	3.9	4.2	4.5	4.8
	0.7	1.6	1.8	2.1	2.4	2.6	2.9	3.1	3.4	3.7	3.9	4.2
	0.6	1.3	1.6	1.8	2	2.2	2.5	2.7	2.9	3.1	3.4	3.6
	0.5	1.1	1.3	1.5	1.7	1.9	2.1	2.2	2.4	2.6	2.8	3
	0.4	0.9	1	1.2	1.3	1.5	1.6	1.8	1.9	2.1	2.2	2.4
	0.3	0.67	0.79	0.9	1	1.1	1.2	1.3	1.5	1.6	1.7	1.8
	0.2	0.45	0.52	0.6	0.67	0.75	0.82	0.9	0.97	1.05	1.12	1.2
0.1	0.22	0.26	0.3	0.34	0.37	0.41	0.45	0.49	0.52	0.56	0.6	
<b>4.3 mm</b>		<b>0.3</b>	<b>0.35</b>	<b>0.4</b>	<b>0.45</b>	<b>0.5</b>	<b>0.55</b>	<b>0.6</b>	<b>0.65</b>	<b>0.7</b>	<b>0.75</b>	<b>0.8</b>
Ring or subdivision width (mm)	3.0	4.7	5.5	6.3	7.1	7.8	8.6	9.4	10.2	11	11.8	12.5
	2.5	3.9	4.6	5.2	5.9	6.5	7.2	7.8	8.5	9.1	9.8	10.5

(continued)



**Table 4.1** (continued)

	Wood density (mg/mm <sup>3</sup> )											
	2.0	3.1	3.7	4.2	4.7	5.2	5.8	6.3	6.8	7.3	7.8	8.4
	1.5	2.4	2.7	3.1	3.5	3.9	4.3	4.7	5.1	5.5	5.9	6.3
	1.0	1.6	1.8	2.1	2.4	2.6	2.9	3.1	3.4	3.7	3.9	4.2
	0.9	1.4	1.6	1.9	2.1	2.4	2.6	2.8	3.1	3.3	3.5	3.8
	0.8	1.3	1.5	1.7	1.9	2.1	2.3	2.5	2.7	2.9	3.1	3.3
	0.7	1.1	1.3	1.5	1.6	1.8	2	2.2	2.4	2.6	2.7	2.9
	0.6	0.94	1.1	1.2	1.3	1.4	1.6	1.7	1.8	2	2.1	2.5
	0.5	0.78	0.91	1.1	1.2	1.3	1.4	1.6	1.7	1.8	2	2.1
	0.4	0.63	0.73	0.84	0.94	1.1	1.2	1.3	1.4	1.5	1.6	1.7
	0.3	0.47	0.55	0.63	0.71	0.78	0.86	0.94	1	1.1	1.2	1.3
	0.2	0.31	0.37	0.42	0.47	0.52	0.58	0.63	0.68	0.73	0.78	0.84
	0.1	0.16	0.18	0.21	0.24	0.26	0.29	0.31	0.34	0.37	0.39	0.42

the ring width or ring subdivision must be at least 0.125 mm. For analysis of either  $\delta^{13}\text{C}$  or  $\delta^{18}\text{O}$  in *Pinus ponderosa*, with two replicates, using the median values typically reported for the analytical masses ( $\delta^{13}\text{C}$  median = 0.3 mg;  $\delta^{18}\text{O}$  median = 0.2 mg), a minimum linear distance (sampling resolution) of 0.3 mm (4.3 mm borer) or 0.2 mm (5.15 mm borer) is required for  $\delta^{13}\text{C}$  and 0.2 mm (4.3 mm borer) or 0.13 mm (5.15 mm borer) is required for  $\delta^{18}\text{O}$ . At least twice the mass is required if both isotopes are to be analyzed. Of course, an assessment that inadequate material will be recovered from a single core can be offset by pooling material from multiple cores (see Sect. 4.3.2 on pooling).

Typically, two cores are sampled per tree, from opposing radial directions across any slope (not upslope or downslope), for establishing tree-ring chronologies, irrespective of the diameter of the increment borer. The same two cores can be used for isotope analyses which will circumvent the potential problem of intra-tree variability (Leavitt and Long 1984) by pooling rings or subdivision of rings while ensuring that sufficient material will be recovered when using smaller diameter increment borers. Albeit, when not constrained by the amount of recovered material, e.g., access to and use of a 12 mm increment borer or analyzing whole rings, it is not unusual to sample one core per tree.

## 4.3 Sample Preparation

### 4.3.1 Sampling Resolution

Most tree rings exhibit anatomical characteristics within annual rings that demarcate tissues with relatively large-diameter tracheids/vessels known as earlywood

(EW) from adjacent tissues with dense, small-diameter tracheids/vessels, which are known as latewood (LW) (Pallardy 2008). In most trees, the EW forms in the spring and the LW in the summer. In some tree species, other wood anatomical characteristics can occasionally be identified, e.g., the so-called false ring, defined as an abrupt intra-annual density fluctuation (IADF), consisting of layers of tracheids with small diameters within the EW and sometimes impinging on the LW (Szejner 2011; Battipaglia et al. 2016; Babst et al. 2016; Pacheco et al. 2018; Belmecheri et al. 2018). Depending on the species, these variations are the expression of phenological processes related to xylogenesis, driven by temperature and water availability (Budelsky 1969; Yoshimura and Suzuki 1975; Vaganov et al. 2006; Zalloni et al. 2016). For example, cell enlargement is driven by turgor pressure and accordingly by water availability (Lockhart 1965; Rathgeber et al. 2016), and extreme or abrupt reductions in water availability can result in the formation of IADFs. These anatomical variations can serve as temporal markers that can be used to investigate intra-seasonal variation in tree-climate interactions using stable isotopes (Castagneri et al. 2018; Belmecheri et al. 2018).

The majority of tree-ring isotope studies are based on the analyses of whole rings or latewood portion of the ring, for both Gymnosperms and Angiosperms (specifically ring-porous angiosperms). Tree-ring stable isotope publications surveyed between 2009 and 2019 report 18 studies based on blocks of rings, 237 studies based on whole rings, 30 studies based on latewood subdivision, 28 studies based on both early-wood/latewood subdivisions, and 35 studies based on subdivisions smaller than early-wood/latewood. For deciduous tree-species, the LW portion of the ring is preferred for isotopic analyses because it corresponds to recent photoassimilates as opposed to remobilized carbon from previous growing seasons used for EW (Kagawa et al. 2006a, b). Therefore, the isotopic composition of LW is imprinted by environmental conditions experienced by trees during the current growing season. In contrast, EW in most conifer species rely almost entirely on current photosynthates.

For Gymnosperms, separating LW and EW is not necessary in some cases (Kress et al. 2010; Daux et al. 2011). Analyses of pine species at the European tree line showed that the  $\delta^{13}\text{C}$  signal was coherent amongst EW and LW (Kress et al. 2010). In this case, the coherence of the  $\delta^{13}\text{C}$  isotopic signal amongst these two portions of growth is related to the short duration of the growing season, and smaller carbohydrate pools. In such cases, analyzing the whole ring offers an advantage in the presence of narrow rings and is more cost-effective for developing long isotopic chronologies.

Recently, analyses of  $\delta^{13}\text{C}$  in EW from *Quercus* species have been used to constrain seasonal dynamics and strategies of carbon storage as they relate the phenological phases to climate trends (e.g. warming) (Kimak and Leuenberger 2015). Using  $\delta^{13}\text{C}$  from EW and LW in mature *Quercus* trees, McCarroll et al. (2017) demonstrated the existence of two pools consisting of only non-structural carbohydrates (NSCs). For EW formation, trees preferably used younger reserves (NSCs from the previous year), but accessed older reserves (NSCs from earlier years) when poor environmental conditions prevailed during the previous growing season (McCarroll et al. 2017). The inter-seasonal  $\delta^{13}\text{C}$  variations described for *Quercus* species are consistent with the highly resolved intra-seasonal variations of  $\delta^{13}\text{C}$  described for several broad-leaf

species (*Fagus*, *Populus*, and *Morus*). Isotopic measurements were conducted at 100  $\mu\text{m}$  resolution for two consecutive years and showed a consistent tri-phasic  $\delta^{13}\text{C}$  pattern of enrichment-depletion-enrichment (Helle et al. 2004). At the beginning of the EW portion,  $\delta^{13}\text{C}$  values rise to reach the maximum observed values, followed by a decline (gradual or abrupt) to the minimum observed values within the LW portion. The end of the LW is marked by an increase of  $\delta^{13}\text{C}$  values and is similar to the next year (ring) EW  $\delta^{13}\text{C}$ . The increase marks the switch-over from current to stored carbohydrates use. This seasonal pattern is interpreted as reflecting isotopic fractionations related to post-photosynthetic processes and downstream metabolism (Gessler et al. 2009; Offermann et al. 2011) (see Chap. 13), which can lead to a decoupling between the signal recorded in the leaf and that stored in the wood or cellulose (Gessler et al. 2014).

In regions with distinct seasonality such as cool and wet spring and hot dry summers, the EW and LW portions will record different climate signals that can be averaged out if the whole ring is analyzed. Beyond EW and LW temporal resolution, a systematic investigation of intra-annual variations of  $\delta^{13}\text{C}$  and  $\delta^{18}\text{O}$  offers the advantage of identifying the seasonality of the climate signal recorded in various portions of the tree-ring throughout the growing season. This then allows reconstruction of the long-term variability of the seasonal climate signal (Roden et al. 2009; Johnstone et al. 2013). Intra-annual  $\delta^{18}\text{O}$  measured from coast redwoods revealed a consistent  $\delta^{18}\text{O}$  pattern across 10 years and from multiple trees/sites, with the most depleted  $\delta^{18}\text{O}$  recorded in the central portion of the ring. The low  $\delta^{18}\text{O}$  values were related to depleted source water  $\delta^{18}\text{O}$  and a reduction of evaporative enrichment related to fog during the summertime, and were interpreted as signaling a switch from stored to current summertime photosynthates. In this study, it was possible to identify the timing of the seasonal climate signal and therefore the portion of the ring suitable for longer-term reconstructions (Johnstone et al. 2013). This one example illustrates the value of considering what portion of the tree ring will be analyzed, and the relevance of such an approach to enhance the interpretation of the isotopic results but also optimize utilization of resources.

In temperate forests, most isotopic studies of tree rings with temporal resolution higher than earlywood and latewood focused on only few years (2–10 years). In contrast, high resolution intra-annual investigation is very common in tropical forests and particularly for tree-species lacking visible growth rings (Verheyden et al. 2004; Anchukaitis et al. 2008), and has been used to develop long and highly-resolved isotopic records (Poussart et al. 2004; Cintra et al. 2019). High-resolution intra-annual tree-ring studies have improved the knowledge and understanding of the underlying physiological processes of tree response to climate and environmental variability (Walcroft et al. 1997; Leavitt et al. 2002; Barbour et al. 2002; Helle et al. 2004; Roden et al. 2009; Kimak and Leuenberger 2015; McCarroll et al. 2017). This is further illustrated by the use of process-based models for interpretation of seasonal variation in  $\delta^{13}\text{C}$  and  $\delta^{18}\text{O}$  (Walcroft et al. 1997; Barbour et al. 2002; Ogée et al. 2009) (see Chap. 26). A detailed model-data comparison for pine trees over two consecutive growing seasons revealed that a single-substrate model (a simple model for carbohydrate reserve) represents a reasonable assumption for interpreting

seasonal variations of tree-ring  $\delta^{13}\text{C}$  and  $\delta^{18}\text{O}$  driven by precipitation and soil moisture (Ogé et al. 2009). Interestingly, a sensitivity analysis of the single substrate model revealed that the modeled EW isotopic signal was sensitive to the onset of the cell-wall thickening phase, during which almost all cellulose is deposited.

Recent insights into xylogenesis have improved the understanding of the timing and duration of cell enlargement and cell-wall thickening phases throughout the tree-ring formation (Cuny et al. 2014, 2015). The duration and rates of cellular differentiation processes are highly variable throughout the growing season (Cuny et al. 2013; Ziaco et al. 2016). For conifers in France, the cell enlargement phase for EW had a longer duration, ~20 days, compared to the cell wall thickening phase of ~5 days. The opposite was observed later in the growing season where LW cells had a shorter enlargement phase and an extended thickening phase, ~50 days (Cuny et al. 2014, 2015). The timing and duration of cell-wall thickening imply that lags between the onset of cell formation and secondary cell-wall formation should be accounted for when aligning climate drivers with isotopic signals recorded in cellulose (Monson et al. 2018; Belmecheri et al. 2018). Until recently, the kinetics of xylogenesis processes were not integrated into the empirical or process-based interpretations of tree-ring isotopic studies (Ogé et al. 2009; Belmecheri et al. 2018). In the absence of such information, tree-ring isotopic studies based on annual or seasonal time resolution can lead to a smoothed or mixed signal of intra-seasonal xylogenesis processes (Chap. 15). For paleoclimatic and ecophysiological inferences, systematic isotopic investigations at high intra-annual resolution offer great potential to gain a better theoretical understanding of the coupling between tree-ring formation, isotopic fractionation and environmental conditions (Wright and Leavitt 2006b; Roden et al. 2009; Vaganov et al. 2011).

The whole ring, EW or LW portions can be accurately and manually separated using a scalpel or a razor blade under a binocular magnifier or stereoscope (e.g. Daux et al. 2011). For high intra-seasonal resolution, a sliding (Barbour et al. 2002; Helle et al. 2004; Ogé et al. 2009) or rotary (Anchukaitis et al. 2008; Szejner et al. 2020b) microtome is used to cut continuous and tangential slices at the desired resolution incrementally. When sampling thin slices with a microtome, it is important to ensure that the ring-boundaries are parallel to each other for an accurate representation of the radial growth progression and that the orientation of the blade is parallel to the fiber direction. Note that the pronounced arc of rings near the pith precludes the use of a microtome for accurate ring subdivision, because of mixing of wood produced during different time periods when cutting with a straight blade across the arc of the ring. Slices as thin as 10  $\mu\text{m}$  can yield enough wood mass for cellulose extraction and isotopic analyses (Table 4.1). This can be achieved using 12 mm tree cores or wood segments (from stem discs).

### 4.3.2 *Sample Pooling*

It is advisable when resources (cost, time) are not limiting to analyze trees individually. The major advantage of analyzing individual trees is the assessment of statistical uncertainties associated with isotopic signal arising from the between-tree variability, but also to correct for age-related trends as discussed above. For physiological and ecological applications, analyzing individual trees enables statistical analysis where a single tree is used as a random or fixed factor when assessing drivers of physiological response of trees to environmental change. This is increasingly used in mixed-effect linear models (Guerrieri et al. 2019).

On the other hand, pooling dated rings from multiple trees reduces sample processing time and resources use. A compromise between these two procedures is a split-pool protocol where rings from multiple trees are pooled for each year but also analyzed separately at a fixed frequency of every 5 or 10 years allowing for inter-tree isotopic errors to be quantified (Wright and Leavitt 2006b; Dorado Liñán et al. 2011; Szejner et al. 2016) (see Chap. 6). Rings from multiple trees for any given year can be pooled independently of their mass differences (but see Dorado Liñán et al. 2011), though adequate sample homogeneity pre- or post-chemical extraction (see following Sect. 4.3.3) is crucial for obtaining a composite (pooled) isotopic time-series that is similar to the average of the individual tree measurements (Leavitt 2010; Dorado Liñán et al. 2011).

Beyond resources, the study aim will determine the sample preparation protocol. For instance, it is possible to pool consecutive years within a tree (blocks of several rings, typically 5 year blocks) to develop long isotope chronologies when the goal is to investigate paleoclimate trends and low-frequency variations (Mayr et al. 2003; Gagen et al. 2012). In such cases, pooling across years seems to be a practical choice that yields a robust isotope-based reconstruction with sufficient sample replication, but the method may not be suitable for some physiological investigations of long-term trends given that pooling adjacent years may involve mixing the isotopic signals of EW and LW sections and their sources, respectively. Nevertheless, multiple-year pooling with individual tree analysis offers the advantage of estimating the confidence interval of an isotope chronology mean and therefore of paleoclimate reconstructions (Boettger and Friedrich 2009). There are different strategies to develop isotope chronologies using multiple-year pooling. The first one consists simply of serial pooling of tree-ring blocks from an individual tree (Leavitt and Lara 1994). The second one consists of pooling tree-ring blocks from an individual tree, but shifted by one year between trees, which produces a “quasi-annual” pooled chronology that retains replication in each year (Boettger and Friedrich 2009). The third strategy consists of supplementing the second strategy by analyzing a larger number of trees where tree-cohorts join (e.g. ~10 trees for cohort-join points vs 5 trees for shifted tree-ring blocks). This technique is termed *Offset-pool plus Join-Point* and was developed by Gagen et al. (2012) to rapidly generate a robust millennial length  $\delta^{13}\text{C}$  chronology by combining living trees and sub-fossil wood. However, such reconstruction relied on prior work in the same site exploring the strength of the climate signal as well as

age-related trends, and consequently can be applied in similar settings to the original study.

In summary a balance between the objectives of the study and available resources will determine the choice and the relevance of analyzing trees individually, pooling rings within individual trees, or pooling the same sampling units from multiple trees prior to chemical extraction of cellulose or isotopic measurements. Yet, the ability to provide uncertainty estimates should remain a central goal and the strategies described above offer a few options to achieve this goal.

### ***4.3.3 Particle Size Requirements for Chemical Extraction and Analytical Repeatability***

When  $\alpha$ -cellulose is to be analyzed for stable isotopes of  $\delta^{13}\text{C}$  and  $\delta^{18}\text{O}$ , we recommend the following steps: (1) reduction of the wood sample prior to chemical extraction, and (2) further particle size reduction using an ultrasonic probe after chemical extraction (Laumer et al. 2009). Large differences in the stable isotope ratios can occur across a tree ring, within the same year, between different sides of the same tree and between neighboring trees of the same species (e.g., Leavitt and Long 1986; Saurer et al. 1997). The current analytical masses used are typically a few hundred micrograms, and usually a subsample from each sample is analyzed, not the entire sample (e.g. whole tree ring or a subdivision of a tree ring). When multiple samples are pooled as described above, homogeneity of the sample is critical for precision (unless the sample mass from which the subsample is drawn is not much larger than the size of the subsample). The subsample must be isotopically representative of the average value for the entire sample within the precision of mass spectrometry, whether pooled or not, or the accuracy and repeatability of the results of the analysis will not be maximized (see Chap. 6 for more details on accuracy and precision). The maximum acceptable particle size that will ensure homogeneity within a pooled or unpooled wood sample is somewhat dependent on the wood density of the tree species, and intra-annual variability in density (e.g. earlywood/latewood), but the most important consideration is the relationship between analytical mass of the sample and of the subsample chosen for stable isotope analysis.

In 1998, Borella et al., published results of a study that considered the number of particles required for analysis given (1) a typical wood density of  $\sim 600 \text{ kg/m}^3$ , (2) a deviation of 1 or 1.5‰ in the measurements of the isotopic ratios within the original sample, (3) the mass of the original sample (immediately prior to analysis), (4) the desired ‰ deviation from the actual value (precision), and (5) the probability that a given particle size will yield a value within  $1\sigma$  or  $2\sigma$  of the actual value. At that time, Borella et al. (1998) stated that “a grain mass of  $<6 \mu\text{g}$  should be achieved to ensure an accuracy of 0.15‰”, which they report as being achievable using a sieve size of 0.15 mm ( $\sim 80$  mesh) for cellulose and 0.10 mm (120 mesh) for whole wood.

Advances in instrumentation now allow analysis of much smaller masses than considered by Borella et al. (1998), where a mass of 1–1.5 mg out of an original post-processing mass of 10–50 mg was used for the online analyses, a range for the subsample of ~2–10% of the original sample mass. Over the last 10 years of publications reporting stable isotope results from wood (2009–2019), the average analytical mass reported for  $\delta^{13}\text{C}$  analyses was  $0.67 \pm 0.6$  mg ( $N = 145$ ; median value = 0.35 mg), and the average mass used for  $\delta^{18}\text{O}$  was  $0.39 \pm 0.3$  mg ( $N = 140$ ; median value = 0.25 mg). The current median values for analytical masses of 0.3 mg ( $\delta^{13}\text{C}$ ) and 0.2 mg ( $\delta^{18}\text{O}$ ) are less than ~20–30% of the analytical values used by Borella et al. (1998), suggesting that the required particle mass under current conditions should be ~20–30% of the 6  $\mu\text{g}$  maximum particle mass recommended by Borella et al. (1998), or between 1 and 2  $\mu\text{g}$ . Particle masses of this size are achievable using some mills, but the resulting particle size is likely to be smaller than the pore size of the filtering media used during cellulose extraction, resulting in sample loss during chemical processing (see below).

Note, however, that Borella et al. (1998) state that the results presented in their Table 1, from which their recommendation was drawn, are for an “extreme case” where two samples that differed by 2‰ were combined. Individual tree rings, or combinations of the same year using multiple cores from the same tree are unlikely to contain two pools that consistently differ by 2‰, at least for  $\delta^{13}\text{C}$ , for which their study was done. The variability of  $\delta^{18}\text{O}$  values across a tree ring and between the same years on different trees is larger than the spread for  $\delta^{13}\text{C}$ . Examples of large intra-annual variations in  $\delta^{18}\text{O}$  in tree-ring  $\alpha$ -cellulose are shown in Fig. 4.3, with intra-annual ranges in the  $\delta^{18}\text{O}$  across thin sections from two years at 4 sites of >6 and >8‰. In this case the within-ring variability is much larger than the between-tree (i.e. between-site) variability.

What is the best method to use for obtaining the particle mass necessary to ensure homogeneity?

Many methods have been employed for reducing the sizes of wood particles prior to chemical extraction (Fig. 4.1), including manual cutting (scalpel, razor blade, etc.), mortar and pestle, and various kinds of milling. Many types of mills are available for wood sample reduction, including grinding/pulverizing mills (Yokoyama and Inoue 2007), impact mills (Nied 2007) and robotic micro-milling (Dodd et al. 2008), although the latter can be extremely time-consuming (Voelker et al. 2018). Milling has been the most common pre-chemical extraction method for particle size reduction prior to chemical extraction over the last 10 years (Fig. 4.1). Reduction methods such as microtome thin sectioning, laser ablation (Drew et al. 2009; Soudant et al. 2016) and the plate method (Li et al. 2011; Kagawa et al. 2015) can circumvent any questions about maximum acceptable particle size, unless the samples are to be pooled, in which case an additional particle reduction step may be required to ensure homogeneity. Yet minimizing the size of the particles prior to chemical extraction is limited by another factor. The resulting particle sizes from some mills are small enough to ensure homogeneity, but most methods for chemical extraction involve the use of filtering media (The Brendel Method is one exception—see Chap. 5 for cellulose

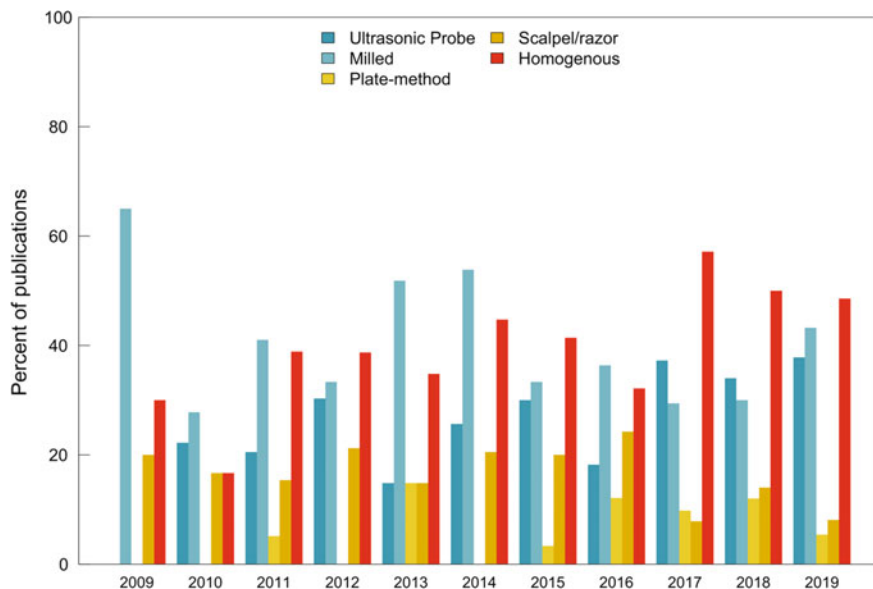


**Fig. 4.1** Methods used to obtain the final particle size analyzed in research published between 2009 and 2019 ( $n = 342$ ). No particle size reduction is involved in the “Plate Method” which is based on cellulose extraction of a whole tree-ring lath (cross-section). Other methods such as laser ablation and microtome thin sectioning are not plotted because they represented only a small percent of the papers. Note the increase in the percentage of papers using the ultrasonic probe method [Dark blue bars] since the method was first described by Laumer et al (2009) and the covariance of the use of this method in recent years with the use of various forms of the word ‘homogenous’ when referring to the analytical subsample [Red bars]

extraction details). Filtering media, such as fritted glass filters (No. 2, porosity 40–100  $\mu\text{m}$ ; e.g., Loader et al. 1997; Rinne et al. 2005) and polymer pouching material (ANKOM F57; porosity 25  $\mu\text{m}$ ; e.g., Szejner et al. 2016, 2018; Belmecheri et al. 2018) have porosities much larger than the particle sizes obtainable through many milling methods. Milling to too fine a particle size will result in substantial sample loss during the subsequent chemical extraction but milling to a very coarse size can result in incomplete chemical extraction. Ideally the particle size after milling will be only slightly larger than the porosity of any filtering media. For example, pre-extraction milling to 20 mesh ( $\sim 840$  microns) can yield adequate particle size. Yet, the suitable particle size for the filtering media is too large to provide adequate homogenization of the sample when small samples masses are being analyzed, we therefore recommend a further reduction of the particle sizes after chemical extraction through the use of an ultrasonic probe (Laumer et al. 2009), which results in complete separation and mixing of the  $\alpha$ -cellulose fibers.

In summary, given the changes in instrumentation that now allow the analysis of  $\delta^{13}\text{C}$  and  $\delta^{18}\text{O}$  from wood-derived samples in the range of 100–200  $\mu\text{g}$ , we recommend reduction of the wood to a particle size larger than the filtering media prior



to chemical extraction, to ensure the completion of the chemical extraction and to reduce the length of the fibers, followed by further particle size reduction using an ultrasonic probe (Laumer et al. 2009). This combination yields samples with the greatest possible homogeneity for the typical methods employed prior to stable isotope analysis of  $\alpha$ -cellulose.

## 4.4 Towards Subseasonal-Resolution Analyses of Tree-Ring Records

### 4.4.1 *Important Considerations*

The appropriate sampling resolution for stable isotope analysis in tree-rings depends on many factors, including the research question, the width of the rings of the chosen trees, and the climate variability and repeating patterns within that variability, factors that are best expressed in the following questions: What temporal resolution would best answer my research question? Is there enough material available in my samples to allow sub-tree-ring sampling? How much does the climate vary across each growing season at my tree site? Are there **intra-annual** climate changes at my site that are temporally consistent on an **inter-annual** basis?

Increasing the number of samples per tree-ring may provide additional data. But to be useful in any given research effort, the increase in the sampling resolution must provide additional information that is pertinent to answering the research question. If finer temporal gradations in the stable isotope data (as a proxy for either environmental or physiological changes) would better inform the research effort and/or increase the certainty of some aspect of the research, then an increase in the sampling resolution is worth considering.

Practical limitations such as narrow tree rings and/or smaller diameter core samples may confound efforts to increase the sampling resolution. The amount of material (wood,  $\alpha$ -cellulose, etc.) required for stable isotope analysis will determine, in part, whether increased sampling resolution is possible. This consideration was addressed in detail earlier in this chapter. The amount of time required to mature the secondary cell wall of each cell (where almost all the “wood” resides) is another consideration that may potentially limit the value of increasing the sampling resolution. The secondary cell wall maturation timing can range from a few weeks to a few months (Cuny et al. 2015), with the maturation of neighboring cells to the inside or outside of the tree ring being slightly ahead or behind any particular cell. The practical result is a smoothing of the stable isotope signal relative to the stable isotope values that would have been present at any given point in time in the newly formed photoassimilates. The degree of overlap in maturation across a tree ring will limit the recoverable temporal resolution of the factor of interest, i.e. environmental changes or physiological changes. Finally, for high resolution sampling to be useful, there must be greater variability in the higher resolution data than in the lower resolution

data, and ideally that variability will recur in a temporally consistent inter-annual pattern. Stable isotope values that vary only slightly across each tree ring will probably not provide enough additional information to justify the additional cost and efforts. Moreover, stable isotope values that vary across each tree ring in each year, but in a non-systematic way, may be difficult to interpret, especially for tree rings formed prior to the existence of local weather data.

Many climate regimes have consistent cool season to warm season shifts in temperature, and some regions also have consistent intra-annual patterns in the precipitation. Monsoonal and Mediterranean climates are good examples of climate regimes with consistent inter-annual and intra-annual climate changes. Such distinct climate variations can result in seasonal and sub-seasonal changes in the stable isotope ratios fixed in the tree-ring cellulose and can even produce visual evidence of the seasonal changes in the wood (i.e. false latewood bands-FLBs, also called inter-annual density fluctuations-IADFs). In these cases, stable isotope analysis at high-resolution within each tree ring (e.g., intra-annual thin sections, or similar) can provide useful seasonal and even sub-seasonal information, both during the period of instrumented weather data and before (Szymczak et al. 2019; Pacheco et al. 2020), with appropriate calibration/verification of the stable isotope time series with the instrumental data.

#### 4.4.2 *Sampling Resolution Comparison*

As an example of the potential value of high-resolution (intra-annual) sampling of tree rings, we combined high-resolution stable isotope values (100  $\mu\text{m}$ ) sampled across two consecutive tree rings to represent a range of sampling resolutions from low resolution (whole tree ring) to high resolution (100  $\mu\text{m}$ ; Fig. 4.2). The stable isotope data used to produce Fig. 4.2 came from  $\alpha$ -cellulose in a tree that grew in a monsoonal climate (i.e. the North American Monsoon in Southwestern US).

*What value was added in this case by having higher resolution data?*

- (1) **Whole-ring**—Note that the whole ring  $\delta^{18}\text{O}$  values (dashed lines) for the two years differ by about 2‰. This 2‰ difference between the two years would be the extent of the information available with whole ring analysis.
- (2) **Earlywood/Latewood**—A further subdivision into earlywood (springwood) and latewood (summerwood) reveals that the latewood  $\delta^{18}\text{O}$  values are enriched compared with the whole ring  $\delta^{18}\text{O}$  values, and that the earlywood  $\delta^{18}\text{O}$  values are slightly depleted compared with the whole ring  $\delta^{18}\text{O}$  values, but the overall pattern is similar between the two years. The Earlywood  $\delta^{18}\text{O}$  values between the two years are similar, but there is a 2‰ difference between the latewood in the two years. Information about differences between the seasons, with similarities between the annual earlywood/latewood pattern, is revealed by using two intra-ring sampling subdivisions.
- (3) **Quartiles**—Further subdivision of the tree-ring  $\delta^{18}\text{O}$  data into quartiles begins to reveal additional intra-annual isotope information when compared with the

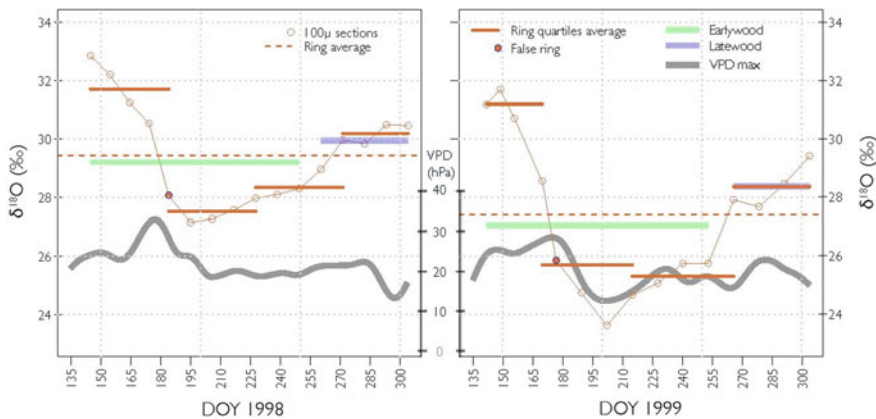


**Fig. 4.2** Subseasonal variation of tree-ring  $\alpha$ -cellulose  $\delta^{18}\text{O}$  recorded across a range of sampling resolutions. Lower resolution  $\delta^{18}\text{O}$  data points were produced by averaging the  $\delta^{18}\text{O}$  values from the  $100\ \mu\text{m}$  thin sections (circles). The whole ring value is indicated by the dashed line. An early-wood/latewood tree-ring subdivision is indicated by the thick green line (earlywood) and the thick blue line (latewood). A 4-part tree-ring subdivision (quartiles) is indicated by the brown lines. The grey line is a 30 day smoothing spline of the maximum daily VPD (hPa) provided here to contextualize environmental drivers of subseasonal  $\delta^{18}\text{O}$  variations recorded in tree-ring  $\alpha$ -cellulose. Note that the Y-axis for the VPD does not extend to the top of the graph. The position of the false ring within each year is indicated with a filled circle. DOY = Day of the Year

whole ring  $\delta^{18}\text{O}$ : (a) the first quartile is very enriched, (b) the second quartile is very depleted, (c) the third quartile reveals differences between the two years, though both are depleted relative to the whole ring value, and (d) the fourth quartile, roughly equivalent to the latewood, is slightly enriched. The variability of the  $\delta^{18}\text{O}$  above and below the tree-ring mean  $\delta^{18}\text{O}$  value would not be recognized with either whole ring or earlywood/latewood analysis.

- (4) **100  $\mu\text{m}$  thin sections**—Values from the original data (circles) indicate transitions across the tree rings, with a very enriched first three slices, a 3–4 slice transition to the most depleted values, followed by a gradual increase in the  $\delta^{18}\text{O}$  values until the end of the growing seasons. Arguably, the results from the quartile analysis provide almost the same information recovered in the  $100\ \mu\text{m}$  thin sections, though information that aids the interpretation will be added in the following case study.

#### 4.4.3 Case Study: *Pinus Ponderosa* Growing in Southwestern US [Southern Arizona]

In the following section, the high-resolution  $\delta^{18}\text{O}$  subseasonal variations presented above, is further replicated in three additional tree sites to investigate the consistency

of the seasonal pattern discussed earlier and its spatial coherence across Southern Arizona.

The annual precipitation in Southern Arizona is consistently bimodal, with a cool-season component and a warm season (monsoon) component (Sheppard et al. 2002). A hot and extremely dry period from April to June always separates these two precipitation modes. During the dry period, tree species growing at high elevations (~2000–2600 m) experience very high transpiration rates caused initially by high vapor pressure deficit (VPD) which is later combined with depleted soil moisture. The combination of extremely dry air and low soil moisture causes the growth in these trees to slow, often resulting in a reduction in the cell sizes (Belmecheri et al. 2018). Following the onset of the North American Monsoon (NAM) precipitation (July 7th  $\pm$  9 days; Higgins et al. 1999), many of the trees are able to resume their cambial activity and growth (Budelsky 1969). In these cases, the smaller lignified cells produced during the dry period are followed by larger cells, forming a visual growth transition. This feature, often called a “false ring”, “interannual density fluctuation (IADF)”, or “false latewood band (FLB)”, when combined with the consistent timing of the onset of the NAM, allows the FLBs to be used as a visual intra-annual time marker, separating spring growth from growth in the summer and autumn.

Examination of the  $\alpha$ -cellulose  $\delta^{18}\text{O}$  extracted from 100  $\mu\text{m}$  thin sections (using a rotary microtome) from high elevation trees growing in two proximate mountain ranges (The Santa Catalina and Pinaleno mountains), at four different elevations (between 2040–2680 m) and during two consecutive years (1998 and 1999) reveals consistent  $\delta^{18}\text{O}$  patterns across the growing seasons in all cases (Fig. 4.3). In general, the  $\delta^{18}\text{O}$  values in cool season precipitation in Arizona are more depleted than those in warm season precipitation, because of the effect of cooler temperatures on the condensation fractionation (Eastoe and Dettman 2016). Stable isotope analyses of precipitation collected at a location close to two of the studied sites (HEL and WCP) show the expected cool season/warm season pattern in precipitation  $\delta^{18}\text{O}$  (Wright 2001). The timing of budburst at one of the sites (HEL) indicated that the growing seasons began in mid-April in both years at a time when soil moisture was close to field capacity (Wright and Leavitt 2006a). The comparisons of the precipitation  $\delta^{18}\text{O}$  values with soil and xylem water  $\delta^{18}\text{O}$  showed strong covariance, indicating little or no groundwater access (Belmecheri et al. 2018). Yet the  $\delta^{18}\text{O}$  values in the first few slices from each year at all the sites were much higher than the  $\delta^{18}\text{O}$  values measured on slices produced during the summer season, the opposite of expectations if the cool season/warm season precipitation  $\delta^{18}\text{O}$  signal was dominating the  $\delta^{18}\text{O}$  values in the photoassimilates.

Approximately 58% of the final  $\delta^{18}\text{O}$  value in xylem  $\alpha$ -cellulose comes from the leaf water, while about 42% of the oxygen atoms in the photoassimilates produced using leaf water subsequently exchange with stem water during cellulose synthesis (Roden and Ehleringer 1999). It is the 58% of the oxygen atoms that retain values related to the leaf water enrichment that provide one possible explanation of the observed cellulose  $\delta^{18}\text{O}$  seasonal pattern. The degree of evaporative enrichment of leaf water  $\delta^{18}\text{O}$  differs greatly with VPD as mediated by water availability in the soil, such that leaf water  $\delta^{18}\text{O}$  values during transpiration may be the same as the source

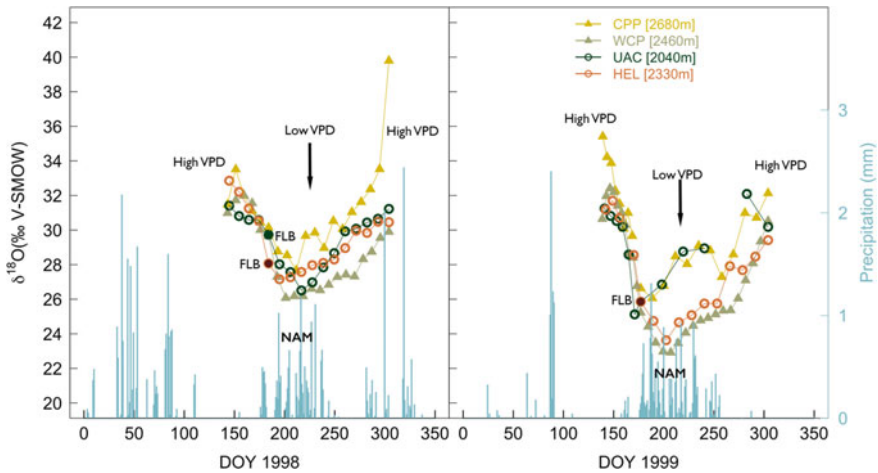


**Fig. 4.3** Tree-ring  $\delta^{18}\text{O}$  (W. E. Wright, *unpublished data*) from 100  $\mu\text{m}$  thin sections for two consecutive years 1998 CE [Left] and 1999 CE [Right]. The data comes from samples taken at four sites located in two Arizona mountain ranges (U.S. Southwest) separated by about 80–90 km. False Latewood Bands (FLBs) occurred in both years at the lower elevation sites [UAC and HEL, circles]. In the 1998 graph, the  $\delta^{18}\text{O}$  values for the FLBs [filled circles] occurred at the same point in time, but their  $\delta^{18}\text{O}$  was different. In the 1999 graph,  $\delta^{18}\text{O}$  values for the FLBs from the two sites plot almost at the same point in time and have very similar  $\delta^{18}\text{O}$ , so the symbols are indistinguishable on the graph. The higher elevation sites [CPP and WCP, triangles] did not form FLBs in these years, though the intra-annual  $\delta^{18}\text{O}$  patterns are very similar. Note that the x-axis values for the  $\delta^{18}\text{O}$  from all the sites are plotted at constant time intervals relative to starting dates of Day 135 (May 15) and ending dates of Day 304 (October 31), based on observed leaf extension timing, which roughly correspond to the growing season (Wright and Leavitt 2006a). Consequently, the placement of the  $\delta^{18}\text{O}$  data points relative to the x-axis is based on estimates for the beginning and end of the growing seasons, and therefore does not include the shift forward in timing required to account for the maturation of the secondary cell walls (i.e. about 4–6 weeks on average)

water  $\delta^{18}\text{O}$  if the atmospheric humidity is 100%, but will become very enriched if transpiration occurs into very dry air. The very enriched early growth in the data shown in Fig. 4.3 is consistent with stable isotope model outputs using local climate data, which suggests that extreme evaporative enrichment caused by high VPD may be the main driver of the high  $\delta^{18}\text{O}$  values (Belmecheri et al. 2018). An alternative interpretation is the use of enriched stored photoassimilates. But the important point here is that coarse resolution sampling would not have revealed the unusual early growing season values.

Another detail that would not have been revealed by coarser sampling is the temporal relationship of the FLBs (IADFs) to the stable isotope values. A FLB is formed during a period of extreme water stress, which causes partial or complete growth cessation resulting in the production of smaller cells. Yet in these examples the summer rains began soon after the formation of the FLB, so most of the maturation occurred under conditions of high humidity (lower vapor pressure deficit). The combined effects of reduced evaporative enrichment of the leaf water and increased

diffusion of depleted water vapor  $^{18}\text{O}$  into the stomata result in leaf water  $\delta^{18}\text{O}$  that is less enriched than during the dry period. Photoassimilates formed using this summer leaf water are then used to mature the small cells in the FLB. Consequently, the  $\delta^{18}\text{O}$  value for the thin section containing the FLB is one of the most depleted in both tree rings (Belmecheri et al. 2018). This pattern can be explained by the kinetics (timing and duration) of cell-wall enlargement and thickening phases for the FLB cells. While cell-wall enlargement of the FLBs is initiated during the arid period, secondary cell-wall deposition begins and extends through the moist monsoon period (July to mid-September).

Evidence for the offset in the timing between the appearance of the small cells and the maturation of the secondary cell walls of the small cells would not be available at a coarser sampling resolution. In addition, thin section analysis allowed us to recognize that the intra-annual patterns in the  $\delta^{18}\text{O}$  of the same years were very similar, and that these  $\delta^{18}\text{O}$  pattern similarities were independent of the presence or absence of a FLB (Fig. 4.3).

#### 4.4.4 Preliminary Assessments

High-resolution intra-annual sampling can also be used in preliminary assessments to inform subsequent sampling for long-term reconstructions. In some instances, answering a research question may require only information from a limited part of the growing season, so information provided by analysis of many tree-ring subdivisions may be superfluous. In one example, the research question involved determining the position of a summer fog drip signal within tree rings of *Sequoia sempervirens* (Roden et al. 2009). The researchers already knew that the stable isotope values in fog drip were always distinguishable from other water sources. Preliminary high-resolution sampling allowed the researchers to focus their subsequent sampling on only the portion of each tree ring that was incorporating fog drip. They were also able to account for some time variance in the fog drip by expanding the sampling increment. The sampling focus and the modification of the width of the sampling unit were facilitated by the preliminary high-resolution sampling.

The data presented in the Southwestern US case study described earlier was also conducted as a preliminary assessment. Initially, the relationships between the presence or absence of FLBs and seasonal transitions in precipitation occurrence were unknown. There was no FLB within the rings in many tree rings at some sites, so an assessment of the high resolution differences between rings with and without FLBs was necessary to be certain that the visual criteria we would use to make subseasonal subdivisions (5 per ring in the case of our studies Szejner et al., 2020) would capture adequate details about intra-annual shifts in the source water and in water stress whether or not there was a FLB present. Careful preliminary assessments can help researchers to optimize information gained from stable isotope analysis when research resources are limited.

## 4.5 Conclusion

As the application of stable isotope measurements in tree rings is becoming essential in the fields of paleoclimate and paleophysiology, its full potential is still limited by time and cost of sample preparation and processing. These constraints persist despite remarkable progress in analytical techniques and a better understanding of biases and uncertainties related to sampling of trees (number and status of trees) and rings (temporal resolution). When planning tree-ring isotope studies, balancing project goals and resources is often unavoidable; however, the goal should still be to produce robust measurements of the sample mean at any chosen temporal-resolution, and to quantify uncertainties of these measurements. Analyzing individual trees allows uncertainties in the paleoclimate or paleophysiology reconstructions to be assessed. Otherwise, choosing between individual trees vs pooling multiple trees, or choosing between whole wood and  $\alpha$ -cellulose should at least be informed by preliminary analyses on a subset of years/trees. In all cases, sample homogeneity (wood or  $\alpha$ -cellulose) is key to achieving precise and representative (within or between tree variability) measurements. Advances in xylogenesis (wood phenology), wood anatomy and mechanistic understanding of how stable isotopes are incorporated in tree-rings offer an opportunity to shift the temporal-scale perspective at which ecophysiological processes, forest-environment interactions, and paleoclimate reconstructions are investigated using tree-ring stable isotopes.

Tree-ring stable isotope studies in conjunction with process-based models, and xylogenesis studies can inform the next generation of vegetation modeling efforts (Zuidema et al. 2018; Friend et al. 2019). With scientific motivations and resource limitations in mind, sampling for isotopic analyses can be approached from the perspective of exploiting and leveraging the same data for both ecophysiology and paleoclimate studies, while reducing uncertainties in estimates and inferences of forest growth, ecophysiology, and climate sensitivity.

## References

- Anchukaitis KJ, Evans MN, Wheelwright NT, Schrag DP (2008) Stable isotope chronology and climate signal calibration in neotropical montane cloud forest trees. *J Geophys Res* 113:G03030
- Babst F, Alexander MR, Szejner P, Bouriaud O, Klesse S, Roden J, Ciais P, Poulter B, Frank D, Moore DJP et al (2014) A tree-ring perspective on the terrestrial carbon cycle. *Oecologia* 176:307–322
- Babst F, Wright WE, Szejner P, Wells L, Belmecheri S, Monson RK (2016) Blue intensity parameters derived from *Ponderosa* pine tree rings characterize intra-annual density fluctuations and reveal seasonally divergent water limitations. *Trees Struct Funct* 30:1403–1415
- Ballantyne AP, Baker PA, Chambers JQ, Villalba R, Argollo J (2011) Regional differences in south American monsoon precipitation inferred from the growth and isotopic composition of tropical trees. *Earth Interact* 15:1–35
- Barbour MM, Andrews TJ, Farquhar GD (2001) Correlations between oxygen isotope ratios of wood constituents of *Quercus* and *Pinus* samples from around the world. *Aust J Plant Physiol* 28:335–348

- Barbour MM, Walcroft AS, Farquhar GD (2002) Seasonal variation in  $\delta^{13}\text{C}$  and  $\delta^{18}\text{O}$  of cellulose from growth rings of *Pinus radiata*. *Plant Cell Environ* 25:1483–1499
- Barbour MM, Roden JS, Farquhar GD, Ehleringer JR (2004) Expressing leaf water and cellulose oxygen isotope ratios as enrichment above source water reveals evidence of a Péclet effect. *Oecologia* 138:426–435
- Barnard HR, Brooks JR, Bond BJ (2012) Applying the dual-isotope conceptual model to interpret physiological trends under uncontrolled conditions. *Tree Physiol* 32:1183–1198
- Battipaglia G, Campelo F, Vieira J, Grabner M, De Micco V, Nabais C, Cherubini P, Carrer M, Bräuning A, Čufar K et al (2016) Structure and function of intra-annual density fluctuations: mind the gaps. *Front Plant Sci* 7:1–8
- Bégin C, Gingras M, Savard MM, Marion J, Nicault A, Bégin Y (2015) Assessing tree-ring carbon and oxygen stable isotopes for climate reconstruction in the Canadian northeastern boreal forest. *Palaeogeogr Palaeoclimatol Palaeoecol* 423:91–101
- Belmecheri S, Wright WE, Szejnjer P, Morino KA, Monson RK (2018) Carbon and oxygen isotope fractionations in tree rings reveal interactions between cambial phenology and seasonal climate. *Plant Cell Environ* 41:2758–2772
- Belmecheri S, Maxwell RS, Taylor AH, Davis KJ, Freeman KH, Munger WJ (2014) Tree-ring  $\delta^{13}\text{C}$  tracks flux tower ecosystem productivity estimates in a NE temperate forest. *Environ Res Lett* 9:074011
- Boettger T, Friedrich M (2009) A new serial pooling method of shifted tree ring blocks to construct millennia long tree ring isotope chronologies with annual resolution. *Isot Environ Health Stud* 45:68–80
- Borella S, Leuenberger M, Saurer M, Siegwolf R (1998) Reducing uncertainties in  $\delta^{13}\text{C}$  analysis of tree rings: Pooling, milling, and cellulose extraction. *J Geophys Res Atmos* 103:19519–19526
- Brienen RJW, Helle G, Pons TL, Guyot J-L, Gloor M (2012) Oxygen isotopes in tree rings are a good proxy for Amazon precipitation and El Niño-Southern oscillation variability. *Proc Natl Acad Sci* 109:16957–16962
- Brienen RJW, Gloor E, Clerici S, Newton R, Arppe L, Boom A, Bottrell S, Callaghan M, Heaton T, Helama S et al (2017) Tree height strongly affects estimates of water-use efficiency responses to climate and  $\text{CO}_2$  using isotopes. *Nat Commun* 8:288
- Budelsky CA (1969) Variation in transpiration and its relationship with growth for *Pinus ponderosa* Lawson in Southern Arizona
- Castagneri D, Battipaglia G, Von Arx G, Pacheco A, Carrer M (2018) Tree-ring anatomy and carbon isotope ratio show both direct and legacy effects of climate on bimodal xylem formation in *Pinus pinea*. *Tree Physiol* 38:1098–1109
- Cerling TE, Hart JA, Hart TB (2004) Stable isotope ecology in the Ituri forest. *Oecologia* 138:5–12
- Cintra BBL, Gloor M, Boom A, Schöngart J, Locosselli GM, Brienen R (2019) Contrasting controls on tree ring isotope variation for Amazon floodplain and terra firme trees (L Cernusak, Ed.). *Tree Physiol* 39:845–860
- Cullen LE, Grierson PF (2006) Is cellulose extraction necessary for developing stable carbon and oxygen isotopes chronologies from *Callitris glaucophylla*? *Palaeogeogr Palaeoclimatol Palaeoecol* 236:206–216
- Cuny HE, Rathgeber CBK, Kiessé TS, Hartmann FP, Barbeito I, Fournier M (2013) Generalized additive models reveal the intrinsic complexity of wood formation dynamics. *J Exp Bot* 64:1983–1994
- Cuny HE, Rathgeber CBK, Frank D, Fonti P, Fournier M (2014) Kinetics of tracheid development explain conifer tree-ring structure. *New Phytol* 203:1231–1241
- Cuny HE, Rathgeber CBK, Frank D, Fonti P, Mäkinen H, Prislán P, Rossi S, del Castillo EM, Campelo F, Vavřík H et al (2015) Woody biomass production lags stem-girth increase by over one month in coniferous forests. *Nat Plants* 1:15160
- D’Almeida C, Vörösmarty CJ, Hurr G, Marengo JA, Dingman SL, Keim BD (2007) The effects of deforestation on the hydrological cycle in Amazonia: a review on scale and resolution. *Int J Climatol* 27:633–647



- Daux V, Edouard JL, Masson-Delmotte V, Stievenard M, Hoffmann G, Pierre M, Mestre O, Danis PA, Guibal F (2011) Can climate variations be inferred from tree-ring parameters and stable isotopes from *Larix decidua*? Juvenile effects, budmoth outbreaks, and divergence issue. *Earth Planet Sci Lett* 309:221–233
- Dawson TE, Ehleringer JR (1991) Streamside trees that do not use stream water. *Nature* 350:335–337
- Dodd JP, Patterson WP, Holmden C, Brasseur JM (2008) Robotic micromilling of tree-rings: a new tool for obtaining subseasonal environmental isotope records. *Chem Geol* 252:21–30
- Dorado Liñán I, Gutiérrez E, Helle G, Heinrich I, Andreu-Hayles L, Planells O, Leuenberger M, Bürger C, Schleser G (2011) Pooled versus separate measurements of tree-ring stable isotopes. *Sci Total Environ* 409:2244–2251
- Drew DM, Schulze ED, Downes GM (2009) Temporal variation in  $\delta^{13}\text{C}$ , wood density and microfibril angle in variously irrigated *Eucalyptus nitens*. *Funct Plant Biol* 36:1–10
- Duffy JE, McCarroll D, Loader NJ, Young GHF, Davies D, Miles D, Bronk RC (2019) Absence of age-related trends in stable oxygen isotope ratios from oak tree rings. *Global Biogeochem Cycles* 33:841–848
- Eastoe CJ, Dettman DL (2016) Isotope amount effects in hydrologic and climate reconstructions of monsoon climates: implications of some long-term data sets for precipitation. *Chem Geol* 430:78–89
- Esper J, Frank DC, Battipaglia G, Büntgen U, Holert C, Treydte K, Siegwolf R, Saurer M (2010) Low-frequency noise in  $\delta^{13}\text{C}$  and  $\delta^{18}\text{O}$  tree ring data: a case study of *Pinus uncinata* in the Spanish Pyrenees. *Global Biogeochem Cycles* 24:1–11
- Esper J, Konter O, Krusic PJ, Saurer M, Holzkaemper S, Buentgen U (2015) Long-term summer temperature variations in the pyrenees from detrended stable carbon isotopes. *Geochronometria* 42:53–59
- Farquhar GD, Hubick KT, Condon AG, Richards RA (1989) Carbon isotope fractionation and plant water-use efficiency. In: Rundel PW, Ehleringer JR, Nagy KA (eds). Springer New York, New York, NY, pp 21–40
- Ferrio JP, Voltas J (2005) Carbon and oxygen isotope ratios in wood constituents of *Pinus halepensis* as indicators of precipitation, temperature and vapour pressure deficit. *Tellus B Chem Phys Meteorol* 57:164–173
- Frank DC, Poulter B, Saurer M, Esper J, Huntingford C, Helle G, Treydte K, Zimmermann NE, Schleser GH, Ahlström A et al (2015) Water-use efficiency and transpiration across European forests during the anthropocene. *Nat Clim Chang* 5:579–583
- Friedman JM, Stricker CA, Csank AZ, Zhou H (2019) Effects of age and environment on stable carbon isotope ratios in tree rings of riparian *Populus*. *Palaeogeogr Palaeoclimatol Palaeoecol* 524:25–32
- Friend AD, Eckes-Shephard AH, Fonti P, Rademacher TT, Rathgeber CBK, Richardson AD, Turton RH (2019) On the need to consider wood formation processes in global vegetation models and a suggested approach. *Ann for Sci* 76:49
- Gagen M, McCarroll D, Robertson I, Loader NJ, Jalkanen R (2008) Do tree ring  $\delta^{13}\text{C}$  series from *Pinus sylvestris* in northern Fennoscandia contain long-term non-climatic trends? *Chem Geol* 252:42–51
- Gagen M, Finsinger W, Wagner-Cremer F, McCarroll D, Loader NJ, Robertson I, Jalkanen R, Young G, Kirchhefer A (2011) Evidence of changing intrinsic water-use efficiency under rising atmospheric  $\text{CO}_2$  concentrations in Boreal Fennoscandia from subfossil leaves and tree ring  $\delta^{13}\text{C}$  ratios. *Glob Change Biol* 17:1064–1072
- Gagen M, McCarroll D, Jalkanen R, Loader NJ, Robertson I, Young GHF (2012) A rapid method for the production of robust millennial length stable isotope tree ring series for climate reconstruction. *Global Planet Change* 82–83:96–103
- Gessler A, Brandes E, Buchmann N, Helle GG, Rennenberg H, Barnard RL, Bernard R (2009) Tracing carbon and oxygen isotope signals from newly assimilated sugars in the leaves to the tree-ring archive. *Plant Cell Environ* 32:780–795

- Gessler A, Ferrio JP, Hommel R, Treydte K, Werner RA, Monson RK (2014) Stable isotopes in tree rings: towards a mechanistic understanding of isotope fractionation and mixing processes from the leaves to the wood. *Tree Physiol* 34:796–818
- Guerrieri R, Jennings K, Belmecheri S, Asbjornsen H, Ollinger S (2017) Evaluating climate signal recorded in tree-ring  $\delta^{13}\text{C}$  and  $\delta^{18}\text{O}$  values from bulk wood and  $\alpha$ -cellulose for six species across four sites in the northeastern US. *Rapid Commun Mass Spectrom* 31:2081–2091
- Guerrieri R, Belmecheri S, Ollinger SV, Asbjornsen H, Jennings K, Xiao J, Stocker BD, Martin M, Hollinger DY, Bracho-Garrillo R et al (2019) Disentangling the role of photosynthesis and stomatal conductance on rising forest water-use efficiency. *Proc Natl Acad Sci USA* 116:16909–16914
- Helama S, Arppe L, Timonen M, Mielikäinen K, Oinonen M (2015) Age-related trends in subfossil tree-ring  $\delta^{13}\text{C}$  data. *Chem Geol* 416:28–35
- Helle G, Schleser GH, Schlessler GH (2004) Beyond  $\text{CO}_2$ -fixation by Rubisco—an interpretation of  $^{13}\text{C}/^{12}\text{C}$  variations in tree rings from novel intra-seasonal studies on broad-leaf trees. *Plant Cell Environ* 27:367–380
- Higgins RW, Chen Y, Douglas AV (1999) Interannual variability of the North American warm season precipitation regime. *J Clim* 12:653–680
- Johnstone JA, Roden JS, Dawson TE (2013) Oxygen and carbon stable isotopes in coast redwood tree rings respond to spring and summer climate signals. *J Geophys Res Biogeosci* 118:1438–1450
- Kagawa A, Sugimoto A, Maximov TC (2006)  $^{13}\text{C}\text{CO}_2$  pulse-labelling of photoassimilates reveals carbon allocation within and between tree rings. *Plant Cell Environ* 29:1571–1584
- Kagawa A, Sugimoto A, Maximov TC (2006) Seasonal course of translocation, storage and remobilization of  $^{13}\text{C}$  pulse-labeled photoassimilate in naturally growing *Larix gmelinii* saplings. *New Phytol* 171:793–804
- Kagawa A, Sano M, Nakatsuka T, Ikeda T, Kubo S (2015) An optimized method for stable isotope analysis of tree rings by extracting cellulose directly from cross-sectional laths. *Chem Geol* 393–394:16–25
- Keeling RF, Graven HD, Welp LR, Resplandy L, Bi J, Piper SC, Sun Y, Bollenbacher A, Meijer HAJ (2017) Atmospheric evidence for a global secular increase in carbon isotopic discrimination of land photosynthesis. *Proc Natl Acad Sci* 201619240
- Keen RM (2019) Using tree-ring growth and stable isotopes to explore ponderosa pine ecophysiological responses to climate variability and the 2012–2015 California Drought 53
- Keller KM, Lienert S, Bozbiyik A, Stocker TF, Churakova Sidorova OV, Frank DC, Klesse S, Koven CD, Leuenberger M, Riley WJ et al (2017) 20th century changes in carbon isotopes and water-use efficiency: tree-ring-based evaluation of the CLM4.5 and LPX-Bern models. *Biogeosciences* 14:2641–2673
- Kimak A, Leuenberger M (2015) Are carbohydrate storage strategies of trees traceable by early-latewood carbon isotope differences? *Trees Struct Funct* 29:859–870
- Klesse S, DeRose RJ, Guiterman CH, Lynch AM, O'Connor CD, Shaw JD, Evans MEK (2018) Sampling bias overestimates climate change impacts on forest growth in the southwestern United States. *Nat Commun* 9:5336
- Klesse S, Weigt R, Treydte K, Saurer M, Schmid L, Siegwolf RTW, Frank DC (2018b) Oxygen isotopes in tree rings are less sensitive to changes in tree size and relative canopy position than carbon isotopes. *Plant Cell Environ* 1–16
- Kress A, Saurer M, Siegwolf RTW, Frank DC, Esper J, Bugmann H (2010) A 350 year drought reconstruction from Alpine tree ring stable isotopes. *Glob Biogeochem Cycles* 24
- Labuhn I, Daux V, Girardclos O, Stievenard M, Pierre M, Masson-Delmotte V (2016) French summer droughts since 1326 CE: a reconstruction based on tree ring cellulose  $\delta^{18}\text{O}$ . *Climate of the past* 12:1101–1117
- Laumer W, Andreu L, Helle G, Schleser GH, Wieloch T, Wissel H (2009) A novel approach for the homogenization of cellulose to use micro-amounts for stable isotope analyses. *Rapid Commun Mass Spectrom* 23:1934–1940

- Lavergne A, Gennaretti F, Risi C, Daux V, Boucher E, Savard MM, Naulier M, Villalba R, Bégin C, Guiot J (2017) Modelling tree ring cellulose  $\delta^{18}\text{O}$  variations in two temperature-sensitive tree species from North and South America. *Climate of the past* 13:1515–1526
- Lavergne A, Graven H, De Kauwe MG, Keenan TF, Medlyn BE, Prentice IC (2019) Observed and modelled historical trends in the water-use efficiency of plants and ecosystems. *Glob Change Biol* 25:2242–2257
- Lavergne A, Voelker S, Csank A, Graven H, de Boer HJ, Daux V, Robertson I, Dorado-Liñán I, Martínez-Sancho E, Battipaglia G et al (2020) Historical changes in the stomatal limitation of photosynthesis: empirical support for an optimality principle. *New Phytol* 225:2484–2497
- Leavitt SW (2010) Tree-ring C–H–O isotope variability and sampling. *Sci Total Environ* 408:5244–5253
- Leavitt SW, Lara A (1994) South American tree rings show declining  $\text{d}^{13}\text{C}$  trend. *Tellus B* 46:152–157
- Leavitt SW, Long A (1984) Sampling strategy for stable carbon isotope analysis of tree rings in pine. *Nature* 311:145–147
- Leavitt SWSW, Long A (1986) Stable-carbon isotope variability in tree foliage and wood. *Ecology* 67:1002–1010
- Leavitt SW, Wright WE, Long A (2002) Spatial expression of ENSO, drought, and summer monsoon in seasonal  $\delta^{13}\text{C}$  of ponderosa pine tree rings in southern Arizona and New Mexico. *J Geophys Res Atmos* 107 ACL 3-1–ACL 3-10
- Leavitt SW, Treydte K, Yu L (2010) Isoscapes 113–135
- Lévesque M, Siegwolf R, Saurer M, Eilmann B, Rigling A (2014) Increased water-use efficiency does not lead to enhanced tree growth under xeric and mesic conditions. *New Phytol* 203:94–109
- Li Q, Nakatsuka T, Kawamura K, Liu Y, Song H (2011) Regional hydroclimate and precipitation  $\delta^{18}\text{O}$  revealed in tree-ring cellulose  $\delta^{18}\text{O}$  from different tree species in semi-arid Northern China. *Chem Geol* 282:19–28
- Loader NJ, Robertson I, Barker AC, Switsur VR, Waterhouse JS (1997) An improved technique for the batch processing of small wholewood samples to  $\alpha$ -cellulose. *Chem Geol* 136:313–317
- Loader NJ, Robertson I, McCarroll D (2003) Comparison of stable carbon isotope ratios in the whole wood, cellulose and lignin of oak tree-rings. *Palaeogeogr Palaeoclimatol Palaeoecol* 196:395–407
- Loader NJ, Young GHF, McCarroll D, Wilson RJS (2013) Quantifying uncertainty in isotope dendroclimatology. *Holocene* 23:1221–1226
- Loader NJ, Young GHF, Grudd H, McCarroll D (2013) Stable carbon isotopes from Torneträsk, northern Sweden provide a millennial length reconstruction of summer sunshine and its relationship to Arctic circulation. *Quatern Sci Rev* 62:97–113
- Lockhart JA (1965) An analysis of irreversible plant cell elongation. *J Theor Biol* 8:264–275
- Mayr C, Frenzel B, Friedrich M, Spurk M, Stichler W, Trimborn P (2003) Stable carbon- and hydrogen-isotope ratios of subfossil oaks in southern Germany: methodology and application to a composite record for the Holocene. *Holocene* 13:393–402
- McCarroll D, Loader NJ (2004) Stable isotopes in tree rings. *Quatern Sci Rev* 23:771–801
- McCarroll D, Whitney M, Young GHF, Loader NJ, Gagen MH (2017) A simple stable carbon isotope method for investigating changes in the use of recent versus old carbon in oak. *Tree Physiol* 37:1021–1027
- McDowell NG, Bond BJ, Dickman LT, Ryan MG, Whitehead D (2011) Relationships between tree height and carbon isotope discrimination. In: Meinzer FC, Lachenbruch B, Dawson T (eds) *Size- and age-related changes in tree structure and function* 255–286
- Medlyn BE, De Kauwe MG, Lin Y-S, Knauer J, Duursma RA, Williams CA, Arneth A, Clement R, Isaac P, Limousin J-M, et al (2017) How do leaf and ecosystem measures of water-use efficiency compare? *New Phytol*
- Miles PD, Smith WB (2009) Specific gravity and other properties of wood and bark for 156 tree species found in North America
- Monserud RA, Marshall JD (2001) Time-series analysis of delta C-13 from tree rings. I. Time trends and autocorrelation. *Tree Physiol* 21:1087–1102

- Monson RK, Szejner P, Belmecheri S, Morino KA, Wright WE (2018) Finding the seasons in tree ring stable isotope ratios. *Am J Bot* 105:1–3
- Moreno-Gutiérrez C, Battipaglia G, Cherubini P, Saurer M, Nicolás E, Contreras S, Querejeta JI (2012) Stand structure modulates the long-term vulnerability of *Pinus halepensis* to climatic drought in a semiarid Mediterranean ecosystem. *Plant Cell Environ* 35:1026–1039
- Nagavciuc V, Ionita M, Perșoiu A, Popa I, Loader NJ, McCarroll D (2019) Stable oxygen isotopes in Romanian oak tree rings record summer droughts and associated large-scale circulation patterns over Europe. *Clim Dyn* 52:6557–6568
- Nehrbass-Ahles C, Babst F, Klesse S, Nötzli M, Bouriaud O, Neukom R, Dobbertin M, Frank D (2014) The influence of sampling design on tree-ring-based quantification of forest growth. *Glob Change Biol* 20:2867–2885
- Nied R (2007) Chapter 5 rotor impact mills. In: *Handbook of powder technology*, vol 12, pp 229–249
- Offermann C, Ferrio JP, Holst J, Grote R, Siegwolf R, Kayler Z, Gessler A (2011) The long way down—are carbon and oxygen isotope signals in the tree ring uncoupled from canopy physiological processes? *Tree Physiol* 31:1088–1102
- Ogée J, Barbour MM, Wingate L, Bert D, Bosc A, Stievenard M, Lambrot C, Pierre M, Bariac T, Loustau D et al (2009) A single-substrate model to interpret intra-annual stable isotope signals in tree-ring cellulose. *Plant Cell Environ* 32:1071–1090
- Pacheco A, Camarero JJ, Ribas M, Gazol A, Gutierrez E, Carrer M (2018) Disentangling the climate-driven bimodal growth pattern in coastal and continental Mediterranean pine stands. *Sci Total Environ* 615:1518–1526
- Pacheco A, Camarero JJ, Pompa-García M, Battipaglia G, Voltas J, Carrer M (2020) Growth, wood anatomy and stable isotopes show species-specific couplings in three Mexican conifers inhabiting drought-prone areas. *Sci Total Environ* 698:134055
- Pallardy SG (2008) *Physiology of Woody plants*. Elsevier
- Perugini L, Caporaso L, Marconi S, Cescatti A, Quesada B, De Noblet-Ducoudré N, House JJ, Arneth A (2017) Biophysical effects on temperature and precipitation due to land cover change. *Environ Res Lett* 12:53002
- Pettersen RC (1984) The chemical composition of wood, pp 57–126
- Poussart PF, Evans MN, Schrag DP (2004) Resolving seasonality in tropical trees: multi-decade, high-resolution oxygen and carbon isotope records from Indonesia and Thailand. *Earth Planet Sci Lett* 218:301–316
- Rathgeber CBK, Cuny HE, Fonti P (2016) Biological basis of tree-ring formation: a crash course. *Front Plant Sci* 7:1–7
- Rinne KT, Boettger T, Loader NJ, Robertson I, Switsur VR, Waterhouse JS (2005) On the purification of  $\alpha$ -cellulose from resinous wood for stable isotope (H, C and O) analysis. *Chem Geol* 222:75–82
- Roden JS, Ehleringer JR (1999) Hydrogen and oxygen isotope ratios of tree-ring cellulose for riparian trees grown long-term under hydroponically controlled environments. *Oecologia* 121:467–477
- Roden JS, Ehleringer JR (2000) Hydrogen and oxygen isotope ratios of tree ring cellulose for field-grown riparian trees. *Oecologia* 123:481–489
- Roden JS, Johnstone JA, Dawson TE (2009) Intra-annual variation in the stable oxygen and carbon isotope ratios of cellulose in tree rings of coast redwood (*Sequoia sempervirens*). *Holocene* 19:189–197
- Salati E, Nobre CA (1991) Possible climatic impacts of tropical deforestation. *Clim Change* 19:177–196
- Saurer M, Borella S, Schweingruber F, Siegwolf R (1997) Stable carbon isotopes in tree rings of beech: Climatic versus site-related influences. *Trees Struct Funct* 11:291–297
- Saurer M, Siegwolf RTW, Schweingruber FH, Saurer M, Siegwolf RT, Schweingruber FH (2004) Carbon isotope discrimination indicates improving water-use efficiency of trees in northern Eurasia over the last 100 years. *Glob Change Biol* 10:2109–2120

- Saurer M, Spahni R, Frank DC, Joos F, Leuenberger M, Loader NJ, McCarroll D, Gagen M, Poulter B, Siegwolf RTW et al (2014) Spatial variability and temporal trends in water-use efficiency of European forests. *Glob Change Biol* 20:3700–3712
- Sheppard PRP, Comrie AAC, Packin GDG, Angersbach K, Hughes MMK (2002) The climate of the US Southeast. *Climate Res* 21:219–238
- Sidorova OV, Siegwolf RTW, Saurer M, Naurzbaev MM, Shashkin AV, Vaganov EA (2010) Spatial patterns of climatic changes in the Eurasian north reflected in Siberian larch tree-ring parameters and stable isotopes. *Glob Change Biol* 16:1003–1018
- Sidorova OV, Siegwolf RTW, Saurer M, Naurzbaev MM, Vaganov EA (2008) Isotopic composition ( $\gamma^{13}\text{C}$ ,  $\gamma^{18}\text{O}$ ) in wood and cellulose of Siberian larch trees for early Medieval and recent periods. *J Geophys Res Biogeosciences* 113
- Soudant A, Loader NJ, Bäck J, Levula J, Kljun N (2016) Intra-annual variability of wood formation and  $\delta^{13}\text{C}$  in tree-rings at Hyytiälä, Finland. *Agric for Meteorol* 224:17–29
- Szejner P, Wright WE, Babst F, Belmecheri S, Trouet V, Leavitt SW, Ehleringer JR, Monson RK (2016) Latitudinal gradients in tree ring stable carbon and oxygen isotopes reveal differential climate influences of the North American Monsoon System. *J Geophys Res Biogeosci* 121:1978–1991
- Szejner P, Wright WE, Belmecheri S, Meko D, Leavitt SW, Ehleringer JR, Monson RK (2018) Disentangling seasonal and interannual legacies from inferred patterns of forest water and carbon cycling using tree-ring stable isotopes. *Glob Change Biol* 24:5332–5347
- Szejner P, Belmecheri S, Ehleringer JR, Monson RK (2020) Recent increases in drought frequency cause observed multi-year drought legacies in the tree rings of semi-arid forests. *Oecologia* 192:241–259
- Szejner P, Clute T, Anderson E, Evans MN, Hu J (2020b) Reduction in lumen area is associated with the  $\delta^{18}\text{O}$  exchange between sugars and source water during cellulose synthesis. *New Phytol*
- Szejner P (2011) Tropical dendrochronology: exploring tree rings of *Pinus oocarpa* in Eastern Guatemala
- Szymczak S, Joachimski MM, Bräuning A, Hetzer T, Kuhlemann J (2011) Comparison of whole wood and cellulose carbon and oxygen isotope series from *Pinus nigra* ssp. *laricio* (Corsica/France). *Dendrochronologia* 29:219–226
- Szymczak S, Brauning A, Hausser M, Garel E, Huneau FF, Santoni SS, Bräuning A, Häusser M, Garel E, Huneau FF et al (2019) The relationship between climate and the intra-annual oxygen isotope patterns from pine trees: a case study along an elevation gradient on Corsica, France. *Ann For Sci* 76:76
- Talbott LD, Rahveh E, Zeiger E (2003) Relative humidity is a key factor in the acclimation of the stomatal response to  $\text{CO}_2$ . *J Exp Bot* 54:2141–2147
- Treydte KS, Schleser GH, Helle G, Frank DC, Winiger M, Haug GH, Esper J (2006) The twentieth century was the wettest period in northern Pakistan over the past millennium. *Nature* 440:1179–1182
- Treydte K, Boda S, Graf Pannatier E, Fonti P, Frank D, Ullrich B, Saurer M, Siegwolf R, Battipaglia G, Werner W et al (2014) Seasonal transfer of oxygen isotopes from precipitation and soil to the tree ring: source water versus needle water enrichment. *New Phytol* 202:772–783
- Vadeboncoeur MA, Jennings KA, Ouimette AP, Asbjornsen H (2020) Correcting tree-ring  $\delta^{13}\text{C}$  time series for tree-size effects in eight temperate tree species (L Cernusak, Ed.). *Tree Physiol* 40:333–349
- Vaganov EA, Hughes MK, Shashkin AV (2006) Growth dynamics of conifer tree rings. Springer-Verlag, Berlin/Heidelberg
- Vaganov EA, Anchukaitis KJ, Evans MN (2011) How well understood are the processes that create dendroclimatic records? A mechanistic model of the climatic control on conifer tree-ring growth dynamics. In: Hughes MK, Swetnam TW, Diaz HF (eds). Springer Netherlands, Dordrecht, pp 37–75

- van der Sleen P, Groenendijk P, Vlam M, Anten NPR, Boom A, Bongers F, Pons TL, Terburg G, Zuidema PA (2014) No growth stimulation of tropical trees by 150 years of CO<sub>2</sub> fertilization but water-use efficiency increased. *Nat Geosci* 8:24–28
- Verheyden A, Helle G, Schleser GH, Dehairs F, Beeckman H, Koedam N (2004) Annual cyclicity in high-resolution stable carbon and oxygen isotope ratios in the wood of the mangrove tree *Rhizophora mucronata*. *Plant Cell Environ* 27:1525–1536
- Voelker SL, Roden JS, Dawson TE (2018) Millennial-scale tree-ring isotope chronologies from coast redwoods provide insights on controls over California hydroclimate variability. *Oecologia* 187:897–909
- Voelker SL, Merschel AG, Meinzer FC, Ulrich DEMM, Spies TA, Still CJ (2019) Fire deficits have increased drought sensitivity in dry conifer forests: fire frequency and tree-ring carbon isotope evidence from Central Oregon. *Glob Change Biol* 25:1247–1262
- Walcroft AS, Silvester WB, Whitehead D, Kelliher FM (1997) Seasonal changes in stable carbon isotope ratios within annual rings of *Pinus radiata* reflect environmental regulation of growth processes. *Aust J Plantphysiology* 24:57–68
- Weigt RB, Bräunlich S, Zimmermann L, Saurer M, Grams TEE, Dietrich HP, Siegwolf RTW, Nikolova PS (2015) Comparison of  $\delta^{18}\text{O}$  and  $\delta^{13}\text{C}$  values between tree-ring whole wood and cellulose in five species growing under two different site conditions. *Rapid Commun Mass Spectrom* 29:2233–2244
- Wigley TML, Briffa KR, Jones PD (1984) On the average value of correlated time series, with applications in dendroclimatology and hydrometeorology. *J Climate Appl Meteorol* 23:201–213
- Wright WE, Leavitt SW (2006) Needle cell elongation and maturation timing derived from pine needle cellulose  $\delta^{18}\text{O}$ . *Plant Cell Environ* 29:1–14
- Wright WE, Leavitt SW (2006) Boundary layer humidity reconstruction for a semiarid location from tree ring cellulose  $\delta^{18}\text{O}$ . *J Geophys Res Atmos* 111:1–9
- Wright WE (2001) Delta-deuterium and delta-oxygen-18 in mixed conifer systems in the United States southwest: the potential of delta-oxygen-18 in *Pinus ponderosa* tree rings as a natural environmental recorder. Department of Geosciences PhD
- Xu G, Liu X, Trouet V, Treydte K, Wu G, Chen T, Sun W, An W, Wang W, Zeng X et al (2019) Regional drought shifts (1710–2010) in East Central Asia and linkages with atmospheric circulation recorded in tree-ring  $\delta^{18}\text{O}$ . *Clim Dyn* 52:713–727
- Xu C, Sano M, Nakatsuka T (2011) Tree ring cellulose  $\delta^{18}\text{O}$  of *Fokienia hodginsii* in northern Laos: a promising proxy to reconstruct ENSO? *J Geophys Res Atmos* 116
- Xu G, Liu X, Sun W, Szejner P, Zeng X, Yoshimura K, Trouet V (2020) Seasonal divergence between soil water availability and atmospheric moisture recorded in intra-annual tree-ring  $\delta^{18}\text{O}$  extremes. *Environ Res Lett*
- Yi K, Maxwell JT, Wenzel MK, Roman DT, Sauer PE, Phillips RP, Novick KA (2019) Linking variation in intrinsic water-use efficiency to isohydrlicity: a comparison at multiple spatiotemporal scales. *New Phytol* 221:195–208
- Yokoyama T, Inoue Y (2007) Chapter 10 selection of fine grinding mills. In: *Handbook of Powder Technology*, vol 12, pp 487–508
- Yoshimura F, Suzuki T (1975) Calcium-stimulated adenosine triphosphatase in the microsomal fraction of tooth germ from porcine fetus. *Biochem Biophys Acta* 410:167–177
- Young GHF, McCarroll D, Loader NJ, Kirchhefer AJ (2010) A 500-year record of summer near-ground solar radiation from tree-ring stable carbon isotopes. *Holocene* 20:315–324
- Young GHF, Demmler JC, Gunnarson BE, Kirchhefer AJ, Loader NJ, McCarroll D (2011) Age trends in tree ring growth and isotopic archives: a case study of *Pinus sylvestris* L. from northwestern Norway. *Glob Biogeochem Cycles* 25
- Zalloni E, de Luis M, Campelo F, Novak K, De Micco V, Di Filippo A, Vieira J, Nabais C, Rozas V, Battipaglia G (2016) Climatic signals from intra-annual density fluctuation frequency in Mediterranean pines at a regional scale. *Front Plant Sci* 7:579

- Zhu M, Stott L, Buckley B, Yoshimura K, Ra K (2012) Indo-Pacific Warm Pool convection and ENSO since 1867 derived from Cambodian pine tree cellulose oxygen isotopes. *J Geophys Res Atmos* 117
- Ziaco E, Biondi F, Rossi S, Deslauriers A (2016) Environmental drivers of cambial phenology in Great Basin bristlecone pine. *Tree Physiol* 36:818–831
- Zuidema PA, Poulter B, Frank DC (2018) A wood biology agenda to support global vegetation modelling. *Trends Plant Sci* 23:1006–1015

**Open Access** This chapter is licensed under the terms of the Creative Commons Attribution 4.0 International License (<http://creativecommons.org/licenses/by/4.0/>), which permits use, sharing, adaptation, distribution and reproduction in any medium or format, as long as you give appropriate credit to the original author(s) and the source, provide a link to the Creative Commons license and indicate if changes were made.

The images or other third party material in this chapter are included in the chapter's Creative Commons license, unless indicated otherwise in a credit line to the material. If material is not included in the chapter's Creative Commons license and your intended use is not permitted by statutory regulation or exceeds the permitted use, you will need to obtain permission directly from the copyright holder.



# Chapter 5

## Stable Isotope Signatures of Wood, its Constituents and Methods of Cellulose Extraction



Gerhard Helle, Maren Pauly, Ingo Heinrich, Karina Schollän, Daniel Balanzategui, and Lucas Schürheck

**Abstract** In this chapter, we give some basic information on the chemical and isotopic properties of wood constituents and describe their relative contribution to the isotopic signature of wood. Based on these considerations we review studies that have compared stable isotope signals of wood with those of corresponding cellulose. We exemplify how relationships of wood-based tree-ring stable isotope sequences with climate can be affected by varying proportions of wood constituents like cellulose, lignin and extractives. A majority of benchmarking studies suggests that cellulose extraction may not be necessary. However, based upon existing research, a general statement cannot be made on the necessity of cellulose extraction. Changes in wood composition can particularly influence environmental signal strength during periods of low isotope variability. Cellulose extraction removes any effects from changing wood composition. We present the three established chemical approaches of extraction, outline how to test the purity of isolated cellulose and present user-friendly efficient experimental setups allowing to simultaneously process hundreds of samples in one batch. Further, we briefly address the analysis of stable isotopes of lignin methoxyl groups because of easy sample preparation and its potential additional value for studies on fossil wood.

---

**Supplementary Information** The online version contains supplementary material available at [https://doi.org/10.1007/978-3-030-92698-4\\_5](https://doi.org/10.1007/978-3-030-92698-4_5).

---

G. Helle (✉) · M. Pauly · I. Heinrich · K. Schollän · D. Balanzategui · L. Schürheck  
GFZ German Research Centre for Geosciences, Telegrafenberg, Potsdam, Germany  
e-mail: [ghelle@gfz-potsdam.de](mailto:ghelle@gfz-potsdam.de)

M. Pauly  
School of Science, Bath Spa University, Bath, UK

I. Heinrich · D. Balanzategui  
German Archaeological Institute DAI, Berlin, Germany



## 5.1 Introduction

At the beginning of tree-ring stable isotope investigations, bulk wood was used without any chemical pre-treatment (e.g. Craig 1954; Farmer and Baxter 1974; Libby and Pandolfi 1974). However, wood is a chemically complex material consisting of various biopolymers (cellulose, lignin, resin etc.) with divergent isotopic signatures (Taylor et al. 2008; Loader et al. 2003; DeNiro and Epstein 1977; Schmidt et al. 1998, 2001; Wilson and Grinsted 1977). Consequently, the use of bulk wood is usually avoided in eco-physiological or climatological stable isotope studies due to potentially changing mass proportions of the different wood constituents relative to each other, different seasonal timing of formation and possible mobility (of extractives) across tree-rings that may cause signal distortion of the tree-ring isotope records. Instead, it is presumed that analysis of one of the major wood constituents, usually cellulose rather than lignin, can ensure isotopic records uninfluenced of changing mass proportions over the life span of a tree. Cellulose ( $\alpha$ -cellulose or, holocellulose which is  $\alpha$ -cellulose and hemicellulose) is the most abundant and most important structural constituent of any terrestrial plant cell wall and it is most frequently chosen for tree-ring stable isotope analyses. It is preferred over lignin because cellulose is a chemically well-defined macromolecule and remains basically immobile during the lifespan of a tree, i.e. the time of polymerization (not necessarily the time of uptake of inorganic precursors by the tree) is always tied to the formation of the annual tree ring. Furthermore, its isolation is relatively simple involving only a few chemicals. Yet, the traditional procedures of cellulose isolation like those described by Green (1963) were tedious. Offline mass spectrometric analysis was the time limiting step in stable isotope analysis, and thus no major efforts in optimizing the methodology of cellulose extraction had to be made. Modern continuous-flow isotope ratio mass spectrometry permits efficient measurement of large sample numbers using minimal sample amounts (few micrograms) (e.g. Loader et al. 2015; Woodley et al. 2012). Sample preparation has become the limiting step in terms of cost and sample throughput and several studies have used bulk wood material with or without prior testing if the bulk wood (or extractives-free wood) and cellulose isotope values are highly cross correlated and show similar relationship, variability and significance to the environmental or climate dynamics against time series of instrumental data. Nonetheless, these approaches are compromises to circumvent the constraints of classical chemical sample preparation. More efficient extraction techniques were developed capable of processing micro-amounts of sample material, while at the same time ensuring high quality in terms of sample purity and homogeneity (e.g. Andreu-Hayles et al. 2019; Schollaen et al. 2017; Kagawa et al. 2015). Ongoing advances in the dissection tree-rings and/or parts thereof using on- and offline UV-laser ablation or UV-laser dissection microscopes (cf. Chap. 7) have challenged the current development of well-adapted sample preparation techniques (e.g. Schollaen et al. 2014, 2017).

Several methodologies have been proposed for the isolation of holo- or  $\alpha$ -cellulose from wood for isotopic analysis. They differ from one another to a greater or lesser

extent concerning the extraction chemistry applied and/or specific devices and reaction vessels developed for improving efficiency by reducing labor time and costs for consumables and laboratory equipment (Andreu-Hayles et al. 2019; Kagawa et al. 2015; Loader et al. 1997; Schollaen et al. 2017; Anchukaitis et al. 2008). Besides the efforts in improving chemical sample preparation for C, O and H isotope analysis of tree-ring cellulose, C and H isotope analysis of lignin methoxyl groups by GC-C/TC-IRMS (Keppler et al. 2007) has been introduced as a novel approach in stable isotope dendroclimatology with a fast and easy preparation method.

In this chapter, we provide some basic information on the chemical and isotopic properties of wood constituents and describe their relative contribution to the isotopic signature of wood. Based on these considerations we review studies that have compared stable isotope signals of wood with those of corresponding cellulose and discuss why the extraction and use of cellulose instead of wood is of benefit. We address the analysis of stable isotopes of lignin methoxyl groups and its additional value. Last, but not least we describe the most commonly used chemical approaches and efficient experimental setups for extracting cellulose and outline how to test the purity of the resulting cellulose.

## 5.2 Whole Wood, Resin Extracted Wood, Lignin or Cellulose?

### 5.2.1 *Basic Considerations from Chemical and Isotopic Properties of Wood Constituents*

Wood is composed of  $\alpha$ -cellulose, hemicellulose, lignin, resin and other extractives that show very different intrinsic isotopic signatures. For carbon, the extent of the general depletion of primary sugars in  $^{13}\text{C}$  relative to the atmospheric  $\text{CO}_2$  pool due to availability of  $\text{CO}_2$  for photosynthesis (Farquhar et al. 1982) is the very foundation of eco-physiological and palaeoclimatological interpretation. Beyond leaf level physiology, photosynthetic intermediates are modified further at various metabolic branching points in primary and secondary plant metabolism. This is due to the involvement of (predominately) kinetic, isotope effects on multiple enzyme reactions during the polymerization or breakdown of precursor substances of the wood constituents (Gleixner et al. 1993; Schmidt et al. 1998). A progressive depletion in  $^{13}\text{C}$  can be usually observed with metabolic distance from a metabolic branching point (Schmidt et al. 1993). Accordingly, carbohydrates from primary plant metabolism like sugars, starch, hemi- or  $\alpha$ -cellulose normally have heavier isotopic signatures than secondary metabolites (e.g. lignin or fatty acids) that originate from different and rather long metabolic pathways. Hemi- and  $\alpha$ -cellulose are usually found enriched in  $^{13}\text{C}$  over lignin and fatty acids by 2 to 4 ‰ on average (Table 5.1) (e.g. Robertson et al. 2004; Schmidt et al. 1998 and citations therein). These differences vary with

**Table 5.1**  $\delta^{13}\text{C}$  and  $\delta^{18}\text{O}$  of lignin and their offsets to corresponding values of cellulose. Only data of pine and oak have been published so far

Species	$\delta^{13}\text{C}_{\text{Lig}} \text{‰}$ vs. VPDB	Offset (C – L)	$\delta^{18}\text{O}_{\text{Lig}} \text{‰}$ vs. SMOW	Offset (C – L)	Reference
<i>P. glauca</i>	NA	NA	$+13.5 \pm 1.5$	10.6	Gray and Thompson (1977) <sup>a</sup>
<i>Quercus spp.</i>	NA	NA	$+22.1 \pm 3.5$	6.9	Barbour et al. (2001) <sup>a</sup>
<i>Pinus spp.</i>	NA	NA	$+21.4 \pm 5.4$	6.4	Barbour et al. (2001) <sup>a</sup>
<i>P. halepensis</i>	$-25.2 \pm 0.6$	2.5	$+22.7 \pm 2.4$	8.6	Ferrio and Voltas (2005) <sup>a</sup>
<i>Q. petraea</i>	$-27.17 \pm 0.8$	2.41	NA	NA	Robertson et al. (2004)
<i>P. radiata</i>	$-28.8 \pm 1.2$	ca. 3.5	NA	NA	Wilson and Grinsted (1977)
<i>P. ponderosa</i>	$-21.0 \pm 0.8$	4.1	NA	NA	Mazany et al. (1980)
<i>Q. robur</i>	ca. $-23.8$	ca. 3	NA	NA	Loader et al. (2003)

NA = Not analysed

<sup>a</sup> Isotope data of lignin obtained gravimetrically from combined mass balance calculations and  $\delta^{18}\text{O}$  analyses of solvent-extracted wood, hemicellulose and  $\alpha$ -cellulose or holocellulose

tree species, tree age, tree organ (e.g. leaf/needle, sapwood, heartwood etc.) and site conditions.

The majority of comparative stable isotope studies on different wood constituents were on carbon and conclusions drawn cannot simply be transferred to hydrogen or oxygen isotopes. Oxygen and hydrogen atoms of chemical wood constituents basically originate from water and, their isotopic signatures are characterized by various exchange reactions of their different precursors at leaf level and beyond (cf. Chaps. 10 and 11 for details), potentially leading to insignificant correlation of  $\delta^{18}\text{O}$  data of cellulose and lignin (Gray and Thompson 1977).

Cellulose is generally enriched in  $^{18}\text{O}$  by  $\sim +27 \pm 4\%$  versus leaf water due to an equilibrium isotope effect between carbonyl groups and water (Sternberg 1989). Hemi- and  $\alpha$ -cellulose were found to have rather similar oxygen isotopic compositions (Gray and Thompson 1977; Richard et al. 2014).

Generally, the  $\delta^{18}\text{O}$  of aromatic compounds like lignin attains values of around  $+12\%$  (vs. V-SMOW) (Schmidt et al. 2001) revealing significantly lower  $\delta^{18}\text{O}$  values than cellulose. However, to our knowledge no data from direct  $\delta^{18}\text{O}$  measurements on chemically extracted lignin do exist, as the extraction procedure (hydrolysis with 72%  $\text{H}_2\text{SO}_4$  at 20 °C, (Klason 1911; TAPPI 1988) usually applied in  $\delta^{13}\text{C}$  studies

may affect  $\delta^{18}\text{O}$  of remaining acid-insoluble lignin. Estimates of  $\delta^{18}\text{O}$  of lignin were obtained gravimetrically from combined mass balance calculations and  $\delta^{18}\text{O}$  analyses of solvent-extracted wood, hemicellulose and  $\alpha$ -cellulose. The calculated  $\delta^{18}\text{O}$  values of lignin were found quite variable and the offsets in  $\delta^{18}\text{O}$  between cellulose and lignin appear to be larger and more variable than the offsets reported for  $\delta^{13}\text{C}$  (Table 5.1).

A similar picture likely holds for hydrogen stable isotopes.  $\delta^2\text{H}$  values of cellulose tend to be higher by 30 to 40‰ than those of corresponding bulk wood due to significantly lower  $\delta^2\text{H}$  values of lignin than those of cellulose (Gori et al. 2013).  $\delta^2\text{H}$  values of wood ( $\delta^2\text{H}_w$ ) collected from various sites between 69°N and 1°S of the equator were always found to be higher ( $\delta^2\text{H}_w = -141$  to  $-29$ ‰ vs. V-SMOW) than  $\delta^2\text{H}$  ( $\delta^2\text{H}_L$ ) obtained from corresponding lignin methoxyl groups ( $\delta^2\text{H}_L = -325$  to  $-153$ ‰ vs. V-SMOW) (Keppler et al. 2007).

While the general differences between the stable isotope values for various wood constituents are a consequence of enzyme-specific fractionations at various metabolic branching points involved in their biosynthesis, the definite extent of isotopic shifts depend on flux rates at metabolic branching points as well as the isotopic signature and the pool sizes of precursor substances which can vary with changing ambient environmental conditions (for details cf. Schmidt et al. 2001, 2003; Keppler et al. 2007; Schmidt 1999).

## 5.2.2 *The Isotope Signatures of Wood as a Result of Relative Contributions of Its Individual Constituents*

### 5.2.2.1 Cellulose and Lignin

The major and also minor wood constituents derived from primary and secondary plant metabolism hold intrinsic differences in their stable isotope C, O and H signatures. Their relative contribution to the isotopic composition of bulk wood depends on the extent of isotopic difference and relative mass contribution of individual constituents.

Hemi- and  $\alpha$ -cellulose together form the largest part within wood (on average 65–75%). They are composed of ca. 45% carbon, 6% hydrogen and 49% oxygen, whereas lignin contains around 60–70% carbon, 6–7% hydrogen and 20–30% oxygen, depending on the relative contribution of monolignols and degree of methoxylation. The lignin content of different woody species can vary between 15 and 36% of the dry weight of wood (e.g. Kürschner and Popik 1962; Pettersen 1984). However, within the same species variability appears to be lower. For pine trees, a range from 25 to 30% has been observed (Zobel and van Buijtenen 1989). On average, gymnosperms have a slightly higher lignin content than angiosperms. Within the same plant lignin can vary also in quantity and composition between different cell types and tissues (Agarwal and Atalla 1986; Boudet 2000). For example, wood formed at the top

of a mature conifer typically has a higher lignin content than wood from further down the stem (Zobel and van Buijtenen 1989). The overall lignin quantity and its composition of different alcohol monomers can also vary depending on location in the cell wall, developmental state of the cell and tissue, and the influence of environmental stress (Zobel and van Buijtenen 1989). Hence, the relative lignin content can vary radially within a tree ring, i.e. from earlywood to latewood (Wilson and Wellwood 1965; Lanvermann et al. 2013; Fergus et al. 1969; Gindl 2001; Fukazawa and Imagawa 1981). Also, radially across the trunk heartwood was found to contain significantly more lignin and less cellulose than sapwood e.g. in *P. abies* (Bertaud and Holmbom 2004) or in *Tectona grandis* (Narayanamurti and Das 1955). This may particularly affect the significance of time series of eco-physiological or climatic signals in tree-ring stable isotope sequences.

### 5.2.2.2 Extractives

Besides cellulose and lignin, extractives, i.e. nonstructural substances that are soluble in organic solvents or water, represent an additional contribution of carbon, oxygen and hydrogen in bulk wood. They are supposed to be rather mobile within the wood and resin or fatty acids can have highly variable carbon and hydrogen contents of up to more than 70% with oxygen contributing not more than around 20%. Extractives in sapwood, often starch, simple sugars or lipids, are generally considered to be energy reserve materials for the tree and carbohydrate and lipid extractives are believed to be converted to compounds during heartwood transformation such as phenols and terpenes (resin) in rather variable amounts contributing to a passive defense to prevent attack by wood destroying insects and fungi (Keith 1969; Hillis 1987; Friedman et al. 2019; Schmidt 1999; Taylor et al. 2002, 2007). Extractives may show a very wide range of  $\delta$ -values, however, as most of them derive from secondary plant metabolism it can be assumed that their stable isotope signatures are considerably depleted as compared to cellulose (Schmidt 1999), but stable isotopes of extractives also revealed significant correlations, at least with respect to carbon (Taylor et al. 2007, 2008). The few studies that have compared bulk wood and extractives-free wood have found no difference or shifts of only up to  $+0.3\text{‰}$  on average in  $\delta^{13}\text{C}$  after removal of extractives (e.g. Harlow et al. 2006; Richard et al. 2014; Ferrio and Voltas 2005). With respect to oxygen positive as well as negative shifts were obtained from *P. pinaster* wood from multiple sites with an average of  $+0.24 \pm 0.6\text{‰}$  (Ferrio and Voltas 2005). From these studies it can be derived that the effects of extractives on the overall isotopic signature of wood might be negligible. However, the amount of extractives in wood can be highly variable. In heartwood of various pine species contents ranging between 5–62% (5–34% *P. sylvestris*, 15–62% *P. nigra*) were found, whereas their content was found fairly stable in sapwood (3–5%). A similar, but smaller radial gradient was found in young trees ranging from 7% (central wood) to 2.5% (outermost rings) (Kurth 1933), and also the chemical properties of extractives can differ between sapwood and heartwood (Keith 1969; Hillis 1987). This can add to the potential differences in lignin and cellulose contents between heartwood and

sapwood resulting in isotopic trends that may mask ecological or climatological long-term information. Extractives obtained from broadleaf woody species growing in temperate climates can constitute up to 10% of dry weight and up to 20% in certain tropical tree species (Pettersen 1984). Besides the general differences found between tree species and gradients across the trunk, the content of extractives can vary in relation to particular environmental incidents such as fire or drought which may induce, for example, resin production or may act as part of the trees' defense mechanism against microbial attack (e.g. Hall 1993; Guest and Brown 1997).

### 5.2.3 *Estimating Potential Effects or Implications of Variable Proportions of Wood Constituents*

Prior to any test measurements the variability of the stable isotope composition of wood due to changing proportions of different wood constituents with their various isotope compositions can be estimated by simple exercises using mass balance equations as demonstrated by e.g. Richard et al. (2014) or Schleser et al. (2015). SM5.2.3 details a general equation for calculating the  $\delta$  value of carbon, oxygen or hydrogen of bulk wood from the relative mass proportions of cellulose, lignin and extractives and their respective isotopic signature. An example calculation of  $\delta^{13}\text{C}$  of bulk wood ( $\delta^{13}\text{C}_{\text{bW}}$ ) for a hypothetical conifer sample is also given. Assuming an average composition of 65% cellulose, 27% lignin and 8% resin and a constant difference of 3.5‰ between cellulose and secondary plant metabolites lignin and resin (i.e. assuming the same  $\delta^{13}\text{C}$  value for lignin and extractives) mass balance calculation results in an offset of  $\delta^{13}\text{C}$  of cellulose ( $\delta^{13}\text{C}_{\text{c}}$ ) to  $\delta^{13}\text{C}_{\text{bW}}$  ( $\delta^{13}\text{C}_{\text{c}} - \delta^{13}\text{C}_{\text{bW}} = 1.59\text{‰}$ ) that is well around the mean of real values observed (Table 5.2a). Compared to  $\delta^{13}\text{C}_{\text{bW}}$ , resin-extracted wood ( $\delta^{13}\text{C}_{\text{eW}}$ ) is calculated slightly less negative by 0.24‰ ( $\delta^{13}\text{C}_{\text{c}} - \delta^{13}\text{C}_{\text{eW}} = 1.35\text{‰}$ ). Such an example indicates that the contribution of extractives like resin to the overall stable isotope value of wood may be negligible if their mass fraction of carbon, oxygen or hydrogen from these extractives make up only a small percentage of the wood and/or if the isotope values of these fractions are mainly in the ranges of the major wood constituents cellulose or lignin. Perhaps more important than the influences of extractives are changing relative proportions of the major constituents cellulose and lignin. As outlined above (Sect. 5.2.2), the proportion of cellulose can increase up to 80% with the lignin content decreasing down to 20% (e.g. in reaction wood). This would lead to an offset of ( $\delta^{13}\text{C}_{\text{c}} - \delta^{13}\text{C}_{\text{eW}} = 0.96\text{‰}$ ). It has to be emphasized that in this example a constant isotopic difference between cellulose and lignin of 3.5‰ has been assumed, however, this isotopic difference not only differs between species (Table 5.1), but potentially changes within a tree and may vary with time, site conditions and wood preservation, as demonstrated in Sect. 5.2.4.3 and Figs. 5.1 and 5.2.

Similar mass balance calculations as for carbon isotopes may suggest that the potential influence of varying cellulose to lignin proportions on  $\delta^{18}\text{O}$  and  $\delta\text{D}$  values

**Table 5.2** Overview of comparative studies on stable isotopes of carbon (a), oxygen (b) and hydrogen (c) in wood and cellulose. See key to abbreviations at the end of the table

Compounds compared	Extraction after <sup>a</sup>	Tree species/sample name	Offset (C–W) % <sub>o</sub>	Correlation r	Remarks	Reference
(a) carbon isotopes						
C – bW	JM(E <sup>1</sup> )/Browning (1967)	<i>P. ponderosa</i>	NA	0.8–0.96	10 yr and 6 yr blocks, CE19820–1045, 22 samples	Mazany et al. (1980)
<b><math>\delta^{13}\text{C}_\text{C}</math> and <math>\delta^{13}\text{C}_\text{Lig}</math> correlate strongly with each other, <math>\delta^{13}\text{C}_\text{C}</math> shows better correlation with regional tree-ring index than <math>\delta^{13}\text{C}_\text{Lig}</math></b>						
C – bW	JW/Green (1963)	<i>J. depeceana</i>	0.9–1.9	0.86	6 intra-annual samples, CE1978–79	6 intra-annual samples, CE1978–79
<b>Similar intra-ring patterns of <math>\delta^{13}\text{C}_\text{bW}</math> and <math>\delta^{13}\text{C}_\text{C}</math></b>						
C – bW	JW/Green (1963)	<i>P. menziesii</i> , <i>P. ponderosa</i>	1.5–2.0	NA	2 yrs, 4 samples per yr, CE1908–1909	Leavitt and Long (1991) <sup>c</sup>
<b>Similar intra-ring patterns of <math>\delta^{13}\text{C}_\text{bW}</math> and <math>\delta^{13}\text{C}_\text{C}</math></b>						
C – tW	JM(E <sup>2</sup> )/Green (1963)	<i>P. menziesii</i>	ca. 2	NA	20 yrs, 3 samples per yr,	Livingston and Spittlehouse (1996) <sup>c</sup>
C – eW			ca. 1	NA	CE1962–1981(SW*), n = 60	
<b>Offset rather stable, half of the difference between <math>\delta^{13}\text{C}_\text{bW}</math> and <math>\delta^{13}\text{C}_\text{C}</math> accounting for extractives</b>						
hC – bW	JM/Leavitt and Danzer (1993)	<i>P. ponderosa</i>	0.65SEW, 2.25SLW; 2.28HEW, 2.78HLW		4 replicates per factorial combination, sapwood/heartwood and earlywood/latewood analysed	Marshall and Monserud (1996)
		<i>P. menziesii</i>	1.75SEW, 2.00SLW; 1.66HEW, 2.02HLW			
		<i>P. monticola</i>	2.13SEW, 2.64SLW; 1.65HEW, 2.40HLW			

(continued)

Table 5.2 (continued)

Compounds compared	Extraction after <sup>a</sup>	Tree species/sample name	Offset (C–W) %	Correlation r	Remarks	Reference
hC – bW	JW(E <sup>2</sup> )/Brenninkmeijer (1983)	<i>Betula sp.</i>	1.81	NA	5 saplings, 1-yr old, pooled, 1989	Borella et al. (1998)
		<i>F. sylvatica</i>	1.68	NA	2 trees, pooled, 1978–1992	
		<i>Quercus sp.</i>	1.02HW	NA	2 trees, pooled, 1930–1970, HW	
		<i>Quercus sp.</i>	1.64SW	NA	1973–1994, SW	
		<i>P. abies</i>	1.37HW	NA	2 trees, pooled, 1950–1960, HW	
		<i>P. abies</i>	1.34SW	NA	5 trees, pooled, 1987–1996, SW	
		Oak Lil171	1.12 + –0.14	0.94	1 tree, n = 14	
		Oak Lil171	1.01 + –0.18	0.93	1 tree, n = 14	
		Oak Sal	0.89 + –0.16	0.995	1 tree, n = 16, LW	
		Oak Sal	1.01 + –0.20	0.95	1 tree, n = 26, LW	
		Oak Sal	0.89 + –0.19	0.97	1 tree, n = 16, EW	
		Oak Sal	1.01 + –0.30	0.90	1 tree, n = 22, EW	
		Beech Lil161	0.99 + –0.13	0.96	1 tree, n = 14	

Good agreement between  $\delta^{13}\text{C}_{\text{bW}}$  and  $\delta^{13}\text{C}_{\text{hC}}$  with similar relationships to climate, if wood is not decayed. Extractives from conifer wood should be removed prior to analysis. Slopes of regression significantly different from 1 except for *Q.* latewood

(continued)



Table 5.2 (continued)

Compounds compared	Extraction after <sup>a</sup>	Tree species/sample name	Offset (C–W) %	Correlation r	Remarks	Reference
$\alpha\text{C} - \text{bW}$	dHCl/Wallis et al. (1997) (modified)	<i>P. pinaster</i> <i>P. radiata</i> <i>E. globulus</i>	0.3–1.6, Ave. = 0.8 0.2–1.3 Ave. = 0.8 0.8–1.3 0.5–1.0	0.94 0.93 0.95 0.96	n = 81 with 3–5 replicates, no information on tree age, SW or HW	MacFarlane et al. (1999)
hC – bW	JM/(Green 1963)					
hC – eW	E <sup>2</sup>					
<b>Strong and consistent correlation between <math>\delta^{13}\text{C}_{\text{bW}}</math> and <math>\delta^{13}\text{C}_{\alpha\text{C}}</math> and <math>\delta^{13}\text{C}_{\alpha\text{C}}</math>; dHCl method removes hC</b>						
$\alpha\text{C} - \text{bW}$	dHCl/MacFarlane et al. (1999)	<i>P. pinaster</i> <i>P. radiata</i>	0.87	0.96	10 trees, planted in 1966 (SW*); pooled wood samples, n $\approx$ 25	Warren et al. (2001)
<b>The difference between <math>\delta^{13}\text{C}_{\text{bW}}</math> and <math>\delta^{13}\text{C}_{\alpha\text{C}}</math> was similar for all treatments, cellulose extraction not necessary</b>						
hC – bW	JM(E <sup>2</sup> )/Leavitt and Danzer (1993) (no NaOH treatment)	<i>P. latifolius</i> , <i>A. falcatus</i> , <i>O. capensis</i> , <i>P. longifolia</i> , <i>C. viridifolium</i> , <i>C. africana</i>	ca. 1	0.92	44 wood samples from 6 tropical tree species	West et al. (2001)
<b>hC extraction necessary in studies with low sample size examining small isotopic shifts. Away from regression, no pattern in the dispersion of residuals found</b>						
C – fbW	JM/Wiesberg (1974)	Unknown gymnosperms	0.1–3.9	0.06	n = 6, fossil wood, early Miocene	Bechtel et al. (2002) <sup>c</sup>

(continued)

Table 5.2 (continued)

Compounds compared	Extraction after <sup>a</sup>	Tree species/sample name	Offset (C–W) %	Correlation r	Remarks	Reference
C – fbW	JM/(Bechtel et al. 2002)	Unknown gymnosperms	3.1–4.6	0.9	n = 7, fossil wood, middle Miocene	Bechtel et al. (2007b) <sup>c</sup>
C – fbW		Unknown gymno- and angiosperms	2.5–4.0	0.97	n = 14, fossil wood, late Miocene	Bechtel et al. (2003a) <sup>c</sup> Bechtel et al. (2007a) <sup>c</sup>
C – fbW		Unknown gymnosperms	1.4–3.6	0.7	n = 8, fossil wood, Pliocene (2.58–5.33Mio a)	Bechtel et al. (2003b) <sup>c</sup>
<b>Higher isotopic difference of ca. 3.5‰ between cellulose and fossil wood ascribed to wood decomposition</b>						
$\alpha\text{C} - \text{bW}$	JM/Loader et al. (1997)	<i>Q. robur</i>	ca. 1	0.981, 0.876 $p < 0.01$	2 trees, CE1946-2000, 55 years, LW	Loader et al. (2003)
		<i>Q. robur</i> (bog oak)	ca. 1	0.965 $p < 0.01$	1 tree, BCE2340-2361, 20 years, LW	
<b><math>\delta^{13}\text{C}_{\text{bW}}</math> shows higher correlations to climate variables than <math>\delta^{13}\text{C}_{\text{eC}}</math>; <math>\delta^{13}\text{C}_{\text{bW}}</math> may be used to provide evidence of inter-annual variance. Some lower-frequency variance could be induced by differential decay</b>						
hC – bW	JW/Sohn and Reiff (1942)	<i>Fagus sylvatica</i>	0.5–1.8	0.94	3yrs, 279 intra-ring samples, CE1994-1996	Helle and Schleser (2004)
<b>Offset between <math>\delta^{13}\text{C}_{\text{bW}}</math> and <math>\delta^{13}\text{C}_{\text{hC}}</math> can be different between years. Overall slope of regression different from 1 (0.86)</b>						

(continued)

Table 5.2 (continued)

Compounds compared	Extraction after <sup>a</sup>	Tree species/sample name	Offset (C–W) %	Correlation r	Remarks	Reference
hC – bW	JW(E <sup>2</sup> )/Leavitt and Danzer (1993)	<i>Q. cerris</i> <i>F. ornus</i> <i>P. radiata</i>	0.04 n.s 0.09 n.s ca. 1.1	0.72 0.57 0.84	3yrs, CE1999-2001 (SW*), n = 44, juvenile trees, 6–7yrs old 3yrs, CE1999-2001(SW*), n = 14 3 tree rings, CE1999-2001 (SW*), n = 6, juvenile trees, 22–24yrs old	D'Alessandro et al. (2004)
<b><math>\delta^{13}\text{C}_{\text{bW}}</math> is suitable for ecophysiological studies. Slope of regression significantly different from one-to-one relationship</b>						
C – bW	dHCl/modified after MacFarlane et al. (1999)	<i>C. odorata</i> <i>S. macrophylla</i>	1.73 ± 0.08 n = 37 1.01 ± 0.23 n = 16	0.87 $p < 0.001$ (all data)	52 samples from tropical species; 10-yr periods pooled	Hietz et al. (2005) <sup>c</sup>
<b>Original dHCl method requires additional NaClO<sub>2</sub> treatment to fully remove lignin</b>						
C – bW	JW/Sohn and Reiff (1942)	<i>Q. sp.</i> (bog oak)	0.6–2.1	0.67	n = 22, 5-yr blocks, BCE137-193	Sass-Klaassen et al. (2005) <sup>c</sup>
<b>Similar intra-ring patterns of <math>\delta^{13}\text{C}_{\text{bW}}</math> and <math>\delta^{13}\text{C}</math></b>						
hC – bW	JM(E <sup>1</sup> )/Leavitt and Danzer (1993)	<i>Rhizophora mucronata</i> (mangrove)	0.97 ± 0.03	0.98 $p < 0.001$	2 trees, n = 27, SW	Verheyden et al. (2005) <sup>c</sup>
<b>Slope of regression not significantly different from one. <math>\delta^{13}\text{C}_{\text{bW}}</math> can be used in studies of sapwood of <i>R. mucronata</i></b>						

(continued)

Table 5.2 (continued)

Compounds compared	Extraction after <sup>a</sup>	Tree species/sample name	Offset (C–W) %	Correlation r	Remarks	Reference
hC – bW	JW(E <sup>2</sup> )/Leavitt and Danzer (1993)	<i>P. halepensis</i>	1.2	0.97	23 sites, 4–6 trees per site, 25yrs, CE1975-1999(SW*), SFT approach	Ferrio and Voltas (2005)
hC – eW	E <sup>2</sup>		1.0	0.49 <i>p</i> < 0.05		
<b><math>\delta^{13}\text{C}_{\text{hC}}</math>, <math>\delta^{13}\text{C}_{\text{eW}}</math> and <math>\delta^{13}\text{C}_{\text{bW}}</math> show significant correlations to climate variables*</b>						
$\alpha\text{C} - \text{bW}$	dHCl/Cullen and MacFarlane (2005)	<i>C. glaucophylla</i>	1.17	0.64	Chronology with replication of 3 to 11 trees; 20yrs, CE1979-1999 (SW*)	Cullen and Grierson (2006)
<b><math>\delta^{13}\text{C}_{\text{bW}}</math> does not record climate in the same way as <math>\delta^{13}\text{C}_{\alpha\text{C}}</math>; <math>\delta^{13}\text{C}_{\alpha\text{C}}</math> is the temporally more stable proxy</b>						
hC – eW	JW(E <sup>2</sup> )/Leavitt and Danzer (1993)	44 species from the US, angiosperms and conifers	1.07 ± 0.09 <sup>b</sup> range 0.5–1.9 1.32 ± 0.10 <sup>b</sup> range 0.3–1.6	0.98 0.98	2 samples per species, various tree portions (stem and branch wood)	Harlow et al. (2006) <sup>c</sup>
<b>hC extraction is unnecessary for most analyses. Simple solvent extraction suitable for many applications. Slopes of regression calculated from different models sometimes significantly different from 1</b>						
hC – eW	JW(E <sup>2</sup> )/Leavitt and Danzer (1993)	<i>P. menziesii</i>	1.48 ± 0.54	0.91	Groups of 3 consecutive rings, 6 trees, 4 SW samples per tree (12 tree rings, CE1990-2001)	Taylor et al. (2008)

Significant correlations between  $\delta^{13}\text{C}_{\text{hC}}$ ,  $\delta^{13}\text{C}_{\text{eW}}$  and  $\delta^{13}\text{C}$  of extractives. hC extraction may not be necessary if low concentration of extractives

(continued)

Table 5.2 (continued)

Compounds compared	Extraction after <sup>a</sup>	Tree species/sample name	Offset (C–W) %	Correlation r	Remarks	Reference
hC – bW	JW(E <sup>2</sup> )/Leavitt and Danzer (1993)	<i>Q. petraea</i>	1 ± 0.7	0.92	2-yr-old saplings, 29 samples	Eglin et al. (2008) <sup>c</sup>
hC – eW			0.9 ± 0.7	0.97		
<b><math>\delta^{13}\text{C}_{\text{eW}}</math> and <math>\delta^{13}\text{C}_{\text{hC}}</math> show practically identical variations; presence of extractives slightly alters variability of <math>\delta^{13}\text{C}_{\text{hW}}</math> compared to <math>\delta^{13}\text{C}_{\text{hC}}</math></b>						
$\alpha\text{C}^5$ – eW	JW(E <sup>2</sup> )/Loader et al. (1997)	<i>Larix cajanderi</i>	1.83–1.99	0.88–0.97, $p < 0.05$	4 trees, >400yrs old, CE1880-2004	Sidorova et al. (2008) <sup>c</sup>
			1.41–1.50	0.80–0.91, $p < 0.05$	CE900-1000	
<b>Offset not stable in time, during some periods <math>\delta^{13}\text{C}_{\text{eW}}</math> showed other and partly stronger relationships to climate variables than <math>\delta^{13}\text{C}_{\alpha\text{C}}</math></b>						
$\alpha\text{C}^5$ – bW	JW/Loader et al. (1997)	<i>Larix gmelinii</i>		0.75, $p < 0.05$	8 trees, >180yrs old, CE1864-2006, annual resolution, material pooled	Sidorova et al. (2009)
<b><math>\delta^{13}\text{C}_{\text{bW}}</math> data showed significant relationship to climate, whereas no climate signals were found in <math>\delta^{13}\text{C}_{\alpha\text{C}}</math></b>						
hC – bW	JW/Kürschner and Popik (1962)	<i>Pinus nigra ssp.</i>	1.2 ± 0.5	0.71	80 yrs, pooled record, CE1905-1985, 5 trees, >200 yrs old	Szymczak et al. (2011)
<b>Offset declining from pith to bark; climatic conditions best reflected in <math>\delta^{13}\text{C}_{\text{hC}}</math>; extraction of cellulose avoids insufficient sample homogenization</b>						

(continued)

Table 5.2 (continued)

Compounds compared	Extraction after <sup>a</sup>	Tree species/sample name	Offset (C–W) %	Correlation r	Remarks	Reference
C – bW	JW/Loader et al. (1997)	<i>Carapa guianensis</i>	0.2 to 1.6	0.88	1 tree, 47 intra-annual samples	Pons and Helle (2011) <sup>c</sup>
		<i>Goupia glabra</i>	0.7 to 1.5	0.89	1 tree, 49 intra-annual samples	
<b>Similar intra-ring patterns of <math>\delta^{13}\text{C}_{\text{bW}}</math> and <math>\delta^{13}\text{C}_{\text{C}}</math></b>						
$\alpha\text{C}^2$ – bW	JW(E <sup>3</sup> )/Loader et al. (1997)	<i>P. radiata</i>	ca. 1	0.99	Seedlings; greenhouse experiment	Roden and Farquhar (2012) <sup>c</sup>
		<i>E. globulus</i>	ca. 1.5	0.98		
<b>Slopes of regression not significantly different from 1:1 relationship, <math>\alpha\text{C}</math> extraction unnecessary</b>						
C – bW	JW/Gaudinski et al. (2005)	<i>L. cajanderi</i>	0.1 to 2.1	0.96	67 yrs, CE1940-2007	Tei et al. (2013) <sup>c</sup>
<b>Climatic information can be satisfactorily obtained using <math>\delta^{13}\text{C}_{\text{bW}}</math></b>						
C – bW	no details given	<i>P. abies</i>	1.35	0.96 $p < 0.001$	1 tree, annual growth rings, n = 60, CE1973-2006 (SW*)	Sohn et al. (2013)

**Bulk wood samples rather than extracted cellulose can be used for isotope analysis as sample sizes were limiting**

(continued)

Table 5.2 (continued)

Compounds compared	Extraction after <sup>a</sup>	Tree species/sample name	Offset (C–W) ‰	Correlation r	Remarks	Reference
C – bW	JW/Loader et al. (1997)	<i>P. abies</i>	ca. 1.4	0.91, 0.88, 0.83 $p < 0.001$	3 sites, 10 trees each site, 4 radii each tree, individual tree rings pooled; CE1860-2009; CE1933-2009; CE1936-2009	Gori et al. (2013)
<b>Extraction of cellulose is unnecessary for trees from the studied sites. High correlation between <math>\delta^{13}\text{C}_{\text{bW}}</math> and <math>\delta^{13}\text{C}_{\text{C}}</math>. Climate signal best preserved in stable isotope ratios of wood</b>						
$\alpha\text{C} - \text{bW}$	JW/Sternberg et al. (1989)	<i>P. sylvestris</i>	0.8 to 1.5	0.95	2 trees, 48 samples	Edvardsson et al. (2014) <sup>c</sup>
<b><math>\delta^{13}\text{C}_{\alpha\text{C}}</math> and <math>\delta^{13}\text{C}_{\text{bW}}</math> are strongly correlated and both show lower isotope values at the onset of growth depressions</b>						
$\text{hC}/\alpha\text{C} - \text{bW}$	JW(E <sup>2</sup> )/Jayme (1942); Wise (1945), different variants	<i>Q. petraea</i>	1.2(hC), 1.3( $\alpha\text{C}$ )	NA	From adult trees, not further specified	Richard et al. (2014)
		<i>P. deltaoides</i> ,	0.8(hC), 0.7( $\alpha\text{C}$ )	NA		
		<i>P. pinaster</i>	1.2(hC), 1.4 ( $\alpha\text{C}$ )	NA		
		<i>F. sylvatica</i>	1.2(hC), NA ( $\alpha\text{C}$ )	NA		
<b>No difference in offset of <math>\delta^{13}\text{C}_{\alpha\text{C}}</math> and <math>\delta^{13}\text{C}_{\text{hC}}</math> to <math>\delta^{13}\text{C}_{\text{bW}}</math> observed</b>						
$\alpha\text{C} - \text{bW}$	BM/Brendel et al. (2000)	<i>P. sylvestris</i>	1.09 ± 0.09	0.96 $p < 0.001$	4 trees, individual tree rings of 4–8 radii pooled, SW, CE1989-2009	Mischel et al. (2015)

(continued)

Table 5.2 (continued)

Compounds compared	Extraction after <sup>a</sup>	Tree species/sample name	Offset (C–W) %	Correlation r	Remarks	Reference
<b><math>\delta^{13}\text{C}_{\text{bW}}</math> records climate in a similar way as <math>\delta^{13}\text{C}_{\alpha\text{C}}</math>. Cellulose extraction may not be mandatory for studies on <i>P. sylvestris</i> from investigated site</b>						
$\alpha\text{C}^3 - \text{bW}$	JW(E <sup>4</sup> )/Green (1963)	<i>F. sylvatica</i>	1.45 ± 0.07	0.72 $p < 0.05$	5 sites, 3 trees per species, 2 radii each, 20 years of sapwood, CE2001–2010 (SW*)	Weigt et al. (2015)
		<i>Q. robur</i>	1.84 ± 0.18	0.85 $p < 0.05$		
		<i>A. alba</i>	1.79 ± 0.09	0.92 $p < 0.05$		
		<i>P. abies</i>	1.73 ± 0.05	0.79 $p < 0.05$		
		<i>P. menziesii</i>	1.75 ± 0.10	0.91 $p < 0.05$		
$\alpha\text{C}^3 - \text{eW}$	E4					
<b><math>\delta^{13}\text{C}_{\text{bW}}</math> from sapwood is as useful as <math>\delta^{13}\text{C}_{\alpha\text{C}}</math> in environmental studies at short-term scale. Variable response of <i>Q.</i> requires further investigations</b>						
hC – bW	JW/Wieloch et al. (2011)	<i>Cariniana micrantha</i>	0.8 to 2.0	0.96 <sup>b</sup> , moving corr. 0.05 to 0.98	1 tropical tree, 253 consecutive yrs, CE1755–2007, SW and HW	Schleser et al. (2015) <sup>c</sup>
<b>High correlation from a subset or subperiod cannot necessarily prove its validity for a longer isotopic record</b>						
$\alpha\text{C} - \text{fbW}$	BM/Brendel et al. (2000); JW(E <sup>2</sup> )/Loader et al. (1997)	<i>Piceoxylon</i>	ca. 3.0	NA	Mummified fossil wood, 2 samples per species, Eocene (53.3 ± 0.6 Ma)	(continued)



Table 5.2 (continued)

Compounds compared	Extraction after <sup>a</sup>	Tree species/sample name	Offset (C–W) %	Correlation r	Remarks	Reference
$\alpha\text{C} - \text{eW}$	$\text{E}^2$		ca. 3.2	NA		
<b>JW method for cellulose extraction from mummified fossil wood favored over BM</b>						
C – bW	BM/Brendel et al. (2000)	<i>P. cembra</i> <i>P. abies</i> <i>L. decidua</i>	0.6–1.6	0.96	Total n = 36, CE1975–2010 (SW*)	Wieser et al. (2016) <sup>c</sup>
<b>Bulk wood samples rather than extracted cellulose can be used for isotope analysis</b>						
$\alpha\text{C} - \text{bW}$	JW( $\text{E}^2$ )/Leavitt and Danzer (1993) and Sternberg et al. (1989)	<i>C. tomentosa</i>	1.2	NA	2 trees per species, ca. 80–100 yrs old; 7 indiv. rings sampled per tree between CE2000–2011(SW*)	Guerrieri et al. (2017) <sup>c</sup>
		<i>Q. rubra</i>	0.1	NA		
		<i>T. canadensis</i>	0.9, 1.5	NA		
		<i>P. rubens</i>	0.9	NA		
		<i>Q. prinus</i>	1.3	NA		
		<i>P. echinata</i>	1.9	NA		

(continued)

Table 5.2 (continued)

Compounds compared	Extraction after <sup>a</sup>	Tree species/sample name	Offset (C-W) %	Correlation r	Remarks	Reference
$\alpha\text{C} - \text{fbW}$	BM/(Gaudinski et al. 2005)	Unknown gymno- and angiosperms	1-4.4 Ave. 2.5	0.98	n = 38, Eocene, Miocene, Oligocene	Lukens et al. (2019)
<b><math>\alpha\text{C}</math> extraction not necessary for climate reconstructions, both <math>\delta^{13}\text{C}_{\text{bW}}</math> and <math>\delta^{13}\text{C}_{\alpha\text{C}}</math> showed significant correlations with climate variables; partly stronger correlations of <math>\delta^{13}\text{C}_{\text{bW}}</math> with climate data</b>						
<b>A strong linear correlation exists between <math>\delta^{13}\text{C}_{\text{bW}}</math> and <math>\delta^{13}\text{C}_{\text{C}}</math> in both deep-time and modern wood samples (augmented data from literature<sup>c</sup>), suggesting that either substrate can provide a reliable record of environmental conditions</b>						
$\alpha\text{C} - \text{bW}$	BM/modified after Gaudinski et al. (2005) and Anchukaitis et al. (2008)	<i>P. deltooides</i>	ca. 0.5-2	0.54	7 trees, indiv. rings of 2 cores pooled, n = 9 to 42; 39 to 220 yrs old; longest sequence: CE1791-1972	Friedman et al. (2019)
<b>Increasing offset between <math>\delta^{13}\text{C}_{\alpha\text{C}}</math> and <math>\delta^{13}\text{C}_{\text{bW}}</math> from pith to bark due to decreasing long term trend in <math>\delta^{13}\text{C}_{\text{bW}}</math></b>						
hC - bW	JW/(E <sup>2</sup> Loader et al. (1997))	<i>P. massoniana</i>	1.26 ± 0.23	0.74 to 0.98 $p < 0.01$	5 site, 216 trees, CE1982-2014 (SW*)	Gu et al. (2020)
$\alpha\text{C}^6 - \text{bW}$			1.31 ± 0.19			
<b><math>\delta^{13}\text{C}_{\text{bW}}</math>, <math>\delta^{13}\text{C}_{\alpha\text{C}}</math> and <math>\delta^{13}\text{C}_{\text{hC}}</math> display uniform year-to-year variations and common significant climatic signals</b>						
Compounds compared	Extraction after <sup>a</sup>	Tree species/sample name	Offset (C-W) %	Correlation r	Remarks	Reference
<b>(b) oxygen isotopes</b>						
$\alpha\text{C} - \text{bW}$	JW/(E <sup>1</sup> )/Green (1963)	<i>P. glauca</i>	4.99 ± 1.1	0.63	1 tree, 5 yr blocks, CE1890-1968, n = 16	Gray and Thompson (1977)
heC - bW						(continued)

Table 5.2 (continued)

Compounds compared	Extraction after <sup>a</sup>	Tree species/sample name	Offset (C-W) %	Correlation r	Remarks	Reference
<b>Good response of <math>\delta^{18}\text{O}_{\text{bW}}</math> to seasonal air temp., but higher correlations of <math>\delta^{18}\text{O}_{\text{eC}}</math> with temp.; <math>\delta^{18}\text{O}_{\text{hC}}</math> not significantly different from <math>\delta^{18}\text{O}_{\text{eC}}</math></b>						
$\alpha\text{C}^1 - \text{bW}$	JW(E <sup>2</sup> )/Borella et al. (1998)	<i>Quercus sp.</i>	4.25 ± 0.55	0.81	1 tree; individual tree-rings, 15yrs, CE1971-1986(SW*), latewood	Borella et al. (1999)
<b>Some climatic information may be lost if <math>\delta^{18}\text{O}_{\text{bW}}</math> is analyzed instead of <math>\delta^{18}\text{O}_{\text{eC}}</math></b>						
bW	no extraction	<i>Abies alba</i>	NA	NA	4 trees, LW only, CE1840-1997	Saurer et al. (2000)
<b>Significant correlations of <math>\delta^{18}\text{O}_{\text{bW}}</math> with climate data</b>						
$\alpha\text{C}^2 - \text{bW}$	JW(E <sup>3</sup> )/Barbour and Farquhar 2000	<i>Quercus spp.</i>	3.7 ± 2.0	NA	16 (Q.) and 26 (P.) samples from around the world; SFT approach	Barbour et al. (2001)
		<i>Pinus spp.</i>	3.9 ± 1.4	NA		
<b><math>\alpha\text{C}</math> extraction unnecessary for isotope studies looking at correlations with site parameters</b>						
hC – bW	JW(E <sup>2</sup> )/Leavitt and Danzer (1993)	<i>P. halepensis</i>	ca. 4	0.49	23 sites, 4–6 trees per site, 25yrs, CE1975-1999 (SW*); SFT approach	23 sites, 4–6 trees per site, 25yrs, CE1975-1999 (SW*); SFT approach
hC – eW			ca. 4	0.41 n.s		

(continued)

Table 5.2 (continued)

Compounds compared	Extraction after <sup>a</sup>	Tree species/sample name	Offset (C-W) ‰	Correlation r	Remarks	Reference
<b><math>\delta^{18}\text{O}_{\text{bW}}</math> show no significant correlations to climate variable, whereas <math>\delta^{18}\text{O}_{\text{HC}}</math> do</b>						
$\alpha\text{C} - \text{bW}$	dHCl/Cullen and MacFarlane (2005)	<i>C. glaucophylla</i>	7.59	0.68	Chronology with replication of 3 to 11 trees, 20yrs, CE1979-1999(SW*)	Cullen and Grierson (2006)
<b><math>\delta^{18}\text{O}_{\text{bW}}</math> does not record climate in the same way as <math>\delta^{18}\text{O}_{\text{eC}}</math>; <math>\delta^{18}\text{O}_{\text{eC}}</math> is the temporally more stable proxy</b>						
$\text{C} - \text{bW}$	JW/Loader et al. (1997)	<i>F. sylvatica</i>	5.1	0.46 $p < 0.01$	6 trees (2 cores, each) per species, CE1916–1950	Battipaglia et al. (2008)
		<i>A. pseudoplatanus</i>	4.4	NA		
<b>Cellulose extraction necessary to investigate climate signals from <math>\delta^{18}\text{O}</math> of broad-leaved species</b>						
$\alpha\text{C} - \text{eW}$	JW(E <sup>3</sup> )/Loader et al. (1997)	<i>L. cajanderi</i>	3.51–3.99	0.56–0.92, $p < 0.05$	CE1880–2004, 4 trees, >400yrs old, CE900–1000	Sidorova et al. (2008)
			2.97–3.43	0.68–0.78, $p < 0.05$		

(continued)

Table 5.2 (continued)

Compounds compared	Extraction after <sup>a</sup>	Tree species/sample name	Offset (C-W) %	Correlation r	Remarks	Reference
<b>Offset not stable in time, during some periods <math>\delta^{18}\text{O}_{\text{hW}}</math> data showed stronger relationship to climate than <math>\delta^{18}\text{O}_{\alpha\text{C}}</math></b>						
$\alpha\text{C}^5 - \text{bW}$	JW/Loader et al. (1997)	<i>Larix gmelinii</i>	NA	0.61, $p < 0.05$	8 trees, >180yrs old, CE1864-2006, annual resolution, material pooled	Sidorova et al. (2009)
<b><math>\delta^{18}\text{O}_{\text{hW}}</math> and <math>\delta^{18}\text{O}_{\alpha\text{C}}</math> do not show similar climatic signals. <math>\delta^{18}\text{O}_{\text{hW}}</math> data showed significant relationship to climate, whereas <math>\delta^{18}\text{O}_{\alpha\text{C}}</math> did not</b>						
hC – bW	JW/Kürschner and Popik (1962)	<i>Pinus nigra ssp.</i>	$4.8 \pm 0.72$	0.77	5 trees, >200 yrs old, 80 yr-long pooled record, CE1905-1985	Szymczak et al. (2011)
<b>Offset declining from pith to bark; climatic conditions best reflected in <math>\delta^{18}\text{O}_{\text{hC}}</math>; hC extraction avoids insufficient sample homogenization</b>						
$\alpha\text{C}^2 - \text{bW}$	JW(E <sup>3</sup> )/Loader et al. (1997)	<i>P. radiata</i>	ca. 4	0.92	Seedlings, greenhouse experiment	Roden and Farquhar (2012)
		<i>E. globulus</i>	ca. 7	0.77		
<b>Slopes of regression significantly different from 1:1 relationship; <math>\alpha\text{C}</math> extraction required</b>						
C – bW	JW/Loader et al. (1997)	<i>P. abies</i>	3.9, 4.0, 3.3	0.67, 0.75, 0.78 $p < 0.001$	3 sites, 10 trees each site, 4 radii each tree, individual tree rings pooled; CE1860-2009; 1933–2009; 1936–2009	Gori et al. (2013)
<b>Extraction of cellulose unnecessary. Significant correlations found between <math>\delta^{18}\text{O}_{\text{hW}}</math> and <math>\delta^{18}\text{O}_{\text{C}}</math>; Climate signal best preserved in <math>\delta^{18}\text{O}_{\text{hW}}</math></b>						

(continued)

Table 5.2 (continued)

Compounds compared	Extraction after <sup>a</sup>	Tree species/sample name	Offset (C-W) %	Correlation r	Remarks	Reference
eW	E <sup>2</sup>	<i>Tectona grandis</i>	NA	NA	7 trees, 107 yr chronology, not pooled, CE1900–2007	Schollaen et al. (2013)
<b>Significant correlations of <math>\delta^{18}\text{O}_{\text{eW}}</math> with climate data</b>						
C – bW	no details given	<i>P. abies</i>	5.9	0.82 $p < 0.001$	1 tree, annual growth rings, n = 30, CE1973–2006(SW*)	Sohn et al. (2013)
<b>bW samples rather than extracted cellulose can be used for isotope analysis as sample sizes were limiting</b>						
$\alpha\text{C} - \text{bW}$	BM/Brendel et al. (2000)	<i>P. sylvestris</i>	$5.58 \pm 0.23$	0.89 $p < 0.001$	4 trees, individual tree rings of 4–8 radii pooled, CE1989 – 2009(SW*)	Mischel et al. (2015)
<b><math>\delta^{13}\text{C}_{\text{bW}}</math> records climate in a similar way as <math>\delta^{13}\text{C}_{\alpha\text{C}}</math>. Cellulose extraction may not be mandatory for carbon isotope analysis</b>						
$\alpha\text{C}^4 - \text{fbW}$ $\alpha\text{C}^4 - \text{feW}$	BM/Brendel et al. (2000); JW(E <sup>2</sup> )/Loader et al. 1997	<i>Piceoxylon</i>	15.5 17	NA	Mummified fossil wood ( $53.3 \pm 0.6$ Ma), 2 samples	Hook et al. (2015)
<b>Cellulose extraction from fossil wood after JM preferred over BM</b>						
$\alpha\text{C}^3 - \text{bW}$	JW(E <sup>2</sup> )/Green (1963)	<i>F. sylvatica</i> <i>Q. robur</i>	$4.95 \pm 0.14$ $5.12 \pm 0.07$	0.5 $p < 0.05$ 0.41 $p < 0.05$	5 sites, 3 trees per species, 2 radii each, 20 years of SW, CE2001–2010	Weigt et al. (2015)

(continued)

Table 5.2 (continued)

Compounds compared	Extraction after <sup>a</sup>	Tree species/sample name	Offset (C-W) %	Correlation r	Remarks	Reference
$\alpha C^3 - eW$	E <sup>4</sup>	<i>A. alba</i>	5.22 ± 0.13	0.84 $p < 0.05$		
		<i>P. abies</i>	5.31 ± 0.11	0.71 $p < 0.05$		
		<i>P. menziesii</i>	5.44 ± 0.11	0.75 $p < 0.05$		
<b><math>\delta^{18}O_{bW}</math> or <math>\delta^{18}O_{eW}</math> of tree rings from sapwood are as useful as <math>\delta^{18}O_{\alpha C}</math> for studying environmental effects at short term scale. Variable response of <math>\delta^{18}O_{bW}</math> of <i>Q. robur</i> requires further investigations</b>						
$\alpha C^6 - bW$	BM/Gaudinski et al. (2005)	<i>P. densiflora</i>	3.8–4.0	0.92	31 stem disks from 13 sites, 5 outermost tree rings (pentads) were sampled	Lee et al. (2015)
<b><math>\delta^{18}O_{bW}</math> is suggested for use as proxy for the geographical origin of Korean Red Pine. <math>\delta^{18}O_{bW}</math> shows similar correlations to <math>\delta^{18}O</math> of surface water than <math>\delta^{18}O_{\alpha C}^*</math> (<math>r^2 = 0.5</math> vs. 0.53). Approx. 50% of <math>\delta^{18}O_{bW}</math> explained by surface water isotopic composition</b>						
C – bW	BM/Brendel et al. (2000)	<i>P. cembra</i>	4.4–4.0	0.85	Total n = 18, CE1975-2010 (SW*)	Wieser et al. (2016) <sup>c</sup>
		<i>P. abies</i>				
		<i>L. decidua</i>				
<b>Bulk wood samples rather than extracted cellulose can be used for isotope analysis</b>						
$\alpha C - bW$	JW(E <sup>2</sup> )/Leavitt and Danzer (1993) and Sternberg et al. (1989)	<i>Carya tomentosa</i>	4.3	NA	2 trees per species, ca. 80–100 yrs old; 7 individual tree rings sampled per tree between CE2000-2011(SW*)	Guerrieri et al. (2017)
		<i>Quercus rubra</i>	3.8	NA		

(continued)

Table 5.2 (continued)

Compounds compared	Extraction after <sup>a</sup>	Tree species/sample name	Offset (C-W) %	Correlation r	Remarks	Reference
		<i>Tsuga canadensis</i>	6.2, 6.5	NA		
		<i>Picea rubens</i>	5.6	NA		
		<i>Quercus prinus</i>	4.9	NA		
		<i>Pinus echinata</i>	6.2	NA		
		Ave. all species	5.6	0.73 $p < 0.001$		
<b><math>\alpha</math>C extraction not necessary for climate reconstructions, both <math>\delta^{18}\text{O}_{\text{hW}}</math> and <math>\delta^{18}\text{O}_{\text{cC}}</math> showed significant correlations with climate variables; partly stronger correlations of <math>\delta^{18}\text{O}_{\text{hW}}</math> with climate data</b>						
Compounds compared	Extraction after <sup>a</sup>	Tree species/sample name	Offset (C-W) %	Correlation r	Remarks	Reference
(c) hydrogen isotopes						
C – bW	JW/Loader et al. (1997)	<i>P. abies</i>	ca. 30–45	0.66–0.88 $p < 0.001$	3 sites, 10 trees each site, 4 radii each tree, individual tree rings pooled: CE1860-2009; CE1933-2009; CE1936-2009	Gori et al. (2013)
<b>Extraction of cellulose unnecessary. Significant correlations found between <math>\delta\text{D}_{\text{hW}}</math> and <math>\delta\text{D}_{\text{c}}</math>; Climate signal best preserved in <math>\delta\text{D}_{\text{hW}}</math></b>						

(continued)

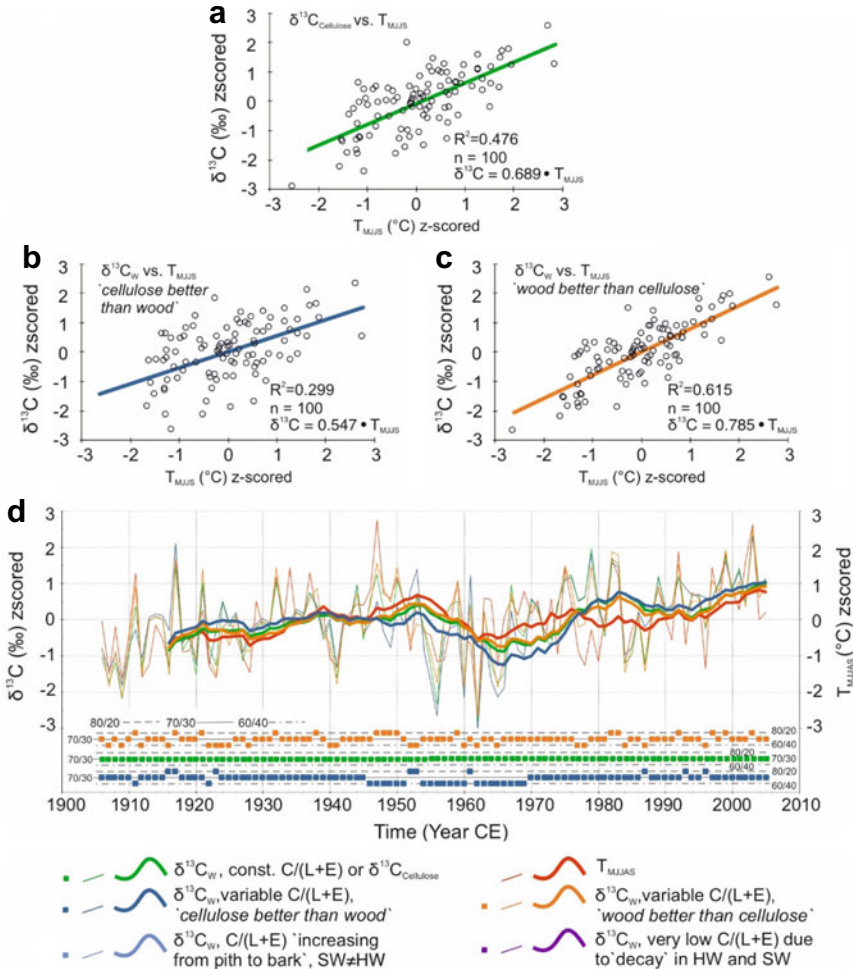


Table 5.2 (continued)

Compounds compared	Extraction after <sup>a</sup>	Tree species/sample name	Offset (C–W) ‰	Correlation r	Remarks	Reference
$\alpha C^6$ – bW	BM/Gaudinski et al. (2005)	<i>P. densiflora</i>	40–43 ± 6	0.89 to 0.92	31 stem disks from 13 sites, 5 outermost tree rings (pentads) were sampled (SW <sup>**</sup> )	Lee et al. (2015)

**$\delta D_{bW}$  is suggested for use as proxy for the geographical origin of Korean Red Pine.  $\delta D_{bW}$  show better correlations to  $\delta D$  of surface water than  $\delta D_{\alpha C}$  ( $r^2 = 0.50$  vs.  $0.28$ ). Approx. 50% of  $\delta D_{bW}$  explained by surface water isotopic composition**

Abbreviations: <sup>a</sup> as referred to in publication; C–W = isotope offset between cellulose and wood; bW = bulk wood; eW = extractive-free or resin-free wood; fbW = fossil bulk wood; W = wood, not further specified; hC = holo-cellulose; heC = hemicellulose; C = cellulose, not further specified;  $\alpha C^1 = 4\%$  NaOH, 70 °C, 24 h;  $\alpha C^2 = 10\%$  NaOH, 70 °C, 5 h;  $\alpha C^3 = 15\%$  NaOH, 45 min, 20 °C;  $\alpha C^4 = 5\%$  NaOH, 2 × 2 h, 70 °C;  $\alpha C^5 = 5\%$  NaOH, 2 × 2 h, 70 °C;  $\alpha C^6 = 17\%$  NaOH, partly various temp.; SW = sapwood; SW\* = probably SW, not explicitly indicated in paper; HW = heartwood; SEW = sapwood, earlywood, HEW = heartwood earlywood; SLW = sapwood, latewood; HLW = heartwood, latewood; EW = earlywood; LW = latewood  
 JW = Jayme-Wise approach, (Jayme 1942; Wise et al. 1946); E<sup>1</sup> = extraction of extractives with benzene/methanol, acetone (mostly using Soxhlet device); E<sup>2</sup> = extraction of extractives with toluene/ethanol; pure ethanol and de-ionized water (mostly using Soxhlet device); E<sup>3</sup> = extraction of extractives with chloroform/ethanol; pure ethanol and de-ionized water (mostly using Soxhlet device); E<sup>4</sup> = extraction of extractives with pure ethanol (24–36 h, at room temperature); dHCL = diglyme-HCL method, (Cullen and MacFarlane 2005; MacFarlane et al. 1999); BM = Brendel-method, (Brendel et al. 2000); NA = Not analysed; SFT = stable isotope-climate relationships from space-for-time approach, not from isotope time series; <sup>b</sup> mean value, <sup>c</sup> compilation of individual data points available in online supplemental material of Lukens et al. (2019)



**Fig. 5.1** Real  $\delta^{13}\text{C}$  time series of tree-ring cellulose ( $\delta^{13}\text{C}_{\text{C}}$ , z-scored) and hypothetical time series for wood ( $\delta^{13}\text{C}_{\text{W}}$ , z-scored) calculated from different proportions of wood constituents (cellulose (C), combined lignin and extractives (L + E)) and linear correlations with instrumental climate data.  $\delta^{13}\text{C}_{\text{W}}$  records were calculated for different C/(L + E) ratios (60/40, 70/30, 80/20) assuming a constant offset of 3.5‰ between C and L + E. Linear correlation of real  $\delta^{13}\text{C}_{\text{C}}$  to air temperature of the vegetation period (May to September) (a). C/(L + E) deviating from 70/30 in individual years or sub-periods causing  $\delta^{13}\text{C}_{\text{W}}$  to correlate better with climate (b) or worse (c) than  $\delta^{13}\text{C}_{\text{C}}$ . d Corresponding time series of  $\delta^{13}\text{C}_{\text{W}}$  calculated from different C/(L + E). Note, z-scored  $\delta^{13}\text{C}_{\text{W}}$  with constant C/(L + E) is not different from z-scored  $\delta^{13}\text{C}_{\text{C}}$ . e  $\delta^{13}\text{C}_{\text{W}}$  records calculated from different levels C/(L + E) hypothetically changing from pith to bark (heartwood (HW) to sapwood (SW)) or due to wood decay (C/(L + E) reduced to 20/80). Corresponding correlations to climate (f, g) show distinct differences to correlation of  $\delta^{13}\text{C}_{\text{C}}$  (a). See 5.2.4.3 SM5.2.4.3 for further details

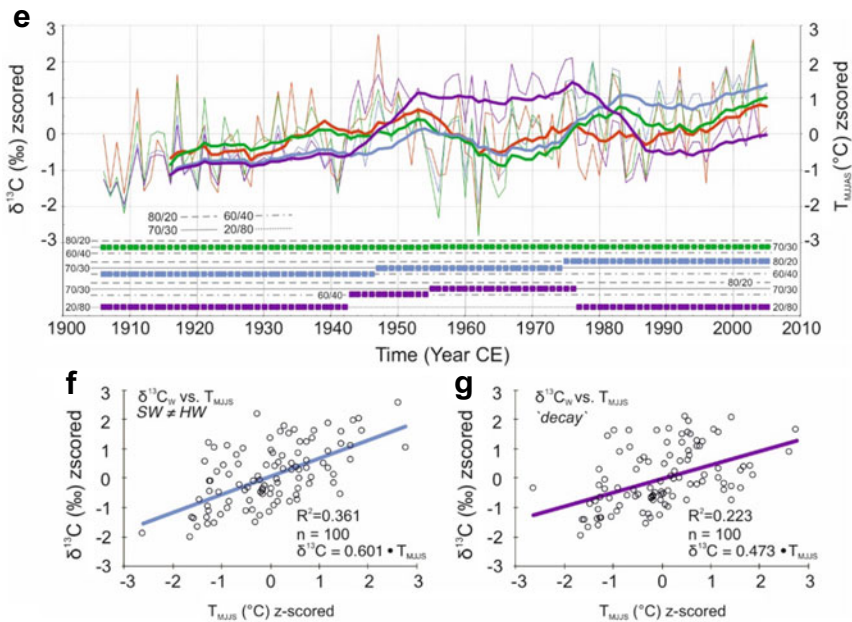


Fig. 5.1 (continued)

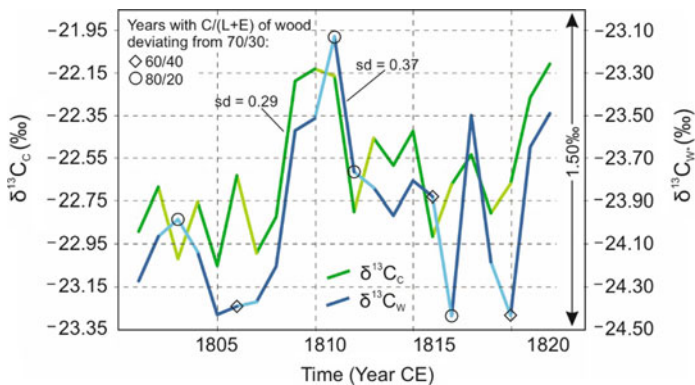


Fig. 5.2 Real  $\delta^{13}\text{C}_C$  time series (green) from *P. sylvestris* with rather low variability for the time period 1801 to 1822CE (22 years). Hypothetical  $\delta^{13}\text{C}_W$  (blue) with 7 years deviating from a C/(L + E) ratio of 70/30. Circles: C/(L + E) = 80/20; diamonds: C/(L + E) = 60/40. Besides different year-to-year variability,  $\delta^{13}\text{C}_W^*$  can even show inverse trends (bright colored lines). See 5.2.4.3 for details

of wood are likely to be lower than the effects on  $\delta^{13}\text{C}$  due to the rather low abundances of hydrogen (6–7%) and oxygen (20–30%) in lignin and the generally much higher content of cellulose in wood.

Mass balance calculations can also help to test the implications of potentially contaminating substances, like chalk or from pencil marks (SM5.2.3; Schollaen et al. 2017).

#### ***5.2.4 Wood Versus Cellulose—A Review of Tree-Ring Stable Isotope Benchmarking Studies***

Stable isotope ratios from cellulose (holo- or  $\alpha$ -cellulose) are usually considered to be the benchmark for eco-physiological and climatological studies using tree rings because any variation due to different biosynthetic pathways of wood constituents have been previously removed. However, many studies have tested whether or not stable isotope ratios of wood are equitable in terms of use and quality. A majority of studies investigated carbon isotopes (40, Table 5.2a), twenty comprised oxygen stable isotopes (Table 5.2b) and two studies focused on hydrogen stable isotopes testing whether or not cellulose extraction is necessary for tracing the geographical origin of wood (Gori et al. 2013; Lee et al. 2015; Table 5.2c). Many trials were focusing on rather short periods of time for comparison (Table 5.2, frequently  $\leq 25$  years) aiming at extrapolating correlation properties of wood and cellulose to other, usually longer time intervals. Associated to these short assessment periods, a few authors indicated that their studies were constrained to sapwood (SW, Table 5.2a, b) (e.g. Weigt et al. 2015; Verheyden et al. 2005; Taylor et al. 2008), but given the information about tree age and sampled time periods, several other studies were also likely limited to the study of sapwood (cf. SW\*; ‘Remarks’ in Table 5.2a–c). Ten studies clearly indicated that longer time periods ( $\geq 50$  years) including sapwood (SW) and heartwood (HW) were investigated. The majority focused on bulk wood, whereas some also used extractives-free wood (mostly from conifers) for comparison with cellulose. All of the peer-reviewed publications we found have assessed the differences (offset, C-W) between isotope values of bulk wood (bW) and/or extractives-free wood (eW) and holocellulose (hC) or  $\alpha$ -cellulose ( $\alpha$ C) for a large number of various species. Holo-, hemi- and  $\alpha$ -cellulose are products of primary plant metabolism. Apparently no significant differences do exist with respect to their carbon and oxygen stable isotope signature (Richard et al. 2014; Gray and Thompson 1977). Hence, except for the details given in Table 5.2 no distinction is being made in the following paragraphs.

### 5.2.4.1 Isotopic Offsets Between Bulk Wood, Extractives-Free Wood and Its Cellulose

Across all studies and species an average offset in  $\delta^{13}\text{C}$  values between wood and cellulose of around 1‰ was found. Usually, the offsets in  $\delta^{13}\text{C}$  were ranging between 0.7 and 2‰, very few studies found no (D' Alessandro et al. 2004) or exceptionally large offsets (Table 5.2a), e.g. ca. 3‰ for fossil wood from the Tertiary geologic period (Lukens et al. 2019 and citations therein; Hook et al. 2015). In a high resolution intra-annual study comprising 279 data pairs across 3 consecutive tree rings, the offset in  $\delta^{13}\text{C}$  varied between 0.5 and 1.8‰, but it was rather stable within years (Helle and Schleser 2004). Generally, intra-seasonal trends revealed a much higher amplitude (up to 5‰) than the variability that might be induced by potentially changing concentrations of individual wood constituents (e.g. Leavitt and Long 1991; Verheyden et al. 2004). However, some phase shift in the relationship between  $\delta^{13}\text{C}$  intra-ring curves of cellulose and lignin was observed (Wilson and Grinstead 1977). The resulting consequences for  $\delta^{13}\text{C}$  of wood were considered to be small with no apparent temporal offset in the climate signal (Loader et al. 2003; Taylor et al. 2008). For more details on intra-annual stable isotope variability see Chap. 15.

Among the ten studies that investigated longer tree-ring sequences, six trials, mostly on  $\delta^{13}\text{C}$ , noted an unstable offset between wood and its cellulose with time. Marshall and Monserud (1996) decided to focus on cellulose after detecting highly variable differences in the  $\delta^{13}\text{C}$  offset between heartwood and sapwood. Particularly, *P. ponderosa* has revealed a considerably higher offset of wood vs. cellulose in heartwood. A similar difference in isotopic offset was observed for sapwood and heartwood of an oak tree (*Quercus sp.*) (Borella et al. 1998). Schleser et al. (2015) reported a variable offset along 253 consecutive tree rings of tropical *C. micrantha* ranging between 0.8 and 2.0‰ with moving correlations (50 years interval length) conspicuously varying from virtually zero to 0.98 (at an average correlation of 0.96). Friedman et al. (2019) found the offset increasing from pith to bark due to a decreasing trend in  $\delta^{13}\text{C}$  of wood that was not observed in  $\delta^{13}\text{C}$  of cellulose. Sidorova et al. (2008) and Sidorova et al. (2009) observed the offsets for both,  $\delta^{13}\text{C}$  and  $\delta^{18}\text{O}$ , being not stable with time. When compared with climate variables, they found slightly, but consistently better relationships to  $\delta^{13}\text{C}$  (and  $\delta^{18}\text{O}$ ) of wood relative to the correlations of corresponding values of cellulose to climate.

Apart from the particular findings for mummified wood ( $\delta^{18}\text{O} \geq 15.5\text{‰}$ , (Hook et al. 2015)), the offsets in  $\delta^{18}\text{O}$  values between wood and cellulose were found generally ranging from 2.97 to 7.59‰, i.e. a considerable higher variability than for  $\delta^{13}\text{C}$  was observed.

With respect to hydrogen stable isotopes Gori et al. (2013) and Lee et al. (2015) have found the  $\delta^2\text{H}$  values of wood about 30–45‰ more negative than those of cellulose at a largely similar interannual variability (Table 5.2c).

#### 5.2.4.2 Statistical Relationship Between the Stable Isotopes of Bulk Wood, Extractives-Free Wood and Corresponding Values of Cellulose

Most studies calculated correlation coefficients ( $r$ ) or coefficients of determination from ordinary least square regression of wood versus cellulose isotope values, and/or applied reduced major axis regression (RMA) or bivariate least squares regression (BLS), for example, to include the measurement errors for calculating confidence intervals (e.g. Verheyden et al. 2005; Harlow et al. 2006). Besides presenting correlation coefficients several authors also examined whether or not slopes of regression were different from one (e.g. Verheyden et al. 2005; Roden and Farquhar 2012; Harlow et al. 2006).

Usually highly significant average correlation coefficients of 0.8 or higher were discovered in the studies comparing  $\delta^{13}\text{C}$  values of wood and corresponding cellulose. A few authors report medium (D'Alessandro et al. 2004; Weigt et al. 2015; Ferrio and Voltas 2005; Schleser et al. 2015) or insignificant (Guerrieri et al. 2017) relationships. For  $\delta^{18}\text{O}$  (wood vs. cellulose values), frequently only medium, nevertheless significant, correlation coefficients were discovered, with  $p$  values often  $<0.05$ , compared to  $<0.01$  or less as was mostly found for  $\delta^{13}\text{C}$ . Whereas one study identified highly variable moving correlations (0.5–0.98; 50 years interval length;  $r_{\text{bar}} = 0.96$ ,  $n = 253$ ) for a tree-ring  $\delta^{13}\text{C}$  sequence from a tropical tree (Schleser et al. 2015), no such test has been reported for  $\delta^{18}\text{O}$  or  $\delta^2\text{H}$ , yet, because time series were too short or not existing.

For hydrogen isotope values for bulk wood and its cellulose, Gori et al. (2013) have found highly significant positive correlation coefficients of 0.7, 0.66 and 0.88 ( $p < 0.001$ ) at three different sites. For *P. densiflora* from a network of sites in South Korea a similar relationship was observed ( $r = 0.89$  to  $0.92$ ) (Lee et al. 2015) (Table 5.2c). These values are slightly lower than those gained for  $\delta^{13}\text{C}$  (Table 5.2a) and lie within the same order of magnitude as the values determined for  $\delta^{18}\text{O}$  (Table 5.2b). This may suggest that hydrogen isotope analysis on wood is as useful as on cellulose. However, in these studies exchangeable hydroxyl-bound hydrogen atoms (ca. 30% of hydrogen in cellulose) have not been quantified or removed prior to the isotope measurements. This is assumed to be not necessary for tracing the geographical origin of timber (Lee et al. 2015; Gori et al. 2013), however it is considered to be important if a measure of the hydrogen (water) taken up by a tree during cellulose synthesis is to be obtained in ecological or paleoclimatic studies using tree-ring time series (Loader et al. 2015; Epstein and Yapp 1976; Sternberg 1989).

### 5.2.4.3 Statistical Relationships of Stable Isotopes of Bulk Wood, Extractives-Free Wood and Corresponding Cellulose to Climate Variables

Several studies tested respective signal strengths of isotope values of wood and corresponding cellulose in relation to climate parameters. This was done by correlating time series of tree-ring isotope data versus instrumental climate variables (e.g. Mazany et al. 1980; Weigt et al. 2015; Guerrieri et al. 2017; Saurer et al. 2000; Gori et al. 2013) or in space-for-time ('SFT', Table 5.2) substitution approaches, by using wood material from trees growing under various eco-climatological conditions at different latitudes and elevations (Barbour et al. 2001; Ferrio and Voltas 2005; Lee et al. 2015; Gori et al. 2013). Barbour et al. (2001) concluded that  $\delta^{18}\text{O}$  from wood contains the same annual average information on climatological site parameters (temperature, rainfall, weighted  $\delta^{18}\text{O}$  of rain) as cellulose. Similarly the two comparative studies on hydrogen stable isotopes suggest that bulk wood is as useful as on cellulose for tracing the geographical origin of timber (Lee et al. 2015; Gori et al. 2013). In another space-for-time substitution study on wood fragments of *P. halepensis* from a network of 23 Mediterranean sites across eastern Spain annual means generally failed to adequately reflect the large range of climate seasonality among the sampled sites (Ferrio and Voltas 2005). In contrast to findings of Barbour et al. (2001), only  $\delta^{18}\text{O}$  values of cellulose revealed weak, but significant correlations to climate variables. Here, the already weak climate signal exhibited by  $\delta^{18}\text{O}$  of cellulose might be further lowered if the analysis of  $\delta^{18}\text{O}$  was conducted on wood, probably because of varying proportions of wood constituents in the sample material combined with their different intrinsic  $\delta^{18}\text{O}$  signatures. Similar to the findings of Ferrio and Voltas (2005), but using  $\delta^{18}\text{O}$  tree-ring time series from two broad-leaved tree species, a study from the Mediterranean (S-Italy) reported that  $\delta^{18}\text{O}$  of the cellulose fraction strongly correlated with monthly and seasonally resolved climate data, while the whole wood fraction generally did not (Battipaglia et al. 2008).

Apart from these two studies with insignificant correlations of  $\delta^{18}\text{O}$  of wood to climate variables statistically significant climate-proxy relationships were generally found for both, wood and cellulose, and for all three isotope species ( $\delta^{13}\text{C}$ ,  $\delta^{18}\text{O}$ ,  $\delta^2\text{H}$ ). The rather coherent response to climate can be expected from the similarity that has been generally observed between the isotopic signatures of wood and its cellulose. For  $\delta^2\text{H}$ , bulk wood showed even stronger relationships to climate or  $\delta^2\text{H}$  of surface waters than  $\delta^2\text{H}$  of cellulose (Gori et al. 2013; Lee et al. 2015). Also,  $\delta^{13}\text{C}$  or  $\delta^{18}\text{O}$  values of wood sometimes showed higher correlations than those of cellulose (Guerrieri et al. 2017; Sidorova et al. 2008, 2009; Loader et al. 2003; Gori et al. 2013), sometimes the opposite was the case, i.e. stronger relationships of cellulose isotopes to climate were reported (Gray and Thompson 1977; Szymczak et al. 2011; Mazany et al. 1980). Furthermore, Cullen and Grierson (2006) found that  $\delta^{18}\text{O}$  of cellulose provides a temporarily more stable climate proxy. Besides differences in signal strength,  $\delta^{18}\text{O}$  of bulk wood and corresponding cellulose were also found to respond to different climatic signals (Sidorova et al. 2008) and hence, Sidorova et al. (2009) suggested to analyze both if enough sample material is available.

#### 5.2.4.4 How Varying Proportions of Wood Constituents Can Affect Climate—Stable Isotope Relations of Bulk Wood Time Series to the Better or Worse

The mixed results in terms of the ranking of climate signal strength in wood and cellulose, respectively, may be just coincidence because correlation coefficients of tree-ring stable isotopes in wood or its cellulose with climate variables were often found to be rather close to each other. Yet, variable proportions of wood constituents with their intrinsic isotope signatures might also be relevant to sometimes either strengthen or weaken the climate signature of isotope values of wood relative to cellulose. In order to figure out how the linear relationship of a tree-ring stable isotope sequence with a climate variable can be affected, we have taken an existing  $\delta^{13}\text{C}$  time series of tree-ring cellulose ( $\delta^{13}\text{C}_\text{C}$ ) and calculated wood time series ( $\delta^{13}\text{C}_\text{W*}$ ) with different hypothetical proportions of wood constituents for linear correlation with instrumental climate data (Fig. 5.1a–g). The  $\delta^{13}\text{C}_\text{C}$  time series was obtained from six trees (not pooled) of a 230-year old pine (*P. sylvestris*) stand located near (approx. 300 m) the long-term meteorological Station Potsdam Telegrafenberg, Germany (PIK-Potsdam 2020). For simplification the hypothetical  $\delta^{13}\text{C}_\text{W*}$  records were calculated from two components only, i.e. cellulose (C) and combined lignin and extractives (L + E) using mass balance equations introduced in Sect. 5.2.3 and SM5.2.3. Assuming that cellulose is constantly about 3.5‰ less negative in  $\delta^{13}\text{C}$  than lignin and extractives three different percentage ratios of C/(L + E), namely 80/20, 70/30 and 60/40 were chosen for calculating  $\delta^{13}\text{C}_\text{W*}$ . This resulted in offsets between  $\delta^{13}\text{C}_\text{C}$  calculated  $\delta^{13}\text{C}_\text{W*}$  well within the real range of offsets reported in the literature (0.7 and 2‰; Table 5.2a). The ratio C/(L + E) of 70/30 was adopted as default for the majority of calculated  $\delta^{13}\text{C}_\text{W}$  values. Different  $\delta^{13}\text{C}_\text{W*}$  curves were obtained by changing this ratio to 80/20 and/or 60/40 for individual years or different periods, e.g. to simulate potential differences between heartwood and sapwood. By changing this ratio for individual years or different periods various  $\delta^{13}\text{C}_\text{W*}$  series were obtained reflecting potential responses to extreme years, effects of reaction wood or differences between heartwood and sapwood, as well as wood decay with a preferential loss of cellulose (cf. SM5.2.4.4. for further details).

$\delta^{13}\text{C}_\text{C}$  is significantly correlated ( $R^2 = 0.76$ ) to air temperature of the vegetation period ( $T_{\text{MJJAS}}$ ; Fig. 5.1a). However, increasing or lowering the average C/(L + E) ratio for some years can cause the resulting  $\delta^{13}\text{C}_\text{W*}$  record to correlate better (Fig. 5.1c) with temperature than  $\delta^{13}\text{C}_\text{C}$  or worse (Fig. 5.1b). The coefficients of determination are quite different ( $R^2 = 0.299$  vs. 0.615) although the time series for  $\delta^{13}\text{C}_\text{W*}$  seem to visually vary in details, only (Fig. 5.1d).

$\delta^{13}\text{C}_\text{W*}$  records correlate better than those of  $\delta^{13}\text{C}_\text{C}$  if low  $\delta^{13}\text{C}$  values (due to low air temperatures) are additionally reduced by lower C/(L + E) ratios and vice versa. In contrast, climate relationship of  $\delta^{13}\text{C}_\text{W*}$  is not as good as of  $\delta^{13}\text{C}_\text{C}$  if the C/(L + E) ratio changes in opposite direction, i.e. when  $\delta^{13}\text{C}_\text{W*}$  is increasing together with decreasing C/(L + E). Changing C/(L + E) over periods of several years or along with specific stem sections the time series for  $\delta^{13}\text{C}_\text{W*}$  can show rather deviating trends (Fig. 5.1e–g). Increasing C/(L + E) ratios from the inner (heartwood, 60/30)



to the outer part (sapwood, 80/20) of a tree-ring sequence can lower the climate relationship of  $\delta^{13}\text{C}_{\text{W}^*}$  as compared to  $\delta^{13}\text{C}_{\text{C}}$  (Fig. 5.1e, f). Likewise, pronounced cellulose decay can not only statistically weaken correlations to climate (Fig. 5.1g), but also can cause distinct differences in the progression of trends (cf. 1950CE to 1980CE, Fig. 5.1e).

Although this simple exercise is based on the assumption of a constant isotope offset between cellulose and lignin and extractives, both having identical values, it illustrates that varying proportions of wood constituents can well explain the observed differences in signal strength reported for isotope ratios of wood, its cellulose and climate data, respectively (Table 5.2).

Generally, changes of the chemical composition of wood can cause rather larger effects during periods in which the isotopic signature governed by environmental conditions varies little in contrast to periods in which the isotopic signature varies strongly. This is exemplified in Fig. 5.2 showing real  $\delta^{13}\text{C}_{\text{C}}$  with rather low variability ( $\text{sd} = 0.29$ ) from Potsdam Scots pine for the time period 1801 to 1822CE (22 years). An artificial  $\delta^{13}\text{C}_{\text{W}^*}$  was calculated with 7 years deviating from a C/(L + E) ratio of 70/30. The resulting  $\delta^{13}\text{C}_{\text{W}^*}$  record shows a higher variability ( $\text{sd} = 0.37$ ) than  $\delta^{13}\text{C}_{\text{C}}$  and, probably more important, sometimes inverse year-to-year changes. Furthermore, this implies that correlations between wood and cellulose isotope values may be reduced during periods of generally low variability of isotopic signature and high when it is changing considerably from a certain level to another one (Schleser et al. 2015).

The illustrated potential effects might be weakened or even be more prominent if the isotope signatures of the different wood constituents do respond differently to environmental or climatic changes, and not in the same way as assumed for the simple exercise here. In this regard, it should be noted, that conclusions drawn from this exercise on carbon stable isotopes cannot be simply transferred to oxygen or hydrogen, because of different proportions of these elements within cellulose, lignin and extractives and different precursors substances with rather different  $\delta^{18}\text{O}$  and  $\delta^2\text{H}$  values (Schmidt et al. 2001).

### 5.2.5 *Benefits of Using Cellulose Instead of Wood*

Before discussing major aspects, the minor benefits of extracting cellulose instead of using wood shall be addressed. Firstly, no carbon transfer across tree-ring boundaries after formation of primary cellulose structures. Secondly, working with cellulose makes the sample homogenization easier. Cellulose can be homogenized rather quickly (ca. 50 samples/hour) with ultrasonic devices after wood slithers or chips of up to 1 mm in thickness and no more than 5 mm in length underwent the chemical extraction procedure (Laumer et al. 2009). Contrastingly, wood material has to be homogenized by grinding, i.e. chopping with subsequent sieving by using certain mills. Although the milling process may only take a few seconds, the necessary cleaning process (vacuum cleaner, compressed air, rinsing with alcohol, etc.)

is usually rather time consuming (ca. 10 samples/hour). Furthermore, sample losses from wood milling are rather high, whereas ultrasonic homogenization virtually leads to no sample loss at all (cf. Sect. 5.3.4 for further details). Thirdly, chemical extraction of cellulose removes contaminants from sampling and handling, e.g. by tree corer or chain saw lubricants and it probably makes an extra removal of extractives obsolete as found for *P. sylvestris* by Rinne et al. (2005). Fourthly, the content of tree-ring cellulose was recently introduced as a potential supplementary proxy in dendroclimatology (Ziehmer et al. 2018).

Major aspects: in theory, the presence of a stable isotopic offset, a significant correlation between isotopes of wood and its cellulose, as well as a slope of regression that is not significantly different from 1 should allow the use of wood instead of cellulose. This seems to be the case for the two studies on  $\delta^2\text{H}$  (Lee et al. 2015; Gori et al. 2013), and for the majority of  $\delta^{13}\text{C}$  and  $\delta^{18}\text{O}$  studies (Table 5.2). However, many authors were usually avoiding generalizing statements as their studies are constrained to certain tree species and/or the specific sites. Nonetheless, a broader validity is suggested simply by the large number of case studies recommending that bulk wood or extractives-free wood (mostly referring to resinous conifers) can be used. This is underlined by two studies that did not assess tree-ring time series but used numerous wood fragments (twigs, branches, stem wood or worked wood) from a wide range of species (Harlow et al. 2006) and/or collected from spatially separated sites along large ecological or environmental gradients (Barbour et al. 2001). Although these studies appear to be very elaborate, Harlow et al. (2006) have investigated 44 different tree species (38 angiosperms; 7 gymnosperms) and Barbour et al. (2001) analyzed 16 samples of different oaks and 26 samples of *Pinus sp.*, it was concluded that cellulose extraction is not necessary for many applications and many wood samples, implying that the conclusions are not unconditional and both studies did not discuss for which species, site conditions or research questions extraction may not be skipped. The uncertainty was indeed highlighted by a Mediterranean site network suggesting that cellulose extraction is required when correlations of isotopes to climate are generally weak so that changes in chemical wood composition can mask the climate signal (Ferrio and Voltas 2005). Other studies from the Mediterranean likewise concluded that cellulose extraction is required for extracting a climate signal from tree-ring  $\delta^{18}\text{O}$  (Battipaglia et al. 2008; Szymczak et al. 2011). In contrast, D'Alessandro et al. (2004) found stable isotopes of bulk wood suitable for ecological studies at their sites in Southern Italy.

In synopsis, the basic question remains whether or not all the studies proposing to skip cellulose extraction are yet adequately systematic in nature, i.e. whether the covered geographical range, species selection, time range and ecological gradients were broad enough for a general conclusive statement. Still, tests seem to be advised for all isotope studies that are not consistent with the framework of the published studies, which is, frequently difficult to define because given site descriptions are lacking in detail.

Many studies that have investigated tree-ring isotope time series of wood and its cellulose and suggest that cellulose extraction is unnecessary have assessed records of no more than 20 to 30 years (e.g. Sohn et al. 2013; Guerrieri et al. 2017; Warren et al.

2001; Weigt et al. 2015), whereas studies on longer sequences were less convincing or even critical about skipping cellulose extraction. They noted some instability in the isotope offsets between wood and its cellulose on inter- and/or intra-annual level, e.g. indicated by variable moving correlations or by slopes of regression being significantly different from a one-to-one relationship (Table 5.2). The results of Schleser et al. (2015), revealing that correlations between  $\delta^{13}\text{C}$  of wood and cellulose can collapse from  $>0.9$  down to virtually zero for 50-year sub-periods of a 273-year record, raise questions whether it is eligible to extrapolate correlation properties from a certain time interval to any other time interval without considering a weakening of signals.

A probable reason for the differences observed might be that the studies on shorter sequences seem to be largely constrained to sapwood, whereas investigations on the longer sequences were comprising heartwood as well (Table 5.2). Sapwood differs from heartwood by chemical and isotopic properties of extractives (Sect. 5.2.2.2). This might have been relevant in the longer-term studies that did not rely on extractives-free wood and hence, were facing differences from pith to bark. However, apart from varying extractives the cellulose to lignin ratio likewise can be very different in sapwood, heartwood and the transition zone in between. Bertaud and Holmbom (2004) not only found that heartwood of *P. abies* contained significantly more lignin and less cellulose than sapwood, but also the transition zone between heartwood and sapwood had a specific composition, with less lignin and lipophilic extractives than heartwood and sapwood. This can explain, at least partly, the varying offsets observed between isotope ratios of (extractives-free) wood and cellulose, and the exercise above (Fig. 5.1e) has demonstrated that potential effects can well cause different curve shapes or trends (from pith to bark) of isotopes between wood and cellulose, respectively, as was also observed in nature (Friedman et al. 2019; Szymczak et al. 2011). Strictly speaking the available literature indicates that only tree-ring stable isotope ratios of sapwood (untreated or extractives-free in case of resinous conifers) may be used in short-term scale studies. Nonetheless, even in short-term studies oak sapwood have shown variable isotope responses and further investigations were suggested (Weigt et al. 2015; Borella et al. 1998).

Isolation of cellulose excludes any potential issue associated with variability in the relative amounts of wood constituents with their different isotope signatures and related to that particular concern was raised regarding the preferential degradation of cellulose in subfossil and fossil wood under both aerobic and anaerobic conditions (Loader et al. 2003; Borella et al. 1998; Hook et al. 2015; Schleser et al. 1999; Savard et al. 2012; Nagavciuc et al. 2018; Lukens et al. 2019). This may impart a low-frequency signal in bulk wood stable isotope values potentially causing trends that are unrelated to climatic or other environmental changes and cause potential problems when using bulk wood for climate reconstructions from long sub-fossil tree-ring chronologies (McCarroll and Loader 2004). Differential degradation of wood constituents can lead to contrasting isotopic trends in trunks (of same age) buried in bogs or deposited lakes (Savard et al. 2012; Bechtel et al. 2007b; Lukens et al. 2019). However, wood decay from infections by fungi and bacteria can already affect stressed or diseased living trees and probably cause much larger damage than

any degradation commencing after wood-preserving burial. In-depth studies (experiments) on the isotopic effects of cellulolytic enzymes of fungi and/or bacteria are lacking and it is quite uncertain to which extent partial decay results in changes in the isotopic signature of cellulose, which would also degrade the environmental or climatic signal. Savard et al. (2012) could show that highly altered wood from boreal lakes shows a decrease not only in cellulose proportion but also in  $\delta^{18}\text{O}$  of cellulose, whereas  $\delta^{13}\text{C}$  ratios were apparently preserved. Despite this one study, there is a need for further research on the effects of different kinds of wood decay, stages of preservation and burial history on the isotopic signatures of wood and its constituents. Loader et al. (2003) and Robertson et al. (2004) suggested to analyze the stable isotope ratios of more resistant lignin to address this issue. Furthermore, the analysis of stable isotope ratios of carbon and hydrogen of lignin methoxyl groups (Mischel et al. 2015; Gori et al. 2013) may also well be used as in case of decayed wood to substitute potentially obscured cellulose isotope data.

### ***5.2.6 The Additional Value of Stable Isotopes of Lignin Methoxyl Groups***

Keppler et al. (2007) and Gori et al. (2013) suggested that stable isotope ratios of carbon and hydrogen of lignin methoxyl groups can be used as palaeoclimate proxies. Particularly, because isotope ratios of hydrogen of lignin methoxyl groups are considered not to undergo significant exchange with plant water during metabolic reactions. Carbon and hydrogen isotope ratios are determined on methyl iodide ( $\text{CH}_3\text{I}$ ) by GC-C/TC-IRMS (Greule et al. 2009; Greule and Keppler 2011).  $\text{CH}_3\text{I}$  gas is obtained from the reaction of hydroiodic acid (HI, 55–58%) with 2 mg/10 mg ( $\delta^{13}\text{C}/\delta^2\text{H}$ ) of wood at 130 °C for 30 min. This method of sample preparation is rather quick, after equilibration of about one hour aliquots of 10–90  $\mu\text{l}$  of  $\text{CH}_3\text{I}$  can be transferred to the autosampler of the GC-C/TC-IRMS (Mischel et al. 2015). A disadvantage of this method might be that not only lignin methoxyl groups are unclosed, but all methoxyl groups being present in a wood sample. Nonetheless, given the high similarity of lignin and corresponding isotope time series of cellulose (Mischel et al. 2015) parallel analyses may help to identify degraded wood sections not only in terms of reduced cellulose content, but also concerning potentially altered isotopic signatures of the remaining cellulose.

## 5.3 Cellulose Extraction Procedures, Reaction Devices and Sample Homogenization

### 5.3.1 *Sample Pre-preparation, Wood Cross Sections and Tree-Ring Dissection*

Analyzing stable isotope ratios of tree rings requires careful sample collection and precise dissection of tree rings or parts thereof (cf. Chap. 4). In the classical approach, wood material from tree rings dissected by scalpel or rotary tools (e.g. Dremel®) is easiest placed into labeled 2 ml transparent microcentrifuge tubes (e.g. Eppendorf Tubes®) for transport and storage. The wood material should be chopped into small pieces of about 1 to <0.5 mm thickness and length of no more than 5 mm prior to extraction described in Sect. 5.3.2 below. The use of small pieces of wood slivers ensures that the chemicals used are effective and the time needed for ultrasonic homogenization after extraction is minimized (Laumer et al. 2009). The chopping procedure is obsolete if micromilling devices are used for sampling tree-ring material, however, precise tree-ring dissection with a scalpel is usually faster than with a semi-automatic micromilling devices. More recently, approaches to cellulose extraction from wood cross-sections (Sect. 5.3.3.3) were proposed that allow for tree-ring dissection from cellulose laths after extraction (Kagawa et al. 2015; Schollaen et al. 2017).

### 5.3.2 *Extraction Chemistry*

Three basic chemical approaches to extract cellulose or  $\alpha$ -cellulose are actually applied in stable isotope studies (Fig. 5.3). The most frequently used approaches to extract cellulose are initially based on a procedure described by Jayme (1942) and improved by Wise et al. (1946) (Jayme-Wise method, often referred to as method after Green (1963)). Two other approaches were established but are far less prevalent: the so-called Brendel-method (Brendel et al. 2000) and the diglyme-HCL method (MacFarlane et al. 1999).

If wood samples are not decayed, extraction procedures proposed here usually yield between about 30 to 45% of cellulose, depending on whether  $\alpha$ -cellulose or holocellulose is targeted. Assuming that about 200  $\mu$ g of cellulose are required for a routine mass spectrometric analysis, a minimum of 2 mg of wood material would allow up to 3 individual measurements.

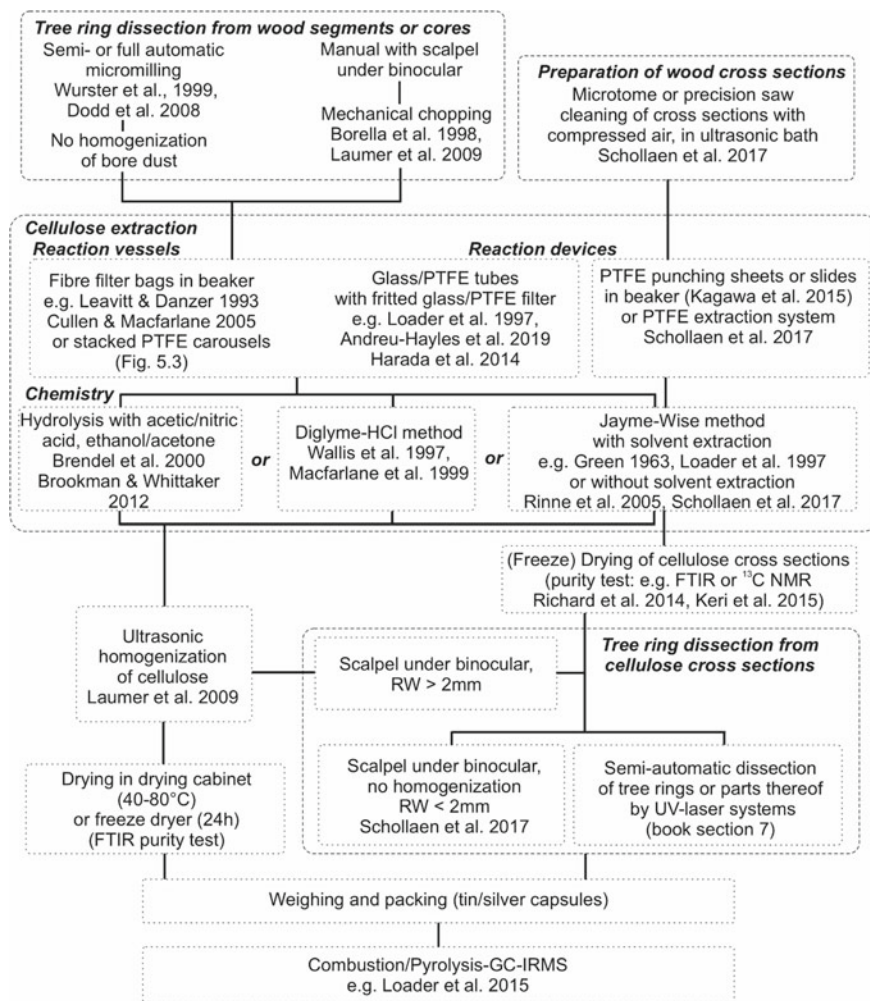


**Fig. 5.3** Overview of procedures of tree-ring stable isotope analysis involving cellulose extraction (modified after Schollaen et al. 2017). Note, removal of extractives from resinous conifers and certain tropical tree species is important. However, this is not highlighted as an extra step on the figure, because FTIR purity tests indicate that resin is removed by the bleaching procedure during cellulose extraction even without prior solvent extraction. For details cf. text, as well as key references given in this figure and citations therein

### 5.3.2.1 Removal of Extractives Prior to Cellulose Extraction

Green (1963) proposed a pretreatment of conifer wood in a Soxhlet apparatus with 2:1 benzene-ethanol and 95% ethanol or 95% ethanol and then ether. He considered a pretreatment to be unnecessary for most non-resinous woods except for tropical

woods. To date, a variety of solvents (ethanol, chloroform, methanol, toluene, deionized water) and solvent-mixtures are applied in isotope studies for removing extractives prior to cellulose extraction (Table 5.2, E<sup>1</sup> to E<sup>4</sup>). In most cases a Soxhlet apparatus is used, however, sometimes wood samples are simply treated with ethanol in a beaker for 1 or 2 days (e.g. Schollaen et al. 2013). Note, FTIR purity tests suggest that a solvent extraction step is unnecessary prior to cellulose extraction when applying the Jayme-Wise method (Sect. 5.3.2.4) to resinous conifers (Schollaen et al. 2017; Andreu-Hayles et al. 2019; Rinne et al. 2005).

### 5.3.2.2 Brendel Method

The Brendel-method applies iterations of acetic acid (80%) and nitric acid (70%) to finely ground wood samples at 120 °C. It has been modified for small samples (Evans and Schrag 2004) and with regards to chemistry (Anchukaitis et al. 2008; Gaudinski et al. 2005; English et al. 2011; Dodd et al. 2008), particularly including sodium hydroxide (NaOH) and extra water rinsing steps to yield pure  $\alpha$ -cellulose instead of holocellulose. The modified Brendel-method is supposed to be particularly attractive to non-specialist researchers new to the field of stable isotope dendroclimatology because it requires only basic equipment and reagents and an advantage over other approaches in terms of minimizing losses associated with filtering and changing of reaction vessels (Brookman and Whittaker 2012). However, even experienced researchers can still face problems with the modified extraction protocol (Berkelhammer and Stott 2011). As a disadvantage of this method it was raised that the proposed reaction temperature (120 °C) to be applied is close to (i) the boiling point for 70% nitric acid and (ii) to melting point of polypropylene microcentrifuge tubes or Eppendorf® vials. Brookman and Whittaker (2012) proposed to digest the samples at lower temperature (115 °C) and provided an update of this method.

### 5.3.2.3 Diglyme-HCL Method

The diglyme-HCL procedure as originally proposed by Wallis et al. (1997) was adapted for tree-ring stable isotope analysis by MacFarlane et al. (1999). It applies a 1:0.25 mixture of diglyme (1-Methoxy-2-(2-methoxyethoxy)ethane) and 10M HCl to ground wood samples at 90 °C (shaking water bath) for 1 h. Depending on the reaction vials used residual cellulose is obtained after cooling by gravity filtration (MacFarlane et al. 1999) or centrifugation and discarding of the supernatant (Hietz et al. 2005). Recovery of cellulose is faster when the wood samples are put into heat-sealed filter bags (e.g. type F57, pore size <30  $\mu$ m, Ankom Technology, NY) for subsequent chemical treatment in a beaker (Cullen and MacFarlane 2005). In adaptation to tropical tree species (*Cedrela odorata*, *Swietenia macrophylla*) Hietz et al. (2005) added an extra step of acidified NaClO<sub>2</sub> (10%, 12 h, 70 °C) ensuring complete removal of lignin.

### 5.3.2.4 Jayme-Wise Method

The Jayme-Wise-method is the prevailing approach to extracting cellulose in stable isotope studies. Originally the procedure results in holocellulose and comprises 3–6 iterations of delignification with sodium chlorite ( $\text{NaClO}_2$ , 1%) acidified with acetic acid to pH 3–4. The reaction temperature is set to about 70 °C and every 60 min fresh portions of acetic acid and sodium chlorite has to be added. A fume hood is required because chlorine dioxide is generated during the delignification. After 3–4 h (softwoods up to 6 h) white (sometimes slightly yellowish) holocellulose is obtained after thorough washing with de-ionized water. At present, the number of iterations with  $\text{NaClO}_2$ , concentration of solution, reaction temperature and reaction time vary by author. In isotope studies pH < 4 should not be used because lower pH will cause higher degradation of final cellulose.

In order to remove hemicelluloses (i.e. non-glucan polysaccharides, in particular xylan and mannan) Green (1963) proposed an additional step with sodium hydroxide (NaOH). He described treatments with various concentrations of NaOH (2–18%) and various reaction temperatures (room temperature to 95 °C) to obtain  $\alpha$ -cellulose. Hence, several different variants of this extraction procedure are currently used in the various stable isotope laboratories around the globe. They basically refer to Green (1963), Leavitt and Danzer (1993) and/or (Loader et al. 1997).

Pure  $\alpha$ -cellulose is usually isolated by a treatment of holocellulose with a NaOH solution (17%) at room temperature followed by repeated washing with deionized water and 1% (w/v) HCl until pH is neutral (e.g. Ziehmer et al. 2018; Loader et al. 1997). However, as indicated in Table 5.2 various other concentrations of the NaOH solution, application times and reaction temperatures were applied intending to isolate  $\alpha$ -cellulose ( $\alpha\text{C}^1$  to  $\alpha\text{C}^6$ ). Most frequently solutions with rather low NaOH concentrations (4–10%) are used but maintaining the relatively high reaction temperature (70–80 °C) of the preceding delignification step with  $\text{NaClO}_2$ . Some authors applying a low concentration, high temperature application of NaOH describe their product still holocellulose or just cellulose, since it has not always been tested whether or not all the xylan and mannan hemicelluloses were effectively removed from the holocellulose. Loader et al. (1997) reported that sequential treatment with a combination of 10% (w/v) NaOH at 80 °C followed by 17% (w/v) NaOH at room temperature maximized the removal of hemicelluloses. Either way, two studies found the carbon and oxygen isotopic compositions of hemicellulose and  $\alpha$ -cellulose to be identical (Gray and Thompson 1977; Richard et al. 2014), so that holocellulose seems to be well suited. More importantly, findings by Rinne et al. (2005) suggest that the 2-step extraction with  $\text{NaClO}_2$  and NaOH can make an extra solvent extraction step unnecessary.

### 5.3.2.5 Testing the Purity of Extracted Cellulose

Despite the various chemical procedures applied no systematic differences seem to prevail between them with respect to the isotopic signature of extracted cellulose. This



is because all the different extraction methods established were tested at some point for the purity of the isolated cellulose in comparison to corresponding wood (Richard et al. 2014; Schollaen et al. 2013; Andreu-Hayles et al. 2019; Keri et al. 2015; Kagawa et al. 2015; Brookman and Whittaker 2012). This is usually done by Infrared Spectrometry (FTIR or IR-ATR; e.g. Richard et al. (2014)) or liquid-state  $^{13}\text{C}$  NMR (Keri et al. 2015). Infrared spectrometry is the most common method to identify the functional groups of resin, lignin,  $\alpha$ -cellulose and hemicellulose. Analyses are usually performed on normalized spectra in the wavenumber region  $1800\text{--}730\text{ cm}^{-1}$ . A specific band at  $1694\text{ cm}^{-1}$  is characteristic of resins occurring only in conifer woods, some FTIR tests indicate that the chemical bleaching during cellulose extraction removes resin even without prior solvent extraction (e.g. Rinne et al. 2005). Further information on relevant FTIR wavenumbers according to literature can be found in SM5.3.2.5.

Apart from IR, liquid state  $^{13}\text{C}$  NMR (DEPT-135  $^{13}\text{C}$  NMR) was chosen as an analytical tool by Keri et al. (2015) in a comparative study testing nine variants of the Jayme-Wise extraction method for the isolation of cellulose from wood. The different approaches mainly varied in concentration of  $\text{NaClO}_2$ ,  $\text{NaOH}$ , and application time and reaction temperatures, as well as rinsing with  $\text{HCl}$ ,  $\text{HNO}_3$  and/or water. They evaluated the purity, degradation and yield of cellulose and stable isotope ratios of carbon and oxygen. All preparation methods tested resulted in pure  $\alpha$ -cellulose samples without hemicellulose and lignin content, and  $\delta^{13}\text{C}$  and  $\delta^{18}\text{O}$  measurements revealed similar values, thus indicating that all the published  $\text{NaClO}_2$  and  $\text{NaOH}$  chemical protocols based on the Jayme-Wise approach are suitable. It might be also best applied in conjunction with the technical devices described below for handling of large sample numbers (Andreu-Hayles et al. 2019; Kagawa et al. 2015; Schollaen et al. 2017).

### ***5.3.3 Extraction Devices—Or How to Keep Order When Processing Large Numbers of Small Samples***

#### **5.3.3.1 From Erlenmeyer Flasks to Custom-Made Filterfunnels**

In the early days of stable isotope analysis cellulose was extracted using Erlenmeyer flasks (Leavitt and Danzer 1993). Because fume hoods have to be used during chemical extraction the number of samples to be processed at a time was limited by the limited space provided for the rather large flasks. A major improvement has been made by introducing small borosilicate extraction thimbles with a sintered glass filter near the bottom end (Loader et al. 1997). Batches (25–50) of (labelled) thimbles could be placed into a beaker containing chemical solutions or deionized water for washing. The beaker containing the thimbles was placed into an ultrasonic bath to promote degassing at  $70\text{ }^\circ\text{C}$ . Removal of chemical solutions or water was achieved by taking out the thimbles from the beaker and vacuum filtration of remaining solvents

from each thimble. This approach was developed further by using filter thimbles with a tapered bottom (Büchner funnels) to make them fit into specially designed PTFE-devices (Wieloch et al. 2011; Andreu-Hayles et al. 2019) that allow simultaneous drainage of 20 interconnected filter funnels from solvents through a single outlet (Fig. 5.4e, f). As commercially available Büchner funnels are relatively expensive and tend to rapidly degrade after a few extractions, custom-made funnels were introduced (Harada et al. 2014; Andreu-Hayles et al. 2019). A borosilicate filter disc is secured between tubings made of glass or PTFE and silicone rubber (Fig. 5.4a, b). Properly labelled custom-made funnels can be placed also into beakers (Fig. 5.4c, d). For further details cf. Andreu-Hayles et al. (2019) and citations therein.

### 5.3.3.2 Filter Fiber Bags

Apart from filter funnels to take up wood material for extraction porous bags are utilized. The samples can be processed simultaneously in a Soxhlet apparatus and/or a beaker glass. A variety of bag materials, e.g., Polytetrafluoroethylene (PTFE), fibre glass are utilised. After the bags have been filled with the samples they are usually heat-sealed. Individual encoding of the bags is complicated since they cannot be simply inscribed with a pencil or felt-tipped pen. Therefore, they are either labelled by cutting out bits and pieces in different shapes from their borders or expensive pre-numbered bags are used. After one time application bags normally need to be replaced.

A handy way of processing a high number of samples within filter fiber bags while maintaining sample organisation and ensuring ease of chemical exchange and washing is to use a filter bag drum tower (FBDT) that is designed to hold filter fiber bags in place during cellulose extraction a 2000 mL beaker (Fig. 5.5). A FBDT contains up to five PTFE sample drums with 25 individually labelled slots placed on top of each other (Fig. 5.5a). Each slot can hold a single filter bag and unlike other methods, the bags do not require inscription. The entire FBDT can be lifted out of the beaker and placed into another one with fresh chemical solution or for neutralizing with boiling water (Fig. 5.5b, c, e).

Individual sample filter bags can be developed by cutting commercially available Ankom F57 filter bags (Fig. 5.5d) into up to 5 individual sample bags (depending on the size of the samples in question) and closed using an inexpensive Polythene Heat Sealer device or soldering iron. The FBDT provides a means of completing cellulose extraction in a single, economical unit which can be heated within a beaker on a single hotplate (Fig. 5.5b) or multiple beakers within a large water bath (Fig. 5.5f). In an optimal arrangement (Fig. 5.5f), five fully equipped beakers can be placed within an ultra-sonic water bath, resulting in 625 samples to be processed in one batch. See SM5.3.3.2 for details on the FBDT and remarks on F57 filter bags.

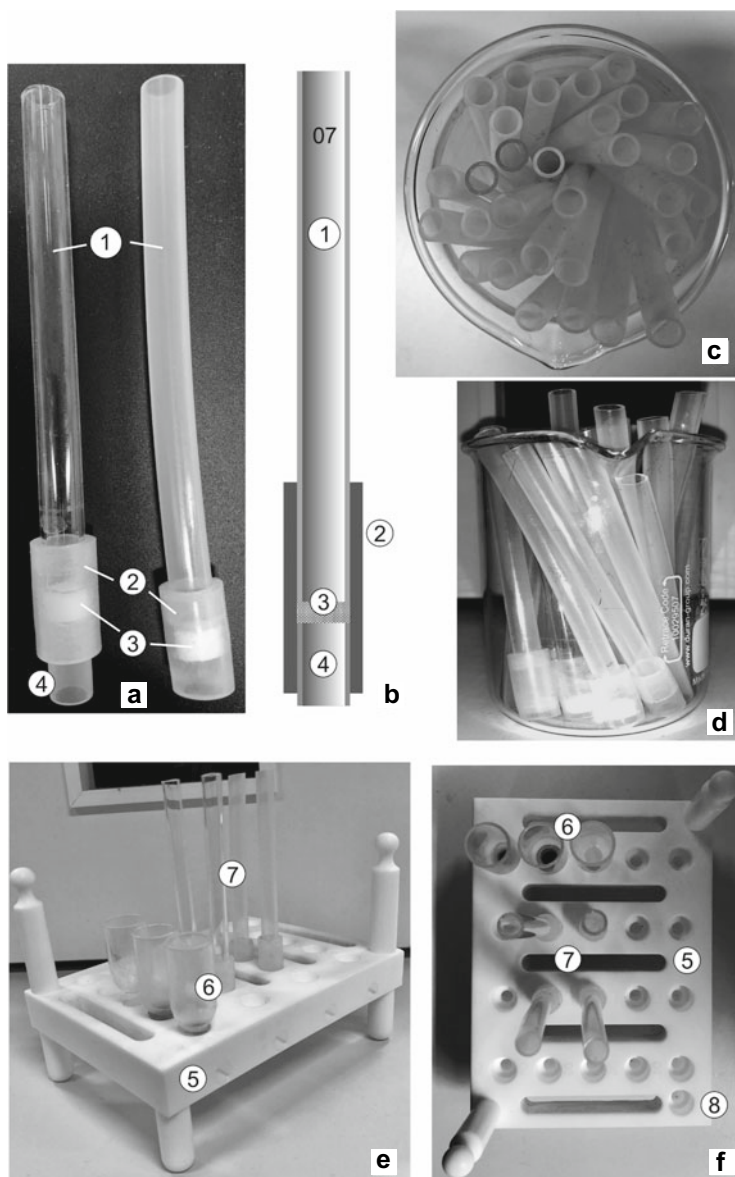


**Fig. 5.4** Custom-made funnel-filter assembly (**a, b**): (1) Glass or PTFE tube, (2) silicone tube, (3) borosilicate filter, (4) PTFE support tube for fitting into PTFE extraction device (**e, f**). **c, d** Several labelled filter funnels placed into a beaker for cellulose extraction without special PTFE device. (5) PTFE extraction device for placing into a water bath. (6) Borosilicate Büchner funnels positioned in PTFE extraction device with slots for up to 20 samples. (7) Custom-made funnels positioned in slots, sealed by silicone tubing. Slots are interconnected by channels leading to an outlet slot allowing simultaneous draining of all filter funnels. For details see Sect. 5.3.3.1, as well as Wieloch et al. (2011), Harada et al. (2014), Andreu-Hayles et al. (2019) and citations therein

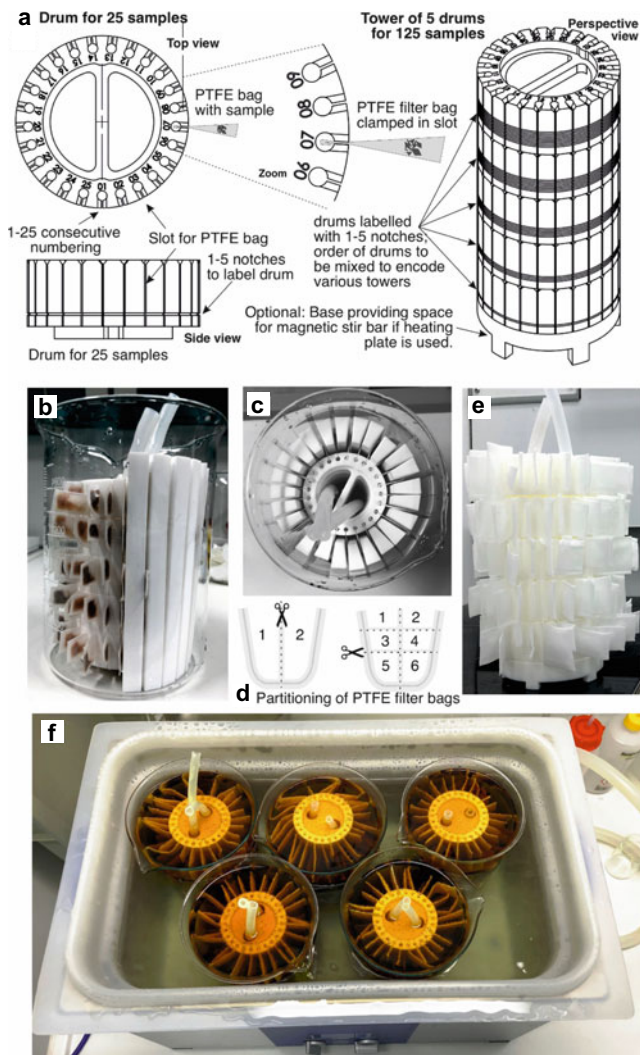


**Fig. 5.5** Filter bag drum tower (FBDT) for holding fiber filter bags in place during cellulose extraction. **a** Sketch drawings showing the design of individual PTFE sample drums for up to 25 filter bags. Up to five labeled PTFE sample drums can be combined forming a tower that can be placed into a 2000 mL beaker (**b**, **c**). FBDTs can be swapped between beakers while maintaining sample organisation by using flexible silicone tubings ensuring ease of chemical exchange and washing (**e**). PTFE segments can be placed vertically between the sample bags along the entire tower (**b**, **c**) to reduce the volume of chemical solution required to ca. 800 mL (in a 2000 mL beaker; 6.4 mL/samples). **d** Individual sample filter bags can be developed by cutting commercially available filter bags up (depending on the size of the samples in question) and using an inexpensive Polythene Heat Sealer device or soldering iron. **f** Five fully equipped beakers placed within an ultra-sonic water bath (Elmasonic S300H, Elma-Schmidbauer GmbH, Singen, Germany) allowing simultaneous treatment of 625 samples

### 5.3.3.3 Cellulose Extraction from Wood Cross-Sections

Loader et al. (2002) made a first attempt to extract cellulose directly from standard increment cores (5 mm Ø). However, this approach was not pursued further, because clear identification of boundaries of narrow tree ring was found difficult to achieve as the cores tend to shrink and twist during extraction and subsequent drying procedure. Instead, Li et al. (2011) reported a technique to extract cellulose from wood cross-sections of 3.5–4 mm thickness (wood laths, Fig. 5.6) using a special perforated PTFE casing to prevent cellulose splines from breaking apart. This method was developed further by Nakatsuka et al. (2011) and Kagawa et al. (2015), by utilizing special containers made of PTFE punching sheet to prevent disintegration of cellulose

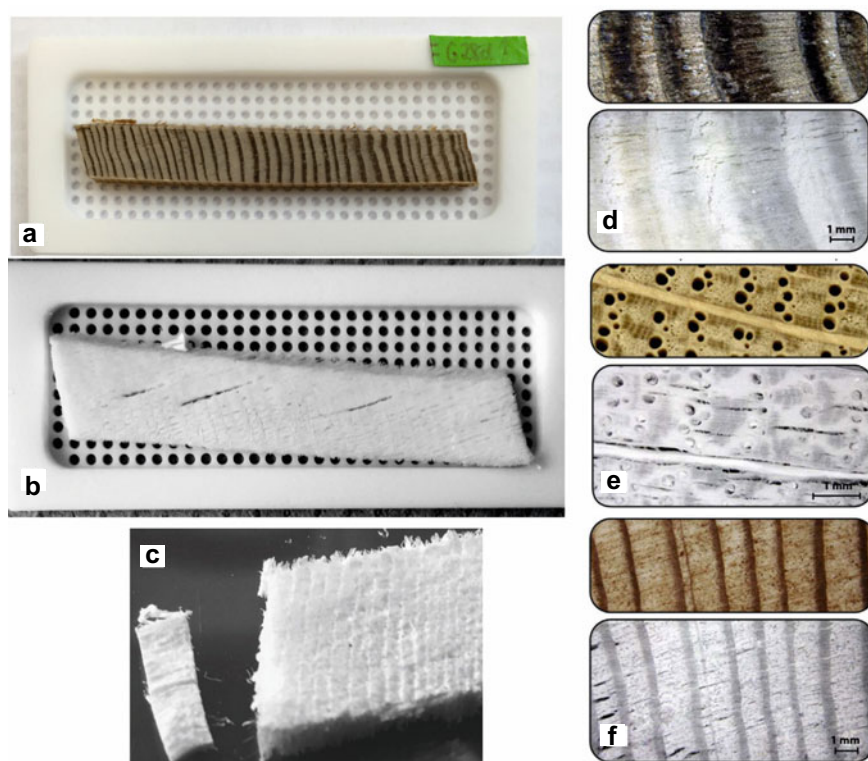


**Fig. 5.6** Cellulose extraction from wood cross-sections in custom made PTFE containers (70 mm × 30 mm). **a** Sub-fossil wood cross-section from pine (*P. sylvestris*, Binz, Switzerland). **b** Cellulose cross-section (ca. 3–4 mm thick). **c** Tree ring dissected from a cellulose cross-sections (10 mm wide, 3 mm thick). **d** Wood and cellulose cross-section from a degraded subfossil pine sample. **e** Wood and cellulose cross-section from oak (*Q. petraea*). **f** wood and cellulose cross-section of larch (*L. decidua*). The upper pictures of each species show wood cross-sections while the lower pictures display the cellulose cross-sections obtained. Tree-ring structures remained clearly visible after the cellulose extraction process. d, e, f modified after Schollaen et al. (2017)

laths (see also Xu et al. 2011). Based upon on the idea of extracting cellulose from wood laths, Schollaen et al. 2017 presented an improved semi-automated cellulose extraction system in conjunction with a comprehensive guide of manual (with scalpel, Fig. 5.6c) or semi-automatic (UV-Laser systems; cf. Chap. 7) sample preparation.

The chemical procedure is not different to methods described above (Sect. 5.3.2), however, wood sample preparation and tree-ring dissection of tree rings from cellulose cross-sections are special. Figure 5.6a, b show wood and white cellulose cross-sections of well-preserved sub-fossil *P. sylvestris* (ca. 14 k a BP) from Switzerland. Tree-ring boundaries can be well identified allowing binocular-aided tree-ring dissection with a scalpel (Fig. 5.6c). Tree rings of a partly decayed wood samples (Fig. 5.6d) are not so clearly visible. However, tree-ring structures of modern oak (Fig. 5.6e) and larch (Fig. 5.6f) are well preserved after the cellulose extraction process. For further details cf. Schollaen et al. 2017 and citations therein.

### 5.3.4 Homogenization of Micro Amounts of Cellulose Samples

As mentioned above, one of the advantages of extracting cellulose is that sample homogenization is simpler. Cellulose can be homogenized rather quickly (100 samples/hour or more) by ultrasonic devices (e.g. UP200s, Hielscher Ultrasonics, Germany) (Laumer et al. 2009). Contrastingly, wood material, if not obtained from full- or semi-automatic micromilling devices (e.g. Dremel<sup>®</sup> rotary tools) has to be homogenized by grinding after dissecting tree rings using a scalpel. Usually (modified) coffee mills (e.g. Borella et al. 1998; Szymczak et al. 2011), ultra-centrifugal mills (ZM200, Retsch GmbH, Haan, Germany) (e.g. Wieloch et al. 2011) or ball mills (e.g. mixer mill MM200, Retsch, Haan, Germany) (e.g. Weigt et al. 2015) are utilized. Although the grinding process itself may only take a few seconds, the necessary cleaning process is usually rather time consuming and sample losses may be high (Laumer et al. 2009).

Homogenization by ultrasonic cracking is virtually without sample loss because sample material does not have to be transferred between storage vials and any special homogenization vessels. Sample material is kept in suspension with water during ultrasound treatment and vacuum freeze-dried thereafter. Laumer et al. (2009) tested and confirmed that neither cellulose soaked in water and stored overnight nor cellulose treated ultrasonically for different time periods showed a significant difference in  $\delta^{18}\text{O}$  from untreated cellulose. No such tests were yet performed with respect to hydrogen isotopes.

## 5.4 Concluding Remarks

Many of the studies that have compared stable isotope ratios in wood and its cellulose suggest that cellulose extraction is not necessary. However, this is not without constraints. Removal of extractives from resinous conifers and certain tropical tree species is required in any case. Studies indicate that this is provided by the chemical bleaching during cellulose extraction even without prior solvent extraction. Furthermore, the basic question remains whether or not the benchmarking studies were broad enough for a general conclusive statement with regard to geographical range, species selection, ecological gradients or time range. Still, tests seem to be advised for environmental or climatological isotope studies, maybe except for those at short-term scale focusing on sapwood. The climatic or ecological signal of a tree-ring stable isotope sequence can be strengthened or weakened by variable relative amounts of wood constituents. In particular, during periods of low isotope variability signals may be weakened or even inverted. Radial changes in relative amounts of wood constituents from pith to bark, e.g. due to conversion of sapwood into heartwood or wood degrading processes can cause trends in isotope chronologies from wood that are unrelated to trends in the desired environmental signal. Hence, varying cellulose to lignin ratios may be critical when analyzing long-term climate trends from old living trees (across heartwood and sapwood) and/or potentially decayed trunks. It may not be required for obtaining information on extreme events such as droughts or high-rainfall years, when large year-to-year isotopic shifts potentially make effects of varying wood constituents insignificant. Nonetheless, a moisture signal in tree-ring  $\delta^{13}\text{C}$  from wood may be enhanced if the fraction of  $^{13}\text{C}$ -depleted secondary metabolites, like lignin or fatty acids, decreases/increases with dry/wet conditions relative to  $^{13}\text{C}$  enriched primary products like cellulose or starch. Correlations may be weakened if the opposite occurs, and the stable isotope signal and wood composition respond differently to certain environmental changes.

Differences in the proportion of the various wood constituents are not the main source of isotope variability within a tree stand. The use of cellulose is likely not reducing this variability (McCarroll and Loader 2004), but changing wood composition adds to the noise in tree-ring stable isotope signals from wood. Hence, cellulose extraction is of benefit. A preceding Soxhlet procedure to remove extractives seems obsolete and homogenization of cellulose is much faster than grinding wood samples. The experimental setups for extraction have dramatically improved over the last decade with respect to handling and costs. Several guidelines for chemical extraction procedures are available. They basically represent modifications of three different chemical approaches (Jayme-Wise, Brendel-, diglyme-HCL method) that are well approved. Any non-specialist or specialist researcher can establish and/or improve their own guideline in accordance to the technical framework of their laboratory, available budget and research aim. Last, but not least, further investigations of wood constituents and their isotope signatures as a function of a tree's life, i.e. across sapwood and heartwood, in response to climate variables, as well as with respect to wood and cellulose decay are advised. Both, tree-ring stable isotope time

series from wood, as well as from cellulose have revealed nonstationary relationships with climate variables. They may respond differently under particular environmental conditions in the surrounding of a tree, such as weather anomalies, changing length in seasonality, tree competition etc. Consequently, the analyses of isotope data from cellulose, wood and lignin methoxyl groups could in part point to different environmental signals, help to assess effects of wood decay and, hence, provide an added value. In parallel to stable isotope analysis, measurements of the chemical composition of wood could enable a potential correction of isotope signals or ensure that changing wood composition is insignificant relative to the variability of the isotopic signals.

## References

- Agarwal UP, Atalla RH (1986) In-situ microprobe studies of plant cell walls: macromolecular organization and compositional variability in the secondary wall of *Picea mariana* (Mill.) B.S.P. *Planta* 169:325–332
- Anchukaitis KJ, Evans MN, Lange T, Smith DR, Leavitt SW, Schrag DP (2008) Consequences of a rapid cellulose extraction technique for oxygen isotope and radiocarbon analyses. *Anal Chem* 80(6):2035–2041. <https://doi.org/10.1021/ac7020272>
- Andreu-Hayles L, Levesque M, Martin-Benito D, Huang W, Harris R, Oelkers R, Leland C, Martin-Fernandez J, Anchukaitis KJ, Helle G (2019) A high yield cellulose extraction system for small whole wood samples and dual measurement of carbon and oxygen stable isotopes. *Chem Geol* 504:53–65. <https://doi.org/10.1016/j.chemgeo.2018.09.007>
- Barbour MM, Andrews TJ, Farquhar GD (2001) Correlations between oxygen isotope ratios of wood constituents of *Quercus* and *Pinus* samples from around the world. *Aust J Plant Physiol* 28(5):335–348. <https://doi.org/10.1071/Pp00083>
- Battipaglia G, Jaeggi M, Saurer M, Siegwolf RTW, Cotrufo MF (2008) Climatic sensitivity of delta O-18 in the wood and cellulose of tree rings: results from a mixed stand of *Acer pseudoplatanus* L. and *Fagus sylvatica* L. *Palaeogeogr Palaeoclimatol Palaeoecol* 261(1–2):193–202. <https://doi.org/10.1016/j.palaeo.2008.01.020>
- Bechtel A, Gruber W, Sachsenhofer RF, Gratzer R, Lucke A, Puttmann W (2003a) Depositional environment of the Late Miocene Hausruck lignite (Alpine Foreland Basin): insights from petrography, organic geochemistry, and stable carbon isotopes. *Int J Coal Geol* 53(3):153–180. [https://doi.org/10.1016/s0166-5162\(02\)00194-5](https://doi.org/10.1016/s0166-5162(02)00194-5)
- Bechtel A, Sachsenhofer RF, Markic M, Gratzer R, Lucke A, Puttmann W (2003b) Paleoenvironmental implications from biomarker and stable isotope investigations on the Pliocene Velenje lignite seam (Slovenia). *Org Geochem* 34(9):1277–1298. [https://doi.org/10.1016/s0146-6380\(03\)00114-1](https://doi.org/10.1016/s0146-6380(03)00114-1)
- Bechtel A, Reischenbacher D, Sachsenhofer RF, Gratzer R, Lucke A (2007a) Paleogeography and paleoecology of the upper Miocene Zillingdorf lignite deposit (Austria). *Int J Coal Geol* 69(3):119–143. <https://doi.org/10.1016/j.coal.2006.03.001>
- Bechtel A, Reischenbacher D, Sachsenhofer RF, Gratzer R, Lucke A, Puttmann W (2007b) Relations of petrographical and geochemical parameters in the middle Miocene Lavanttal lignite (Austria). *Int J Coal Geol* 70(4):325–349. <https://doi.org/10.1016/j.coal.2006.07.002>
- Bechtel A, Sachsenhofer RF, Gratzer R, Lucke A, Puttmann W (2002) Parameters determining the carbon isotopic composition of coal and fossil wood in the Early Miocene Oberdorf lignite seam (Styrian Basin, Austria). *Org Geochem* 33(8):1001–1024. [https://doi.org/10.1016/s0146-6380\(02\)00054-2](https://doi.org/10.1016/s0146-6380(02)00054-2)



- Berkelhammer M, Stott L (2011) Correction to “Recent and dramatic changes in Pacific storm trajectories as recorded in the  $\delta^{18}\text{O}$  of Bristlecone Pine tree ring cellulose”. *Geochem Geophys Geosyst* 12 (9):n/a–n/a. <https://doi.org/10.1029/2011GC003765>
- Bertaud F, Holmbom B (2004) Chemical composition of earlywood and latewood in Norway spruce heartwood, sapwood and transition zone wood. *Wood Sci Technol* 38(4):245–256. <https://doi.org/10.1007/s00226-004-0241-9>
- Borella S, Leuenberger M, Saurer M (1999) Analysis of delta O-18 in tree rings: wood-cellulose comparison and method dependent sensitivity. *J Gerontol Ser A Biol Med Sci* 104(D16):19267–19273. <https://doi.org/10.1029/1999jd900298>
- Borella S, Leuenberger M, Saurer M, Siegwolf R (1998) Reducing uncertainties in delta C-13 analysis of tree rings: pooling, milling, and cellulose extraction. *J Geophys Res-Atmos* 103(D16):19519–19526. <https://doi.org/10.1029/98jd01169>
- Boudet AM (2000) Lignins and lignification: selected issues. *Plant Physiol Biochem* 38:81–96. [https://doi.org/10.1016/S0981-9428\(00\)00166-2](https://doi.org/10.1016/S0981-9428(00)00166-2)
- Brendel O, Iannetta PPM, Stewart D (2000) A rapid and simple method to isolate pure alpha-cellulose. *Phytochem Anal* 11(1):7–10. [https://doi.org/10.1002/\(SICI\)1099-1565\(200001/02\)11:1%3c7::AID-PCA488%3e3.0.CO;2-U](https://doi.org/10.1002/(SICI)1099-1565(200001/02)11:1%3c7::AID-PCA488%3e3.0.CO;2-U)
- Breninkmeijer CAM (1983) Deuterium, Oxygen-18 and Carbon-13 in tree rings and peat deposits in relation to climate. Ph.D. thesis, Rijksuniversiteit te Groningen, Groningen, The Netherlands
- Brookman T, Whittaker T (2012) Experimental assessment of the purity of alpha-cellulose produced by variations of the Brendel method: Implications for stable isotope (delta C-13, delta O-18) dendroclimatology. *Geochem Geophys Geosyst* 13. <https://doi.org/10.1029/2012gc004215>
- Browning BL (1967) 19. The isolation and determination of cellulose / 20. Solubility in alkaline solvents. In: *Methods of wood chemistry, vol II*. Interscience Publishers (Wiley), New York-London-Sydney, pp 387–427
- Craig H (1954) Carbon-13 variations in Sequoia rings and the atmosphere. *Science* 119:141–143
- Cullen LE, Grierson PF (2006) Is cellulose extraction necessary for developing stable carbon and oxygen isotopes chronologies from *Callitris glaucophylla*? *Palaeogeogr Palaeoclimatol Palaeoecol* 236(3–4):206–216. <https://doi.org/10.1016/j.palaeo.2005.11.003>
- Cullen LE, MacFarlane C (2005) Comparison of cellulose extraction methods for analysis of stable isotope ratios of carbon and oxygen in plant material. *Tree Physiol* 25(5):563–569. <https://doi.org/10.1093/treephys/25.5.563>
- D’Alessandro CM, Guerrieri MR, Saracino A (2004) Comparing carbon isotope composition of bulk wood and holocellulose from *Quercus cerris*, *Fraxinus ornus* and *Pinus radiata* tree rings. *Forest@ - J Silvicult For Ecol* 1(1):51–57. <https://doi.org/10.3832/efor0217-0010051>
- DeNiro MJ, Epstein S (1977) Mechanism of carbon isotope fractionation associated with lipid synthesis. *Science* 197(4300):261–263. <https://doi.org/10.1126/science.327543>
- Dodd JP, Patterson WP, Holmden C, Brasseur JM (2008) Robotic micromilling of tree-rings: a new tool for obtaining subseasonal environmental isotope records. *Chem Geol* 252(1–2):21–30. <https://doi.org/10.1016/j.chemgeo.2008.01.021>
- Edvardsson J, Edwards TWD, Linderson H, Hammarlund D (2014) Exploring climate forcing of growth depression in subfossil South Swedish bog pines using stable isotopes. *Dendrochronologia* 32(1):55–61. <https://doi.org/10.1016/j.dendro.2013.08.002>
- Eglin T, Maunoury-Danger F, Fresneau C, Lelarge C, Pollet B, Lapierre C, Francois C, Damesin C (2008) Biochemical composition is not the main factor influencing variability in carbon isotope composition of tree rings. *Tree Physiol* 28(11):1619–1628. <https://doi.org/10.1093/treephys/28.11.1619>
- English NB, McDowell NG, Allen CD, Mora C (2011) The effects of alpha-cellulose extraction and blue-stain fungus on retrospective studies of carbon and oxygen isotope variation in live and dead trees. *Rapid Commun Mass Spectrom* 25(20):3083–3090. <https://doi.org/10.1002/rcm.5192>
- Epstein S, Yapp CJ (1976) Climatic implications of the D/H ratio of hydrogen in C-H groups in tree cellulose. *Earth Planet Sci Lett* 30:252–261

- Evans MN, Schrag DP (2004) A stable isotope-based approach to tropical dendroclimatology. *Geochim Cosmochim Acta* 68(16):3295–3305. <https://doi.org/10.1016/j.gca.2004.01.006>
- Farmer JG, Baxter MS (1974) Atmospheric carbon-dioxide levels as indicated by stable isotope records in wood. *Nature* 247(5439):273–275
- Farquhar GD, O’Leary MH, Berry JA, (1982) On the relationship between carbon isotope discrimination and the intercellular carbon dioxide concentration in leaves. *Aust J Plant Physiol* 9:121–137
- Fergus BJ, Procter AR, Scott JAN, Goring DAI (1969) Distribution of lignin in sprucewood as determined by ultraviolet microscopy. *Wood Sci Technol* 3(2):117–138
- Ferrio JP, Voltas J (2005) Carbon and oxygen isotope ratios in wood constituents of *Pinus halepensis* as indicators of precipitation, temperature and vapour pressure deficit. *Tellus* 57B(2):164–173. <https://doi.org/10.1111/j.1600-0889.2005.00137.x>
- Friedman JM, Stricker CA, Csank AZ, Zhou HH (2019) Effects of age and environment on stable carbon isotope ratios in tree rings of riparian *Populus*. *Palaeogeogr Palaeoclimatol Palaeoecol* 524:25–32. <https://doi.org/10.1016/j.palaeo.2019.03.022>
- Fukazawa K, Imagawa H (1981) Quantitative analysis of lignin using an UV microscopic image analyzer—variation within one growth increment. *Wood Sci Technol* 15(1):45–55
- Gaudinski JB, Dawson TE, Quideau S, Schuur EAG, Roden JS, Trumbore SE, Sandquist DR, Oh SW, Wasylishen RE (2005) Comparative analysis of cellulose preparation techniques for use with C-13, C-14, and O-18 isotopic measurements. *Anal Chem* 77(22):7212–7224. <https://doi.org/10.1021/ac050548u>
- Gindl W (2001) Cell-wall lignin content related to tracheid dimensions in drought-sensitive Austrian pine (*Pinus nigra*). *IAWA J* 22(2):113–120. <https://doi.org/10.1163/22941932-90000272>
- Gleixner G, Danier HJ, Werner RA, Schmidt HL (1993) Correlations between the delta 13-C content of primary and secondary plant products in different cell compartments and that in decomposing basidiomycetes. *Plant Physiol* 102:1287–1290
- Gori Y, Wehrens R, Greule M, Keppler F, Ziller L, La Porta N, Camin F (2013) Carbon, hydrogen and oxygen stable isotope ratios of whole wood, cellulose and lignin methoxyl groups of *Picea abies* as climate proxies. *Rapid Commun Mass Spectrom* 27(1):265–275. <https://doi.org/10.1002/rcm.6446>
- Gray J, Thompson P (1977) Climatic information from <sup>18</sup>O/<sup>16</sup>O analysis of cellulose, lignin and whole wood from tree rings. *Nature* 270:708–709
- Green JW (1963) Wood cellulose. In: Whistler RL, Green JW, BeMiller JN, Wolfrom ML (eds) *Methods in carbohydrate chemistry, vol III, cellulose*. Academic Press, New York, pp 9–21
- Greule M, Keppler F (2011) Stable isotope determination of ester and ether methyl moieties in plant methoxyl groups. *Isot Environ Health Stud* 47(4):470–482. <https://doi.org/10.1080/10256016.2011.616270>
- Greule M, Mosandl A, Hamilton JTG, Keppler F (2009) A simple rapid method to precisely determine C-13/C-12 ratios of plant methoxyl groups. *Rapid Commun Mass Spectrom* 23(11):1710–1714. <https://doi.org/10.1002/rcm.4057>
- Gu HL, Wang J, Lei C (2020) Climate-sensitivity comparisons for whole wood, holocellulose, and alpha-cellulose carbon isotope series in masson pine. *Arab J Sci Eng*. <https://doi.org/10.1007/s13369-020-04629-w>
- Guerrieri R, Jennings K, Belmecheri S, Asbjornsen H, Ollinger S (2017) Evaluating climate signal recorded in tree-ring delta C-13 and delta O-18 values from bulk wood and alpha-cellulose for six species across four sites in the northeastern US. *Rapid Commun Mass Spectrom* 31(24):2081–2091. <https://doi.org/10.1002/rcm.7995>
- Guest D, Brown J (1997) *Plant pathogens and plant diseases*. Rockvale publications National library of Australia
- Hall C (1993) *Wood: decay, pests and protection*. Chapman & Hall, London, UK
- Harada M, Watanabe Y, Nakatsuka T, Tazuru-Mizuno S, Horikawa Y, Sugiyama J, Tsuda T, Tagami T (2014) Alpha-cellulose extraction procedure for the tropical tree sungkai (*Peronema canescens*

- Jack) by using an improved vessel for reliable paleoclimate reconstruction. *Geochem J* 48(3):299–307. <https://doi.org/10.2343/geochemj.2.0306>
- Harlow BA, Marshall JD, Robinson AP (2006) A multi-species comparison of delta C-13 from whole wood, extractive-free wood and holocellulose. *Tree Physiol* 26(6):767–774. <https://doi.org/10.1093/treephys/26.6.767>
- Helle G, Schleser GH (2004) Beyond CO<sub>2</sub>-fixation by Rubisco—an interpretation of C-13/C-12 variations in tree rings from novel intra-seasonal studies on broad-leaf trees. *Plant Cell Environ* 27(3):367–380
- Hietz P, Wanek W, Dunisch O (2005) Long-term trends in cellulose delta C-13 and water-use efficiency of tropical *Cedrela* and *Swietenia* from Brazil. *Tree Physiol* 25(6):745–752. <https://doi.org/10.1093/treephys/25.6.745>
- Hillis WE (1987) Heartwood and tree exudates. Springer Series in wood science, vol 4. Springer, Berlin. <https://doi.org/10.1007/978-3-642-72534-0>
- Hook BA, Halfar J, Bollmann J, Gedalof Z, Rahman MA, Reyes J, Schulze DJ (2015) Extraction of alpha-cellulose from mummified wood for stable isotopic analysis. *Chem Geol* 405:19–27. <https://doi.org/10.1016/j.chemgeo.2015.04.003>
- Jayme G (1942) Preparation of holocellulose and cellulose with sodium chlorite. *Cellul Chem Technol* 20:43–49
- Kagawa A, Sano M, Nakatsuka T, Ikeda T, Kubo S (2015) An optimized method for stable isotope analysis of tree rings by extracting cellulose directly from cross sectional laths. *Chem Geol* 393–394:16–25. <https://doi.org/10.1016/j.chemgeo.2014.11.019>
- Keith CT (1969) Resin content of red pine wood and its effect on specific gravity determinations. *For Chron* 10:338–343
- Keppler F, Harper DB, Kalin RM, Meier-Augenstein W, Farmer N, Davis S, Schmidt HL, Brown DM, Hamilton JTG (2007) Stable hydrogen isotope ratios of lignin methoxyl groups as a paleoclimate proxy and constraint of the geographical origin of wood. *New Phytol* 176(3):600–609. <https://doi.org/10.1111/j.1469-8137.2007.02213.x>
- Keri M, Palcsu L, Turi M, Heim E, Czebely A, Novak L, Banyai I (2015) C-13 NMR analysis of cellulose samples from different preparation methods. *Cellulose* 22(4):2211–2220. <https://doi.org/10.1007/s10570-015-0642-y>
- Klason P (1911) Beiträge zur Kenntnis der chemischen Zusammensetzung des Fichtenholzes. *Schriften des Vereins der Zellstoff- und Papier-Chemiker* 2
- Kürschner K, Popik MG (1962) Zur Analyse von Hölzern. *Mitteilungen zur Chemie, Physik, Biologie Und Technik Des Holzes* 1:1–11
- Kurth EF (1933) Distribution and nature of extractives in longleaf and shortleaf pine. *Ind Eng Chem* 25(2):192–195
- Lanvermann C, Evans R, Schmitt U, Hering S, Niemz P (2013) Distribution of structure and lignin within growth rings of Norway spruce. *Wood Sci Technol* 47(3):627–641. <https://doi.org/10.1007/s00226-013-0529-8>
- Laumer W, Andreu L, Helle G, Schleser GH, Wieloch T, Wissel H (2009) A novel approach for the homogenization of cellulose to use micro-amounts for stable isotope analyses. *Rapid Commun Mass Spectrom* 23(13):1934–1940. <https://doi.org/10.1002/Rcm.4105>
- Leavitt SW, Danzer SR (1993) Method for batch processing small wood samples to holocellulose for stable-carbon isotope analysis. *Anal Chem* 65(1):87–89. <https://doi.org/10.1021/ac00049a017>
- Leavitt SW, Long A (1982) Stable carbon isotopes as a potential supplemental tool in dendrochronology. *Tree-Ring Bulletin* 42:49–55
- Leavitt SW, Long A (1991) Seasonal stable-carbon isotope variability in tree rings: possible paleoenvironmental signals. *Chem Geol (Isot Geosci Sect)* 87(1):59–70. [https://doi.org/10.1016/0168-9622\(91\)90033-S](https://doi.org/10.1016/0168-9622(91)90033-S)
- Lee S, Park BS, Lee D, Chung H, Lee KS (2015) Spatial variability in hydrogen and oxygen isotopic composition of Korean Red Pine and its implication for tracing wood origin. *Environ Earth Sci* 73(12):8045–8052. <https://doi.org/10.1007/s12665-014-3960-8>

- Li Z-H, Labbé N, Driese SG, Grissino-Mayer HD (2011) Micro-scale analysis of tree-ring  $\delta^{18}\text{O}$  and  $\delta^{13}\text{C}$  on  $\alpha$ -cellulose spline reveals high-resolution intra-annual climate variability and tropical cyclone activity. *Chem Geol* 284(1–2):138–147. <https://doi.org/10.1016/j.chemgeo.2011.02.015>
- Libby LM, Pandolfi LJ (1974) Temperature dependence of isotope ratios in tree rings. *Proc Natl Acad Sci* 71(6):2482–2486
- Livingston NJ, Spittlehouse DL (1996) Carbon isotope fractionation in tree ring early and late wood in relation to intra-growing season water balance. *Plant, Cell Environ* 19(6):768–774. <https://doi.org/10.1111/j.1365-3040.1996.tb00413.x>
- Loader NJ, Robertson I, Barker AC, Switsur VR, Waterhouse JS (1997) An improved technique for the batch processing of small wholewood samples to  $\alpha$ -cellulose. *Chem Geol* 136(3–4):313–317. [https://doi.org/10.1016/S0009-2541\(96\)00133-7](https://doi.org/10.1016/S0009-2541(96)00133-7)
- Loader NJ, Robertson I, Luecke A, Helle G (2002) Preparation of hollocellulose from standard increment cores for stable carbon isotope analysis. *Swansea Geographer* 37:1–9
- Loader NJ, Robertson I, McCarroll D (2003) Comparison of stable carbon isotope ratios in the whole wood, cellulose and lignin of oak tree-rings. *Palaeogeogr Palaeoclimatol Palaeoecol* 196(3–4):395–407. [https://doi.org/10.1016/S0031-0182\(03\)00466-8](https://doi.org/10.1016/S0031-0182(03)00466-8)
- Loader NJ, Street-Perrott FA, Daley TJ, Hughes PD, Kimak A, Levanic T, Mallon G, Mauquoy D, Robertson I, Roland TP, van Bellen S, Ziehmer MM, Leuenberger M (2015) Simultaneous determination of stable carbon, oxygen, and hydrogen isotopes in cellulose. *Anal Chem* 87(1):376–380. <https://doi.org/10.1021/ac502557x>
- Lukens WE, Eze P, Schubert BA (2019) The effect of diagenesis on carbon isotope values of fossil wood. *Geology* 47(10):987–991. <https://doi.org/10.1130/g46412.1>
- MacFarlane C, Warren CR, White DA, Adams MA (1999) A rapid and simple method for processing wood to crude cellulose for analysis of stable carbon isotopes in tree rings. *Tree Physiol* 19(12):831–835. <https://doi.org/10.1093/treephys/19.12.831>
- Marshall JD, Monsrud RA (1996) Homeostatic gas-exchange parameters inferred from C-13/C-12 in tree rings of conifers. *Oecologia* 105(1):13–21. <https://doi.org/10.1007/Bf00328786>
- Mazany T, Lerman JC, Long A (1980) Carbon-13 in tree-ring cellulose as an indicator of past climates. *Nature* 287:432–435
- McCarroll D, Loader NJ (2004) Stable isotopes in tree rings. *Quatern Sci Rev* 23(7–8):771–801
- Mischel M, Esper J, Keppler F, Greule M, Werner W (2015) Delta H-2, delta C-13 and delta O-18 from whole wood, alpha-cellulose and lignin methoxyl groups in *Pinus sylvestris*: a multi-parameter approach. *Isot Environ Health Stud* 51(4):553–568. <https://doi.org/10.1080/10256016.2015.1056181>
- Nagavciuc V, Kern Z, Perşoiu A, Kesjár D, Popa I (2018) Aerial decay influence on the stable oxygen and carbon isotope ratios in tree ring cellulose. *Dendrochronologia* 49:110–117. <https://doi.org/10.1016/j.dendro.2018.03.007>
- Nakatsuka T, Zhang C, Yasue K, Kagawa A (2011) Extracting  $\alpha$ -cellulose from tree-ring laths—a new method for tree ring stable isotope analysis. In: 2nd International Asian dendrochronological conference, Xian, China, 20–24 August 2011
- Narayanamurti D, Das NR (1955) Die Abhängigkeit der chemischen Zusammensetzung des Holzes einiger indischer Holzarten von seiner Lage innerhalb des Stammes. *Holz Als Roh- Und Werkstoff* 13(2):52–56
- Pettersen RC (1984) The chemical composition of wood. In: Rowell R (ed) *The chemistry of solid wood*. Advances in chemistry series. 207. American Chemical Society, Washington, DC, pp 57–126
- PIK-Potsdam (2020) Long term meteorological weather station Potsdam Telegrafenberg. Potsdam Institute for Climate Impact Research. [www.pik-potsdam.de/services/climate-weather-potsdam](http://www.pik-potsdam.de/services/climate-weather-potsdam). Accessed 19 April 2020
- Pons TL, Helle G (2011) Identification of anatomically non-distinct annual rings in tropical trees using stable isotopes. *Trees-Struct Funct* 25(1):83–93. <https://doi.org/10.1007/s00468-010-0527-5>

- Richard B, Quiles F, Carteret C, Brendel O (2014) Infrared spectroscopy and multivariate analysis to appraise alpha-cellulose extracted from wood for stable carbon isotope measurements. *Chem Geol* 381:168–179. <https://doi.org/10.1016/j.chemgeo.2014.05.010>
- Rinne KT, Boettger T, Loader NJ, Robertson I, Switsur VR, Waterhouse JS (2005) On the purification of alpha-cellulose from resinous wood for stable isotope (H, C and O) analysis. *Chem Geol* 222(1–2):75–82. <https://doi.org/10.1016/j.chemgeo.2005.06.010>
- Robertson I, Loader NJ, McCarroll D, Carter AHC, Cheng L, Leavitt SW (2004)  $\delta^{13}\text{C}$  of tree-ring lignin as an indirect measure of climate change. *Water Air Soil Pollut Focus* 4:531–544
- Roden JS, Farquhar GD (2012) A controlled test of the dual-isotope approach for the interpretation of stable carbon and oxygen isotope ratio variation in tree rings. *Tree Physiol* 32(4):490–503. <https://doi.org/10.1093/treephys/tps019>
- Sass-Klaassen U, Poole I, Wils T, Helle G, Schleser GH, van Bergen PF (2005) Carbon and oxygen isotope dendrochronology in sub-fossil bog oak tree rings—a preliminary study. *IAWA J* 26(1):121–136. <https://doi.org/10.1163/22941932-90001607>
- Saurer M, Cherubini P, Siegwolf R (2000) Oxygen isotopes in tree-rings of *Abies alba*: the climatic significance of interdecadal variations. *J Geophys Res* 105(D10):12461–12470. <https://doi.org/10.1029/2000jd900160>
- Savard MM, Begin C, Marion J, Arseneault D, Begin Y (2012) Evaluating the integrity of C and O isotopes in sub-fossil wood from boreal lakes. *Palaeogeogr Palaeoclimatol Palaeoecol* 348:21–31. <https://doi.org/10.1016/j.palaeo.2012.06.003>
- Schleser GH, Anhof D, Helle G, Vos H (2015) A remarkable relationship of the stable carbon isotopic compositions of wood and cellulose in tree-rings of the tropical species *Cariniana micrantha* (Ducke) from Brazil. *Chem Geol* 401:59–66. <https://doi.org/10.1016/j.chemgeo.2015.02.014>
- Schleser GH, Frielingsdorf J, Blair A (1999) Carbon isotope behaviour in wood and cellulose during artificial aging. *Chem Geol* 158(1–2):121–130. [https://doi.org/10.1016/S0009-2541\(99\)00024-8](https://doi.org/10.1016/S0009-2541(99)00024-8)
- Schmidt HL (1999) Isotope discriminations upon biosynthesis in natural systems: general causes and individual factors of the different bioelements. *Isot Environ Health Stud* 35(1–2):11–18. <https://doi.org/10.1080/10256019908234076>
- Schmidt HL, Gleixner G, Griffiths H (1998) Carbon isotope effects on key reactions in plant metabolism and  $^{13}\text{C}$  patterns in natural compounds. *Stable isotopes—integration of biological, ecological and geochemical processes*. Environmental plant biology. BIOS Scientific Publishers, Oxford, UK, pp 13–26
- Schmidt HL, Kexel H, Butzenlechner M, Schwarz S, Gleixner G, Thimet S, Werner RA, Gensler M (1993) Non-statistical isotope distribution in natural compounds: mirror of their biosynthesis and key for their origin assignment. In: Wada E (ed) *Isotopes in nature*, Tokyo
- Schmidt HL, Werner RA, Eisenreich W (2003) Systematics of  $^2\text{H}$  patterns in natural compounds and its importance for the elucidation of biosynthetic pathways. *Phytochem Rev* 2(61–79)
- Schmidt HL, Werner RA, Rossmann A (2001) O-18 pattern and biosynthesis of natural plant products. *Phytochemistry* 58(1):9–32. [https://doi.org/10.1016/S0031-9422\(01\)00017-6](https://doi.org/10.1016/S0031-9422(01)00017-6)
- Schollaen K, Baschek H, Heinrich I, Slotta F, Pauly M, Helle G (2017) A guideline for sample preparation in modern tree-ring stable isotope research. *Dendrochronologia* 44:133–145. <https://doi.org/10.1016/j.dendro.2017.05.002>
- Schollaen K, Heinrich I, Helle G (2014) UV-laser-based microscopic dissection of tree rings—a novel sampling tool for  $\delta^{13}\text{C}$  and  $\delta^{18}\text{O}$  studies. *New Phytol* 201(3):1045–1055. <https://doi.org/10.1111/nph.12587>
- Schollaen K, Heinrich I, Neuwirth B, Krusic PJ, D'Arrigo RD, Karyanto O, Helle G (2013) Multiple tree-ring chronologies (ring width,  $\delta^{13}\text{C}$  and  $\delta^{18}\text{O}$ ) reveal dry and rainy season signals of rainfall in Indonesia. *Quat Sci Rev* 73:170–181. <https://doi.org/10.1016/j.quascirev.2013.05.018>
- Sidorova OV, Siegwolf RTW, Saurer M, Naurzbaev MM, Vaganov EA (2008) Isotopic composition ( $\delta^{13}\text{C}$ ,  $\delta^{18}\text{O}$ ) in wood and cellulose of Siberian larch trees for early Medieval and recent periods. *J Geophys Res Biogeosci* 113(G2). <https://doi.org/10.1029/2007JG000473>

- Sidorova OV, Siegwolf RTW, Saurer M, Shashkin AV, Knorre AA, Prokushkin AS, Vaganov EA, Kirdyanov AV (2009) Do centennial tree-ring and stable isotope trends of *Larix gmelinii* (Rupr.) Rupr. indicate increasing water shortage in the Siberian north? *Oecologia* 161(4):825–835. <https://doi.org/10.1007/s00442-009-1411-0>
- Sohn AW, Reiff F (1942) Natriumchlorit Als Aufschlussmittel. *Der Papierfabrikant* 1(2):5–7
- Sohn JA, Gebhardt T, Ammer C, Bauhus J, Haberle KH, Matyssek R, Grams TEE (2013) Mitigation of drought by thinning: short-term and long-term effects on growth and physiological performance of Norway spruce (*Picea abies*). *For Ecol Manag* 308:188–197. <https://doi.org/10.1016/j.foreco.2013.07.048>
- Sternberg L (1989) Oxygen and hydrogen isotope ratios in plant cellulose. Mechanisms and applications. In: Rundel PW, Ehleringer JR, Nagy KA (eds) *Applications of stable isotopes in ecological research*. Springer-Verlag, New York, pp 124–141
- Sternberg L, Linskens HF, Jackson JF (1989) Oxygen and hydrogen isotope measurement in plant cellulose. Analysis. In: *Plant fibres. Modern methods of plant analysis*. Springer, Berlin, pp 89–99
- Szymczak S, Joachimski MM, Braeuning A, Hetzer T, Kuhlemann J (2011) Comparison of whole wood and cellulose carbon and oxygen isotope series from *Pinus nigra* ssp *laricio* (Corsica/France). *Dendrochronologia* 29(4):219–226. <https://doi.org/10.1016/j.dendro.2011.04.001>
- TAPPI TAotPaPI (1988) Test method T222 om-83. TAPPI. Atlanta, GA
- Taylor AM, Brooks JR, Lachenbruch B, Morrell JJ (2007) Radial patterns of carbon isotopes in the xylem extractives and cellulose of Douglas-fir. *Tree Physiol* 27(6):921–927. <https://doi.org/10.1093/treephys/27.6.921>
- Taylor AM, Brooks JR, Lachenbruch B, Morrell JJ, Voelker S (2008) Correlation of carbon isotope ratios in the cellulose and wood extractives of Douglas-fir. *Dendrochronologia* 26(2):125–131. <https://doi.org/10.1016/j.dendro.2007.05.005>
- Taylor AM, Gartner BL, Morrell JJ (2002) Heartwood formation and natural durability—a review. *Wood Fiber Science* 34(4):587–591
- Tei S, Sugimoto A, Yonenobu H, Hoshino Y, Maximov TC (2013) Reconstruction of summer palmer drought severity index from delta C-13 of larch tree rings in East Siberia. *Quat Int* 290:275–281. <https://doi.org/10.1016/j.quaint.2012.06.040>
- Verheyden A, Helle G, Schleser GH, Dehairs F, Beeckman H, Koedam N (2004) Annual cyclicity in high-resolution stable carbon and oxygen isotope ratios in the wood of the mangrove tree *Rhizophora mucronata*. *Plant, Cell Environ* 27(12):1525–1536
- Verheyden A, Roggeman M, Bouillon S, Elskens M, Beeckman H, Koedam N (2005) Comparison between delta C-13 of alpha-cellulose and bulk wood in the mangrove tree *Rhizophora mucronata*: Implications for dendrochemistry. *Chem Geol* 219(1–4):275–282. <https://doi.org/10.1016/j.chemgeo.2005.02.015>
- Wallis FA, Wearne RH, Wright PJ (1997) New approaches to rapid analysis of cellulose in wood. In: *ISWPC: 9th international symposium on wood and pulping chemistry*, Montreal, pp 1–4
- Warren CR, McGrath JF, Adams MA (2001) Water availability and carbon isotope discrimination in conifers. *Oecologia* 127(4):476–486. <https://doi.org/10.1007/s004420000609>
- Weigt RB, Braunlich S, Zimmermann L, Saurer M, Grams TEE, Dietrich HP, Siegwolf RTW, Nikolova PS (2015) Comparison of delta O-18 and delta C-13 values between tree-ring whole wood and cellulose in five species growing under two different site conditions. *Rapid Commun Mass Spectrom* 29(23):2233–2244. <https://doi.org/10.1002/rcm.7388>
- West AG, Midgley JJ, Bond WJ (2001) The evaluation of delta C-13 isotopes of trees to determine past regeneration environments. *For Ecol Manag* 147(2–3):139–149. [https://doi.org/10.1016/S0378-1127\(00\)00474-6](https://doi.org/10.1016/S0378-1127(00)00474-6)
- Wieloch T, Helle G, Heinrich I, Voigt M, Schyma P (2011) A novel device for batch-wise isolation of alpha-cellulose from small-amount wholewood samples. *Dendrochronologia* 29(2):115–117. <https://doi.org/10.1016/j.dendro.2010.08.008>
- Wiesberg L (1974) Die 13 C-Abnahme in Holz von Baumjahresringen, eine Untersuchung zur anthropogenen Beeinflussung des CO<sub>2</sub>-Haushaltes der Atmosphre. Dissertation, RWTH Aachen

- Wilson AT, Grinsted MJ (1977) 12C/13C in cellulose and lignin as palaeothermometers. *Nature* 265:133–135
- Wilson JW, Wellwood RW (1965) Intra-increments chemical properties of certain western Canadian coniferous species. In: Cote WA (ed) *Cellular ultrastructure of woody plants*. Syracuse University Press, Syracuse, USA, pp 551–559
- Wieser G, Oberhuber W, Gruber A, Leo M, Matyssek R, Grams TEE (2016) Stable water use efficiency under climate change of three sympatric conifer species at the alpine treeline. *Front Plant Sci* 7. <https://doi.org/10.3389/fpls.2016.00799>
- Wise LE (1945) Quantitative isolation of hemicelluloses from coniferous woods. *Ind Eng Chem Anal* 17:63–64
- Wise LE, Murphy M, D'Addieco AA, (1946) Chlorite holocellulose, its fractionation and bearing on summative wood analysis and on studies on the hemicelluloses. *Paper Trade J* 122(2):35–43
- Woodley EJ, Loader NJ, McCarroll D, Young GHF, Robertson I, Heaton THE, Gagen MH, Warham JO (2012) High-temperature pyrolysis/gas chromatography/isotope ratio mass spectrometry: simultaneous measurement of the stable isotopes of oxygen and carbon in cellulose. *Rapid Commun Mass Spectrom* 26(2):109–114. <https://doi.org/10.1002/Rcm.5302>
- Xu C, Sano M, Nakatsuka T (2011) Tree ring cellulose delta <sup>18</sup>O of *Fokienia hodginsii* in northern Laos: a promising proxy to reconstruct ENSO? *J Geophys Res* 116(D24):D24109. <https://doi.org/10.1029/2011jd016694>
- Ziehmer MM, Nicolussi K, Schluchter C, Leuenberger M (2018) Preliminary evaluation of the potential of tree-ring cellulose content as a novel supplementary proxy in dendroclimatology. *Biogeosciences* 15(4):1047–1064. <https://doi.org/10.5194/bg-15-1047-2018>
- Zobel BJ, van Buijtenen JP (1989) *Wood variation: its causes and control*. Springer Series in wood science. Springer-Verlag, Berlin, Heidelberg. <https://doi.org/10.1007/978-3-642-74069-5>

**Open Access** This chapter is licensed under the terms of the Creative Commons Attribution 4.0 International License (<http://creativecommons.org/licenses/by/4.0/>), which permits use, sharing, adaptation, distribution and reproduction in any medium or format, as long as you give appropriate credit to the original author(s) and the source, provide a link to the Creative Commons license and indicate if changes were made.

The images or other third party material in this chapter are included in the chapter's Creative Commons license, unless indicated otherwise in a credit line to the material. If material is not included in the chapter's Creative Commons license and your intended use is not permitted by statutory regulation or exceeds the permitted use, you will need to obtain permission directly from the copyright holder.



# Chapter 6

## Tree-Ring Stable Isotope Measurements: The Role of Quality Assurance and Quality Control to Ensure High Quality Data



**J. Renée Brooks, William D. Rugh, and Roland A. Werner**

**Abstract** Quality assurance and quality control (QA/QC) are important components of every study. In this chapter, we give an overview of QA/QC specific for tree-ring stable-isotope analysis from the perspective of the entire research project, rather than from the operation of Isotope Ratio Mass Spectrometers (IRMS). We address how users of stable isotope tree-ring data can quantify the quality of their data for reporting in publications by calculating accuracy and precision. We cover some of the potential sources of error that can occur during sample processing and isotopic measurements, basic principles of calibration to the appropriate isotopic scales, and how researchers can detect error and calculate uncertainty using duplicates and quality control standards.

### 6.1 Introduction

This chapter addresses how you can determine the analytical quality of your stable isotope tree-ring data for reporting in publications and with the data when made public. Jardine and Cunjak (2005) summarized the wide disparity in reporting analytical error of stable isotopic data in the ecological literature. We provide guidance on the necessary data and methods for estimating the uncertainty around stable isotope data for one's research project. Our approach is from the perspective of the researcher designing a project that uses the stable isotopes contained within tree rings, rather than from the perspective of a laboratory conducting stable isotope analysis for a wide array of projects and individuals. Ultimately, the researcher is responsible for quantifying the quality of the data generated within the project and needs to report

---

J. R. Brooks (✉) · W. D. Rugh  
Pacific Ecological Systems Division, Center for Public Health and Environmental Assessment,  
Office of Research and Development, U. S. Environmental Protection Agency, 200 SW 35th St.,  
Corvallis, OR 97333, USA  
e-mail: [Brooks.ReneeJ@EPA.gov](mailto:Brooks.ReneeJ@EPA.gov)

R. A. Werner  
Department of Environmental Systems Science, Institute of Agricultural Sciences, ETH Zürich,  
Universitätsstrasse 2, 8092 Zürich, Switzerland



that uncertainty in final reports and published papers. Ideally, measures of uncertainty should stay with the data when the data are made publicly available.

### **6.1.1 What is QA/QC?**

Quality assurance (QA) is the overall framework or plan that describes your experimental design to address your research questions and what steps you will take to detect and minimize errors in the data you are generating within the project. Quality control (QC) is the system of procedures or actual steps you take to quantify and minimize potential errors and assure data integrity. In other words, quality assurance is the plan you develop, whereas quality control is implementing that plan and documenting those steps. For example, your quality assurance plan might call for a certain frequency of sample duplication (see Sect. 6.2.3.1) to be included in each sample set analyzed on the Isotope Ratio Mass Spectrometers (IRMS) for calculating precision and that a QC standard be used in each sample set to test the accuracy of calibration procedure. The quality control would be the actual inclusion of those duplicates and QC standards, and then an estimation of precision with duplicates, and accuracy with the QC standard. A good quality assurance plan with appropriate quality control measures is a critical component of every study and needs to be developed at the very beginning of every project.

A QA plan should be developed around a project's objectives and experimental design and include the information in the methods section of one's publication(s). The QA plan is not static, it evolves as the project proceeds and is updated to address new or emerging issues not foreseen at the beginning of the project. Individual procedures used in the study such as methods for ring separation and cellulose extraction should be written into standard operating procedures (SOPs), which provide step-by-step instructions for carrying out each procedure. The purpose of SOPs is to ensure that everyone is following the same methods for every sample within the study, and to limit variation that may be introduced by different people conducting the procedure. All personnel conducting those procedures must be required to read and follow the study SOPs. Developing a good QA plan and SOPs is the first step to ensuring your data are of the quality you need to address your research objectives.

Quality control steps should be described in both the QA plan and in individual SOPs. Quality control steps would be measures that would allow for quantifying variation introduced by the procedure. For example, including a QC sample, such as a uniformly homogenized wood sample of sufficient volume for many samples, into each set of samples processed or analyzed together would allow for quantification of the uncertainty with sample processing and measurement (Porter and Middlestead 2012). This chapter will discuss many of the sources of uncertainty in tree-ring stable isotope analysis, and QC steps to assess the quality of your data even if you are not conducting the stable isotope measurements yourself.

## 6.1.2 *Taking Ownership of Your Data Quality*

The following are a set of questions to consider during development of your QA plan and develop QC steps to address them:

- Can I detect the isotopic differences I am expecting with my study design?

This is the primary study question being asked of the isotopic data. Do you have sufficient replication and sample precision so that the signal variation within the study is much larger than the variation between sample replicates? In order to answer this question, you must understand some more basic levels of isotopic variation, and what might be causing that variation: signal variation is what you are hoping to show using stable isotopes, and noise-variation is unrelated to your study question which could be natural variation of the system or measurement noise. A good experimental design might be able to control for natural system variation, and good QA/QC should minimize the measurement noise.

- What is the range of isotopic variation within my study?

Is your isotopic variation within the study sufficiently large relative to analytical error in order to detect biologically meaningful patterns? Are the isotopic values a useful measure to address the question you have? Is the variation between replicates (two trees from the same stand expected to show similar patterns) small relative to the variation across time? Generally, background literature of similar studies will provide some guiding expectations and will help in designing experiments that will maximize the signal around your study questions.

- How variable are my samples (variation within a sample)?

This is an area of which you have control and relates to sample homogenization (see Sect. 6.3.1.1) and is measured by sample precision of duplicates (see Sect. 6.2.3).

- Have my samples been isotopically altered since collection?

This question addresses potential problems with sample extraction methods or storage issues that alter the isotopic ratio of the sample in unintended ways. Clear and detailed SOPs will help ensure that all personnel are conducting analyses correctly and minimizing mistakes. The use of replicates, duplicates and a study standard can be useful in detecting any issues that do occur (see Sects. 6.2.3.1, 6.3.1.1 and 6.4.2.3).

- Do the stable isotope values I received from a lab accurately reflect the isotopic values of the samples I submitted?

This question relates to whether the IRMS was functioning normally, and the samples were accurately calibrated to the international scale (see Sect. 6.3). Generally, you are not in control of how your samples are calibrated but obtaining information about the calibration standards and independent QC standards as well as your sample duplicates should enable you to answer this question by calculating the accuracy and precision

as outlined below. We encourage you to compile your QC data from each set of samples submitted for analysis on the IRMS and calculate your own study accuracy and precision to be reported in your final manuscripts as well as kept with the data when made publicly available.

## 6.2 Measurements of Uncertainty

All measurements have some uncertainty around a reported value, and this uncertainty should be reported with the value to allow for accurate interpretation. In the Eurachem/CITAC guide (<https://www.eurachem.org/index.php/publications/guides/quam>), the term measurement ‘uncertainty’ is defined as the “parameter associated with the result of a measurement that characterizes the dispersion of the measured values that could reasonably be attributed to the measurand” (Ellison and Williams 2012). In this section, we outline the steps to accurately quantify uncertainty around tree-ring stable isotope values used in a research project.

### 6.2.1 *Identical Treatment Principle*

The Identical Treatment Principle (IT Principle) is the principle that standards (both for calibration and QC purposes) shall be treated the same as the samples (Werner and Brand 2001). Following this principle, the standards will go through the same transformations as the sample from cellulose to the final gas that is measured in the IRMS, and any alteration to the isotopic composition will affect both standards and samples equally. For example, calibration and QC standards (and preferably one or two cellulose standards) need to be transformed from sample matrix into the measured gases along with each set of samples analyzed on the IRMS for accurate isotopic measurements. Isotopic reference gas, which is injected directly to the IRMS without the transformation step, should never be used alone to establish the calibration. By using this principle, calibration standards should accurately correct for isotopic alterations during the transformation process. The IT Principle should be standard practice in all IRMS laboratories, but it can also be applied within a study to other transformation steps such as cellulose extraction (see Chap. 5). However, no wood standard with a certified isotopic ratio for cellulose exists, so applying the IT Principle to cellulose extraction must be modified. The key is to develop a study standard that can be used to assess the influence of the process or transformation that the samples go through (see Sect. 6.4.2.3 in this chapter). For example, Porter and Middlestead (2012) developed a study standard using a large amount of homogenized wood particles similar in particle size to their samples, and included one sample in every sample set extracted for cellulose within a study to account for the variance the extraction process may have imposed on their samples. While they didn’t know a priori the isotopic composition of cellulose within this wood study standard, they

could calculate the uncertainty introduced by variation in cellulose extraction and isotopic measurement over the duration of their study. Another approach would be to construct an “artificial” wood sample mixing wood components (lignin, cellulose and other materials) using reagent grade cellulose where the isotopic composition could be measured prior to and after extraction (See Richter et al. 2009 for an example of an artificial leaf). For hydrogen isotopes in cellulose samples, hydrogen exchange of hydroxyl groups with local water vapor is another important isotopic transformation that must be corrected for using standards that have been treated identically to the samples (see Chap. 11). To apply the IT Principle, researchers should include some form of standards along with their samples whenever samples are transformed from their original state to the final gas introduced into the IRMS.

### 6.2.2 Accuracy

Accuracy is a measure of systematic bias and is calculated as the difference between a measured value from the “true” value (measured—true). For stable isotope measurements, accuracy is determined from a QC standard with a known isotopic value. A QC standard cannot be used for any calibration or normalization of the isotopic results but is used as an independent test of the calibration and normalization process (see Sect. 6.3). Generally, one or two QC standards are included into each set of samples analyzed by the IRMS, following the IT Principle.

A research study is generally composed of multiple sets of samples that have been measured on the IRMS over time, and thus contain multiple measurements of a QC standard (Table 6.1). To calculate accuracy across the entire study, researchers should calculate the average and the standard deviation of the difference value (measured—true). The average difference value is the systematic bias within the study, and if the isotope data are adequately calibrated, the average should be very close to zero. The standard deviation of the difference values is the random error around the accuracy measurement, and it should be similar to sample precision (see next section) or smaller. In Table 6.1, accuracy, or study bias is average difference ( $\mu$ ) and was estimated to be  $-0.01\text{‰}$ , while random error represented by the standard deviation ( $\sigma$ ) was  $0.12\text{‰}$ , which is typical for carbon isotope values of homogenized internal laboratory standards. If the study bias was larger than the standard deviation, then the study data could have a significant bias that the calibration procedures did not correct; however, a low number of QC samples could lead to a false indication of bias as well. For the example in Table 6.1, the accuracy of the study should be reported as  $-0.01 \pm 0.12\text{‰ SD}$ .

**Table 6.1** Example calculation of accuracy from QC standards from six IRMS sets of study samples. A set is a sequence of samples analyzed continuously on the IRMS, usually overnight. In this example, QC samples were analyzed at the 68th position in the sample set, and the 93rd position

Internal QC Standard	Sample set	Sample position	$\delta^{13}\text{C}^c$ (calibrated <sup>d</sup> )	$\delta^{13}\text{C}$ (actual <sup>e</sup> )	$\delta^{13}\text{C}$ (difference)
ISIRF <sup>a</sup> Cellulose	1	68	-24.71	-24.88	0.17
ISIRF Cellulose	1	93	-24.76	-24.88	0.12
NBS <sup>b</sup> Apple	2	68	-27.10	-27.03	-0.07
NBS Apple	2	93	-27.03	-27.03	0.00
ISIRF Cabbage	3	68	-25.72	-25.61	-0.11
ISIRF Cabbage	3	93	-25.74	-25.61	-0.13
ISIRF Cabbage	4	68	-25.46	-25.61	0.15
ISIRF Cabbage	4	93	-25.61	-25.61	0.00
ISIRF Cellulose	5	68	-24.89	-24.88	-0.01
ISIRF Cellulose	5	93	-24.82	-24.88	0.06
NBS Citrus	6	68	-27.70	-27.49	-0.21
NBS Citrus	6	93	-27.52	-27.49	-0.03
		Accuracy	Bias	$\mu$ :	-0.01
			Random error	$\sigma$ :	0.12

<sup>a</sup>ISIRF Integrated Stable Isotope Research Facility at the US EPA in Corvallis, Oregon

<sup>b</sup>NBS National Bureau of Standards, currently National Institute of Standards and Technology (NIST)

<sup>c</sup> $\delta^{13}\text{C}$  is carbon isotope ratio as defined in Eq. 6.3, Sect. 6.4.2.1. All units are in parts per thousand (‰)

<sup>d</sup>Calibrated values are those reported to you by the IRMS facility after data corrections and scale calibration have been complete for that sample set

<sup>e</sup>Actual values are those assigned to the standard by the IRMS laboratory after multiple calibrations with certified reference materials, and repeatedly measured to determine a long-term average value with associated uncertainty

### 6.2.3 Precision

Precision is the random error of the measurement for study samples, generally calculated as the standard deviation of repeated measures from study samples. Standard deviation is a statistical description of population variance and for precision, that population is repeated measures of the same study sample. One standard deviation away from the mean captures 68% of the observations (assuming a normal distribution), and two standard deviations capture 95% of the observations. Another common measurement for precision is the coefficient of variation (CV) which is calculated as  $\sigma/\mu$ . However, because stable isotope measures are ratios (see Chap. 8) and are referenced to a standard (zero means the same as the scaling standard), CV should never be used for precision of stable isotope ratios.

Precision reported for a study should always be based on repeated measures of study samples and not from laboratory standards, or the QC standards. IRMS laboratories base their long-term analytical precision on those standards, but laboratory analytical precision is not the same as precision for a study. Precision based on study samples will include variance from sample preparation, and homogenization. If the repeated measures are from duplicates created during the tree-ring grinding process, then variation introduced from storage and cellulose extraction will also be included in the precision measurement (see Sect. 6.2.3.1).

Study precision reported in a paper should be based on the aggregate of repeated samples for an entire study and not just a typical value from the results of a single IRMS sequence, or from the long-term precision of laboratory standards from the laboratory conducting the analysis. For each set of samples analyzed on the IRMS, 2–3 samples are generally duplicated, and precision is determined from these for that set. This type of precision is a measure of *repeatability*: the agreement between measures of the *same sample analyzed under the same conditions* (the same operator, instrument, over a short period of time). To calculate precision of a study, these repeated measures need to be accumulated across sample sets, which is closer to a measure of *reproducibility*: the agreement between measures of the *same sample analyzed under the different conditions*. Equation 6.1 is used to calculate precision when samples that are duplicated don't have identical isotopic values but span a range of isotopic values:

$$s = \sqrt{\frac{\sum s^2(n-1)}{\sum(n-1)}} \quad (6.1)$$

where  $s^2$  is the variance between the duplicates, and  $n$  is the number of times the sample was analyzed, generally two. In the case of a study standard (see Sect. 6.4.2.3) that is included in every sample set,  $n$  would be much larger equaling the number of sample sets in which the study standard was included. Equation 6.1 sums the variance of all duplicated samples, and weights them by the degrees of freedom ( $n - 1$ ), before taking the square root to estimate standard deviation. Table 6.2 contains an example of how precision for a study should be calculated. Precision for this set of samples was  $\pm 0.06 \%$ , slightly better than the uncertainty around the accuracy estimate in Table 6.1.

### 6.2.3.1 Duplication Versus Replication

Duplicate samples are not statistical replicates but are considered the same sample collected twice or more, and are used to calculate precision only. Duplicates are collected to answer the questions “how much variation exists within the same sample” and “have my samples been unintentionally fractionated since collection”. Tree-ring samples are often composed of combining a particular year (or sub-year) of growth

**Table 6.2** Example calculation of precision for a study compiled from four sets of samples on an IRMS for  $\delta^{13}\text{C}$ . Three duplicates were analyzed within each sample set, and sample sequence indicates when in the order of samples that the duplicates were analyzed. Note that the first replicate within a sequence is split between the beginning (Sample Position 7) and the end of the IRMS set (Sample Position 92)

Sample ID		Sample set	Sample position	$\delta^{13}\text{C}$ (Calibrated)	$\delta^{13}\text{C}$ (Variance)	Degrees of freedom
Sample 20	Dup 1	1	7	-24.65	0.00045	1
	Dup 2	1	92	-24.68		
Sample 40	Dup 1	1	46	-21.85	0.00980	1
	Dup 2	1	47	-21.99		
Sample 60	Dup 1	1	70	-25.21	0.00405	1
	Dup 2	1	71	-25.30		
Sample 80	Dup 1	2	7	-24.60	0.00405	1
	Dup 2	2	92	-24.51		
Sample 100	Dup 1	2	46	-22.79	0.02420	1
	Dup 2	2	47	-23.01		
Sample 120	Dup 1	2	70	-23.95	0.00605	1
	Dup 2	2	71	-23.84		
Sample 140	Dup 1	3	7	-23.48	0.00245	1
	Dup 2	3	92	-23.41		
Sample 160	Dup 1	3	46	-23.25	0.00080	1
	Dup 2	3	47	-23.29		
Sample 180	Dup 1	3	70	-24.24	0.00020	1
	Dup 2	3	71	-24.26		
Sample 200	Dup 1	4	7	-23.78	0.00045	1
	Dup 2	4	92	-23.75		
Sample 220	Dup 1	4	46	-22.90	0.00180	1
	Dup 2	4	47	-22.96		
Sample 240	Dup 1	4	70	-24.61	0.00320	1
	Dup 2	4	71	-24.69		
Study Standard	QC	1	50	-24.92	0.00113	3

(continued)

**Table 6.2** (continued)

Sample ID		Sample set	Sample position	$\delta^{13}\text{C}$ (Calibrated)	$\delta^{13}\text{C}$ (Variance)	Degrees of freedom
Study Standard	QC	2	50	-24.90		
Study Standard	QC	3	50	-24.95		
Study Standard	QC	4	50	-24.87		
			Precision	Sum	0.0609	15
				<i>s</i>	0.064	

from multiple cores collected from the same tree. These multiple core pieces are then homogenized to make a sample (see Chap. 4). For sample duplication, the sample should be split after homogenization, and stored in separate containers. Variance between these samples will include variance from lack of homogenization, cellulose extraction, sample storage, and analysis on the IRMS. Samples that are split just prior to analysis contain only the variance of homogenization and the analysis on the IRMS.

We recommend creating a duplicate for every twenty samples. Sample size for creating duplicates may be an issue depending on the growth rate of the sampled trees, and the sectioning requirements of the study (i.e. annual increments, separating late- and earlywood). In these cases, duplicates might be created for only larger growth rings, and a lower frequency of duplicates may be necessary.

Only one value from the duplicates should be analyzed in any statistical or other analysis as part of the study. Duplicates are for quality assurance only, and to use them in statistical analysis would be considered pseudo-replication (Hurlbert 1984). The duplicate value used should not be the mean of the two values as that value would be less variable than all the other samples that were not duplicated. Statistical replicates are independent samples collected from a population or group that is to be compared with another population or group. For tree-ring stable isotopes, individual trees are generally considered replicates, but that depends on the study objective.

#### 6.2.4 Study Uncertainty and the Propagation of Error

In the examples from Tables 6.1 and 6.2 which are from the same study, accuracy was  $0.02 \pm 0.12 \%$ , and our measured precision was  $\pm 0.06 \%$ , which was lower than the uncertainty around the accuracy estimate. Both of these values should be reported in the methods section of a study, but the larger value of uncertainty is a better reflection of actual study uncertainty. For example, because the uncertainty around accuracy was larger than precision, it was a better reflection of the study uncertainty for comparing numbers within the study to each other.



Uncertainty is also used to determine the number of significant digits to report. Because the uncertainty within the study in Tables 6.1 and 6.2 was approximately 0.1 ‰ for  $\delta^{13}\text{C}$ , then values of  $\delta^{13}\text{C}$  reported for this study should not include digits below 0.1 ‰, even though values with more digits are often provided by output from the IRMS. We included more digits in Tables 6.1 and 6.2 so that variation between values were apparent.

For data included in meta-analysis, where the  $\delta^{13}\text{C}$  values are to be compared to  $\delta^{13}\text{C}$  values from other studies analyzed in other laboratories, then additional uncertainty must be considered. The values assigned to the QC standards have uncertainty around them, and that uncertainty must be propagated along with the uncertainty described above. The root mean squared error is used for propagating error (Eq. 6.2).

$$S_{Meta} = \sqrt{S_{QC}^2 + S_{Study}^2} \quad (6.2)$$

If the assigned values of the QC standards had uncertainties of 0.2 ‰ when calibrated to the internationally certified standard reference material (see Sect. 6.4.2), and the study uncertainty was 0.12 ‰, then the combined uncertainty using Eq. 6.2 would be 0.23 ‰. This uncertainty value should be used with the data for any meta-analysis across studies as it reflects the uncertainty to the international scale (see Sect. 6.3.3). The patterns and trends within a single study with samples all calibrated to the same standards in the same way by the same lab have inherently less uncertainty (0.12 ‰ in this case) relative to each other, as compared to samples that originated from different studies with different calibration procedures and standards.

### 6.3 IRMS Errors and Calibration

Errors introduced into isotopic analysis can come from sample collection, cross-dating, sub-sectioning cores, sample handling, extraction processes, from the sample conversion into gases introduced to the IRMS, or from analysis on the IRMS directly. These errors have random and systematic components. Random error cannot be corrected and is the major component of uncertainty. Systematic errors can potentially be corrected with accurate calibration if standards were also subjected to the same process. Errors from sample collection, cross-dating, sub-sectioning cores, handling and extraction are mostly random and cannot be corrected. However, both sample conversion to gases and isotopic analysis of the gases contain both elements of error.

The IRMS and associated peripherals (i.e. elemental analyzers,) need to be optimized for *precision* and *accuracy* for the samples being measured, thus laboratory accuracy and precision can vary dramatically depending on instrument maintenance and attention to measurement details. For example, sample volumes need to be within the *linear working range* of the instrument when the ratio output to input signal is

constant and in a direct proportion over the range of instrument voltage output generated by the samples. The introduced gases need to produce appropriate peak shapes. The reasons for increasing errors in isotopic analysis are extensive, and can be related to the ionizing process in the ion source of the mass spectrometer or due to problems with the conversion of the sample to the measuring gas. We advise carefully selecting an IRMS laboratory with experience in the type of analysis required for a study, and with documented and defensible QA/QC procedures. In addition, we advise including an independent QC standard with a known isotopic value with each set of samples if possible. Study standards (see Sect. 6.4.2) can be that independent QC standard if its isotopic value is from multiple IRMS labs.

Measurements of  $\delta^{13}\text{C}$  of wood or cellulose and  $\delta^{18}\text{O}$  of cellulose are relatively standard isotopic measurements that can be made with high precision and accuracy (see Chaps. 9 and 10). Both wood and cellulose have consistent stoichiometry for C and O, thus sample weights can be optimized for isotopic analysis. However, measurements of  $\delta^{15}\text{N}$  and  $\delta^2\text{H}$  in tree rings can be particularly challenging. For  $\delta^{15}\text{N}$ , the challenge comes from the low amount of nitrogen contained in wood compared to the abundance of carbon (C:N ratio of  $\sim 300$ , see Chap. 12), and for  $\delta^2\text{H}$ , the problem is from isotopic exchange of hydroxyl H atoms on cellulose with the last water in which the sample was in contact (see Chap. 11). For measuring  $\delta^{15}\text{N}$  in wood samples,  $\text{CO}_2$  volumes far exceed  $\text{N}_2$ , and large sample sizes are required to obtain enough N atoms for accurate analysis. As a result, laboratories need to take special action to ensure the large sample is completely converted to  $\text{CO}_2$  and  $\text{N}_2$  and that the volume of  $\text{CO}_2$  from the previous sample does not interfere with the  $\text{N}_2$  peak of the current sample for accurate measures of  $\delta^{15}\text{N}$  (e.g. Brooks et al. 2003). Most laboratories making  $\delta^{15}\text{N}$  analysis on wood will optimize for  $\delta^{15}\text{N}$ , and not measure  $\delta^{13}\text{C}$  on the same sample, and thus, require two separate analyses to provide  $\delta^{13}\text{C}$  and  $\delta^{15}\text{N}$  values. Below, we briefly describe some of the potential errors and calibration procedures so that readers understand some of the complexity into making accurate and precise isotopic analysis.

### 6.3.1 *Random Measurement Error*

Random errors influence the measurement in unpredictable ways, hence showing no statistical pattern, and thus cannot be corrected. For example, unknown parameters in the IRMS such as electronic noise in the detector can introduce random error into the isotopic measurement. This random variance is quantified within the precision measurements described above. Increases in random error within and between sample sets analyzed on the IRMS are often a sign of needed maintenance for the IRMS, as they are often caused by instrument parameters influencing the robustness and ruggedness of an isotopic measurement method. Increased random error must be recognized by the IRMS operator, and the causal factor repaired to improve precision. Laboratories conducting IRMS measurements should monitor the long-term

stability of the measurement system or method, by regular measurement of QC standards in every sample set. The long-term instrument stability should be visualized in quality control charts showing QC standard variation over time to allow detection of possible systematic deviations, or increased noise. When such problems are noticed, laboratory personnel should have rules of action for maintenance and troubleshooting possible problems. IRMS laboratories can vary greatly in the degree of quality assurance exercised contributing to overall uncertainty in isotopic analysis. The analysis of duplicate samples and QC standards over time should allow for quantification of random error in precision and accuracy measures described above.

### **6.3.1.1 Errors from Sample Tracking, Preparation, and Homogenization**

Sample tracking, homogenization and preparation can cause significant random error if good QA practices are not followed. The preparation of tree-ring samples for isotopic analysis requires many steps, each of which can introduce error and mistakes. The process of accurately dating cores, subdividing cores, and combining increments from multiple cores from a single tree into a single sample leads to many points where irreversible mistakes can happen. Duplicates will not capture this type of error because duplicates are generally created after these steps. However, replicate trees within a study design will. Because of sample sizes or cost of analysis, some studies end up pooling replicate trees but doing so can mask these types of errors. Liñán et al. (2011) found good agreement between individual tree and samples pooled across trees, but sacrificed the ability to quantify uncertainty between trees. Sample homogenization and extraction will also lead to random variance, but adequate duplication will account for this error. As IRMS technical advancements allow for analysis on smaller and smaller samples, homogenization becomes more and more important to reduce variance between duplicate samples. Borella et al. (1998) recommended particle sizes of 0.1 mm or smaller for samples weighing 1.5 mg (~250 particles per sample) in  $\delta^{13}\text{C}$  analysis. The nested nature of tree-ring stable isotope analysis, with many years (or sub-years) of samples from multiple trees can also lead to sample tracking problems, particularly if samples are moved through multiple containers for grinding and extraction. A good quality assurance plan should develop a system to make sure that samples are uniquely identifiable so that they don't get easily confused with one another, allowing for accurate chain of custody and traceability for all samples.

### **6.3.2 Systematic Measurement Error**

Systematic errors influence the accuracy of the result in the same direction, in a reproducible fashion. Generally, they can be detected and corrected by using calibration standards (see Sect. 6.3.3). Systematic errors are normally caused by erratic

instruments, wrong handling of instruments, or changing environmental conditions during analysis of a sample set on the IRMS. Systematic errors are classified into two types: offset and scale factor errors (Fig. 6.1). Offset errors are considered constant across the range of isotopic values being measured. However, the offset may not be constant over time, and is then known as instrument drift. Drift can be defined as a slow change over time of an output signal to the same input parameter. Within the IRMS, drift can occur because the ionizing conditions in the ion source of the mass spectrometer are not constant over time. While a constant offset can be detected by calibration standards measured at one time within the sample set, drift can only be detected and corrected by calibration standards that were analyzed throughout the entire sequence of samples (see below).

Scale factor errors are associated with measurement compression or expansion of the actual range in isotopic values, and can be corrected by measuring calibration standards that span an appropriate isotopic range, ideally a range larger than the isotopic range of samples being analyzed, and that brackets the sample measurements. Scale factor errors (often scale compression effects) in isotope ratio mass spectrometry are often caused by mass discriminatory effects (the heavy isotope moves more slowly than the light isotope) during the transport of the sample gases towards the ion detection in the mass spectrometer (Meier-Augenstein and Schimmelmann 2019). Examples of mass discriminatory effects are peak tailing on GC columns and adsorption in the ion source. Large compressions of the isotopic scale

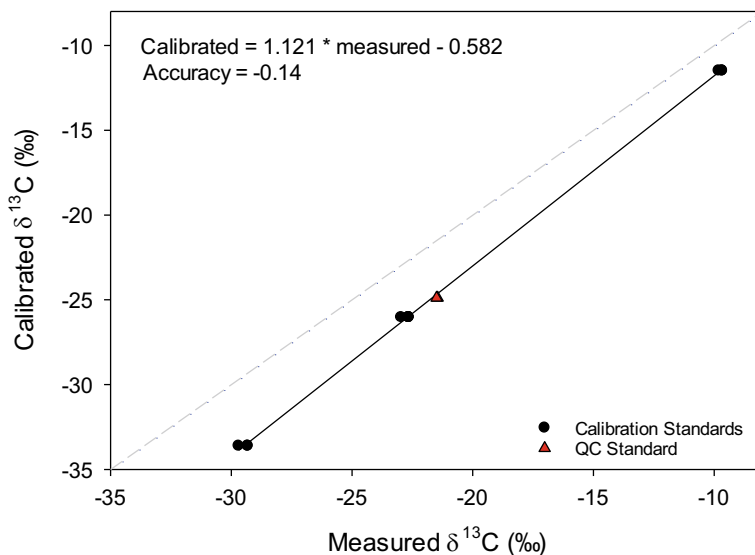


**Fig. 6.1** Typical calibration for adjusting measured sample values to the correct  $\delta$  scale illustrating the two types of systematic error affecting  $\delta^{13}\text{C}$ . The intercept represents the offset correction error, and the slope the scale factor error. The gray dashed line is a 1:1 line between measured and calibrated isotopic values

can lead to lower accuracy because the relative variation between samples is reduced, and the overall signal is reduced relative to the noise of the measurement. Scale-factor errors influence the slope of the calibration curve (Fig. 6.1).

### 6.3.3 Calibration

Proper calibration of isotopic measurements is essential to providing accurate results. In analytical sciences, the term “calibration” describes a series of operations that connect the measured value of a sample with its real analytical value (true value) using calibration standards that have followed the IT Principle (see Sect. 6.2.1). Calibration standards are certified standard reference materials (SRMs) with known composition (true value including a statement on the measurement uncertainty if applicable). Mathematical equations relating the difference between the certified SRMs measured values and the analytical “true” value are used to correct the measured sample values to deliver accurate results in a reproducible fashion (Fig. 6.1).

Isotopic analysis and data calibration must be performed in an accurate and reliable way under specified conditions (constant environmental conditions like temperature, air humidity etc.), and using certified SRMs spanning a quantified range of isotopic values. As mentioned above, the IRMS needs to be optimally adjusted for accurate and precise measurements, and the amount of sample introduced needs to be within the linear working range of the instrument. Introducing sample volumes that are too small or too large can produce results outside the *limits of detection* or *quantification*. Thus, the IRMS and peripheral equipment need to be routinely maintained in working order for samples to be accurately calibrated, correcting for offset problems, and adjusted to the appropriate  $\delta$  scale.

The first step in calibration is to correct the data for systematic offset errors that change over time or with sample volume such as drift. For sample drift, calibration standards need to be analyzed throughout the set of samples. A systematic long-term drift might be correctable if the trend can be mathematically estimated, whereas a highly variable drift is not correctable and becomes random error, and an increase in measurement uncertainty. Once these systematic drift errors are corrected, the data can then be calibrated to the appropriate isotopic  $\delta$  scale. Additionally, separating duplicates within the sample set such that one is analyzed early, and one is analyzed towards the end of a set will help capture the variance not corrected by drift corrections into the precision estimate (Table 6.2).

The last step in the calibration process is calibrating to the appropriate international scale (Sect. 6.4.2.1). The isotopic  $\delta$  scale is determined by two primary *scale-defining* international standards (Table 6.3), where one standard sets the zero ‰ value, and the second sets the ‰ distance. For example, Vienna Standard Mean Ocean Water (V-SMOW) is defined as 0 ‰ and Standard Light Antarctic Precipitation (SLAP) has the  $\delta^2\text{H}$  value of  $-428$  ‰, so the distance between these two measurements is 428 ‰, setting the hydrogen isotopic  $\delta$  scale. All standard reference materials need to be

**Table 6.3** International scales for isotope ratio determination (Accepted isotope ratios and R values for certified SRM can change over time. The most current values can be obtained from the CIAAW website: [www.ciaaw.org](http://www.ciaaw.org))

Ratio	International scale	primary SRM defining scale	Accepted ratio R [ $\times 10^6$ ]	Error of ratio R [ $\times 10^6$ ]	References
$^2\text{H}/^1\text{H}$	VSMOW	VSMOW: 0 ‰	155.75	$\pm 0.08$	de Wit et al. (1980)
		SLAP: $-428$ ‰			Gonfiantini (1978)
$^{13}\text{C}/^{12}\text{C}$	VPDB	NBS 19: $+1.95$ ‰	11,180.2	$\pm 2.8$	Zhang and Li (1990)
		USGS64: $-40.81$ ‰			Schimmelmann et al. (2016)
$^{15}\text{N}/^{14}\text{N}$	AIR-N <sub>2</sub>	AIR-N <sub>2</sub> : 0 ‰	3678.2	$\pm 1.5$	de Bièvre et al. (1996)
		IAEA-N-1 + $0.43$ ‰			Boehlke and Coplen (1993)
		USGS32 + 180 ‰			Boehlke and Coplen (1993)
$^{18}\text{O}/^{16}\text{O}$	VSMOW	VSMOW: 0 ‰	2005.2	$\pm 0.45$	Baertschi (1976)
		SLAP: $-55.5$ ‰			Gonfiantini (1978)
$^{17}\text{O}/^{16}\text{O}$	VSMOW	VSMOW: 0 ‰	379.9	$\pm 0.8$	Li et al. (1988)
		SLAP: $-29.6986$ ‰ <sup>a</sup>			Schoenemann et al. (2013)

<sup>a</sup>Exact values defining the  $\delta^{17}\text{O}$  VSMOW/SLAP scale. The  $\delta^{17}\text{O}$  values for SLAP are calculated assuming that the accepted mass-dependent isotope fractionation with  $\lambda = 0.528$  is valid for ocean water (c.f. Brand et al. 2014)

calibrated to these scale-defining international standards for isotopic measurements to be meaningful and comparable across laboratories, studies and through time.

This final scaling correction can contain both scale-factor and offset errors and requires at least two or more independent calibration standards with isotope ratios that span the isotopic range of sample values but have similar chemical properties. In the example in Fig. 6.1, three calibration standards were used that spanned 22.1 ‰ in the Vienna Pee Dee Belemnite (VPDB)  $\delta^{13}\text{C}$  scale. The measured span between the calibration standards was only 20 ‰, indicating scale compression error. The correction equation slope reflects this compression with a slope greater than 1, and thus would stretch the data back to the correct  $\delta$  value (Coplen 1988), and this stretching increases the error associated with each measurement in the set. The measured  $\delta$  values were also higher than the actual  $\delta$  values leading to an intercept of  $-0.58$  ‰ which represents the offset factor. Three calibration standards were used in this example, and one independent QC sample that was not used to calculate any correction equations, and is the only standard used to calculate accuracy (see Sect. 6.2.2).

The advantage of three calibration standards that span the range of samples is that it would be apparent if one standard has become compromised for any reason. This would be an additional QC check on the calibration equation.

### **6.3.3.1 Calibration Error**

Improper and inconsistent calibration of data to the correct  $\delta$  scale is major source of error and data discrepancy between laboratories (Wassenaar et al. 2018; Meier-Augenstein and Schimmelmann 2019). Wassenaar et al. (2018) found that laboratories reporting inaccurate data during a round-robin comparison had four common problems: incorrect data calibration to the  $\delta$  scale (sometimes called normalization), insufficient coverage of the  $\delta$ -scale, instrument problems, and/or compromised standard reference material. While their study compared laboratories analyzing water samples, similar problems can be found in laboratories measuring isotopic ratios of other materials. This potential difference between laboratories measuring the same sample is concerning for studies that switch laboratories during a study, or for meta-analysis of isotopic data. For studies that need to switch IRMS laboratories mid-study, we highly recommend conducting repeat analysis at both IRMS laboratories for 10% of samples spanning a range of isotopic values. The researcher should calculate any systematic differences between the laboratories, and correct all data to one laboratory scale. In addition, the researcher should quantify the remaining random differences (after correcting for systematic differences) between the 10% repeated measures using Eq. 6.1 and include that uncertainty using Eq. 6.2. Anyone conducting meta-analysis using stable isotope data from tree rings needs to be aware of this problem as well and increase the uncertainty around the compiled data to reflect the actual reproducibility rather than the repeatability, which is precision based on results from a single laboratory over a short period of time.

## **6.4 Traceability and Standards**

### **6.4.1 Traceability**

Traceability is defined as “the value of a standard, whereby it can be related to stated references, usually national or international standards, through an unbroken chain of comparisons all having stated uncertainties” (ISO 15189). For isotope ratio mass spectrometry without real SI units, traceability implies a connection of all measured  $\delta$  values to an internationally accepted measurement scale related to a scale defining primary reference material (de Bièvre et al. 1997). This unbroken calibration chain must be connected to carefully measured and estimated uncertainties of all involved intermediate materials and used procedures. The combined uncertainty of the whole comparison chain will define the quality of the connection

to the internationally agreed scale unit (Table 6.3) and consequently will be also a quality factor for the measured values themselves. To arrive at a combined uncertainty budget (see Sect. 6.2.4 on uncertainty) for any certified reference material, the uncertainty value must include the uncertainty around the international certified standard reference materials that were used in the calibration as well as the uncertainty estimated from all the steps in the isotopic measurement (from conversion to gases for analysis, to the actual measurement of the ion current ratios of a sample, to the reported  $\delta$  values). This list can contain typical laboratory corrections like  $^{17}\text{O}$  correction, linearity, blank, drift, memory and/or offset correction as well as normalization (Dunn et al. 2015). Every certified reference material should have its isotopic value and associated uncertainty reevaluated and connected back to internationally certified scale-defining standard reference material regularly, and this uncertainty should be propagated forward to the measurement of samples. Ideally, studies should report the certified reference materials used in calibration and associated values, as the assigned values to certified reference materials can change over time.

Traceability also relates to the chain of custody and treatment of samples from collection through analysis to the final data analysis and publication (see Sect. 6.3.1.1). Significant error and uncertainty can be introduced without a proper plan for tracking samples from collection to publication of the data. Assigning sample IDs that avoid confusion and errors is critical, and with the nested nature of tree-ring samples, can be very challenging. Additionally, samples go through many steps from collection to accurate dating of rings, to separating rings, to homogenization to cellulose extraction to weighing for isotopic analysis. Sample identity and accurate sample tracking needs to be maintained throughout all these steps. Details of assigning sample IDs and sample tracking should be thought out carefully and explained clearly in a QA plan and appropriate SOPs.

## ***6.4.2 Types of Isotopic Standards for Tree-Ring Analysis***

Three classes of standards are used in isotopic studies: international certified standard reference materials (SRM) (Sect. 6.4.2.1), laboratory standard reference materials (Sect. 6.4.2.2) and study standards (Sect. 6.4.2.3). International-certified SRM are reference materials with certified accuracy and uncertainty including a stated confidence level and supplied by supranational organizations like the International Atomic Energy Agency (IAEA) in highly controlled and limited quantities. Laboratory SRMs are SRMs used in day-to-day operation of the IRMS for calibration and QC. These laboratory SRMs must be routinely calibrated to the appropriate  $\delta$  scale using international certified SRM and assigned a level of accuracy and uncertainty to their assessed isotopic value. Study standards are large quantities of homogenized material in which the isotopic value may or may not have been previously determined. These standards are used to check for consistency and estimating of processing influences on study precision.



### 6.4.2.1 International Certified Standard Reference Material

Measured isotope ratios are typically reported as the deviation from a primary reference material that defines the zero point for a respective scale for each element. These *primary* SRMs are then *scale defining* international standards (Table 6.3) and are often defined without uncertainty. Using carbon as an example, the scale-defining primary international SRM is Vienna Pee Dee Belemnite (VPDB, Table 6.3), thus a measured ratio of  $^{13}\text{C}/^{12}\text{C}$  ( $^{13}\text{R}_{\text{sample}}$ ) would be compared to the  $^{13}\text{C}/^{12}\text{C}$  of VPDB ( $^{13}\text{R}_{\text{VPDB}}$ , Eq. 6.3).

$$\delta_{\text{C}_{\text{VPDB}}}^{13} = \frac{^{13}\text{R}_{\text{Sample}} - ^{13}\text{R}_{\text{VPDB}}}{^{13}\text{R}_{\text{VPDB}}} = \frac{^{13}\text{R}_{\text{Sample}}}{^{13}\text{R}_{\text{VPDB}}} - 1 \quad (6.3)$$

The resulting  $\delta$  value is typically reported in parts per thousand (‰) by multiplying by 1000. This “‰ unit” is not compatible with the SI system; in recent years the term milli-Urey (mUr) as an attributed SI unit replacing “‰” was suggested (Brand and Coplen 2012). The storage and distribution of international certified scale-defining SRMs are under control of the International Union of Pure and Applied Chemistry (IUPAC), Commission for Isotope Abundances and Atomic Weights (CIAAW, [www.ciaaw.org](http://www.ciaaw.org), Brand et al. 2014), and can be ordered from IAEA only once in 3 years per lab.

Interestingly, the corresponding isotope ratios of the international scale-defining primary SRMs are not always known exactly. The original reference material Pee Dee Belemnite (PDB) acting as scale anchor for  $^{13}\text{C}/^{12}\text{C}$  and  $^{18}\text{O}/^{16}\text{O}$  since the 1950s was used up a long time ago. To preserve the scale in a consistent way, the virtual standard VPDB was defined via the reference material NBS 19. The original Standard Mean Ocean Water (SMOW) for  $^{18}\text{O}/^{16}\text{O}$  and  $^2\text{H}/^1\text{H}$  virtually did not exist but was defined via reference material NBS-1. As a replacement of the exhausted NBS-1, a large batch of water with an isotopic composition close to SMOW was prepared and termed “VSMOW”, with the V standing for Vienna where IAEA is located. Recently, a new reference water set VSMOW-2 and SLAP-2 was produced to be available as SRM set for the oxygen and hydrogen isotope scale. VSMOW-2 and SLAP-2 are now associated with an uncertainty relative to VSMOW and SLAP. AIR-N<sub>2</sub> serves as scale anchor for  $^{15}\text{N}/^{14}\text{N}$  measurements.

To overcome the constraints of limited supply of the primary SRMs and to ensure a more general applicability of SRMs, several materials of natural and/or synthetic origin have been produced to act as secondary SRMs. These reference materials must satisfy special conditions:

- Homogeneous material in the isotope range used for measurements and certified as homogeneous to a certain sample size.
- High purity of the reference material. No extra purification needed when SRM is used with described dedicated analysis techniques. Single chemical compound preferred.

- Stable and inert material. No need for special treatment during storage or handling of the SRM (no reaction “autodecomposing” with water, air-O<sub>2</sub> under normal conditions). Non-hygroscopic.
- No change of isotope ratio when stored or handled properly under normal conditions. In case SRM should work for oxygen and hydrogen isotope ratios: no or low (and documented) exchangeable hydrogen and/or oxygen atoms in the SRM molecule.
- Easy handling of SRM (no autodecomposition, no “electrostatic” property, not toxic or explosive). Easily replaceable when exhausted.
- SRM with chemical form similar to samples available (carbonate for carbonate analysis, water for water analysis, organic when organic samples should be analyzed).
- Identical chemical form preferably with different isotope ratios available (calibration).

The  $\delta$  values of these internationally available secondary SRM are derived from careful calibration versus the primary scale-defining SRMs. For this reason, all secondary SRMs have uncertainties assigned with the internationally adopted and agreed  $\delta$  values, which can change over time. All these properties are also desirable for any reference material used for calibration or QC in isotopic analysis. However, not all certified SRMs can be accurately measured on all peripheral devices used for IRMS analysis. For example, Schimmelmann et al. (2016) found that  $\delta^2\text{H}$  values of caffeine cannot be measured accurately in a TC/EA, but need a chromium reactor, thus would be an inappropriate SRM for TC/EA analysis. Nitrogen bearing organic compounds interfere with  $\delta^2\text{H}$  analysis during pyrolysis (Nair et al. 2015). The CIAAW provides a list of certified SRM with their isotopic values (<http://ciaaw.org/reference-materials.htm>).

#### 6.4.2.2 Laboratory Standard Reference Materials

Because of the limited availability of International certified scale-defining and most secondary SRMs, IRMS laboratories use “laboratory SRMs” for calibration and quality control during routine isotopic analysis. IRMS laboratories must calibrate all of their laboratory SRMs with international certified SRMs. Many laboratories have a large range of laboratory SRMs because the chemical properties of the SRMs used for correcting and calibrating isotopic measurement should be as similar as possible to the samples under investigation following the IT Principle (Werner and Brand 2001; Brand et al. 2009). To the extent possible, these laboratory SRMs should be composed of material that adheres to the special conditions listed above for international certified SRMs. For tree-ring cellulose analysis, IAEA-CH-3 is a certified cellulose standard that laboratories can use. Laboratories are always searching for reference materials that can span a range of isotopic values for proper calibration across the relevant  $\delta$  scales (see Sect. 6.3). To that end, Qi et al. (2016) developed three whole-wood reference materials that span a range of isotopic values for  $\delta^2\text{H}$ ,

$\delta^{18}\text{O}$ ,  $\delta^{13}\text{C}$  and  $\delta^{15}\text{N}$ , and they provide the fraction of exchangeable hydrogen for each. These would be ideal laboratory SRMs for tree-ring studies for both calibration and QC. However, they were not certified for their cellulose isotopic values, so they would require in-house calibration with other international SRMs before being used for the IT Principle through cellulose extractions. In addition to IAEA-CH-3, certified wood samples are an excellent start at providing appropriate SRM for isotopic analysis for any study using wood or cellulose from tree rings.

### 6.4.2.3 Study Standards

Study standards provide additional information to assess error or for calculating precision for a study (Table 6.2). A study standard is a bulk sample of similar chemical composition as the samples within the study. For tree-ring analysis, this would be a large highly homogenized wood sample that can be used as a QC sample throughout all the steps of preparation such as cellulose extraction (Porter and Middlestead 2012). QC standards added by the IRMS laboratory during isotopic analysis will quantify the accuracy of isotopic analysis, but would not capture the uncertainty associated with sample processing or storage. Sample duplicates will capture some processing and storage uncertainty, but duplicates are often processed and analyzed together in the same sample set through cellulose extraction to analysis on the IRMS. A study standard will allow for assessing error across the entire study. By including one or more study standards into each set of samples that are processed as a unit throughout the study, inter-set variation can be quantified and study standards can potentially identify batches that were compromised during processing (Porter and Middlestead 2012) Comparing a single result with a longer record of data can additionally help researchers to detect isotope fractionation problems during processing of tree-ring samples.

## 6.5 Conclusions

A proper quality assurance plan along with proper quality control steps and measures should be a part of every research project. Our purpose in this chapter was to provide tools for researchers to quantify the accuracy and precision of their isotopic data within tree-ring studies, although many of the principles apply to all studies. We discussed some of the challenges with making high quality isotopic measurements, but this chapter was not intended to guide anyone through the details of how to properly operate an IRMS. Instead, we discussed these challenges to highlight how critical it is to use a high-quality laboratory for conducting stable isotope analysis, and how critical instrument condition and proper use of standards are to accurate and precise isotopic data. The use of duplicates and study standards gives researchers the ability to quantify the precision of their analysis as outlined in Sect. 6.2. Following the principles outlined in this chapter, researchers should be able to design a quality

assurance plan to minimize potential errors in tree-ring isotopic analysis and quantify the uncertainty around the isotopic values in their study for reporting in the final published manuscripts and to provide with the data when made public. In the methods and materials section of manuscripts, researchers should include at a minimum the accuracy as  $\mu \pm \sigma$  of the QC standards (Table 6.1) and the precision based on sample duplicates (Table 6.2) along with the number of QC standards and duplicates, the standard reference material used for the QC standard, and the isotopic range of calibration standards used during analysis.

**Acknowledgements** We thank Leslie Chesson, Willi Brand, Andrew Schauer, and Jim Markwiese for their thoughtful and detailed reviews of this chapter. This chapter has been subjected to Agency review and has been approved for publication. The views expressed in this paper are those of the author(s) and do not necessarily reflect the views or policies of the U.S. Environmental Protection Agency. Mention of trade names or commercial products does not constitute endorsement or recommendation for use.

## References

- Baertschi P (1976) Absolute  $^{18}\text{O}$  content of standard mean ocean water. *Earth Planet Sci Lett* 31:341–344
- Boehlke JK, Coplen TB (1993) Interlaboratory comparison of reference materials for nitrogen-isotope-ratio measurements. In: Reference and intercomparison materials for stable isotopes of light elements. IAEA, Vienna IAEA-TECDOC-825
- Borella S, Leuenberger M, Saurer M, Siegwolf R (1998) Reducing uncertainties in  $\delta^{13}\text{C}$  analysis of tree rings: pooling, milling and cellulose extraction. *J Geophys Res* 103(19):515–19526
- Brand WA, Coplen TB (2012) Stable isotope deltas: tiny, yet robust signatures in nature. *Isot Environ Health Stud.* <https://doi.org/10.1080/10256016.2012.666977>
- Brand WA, Coplen TB, Aerts-Bijma AT, Böhlke JK, Gehre M, Geilmann H, Gröning M, Jansen HG, Meijer HA, Mroczkowski SJ, Qi H, Soergel K, Stuart-Williams H, Weise SM, Werner RA (2009) Comprehensive inter-laboratory calibration of reference materials for  $\delta^{18}\text{O}$  versus VSMOW using various on-line high-temperature conversion techniques. *Rapid Commun Mass Spectrom* 23:999–1019
- Brand WA, Coplen TB, Vogl J, Rosner M, Prohaska T (2014) Assessment of international reference materials for isotope-ratio analysis (IUPAC Technical Report). *Pure Appl Chem* 86. <https://doi.org/10.1515/pac-2013-1023>
- Brooks PD, Geilmann H, Werner RA, Brand WA (2003) Letter to the editor. *Rapid Commun Mass Spectrom* 17:1924–1926
- Coplen TB (1988) Normalization of oxygen and hydrogen isotope data. *Chem Geol* 72:293–297
- de Bièvre P, Kaarls R, Peiser HS, Rasberry SD, Reed WP (1997) Protocols for traceability in chemical analysis. Part I: definitions and terminology. *Accred Qual Assur* 2:168–179
- de Bièvre P, Valkiers S, Peiser SH, Taylor PDP, Hansen P (1996) Mass-spectrometric methods for determining isotopic composition and molar mass traceable to the SI, exemplified by improved values for nitrogen. *Metrologia* 33:447–455
- de Wit JC, van der Straaten CM, Mook WG (1980) Determination of the absolute hydrogen isotopic ratio of V-SMOW and SLAP. *Geostand Newsl* 4:33–36
- Dunn PJH, Hai L, Malinovsky D, Goenaga-Infante H (2015) Simple spreadsheet templates for the determination of the measurement uncertainty of stable isotope delta values. *Rapid Commun Mass Spectrom* 29:2184–2186

- Ellison SLR, Williams A (2012) EURACHEM/CITAC guide CG 4 quantifying uncertainty in analytical measurement
- Gonfiantini R (1978) Standards for stable isotope measurements in natural compounds. *Nature* 271:534–536
- Hurlbert SH (1984) Pseudoreplication and the design of ecological field experiments. *Ecol Monogr* 54:187–211
- Jardine TD, Cunjak RA (2005) Analytical error in stable isotope ecology. *Oecologia* 144:528–533
- Li WJ, Ni B, Jin D, Zhang Q-L (1988) Measurement of the absolute abundance of oxygen-17 in V-SMOW. *Chin Sci Bull* 33:1610–1613
- Liñán ID, Gutiérrez E, Helle G, Heinrich I, Andreu-Hayles L, Planells O, Leuenberger M, Bürger C, Schleser GH (2011) Pooled versus separate measurements of tree-ring stable isotopes. *Sci Total Environ* 409:2244–2251
- Meier-Augenstein W, Schimmelmann A (2019) A guide for proper utilisation of stable isotope reference materials. *Isot Environ Health Stud* 55:113–128
- Nair S, Geilmann H, Coplen TB, Qi H, Gehre M, Schimmelmann A, Brand WA (2015) Isotopic disproportionation during hydrogen isotopic analysis of nitrogen-bearing organic compounds. *Rapid Commun Mass Spectrom* 29:878–884
- Porter TJ, Middlestead P (2012) On estimating the precision of stable isotope ratios in processed tree-rings. *Dendrochronologia* 30:239–242
- Qi H, Coplen TB, Jordan JA (2016) Three whole-wood isotopic reference materials, USGS54, USGS55, and USGS56, for  $\delta^2\text{H}$ ,  $\delta^{18}\text{O}$ ,  $\delta^{13}\text{C}$ , and  $\delta^{15}\text{N}$  measurements. *Chem Geol* 442:47–53
- Richter A, Wanek W, Werner RA, Ghashghaie J, Jaggi M, Gessler A, Brugnoli E, Hettmann E, Gottlicher SG, Salmon Y, Bathellier C, Kodama N, Nogues S, Søe A, Volders F, Sorgel K, Blochl A, Siegwolf R, Buchmann N, Gleixner G (2009) Preparation of starch and soluble sugars of plant material for the analysis of carbon isotope composition: a comparison of methods. *Rapid Commun Mass Spectrom* 23:2476–2488
- Schimmelmann A, Qi H, Coplen TB, Brand WA, Fong J, Meier-Augenstein W, Kemp HF, Toman B, Ackermann A, Assonov S, Aerts-Bijma AT, Brejcha R, Chikaraishi Y, Darwish T, Elsner M, Gehre M, Geilmann H, Gröning M, Hélie J-F, Herrero-Martín S, Meijer HA, Sauer PE, Sessions AL, Werner RA (2016) Organic reference materials for hydrogen, carbon, and nitrogen stable isotope-ratio measurements: caffeine, n-alkanes, fatty acid methyl esters, glycines, l-valines, polyethylenes, and oils. *Anal Chem* 88:4294–4302
- Schoenemann SW, Schauer AJ, Steig EJ (2013) Measurement of SLAP2 and GISP  $\delta^{17}\text{O}$  and proposed VSMOW-SLAP normalization for  $\delta^{17}\text{O}$  and  $^{17}\text{O}_{\text{excess}}$ . *Rapid Commun Mass Spectrom* 27:582–590
- Wassenaar LI, Terzer-Wassmuth S, Douence C, Araguas-Araguas L, Aggarwal PK, Coplen TB (2018) Seeking excellence: an evaluation of 235 international laboratories conducting water isotope analyses by isotope-ratio and laser-absorption spectrometry. *Rapid Commun Mass Spectrom* 32:393–406
- Werner RA, Brand WA (2001) Referencing strategies and techniques in stable isotope ratio analysis. *Rapid Commun Mass Spectrom* 15:501–519
- Zhang Q-L, Li WJ (1990) A calibrated measurement of the atomic weight of carbon. *Chin Sci Bull* 35:290–296

**Open Access** This chapter is licensed under the terms of the Creative Commons Attribution 4.0 International License (<http://creativecommons.org/licenses/by/4.0/>), which permits use, sharing, adaptation, distribution and reproduction in any medium or format, as long as you give appropriate credit to the original author(s) and the source, provide a link to the Creative Commons license and indicate if changes were made.

The images or other third party material in this chapter are included in the chapter's Creative Commons license, unless indicated otherwise in a credit line to the material. If material is not included in the chapter's Creative Commons license and your intended use is not permitted by statutory regulation or exceeds the permitted use, you will need to obtain permission directly from the copyright holder.



# Chapter 7

## Newer Developments in Tree-Ring Stable Isotope Methods



**Katja T. Rinne-Garmston, Gerhard Helle, Marco M. Lehmann, Elina Sahlstedt, Jürgen Schleucher, and John S. Waterhouse**

**Abstract** The tree-ring stable C, O and H isotope compositions have proven valuable for examining past changes in the environment and predicting forest responses to environmental change. However, we have not yet recovered the full potential of this archive, partly due to a lack understanding of fractionation processes resulting from methodological constraints. With better understanding of the biochemical and tree physiological processes that lead to differences between the isotopic compositions of primary photosynthates and the isotopic compositions of substrates deposited in stem xylem, more reliable and accurate reconstructions could be obtained. Furthermore, by extending isotopic analysis of tree-ring cellulose to intra-molecular level, more information could be obtained on changing climate, tree metabolism or ecophysiology. This chapter presents newer methods in isotope research that have become available or show high future potential for fully utilising the wealth of information available in tree-rings. These include compound-specific analysis of sugars and cyclitols, high spatial resolution analysis of tree rings with UV-laser, and position-specific isotope analysis of cellulose. The aim is to provide the reader with understanding of

---

K. T. Rinne-Garmston (✉) · E. Sahlstedt  
Natural Resources Institute Finland (Luke), Latokartanonkaari 9, 00790 Helsinki, Finland  
e-mail: [katja.rinne-garmston@luke.fi](mailto:katja.rinne-garmston@luke.fi)

E. Sahlstedt  
e-mail: [elina.sahlstedt@luke.fi](mailto:elina.sahlstedt@luke.fi)

G. Helle  
Helmholtz-Centre Potsdam, GFZ German Centre for GeoSciences Section 4.3 Climate Dynamics and Landscape Evolution, Potsdam, Germany  
e-mail: [gerhard.helle@gfz-potsdam.de](mailto:gerhard.helle@gfz-potsdam.de)

M. M. Lehmann  
Swiss Federal Institute for Forest, Snow and Landscape Research WSL, Birmensdorf, Switzerland  
e-mail: [marco.lehmann@alumni.ethz.ch](mailto:marco.lehmann@alumni.ethz.ch)

J. Schleucher  
Department of Medical Biochemistry and Biophysics, Umeå University, 90187 Umeå, Sweden  
e-mail: [jurgen.schleucher@umu.se](mailto:jurgen.schleucher@umu.se)

J. S. Waterhouse  
School of Life Sciences, Anglia Ruskin University, East Road, Cambridge CB1 1PT, UK  
e-mail: [john.waterhouse@aru.ac.uk](mailto:john.waterhouse@aru.ac.uk)

the advantages and of the current challenges connected with the use of these methods for stable isotope tree-ring research.

## 7.1 Introduction

Significant gaps still exist in our understanding about how a given isotopic composition of a tree ring is formed. This mainly concerns the metabolic processes and isotopic fractionations that occur post-photosynthetically in the leaf and phloem and also during tree-ring formation (see Chap. 13). To achieve a profound level of knowledge of these processes that impact the environmental signal extractable from tree-ring  $\delta^2\text{H}$ ,  $\delta^{13}\text{C}$  and  $\delta^{18}\text{O}$  values, it is necessary to go beyond the conventional analytical methods in isotope analysis, which utilize “bulk” matter (e.g. leaves or sugar extract) and to focus on studies at intra-annual level and at intra-molecular level. New methodological developments have been made during the last decade that have shown high potential in this respect. These developments enable us to study isotopic fractionation processes and environmental signals in  $\delta^{13}\text{C}$ ,  $\delta^{18}\text{O}$  and to some extent also in  $\delta^2\text{H}$  values at molecular (compound-specific isotope analysis, “CSIA”) and even at intra-molecular (position-specific isotope analysis) level. Combined with methodological advancements in intra-annual tree-ring analysis (application of UV-laser), these new applications will improve our understanding of the relationships between climatic and isotope variability in tree rings. This chapter describes the new methodological developments of stable isotope analysis established for non-structural carbohydrates and tree rings.

## 7.2 Compound-Specific $\delta^{13}\text{C}$ and $\delta^{18}\text{O}$ Analysis of Sugars and Cyclitols

CSIA was introduced already in 1984 for  $\delta^{13}\text{C}$ , which was accomplished by coupling on-line Gas Chromatography (GC) to an Isotope Ratio Mass Spectrometer (IRMS) (Barrie et al. 1984). However,  $\delta^{13}\text{C}$  analysis of carbohydrates using a GC/combustion-IRMS requires substantial derivatization, which incorporates external carbon atoms into the molecule and can cause kinetic isotope effects (Boschker et al. 2008; Macko et al. 1998). The development of a new interface for on-line coupling of high-performance liquid chromatography (HPLC) to an IRMS by Krummen et al. (2004) overcame these issues by removing the need for sample derivatization. Hence, it has become the method of choice for  $\delta^{13}\text{C}$  analysis of sugars and sugar-like compounds (Boschker et al. 2008; Rinne et al. 2012).  $\delta^{18}\text{O}$  analysis of carbohydrates has been recently achieved with GC/pyrolysis-IRMS (Zech and Glaser 2009; Zech et al. 2013a), where CSIA has been finally accomplished without the introduction of external O into the derivative (Lehmann et al. 2016). So far, no literature has been



published on compound-specific hydrogen isotope analysis of carbohydrates using chromatographic separation, presumably because of the oxygen-bound hydrogen that exchanges with surrounding water during sample processing or the addition of external hydrogen to the sugar molecule during derivatization.

### **7.2.1 $\delta^{13}\text{C}$ Analysis of Tree Sugars and Cyclitols Using Liquid Chromatography**

Tree-ring  $\delta^{13}\text{C}$  composition does not directly record changes in the ratio of leaf internal to ambient  $\text{CO}_2$  concentrations ( $c_i/c_a$ ), which would relate to changes in environmental conditions and their impact on photosynthetic rate and stomatal conductance (Barbour and Song 2014; Cernusak et al. 2009; Gessler et al. 2014). A multitude of mechanisms have been proposed that may modify the original environmental signal imprinted in primary photosynthates (Farquhar et al. 1982) during the pathway from leaf sucrose production to its consumption for stem wood production. These include respiration, enzymatic isotope fractionation, carbohydrate storage effects and fractionation during xylem cell formation (Gleixner et al. 1998; Helle and Schleser 2004; Panek and Waring 1997; Rinne et al. 2015a) (see Chap. 13). Detailed understanding of post-photosynthetic fractionations and processes is necessary for improved interpretation of  $\delta^{13}\text{C}$  signal in tree rings. To achieve a profound level of understanding for a single biochemical process, studies must be conducted on a molecular level. This is because individual compounds within the “bulk” matter may have a  $\delta^{13}\text{C}$  signal that contains substantially different environmental or biochemical information. For tree rings, the need for CSIA was recognized quite early, and cellulose extraction is nowadays a common, and recommended practice in stable isotope laboratories developing tree-ring isotopic chronologies. For metabolic studies, isolation of other compounds, such as sugars, starch and organic acids, is also needed. This section discusses CSIA of sugars and sugar-like substances (cyclitols), which are involved in various biochemical processes and are essential for the accurate interpretation of the tree-ring  $\delta^{13}\text{C}$  archive.

#### **7.2.1.1 Analytical Methodology**

Isotope analysis of bulk material, such as whole leaves or bulk compounds extracted by water, has been the mainstay in biochemical studies. However, bulk isotope ratios reflect the average value of compound-specific isotope ratios in a mixture, where the individual compounds may substantially differ in their isotopic value due to differences in their genesis. Hence, the recent literature has started to explore the application of chromatographic separation on bulk matter prior to isotope analysis, which is possible on-line using high-performance liquid chromatography (HPLC), ion chromatography (IC) or gas chromatography (GC) connected via an interface to

an IRMS. HPLC and IC separation are best suited for the analysis of non-volatile, polar and thermally labile sugars and cyclitols (e.g. pinitol and myo-inositol), because no modifications (i.e. derivatization) are required for the analyte prior to its introduction to an HPLC/IC-IRMS system. For HPLC (Krummen et al. 2004) and IC (Morrison et al. 2010) separation, a small amount of purified sugar extract is injected into a moving stream of liquid (i.e. mobile phase, dilute NaOH), which passes through a column packed with particles of stationary phase. The most commonly used column for CSIA of sugars has been the Dionex CarboPac PA20 (Thermo Fisher Scientific) due to its capabilities at separating individual chromatography peaks (Boschker et al. 2008; Rinne et al. 2012). Column oven temperatures of 15 or 20 °C have been typically used for plant sugars (Rinne et al. 2015a). At higher temperatures isomerization will distort  $\delta^{13}\text{C}$  values of hexoses (Rinne et al. 2012). Different compounds pass through a column at different times, i.e. they have different elution rates. The eluting compounds are oxidized to  $\text{CO}_2$ , when still in the mobile phase, using sodium persulfate ( $\text{Na}_2\text{S}_2\text{O}_8$ ) under acidic conditions ( $\text{H}_3\text{PO}_4$ ) at 99 °C. Since oxidation is done in the mobile phase, which contains dissolved  $\text{CO}_2$  and a high abundance of O atoms from the chemicals used, these instruments are not suitable for compound-specific  $\delta^{18}\text{O}$  analyses (for  $\delta^{18}\text{O}$  analysis see Sect. 7.2.2). For  $\delta^{13}\text{C}$  determination, the  $\text{CO}_2$  produced from each carbohydrate is separated from the mobile phase in a capillary gas separator flushed with helium gas, dried and led to the IRMS for analysis. The analytical instruments enable accurate and reproducible  $\delta^{13}\text{C}$  measurements of sample sizes down to 400 ng of C per compound. In addition, the produced  $\text{CO}_2$  can be also used to obtain the concentration of each carbohydrate. An example of a HPLC-IRMS chromatogram of larch needle sugars is presented in Fig. 7.1.

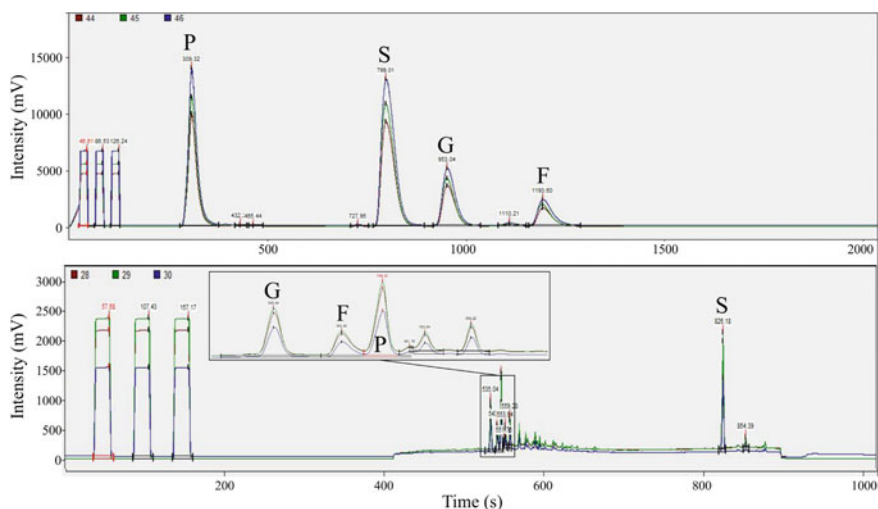


**Fig. 7.1** Larch needle sugar HPLC-IRMS (top graph) and GC/Py-IRMS (bottom) chromatograms for compound-specific  $\delta^{13}\text{C}$  and  $\delta^{18}\text{O}$  analysis, respectively. The four compounds with adequate amount of material for isotope analysis are pinitol (P), sucrose (S), glucose (G) and fructose (F)

### 7.2.1.2 Sample Preparation

In the field, collected plant samples for sugar extraction are placed immediately in a cold box below 0 °C and microwaved soon after (60 s at 600 W) to stop enzymatic activities (Wanek et al. 2001). Sampled tissues are subsequently dried for 24 h at 60 °C and ground to fine powder. Typically, the water soluble fraction is extracted using a method modified after Wanek et al. (2001) and Rinne et al. (2012). According to this method, reaction vials are filled with 60 mg of the homogenized needle powder and 1.5 mL of Milli-Q water (18.2 MΩ, total organic C < 5 ppb). The mixture is stirred with vortex until the powder is fully suspended. The tubes are then placed in a water bath at 85 °C for 30 min. The samples are then centrifuged at 10,000 g for 2 min. For phloem samples, the exudation method has been used for obtaining sugars for isotope analysis (Gessler et al. 2004; Treydte et al. 2014), and described in detail in Chap. 13. After extraction, neutral carbohydrates are purified from ionic compounds using anion and cation exchange cartridges (Fionex OnGuard II H and OnGuard II A, Thermo Fisher Scientific; Wild et al. 2010) and from phenolic compounds (Dionex OnGuard II P) as described in detail in Rinne et al. (2012). Purification is necessary not only to simplify the chromatogram but also to remove compounds that could affect the column performance and lifetime (Boschker et al. 2008).

### 7.2.1.3 Research Applications

So far only a few studies have been published on compound-specific  $\delta^{13}\text{C}$  analysis of tree sugars and cyclitols. CSIA has been applied on leaf (Bogelein et al. 2019; Churakova (Sidorova) et al. 2018; Churakova (Sidorova) et al. 2019; Galiano et al. 2017; Rinne et al. 2015a), twig and stem phloem (Bogelein et al. 2019; Smith et al. 2016), shoot (Streit et al. 2013) and coarse root (Galiano et al. 2017) samples for tree physiological and environmental studies, both at natural isotope abundance and after  $^{13}\text{CO}_2$  labelling. In addition to trees, CSIA of sugars has been used on a CAM plant *Kalanchoë daigremontiana* to study the flux of carbon from PEPC and direct Rubisco fixation (Wild et al. 2010), on potato plants to study source of leaf respired  $\text{CO}_2$  (Lehmann et al. 2015) and on common bean to determine the influence of sugars and cyclitols on predictions of plant water use efficiency (Smith et al. 2016).

For leaf sugars of larch (*Larix gmelinii* Rupr. in Siberia and *Larix decidua* Mill. in Swiss mountains), high resolution sampling during a growing season has shown a significant climatic signal with little or no sign of the use of carbohydrate reserves in  $\delta^{13}\text{C}$  values of sucrose or hexoses (glucose and fructose) in studies at natural abundance (Churakova (Sidorova) et al. 2019; Rinne et al. 2015a). Also, Streit et al. (2013) combined  $^{13}\text{C}$ -labelling with subsequent CSIA on larch (*Larix decidua*), and showed that sucrose  $\delta^{13}\text{C}$  value was not much affected by old stored carbon. The intra-seasonal low-frequency trends of climatic variability observed in leaf sucrose, which is the sugar transported from leaves to phloem (Dennis and Blakeley 2000; Streit et al. 2013), of *Larix gmelinii* (Rinne et al. 2015a) were retained in the corresponding intra-annual tree-ring  $\delta^{13}\text{C}$  records (Rinne et al. 2015b). This matching of seasonal signals

may indicate a better chance to reconstruct seasonal climate information from larch trees compared with other species that have shown more dependency on reserves. To improve knowledge on the use of C reserves for leaf sugar formation and to determine how the intra-seasonal climate signal in leaf sugars is preserved in intra-annual tree-ring  $\delta^{13}\text{C}$  record, similar studies are needed also for other tree species and for different growing conditions.

CSIA analysis has shown that individual sugars and sugar-like compounds have differences in the environmental signal stored in their  $\delta^{13}\text{C}$  values due to differences in their genesis (Fig. 7.2). In contrast to sugars, which have been reported to record well day-to-day variability of the ambient weather conditions (Rinne et al. 2015a), leaf pinitol is isotopically relatively invariable from one day to another suggesting a slow turnover rate for this compound (Bogelein et al. 2019; Churakova (Sidorova) et al. 2019; Rinne et al. 2015a). A significant carbon reserve signal in pinitol  $\delta^{13}\text{C}$  was suggested also by the study of Streit et al. (2013). Yet, the abundance and  $\delta^{13}\text{C}$  value of pinitol have been observed to correlate with stress-related processes, such as drought and cold temperatures (Churakova (Sidorova) et al. 2019; Ford 1984; Moing 2000; Rinne et al. 2015a). In addition to the significant differences in intra-seasonal trends between pinitol and sugars, also the absolute  $\delta^{13}\text{C}$  values differ: pinitol is in general relatively  $^{13}\text{C}$ -depleted. For these reasons, climatic and physiological signals

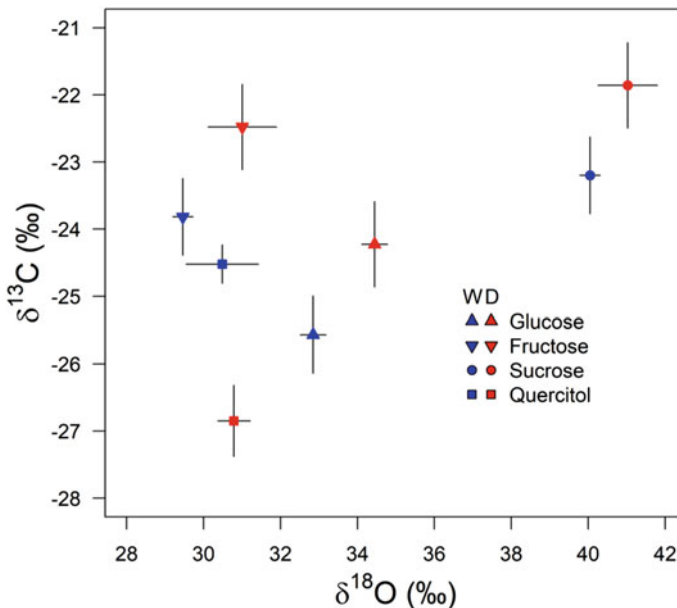


**Fig. 7.2** CSIA of individual leaf sugars.  $\delta^{13}\text{C}$  and  $\delta^{18}\text{O}$  values in glucose, fructose, sucrose, and quercitol in 2 year old oak (*Quercus robur*) saplings under well-watered (W) and dry (D) soil moisture conditions measured by HPLC- and GC/Pyr-IRMS, respectively. Dry conditions were induced by no water addition for 3 weeks. Experimental details of the greenhouse experiment can be derived from (Lehmann et al. 2018). Mean  $\pm$  SE (n = 4–5)

extractable from leaf photosynthates can be reduced or even distorted, if bulk  $\delta^{13}\text{C}$  analysis (vs. CSIA) is used for samples with high pinitol content. For example, (Bogelein et al. 2019) reported absence of diel variation in  $\delta^{13}\text{C}$  of leaf and twig phloem water soluble organic matter of Douglas fir, which was connected with the large amount of isotopically relatively invariable cyclitols. Further, the CSIA studies of Rinne et al. (2015a) and Rinne et al. (2015b) on larch suggested that the widely reported and debated  $^{13}\text{C}$ -depletion of leaf bulk sugars relative to tree rings (Gessler et al. 2009; Gleixner et al. 1993) is in large parts due to the high abundance of  $^{13}\text{C}$ -depleted pinitol in the leaves, as well as due to the  $^{13}\text{C}$ -enrichment of the transport sugar sucrose relative to hexoses (Bogelein et al. 2019; Churakova (Sidorova) et al. 2018; Churakova (Sidorova) et al. 2019; Rinne et al. 2015a). Bulk sugar  $\delta^{13}\text{C}$  analysis can also lead to erroneous conclusions on the use of reserves for leaf sugar formation, if pinitol is abundant in the studied leaves, as is typical for areas with cold winters where pinitol is needed for cryoprotection (Lipavská et al. 2000).

The  $^{13}\text{C}$ -enrichment of leaf sucrose relative to hexoses is likely caused by invertase enzyme (Rinne et al. 2015b), which causes fractionation at the C-2 position of fructose leading to  $\sim 1\%$  relative enrichment of sucrose (Gilbert et al. 2011; Mauve et al. 2009). The  $\delta^{13}\text{C}$  difference between leaf sucrose and hexoses can be sustained with continuous synthesis (hexoses) and transport (sucrose) reactions (i.e. branching points) (Hobbie and Werner 2004). However, the level of leaf sucrose  $^{13}\text{C}$ -enrichment relative to hexoses is not constant in the published studies (Bogelein et al. 2019; Churakova (Sidorova) et al. 2018; Churakova (Sidorova) et al. 2019), not even within a growing season (Rinne et al. 2015a). This may indicate, for example, a varying level of activity of the fractionating invertase enzyme (Rinne et al. 2015b), the presence of readily available residual remobilized carbohydrates (Rinne et al. 2015b), tree health status (Churakova (Sidorova) et al. 2018) or species specific differences (*Pinus mugo* ssp. *uncinata* and *Larix decidua*) (Churakova (Sidorova) et al. 2019).

The  $^{13}\text{C}$ -enrichment of sucrose relative to hexoses and cyclitols could also explain the reported  $^{13}\text{C}$ -enrichment of phloem (where sucrose is loaded for downstream transport) relative to leaves in studies that have analysed bulk sugar  $\delta^{13}\text{C}$  values (Brandes et al. 2006). Indeed, for Douglas fir trees (*Pseudotsuga menziesii*), Bogelein et al. (2019) reported a one-to-one relationship between leaf sucrose  $\delta^{13}\text{C}$  and twig bulk sugar  $\delta^{13}\text{C}$  values supporting the hypothesis. However, for broad-leaved species, compartmentalization of sugars with different  $\delta^{13}\text{C}$  composition in leaf mesophyll may induce an additional isotopic fractionation during phloem loading (Bogelein et al. 2019). More studies are needed to understand how leaf-to-phloem isotope fractionation differs between tree species. Further isotopic discrimination may occur during tree-ring formation due to the kinetic isotope effect of invertase, if a branching point is present also during wood formation (Rinne et al. 2015b). Concomitant CSIA analysis of sugars obtained from different tree compartments on a seasonal scale combined with high-resolution tree-ring analysis are needed to construct isotope fractionation transfer models, including storage and later remobilization. This will lead to a better knowledge of the formation of tree-ring isotope signal enabling utilization of tree-ring isotope chronologies at their full potential.

### 7.2.2 $\delta^{18}\text{O}$ Analysis of Tree Sugars and Cyclitols Using Gas Chromatography

During the last decade, several gas chromatograph pyrolysis IRMS (GC/Pyr-IRMS) methods have been developed for  $\delta^{18}\text{O}$  analysis of individual carbohydrates (Lehmann et al. 2016; Zech and Glaser 2009; Zech et al. 2013a). The primary aim of each method is to convert the very hydrophilic carbohydrates into volatile and hydrophobic compounds by chemical conversion, a process which is commonly known as “derivatization”. All common derivatization reactions for  $\delta^{18}\text{O}$  analysis of individual carbohydrates permanently add new functional groups to oxygen atoms of the hydrophilic hydroxyl groups (i.e. C–OH) of carbohydrate molecules. The ideal method avoids oxygen isotope fractionation and addition of new oxygen isotopes during the derivatization reaction. The methylboronic acid (MBA) derivatization allows  $\delta^{18}\text{O}$  analysis of individual carbohydrates derived from hemicellulose such as arabinose, xylose, rhamnose, or fucose (Zech and Glaser 2009), which was widely applied on plant hemicellulose in soils and thus for (paleo-)climate reconstructions (Hepp et al. 2016; Zech et al. 2013b). However, the MBA derivatization does not work with recent photosynthetic assimilates such as hexoses or sucrose. A trimethylsilyl (TMS) derivatization method produces more reliable  $\delta^{18}\text{O}$  results for sucrose and raffinose, but not for hexoses and cyclitols (Zech et al. 2013a). The most recent method for compound-specific  $\delta^{18}\text{O}$  analysis of carbohydrates is the methylation derivatization, which was found to produce precise and accurate  $\delta^{18}\text{O}$  results for a wide variety of sugars (Lehmann et al. 2016). This includes common plant sugars, such as glucose, fructose, sucrose and cyclitols, as well as levoglucosan, a biomarker for biomass (e.g. wood or grass) burning. Therefore, the method has been widely applied in plant ecophysiological research (Blees et al. 2017; Lehmann et al. 2016, 2017, 2018, 2019).

In general, a minimum of about one milligram of sugars from plant material should be used for methylation derivatization to achieve adequate amount oxygen for  $\delta^{18}\text{O}$  analysis. An addition of silver oxide, methyl iodide, acetonitrile, and dimethyl sulfide starts the (overnight) methylation process. After a centrifugation step, the methylated sugars in acetonitrile can be injected into a hot injector (250 °C) for separation on a GC column (e.g. SemiVolatiles, 60 m × 0.25 mm × 0.25 μm, Zebron, Phenomenex, Torrance, CA, USA). The GC is coupled via an IsoLink interface and a reference control unit to an IRMS (all Thermo Fisher Scientific, Bremen, Germany). The IsoLink holds space for a 32 cm oxygen isotope reactor (0.8 mm outer diameter) consisting of outer ceramic and an inner platinum tube filled with nickel wires. The reactor is heated to 1280 °C in a high temperature conversion oven causing pyrolysis of individual methylated sugars that elute from the GC and pass the reactor in a flow consisting of helium (1.4 mL min<sup>-1</sup>) and 1% hydrogen in helium (ca. 0.6 ml/min). The oxygen isotope ratio of each individual sugar is then measured on the produced CO gas peak (mass 28/mass 30) using an IRMS (Fig. 7.1). Importantly, triplicates of standard sugar mixes of different concentrations should be interspersed into a measurement sequence for drift, amount, and pyrolysis offset corrections.

### 7.2.2.1 Sample Preparation for GC/Pyr-IRMS

Sample preparation including hot water extraction from plant material and sugar purification with ion-exchange cartridges generally follows the protocol of Sect. 7.2.1.2 in this chapter. However, a few points should be additionally considered for  $\delta^{18}\text{O}$  analysis. (1) For a better understanding of oxygen isotope fractionations in plants, it is important to have also the information on  $\delta^{18}\text{O}$  values of water in leaves and other tissues. Plant samples should therefore be ideally transferred into gas-tight glass vials (Labco, UK) and stored as cold as possible in the dark shortly after sampling to avoid metabolic activity. The vials allow the extraction of water by vacuum distillation (West et al. 2006) and the remaining dry material can be milled to powder and used for sugar extraction and purification (Lehmann et al. 2018). (2) Although oxygen isotope exchange between water and sugars have been observed to be negligible for the above-described sugar sample preparation (Lehmann et al. 2017), it is recommended to keep water extracts and purified sugars frozen at all times, if they are not used for further analysis. (3) Furthermore, prior to derivatization, it is generally recommended to freeze-dry each sugar sample to remove excess water, avoiding any potential isotope fractionation that can be caused by oven-drying (Lehmann et al. 2020).

### 7.2.2.2 Research Application ( $\delta^{18}\text{O}$ of Individual Sugars)

Given the relatively new methodological development, research applications of the compound-specific  $\delta^{18}\text{O}$  analysis of individual sugars in ecophysiological or dendrochronological research are still rare (Blees et al. 2017; Lehmann et al. 2016, 2017, 2018; Zech et al. 2013a). First applications on leaves from grasses and trees showed that sucrose is generally  $^{18}\text{O}$ -enriched compared to hexoses and cyclitols. In grasses, biosynthetic fractionation factors ( $\varepsilon_{\text{bio}}$ ) of  $\sim 33$  and  $\sim 30\text{‰}$  were found for sucrose and hexoses (Lehmann et al. 2017), respectively, both exceeding the commonly reported value of  $27\text{‰}$  (Sternberg and DeNiro 1983). Moreover, the  $\varepsilon_{\text{bio}}$  values of the individual sugars were found to depend on changes in relative humidity, and this dependence was stronger for sucrose than for other carbohydrates (Lehmann et al. 2017). The  $\varepsilon_{\text{bio}}$  was also found to be species dependent, so that  $\varepsilon_{\text{bio}}$  was higher in larch than in oak trees under similar environmental conditions. The results indicate that processes controlling the imprint of the leaf water isotopic signal on carbohydrates can differ with environmental conditions and between tree species, which should be considered in studies comparing  $\delta^{18}\text{O}$  responses across sites and species (Treydte et al. 2007).

Leaf water, which reflects the synthesis water for carbohydrates, was found to be increasingly  $^{18}\text{O}$ -enriched from the bottom to the tip or from the vein to the margin of a leaf (Cernusak et al. 2016). The extent of this  $^{18}\text{O}$ -enrichment in leaf water has been observed to increase with a decrease in air humidity (Cernusak et al. 2016; Helliker and Ehleringer 2002). In addition to this  $^{18}\text{O}$ -enrichment, the relative location of sucrose and hexose syntheses may differ within a leaf, e.g. higher sucrose

synthesis rates have been observed in tips of a grass leaf blade compared to the bottom (Williams et al. 1993). Thus, relatively higher synthesis rates of sucrose in  $^{18}\text{O}$ -enriched leaf water compartments might therefore explain the  $^{18}\text{O}$ -enrichment of sucrose compared of hexoses and thus oxygen isotope fractionations among individual carbohydrates (Lehmann et al. 2017). If true, a similar mechanism might explain the tree-specific  $\delta^{18}\text{O}$  differences in carbohydrates between larch and oak. Relatively higher sugar synthesis in  $^{18}\text{O}$ -depleted leaf water in the bottom of a needle may cause lower  $\delta^{18}\text{O}$  values in leaf sugars compared to those in broadleaf oaks. In fact, the differences in leaf sugars are likely translated to tree-rings and should be considered if species responses to environmental changes are compared.

In contrast, only a few  $\delta^{18}\text{O}$  data are currently available for cyclitols, also known as sugar alcohols or alditols (Lehmann et al. 2016). Overall,  $\delta^{18}\text{O}$  values in sugar alcohols tend to be lower compared to sucrose and hexoses across different tree species. As described above (Sect. 7.2.1.3), biochemical pathways for sugar alcohols are different and their seasonal turnover is slower compared to photosynthetic assimilates. For instance, rapid changes in the isotopic composition of leaf water are only barely incorporated into cyclitols compared to other photosynthetic assimilates (Lehmann et al. 2017, 2018). High abundances of cyclitols, such as pinitol or quercitol, can therefore strongly dampen the  $\delta^{18}\text{O}$  response of leaf sugars to recent environmental changes, if measured with standard  $\delta^{18}\text{O}$  analysis for total organic matter (Kornexl et al. 1999a, b).

The different response of sugars and cyclitols in leaves to environmental stress can be deduced from Fig. 7.2. In a greenhouse experiment, 2 year old oak trees were kept for 3 weeks without water to induce drought stress, while a control was well-watered (see Lehmann et al. 2018 for experimental details). The drought stress caused no change in  $\delta^{18}\text{O}$  values but lower  $\delta^{13}\text{C}$  values in the cyclitol quercitol, while  $\delta^{13}\text{C}$  and  $\delta^{18}\text{O}$  values increased in sucrose and hexoses. These differences between cyclitol and sugars would have opposite physiological interpretations for dual isotope applications (Chap. 16) where the isotopic response of quercitol would be interpreted as lower assimilation rates without a change in stomatal conductance, and the isotopic response of sucrose and hexoses would indicate no change in assimilation rates but lower stomatal conductance (Scheidegger et al. 2000). Compared to the cyclitol quercitol, the isotopic response of sucrose and hexoses likely reflects the more realistic physiological adaptation to the drought treatment, given that no water was given for 3 weeks and the oak saplings had to close their stomata to avoid unwanted water loss. Thus, our result demonstrates that high amounts of cyclitols in a sample may lead to dampened or falsified isotopic responses to environmental stresses, if only bulk sugar fractions are measured, and therefore may cause misleading interpretations. Compound-specific isotope analysis of sugars allow to avoid these biases as the isotopic response of individual compounds is specifically measured.

Further studies showed that individual sugars were up to 8‰ enriched in  $^{18}\text{O}$  compared to cellulose in grass leaves under controlled conditions, with  $\delta^{18}\text{O}$  values of sucrose showing the highest correlation with those of cellulose among other individual sugars (Lehmann et al. 2017). This indicates a strong biochemical link between sucrose and cellulose synthesis, but also a strong  $^{18}\text{O}$ -depletion of sugars during



cellulose synthesis (Cernusak et al. 2005; Farquhar et al. 1998; Roden et al. 2000). Moreover, sucrose has been observed to better integrate rapid isotopic changes in leaf water than other carbohydrates (e.g. hexoses, cyclitols) (Lehmann et al. 2018, 2019). Sucrose might therefore be the ideal candidate to trace  $\delta^{18}\text{O}$  variations from leaves to stem cambium cells where tree-rings are produced. However, studies on a compound-specific level tracing the translocation of sucrose in the phloem to sink tissues, such as tree-rings, are very scarce and limited so far to leaf and twig level (Cernusak et al. 2003; Lehmann et al. 2018). The compound-specific approach may therefore be applied on twig and stem phloem in mature trees to better understand how the isotopic signal in leaves is transported and incorporated into tree-ring archives (Gessler et al. 2013; Treydte et al. 2014).

In summary, the newest findings by CSIA studies reveal high  $\delta^{18}\text{O}$  variation between individual sugars, which can be much higher than year-to-year variations in tree-ring cellulose. The leaf water signal is differently incorporated by different sugars (e.g. sucrose vs. hexoses versus cyclitols) and depends on environmental conditions (e.g. relative humidity, drought) and species. The recent CSIA results are particularly important for modelling studies, which aim to reconstruct the leaf water isotopic enrichment and thus the physiological responses to environmental conditions from tree-ring isotope ratios. Studies comparing tree-ring  $\delta^{18}\text{O}$  values of different species and/or across different sites should also consider these newest developments.

### **7.3 UV-Laser Aided Sampling and Isotopic Analysis of Tree Rings**

Two new approaches to tree-ring stable isotope analysis have been established, which both utilize UV-laser systems. One of them is UV-laser assisted microdissection, which can be used to cut subsamples of tree rings that are subsequently manually prepared for isotopic analysis using the conventional methods (e.g. cellulose extraction, EA/HTC-IRMS analysis). The other UV-laser-based method enables on-line isotope analysis of tree rings, which is accomplished via laser ablation (as opposed to laser cutting). Both methods take advantage of the features of modern UV-laser systems, which support the sampling of tree tissues at a very high spatial resolution and accuracy.

#### ***7.3.1 UV-Laser Microscopic Dissection (LMD) of Tree Rings***

UV-laser-assisted microdissection (LMD or LAM) or laser capture microdissection (LCM) is a technology allowing for isolating areas of interest from cell tissues under direct microscopic visualization. LMD systems are typically used for isolating

DNA and RNA in e.g. genomics, transcriptomics, metabolomics and next generation sequencing, as well as for live cell culture manipulation in cloning and re-cultivation experiments (c.f. Leica Microsystems GmbH 2018; Carl Zeiss Microscopy GmbH 2013 for comprehensive lists of publications). A key advantage of using the LMD technique is on-screen selection of sample areas enabling accurate sub-seasonal sampling of single cell rows or dissection of complete tree rings with irregular shapes or narrow ring widths, as documented in recent studies (Blokhina et al. 2017; Kuroda et al. 2014; Schollaen et al. 2014, 2017). Furthermore, the technique provides electronic documentation of the dissection processes by photo or video sequences, as well as a report of labelled and dissected elements.

### 7.3.1.1 Instrumentation and Principle of the LMD Methodology

The LMD approach to dissecting and sampling wood cells of tree rings for downstream analysis has first been described in detail by Schollaen et al. (2014). Two different UV-laser microdissection microscopes (i) LMD7000 by Leica Microsystems GmbH, Wetzlar, Germany and (ii) PALM MicroBeam by Carl Zeiss Microscopy GmbH, Jena, Germany, implemented at the GFZ German Research Centre for Geosciences, Potsdam, were tested and their advantages and constraints of the use in tree-ring stable isotope research was discussed. The LMD systems are basically used off-line and generally consist of a microscope equipped with objectives of high UV transmission, a UV-laser cutting unit, a motorized stage for various sample holders and specimen collectors. Sample holders can carry thin sections of up to 50 mm × 76 mm in area and a variety of vials like PCR tubes or 96-well plates can be employed for receiving specimens from the dissection of the tree-ring samples.

The preparation and analysis scheme comprises five steps:

- (1) manual preparation of thin wood cross-sections (max. 1500  $\mu\text{m}$  thickness) with a microtome or a high-precision saw,
- (2) microscopic identification and pen-screen selection of woody tissues of interest,
- (3) automatic UV-laser-assisted microscopic dissection of inter-or intra-annual wood sections,
- (4) automatic sample collection by gravity (Leica LMD 7000) or forceps (PALM Microbeam) into PCR tubes or 96-well plates, optional chemical treatment (e.g. cellulose extraction), and
- (5) stable isotope analysis via conventional isotope ratio mass spectrometry (IRMS) coupled online to a combustion or pyrolysis furnace ( $\delta^2\text{H}$ ,  $\delta^{13}\text{C}$  and  $\delta^{18}\text{O}$ ).

In general, wood samples of 100–1500  $\mu\text{m}$  thickness can be dissected without any major constraints. The use of cross-sections thinner than 100  $\mu\text{m}$  may not be advised. Wood of certain tree species, e.g. *Adansonia digitata* (baobab) can have densities varying between 0.09 and 0.2  $\text{mg}/\text{mm}^3$ . The density of cellulose extracted from conifers can be in a similar range. Specimen dissected from corresponding

cross sections of about  $0.15 \text{ mm}^3$  (e.g. from a  $0.3 \times 5 \text{ mm}$  wide and  $0.1 \text{ mm}$  thick cross-section) yield a mass range of  $13.5\text{--}30 \mu\text{g}$ , which can be challenging for routine mass spectrometry with conventional combustion/pyrolysis systems. Dissection of samples of up to  $1500 \mu\text{m}$  thickness requires a number of cutting iterations to be preselected in the LMD software resulting in automatic adjustment of the in-focus depth of the Z-axis of the UV-laser beam during repeated lasering of the pre-defined cutting line. Unlike UV-ablation lasers, LMD systems are producing sharp-contoured pieces of sample tissue instead of wood dust.

Relevant plant cells/tissues can be selected on-screen, while non-relevant tissues (e.g. resin ducts, wood rays) may not be selected or be removed, i.e. cut away before sampling. Any size and area within the given range of the size of the sample holder (max.  $50 \text{ mm} \times 76 \text{ mm}$ ) can be dissected. This allows for the precise dissection of asymmetric tree rings or parts thereof, for example by lobate growth, intra-ring density fluctuations or wedging tree rings. Furthermore, it is possible to cut serial sections or even to pool sample material, for example, if the weight of the dissected tissue from one thin section is found insufficient for a stable isotope measurement (for details c.f. Schollaen et al. 2014, 2017). Sample material from the same array of wood cells can be identified unambiguously on a second or third cross-section and may be pooled for chemical treatment, e.g. cellulose extraction before IRMS analysis. However, thin wood cross-sections may also be subject to LMD after cellulose extraction. (Schollaen et al. 2017) showed that tree-ring structures of cellulose laths, which represented a variety of tree species (coniferous and angiosperm wood) with different wood growth rates and differently shaped tree-ring boundaries, largely remained well identifiable and suited for UV-dissection at annual and intra-annual resolution. Nevertheless, it can be challenging to work with cellulose cross sections originating from very soft and light wood like e.g. from baobabs (*Adansonia digitata*), which contain a high percentage of parenchyma tissue (up to 80%) (Schollaen et al. 2017). In order to get enough sample material for a stable isotope measurement, either the radial cutting width or the thickness of the thin section needs to be adjusted accordingly. A wider sample reduces the possible data points per tree ring, whereas a thicker sample increases the time required to dissect the sample. For example, ten cutting processes on the same sample were needed to successfully separate a baobab cellulose sample from a cross section of  $1300 \mu\text{m}$  thickness.

### 7.3.1.2 Comparison of the LMD Systems and their Operation

The two commercially available LMD systems differ concerning their practical implementations and applications. The laser from Leica is moved via optics and the cross-section samples are mounted on a stage that is fixed during actual laser cutting. The Leica system uses high precision optics to steer the laser beam by means of prisms along the desired cut lines on the tissue. Limitations of earlier software (v6.7.1.3952; Schollaen et al. 2014) have been overcome, so that the laser cutting of the LMD7000 is no longer restricted to the actual microscopic field of view. Larger areas, for example whole tree rings, can now be marked. The dissected sample tissues

principally fall down by gravity into collection vessels like 96-well plates, which can be equipped with tin or silver capsules for direct uptake of sample tissue. Thus, samples can be prepared directly for conventional autosampler systems coupled to IRMS. Another limitation of the Leica system was the lack of an automatic z-focus adjustment to allow repeated laser cutting of thicker cross-sections (Schollaen et al. 2014) but this function has been available since 2017.

Compared to the Leica microscope, the objectives of the Zeiss microscope are installed inversely, or underneath the sample holder, i.e. dissected specimen cannot be collected by gravity. Hence, tissues of interests are marked via mouse or screen pen on the lower sample side and can be selected beyond the visible screen. The laser stays fixed while the sample is moved by the high-precision stage during the dissection process. The UV laser passes through the glass slide and the dissected sample tissues remain in position. After all of the marked tissue has been dissected, specimens are picked up manually with a forceps and transferred into tin or silver capsules for stable isotope measurements. Dissected tree-ring sample tissues were observed to be too heavy for patented ZEISS laser catapult that was designed to toss upwards individual cells or even smaller specimen up into collection vessels (Schollaen et al. 2014). The Zeiss system also comes with an automatic z-focus feature that allows easy definition of the number of automatic cutting iterations. As the Zeiss laser (100  $\mu\text{J}$ , wavelength 355 nm) is less powerful than the laser from Leica (120  $\mu\text{J}$ , wavelength 349 nm), more cutting iterations are generally required.

Together with the manual collection of dissected specimens, the overall sampling process with the Zeiss system takes longer than with the Leica system. In general, the use of UV-laser microdissection microscopes is not necessarily faster than traditional methods for the dissection of wood tissue. The cutting process of selected tissue lasts ca. 1–2 min, depending on the size of the selected area, the thickness of the cross-section, density of the wood material and the UV laser settings. If further cutting iterations are required, more time is needed. The average sample throughput per 8-h day may vary between 20 and 120 samples. This includes the on-screen selection of area, the automatic UV-laser-based microscopic dissection and the collection of specimens, as well as unpredictable interferences such as stuck specimens (Leica LMD7000). With some modification of the current sample collection methods the Leica system could be run automatically overnight, which would increase sample throughput drastically, allowing more cuts than manual methods.

### ***7.3.2 On-line Analysis of Tree-Ring $\delta^{13}\text{C}$ by Laser Ablation IRMS***

Laser ablation-combustion-gas chromatography-IRMS method (hereafter LA-IRMS) to analyze carbon isotope composition of wood was introduced by Schulze et al. (2004). In the method, the labor intensive process of sectioning wood manually or by microtome to produce samples for intra-annual isotope studies (Helle and

Schleser 2004; Kagawa et al. 2003) is replaced by a spatially precise, high resolution sampling of tree rings in situ using a UV-laser (Schulze et al. 2004). In contrast to the newly developed LMD technique (see Sect. 7.3.1.), the LA-IRMS combines the sampling and isotope analysis by transportation of the ablated sample material directly to IRMS via a modified combustion unit (Loader et al. 2017; Schulze et al. 2004). Unlike the LMD technique, the LA-IRMS applications have so far been limited to  $\delta^{13}\text{C}$  analysis.

### 7.3.2.1 Instrumentation and Principle of Analysis

Similar to a conventional EA-IRMS, which is used for “bulk” isotope analysis of, for example, tree rings, a LA-IRMS operates as a continuous flow IRMS (Schulze et al. 2004). A wood sample is placed in a He-flushed chamber connected to a UV-laser, where a subsample of the wood is removed by laser ablation, and the released particles are directed by the He flow to a miniaturized combustion unit. Water vapor is removed from the formed  $\text{CO}_2$ , which can then be introduced into a liquid nitrogen trap that concentrates  $\text{CO}_2$  from a single ablation run in a small volume of carrier gas (Loader et al. 2017). The cryogenic trapping is beneficial for high resolution  $\delta^{13}\text{C}$  analysis, where the amount of ablated wood is at the minimum (Rinne et al. 2015b). After the  $\text{CO}_2$  is released from the cold trap, it is separated from other gaseous products in a GC-column prior to its introduction into an IRMS for  $\delta^{13}\text{C}$  analysis (Loader et al. 2017; Schulze et al. 2004).

The size of the sample  $\text{CO}_2$  peak detected by IRMS can be tuned by adjusting the laser output power settings, the laser spot size and the length of the ablated track (Loader et al. 2017; Schulze et al. 2004), which is positioned along a line parallel to the corresponding tree-ring boundary (Fig. 7.3). The ablation track is positioned using a camera connected with the laser unit and controlled by the laser software.

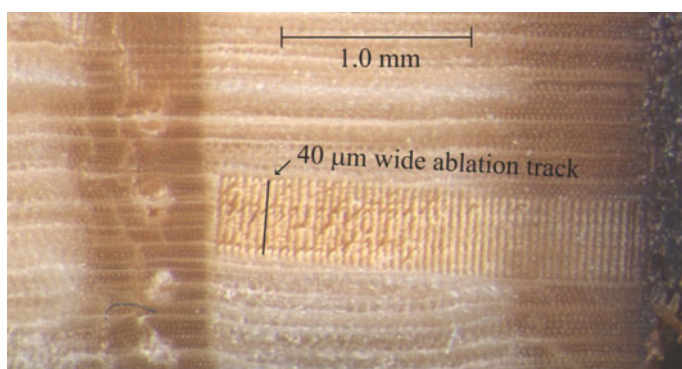


**Fig. 7.3** Picture of an annual ring of larch (*Larix gmelinii* Rupr.) analysed using a LA-IRMS (modified after Rinne et al. 2015b). 53 laser ablation tracks with a 40  $\mu\text{m}$  diameter laser spot size and 40  $\mu\text{m}$  were analysed within the annual ring. The width of the annual ring was 2.3 mm.

A spatial resolution of 80  $\mu\text{m}$  has been reached in LA-IRMS analysis using 40  $\mu\text{m}$  diameter spot size for ablation tracks and 40  $\mu\text{m}$  spacing between each track (Fig. 7.3; Rinne et al. 2015b, Schulze et al. 2004). The maximum number of ablation tracks (i.e.  $\delta^{13}\text{C}$  data points) in an intra-annual tree-ring  $\delta^{13}\text{C}$  profile depends on the width of the tree ring and on the selected laser spot size (Fig. 7.3).

Following the principle of identical treatment (Chap. 6), at least one or preferably three reference materials with known isotope composition should be measured with LA-IRMS together with the analytes for correcting the produced  $\delta^{13}\text{C}$  results. Ideally, the reference material should be matrix matched to the sample and isotopically homogenous to a very fine spatial scale. Unfortunately, certified reference materials of this type do not exist, and as a substitute, the IAEA-C3 cellulose paper has been used (Loader et al. 2017; Schulze et al. 2004). Analysis of this material has shown that the precision of LA-IRMS measurements (the standard deviation of repeated measurements (SD): 0.1–0.2‰; Loader et al. 2017; Schulze et al. 2004) is comparable to conventional EA-IRMS  $\delta^{13}\text{C}$  measurements (SD:  $\leq 0.1\%$ ). However, a  $\delta^{13}\text{C}$  offset correction may be required for tree-ring LA-IRMS data to correct for a matrix effect caused by using a non-matrix-matched reference material, such as the cellulose IAEA-C3 (Míková et al. 2014; Rinne et al. 2015b).

### 7.3.2.2 Sample Preparation for LA-IRMS

Due to the mobility of resin in tree rings (Long et al. 1979), resinous tree cores obtained from conifers should be treated in a Soxhlet apparatus with hot ethanol over a period of 50 h followed by repeated washing with boiling deionized water to remove the solvents completely (Loader et al. 2017; Rinne et al. 2015b). Tree cores can then be dried at 40 °C in an oven for 2 days to speed up the drying process (Rinne et al. 2015b). Despite of the Soxhlet extraction procedure, some resins have occasionally been observed to persist in resin ducts, as indicated by ATR-FTIR analysis (Rinne et al. 2005) and deviant  $\delta^{13}\text{C}$  values obtained during laser ablation (Loader and Rinne, unpublished data). Consequently, resin ducts should be avoided, when positioning ablation tracks, in case of incomplete resin removal (Rinne et al. 2015b).

For laser ablation, the surface of the analyzed tree-ring sample should be even to enable accurate focusing of the laser beam. This can be achieved by treating the wood surface with a microtome, razorblade or sandpaper (Loader et al. 2017; Schulze et al. 2004; Soudant et al. 2016). Finally, the resin extracted (for conifers) and polished sample is cut into sections that fit into the laser chamber together with the reference material. LA-IRMS analysis of resin extracted wood takes advantage of the reported generally similar climatic signal in  $\delta^{13}\text{C}$  values of wood compared to extracted cellulose (e.g. Helle and Schleser 2004; Schulze et al. 2004; Weigt et al. 2015). If the objectives of the study require the analysis of cellulose instead of resin-free wood, cellulose extraction can be performed prior to LA-IRMS using methods designed for whole wood sections as described in Loader et al. (1997) and Schollaen et al. (2017) (cf. Schulze et al. 2004). However, the extraction procedure will cause

some distortion to the wood sections (e.g. shortening and bending) (Schollaen et al. 2017; Schulze et al. 2004), which may complicate the selection of ablation spots as well as the connection of the individual  $\delta^{13}\text{C}$  results with tracheid formation times, especially in very high resolution studies. See Chapter 5 for further details on chemical pre-treatments, review and discussion of the use of wood, resin extracted wood and cellulose in stable isotope studies.

### ***7.3.3 Conversion of High Resolution Tree-Ring Isotope Data into a Temporal Scale***

To fully utilize high resolution stable isotope data from tree rings, special consideration should be given on how to link tree-ring isotopic profiles obtained by LMD ( $\delta^2\text{H}$ ,  $\delta^{13}\text{C}$  or  $\delta^{18}\text{O}$ ) or LA-IRMS ( $\delta^{13}\text{C}$ ) methods with other seasonal data that has been collected from the studied tree (e.g. carbohydrate dynamics of the growing season) and how to relate the isotopic profiles with climatic events (Schulze et al. 2004). To accomplish this, the isotopic profiles can be transformed into a temporal scale using direct (dendrometer band) or indirect (e.g. cell size, cell number) seasonal growth measurements of tree rings (Skomarkova et al. 2006; Walcroft et al. 1997; Vysotskaya et al. 1985). However, a tree-ring stable isotope signal is not formed only during the phenophase of wood expansion but also during the phase of lignification, whose start and end dates occur later in the growing season in comparison to those of the expansion phase (Cuny et al. 2013; Rinne et al. 2015b). Consequently, for laser-assisted, high resolution isotopic analysis of woody tissue, ideally both the seasonal expansion and lignification development of the tree ring should be determined.

Although somewhat laborious, periodical collection of micro-cores provides a way of monitoring wood formation stages without causing undue damage to the trees under study (Forster et al. 2000). Several methods of obtaining micro-cores exist, including different types of needles, punchers and miniaturized borers (Forster et al. 2000; Rossi et al. 2006). Samples are collected from the trees during the growing season (e.g. weekly) following an oblique pattern around the tree trunk (Fonti et al. 2018; Rinne et al. 2015b). Distance between coring spots should be  $\geq 1$  cm to avoid wood tissue affected by previous sampling (Forster et al. 2000). In the field micro-cores are placed in ethanol solution and subsequently stored in a fridge until further processing. Sample processing and analysis for xylogensis parameter measurements is described in detail in (Schweingruber et al. 2006). Careful comparison of the laser ablation spots or laser dissection areas to tree-ring structure, together with the information on timing of tracheid formation obtained from micro-core time series, allows one to estimate the corresponding timing of each individual isotopic measurement within the calendar year (Fonti et al. 2018; Rinne et al. 2015b).

### 7.3.4 Research Applications

The laser assisted methods have provided an unprecedented spatial accuracy in sampling for isotopic analysis compared to conventional use of handheld instruments or microtomes (De Micco et al. 2012; Rinne et al. 2015b; Schollaen et al. 2014; Schulze et al. 2004). Both LMD and LA methods are capable of sampling very small scale features in tree rings, such as small growth defects (Battibaglia et al. 2010; De Micco et al. 2012) and ray parenchyma (Schollaen et al. 2014), and provide material for high resolution intra-annual isotope analysis (Bruykhanova et al. 2011; Fonti et al. 2018; Rinne et al. 2015b; Schollaen et al. 2014; Skomarkova et al. 2006; Soudant et al. 2016; Vaganov et al. 2009) either on-line ( $\delta^{13}\text{C}$ : LA-IRMS) or off-line (LMD:  $\delta^{13}\text{C}$ ,  $\delta^{18}\text{O}$ ,  $\delta^2\text{H}$ ).

The studies utilizing laser assisted methods have combined the resulting knowledge of intra-annual  $\delta^{13}\text{C}$  variability with other tree-ring characteristics that can be measured in equal spatial resolution, such as wood density (Schollaen et al. 2014; Skomarkova et al. 2006) and wood anatomical traits (Battibaglia et al. 2010; Bruykhanova et al. 2011; De Micco et al. 2012; Fonti et al. 2018; Vaganov et al. 2009), for the better understanding of intra-ring proxy signals. The isotopic profiles together with other seasonal data can then be compared with environmental variables for deepening our understanding about the mechanisms controlling the isotope variability in tree rings (see Chap. 15 for further discussions). The outcomes of such studies, where the UV-laser assisted analytical methods have been employed, include (1) evaluation of a dependency on carbohydrate reserves (Bruykhanova et al. 2011; Fonti et al. 2018; Rinne et al. 2015b; Skomarkova et al. 2006; Vaganov et al. 2009), (2) influence of stand structure (Skomarkova et al. 2006), tree age (Fonti et al. 2018) and tree growth rates (Vaganov et al. 2009) on the intra-annual  $\delta^{13}\text{C}$  signal, (3) preservation of seasonal rainfall patterns in tree-ring  $\delta^{18}\text{O}$  (Schollaen et al. 2014) and (4) linking of intra-annual tree-ring  $\delta^{13}\text{C}$  profiles to upstream post-photosynthetic processes by analyzing the seasonal variation of  $\delta^{13}\text{C}$  in different leaf sugars within growing seasons (Rinne et al. 2015b). In the future, these methods will continue to broaden our understanding of the fine scale variation of the isotopic composition of tree rings. In addition, LA-IRMS has potential for it to be used as a tool for selecting tree cores for conventional isotopic analysis, for analyzing exceptionally narrow rings and for constructing long  $\delta^{13}\text{C}$  tree-ring chronologies in a relatively less labor intensive manner (Loader et al. 2017).

## 7.4 Position-Specific Isotope Analysis of Cellulose

Intra-molecular isotope analysis of tree-ring cellulose has been established for all the constituent chemical elements. For  $\delta^2\text{H}$  and  $\delta^{13}\text{C}$  analysis, the methodology utilizes the nuclear spin of  $^2\text{H}$  and  $^{13}\text{C}$ , which produces a nuclear magnetic resonance (NMR) signal that can be used for position-specific measurements. For  $\delta^{18}\text{O}$  analysis, on the



other hand, a different approach has been necessary, since  $^{18}\text{O}$  does not have a nuclear spin. The published methods involved for  $\delta^{18}\text{O}$  requires a substantial amount of synthetic organic chemistry, which is needed to isolate or remove oxygen atoms from particular positions for  $\delta^{18}\text{O}$  determination.

Significant intra-molecular isotope variation has been reported for cellulose, for all the three elements. If changes occur in the intra-molecular isotope pattern, this can influence the  $\delta$  values of cellulose, but this influence cannot be inferred without intra-molecular isotope data. Applied to isotope studies of tree rings, trends in a  $\delta$  value of cellulose might be attributed to changing climate, while the intra-molecular location of the effect would point to changes in metabolic regulation along the tree-ring series. Further, because intra-molecular variation is created by enzyme reactions, it can in principle carry ecophysiological information, as illustrated by Gleixner and Schmidt (1997). Researchers have barely begun to explore this potential wealth of information, largely because intra-molecular isotope variation was for a long time extremely cumbersome to measure.

#### 7.4.1 Position-Specific $\delta^2\text{H}$ and $\delta^{13}\text{C}$

In tree-ring studies, stable isotope composition is measured for the whole molecule, that is, for the glucose units of cellulose. However, a glucose unit contains for each of the elements several intra-molecular positions, which are biochemically distinct. Thus, the question arises how these distinct positions behave in terms of isotope abundance. Kinetic isotope effects modify the abundance of heavy isotopes that are connected to a particular chemical bond. Because isotope effects of enzymes synthesizing glucose vary, it must be expected that isotope abundance varies among the intra-molecular positions. This conclusion holds for all isotopes in non-symmetrical molecules. Indeed, it has also been demonstrated for many other metabolites that stable isotope abundance varies among intra-molecular positions. This was concluded in an earlier study for  $^{13}\text{C}$  in acetyl-CoA (De Niro and Epstein 1977) and later for deuterium (D) in several metabolites (Martin et al. 1992). For photosynthetic glucose, Rossmann et al. (1991) observed substantial intra-molecular  $^{13}\text{C}$  variation, which could be explained mechanistically as equilibrium isotope effect of aldolase (Gleixner and Schmidt 1997). This example demonstrates an important advantage of intra-molecular isotope data: the intra-molecular localization of isotope fractionation directly suggests which enzyme might be responsible, and this hypothesis can then be compared to the enzyme's isotope effect or be tested in experiments.

For deuterium, Martin et al. (1992) summarized the knowledge on various metabolites. They describe intra-molecular  $\delta^2\text{H}$  variation for sugars, amino acids and monoterpene biosynthesis, with typical intra-molecular variation of hundreds of ‰. For  $^{13}\text{C}$ , the typical intra-molecular isotope variation is 10‰ (Schmidt 2003) (for intra-molecular oxygen isotope variation, see Sect. 7.4.2). From the size of this intra-molecular variation, it must be concluded that  $\delta$  values are averages of the intra-molecular isotope data, with important consequences.

### 7.4.1.1 Sample Preparation and Analytical Methodology

Measurements of intra-molecular  $^{13}\text{C}$ -abundance of glucose were first performed by controlled breakdown of the molecule and subsequent IRMS analysis of the fragments (Rossmann et al. 1991). However, such wet-chemical methods are extremely labour-intensive and need to be tailor-made for each metabolite. In the meantime,  $^{13}\text{C}$  NMR has been established as a tool for intra-molecular  $^{13}\text{C}$ -measurements. In a  $^{13}\text{C}$  NMR spectrum, each structurally distinct C gives rise to a specific signal (Fig. 7.4). Careful optimization of parameters is needed so that the signal integrals reflect relative isotopomer abundances (Chaintreau et al. 2013), but when this is achieved, this general method has been applied to various metabolites including tree-ring cellulose (Romek et al. 2017; Wieloch et al. 2018). NMR has the fundamental advantage that the intra-molecular isotope composition of the intact molecule is determined, avoiding a risk for isotope fractionation during chemical breakdown, pyrolysis or fragmentation. On the other hand, NMR gives relative abundances of isotopomers, but no information about the ratio of heavy to light isotopes.

For measurements of intra-molecular  $^2\text{H}$  variation, deuterium NMR spectroscopy has been the method of choice. NMR can be done both on solid and solution samples, but solution NMR achieves the resolution required for isotopomer analysis, therefore polymeric analytes such as cellulose have to be broken down first. Although the 7 carbon-bound deuterons of glucose in principle give separate NMR signals, these are in practice not resolved. Therefore, glucose must be converted into a derivative that gives resolved signals by locking the anomeric equilibrium and by lowering the polarity of the molecule so that it can be dissolved in low-viscosity organic solvents yielding narrow signals (Betson et al. 2006). As seen in Fig. 7.5, deuterium isotopomer variation is directly visible in the NMR spectrum. But as for  $^{13}\text{C}$ , quantification of the isotopomers is done by integration of the signals by lineshape fitting. NMR spectra give ratios of isotopomer abundances, but do not directly reflect the ratio of heavy to light isotope. From isotopomer patterns, site-specific isotope ratios can be calculated in two ways: Either the  $\delta^2\text{H}$  of the analyte is measured independently and isotope ratios for the intramolecular positions are calculated by isotope

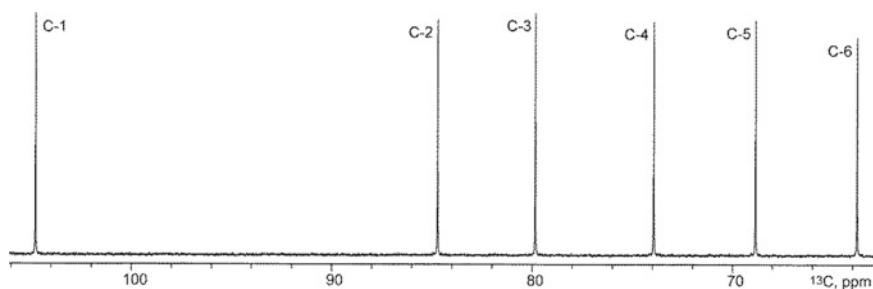


**Fig. 7.4**  $^{13}\text{C}$  NMR of a glucose derivative. Each signal originates from one  $^{13}\text{C}$  isotopomer. The x-axis is the so-called chemical shift. The “ppm” units are unrelated to isotope abundance but describe the signal positions that are governed by the intra-molecular chemical environment of each  $^{13}\text{C}$

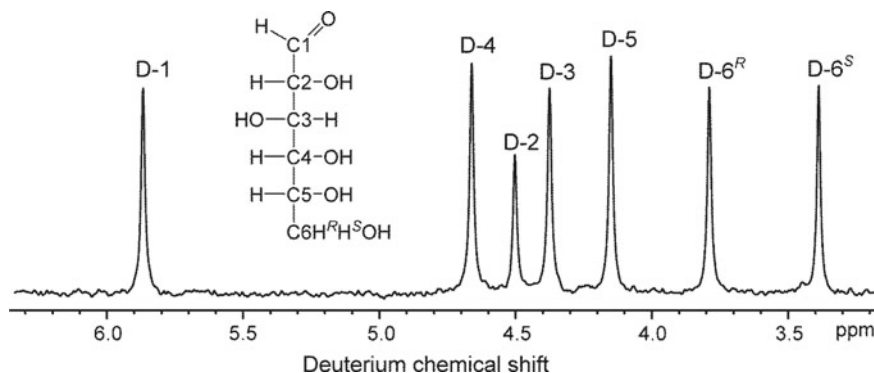


**Fig. 7.5**  $^2\text{H}$  NMR spectrum of a glucose derivative designed to give highly resolved spectra. The formula of glucose shows the assignment of the signals to isotopomers of glucose. Reproduced from Ehlers et al. (2015)

mass balance, or a reference molecule with known  $\delta^2\text{H}$  is added to the NMR sample so that integrals in the  $^2\text{H}$  spectrum can be linked to the  $\delta^2\text{H}$  scale (Spahr et al. 2015).

#### 7.4.1.2 Research Applications

As expected from the results on other metabolites, the intra-molecular  $^2\text{H}$  distribution of tree-ring derived glucose is non-random (Betson et al. 2006). The intra-molecular variation is hundreds of ‰ large, much larger than for example the seasonal variation of  $\delta^2\text{H}$  of precipitation. Because the intra-molecular variation influences  $\delta^2\text{H}$  of the whole molecule, correlations of tree-ring  $\delta^2\text{H}$  with climate variables are fraught with difficulty. Betson et al. (2006) also showed that the intra-molecular pattern of tree-ring cellulose is independent of the source water  $\delta^2\text{H}$ . For metabolites on the leaf level, this can be expected, because when a metabolite is synthesized in a cellular compartment, all hydrogen that is incorporated into the molecule originates from the same water with a certain  $\delta^2\text{H}$ . When tree-ring cellulose is synthesized, the  $^2\text{H}$  isotopomer pattern may be modified by hydrogen exchange; that clear signals can be obtained from tree-ring cellulose may indicate that this exchange is constant over time. That the intramolecular pattern is independent of  $\delta^2\text{H}$  means that signals that are based on isotopomer ratios can be extracted and interpreted without knowledge of  $\delta^2\text{H}$ .

As mentioned above, intra-molecular isotope patterns reflect regulation of enzymes or metabolic pathways. Thus, they might respond to changes in metabolic fluxes. This was tested on glucose formed by plants using the  $\text{C}_3$  photosynthetic pathway. In  $\text{C}_3$  plants, the  $\text{CO}_2$ -fixing enzyme Rubisco can react with oxygen instead, in a side reaction that leads to C loss of the plant and which therefore is highly relevant for the global C cycle. Metabolites formed upon  $\text{O}_2$  fixation are partly recycled to glucose in the so-called photorespiration cycle; therefore the isotopomer pattern of

C<sub>3</sub> glucose might reflect the ratio of O<sub>2</sub> to CO<sub>2</sub> fixation. As shown in Fig. 7.6a, the <sup>2</sup>H isotopomer pattern of C<sub>3</sub> glucose indeed depends on atmospheric CO<sub>2</sub> concentration during growth, expressed as function of 1/CO<sub>2</sub> to reflect the O<sub>2</sub>:CO<sub>2</sub> competition. The high correlation observed indicates that this isotopomer ratio is a clean measure

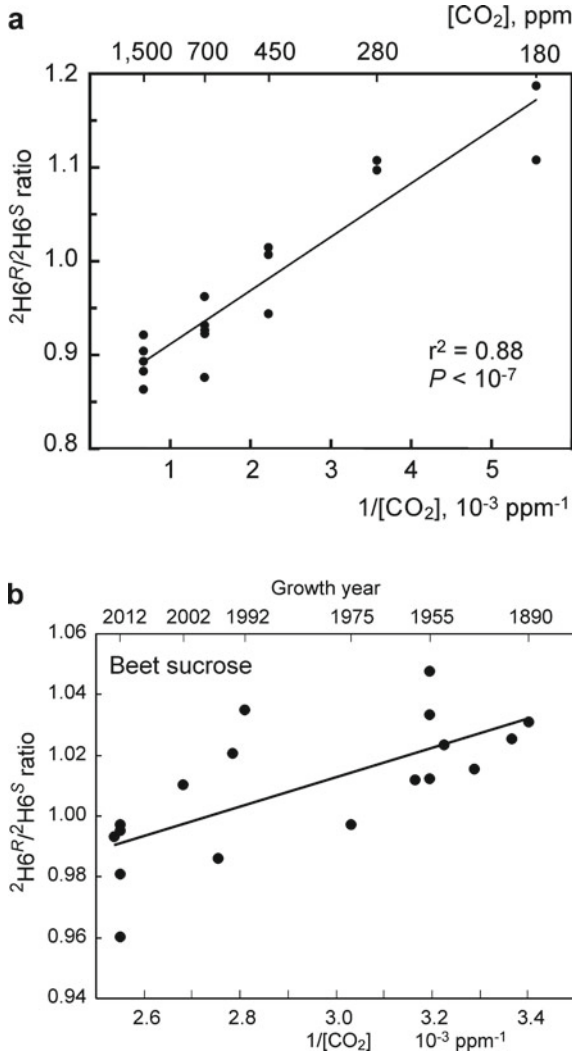


**Fig. 7.6** Dependence of the <sup>2</sup>H-6<sup>R</sup>/<sup>2</sup>H-6<sup>S</sup> isotopomer ratio (see Fig. 7.5) on 1/CO<sub>2</sub> in **a** chamber-grown sunflowers ( $r^2 = 0.88$ ,  $P < 10^{-7}$ , slope  $0.057 \pm 0.006$  (SEM)) and **b** beet sugar samples formed between 1890 and 2012 ( $r^2 = 0.49$ ,  $P = 0.001$ , slope  $= 0.048 \pm 0.012$ ). The slopes of the isotopomer ratio as function of 1/CO<sub>2</sub> are not significantly different. Reproduced from Ehlers et al. (2015)

of this metabolic flux ratio. This information cannot be achieved with  $\delta^2\text{H}$  measurements on the whole molecule, because the dependence on the level of isotopomers gets averaged into the  $\delta^2\text{H}$  of the whole molecule. The quantitative dependence of the  $^2\text{H}$  isotopomer ratio on  $1/\text{CO}_2$  was compared between plants grown in a  $\text{CO}_2$  manipulation experiment and plants that grew at different times during the rise of atmospheric  $\text{CO}_2$  concentration. Because there was no significant difference between the two data sets, it was concluded that increasing  $\text{CO}_2$  concentration suppressed photorespiration to the same degree in the chamber studies and over the twentieth century. This also suggests that there was no acclimation response of plants over nearly a century, and demonstrates how long-term physiological information can be derived from isotopomers.

In contrast to the high correlations observed in Fig. 7.6, correlations of  $\delta$  values with environmental parameters in tree-ring studies usually do not exceed  $r^2 = 0.25$  (McCarroll and Loader 2004). We hypothesize that this is a general consequence of the averaging of isotopomer abundances into the  $\delta$  value for the whole molecule of the respective isotope. The high correlations observed indicate that the  $^2\text{H}\text{-}6^{\text{R}}/^2\text{H}\text{-}6^{\text{S}}$  ratio is determined by one metabolic process, namely the ratio of oxygenation to carboxylation, which is driven by atmospheric  $\text{CO}_2$ . Other isotopomer ratios may reflect other metabolic processes that may be driven by other environmental drivers (see below for  $^{13}\text{C}$ ). When a  $\delta$  value is correlated with one environmental driver, it must be expected that isotopomer variation introduced by other environmental variables degrades this correlation, hence the curtailed correlation coefficients observed.

As glucose shows a non-random intra-molecular  $^{13}\text{C}$  pattern (Gilbert et al. 2012; Gleixner and Schmidt 1997), the glucose units of tree-ring cellulose should also show a  $^{13}\text{C}$  pattern. This expectation has been tested using a pine (*Pinus nigra*) tree-ring series (Wieloch et al. 2018). Figure 7.7 shows the observed  $^{13}\text{C}$  isotopomer pattern. The  $^{13}\text{C}$  variation of about  $\pm 5\%$  is important for  $^{13}\text{C}$  signals in the C cycle: When cellulose is decomposed in the environment, the  $\delta^{13}\text{C}$  of the released  $\text{CO}_2$  differs among the intra-molecular C positions. Thus, the  $\delta^{13}\text{C}$  of respired  $\text{CO}_2$  can vary, depending on whether the glucose units are completely respired to  $\text{CO}_2$ , or if the active metabolic pathway (such as fermentation) only releases some C positions as  $\text{CO}_2$ . Furthermore, it was observed that this  $^{13}\text{C}$  pattern is variable over the tree-ring series (Wieloch et al. 2018). This variation must be caused by changes in environmental variables and hence it carries ecophysiological information. To analyse this, a hierarchical cluster analysis identified groups of  $^{13}\text{C}$  isotopomers that vary independently of each other, which implies that they carry independent ecophysiological signals. One of these signals originates from the  $^{13}\text{C}$  fractionation of diffusion and the  $^{13}\text{C}$  isotope effect of Rubisco. The others are caused by yet unidentified  $^{13}\text{C}$  fractionations downstream of Rubisco, and will hence carry new information. We hypothesize that isotopomer signals originating from such fractionations will shed light on processes such as C allocation. We anticipate that extracting such signals from tree-ring series can unravel acclimation responses of plants to environmental changes, a subject of great importance for the future of the biosphere as a C sink, and for crop productivity.

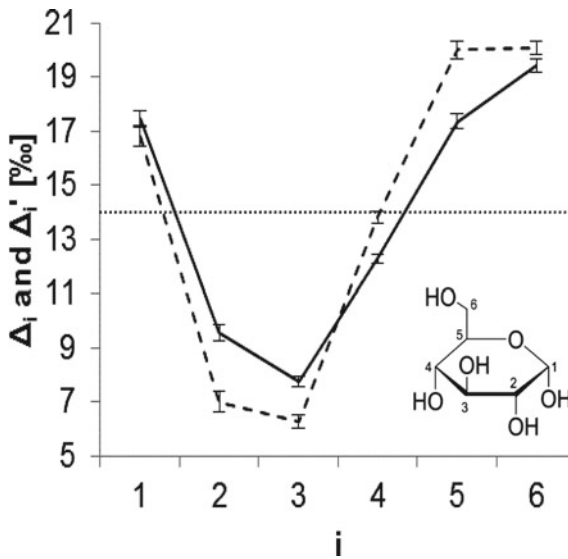


**Fig. 7.7**  $^{13}\text{C}$  isotopomer pattern of glucose units of tree-ring cellulose. The pattern connected by a solid line is the observed distribution, expressed as  $^{13}\text{C}$  fractionation  $\Delta_i$  for carbon  $i = 1\text{--}6$ ; and the dashed line is a fractionation pattern  $\Delta_i'$  that has been back-calculated to remove the isotope scrambling effect of triose phosphate cycling. Reproduced from Wieloch et al. (2018)

### 7.4.2 Position-Specific $\delta^{18}\text{O}$

Oxygen isotope ratios ( $\delta^{18}\text{O}$ ) in the annual growth rings of trees are considered to hold a valuable climatic and physiological records (Farquhar et al. 1998; Lehmann et al. 2017; McCarroll and Loader 2004; Sternberg et al. 2006) (see Chaps. 10, 16 and 19 for a more detailed discussion on climatic and physiological aspects of  $\delta^{18}\text{O}$ ). The original source of the oxygen atoms in tree-ring cellulose is soil moisture, generally obtained from precipitation, the  $\delta^{18}\text{O}$  of which are closely linked to temperature (Chap. 18; Dansgaard 1964). Early hopes that  $\delta^{18}\text{O}$  values of tree rings (e.g. Gray and Thompson 1976) could directly serve as a record for past temperature were overly optimistic. This is because the isotopic history of oxygen atoms from source water taken up by the tree and their final destination in trunk cellulose is complicated and, indeed, not fully understood (see Chap. 10 for more details). As a result of the processes involved, tree-ring cellulose is expected to carry a mixed soil water and leaf water signal in its oxygen atoms, complicating the process of abstracting climatic and physiological information from the oxygen isotope record (Roden et al. 2000). Position-specific isotope analysis of the oxygen atoms of cellulose holds out the hope of separating the leaf water and source water signals, especially if oxygen atoms at specific positions exchange either fully or not at all with stem water: the former group of oxygen atoms would be expected to provide a good record of source water, hence temperature, while the latter group would provide a good record of

leaf water, hence relative humidity. Progress in this field, however, has been much slower than is the case for position-specific carbon and hydrogen isotope analysis of cellulose (see Sect. 7.4.1). This is chiefly because, unlike  $^{13}\text{C}$  and  $^2\text{H}$ ,  $^{18}\text{O}$  does not have a nuclear spin and so does not produce an NMR signal. The lighter isotope ( $^{17}\text{O}$ ) has a nuclear spin of  $5/2$ ; so that the  $^{17}\text{O}$  nucleus has a quadrupole moment, which results in broad NMR peaks with poor resolution. This, combined with very low signal strengths resulting from the low natural abundance of  $^{17}\text{O}$  (ca. 0.038%) means that  $^{17}\text{O}$  NMR cannot at present be used to determine intra-molecular  $\delta^{17}\text{O}$  values of samples with isotopes of natural abundance.

#### 7.4.2.1 Sample Preparation and Analytical Methodology

To date, all methods published for the determination of  $\delta^{18}\text{O}$  values at specific positions in the glucose rings of cellulose have involved a significant amount of synthetic organic chemistry in order to isolate or remove oxygen atoms from particular positions. Sternberg et al. (2003) reported the first of these methods, which was designed to determine the value of  $\delta^{18}\text{O}$ -2 of cellulose<sup>1</sup> by hydrolysing cellulose to glucose and then converting this to phenylglucosazone (Fig. 7.8a). Values of  $\delta^{18}\text{O}$ -2 were calculated from measured oxygen isotope ratios of cellulose ( $\delta^{18}\text{O}_{\text{cell}}$ ) and phenylglucosazone ( $\delta^{18}\text{O}_{\text{PG}}$ ) using an isotopic mass balance equation. The authors used cellulose from wheat seedlings (*Triticum aestivum*), which were grown in the dark in water samples differently enriched in  $^{18}\text{O}$ , in order to simulate heterotrophic synthesis of cellulose in trunks of trees. The amount of cellulose required (1.5 g), however, is very high considering the amount of wood present in individual growth rings of trees. Results indicated that oxygen atoms at position 2 in cellulose completely exchanged with water, suggesting that  $\delta^{18}\text{O}$ -2 would be a better recorder of oxygen isotope ratios of soil water than is  $\delta^{18}\text{O}_{\text{cell}}$ . In a later study, however, Sternberg et al. (2006), using the same general synthetic method but with modified methods for hydrolysis of cellulose, obtained results indicating that only about 65–70% of the oxygen atoms at position 2 exchanged with water during cellulose synthesis. Importantly, the authors showed that there was no exchange between the oxygen atoms of cellulose and water during cellulose hydrolysis.

A different approach was made by Waterhouse et al. (2013), who described a method for the determination of the  $\delta^{18}\text{O}$  value for each of the five oxygen positions in the glucose ring of cellulose. The overall process involved multiple synthetic steps, in which oxygen atoms from specific positions were removed and incorporated into molecules of benzoic acid (Fig. 7.8b). Benzoic acid samples were used for isotopic ratio measurement using GC/Pyr-IRMS. Reaction conditions had to be optimized to minimize the risk of isotopic fractionation during each step. As the authors acknowledge, a process with so many steps and the consequent need for large wood samples is unlikely to be practical for routine isotope analysis of tree-ring cellulose. The

---

<sup>1</sup> Oxygen atoms at specific positions in the cellulose molecule are designated 'O-n', where n is the same number as that of the carbon to which the oxygen atom is bonded—see Fig. 7.8a.

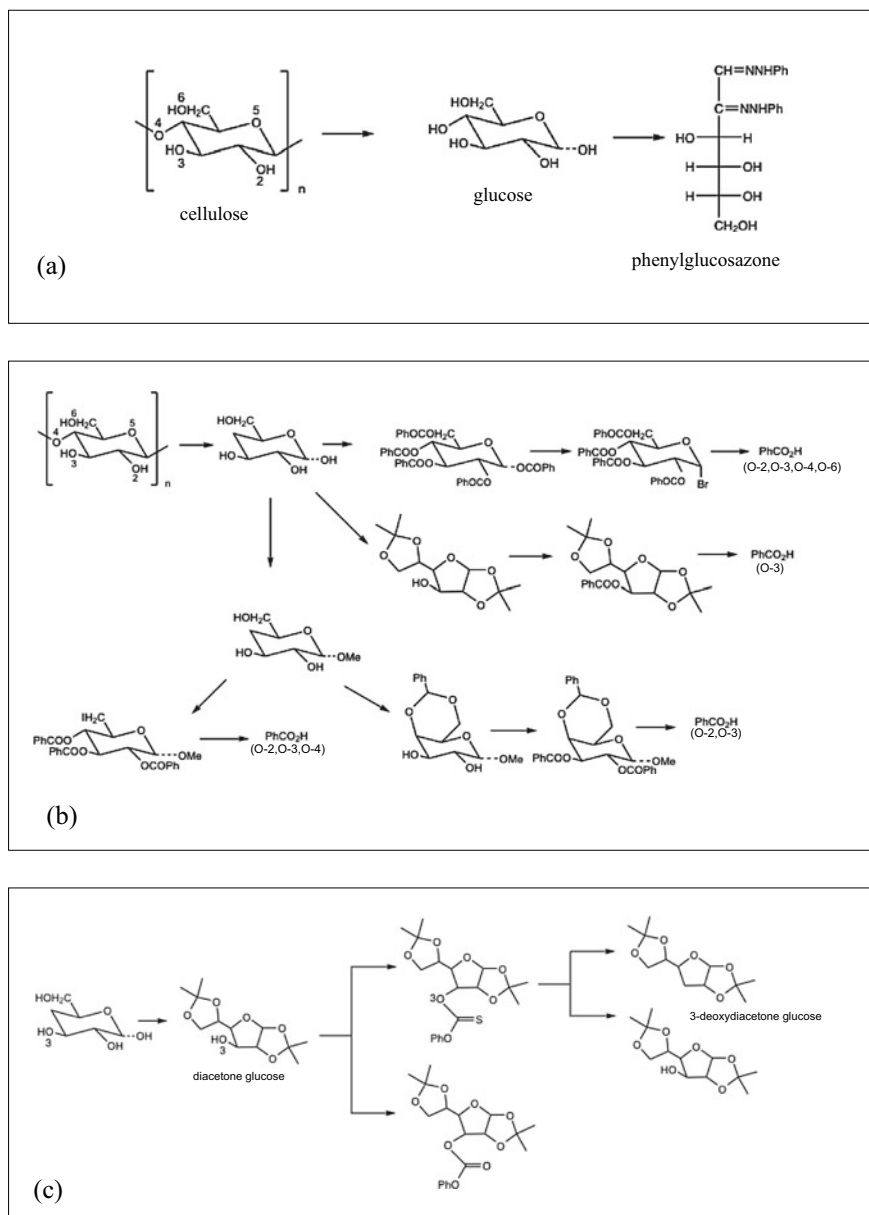


**Fig. 7.8** Summaries of synthetic chemical steps involved in preparing samples for measuring oxygen isotope ratios at specific positions in cellulose. See cited literature for reagents and conditions. **a** Preparation of phenylglucosazone from cellulose (after Sternberg et al. 2003)—note numbering of oxygen atoms in the cellulose molecule. **b** Selective incorporation into benzoic acid ( $\text{PhCO}_2\text{H}$ ) of oxygen atoms from indicated positions of cellulose (after Waterhouse et al. 2013). **c** Selective removal of O-3 from glucose by conversion of diacetone glucose to 3-deoxyacetone glucose (after Ma et al. 2018)



method was applied to  $\alpha$ -cellulose samples obtained from wheat seedlings germinated in water of differing values of  $\delta^{18}\text{O}$  (Sternberg et al. 2003), in order to determine the degree of isotopic exchange at each position during heterotrophic cellulose synthesis. Significant differences in the percentage exchange of oxygen with water at each position were detected: O-2 and O-4 showed little or no exchange; O-3, 48% exchange; O-5 and O-6, ca. 80% exchange. O-1, on the other hand, is derived from the water used in acid hydrolysis of cellulose. These results suggest that it is O-2 and O-4 that maintain chiefly a leaf water signal, whereas O-5 and O-6 should be the best targets for reconstructing source water isotope ratios. Significantly, the average of these percentage figures (41%) is close to the previously reported value (ca. 42%) for the percentage of oxygen exchange with trunk water during cellulose (Roden et al. 2000). The result that O-2 does not exchange is contrary to those of Sternberg et al. (2003) and Sternberg et al. (2006) but consistent with later results from samples from trees (Ellsworth et al. 2013; Sternberg et al. 2007)—see above; moreover, the enriched values of  $\delta^{18}\text{O}$ -2 (Ellsworth et al. 2013) are consistent with  $\delta^{18}\text{O}$ -2 of cellulose carrying a leaf-water signal enriched by evapotranspiration. However, oxygen at position 2 should have several opportunities to exchange with water during cellulose synthesis via reversible addition at carbonyl (Farquhar et al. 1998; Hill et al. 1995; Sternberg and DeNiro 1983); the fact that it seems not to exchange requires explanation.

More recently, a method for the determination of  $\delta^{18}\text{O}$ -3 of cellulose has been described (Ma et al. 2018). Like earlier methods, it comprises a sequence of synthetic steps and involves the same general strategy of Sternberg and colleagues described above: removal of the oxygen in question and calculation of its isotope ratio using an isotopic mass balance equation. In this case, glucose (from e.g. cellulose) is converted to diacetone glucose and O-3 removed by conversion to 3-deoxydiacetone glucose in a 2-step process (Fig. 7.8c). Values of  $\delta^{18}\text{O}$ -3 are calculated from  $\delta^{18}\text{O}$  values of these two products measured using GC/Pyr-IRMS. One complication with the overall procedure is that the second and third synthetic steps each yield two products, allowing the possibility of a consequential change in the  $\delta^{18}\text{O}$  value of 3-deoxydiacetone glucose. The authors calculate, however, that this is not significant. They also address the potential problem of error propagation, and show that overall the uncertainty in values of  $\delta^{18}\text{O}$ -3 could be as high as 1.3‰. Calculation of  $\delta^{18}\text{O}$ -3 of glucose derived from a  $\text{C}_4$  plants suggested that this oxygen was isotopically enriched by around 12‰ relative to the average values of O-2 to O-6, confirming that there is isotopic inhomogeneity within the glucose molecule. Although the authors claim that their method would be suitable for a 50 mg sample of glucose, this still represents an inconveniently large amount of wood for routine application to samples from individual tree rings.

Despite the novelty of the above methods, they all require time-consuming synthetic procedures, which risk isotopic fractionation, and comparatively large amounts of material; there are also uncertainties regarding propagation of errors throughout the many procedures involved. Much still needs to be done before position-specific oxygen isotope analysis can be routinely applied to tree-ring samples.

### 7.4.2.2 Research Applications

There are only two reports in the literature on the application of position specific  $\delta^{18}\text{O}$  analysis to tree samples, and both of them use the phenylglucosazone technique to obtain values of  $\delta^{18}\text{O}$ -2. In the first of these (Sternberg et al. 2007), trees were sampled from a wide range of latitudes across the northern hemisphere. Phenylglucosazone was prepared from glucose after acid hydrolysis of cellulose obtained from stem samples. Each sample of phenylglucosazone required comparatively large amounts (0.3 g) of wood. Comparison of values of  $\delta^{18}\text{O}_{\text{cell}}$ ,  $\delta^{18}\text{O}_{\text{PG}}$  and  $\delta^{18}\text{O}$ -2 (the latter was calculated from measured  $\delta^{18}\text{O}_{\text{cell}}$ , and  $\delta^{18}\text{O}_{\text{PG}}$ ) with  $\delta^{18}\text{O}_{\text{sw}}$  (measured from water removed from the stem) showed that  $\delta^{18}\text{O}_{\text{PG}}$  was most closely related to  $\delta^{18}\text{O}_{\text{sw}}$ , whereas  $\delta^{18}\text{O}$ -2 was very poorly correlated with  $\delta^{18}\text{O}_{\text{sw}}$ . This result was unexpected, as O-2 had been previously reported to undergo exchange with source water to a high degree during heterotrophic cellulose synthesis (see above). The authors proposed that the lack of correlation resulted from ‘isotopic noise’ in values of  $\delta^{18}\text{O}$ -2 caused by the variety of species sampled and widely different values of  $\delta^{18}\text{O}_{\text{sw}}$  across the wide geographical area of the study. One of the main conclusions was that phenylglucosazone presents a better record of  $\delta^{18}\text{O}_{\text{sw}}$ , and hence precipitation, than does cellulose itself.

In the second study (Ellsworth et al. 2013), phenylglucosazone was prepared from  $\alpha$ -cellulose extracted from annual growth rings of trees growing in Finland, Switzerland and New Zealand. An innovation of the work was the modification of the synthesis of phenylglucosazone so that a smaller amount (25 mg) of cellulose could be used. This makes the technique more appropriate for the routine analysis of annual growth rings. As expected, removing O-2 from cellulose resulted in  $^{18}\text{O}_{\text{PG}}$  having a much stronger relationship with  $\delta^{18}\text{O}_{\text{sw}}$ , hence higher potential for climatic reconstruction, than either  $\delta^{18}\text{O}_{\text{cell}}$  or  $\delta^{18}\text{O}$ -2. Furthermore, the authors showed that values of  $\delta^{18}\text{O}_{\text{sw}}$  calculated from measured  $^{18}\text{O}_{\text{PG}}$  closely followed observed values of  $\delta^{18}\text{O}_{\text{sw}}$  in both magnitude and temporal variability, whereas values of  $\delta^{18}\text{O}_{\text{sw}}$  calculated from  $\delta^{18}\text{O}$ -2 were both significantly enriched and much more variable than observed values.

**Acknowledgement** We would like to acknowledge funding from European Research Council (ERC, No. 755865, granted to KRG); Academy of Finland (295319, KRG and ES); SNF Ambizione (179978, MML); Swedish Research Council VR (JS); KAW, Trygger and Kempe foundations (JS); and EU FP6 project “Millennium” (17008, JW).

## References

- Barbour MM, Song X (2014) Do tree-ring stable isotope compositions faithfully record tree carbon/water dynamics? *Tree Physiol* 34:792–795
- Barrie A, Bricout J, Koziat J (1984) Gas chromatography—stable isotope ratio analysis at natural abundance levels. *Biomed Mass Spectrom* 11:583

- Battibaglia G, De Micco V, Brand WA, Linke P, Aronne G, Saurer M, Cherubini P (2010) Variations of vessel diameter and  $\delta^{13}\text{C}$  in false rings of *Arbutus unedo* L. reflect different environmental conditions. *New Phytol* 188:1099–1112
- Betson TR, Augusti A, Schleucher J (2006) Quantification of deuterium isotopomers of tree-ring cellulose using nuclear magnetic resonance. *Anal Chem* 78:8406–8411
- Blees J, Saurer M, Siegwolf R, Ulevicius V, Prevôt A, Dommen J, Lehmann M (2017) Oxygen isotope analysis of levoglucosan, a tracer of wood burning, in experimental and ambient aerosol samples. *Rapid Commun Mass Spectrom* 31:2101–2108
- Blokhina O, Valerio C, Sokolowska K, Zhao L, Karkonen A, Niittyta T, Fagerstedt K (2017) Laser capture microdissection protocol for xylem tissues of woody plants. *Front Plant Sci* 7
- Bogelein R, Lehmann MM, Thomas FM (2019) Differences in carbon isotope leaf-to-phloem fractionation and mixing patterns along a vertical gradient in mature European beech and Douglas fir. *New Phytol* 222:1803–1815
- Boschker HT, Moerdijk-Poortvliet TC, van Breugel P, Houtekamer M, Middelburg JJ (2008) A versatile method for stable carbon isotope analysis of carbohydrates by high-performance liquid chromatography/isotope ratio mass spectrometry. *Rapid Commun Mass Spectrom* 22:3902–3908
- Brandes E, Kodama N, Whittaker K, Weston C, Rennenberg H, Keitel C, Adams MA, Gessler A (2006) Short-term variation in the isotopic composition of organic matter allocated from the leaves to the stem of *Pinus sylvestris*: effects of photosynthetic and postphotosynthetic carbon isotope fractionation. *Glob Chang Biol* 12:1922–1939
- Bruykanova MV, Vaganov EA, Wirth C (2011) Influence of climatic factors and reserve assimilates on the radial growth and carbon isotope composition in tree rings of deciduous and coniferous species. *Contemp Probl Ecol* 4:126–132
- Cernusak LA, Wong SC, Farquhar GD (2003) Oxygen isotope composition of phloem sap in relation to leaf water in *Ricinus communis*. *Funct Plant Biol* 30:1059–1070
- Cernusak LA, Farquhar GD, Pate JS (2005) Environmental and physiological controls over oxygen and carbon isotope composition of Tasmanian blue gum, *Eucalyptus globulus*. *Tree Physiol* 25:129–146
- Cernusak LA, Tcherkez G, Keitel C, Cornwell WK, Santiago LS, Knohl A, Barbour MM, Williams DG, Reich PB, Ellsworth DS, Dawson TE, Griffiths HG, Farquhar GD, Wright IJ (2009) Why are non-photosynthetic tissues generally  $^{13}\text{C}$  enriched compared with leaves in  $\text{C}_3$  plants? Review and synthesis of current hypotheses. *Funct Plant Biol* 36:199
- Cernusak LA, Barbour MM, Arndt SK, Cheesman AW, English NB, Feild TS, Helliker BR, Holloway-Phillips MM, Holtum JAM, Kahmen A, McInerney FA, Munksgaard NC, Simonin KA, Song X, Stuart-Williams H, West JB, Farquhar GD (2016) Stable isotopes in leaf water of terrestrial plants. *Plant Cell Environ* 39:1087–1102
- Chaintreau A, Fieber W, Sommer H, Gilbert A, Yamada K, Yoshida N, Pagelot A, Moskau D, Moreno A, Schleucher J, Reniero F, Holland M, Guillou C, Silvestre V, Akoka S, Remaud GS (2013) Site-specific  $^{13}\text{C}$  content by quantitative isotopic  $^{13}\text{C}$  nuclear magnetic resonance spectrometry: a pilot inter-laboratory study. *Anal Chim Acta* 788:108–113
- Churakova (Sidorova) O, Lehmann M, Saurer M, Fonti M, Siegwolf R, Bigler C (2018) Compound-specific carbon isotopes and concentrations of carbohydrates and organic acids as indicators of tree decline in Mountain pine. *Forests* 9:363
- Churakova (Sidorova) OV, Lehmann MM, Siegwolf RTW, Saurer M, Fonti MV, Schimid L, Timofeeva G, Rinne-Garmston KT, Bigler C (2019) Compound-specific carbon isotope patterns in needles of conifer tree species from the Swiss National Park under recent climate change. *Plant Physiol Biochem* 139:264–272
- Cuny HE, Rathgeber CBK, Senga Kiessé T, Hartmann FP, Barbeito I, Fournier M (2013) Generalized additive models reveal the intrinsic complexity of wood formation dynamics. *J Exp Bot* 64:1983–1994
- Dansgaard W (1964) Stable isotopes in precipitation. *Tellus* 16:436–468
- De Niro MJ, Epstein S (1977) Mechanisms of carbon isotope fractionation associated with lipid-synthesis. *Science* 197:261–263

- De Micco V, Battibaglia G, Brand WA, Linke P, Saurer M, Aronne G, Cherubini P (2012) Discrete versus continuous analysis of anatomical and  $\delta^{13}\text{C}$  variability in tree rings with intra-annual density fluctuations. *Trees* 26:513–524
- Dennis DT, Blakeley SD (2000) Carbohydrate metabolism. In: *Biochemistry and molecular biology of plants*. American Society of Plant Physiologists, Rockville MD, USA
- Ehlers I, Augusti A, Betson TR, Nilsson MB, Marshall JD, Schleucher J (2015) Detecting long-term metabolic shifts using isotopomers:  $\text{CO}_2$ -driven suppression of photorespiration in C3 plants over the 20th century. *Proc Natl Acad Sci* 112:15585–15590
- Ellsworth PV, Anderson WT, Somninen E, Barbour MM, Sternberg LSL (2013) Reconstruction of source water using the  $\delta^{18}\text{O}$  of tree ring phenylglucosazone: a potential tool in paleoclimate studies. *Dendrochronologia* 31:153–158
- Farquhar GD, O'Leady MH, Berry JA (1982) On the relationship between carbon isotope discrimination and the intercellular carbon dioxide concentration in leaves. *Aust J Plant Physiol* 9:121–137
- Farquhar GD, Barbour MM, Henry BK (1998) Interpretation of oxygen isotope composition of leaf material. In: *Stable isotopes: the integration of biological, ecological and geochemical processes*. BIOS Scientific, Oxford, pp 27–62
- Fonti MV, Vaganov EA, Wirth C, Shashkin AV, Astrakhantseva NV, Schulze ED (2018) Age-effect on intra-annual  $\delta^{13}\text{C}$ -variability within Scots pine tree-rings from central Siberia. *Forests* 9:1–14
- Ford CW (1984) Accumulation of low molecular weight solutes in waterstressed tropical legumes. *Phytochemistry* 23:1007–1015
- Forster T, Schweingruber FH, Denneler B (2000) Increment puncher: a tool for extracting small cores of wood and bark from living trees. *IAWA J* 21:169–180
- Galiano L, Timofeeva G, Saurer M, Siegwolf R, Martinez-Vilalta J, Hommel R, Gessler A (2017) The fate of recently fixed carbon after drought release: towards unravelling C storage regulation in *Tilia platyphyllos* and *Pinus sylvestris*. *Plant Cell Environ* 40:1711–1724
- Gessler A, Brandes E, Keitel C, Boda S, Kayler ZE, Granier A, Barbour M, Farquhar GD, Treydte K (2013) The oxygen isotope enrichment of leaf-exported assimilates—does it always reflect lamina leaf water enrichment? *New Phytologist* 200:144–157
- Gessler A, Rennenberg H, Keitel C (2004) Stable isotope composition of organic compounds transported in the phloem of European beech—evaluation of different methods of phloem sap collection and assessment of gradients in carbon isotope composition during leaf-to-stem transport. *Plant Biol* 6:721–729
- Gessler A, Tcherkez G, Karyanto O, Keitel C, Ferrio JP, Ghashghaie J, Kreuzwieser J, Farquhar GD (2009) On the metabolic origin of the carbon isotope composition of  $\text{CO}_2$  evolved from darkened light-acclimated leaves in *Ricinus communis*. *New Phytol* 181:374–386
- Gessler A, Ferrio JP, Hommel R, Treydte K, Werner RA, Monson RK (2014) Stable isotopes in tree rings: towards a mechanistic understanding of isotope fractionation and mixing processes from the leaves to the wood. *Tree Physiol* 34:796–818
- Gilbert A, Silvestre V, Robins RJ, Tcherkez G, Remaud GS (2011) A  $^{13}\text{C}$  NMR spectrometric method for the determination of intramolecular  $\delta^{13}\text{C}$  values in fructose from plant sucrose samples. *New Phytol* 191:579–588
- Gilbert A, Silvestre V, Robins RJ, Remaud GS, Tcherkez G (2012) Biochemical and physiological determinants of intramolecular isotope patterns in sucrose from C-3, C-4 and CAM plants accessed by isotopic  $^{13}\text{C}$  NMR spectrometry: a viewpoint. *Nat Prod Rep* 29:476–486
- Gleixner G, Schmidt H-L (1997) Carbon isotope effects on the fructose-1,6-bisphosphate aldolase reaction, origin for non-statistical  $^{13}\text{C}$  distributions in carbohydrates. *J Biol Chem* 272:5382–5387
- Gleixner G, Danier H-J, Werner RA, Schmidt H-L (1993) Correlations between the  $^{13}\text{C}$  content of primary and secondary plant products in different cell compartments and that in decomposing basidiomycetes. *Plant Physiol* 102:287–290
- Gleixner G, Scrimgeour C, Schmidt H-L, Viola R (1998) Stable isotope distribution in the major metabolites of source and sink organs of *Solanum tuberosum* L.: a powerful tool in the study of metabolic partitioning in intact plants. *Planta* 207:241–245

- Gray J, Thompson P (1976) Climatic information from  $^{18}\text{O}/^{16}\text{O}$  ratios of cellulose in tree-rings. *Nature* 262:481–482
- Helle G, Schleser GH (2004) Beyond  $\text{CO}_2$ -fixation by Rubisco—an interpretation of  $^{13}\text{C}/^{12}\text{C}$  variations in tree rings from novel intra-seasonal studies on broad-leaf trees. *Plant Cell Environ* 27:367–380
- Helliker BR, Ehleringer JR (2002) Differential  $^{18}\text{O}$  enrichment of leaf cellulose in  $\text{C}_3$  versus  $\text{C}_4$  grasses. *Funct Plant Biol* 29:435–442
- Hepp J, Rabus M, Anhauser T, Bromm T, Laforsch C, Sirocko F, Glaser B, Zech M (2016) A sugar biomarker proxy for assessing terrestrial versus aquatic sedimentary input. *Org Geochem* 98:98–104
- Hill SA, Waterhouse JS, Field EM, Switsur VR, Ap Rees T (1995) Rapid recycling of triose phosphates in oak stem tissue. *Plant Cell Environ* 18:931–936
- Hobbie EA, Werner RA (2004) Intramolecular, compound-specific, and bulk carbon isotope patterns in  $\text{C}_3$  and  $\text{C}_4$  plants: a review and synthesis. *New Phytol* 161:371–385
- Kagawa A, Naito D, Sugimoto A, Maximov TC (2003) Effects of spatial and temporal variability in soil moisture on widths and  $\delta^{13}\text{C}$  values of eastern Siberian tree rings. *J Geophys Res* 108
- Kornel BE, Werner RA, Gehre M (1999) Standardization for oxygen isotope ratio measurement—still an unsolved problem. *Rapid Commun Mass Spectrom* 13:1248–1251
- Kornel BE, Gehre M, Hofling R, Werner RA (1999) On-line  $\delta^{18}\text{O}$  measurement of organic and inorganic substances. *Rapid Commun Mass Spectrom* 13:1685–1693
- Krummen M, Hilkert AW, Juchelka D, Duhr A, Schluter HJ, Pesch R (2004) A new concept for isotope ratio monitoring liquid chromatography/mass spectrometry. *Rapid Commun Mass Spectrom* 18:2260–2266
- Kuroda K, Fujiwara T, Hashida K, Imai T, Kushi M, Saito K, Fukushima K (2014) The accumulation pattern of ferruginol in the heartwood-forming *Cryptomeria japonica* xylem as determined by time-of-flight secondary ion mass spectrometry and quantity analysis. *Ann Bot* 113:1029–1036
- Lehmann MM, Rinne KT, Blessing C, Siegwolf RT, Buchmann N, Werner RA (2015) Malate as a key carbon source of leaf dark-respired  $\text{CO}_2$  across different environmental conditions in potato plants. *J Exp Bot* 66:5769–5781
- Lehmann MM, Fischer M, Blees J, Zech M, Siegwolf RT, Saurer M (2016) A novel methylation derivatization method for  $\delta^{18}\text{O}$  analysis of individual carbohydrates by gas chromatography/pyrolysis-isotope ratio mass spectrometry. *Rapid Commun Mass Spectrom* 30:221–229
- Lehmann MM, Gamarra B, Kahmen A, Siegwolf RTW, Saurer M (2017) Oxygen isotope fractionations across individual leaf carbohydrates in grass and tree species. *Plant Cell Environ* 40:1658–1670
- Lehmann MM, Goldsmith GR, Schmid L, Gessler A, Saurer M, Siegwolf RTW (2018) The effect of ( $^{18}\text{O}$ ) O-labelled water vapour on the oxygen isotope ratio of water and assimilates in plants at high humidity. *New Phytol* 217:105–116
- Lehmann MM, Egli M, Brinkmann N, Werner RA, Saurer M, Kahmen A (2020). Improving the extraction and purification of leaf and phloem sugars for oxygen isotope analyses. *Rapid Communications in Mass Spectrometry* 34 (19):8854
- Lehmann MM, Goldsmith GR, Mirande-Ney C, Weigt RB, Schönbeck L, Kahmen A, Gessler A, Siegwolf RTW, Saurer M (2019) The  $^{18}\text{O}$ -signal transfer from water vapour to leaf water and assimilates varies among plant species and growth forms. *Plant Cell Environ*
- Lipavská H, Svobodová H, Albrechtová J (2000) Annual dynamics of the content of non-structural saccharides in the context of structural development of vegetative buds of Norway spruce. *J Plant Physiol* 157:365–373

- Loader NJ, Robertson I, Barker AC, Switsur VR, Waterhouse JS (1997) An improved method for the batch processing of small whole wood samples to  $\alpha$ -cellulose. *Chem Geol* 136:313–317
- Loader NJ, McCarroll D, Barker S, Jalkanen R, Grudd H (2017) Inter-annual carbon isotope analysis of tree-rings by laser ablation. *Chem Geol* 466:323–326
- Long A, Arnold LD, Larry D, Damon PE, Lerman JC, Wilson AT (1979) Radial translocation of carbon in bristlecone pine. *Proceedings ninth international conference on radiocarbon dating, Los Angeles and La Jolla. Berkeley, University of California Press*, pp 532–537
- Ma R, Zhu Z, Wang B, Zhao Y, Yin X, Lu F, Wang Y-P, Su J, Hocart CH, Zhou Y (2018) Novel position-specific  $^{18}\text{O}/^{16}\text{O}$  Measurement of carbohydrates. I. O-3 of glucose and confirmation of  $^{18}\text{O}/^{16}\text{O}$  heterogeneity at natural abundance levels in glucose from starch of  $\text{C}_4$  plants. *Anal Chem* 90:10293–10301
- Macko SA, Ryan M, Engel M (1998) Stable isotopes analysis of individual carbohydrates by GC/C/IRMS. *Chem Geol* 152:205–210
- Martin GJ, Martin ML, Zhang BL (1992) Site-specific natural isotope fractionation of hydrogen in plant products studied by nuclear magnetic resonance. *Plant Cell Environ* 15:1037–1050
- Mauve C, Bleton J, Bathellier C, Lelarge-Trouverie C, Guerard F, Ghashghaie J, Tchaplà A, Tcherkez G (2009) Kinetic  $^{12}\text{C}/^{13}\text{C}$  isotope fractionation by invertase: evidence for a small in vitro isotope effect and comparison of two techniques for the isotopic analysis of carbohydrates. *Rapid Commun Mass Spectrom* 23:2499–2506
- McCarroll D, Loader NJ (2004) Stable isotopes in tree rings. *Quat Sci Rev* 23:771–801
- Miková J, Košler J, Wiedenbeck M (2014) Matrix effects during laser ablation MC ICP-MS analysis of boron isotopes in tourmaline. *J Anal At Spectrom* 29:903–914
- Moing A (2000) Sugar alcohols as carbohydrate reserves in some higher plants. In: *Carbohydrate reserves in plant—synthesis and regulation*. Elsevier Science BV, Amsterdam, The Netherlands
- Morrison DJ, Taylor K, Preston T (2010) Strong anion-exchange liquid chromatography coupled with isotope ratio mass spectrometry using a Liqueface interface. *Rapid Commun Mass Spectrom* 24:1755–1762
- Panek JA, Waring RH (1997) Stable carbon isotopes as indicators of limitations to forest growth imposed by climate stress. *Ecol Appl* 7:854–863
- Rinne KT, Boettger T, Loader NJ, Robertson I, Switsur VR, Waterhouse JS (2005) On the purification of  $\alpha$ -cellulose from resinous wood for stable isotope (H, C and O) analysis. *Chem Geol* 222:75–82
- Rinne KT, Saurer M, Streit K, Siegwolf RT (2012) Evaluation of a liquid chromatography method for compound-specific  $\delta^{13}\text{C}$  analysis of plant carbohydrates in alkaline media. *Rapid Commun Mass Spectrom* 26:2173–2185
- Rinne KT, Saurer M, Kirilyanov AV, Loader NJ, Bryukhanova MV, Werner RA, Siegwolf RT (2015) The relationship between needle sugar carbon isotope ratios and tree rings of larch in Siberia. *Tree Physiol* 35:1192–1205
- Rinne KT, Saurer M, Kirilyanov AV, Bryukhanova MV, Prokushkin AS, Churakova (Sidorova) OV, Siegwolf RTW (2015a) Examining the response of needle carbohydrates from Siberian larch trees to climate using compound-specific  $\delta^{13}\text{C}$  and concentration analyses. *Plant Cell Environ* 38:2340–2352
- Roden JS, Lin G, Ehleringer JR (2000) A mechanistic model for interpretation of hydrogen and oxygen isotope ratios in tree-ring cellulose. *Geochim Cosmochim Acta* 64:21–35
- Romek KM, Krzeminska A, Remaud GS, Julien M, Paneth P, Robins RJ (2017) Insights into the role of methionine synthase in the universal C-13 depletion in O- and N-methyl groups of natural products. *Arch Biochem Biophys* 635:60–65

- Rossi S, Anfodillo T, Menardi R (2006) Trephor: a new tool for sampling microcores from tree stems. *IAWA J* 27:89–97
- Rossmann A, Butzenlechner M, Schmidt HL (1991) Evidence for a nonstatistical carbon isotope distribution in natural glucose. *Plant Physiol* 96:609–614
- Scheidegger Y, Saurer M, Bahn M, Siegwolf R (2000) Linking stable oxygen and carbon isotopes with stomatal conductance and photosynthetic capacity: a conceptual model. *Oecologia* 125:350–357
- Schmidt HL (2003) Fundamentals and systematics of the non-statistical distributions of isotopes in natural compounds. *Naturwissenschaften* 90:537–552
- Schollaen K, Heinrich I, Helle G (2014) UV-laser-based microscopic dissection of tree rings—a novel sampling tool for  $\delta(13)C$  and  $\delta(18)O$  studies. *New Phytol* 201:1045–1055
- Schollaen K, Baschek H, Heinrich I, Slotta F, Pauly M, Helle G (2017) A guideline for sample preparation in modern tree-ring stable isotope research. *Dendrochronologia* 44:133–145
- Schulze B, Wirth C, Linke P, Brand WA, Kuhlmann I, Horna V, Schulze ED (2004) Laser ablation-combustion-GC-IRMS—a new method for online analysis of intra-annual variation of  $\delta^{13}C$  in tree rings. *Tree Physiol* 24:1193–1201
- Schweingruber FH, Börner A, Schulze E-D (2006) Atlas of woody plant stems: evolution, structure, and environmental modifications. Springer, Berlin
- Skomarkova MV, Vaganov EA, Mund M, Knohl A, Linke P, Boerner A, Schulze ED (2006) Inter-annual and seasonal variability of radial growth, wood density and carbon isotope ratios in tree rings of beech (*Fagus sylvatica*) growing in Germany and Italy. *Trees* 20:571–586
- Smith M, Wild B, Richter A, Simonin K, Merchant A (2016) Carbon isotope composition of carbohydrates and polyols in leaf and phloem sap of *Phaseolus vulgaris* L. influences predictions of plant water use efficiency. *Plant Cell Physiol* 57:1756–1766
- Soudant A, Loader NJ, Bäck J, Levula J, Kljun N (2016) Intra-annual variability of wood formation and  $\delta^{13}C$  in tree-rings at Hyytiälä, Finland. *Agric For Meteorol* 224:17–29
- Spahr S, Bolotin J, Schleucher J, Ehlers I, von Gunten U, Hofstetter TB (2015) Compound-specific carbon, nitrogen, and hydrogen isotope analysis of N-nitrosodimethylamine in aqueous solutions. *Anal Chem* 87:2916–2924
- Sternberg LSL, DeNiro MJ (1983) Biogeochemical implications of the isotopic equilibrium fractionation factor between the oxygen atoms of acetone and water. *Geochim Cosmochim Acta* 47:2271–2274
- Sternberg LSL, Anderson WT, Morrison K (2003) Separating soil and leaf water  $^{18}O$  isotopic signals in plant stem cellulose. *Geochim Cosmochim Acta* 67:2561–2566
- Sternberg LSL, Pinzon MC, Anderson WT, Jahren AH (2006) Variation in oxygen isotope fractionation during cellulose synthesis: intramolecular and biosynthetic effects. *Plant Cell Environ* 29:1881–1889
- Sternberg LSL, Pinzon MC, Vendramini PF, Anderson WT, Jahren AH, Beuning K (2007) Oxygen isotope ratios of cellulose-derived phenylglucosazone: an improved paleoclimate indicator of environmental water and relative humidity. *Geochim Cosmochim Acta* 71:2463–2473
- Streit K, Rinne KT, Hagedorn F, Dawes MA, Saurer M, Hoch G, Werner RA, Buchmann N, Siegwolf RT (2013) Tracing fresh assimilates through *Larix decidua* exposed to elevated  $CO_2$  and soil warming at the alpine treeline using compound-specific stable isotope analysis. *New Phytol* 197:838–849
- Treydte K, Boda S, Graf Pannatier E, Fonti P, Frank D, Ullrich B, Saurer M, Siegwolf R, Battipaglia G, Werner W, Gessler A (2014) Seasonal transfer of oxygen isotopes from precipitation and soil to the tree ring: source water versus needle water enrichment. *New Phytol* 202:772–783

- Treydte K, Frank D, Esper J, Andreu L, Bednarz Z, Berninger F, Boettger T, D'Alessandro CM, Etien N, Filot M, Grabner M, Guillemin MT, Gutierrez E, Haupt M, Helle G, Hilasvuori E, Jungner H, Kalela-Brundin M, Krapiec M, Leuenberger M, Loader NJ, Masson-Delmotte V, Pazdur A, Pawelczyk S, Pierre M, Planells O, Pukiene R, Reynolds-Henne CE, Rinne KT, Saracino A, Saurer M, Sonninen E, Stievenard M, Switsur VR, Szczepanek M, Szychowska-Krapiec E, Todaro L, Waterhouse JS, Weigl M, Schleser GH (2007) Signal strength and climate calibration of a European tree-ring isotope network. *Geophys Res Lett* 34
- Vaganov EA, Schulze ED, Skomarkova MV, Knohl A, Brand WA, Roscher C (2009) Intra-annual variability of anatomical structure and  $\delta^{13}\text{C}$  values within tree rings of spruce and pine in alpine, temperate and boreal Europe. *Oecologia* 161:729–745
- Vysotskaya LG, Shashkin AV, Vaganov EA (1985) Analysis of the size distribution of tracheids in the annual rings of pines growing under various moisture conditions. *Sov J Ecol* 16:29–34
- Walcroft AS, Silvester WB, Whitehead D, Kelliher FM (1997) Seasonal changes in stable carbon isotope ratios within annual rings of *Pinus radiata* reflect environmental regulation of growth processes. *Aust J Plant Physiol* 24:57–68
- Wanek W, Heintel S, Richter A (2001) Preparation of starch and other carbon fractions from higher plant leaves for stable carbon isotope analysis. *Rapid Commun Mass Spectrom* 15:1136–1140
- Waterhouse JS, Cheng S, Juchelka D, Loader NJ, McCarroll D, Switsur VR, Gautam L (2013) Position-specific measurement of oxygen isotope ratios in cellulose: isotopic exchange during heterotrophic cellulose synthesis. *Geochim Cosmochim Acta* 112:178–191
- Weigt RB, Braunlich S, Zimmermann L, Saurer M, Grams TE, Dietrich HP, Siegwolf RT, Nikolova PS (2015) Comparison of  $\delta^{18}\text{O}$  and  $\delta^{13}\text{C}$  values between tree-ring whole wood and cellulose in five species growing under two different site conditions. *Rapid Commun Mass Spectrom* 29:2233–2244
- West AG, Patrickson SJ, Ehleringer JR (2006) Water extraction times for plant and soil materials used in stable isotope analysis. *Rapid Commun Mass Spectrom* 20:1317–1321
- Wieloch T, Ehlers I, Yu J, Frank D, Grabner M, Gessler A, Schleucher J (2018) Intramolecular  $^{13}\text{C}$  analysis of tree rings provides multiple plant ecophysiology signals covering decades. *Sci Rep* 8:5048
- Wild B, Wanek W, Postl W, Richter A (2010) Contribution of carbon fixed by Rubisco and PEPC to phloem export in the Crassulacean acid metabolism plant *Kalanchoe daigremontiana*. *J Exp Bot* 61:1375–1383
- Williams JHH, Collis BE, Pollock CJ, Williams ML, Farrar JF (1993) Variability in the distribution of photoassimilates along leaves of temperate Gramineae. *New Phytol* 123:699–703
- Zech M, Glaser B (2009) Compound-specific  $\delta^{18}\text{O}$  analyses of neutral sugars in soils using gas chromatography-pyrolysis-isotope ratio mass spectrometry: problems, possible solutions and a first application. *Rapid Commun Mass Spectrom* 23:3522–3532
- Zech M, Saurer M, Tuthorn M, Rinne KT, Werner RA, Siegwolf R, Glaser B, Juchelka D (2013) A novel methodological approach for  $\delta^{18}\text{O}$  analysis of sugars using gas chromatography-pyrolysis-isotope ratio mass spectrometry. *Isot Environ Health Stud* 49:492–502
- Zech M, Tuthorn M, Detsch F, Rozanski K, Zech R, Zoller L, Zech W, Glaser B (2013) A 220 ka terrestrial  $\delta^{18}\text{O}$  and deuterium excess biomarker record from an eolian permafrost paleosol sequence, NE-Siberia. *Chem Geol* 360:220–230



**Open Access** This chapter is licensed under the terms of the Creative Commons Attribution 4.0 International License (<http://creativecommons.org/licenses/by/4.0/>), which permits use, sharing, adaptation, distribution and reproduction in any medium or format, as long as you give appropriate credit to the original author(s) and the source, provide a link to the Creative Commons license and indicate if changes were made.

The images or other third party material in this chapter are included in the chapter's Creative Commons license, unless indicated otherwise in a credit line to the material. If material is not included in the chapter's Creative Commons license and your intended use is not permitted by statutory regulation or exceeds the permitted use, you will need to obtain permission directly from the copyright holder.



**Part III**  
**Isotopic Fractionations from Source**  
**to Wood**

# Chapter 8

## Isotopes—Terminology, Definitions and Properties



Roland A. Werner and Marc-André Cormier

**Abstract** The intention of this chapter is to give insight into the properties and peculiarities of the stable isotopes of the bioelements. Following an overview about the terminology and ‘technical jargon’ used in stable isotope sciences, methods to calculate and express isotopic abundances are presented. Subsequently, a short description of the physicochemical basis of equilibrium and kinetic (mass-dependent) isotope effects (EIEs and KIEs) as origin of isotope fractionation in chemical and biological systems is given. Further, measures for calculation and presentation of isotope fractionation are introduced and the corresponding properties of these quantities are critically discussed. Finally, examples for equilibrium and kinetic isotope fractionation in biochemical reactions are presented in more details and subsequent effects and consequences including the relationship between EIEs and KIEs are reviewed.

---

R. A. Werner (✉)

Institute of Agricultural Sciences, Department of Environmental Systems Science, ETH Zurich, Universitätstrasse 2, 8092 Zurich, Switzerland  
e-mail: [roland.werner@usys.ethz.ch](mailto:roland.werner@usys.ethz.ch)

M.-A. Cormier

Department of Earth Sciences, University of Oxford, South Parks Road, Oxford, UK  
e-mail: [ma\\_cormier@alumni.ethz.ch](mailto:ma_cormier@alumni.ethz.ch)

© The Author(s) 2022

R. T. W. Siegwolf et al. (eds.), *Stable Isotopes in Tree Rings*, Tree Physiology 8,  
[https://doi.org/10.1007/978-3-030-92698-4\\_8](https://doi.org/10.1007/978-3-030-92698-4_8)

253

## 8.1 Introduction

The bioelements H, C, N, O and S occur in nature as mixtures of stable isotopes.<sup>1</sup> As a consequence, all organic material also consists of a mixture of stable isotopes. With the exception of sulfur, the natural mean global abundance of the heavy stable isotopes of the bioelements is around one percent or less. The isotopic composition of organic compounds is primarily dependent on the isotopic composition of the precursor molecules and on isotope fractionation during (bio)synthesis or (bio)degradation reactions. The extent of the observable isotope fractionation is also dependent on environmental and climatic variables and their impact on the source organism producing the biomass. Plants record these isotope fractionations annually e.g. in tree rings. Therefore, with a proper understanding of the processes involving isotope fractionation, it will be possible to use the information behind the isotopic signatures of tree rings to reconstruct the climatic conditions (climate proxy) during tree ring growth. The principles and techniques of tree ring research will be explained in the following chapters of this book. The aim of the present chapter is to provide key knowledge on isotope terminology and related ‘technical jargon’, as well as on properties and behavior of stable isotopes in biochemical reactions and/or physical processes. The chapter gives definitions, thereby explaining terms in simple examples with reference to mono-, disaccharides and cellulose (and other wood ingredients) where possible.

## 8.2 Terminology

### 8.2.1 *Isotopes*

Atoms consist of a nucleus and an electron shell; the mass of an atom is concentrated mainly in the nucleus. The nucleus contains nucleons (positively charged protons and neutrons without charge). The much lighter electrons with negative charge “orbit”<sup>2</sup>

---

<sup>1</sup> In this chapter the authors follow in principle below listed recommendations with the following supplement: the terms ‘isotope fractionation (factor)’ and ‘isotopic fractionation (factor)’ are used synonymously.

Official terms used in “isotope chemistry” according to the IUPAC Compendium of Chemical Terminology (Gold Book) and related glossary recommendations (Muller 1994; Coplen 2011; Brand et al. 2014) are:

(1) Isotope effect (IE → equilibrium, heavy atom, intramolecular, inverse, kinetic, normal, primary, secondary, solvent, thermodynamic IE), isotope exchange, isotope ratio, isotope scale.

(2) Isotopic abundance, isotopic atom, isotopic composition, isotopic enrichment (factor), isotopic exchange, isotopic fractionation (factor), isotopic mass, isotopic separation, isotopic signature, isotopic substitution, isotopic tracer.

(3) Isotopically enriched, isotopically labelled, isotopically substituted.

<sup>2</sup> In quantum mechanics there is no orbiting motion of electrons, but only a probability to find an electron in a certain location in the electron shell.

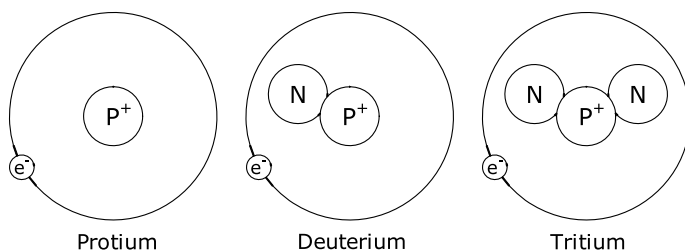


**Fig. 8.1** Schematic representation of the three naturally occurring hydrogen isotopes. The origin of the names protium, deuterium and tritium are the ancient greek terms *prōtos* (πρῶτος—first), *deúteros* (δεύτερος—second) and *trítos* (τρίτος—third) Urey et al. (1933). The three hydrogen isotopes differ only in mass of the nucleus (atomic mass) and not in the arrangement of the electron(s)

around the central nucleus in the electron shell. Electrons and protons are mutually attracted to each other by electromagnetic force. The term *nuclide* is used to describe atomic species by the composition of the nucleus e.g. by the number of protons ( $Z$ ) and the number of neutrons ( $N$ ). Nuclides with the same number of protons are described as **isotopes**. In this context **isobaric nuclides (Isobars)** have the same nominal mass while **isotones** are nuclides having the same number of neutrons. The term ‘isotope’ was introduced by Nobel laureate Frederick Soddy (1923) through merging the Greek words for ‘equal’ (*ισο*—iso) and ‘place’ (*τόπος*—topos) indicating that all isotopes of the same chemical element share the same position in the periodic table of the elements (IUPAC periodic table of the elements and isotopes (IPTEI), Holden et al. 2018). As an example, the isotopes with the simplest schematic structure are shown in Fig. 8.1. The most abundant hydrogen atom, ‘protium’ consists of a single proton and one electron. ‘Deuterium’ is the heavier stable hydrogen isotope possessing an additional neutron. ‘Tritium’ possessing two neutrons is the only naturally occurring, not stable, radioactive hydrogen isotope (Fig. 8.1).

Isotopes of the same element have different masses owing to the various number of neutrons at constant proton number in the nucleus. Universally, the mass number of nuclides (sum of protons and neutrons) is denoted on the left side of the atomic symbol as a superscript and the atomic number (number of protons) is noted as the left subscript (International Union of Pure and Applied Chemistry 1959). For example,  ${}^{12}_6\text{C}$  and  ${}^{13}_6\text{C}$  are the stable isotopes of carbon and  ${}^{14}_6\text{C}$  is the naturally occurring radioactive carbon isotope with the masses ( $N + Z$ ) changing from 12 to 14, respectively. By definition, all of them have six protons ( $Z = 6$ ); the number of neutrons varies from six ( ${}^{12}\text{C}$ ;  $N = 6$ ) to eight ( ${}^{14}\text{C}$ ;  $N = 8$ ) for the naturally occurring carbon isotopes. Additionally, other radioactive carbon isotopes like  ${}^{11}_6\text{C}$  ( $N = 5$ ) can be artificially produced, but are highly unstable (very short half-life time). The atomic weight of the elements is not considered as a constant of nature (Coplen and Holden 2011; Brand 2013); it could be calculated from the number of stable isotopes and the corresponding global mean natural abundances (with the natural isotopes of the bioelements as example). In the case of carbon, about 98.93%  ${}^{12}\text{C}$  and 1.07%  ${}^{13}\text{C}$  (with negligible amounts of  ${}^{14}\text{C}$ ) are occurring naturally. Multiplying these numbers

**Table 8.1** Natural abundance of the stable isotopes of the bioelements. The standard atomic weight of these elements is derived from best estimates by the IUPAC of atomic weights occurring in terrestrial materials (Meija et al. 2016; IUPAC 2018)

Element	Atomic mass	Range of atomic mass	Mean natural abundance
Hydrogen	1.008	1.00784–1.00811	99.9885% $^1\text{H}$
			0.0115% $^2\text{H}$
Carbon	12.011	12.0096–12.0116	98.93% $^{12}\text{C}$
			1.07% $^{13}\text{C}$
Nitrogen	14.007	14.00643–14.00728	99.636% $^{14}\text{N}$
			0.364% $^{15}\text{N}$
Oxygen	15.999	15.99903–15.99977	99.757% $^{16}\text{O}$
			0.038% $^{17}\text{O}$
			0.205% $^{18}\text{O}$
Sulfur	32.06	32.059–32.076	94.99% $^{32}\text{S}$
			0.75% $^{33}\text{S}$
			4.25% $^{34}\text{S}$
			0.01% $^{36}\text{S}$

with the corresponding mass numbers (12 Da<sup>3</sup> for  $^{12}\text{C}$  and 13.003354835 Da for  $^{13}\text{C}$ ; Meija et al. 2016, IUPAC 2018) will result in an average atomic weight of 12.011 Da for the element carbon (IUPAC 2018).<sup>4</sup>

As mentioned above, isotopes of an element are either stable or radioactive. In the following we will focus on the stable isotopes of the bioelements H, C, N, O and S. The natural abundance of the primordial isotopes (or primordial nuclides) on Earth, including the stable and the long-lived radionuclides have been determined during the formation of our solar system (Chown 2001).

Table 8.1 lists the atomic weight in intervals because the natural abundance of the isotopes of the bioelements on Earth varies compound-wise on spatial and temporal scales.

<sup>3</sup> The mass of nuclides (and nucleons) can be expressed in dalton Da or in unified atomic mass units u (IUPAC Green book: Quantities, Units and Symbols in Physical Chemistry, 3rd ed.; <https://doi.org/10.1039/9781847557889> (February 2022). Da and u both are defined as exactly 1/12 of the mass of a single  $^{12}\text{C}$  atom (BIPM 2019).

<sup>4</sup> Please refer to the web site of the Commission on Isotopic Abundances and Atomic Weights (CIAAW) of the International Union of Pure and Applied Chemistry (IUPAC) for relevant and recent authoritative literature: <https://www.ciaaw.org> (December 2021).

## 8.2.2 Isotopocule, Isotopologue and Isotopomer

The umbrella term used for molecules having identical chemical constitution, but differing in isotopic composition and different number of isotopic substituents or different chemical positions of the specific isotope substituent(s) in these molecules is **isotopocules** (Kaiser and Röckmann 2008). The term is a short form of the description “all *isotopically* substituted species of a *molecule*”. Molecules that differ only in the number of isotope substituents are designated as **isotopologues** (derived from contracting “*isotopic homologues*”; Seeman et al. 1992; Seeman and Paine 1992). Isotopologues can have different masses. However, in some cases also isobaric isotopologues are possible (e.g.  $^{14}\text{N}^{15}\text{N}^{16}\text{O}$  and  $^{14}\text{N}^{14}\text{N}^{17}\text{O}$  in case of nitrous oxide). Molecules differing in the chemical positions of isotopic substituents (and not in bulk isotopic composition) are named **isotopomers** (abbreviated from “*isotopic isomer*”; Seeman et al. 1992; Seeman and Paine 1992). These isotopomer molecules do have identical mass.

This terminology is best explained with a simple molecule like nitrous oxide ( $\text{N}_2\text{O}$ ) having both isotopologues and isotopomeric variants. Nitrous oxide is a linear asymmetric molecule; each nitrogen atom has different chemical bonding partners (Fig. 8.2 left side). The most abundant ‘isotopic’ nitrous oxide molecule is  $^{14}\text{N}_2^{16}\text{O}$ . With two stable nitrogen isotopes and three stable oxygen isotopes a total of twelve stable nitrous oxide isotopocules are possible with masses from 44 ( $^{14}\text{N}_2^{16}\text{O}$ ) to 48 ( $^{15}\text{N}_2^{18}\text{O}$ ) (Fig. 8.2 right side; Magyar et al. 2016). Among them, nine isotopologues and six isotopomers (corresponding to three ‘isotopomer pairs’) can occur. Isotopomer molecules have the same mass but the heavy isotope(s) are located at different chemical positions in the molecule. In case of  $\text{N}_2\text{O}$ , the two nitrogen atoms have different bonding partners allowing isotopomer molecules with one  $^{14}\text{N}$  and one  $^{15}\text{N}$  atom. The  $^{15}\text{N}$  can be either positioned as terminal or central N atom (Fig. 8.2).

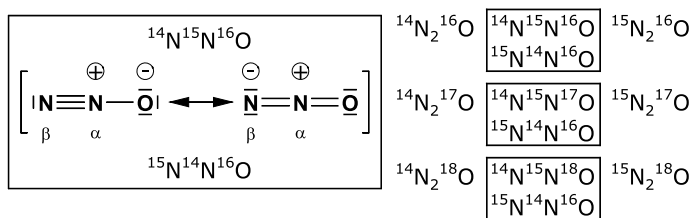


**Fig. 8.2** Left side: The chemical bonding inside the nitrous oxide molecule can be described by two stable resonance structures with a delocalized electron system. Nitrous oxide molecules with one  $^{14}\text{N}$  and one  $^{15}\text{N}$  atom can have two ‘constitutional isotopomers’.  $^{15}\text{N}$  can be either in the central ( $\alpha$ ) or terminal ( $\beta$ ) N position. The concept of ‘site preference’ with  $\alpha$  and  $\beta$  denotation of the N atoms in  $\text{N}_2\text{O}$  was introduced by Toyoda and Yoshida (1999). Right side: Twelve stable isotopocule molecules of nitrous oxide. The three isotopomer pairs are marked with rectangular boxes. Only one member of each isotopomer pair can be counted as isotopologue; giving in total nine isotopologues

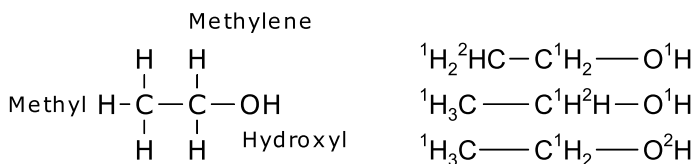


**Fig. 8.3** Left side: Ethanol—structural formula and functional groups. Right side: Three different ‘constitutional isotopomers’ of ethanol molecules labelled with one  ${}^2\text{H}$  atom. This  ${}^2\text{H}$  atom can be positioned in either the methyl, the methylene or the hydroxyl group of ethanol

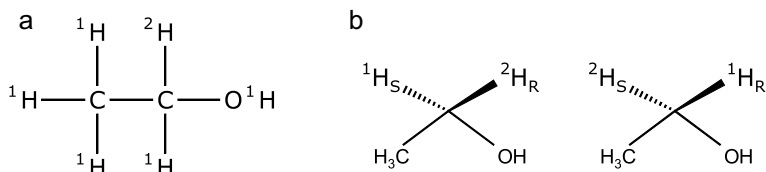


**Fig. 8.4** **a** Structural formula of ethanol. **b** Fischer projections of the two optical ‘stereo isotopomers’ of ethanol position-specifically labelled with one  ${}^2\text{H}$  atom (‘isotopically labelled’) in the methylene group. The  ${}^2\text{H}$  atom can be either in (*R*)- or (*S*)-position<sup>5</sup>

Isotopomers can be either constitutional isotopomers (‘constitutional isotopomer’, see  ${}^{14}\text{N}{}^{15}\text{N}{}^{16}\text{O}$  and  ${}^{15}\text{N}{}^{14}\text{N}{}^{16}\text{O}$  molecules above) or isotopic stereo isomers (‘stereoisotopomer’). Constitutional isotopomers have the same molecular formula and same isotopic mass, but a different spatial arrangement of the atoms and a different chemical connectivity inside the molecule.

As an example, the three possible constitutional  ${}^2\text{H}$  isotopomers of ethanol are shown in Fig. 8.3 (right side).  ${}^2\text{H}$  could be found either in the methyl, or in the methylene or the hydroxyl group of the molecule. All three hydrogen atoms in the methyl group of ethanol are chemically indistinguishable, but the H atoms in the methylene group can be differentiated as *pro-R*- and *pro-S*-H atoms (prochiral ethanol molecule<sup>5</sup>; Zhang and Pionnier 2002) allowing two possible enantiomeric optical stereo isotopomer molecules of 1-( ${}^2\text{H}$ )-ethanol (Fig. 8.4).

The two hydrogen atoms bound to position C-6 of glucose can be differentiated as (*R*)- and (*S*)-position (Zhang et al. 2002). The position-specific hydrogen isotopic signature in these two positions of glucose hydrolyzed from plant cellulose bears also information on the photorespiration/ photosynthesis ratio of the respective plant (Ehlers et al. 2015).

Geometric stereo isotopomers show a usually small restricted rotation of two different isotopic substituents around a carbon–carbon double bond allowing a

<sup>5</sup> Prochiral molecules can be converted to chiral molecules by a single desymmetrization step; the two hydrogen atoms in the methylene group of ethanol are enantiotopic, but can be differentiated in an asymmetric environment (e.g. by enzymes; Smith 2013, pp. 170–171). Substitution of the two hydrogen atoms in the  $\text{CH}_2$  position-specifically with  ${}^1\text{H}$  and  ${}^2\text{H}$  produces monodeuterated isotopic enantiomers → chiral isotopomers (see e.g. Zhang and Pionnier 2002).



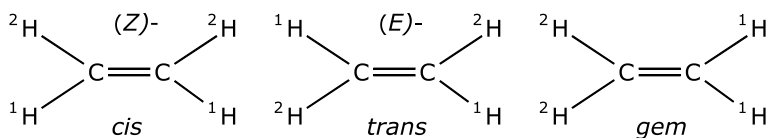


**Fig. 8.5** Lewis structures of three isotopomers of dideuteroethene: *cis*-1,2-<sup>2</sup>H<sub>2</sub> ethene and *trans*-1,2-<sup>2</sup>H<sub>2</sub> ethene are diastereomeric isotopomers. Meanwhile IUPAC prefers the *(Z)*-/*(E)*-notation to describe the absolute stereochemistry for alkenes. In contrast 1,1-dideuteroethene (“*gem*-dideuteroethene”) is a constitutional isotopomer. All of them have different physical properties (Bigeleisen et al. 1977)

different spatial positioning of the two different isotopic substituents relative to the double bond. This is best explained with e.g. ethene molecules consisting of two <sup>1</sup>H and two <sup>2</sup>H atoms (Fig. 8.5). The two <sup>1</sup>H (and the two <sup>2</sup>H) atoms can be oriented on the same side of the carbon double bond (*cis*) or on the opposite side (*trans*). The resulting diastereomeric isotopomer molecules are termed *cis*- and *trans*-1,2-<sup>2</sup>H<sub>2</sub> ethene or *(Z)*- and *(E)*-1,2-<sup>2</sup>H<sub>2</sub> ethene (latter terms now preferred IUPAC notation for alkenes).

In contrast 1,1-dideuteroethene with the two <sup>2</sup>H atoms as substituents at the same carbon atom (“*gem*-dideuteroethene”) is a constitutional isotopomer.

Isotope ratio analysis of tree ring cellulose has been used since the 1970s to reconstruct past climate conditions. The site-specific isotopic signature (isotopomer analysis) of glucose hydrolyzed from the extracted cellulose fraction shows high intramolecular differences for <sup>2</sup>H (seven carbon-bound hydrogen isotopomers<sup>6</sup> of glucose; Augusti et al. 2006, Betson et al. 2006) and <sup>13</sup>C (six carbon isotopomers of glucose; Wieloch et al. 2018, 2021). This site-specific isotopic signature has its origin in position-specific isotope effects on enzyme reactions during glucose and/or cellulose biosynthesis and might help to elucidate the mechanism of biochemical reactions causing plant-specific adaption to environmental and climatic changes. A corresponding site-specific oxygen isotopic signature (<sup>18</sup>O isotopomers) of glucose (from soluble sugars and cellulose monomers) has been proven (c.f. Schmidt et al. 2001; Sternberg 2009; Ma et al. 2018) with six possible oxygen isotopomers of glucose. Recently the possible application of the analysis of lignin isotopomers (i.e. carbon and hydrogen isomers in the methoxy groups of lignin) isolated from tree ring wood in reconstructing paleoclimate has been described by Gori et al. (2013) and Mischel et al. (2015). Wang et al. (2021) analyzed the position-specific oxygen isotopic signature of lignin monomeric units.

<sup>6</sup> Hydrogen atoms bound to heteroatoms like O, N or S are easily exchangeable with hydrogen atoms from (polar) solvents (Bonhoeffer and Brown 1933; Gold and Satchell 1955). Carbon-bound hydrogen atoms preserve the isotopic signature originally imprinted during synthesis reactions with the exception of H atoms bound to enol tautomers (see e.g. Zhang et al. 1993).

**Table 8.2** Masses and abundances of the twelve isotopocules of nitrous oxide assuming random distribution (without mass selective processes). Proportional abundances of the isotopocule N<sub>2</sub>O molecules have been calculated using the natural abundances of the nitrogen (<sup>14</sup>N 99.636 and <sup>15</sup>N 0.0364%) and oxygen isotopes (<sup>16</sup>O 0.99757, <sup>17</sup>O 0.00038 and <sup>18</sup>O 0.00205%) given by IUPAC (2018)

Mass	Isotopocule	Proportional abundance
44	<sup>14</sup> N <sup>14</sup> N <sup>16</sup> O	$9.90 \times 10^{-1}$
45	<sup>14</sup> N <sup>15</sup> N <sup>16</sup> O	$3.62 \times 10^{-3}$
45	<sup>15</sup> N <sup>14</sup> N <sup>16</sup> O	$3.62 \times 10^{-3}$
45	<sup>14</sup> N <sup>14</sup> N <sup>17</sup> O	$3.77 \times 10^{-4}$
46	<sup>15</sup> N <sup>15</sup> N <sup>16</sup> O	$1.32 \times 10^{-5}$
46	<sup>14</sup> N <sup>15</sup> N <sup>17</sup> O	$1.38 \times 10^{-6}$
46	<sup>15</sup> N <sup>14</sup> N <sup>17</sup> O	$1.38 \times 10^{-6}$
46	<sup>14</sup> N <sup>14</sup> N <sup>18</sup> O	$2.04 \times 10^{-3}$
47	<sup>15</sup> N <sup>15</sup> N <sup>17</sup> O	$5.03 \times 10^{-9}$
47	<sup>14</sup> N <sup>15</sup> N <sup>18</sup> O	$7.43 \times 10^{-6}$
47	<sup>15</sup> N <sup>14</sup> N <sup>18</sup> O	$7.43 \times 10^{-6}$
48	<sup>15</sup> N <sup>15</sup> N <sup>18</sup> O	$2.72 \times 10^{-8}$

### 8.2.3 Clumped Isotopes

Molecules containing more than one heavy isotope (multiply-substituted isotopocules) are labeled as showing the “clumped isotopes” effect. For molecules with “clumped isotopes” the chemical bonds between the heavy isotopes are the focus. Due to their often low isotopic abundances, these molecules usually are difficult to observe in tree rings. Interestingly, the analysis of clumped isotopes in methoxy groups extracted from organic material was recently shown by Lloyd et al. (2018, 2021). This opens a door for possible applications of “clumped isotopes” in methoxy groups of lignin extracted from tree rings.

The stochastic proportional abundance (Table 8.2) of the ‘clumped isotopocules’ of nitrous oxide can be calculated using the known numbers for the natural abundance of the nitrogen and oxygen isotopes shown in Table 8.1. In nature, the isotopocule molecules of nitrous oxide do not exhibit a stochastic distribution because of equilibrium and kinetic isotope effects influencing thermodynamic stability and/ or kinetic reaction rates of the involved synthesis or degradation reactions of each isotopocule showing “clumped isotopes”.

## 8.3 Notation and Measurement Units

### 8.3.1 Atom Fraction

Abundances of isotopes should be reported in terms of atom fraction ( $x$ ). The new term atom fraction is compatible with the International System of Units (SI) and should replace the old term atom percent (atom %). For example, the <sup>13</sup>C fraction of

a substance A is given by:

$$x(^{13}\text{C})_A = \frac{n(^{13}\text{C})_A}{n(^{13}\text{C})_A + n(^{12}\text{C})_A} \quad (8.1)$$

where  $n$  = amount of  $^{13}\text{C}$  or  $^{12}\text{C}$  atoms in substance A<sup>7</sup>. Atom fraction is a dimensionless quantity (Coplen 2011); therefore, a specification of results in form of a relative indication in per cent<sup>8</sup> is possible (see Table 8.1 with estimates of the natural isotopic abundances given in relative form in per cent).

### 8.3.2 Isotope Delta

The measurement of the absolute isotopic abundances of the bioelements is too labor-intensive, error-prone and costly relative to used methods and techniques to perform it on a daily basis (Nier 1946; De Bièvre et al. 1996). In contrast, the “simultaneous” measurement of isotope ratios<sup>9</sup> (e.g.  $^{13}\text{C}/^{12}\text{C}$ ) of a sample relative to that of a standard with an isotope ratio mass spectrometer allows a high-precision determination (error cancelling; Nier 1946; Werner and Brand 2001; Brand 2004).

Changes of isotope ratios through natural processes are very small and the isotope ratios generally vary only at the third decimal place or beyond. To better illustrate changes in isotope ratios caused by natural processes, the term ‘isotope delta’ (relative isotope-ratio difference; Coplen 2011) has been accepted showing the difference of the sample isotope ratio from the standard one. The isotope delta was first formally defined by McKinney et al. (1950). Meanwhile the definition of the isotope delta was made compatible (see Coplen 2011) to the requirements of the International System of Units (SI). Equations (8.2a and 8.2b) show the isotope delta formula (in the two common notations) applied for stable carbon isotopes (i.e.  $\delta^{13}\text{C}$ ).

$$\delta^{13}\text{C}_{\text{VPDB}} = \frac{{}^{13}R_{\text{Sample}} - {}^{13}R_{\text{VPDB}}}{{}^{13}R_{\text{VPDB}}} \quad (8.2a)$$

$$\delta^{13}\text{C}_{\text{VPDB}} = \frac{{}^{13}R_{\text{Sample}}}{{}^{13}R_{\text{VPDB}}} - 1 \quad (8.2b)$$

<sup>7</sup>  $^{14}\text{C}$  is neglected due to very low natural abundance.

<sup>8</sup> It is recommended to use ‘per cent’ in the text of manuscripts and the ‘%’ sign only in tables and figures or behind numbers in the text (Coplen 2011).

<sup>9</sup> By convention the ratio is always determined as the ratio of the heavy to the light isotope (O’Neil 1986b).

$^{13}R_{\text{Sample}}$  represents the  $^{13}\text{C}/^{12}\text{C}$  ratio of the sample.  $^{13}R_{\text{VPDB}}$  is the  $^{13}\text{C}/^{12}\text{C}$  ratio of the international VPDB (Vienna Peedee Belemnite) ‘standard’,<sup>10</sup> defining the carbon isotope scale (c.f. Werner and Brand 2001; Brooks et al. Chap. 6); corresponding scale defining standards and reference materials for the bioelements can be found in Chap. 6 (Table 6.3). Up to few years ago, this equation contained an additional multiplying factor 1000 and the resulting  $\delta^{13}\text{C}$  values were written in per mill (‰) “units”.<sup>11</sup> To ensure comparability of the old and the actual valid definition of isotope delta values, it is recommended to avoid ‰ or the factor 1000 when including the isotope delta equation in manuscripts. A  $\delta^{13}\text{C}$  value of ‘ $-0.010$ ’ according to Eqs. (2a and 2b) can be also expressed as ‘ $-10$  ‰’. According to Coplen (2011), it is recommended to replace the old “traditional” ‰ sign by e.g. ‘ $10^3 \delta^{13}\text{C}$ ’ (here exemplarily shown for carbon isotopes) in tables and figures of articles and presentations. To prevent possible confusion with two otherwise identical equations differing only by multiplication with a factor of 1000, Brand and Coplen (2012) suggested the new unit ‘milli-Urey’ (mUr) replacing the old ‰.<sup>12</sup> The use of the ‰ symbol is not encouraged any further by IUPAC. Consequently, all  $\delta$  values in this chapter will be expressed in the unit ‘mUr’.<sup>13</sup>

### 8.3.3 Isotope phi

Isotope delta values can be added or subtracted linearly allowing the use in mass balance equations or correction procedures for (analytical) blanks. This is strictly valid only in the natural isotopic abundance range of  $^{13}\text{C}$ ,  $^{15}\text{N}$ ,  $^{18}\text{O}$  (and  $^{34}\text{S}$ ). For hydrogen isotopes with a wide natural range of  $\delta^2\text{H}$  values from  $-500$  to  $+300$  mUr and applications of artificially heavy isotope enriched tracer of the other isotopes (‘isotopic tracer’) it is recommended to use the phi notation in mass balance equations ( $\Phi$  defined in Eq. 8.3 exemplarily shown for carbon isotopes) instead of  $\delta$  values (Corso and Brenna 1997) because the isotope delta is not linearly connected to the isotopic abundance. Brand and Coplen (2012); Coplen (2011).

<sup>10</sup> VPDB is not a physical existing standard; the VPDB scale can be traced back to the now exhausted carbonate standard PDB and the  $^{13}\text{C}/^{12}\text{C}$  and  $^{18}\text{O}/^{16}\text{O}$  ratios of VPDB are now defined via NBS 19 reference material.

<sup>11</sup> The official diction for “‰” is ‘per mill’ and not ‘per mil’, ‘permil’ or ‘per mille’ (International Organization for Standardization 1992). But keep in mind, ‘per mill’ is a fraction or comparator sign and not a true unit. The extraneous factor 1000 is not permitted in quantity equations (Coplen 2011).

<sup>12</sup> Especially as the original isotope delta equation with the factor 1000 was introduced to avoid giving results with several decimal places.

<sup>13</sup> The term ‘mUr’ can be used for all isotope scales of the bioelements. A  $\delta$  value of 1 ‰ in the old form (McKinney et al. 1950) corresponds to 0.001 (“modern”  $\delta$  equation according to Coplen 2011) and 1 mUr (Brand and Coplen 2012).

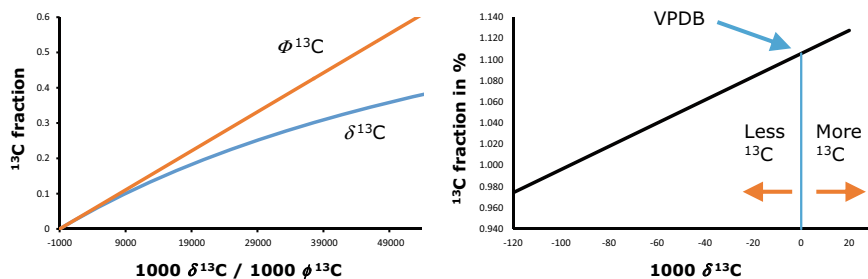


**Fig. 8.6** Left side:  $\delta^{13}\text{C}$  versus  $\phi^{13}\text{C}$  values in dependence of  $^{13}\text{C}$  atom fraction:  $\phi^{13}\text{C}$  values show a perfectly linear connection to  $^{13}\text{C}$  atom fraction whereas  $\delta^{13}\text{C}$  values do not. Right side: For carbon isotope ratio measurements the international scale-defining standard is VPDB with an accepted  $^{13}\text{C}/^{12}\text{C}$  ratio of  $11180.2 \times 10^{-6}$  (Zhang and Li 1990 cited in Werner and Brand 2001). VPDB is a virtual standard (based on exhausted carbonate standard PDB) and defined via NBS 19 reference material

$$\phi^{13}\text{C} = \frac{\delta^{13}\text{C}}{^{13}R_{\text{Sample}} + 1} \quad (8.3)$$

The  $^{13}R_{\text{Sample}}$  needed to calculate  $\phi^{13}\text{C}$  values can be derived from Eq. 8.2b.

In Fig. 8.6 the relationship between ‘isotope delta’ values, ‘isotope phi’ values and corresponding ‘atom fraction’ values is exemplarily shown for carbon isotopes.

A sample that contains relatively more  $^{13}\text{C}$  than the standard, is enriched in  $^{13}\text{C}$  relative to the standard and will therefore show more positive or higher  $\delta^{13}\text{C}$  values relative to the standard. In contrast samples with relatively less  $^{13}\text{C}$  as compared to the standard will be depleted in  $^{13}\text{C}$  relative to the standard and correspondingly will have more negative or lower  $\delta^{13}\text{C}$  values than the standard (Fig. 8.6 right side). The isotope delta value of the scale-defining standard is per definition set to zero ( $0.000 = 0\text{‰} = 0 \text{ mUr}$ ) on all the corresponding isotope scales. Per definition (see Eqs. 8.2a and 8.2b) the minimum  $\delta^{13}\text{C}$  value is  $-1000 \text{ mUr}$ . A special feature of the international carbon isotope scale with the virtual VPDB standard is its relatively high  $^{13}\text{C}/^{12}\text{C}$  ratio with the consequence that nearly all natural organic carbonaceous material is  $^{13}\text{C}$  depleted relative to VPDB and will therefore show negative  $\delta^{13}\text{C}$  values.

**Table 8.3** Selected properties of the water isotopologue  $^2\text{H}_2\text{O}$  in relation to  $\text{H}_2\text{O}$ . Data from Krumbiegel (1970)<sup>15</sup>

Property	$\text{H}_2\text{O}$	$^2\text{H}_2\text{O}$	Difference (%)
Molecular weight in g/mol	18.01558	20.02823	11.2
Melting point in °C, 1013.25 hPa	0	3.813	1.4 <sup>a</sup>
Boiling point in °C, 1013.25 hPa	100	101.43	0.4 <sup>a</sup>
Vapor pressure in hPa, 20 °C	23.38	20.32	-13.1
Vapor pressure in hPa, 100 °C	1013.25	962.05	-5.1
Density in g/mL 20 °C	0.998232	1.10536	10.7
Ionic product 25 °C in mol <sup>2</sup> /L <sup>2</sup>	$1.01 \times 10^{-14}$	$1.38 \times 10^{-15}$	-86.3
Solubility of NaCl, 25 °C in g salt / 100 g water	35.92	30.56	-14.9

<sup>a</sup>Relative to 0 K (-273.15 °C)

## 8.4 Properties of Isotopes

The term mass-dependent<sup>14</sup> ‘isotope effect’ in a wider sense describes small changes in physical and/ or chemical properties of isotopic atoms of elements and/ or of isotopocules caused by differences in nuclear mass. The following chapters deal exclusively with mass-dependent isotope effects.

### 8.4.1 Isotope Effects—Physical Effects

The mass variance of isotopic atoms and/or isotopocule molecules can influence their physical properties. Isotopes of the same element may be separated using physical processes like diffusion, fractional distillation, centrifugation, electrolysis etc. The large relative mass difference of hydrogen isotopes in the water molecule as an example is responsible for the considerable differences in vapor pressure, melting and boiling points of normal  $\text{H}_2\text{O}$  and  $^2\text{H}_2\text{O}$  (Table 8.3), but obviously has no significant influence on the organoleptic tasting of both water samples (Urey and Failla 1935). The different water isotopologues also have different molar volumes ( $^2\text{H}_2\text{O} > \text{H}_2^{16}\text{O} > \text{H}_2^{18}\text{O}$ ; Jancsó 2011). The crossover of the lighter water molecules from liquid to gaseous phase is facilitated in contrast to the heavier ones. Physical processes with

<sup>14</sup> Mass dependent isotope effects on physical processes and/or (bio)chemical reactions lead to changes in isotope ratios between reactant(s) and product(s) with the size of the change being proportional to the relative difference in mass between the isotopes. Non-mass-dependent isotope fractionation (e.g. Thieme 2006) often occurs in high energy systems (e.g. ozone formation by photolysis or electrical discharge).

<sup>15</sup> See similar data collection by Horita and Cole (2004), Jancsó (2011), Brand and Coplen (2012) and Haynes et al. (2014) and [https://water.lsbu.ac.uk/water/water\\_properties.html](https://water.lsbu.ac.uk/water/water_properties.html) (December 2021).

phase transitions (e.g. evaporation or condensation of water molecules) are known to be (partly) ‘isotope-selective’ and can be used for example to enrich heavier water isotopocules in the liquid phase. Similarly, heavier isotopocule molecules will be enriched in the solid phase (‘isotopically enriched’) during a phase transition between solid and liquid phase.

Other examples for ‘isotope-selective’ physical processes are a.o. diffusion and deflection in magnetic fields. Having the same kinetic energy  $E_{kin}$  (in the gas phase at a given temperature, Eqs. 8.4 and 8.5), heavier isotopologues (with  $m_h$ ) will show a smaller average velocity  $v$  (White 2015) in contrast to lighter isotopologues (with  $m_l$ ) when diffusing along a concentration gradient into a low-pressure system (Young et al. 2002). The basis for the measurement of isotope ratios by isotope ratio mass spectrometry (IRMS) is also the behavior of ionized isotopologue molecules in a magnetic field. The radius of deflection ( $r$ ) of the accelerated ions generated from the isotopologue molecules in the magnetic field can be described by the Eq. (8.6) with  $m$  = mass of the ion,  $e$  = electric charge unit,  $B$  = magnetic field strength and  $U$  = acceleration voltage (e.g. Ardenne 1944; Love 1973).

$$E_{kin} = 1/2m_l v_l^2 = 1/2m_h v_h^2 \quad (8.4)$$

$$\frac{v_l}{v_h} = \sqrt{\frac{m_h}{m_l}} \quad (8.5)$$

$$r = \frac{1}{B} \sqrt{\frac{2mU}{e}} \quad (8.6)$$

The mass of the ion is proportional to the square radius of deflection of the ion in the magnetic field of an isotope ratio mass spectrometer.<sup>16</sup>

### 8.4.2 Isotope Effects—Chemical Effects

Chemistry textbooks teach that isotopes of an element have identical chemical properties because the chemical ‘reactivity’ of atoms and molecules is determined by the electrons in the outermost shell (i.e. valence electrons) of the atom(s). These electrons participate in the formation (or cleavage) of chemical bonds between different atoms. Isotopes of the same element have the same number of electrons in the same electron shell; therefore also isotopocules have the same electron bonding system. But isotopes of an element do not behave like identical twins. The type of the chemical ‘behavior’ is nearly identical, but the rate of kinetic reactions and/or the position of the chemical equilibria of certain thermodynamic reactions can be ‘isotope-selective’.

<sup>16</sup> An isotope enrichment method by electromagnetic separation has been used for enrichment of <sup>235</sup>U for the Manhattan Project (development of the Hiroshima bomb), starting in 1942 in Oak Ridge, TN, USA (Groves 1962; Love 1973).

Chemical reactions of isotopocule molecules are qualitatively equal but can be quantitatively different (c.f. Hoefs 2018). Different nuclear mass (and increasing nuclear volumes) of the isotopes will influence the intramolecular binding forces and therefore lead to a shift of lines in e.g. Raman and IR spectra of isotopocule molecules due to affecting the frequencies of the vibrational modes of a molecule (“isotopic shift”). Molecules in which positions are substituted with heavy isotopes (isotopic substitution) are more stable and more energy (‘bond-dissociation energy’) is needed to cleave a covalent bond homolytically<sup>17</sup> between atoms when heavier isotopes are involved. This implies that covalent chemical bonds between  $^{12}\text{C}-^1\text{H}$  are weaker and easier to split than between  $^{13}\text{C}-^1\text{H}$  or  $^{12}\text{C}-^2\text{H}$  (even more energy would be needed for  $^{13}\text{C}-^2\text{H}$ ). The cleavage reaction of bonds between lighter isotopes normally will also have a higher reaction velocity. Correspondingly, higher energy (‘bond enthalpy’) is released during bond formation with heavier isotopes.

According to the IUPAC Gold Book<sup>18</sup> the term ‘isotope effect’ (IE) is defined more scientifically as the “effect on the rate or equilibrium constant of two reactions that differ only in the isotopic composition of one or more of their otherwise chemically identical components”. Effects on rate constants are known as ‘kinetic isotope effects’ (KIE); effects on equilibrium constants are designated as ‘thermodynamic’ or ‘equilibrium isotope effects’ (EIE). The isotope effect is mathematically expressed as the ratio of the rate constants (in case of KIE) or equilibrium constants (in case of EIE) of the respective reaction; both exemplarily shown for carbon isotopes (after Coplen 2011):

$$^{13}\text{KIE} = ^{12}\text{k}/^{13}\text{k} \quad (8.7)$$

$$^{13}\text{EIE} = ^{12}\text{K}/^{13}\text{K} \quad (8.8)$$

Cautionary note: in other science fields  $^{13}\text{KIE} = ^{13}\text{k}/^{12}\text{k}$  and  $^{13}\text{EIE} = ^{13}\text{K}/^{12}\text{K}$  is used rather than Eqs. (8.7) and (8.8).  $^{12}\text{k}$  and  $^{13}\text{k}$  are the rate constants and  $^{12}\text{K}$  and  $^{13}\text{K}$  the equilibrium constants for reactions involving  $^{12}\text{C}$  and  $^{13}\text{C}$  isotopocules, respectively. According to Eq. (8.7) KIEs larger than 1 are termed ‘normal’ and smaller than 1 are called ‘inverse’. Isotope effects related to the atoms (as part of molecules) directly taking part in bond formation or cleavage are named ‘primary IE’; IE related to more remote atoms or molecule positions are designated as ‘secondary’. Furthermore, the bond formation or split can be in the rate-determining step (KIE) or pre-equilibrating step (EIE). Secondary IE are typically smaller than primary IE and the dimension is usually dependent also on the distance of the respective atom or molecule position from the site of bond formation or cleavage (secondary IE in  $\alpha$  position > secondary IE in  $\beta$  position and so on, relative to the positions directly involved in bond cleavage or bond formation; Van Hook 2011). Isotope effects caused

<sup>17</sup> During a homolytic bond cleavage the shared electrons of the chemical bond to be split will be divided equally between the binding partners.

<sup>18</sup> IUPAC Gold Book: Compendium of Chemical Terminology <https://goldbook.iupac.org/> (December 2021).



by the isotopic substitution of elements heavier than hydrogen ( $^1\text{H}$ ,  $^2\text{H}$ ,  $^3\text{H}$ ) can be named ‘heavy atom isotope effects’. Substrates with equivalent molecule positions (two or more identical functional groups) can be subject to ‘intramolecular IEs’ (e.g. decarboxylation reaction of carboxylic acids with two or more carboxyl groups, e.g. Yankwich and Belford 1954). Isotope effects often influence only the isotope ratio of a specific position in a molecule (‘position-specific’ or ‘site-specific’ isotope effect); a corresponding site-specific isotope ratio analysis (“isotopomer analysis”) can be performed by quantitative NMR or by IRMS coupled to chemical degradation of the chemical molecules in question. This has been shown by measuring site-specific  $\delta^{13}\text{C}$  values of all six carbon positions of glucose with IRMS by Rossmann et al. (1991) and with NMR by Gilbert et al. (2012); c.f. a recent review by Gilbert (2021). EIEs can be larger or smaller than unity depending on the potential enrichment of the heavier isotope in reactant(s) or product(s). Solvent isotope effects<sup>18</sup> are either KIEs or EIEs caused by changes of the isotope ratio of the solvent<sup>19</sup>.

In the following the physicochemical basics of the theory of (kinetic and equilibrium) isotope effects will be discussed briefly. A more detailed discussion of the theoretical background of isotope effects as origin of isotope fractionation has been provided by a.o. Bigeleisen and Goepfert-Mayer (1947), Urey (1947) and Bigeleisen (1965) for equilibrium isotope effects and by Bigeleisen and Wolfsberg (1958), Saunders (1966) and Wolfsberg et al. (2010) for kinetic isotope effects.

#### 8.4.2.1 Fundamentals of Mass-Dependent Isotope Fractionation in Chemical Reactions

Atoms in molecules are in constant movement (in translational, rotational and vibrational mode). Translational and rotational motions are of minor relevance for chemical isotope effects (Hoefs 2018) as they have limited effect on intramolecular bonds. Only (intramolecular) vibrations are influencing the atomic distances of chemical bonds in molecules. The energy at a specific quantum level  $n$  ( $E_n$ ) associated to these stretching and bending (deformation) vibration modes<sup>20</sup> of the bond in question according to the quadratic harmonic oscillator approximation (see text below

---

<sup>19</sup> Solvent molecules can interact in(bio)chemical reactions mostly in three ways: (1) Solvent molecules can be reaction partners (direct participation of water molecules, e.g. as  $\text{H}_2\text{O}$  or  $\text{H}_3\text{O}^+$  in hydrolysis reactions interacting with reactant state, transition state and/or product state of the reaction; Schowen 2007). (2) Protic solvents can modify properties of involved reaction partners by exchanging (hydrogen) isotopes with reactants, products and/or involved enzymes possibly affecting enzyme activity and structure (Fitzpatrick 2015). (3) Solvent–solute interactions are known to stabilize the transition state of a reaction by influencing both, the free energy of the transition state and the activation energy of the specific reaction. The extent and nature of these interactions can be influenced by the isotope ratio of the used solvents (Smith 2013, p. 288).

<sup>20</sup> Depending on the degrees of freedom polyatomic molecules can show vibration modes influencing the length of a specific chemical bond (stretching mode) in the molecule or vibration modes that are related to the change in the angle between two bonds in the molecule. All these vibration modes influence the inner energy of the molecule. Asymmetric or symmetric stretching is important for the splitting (and formation) of that specific bond.

and Fig. 8.7) is:

$$E_n = (n + 1/2)hv \quad (8.9)$$

where  $h$  is the Planck constant,  $n = \text{vibrational quantum number}$  (0 plus positive integers) and  $\nu$  the vibrational frequency. The origin of isotope effects can be attributed to the dependence of the vibration frequency on the reduced mass ( $\mu$ ) of the binding partners and a molecule-specific force constant  $k$  of the bond involved (Eq. (8.10), analogous to the spring constant in Hooke's law). The force constant is identical for isotopologue molecules (Fujii et al. 2009) and the potential energy surface (Fig. 8.7)

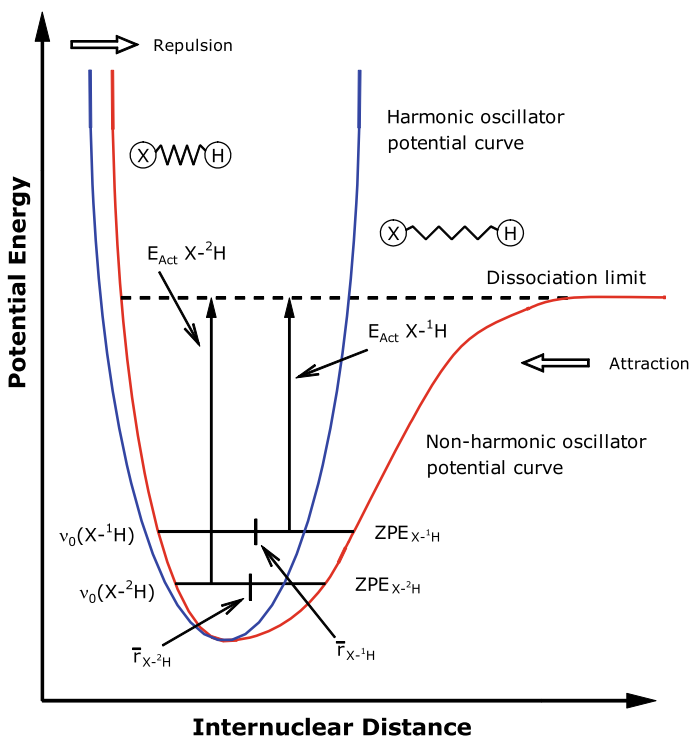


**Fig. 8.7** Schematics of a potential energy curve for the diatomic molecule X–H, adapted and modified from Vogel and Houk (2019). Blue line represents the quantum harmonic oscillator energy well; whereas the red line shows the more realistic anharmonic oscillator (Morse potential).  $E_{\text{Act}}$  = activation energy needed to drive the corresponding bond to the dissociation limit (splitting of the chemical bond). ZPE = zero-point energy, corresponds to the energy at the lowest vibrational level  $\nu_0$ . The anharmonic oscillator shows the minimum and maximum position (left and right side of the red line) of the H atom relative to the X atom positioned at 0 distance symbolized by the “two balls - spring model”. Consequently, the difference from the X atom to the  $X-^1\text{H}$  and  $X-^2\text{H}$  marks in the horizontal ZPE lines corresponds to the average bond lengths of the  $X-^1\text{H}$  or  $X-^2\text{H}$  bond. The bond involving  $^2\text{H}$  is shorter than the bond with  $^1\text{H}$  (Vogel and Houk 2019)

is then essentially independent from isotopic substitution (Bennet 2012).

$$v = \frac{1}{2\pi} \sqrt{\frac{k}{\mu}} \quad (8.10)$$

Key influencing factor on the vibrational frequency is then the reduced mass  $\mu$  (Eq. 8.11) of the two bonded atoms. Increasing reduced mass  $\mu$  lowers the vibration frequency  $v$ . According to Young et al. (2002) the reduced mass is relevant for bond-breaking reactions, whereas molecular or atomic mass is relevant for transport processes.

$$\mu = \frac{m_1 \times m_2}{m_1 + m_2} \quad (8.11)$$

The reduced mass  $\mu$  is increasing with increasing mass  $m$ . Substituting one of the bonding partners in a molecule with a heavy isotope will change neither nuclear charge, nor electron distribution in the molecule nor the potential energy curve of the “isotopic” molecule. But the vibrational frequency of a bond and the average bond length will be influenced (Vogel and Houk 2019). This is best shown schematically in Fig. 8.7 by drawing the potential energy of the most simple example, a diatomic molecule (X–H) in dependence to the internuclear distance in the molecule (potential energy surface). This course of the potential energy relative to the internuclear distance can be either modeled by the quantum harmonic oscillator (blue line in Fig. 8.7) or by the more realistic Morse potential (red line in Fig. 8.7) that includes a.o. corrections for anharmonicity of real chemical bonds. The anharmonic oscillator postulates different average bond lengths for e.g. X-<sup>1</sup>H and X-<sup>2</sup>H bonds (Vogel and Houk 2019). The two bonded atoms influence each other by repulsive and attractive forces, building an average bond length between them. In Fig. 8.7 the X atom would be near the vertical axis and the bonded H atom then would vibrate following the black horizontal lines (either at  $v_0(\text{X-}^1\text{H})$  or  $v_0(\text{X-}^2\text{H})$  depending on the isotopic mass of the H atom) represented by the two end positions of the “two balls—spring model” as an analogue for the chemical bond in the diatomic molecule shown in Fig. 8.7 (Mook 2001). The red line models the minimum potential energy in dependence of the internuclear distance (*energy well* or *potential well*) between the two atoms. The energy of such a system at the lowest vibrational energy level (ground state  $n = 0$ ; at room temperature the majority of the molecules are in vibrational ground state) is defined as zero-point energy (ZPE) corresponding to the energy of the respective system at 0 K (−273.15 °C). The energy level of the atom in the energy well (the bottom of the well will not be reached even at 0 K) is then depending on its mass and is labelled as  $\text{ZPE}_{\text{X-}^1\text{H}}$  and  $\text{ZPE}_{\text{X-}^2\text{H}}$  in Fig. 8.7. To reach the dissociation limit with the effect to split the X–H bond, a certain amount of (kinetic) activation energy ( $E_{\text{Act}}$ ) has to be applied. Correspondingly, this energy (‘bond enthalpy’) will be released during the bond formation process. Bonds with heavier isotopes show lower vibrational frequencies and therefore will have a lower ZPE. The heavier hydrogen isotope

is located at a lower level in the energy well than the lighter hydrogen isotope and needs therefore more energy (higher activation energy) to leave the chemical bond, which means, that it has a higher bond enthalpy.

To summarize the above: Chemical bonds with heavier isotopes have a lower vibrational frequency as compared to lighter ones. Therefore chemical bonds with heavier isotopes have a lower ZPE. Consequently, more energy (higher activation energy  $E_{\text{Act}}$ ) is needed to cleave bonds with heavier isotopes (Fig. 8.7), and formation of bonds with heavier isotopes will then also release more energy (bond enthalpy) and are stronger. Therefore, heavier isotopocules are more stable than light isotopocules.

#### 8.4.2.2 Thermodynamic or Equilibrium Isotope Effects for Reversible Reactions at Equilibrium

Reversible chemical reactions approach equilibrium with the consequence that forward and backward reaction then occur simultaneously and at chemical equilibrium also with equal rates. The concentration of reactants and products will change until a chemical equilibrium is established. Such reversible reactions can be described with equilibrium constants. In many cases also the position of the equilibrium in such reversible reactions is ‘isotope-selective’. Reactants and products are then also ‘isotopically’ different. Such isotope exchange reactions tend to reach additionally an isotopic equilibrium. In these isotopic exchange reactions two different chemical structures in which the isotopes of the element in question are bonded in different ways are connected to each other. The distribution of the isotopes between the two structures in this system will occur ensuring that the free energy of the total system is at the minimum in equilibrium conditions (White 2015).

It can then be deduced that in a chemical and isotopic equilibrium<sup>21</sup> the heavier isotope will concentrate at the molecular site where it is bonded stronger (Fig. 8.8). A measure for the bond strength is the force constant  $k$  from Eq. (8.10). The force constant  $k$  in the harmonic oscillator model is independent from the nuclear masses of the isotopic bond partner (Fujii et al. 2009) and is directly proportional to the strength of the vibrating chemical bond. The small difference in ZPEs between the isotopologue molecules drives the isotopic exchange reaction; the size of  $\Delta\text{ZPE}$  is controlling the isotope effect. The extent of equilibrium isotope fractionation is mostly decreasing with increasing temperature (c.f. O’Neil 1986a; Hoefs 2018). The heavy isotope is usually concentrated in the molecule or ion with the more constrained site (O’Leary et al. 1992), the chemical structure in which the element in question is “bound most strongly” (Bigeleisen 1965). The heavy isotopes can preferentially be found in chemical structures connected to strong and short chemical

---

<sup>21</sup> The free energy change (standard Gibbs energy change  $\Delta G^0$ ) for such an isotope exchange reaction typically is relative small (e.g.  $\sim -5$  J/mole for the oxygen isotope equilibrium between  $\text{H}_2\text{CO}_3/\text{H}_2\text{O}$  at pH 0, whereas the free energy of the hydration of  $\text{CO}_2$  at same pH is around  $-17$  kJ/mole; Usdowski and Hoefs 1993). Therefore it can be assumed that chemical systems in isotopic equilibrium are also in chemical equilibrium. But see Schimerlik et al. (1975) and footnote 26.

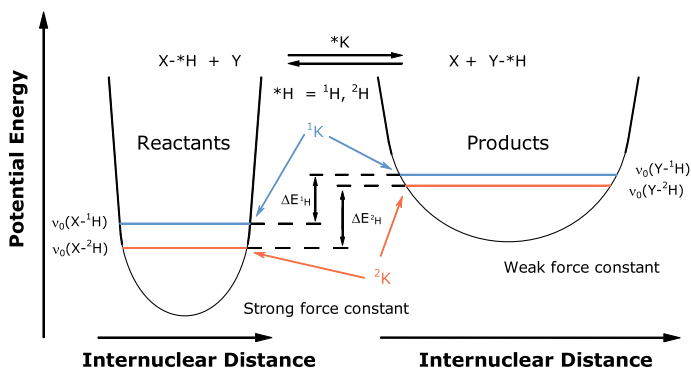


**Fig. 8.8** Schematics of the potential energy curves (illustrating the harmonic oscillator curves only) for a reversible reaction between reactant(s) and product(s), approaching isotopic (and chemical) equilibrium (adapted and modified from Vogel and Houk 2019). A strong (stiff) X–H bond in the reactant is exchanged with a weak Y–H bond in the product. The difference  $\Delta E_{\text{H}}^1$  ( $ZPE_{\text{Y-}^1\text{H}} - ZPE_{\text{X-}^1\text{H}}$ ) is smaller than the difference  $\Delta E_{\text{H}}^2$  ( $ZPE_{\text{Y-}^2\text{H}} - ZPE_{\text{X-}^2\text{H}}$ ). This will lead to a normal equilibrium isotope effect with  ${}^1K > {}^2K$  and following  ${}^1K/{}^2K > 1$  (Vogel and Houk 2019)

bonds showing higher bond enthalpy (higher bond stiffness—the oscillator with the highest frequency; Bigeleisen 1965; Vogel and Houk 2019; Fig. 8.8). The bond stiffness is related to the force constant  $k$  in Eq. (8.10). A strong bond corresponds to a force constant with a high value and vice versa. In summary, heavy isotopes are concentrated in chemical structures which have the more constrained environment with bonds with the highest stiffness (low-energy systems having most stable bonds). Usually for carbon isotopes, the chemical state with four bonds is preferred under equilibrium conditions: Bicarbonate is  $^{13}\text{C}$  enriched relative to  $\text{CO}_2$  and carboxyl groups in organic acids are enriched in  $^{13}\text{C}$  relative to  $\text{CO}_2$  (O’Leary et al. 1992). In the review article by Rishavy and Cleland (1999) many isotope fractionation factors for (organic) molecules are tabulated.

#### 8.4.2.3 Kinetic Isotope Effects on Unidirectional (One-Way) or Irreversible Reactions

The progress of a kinetically controlled chemical reaction can be characterized by showing the energy profile along the reaction coordinate<sup>22</sup> during transformation of reactant(s) to product(s). The reaction coordinate connects the reactant(s) and product(s), both at local energy minima via an intermediary transition state at maximum energy (Fig. 8.9). Reactants are separated from the products by a potential wall; the transition state correspond to the highest potential energy on the reaction

<sup>22</sup> According to Van Hook (2011) the reaction coordinate describes the progress through the respective chemical reaction. The reaction coordinate thereby displays the reaction path at minimum energy level between the reactant(s) and product(s), both shown as (local) energy minima.

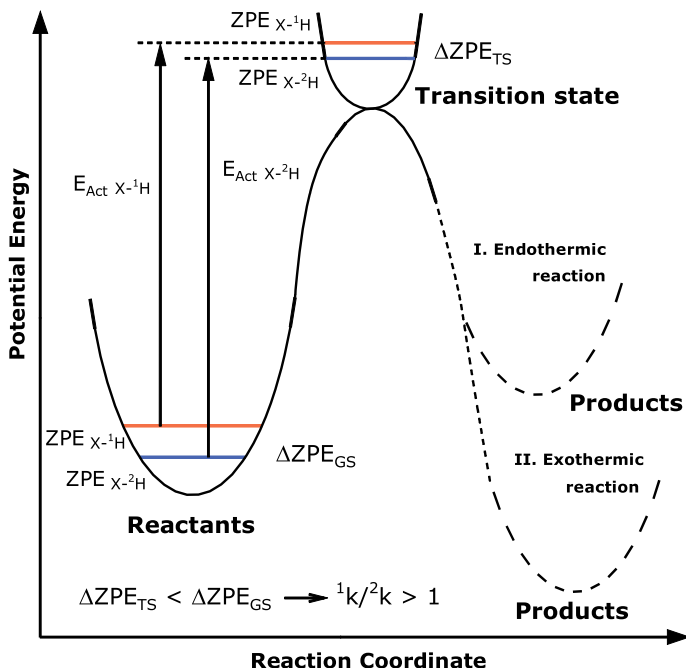


**Fig. 8.9** Schematics of a potential energy diagram (potential energy following the reaction coordinate<sup>22</sup>) of a hypothetical reaction (X-H cleavage) from the ground state (GS) via the transition state (TS) to the product state. The activation energy ( $E_{\text{Act}}$ ) of the X-<sup>2</sup>H bond between GS and TS is higher than the corresponding activation energy of the X-<sup>1</sup>H bond describing a reaction with normal kinetic isotope effect. The reaction can be either endothermic or exothermic. Scheme modified after Bennet (2012)

coordinate. Ground state (reactants) and activated transition state (TS) are in equilibrium, whereas the further reaction path from transition state to the product(s) is irreversible. The total reaction can be exothermic thereby releasing energy from the system to the environment during the reaction or endothermic with the need to absorb energy from the environment. Figure 8.9 illustrates the change of the potential energy surface of a homolysis<sup>17</sup> reaction (X-H bond) from the initial (ground) state via the transition state towards the products along the reaction coordinate. Both ground state and transition state of a reaction can be characterized by vibrational modes with associated ZPEs. The corresponding activation energies of the reactants are primarily determining the extent of the kinetic isotope effect. As stated above, chemical bonds with heavier isotopes have lower vibrational frequencies and a lower ZPE than bonds in the lighter isotopologues. These bonds are therefore located deeper in the potential energy surface (as can be seen in Fig. 8.7). Consequently, a higher activation energy is needed to reach the transition state (or the dissociation limit) of the respective chemical bond. This corresponds also to a slower reaction rate. In case of a 'normal' hydrogen isotope effect the difference in ZPEs of the isotopologue

molecules in the transition state is lower than the corresponding difference in ground state ( $\Delta ZPE_{TS} < \Delta ZPE_{GS}$ ; Wolfsberg et al. 2010) because of and due to the different activation energies between the C-<sup>1</sup>H and C-<sup>2</sup>H bond.

To summarize: Bonds with heavier isotopes vibrate at lower frequency and have therefore a lower ZPE. This implies a higher activation energy for the specific chemical bond in the heavy isotopologue to approach a transition state or the dissociation limit of the bond in question. Heavier isotopologues are more stable and correspondingly react more slowly as compared to lighter isotopologues (Elsner 2010). This results in lower turnover rates causing (normal) isotope fractionation in irreversible or one-way reactions without complete turnover of reactants to products (non-quantitative reaction). Kinetic isotope effects are depending on the mechanism of the involved (bio)chemical reaction and are therefore an effective instrument to get insights in (enzyme) reaction mechanisms (e.g. Elsner and Hofstetter 2011).

## 8.5 Isotope Fractionation

**Isotope effects** on (chemical) reactions are physical phenomena which cannot be directly measured by itself, but can lead to observable **isotope fractionation** (partial isotopic separation) between products and reactants in case of a non-quantitative turnover or a (quantitative) allocation of the isotopic composition of e.g. one reactant to two or more products. To get a KIE (or EIE) expressed in form of an isotope fractionation in reaction networks needs branching points involved (e.g. Hayes 2001; Schmidt et al. 2015). Isotope effects on enzyme reactions normally are position-specific (site-specific) thereby influencing the isotope ratio of one specific molecule position. The relative isotopic abundance (and the corresponding atom weight) of chemical compounds and biological materials are not precisely constant at a local scale. Isotope effects on (bio)chemical reactions and/ or physical processes will influence the isotope ratio of involved compounds by fractionating isotopes during the reaction and/or the process. Thereby, the corresponding isotope ratio of these compounds will be changed leading to an enrichment or depletion of the relative abundance of one isotope compared to the other(s) during the chemical reaction or physical process. In the following, isotope fractionation in (bio)chemical reactions on the way from the reactant(s) to the product(s) during establishing an equilibrium in reversible reactions or in an irreversible kinetically controlled reaction will be discussed. The change in isotope ratio is proportional to the size of the involved isotope effect.

Isotope fractionation can be caused by:

- Thermodynamic or equilibrium isotope effects on reversible reactions reaching a chemical (and isotopic) equilibrium.
- Kinetic isotope effects on (irreversible) unidirectional reactions and reactions not leading to (full) chemical equilibrium.

Often the situation is more complex; there are (bio)chemical reactions (and physical processes) that are not completely unidirectional, but also a full (chemical) equilibrium is not accomplished. In such systems the net isotope fractionation can vary between the kinetic isotope fractionation of e.g. the forward reaction and an isotope fractionation near the equilibrium isotope fractionation depending on the realized ratio of forward to backward flux in relation to the equilibrium fluxes (e.g. Sade and Halevy 2017). An example for such a (physical) system combining kinetic and equilibrium isotope fractionation would be the relationship between the isotope ratios of  $\text{H}_2\text{O}(\text{l})$  and  $\text{H}_2\text{O}(\text{g})$  in an open system with liquid and gaseous water. Kinetic isotope fractionation dominates the evaporative transition of  $\text{H}_2\text{O}(\text{l})$  to  $\text{H}_2\text{O}(\text{g})$  up to the point when the vapor phase above the liquid water gets saturated, but complete irreversibility of the evaporation cannot be ensured and the proportion of incipient condensation is difficult to measure (Mook 2001). With starting saturation the kinetic isotope  $^{18}\text{O}$  depletion of  $\text{H}_2\text{O}(\text{g})$  reduces to the equilibrium one (see Chap. 10). Evaporation and condensation of  $\text{H}_2\text{O}(\text{g})$  in a closed system is then an equilibrium process (Chaps. 10 and 18). As consequence the extent of the  $^{18}\text{O}$  depletion of the  $\text{H}_2\text{O}(\text{g})$  above  $\text{H}_2\text{O}(\text{l})$  depends on the degree of saturation in the system under observation (O'Neil 1986a; Mook 2001). A plant physiological example for the combined effect of kinetic and equilibrium isotope fractionation is the  $\text{CO}_2$  exchange between leaves (stomata) and atmosphere: The oxygen isotopic information of  $\text{CO}_2$  that is back diffusing from the stomata in leaves to the atmosphere is depending on the reaction conditions of the oxygen isotope exchange reaction between leaf water and  $\text{CO}_2$  catalyzed by the enzyme carbonic anhydrase (CA) in plant leaves. Depending a.o. on the activity of CA the actual  $^{18}\text{O}$  enrichment of the  $\text{CO}_2$  from back diffusion out of the stomata can be lower as the theoretically expected equilibrium isotope enrichment in  $^{18}\text{O}$  (Gillon and Yakir 2000).

Enzyme catalyzed reactions should show identical equilibrium isotope fractionation than the not catalyzed reaction as enzymes in fact take part in the reaction but are not altering the position of the chemical and isotopic equilibrium (see e.g. Uchikawa and Zeebe 2012). Isotope fractionation by equilibrium isotope effects in multi-reaction sequences can be additive to other isotope fractionation caused either by equilibrium or kinetic isotope effects. Enzyme-catalyzed reactions often show lower kinetic isotope fractionation than their non-catalyzed analogues (O'Leary et al. 1992). Isotope fractionation caused by irreversible or unidirectional kinetically controlled reactions is often larger than related equilibrium isotope fractionation (O'Leary et al. 1992). Kinetic isotope fractionation is often related to one rate-limiting step in a chemical reaction or reaction network.

### 8.5.1 *Quantities to Express Isotope Fractionation*

The distribution of the stable isotopes between two compounds A and B can be displayed in several mathematical forms. The following equations will be exemplary for carbon isotope fractionation.



(A) The isotope fractionation factor<sup>1</sup>  $\alpha$  describes the isotopic relationship between compounds A and B that can either be in equilibrium ( $A \rightleftharpoons B$  or  $B \rightleftharpoons A$ ) or in an one-way (irreversible) relationship ( $A \rightarrow B$ ). The isotope fractionation factors for equilibrium reactions can be identified as  $\alpha_{\text{eq}}^{13}\text{C}_{A/B}$  and for kinetic reactions as  $\alpha_{\text{kin}}^{13}\text{C}_{A/B}$ .

$$\alpha^{13}\text{C}_{A/B} = \frac{{}^{13}R_A}{{}^{13}R_B} = \frac{\delta^{13}\text{C}_A + 1}{\delta^{13}\text{C}_B + 1} \quad (8.12)$$

The isotopic fractionation factor  $\alpha^{13}\text{C}_{A/B}$  can be easily determined by measuring the corresponding  $\delta^{13}\text{C}$  values of the compounds in question. It is common use to list isotope fractionation factors for isotope exchange reactions of the molecules or ions of interest relative to so called ‘reference molecules’ (Rishavy and Cleland 1999). The reference molecule for  ${}^2\text{H}/{}^1\text{H}$  and  ${}^{18}\text{O}/{}^{16}\text{O}$  systems is usually water. For  ${}^{13}\text{C}/{}^{12}\text{C}$  often (aqueous) carbon dioxide is used (Rishavy and Cleland 1999). Corresponding  $\alpha$  factors would be e.g.  $\alpha_{\text{eq}}^{13}\text{C}_{\text{HCO}_3^-/\text{CO}_2}$  for the bicarbonate/carbon dioxide  ${}^{13}\text{C}/{}^{12}\text{C}$  system and  $\alpha_{\text{eq}}^{18}\text{O}_{\text{CO}_2/\text{H}_2\text{O}}$  for the carbon dioxide/water  ${}^{18}\text{O}/{}^{16}\text{O}$  system.  $\alpha_{\text{eq}}$  Values larger than unity indicate an enrichment of the heavier isotope in the molecule or ion of interest. Values smaller than unity would show an enrichment of the heavier isotope in the corresponding reference molecule (Rishavy and Cleland 1999).

The kinetic carbon isotope fractionation factor  $\alpha_{\text{kin}}^{13}\text{C}$  is defined analogous to Eqs. (8.7) and (8.12) for the reaction  $A \rightarrow B$ ; reactant A (‘source’) is converted to product B. This mode of designation for the quantities describing isotope fractionation, especially connected to  ${}^{13}\text{C}$  fractionation during photosynthesis, is used by Farquhar et al. (1989), O’Leary et al. (1992), Hayes (2001), Fry (2006) and many others. Authors working in other scientific disciplines prefer a reciprocal diction of Eq. 8.12 with  $\alpha_{\text{kin}}^{13}\text{C}_{B/A} = (\delta^{13}\text{C}_B + 1)/(\delta^{13}\text{C}_A + 1)$  as recommended by Coplen (2011). The latter way of designation is more commonly used with hydrogen isotopes (see Hayes 2001, Sachse et al. 2012, Cormier et al. 2018 and many others).

In equilibrium reactions the isotopic fractionation factor  $\alpha$  is related to the equilibrium constant  $K$ :

$$\alpha = K^{1/n} \quad (8.13)$$

with  $n$  describing the number of atoms exchanged in the reaction. Normally reactions are written for the case  $n = 1$  (only one isotopic atom is exchanged) to keep the mathematics involved at low level (O’Neil 1986b). It is important to note that, the equilibrium constant of an isotope exchange reaction depends on how the chemical equation for the isotope exchange reaction is written (O’Neil 1986b).<sup>23</sup> This then

<sup>23</sup> As an example, the equilibrium reaction between  $\text{CO}_2$  and  $\text{HCO}_3^-$  can be written either as (i)  ${}^{13}\text{CO}_2 + {}^{12}\text{HCO}_3^- \rightleftharpoons {}^{12}\text{CO}_2 + {}^{13}\text{HCO}_3^-$  or as (ii)  ${}^{12}\text{CO}_2 + {}^{13}\text{HCO}_3^- \rightleftharpoons {}^{13}\text{CO}_2 + {}^{12}\text{HCO}_3^-$ . The corresponding isotopic fractionation factor  $\alpha$  for equilibrium (i) would be  $\alpha_{\text{eq}}^{13}\text{C}_{\text{HCO}_3^-/\text{CO}_2}$  and that for equilibrium (ii) would be  $\alpha_{\text{eq}}^{13}\text{C}_{\text{CO}_2/\text{HCO}_3^-}$ . Isotope fractionation factor  $\alpha$  from

affects the definition of EIE (Eq. (8.8)) as well as the isotope fractionation factor  $\alpha$  (leading correspondingly to values  $\alpha_{A/B} > 1$  or  $\alpha_{B/A} < 1$ , or vice versa).

(B) Isotope fractionation can also be described with the epsilon notation (previous name ‘isotopic enrichment factor’ is not biuniquely used see IUPAC Gold Book<sup>18</sup>).

$$\varepsilon^{13}\text{C}_{A/B} = \alpha^{13}\text{C}_{A/B} - 1 \quad (8.14)$$

The factor epsilon should be named ‘isotopic fractionation’ (Coplen 2011) or ‘isotope fractionation’<sup>1</sup>; a specification for equilibrium and kinetic reactions is possible. In principle  $\alpha$  and  $\varepsilon$  values can be used to describe isotope fractionation in equilibrium systems and kinetic processes with irreversible reactions.  $\varepsilon$  values can be expressed as ‘ $10^3 \varepsilon$ ’ or like the  $\delta$  values in mUr.

(C) The isotope fractionation between the two compounds A and B can be approximated as the difference of two (measurable)  $\delta$  values (shown here for two  $\delta^{13}\text{C}$  values).

$$\Delta^{13}\text{C}_{A/B} = \delta^{13}\text{C}_A - \delta^{13}\text{C}_B \quad (8.15)$$

All these quantities are related to each other by the following equation.

$$\Delta^{13}\text{C}_{A/B} \approx \varepsilon^{13}\text{C}_{A/B} = \alpha^{13}\text{C}_{A/B} - 1 \quad (8.16)$$

In geological studies “ $\ln\alpha$  values” are often used to relate (equilibrium) isotope fractionation between solids (e.g. minerals) to their formation temperature (Sharp and Kirschner 1994). The term ‘ $10^3 \ln\alpha$ ’ is indicated as ‘per mill isotope fractionation’<sup>11</sup> in prominent geological literature (Friedman and O’Neil 1977; O’Neil 1986b). This ‘per mill isotope fractionation’ is often (depending on the temperature range) a linear function of  $T^{-1}$  (low temperature processes) or  $T^{-2}$  (high temperature processes) (O’Neil 1986a; Hoefs 2018). Such resulting isotope fractionation curves can then be applied in isotope thermometry (Clayton 1981). The interrelation between the isotopic difference  $\Delta$  and  $\ln\alpha$  is shown (for  $^{13}\text{C}$ ) in equation

$$\Delta^{13}\text{C}_{A/B} \approx \ln(\alpha^{13}\text{C}_{A/B}) \quad (8.17)$$

This is mostly valid for  $\alpha$  values around 1, small numerical values for both  $\delta^{13}\text{C}_A$  and  $\delta^{13}\text{C}_B$  and for small differences between  $\delta^{13}\text{C}_A$  and  $\delta^{13}\text{C}_B$ . O’Neil (1986b)

---

(i) is the inverse of  $\alpha$  from (ii).  $\alpha_{eq}^{13}\text{C}_{\text{HCO}_3^-/\text{CO}_2} > 1$  (e.g. Marlier and O’Leary 1984) and  $\alpha_{eq}^{13}\text{C}_{\text{CO}_2/\text{HCO}_3^-} < 1$  (e.g. Mook et al. 1974), both describing the identical  $^{13}\text{C}$  enrichment of  $\alpha_{eq}^{13}\text{C}_{\text{CO}_2/\text{HCO}_3^-} < 1$  in equilibrium with  $\text{CO}_2$ . The equilibrium isotope effect ( $^{13}\text{EIE}$  in case of carbon isotopes) on an exchange reaction of one (carbon) atom as defined in eq. 8.8 is exactly the inverse of the equilibrium constant  $K$  (eq. 8.13; e.g. eq. 8.21 for the bicarbonate/carbon dioxide  $^{13}\text{C}$  exchange) and correspondingly the equilibrium isotope fractionation factor ( $\alpha_{eq}^{13}\text{C}$  in case of carbon isotopes) as defined in equation 8.12 (when the exchange reaction is written in the same direction, as discussed by Coplen 2011, p. 2549).

suggested a preferred use of the  $\ln\alpha$  values over  $\Delta$  values when either the difference  $\Delta$  or the involved  $\delta^{13}\text{C}$  values of A and B are larger than 10 mUr (see Table 8.4).<sup>24</sup>

In the scientific literature, there are different definitions available for  $\alpha$ ,  $\varepsilon$  and  $\Delta$  (e.g. Fry 2006). In disciplines like geochemistry and hydrology for example, it is more common to define  $\alpha_{\text{kin}} = \text{h}^{\text{k}}/\text{l}^{\text{k}}$  with the heavy isotope in the numerator and the light one in the denominator (e.g. Mook 2001; Harris et al. 2012). To avoid any confusion, it is recommended on the one side to carefully verify how the particular values are given in the respective source article. On the other side, a clear definition and precise wording should be provided to the reader when writing new manuscripts.

In practice, one often needs to discuss the isotopic difference between two samples for which only  $\delta$  values without information on turnover rates are available. The above mentioned quantities for isotope fractionation  $\varepsilon$ ,  $\alpha$ ,  $\ln\alpha$  and  $\Delta$  will be exemplified for the following arbitrary systems. The mode of designation for  $^{13}\text{C}$  fractionation developed above (Eqs. 8.12–8.17) has been applied:

- (I) A precursor material with a  $\delta^{13}\text{C}_{\text{Source}}$  value of  $-8.00$  mUr should be converted to a) product A with a  $\delta^{13}\text{C}$  value of  $-14.00$  mUr, b) product B with a  $\delta^{13}\text{C}$  value of  $-28.00$  mUr and c) product C with a  $\delta^{13}\text{C}$  value of  $-90.00$  mUr.
- (II) (a) A precursor material A with a  $\delta^{13}\text{C}$  value of  $-14.00$  mUr, (b) product B with a  $\delta^{13}\text{C}$  value of  $-28.00$  mUr and (c) product C with a  $\delta^{13}\text{C}$  value  $-90.00$  mUr each should be converted to a product with a  $\delta^{13}\text{C}$  value of  $-8.00$  mUr (reversed case I).

The corresponding calculated values for  $\Delta$ ,  $\ln\alpha$ ,  $\alpha$  and  $\varepsilon$  for both scenarios are presented in Table 8.4. Simply subtracting the  $\delta^{13}\text{C}$  values ( $\Delta^{13}\text{C}$ ) delivers a good approximation to the involved isotope fractionation for case Ia) with a difference ( $\delta^{13}\text{C}_{\text{Source}} - \delta^{13}\text{C}_{\text{Product}} < 10$  mUr). The difference of both  $\Delta^{13}\text{C}_{\text{Source/Product}}$  and  $\ln\alpha^{13}\text{C}_{\text{Source/Product}}$  to  $\varepsilon^{13}\text{C}_{\text{Source/Product}}$  is within the limits of the analytical error of a measurement of the  $\delta^{13}\text{C}$  value (we assume here  $\pm 0.1$  mUr for measurement with an elemental analyzer coupled to IRMS). For case Ib) with a difference of 20 mUr between  $\delta^{13}\text{C}_{\text{Source}}$  and  $\delta^{13}\text{C}_{\text{Product}}$ , the difference between  $\Delta^{13}\text{C}_{\text{Source/Product}}$  and  $\varepsilon^{13}\text{C}_{\text{Source/Product}}$  increases quite considerably, whereas the difference between  $\ln\alpha^{13}\text{C}_{\text{Source/Product}}$  and  $\varepsilon^{13}\text{C}_{\text{Source/Product}}$  would be still in the range of  $2\sigma$  (analytical error). Nevertheless, the  $\Delta^{13}\text{C}$  notation is in quite common use for estimating the photosynthetic isotope fractionation (Farquhar et al. 1989). In case Ic (with differences in  $\delta^{13}\text{C}$  of  $>20$  mUr between source and product and one of the involved  $\delta^{13}\text{C}$  values more than 10 mUr distant from the 0 mUr of the standard) only  $\alpha^{13}\text{C}$  values and/or the  $\varepsilon^{13}\text{C}$  notation should be used. In case II, it is obvious that  $\Delta$  and  $\ln\alpha$  show the same relation than in case I, except for the algebraic sign. In contrast  $\alpha^{13}\text{C}$  and  $\varepsilon^{13}\text{C}$  show always different numerical values. The  $\varepsilon^{13}\text{C}$  values for case Ia and IIa still show similar mathematical absolute values, but with increasing mathematical distance from the 0 mUr of the standard (case Ib to IIb and Ic to IIc) the absolute  $\varepsilon^{13}\text{C}$  values are getting more and more different (Table 8.4). The numerical values for

<sup>24</sup> Therefore  $\Delta$  values should not be used to describe hydrogen isotope fractionation.

**Table 8.4** Comparison of the different measures for isotope fractionation ( $\Delta$ ,  $\ln\alpha$ ,  $\alpha$  and  $\epsilon$  exemplarily shown for carbon stable isotopes) for two cases. Case II is the reversed form of case I. The  $\delta^{13}\text{C}$  and  $\Delta^{13}\text{C}$  values are given in 'mUr' corresponding to ' $10^{-3}$   $\delta$  values'. The calculated ' $\ln\alpha$  values' are presented in form of ' $\ln\alpha \times 10^3$ '. Isotope fractionation  $\epsilon$  values are given as ' $\epsilon \times 10^3$ '. In case II the sources and sinks have been exchanged relative to case I resulting in different values for  $\alpha$  and  $\epsilon$ , whereas both  $\Delta$  and  $\ln\alpha$  values have the same values except for the algebraic sign

$\delta^{13}\text{C}_{\text{Source}}$ in mUr	$\delta^{13}\text{C}_{\text{Product}}$ in mUr	$\Delta^{13}\text{C}_{\text{Source/Product}}$ in mUr	$\ln(\alpha^{13}\text{C}_{\text{Source/Product}})$ $\times 10^3$ or in mUr <sup>25</sup>	$\alpha^{13}\text{C}_{\text{Source/Product}}$	$\epsilon^{13}\text{C}_{\text{Source/Product}}$ $\times 10^3$ or in mUr
<b>I</b>					
8.00	-14.00	6.00	6.0668	1.0061	6.0852
-8.00	-28.00	20.00	20.3673	1.0206	20.5761
-8.00	-90.00	82.00	86.2785	1.0901	90.1099
<b>II</b>					
-14.00	-8.00	-6.00	-6.0668	0.9940	-6.0484
-28.00	-8.00	-20.00	-20.3673	0.9798	-20.1613
-90.00	-8.00	-82.00	-86.2785	0.9173	-82.6613

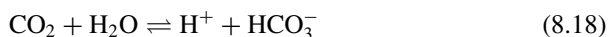
<sup>25</sup>  $\ln\alpha$  values of the examples presented in Table 8.4 (case I and case II (reversed case I) are identical except for the algebraic sign, although the  $\alpha$  values of case I and case II are different. According to the 2<sup>nd</sup> law of logarithms:  $\ln(x/y) = \ln(x) - \ln(y) = -[\ln(y) - \ln(x)] = -\ln(y/x)$ .

$\alpha^{13}\text{C}$  and  $\varepsilon^{13}\text{C}$  are depending on which mode of designation for isotope fractionation is used.  $\alpha_{\text{kin}}^{13}\text{C}$  values  $>1$  (case I) deliver positive values for  $\Delta^{13}\text{C}$ ,  $\ln\alpha^{13}\text{C}$  and  $\varepsilon^{13}\text{C}$  indicating that the products are depleted in  $^{13}\text{C}$ , whereas  $\alpha_{\text{kin}}^{13}\text{C}$  values  $<1$  (case II) lead to negative values for  $\Delta^{13}\text{C}$ ,  $\ln\alpha^{13}\text{C}$  and  $\varepsilon^{13}\text{C}$  showing an  $^{13}\text{C}$  enrichment of the products.

In special cases, a combined use of the above described quantities can be applied in scientific literature: For instance, a simple subtraction ( $\Delta$ ) of different  $\varepsilon^2\text{H}$  values was recently used to compare the different hydrogen isotopic fractionations occurring during the biosynthesis of *n*-alkanes (i.e.  $^2\text{H}$ - $\varepsilon_{\text{bio}}$  quantifying the  $^2\text{H}$  isotope fractionation between leaf water and synthesized leaf compounds) in plants growing under different environmental regimes implying different physiological plant metabolism (Cormier et al. 2018). In that context, this was expressed as the  $\Delta^2\text{H}$ - $\varepsilon_{\text{bio}}$  of *n*-alkanes between heterotrophic and autotrophic metabolisms, but the concept could be used to estimate other differences occurring in other complex isotope systems (e.g. systems encompassing many biochemical pathways).

### 8.5.2 Example for Equilibrium Isotope Effects

Reversible reactions aim at approaching a chemical equilibrium with forward and backward reactions then proceeding simultaneously at the same rate (principle of Le Chatelier). The concentrations of all reaction partners at this ‘dynamic’ equilibrium will be constant without a net change. The equilibrium constant of a reversible chemical reaction is related to the ratio of the stoichiometrically balanced product concentrations to reactant concentrations at equilibrium. In case of  $\text{CO}_2$  hydration and  $\text{HCO}_3^-$  dehydration in water:



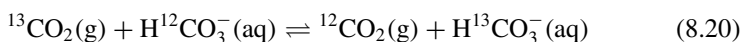
the equilibrium constant will be:

$$K_{\text{eq}} = \frac{[\text{HCO}_3^-][\text{H}^+]}{[\text{CO}_2]} \quad (8.19)$$

Adding of reactant(s) will increase the forward reaction, by adding product(s) the backward reaction will be strengthened. A change of temperature will change the equilibrium concentration of reactants and products and correspondingly the equilibrium constant. The reversible reactions tend to approach both a chemical and an isotopic equilibrium (see Schimerlik et al. 1975; Rishavy and Cleland 1999).<sup>26</sup> Isotope exchange reactions are reversible reactions involving a redistribution of

<sup>26</sup> Schimerlik et al. (1975) observed that a reversible system at chemical but not “isotopic equilibrium” is perturbed away from the (chemical) equilibrium after starting the reaction by adding the enzyme. Finally, a new equilibrium was achieved where both conditions are met. Consequently, a

isotopes between the reactants and products by substituting lighter isotopes in a chemical compound with a heavier one and vice versa. As an example the carbon isotope exchange between  $\text{CO}_2$  and  $\text{HCO}_3^-$  will be discussed <sup>23</sup>:



The equilibrium constant for that reaction is then:

$$K = \frac{[^{12}\text{CO}_2][\text{H}^{13}\text{CO}_3^-]}{[^{13}\text{CO}_2][\text{H}^{12}\text{CO}_3^-]} \quad (8.21)$$

The corresponding isotope fractionation factor  $\alpha_{\text{eq}}^{13}\text{C}$  for the  $\text{HCO}_3^-/\text{CO}_2$  system can be calculated according to Eq. 8.13:

$$\alpha^{13}\text{C}_{\text{HCO}_3^-/\text{CO}_2} = \frac{^{13}R_{\text{HCO}_3^-}}{^{13}R_{\text{CO}_2}} \quad (8.22)$$

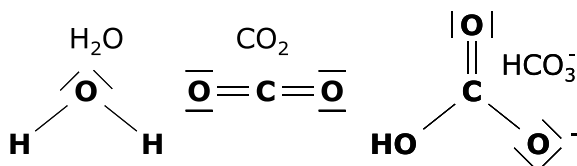
The  $K$  values for the equilibrium constant are temperature dependent (Le Chatelier's principle). In addition, the EIE values for the isotope exchange reaction are temperature dependent and can be theoretically calculated using statistical mechanical methods on the basis of spectroscopic data (Urey and Greiff 1935; Urey 1947, Bigeleisen and Goepfert Mayer 1947). The  $K$  value for the equilibrium reaction between carbon dioxide and bicarbonate for example has been determined to be 1.0093 at 0 °C and 1.0068 at 30 °C (Friedman and O'Neil 1977). As a consequence, at 30 °C the bicarbonate is only by 6.8 mUr enriched in  $^{13}\text{C}$  relative to the  $\text{CO}_2$ . In contrast, the  $^{13}\text{C}$  equilibrium enrichment of bicarbonate at 0 °C is 9.3 mUr. Raising the temperature 'diminishes' the extent of  $^{13}\text{C}$  enrichment by favoring the reaction towards the reactant(s) of the reaction because the (endothermic) back reaction is absorbing heat. As a rule of thumb one should keep in mind that the heavier isotopes prefer to concentrate in the more constrained chemical system with more and stronger chemical bonds (O'Leary 1978; O'Leary et al. 1992). In physical phase separations the lighter isotope is more 'volatile' with the effect that the heavier isotope will concentrate in the more condensed phase.

Both the oxygen isotope exchange reaction between  $\text{H}_2\text{O}$  and  $\text{CO}_2$  and the carbon isotope exchange reaction between  $\text{CO}_2$  and  $\text{HCO}_3^-$  explain this very well. Oxygen in  $\text{CO}_2$  is bonded with two double bonds in contrast to two single bonds in  $\text{H}_2\text{O}$  (Fig. 8.10). The carbon atom in  $\text{HCO}_3^-$  is connected to three oxygen atoms with double and single bonds in contrast to two double bonds between C and O in  $\text{CO}_2$  (Fig. 8.10). This leads to the  $^{13}\text{C}$  enrichment of the bicarbonate ion relative to  $\text{CO}_2$  and the  $^{18}\text{O}$  enrichment of  $\text{CO}_2$  relative to  $\text{H}_2\text{O}$  under equilibrium conditions. Equilibrium isotope effects are temperature-dependent; the resulting isotope fractionation normally decreases with increasing temperature. Oxygen isotope exchange of

---

system at isotopic equilibrium implies that the system is also at chemical equilibrium, but more time is needed to reach isotopic equilibrium (Rishavy and Cleland 1999).

**Fig. 8.10** Structural formulas of  $\text{H}_2\text{O}$ ,  $\text{CO}_2$  and  $\text{HCO}_3^-$



oxygen atoms in carbonyl groups of aldehydes and ketones with surrounding water is occurring under physiological conditions (c.f. Schmidt et al. 2001) during cellulose biosynthesis. This reversible hydration of carbonyl compounds easily establishes an equilibrium oxygen isotope enrichment of the oxygen function in the  $\text{C}=\text{O}$  group relative to the oxygen in water via a *gem*-diol ( $\text{HO-CR}_2\text{-OH}$ ) intermediate. This isotope exchange reaction of intermediates leads to the well-known  $^{18}\text{O}$  enrichment of cellulose relative to the water present during biosynthesis of glucose/ cellulose by  $+27 \pm 3$  mUr (Sternberg et al. 1986). Oxygen isotope analysis of cellulose in tree rings allows to infer climatic conditions during biosynthesis of cellulose in the trees via the oxygen isotopic composition of (leaf) water as long as the extent of  $^{18}\text{O}$  enrichment is constant under physiological conditions.

### 8.5.3 Example for Kinetic Isotope Effects

Irreversible unidirectional reactions are reactions where only the forward reaction takes place without the possibility of a backward reaction. An irreversible reaction is characterized by a reaction rate that corresponds to the velocity of the conversion of reactant(s) to product(s). The reaction rate is directly proportional to the concentrations of the reactant(s) via the rate constant  $k$ . This rate constant  $k$  is related to the Gibbs free energy. Substituting the bond partners of a chemical bond with heavier isotopes will decrease the rate constant for the heavier isotopocule via the Gibbs free energy of the molecule. The KIE (kinetic isotope effect) of a reaction is defined as the ratio of the rate constants of the corresponding irreversible reaction according to Coplen (2011), exemplarily shown for  $^{13}\text{C}$  in Eq. (8.7).

A kinetic isotope effect occurs when the rate of an irreversible chemical reaction is sensitive to the atomic mass. An example for a unidirectional reaction with kinetic isotope effect is the pyruvate dehydrogenase (PDH) reaction.

Pyruvate is decarboxylated to acetyl-CoA with gain of NADH. In plants the produced  $\text{CO}_2$  can be either re-assimilated (during the day) or is respired (during night). The PDH catalyzed reaction is regulating an important interface between plant catabolic and anabolic metabolism (Tovar-Méndez et al. 2003) and PDH is a key enzyme in plant (dark) respiration (Werner et al. 2011). During the reaction the bond between C-1 and C-2 of pyruvate (Fig. 8.11) is cleaved. Melzer and Schmidt (1987) measured the KIEs on the PDH catalyzed reaction (PDH from *S. cerevisiae*) for all three carbon atoms of pyruvate; namely primary  $^{13}\text{C}$ KIEs on C-1 and C-2 and a secondary  $^{13}\text{C}$ KIE on C-3 of pyruvate.

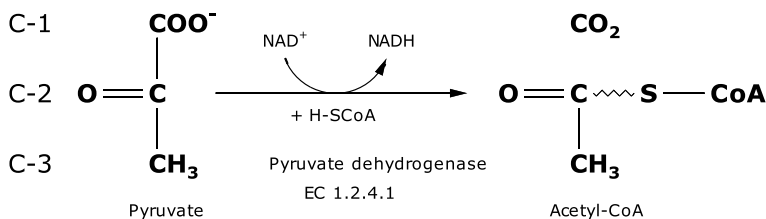


**Fig. 8.11** Pyruvate dehydrogenase catalyzes the oxidative decarboxylation of pyruvate under production of acetyl-CoA and NADH. This reaction takes place in plant mitochondria and chloroplasts and is irreversible under physiological conditions

$${}^{13}\text{KIE}_{\text{C-1}} = 1.0238 \pm 0.0013 \quad (8.23\text{a})$$

$${}^{13}\text{KIE}_{\text{C-2}} = 1.0254 \pm 0.0016 \quad (8.23\text{b})$$

$${}^{13}\text{KIE}_{\text{C-3}} = 1.0031 \pm 0.0003 \quad (8.23\text{c})$$

The primary  ${}^{13}\text{KIE}$ s on C-1 (1.0238) and C-2 (1.0254) of pyruvate are of a comparable dimension, whereas the  ${}^{13}\text{KIE}$  on C-3 (1.0031) is one size smaller, typical for a secondary KIE on carbon atoms not involved in the bond cleavage (Melzer and Schmidt 1987). In case of a non-quantitative conversion of pyruvate to acetyl-CoA the C-1 and C-2 of pyruvate will be strongly enriched in  ${}^{13}\text{C}$ . The produced acetyl-CoA will be depleted in  ${}^{13}\text{C}$  leading to the prominent  ${}^{13}\text{C}$  depletion of acetogenic lipids relative to their precursor glucose (see cited literature in Hayes 2001 and Hobbie and Werner 2004). Acetyl-CoA is  ${}^{13}\text{C}$  depleted in C-1 (former C-2 of pyruvate) and enriched in  ${}^{13}\text{C}$  in C-2 (former C-3 of pyruvate) relative to the  ${}^{13}\text{C}/{}^{12}\text{C}$  ratio of the whole acetyl-CoA molecule. This alternating  ${}^{13}\text{C}$  pattern can be again found in the  ${}^{13}\text{C}$  pattern of fatty acids biosynthesized from acetyl-CoA units. The odd-numbered carbon positions in fatty acids (originating from C-1 of acetyl-CoA) are depleted in  ${}^{13}\text{C}$ . In contrast, the even-numbered carbon positions (methyl position of acetyl-CoA acts as precursor) are enriched in  ${}^{13}\text{C}$  relative to glucose (c.f. Hayes 2001).

The extent of isotope fractionation in natural systems is usually decreasing with increasing temperatures; approaching zero at very high (geological) temperatures (Hoefs 2018). Also heavy atom isotope effects per se tend to decrease with higher temperature (O’Leary 1978). Living organic systems are adapted to an environment with limited temperature and pH range (“physiological” temperature and pH values) that allows enzymes in reaction networks to function. As a consequence isotope effects in living organic systems are largely invariant with temperature (O’Leary 1978). For instance, the  $27 \pm 3 \text{ mUr}$   ${}^{18}\text{O}$  enrichment of cellulose relative to water during its biosynthesis appears constant in the range of temperatures where trees can grow. However, the resulting isotope fractionation in organisms may nevertheless show some temperature effects. This can be the case because pool sizes, flow



rates, and enzymatic activities in these reaction networks may depend on temperature (O’Leary et al. 1992). Moreover, the environmental sources of reactants in these reaction networks (e.g. environmental water) may also be affected by temperature (e.g. the temperature of precipitation in rain and snow events will affect the isotopic composition of the water available to plants). As such, although isotope effects in living organic systems are largely invariant with temperature, a temperature signal may yet be recorded in the isotopic composition of organic material and used, if disentangled from other signals, to reconstruct temperatures at the moment of production.

### 8.5.4 Connection of EIE and KIE

Reversible chemical reactions approach chemical and isotopic equilibrium. The two involved (forward and backward) reactions can be associated with kinetic isotope effects (e.g. Jones 2003). If the reaction system is in chemical and isotopic equilibrium the fluxes of the forward and backward reactions are equal. As an example the hydration reaction of  $\text{CO}_2$  and the dehydration of  $\text{HCO}_3^-$  is shown (Eq. (8.18)). Marlier and O’Leary (1984) measured the KIEs for the  $\text{CO}_2$  hydration (forward) and the  $\text{HCO}_3^-$  dehydration (backward reaction) at 24 °C under conditions that secure the irreversibility of both reactions. The corresponding equilibrium isotope effect was calculated ( $^{13}\text{EIE}_{\text{HCO}_3^-/\text{CO}_2} = ^{13}\text{KIE}_{\text{HCO}_3^-/\text{CO}_2} / ^{13}\text{KIE}_{/\text{CO}_2/\text{HCO}_3^-}$ ) and fits very well to experimentally determined  $^{13}\text{EIE}$  values (Mook et al. 1974; c.f. Friedman and O’Neil 1977).

$$^{13}\text{KIE}_{\text{CO}_2/\text{HCO}_3^-} = 1.0069 \pm 0.0003 \quad (8.24a)$$

$$^{13}\text{KIE}_{\text{HCO}_3^-/\text{CO}_2} = 1.0147 \pm 0.0007 \quad (8.24b)$$

$$^{13}\text{EIE}_{\text{HCO}_3^-/\text{CO}_2} = 1.0077 \pm 0.0008 \quad (8.24c)$$

According to O’Leary et al. (1992) the equilibrium isotope fractionation can be calculated from the two kinetic isotope fractionations (on forward and backward reactions) via:

$$\Delta^{13}\text{C}_{(\text{A}/\text{B})} = \Delta^{13}\text{C}_{(\text{A}\rightarrow\text{B})} - \Delta^{13}\text{C}_{(\text{B}\rightarrow\text{A})} \quad (8.25)$$

but compare with Table 8.4 and related text.

EIE reactions are sensitive to temperature but KIE reactions are not (at least not with the same level of “sensitivity”). These two facts are interconnected versus the Le Chatelier principle. The size of the equilibrium constant will change when the temperature is changing. This has as consequence that the ratio of the fluxes

of forward and backward reaction is changing but the values of the kinetic isotope effects on forward and backward reaction will not be influenced to the same extent by the temperature itself.

## 8.6 Conclusion

The measurement of stable isotope ratios of the bioelements is a technique used in many different scientific areas, and not all communities seem to use the same set of parameters and equations. While following the terminological recommendations by Coplen (2011), the present manuscript explains the basic principles and concepts underlying the use of stable isotopes in many diverse fields of study. It strongly suggests to thoroughly check the exact definitions and equations to derive specific parameters, e.g. to express isotope fractionation. Authors are encouraged to carefully select corresponding suitable parameters (cf. Table 8.4) and to use proper terminology and notation. They are also advised to provide a traceable derivation (e.g. in form of equations) in their texts to avoid confusion when reporting results of stable isotope measurements. This clarification should foster and grow the understanding and interpretation of stable isotope data, also across discipline borders.

**Acknowledgements** We would like to thank Shiva Ghiasi (IAS, ETH Zurich, Switzerland) for helpful discussion and Luca L.E. Werner (MNG Rämibühl, Zurich, Switzerland) for helpful comments and mathematical support. We would like to thank Willi A. Brand (MPI-BGC, Jena, Germany), Gerhard Strauch (Helmholtz Centre for Environmental Research—UFZ, Leipzig, Germany) and an anonymous reviewer for critically reading and suggesting substantial improvements that helped to complete and clarify the manuscript. M.-A.C. received funding from the UK Biotechnology and Biological Sciences Research Council.

## References

- Ardenne M von (1944) Die physikalischen Grundlagen der Anwendung radioaktiver oder stabiler Isotope als Indikatoren. Springer-Verlag, Berlin, D
- Augusti A, Betson TR, Schleucher J (2006) Hydrogen exchange during cellulose synthesis distinguishes climatic and biochemical isotope fractionations in tree rings. *New Phytol* 172:490–499
- Bennet AJ (2012) Kinetic isotope effects for studying post-translational modifying enzymes. *Curr Opin Chem Biol* 16:472–478
- Betson TR, Augusti A, Schleucher J (2006) Quantification of deuterium isotopomers of tree-ring cellulose using magnetic resonance. *Anal Chem* 78:8406–8411
- Bigeleisen J (1965) Chemistry of isotopes. *Science* 147:463–471
- Bigeleisen J, Goepfert-Mayer M (1947) Calculation of equilibrium constants for isotopic exchange reactions. *J Chem Phys* 15:261–267
- Bigeleisen J, Fuks S, Ribnikar SV, Yato Y (1977) Vapor pressures of the isotopic ethylenes. V. Solid and liquid ethylene-d<sub>1</sub>, ethylene-d<sub>2</sub> (*cis*, *trans*, and *gem*), ethylene-d<sub>3</sub>, and ethylene-d<sub>4</sub>. *J Chem Phys* 66:1689–1700

- Bigeleisen J, Wolfsberg M (1958) Theoretical and experimental aspects of isotope effects in chemical kinetics. In: Prigogine I (ed) *Advances in Chemical Physics* Vol. 1, Interscience Publishers Inc., New York, pp 15–76
- BIPM (2019) *The International Systems of Units (SI). 9th SI Brochure*. BIPM, Sèvres Cedex, France. ISBN 978-92-822-2272-0
- Bonhoeffer KF, Brown GW (1933) Über den Austausch von Wasserstoff zwischen Wasser und darin gelösten wasserstoffhaltigen Verbindungen. *Z Phys Chem B* 23:171–174
- Brand WA (2004) Mass spectrometer hardware for analyzing stable isotope ratios. In: de Groot PA (ed) *Handbook of Stable Isotope Analytical Techniques*, vol 1. Elsevier, Amsterdam, pp 835–856
- Brand WA (2013) Atomic weights: not so constant after all. *Anal Bioanal Chem* 405:2755–2761
- Brand WA, Coplen TB (2012) Stable isotope deltas: tiny, yet robust signatures in nature. *Isot Environ Health Stud* 48:393–409
- Brand WA, Coplen TB, Vogl J, Rosner M, Prohaska (2014) Assessment of international reference materials for isotope-ratio analysis (IUPAC Technical Report). *Pure Appl Chem* 86:425–467
- Chown M (2001) *The magic furnace: the search for the origins of atoms*. Oxford University Press, New York
- Clayton RN (1981) Isotopic thermometry. In: Newton RC, Navrotsky A, Wood BJ (1981) *Thermodynamics of minerals and melts*. Springer, New York, Heidelberg, Berlin. *Adv Physical Geochem* 1:85–109
- Coplen TB (2011) Guidelines and recommended terms for expression of stable-isotope-ratio and gas-ratio measurement results. *Rapid Commun Mass Spectrom* 25:2538–2560
- Coplen TB, Holden NE (2011) No longer constants of nature. *Chem Int* 33:10–15
- Cormier M-A, Werner RA, Sauer PE, Gröcke DR, Leuenberger MC, Wieloch T, Schleucher J, Kahmen A (2018)  $^2\text{H}$ -fractionations during the biosynthesis of carbohydrates and lipids imprint a metabolic signal on the  $\delta^2\text{H}$  values of plant organic compounds. *New Phytol* 218:479–491
- Corso TN, Brenna JT (1997) High-precision position-specific isotope analysis. *Proc Natl Acad Sci USA* 94:1049–1053
- De Bièvre P, Valkiers S, Peiser HS, Taylor PDP, Hansen P (1996) Mass-spectrometric methods for determining isotopic composition and molar mass traceable to the SI, exemplified by improved values for nitrogen. *Metrologia* 33:447–455
- Ehlers I, Augusti A, Betson TR, Nilsson MB, Marshall JD, Schleucher J (2015) Detecting long-term metabolic shifts using isotopomers:  $\text{CO}_2$ -driven suppression of photorespiration in  $\text{C}_3$  plants over the 20th century. *Proc Natl Acad Sci USA* 122:15585–15590
- Elsner M (2010) Stable isotope fractionation to investigate natural transformation mechanisms of organic contaminants: principles, prospects and limitations. *J Environ Monit* 12:2005–2031
- Elsner M, Hofstetter TB (2011) Current perspectives on the mechanisms of chlorohydrocarbon degradation in subsurface environments: insight from kinetics, product formation, probe molecules, and isotope fractionation. In: Tratnyek PG, Grundl TJ, Haderlein SB (eds) *ACS symposium series*, vol 1071, *Aquatic Redox Chemistry*, pp 407–439
- Farquhar GD, Ehleringer JR, Hubick KT (1989) Carbon isotope discrimination and photosynthesis. *Ann Rev Plant Physiol Plant Mol Biol* 40:503–537
- Fitzpatrick PF (2015) Combining solvent isotope effects with substrate isotope effects in mechanistic studies of alcohol and amine oxidation by enzymes. *Biochim Biophys Acta* 1854:1746–1755
- Friedman I, O’Neil JR (1977) Compilation of stable isotope fractionation factors of geochemical interest. Chapter KK in Fleischer M. (ed.) *Data of Geochemistry*, 6th Ed. Geological Survey Professional Paper 440-KK. United States Government Printing Office, Washington USA
- Fry B (2006) *Stable isotope ecology*. Springer Science + Business Media, New York, pp 26–28; 285ff
- Fujii T, Moynier F, Albarède F (2009) The nuclear field shift effect in chemical exchange reactions. *Chem Geol* 267:139–156
- Gilbert A (2021) The organic isotopologue frontier. *Annu Rev Earth Planet Sci* 49:435–464
- Gilbert A, Robins RJ, Remaud GS, Tcherkez GGB (2012) Intramolecular  $^{13}\text{C}$  pattern in hexoses from autotrophic and heterotrophic  $\text{C}_3$  plant tissues. *Proc Natl Acad Sci USA* 109:18204–18209

- Gold V, Satchell DPN (1955) The principles of hydrogen isotope exchange reactions in solution. *Q Rev Chem Soc* 9:51–72
- Gori Y, Wehrens R, Greule M, Keppler F, Ziller L, La Porta N, Camin F (2013) Carbon, hydrogen and oxygen stable isotope ratios of whole wood, cellulose and lignin methoxyl groups of *Picea abies* as climate proxies. *Rapid Commun Mass Spectrom* 27:265–275
- Gillon JS, Yakir D (2000) Naturally low carbonic anhydrase activity in C<sub>4</sub> and C<sub>3</sub> plants limits discrimination against C<sup>18</sup>O during photosynthesis. *Plant Cell Environ* 23:903–915
- Groves LR (1962) Now it can be told—the story of the Manhattan project. Harper, New York, USA
- Harris E, Sinha B, Hoppe P, Crowley JN, Ono S, Foley S (2012) Sulfur isotope fractionation during oxidation of sulfur dioxide: gas-phase oxidation by OH radicals and aqueous oxidation by H<sub>2</sub>O<sub>2</sub>, O<sub>3</sub> and iron catalysis. *Atmos Chem Phys* 12:407–424
- Hayes JM (2001) Fractionation of the isotopes of carbon and hydrogen in biosynthetic processes. In: Valley JW, Cole DR (eds) *Stable isotope geochemistry*. *Rev Mineral Geochem* 43:225–277
- Haynes WM, Lide DR, Bruno TJ (2014) *CRC Handbook of chemistry and physics*. 95th Ed. CRC Press, Taylor & Francis Group, Boca Raton, USA
- Hobbie EA, Werner RA (2004) Intramolecular, compound-specific, and bulk carbon isotope patterns in C<sub>3</sub> and C<sub>4</sub> plants: a review and synthesis. *New Phytol* 161:371–385
- Hoefs J (2018) *Stable isotope geochemistry*, 8th Ed. Springer Textbooks in Earth Sciences, Geography and Environment, Berlin und Heidelberg, D
- Holden NE, Coplen TB, Böhlke JK, Tarbox LV, Benefield J, de Laeter JR, Mahaffy PG, O'Connor G, Roth E, Tepper DH, Walczyk T, Wieser ME, Yoneda S (2018) IUPAC periodic table of the elements and isotopes (IPTEI) for the education community (IUPAC Technical Report). *Pure Appl Chem* 90:1833–2092
- Horita J, Cole DR (2004) Stable isotope partitioning in aqueous and hydrothermal systems to elevated temperatures. In: Palmer DA, Fernández-Prini R, Harvey AH (eds) *Aqueous systems at elevated temperatures and pressures: physical chemistry in water, steam and hydrothermal solutions*. Elsevier, Amsterdam, pp 277–319
- International Organization for Standardization (1992) ISO-31-0. Quantities and units - Part 0: General principles, Amendment 1. 2.3.3 The unit one. International Organization for Standardization, Geneva, Switzerland, pp 7–8
- International Union of Pure and Applied Chemistry (1959) *Nomenclature of inorganic chemistry: definitive rules for nomenclature of inorganic chemistry* (1957) Report of the Commission on the Nomenclature of Inorganic Chemistry. Butterworths Scientific Publications, London, p 10
- IUPAC (2018) Periodic table of the elements. Version dated 1 December 2018: Interactive Version February 2022: <https://applets.kcvs.ca/IPTEI/IPTEI.html>.
- Jancsó G (2011) Isotope effects. In: Vértes A, Nagy S, Klencsár Z, Lovas RG, Rösch F (eds) *Handbook of nuclear chemistry*, Vol. 1, 2nd Ed. Springer, Dordrecht, pp 699–725
- Jones WD (2003) Isotope effects in C-H bond activation reactions by transition metals. *Acc Chem Res* 36:140–146
- Kaiser J, Röckmann T (2008) Correction of mass spectrometric isotope ratio measurements for isobaric isotopologues of O<sub>2</sub>, CO, CO<sub>2</sub>, N<sub>2</sub>O and SO<sub>2</sub>. *Rapid Commun Mass Spectrom* 22:3997–4008
- Krumbiegel P (1970) *Isotopieeffekte*. Akademie-Verlag GmbH, Berlin
- Lloyd M, Dawson K, Douglas P, Eiler J (2018) How reversible is methylotrophic methanogenesis? Distinguishing gross from net uptake using clumped isotopes in methanol. *Goldschmidt Abstracts*, 2018 1585. <https://goldschmidt.info/2018/abstracts/abstractView?id=2018004311>
- Love LO (1973) Electromagnetic separation of isotopes at Oak Ridge. An informal account of history, techniques and accomplishments. *Science* 182:343–352
- Lloyd MK, Eldridge DL, Stolper DA (2021) Clumped <sup>13</sup>CH<sub>2</sub>D and <sup>12</sup>CHD<sub>2</sub> compositions of methyl groups from wood and synthetic monomers: methods, experimental and theoretical calibrations, and initial results. *Geochim Cosmochim Acta* 297:233–275
- Ma R, Zhu Z, Wang B, Zhao Y, Yin X, Lu F, Wang Y, Su J, Hocart CH, Zhou Y (2018) Novel position-specific <sup>18</sup>O/<sup>16</sup>O measurement of carbohydrates. I. O-3 of glucose and confirmation of

- $^{18}\text{O}/^{16}\text{O}$  heterogeneity at natural abundance levels in glucose from starch in a  $\text{C}_4$  plant. *Anal Chem* 90:10293–10301
- Magyar PM, Orphan VJ, Eiler JM (2016) Measurement of rare isotopologues of nitrous oxide by high-resolution multi-collector mass spectrometry. *Rapid Commun Mass Spectrom* 30:1923–1940
- Marlier JF, O’Leary MH (1984) Carbon kinetic isotope effects on the hydration of carbon dioxide and the dehydration of bicarbonate ion. *J Am Chem Soc* 106:5054–5057
- McKinney CR, McCrea JM, Epstein S, Allen HA, Urey HC (1950) Improvements in mass spectrometers for the measurement of small differences in isotope abundance ratios. *Rev Sci Instrum* 21:724–730
- Meija J, Coplen TB, Berglund M, Brand WA, De Bièvre P, Gröning M, Holden NE, Irrgeher J, Loss RD, Walczyk T, Prohaska T (2016) Atomic weights of the elements 2013 (IUPAC Technical Report). *Pure Appl Chem* 88:265–291
- Melzer E, Schmidt H-L (1987) Carbon isotope effects on the pyruvate dehydrogenase reaction and their importance for relative carbon-13 depletion in lipids. *J Biol Chem* 262:8159–8164
- Mischel M, Esper J, Keppler F, Greule M, Werner W (2015)  $\delta^2\text{H}$ ,  $\delta^{13}\text{C}$  and  $\delta^{18}\text{O}$  from whole wood,  $\alpha$ -cellulose and lignin methoxyl groups in *Pinus sylvestris*: a multi-parameter approach. *Isot Environ Health Stud* 51:553–568
- Mook WG (2001) Environmental isotopes in the hydrological cycle—principles and applications. Volume 1: Introduction—Theory, Methods, Review. International Atomic Energy Agency and United Nations Educational Scientific and Cultural Organization. Chapter 3:23–32
- Mook WG, Bommerson JC, Staverman WH (1974) Carbon isotope fractionation between dissolved bicarbonate and gaseous carbon dioxide. *Earth Planet Sci Lett* 22:169–176
- Muller P (1994) Glossary of terms used in physical organic chemistry (IUPAC Recommendations 1994). *Pure Appl Chem* 66:1077–1184
- Nier AOC (1946) The mass spectrometer and its application to isotope abundance measurements in tracer isotope experiments. In: Wilson DW, Nier AOC, Reimann SP (eds) Preparation and measurement of isotopic tracers. JW Edwards, Ann Arbor, Michigan USA, pp 11–30
- O’Leary MH (1978) Heavy-atom isotope effects in enzyme-catalyzed reactions. In: Gandour RD, Schowen RL (eds) Transition states of biochemical processes. Springer Science + Business Media, LLC, New York USA, pp 285–316
- O’Leary MH, Madhavan S, Paneth P (1992) Physical and chemical basis of carbon isotope fractionation in plants. *Plant Cell Environ* 15:1099–1104
- O’Neil JR (1986a) Theoretical and experimental aspects of isotopic fractionation. In: Valley JW, Taylor HP, O’Neil JR (eds) Stable isotopes in high temperature geological processes. *Rev Mineral* 16:1–40
- O’Neil JR (1986b) Appendix: terminology and standards. In: Valley JW, Taylor HP, O’Neil JR (eds) Stable isotopes in high temperature geological processes. *Rev Mineral* 16:561–570
- Rishavy MA, Cleland WW (1999)  $^{13}\text{C}$ ,  $^{15}\text{N}$  and  $^{18}\text{O}$  equilibrium isotope effects and fractionation factors. *Can J Chem* 77:967–977
- Rossmann A, Butzenlechner M, Schmidt H-L (1991) Evidence for a nonstatistical carbon isotope distribution in natural glucose. *Plant Physiol* 96:609–614
- Sachse D, Billault I, Bowen GJ, Chikaraishi Y, Dawson TE, Feakins SJ, Freeman KH, Magill CR, McInerney FA, van der Meer MTJ, Polissar P, Robins RJ, Sachs JP, Schmidt H-L, Sessions AL, White JWC, West JB, Kahmen A (2012) Molecular paleohydrology: interpreting the hydrogen-isotopic composition of lipid biomarkers from photosynthesizing organisms. *Annu Rev Earth Planet Sci* 40:221–249
- Sade Z, Halevy I (2017) New constraints on kinetic isotope effects during  $\text{CO}_{2(\text{aq})}$  hydration and hydroxylation: revisiting theoretical and experimental data. *Geochim Cosmochim Acta* 214:246–265. Corrigendum: *Geochim Cosmochim Acta* (2018) 225:237–240
- Saunders WH (1966) Kinetic isotope effects. *Survey Progr Chem* 3:109–146
- Schimerlik MI, Rife JE, Cleland WW (1975) Equilibrium perturbation by isotope substitution. *Biochem* 14:5347–5354

- Schowen RL (2007) The use of solvent isotope effects in the pursuit of enzyme mechanisms. *J Label Compd Radiopharm* 50:1052–1062
- Schmidt H-L, Robins RJ, Werner RA (2015) Multi-factorial *in vivo* stable isotope fractionation: causes, correlations, consequences and applications. *Isot Environ Health Stud* 51:155–199
- Schmidt H-L, Werner RA, Rossmann A (2001)  $^{18}\text{O}$  Pattern and biosynthesis of natural plant products. *Phytochem* 58:9–32
- Seeman JI, Paine JB (1992) Isotopomers, isotopologs. *Chem Eng News* 70(49) December 7:2
- Seeman JI, Secor HV, Disselkamp R, Bernstein ER (1992) Conformational analysis through selective isotopic substitution: supersonic jet spectroscopic determination of the minimum energy conformation of *o*-xylene. *J Chem Soc Chem Commun* 1992:713–714
- Sharp ZD, Kirschner DL (1994) Quartz-calcite oxygen isotope thermometry: a calibration based on natural isotopic variations. *Geochim Cosmochim Acta* 58:4491–4501
- Smith MB (2013) March's advanced organic chemistry. Reactions, mechanisms, and structure. 7th Ed. John Wiley & Sons, Hoboken, New Jersey, USA
- Soddy F (1923) The origins of the conception of isotopes. *Nature* 112:208–213
- Sternberg LdSL, DeNiro MJ, Savidge RA (1986) Oxygen isotope exchange between metabolites and water during biochemical reactions leading to cellulose synthesis. *Plant Physiol* 82:423–427
- Sternberg LdSLOR (2009) Oxygen stable isotope ratios of tree-ring cellulose: the next phase of understanding. *New Phytol* 181:553–562
- Thiemens MH (2006) History and applications of mass-independent isotope effects. *Annu Rev Earth Planet Sci* 34:217–262
- Tovar-Méndez A, Miernyk JA, Randall DD (2003) Regulation of pyruvate dehydrogenase complex activity in plant cells. *Eur J Biochem* 270:1043–1049
- Toyoda S, Yoshida N (1999) Determination of nitrogen isotopomers of nitrous oxide on a modified isotope ratio mass spectrometer. *Anal Chem* 71:4711–4718
- Uchikawa J, Zeebe RE (2012) The effect of carbonic anhydrase on the kinetics and equilibrium of the oxygen isotope exchange in the  $\text{CO}_2\text{-H}_2\text{O}$  system: implications for  $\delta^{18}\text{O}$  vital effects in biogenic carbonates. *Geochim Cosmochim Acta* 95:15–34
- Urey HC (1947) The thermodynamic properties of isotopic substances. *J Chem Soc* 1947:562–581
- Urey HC, Failla G (1935) Concerning the taste of heavy water. *Science* 81:273
- Urey HC, Greiff LJ (1935) Isotopic exchange equilibria. *J Am Chem Soc* 57:321–327
- Urey HC, Murphy GM, Brickwedde FG (1933) A name and symbol for  $\text{H}^2$ . *J Chem Phys* 1:512–513
- Usdowski E, Hoefs J (1993) Oxygen isotope exchange between carbonic acid, bicarbonate, carbonate, and water: a re-examination of the data of McCrea (1950) and an expression for the overall partitioning of oxygen isotopes between the carbonate species and water. *Geochim Cosmochim Acta* 57:3815–3818
- Van Hook WA (2011) Isotope effects in chemistry. *Nukleonika* 56:217–240
- Vogel P, Houk KN (2019) Organic chemistry—theory, reactivity and mechanisms in modern synthesis. Wiley-VCH Verlag GmbH & Co. KGaA, Weinheim, Germany, pp 49–52; 231–240
- Wang Y, Zhu Z, Xia Y, Zhong M, Ma R, Zhao Y, Yan Q, Miao Q, Wang B, Ma Y, Yin X, Zhou Y (2021) Accessing the position-specific  $^{18}\text{O}/^{16}\text{O}$  ratios of lignin monomeric units from higher plants with highly selective hydrogenolysis followed by GC/Py/IRMS analysis. *Anal Chim Acta* 1171:338667. <https://doi.org/10.1016/j.aca.2021.338667>
- Werner RA, Brand WA (2001) Referencing strategies and techniques in stable isotope ratio analysis. *Rapid Commun Mass Spectrom* 15:501–519
- Werner RA, Buchmann N, Siegwolf RTW, Kornel BE, Gessler A (2011) Metabolic fluxes, carbon isotope fractionation and respiration—lessons to be learned from plant biochemistry. *New Phytol* 191:10–15
- White WM (2015) Isotope geochemistry. John Wiley & Sons, Chichester, UK, pp 246–276
- Wieloch T, Ehlers I, Yu J, Frank D, Grabner M, Gessler A, Schleucher J (2018) Intramolecular  $^{13}\text{C}$  analysis of tree rings provides multiple plant ecophysiology signals covering decades. *Sci Rep* 8:5048. <https://doi.org/10.1038/s41598-018-23422-2>

- Wieloch T, Werner RA, Schleucher J (2021) Carbon flux around leaf-cytosolic glyceraldehyde-3-phosphate dehydrogenase introduces a  $^{13}\text{C}$  signal in plant glucose. *J Exp Bot* 72:7136–7144
- Wolfsberg M, Van Hook WA, Paneth P (2010) Kinetic isotope effects on chemical reactions. Chapter 10 in: *Isotope Effects in the Chemical, Geological, and Bio Sciences*. Springer, Dordrecht, pp 313–342
- Yankwich PE, Belford RL (1954) Intramolecular carbon isotope effect in the decarboxylation of normal malonic acid in quinoline solution. *J Am Chem Soc* 76:3067–3070
- Young ED, Galy A, Nagahara H (2002) Kinetic and equilibrium mass-dependent isotope fractionation laws in nature and their geochemical and cosmochemical significance. *Geochim Cosmochim Acta* 66:1095–1104
- Zhang B-L, Pionnier S (2002) Natural stereospecific hydrogen isotope transfer in alcohol dehydrogenase-catalysed reduction. *Nukleonika* 47:S29–S31
- Zhang B-L, Billault I, Li X, Mabon F, Remaud G, Martin ML (2002) Influence of the photosynthetic pathway on the hydrogen isotopic profile of glucose. *Nukleonika* 47:S63–S65
- Zhang BL, Mabon F, Martin ML (1993) Simultaneous determination of primary and secondary thermodynamic isotope effects in tautomeric equilibria. *J Phys Org Chem* 6:367–373
- Zhang Q-L (Chang TL), Li W-J (1990) A calibrated measurement of the atomic weight of carbon. *Chin Sci Bull* 35:290–296

**Open Access** This chapter is licensed under the terms of the Creative Commons Attribution 4.0 International License (<http://creativecommons.org/licenses/by/4.0/>), which permits use, sharing, adaptation, distribution and reproduction in any medium or format, as long as you give appropriate credit to the original author(s) and the source, provide a link to the Creative Commons license and indicate if changes were made.

The images or other third party material in this chapter are included in the chapter's Creative Commons license, unless indicated otherwise in a credit line to the material. If material is not included in the chapter's Creative Commons license and your intended use is not permitted by statutory regulation or exceeds the permitted use, you will need to obtain permission directly from the copyright holder.



# Chapter 9

## Carbon Isotope Effects in Relation to CO<sub>2</sub> Assimilation by Tree Canopies



Lucas A. Cernusak and Nerea Ubierna

**Abstract** The carbon atoms deposited in tree rings originate from the CO<sub>2</sub> in the atmosphere to which the tree's canopy is exposed. Thus, the first control on the stable carbon-isotope composition of tree rings is by  $\delta^{13}\text{C}$  of atmospheric CO<sub>2</sub>. There has been an inter-annual trend of decreasing  $\delta^{13}\text{C}$  of atmospheric CO<sub>2</sub> over the past two centuries as a result of combustion of fossil fuels and land-use change. Atmospheric CO<sub>2</sub> is, for the most part, well mixed, but the sub-canopy air space can become depleted in <sup>13</sup>C due to inputs from soil and plant respiration when turbulent exchange with the troposphere is hindered, for example by a high leaf area index at night. This is less likely to occur during daytime when turbulence is higher and photosynthesis takes place. Discrimination against <sup>13</sup>C ( $\Delta^{13}\text{C}$ ) occurs upon assimilation of atmospheric CO<sub>2</sub> by C<sub>3</sub> photosynthesis. Trees using the C<sub>3</sub> photosynthetic pathway comprise the overwhelming majority of all trees. The primary control on the extent of discrimination during C<sub>3</sub> photosynthesis is the drawdown in CO<sub>2</sub> concentration from the air outside the leaf to the site of carboxylation in the chloroplast. Part of this drawdown is captured by  $c_i/c_a$ , that is, the ratio of intercellular to ambient CO<sub>2</sub> concentrations. The  $c_i/c_a$  represents the balance between the CO<sub>2</sub> supply by stomata and its demand by photosynthesis. It can be related to water-use efficiency, the amount of CO<sub>2</sub> taken up by photosynthesis for a given amount of water loss to the atmosphere, assuming a given evaporative demand. To predict time-averaged  $c_i/c_a$  from wood  $\Delta^{13}\text{C}$ , a simplified, linear model can be employed. In this linear model, the slope is determined by  $\bar{b}$ , the effective enzymatic discrimination. The value of  $\bar{b}$  can be estimated by comparing wood  $\Delta^{13}\text{C}$  to representative measurements of  $c_i/c_a$ . The  $\bar{b}$  was originally estimated from observations of leaf tissue to have a value of 27‰. We compiled data for woody stem tissue here, and our analysis suggests that a lower  $\bar{b}$  should be used in the simplified model for wood ( $\bar{b} = 25.5\%$ ) than for leaves ( $\bar{b} = 27\%$ ). This is also consistent with widespread observations that woody tissues are enriched in <sup>13</sup>C compared to leaves.

---

L. A. Cernusak (✉)

College of Science and Engineering, James Cook University, Cairns, QLD 4878, Australia  
e-mail: [lucas.cernusak@jcu.edu.au](mailto:lucas.cernusak@jcu.edu.au)

N. Ubierna

The Australian National University, Canberra, ACT 0200, Australia

© The Author(s) 2022

R. T. W. Siegwolf et al. (eds.), *Stable Isotopes in Tree Rings*, Tree Physiology 8,  
[https://doi.org/10.1007/978-3-030-92698-4\\_9](https://doi.org/10.1007/978-3-030-92698-4_9)

291



## 9.1 Introduction

The abundance of the heavier stable carbon isotope,  $^{13}\text{C}$ , in plant material is modulated both by its environment and by plant metabolism. The ratio  $^{13}\text{C}/^{12}\text{C}$  is typically expressed as  $\delta^{13}\text{C}$ , which is the relative deviation of the ratio in the sample of interest from that of an internationally accepted standard, Vienna Pee Dee Belemnite (Craig 1957; Coplen 2011). With respect to plant metabolism, stable isotopes have the unique feature of integrating plant responses over time and space. Thus, they offer a powerful tool to investigate photosynthetic processes and responses to environmental change from the leaf to the ecosystem. In this chapter, we focus on  $\delta^{13}\text{C}$  in tree rings and how it is related to assimilation of  $\text{CO}_2$  by the tree's canopy.

Tree rings have the potential to provide a time-structured archive of information related to a tree's growth environment and its physiological responses to changes in that environment (Fritts and Swetnam 1989; Briffa et al. 2004). Tree ring analyses have provided an indispensable tool in efforts to understand how the terrestrial biosphere is responding to the accelerating impacts of the Anthropocene (Saurer et al. 2004; Peñuelas et al. 2011; Frank et al. 2015; van der Sleen et al. 2015). One of the more tractable analyses that can be conducted on tree rings is to measure the  $\delta^{13}\text{C}$  of the wood that comprises the individual rings or sequences of rings. This represents an integration of carbon laid down over a period of time. For annual rings, this is taken as the course of a growing season (Chap. 14), or the full year in the case of tropical trees without distinct non-growing seasons (Chap. 22). In the latter case, there may also be a lack of clear annual rings. It is assumed that the majority of carbon will have originated from canopy photosynthesis in that same time period, although there can also be a contribution from stored carbon produced in previous years (Monserud and Marshall 2001; Drew et al. 2009; Belmecheri et al. 2018).

The carbon isotope ratio of the photosynthate produced by a tree's canopy is determined primarily by two factors: the  $\delta^{13}\text{C}$  of the atmospheric  $\text{CO}_2$ , which provides the substrate for photosynthesis, and the discrimination against  $^{13}\text{C}$  ( $\Delta^{13}\text{C}$ ) which takes place during conversion of gaseous  $\text{CO}_2$  into carbohydrates through the process of photosynthesis. When these two factors are sufficiently understood, one can use the measured  $\delta^{13}\text{C}$  in a tree ring to make inferences about how the process of  $^{13}\text{C}$  discrimination responded to climatic and other environmental changes. Also, because the  $\Delta^{13}\text{C}$  is responsive to climate, there exists the possibility to reconstruct climate from measured changes in  $\Delta^{13}\text{C}$  once a calibration relating the two has been developed (McCarroll and Loader 2004; Hartl-Meier et al. 2015). Perhaps the most widespread use of tree ring analyses of  $\delta^{13}\text{C}$  has been to reconstruct changes in intrinsic water-use efficiency, the ratio of photosynthesis to stomatal conductance to water vapour, over the course of a tree's adult life in response to climatic change, mainly rising atmospheric  $\text{CO}_2$  concentration (Francey and Farquhar 1982; Saurer et al. 2004; Peñuelas et al. 2011; Frank et al. 2015; van der Sleen et al. 2015). This is possible because there is a reliable relationship between  $\Delta^{13}\text{C}$ , as recorded in plant biomass, and the ratio of intercellular to ambient  $\text{CO}_2$  concentrations,  $c_i/c_a$ , which in turn is related to the intrinsic water-use efficiency (Farquhar et al. 1982a, b; Farquhar and

Richards 1984). The latter represents an index of the amount of carbon that a tree took up by photosynthesis relative to its potential for releasing water to the atmosphere through transpiration (see Chap. 17). If the atmospheric vapour pressure deficit is known, then the intrinsic water use efficiency can be converted to an actual water use efficiency in terms of molar or mass units of water exchanged for carbon. More detailed physiological conclusions can be drawn when the  $\delta^{13}\text{C}$  values are combined with  $\delta^{18}\text{O}$  from the same sample (e.g. Chap. 16).

## 9.2 The $\delta^{13}\text{C}$ of Atmospheric CO<sub>2</sub>

Prior to the industrial revolution, the  $\delta^{13}\text{C}$  of atmospheric CO<sub>2</sub> fluctuated between about  $-7.5$  and  $-6.2\text{‰}$  for the previous 160,000 years (Fig. 9.1). These data are based on analysis of air that was trapped in ice cores. The onset of industrial activity saw increasing combustion of fossil fuels, made up of plant carbon deposited in geological reservoirs millions of years ago. This fossil carbon carries a  $\delta^{13}\text{C}$  signature reflecting photosynthetic discrimination against  $^{13}\text{C}$ , and has  $\delta^{13}\text{C}$  roughly similar to C<sub>3</sub> plants of today, with global emissions having a weighted mean  $\delta^{13}\text{C}$  of  $\sim -28\text{‰}$  in recent decades (Andres et al. 1996, 2000). The CO<sub>2</sub> released from combustion of fossil fuels associated with the industrial revolution began to accumulate in the atmosphere after the mid-18<sup>th</sup> Century, and the atmospheric CO<sub>2</sub> concentration increased from a pre-industrial value of  $\sim 280 \mu\text{mol mol}^{-1}$  to  $\sim 407 \mu\text{mol mol}^{-1}$  in 2018. Associated with this, the  $\delta^{13}\text{C}$  of atmospheric CO<sub>2</sub> began to decline (Fig. 9.1). From about 1960 onwards, it declined at a steeper rate, reaching  $-8.5\text{‰}$  in 2018 (Table 9.1). This was associated with an acceleration in the rate of fossil fuel emissions around this time (Andres et al. 2012). The depletion in  $^{13}\text{C}$  of atmospheric CO<sub>2</sub> caused by the addition of CO<sub>2</sub> from combustion of fossil fuels during the industrial period is referred to as the  $^{13}\text{C}$  Suess Effect (Keeling 1979), by analogy to the decrease in  $^{14}\text{C}$  of CO<sub>2</sub> discovered by Hans Suess (1955).

Both the atmospheric CO<sub>2</sub> concentration and its  $\delta^{13}\text{C}$  show an intra-annual, or seasonal, cycle associated with photosynthesis in summer months and respiration in winter months in the northern hemisphere (Fig. 9.1). This seasonal cycle is most pronounced at high latitudes in the northern hemisphere, less pronounced at tropical latitudes, and essentially absent at high latitudes of the southern hemisphere, where there is very little land mass and therefore little terrestrial productivity (Keeling et al. 2005). In addition to this latitudinal and hemispheric gradient in the seasonal cycle of CO<sub>2</sub> concentration and isotopic composition, there is also an interhemispheric gradient in seasonally adjusted values for these variables; that is, their values when the seasonal cycle has been statistically removed. The interhemispheric gradient is such that the atmospheric CO<sub>2</sub> concentration is higher in the northern than in the southern hemisphere, and this concentration difference has been increasing since direct atmospheric measurements commenced around 1960 (Keeling et al. 2011). It is accompanied by a difference in seasonally adjusted atmospheric  $\delta^{13}\text{C}$  of CO<sub>2</sub> on the order of  $0.1\text{‰}$ , in which  $\delta^{13}\text{C}$  of CO<sub>2</sub> in the northern hemisphere is more negative

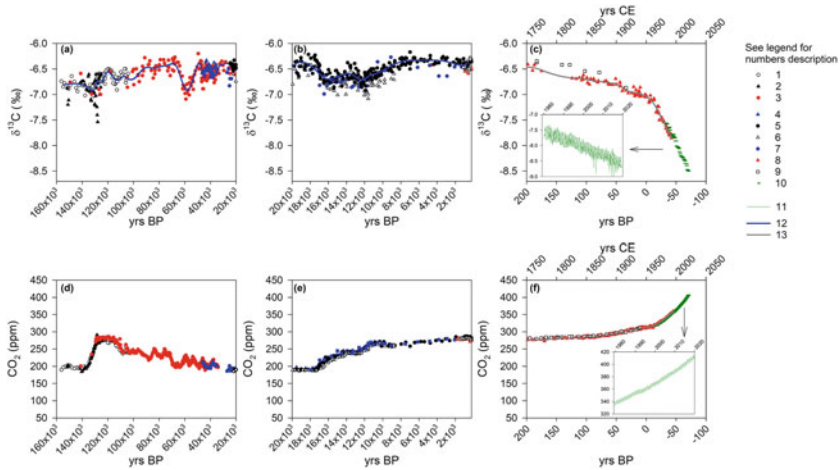


**Fig. 9.1** The stable isotope composition ( $\delta^{13}\text{C}$ , panels **a** to **c**) and  $\text{CO}_2$  concentration ( $[\text{CO}_2]$ , panels **d** to **f**) of atmospheric  $\text{CO}_2$  over the last ~160,000 years. Time is in years before present (yrs BP), where zero corresponds to the year 1950 of the current era (CE). In panels **c** and **f** both yrs BP and CE zero are presented. Data are from studies reporting both  $\delta^{13}\text{C}$  and  $[\text{CO}_2]$  in either ice cores or atmospheric air samples. For each data series the information presented next corresponds to the number in the legend—*symbol*—time span (Kyrs BP or CE)—sample origin (ice core drilling location or atmospheric station)—reference. Data series: 1—*White circles*—156.3 to 104.3 Kyrs BP—European Project for IceCoring in Antarctica (EPICA) Dome C (EDC) and Talos Dome—Schneider et al. (2013); 2—*Black triangles*—151.7 to 125.2 Kyrs BP—EDC—Lourantou et al. (2010); 3—*Red circles*—149.5 to 1.5 Kyrs BP – EDC, Talos Dome and EPICA Lronning Maud Land (EDML) – Eggleston et al. (2016); 4—*Blue triangles*—46.4 to 10.9 Kyrs BP—Taylor Dome—Bauska et al. (2016, 2018); 5—*Black circles*—24.4 to 0.5 Kyrs BP—EDC and Talos Dome—Schmitt et al. (2012); 6—*White triangles*—22.0 to 8.8 Kyrs BP—EDC—Lourantou et al. (2010); 7—*Blue circles*—27.1 to 1.3 Kyrs BP—Taylor Dome—Indermuhle et al. (1999); Smith et al. (1999); 8—*Red triangles*—1.8 to -0.04 Kyrs BP—Law Dome—Rubino et al. (2019); 9—*White squares*—1.2 to -0.01 Kyrs BP—WAIS Divide—Bauska et al. (2015); 10 – *Green horizontal lines* – air samples at Mauna Loa and South Pole – 1960 to 2018 CE—Keeling et al. (2001, 2017), Table S3 in Supplemental Materials). Series 10 shows seasonally detrended monthly records while Series 11 (*Green line* in the inserts of panels **c** and **f**) show the seasonal trends for  $\delta^{13}\text{C}$  (Keeling et al. 2001) and  $[\text{CO}_2]$  (NOAA ESRL-Global Monitoring Division) in air samples from Mauna Loa. The *Blue line* (12) is the Monte Carlo spline fitted to the  $\delta^{13}\text{C}$  data in series 1, 3 and 5 by Eggleston et al. (2016). The *Grey lines* (13) are the splines fitted to Law Dome ice core records of  $\delta^{13}\text{C}$  and  $[\text{CO}_2]$  by Rubino et al. (2019). Online resources: 1. <https://doi.pangaea.de/10.1594/PANGAEA.817041> 2. [ftp://ftp.ncdc.noaa.gov/pub/data/paleo/icecore/antarctica/epica\\_domec/edc2010d13co2-t2.txt](ftp://ftp.ncdc.noaa.gov/pub/data/paleo/icecore/antarctica/epica_domec/edc2010d13co2-t2.txt) 3. <https://doi.org/10.1594/PANGAEA.859209>, <https://doi.org/10.1594/PANGAEA.859179> 4. <https://www1.ncdc.noaa.gov/pub/data/paleo/icecore/antarctica/taylor/taylor2018d13co2.txt> 5. <https://doi.org/10.1594/PANGAEA.772713> 6. [ftp://ftp.ncdc.noaa.gov/pub/data/paleo/icecore/antarctica/epica\\_domec/edc2010d13co2.txt](ftp://ftp.ncdc.noaa.gov/pub/data/paleo/icecore/antarctica/epica_domec/edc2010d13co2.txt) 7. [ftp://ftp.ncdc.noaa.gov/pub/data/paleo/icecore/antarctica/taylor/taylor\\_co2-lat\\_equat.txt](ftp://ftp.ncdc.noaa.gov/pub/data/paleo/icecore/antarctica/taylor/taylor_co2-lat_equat.txt) 8 and 13. <https://doi.org/10.25919/5bfe29ff807fb> 9. <ftp://ftp.ncdc.noaa.gov/pub/data/paleo/icecore/antarctica/wais2015d13co2.txt> and <ftp://ftp.ncdc.noaa.gov/pub/data/paleo/icecore/antarctica/wais2015co2.txt> 10. <https://scrippsco2.ucsd.edu> 11. [https://scrippsco2.ucsd.edu/assets/data/atmospheric/stations/flask\\_isotopic/daily/flask\\_c13\\_mlo.csv](https://scrippsco2.ucsd.edu/assets/data/atmospheric/stations/flask_isotopic/daily/flask_c13_mlo.csv) and [ftp://afpt.cmdl.noaa.gov/products/trends/co2/co2\\_mm\\_mlo.txt](ftp://afpt.cmdl.noaa.gov/products/trends/co2/co2_mm_mlo.txt) 12. <http://www1.ncdc.noaa.gov/pub/data/paleo/icecore/antarctica/eggleston2016d13co2.txt>. The age chronologies are: AICC2012 (Bazin et al. 2013) for series 1 and 3, EDC3\_gas\_a according to the 4th scenario (Loulergue et al. 2007) for series 2 and 6, LDC 2010 (Lemieux-Dudon et al. 2010) for series 5, Baggenstos et al. (2017) for series 4, and st9810 (Steig et al. 1998) for series 7

**Table 9.1** Annual values for  $\delta^{13}\text{C}$  (‰) and CO<sub>2</sub> concentration (ppm) of atmospheric CO<sub>2</sub> for the period 1850 to 2018. Data from 1850 to 1979 are the splines fitted by Rubino et al. (2019) to ice core records from Law Dome, Antarctica. Data from 1980 to 2018 are the average of annual records of atmospheric samples collected at Mauna Loa, Hawaii and the South Pole Observatory (Keeling et al. 2001)

Year	$\delta^{13}\text{C}$	[CO <sub>2</sub> ]	Year	$\delta^{13}\text{C}$	[CO <sub>2</sub> ]	Year	$\delta^{13}\text{C}$	[CO <sub>2</sub> ]	Year	$\delta^{13}\text{C}$	[CO <sub>2</sub> ]
1850	-6.71	285.5	1893	-6.78	293.5	1936	-6.98	308.4	1979	-7.54	334.9
1851	-6.71	285.6	1894	-6.78	293.5	1937	-6.98	309.0	1980	-7.56	337.9
1852	-6.71	285.6	1895	-6.78	293.6	1938	-6.98	309.6	1981	-7.58	339.2
1853	-6.71	285.5	1896	-6.78	293.8	1939	-6.99	310.1	1982	-7.57	340.2
1854	-6.72	285.4	1897	-6.78	294.0	1940	-6.99	310.5	1983	-7.65	341.9
1855	-6.72	285.2	1898	-6.78	294.3	1941	-6.99	311.0	1984	-7.70	343.5
1856	-6.72	285.0	1899	-6.79	294.7	1942	-7.00	311.4	1985	-7.66	344.8
1857	-6.72	284.9	1900	-6.79	295.1	1943	-7.00	311.7	1986	-7.64	346.2
1858	-6.72	285.0	1901	-6.79	295.5	1944	-7.01	311.9	1987	-7.70	348.0
1859	-6.72	285.0	1902	-6.80	296.0	1945	-7.01	311.8	1988	-7.77	350.3
1860	-6.73	285.1	1903	-6.81	296.4	1946	-7.02	311.7	1989	-7.80	351.7
1861	-6.73	285.2	1904	-6.81	296.9	1947	-7.02	311.6	1990	-7.82	353.1
1862	-6.73	285.3	1905	-6.82	297.3	1948	-7.03	311.6	1991	-7.80	354.4
1863	-6.73	285.5	1906	-6.83	297.6	1949	-7.03	311.6	1992	-7.81	355.4
1864	-6.73	285.7	1907	-6.84	297.9	1950	-7.04	311.8	1993	-7.78	356.1
1865	-6.73	286.0	1908	-6.84	298.1	1951	-7.05	312.1	1994	-7.83	357.6
1866	-6.73	286.3	1909	-6.85	298.3	1952	-7.06	312.4	1995	-7.85	359.5
1867	-6.74	286.6	1910	-6.86	298.5	1953	-7.06	312.9	1996	-7.91	361.3
1868	-6.74	287.0	1911	-6.87	298.8	1954	-7.07	313.4	1997	-7.91	362.4
1869	-6.74	287.4	1912	-6.88	299.3	1955	-7.08	313.9	1998	-8.01	365.1
1870	-6.74	287.7	1913	-6.89	299.9	1956	-7.09	314.4	1999	-8.02	366.9
1871	-6.74	288.1	1914	-6.90	300.6	1957	-7.10	314.8	2000	-8.03	368.4
1872	-6.74	288.4	1915	-6.90	301.2	1958	-7.11	315.0	2001	-8.04	369.8
1873	-6.74	288.7	1916	-6.91	301.9	1959	-7.13	315.2	2002	-8.06	371.8
1874	-6.75	288.9	1917	-6.92	302.6	1960	-7.14	315.5	2003	-8.12	374.3
1875	-6.75	289.1	1918	-6.92	303.2	1961	-7.15	316.0	2004	-8.16	376.0
1876	-6.75	289.2	1919	-6.93	303.7	1962	-7.17	316.9	2005	-8.20	378.2
1877	-6.75	289.1	1920	-6.93	304.1	1963	-7.19	317.8	2006	-8.21	380.1
1878	-6.75	289.1	1921	-6.94	304.5	1964	-7.20	318.6	2007	-8.22	382.1
1879	-6.75	289.1	1922	-6.94	304.8	1965	-7.22	319.4	2008	-8.23	384.0
1880	-6.76	289.1	1923	-6.94	304.9	1966	-7.24	320.1	2009	-8.24	385.6
1881	-6.76	289.3	1924	-6.95	305.0	1967	-7.27	321.0	2010	-8.27	387.8
1882	-6.76	289.5	1925	-6.95	305.1	1968	-7.29	321.9	2011	-8.28	389.7

(continued)

**Table 9.1** (continued)

Year	$\delta^{13}\text{C}$	[CO <sub>2</sub> ]	Year	$\delta^{13}\text{C}$	[CO <sub>2</sub> ]	Year	$\delta^{13}\text{C}$	[CO <sub>2</sub> ]	Year	$\delta^{13}\text{C}$	[CO <sub>2</sub> ]
1883	-6.76	289.8	1926	-6.95	305.2	1969	-7.31	322.9	2012	-8.30	391.8
1884	-6.77	290.0	1927	-6.95	305.5	1970	-7.33	324.1	2013	-8.35	394.8
1885	-6.77	290.3	1928	-6.96	305.9	1971	-7.36	325.3	2014	-8.35	396.9
1886	-6.77	290.6	1929	-6.96	306.1	1972	-7.38	326.6	2015	-8.39	399.2
1887	-6.77	291.1	1930	-6.96	306.3	1973	-7.40	327.9	2016	-8.47	402.3
1888	-6.77	291.6	1931	-6.96	306.5	1974	-7.43	329.2	2017	-8.49	404.6
1889	-6.77	292.1	1932	-6.97	306.8	1975	-7.45	330.4	2018	-8.50	406.9
1890	-6.78	292.5	1933	-6.97	307.1	1976	-7.47	331.6			
1891	-6.78	292.9	1934	-6.97	307.4	1977	-7.49	332.7			
1892	-6.78	293.3	1935	-6.97	307.9	1978	-7.52	333.8			

than that in the southern hemisphere. These interhemispheric gradients largely reflect the greater intensity of fossil fuel emissions in the northern hemisphere compared to the southern hemisphere. However, there is also a natural gradient that can be seen if fossil fuel emissions are statistically removed; this appears to be related to oceanic transport processes (Keeling et al. 2011).

Despite these complexities, it is still true from a broader perspective that in the troposphere, the concentration of CO<sub>2</sub> and its  $\delta^{13}\text{C}$  are generally well mixed. For example, the interhemispheric gradient in  $\delta^{13}\text{C}$  of CO<sub>2</sub> of ~0.1‰ is of the same order of magnitude as the measurement uncertainty for  $\delta^{13}\text{C}$  in wood samples. Thus, it is probably not relevant for tree ring studies. However, at the land surface, in ecosystems where vegetation canopies are dense and fluxes of carbon into and out of vegetation and soils are large, the air CO<sub>2</sub> concentration and  $\delta^{13}\text{C}$  can become partly uncoupled from the free troposphere above. This uncoupling should be most pronounced where carbon cycling is vigorous and leaf area indices are high, such as in tropical rainforests. An example of the air CO<sub>2</sub> concentration and its  $\delta^{13}\text{C}$  for a tropical rainforest in French Guiana is shown in Fig. 9.2. There is a notable build-up of CO<sub>2</sub> beneath the canopy at night, with the highest values near the forest floor fed by respiration from soils that are relatively warm and moist, and have large root biomass. The build-up of CO<sub>2</sub> shifts the  $\delta^{13}\text{C}$  toward that of C<sub>3</sub> plants, because the additional CO<sub>2</sub> comes from respiration fuelled by carbohydrates captured in photosynthesis and decomposition of dead plant material. As a result, the  $\delta^{13}\text{C}$  of atmospheric CO<sub>2</sub> in the forest understory can be as low as -12‰ (Buchmann et al. 1997; Pataki et al. 2003). However, such pronounced build-up of respired CO<sub>2</sub> is generally limited to night time conditions when there is little atmospheric turbulence and therefore less effective mixing of air beneath the canopy with that above.

Under photosynthetic conditions, when the sun shines, the land surface heats causing turbulence, and atmospheric mixing is therefore more effective. Buchmann et al. (1997) estimated that at 2 m height in a tropical rainforest the daytime  $\delta^{13}\text{C}$  of CO<sub>2</sub> weighted by the top of canopy photosynthetically active radiation was only about 1‰ more negative than the free tropospheric value. In contrast to this relatively

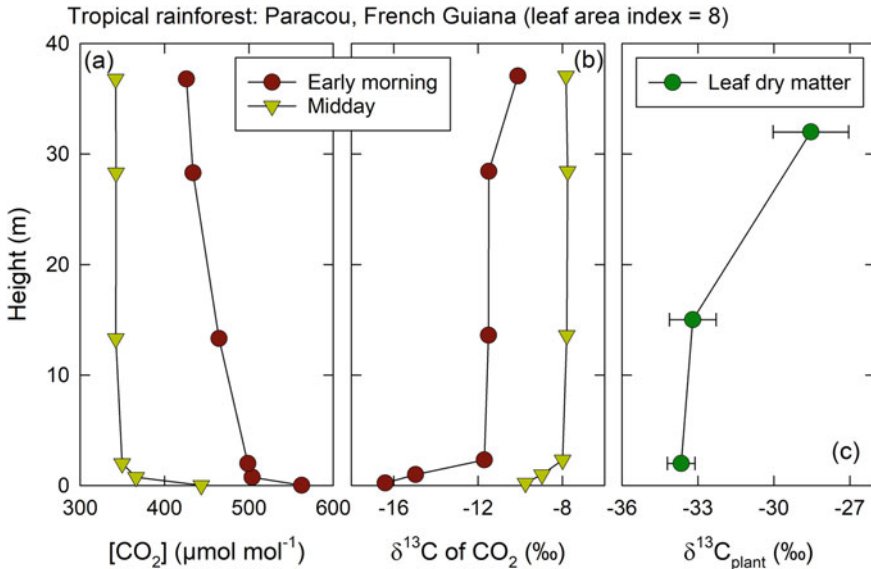


**Fig. 9.2** The CO<sub>2</sub> concentration (a) and its δ<sup>13</sup>C (b) measured in a tropical rainforest in early morning, before the onset of turbulent mixing, and at midday, when the canopy air space is typically well mixed. The more negative δ<sup>13</sup>C of CO<sub>2</sub> in the understory is also reflected in the δ<sup>13</sup>C of leaf dry matter (c), explaining part of the gradient in leaf dry matter δ<sup>13</sup>C from top of canopy to the understory. Comparison of panels b and c shows that other factors in addition to δ<sup>13</sup>C of CO<sub>2</sub> must be driving the reduction in δ<sup>13</sup>C<sub>plant</sub> from canopy top to understory, with reduction in light likely the most important of these. The figure is redrawn from Buchmann et al. (1997), using data they presented for the dry season

modest daytime shift in δ<sup>13</sup>C of atmospheric CO<sub>2</sub> with canopy depth, the gradient in δ<sup>13</sup>C of leaf biomass (δ<sup>13</sup>C<sub>p</sub>) from upper canopy to understory can be up to 5‰ (Fig. 9.2c). The much steeper gradient in leaf δ<sup>13</sup>C<sub>p</sub> compared to that in daytime δ<sup>13</sup>C of CO<sub>2</sub> suggests that physiological effects predominate in driving the changes in leaf biomass δ<sup>13</sup>C (Le Roux et al. 2001; Buchmann et al. 2002; Duursma and Marshall 2006; Ubierna and Marshall 2011). These physiological effects are likely driven by the reduction in light with canopy depth. The amount of photosynthetically active radiation in the understory of a forest with leaf area index of 8, for example, can be as little as 1% of that above the canopy (Duursma and Mäkelä 2007). Such strong gradients in light result in lower chloroplastic CO<sub>2</sub> concentrations at top of the canopy than at depth, and therefore lower photosynthetic <sup>13</sup>C discrimination in sun than in shade foliage.

For trees that grow with their crowns in the forest canopy or in communities with lower leaf area indices, the δ<sup>13</sup>C of atmospheric CO<sub>2</sub> that forms the source for photosynthesis can be assumed similar to that of the free troposphere (Buchmann et al. 2002). For trees with their crowns near the forest floor in communities with dense canopies, Buchmann et al. (2002) provide a relatively simple, empirical approach to estimating the daytime depletion of δ<sup>13</sup>C of atmospheric CO<sub>2</sub> as a function of canopy

height. This is most relevant to the lowermost 2 m of the canopy air space near the forest floor.

Typically for tree ring studies, an annually averaged value for the  $\delta^{13}\text{C}$  of  $\text{CO}_2$  in the troposphere is needed. This can be compiled for years prior to 1980 based on ice core data, and for years after 1980 from flask measurements of atmospheric  $\text{CO}_2$  that can be accessed online ([https://scrippsco2.ucsd.edu/data/atmospheric\\_co2/sampling\\_stations.html](https://scrippsco2.ucsd.edu/data/atmospheric_co2/sampling_stations.html)), with details of the measurements described in Keeling et al. (2001). In Table 9.1, we compile annually averaged values which are updated since the values given by McCarroll and Loader (2004). The ice core  $\delta^{13}\text{C}$  record was revised recently (Rubino et al. 2019), such that the value in 1850 is best estimated as  $\sim -6.7\text{‰}$ , rather than about  $\sim -6.4\text{‰}$  at the time that McCarroll and Loader (2004) compiled their table. In Table 9.1, we list the spline fitted data from Rubino et al. (2019) for the years 1850 to 1979, because the directly measured ice core data are not annually resolved. For years from 1980 to 2018, we list the average of flask measurements from Mauna Loa and South Pole (Graven et al. 2017; Keeling et al. 2017). The interhemispheric gradient in  $\delta^{13}\text{C}$  of  $\text{CO}_2$  between Mauna Loa and South Pole is small, less than  $0.1\text{‰}$  for most years, and the continuity with the ice core record at the changeover point from 1979 to 1980 is good (Table 9.1). An alternative to using spline fitted data is to use separate regression equations for prior to 1960 and following 1960, an approach favoured by McCarroll and Loader (2004). For comparison to their values, we provide such regression equations in Fig. 9.3. Note, however, that the annual values listed in Table 9.1 are not from these regression equations, but rather from the sources described above. During preparation of this book chapter, Belmecheri and Lavergne (2020) also published a new up-to-date compilation of atmospheric  $\text{CO}_2$  concentrations and  $\delta^{13}\text{C}$  for use in tree ring studies. Although they used different datasets for their compilation than we did for Table 9.1, the two compilations agree to within 1.6 ppm for  $[\text{CO}_2]$  and  $0.1\text{‰}$  for  $\delta^{13}\text{C}$  for individual years, with mean differences of 0.5 ppm and  $0.03\text{‰}$  for  $[\text{CO}_2]$  and  $\delta^{13}\text{C}$ , respectively.

### 9.3 Photosynthetic Discrimination Against $^{13}\text{C}$

Once an estimate for the  $\delta^{13}\text{C}$  of the air that a plant was exposed to ( $\delta^{13}\text{C}_a$ ) has been obtained, and the  $\delta^{13}\text{C}$  of plant tissue measured ( $\delta^{13}\text{C}_p$ ), the  $^{13}\text{C}$  discrimination of the plant tissue ( $\Delta^{13}\text{C}_p$ ) can be calculated (Farquhar et al. 1989),

$$\Delta^{13}\text{C}_p = \frac{\delta^{13}\text{C}_a - \delta^{13}\text{C}_p}{1 + \delta^{13}\text{C}_p} \quad (9.1a)$$

The delta values are typically expressed in per mil, which means that they will have been multiplied by 1000. When Eq. (9.1a) is scaled to per mil, the left side of the equation and the terms in the numerator of the right side will be multiplied by

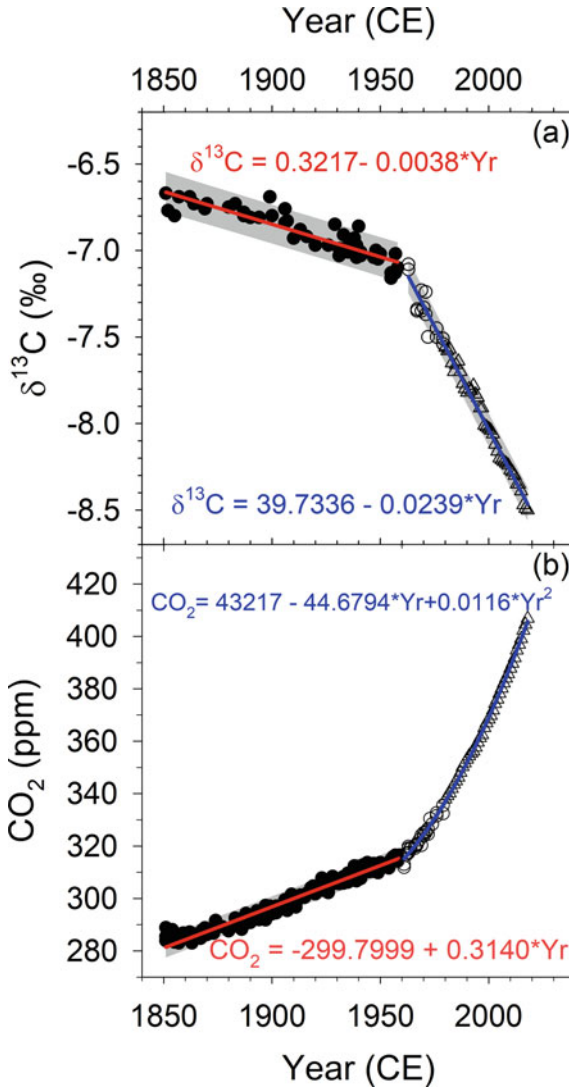


**Fig. 9.3** Alternatively to values given in Table 9.1, annual  $\delta^{13}\text{C}$  and  $\text{CO}_2$  concentration can be estimated from fitted functions. In this case, two time periods are considered as distinct (McCarroll and Loader, 2004): from 1850 to 1960 (*Period 1*), and from 1961 to 2018 (*Period 2*). Data used for *Period 1* are the original ice core records from Rubino et al. (2019) (black circles in panels **a** and **b**), which differ from the spline fitted values displayed in Table 9.1. Data used for *Period 2* are a combination of ice cores (clear circles, from 1961 to 1979, Rubino et al. 2019 original values) and atmospheric  $\text{CO}_2$  records (clear triangles, from 1980 to 2018, Keeling et al. 2001). The grey shaded areas around each fitted line represent the 95% prediction limits. Functions for  $\delta^{13}\text{C}$  are: *Period 1*)  $\delta^{13}\text{C} = (0.3217 \pm 0.4487) - (-0.0038 \pm 0.0002) \cdot \text{Year}$ ,  $R^2 = 0.83$ ,  $P < 0.0001$ ,  $\text{df} = 51$ ; *Period 2*)  $\delta^{13}\text{C} = (39.7336 \pm 0.7971) - (0.0239 \pm 0.0004) \cdot \text{Year}$ ,  $R^2 = 0.99$ ,  $P < 0.0001$ ,  $\text{df} = 51$ . Functions for  $[\text{CO}_2]$  are: *Period 1*)  $[\text{CO}_2] = (-299.7999 \pm 9.8124) - (0.3140 \pm 0.0051) \cdot \text{Year}$ ,  $R^2 = 0.96$ ,  $P < 0.0001$ ,  $\text{df} = 158$ ; *Period 2*)  $[\text{CO}_2] = (43,217 \pm 2120.2725) - (44.6794 \pm 2.1335) \cdot \text{Year} + (0.0116 \pm 0.0005) \cdot \text{Year}^2$ ,  $R^2 = 1$ ,  $P < 0.0001$ ,  $\text{df} = 68$



the factor 1000. Therefore, if the  $\delta^{13}\text{C}_a$  and  $\delta^{13}\text{C}_p$  are already expressed in per mil, Eq. (9.1a) will be written as,

$$\Delta^{13}\text{C}_p(^{\circ}/_{\infty}) = \frac{\delta^{13}\text{C}_a(^{\circ}/_{\infty}) - \delta^{13}\text{C}_p(^{\circ}/_{\infty})}{1 + \frac{\delta^{13}\text{C}_p(^{\circ}/_{\infty})}{1000}} \quad (9.1b)$$

Thus, the  $^{13}\text{C}$  discrimination essentially expresses the difference between the  $\delta^{13}\text{C}$  of atmospheric  $\text{CO}_2$  and that of plant tissue, with the denominator on the right side of the equation typically increasing that value by a factor of 1.02 to 1.03.

For  $\text{C}_3$  plants, which include the vast majority of all tree species, the  $\Delta^{13}\text{C}_p$  can then be related to  $c_i/c_a$  according to the theoretical model of Farquhar et al. (1982b). In its simplest form, this model can be expressed as,

$$\Delta^{13}\text{C}_p \approx a_s + (\bar{b} - a_s) \frac{c_i}{c_a} \quad (9.2)$$

Here,  $a_s$  is the  $^{13}\text{C}/^{12}\text{C}$  fractionation that takes place during diffusion of  $\text{CO}_2$  through static air, such as in the stomatal pore. The  $a_s$  has a theoretical value of 4.4‰. The term  $\bar{b}$  represents discrimination against  $^{13}\text{CO}_2$  by carboxylating enzymes, mainly Rubisco. In this simplified form of the model, the term  $\bar{b}$  also encompasses some other known sources of variation in  $\delta^{13}\text{C}_p$ , such as the diffusion resistance from the intercellular air spaces to the sites of carboxylation in the chloroplasts (Ubierna and Farquhar 2014). The value that is commonly assumed for  $\bar{b}$  is 27‰. This estimate was first based on comparison of instantaneous measurements of  $c_i/c_a$  from leaf gas exchange with  $\Delta^{13}\text{C}_p$  measured in leaf tissue (Farquhar et al. 1982a). Subsequent measurements of instantaneous gas exchange and leaf tissue  $\delta^{13}\text{C}_p$  have also generally supported a value for  $\bar{b}$  of 27‰ with respect to leaf dry matter (Farquhar et al. 1989; Cernusak et al. 2013; Cernusak 2020).

The objective for tree ring studies is often to retrieve an estimate of  $c_i/c_a$  from measurements of  $\Delta^{13}\text{C}_p$ . For this, Eq. (9.2) can be rearranged,

$$\frac{c_i}{c_a} \approx \frac{\Delta^{13}\text{C}_p - a_s}{\bar{b} - a_s} \quad (9.3)$$

Finally, the intrinsic water use efficiency,  $A/g_s$ , where  $A$  is net photosynthesis and  $g_s$  is stomatal conductance to water vapour, can be calculated as,

$$\frac{A}{g_s} \approx \frac{c_a \left(1 - \frac{c_i}{c_a}\right)}{1.6} \quad (9.4)$$

The factor of 1.6 in the denominator represents the ratio between the stomatal conductance to water vapour and that to  $\text{CO}_2$ . Note that Eq. (9.4) ignores both boundary layer resistance and ternary effects, and is thus a reasonable simplification of a more precise treatment (von Caemmerer and Farquhar 1981).

As noted above, Eq. (9.2) represents a simplified version of a more elaborate model for  $\Delta^{13}\text{C}$  during C<sub>3</sub> photosynthesis (Farquhar et al. 1982b; Farquhar and Cernusak 2012; Busch et al. 2020),

$$\Delta^{13}\text{C} \approx \frac{1}{1-t} \left( a_b \frac{c_a - c_s}{c_a} + a_s \frac{c_s - c_i}{c_a} \right) + \frac{1+t}{1-t} \left( a_m \frac{c_i - c_c}{c_a} + b \frac{c_c}{c_a} - e \frac{\mathcal{R}_d}{A} \frac{c_c}{c_a} - f \frac{\Gamma^*}{c_a} \right) \quad (9.5)$$

Here,  $a_b$  is the  $^{13}\text{C}/^{12}\text{C}$  fractionation during diffusion of CO<sub>2</sub> through the boundary layer (2.9‰), and  $a_m$  is that for dissolution and diffusion from the intercellular air spaces to the sites of carboxylation in the chloroplasts (1.8‰). The term  $b$  represents fractionation by Rubisco (~29‰),  $e$  is fractionation during day respiration, and  $f$  is fractionation during photorespiration. The fractionation factor assigned for  $e$  should take into account both respiratory fractionation, estimated at between 0 and 5‰ (Tcherkez et al. 2010, 2011) and any offset between  $\delta^{13}\text{C}$  of respiratory substrate and the substrate currently being produced by photosynthesis (Wingate et al. 2007; Busch et al. 2020). Estimates of fractionation for photorespiration,  $f$ , range from 8 to 16‰ (Gillon and Griffiths 1997; Lanigan et al. 2008; Evans and von Caemmerer 2013). The  $R_d$  is the rate of day respiration, and  $\Gamma^*$  is the CO<sub>2</sub> compensation point in the absence of day respiration. The terms  $c_s$  and  $c_c$  represent the CO<sub>2</sub> concentrations at the leaf surface and at the sites of carboxylation, respectively. The term  $t$  is a ternary correction factor, defined approximately as  $t \approx E/2g_c$ , where  $E$  is transpiration rate and  $g_c$  is stomatal conductance to CO<sub>2</sub> (Farquhar and Cernusak 2012). For further description of the terms in Eq. (9.5), the reader is referred to Ubierna et al. (2018).

The reader will notice that the value taken for  $b$ , discrimination by Rubisco, in the more complete model, Eq. (9.5), is typically 29‰, whereas the value taken for  $\bar{b}$  in the simple model, Eq. (9.2), for leaf tissue is smaller at 27‰. Below we discuss an even smaller value that should be used in the simple model for woody tissue. The difference arises because  $\bar{b}$  becomes something of a catch all for several less important terms that are in Eq. (9.5), but neglected from Eq. (9.2). A hierarchical approach to removing these terms was provided by Ubierna and Farquhar (2014), from which the impacts can be explored. Interestingly, such a bottom up approach suggested that the expected value for  $\bar{b}$  is actually less than 27‰, and the estimate of 27‰ likely includes developmental effects in leaf tissue  $\delta^{13}\text{C}$  (Cernusak et al. 2009a; Vogado et al. 2020) and possibly other post-photosynthetic processes (Ubierna and Farquhar 2014). The largest impact on the difference between  $b$  and  $\bar{b}$  comes from the drawdown in CO<sub>2</sub> concentration between the intercellular air spaces and the sites of carboxylation in the chloroplasts. This is the effect of a finite mesophyll conductance to diffusion of CO<sub>2</sub>. An additional term that could be of interest in tree ring studies is the photorespiratory fractionation,  $f(\Gamma^*/c_a)$ . Over large changes in atmospheric CO<sub>2</sub> concentration, there is a discernible impact on  $\Delta^{13}\text{C}$  from changes in  $\Gamma^*/c_a$ , independent of impacts caused by changes in  $c_i/c_a$  (Schubert and Jahren 2012, 2018; Porter et al. 2019).

Equation (9.5) is thought to include all processes that impact upon discrimination against  $^{13}\text{C}$  in photosynthetic CO<sub>2</sub> uptake by C<sub>3</sub> photosynthesis. Even so, there

are further modifications that could take place depending on the arrangement of mitochondria with respect to chloroplasts (Tholen et al. 2012; Ubierna et al. 2019), and the model does not address allocation of the products of photosynthesis, for example to starch versus export from the chloroplast (Tcherkez et al. 2004). Post photosynthetic fractionation is discussed further in Chap. 13. Equation (9.5) requires several additional parameters compared to Eq. (9.2) which are difficult to estimate retrospectively, as would be required for application to tree rings. Therefore, Eq. (9.2) represents a good compromise between mechanistic representation and tractability with respect to parameterisation. For situations where other parameters can also be measured or where accompanying datasets are available, application of the more complete model to tree rings could yield more subtle, but important, insights about past climate, leaf gas exchange, and carbon allocation dynamics within trees (Ogee et al. 2009). However, there remain challenges in understanding time integration and post-photosynthetic fractionation with respect to the  $\delta^{13}\text{C}$  signal in tree rings, and these create additional complexities for knowing how and when Eq. (9.5) can be applied effectively.

## 9.4 Relating the $\delta^{13}\text{C}$ of Wood to Leaf Gas Exchange

As mentioned above, the value originally estimated for  $\bar{b}$  in Eq. (9.2) of 27‰ was based on comparison of instantaneous measurements of  $c_i/c_a$  by leaf gas exchange with  $\delta^{13}\text{C}_p$  measured in leaf tissue (Farquhar et al. 1982a). At the same time, it has long been recognized that  $\delta^{13}\text{C}_p$  of wood is typically less negative than that of the leaf tissue which supplies it with photosynthate (Craig 1953; Leavitt and Long 1982; Francey et al. 1985; Leavitt and Long 1986; Badeck et al. 2005; Cernusak et al. 2009a). Differences are typically such that  $\delta^{13}\text{C}_p$  of leaves is more negative than that of stem or branch wood by about 1 to 3‰. A number of hypotheses have been suggested to account for this difference, none of which are mutually exclusive (Cernusak et al. 2009a). Part of the explanation involves a depletion in leaf  $\delta^{13}\text{C}_p$  that takes place during leaf expansion, such that when leaves mature, they export carbon less negative in  $\delta^{13}\text{C}$  compared to their structural carbon (Evans 1983; Francey et al. 1985; Cernusak et al. 2009a; Vogado et al. 2020). There are likely additional processes during the transfer of photosynthate from chloroplasts to newly differentiating woody tissue that could contribute (Offermann et al. 2011; Gessler et al. 2014; Bögelein et al. 2019), with further discussion in Chap. 13.

Although it is difficult to define the exact processes involved, it would nevertheless seem reasonable that the value of  $\bar{b}$  assigned for woody tissue in Eq. (9.2) could be less than that which would be assigned for leaf tissue. In Fig. 9.4, we compile data for 33 woody plant species in which  $c_i/c_a$  was measured by leaf gas exchange and the  $\delta^{13}\text{C}_p$  was measured in both leaves and woody stem tissue. We present the data for individual plants, rather than as species averages, because in many cases treatments were imposed within a species that resulted in a within species range of  $c_i/c_a$  and  $\delta^{13}\text{C}_p$ . The full dataset is available in a Dryad Digital Repository (<https://doi.org/10.>

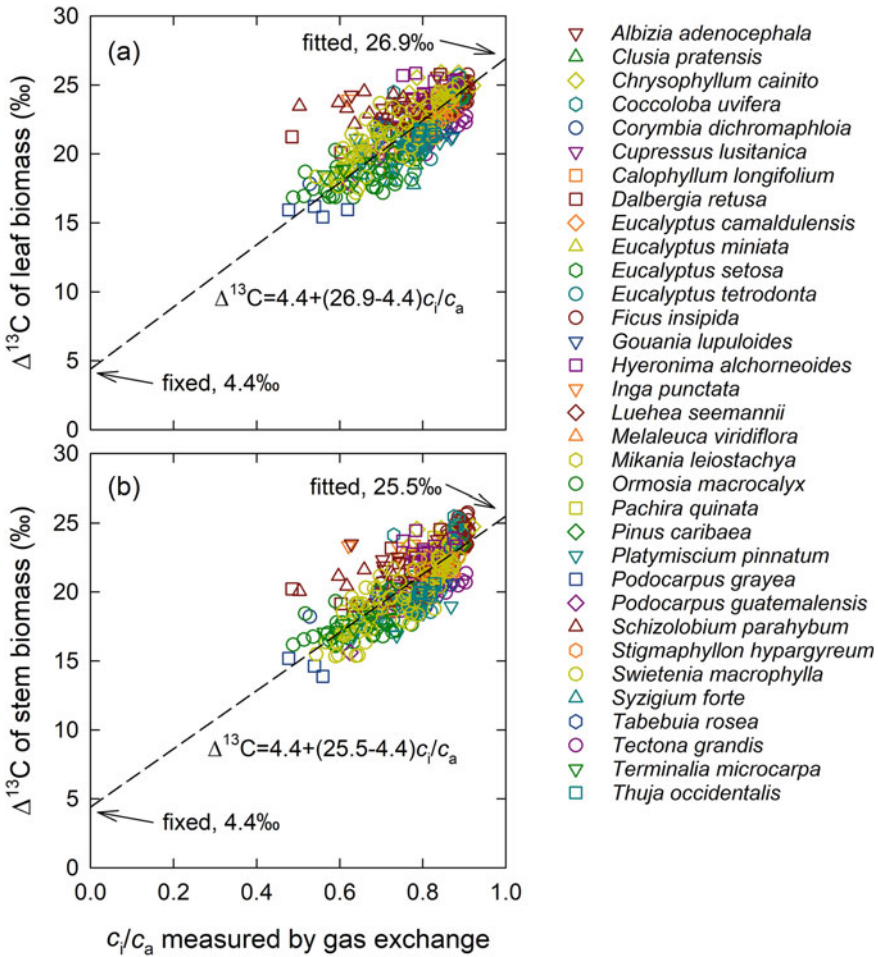


**Fig. 9.4** Carbon isotope discrimination ( $\Delta^{13}\text{C}$ ) measured in leaf biomass **a** and in stem biomass **b** plotted against the ratio of intercellular to ambient CO<sub>2</sub> concentrations ( $c_i/c_a$ ) measured by instantaneous gas exchange in 33 woody plant species. Further details of the measurements can be found in the original publications (Cernusak et al. 2007, 2008, 2009b, 2011; Garrish et al. 2010; Cernusak 2020). The data are available in a Dryad Digital Repository (<https://doi.org/10.5061/dryad.jm63xsjct>). Dashed lines show regression lines fitted with the intercepts fixed at 4.4‰. The inset equations show the regression slopes applied to the simplified model of Farquhar et al. (1982b)

5061/dryad.jm63xsjct). The fitted value for  $\bar{b}$  for the leaf tissue dataset, with  $a_s$  fixed at 4.4‰, was  $26.9 \pm 0.1\text{‰}$  (coefficient  $\pm$  SE;  $R^2 = 0.52$ ,  $n = 451$ ). This estimate is consistent with previous estimates of  $\bar{b} = 27\text{‰}$  for leaf tissue. On the other hand, the estimate of  $\bar{b}$  for stem tissue was  $25.5 \pm 0.1\text{‰}$  ( $R^2 = 0.63$ ,  $n = 449$ ), consistent with the idea that wood is less negative in  $\delta^{13}\text{C}_p$  than leaves of the same plant. Therefore, we recommend that if one aims to reconstruct  $c_i/c_a$  from leaf  $\delta^{13}\text{C}_p$ , a value for  $\bar{b}$

of 27‰ should be used in Eq. (9.3), as is typically done. On the other hand, if one aims to reconstruct  $c_i/c_a$  from woody tissue, as is the case for tree rings, one should use a value for  $\bar{b}$  of 25.5‰. The difference in  $c_i/c_a$  estimates will vary depending on the measured  $\delta^{13}\text{C}_p$ , but will be on the order of 0.05 in  $c_i/c_a$ . Thus, the difference is not large, but at the same time it will better align estimates of  $c_i/c_a$  from leaf and woody tissue with each other. Also, when carried through to the calculation of intrinsic water-use efficiency, the proportional change is larger, about 17% decrease in estimated  $A/g_s$  when  $c_i/c_a$  shifts from 0.7 to 0.75, for example. Note that if some parameters from Eq. (9.5) are brought in to Eq. (9.2), but Eq. (9.5) is not adopted in its entirety, then  $\bar{b}$  will need to be adjusted. This would create a challenge in merging the empirically determined value of  $\bar{b}$  from organic material analyses with parameters drawn from other contexts, and should be approached with caution (Vogado et al. 2020).

In order to test for species specificity in the value of  $\bar{b}$  for woody tissues, we constructed a mixed effects model for wood  $\Delta^{13}\text{C}$  as a function of  $c_i/c_a$  with a fixed intercept of 4.4‰; species  $\times c_i/c_a$  was additionally taken as a random effect. The model thus allowed us to test for different slopes among species (indicating different  $\bar{b}$  among species). The random effect was shown to be significant, with 14 out of 33 species having a slope significantly different than the overall mean slope, suggesting that  $\bar{b}$  can indeed vary among species. Thus, the value for  $\bar{b}$  for woody stems of 25.5‰ is a cross-species average value. However, the situation is entirely analogous to taking  $\bar{b} = 27‰$  based on the average estimate for leaf tissue, as this is also a cross-species average and varies by species, as shown in Fig. 9.4a. Thus, we are suggesting moving the average from 27 to 25.5‰ for woody tissues, to correct for the overall average difference between leaf and wood  $\Delta^{13}\text{C}$ , but this does not address the variance around this average due to species or environment. It is an incremental step, but nonetheless seems an easy and appropriate one to take.

Often for tree-ring studies, investigators prefer to extract cellulose prior to isotopic analysis, which has both advantages and disadvantages (McCarroll and Loader 2004). The  $\delta^{13}\text{C}$  of cellulose is typically less negative than that of whole wood by about 1‰ (Leavitt and Long 1982; Loader et al. 2003; Harlow et al. 2006). We recommend that if cellulose is analysed for  $\delta^{13}\text{C}$ , that an approximation of the offset between this and whole wood  $\delta^{13}\text{C}$  be subtracted from the cellulose  $\delta^{13}\text{C}$  before application of Eq. (9.3) with  $\bar{b} = 25.5‰$ , since this value of  $\bar{b}$  was determined for whole wood.

## 9.5 Conclusions

In this chapter, we have reviewed the primary influences on the  $\delta^{13}\text{C}$  of carbon captured by photosynthesis in  $\text{C}_3$  plants. The first control is the  $\delta^{13}\text{C}$  of atmospheric  $\text{CO}_2$  that the plant canopy was exposed to. The  $\delta^{13}\text{C}$  of atmospheric  $\text{CO}_2$  has decreased since the onset of the industrial revolution due to release of carbon from geological reservoirs. The  $\delta^{13}\text{C}$  of atmospheric  $\text{CO}_2$  inferred from ice cores was recently revised down slightly, so that the value in 1850 is now estimated at

~−6.7‰. The mean value for 2018 was −8.5‰. The δ<sup>13</sup>C of CO<sub>2</sub> beneath forest canopies can be more negative than that in the free troposphere above due to the influence of soil and plant respired CO<sub>2</sub>. This decrease in δ<sup>13</sup>C occurs mainly at night, and is most pronounced in forests with high leaf area indices. During daytime when photosynthesis takes place, turbulent exchange of canopy air with that in the troposphere diminishes this effect. Thus, forest respiration can reduce the δ<sup>13</sup>C of the CO<sub>2</sub> that forms the source for photosynthesis of understory plants and small statured trees, but the decrease is probably not more than about 1‰ under photosynthetic conditions. A simplified model provides a means of calculating  $c_i/c_a$ , the ratio of intercellular to ambient CO<sub>2</sub> concentrations, from measurements of δ<sup>13</sup>C of plant tissues and an inference of the δ<sup>13</sup>C of atmospheric CO<sub>2</sub> at the time when the plant tissue was formed. The long standing observation that woody tissues are less negative in δ<sup>13</sup>C than the leaves that supply them with photosynthate suggests that the coefficient relating  $c_i/c_a$  to δ<sup>13</sup>C should differ for the two tissue types (see also Chap. 13). We used a dataset comprising measurements in 33 woody plant species to estimate that the coefficient  $\bar{b}$  should be taken as 27‰ in the simplified model for leaf tissue, and as 25.5‰ for woody tissue, including tree rings. While the difference in estimated  $c_i/c_a$  using the two coefficients is not large, the revision will aid in aligning  $c_i/c_a$  inferred from tree rings with that which would be measured by instantaneous gas exchange.

## References

- Andres RJ, Marland G, Boden T, Bischof S (2000) Carbon dioxide emissions from fossil fuel consumption and cement manufacture, 1751–1991, and an estimate of their isotopic composition and latitudinal distribution. In: Schimel DS, Wigley TML (eds) *The carbon cycle*. Cambridge University Press, Cambridge, pp 53–62
- Andres RJ, Boden TA, Breon FM, Ciais P, Davis S, Erickson D, Gregg JS, Jacobson A, Marland G, Miller J, Oda T, Olivier JGJ, Raupach MR, Rayner P, Treanton K (2012) A synthesis of carbon dioxide emissions from fossil-fuel combustion. *Biogeosciences* 9:1845–1871
- Andres RJ, Boden TA, Marland G. 1996. Annual fossil-fuel CO<sub>2</sub> emissions: global stable carbon isotopic signature. Environmental System Science Data Infrastructure for a Virtual Ecosystem, Carbon Dioxide Information Analysis Center (CDIAC), Oak Ridge National Laboratory (ORNL), Oak Ridge, TN (United States)
- Badeck FW, Tcherkez G, Nogues S, Piel C, Ghashghaie J (2005) Post-photosynthetic fractionation of stable carbon isotopes between plant organs—a widespread phenomenon. *Rapid Commun Mass Spectrom* 19:1381–1391
- Bagenstos D, Bauska TK, Severinghaus JP, Lee JE, Schaefer H, Buizert C, Brook EJ, Shackleton S, Petrenko VV (2017) Atmospheric gas records from Taylor Glacier, Antarctica, reveal ancient ice with ages spanning the entire last glacial cycle. *Clim Past* 13:943–958
- Bauska TK, Joos F, Mix AC, Roth R, Ahn J, Brook EJ (2015) Links between atmospheric carbon dioxide, the land carbon reservoir and climate over the past millennium. *Nat Geosci* 8:383–387
- Bauska TK, Bagenstos D, Brook EJ, Mix AC, Marcott SA, Petrenko VV, Schaefer H, Severinghaus JP, Lee JE (2016) Carbon isotopes characterize rapid changes in atmospheric carbon dioxide during the last deglaciation. *Proc Natl Acad Sci* 113:3465–3470

- Bauska TK, Brook EJ, Marcott SA, Baggenstos D, Shackleton S, Severinghaus JP, Petrenko VV (2018) Controls on millennial-scale atmospheric CO<sub>2</sub> variability during the last glacial period. *Geophys Res Lett* 45:7731–7740
- Bazin L, Landais A, Lemieux-Dudon B, Kele HTM, Veres D, Parrenin F, Martinier P, Ritz C, Capron E, Lipenkov V, Loutre M-F, Raynaud D, Vinther B, Svensson A, Rasmussen SO, Severi M, Blunier T, Leuenberger M, Fischer H, Masson-Delmotte V, Chappellaz J, Wolff E (2013) An optimized multi-proxy, multi-site Antarctic ice and gas orbital chronology (AICC2012): 120–800 ka. *Clim Past* 9:1715–1731
- Belmecheri S, Wright WE, Szejner P, Morino KA, Monson RK (2018) Carbon and oxygen isotope fractionations in tree rings reveal interactions between cambial phenology and seasonal climate. *Plant Cell Environ* 41:2758–2772
- Belmecheri S, Lavergne A (2020) Compiled records of atmospheric CO<sub>2</sub> concentrations and stable carbon isotopes to reconstruct climate and derive plant ecophysiological indices from tree rings. *Dendrochronologia* 63: 125748
- Bögelein R, Lehmann MM, Thomas FM (2019) Differences in carbon isotope leaf-to-phloem fractionation and mixing patterns along a vertical gradient in mature European beech and Douglas fir. *New Phytol* 222:1803–1815
- Briffa KR, Osborn TJ, Schweingruber FH (2004) Large-scale temperature inferences from tree rings: a review. *Global Planet Change* 40:11–26
- Buchmann N, Guehl JM, Barigah TS, Ehleringer JR (1997) Interseasonal comparison of CO<sub>2</sub> concentrations, isotopic composition, and carbon dynamics in an Amazonian rainforest (French Guiana). *Oecologia* 110:120–131
- Buchmann N, Brooks JR, Ehleringer JR (2002) Predicting daytime carbon isotope ratios of atmospheric CO<sub>2</sub> within forest canopies. *Funct Ecol* 16:49–57
- Busch FA, Holloway-Phillips M, Stuart-Williams H, Farquhar GD (2020) Revisiting carbon isotope discrimination in C<sub>3</sub> plants shows respiration rules when photosynthesis is low. *Nat Plants* 6:245–258
- Cernusak LA (2020) Gas exchange and water-use efficiency in plant canopies. *Plant Biol* 22(Suppl. 1):52–67
- Cernusak LA, Winter K, Aranda J, Turner BL, Marshall JD (2007) Transpiration efficiency of a tropical pioneer tree (*Ficus insipida*) in relation to soil fertility. *J Exp Bot* 58:3549–3566
- Cernusak LA, Winter K, Aranda J, Turner BL (2008) Conifers, angiosperm trees, and lianas: growth, whole-plant water and nitrogen use efficiency, and stable isotope composition ( $\delta^{13}\text{C}$  and  $\delta^{18}\text{O}$ ) of seedlings grown in a tropical environment. *Plant Physiol* 148:642–659
- Cernusak LA, Winter K, Turner BL (2009a) Physiological and isotopic ( $\delta^{13}\text{C}$  and  $\delta^{18}\text{O}$ ) responses of three tropical tree species to water and nutrient availability. *Plant Cell Environ* 32:1441–1455
- Cernusak LA, Tcherkez G, Keitel C, Cornwell WK, Santiago LS, Knohl A, Barbour MM, Williams DG, Reich PB, Ellsworth DS, Dawson TE, Griffiths H, Farquhar GD, Wright IJ (2009b) Why are non-photosynthetic tissues generally <sup>13</sup>C enriched compared to leaves in C<sub>3</sub> plants? Review and synthesis of current hypotheses. *Funct Plant Biol* 36:199–213
- Cernusak LA, Winter K, Martinez C, Correa E, Aranda J, Garcia M, Jaramillo C, Turner BL (2011) Responses of legume versus nonlegume tropical tree seedlings to elevated CO<sub>2</sub> concentration. *Plant Physiol* 157:372–385
- Cernusak LA, Ubierna N, Winter K, Holtum JAM, Marshall JD, Farquhar GD (2013) Environmental and physiological determinants of carbon isotope discrimination in terrestrial plants. *New Phytol* 200:950–965
- Coplen TB (2011) Guidelines and recommended terms for expression of stable-isotope-ratio and gas-ratio measurement results. *Rapid Commun Mass Spectrom* 25:2538–2560
- Craig H (1953) The geochemistry of the stable carbon isotopes. *Geochim Cosmochim Acta* 3:53–92
- Craig H (1957) Isotopic standards for carbon and oxygen and correction factors for mass-spectrometric analysis of carbon dioxide. *Geochim Cosmochim Acta* 12:133–149
- Drew DM, Schulze ED, Downes GM (2009) Temporal variation in  $\delta^{13}\text{C}$ , wood density and microfibril angle in variously irrigated *Eucalyptus nitens*. *Funct Plant Biol* 36:1–10

- Duursma RA, Mäkelä A (2007) Summary models for light interception and light-use efficiency of non-homogeneous canopies. *Tree Physiol* 27:859–870
- Duursma RA, Marshall JD (2006) Vertical canopy gradients in  $\delta^{13}\text{C}$  correspond with leaf nitrogen content in a mixed-species conifer forest. *Trees Struct Funct* 20:496–506
- Eggleston S, Schmitt J, Bereiter B, Schneider R, Fischer H (2016) Evolution of the stable carbon isotope composition of atmospheric CO<sub>2</sub> over the last glacial cycle. *Paleoceanography* 31:434–452
- Evans JR, von Caemmerer S (2013) Temperature response of carbon isotope discrimination and mesophyll conductance in tobacco. *Plant Cell Environ* 36:745–756
- Evans JR (1983) Photosynthesis and nitrogen partitioning in leaves of *Triticum aestivum* L. and related species. PhD thesis, Australian National University, Canberra
- Farquhar GD, Cernusak LA (2012) Ternary effects on the gas exchange of isotopologues of carbon dioxide. *Plant Cell Environ* 35:1221–1231
- Farquhar GD, Richards RA (1984) Isotopic composition of plant carbon correlates with water-use efficiency in wheat genotypes. *Aust J Plant Physiol* 11:539–552
- Farquhar GD, O'Leary MH, Berry JA (1982a) On the relationship between carbon isotope discrimination and the intercellular carbon dioxide concentration in leaves. *Aust J Plant Physiol* 9:121–137
- Farquhar GD, Ball MC, von Caemmerer S, Roksandic Z (1982b) Effect of salinity and humidity on  $\delta^{13}\text{C}$  value of halophytes- evidence for diffusional isotope fractionation determined by the ratio of intercellular/atmospheric partial pressure of CO<sub>2</sub> under different environmental conditions. *Oecologia* 52:121–124
- Farquhar GD, Ehleringer JR, Hubick KT (1989) Carbon isotope discrimination and photosynthesis. *Annu Rev Plant Physiol Plant Mol Biol* 40:503–537
- Francey RJ, Farquhar GD (1982) An explanation of  $^{13}\text{C}/^{12}\text{C}$  variations in tree rings. *Nature* 297:28–31
- Francey RJ, Gifford RM, Sharkey TD, Weir B (1985) Physiological influences on carbon isotope discrimination in huon pine (*Lagarostrobos franklinii*). *Oecologia* 66:211–218
- Frank DC, Poulter B, Saurer M, Esper J, Huntingford C, Helle G, Treydte K, Zimmermann NE, Schleser GH, Ahlstrom A, Ciais P, Friedlingstein P, Levis S, Lomas M, Sitch S, Viovy N, Andreu-Hayles L, Bednarz Z, Berninger F, Boettger T, D'Alessandro CM, Daux V, Filot M, Grabner M, Gutierrez E, Haupt M, Hiltavuori E, Jungner H, Kalela-Brundin M, Krapiec M, Leuenberger M, Loader NJ, Marah H, Masson-Delmotte V, Pazdur A, Pawelczyk S, Pierre M, Planells O, Pukiene R, Reynolds-Henne CE, Rinne KT, Saracino A, Sonninen E, Stievenard M, Switsur VR, Szczepanek M, Szychowska-Krapiec E, Todaro L, Waterhouse JS, Weigl M (2015) Water-use efficiency and transpiration across European forests during the Anthropocene. *Nat Clim Change* 5:579–583
- Fritts HC, Swetnam TW (1989) Dendroecology: a tool for evaluating variations in past and present forest environments. In: Begon M, Fitter AH, Ford ED, MacFadyen A (eds) *Academic Press, Advances in Ecological Research*, pp 111–188
- Garrish V, Cernusak LA, Winter K, Turner BL (2010) Nitrogen to phosphorus ratio of plant biomass versus soil solution in a tropical pioneer tree, *Ficus insipida*. *J Exp Bot* 61:3735–3748
- Gessler A, Ferrio JP, Hommel R, Treydte K, Werner RA, Monson RK (2014) Stable isotopes in tree rings: towards a mechanistic understanding of isotope fractionation and mixing processes from the leaves to the wood. *Tree Physiol* 34:796–818
- Gillon JS, Griffiths H (1997) The influence of (photo)respiration on carbon isotope discrimination in plants. *Plant Cell Environ* 20:1217–1230
- Graven H, Allison CE, Etheridge DM, Hammer S, Keeling RF, Levin I, Meijer HAJ, Rubino M, Tans PP, Trudinger CM, Vaughn BH, White JWC (2017) Compiled records of carbon isotopes in atmospheric CO<sub>2</sub> for historical simulations in CMIP6. *Geosci Model Dev* 10:4405–4417
- Harlow BA, Marshall JD, Robinson AP (2006) A multi-species comparison of  $\delta^{13}\text{C}$  from whole wood, extractive-free wood and holocellulose. *Tree Physiol* 26:767–774



- Hartl-Meier C, Zang C, Buntgen U, Esper J, Rothe A, Gottlein A, Dirnback T, Treydte K (2015) Uniform climate sensitivity in tree-ring stable isotopes across species and sites in a mid-latitude temperate forest. *Tree Physiol* 35:4–15
- Indermuhle A, Stocker TF, Joos F, Fischer H, Smith HJ, Wahlen M, Deck B, Mastroianni D, Tschumi J, Blunier T, Meyer R, Stauffer B (1999) Holocene carbon-cycle dynamics based on CO<sub>2</sub> trapped in ice at Taylor Dome, Antarctica. *Nature* 398:121–126
- Keeling CD (1979) The Suess effect: <sup>13</sup>C/Carbon-<sup>14</sup>C interrelations. *Environ Int* 2:229–300
- Keeling CD, Piper SC, Whorf TP, Keeling RF (2011) Evolution of natural and anthropogenic fluxes of atmospheric CO<sub>2</sub> from 1957 to 2003. *Tellus B* 63:1–22
- Keeling RF, Graven HD, Welp LR, Resplandy L, Bi J, Piper SC, Sun Y, Bollenbacher A, Meijer HAJ (2017) Atmospheric evidence for a global secular increase in carbon isotopic discrimination of land photosynthesis. *Proc Natl Acad Sci USA* 114:10361–10366
- Keeling CD, Piper SC, Bacastow RB, Wahlen M, Whorf TP, Heimann M, Meijer HA (2001) Exchanges of atmospheric CO<sub>2</sub> and <sup>13</sup>CO<sub>2</sub> with the terrestrial biosphere and oceans from 1978 to 2000. I. Global aspects, SIO Reference Series, No. 01-06: Scripps Institution of Oceanography, San Diego
- Keeling CD, Piper SC, Bacastow RB, Wahlen M, Whorf TP, Heimann M, Meijer HA (2005) Atmospheric CO<sub>2</sub> and <sup>13</sup>CO<sub>2</sub> exchange with the terrestrial biosphere and oceans from 1978 to 2000: observations and carbon cycle implications. In: Baldwin IT, Caldwell MM, Heldmaier G, Jackson RB, Lange OL, Mooney HA, Schulze ED, Sommer U, Ehleringer JR, Denise Dearing M, Cerling TE (eds) *A history of atmospheric CO<sub>2</sub> and its effects on plants, animals, and ecosystems*. Springer, New York, pp 83–113
- Lanigan GJ, Betson N, Griffiths H, Seibt U (2008) Carbon isotope fractionation during photorespiration and carboxylation in *Senecio*. *Plant Physiol* 148:2013–2020
- Le Roux X, Bariac T, Sinoquet H, Genty B, Piel C, Mariotti A, Girardin C, Richard P (2001) Spatial distribution of leaf water-use efficiency and carbon isotope discrimination within an isolated tree crown. *Plant Cell Environ* 24:1021–1032
- Leavitt SW, Long A (1982) Evidence for <sup>13</sup>C/<sup>12</sup>C fractionation between tree leaves and wood. *Nature* 298:742–744
- Leavitt SW, Long A (1986) Stable-carbon isotope variability in tree foliage and wood. *Ecology* 67:1002–1010
- Lemieux-Dudon B, Blayo E, Petit J-R, Waelbroeck C, Svensson A, Ritz C, Barnola J-M, Narcisi BM, Parrenin F (2010) Consistent dating for Antarctic and Greenland ice cores. *Quatern Sci Rev* 29:8–20
- Loader NJ, Robertson I, McCarroll D (2003) Comparison of stable carbon isotope ratios in the whole wood, cellulose and lignin of oak tree-rings. *Palaeogeogr Palaeoclimatol Palaeoecol* 196:395–407
- Loulergue L, Parrenin F, Blunier T, Barnola J-M, Spahni R, Schilt A, Raisbeck G, Chappellaz J (2007) New constraints on the gas age-ice age difference along the EPICA ice cores, 0–50 kyr. *Clim Past* 3:527–540
- Lourantou A, Chappellaz J, Barnola JM, Masson-Delmotte V, Raynaud D (2010) Changes in atmospheric CO<sub>2</sub> and its carbon isotopic ratio during the penultimate deglaciation. *Quatern Sci Rev* 29:1983–1992
- McCarroll D, Loader NJ (2004) Stable isotopes in tree rings. *Quatern Sci Rev* 23:771–801
- Monserud RA, Marshall JD (2001) Time-series analysis of  $\delta^{13}\text{C}$  from tree rings 1: time trends and autocorrelations. *Tree Physiol* 21:1087–1102
- Offermann C, Ferrio JP, Holst J, Grote R, Siegwolf R, Kayler Z, Gessler A (2011) The long way down—are carbon and oxygen isotope signals in the tree ring uncoupled from canopy physiological processes? *Tree Physiol* 31:1088–1102
- Ogee J, Barbour MM, Wingate L, Bert D, Bosc A, Stievenard M, Lambrot C, Pierre M, Bariac T, Loustau D, Dewar RC (2009) A single-substrate model to interpret intra-annual stable isotope signals in tree-ring cellulose. *Plant Cell Environ* 32:1071–1090

- Pataki DE, Ehleringer JR, Flanagan LB, Yakir D, Bowling DR, Still CJ, Buchmann N, Kaplan JO, Berry JA (2003) The application and interpretation of Keeling plots in terrestrial carbon cycle research. *Global Biogeochem Cycles* 17:15
- Peñuelas J, Canadell JG, Ogaya R (2011) Increased water-use efficiency during the 20<sup>th</sup> century did not translate into enhanced tree growth. *Glob Ecol Biogeogr* 20:597–608
- Porter AS, Gerald CEF, Yiotis C, Montanez IP, McElwain JC (2019) Testing the accuracy of new paleoatmospheric CO<sub>2</sub> proxies based on plant stable carbon isotopic composition and stomatal traits in a range of simulated paleoatmospheric O<sub>2</sub>:CO<sub>2</sub> ratios. *Geochim Cosmochim Acta* 259:69–90
- Rubino M, Etheridge DM, Thornton DP, Howden R, Allison CE, Francey RJ, Langenfelds RL, Steele LP, Trudinger CM, Spencer DA, Curran MAJ, van Ommen TD, Smith AM (2019) Revised records of atmospheric trace gases CO<sub>2</sub>, CH<sub>4</sub>, N<sub>2</sub>O, and δ<sup>13</sup>C-CO<sub>2</sub> over the last 2000 years from Law Dome, Antarctica. *Earth Syst Sci Data* 11:473–492
- Saurer M, Siegwolf RTW, Schweingruber FH (2004) Carbon isotope discrimination indicates improving water-use efficiency of trees in northern Eurasia over the last 100 years. *Glob Change Biol* 10:2109–2120
- Schmitt J, Schneider R, Elsigs J, Leuenberger D, Lourdantou A, Chappellaz J, Köhler P, Joos F, Stocker TF, Leuenberger M, Fischer H (2012) Carbon isotope constraints on the deglacial CO<sub>2</sub> rise from ice cores. *Science* 336:711–714
- Schneider R, Schmitt J, Köhler P, Joos F, Fischer H (2013) A reconstruction of atmospheric carbon dioxide and its stable carbon isotopic composition from the penultimate glacial maximum to the last glacial inception. *Clim Past* 9:2507–2523
- Schubert BA, Jahren AH (2012) The effect of atmospheric CO<sub>2</sub> concentration on carbon isotope fractionation in C<sub>3</sub> land plants. *Geochim Cosmochim Acta* 96:29–43
- Schubert BA, Jahren AH (2018) Incorporating the effects of photorespiration into terrestrial paleoclimate reconstruction. *Earth Sci Rev* 177:637–642
- Smith HJ, Fischer H, Mastroianni D, Deck B, Wahlen M (1999) Dual modes of the carbon cycle since the Last Glacial Maximum. *Nature* 400:248–250
- Steig EJ, Brook EJ, White JWC, Sucher CM, Bender ML, Lehman SJ, Morse DL, Waddington ED, Clow GD (1998) Synchronous climate changes in Antarctica and the North Atlantic. *Science* 282:92–95
- Suess HE (1955) Radiocarbon concentration in modern wood. *Science* 122:415
- Tcherkez G, Farquhar G, Badeck F, Ghashghaie J (2004) Theoretical considerations about carbon isotope distribution in glucose of C<sub>3</sub> plants. *Funct Plant Biol* 31:857–877
- Tcherkez G, Schauffele R, Noguees S, Piel C, Boom A, Lanigan G, Barbaroux C, Mata C, Elhani S, Hemming D, Maguas C, Yakir D, Badeck FW, Griffiths H, Schnyder H, Ghashghaie J (2010) On the <sup>13</sup>C/<sup>12</sup>C isotopic signal of day and night respiration at the mesocosm level. *Plant Cell Environ* 33:900–913
- Tcherkez G, Mauve C, Lamothe M, Le Bras C, Grapin A (2011) The <sup>13</sup>C/<sup>12</sup>C isotopic signal of day-respired CO<sub>2</sub> in variegated leaves of *Pelargonium x hortorum*. *Plant Cell Environ* 34:270–283
- Tholen D, Ethier G, Genty B, Pepin S, Zhu XG (2012) Variable mesophyll conductance revisited: theoretical background and experimental implications. *Plant Cell Environ* 35:2087–2103
- Ubierna N, Farquhar GD (2014) Advances in measurements and models of photosynthetic carbon isotope discrimination in C<sub>3</sub> plants. *Plant Cell Environ* 37:1494–1498
- Ubierna N, Marshall JD (2011) Vertical and seasonal variation in the δ<sup>13</sup>C of leaf-respired CO<sub>2</sub> in a mixed conifer forest. *Tree Physiol* 31:414–427
- Ubierna N, Cernusak LA, Holloway-Phillips M, Busch FA, Cousins AB, Farquhar GD (2019) Critical review: incorporating the arrangement of mitochondria and chloroplasts into models of photosynthesis and carbon isotope discrimination. *Photosynth Res* 141:5–31
- Ubierna N, Holloway-Phillips MM, Farquhar GD (2018) Using stable carbon isotopes to study C<sub>3</sub> and C<sub>4</sub> photosynthesis: models and calculations. In: Covshoff S (ed) *Photosynthesis: methods and protocols*. Springer, New York, pp 155–196

- van der Sleen P, Groenendijk P, Vlam M, Anten NPR, Boom A, Bongers F, Pons TL, Terburg G, Zuidema PA (2015) No growth stimulation of tropical trees by 150 years of CO<sub>2</sub> fertilization but water-use efficiency increased. *Nat Geosci* 8:24–28
- Vogado NO, Winter K, Ubierna N, Farquhar GD, Cernusak LA (2020) Directional change in leaf dry matter  $\delta^{13}\text{C}$  during leaf development is widespread in C<sub>3</sub> plants. *Annals Botany* 126:981–990
- von Caemmerer S, Farquhar GD (1981) Some relationships between the biochemistry of photosynthesis and the gas exchange of leaves. *Planta* 153:376–387
- Wingate L, Seibt U, Moncrieff JB, Jarvis PG, Lloyd J (2007) Variations in <sup>13</sup>C discrimination during CO<sub>2</sub> exchange by *Picea sitchensis* branches in the field. *Plant Cell Environ* 30:600–616

**Open Access** This chapter is licensed under the terms of the Creative Commons Attribution 4.0 International License (<http://creativecommons.org/licenses/by/4.0/>), which permits use, sharing, adaptation, distribution and reproduction in any medium or format, as long as you give appropriate credit to the original author(s) and the source, provide a link to the Creative Commons license and indicate if changes were made.

The images or other third party material in this chapter are included in the chapter's Creative Commons license, unless indicated otherwise in a credit line to the material. If material is not included in the chapter's Creative Commons license and your intended use is not permitted by statutory regulation or exceeds the permitted use, you will need to obtain permission directly from the copyright holder.



# Chapter 10

## Environmental, Physiological and Biochemical Processes Determining the Oxygen Isotope Ratio of Tree-Ring Cellulose



Xin Song, Andrew Lorrey, and Margaret M. Barbour

**Abstract** Analysis of the oxygen isotope ratio of tree-ring cellulose ( $\delta^{18}\text{O}_{\text{cell}}$ ) is a promising tool for reconstructing past climatic variations and their influence on terrestrial ecosystems, but control mechanisms of  $\delta^{18}\text{O}_{\text{cell}}$  are multi-faceted, involving a number of fractionation steps along the oxygen transfer pathway from precipitation water to the site of cellulose formation. The goal of the current chapter is to provide an overview of the current knowledge concerning fractionation mechanisms related to  $\delta^{18}\text{O}_{\text{cell}}$ . The review is organized by using the currently widely-used  $\delta^{18}\text{O}_{\text{cell}}$  model as a reference context, and is focused on three main determinants of  $\delta^{18}\text{O}_{\text{cell}}$ : source water isotope ratio ( $\delta^{18}\text{O}_{\text{sw}}$ ), leaf water isotope enrichment ( $\Delta^{18}\text{O}_{\text{lw}}$ ), and biochemical fractionations downstream of  $\Delta^{18}\text{O}_{\text{lw}}$ . For each component, we summarize environmental, physiological, and/or biochemical processes underlying  $^{18}\text{O}$  fractionations, and provide explanations of how these processes are critically relevant for linking  $\delta^{18}\text{O}_{\text{cell}}$  to climatic factors in real-world scenarios. We identify knowledge gaps in mechanistic controls of  $\delta^{18}\text{O}_{\text{cell}}$ , and highlight opportunities for more research to improve upon the existing model.

---

X. Song (✉)

College of Life and Marine Sciences, Shenzhen University, Shenzhen 518000, Guangdong Province, China

e-mail: [xin.song@szu.edu.cn](mailto:xin.song@szu.edu.cn)

Shenzhen Key Laboratory of Marine Biological Resources and Ecological Environment, Shenzhen University, Shenzhen 518000, Guangdong Province, China

A. Lorrey

National Institute of Water and Atmospheric Research Ltd., Auckland, New Zealand

M. M. Barbour

The University of Sydney, School of Life and Environmental Sciences, Sydney, Australia

© The Author(s) 2022

R. T. W. Siegwolf et al. (eds.), *Stable Isotopes in Tree Rings*, Tree Physiology 8, [https://doi.org/10.1007/978-3-030-92698-4\\_10](https://doi.org/10.1007/978-3-030-92698-4_10)

## 10.1 Introduction

Stable oxygen isotope composition of tree ring cellulose ( $\delta^{18}\text{O}_{\text{cell}}$ ) has been demonstrated to reflect a suite of biotic and abiotic factors (i.e. air temperature, precipitation, relative humidity, leaf temperature, transpiration) during the period of tree growth. There is widespread interest in the employment of  $\delta^{18}\text{O}_{\text{cell}}$  as a reconstructive proxy to these various factors, and such interest spans a range of research areas including paleoclimatic studies (Anchukaitis and Evans 2010; Saurer et al. 2012; Voelker et al. 2014; Zeng et al. 2017), plant ecophysiology (Helliker and Richter 2008; Brooks and Coulombe 2009; Ulrich et al. 2019), and environmental sciences (Savard 2010; Wagner and Wagner 2006; Guerrieri et al. 2011).

Central to many of the  $\delta^{18}\text{O}_{\text{cell}}$ -based applications is a solid understanding of the isotopic fractionation mechanisms underlying  $\delta^{18}\text{O}_{\text{cell}}$ . Over the last 30 years, plant scientists have made significant progress in characterizing physiology- and biochemistry-related fractionation processes and their influences on  $\delta^{18}\text{O}_{\text{cell}}$ . These efforts have led to an accumulation of knowledge about  $\delta^{18}\text{O}_{\text{cell}}$ -associated mechanisms, and consequently the development of a process-based model which can be mathematically expressed as the following (Roden et al. 2000; Barbour and Farquhar 2000):

$$\delta^{18}\text{O}_{\text{cell}} = \delta^{18}\text{O}_{\text{sw}} + (1 - p_{\text{ex}})\Delta^{18}\text{O}_{\text{lw}} + \varepsilon_0 \quad (10.1)$$

where  $p_{\text{ex}}$  is the fraction of oxygen in the cellulose molecule that exchanges with water at the site of cellulose synthesis, and  $\varepsilon_0$  is the biochemical fractionation factor associated with the exchange of oxygen atoms between carbonyl group and the tissue water.  $\Delta^{18}\text{O}_{\text{lw}}$  refers to isotope enrichment of bulk leaf water above source water and can be approximated as isotopic difference between leaf and source water or  $\delta^{18}\text{O}_{\text{lw}} - \delta^{18}\text{O}_{\text{sw}}$ .

In this chapter, we will review the current knowledge of the factors/processes affecting stable isotope compositions in tree ring cellulose, by using the tree-ring isotope model (Eq. 10.1) as a reference context. We will focus on the three main determinants of  $\delta^{18}\text{O}_{\text{cell}}$  as represented by the mechanistic model: source water isotope ratio, leaf water isotopic enrichment, and biochemical fractionation at the site of sucrose production and cellulose synthesis. For each of the components we will present current understanding as well as highlight knowledge gaps that remain to be answered with future research. Further, recent evidence for the presence of biochemical fractionation during phloem loading and transport, a process not represented by the current model, will also be discussed.

## 10.2 Oxygen Isotope Ratio of Source Water ( $\delta^{18}\text{O}_{\text{sw}}$ )

### 10.2.1 $\delta^{18}\text{O}_{\text{sw}}$ and Climatic Signals

Source water is here defined as water in the soil available to be taken up by roots. Previous studies have produced convincing evidence that root uptake and subsequent xylem transport of the source water do not alter the original  $\delta^{18}\text{O}$  signature (i.e., no occurrence of isotopic fractionation during these processes; Wershaw et al. 1966; Dawson and Ehleringer 1991; Dawson 1993). As such, it is now common practice for researchers to analyse stem xylem water when determining  $\delta^{18}\text{O}_{\text{sw}}$ .

In a general sense, the ultimate “source” of the source water originates from local precipitation. Hence, in situations where  $\delta^{18}\text{O}_{\text{xw}}$  information is not available, use of  $\delta^{18}\text{O}$  of precipitation ( $\delta^{18}\text{O}_{\text{ppt}}$ ) as a proxy for  $\delta^{18}\text{O}_{\text{sw}}$  is an alternative. The past several decades have seen great efforts to document natural variation in  $\delta^{18}\text{O}_{\text{ppt}}$  in space and time (Bowen 2018). As a result, GIS-based, data-driven models (i.e., isoscape models) are now available enabling prediction of  $\delta^{18}\text{O}_{\text{ppt}}$  at any given site on the Earth with high accuracy (Bowen and Revenaugh 2003). The availability of isoscape-type  $\delta^{18}\text{O}_{\text{ppt}}$  data has provided a convenient and effective means for researchers to constrain  $\delta^{18}\text{O}_{\text{sw}}$  with  $\delta^{18}\text{O}_{\text{ppt}}$  under different field settings (Bowen 2010).

Regarding climatic effects on  $\delta^{18}\text{O}_{\text{ppt}}$ , the pioneering work of Dansgaard (1964) has demonstrated that  $\delta^{18}\text{O}_{\text{ppt}}$  can be influenced by several abiotic factors including altitude, latitude, distance from coast and amount of precipitation. Both the altitude and latitude effects are derived from the decreasing temperature as latitude and altitude increase, where the temperature influences the condensation rate and the equilibrium fractionation between vapour and liquid (Gat 1996). The distance from coast, known as the continental effect, is caused by a Rayleigh distillation process by which preferential precipitation of the heavier water isotopes ( $^{18}\text{O}$  and  $^2\text{H}$ ) leaves subsequent precipitation depleted as a weather system moves over land. The fourth effect noted by Dansgaard (1964), is the amount effect that is also caused by a Rayleigh process, resulting in a negative correlation between the amount of precipitation and its isotope composition, as typically observed in tropical regions.

The isotope processes described in Dansgaard (1964) suggest that  $\delta^{18}\text{O}_{\text{ppt}}$  variation in space and time is mainly a function of two climatic variables; temperature and precipitation amount. It has been shown that temperature effect is often markedly present in the mid- and high-latitudinal regions whereas precipitation amount is more likely a significant controlling factor for low-latitudinal  $\delta^{18}\text{O}_{\text{ppt}}$  variation (Bowen and Revenaugh 2003). Accordingly,  $\delta^{18}\text{O}$  of tree rings, with  $\delta^{18}\text{O}_{\text{ppt}}$  as one of its critical determinants, has also been shown by numerous studies to provide proxy information about precipitation amount in tropical ecosystems (Anchukaitis and Evans 2010; Brienen et al. 2012) and air temperature in boreal and temperate ecosystems (Rebetez et al. 2003; Etien et al. 2008). Modelled and measured  $\delta^{18}\text{O}_{\text{ppt}}$  has also been included in mechanistic models of  $\delta^{18}\text{O}_{\text{cell}}$  that couple variable climate measurements with environmental and ecophysiological parameters, which show

strong relationships for the inter-annual tree responses to vapour pressure deficit and relative humidity (Lorrey et al. 2016). On interglacial to glacial timescales, tree ring  $\delta^{18}\text{O}_{\text{cell}}$  measurements are rare (Poussart 2004), but some species like New Zealand kauri offer this potential (Lorrey et al. 2018). Differences between interglacial and glacial oceanic  $\delta^{18}\text{O}_{\text{seawater}}$  as a result of continental ice sheet expansion and eustatic sea level lowering drives  $\delta^{18}\text{O}_{\text{ppt}}$  toward more negative values during glacial phases. This suggests an ice volume correction for  $\delta^{18}\text{O}_{\text{cell}}$  may be required when tree rings outside of interglacial epochs are analysed.

### 10.2.2 Isotopic Transfer from Precipitation to Source Water

Other than studies that investigated the relationships between  $\delta^{18}\text{O}_{\text{cell}}$  and  $\delta^{18}\text{O}_{\text{ppt}}$  contained climatic factors, there are also studies performed to examine how  $\delta^{18}\text{O}_{\text{cell}}$  is related to  $\delta^{18}\text{O}_{\text{ppt}}$  itself (Saurer et al. 1997a; Barbour et al. 2001; Song et al. 2011). These studies generally showed good correlations between  $\delta^{18}\text{O}_{\text{cell}}$  and  $\delta^{18}\text{O}_{\text{ppt}}$ , substantiating the role of  $\delta^{18}\text{O}_{\text{ppt}}$  in controlling  $\delta^{18}\text{O}_{\text{cell}}$ . Notably, several large spatial-scale studies have presented data to show that  $\delta^{18}\text{O}_{\text{cell}}$  is strongly correlated with amount-weighted average of  $\delta^{18}\text{O}_{\text{ppt}}$  throughout the year ( $\delta^{18}\text{O}_{\text{ppt\_annual}}$ ). Such observations indicate that source water utilized by trees during the period of tree-ring growth (i.e., the growing season) may not derive solely from water precipitated over the growing season, but rather is more likely from a combination of both growing and non-growing season precipitation water. As an example, Fig. 10.1 presents the results from a re-analysis of a published, world-wide collection of tree wood cellulose sampled from a number of *Quercus* and *Pinus* tree species (Barbour et al. 2001). As can be seen from Fig. 10.1(a), at this large, geographic scale  $\delta^{18}\text{O}_{\text{cell}}$  was strongly positively correlated with the variation in  $\delta^{18}\text{O}_{\text{ppt\_annual}}$ , with a correlation coefficient of 0.79 ( $P < 0.001$ ). By comparison, the correlation coefficient for the relationship between  $\delta^{18}\text{O}_{\text{cell}}$  and growing-season averaged  $\delta^{18}\text{O}_{\text{ppt}}$  (or  $\delta^{18}\text{O}_{\text{ppt\_grs}}$ ) is only 0.61 (Fig. 10.1b), lower than the  $\delta^{18}\text{O}_{\text{cell}} - \delta^{18}\text{O}_{\text{ppt\_annual}}$  relationship. Further evidence in support of the notion that trees utilize a combination of both growing- and non-growing-season rainwater can be obtained from Sternberg et al. (2007) in which tree xylem water was directly sampled and analysed for  $\delta^{18}\text{O}$  across a continental scale in the United States. For this study  $\delta^{18}\text{O}$  of xylem water was found to be related more strongly to  $\delta^{18}\text{O}_{\text{ppt\_annual}}$  than to  $\delta^{18}\text{O}_{\text{ppt\_grs}}$  (see Fig. 10.2), in agreement with the pattern seen at the cellulose level.

Stored meteoric water in soil and regolith that interacts with tree roots (Sprenger et al. 2016) has an isotopic composition related to multiple precipitation events, including rainfall from the growing season and pre-growing season dormancy intervals. This highlights the fact that trees utilise a heterogeneous precipitation resource from both the current and past seasons. Recently, capitalizing on a four-year collection of isotope compositions of precipitation, soil and tree xylem water, Brinkmann et al. (2018) conducted a rigorous, quantitative evaluation of the residence time of

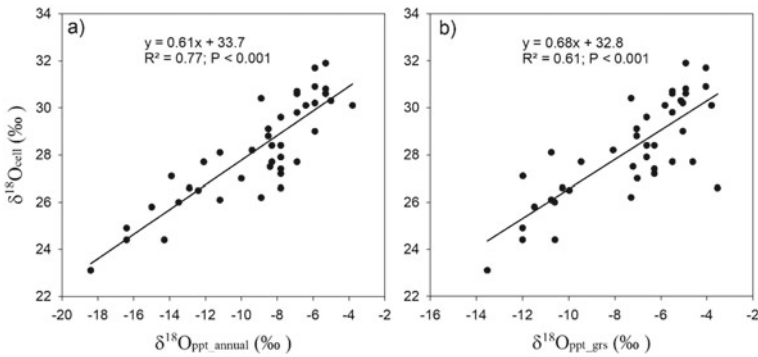


**Fig. 10.1** The relationships between  $\delta^{18}\text{O}$  of tree-ring cellulose ( $\delta^{18}\text{O}_{\text{cell}}$ ) and annual-weighted ( $\delta^{18}\text{O}_{\text{ppt\_annual}}$ ; **a**), and growing-season-weighted ( $\delta^{18}\text{O}_{\text{ppt\_grs}}$ ; **b**)  $\delta^{18}\text{O}$  of precipitation. The  $\delta^{18}\text{O}_{\text{ring}}$  data presented in this figure were obtained from Barbour et al. (2001). Each of the  $\delta^{18}\text{O}_{\text{ring}}$  data points represents integration of 3–10 year of tree-ring isotope signal in the late 1990s.  $\delta^{18}\text{O}_{\text{ppt\_annual}}$  and  $\delta^{18}\text{O}_{\text{ppt\_grs}}$  were calculated based on the site information (latitude, longitude and elevation) presented in Barbour et al. (2001), using the online precipitation isotope calculator at <http://www.waterisotopes.org> (Bowen and Revenaugh 2003). The criterion set out in Song et al. (2011) was used to define growing-season months for each sampling site. For more information about this world-wide collection of  $\delta^{18}\text{O}_{\text{ring}}$  data refer to Barbour et al. (2001)

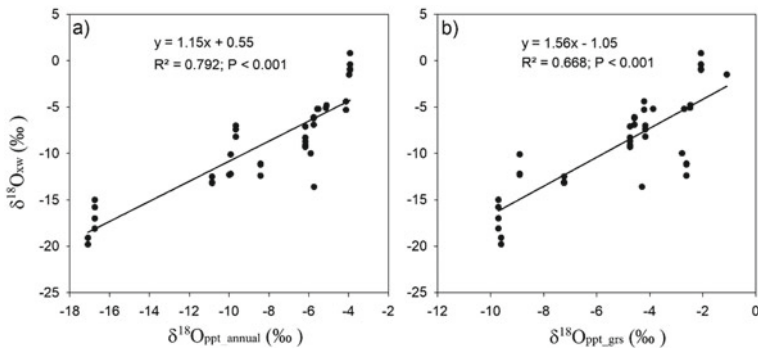


**Fig. 10.2** The relationships between  $\delta^{18}\text{O}$  of stem xylem water ( $\delta^{18}\text{O}_{\text{xw}}$ ) and annual-weighted ( $\delta^{18}\text{O}_{\text{ppt\_annual}}$ ; **a**), and growing-season-weighted ( $\delta^{18}\text{O}_{\text{ppt\_grs}}$ ; **b**)  $\delta^{18}\text{O}$  of precipitation across a wide range of sites in the United States. **(a)** is an adaptation from Fig. 1 of Sternberg et al. (2007). For **(b)**,  $\delta^{18}\text{O}_{\text{ppt\_grs}}$  values were calculated based on the site information presented in Sternberg et al. (2007), using the online precipitation isotope calculator at <http://www.waterisotopes.org> (Bowen and Revenaugh 2003). The criterion set out in Song et al. (2011) was used to define growing-season months for each sampling site

precipitation in the soil of a temperate forest. Their results showed that the residence time of soil water can be months or even years long, depending on the relative strengths of the precipitation input and the amount of water removal through evapotranspiration and infiltration. A significant finding of the Brinkmann et al. (2018)



is that contributions of growing season and non-growing season precipitation are of similar magnitude as far as the total water supply of temperate trees is concerned. This finding is consistent with the pattern seen at the spatial scale that demonstrates strong correlations of  $\delta^{18}\text{O}_{\text{cell}}$  or  $\delta^{18}\text{O}_{\text{xw}}$  with  $\delta^{18}\text{O}_{\text{ppt\_annual}}$ .

It is worth pointing out that the close linkage between precipitation water and source water notwithstanding,  $\delta^{18}\text{O}_{\text{ppt}}$  inherently represents an approximation to  $\delta^{18}\text{O}_{\text{sw}}$  regardless of the temporal scale over which it is integrated. In some cases, there is evidence that rapid uptake of meteoric rainfall (via increased soil moisture availability) corresponds to incremental growth of trees (Wunder et al. 2013), suggesting in some cases there may be low  $\delta^{18}\text{O}_{\text{ppt}}$  residence time prior to incorporation in  $\delta^{18}\text{O}_{\text{cell}}$ . On the other hand, the transfer of the isotope signal from precipitation to the plant-available source water pool may not be a straightforward process, but instead, could be complicated by several factors. For example, after infiltrating into the soil, the precipitation signal can be damped or even masked after mixing with the existing soil water, and there is potential for precipitation and soil water to mix with short- and long-residence stem water, and/or precipitation may be further altered by extreme events such as tropical cyclones that often bring in large amount of water with distinctively low  $\delta^{18}\text{O}$  values (Miller et al. 2006), or by evaporative enrichment of soil water or the influence of the ground water (Cernusak et al. 2016; Sprenger et al. 2016). In addition,  $\delta^{18}\text{O}_{\text{ppt}}$  is known to be seasonally variable for many regions (Bowen 2018), which means the season of growth response that dominates incremental ring addition (and therefore  $\delta^{18}\text{O}_{\text{cell}}$ ) may require consideration. Furthermore, according to the recently proposed “two-water worlds” theory, it is possible that in some circumstances the precipitation signal may not be present in  $\delta^{18}\text{O}_{\text{xw}}$  at all, i.e., after soil pores are filled with tightly-bound water from early rainfall events, the subsequent, recurrent precipitation would only act as the so-called “mobile water” contributing mainly to the soil water flow, without interacting much with the plant-accessible pore water (Brooks et al. 2010). Nevertheless, the “two-water worlds” theory suggests that substantial energy will need to be overcome during root uptake of the tightly-bound water, and thus is incompatible with water movement along water potential gradients within the soil–plant–atmosphere continuum (Bowling et al. 2017). Because of these complications, we recommend caution in the use of  $\delta^{18}\text{O}_{\text{ppt}}$  to parameterize  $\delta^{18}\text{O}_{\text{sw}}$  in applications where very precise information about  $\delta^{18}\text{O}_{\text{sw}}$  is needed.

## 10.3 Oxygen Isotope Enrichment of Leaf Water ( $\Delta^{18}\text{O}_{\text{lw}}$ )

### 10.3.1 The Craig-Gordon Model and Humidity Effect

During plant transpiration, the heavier  $\text{H}_2^{18}\text{O}$  evaporates and diffuses more slowly through the stomata than does  $\text{H}_2^{16}\text{O}$ , leaving leaf water enriched in  $^{18}\text{O}$ . Early studies of leaf water enrichment usually treated the leaf as a single, well-mixed and

isotopically uniform water pool such that  $\Delta^{18}\text{O}_{\text{lw}}$  is the same as  $^{18}\text{O}$  enrichment of water at the evaporative sites within the leaf ( $\Delta^{18}\text{O}_{\text{e}}$ ). At steady state,  $\Delta^{18}\text{O}_{\text{e}}$  can be well described by the Craig-Gordon model, as the following (Craig and Gordon 1965; Farquhar et al. 2007):

$$\Delta^{18}\text{O}_{\text{e}} = \varepsilon^+ + \varepsilon^{\text{k}} + (\Delta^{18}\text{O}_{\text{v}} - \varepsilon^{\text{k}}) \left( \frac{e_{\text{a}}}{e_{\text{i}}} \right) \quad (10.2)$$

where  $\varepsilon^+$  and  $\varepsilon^{\text{k}}$  are temperature dependent equilibrium fractionation factor for the water evaporation and the cumulative kinetic fractionation factor of water vapor diffusing out of the leaf respectively,  $\Delta^{18}\text{O}_{\text{v}}$  denotes  $^{18}\text{O}$  enrichment of atmospheric water vapour relative to the source water, and  $\frac{e_{\text{a}}}{e_{\text{i}}}$  is the ratio of the water vapor mole fraction in the air relative to that in the intercellular air spaces within the leaf.

With regard to tree-ring isotope modelling, atmospheric water vapor is often assumed to be in isotopic equilibrium with the source water. This assumption has been examined in several studies that employed either isotope ratio infrared spectrometry for making high-frequency, in-situ measurement of  $\delta^{18}\text{O}$  of water vapour ( $\delta^{18}\text{O}_{\text{v}}$ ) throughout the year (Lee et al. 2006), or a novel, epiphyte-based proxy for estimating a  $\delta^{18}\text{O}_{\text{v}}$  signal that integrates over the growing season (Helliker and Griffiths 2007; Helliker 2014). The results of these studies, albeit obtained through remarkably different types of methods, showed consistent evidence supporting the general validity of the equilibrium assumption. In the case of equilibrium,  $\Delta^{18}\text{O}_{\text{v}}$  is equivalent to  $-\varepsilon^+$ . In such a case, Eq. 10.2 can be further simplified to:

$$\Delta^{18}\text{O}_{\text{lw}} = (\varepsilon^+ + \varepsilon^{\text{k}}) \left( 1 - \frac{e_{\text{a}}}{e_{\text{i}}} \right) \quad (10.3)$$

Note that  $\varepsilon^{\text{k}}$  is dependent on weighted diffusional fractionations through the stomata and leaf boundary layer, so a weak negative dependence of  $\varepsilon^{\text{k}}$  on stomatal conductance ( $g_{\text{s}}$ ) is expected. Further,  $\varepsilon^+$  may also be slightly (but in a positive manner) influenced by  $g_{\text{s}}$ , given that a lower  $g_{\text{s}}$  is generally associated with an elevation in leaf temperature. Nevertheless, in natural conditions both  $\varepsilon^+$  and  $\varepsilon^{\text{k}}$  can vary only in a very limited range, and Eq. 10.3 essentially demonstrates that  $\Delta^{18}\text{O}_{\text{lw}}$  is strongly related to  $\frac{e_{\text{a}}}{e_{\text{i}}}$  in a negative manner. The  $\frac{e_{\text{a}}}{e_{\text{i}}}$  term in Eq. 10.3 can be further approximated by the ambient relative humidity (RH) if tree canopies are generally assumed to be aerodynamically coupled to the ambient environment. Such an approximation in turn gives rise to the expectation that  $\Delta^{18}\text{O}_{\text{e}}$  and by extension  $\delta^{18}\text{O}_{\text{cell}}$  should contain a record of RH.

Assessment of the RH influence on  $\Delta^{18}\text{O}_{\text{e}}$  has been included in numerous studies in a variety of plants (Farquhar et al. 2007). Some studies showed evidence of a RH signal in  $\delta^{18}\text{O}_{\text{cell}}$  (Ramesh et al. 1986; Saurer et al. 1997b; Porter et al. 2009; Lorrey et al. 2016), whilst many others reported no significant relationship between  $\delta^{18}\text{O}_{\text{cell}}$  and RH. The mixed results at the tree-ring level are not surprising given that  $\delta^{18}\text{O}_{\text{cell}}$  is subject to the control of isotope signatures of two different water pools ( $\delta^{18}\text{O}_{\text{sw}}$  and

$\Delta^{18}\text{O}_{\text{lw}}$ ; refer to Eq. 10.1). In view of the “dual control” nature, we can reasonably infer that the  $\Delta^{18}\text{O}_e$ -contained RH signal could be better revealed in circumstances where  $\delta^{18}\text{O}_{\text{sw}}$  remains relatively constant and thus does not add a confounding factor, i.e., in deep-rooted trees that mainly utilize deep soil water or ground water; whereas when  $\delta^{18}\text{O}_{\text{sw}}$  variation is considerable and becomes a dominant source of variation in  $\delta^{18}\text{O}_{\text{cell}}$ , the leaf-level signal may become dampened or even completely masked, resulting in a lack of significant correlation between  $\delta^{18}\text{O}_{\text{cell}}$  and RH (see Tsuji et al. (2006) and Cintra et al. (2019) for examples illustrating this point).

It is worth pointing out that the above inference inherently assumes that RH as a climatic factor is only related to variation in  $\Delta^{18}\text{O}_e$  but not with  $\delta^{18}\text{O}_{\text{sw}}$ . Clearly, this assumption is an over-simplification of the complex dynamics between isotopes and climates in nature, and thus may not be valid in some circumstances. For example, in regions where the “amount effect” dominates, a decrease in RH could act to increase  $\delta^{18}\text{O}_{\text{cell}}$  not only because of its effect on enriching  $\Delta^{18}\text{O}_{\text{lw}}$ , but also because a lower RH (or drier atmosphere) is usually accompanied with a reduction in precipitation, which, in the event of the “amount effect” corresponds to higher  $\delta^{18}\text{O}_{\text{sw}}$  values. In such a case, the amount-effect caused variation in  $\delta^{18}\text{O}_{\text{sw}}$  (and the associated variation in RH) essentially acts to strengthen the  $\delta^{18}\text{O}_{\text{cell}}$ -RH link instead of confounding it; this is in contrast with the general case as pointed out in the preceding paragraph. This type of response has been observed for some tree species in monsoon-affected East Asia or tropical ecosystems (Xu et al. 2015; Zeng et al. 2015).

As far as detection of a leaf water signal in  $\delta^{18}\text{O}_{\text{cell}}$  is concerned, plant physiologists have demonstrated the value of removing the influence of  $\delta^{18}\text{O}_{\text{sw}}$  by expressing cellulose isotope signatures as enrichments above the source water (i.e.,  $\Delta^{18}\text{O}_{\text{cell}} = \delta^{18}\text{O}_{\text{cell}} - \delta^{18}\text{O}_{\text{sw}}$ ). Expressing Eq. 10.1 in the form of  $\Delta^{18}\text{O}_{\text{cell}}$  notation yields the following:

$$\Delta^{18}\text{O}_{\text{cell}} = (1 - p_{\text{ex}})\Delta^{18}\text{O}_{\text{lw}} + \varepsilon_o \quad (10.4)$$

From Eq. 10.4 it can be seen that  $\delta^{18}\text{O}_{\text{sw}}$  is no longer a parameter influencing  $\Delta^{18}\text{O}_{\text{cell}}$ . Therefore we should expect that  $\Delta^{18}\text{O}_{\text{cell}}$  is related to  $\Delta^{18}\text{O}_{\text{lw}}$  or  $\Delta^{18}\text{O}_{\text{lw}}$ -contained RH signal in a more clear-cut manner, without relying on whether there is significant  $\delta^{18}\text{O}_{\text{sw}}$  variation or not. However, counter to this theoretical expectation, in neither of the two studies that analysed large-scale collection of tree-ring datasets was  $\Delta^{18}\text{O}_{\text{cell}}$  observed to exhibit strongly negative correlation with RH (Helliker and Richter 2008; Song et al. 2011; Fig. 10.3a, b). Such an inconsistency with what is predicted by theory (i.e. Equations 10.3 and 10.4) has prompted the suggestion that assumptions implicit in models where tree canopies are aerodynamically coupled to the ambient environment (such that  $e_a/e_i$  is equal to RH) are invalid (Helliker and Richter 2008). Subsequent calculations based on inverting of Eq. 10.4 led to the unexpected finding of boreal-to-subtropical convergence of photosynthesis-weighted tree leaf temperatures toward ca. 21 °C (Helliker and Richter 2008).

Of interest, a similar absence of a negative association between RH and  $\Delta^{18}\text{O}$  of tree-stem cellulose was also observed in a more recent study performed across

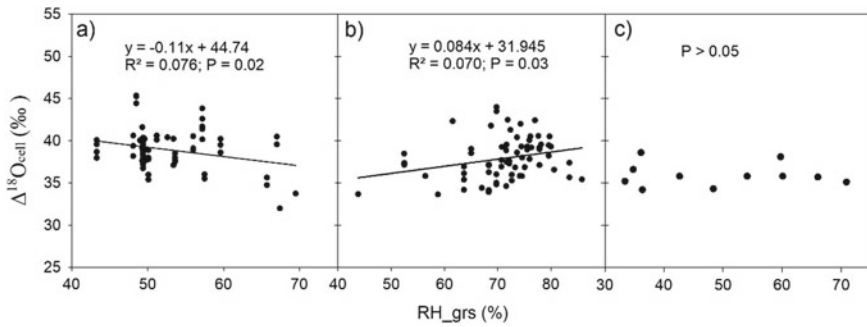


**Fig. 10.3** The relationships between  $\Delta^{18}\text{O}_{\text{cell}}$  and relative humidity (RH) across geographic scales. Data presented in (a) and (b) were obtained from Helliker and Richter (2008) and Song et al. (2011) respectively. (c) was  $\Delta$  adapted from Fig. 3 of Cheeseman and Cernusak (2017).  $^{18}\text{O}_{\text{cell}}$  values in (a) and (b) were derived from tree-ring cellulose samples while in (c) were from tree-branch cellulose samples. Data in (a) and (b) spanned a wide range of latitudes at the continental and global scale respectively; data in (c) spanned an aridity gradient in the northeastern part of Australia. RH values shown in (a) and (b) represent growing-season averaged values and in (c) were averaged from site averages of 9 a.m. and 3 p.m. measurements and thus also likely represent the conditions during which the majority of photosynthesis occurs

11 sampling sites that spanned an aridity gradient in NE Australia (Cheeseman and Cernusak 2017; Fig. 10.3c). However, this observation cannot be fully explained by leaf-air temperature uncoupling, as along this same gradient a strongly negative correlation was observed between RH and leaf cellulose enrichment. In view of the different patterns between stem- and leaf-cellulose enrichment, Cheeseman and Cernusak (2017) proposed that the nil trend of stem cellulose enrichment along the RH gradient is a result of variation in the biochemical term “ $p_{\text{ex}}$ ” (a topic that will be explored in more detail in the next section) and especially that  $p_{\text{ex}}$  is related to aridity. As of now, whether it is leaf temperature or  $p_{\text{ex}}$  that represents the true mechanism for the observed stem or tree-ring cellulose patterns remains to be further tested. Future studies explicitly designed to examine the relevant assumptions (as recently attempted by Helliker et al. (2018)) will hold the key to unravelling this uncertainty.

### 10.3.2 The Péclet Effect Model

The Craig-Gordon model has been shown to predict general trends in leaf water enrichment quite well. However, if examined more closely, measured bulk leaf water enrichment in many cases was found to be somewhat less enriched than that predicted by the Craig-Gordon equation (Walker et al. 1989; Flanagan et al. 1991). This has led to the realization that the Craig-Gordon equation may only predict the  $^{18}\text{O}$  enrichment at the evaporative sites within the leaf water, but not the bulk leaf water. The latter instead can be highly heterogeneous, likely as a result of mixing processes within the leaf lamina involving both unenriched and enriched water. This process was

rigorously treated by Farquhar and Lloyd (1993), who introduced a Péclet effect into the leaf model to mathematically account for the ratio of advection of unenriched vein water via transpiration stream to back-diffusion of the enriched water from the evaporative site. With the incorporation of the Péclet effect,  $\Delta^{18}\text{O}_{\text{lw}}$  model can be further modified into the following form:

$$\Delta^{18}\text{O}_{\text{lw}} = \Delta^{18}\text{O}_e - \frac{1 - e^{-P}}{P} \quad (10.5)$$

where  $\Delta^{18}\text{O}_e$ , as aforementioned, refers to  $^{18}\text{O}$  enrichment of evaporative site water and can be predicted by the Craig-Gordon model (Eq. 10.2) and  $P = \frac{EL}{CD}$ .  $E$  is leaf transpiration rate,  $L$  is the scaled effective pathlength (m) for water movement within the leaf lamina,  $C$  is the density of water ( $55.56 \times 10^3 \text{ mol m}^{-3}$ ) and  $D$  is the diffusivity of  $\text{H}_2^{18}\text{O}$  in water (Cuntz et al. 2007). A detailed, theoretical analysis of Eq. 10.5 revealed that for plants experiencing similar atmospheric conditions (i.e., similar  $\delta^{18}\text{O}_v$  and RH), there should be a negative correlation between  $\Delta^{18}\text{O}_{\text{lw}}$  and stomatal conductance and/or transpiration rate (Barbour et al. 2000a). The demonstrated potential for  $\Delta^{18}\text{O}_{\text{lw}}$  to record transpirative physiology in turn stimulated considerable interest among plant scientists to explore the use of plant oxygen isotopes as a phenotypic trait for various applications in crop breeding, forest management, and global change ecology (Barbour et al. 2000b; Brooks and Coulombe 2009; Cabrera-Bosquet et al. 2009; Battipaglia et al. 2013). For more details on this topic, the reader is referred to the “dual isotope” chapter (Chap. 16) of this book.

Although the Péclet effect is a theoretically sound concept, until now the available evidence in support of this concept remains limited. The standard procedure for experimentally testing the Péclet effect relies on examination of the relationship between transpiration rate ( $E$ ) and the proportional difference between  $\Delta^{18}\text{O}_{\text{lw}}$  and  $\Delta^{18}\text{O}_e$  ( $f$ ). A positive correlation between  $f$  and  $E$  is compatible with that predicted from the Péclet theory (Flanagan et al 1991; Barbour et al. 2000a), and consequently is used as a criterion by which to determine the validity of the Péclet concept. However, to date a significantly positive  $f$ – $E$  relationship was only observed in some studies (Flanagan et al. 1994; Barbour et al. 2000a; Rippulone et al. 2008), but not in many others (Roden and Ehleringer 1999; Cernusak et al. 2003; Song et al. 2015; Roden et al. 2015).

The limited support for the Péclet theory may be viewed as an indication that the Péclet effect is insignificant in determining leaf water enrichment for many species. However, this indication is far from being conclusive, given that methodological issues common in the published experiments could have biased the results. For example, one methodological issue is related to the adoption by many early studies of a somewhat arbitrary procedure to determine isotopic steady state and  $\delta^{18}\text{O}$  of leaf transpiration ( $\delta^{18}\text{O}_E$ ) (Simonin et al. 2013); this could have led to uncertainty in estimating  $\delta^{18}\text{O}_e$  and  $f$ , and by extension in assessing the  $f$ – $E$  relationship (Loucos et al. 2015). Another methodological issue lies in that all currently available methods for measuring  $\delta^{18}\text{O}_{\text{lw}}$  involve a step of destructive sampling of the leaf before isotopic

analysis. This dictates the need for collection of multiple leaves for generating a single  $f-E$  plot (i.e., each data point in the  $f-E$  plot corresponds to an individual leaf) (Cernusak and Kahmen 2013). Such a multi-leaf based approach is not ideal, because among-leaf variation in anatomical, morphological and physiological variables may be confounding factors that result in “noise” within the  $f-E$  plot (i.e., among-leaf variation *per se* results in much variation in  $f$ ), potentially posing an obstacle to detecting the true Péclet signal.

Encouragingly, with the recent emergence of laser-based measurement instruments that permit online quantification of  $\delta^{18}\text{O}_E$  at both steady and non-steady states, the above-mentioned first methodological issue can now be readily overcome (Song et al. 2015; Holloway-Phillips et al. 2016). Addressing the second issue will rest on development of new methods to allow for repeated determination of  $\delta^{18}\text{O}_{lw}$  on a single leaf. In this context, we note that previous studies have attempted to indirectly estimate  $\delta^{18}\text{O}_{lw}$  at different time points in a single castor bean leaf through repeated sampling and measurement of  $\delta^{18}\text{O}$  of phloem sugar transported out of the leaf under different VPD conditions (Barbour et al. 2000a, Cernusak et al. 2003). The phloem-based “single-leaf” method is a novel attempt; nevertheless, this method has limitations in that: (1) it requires assumptions regarding the biochemical fractionation factor and/or time lags from isotopic transfer of leaf water to phloem organic matter, and (2) the method relies on a phloem-bleeding technique, yet this technique is only applicable to a few plant species. As such, future studies should focus on development of a method that would permit multiple direct measurements of isotopic signals from leaf water in a non-destructive manner, and also be generally applicable to different types of species.

Undoubtedly, continued mechanistic investigations will enlighten us as to whether the Péclet theory is a valid concept in different plant types. Nevertheless, it has been argued that the Péclet effect, even if present, is unlikely to exert a significant impact on  $\delta^{18}\text{O}_{cell}$  when the effect is relatively small, because the transfer of the Péclet signal from leaf water down to tree-ring cellulose necessarily involves multiple steps that serve to further damp the original signal, to the point that the association of the Péclet effect to  $\delta^{18}\text{O}_{cell}$  becomes weak or even negligible (Ogee et al. 2009). Furthermore, in many paleo-related contexts applying a single-value based correction (the so-called “damping factor”) to the Craig-Gordon equation and the tree-ring model seems to serve the study purposes well (Saurer et al. 1997a; Saurer et al. 2016). In such cases there may be limited value of considering the more complicated Péclet correction. As such, we recommend that researchers carefully consider several factors including the strength of the Péclet signal and the scale and purpose of the planned investigation when it comes to deciding whether to include the Péclet correction for modelling  $\delta^{18}\text{O}_{cell}$  in practice (Cernusak et al. 2016).

## 10.4 Biochemical Fractionation

### 10.4.1 *Oxygen Isotope Exchange at the Sites of Sucrose Production and Cellulose Synthesis*

Exchange of oxygen atoms between water and organic molecules can occur for oxygen in carbonyl groups via formation of short-lived gem-diol intermediates (Sternberg et al. 1986). Hydration of a carbonyl oxygen is closely coupled with subsequent dehydration and the oxygen atom retained in the organic molecule can be from either the original molecule or the reaction water (Sternberg 2009). Importantly, when this type of oxygen exchange reaction reaches equilibrium, the carbonyl oxygen will become ca. 27‰ more enriched in  $^{18}\text{O}$  than the reaction water because of a biochemical fractionation effect (Sternberg and DeNiro 1983). This explains why  $\epsilon_{\text{o}}$  (the biochemical fractionation factor) is treated as a constant of 27‰ in the tree-ring model (but see Sternberg and Ellsworth (2011) and Zech et al. (2014) for a slight temperature effect on  $\epsilon_{\text{o}}$ ).

According to the tree-ring model, carbonyl-water exchange of oxygen occurs during two distinct metabolic steps: the photosynthetic production of sucrose in the leaf and sucrose-cellulose conversion within the stem (Sternberg 2009). Of relevance to oxygen exchange at the leaf level, is the fact that all of the oxygen atoms in a sucrose molecule will pass through a carbonyl group at some point in the Calvin cycle leading to production of sucrose (Farquhar et al. 1998). For this reason, leaf sucrose is expected to be in equilibrium with the reaction water (i.e., leaf water). This expectation is well supported by published data proving that leaf soluble organic matter (a proxy for sucrose) is ca. 27‰ more enriched than leaf water in a diversity of plant species (Cernusak et al. 2003; Gessler et al. 2007, 2013; Barnard et al. 2007). The oxygen exchange at the site of cellulose synthesis is made possible by the requirement that sucrose be cleaved into carbonyl-containing hexoses (glucose and fructose) before it can be converted into cellulose. Further, it has been demonstrated that a proportion of hexose phosphate molecules also undergo futile cycling through triose phosphates before being incorporated to cellulose (Hill et al. 1995). This triose cycling process would expose more carbonyl oxygen to the local water (i.e., xylem water), allowing additional isotopic exchange.

As already mentioned, the proportion of oxygen exchange with xylem water during the sucrose-cellulose conversion is termed  $p_{\text{ex}}$  in the tree-ring model. Regarding  $p_{\text{ex}}$ , the conventional assumption is that it is a rather invariable parameter, with a value close to 0.4 regardless of species or environmental conditions. Support for this assumption comes from a number of experimental and observational studies performed on a range of species and growth conditions (Sternberg et al. 1986; Yakir and Deniro 1990; Roden et al. 2000; Cernusak et al. 2005), over which average  $p_{\text{ex}}$  is ca. 0.42 (summarized by Cernusak et al. 2005). Nevertheless, several more recent studies have suggested that  $p_{\text{ex}}$  may exhibit considerable variation in association with variation in aridity (Cheeseman and Cernusak 2017), salinity (Ellsworth and Sternberg 2014), or turnover time ( $\tau$ ) of the sucrose pool available for cellulose synthesis

(Song et al. 2014). A relationship between  $p_{\text{ex}}$  and  $\tau$  was suggested by Farquhar et al. (1998) through consideration of biochemical pathways leading to cellulose synthesis. When  $\tau$  is small such that the sucrose pool turns over rapidly, there should be less opportunity for hexose phosphates to cycle through triose, potentially resulting in a smaller  $p_{\text{ex}}$  compared to the case of a slow turnover pool of sucrose. Further, it is known that  $\tau$  is a parameter that can be readily influenced by plant growth environments, and hence the observed aridity- or salinity-dependence of  $p_{\text{ex}}$  may well be an indirect reflection of  $\tau$  influence on  $p_{\text{ex}}$ . However, despite these plausible explanations, Waterhouse et al. (2013) demonstrated that position-specific isotopic exchange rates in cellulose cannot be fully accounted for by the carbonyl-exchange theory, with or without consideration of cycling via trioses. That is, our current understanding of the biochemical fractionation is incomplete and more research is needed to explore potential variations in  $p_{\text{ex}}$  and the associated mechanisms.

### ***10.4.2 Oxygen Isotope Exchange During Phloem Loading and Transport of Sucrose***

Lying between the above mentioned two metabolic steps is the sucrose translocation pathway, where sucrose is loaded into the minor-vein phloem of the leaf and subsequently transported downwards in phloem towards the cellulose synthesis site. The current tree-ring model assumes no isotopic effect during sucrose translocation. However, this assumption may be problematic, as both phloem loading and transport involve highly dynamic and complex mechanisms (i.e., multiple pathways during loading and the leakage-retrieval dynamics persisting throughout transport) (van Bel 2003), which may give rise to metabolic conversion of sucrose into carbonyl-containing intermediates and consequently to isotopic oxygen exchange (Barnard et al. 2007; Offermann et al. 2011; Gessler et al. 2013, 2014).

Indeed, several studies have documented significant leaf-to-phloem or phloem-basipetal isotopic gradients in sucrose (Gavrishkova et al. 2011; Offermann et al. 2011; Gessler et al. 2013), hinting at the possibility of biochemical fractionation during phloem loading and transport. In a field investigation involving five different species, Gessler et al. (2013) found that twig phloem-transported sucrose was significantly less enriched than its leaf counterpart in three evergreen species, but not in the other two deciduous species. Gessler et al. (2013) presented a detailed discussion of the anatomical and physiological variations in the studied species, and suggested that these variations may at least be partially responsible for species-specific variation in the extent of phloem-loading/transport associated oxygen exchange, in turn causing the observed variation in the isotopic difference between phloem sucrose and leaf water among species. The dataset presented in Gessler et al. (2013) does not allow for quantitative assessment of the contribution of bark photosynthesis (a critical confounding factor) to the  $\delta^{18}\text{O}$  signature in phloem so that no definitive conclusion can be drawn yet regarding whether and to what extent carbonyl-oxygen



exchange during phloem loading/transport may influence the phloem-leaf isotopic difference in different species. Nevertheless, the observed isotopic effect during phloem loading/transport highlights knowledge gaps that need to be filled in order to put our understanding of the  $\delta^{18}\text{O}_{\text{cell}}$ -associated mechanisms on a firmer ground. To this end, future experimental studies should be performed not only to advance understanding of the biochemical/physiological mechanisms underlying the phloem-related oxygen exchange process, but also to quantify the mean and variation of the *apparent* fractionation factor associated with this process among different species and/or environmental conditions. This understanding should then be incorporated into the existing tree-ring isotope model, to improve our ability to interpret climatic and physiological signals from  $\delta^{18}\text{O}_{\text{cell}}$  under various contexts.

## 10.5 Conclusions

The oxygen isotope composition of tree rings records environmental conditions, such as temperature and relative humidity, and to a lesser extent physiological and biochemical responses such as stomatal regulation of water loss and the balance between sources and sinks for carbohydrates. However, there are a number of gaps in our understanding that need to be addressed, the three most pressing being: (1) the relevance of the Péclet effect in leaves from different species; (2) the role of variability in the proportion of exchangeable oxygen during cellulose synthesis; and (3) isotope effects during phloem loading, unloading and transport. We envision that use of high-resolution isotope sampling/measurements techniques (see Chap. 7 for more details), combined with detailed physiological and environmental monitoring across a range of species and geographies would be helpful in resolving some of these uncertainties.

## References

- Anchukaitis KJ, Evans MN (2010) Tropical cloud forest climate variability and the demise of the Monteverde golden toad. *Proc Natl Acad Sci USA* 107:5036–5040
- Barbour MM, Farquhar GD (2000) Relative humidity- and ABA-induced variation in carbon and oxygen isotope ratios of cotton leaves. *Plant, Cell Environ* 23:473–485
- Barbour MM, Fischer RA, Sayre KD, Farquhar GD (2000) Oxygen isotope ratio of leaf and grain material correlates with stomatal conductance and grain yield in irrigated wheat. *Aust J Plant Physiol* 27:625–637
- Barbour MM, Schurr U, Henry BK, Wong SC, Farquhar GD (2000) Variation in the oxygen isotope ratio of phloem sap sucrose from castor bean. Evidence in support of the Péclet effect. *Plant Physiol* 123:671–679
- Barbour MM, Andrews TJ, Farquhar GD (2001) Correlations between oxygen isotope ratios of wood constituents of *Quercus* and *Pinus* samples from around the world. *Aust J Plant Physiol* 28:335–348

- Barnard RL, Salmon Y, Kodama N, Sorgel K, Holst J, Rennenberg H, Gessler A, Buchmann N (2007) Evaporative enrichment and time lags between  $\delta^{18}\text{O}$  of leaf water and organic pools in a pine stand. *Plant, Cell Environ* 30:539–550
- Battipaglia G, Saurer M, Cherubini P, Calfapietra C, McCarthy HR, Norby RJ, Cotrufo MF (2013) Elevated  $\text{CO}_2$  increases tree-level intrinsic water use efficiency: insights from carbon and oxygen isotope analyses in tree rings across three forest FACE sites. 197:544–554
- Bowen GJ (2010) Isoscapes: spatial pattern in isotopic biogeochemistry. *Annu Rev Earth Planet Sci* 38:161–187
- Bowen GJ, Revenaugh J (2003) Interpolating the isotopic composition of modern meteoric precipitation. *Water Resour Res* 39:1299
- Bowen, GJ (2018) The online isotopes in precipitation calculator, version 3.2. [http://wateriso.utah.edu/waterisotopes/pages/information/oipc\\_info.html](http://wateriso.utah.edu/waterisotopes/pages/information/oipc_info.html)
- Bowling DR, Schulze ES, Hall SJ (2017) Revisiting streamside trees that do not use stream water: can the two water worlds hypothesis and snowpack isotopic effects explain a missing water source? *Ecohydrol* 10:1–12
- Brienen RJW, Helle G, Pons TL, Guyot JL, Gloor M (2012) Oxygen isotopes in tree rings are a good proxy for Amazon precipitation and ElNino-Southern Oscillation variability. *Proc Natl Acad Sci USA* 109:16957–16962
- Brinkmann N, Seeger S, Weiler M, Buchmann N, Eugster W, Kahmen A (2018) Employing  $\delta^2\text{H}$  and  $\delta^{18}\text{O}$  values to estimate mean residence time and temporal origin of soil and xylem water in a temperate forest. *New Phytol* 219:1300–1313
- Brooks JR, Coulombe R (2009) Physiological responses to fertilization recorded in tree rings: isotopic lessons from a long-term fertilization trial. *Ecol Appl* 19:1044–1060
- Brooks JR, Barnard HR, Coulombe R, McDonnell JJ (2010) Ecohydrologic separation of water between trees and streams in a Mediterranean climate. *Nat Geosci* 3:100–104
- Cabrera-Bosquet L, Sanchez C, Araus JL (2009) Oxygen isotope enrichment ( $\delta^{18}\text{O}$ ) reflects yield potential and drought resistance in maize. *Plant, Cell Environ* 32:1487–1499
- Cernusak LA, Kahmen A (2013) The multifaceted relationship between leaf water  $^{18}\text{O}$  enrichment and transpiration rate. *Plant, Cell Environ* 36:1239–1241
- Cernusak LA, Wong SC, Farquhar GD (2003) Oxygen isotope composition of phloem sap in relation to leaf water in *Ricinus communis*. *Funct Plant Biol* 30:1059–1070
- Cernusak LA, Farquhar GD, Pate JS (2005) Environmental and physiological controls over oxygen and carbon isotope composition of Tasmanian blue gum, *Eucalyptus globulus*. *Tree Physiol* 25:129–146
- Cernusak LA, Barbour MM, Stefan KA, Cheesman AW, English NB, Feild TS, Helliker BR, Holloway-Phillips MM, Holtum JA, Kahmen A et al (2016) Stable isotope enrichment in leaf water of terrestrial plants. *Plant, Cell Environ* 39:1087–1102
- Cheesman AW, Cernusak LA (2017) Infidelity in the outback: climate signal recorded in  $\Delta^{18}\text{O}$  of leaf but not branch cellulose of eucalypts across an Australian aridity gradient. *Tree Physiol* 37(5):554–564
- Cintra BBL, Gloor M, Boom A, Schöngart J, Locosselli GM, Brienen R (2019) Contrasting controls on tree ring isotope variation for Amazon floodplain and terra firme trees. *Tree Physiol* 39:845–860
- Craig H, Gordon LI (1965) Deuterium and oxygen-18 variations in the ocean and the marine atmosphere. In: Tongiorgi E (ed) *Proceedings of a Conference on stable isotopes in oceanographic studies and paleo temperatures*. Lischi and Figli, Pisa, Italy, pp 9–130
- Cuntz M, Ogee J, Farquhar GD, Peylin P, Cernusak LA (2007) Modelling advection and diffusion of water isotopologues in leaves. *Plant, Cell Environ* 30:892–909
- Dansgaard W (1964) Stable isotopes in precipitation. *Tellus* 16(4):436–468
- Dawson TE (1993) Water sources of plants as determined from xylem-water isotopic composition: perspectives on plant competition, distribution, and water relations. In: Ehleringer JR, Hall AE, Farquhar GD (eds) *Stable isotopes and plant carbon/water relations*. Academic Press, New York, USA, pp 465–496
- Dawson TE, Ehleringer JR (1991) Streamside trees that do not use stream water. *Nature* 350:335–337

- Ellsworth PFV, Sternberg LDL (2014) Biochemical effects of salinity on oxygen isotope fractionation during cellulose synthesis. *New Phytol* 202:784–789
- Etien, N, Daux, V, Masson-Delmotte V, Steievenard M, Bernard V, Durost S, Guillemin MT, Mestre O, Pierre M (2008) A bi-proxy reconstruction of Fontainebleau (France) growing season temperature from AD 1596 to 2000. *Clim Past* 4:91–106
- Farquhar GD, Lloyd J (1993) Carbon and oxygen isotope effects in the exchange of carbondioxide between terrestrial plants and the atmosphere. In: Ehleringer JR, Hall AE, Farquhar GD (eds) *Stable isotopes and plant carbon/water relations*. Academic Press, New York, USA, pp 47–79
- Farquhar GD, Cernusak LA, Barnes B (2007) Heavy water fractionation during transpiration. *Plant Physiol* 143:11–18
- Farquhar GD, Barbour MM, Henry BK (1998) Interpretation of oxygen isotope composition of leaf material. In: Griffiths H (ed) *Stable isotopes: integration of biological, ecological and geochemical processes*. BIOS Scientific Publishers, Oxford, pp 27–61
- Flanagan LB, Comstock JP, Ehleringer JR (1991) Comparison of modeled and observed environmental-influences on the stable oxygen and hydrogen isotope composition of leaf water in *Phaseolus-vulgaris* l. *Plant Physiol* 96:588–596
- Flanagan LB, Phillips SL, Ehleringer JR, Lloyd J, Farquhar GD (1999) Effect of changes in leaf water oxygen isotopic composition on discrimination against  $C^{18}O^{16}O$  during photosynthetic gas-exchange. *Aust J Plant Physiol* 21:221–234
- Gat JR (1996) Oxygen and hydrogen isotopes in the hydrologic cycle. *Annu Rev Earth Planet Sci* 24:255–262
- Gavrichkova O, Proietti I S, Moscatello S, Portarena S, Battistelli A, Matteucci G, Brugnoli E (2011) Short-term natural  $^{13}C$  and  $^{18}O$  variations in pools and fluxes in a beech forest: the transfer of isotopic signal from recent photosynthates to soil respired  $CO_2$ . 8: 2833–2846
- Gessler A, Peuke AD, Keitel C, Farquhar GD (2007) Oxygen isotope enrichment of organic matter in *Ricinus communis* during the diel course and as affected by assimilate transport. *New Phytol* 174:600–613
- Gessler A, Brandes E, Keitel C, Boda S, Kayler ZE, Granier A, Treydte K (2013) The oxygen isotope enrichment of leaf-exported assimilates-does it always reflect lamina leaf water enrichment? *New Phytol* 200:144–157
- Gessler A, Ferrio JP, Hommel R, Treydte K, Werner RA, Monson RK (2014) Stable isotopes in tree rings: towards a mechanistic understanding of isotope fractionation and mixing processes from the leaves to the wood. *Tree Physiol* 34:796–818
- Guerrieri R, Mencuccini M, Sheppard LJ, Saurer M, Perks MP, Levy P, Sutton MA, Borghetti M, Grace J (2011) The legacy of enhanced N and S deposition as revealed by the combined analysis of  $\delta^{13}C$ ,  $\delta^{18}O$  and  $\delta^{15}N$  in tree rings. *Glob Change Biol* 17:1946–1962
- Helliker BR (2014) Reconstructing the  $\delta^{18}O$  of atmospheric water vapour via the CAM epiphyte *Tillandsia usneoides*: seasonal controls on  $\delta^{18}O$  in the field and large-scale reconstruction of  $\delta^{18}O_a$ . *Plant, Cell Environ* 37:541–556
- Helliker BR, Griffiths H (2007) Toward a plant-based proxy for the isotope ratio of atmospheric water vapor. *Glob Change Biol* 13:723–733
- Helliker BR, Richter SL (2008) Subtropical to boreal convergence of tree-leaf temperatures. *Nature* 454:511–516
- Helliker BR, Song X, Goulden ML, Clark K, Bolstad P, Munger JM, Chen J, Noormets A, Hollinger D, Wofsy S, Martin T, Baldocchi D, Euskirchen E, Desai A, Burns SP (2018) Assessing the interplay between canopy energy balance and photosynthesis with cellulose  $\delta^{18}O$ : large-scale patterns and independent ground-truthing. *Oecologia* 187:995–1007
- Hill SA, Waterhouse JS, Field EM, Switsur VR, Apreses T (1995) Rapid recycling of triose phosphates in oak stem tissue. *Plant, Cell Environ* 18:931–936
- Holloway-Phillips M, Cernusak LA, Barbour MM, Song X, Cheesman A, Munksgaard N, Stuart-Williams H, Farquhar GD (2016) Leaf vein fraction influences the Péclet effect and  $^{18}O$  enrichment in leaf water. *Plant, Cell Environ* 39:2414–2427

- Lee X, Smith R, Williams J (2006) Water vapor  $^{18}\text{O}/^{16}\text{O}$  isotope ratio in surface air in New England, USA. *Tellus B* 58:293–304
- Lorrey AM, Brookman T, Evans MN, Fauchereau NC, Barbour MM, Macinnis-Ng C, Criscitiello AS, Eischeid G, Horton TW, Fowler AM, Schrag DP (2016) Stable oxygen isotope signatures of early season wood in New Zealand kauri (*Agathis australis*) tree rings: Prospects for palaeoclimate reconstruction. *Dendrochronologia* 40:50–63
- Lorrey AM, Boswijk G, Hogg A, Palmer JG, Turney CSM, Fowler AM, Ogden J, Woolley JM (2018) The scientific value and potential of New Zealand swamp kauri. *Quat Sci Rev* 183:124e139
- Loucos KE, Simonin KA, Song X, Barbour MM (2015) Observed relationships between leaf  $\text{H}_2^{18}\text{O}$  Péclet effective length and leaf hydraulic conductance reflect assumptions in Craig-Gordon model calculations. *Tree Physiol* 35:16–26
- Miller DL, MC, Grissino-Mayer HD, Mock CJ, Uhle ME, Sharp Z (2006) Tree-ring isotope records of tropical cyclone activity. *Proc Natl Acad Sci USA* 103:14294–14297
- Offermann C, Ferrio JP, Holst J, Grote R, Siegwolf R, Kayler Z, Gessler A (2011) The long way down—are carbon and oxygen isotope signals in the tree ring uncoupled from canopy physiological processes? *Tree Physiol* 31:1088–1102
- Ogee J, Barbour MM, Wingate L, Bert D, Bosc A, Stievenard M, Lambrot C, Pierre M, Bariac T, Loustau D (2009) A single substrate model to interpret intra-annual stable isotope signals in tree ring cellulose. *Plant, Cell Environ* 32:1071–1090
- Porter TJ, Pisaric MFJ, Kokelj SV, Edwards TWD (2009) Climatic signals in  $\delta^{13}\text{C}$  and  $\delta^{18}\text{O}$  of tree-rings from white spruce in the Mackenzie Delta region, northern Canada. *Arct Antarct Alp Res* 41:497–505
- Poussart PF (2004) Isotopic investigations of tropical trees. PhD Dissertation. Department of earth and planetary sciences. Harvard University, Cambridge, Massachusetts
- Ramesh R, Bhattacharya SK, Gopalan K (1986) Climatic correlations in the stable isotope records of silver fir (*Abies pindrow*) trees from Kashmir, India. *Earth Planet Sci Lett* 79:66–74
- Rebetez M, Saurer M, Cherubini P (2003) To what extent can oxygen isotopes in tree rings and precipitation be used to reconstruct past atmospheric temperature? A case study. *Clim Change* 61:237–248
- Rippulone F, Matsuo N, Stuart-Williams H, Wong SC, Borghetti M, Tani M, Farquhar G (2008) Environmental effects on oxygen isotope enrichment of leaf water in cotton leaves. *Plant Physiol* 146:729–736
- Roden JS, Ehleringer JR (1999) Observations of hydrogen and oxygen isotopes in leaf water confirm the Craig-Gordon model under wide-ranging environmental conditions. *Plant Physiol* 120:1165–1173
- Roden JS, Lin GH, Ehleringer JR (2000) A mechanistic model for interpretation of hydrogen and oxygen isotope ratios in tree-ring cellulose. *Geochim Cosmochim Acta* 64:21–35
- Roden J, Kahmen A, Buchmann N, Siegwolf R (2015) The enigma of effective path length for  $^{18}\text{O}$  enrichment in leaf water of conifers. *Plant, Cell Environ* 38:2551–2565
- Saurer M, Aellen K, Siegwolf RTW (1997) Correlating  $\delta^{13}\text{C}$  and  $\delta^{18}\text{O}$  in cellulose of trees. *Plant Cell Environ* 20:1543–1550
- Saurer M, Kress A, Leuenberger M, Rinne KT, Treydte KS, Siegwolf RTW (2012) Influence of atmospheric circulation patterns on the oxygen isotope ratio of tree rings in the Alpine region. *J Geophys Res* 117(D50):5118
- Saurer M, Kirdyanov AV, Prokushkin AS, Rinne KT, Siegwolf RTW (2016) The impact of an inverse climate–isotope relationship in soil water on the oxygen isotope composition of *Larix gmelinii* in Siberia. *New Phytol* 209:955–964
- Saurer M, Borella S, Leuenberger M (1997b)  $\delta^{18}\text{O}$  of tree rings of beech (*Fagus sylvatica*) as a record of  $\delta^{18}\text{O}$  of the growing season precipitation. *Tellus* 49b:80–92
- Savard MM (2010) Tree-ring stable isotopes and historical perspectives on pollution—an overview. *Environ Pollut*

- Simonin KA, Roddy AB, Link P, Apodaca R, Tu KP, Hu J, Dawson TE, Barbour MM (2013) The isotopic composition of transpiration and rates of change in leaf water isotopologue storage in response to environmental variables. *Plant, Cell Environ* 36:2190–2206
- Song X, Barbour MM, Saurer M, Helliker BR (2011) Examining the large-scale convergence of photosynthesis-weighted tree leaf temperatures through stable oxygen isotope analysis of multiple data sets. *New Phytol* 192:912–924
- Song X, Farquhar GD, Gessler A, Barbour MM (2014) Turnover time of the non-structural carbohydrate pool influences  $\delta^{18}\text{O}$  of leaf cellulose. *Plant Cell Environ* 37:2500–2507
- Song X, Loucos KE, Simonin KA, Farquhar GD, Barbour MM (2015) Measurements of transpiration isotopologues and leaf water to assess enrichment models in cotton. *New Phytol* 206(2):637–646
- Sprenger M, Leistert H, Gimbel K, Weiler M (2016) Illuminating hydrological processes at the soil-vegetation-atmosphere interface with water stable isotopes. *Rev Geophys* 54:674–704
- Sternberg L (2009) Oxygen stable isotope ratios of tree-ring cellulose: the next phase of understanding. *New Phytol* 181:553–562
- Sternberg LDL, DeNiro MJ (1983) Biogeochemical implications of the isotopic equilibrium fractionation factor between the oxygen-atoms of acetone and water. *Geochim Cosmochim Acta* 47:2271–2274
- Sternberg LDL, Deniro MJ, Savidge RA (1986) Oxygen isotope exchange between metabolites and water during biochemical reactions leading to cellulose synthesis. *Plant Physiol* 82:423–427
- Sternberg LDL, Pinzon MC, Vendramini PF, Anderson WT, Jahren AH, Beuning K (2007) Oxygen isotope ratios of cellulose-derived phenylglucosazone: an improved paleoclimate indicator of environmental water and relative humidity. *Geochim Cosmochim Acta* 71:2463–2473
- Sternberg L, Ellsworth PFV (2011) Divergent biochemical fractionation, not convergent temperature, explains cellulose oxygen isotope enrichment across latitudes. *PLoS One* 6:e28040
- Tsuji H, Nakatsuka T, Takagi K (2006)  $\delta^{18}\text{O}$  of tree-ring cellulose in two species (spruce and oak) as proxies of precipitation amount and relative humidity in northern Japan. *Chem Geol* 231:67–76
- Ulrich DEM, Still C, Brooks JR, Kim Y, Meinzer FC (2019) Investigating old-growth ponderosa pine physiology using tree-rings,  $\delta^{13}\text{C}$ ,  $\delta^{18}\text{O}$ , and a process-based model. *Ecology* 100:e02656
- van Bel AJE (2003) The phloem, a miracle of ingenuity. *Plant, Cell Environ* 26:125–149
- Voelker SL, Brooks JR, Meinzer FC, Roden J, Pazdur A, Pawelczyk S, Hartsough P, Snyder K, Plavcova L, Santrucek J (2014) Reconstructing relative humidity from plant  $\delta^{18}\text{O}$  and  $\delta\text{D}$  as deuterium deviations from the global meteoric water line. *Ecol Appl* 24(5):960–975
- Wagner R, Wagner E (2006) Influence of air pollution and site conditions on trends of carbon and oxygen isotope ratios in tree ring cellulose. *Isot Environ Health Stud* 42:351–365
- Walker CD, Leaney FW, Dighton JC, Allison GB (1989) The influence of transpiration on the equilibration of leaf water with atmospheric water vapour. *Plant, Cell Environ* 12:221–234
- Waterhouse JS, Cheng SY, Juchelka D, Loader NJ, McCarroll D, Switsur VR, Gautam L (2013) Position-specific measurement of oxygen isotope ratios in cellulose: isotopic exchange during heterotrophic cellulose synthesis. *Geochim Cosmochim Acta* 112:178–191
- Wershaw RL, Friedman I, Heller SJ, Frank PA (1966) Hydrogen isotope fractionation of water passing through trees. In: Hobson GD (ed) 'Advances in organic geochemistry'. Pergamon Press: Oxford, pp 55–67
- Wunder J, Fowler AM, Cook ER, Pirie M, McCloskey SPJ (2013) On the influence of tree size on the climate–growth relationship of New Zealand kauri (*Agathis australis*): insights from annual, monthly and daily growth patterns. *Trees* 27:937–948
- Xu C, Sano M, Nakatsuka T (2015) Tree ring cellulose  $\delta^{18}\text{O}$  of *Fokienia hodginsii* in northern Laos: a promising proxy to reconstruct ENSO? *J Geophys Res—Atmos* 116:D24109
- Yakir D, DeNiro MJ (1990) Oxygen and hydrogen isotope fractionation during cellulose metabolism in *Lemna gibba* L. *Plant Physiol* 93:325–332

- Zech M, Mayr C, Tuthorn M, Leiber-Sauheitl K, Glaser B (2014) Oxygen isotope ratios ( $^{18}\text{O}/^{16}\text{O}$ ) of hemicellulose-derived sugar biomarkers in plants, soils and sediments as paleoclimate proxy I: insight from a climate chamber experiment. *Geochim Cosmochim Acta* 126:614–662
- Zeng X, Liu X, Evans MN, Wang W, An W, Xu G, Wu G (2015) Seasonal incursion of Indian Monsoon humidity and precipitation into the southeastern Qinghai-Tibetan Plateau inferred from tree ring  $\delta^{18}\text{O}$  values with intra-seasonal resolution. *Earth Planet Sci Lett* 443:9–19
- Zeng X, Liu X, Treyde K, Evans M, Wang W, An W, Sun W, Xu G, Zhang X (2017) Climate signals in tree-ring  $\delta^{18}\text{O}$  and  $\delta^{13}\text{C}$  from southeastern Tibet: insights from observations and forward modeling of intra-to interdecadal variability. *New Phytol* 216:1104–1118

**Open Access** This chapter is licensed under the terms of the Creative Commons Attribution 4.0 International License (<http://creativecommons.org/licenses/by/4.0/>), which permits use, sharing, adaptation, distribution and reproduction in any medium or format, as long as you give appropriate credit to the original author(s) and the source, provide a link to the Creative Commons license and indicate if changes were made.

The images or other third party material in this chapter are included in the chapter's Creative Commons license, unless indicated otherwise in a credit line to the material. If material is not included in the chapter's Creative Commons license and your intended use is not permitted by statutory regulation or exceeds the permitted use, you will need to obtain permission directly from the copyright holder.



# Chapter 11

## The Stable Hydrogen Isotopic Signature: From Source Water to Tree Rings



Marco M. Lehmann, Philipp Schuler, Marc-André Cormier, Scott T. Allen,  
Markus Leuenberger, and Steve Voelker

**Abstract** The hydrogen isotopic signature ( $\delta^2\text{H}$ ) of water in trees contains information on plant functional responses to climatic changes and on the origin of the water. This is also true for the non-exchangeable hydrogen isotopic signature ( $\delta^2\text{H}_{\text{NE}}$ ) of plant organic matter, which contains additional physiological and biochemical information that can be dated to specific years if extracted from annual rings of trees. Despite this potential for gaining unique insights from  $\delta^2\text{H}_{\text{NE}}$  of tree-ring cellulose ( $\delta^2\text{H}_{\text{TRC}}$ ), it has not been widely used compared to other isotope signals, likely due to challenging methodological constraints and interpretations of these isotopic signals. In this chapter, we first summarize hydrogen isotope ( $^2\text{H}$ -) fractionation that occurs between source water and tree rings and review methods (e.g. nitration, equilibration, position-specific applications) and calculations to determine  $\delta^2\text{H}_{\text{NE}}$  in tree material. Building upon a summary of the current state of knowledge, this chapter also provides an exhaustive synthesis of  $\delta^2\text{H}_{\text{TRC}}$  papers, applications, and associated data from approximately 180 sites across the globe (paired with

---

**Supplementary Information** The online version contains supplementary material available at [https://doi.org/10.1007/978-3-030-92698-4\\_11](https://doi.org/10.1007/978-3-030-92698-4_11).

---

M. M. Lehmann (✉) · P. Schuler  
Forest Dynamics, Swiss Federal Institute for Forest, Snow and Landscape Research, WSL,  
Birmensdorf, Switzerland  
e-mail: [marco.lehmann@alumni.ethz.ch](mailto:marco.lehmann@alumni.ethz.ch)

M.-A. Cormier  
Department of Earth Sciences, University of Oxford, South Parks Road, Oxford OX1 3AN, UK

S. T. Allen  
Department of Natural Resources and Environmental Sciences, University of Nevada, Reno, NV  
89557, USA

M. Leuenberger  
Climate and Environmental Physics, Physics Institute and Oeschger Centre for Climate Change  
Research, University of Bern, Sidlerstrasse 5, 3012 Bern, Switzerland

S. Voelker  
College of Forest Resources and Environmental Science, Michigan Technological University,  
Houghton, MI 49931, USA

modelled precipitation  $\delta^2\text{H}$  values and climate data). The data allow us to investigate the hydrological-climatic effects driving  $\delta^2\text{H}_{\text{TRC}}$  pattern on a global scale, the relationship of hydrogen with oxygen isotopes in the same tree-ring material, as well as the influence of physiological-biochemical effects (e.g., species differences, tree growth) that appear to be more important on local or temporal scales than on a large spatial scales. Thus, when local hydro-climatic influences on source water  $\delta^2\text{H}$  can be isolated,  $\delta^2\text{H}_{\text{TRC}}$  gives novel insights on tree physiological responses to abiotic and biotic stresses. We conclude that the growing constellation of tree-ring metrics, including advancements in  $^2\text{H}$ -processing (i.e., equilibration techniques allowing rapid determinations of  $\delta^2\text{H}_{\text{NE}}$ ) and further refinements to the understanding of post-photosynthetic  $^2\text{H}$ -fractionations will together provide many new opportunities to understand past climates and ecophysiology by using  $\delta^2\text{H}$  in tree rings.

## 11.1 General Introduction

Hydrogen isotopes in various biomarkers have been widely used by geochemists and paleo-climatologists to reconstruct past hydrological and climatic changes (Feng and Epstein 1994; Sachse et al. 2012). The underlying assumption of these studies has been that the hydrogen isotope ratio ( $\delta^2\text{H}$ ) in a compound reflects the  $\delta^2\text{H}$  of water used during photosynthesis and during biosynthesis of these compounds in various plant organs. Given that  $\delta^2\text{H}$  of precipitation water is well known to be under the control of air humidity during evaporation and temperature during condensation,  $\delta^2\text{H}$  of plant compounds have primarily been used to reconstruct those two climatic variables (Libby et al. 1976; Voelker et al. 2014a). The more abundant protium (99.98%) is the lighter of the two stable hydrogen isotopes, consisting of one proton and one electron (mass 1). The less abundant deuterium (0.02%) is the heavier of the two, holding an additional neutron (mass 2). The large difference in mass between the two hydrogen isotopes is physically expressed as strong kinetic and equilibrium isotope fractionation that can cause  $\delta^2\text{H}$  variation of up to 550‰ in water and organic (plant) samples (Schmidt et al. 2007). Moreover, there are strong differences in  $^2\text{H}$ -fractionation among plant metabolic pathways leading to  $\delta^2\text{H}$  variation between carbohydrates, lipids, and proteins. In recent decades, measurements of  $\delta^2\text{H}$  have been increasingly applied on plant-derived lipids such as n-alkanes, that are highly recalcitrant to environmental degradation over timescales of thousands of years. These compounds can be extracted from soil or sediment cores, or other sources that are often dated using radiocarbon or other dating methods (Sachse et al. 2012). Yet, we are just beginning to understand the physiological and hydrological driving factors causing isotopic variations of plant-derived lipids (Kahmen et al. 2013; Newberry et al. 2015). In contrast, analyses of non-exchangeable  $\delta^2\text{H}$  of tree-ring cellulose ( $\delta^2\text{H}_{\text{TRC}}$ ) is still rarely applied, which is mainly caused by what has appeared to be a low sensitivity to local climatic changes and associated difficulties interpreting  $\delta^2\text{H}$  signals (Boettger et al. 2014; Lipp et al. 1991), as well as due to



methods that hinder the rate of sample processing (Epstein and Yapp 1976; Schimmelmann 1991). However, further developments during the last two decades led to high-throughput methods for  $\delta^2\text{H}_{\text{NE}}$  analyses of plant organic material (including  $\delta^2\text{H}_{\text{TRC}}$ ) and important new interpretations of metabolic controls over  $\delta^2\text{H}_{\text{NE}}$  in plant material (Cormier et al. 2018; Sanchez-Bragado et al. 2019) and tree-ring cellulose (Kimak 2015; Lehmann et al. 2021; Mayr 2003). The coming decade promises more rapid developments in this field that should lead to more studies employing  $\delta^2\text{H}_{\text{TRC}}$  to understand past climates and plant ecophysiology.

## 11.2 The Hydrogen Isotopic Signature of Water in Trees

The hydrogen isotopic compositions of precipitation and atmospheric water represent the primary determinants of  $\delta^2\text{H}$  in terrestrial plant tissues including tree rings. Establishment of the temporal and spatial dynamics of the hydrogen isotopic composition of source water ( $\delta^2\text{H}_\text{S}$ , but see also Chapter 18), via measurements and modelling, is therefore an important prerequisite for optimal interpretation of  $\delta^2\text{H}$  values in tree rings (Allen et al. 2019; Dawson et al. 2002; Saurer et al. 2012). As  $\delta^2\text{H}$  values in precipitation and water progressively change due to various factors including temperature, elevation, latitude, distance to coast, amount of a rain event, weather events, and atmospheric circulation pattern, the variability of water isotopes across land surfaces are substantial. Ocean water is used as international reference point for isotope measurements (Vienna Standard Mean Ocean Water, VSMOW), with a  $\delta^2\text{H}$  value of 0‰. After evaporation from a water surface or from vegetation, vapor is depleted in  $^2\text{H}$  (lower  $\delta^2\text{H}$ ) compared to its origin due to fractionation during phase transition from liquid to gas form; that transition favors the preferential evaporation of lighter isotopologues (e.g.,  $^1\text{H}^{16}\text{O}$ ) over heavier ones (e.g.,  $^2\text{H}^{18}\text{O}$ ). In contrast, when water condenses in clouds, precipitation is enriched in  $^2\text{H}$  (higher  $\delta^2\text{H}$ ) than the water vapor remaining in the air (Fig. 11.1). Therefore, precipitation will become more depleted in  $^2\text{H}$  with each rain event as an air mass undergoes successive condensation and precipitation while moving inland or to higher elevations. This process, commonly termed “rainout”, depends strongly on temperature conditions during condensation, partially explaining the strong temperature dependency of precipitation  $\delta^2\text{H}$  values (Dansgaard 1964; Libby et al. 1976). Given that the isotopic composition of precipitation is not always available, global maps of average water isotope values have been modelled and can be used to infer  $\delta^2\text{H}$  values of precipitation in the absence of measurements (Bowen and Revenaugh 2003). The isotopic signals of precipitation can be modified by evaporation effects prior to when trees take up water in the soil, which has often been characterized by an enrichment in  $^2\text{H}$  from deep to more shallow soil layers (Allison et al. 1983; Lin and Sternberg 1993). On the other hand,  $\delta^2\text{H}$  of soil water that is taken up by trees is an admixture of recent and older precipitation that can depend on the size, depth, and geological properties of water catchments and groundwater aquifers, as well as on water turnover rates in concert with soil characteristics, vegetation rooting depths and other

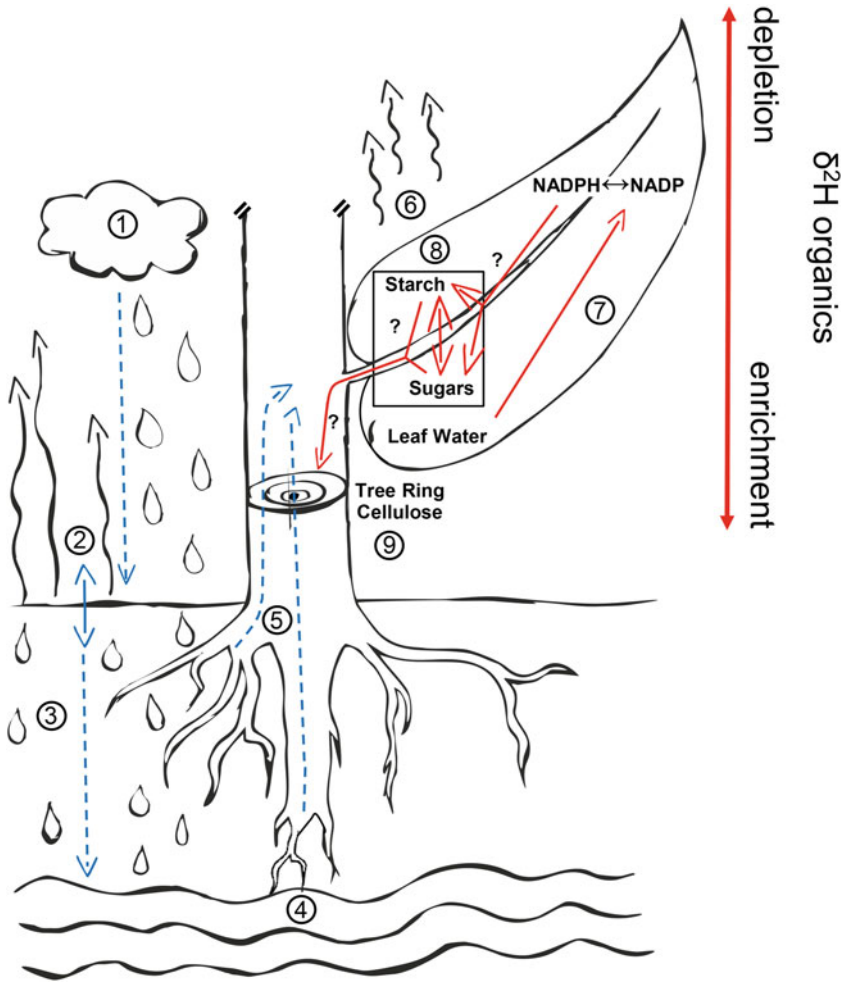


**Fig. 11.1** ① The hydrogen isotope composition in tree rings is dependent on the origin of the rain (water vapor source). The higher the latitude (latitude effect) and altitude (altitude effect), and the more continental the formation area of the clouds is, the more  $^2\text{H}$ -depleted the precipitation will become. ② Surface water becomes  $^2\text{H}$ -enriched due to evaporation of isotopically lighter water. ③ Water infiltrating deeper soil layers mixes with water of previous precipitation events, which is often  $^2\text{H}$ -depleted compared to surface water as it experiences no evaporative effects. ④ The isotopic composition of groundwater can deviate strongly from rainwater as it may have a different catchment area and a different temporal origin. ⑤ Depending on the root depth and transpiration rates, tree xylem water can show a mixed isotopic composition of soil and groundwater, with generally no further  $^2\text{H}$ -fractionation during uptake. ⑥ Leaf water is  $^2\text{H}$ -enriched due to transpiration of isotopically lighter water. This effect can be influenced by changes in stomatal aperture, temperature, and air humidity. ⑦  $^2\text{H}$ -enriched leaf water and  $^2\text{H}$ -depleted NADPH derived from photolysis of  $\text{H}_2\text{O}$  are the main isotopic sources of primary assimilates. ⑧ Unresolved  $^2\text{H}$ -fractionation processes linked to carbon fixation, starch synthesis, re-mobilization, and downstream transport of sugars lead to a  $^2\text{H}$ -enrichment of tree-ring cellulose compared to leaf assimilates. Blue lines refers to water, with dashed lines indicating processes that show little or no  $^2\text{H}$ -fractionation. Red lines and axis refers only to  $^2\text{H}$ -fractionations in organic molecules, including NADPH and carbohydrates (i.e. sugars, starch, and cellulose)

processes modifying the mixing and uptake of water by tree roots (Brooks et al. 2010; Lin and Sternberg 1993). Overall, the isotopic composition of precipitation and source water taken up by trees can lag precipitation inputs by weeks to years, and can vary markedly among individuals and across regions (Allen et al. 2019; Voelker et al. 2019; Volkman et al. 2016).

Source water ( $\delta^2\text{H}_\text{S}$ ) becomes enriched in heavy isotopes after reaching leaves due to preferential evaporation loss of lighter isotopologues from the leaf water pool during transpiration. The fractionation from  $\delta^2\text{H}_\text{S}$  to  $\delta^2\text{H}$  of leaf water ( $\delta^2\text{H}_\text{L}$ ) has been closely predicted by the Craig-Gordon model (Dongmann et al. 1974), describing the isotopic enrichment at the evaporative site of a water pool as (Craig and Gordon 1965):

$$\delta^2\text{H}_\text{L} = \delta^2\text{H}_\text{S} + \varepsilon_e + \varepsilon_k + (\delta^2\text{H}_\text{V} - \varepsilon_k - \delta^2\text{H}_\text{S}) * e_a/e_i \quad (11.1)$$

where  $\varepsilon_e$  is the temperature-dependent equilibrium isotope fractionation between vapor and liquid water (Horita and Wesolowski 1994),  $\varepsilon_k$  is the kinetic isotope fractionation occurring during the diffusion of water molecules through the stomata cavity and the boundary layer (Merlivat 1978),  $\delta^2\text{H}_\text{V}$  is the hydrogen isotope ratio of atmospheric water vapor, and  $e_a/e_i$  is the ratio between the partial pressures of the atmosphere and intracellular water vapor. As implied by Eq. 11.1,  $\delta^2\text{H}_\text{L}$  values are mainly driven by the leaf-to-air vapor pressure ratio, similar to relative humidity (i.e., which is often used as an estimate for  $e_a/e_i$ ) or by the vapor pressure deficit (VPD, difference between saturated and ambient pressure) and have found widespread application for reconstruction of environmental and hydrological conditions from plant organic compounds (Sachse et al. 2012; Voelker et al. 2014a; Zech et al. 2013). Importantly, at high relative humidity (ca. > 60%), the isotopic value of water vapor dominates the isotopic signal of leaf water (Gerlein-Safdi et al. 2018; Lehmann et al. 2018; Roden et al. 2000). The basic leaf water model (Eq. 11.1) tends to overestimate  $\delta^2\text{H}_\text{L}$  values; corrections include representing leaves as two pools as well as Péclet effects, to account for unenriched water pools (e.g., lignified leaf veins) or progressive leaf water enrichment (e.g., from the bottom to the tip or from the main vein to the margin in leaves) (Roden et al. 2015). Variation in  $\delta^2\text{H}_\text{L}$  strongly influences  $\delta^2\text{H}$  of assimilates (Cormier et al. 2018) and thus  $\delta^2\text{H}_\text{TRC}$  (Roden et al. 2000). The following section will therefore focus on the manifold isotope fractionations influencing  $\delta^2\text{H}_\text{TRC}$  chronologies.

### 11.3 The Hydrogen Isotopic Signature of Tree-Ring Cellulose

$^2\text{H}$ -fractionations occurring in trees during the biosynthesis of organic compounds from leaf water and  $\text{CO}_2$  to sugars and subsequent molecules result from several biochemical processes (Luo and Sternberg 1992; Schmidt et al. 2003; Sternberg et al.

1984; Yakir 1992). The biosynthetic hydrogen isotope fractionation ( $\epsilon_{\text{bio}}$ ) between leaf water and organic compounds was (and still is) largely treated as a constant in practice in paleo-biogeochemical studies (Sachse et al. 2012). However,  $\epsilon_{\text{bio}}$  may vary among species and compounds, as related to plant enzymatic reactions and the specific biochemical origin of H atoms during their biosynthesis (Cormier et al. 2019, 2018; Estep and Hoering 1981; Ziegler et al. 1976). For biosynthesis of compounds in plants, three origins of H are important in this respect (Fig. 11.1):

- (1) The organic precursor molecules in a biosynthetic pathway; for example, the H atoms of ribulose-1,5-bisphosphate that are transferred to the two triose phosphates synthesized in the Calvin cycle.
- (2) Redox cofactors (e.g. the biological reducing agent NADPH) that provide an important part of the H atoms in the biosynthesis of organic compounds.
- (3) The cellular water.

Yakir and DeNiro (1990) suggested that the overall  $^2\text{H}$ -fractionation factor occurring between leaf water ( $\delta^2\text{H}_{\text{L}}$ ) and carbohydrates ( $\delta^2\text{H}_{\text{Carbo}}$ ) can be divided into photosynthetic (F1) and post-photosynthetic  $^2\text{H}$ -fractionations (F2), and that the relative fraction (f) of these two processes drives the  $\epsilon_{\text{bio}}$  according to the following equations:

$$\delta^2\text{H}_{\text{Carbo}} = \delta^2\text{H}_{\text{L}} + \epsilon_{\text{bio}} \quad (11.2)$$

$$\epsilon_{\text{bio}} = f * \text{F1} + (1 - f) * \text{F2} \quad (11.3)$$

The photosynthetic  $^2\text{H}$ -fractionation (F1) occurs in the chloroplast during the light reaction of photosynthesis where ferredoxin-NADP + reductase produces NADPH with reduced H that is strongly  $^2\text{H}$ -depleted compared with leaf water (Luo et al. 1991). This  $^2\text{H}$ -depleted H pool in NADPH is subsequently introduced into organic compounds in the Calvin cycle, causing the first building blocks of sugar pools to be  $^2\text{H}$ -depleted compared with leaf water. Cormier et al. (2018) suggests that this initial process is independent of the rate of photosynthesis within a species and possibly stable for any given species. In turn, this suggests variation in  $\epsilon_{\text{bio}}$  of carbohydrates are driven by post-photosynthetic  $^2\text{H}$ -fractionations.

Post-photosynthetic  $^2\text{H}$ -fractionation (F2) processes are assumed to have strong  $^2\text{H}$ -enrichment effects, commencing in sugars produced by the Calvin cycle and reflecting several overlapping processes and enzymatic reactions. Triose phosphates (TP) synthesis in the Calvin cycle allows (partial) exchange of C-bound H atoms with ( $^2\text{H}$ -enriched) cellular water in  $\text{CH}_2$  groups adjacent to CO groups via an enolic structure (Knowles and Albery 1977). Moreover, only one out of four C-bound H atoms in TPs is derived from  $^2\text{H}$ -depleted NADPH from the light reaction of photosynthesis; alternatively, the others derive from precursor molecules that become  $^2\text{H}$ -enriched after exchange with cellular water, as described earlier. During the fructose-1,6-bisphosphate aldolase reaction, two TPs are used to build one hexose phosphate and one out of four C-bound H atoms is lost to the surrounding water (Schmidt et al. 2015).

Phosphoglucose isomerase, used to inter-convert glucose 6-phosphate and fructose 6-phosphate, might further  $^2\text{H}$ -enrich the sugar pool by allowing partial exchange of specific H atoms with the surrounding cellular water (Schleucher et al. 1999). In non-autotrophic plants and plant tissues, NADPH is likely strongly  $^2\text{H}$ -enriched as it derives from the oxidative pentose phosphate pathway reactions. Overall,  $\delta^2\text{H}_{\text{NE}}$  values of carbohydrates typically do not deviate as strongly from those in leaf water as we would expect from the primary  $^2\text{H}$ -depletion of the NADPH pool that is generated in the light reaction of photosynthesis because post-photosynthetic  $^2\text{H}$ -enrichment of the sugar pool provides nearly a net balance of isotopic fractionation events affecting tree rings and other plant tissues.

The  $^2\text{H}$ -fractionations in sugar pools of trees do not only occur at the leaf level. Roden and Ehleringer (1999) experimentally showed that about 36% of the leaf isotopic signature in a given tree-ring was replaced by the source water isotopic signal during cellulose biosynthesis. From their findings, the authors developed a mechanistic model for  $\delta^2\text{H}_{\text{TRC}}$ :

$$\delta^2\text{H}_{\text{TRC}} = f * (\delta^2\text{H}_{\text{S}} + \text{F2}) + (1 - f) * (\delta^2\text{H}_{\text{L}} + \text{F1}) \quad (11.4)$$

The estimates of  $^2\text{H}$ -fractionation factors were derived from various experimental systems (Luo and Sternberg 1992; Yakir and DeNiro 1990), with F1 and F2 as  $-171\text{‰}$  and  $+158\text{‰}$ , respectively. The Roden et al. (2000) model provided a 1:1 relationship between observed and modeled  $\delta^2\text{H}_{\text{TRC}}$  under two different relative humidity conditions. Similarly, the Roden model has been applied to paired tree-ring oxygen and hydrogen isotopes for reconstruction of relative humidity over space and time (Voelker et al. 2014a). Although the Roden model has found practical applications for tree-ring studies it is known to neglect that the compensating effects of F1 and F2 simultaneously determine  $\delta^2\text{H}_{\text{Carbo}}$  (Eqs. 11.2 and 11.3) and that  $\delta^2\text{H}_{\text{NE}}$  of leaf sugars are lower than  $\delta^2\text{H}_{\text{TRC}}$ . Moreover, as discussed toward the end of this chapter, the use of heterotrophic  $^2\text{H}$ -enriched starch might play an important role for  $\delta^2\text{H}_{\text{TRC}}$  values of mature trees (Kimak et al. 2015; Lehmann et al. 2021; Mayr 2003). Thus, further improvements to the Roden et al. (2000) model are needed to more accurately understand drivers of plant tissue  $\delta^2\text{H}$  and, consequently, better realize the research potential that  $\delta^2\text{H}_{\text{TRC}}$  can provide.

## 11.4 Methods and Calculations for $\delta^2\text{H}$ Analysis of Tree Carbohydrates

There are two kinds of hydrogen in carbohydrates or hydrocarbons such as sugars and cellulose. Hydrogen linked to carbon atoms (C-H) is called non-exchangeable hydrogen and cannot be easily exchanged without enzymatic catalysis in biochemical pathways. The  $\delta^2\text{H}$  ratio of such carbon-bound non-exchangeable hydrogen

(often termed  $\delta^2\text{H}_{\text{NE}}$ ) in carbohydrates holds meaningful information on hydrological, climatic, or biochemical conditions during their synthesis and is therefore of interest in dendrochronological studies. In contrast, hydrogen that is linked to oxygen atoms in hydroxyl (O–H) groups of carbohydrate molecules is called exchangeable hydrogen. Exchangeable hydrogen is in equilibrium with the hydrogen of the surrounding water such as recent sap water or environmental water and thus does not reflect the hydrological, climatic, or biochemical conditions during cellulose synthesis. Moreover, during extraction of carbohydrates such as sugars or cellulose, the exchangeable hydrogen will be exchanged with extraction water or solutions and therefore its original isotopic composition will be again overwritten. Therefore, it is crucial to exclude the exchangeable hydrogen for an accurate determination of  $\delta^2\text{H}_{\text{NE}}$  values in carbohydrates. Several methods have been developed to overcome this problem over the last decades to isolate the  $\delta^2\text{H}_{\text{NE}}$  values of sugars and cellulose in plants. In Table 11.1, we summarized the different available  $\delta^2\text{H}_{\text{NE}}$  methods and in the following section we explain the main principles.

**Table 11.1** Overview of methods to determine  $\delta^2\text{H}_{\text{NE}}$  in plant carbohydrates. The given references reflect seminal papers that provide detailed descriptions of the methods and demonstrate some applications. “Hot equilibration” is performed in an oven or in a heated operational unit, while “cold equilibration” is conducted at room temperature. “Online” means that individual samples (of a batch) are equilibrated with water vapor and subsequently analyzed by IRMS. “Offline” means that sample equilibration with water vapor is performed independently of the actual IRMS analysis

Methods	Compounds	Sample amount	References
Nitration	Cellulose, Starch	Individual samples	Alexander and Mitchell (1949), Boettger et al. (2007)
Nitration	Sugars	Individual samples	Doner et al. (1987), Dunbar and Schmidt (1984)
Hot offline equilibration	Cellulose, Starch, Sugars	Batch of samples	Sauer et al. (2009), Schuler et al. (2022), Wassenaar et al. (2015)
Hot online equilibration	Cellulose	Batch of samples	Filot et al. (2006), Loader et al. (2015)
Cold offline equilibration	Dry Matter, Cellulose, Water soluble organic compounds	Batch of samples	Qi and Coplen (2011), Sanchez-Bragado et al. (2019)
NMR	Cellulose, Starch, Sugars	Individual samples	Betson et al. (2006), Schleucher et al. (1999)
Lignin methoxyl groups	Lignin	Individual samples	Anhauser et al. (2017), Greule et al. (2008)

### 11.4.1 Nitration Methods

Nitration is the most commonly employed method (Table 11.1) for determination of  $\delta^2\text{H}_{\text{NE}}$  values in cellulose and particularly helpful to establish  $\delta^2\text{H}_{\text{NE}}$  reference material (Boettger et al. 2007). The nitration of cellulose is a reaction where the hydroxyl groups are replaced by nitro groups ( $\text{NO}_2$ ) via an electrophilic substitution. The reaction can be performed using a mixture of  $\text{HNO}_3$  (90%) and  $\text{H}_2\text{SO}_4$  (~98%) with a final concentration of  $\text{HNO}_3$  of about 25% in a 150 times weight excess at room temperature for  $\geq 12$  h. Alternatively, cellulose can also be nitrated with a 40 times weight excess of a solution of 28.7 m%  $\text{P}_2\text{O}_5$  in  $\text{HNO}_3$  (90%) at room temperature (RT) for 4 h (modified after Alexander and Mitchell 1949). For both methods, the mixing of the two components is highly exergonic and the solution needs to be cooled down to 4 °C, e.g., in an ice-water bath. The complete dissolving of  $\text{P}_2\text{O}_5$  can take several hours or overnight, where a slow temperature increase to RT is uncritical. For achieving highly nitrated cellulose, it is recommended to constantly stir the reaction solution and to keep the water content as low as possible. After the nitration, the product can be washed with distilled water and stabilised with methanol. Incompletely nitrated side products can be removed via the dissolution of the highly nitrated product in acetone and centrifugation. Cellulose nitrate with a nitrogen content of  $> 12.7\%$  is assumed to reflect a nearly complete nitration, but more than 13.5% N are not achievable (de la Ossa et al. 2011). To complete these steps noted in the methods above and produce cellulose nitrate with an acceptably high nitrogen content, there is probably an upper limit of about 50 samples per week that can be processed by one person, which has limited its application in attempts to understand inter-annual variation in  $\delta^2\text{H}$  of tree rings. Note that cellulose nitrate is an explosive material and should be stored in a refrigerator to reduce degradation. In addition, nitration methods for sugars have been developed (Dunbar and Schmidt 1984) and applied in food authenticity studies (Doner et al. 1987). However, sugar nitration should be performed very carefully under constant cooling as temperature above 20 °C can cause an extremely vigorous reaction and explosion. Finally,  $\delta^2\text{H}$  analysis of cellulose nitrate with a TC/EA-IRMS system might be best performed in a reactor consisting of a mix of chromium and quartz chips to avoid potential isotope fractionation during pyrolysis of nitrogen-rich compounds (Gehre et al. 2015).

### 11.4.2 Equilibration Methods

In contrast to the cellulose nitration method, where the exchangeable H on hydroxyl (OH) groups is replaced by a nitro group ( $\text{NO}_2$ ), the equilibration method is based on a physico-chemical principle of exchanging the OH groups with those of standard water. This process of H isotope exchange happens naturally with ambient water or vapor. In order to guarantee stable and robust  $\delta^2\text{H}_{\text{NE}}$  values, which makes up 70% of the hydrogen atoms in a cellulose molecule, it is accepted to follow an equilibration

with in-house-standard water of known isotopic composition before sample analysis with a TC/EA-IRMS system. Samples are decomposed by pyrolysis at ca. 1400 °C to hydrogen (H<sub>2</sub>) and carbon monoxide (CO) gases, with the former being used to determine  $\delta^2\text{H}$  values. Given strong methodological improvements over the last decades, the equilibration method has become more popular for determining  $\delta^2\text{H}_{\text{NE}}$  in cellulose.

First, offline methods were used to perform the equilibration (Feng et al. 1993; Grinsted and Wilson 1979; Schimmelmann 1991; Wassenaar and Hobson 2000). They followed different temperature regimes but all of them suffered from disadvantages: (1) slow equilibration process at low temperatures, (2) difficult and time-consuming removal of the excess water through sublimation for the method of Feng et al. (1993), (3) isotope fractionation potential between water and exchangeable hydrogen during the different process steps and (4) a rather large amount of sample (3–12 mg) that is required. Wassenaar and Hobson (2000) described a similar method with static offline equilibration that can be applied for cellulose, as well as for complex organic materials, for example, feathers or keratin. More recent developments in offline methods allow equilibration of a batch of cellulose, starch, or sugar samples in a metal chamber under a continuous flow of vapor with a known isotopic composition at high temperature conditions (ca. 70 to 130 °C; “Hot offline equilibration”, Table 11.1) in an oven and to dry them before TC/EA-IRMS analysis (Sauer et al. 2009; Schuler et al. 2022). This system was further optimized, enabling sample equilibration and drying to occur directly in a heated and helium purged autosampler to prevent contamination with humid laboratory air. The autosampler is placed on an TC/EA-IRMS system, so that multiple samples can be equilibrated with injected water vapor, dried, and directly measured (Wassenaar et al. 2015). Equilibrations are mostly performed at high temperatures to vaporize a water source and to accelerate the equilibration process. However, other studies showed that sufficient equilibration of plant material with a water source can also be achieved at room temperature in an evacuated glass desiccator over a longer time period (“Cold offline equilibration”, Table 11.1), followed by drying of the samples in a vacuum oven over several days (Qi and Coplen 2011; Sanchez-Bragado et al. 2019).

In addition to offline equilibration systems, Pilot et al. (2006) developed an online equilibration method. An equilibration chamber temperature controlled at 110 °C with a moving piston selecting between three positions to load (sample derived from an autosampler), equilibrate and inject a sample for subsequent isotope ratio analysis. The equilibration chamber is flushed with helium and in-house-standard water that is immediately vaporized when entering the heated equilibration chamber. An analytical batch consists of 94 measurements (i.e. 55 samples and 39 standard materials), allowing the analysis of about 165 samples per week. Samples and standard materials are equilibrated sequentially within 600 s and then pyrolyzed by a TC/EA-IRMS to determine  $\delta^2\text{H}$  values. A GC-column held at 70 °C was used to separate H<sub>2</sub> and CO gases to the degree that sequential isotope ratio measurements are feasible on IRMS, enabling to do triple isotope analysis (Loader et al. 2015). The “hot online equilibration” method (see Table 11.1) can actually be used for the quadruple isotope



ratio determination by a corresponding adjustment of the GC-column that allows the separation of N<sub>2</sub> from CO.

### ***11.4.3 Position-Specific Methods to Determine $\delta^2\text{H}_{\text{NE}}$ in Wood Material***

Deuterium in plant carbohydrates can also be position-specifically determined by nuclear magnetic resonance (NMR, Table 11.1) spectroscopy.  $\delta^2\text{H}_{\text{NE}}$  methods have been developed for starch and sugars from different herb and tree species (Schleucher et al. 1999; Zhang et al. 2002) and for plant and tree-ring cellulose (Betson et al. 2006). The intra-molecular analysis reveals strong  $\delta^2\text{H}$  differences for carbon-bound hydrogen atoms within carbohydrate molecules. Thus for interpretation of  $\delta^2\text{H}_{\text{TRC}}$  values the underlying  $\delta^2\text{H}_{\text{NE}}$  variations on individual positions should be considered (but see Chapter 7 for more information). Moreover, a novel and simple preparation method was developed to measure the  $\delta^2\text{H}$  value of lignin methoxyl groups ( $\delta^2\text{H}_{\text{meth}}$ , Table 11.1) by gas chromatograph/pyrolysis-IRMS (Greule et al. 2008).  $\delta^2\text{H}_{\text{meth}}$  values of wood samples were strongly correlated with the  $\delta^2\text{H}_{\text{P}}$  on a global scale.  $\delta^2\text{H}_{\text{meth}}$  might therefore reflect a new climate proxy for temperature changes over time if extracted from annual rings of trees (Gori et al. 2013). However, the biosynthetic isotope fractionation between  $\delta^2\text{H}_{\text{meth}}$  and  $\delta^2\text{H}_{\text{P}}$  of ca. -217 ‰ can vary among different tree species and therefore care should be taken if used for climate reconstructions (Anhauser et al. 2017).  $\delta^2\text{H}_{\text{meth}}$  might be of particular interest for paleo-wood samples, which have often been buried under anoxic conditions and have undergone substantial or nearly complete losses in cellulose due to degradation, but may still contain lignin.

### ***11.4.4 Calculation of Non-exchangeable Hydrogen Isotopic Composition, International Standards, and Referencing***

During our review for this chapter, we found that equations regarding  $\delta^2\text{H}_{\text{NE}}$  can vary among studies using equilibration methods. To facilitate comparisons among past and future  $\delta^2\text{H}_{\text{TRC}}$  values, we propose the following systematics and syntax. The total  $\delta^2\text{H}$  values ( $\delta^2\text{H}_{\text{T}}$ ), which is the result of an isotopic analysis of equilibrated samples, can be calculated as follows:

$$\delta^2\text{H}_{\text{T}} = f_e * \delta^2\text{H}_{\text{E}} + (1 - f_e) * \delta^2\text{H}_{\text{NE}} \quad (11.5)$$

where  $f_e$  is the fraction of total exchangeable hydrogen in the total H pool and  $\delta^2\text{H}_{\text{E}}$  the  $\delta^2\text{H}$  value of the exchangeable hydrogen atoms. For a precise estimation of  $\delta^2\text{H}_{\text{NE}}$ ,

a comprehensive evaluation of different potential cases for  $f_e$  are needed. Theoretically, 30% of the hydrogen in cellulose should be exchanged, but in most cases less were exchanged, most probably due to difficulties in accessing all exchangeable hydrogen and to inhomogeneities of the cellulose preparation steps. Therefore, the range for  $f_e$  of cellulose varies between 0 and 0.3 (Schimmelmann 1991; Wassenaar and Hobson 2000). The higher  $f_e$  values of a measurement, the better the equilibration processes and the precision and accuracy of the  $\delta^2\text{H}_{\text{NE}}$  analysis:

$$f_e = (\delta^2\text{H}_{\text{T}} - \text{A} - \delta^2\text{H}_{\text{T}} - \text{B}) / (\delta^2\text{H}_{\text{W}} - \text{A} - \delta^2\text{H}_{\text{W}} - \text{B}) * (1 - \epsilon_e/1000) \quad (11.6)$$

where  $\delta^2\text{H}_{\text{T-A}}$  and  $\delta^2\text{H}_{\text{T-B}}$  are  $\delta^2\text{H}_{\text{T}}$  values of cellulose that have been equilibrated with in-house-standard water (A or B) and thus with water vapor of a known isotope ratio ( $\delta^2\text{H}_{\text{W-A}}$ ,  $\delta^2\text{H}_{\text{W-B}}$ ), respectively. The isotopic differences between the two in-house-standard waters A and B is mostly several 100‰ and allow for the determination of  $f_e$  (approximately the slope of relationship between  $\delta^2\text{H}_{\text{T}}$  and  $\delta^2\text{H}_{\text{W}}$  of both waters). The  $^2\text{H}$ -fractionation ( $\epsilon_e$ ) occurring between  $\delta^2\text{H}_{\text{E}}$  and  $\delta^2\text{H}$  of water vapor has been found to vary between 60‰ and 100‰ for most plant derived compounds. Most methods set  $\epsilon_e$  to ca. 80‰, as it has been found to be an average isotope fractionation factor for most cellulose samples (Schimmelmann 1991; Wassenaar and Hobson 2000). Both,  $\epsilon_e$  and  $f_e$  are temperature dependent, so temperature needs to be tightly controlled during equilibration and also held constant among batches to provide consistent results.

A mass balance allows the determination of  $\delta^2\text{H}_{\text{NE}}$  from the  $\delta^2\text{H}_{\text{TA}}$  or  $\delta^2\text{H}_{\text{TB}}$  where  $\delta^2\text{H}_{\text{T}}$  values are normalized to the international VSMOW scale using an international standard, which has no exchangeable hydrogen (e.g., polyethylene foil, IAEA-CH-7) following Filot et al. (2006):

$$\delta^2\text{H}_{\text{NE}} = (\delta^2\text{H}_{\text{TA}} - 1000 * f_e * (\epsilon_e - 1) - f_e * \epsilon_e * \delta^2\text{H}_{\text{WA}}) / (1 - f_e) \quad (11.7)$$

$\delta^2\text{H}_{\text{NE}}$  values of equilibrated cellulose samples should be checked against cellulose standards with known  $\delta^2\text{H}_{\text{NE}}$  values to verify method accuracy. Cellulose nitrate derived from different wood material or chronologies might be ideal for verification of these methods (Filot et al. 2006; Schuler et al. 2022). Recently published international wood standards (USGS 54–56) might also be used for  $\delta^2\text{H}$  calibration (Qi et al. 2016). There is also an international cellulose standard available (IAEA-CH-3), however, there is no agreement yet on its actual  $\delta^2\text{H}_{\text{NE}}$  value (Loader et al. 2015; Sauer et al. 2009). Equilibration can also be performed on other organic matter, however, the degree of exchangeable hydrogen and the exchangeability of hydrogen atoms itself can differ among substances.

## 11.5 Synthesis of $\delta^2\text{H}_{\text{TRC}}$ Data, Applications, and Interpretations

For this book chapter, we reviewed ca. 50 studies and unpublished records showing information on  $\delta^2\text{H}_{\text{NE}}$  of tree-ring cellulose ( $\delta^2\text{H}_{\text{TRC}}$ ; mainly derived via equilibration or nitration methods) from ca. 180 sites. We approximated the mean  $\delta^2\text{H}_{\text{TRC}}$  values for each site chronology and plotted the distribution on a global map (Fig. 11.2). Table S1 holds all information on publications, sample preparation and material, tree species, temporal resolutions, location, and tree-ring isotope data. For each site, we estimated the mean annual temperature (MAT) and mean annual sum of precipitation (MAP) using a gridded data product at 5-arc-minute resolution (Fick and Hijmans 2017). We also modelled long-term mean annual  $\delta^2\text{H}$  and  $\delta^{18}\text{O}$  of precipitation ( $\delta^2\text{H}_{\text{P}}$  and  $\delta^{18}\text{O}_{\text{P}}$ ) for each site using grids available on Bowen and Revenaugh (2003). For studies that reported site elevation,  $\delta^2\text{H}_{\text{P}}$  values were adjusted by a value calculated from multiplying the isotopic lapse rate, assumed to be  $-2.24\text{‰}$   $\delta^2\text{H}$  per 100 m (Poage and Chamberlain 2001) for the difference between site elevation and pixel-mean elevation; for studies that did not report site elevation, the gridded values were used without adjustment.

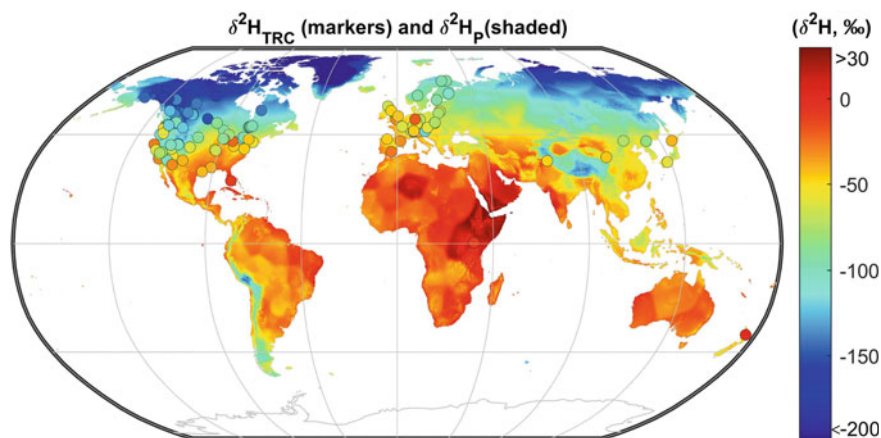


**Fig. 11.2** Global map for  $\delta^2\text{H}_{\text{NE}}$  of tree-ring cellulose ( $\delta^2\text{H}_{\text{TRC}}$ , VSMOW, markers) and  $\delta^2\text{H}$  of precipitation ( $\delta^2\text{H}_{\text{P}}$ , VSMOW, shaded) for ca. 140 sites derived from literature data (Table S1). Paleo sites ( $< 1000$  years before 2000 AD) are not shown due to climatic and sampling uncertainties

### 11.5.1 Global $\delta^2\text{H}_{\text{TRC}}$ Patterns and Hydro-Climatic Effects

For more than four decades,  $\delta^2\text{H}_{\text{NE}}$  of wood or tree-ring cellulose has been recognized to closely correlate with MAT and that  $\delta^2\text{H}_{\text{NE}}$  is generally sensitive to continental-scale climatic trends (Epstein and Yapp 1976; Gray and Song 1984; Libby et al. 1976; Schiegl 1974). In retrospect, the temperature dependence of  $\delta^2\text{H}_{\text{TRC}}$  at these large scales is partially due to the isotopic composition of meteoric water, which also correlates with temperature variations (Dansgaard 1964; Yapp and Epstein 1982). Here we investigated the global relationship of  $\delta^2\text{H}_{\text{TRC}}$  with  $\delta^2\text{H}_{\text{P}}$  and MAT across various tree species and study sites (Fig. 11.3). Including  $\delta^2\text{H}_{\text{TRC}}$  values from paleo study sites (< 1000 years before 2000 AD) only slightly affected the relationship. However, to be conservative, we excluded paleo studies (ca. 40 sites) from this analysis due to large uncertainties related to time-transgressive estimates of paleoclimate temperatures and associated estimates of  $\delta^2\text{H}_{\text{P}}$ .

As expected,  $\delta^2\text{H}_{\text{P}}$  is indeed significantly related to  $\delta^2\text{H}_{\text{TRC}}$  ( $r^2 = 0.69$ ), demonstrating that spatial variability in  $\delta^2\text{H}_{\text{P}}$  of precipitation determines more than two thirds of the spatial variation in tree-ring isotope ratios. Interestingly, the relationship between  $\delta^2\text{H}_{\text{P}}$  and  $\delta^2\text{H}_{\text{TRC}}$  largely envelopes the 1:1 line, albeit with a slightly shallower slope of  $0.9 \pm 0.05$ . The overlap of the 1:1 line is somewhat surprising, given that  $\delta^2\text{H}_{\text{TRC}}$  is modified by  $^2\text{H}$ -enrichment of leaf water and by various  $^2\text{H}$ -fractionation in carbohydrates in leaf and sink tissues. Roden et al. (2000) showed that it is rather unlikely that the leaf water signal is fully lost during tree-ring cellulose synthesis for both oxygen and hydrogen isotopes. We therefore assume that the sum of the  $^2\text{H}$ -enrichment during leaf water evaporation and  $^2\text{H}$ -fractionations of carbohydrates (Eqs. 11.2 and 11.3) cancel each other out, so that the mean  $\delta^2\text{H}_{\text{TRC}}$  of a chronology approximately reflects the average  $\delta^2\text{H}_{\text{P}}$  of a site. While MAP showed no clear relationship with  $\delta^2\text{H}_{\text{TRC}}$  (not shown), we found a significant relationship between MAT and  $\delta^2\text{H}_{\text{TRC}}$  ( $r^2 = 0.47$ ), with a slope-derived change of  $5.2 \pm 0.5\text{‰}/^\circ\text{C}$  and an intercept of  $-21.5 \pm 4.0\text{‰}$ . The linear relationship was very similar between MAT and  $\delta^2\text{H}_{\text{P}}$  ( $r^2 = 0.67$ , not shown), with a slope-derived change of  $5.8 \pm 0.3\text{‰}/^\circ\text{C}$  and an intercept of  $-122.2 \pm 3.0\text{‰}$ . Our results agree with  $5.5\text{‰}/^\circ\text{C}$  that was observed by Gray and Song (1984), demonstrating that the temperature-dependent equilibrium isotope effect in precipitation water is the dominant factor influencing  $\delta^2\text{H}_{\text{TRC}}$  on a global scale (however, not on a local scale as discussed later).

Moreover, we additionally investigated the global  $\delta^2\text{H}$ - $\delta^{18}\text{O}$  relationship for tree-ring cellulose of about 110 sites (70 modern/40 paleo) (Fig. 11.4). Previously, these two types of data had been used to model leaf water isotope across continental climate gradients (Voelker et al. 2014a). However, to our knowledge, a global  $\delta^2\text{H}$ - $\delta^{18}\text{O}$  relationship for tree-ring cellulose across diverse tree species has not previously been presented. We found that the global  $\delta^2\text{H}$ - $\delta^{18}\text{O}$  of tree-ring cellulose is shifted by an average  $\delta^{18}\text{O}$  offset of  $+38.6\text{‰}$  between precipitation and the signal incorporated in tree-ring cellulose. This offset approximates the difference between measured  $\delta^{18}\text{O}$  values of xylem water and tree-ring cellulose (Roden and Ehleringer 2000). The

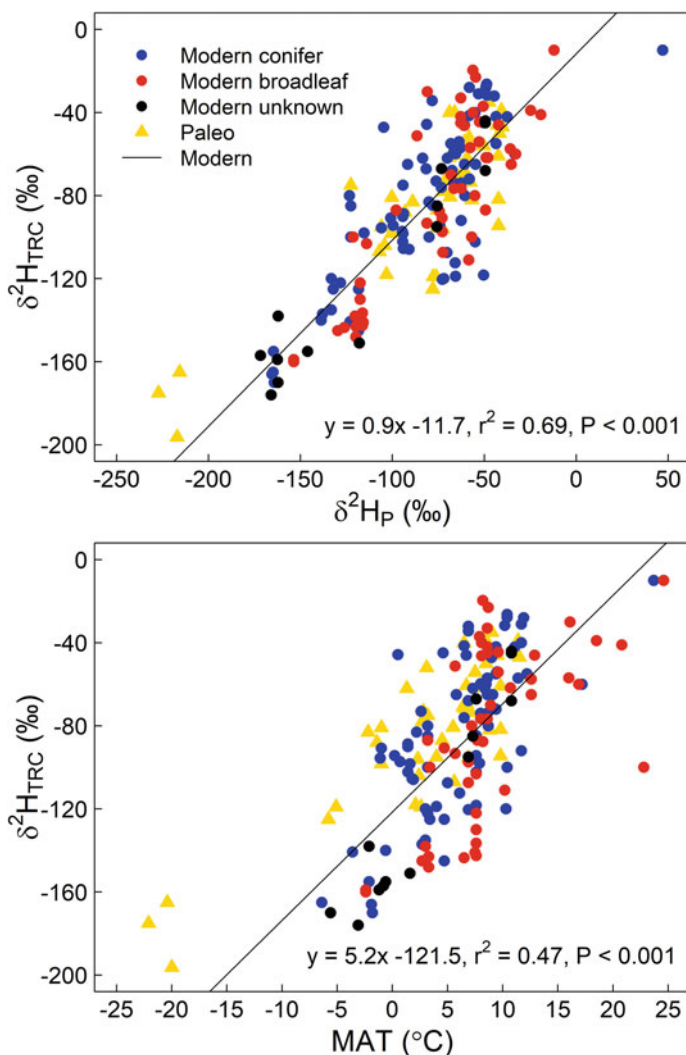


**Fig. 11.3** Relationships between  $\delta^2\text{H}_{\text{NE}}$  of tree-ring cellulose ( $\delta^2\text{H}_{\text{TRC}}$ , VSMOW) with modelled  $\delta^2\text{H}$  of precipitation water ( $\delta^2\text{H}_{\text{P}}$ ) and mean annual temperature (MAT). Mean values of ca. 180 sites derived from ca. 50 publications and unpublished records (Table S1) are given. Paleo sites (< 1000 years before 2000 AD) were excluded from the regression line due to climatic and sampling uncertainties. Unknown = tree species could not be identified

changes in  $\delta^2\text{H}_{\text{TRC}}$  values are low (Fig. 11.4), which can be explained by the close relationship to  $\delta^2\text{H}_{\text{P}}$  (Fig. 11.3). The slope of the  $\delta^2\text{H}$ - $\delta^{18}\text{O}$  relationship for tree-ring cellulose is 8.1 and thus closely mirrors that of the global meteoric water line (the GMWL is here derived from the modelled precipitation isotope data), reflecting the dominance of isotope fractionations driving spatial variation in the signals of  $\delta^2\text{H}_{\text{P}}$

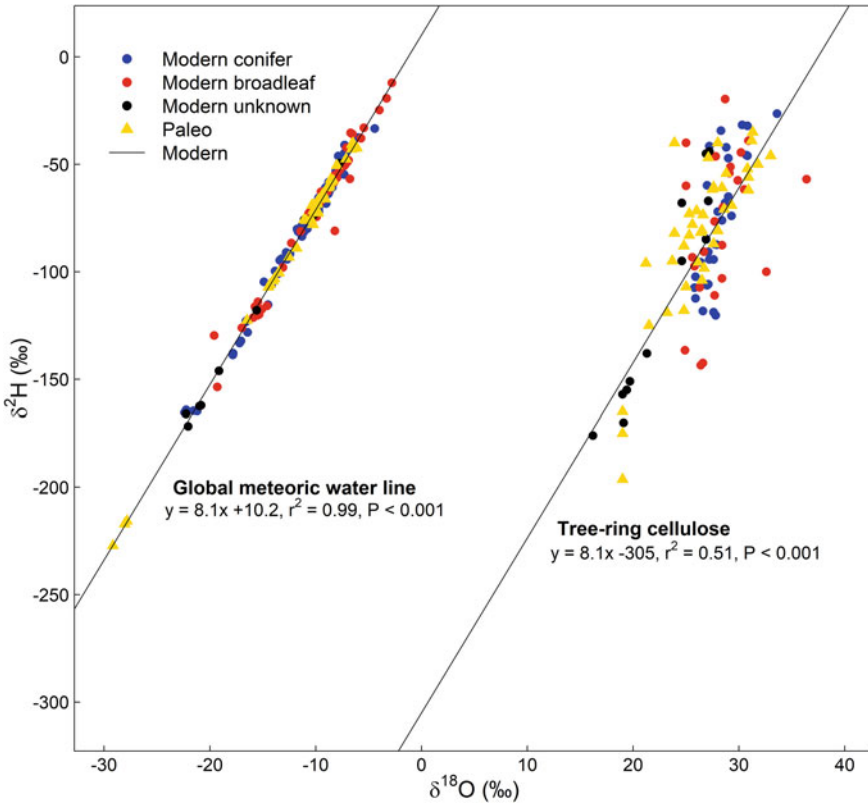


**Fig. 11.4** Global relationships between  $\delta^{18}\text{O}$  and  $\delta^2\text{H}$  values (both VSMOW) for precipitation (modelled) and tree-ring cellulose. Mean values of ca. 180 sites are given for precipitation and of ca. 110 sites for tree-ring cellulose (Table S1). Paleo sites (< 1000 years before 2000 AD) were excluded from the regression line due to climatic and sampling uncertainties. Isotope data of precipitation follow the typical equation of the global meteoric water line (GMWL). Isotope data of tree-ring cellulose follow the same slope as the GMWL. Unknown = tree species could not be identified

and  $\delta^{18}\text{O}_\text{P}$  taken up by trees. Global  $\delta^2\text{H}$ - $\delta^{18}\text{O}$  relationships of tree-ring cellulose were not clearly influenced by broadleaf or coniferous tree species (Fig. 11.3 & 11.4) and species-effects might not play a significant role at this scale (but see species effects on the local scale below). Perhaps more importantly, variability of how  $\delta^2\text{H}$  vs  $\delta^{18}\text{O}$  diverge from this global relationship spatiotemporally and among and within species certainly has the potential to yield unique insights on climatic variability, ecohydrology and tree ecophysiology that needs further exploration.

### 11.5.2 *Paleo-Climatic $\delta^2H_{TRC}$ Applications*

Due to the strong temperature response,  $\delta^2H_{TRC}$  analyses were undertaken to provide early paleoclimate or “paleo-thermometer” proxies that could be applied to ancient wood samples (Feng and Epstein 1994; Yapp and Epstein 1977). Other studies on ancient wood material combined  $\delta^2H_{NE}$  and  $\delta^{18}O$  for the reconstruction of relative humidity (Edwards and Fritz 1986; Voelker et al. 2014a) and atmospheric circulations patterns (Feng et al. 2007). Some studies used the  $\delta^2H_{TRC}$  difference between ancient and modern wood to infer climatic changes or monsoon intensity (Boettger et al. 2003; Feng et al. 1999). Moreover,  $\delta^2H_{TRC}$  can function as a supplementary information, helping to date tree rings in wood of unknown sources (Becker et al. 1991). This is particularly important for dating of ancient wood samples, which are rarer and thus can be more difficult to cross date using conventional dendrochronological methods. The longest published  $\delta^2H_{TRC}$  record so far (over 8000 years before 1950, at 50-year resolution) was established by Feng and Epstein (1994) from bristlecone pine trees. However,  $\delta^2H_{TRC}$  was also analyzed from much older individual wood samples from the Late Glacial/Holocene (14 to 8 Ka) (Boettger et al. 2003; Edwards and Fritz 1986; Epstein 1995; Feng et al. 2007), Late Pleistocene (60 to 30 Ka) (Stojakowits et al. 2020), Early Pliocene (~4.5 Ma) (Csank et al. 2011), and Eocene (~45 Ma) (Jahren and Sternberg 2008). Despite this past work, hydrogen isotope analysis of tree rings is rarely conducted compared to the use of hydrogen isotopes from other paleo isotope archives (e.g., ice or sediment cores). Hence, novel approaches that combine  $\delta^2H_{TRC}$  with carbon and oxygen isotope analyses and other tree-ring properties at inter-annual resolution may provide promising new multi-proxy tools for understanding past climates and their impact on plant ecophysiology.

### 11.5.3 *Local $\delta^2H_{TRC}$ Pattern and Physio-Biochemical Effects*

Despite known correlations between climate variables and  $\delta^2H_{TRC}$  across large spatial scales, temporal variations in local  $\delta^2H_{TRC}$  chronologies often do not strongly correlate with local climatic changes or hydrological influences (Boettger et al. 2014; Lipp et al. 1991; Loader et al. 2008; Pendall 2000). Oxygen and hydrogen isotopes in an individual tree should theoretically be derived from the same water sources and thus be correlated (as shown in Fig. 11.4), however, only weak relationships between  $\delta^2H$  and  $\delta^{18}O$  chronologies of tree-ring cellulose have been observed on local scales (Fig. 11.5). Early research indicates that climatic information in water-derived hydrogen isotopes is potentially overwritten by physiological factors driving changes in  $\delta^2H_{TRC}$ , including differences in  $^2H$ -fractionation between autotrophic and heterotrophic tissues and metabolic pathways (Luo and Sternberg 1992; Yakir

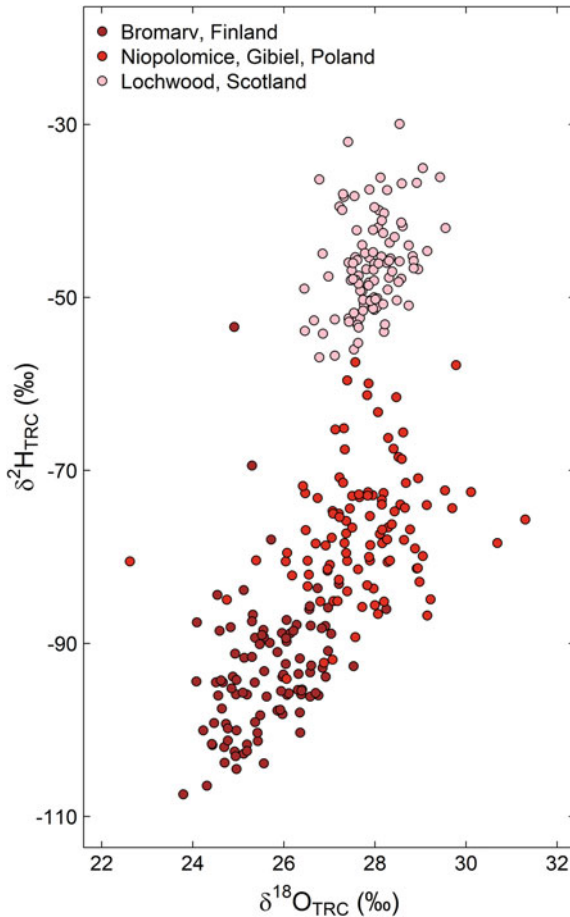


**Fig. 11.5** Local relationships between  $\delta^{18}\text{O}$  and  $\delta^2\text{H}$  chronologies of tree-ring late wood cellulose (TRC, both VSMOW) for three European *Quercus robur* forest sites (Haupt et al. 2011; Hilarvuori and Berninger 2010; Szczepanek et al. 2006). The chronologies are annually resolved for the period 1901–2003. Relationships are low for all sites ( $r^2 < 0.1$ )

and DeNiro 1990). The following text reviews a growing body of evidence documenting strong physio-biochemical isotope effects on  $\delta^2\text{H}$  of plant-derived carbohydrates that are eventually incorporated into  $\delta^2\text{H}_{\text{TRC}}$  and may explain the difference between global versus local isotopic patterns.

(1) **Maturation effect:** In Germany,  $\delta^2\text{H}_{\text{TRC}}$  of oaks was shown to increase by about 20‰ between approximately age 0 and 150, with little change thereafter (Lipp et al. 1993; Mayr 2003). We term this trend over 100+ years a “maturation effect” because the juvenile stage for many oaks, biologically, usually only lasts up to about 40–50 years and sometimes much less if trees are from sprout rather than seed origin. This increase in  $\delta^2\text{H}_{\text{TRC}}$  with age is the opposite of that which would be expected



if rooting depths increased with development, leading to them tapping deeper soil water sources with more negative  $\delta^2\text{H}_\text{S}$  values. Changes in  $\delta^2\text{H}_\text{TRC}$  values with tree age might be related to an age-related increase in the availability or use of non-structural carbohydrates for growth (i.e. fresh assimilates vs. carbon storage) and/or increased phloem transport distance between canopy leaf area and the stem base (i.e. tree height) where wood samples are typically extracted for isotopic analyses. The aforementioned ideas should be tested with species that differ in growth rate and maturation as only a few  $\delta^2\text{H}_\text{TRC}$  studies have investigated the maturation effect so far (Arosio et al. 2020).

(2) **Intra-annual effects:** An early  $\delta^2\text{H}_\text{TRC}$  study investigated intra-annual variation (Epstein and Yapp 1976) and documented that earlywood was  $^2\text{H}$ -enriched by 7 to 52‰ compared to latewood within the same tree and year, with some exceptions;  $^2\text{H}$ -enriched earlywood was confirmed by other studies (Kimak 2015; Mayr 2003). Higher-resolution intra-annual measurements in fossil (*Metasequoia sp.*) or in modern (*Quercus crispula*, *Pinus radiata*) wood demonstrated that cellulose is most  $^2\text{H}$ -depleted in the center of an annual tree-ring, while the start and end are more  $^2\text{H}$ -enriched (Jahren and Sternberg 2008; Nabeshima et al. 2018; Wilson and Grinsted 1978). Leaf cellulose of two deciduous trees in Switzerland were also observed to be more  $^2\text{H}$ -enriched in the early than in the late growing season, while the opposite pattern was observed for an evergreen conifer (Kimak et al. 2015). The drivers of these intra-annual effects are not simply explained by changes in source water or environmental conditions. Winter/spring source water from temperate and boreal zones is  $^2\text{H}$ -depleted, which is in contrast to higher  $\delta^2\text{H}_\text{TRC}$  values in wood formed at the growing season, assuming much of the water used by trees during this time are from dormant season precipitation recharge of soil moisture. The VPD-driven leaf water  $^2\text{H}$ -enrichment would also be lesser during the early growing season than in summer, which is again in contrast to the observed intra-annual  $\delta^2\text{H}_\text{NE}$  pattern in leaf and tree-ring cellulose. It is likely, the intra-annual effects are caused by a higher relative use of  $^2\text{H}$ -enriched storage pools for the formation of earlywood and consequently  $^2\text{H}$ -depleted photosynthetic assimilates for the formation of late wood (Lehmann et al. 2021; Vitali et al. 2022). Clearly, the drivers of intra-annual isotope variation needs further exploration to provide better insights on seasonal changes in plant-water relations and physiology.

(3) **Growth effects:** Change in biomass productivity, as indicated by various metrics of tree-ring growth, have often been used as primary indicator of plant physiological performance under changing climatic conditions. Here we combined growth and  $\delta^2\text{H}_\text{TRC}$  data of bur oaks (*Quercus macrocarpa* Michx.) at three North American sites with a range in environmental conditions (Voelker et al. 2014a, b). Using the Roden model (Eq. 11.4), we calculated the expected  $\delta^2\text{H}_\text{TRC}$  for at least fifteen years at each of those three sites and then subtracted these modeled values from the observed  $\delta^2\text{H}_\text{TRC}$  values and plotted these residuals versus growth rates as calculated by Voelker et al. (2014b), which yielded a significant negative relationship ( $r^2 = 0.30$ ; Fig. 11.6). For the model, we assumed constant  $\delta^2\text{H}_\text{S}$  values for each year, as the species is known to be very deeply rooted, and  $\delta^2\text{H}$  values of vapor to be in equilibrium with those

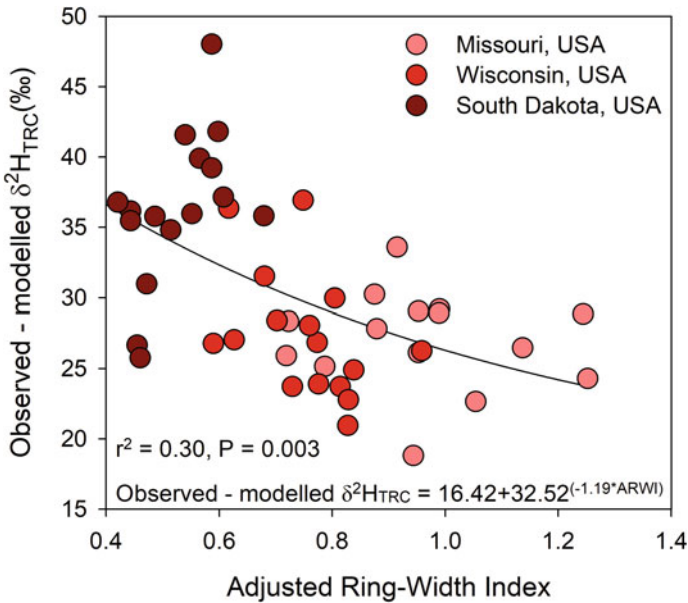


**Fig. 11.6** The  $\delta^2\text{H}$  differences between observed and modeled tree-ring cellulose ( $\delta^2\text{H}_{\text{TRC}}$ , VSMOW) following (Voelker et al. 2014a), plotted against adjusted growth rate index values following (Voelker et al. 2014b). Each data point represents a cross-dated tree-ring year within a site pooled across > 10 trees of bur oak (*Quercus macrocarpa*). The three sites were sampled across continental gradients in temperature and humidity. The relationships within sites are not significant ( $P > 0.05$ ), which likely reflects a lack of data for changes in precipitation  $\delta^2\text{H}$  across years. The significant relationship across sites supports the contention of Cormier et al. (2018) that constraints on metabolic rates can increase  $\delta^2\text{H}$

of source water. If the Roden model would have accounted for all  $\delta^2\text{H}_{\text{TRC}}$  variation, then there should be no offset and no trend in data shown. There are two possibilities explaining the trend. The first is that the modelled  $\delta^2\text{H}_\text{S}$  used in the Roden model were increasingly underestimated across regions with slower growth rates, which is unlikely, because the slower growth rates arise from a complex combination of climatic phenomena that would not have provided such shifts in modeled  $\delta^2\text{H}_\text{S}$  values. The second explanation for this trend is that low growth rates are inherently associated with greater  $^2\text{H}$ -fractionation, which correspond to how slow-growing oak trees used a greater proportion of stored carbohydrates that were  $^2\text{H}$ -enriched. To some extent this would be expected, particularly in oak trees, because their earlywood vessels are largely formed early in the spring (i.e. before leaf expansion is complete) from stored carbohydrates and as oaks grow more slowly, a larger proportion of the tree-ring tissue in any given year is earlywood vessels (Voelker et al. 2012). Figure 11.6 demonstrates that correlations were weak within sites, which would be expected given a lack of year-specific knowledge of water  $\delta^2\text{H}$  values to plug into the Roden model. Importantly, the significant relationship across sites provides the first tree-ring based support for the contention of Cormier et al. (2018) that constraints on

metabolic rates can increase  $\delta^2\text{H}$  in plant compounds. Besides, a recent publication suggest the use of carbon storage under stress conditions by observing a negative relationship between  $\delta^2\text{H}_{\text{TRC}}$  values and tree-ring width chronologies on four sites in Europe and Asia, where growth is limited by precipitation or light (Lehmann et al. 2021). However, on a site where temperature was the growth-limiting factor, the relationship between  $\delta^2\text{H}_{\text{TRC}}$  and TRW was slightly positive. Thus, further studies are needed to determine the driving factors of  $^2\text{H}$ -fractionations related to annual growth (Vitali et al. 2022).

(4) **Herbaceous tissue effects:** Tissue-specific  $\delta^2\text{H}_{\text{NE}}$  effects represent important physiological processes, but have rarely been analyzed in trees (e.g. stem vs. root cellulose, Roden and Ehleringer 1999). We thus focused on  $\delta^2\text{H}_{\text{NE}}$  reports working with herbaceous plant tissues and assume that this knowledge is helpful to understand tree physiological responses. Sanchez-Bragado et al. (2019) documented the lowest  $\delta^2\text{H}_{\text{NE}}$  values in plant assimilates of autotrophic flag leaf tissues of wheat, intermediate  $\delta^2\text{H}_{\text{NE}}$  values in semi-autotrophic ears, and highest  $\delta^2\text{H}_{\text{NE}}$  values in heterotrophic roots and grain tissues. These results indicate the importance of the photosynthetic reactions causing  $^2\text{H}$ -depleted NADPH pools in autotrophic tissues. The findings are supported by  $\delta^2\text{H}_{\text{NE}}$  responses of leaf cellulose to light intensity and  $\text{CO}_2$  concentrations (Cormier et al. 2018),  $\delta^2\text{H}_{\text{NE}}$  differences in leaves of different morphology between parasitic plants and their hosts (Cormier et al. 2019), leaf blade and vein tissues (Kimak et al. 2015), and photosynthetic pathways (Sternberg and DeNiro 1983). These findings collectively indicate that autotrophic leaf tissues and their compounds are likely more  $^2\text{H}$ -depleted compared to all other plant tissues of trees (Ruppenthal et al. 2015). It will remain a future challenge to determine  $\delta^2\text{H}_{\text{NE}}$  values of compounds in different tree tissues and to better understand the most relevant processes leading to  $^2\text{H}$ -fractionations that occur during photosynthesis, transport of freshly assimilated sugars, and during cellulose biosynthesis in woody tissues.

(5) **Species effects:** We analyze the previously described synthesized dataset for species effects because they are under-described in the literature (but see Ziehmer et al. (2018)). Using sub-fossil wood remains from alpine locations in the European Alps, we show that  $\delta^2\text{H}_{\text{TRC}}$  is consistently 40‰ lower in the deciduous *Larix decidua* than in evergreen *Pinus cembra* across a 9000-year chronology (Fig. 11.7). Such differences might be partly driven by  $\delta^2\text{H}_\text{S}$  difference, or, on the other hand, they might indicate divergent metabolic  $^2\text{H}$ -fractionations associated with leaf formation, translocation of assimilates, and tree-ring formation (Arosio et al. 2020). To investigate this further, we corrected the  $\delta^2\text{H}_{\text{TRC}}$  value from each site in the literature data with modelled  $\delta^2\text{H}$  values of precipitation ( $\Delta^2\text{H}_{\text{TRC}}$ ). As global-scale isotope variations in precipitation water are taken into account by this correction (see Fig. 11.3),  $\Delta^2\text{H}_{\text{TRC}}$  can be compared between tree species from different sites. However, no clear  $\Delta^2\text{H}_{\text{TRC}}$  pattern were observed on a global scale (Fig. 11.8), suggesting that  $\Delta^2\text{H}_{\text{TRC}}$  variations must be related to some combination of species/genus and regional climatic differences (i.e. MAT, MAP). We further investigated the  $\Delta^2\text{H}_{\text{TRC}}$  values across genus and species, with mean values ranging strongly between  $-57$  and  $30$ ‰ and  $-19$  and

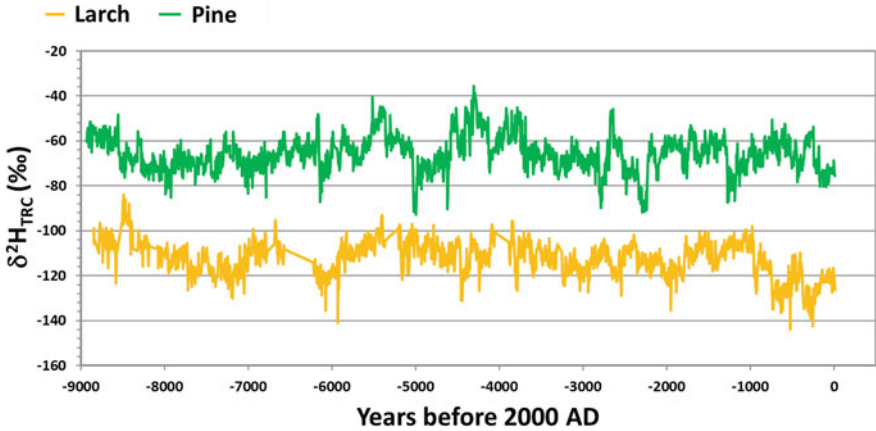


**Fig. 11.7** δ<sup>2</sup>H<sub>NE</sub> of tree-ring cellulose (δ<sup>2</sup>H<sub>TRC</sub>, VSMOW) for deciduous *Larix decidua* and ever-green *Pinus cembra* over the course of 9000 years in 5-year resolution. These records were established on subfossil wood remains based on 201 trees of the Eastern Alpine Conifer Chronology (EACC) established by the Department of Geography of the University of Innsbruck, where these samples has been calendar-dated (Nicolussi et al. 2009)

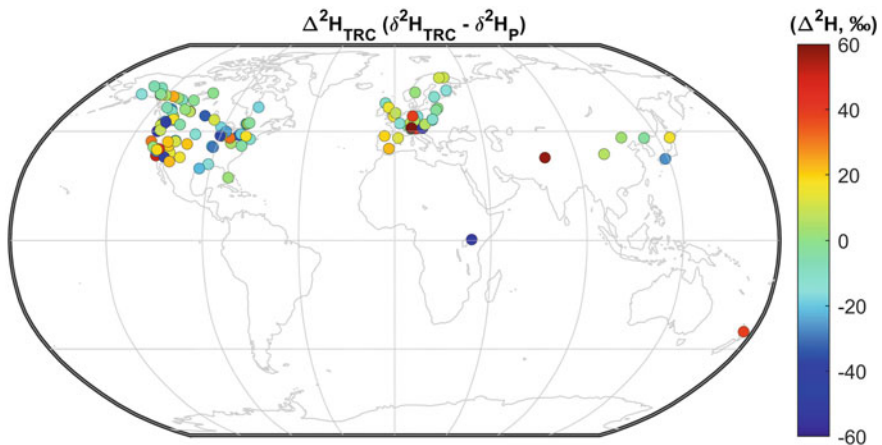


**Fig. 11.8** Global map for δ<sup>2</sup>H of tree-ring cellulose corrected for δ<sup>2</sup>H of precipitation (Δ<sup>2</sup>H<sub>TRC</sub>, VSMOW, circles) for ca. 140 sites derived from literature data (Table S1). Paleo sites (< 1000 years before 2000 AD) are not shown due to climatic and sampling uncertainties

34.5%, respectively (Fig. 11.9). Δ<sup>2</sup>H<sub>TRC</sub> values were significantly different for some genera ( $P < 0.001$ ) and species ( $P \leq 0.02$ ), showing that taxon-specific information is likely imprinted on the <sup>2</sup>H-fractionations in mature trees. Interestingly, we found that Δ<sup>2</sup>H<sub>TRC</sub> values at the genus level were co-influenced by MAP ( $P \leq 0.02$ , ANCOVA), indicating that regional climate conditions at a given site, likely a combination of precipitation and strongly co-varying relative humidity, also contributes to variation

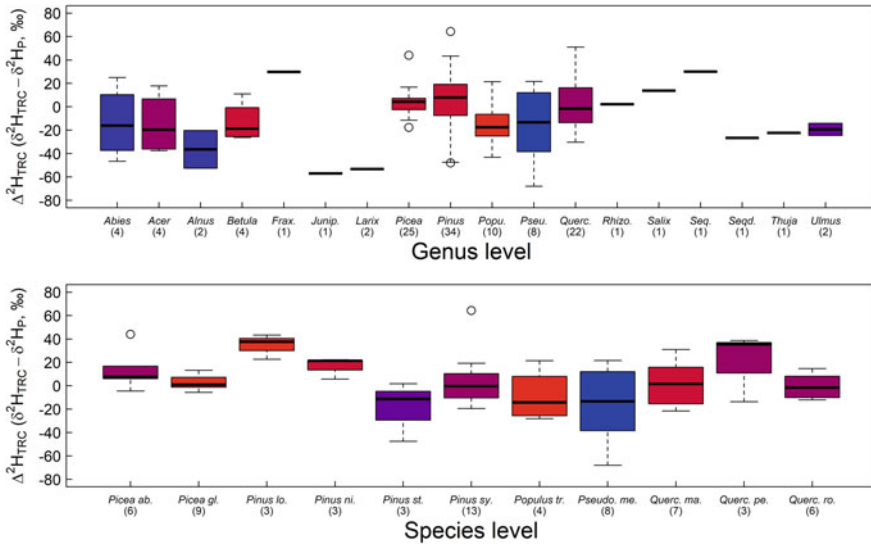


**Fig. 11.9** Variations in  $\delta^2\text{H}$  of tree-ring cellulose corrected for  $\delta^2\text{H}$  of precipitation ( $\Delta^2\text{H}_{\text{TRC}}$ , VSMOW) for species and genus level across different sites on a global scale. For genus, the number of sites strongly varies ( $n = 1$  to 34, given in parenthesis). For species, a minimum of three sites were considered ( $n = 3$  to 13). The color-coding indicates the average mean annual precipitation (MAP) for each species and genus varying between  $< 500$  mm (red) and  $> 1500$  mm (blue). Paleo studies were excluded ( $< 1000$  years before 2000 AD; Table S1). Abbreviations: Junip. = Juniperus, Pseu./Pseudo. = Pseudotsuga, Querc. = Quercus, Rhizo. = Rhizophora, Popu. = Populus, Seq. = Sequoia, Seqd. = Sequoiadendron, ab. = abies, gl. = glauca, lo. = longaeava, ni. = nigra, st. = strobis, sy. = sylvestris, tr. = tremuloides, me. = menziesii, ma. = macrocarpa, pe. = petraea, ro. = robur

in  $^2\text{H}$ -fractionations. The influence of water availability on  $\Delta^2\text{H}_{\text{TRC}}$  would make sense, since growth sometimes depends on carbon storage and thus on  $^2\text{H}$ -enriched heterotrophic starch rather than on  $^2\text{H}$ -depleted sugars from recent photoassimilates, particularly in extreme dry years or during defoliation events (Vitali et al. 2022). Thus, it is likely that the highly negative and positive  $\Delta^2\text{H}_{\text{TRC}}$  variations at the species and genus levels mainly reflect plastic  $^2\text{H}$ -fractionations related to the carbohydrate metabolism in trees. In this sense, broad surveys of  $\delta^2\text{H}_{\text{NE}}$  values of non-structural carbohydrates and cellulose in different tree species might be helpful to disentangle the drivers of  $^2\text{H}$ -fractionations and potential phylogenetic effects.

### 11.6 Conclusions

Our chapter reveals that we are at the beginning of a new phase of understanding the hydrogen isotopic signals in trees. Overall, deriving robust inter-annual climate signals from  $\delta^2\text{H}_{\text{TRC}}$  is currently challenging, but  $\delta^2\text{H}_{\text{TRC}}$  may retain important low-frequency climate variation and allow for additional and complementary inferences on tree physiology and carbon metabolism when paired with other isotopic signals

and tree-ring growth. To maximize this potential the  $\delta^2\text{H}_{\text{TRC}}$  signals need further study and calibration. Toward this end, the foremost need is to investigate the  $^2\text{H}$ -fractionation processes between water, photosynthetic assimilates, carbon storage, and cellulose at the leaf and stem level. More specifically, studies should be carefully designed to address how this varies with abiotic or biotic stressors, among species and genus, and across diel and seasonal cycles. Second, we need to develop new isotope modeling approaches that can better isolate hydrological  $^2\text{H}$ -fractionations (leaf water, source water) from the proportionally larger biochemical  $^2\text{H}$ -fractionations. Third, the new knowledge on  $^2\text{H}$ -fractionation processes need to be applied to  $\delta^2\text{H}_{\text{TRC}}$  chronologies to assess the potential for obtaining improved multi-proxy climate reconstructions or improved understanding of changes in ecophysiology in response to climate variability or other environmental influences. Great progress has been made in understanding and calibrating the  $\delta^2\text{H}_{\text{TRC}}$  signal. Continuing advancements in  $^2\text{H}$ -processing that allow for rapid determinations of  $\delta^2\text{H}_{\text{NE}}$ , a growing constellation of ancillary tree-ring metrics, and advances in knowledge on post-photosynthetic  $^2\text{H}$ -fractionations together foretell that applications of  $\delta^2\text{H}_{\text{TRC}}$  will be increasingly used in dendroclimatology and forest ecophysiology.

**Acknowledgements** We thank Neil Loader (Swansea University) and Christoph Mayr (Friedrich Alexander University Erlangen-Nuremberg) for reviewing this book chapter. We also thank Kurt Nicolussi for the organization and cross-dating of the EACC wood material. Steve Voelker was supported by US-NSF Award #1903721. Marco M. Lehmann was supported by the SNSF Ambizione grant (No. 179978).

## References

- Alexander WJ, Mitchell RL (1949) Rapid measurement of cellulose viscosity by the nitration method. *Anal Chem* 21:1497–1500
- Allen ST, Kirchner JW, Braun S, Siegwolf RTW, Goldsmith GR (2019) Seasonal origins of soil water used by trees. *Hydrol Earth Syst Sci* 23:1199–1210
- Allison GB, Barnes CJ, Hughes MW (1983) The distribution of deuterium and  $^{18}\text{O}$  in dry soils. 2. Experimental. *J Hydrol* 64:377–397
- Anhauser T, Greule M, Keppler F (2017) Stable hydrogen isotope values of lignin methoxyl groups of four tree species across Germany and their implication for temperature reconstruction. *Sci Total Environ* 579:263–271
- Arosio T, Ziehmer-Wenz MM, Nicolussi K, Schlüchter C, Leuenberger M (2020) Alpine Holocene tree-ring dataset: age-related trends in the stable isotopes of cellulose show species-specific patterns. *Biogeosci* 17:4871–4882. <https://doi.org/10.5194/bg-17-4871-2020>
- Becker B, Kromer B, Trimborn P (1991) A stable isotope tree-ring timescale of the late glacial holocene boundary. *Nature* 353:647–649
- Betson TR, Augusti A, Schleucher J (2006) Quantification of deuterium isotopomers of tree-ring cellulose using nuclear magnetic resonance. *Anal Chem* 78:8406–8411
- Boettger T, Haupt M, Friedrich M, Waterhouse JS (2014) Reduced climate sensitivity of carbon, oxygen and hydrogen stable isotope ratios in tree-ring cellulose of silver fir (*Abies alba* Mill.) influenced by background  $\text{SO}_2$  in Franconia (Germany, Central Europe). *Environ Pollut* 185:281–294

- Boettger T, Haupt M, Knoller K, Weise SM, Waterhouse JS, Rinne KT, Loader NJ, Somninen E, Jungner H, Masson-Delmotte V, Stievenard M, Guillemain MT, Pierre M, Pazdur A, Leuenberger M, Filot M, Saurer M, Reynolds CE, Helle G, Schleser GH (2007) Wood cellulose preparation methods and mass spectrometric analyses of  $\delta^{13}\text{C}$ ,  $\delta^{18}\text{O}$ , and nonexchangeable  $\delta^2\text{H}$  values in cellulose, sugar, and starch: an interlaboratory comparison. *Anal Chem* 79:4603–4612
- Boettger T, Hiller A, Kremenetski K (2003) Mid-Holocene warming in the northwest Kola Peninsula, Russia: northern pine-limit movement and stable isotope evidence. *Holocene* 13:403–410
- Bowen GJ, Revenaugh J (2003) Interpolating the isotopic composition of modern meteoric precipitation. *Water Resour Res* 39
- Brooks JR, Barnard HR, Coulombe R, McDonnell JJ (2010) Ecohydrologic separation of water between trees and streams in a Mediterranean climate. *Nat Geosci* 3:100–104
- Cormier MA, Werner RA, Leuenberger MC, Kahmen A (2019)  $^2\text{H}$ -enrichment of cellulose and n-alkanes in heterotrophic plants. *Oecologia* 189:365–373
- Cormier MA, Werner RA, Sauer PE, Grocke DR, Leuenberger MC, Wieloch T, Schleucher J, Kahmen A (2018)  $^2\text{H}$ -fractionations during the biosynthesis of carbohydrates and lipids imprint a metabolic signal on the  $\delta^2\text{H}$  values of plant organic compounds. *New Phytol* 218:479–491
- Craig H, Gordon LI (1965) Deuterium and oxygen 18 variations in the ocean and marine atmosphere. In: Tongiorgi E (ed) *Proceedings of a conference on stable isotopes in oceanographic studies and paleotemperatures*. Lischi and Figli, Spoleto, Italy, pp 9–130
- Csank AZ, Patterson WP, Eglinton BM, Rybczynski N, Basinger JF (2011) Climate variability in the Early Pliocene Arctic: Annually resolved evidence from stable isotope values of sub-fossil wood, Ellesmere Island Canada. *Palaeogeogr Palaeoclimatol Palaeoecol* 308:339–349
- Dansgaard W (1964) Stable isotopes in precipitation. *Tellus* 16:436–468
- Dawson TE, Mambelli S, Plamboeck AH, Templer PH, Tu KP (2002) Stable isotopes in plant ecology. *Annu Rev Ecol Syst* 33:507–559
- de la Ossa MAF, Lopez-Lopez M, Torre M, Garcia-Ruiz C (2011) Analytical techniques in the study of highly-nitrated nitrocellulose. *Trac-Trends Anal Chem* 30:1740–1755
- Doner LW, Ajie HO, Sternberg LDL, Milburn JM, Deniro MJ, Hicks KB (1987) Detecting sugar-beet syrups in orange juice by D/H and  $^{18}\text{O}/^{16}\text{O}$  analysis of sucrose. *J Agric Food Chem* 35:610–612
- Dongmann G, Nurnberg HW, Forstel H, Wagener K (1974) Enrichment of  $\text{H}_2^{18}\text{O}$  in leaves of transpiring plants. *Radiat Environ Biophys* 11:41–52
- Dunbar J, Schmidt HL (1984) Measurement of the  $^2\text{H}/^1\text{H}$  ratios of the carbon bound hydrogen atoms in sugars. *Fresen Z Anal Chem* 317:853–857
- Edwards TWD, Fritz P (1986) Assessing meteoric water composition and relative humidity from  $\delta^{18}\text{O}$  and  $\delta^2\text{H}$  in wood cellulose: paleoclimatic implications for southern Ontario Canada. *Appl Geochem* 1:715–723
- Epstein S (1995) The isotopic climatic records in the Alleröd-Bølling-Younger Dryas and post-Younger Dryas events. *Global Biogeochem Cycles* 9:557–563
- Epstein S, Yapp CJ (1976) Climatic implications of the D/H ratio of hydrogen in C-H groups in tree cellulose. *Earth Planet Sci Lett* 30:252–261
- Estep MF, Hoering TC (1981) Stable hydrogen isotope fractionations during autotrophic and mixotrophic growth of microalgae. *Plant Physiol* 67:474–477
- Feng XH, Cui HT, Tang KL, Conkey LE (1999) Tree-ring  $\delta\text{D}$  as an indicator of Asian monsoon intensity. *Quatern Res* 51:262–266
- Feng XH, Epstein S (1994) Climatic implications of an 8000-year hydrogen isotope time series from bristlecone pine trees. *Science* 265:1079–1081
- Feng XH, Krishnamurthy RV, Epstein S (1993) Determination of D/H ratios of nonexchangeable hydrogen in cellulose: A method based on the cellulose-water exchange reaction. *Geochim Cosmochim Acta* 57:4249–4256
- Feng XH, Reddington AL, Faiia AM, Posmentier ES, Shu Y, Xu XM (2007) The changes in North American atmospheric circulation patterns indicated by wood cellulose. *Geology* 35:163–166
- Fick SE, Hijmans RJ (2017) WorldClim 2: new 1-km spatial resolution climate surfaces for global land areas. *Int J Climatol* 37:4302–4315

- Filot MS, Leuenberger M, Pazdur A, Boettger T (2006) Rapid online equilibration method to determine the D/H ratios of non-exchangeable hydrogen in cellulose. *Rapid Commun Mass Spectrom* 20:3337–3344
- Gehre M, Renpenning J, Gilevska T, Qi HP, Coplen TB, Meijer HAJ, Brand WA, Schimmelmann A (2015) On-line hydrogen-isotope measurements of organic samples using elemental chromium: an extension for high temperature elemental-analyzer techniques. *Anal Chem* 87:5198–5205
- Gerlein-Safdi C, Gauthier PPG, Caylor KK (2018) Dew-induced transpiration suppression impacts the water and isotope balances of *Colocasia* leaves. *Oecologia* 187:1041–1051
- Gori Y, Wehrens R, Greule M, Keppler F, Ziller L, La Porta N, Camin F (2013) Carbon, hydrogen and oxygen stable isotope ratios of whole wood, cellulose and lignin methoxyl groups of *Picea abies* as climate proxies. *Rapid Commun Mass Spectrom* 27:265–275
- Gray J, Song SJ (1984) Climatic implications of the natural variations of D/H ratios in tree ring cellulose. *Earth Planet Sci Lett* 70:129–138
- Greule M, Mosandl A, Hamilton JTG, Keppler F (2008) A rapid and precise method for determination of D/H ratios of plant methoxyl groups. *Rapid Commun Mass Spectrom* 22:3983–3988
- Grinsted MJ, Wilson AT (1979) Hydrogen isotopic chemistry of cellulose and other organic material of geochemical interest. *NZ J Sci* 22:281–287
- Haupt M, Weigl M, Grabner M, Boettger T (2011) A 400-year reconstruction of July relative air humidity for the Vienna region (eastern Austria) based on carbon and oxygen stable isotope ratios in tree-ring latewood cellulose of oaks (*Quercus petraea* Matt. Liebl.). *Clim Change* 105:243–262
- Hilasvuori E, Berninger F (2010) Dependence of tree ring stable isotope abundances and ring width on climate in Finnish oak. *Tree Physiol* 30:636–647
- Horita J, Wesolowski DJ (1994) Liquid-vapor fractionation of oxygen and hydrogen isotopes of water from the freezing to the critical temperature. *Geochim Cosmochim Acta* 58:3425–3437
- Jahren AH, Sternberg LSL (2008) Annual patterns within tree rings of the Arctic middle Eocene (ca. 45 Ma): Isotopic signatures of precipitation, relative humidity, and deciduousness. *Geology* 36:99–102
- Kahmen A, Hoffmann B, Schefuß E, Arndt SK, Cernusak LA, West JB, Sachse D (2013) Leaf water deuterium enrichment shapes leaf wax n-alkane  $\delta D$  values of angiosperm plants II: Observational evidence and global implications. *Geochim Cosmochim Acta* 111:50–63
- Kimak A (2015) Dissertation: tracing physiological processes of long living tree species and their response on climate change using triple isotope analyses. University of Bern, Climate and Environmental Physics
- Kimak A, Kern Z, Leuenberger M (2015) Qualitative distinction of autotrophic and heterotrophic processes at the leaf level by means of triple stable isotope (C-O-H) patterns. *Front Plant Sci* 6:1008
- Knowles JR, Albery WJ (1977) Perfection in enzyme catalysis: the energetics of triosephosphate isomerase. *Acc Chem Res* 10:105–111
- Lehmann MM, Goldsmith GR, Schmid L, Gessler A, Saurer M, Siegwolf RTW (2018) The effect of  $^{18}O$ -labelled water vapour on the oxygen isotope ratio of water and assimilates in plants at high humidity. *New Phytol* 217:105–116
- Lehmann MM, Vitali V, Schuler P, Leuenberger M, Saurer M (2021) More than climate: Hydrogen isotope ratios in tree rings as novel plant physiological indicator for stress conditions. *Dendrochronologia* 65:125788. <https://doi.org/10.1016/j.dendro.2020.125788>
- Libby LM, Pandolfi LJ, Payton PH, Marshall J, Becker B, Giertz-Siebenlist V (1976) Isotopic tree thermometers. *Nature* 261:284–288
- Lin G, Sternberg L (1993) Hydrogen isotopic fractionation by plant roots during water uptake in coastal wetland plants. In: Ehleringer J, Hall AE, Farquhar GD (eds) Stable isotopes and plant carbon-water relations. Academic Press, pp 497–510
- Lipp J, Trimborn P, Fritz P, Moser H, Becker B, Frenzel B (1991) Stable isotopes in tree ring cellulose and climatic change. *Tellus B Chem Phys Meteorol* 43:322–330



- Lipp J, Trimborn P, Graf W, Becker B (1993) Climatic significance of D/H ratios in the cellulose of late wood in tree rings from spruce (*Picea abies* L.). In: Isotope techniques in the study of past and current environmental change in the hydrosphere and atmosphere. IAEA, Vienna, pp 395–405
- Loader NJ, Santillo PM, Woodman-Ralph JP, Rolfe JE, Hall MA, Gagen M, Robertson I, Wilson R, Froyd CA, McCarroll D (2008) Multiple stable isotopes from oak trees in southwestern Scotland and the potential for stable isotope dendroclimatology in maritime climatic regions. *Chem Geol* 252:62–71
- Loader NJ, Street-Perrott FA, Daley TJ, Hughes PDM, Kimak A, Levanic T, Mallon G, Mauquoy D, Robertson I, Roland TP, van Bellen S, Ziehmer MM, Leuenberger M (2015) Simultaneous determination of stable carbon, oxygen, and hydrogen isotopes in cellulose. *Anal Chem* 87:376–380
- Luo YH, Sternberg L, Suda S, Kumazawa S, Mitsui A (1991) Extremely low D/H ratios of photoproduced hydrogen by cyanobacteria. *Plant Cell Physiol* 32:897–900
- Luo YH, Sternberg LDL (1992) Hydrogen and oxygen isotopic fractionation during heterotrophic cellulose synthesis. *J Exp Bot* 43:47–50
- Mayr C (2003) Dissertation: Möglichkeiten der Klimarekonstruktion im Holozän mit  $\delta^{13}\text{C}$ - und  $\delta^2\text{H}$ -Werten von Baum-Jahringen auf der Basis von Klimakammerversuchen und Rezentstudien. GSF-Forschungszentrum für Umwelt und Gesundheit
- Merlivat L (1978) Molecular diffusivities of  $\text{H}_2^{16}\text{O}$ ,  $\text{HD}^{16}\text{O}$ , and  $\text{H}_2^{18}\text{O}$  in gases. *J Chem Phys* 69:2864–2871
- Nabeshima E, Nakatsuka T, Kagawa A, Hiura T, Funada R (2018) Seasonal changes of  $\delta\text{D}$  and  $\delta^{18}\text{O}$  in tree-ring cellulose of *Quercus crispula* suggest a change in post-photosynthetic processes during earlywood growth. *Tree Physiol* 38:1829–1840
- Newberry SL, Kahmen A, Dennis P, Grant A (2015) n-Alkane biosynthetic hydrogen isotope fractionation is not constant throughout the growing season in the riparian tree *Salix viminalis*. *Geochim Cosmochim Acta* 165:75–85
- Nicolussi K, Kaufmann M, Melvin TM, van der Plicht J, Schiessling P, Thurner A (2009) A 9111 year long conifer tree-ring chronology for the European Alps: a base for environmental and climatic investigations. *Holocene* 19:909–920
- Pendall E (2000) Influence of precipitation seasonality on pinon pine cellulose  $\delta\text{D}$  values. *Glob Change Biol* 6:287–301
- Poage MA, Chamberlain CP (2001) Empirical relationships between elevation and the stable isotope composition of precipitation and surface waters: Considerations for studies of paleoelevation change. *Am J Sci* 301:1–15
- Qi HP, Coplen TB (2011) Investigation of preparation techniques for  $\delta^2\text{H}$  analysis of keratin materials and a proposed analytical protocol. *Rapid Commun Mass Spectrom* 25:2209–2222
- Qi HP, Coplen TB, Jordan JA (2016) Three whole-wood isotopic reference materials, USGS54, USGS55, and USGS56, for  $\delta^2\text{H}$ ,  $\delta^{18}\text{O}$ ,  $\delta^{13}\text{C}$ , and  $\delta^{15}\text{N}$ . *Chem Geol* 442:47–53
- Roden J, Kahmen A, Buchmann N, Siegwolf R (2015) The enigma of effective path length for  $^{18}\text{O}$  enrichment in leaf water of conifers. *Plant Cell Environ* 38:2551–2565
- Roden JS, Ehleringer JR (1999) Hydrogen and oxygen isotope ratios of tree-ring cellulose for riparian trees grown long-term under hydroponically controlled environments. *Oecologia* 121:467–477
- Roden JS, Ehleringer JR (2000) Hydrogen and oxygen isotope ratios of tree ring cellulose for field-grown riparian trees. *Oecologia* 123:481–489
- Roden JS, Lin GG, Ehleringer JR (2000) A mechanistic model for interpretation of hydrogen and oxygen isotope ratios in tree-ring cellulose. *Geochim Cosmochim Acta* 64:21–35
- Ruppenthal M, Oelmann Y, del Valle HF, Wilcke W (2015) Stable isotope ratios of nonexchangeable hydrogen in organic matter of soils and plants along a 2100-km climosequence in Argentina: New insights into soil organic matter sources and transformations? *Geochim Cosmochim Acta* 152:54–71

- Sachse D, Billault I, Bowen GJ, Chikaraishi Y, Dawson TE, Feakins SJ, Freeman KH, Magill CR, McInerney FA, van der Meer MTJ, Polissar P, Robins RJ, Sachs JP, Schmidt HL, Sessions AL, White JWC, West JB, Kahmen A (2012) Molecular paleohydrology: interpreting the hydrogen-isotopic composition of lipid biomarkers from photosynthesizing organisms. *Annu Rev Earth Planet Sci* 40:221–249
- Sanchez-Bragado R, Serret MD, Marimon RM, Bort J, Araus JL (2019) The hydrogen isotope composition  $\delta^2\text{H}$  reflects plant performance. *Plant Physiol* 180:793–812
- Sauer PE, Schimmelmann A, Sessions AL, Topalov K (2009) Simplified batch equilibration for D/H determination of non-exchangeable hydrogen in solid organic material. *Rapid Commun Mass Spectrom* 23:949–956
- Saurer M, Kress A, Leuenberger M, Rinne KT, Treydte KS, Siegwolf RTW (2012) Influence of atmospheric circulation patterns on the oxygen isotope ratio of tree rings in the Alpine region. *J Geophys Res Atmos* 117:D05118
- Schiegl WE (1974) Climatic significance of deuterium abundance in growth rings of *Picea*. *Nature* 251:582–584
- Schimmelmann A (1991) Determination of the concentration and stable isotopic composition of nonexchangeable hydrogen in organic matter. *Anal Chem* 63:2456–2459
- Schleucher J, Vanderveer P, Markley JL, Sharkey TD (1999) Intramolecular deuterium distributions reveal disequilibrium of chloroplast phosphoglucose isomerase. *Plant Cell Environ* 22:525–533
- Schmidt H-L, Werner RA, Eisenreich W (2003) Systematics of  $^2\text{H}$  patterns in natural compounds and its importance for the elucidation of biosynthetic pathways. *Phytochem Rev* 2:61–85
- Schmidt HL, Werner RA, Rossmann A, Mosandl A, Schreier P (2007) Stable isotope ratio analysis in quality control of flavourings. In: Ziegler H (ed) *Flavourings : production, composition, applications, regulations*. Wiley-VCH, Weinheim, Germany, pp. 589–663
- Schmidt HL, Robins RJ, Werner RA (2015) Multi-factorial in vivo stable isotope fractionation: causes, correlations, consequences and applications. *Isot Environ Health Stud* 51:155–199
- Schuler P, Cormier MA, Werner RA, Buchmann N, Gessler A, Vitali V, Saurer M, Lehmann MM (2022) A high-temperature water vapor equilibration method to determine non-exchangeable hydrogen isotope ratios of sugar, starch and cellulose. *Plant Cell Environ* 45(1):12–22. <https://doi.org/10.1111/pce.14193>
- Sternberg L, DeNiro MJ (1983) Isotopic composition of cellulose from C<sub>3</sub>, C<sub>4</sub>, and CAM plants growing near one another. *Science* 220:947–949
- Sternberg L, Deniro MJ, Ajje H (1984) Stable hydrogen isotope ratios of saponifiable lipids and cellulose nitrate from CAM, C<sub>3</sub> and C<sub>4</sub> plants. *Phytochemistry* 23:2475–2477
- Stojakowits P, Mayr C, Lücke A, Wissel H, Hedenäs L, Lempe B, Friedmann A, Diersche V (2020) Impact of climatic extremes on Alpine ecosystems during MIS 3. *Quatern Sci Rev* 239:106333
- Szczepanek M, Pazdur A, Pawelczyk S, Bottger T, Haupt M, Halas S, Bednarz Z, Krapiec M, Szychowska-Krapiec E (2006) Hydrogen, carbon and oxygen isotopes in pine and oak tree rings from Southern Poland as climatic indicators in years 1900–2003. *Geochronometria* 25:67–76
- Vitali V, Martínez-Sancho E, Treydte K, Andreu-Hayles L, Dorado-Liñán I, Gutierrez E, Helle G, Leuenberger M, Loader NJ, Rinne-Garmston KT, Schleser GH (2022) The unknown third—Hydrogen isotopes in tree-ring cellulose across Europe. *Sci Total Environ* 813:152281. <https://doi.org/10.1016/j.scitotenv.2021.152281>
- Voelker SL, Brooks R, Meinzer FC, Roden J, Pazdur A, Pawelczyk S, Hartsough P, Snyder K, Plavcova L, Santrucek J (2014a) Reconstructing relative humidity from plant  $\delta^{18}\text{O}$  and  $\delta\text{D}$  as deuterium deviations from the global meteoric water line. *Ecol Appl* 24:960–975
- Voelker SL, Meinzer FC, Lachenbruch B, Brooks JR, Guyette RP (2014b) Drivers of radial growth and carbon isotope discrimination of bur oak (*Quercus macrocarpa* Michx.) across continental gradients in precipitation, vapour pressure deficit and irradiance. *Plant Cell Environ* 37:766–779
- Voelker SL, Noirot-Cosson PE, Stambaugh MC, McMurry ER, Meinzer FC, Lachenbruch B, Guyette RP (2012) Spring temperature responses of oaks are synchronous with North Atlantic conditions during the last deglaciation. *Ecol Monogr* 82:169–187

- Voelker SL, Wang SYS, Dawson TE, Roden JS, Still CJ, Longstaffe FJ, Ayalon A (2019) Tree-ring isotopes adjacent to Lake Superior reveal cold winter anomalies for the Great Lakes region of North America. *Scientific Reports*, no 9
- Volkman THM, Kuhnhammer K, Herbstritt B, Gessler A, Weiler M (2016) A method for in situ monitoring of the isotope composition of tree xylem water using laser spectroscopy. *Plant Cell Environ* 39:2055–2063
- Wassenaar LI, Hobson KA (2000) Improved method for determining the stable-hydrogen isotopic composition ( $\delta D$ ) of complex organic materials of environmental interest. *Environ Sci Technol* 34:2354–2360
- Wassenaar LI, Hobson KA, Sisti L (2015) An online temperature-controlled vacuum-equilibration preparation system for the measurement of  $\delta^2H$  values of non-exchangeable-H and of  $\delta^{18}O$  values in organic materials by isotope-ratio mass spectrometry. *Rapid Commun Mass Spectrom* 29:397–407
- Wilson AT, Grinsted MJ (1978) The possibilities of deriving past climate information from stable isotope studies on tree rings. In: Robinson BW (ed) *Stable isotopes in the Earth Sciences*. Science information division, New Zealand department of scientific and industrial research, pp 61–66
- Yakir D (1992) Variations in the natural abundance of oxygen-18 and deuterium in plant carbohydrates. *Plant Cell Environ* 15:1005–1020
- Yakir D, DeNiro MJ (1990) Oxygen and hydrogen isotope fractionation during cellulose metabolism in *Lemma gibba* L. *Plant Physiol* 93:325–332
- Yapp CJ, Epstein S (1977) Climatic implications of D/H ratios of meteoric water over North America (9500–22,000 B.P.) as inferred from ancient wood cellulose C-H hydrogen. *Earth Planet Sci Lett* 34:333–350
- Yapp CJ, Epstein S (1982) A reexamination of cellulose carbon-bound hydrogen  $\delta D$  measurements and some factors affecting plant-water D/H relationships. *Geochim Cosmochim Acta* 46:955–965
- Zech M, Tuthorn M, Detsch F, Rozanski K, Zech R, Zoller L, Zech W, Glaser B (2013) A 220 ka terrestrial  $\delta^{18}O$  and deuterium excess biomarker record from an eolian permafrost paleosol sequence NE-Siberia. *Chem Geol* 360:220–230
- Zhang BL, Billault I, Lo XB, Mabon F, Remaud G, Martin ML (2002) Hydrogen isotopic profile in the characterization of sugars. Influence of the metabolic pathway. *J Agric Food Chem* 50:1574–1580
- Ziegler H, Osmond CB, Stichler W, Trimborn P (1976) Hydrogen isotope discrimination in higher plants: Correlations with photosynthetic pathway and environment. *Planta* 128:85–92
- Ziehmer MM, Nicolussi K, Schluchter C, Leuenberger M (2018) Preliminary evaluation of the potential of tree-ring cellulose content as a novel supplementary proxy in dendroclimatology. *Biogeosciences* 15:1047–1064

**Open Access** This chapter is licensed under the terms of the Creative Commons Attribution 4.0 International License (<http://creativecommons.org/licenses/by/4.0/>), which permits use, sharing, adaptation, distribution and reproduction in any medium or format, as long as you give appropriate credit to the original author(s) and the source, provide a link to the Creative Commons license and indicate if changes were made.

The images or other third party material in this chapter are included in the chapter's Creative Commons license, unless indicated otherwise in a credit line to the material. If material is not included in the chapter's Creative Commons license and your intended use is not permitted by statutory regulation or exceeds the permitted use, you will need to obtain permission directly from the copyright holder.



# Chapter 12

## Nitrogen Isotopes in Tree Rings—Challenges and Prospects



Martine M. Savard and Rolf T. W. Siegwolf

**Abstract** Nutritive, but detrimental if at high levels, several nitrogen (N) forms involved in air and soil biogeochemical reactions constitute the N load trees assimilate. Although a large body of literature describes series of tree-ring N isotopes ( $\delta^{15}\text{N}$ ) as archival systems for environmental changes, several questions relative to the isotopic integrity and reproducibility of trends still linger in the dendroisotopist community. This chapter reviews the fundamentals of forest N cycling and examines trees as N receptors in their very position, at the interface between the atmosphere and pedosphere. The related scrutiny of intrinsic and extrinsic mechanisms regulating isotopic changes also underlines flaws and forces of tree-ring  $\delta^{15}\text{N}$  series as environmental indicators.

### 12.1 Introduction

Key nutrient for trees, but forming reactive molecules potentially detrimental to forest ecosystems (e.g., Etzold et al. 2020), N constitutes a central object of research in terrestrial biogeochemistry. After several decades, the substantial body of literature on N in trees reflects the complexity of N cycling through trees, and how some intrinsic and extrinsic processes remain elusive. With anthropogenic emissions of reactive N ( $\text{N}_r$ ) rising globally and driving atmosphere-pedosphere exchanges that can perturb the external terrestrial N cycle, tree-ring  $\delta^{15}\text{N}$  series may record past changes in forest-N cycling.

Studies of long tree-ring  $\delta^{15}\text{N}$  series are rare, largely because ring wood includes very low amounts of N relative to carbon, evidently making tree rings difficult for

---

M. M. Savard (✉)

Geological Survey of Canada (Natural Resources Canada), 490 de la Couronne, Québec (QC) G1 K 99, Canada

e-mail: [martinem.savard@canada.ca](mailto:martinem.savard@canada.ca)

R. T. W. Siegwolf

Swiss Federal Institute for Forest, Snow and Landscape Research WSL, Birmensdorf, Switzerland

Lab of Atmospheric Chemistry, Paul Scherrer Institute (PSI), Villigen, Switzerland

© The Author(s) 2022

R. T. W. Siegwolf et al. (eds.), *Stable Isotopes in Tree Rings*, Tree Physiology 8,  
[https://doi.org/10.1007/978-3-030-92698-4\\_12](https://doi.org/10.1007/978-3-030-92698-4_12)

361

isotopic determination. Additionally, N translocates between trunk rings, dampening environmental isotopic effects in time series. Nevertheless, several studies report  $\delta^{15}\text{N}$  trends interpreted in relations to changes in soil and air conditions.

How does N assimilation in non  $\text{N}_2$ -fixing trees operate? Do trees react to changes in air and soil  $\text{N}_r$  contents? Can tree-ring  $\delta^{15}\text{N}$  series help understand environmental changes? The purpose of this review primarily consists in scrutinizing the current understanding of mechanisms responsible for determining  $\delta^{15}\text{N}$  values in tree rings, appraising the type of information  $\delta^{15}\text{N}$  series can provide, and synthesizing the knowledge gaps of this research domain.

## 12.2 Sample Preparation and Analytical Procedures

The habitual mechanical separation of tree rings from stem samples using fine blades or microtome at the sought time resolution produces wood sub-samples for  $\delta^{15}\text{N}$  analysis. Treating these sub-samples prior to their isotopic analysis generates a debate regarding the utility of removing their mobile N (resins) to prevent producing false trends. But recent investigations suggest this type of pre-treatment does not modify significantly the final  $\delta^{15}\text{N}$  values (Elhani et al. 2005; Bukata and Kyser 2007; Couto-Vázquez and González-Prieto 2010; Caceres et al. 2011; Doucet et al. 2011; Tomlinson et al. 2014). Another observation arguing against pre-treatment is that samples from several species, for instance *Pinus ponderosa*, *Fagus grandifolia* and *Picea rubens*, show no change of concentrations after resin removal (Hart and Classen 2003; Doucet et al. 2011).

On another note, regardless of pre-treating wood samples or not, several studies have clearly shown trends of higher N concentrations in rings (and coniferous leaves) grown during sampling years, relative to concentrations in previous years. The general pattern forms an increasing trend from the heartwood-sapwood transition to the most recent ring; a physiological effect typical of N translocation. In addition, tree-ring N concentrations show poor inter-tree and inter-species coherence. These observations make N concentrations in tree rings (and dated coniferous leaves) useless in environmental research (Hart and Classen 2003; Saurer et al. 2004; Savard et al. 2009; Gerhart and McLaughlan 2014). However, this inter-ring N mobility does not seem to affect the final tree-ring  $\delta^{15}\text{N}$  values (Doucet et al. 2011).

For isotopic analysis, wood samples wrapped in tin capsules drop automatically from a carousel into an elemental analyser (EA) in continuous flow (CF) with an isotope ratio mass spectrometer (IRMS). The analytical procedure involves combustion in a reaction tube producing  $\text{N}_2\text{O}$ , followed by a reduction to  $\text{N}_2$ , which produces the analyses calibrated relative to air  $\text{N}_2$  (set at 0‰). Tree-ring wood harbors very low concentrations relative to roots or leaves (Scarascia-Mugnozza et al. 2000), and high C/N ratios, making its isotopic analysis difficult. For that reason, the EA-CF IRMS system for  $\delta^{15}\text{N}$  analysis needs close monitoring for performing complete combustion to prevent  $\text{CO}^+$  derived interferences at masses 28 and 29. A CO trap installed between ovens and GC columns helps for that step. The low N concentrations in wood

make internal standards a requirement to avoid poor analytical accuracy from low peak to background ratios (Couto-Vázquez and González-Prieto 2010). Inserting several internal wood standards in sample batches allows monitoring the external precision and accuracy of the complete laboratory procedure. Whole wood materials from three species of trees recently proposed as references may also support this essential task (Qi et al. 2016), although the  $\delta^{15}\text{N}$  range they cover is narrower ( $-2.4$  to  $+1.8\text{‰}$ ) than the natural extent in tree rings (generally between  $-10$  and  $+5\text{‰}$ ).

## 12.3 Assimilation, Storage and Fractionation of Nitrogen by Trees

Numerous tree-ring studies dealing with natural  $\delta^{15}\text{N}$  values or  $^{15}\text{N}$ -labelled N assume that uptake of soil inorganic N dominates the N assimilated in stems of non  $\text{N}_2$ -fixing trees. However, other means such as soil organic N assimilation and foliar uptake of various atmospheric N forms may significantly contribute to the N loads commonly characterized for  $\delta^{15}\text{N}$  values (Fig. 12.1). This section discusses the knowledge gains from controlled experiments, studies under natural conditions, recent developments in understanding the ultimate source and pathways of N to tree rings, and the role of N remobilization in determining the tree-ring  $\delta^{15}\text{N}$  values.

### 12.3.1 Nitrogen through Foliage

Many studies reveal that soil fertilization has direct impacts on foliar N characteristics, however, leaves also assimilate N (e.g., Gebauer and Schulze 1991; Arain et al. 2006; Pardo et al. 2007; Vizoso et al. 2008; Balster et al. 2009; Averill and Finzi 2011). Similarly, articles specifically addressing canopy functions report operational foliar uptake from air for all atmospheric N forms (Garten and Hanson 1990; Rennenberg and Gessler 1999; Krupa 2003; Sparks et al. 2003; Vallano and Sparks 2007; Chaparro-Suarez et al. 2011). In other words, it is widely accepted now that the foliar N loads come from soil as well as from air (e.g., Vallano and Sparks 2013). For its nutritive functions, leaf N plays a crucial role in enhancing activities of Rubisco, the proteins of photosynthesis (Warren et al. 2003; Wright et al. 2004). However, higher atmospheric N availability does not always translate into higher growth rates of stems. The crucial point for the present chapter lies with estimating the atmospheric foliar N contribution to the loads in stems of deciduous and coniferous trees, as atmospheric N transferred from leaves to stems may have a direct impact on the tree-ring  $\delta^{15}\text{N}$  series.

Atmospheric  $\text{N}_r$ -forms include N in ammonia gases ( $\text{NH}_4^+$ ,  $\text{NH}_3$ ), oxides ( $\text{NO}_3^-$ ,  $\text{NO}_2$ ,  $\text{NO}$ ), nitric acid ( $\text{HNO}_3$ ), and organic compounds (amino acids, peroxyacetyl nitrate PAN). These N-forms get to ground through wet scavenging or dry deposition

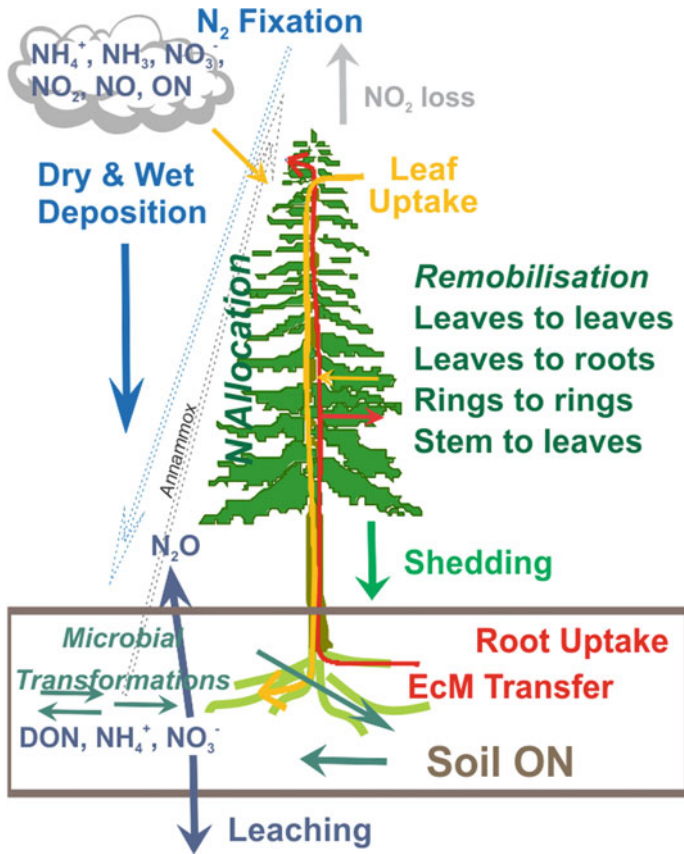


**Fig. 12.1** Representation of the forest nitrogen cycle. Processes influencing the bioavailability of N forms taken up by boreal and temperate trees are included;  $\text{NO}_2$  loss is significant mostly in wetlands and tropical settings; the tropical cycle would include  $\text{N}_2$  fixation by trees (not shown). EcM stand for ectomycorrhiza (Sect. 12.3.2)

upon contact with surfaces such as leaves. The N forms enter leaves either as wet or dry (gaseous) phases through stomata, although the liquid phases appear to pass in the foliar system more readily (Rennenberg and Gessler 1999; Harrison et al. 2000b; Krupa 2003; Choi et al. 2005; Gerhart and McLauchlan 2014). A series of enzymatic reactions transform  $\text{NH}_4^+$  and  $\text{NO}_3^-$  into amino acids, which generally enriches the reactants and depletes the products in  $^{15}\text{N}$  (e.g., Rennenberg and Gessler 1999). Once incorporated in organic compounds within leaves, N shortly resides in active and non-active parts (Millard and Grelet 2010). Experiments using  $^{15}\text{N}$ -labelled N show that the remobilized N can reach down to the root systems (Macklon et al. 1996; Rennenberg and Gessler 1999; Bazot et al. 2016).

Studies rarely quantify stem N originating from foliar uptake. In one known experimental example, the estimated proportions of N from previous-year needles

exported to support the growth of shoots vary between 10 and 37% in 5 year-old or younger coniferous trees (Millard and Grelet 2010). Otherwise, in 30-year-old spruce trees, between 8 and 22% of the annual N demands come from leaves, the range depending on the N forms selected for experiments (Harrison et al. 2000a, and references therein). Also, natural abundance of  $^{15}\text{N}$  has helped estimating foliar assimilation at 10% in 10- to 20 year-old Norway spruce trees, given that the signal of car exhaust, the single local source of anthropogenic  $\text{NO}_2$  emissions, was known to strongly deviate from the natural N sources (Ammann et al. 1999). However, in general, the precise quantification of anthropogenic N in the canopy constitutes a complex task because the isotopic signals of N in air can significantly change in space and time, and an array of emitters show overlapping  $\delta^{15}\text{N}$  ranges (e.g., Savard et al. 2017).

In deciduous specimens, the proportion of canopy N uptake used up for annual wood production appears to vary between <5 to >40% (Harrison et al. 2000b). In the case of young poplars exposed to  $\text{NO}_2$ -enriched air with low  $\delta^{15}\text{N}$  values, and grown on high and low N-supplied soils, the calculated foliar contributions were 14 and 18% of the total amount of plant N, respectively, based on  $\delta^{15}\text{N}$  measurements of plant material and the known isotopic signal of  $\text{NO}_2$  (Siegwolf et al. 2001). In another example, with labelled fertilizers applied at both the foliage and root levels of oak trees, soil N and internal storage contributed 60 and 40%, respectively, to the N of spring leaves (Bazot et al. 2016). Whereas the total autumn root N reserves included 73% from leaves and 27% from soils. At the broad scale, modeling studies reported the canopy to contribute between 3 and 16% of the total N demands for new growth in plants (Vallano and Sparks 2007, and references therein). Thus, on one hand, N in leaves comes partly from soils, and several studies clearly demonstrated partial remobilization of this N. On the other hand, the estimated contributions from leaves to the demands of trees may be more variable than the range covered in the literature because they largely depend on the atmospheric concentrations and the involved N-forms, the studied tree species, and the methodology selected for quantifying the foliar uptake/contribution.

Although trees acquire atmospheric N directly through leaves and without intermediate transformation steps as through soils before root uptake, the overall influence foliar uptake has on the tree-ring N loads is difficult to determine. To our knowledge, research efforts never estimated its contribution to stem N loads of mature trees. Accordingly, the remaining key questions regarding foliar uptake does not relate to its assessment but to the magnitude of its contribution in determining the final tree-ring  $\delta^{15}\text{N}$  values.



## 12.3.2 From Soils through Roots to the Stems

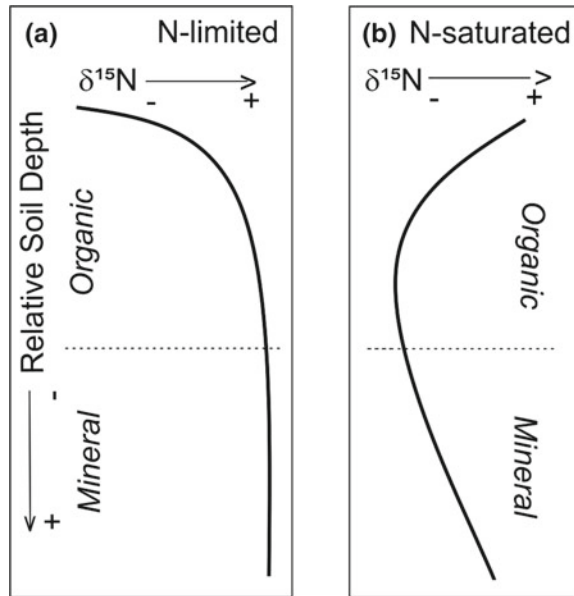
### 12.3.2.1 Soil Nitrogen Species and Processes

Dinitrogen-fixing microbes and forest organic matter represent the ultimate sources of N in soils of non-disturbed forests (Fig. 12.1). Geological N from rocks and minerals can provide a background influencing the forest N cycling and the overall  $\delta^{15}\text{N}$  values of organic soils, particularly if developed over clay-rich mineral horizons or sedimentary rocks, which generally have high  $\delta^{15}\text{N}$  values (Holloway and Dahlgren 2002; Craine et al. 2015; Houlton et al. 2018). Variability in the distribution of geological N contributes to the heterogeneity of soil N properties. Several studies also report evidence for microbial communities (fungi and bacteria) involved in mineral weathering (e.g., Courty et al. 2010).

Even though the absolute amount of N in soils is large, the dominant proportion of N is immobilized (carbon bound) in organic matter (Knicker 2004; Näsholm et al. 2009), with a small part of this matter available for nutrition (labile N or dissolved organic N—DON). The main N-rich constituents of DON, amino acids, derive from rapid hydrolysis of soil proteins (Näsholm et al. 2009). Furthermore, the soil inorganic ( $\text{NH}_4^+$  and  $\text{NO}_3^-$ ) parts, largely derived from organic matter constitute only about 1% of the total soil N (Kendall et al. 2007). Forest N demands generally exceed the inputs in bioavailable N forms, limiting the net productivity in most of the boreal and temperate forests. As a consequence, trees compete for soil  $\text{NH}_4^+$ ,  $\text{NO}_3^-$  and DON. Anthropogenic N emissions can add to the regional N loads by wet or dry deposition, and enter the series of transformations leading to the bioavailable N pool mined by tree roots (Fig. 12.1).

The main transformation processes affecting the concentration and  $\delta^{15}\text{N}$  values of inorganic and organic bioavailable N in soils consist in fixation, immobilization, ammonification (mineralization), volatilization, nitrification and denitrification (Hopkins et al. 1998), and the rates of these N transformations vary seasonally and regionally (Handley et al. 1998). Whereas fixation and ammonification generally create minor isotopic N fractionation, volatilization of  $\text{NH}_4^+$ , nitrification and denitrification tend to significantly increase the  $^{15}\text{N}$  content in the reacting substrates and decrease it in the products (Högberg 1997; Pardo and Nadelhoffer 2010; Hobbie and Högberg 2012). Consequence to the interplaying N transformation processes, nitrate, ammonium and DON generally show  $\delta^{15}\text{N}$  values in increasing order. In addition, in N-limited forests,  $\delta^{15}\text{N}$  values of bulk N tend to increase with sample depth, and its concentration, to decrease (Fig. 12.2a). The general explanations for this pattern are that low nitrification rates and leaching from top horizons depletes the components of the organic horizons in  $^{15}\text{N}$ . Shedding of leaves depleted in  $^{15}\text{N}$  relative to soil and preferential uptake of  $^{15}\text{N}$  by fungi associated to roots (see Sect. 12.3.2.2) may accentuate this pattern (Hobbie and Colpaert 2002; Compton et al. 2007; Högberg et al. 2011). However, in less N-limited forests, the top horizons may show high  $\delta^{15}\text{N}$  values in soil N-species due to increased rates of nitrification in the N- and organic-rich horizons (Fig. 12.2b; Högberg 1997; Mayor et al. 2012; Shi et al. 2014).

**Fig. 12.2** The general  $\delta^{15}\text{N}$  trends of soil bulk N as a function of sample depth for N-limited **a** and N-saturated **b** forests (see text)



Hence, the overall N status of the forest, the proportions of the various soil N forms trees use up, and the depth of root N uptake from the soil all have direct influence on the final  $\delta^{15}\text{N}$  values of tree tissues. A key point to note here is that isotopic studies rarely characterize root (or tree-ring) samples along with individual bioavailable soil N forms, even though this combination would greatly help determining fractionation steps before N uptake by trees.

### 12.3.2.2 Direct and Ectomycorrhizal Root Uptake

Trees can use up inorganic N forms and DON directly through their roots (Näsholm et al. 2009; Averill and Finzi 2011). This direct uptake by physical transport shows no evidence of fractionation; N isotopic fractionation occurs during assimilation processes involving enzymatic functions (Handley et al. 1998; Pardo et al. 2013). Alternatively, trees can gain N (and other nutrients) while providing C, through symbiotic associations with fungi (ectomycorrhiza EcM; e.g., Näsholm et al. 2009; Courty et al. 2010; Lilleskov et al. 2019). It is well accepted that EcM generally show higher  $\delta^{15}\text{N}$  values relative to N sources in soils, and to roots and stems of trees. In the process of N uptake, they preferentially incorporate the heavy  $^{15}\text{N}$  during the production of their tissues, and provide light N to their hosts (Gebauer and Taylor 1999; Hobbie and Högberg 2012). The extent of this biogenic fractionation and thus the isotopic values of fungi vary widely (Trudell et al. 2004; Mayor et al. 2009; Hobbie and Högberg 2012), inasmuch as different EcM communities may efficiently assimilate specific soil N-compounds. Also, it is established that EcM communities

change in structure and abundance under varying soil chemistry (pH), N deposition, N transformation rates, and climatic conditions (Chalot et al. 1995; Wallander et al. 1997; Qian et al. 1998; Schulze et al. 2000; Lilleskov et al. 2002; Averill and Finzi 2011; Högberg et al. 2011; Kjoller et al. 2012; Kluber et al. 2012; van der Linde et al. 2018). The role of EcM in regulating  $\delta^{15}\text{N}$  values in plants during N assimilation in field conditions is illustrated by the measured  $\delta^{15}\text{N}$  patterns in Alaskan trees, EcM and soils (Hobbie et al. 1999). Modeling of these results indicates a net fractionation during the N transfer from EcM to trees.

Another example compares the foliar  $\delta^{15}\text{N}$  values of *Acer rubrum* seedlings from seven sites distributed along a gradient of atmospheric  $\text{NO}_2$ , with active EcM or manipulated absence of EcM in native soils of New York state (Vallano and Sparks 2013). The foliar  $\delta^{15}\text{N}$  results for seedlings devoid of EcM show no influence of increasing N, but for EcM seedlings, they correlate significantly with ambient  $\text{NO}_2$  levels, indicating the aid EcM provides to trees for N assimilation. These examples and the above observations make EcM causative agents for changes in tree-ring (and foliar)  $\delta^{15}\text{N}$  series, a key point for understanding the overall  $\delta^{15}\text{N}$  values of N transferred from soils to trees. However, the inventory of responses and functionalities of EcM communities under various environmental conditions, particularly the extent of their isotopic fractionation and implication during N uptake by roots, is not yet comprehensive. Research in that domain could help elucidate the causes of shifts in tree-ring  $\delta^{15}\text{N}$  series.

### 12.3.2.3 Preference of Trees for Soil N Species

Most trees absorb  $\text{NH}_4^+$  and  $\text{NO}_3^-$ , but experiments conducted using fertilization with  $^{15}\text{N}$ -labelled N demonstrated that various species of trees show improved performances if grown with a specific soil N form (Kronzucker et al. 1997; Zhang et al. 2016; Miller and Hawkins 2007). The relative preferences for specific N forms mostly derive from the energy requirement for the production of proteins and the needed level of carboxylates (Arnold and van Diest 1991). Many species of deciduous trees take up  $\text{NO}_3^-$  preferentially (e.g., *Quercus alba*, *Fagus grandifolia*), whereas it is well established that most coniferous trees lacking the enzyme nitrate reductase assimilate  $\text{NH}_4^+$  more favorably, up to 20 times more than  $\text{NO}_3^-$  (Kronzucker et al. 1997; Templer and Dawson 2004; Islam and Macdonald 2009). Other studies have addressed the question of assimilation of DON, and found that coniferous trees such as *Chamaecyparis obtusa* do not use this form of N-compound (Takebayashi et al. 2010), while *Pinus sylvestris* and *Picea abies* assimilate as much DON as  $\text{NH}_4^+$  if the soil contains similar amounts of each N form (Ohlund and Näsholm 2002). To explain long-term deviations between tree-ring  $\delta^{15}\text{N}$  series of various deciduous species, McLauchlan and Craine (2012) linked differences to N-form preferences. Given that soil N compounds undergo different transformation paths and carry distinct  $\delta^{15}\text{N}$  signals, diverse N preferences by trees growing at the same site or under similar conditions ought to generate distinct tree-ring  $\delta^{15}\text{N}$  trends over time.

### ***12.3.3 N Remobilization, Inter-ring Translocation and Fractionation Within Stems***

Many studies explain well the fractionation along the length of trees, from root to stems and leaves (Yoneyama et al. 1998; Gebauer et al. 2000; Evans 2001). Briefly, after assimilation of N-species by trees, enzymatic functions transform  $\text{NH}_4^+$  and  $\text{NO}_3^-$  into amino acids (Handley et al. 1998). As mentioned previously, these steps generally enrich the reactants in  $^{15}\text{N}$  and deplete the products (Yoneyama et al. 1998; Gebauer et al. 2000). Research efforts also indicated that deciduous trees store N in their bark and wood, whereas coniferous trees predominantly store N as photosynthetic proteins in their youngest needles. The remobilization of these amino acids is seasonal. During spring, deciduous trees transfer non-structural N compounds (arginine and asparagine) from twigs and coarse roots (and stems) to forming leaves (Bazot et al. 2013; Brereton et al. 2014). For instance, N proportion in twigs of oak trees decreases by 55% during that period. During summer, leaves are the dominant storage of N (>50% in June, compared to only 10% in stems; see also Sect. 12.3.1). During autumn, while leaves are shedding, storage begins in stems, coarse roots and twigs. For willow trees, the stems become a major N reserve (Brereton et al. 2014), a pool that new leaves will solicit later on.

During spring, coniferous trees transfer N stored in their youngest needles to support new growth of leaves and stems (Millard and Proe 1993; Bauer et al. 2000; Krupa 2003; Millard and Grelet 2010; Couto-Vázquez and González-Prieto 2014). Translocation generates fractionation and systematically decreases  $\delta^{15}\text{N}$  values in old needles relative to young needles (Gebauer and Schulze 1991; Couto-Vázquez and González-Prieto 2010). In contrast, there is no systematic difference between recent and old tree rings as mentioned in Sect. 12.2. The remobilization steps described above may largely explain why foliage and tree-ring  $\delta^{15}\text{N}$  trends in coniferous trees are different from broad-leave trees (Pardo et al. 2006; Gerhart and McLauchlan 2014; Tomlinson et al. 2015).

For further assessing the impact of N mobility in stems on growth ring  $\delta^{15}\text{N}$  values, various research groups investigated the distribution of  $^{15}\text{N}$  after fertilization or misting labelled-N compounds (e.g., Elhani et al. 2005; Tomlinson et al. 2014). In such studies, labelled N detected in rings predating and postdating the marking events, clearly indicate that rings include both C-bound and mobile N (not removable by sample pretreatments). However, in most cases, the  $^{15}\text{N}$  maximal contents always peak in rings of the marking years (Schleppi et al. 1999; Elhani et al. 2003, 2005; Tomlinson et al. 2014). These experiments indicate that the inter-ring translocation of N does not erase the record (direction and year of changes) of environmental events, but may minimize the extent of its isotopic impact.

## 12.4 Tree-Ring $\delta^{15}\text{N}$ Responses to Changing Conditions

### 12.4.1 *Physiological Changes*

Some studies suggested that physiological functions, for instance lignification, may modify the  $\delta^{15}\text{N}$  values of rings with age of Spanish *Pinus radiata*, and proposed further experimentation in order to assess the validity of the hypothesis (Couto-Vázquez and González-Prieto 2010). *Acer saccharum* and *Fagus grandifolia* trees investigated for assessing the importance of potentially changing root depth with age on the evolution of  $\delta^{15}\text{N}$  values in leaves (and tree rings by extension) show no significant changes with age, but significant  $\delta^{15}\text{N}$  differences between root, stems and leaves, and averages between the two species (Pardo et al. 2013). These results suggest fractionation during transport and assimilation of N, and physiological differences between species. Such a finding agrees with former studies of temperate trees reporting a general increasing  $\delta^{15}\text{N}$  trend along the height of trees (Kolb and Evans 2002; Couto-Vázquez and González-Prieto 2010), with differences existing between species.

### 12.4.2 *Regional and Global Climate*

Based on the concepts explored in the former sections, in theory climatic conditions can imprint the  $\delta^{15}\text{N}$  values transferred to tree rings. Namely, temperature and precipitation variations may modify the soil bioavailable N pools through changes in organic matter degradation, ammonification and nitrification rates, functions of EcM communities, and depth of drawing available soil water and N species (Savard et al. 2009; Courty et al. 2010; Durán et al. 2016). Such changes modify the overall isotopic signal of bioavailable N, which will reverberate in the  $\delta^{15}\text{N}$  values of trees. Indeed, several studies have linked foliar  $\delta^{15}\text{N}$  results from various species of trees with precipitation, showing either direct or inverse correlations depending on the amounts of precipitation considered (Pardo et al. 2006; and references therein). Likewise, in rain exclusion experiments (simulated droughts) deciduous trees clearly increased their foliar  $\delta^{15}\text{N}$  values due to a relative decrease in soil N availability (Ogaya and Peñuelas 2008). At large scales, plant foliar  $\delta^{15}\text{N}$  trends correlate inversely with mean annual precipitation, but directly with mean annual temperature (MAT) possibly due to higher soil N availability under moist and warm conditions (Craine et al. 2009; Dawes et al. 2017). Instead, inverse correlation of temperature with foliar  $\delta^{15}\text{N}$  values of *Populus balsamifera* may reflect changing dominance in soil N transformation pathways, from DON leaching (low MAT) to denitrification (high MAT; Elmore et al. 2017). In general, we must keep in mind that soil N availability derives from microbial activity, and thus hinges on temperature and soil water content. Depending on the habitat, microbial activity reaches an optimum at a specific range of soil temperature and water content: too much or too little water reduces or inhibits microbial activity. The

same is true for temperature. As such, N availability depends on soil temperature and water content, which ultimately leave their fingerprints on the  $\delta^{15}\text{N}$  values of soil N compounds.

If leaf  $\delta^{15}\text{N}$  values of a given time contain climatic information, tree-ring  $\delta^{15}\text{N}$  series should also record this information. This suggestion is supported by a few studies reporting significant statistical correlations between precipitation or temperature with  $\delta^{15}\text{N}$  series from *Fagus grandifolia*, *Pinus strobus*, *Pinus massioniana*, *Fagus sylvatica* and *Pinus radiata* (Savard et al. 2009; Sun et al. 2010; Härdtle et al. 2013; Couto-Vázquez and González-Prieto 2014). Causes for the climate-induced  $\delta^{15}\text{N}$  variations include modified ratios of soil  $\text{NH}_4^+/\text{NO}_3^-$ , and change in soil depths of root uptake.

Despite these expressions of climatic triggers for changes in tree-ring  $\delta^{15}\text{N}$  series, one has to consider the potential limitations when evaluating potential climatic effects. High frequency changes in climatic parameters may be impractical to resolve using  $\delta^{15}\text{N}$  values of annually sampled tree rings, as remobilization and translocation of N tend to minimize the isotopic responses (Sect. 12.3.3). Such attempt for quantitative climatic–isotopic correspondence at this resolution may fail. However, tree-ring  $\delta^{15}\text{N}$  series may record low-frequency climate variability. This proposition is supported by a recent investigation of  $\delta^{15}\text{N}$  series in six and ten *Picea glauca* trees from two Canadian sites (Savard et al. 2020). The results indicate that short-term variations (<7 years) show no inter-tree coherence, whereas middle- (7–15 years) to long-term (>15 years) isotopic changes show strong coherence, encouraging their use as an environmental indicator. One option that may deserve further testing is to pass running averages through long tree-ring  $\delta^{15}\text{N}$  series, and evaluate their correlations with similarly treated climatic series (Savard et al. 2009; similarly treated for global climatic changes, see Sect. 12.4.3—cause number 4). As can be seen, climatic tree-ring  $\delta^{15}\text{N}$  studies require further exploration considering that climatic effects may interplay with anthropogenic impacts, and that improved knowledge on that front may help deciphering intricate  $\delta^{15}\text{N}$  responses of trees to intrinsic and extrinsic triggers.

### 12.4.3 Anthropogenic Impacts

There are four main reasons why anthropogenic N emissions are expected to affect the  $\delta^{15}\text{N}$  values in rings of specific species of trees. (1) Shifts in signals in N forms assimilated by trees through addition of large anthropogenic N loads with isotopic ratios markedly different from natural N isotopic abundance. (2) Change in N availability of the forest ecosystem due to high anthropogenic N supply relative to demands, modifying the overall soil N isotopic contents. (3) Modifications of the overall soil microbial structure and related N dynamics having an impact on the signal of N assimilated by stems under moderate anthropogenic N deposition. (4) Global change (climate and  $\text{pCO}_2$ ) interplaying with one or a combination of the former causes.

In the first case, much of the N in trees derives from the inorganic soil N pool ( $\text{NH}_4^+$  and  $\text{NO}_3^-$ ), which forms only a small portion of the total soil N, but that has  $\delta^{15}\text{N}$  signals that may vary with changes in environmental conditions, particularly with enhanced N deposition from anthropogenic emissions. After transition of N contaminants in the soil compartments, trees assimilate anthropogenic N through roots, or root N possibly combines in stems with anthropogenic N transiting through leaves. Key studies have invoked changes in the isotopic signals of assimilated N to account for shifts in tree-ring  $\delta^{15}\text{N}$  values (Saurer et al. 2004; Savard et al. 2009). However, determining the cause of changes in tree-ring  $\delta^{15}\text{N}$  series is possible only when N deposits chronically and in abundance, from a dominant source with  $\delta^{15}\text{N}$  values deviate significantly from soil N, and if the other potential causes for change do not blur this effect.

In the second case, increased N deposition in temperate and boreal forest ecosystems may cause acidification of soils, and nutrient nitrogen imbalances in trees (Aber et al. 1998; Högberg et al. 2007). The soil N status may pass from semi-closed to open, if a high N supply exceeds demands. Such a forest soil would see a high rate of  $^{15}\text{N}$ -poor nitrate loss through leaching, increasing the overall  $\delta^{15}\text{N}$  values of the residual pool (Fig. 12.2). The chronic exposure of a forest to such a rate of N input would generate a long-term  $\delta^{15}\text{N}$  increase in tree rings. In contrast, a decrease of anthropogenic N supply would generate a decrease in long-term tree-ring  $\delta^{15}\text{N}$  series in the recovering forests. This interpretation explains the declining  $\delta^{15}\text{N}$  series over 75 years in *Picea rubens* trees of the central Appalachians (Mathias and Thomas 2018).

In the third case, a combination of modified biogeochemical processes under low to moderate long-term exposure to anthropogenic N inputs alters the overall signal of soil N species prior to their assimilation by trees. On a theoretical basis, one can conceive that microbial communities in forest soils with very low N availability ( $<1$  kg/ha/y) will quickly adapt to enhanced input and chronic exposure to anthropogenic N. As mentioned in Sect. 12.3.2, in such conditions, existing EcM communities may thrive or shift in terms of diversity, and rates of bacterial N transformation may change. A study of four different deciduous species of trees in Indiana (USA), found long-term increasing and decreasing  $\delta^{15}\text{N}$  trends explained by species-specific preferences for inorganic N forms while nitrification increases (McLauchlan and Craine 2012).

In the fourth potential cause for  $\delta^{15}\text{N}$  changes in plant tissue, climatic conditions or rising  $\text{pCO}_2$  generate long-term changes in soil N processes and N availability. At a continental scale, centennial, standardized, 10 year resolution tree-ring  $\delta^{15}\text{N}$  series of temperate forests seem to evolve independently from anthropogenic N deposition in the USA (McLauchlan et al. 2017). The series instead may reflect changes in N transformation rates and EcM assimilation, and the declining N availability under rising  $\text{pCO}_2$ . Further along this line, at the global scale, rising atmospheric  $\text{CO}_2$  may have generated decreasing foliage and tree-ring  $\delta^{15}\text{N}$  trends through the last 150 years due to prolonged growing seasons, increased photosynthesis and overall enhanced plant-N demands, ultimately lowering the terrestrial N availability (Craine et al. 2019).

To summarize, tree-ring series may record changes in the forest N cycle or reflect successive N-cycling patterns, but the potential causes for these changes are complex and rigorous interpretations require excellent knowledge of the setting in which trees are growing. Given the attenuated nature of the isotopic changes due to intra-tree N remobilization and intricate enzymatic fractionations along the assimilation path within trees, attempts to quantify anthropogenic impacts on the forest N cycle using tree rings or leaves could be scant. On a more positive note, recognizing and dating perturbations of the forest N cycle using tree-ring  $\delta^{15}\text{N}$  series appears achievable.

#### **12.4.4 Other Applications**

The literature also documents several applications other than the ones presented in Sects. 12.4.1, 12.4.2 and 12.4.3. For tropical and  $\text{N}_2$ -fixing trees, the reader can consult Craine et al. (2015). Boreal wetland and tropical trees emit  $\text{N}_2\text{O}$  (Rusch and Rennenberg 1998; Welch et al. 2019), a process significant for understanding the global N cycling, for which  $\delta^{15}\text{N}$  results in stems and emitted gasses may turn useful. Moreover, tree-ring  $\delta^{15}\text{N}$  applications exist on effects of wild fires (Cook 2002; Beghin et al. 2011; Hyodo et al. 2012), clear cutting (Pardo et al. 2002; Bukata and Kyser 2005), and bird nesting (Mizota 2009; Holdaway et al. 2010; Larry et al. 2010). Understandably, researchers should select sites devoid of these perturbations in order to achieve meaningful results and refine our understanding of climatic and anthropogenic influences on tree-ring  $\delta^{15}\text{N}$  series.

### **12.5 Knowledge Gaps and Future Directions**

Studies dealing with the assimilation of N through either leaves or roots have mostly operated independently, with root assimilation experiments disregarding the potential foliar assimilation, and vice versa. As a consequence, the proportions of N in stems contributed from the foliar and rooting systems still need resolving even if these proportions are highly pertinent for relating tree-ring  $\delta^{15}\text{N}$  values to mechanistic processes and environmental changes.

As with ice cores, lakes sediments and skeletal corals reflecting complex and irrefutable anthropogenic impacts on the atmospheric, aquatic, and marine N cycling, tree-ring series likely represent another natural archive offering potential for unravelling impacts on forest N cycling. Although each archival system potentially offers many applications, in all cases the interplaying mechanisms responsible for changes through time need to be further constrained. With trees, difficulties arise from the requirement to have an excellent understanding of soil conditions to interpret tree-ring trends adequately. Further research should address the knowledge gaps on the steps of fractionation of individual bioavailable N forms in the soil compartments. Similarly, the role of EcM should be explored as it might be effective or non-effective



during the transfer of N forms to roots under the broad ranges of existing soil conditions. Tree-ring studies seldom involve the investigation of the full spectrum of N transformations in the air–soil–tree continuum. However, such an interdisciplinary approach may solve several questions regarding the extrinsic controls on tree-ring  $\delta^{15}\text{N}$  changes, perhaps with the combination of running well-adapted models of soil N budgets.

**Acknowledgements** The authors are grateful to G. Bordeleau and P. van der Sleen for a pre-submission and official referee reviews of the manuscript. Natural Resources Canada Contribution number: 20190279.

## References

- Aber J, McDowell W, Nadelhoffer K, Magill A, Berntson G, Kamakea M, McNulty S, Currie W, Rustad L, Fernandez I (1998) Nitrogen saturation in temperate forest ecosystems. *Bioscience* 48(11):921–934
- Ammann M, Siegwolf R, Pichlmayer F, Suter M, Saurer M, Brunold C (1999) Estimating the uptake of traffic-derived  $\text{NO}_2$  from  $^{15}\text{N}$  abundance in Norway spruce needles. *Oecologia* 118(2):124–131
- Arain MA, Yuan F, Andrew Black T (2006) Soil–plant nitrogen cycling modulated carbon exchanges in a western temperate conifer forest in Canada. *Agric For Meteorol* 140(1–4):171–192
- Arnold G, van Diest A (1991) Nitrogen supply, tree growth and soil acidification. *Fertil Res* 27:29–38
- Averill C, Finzi A (2011) Increasing plant use of organic nitrogen with elevation is reflected in nitrogen uptake rates and ecosystem  $\delta^{15}\text{N}$ . *Ecology* 92(4):883–891
- Bazot S, Barthes L, Blanot D, Fresneau C (2013) Distribution of non-structural nitrogen and carbohydrate compounds in mature oak trees in a temperate forest at four key phenological stages. *Trees* 27(4):1023–1034
- Bazot S, Fresneau C, Damesin C, Barthes L (2016) Contribution of previous year's leaf N and soil N uptake to current year's leaf growth in sessile oak. *Biogeosciences* 13(11):3475–3484
- Beghin R, Cherubini P, Battipaglia G, Siegwolf R, Saurer M, Bovio G (2011) Tree-ring growth and stable isotopes ( $^{13}\text{C}$  and  $^{15}\text{N}$ ) detect effects of wildfires on tree physiological processes in *Pinus sylvestris* L. *Trees* 25(4):627–636
- Brereton NJ, Pitre FE, Shield I, Hanley SJ, Ray MJ, Murphy RJ, Karp A (2014) Insights into nitrogen allocation and recycling from nitrogen elemental analysis and  $^{15}\text{N}$  isotope labelling in 14 genotypes of willow. *Tree Physiol* 34(11):1252–1262
- Bukata AR, Kyser KT (2005) Response of the nitrogen isotopic composition of tree-rings following tree-clearing and land-use change. *Environ Sci Technol* 39:7777–7783
- Bukata AR, Kyser TK (2007) Carbon and nitrogen isotope variations in tree-rings as records of perturbations in regional carbon and nitrogen cycles. *Environ Sci Technol* 41(4):1331–1338
- Caceres ML, Mizota C, Yamanaka T, Nobori Y (2011) Effects of pre-treatment on the nitrogen isotope composition of Japanese black pine (*Pinus thunbergii*) tree-rings as affected by high N input. *Rapid Commun Mass Spectrom* 25(21):3298–3302
- Chalot M, Kytöviita MM, Brun A, Finlay RD, Söderström B (1995) Factors affecting amino acid uptake by the ectomycorrhizal fungus *Paxillus involutus*. *Mycol Res* 99(9):1131–1138
- Chaparro-Suarez IG, Meixner FX, Kesselmeier J (2011) Nitrogen dioxide ( $\text{NO}_2$ ) uptake by vegetation controlled by atmospheric concentrations and plant stomatal aperture. *Atmos Environ* 45(32):5742–5750
- Choi W-J, Lee S-M, Chang SX, Ro H-M (2005) Variations of  $\delta^{13}\text{C}$  and  $\delta^{15}\text{N}$  in *Pinus densiflora* tree-rings and their relationship to environmental changes in Eastern Korea. *Water Air Soil Pollut* 164(1):173–187

- Compton JE, Hooker TD, Perakis SS (2007) Ecosystem N distribution and  $\delta^{15}\text{N}$  during a century of forest regrowth after agricultural abandonment. *Ecosystems* 10(7):1197–1208
- Cook G (2002) Effects of frequent fires and grazing on stable nitrogen isotope ratios of vegetation in northern Australia. *Aust Ecol* 26:630–636
- Courty P-E, Buée M, Diedhiou AG, Frey-Klett P, Le Tacon F, Rineau F, Turpault M-P, Uroz S, Garbaye J (2010) The role of ectomycorrhizal communities in forest ecosystem processes: new perspectives and emerging concepts. *Soil Biol Biochem* 42(5):679–698
- Couto-Vázquez A, González-Prieto SJ (2010) Effects of climate, tree age, dominance and growth on  $\delta^{15}\text{N}$  in young pinewoods. *Trees* 24(3):507–514
- Couto-Vázquez A, González-Prieto SJ (2014) Effects of biotic and abiotic factors on  $\delta^{15}\text{N}$  in young *Pinus radiata*. *Eur J For Res* 133(4):631–637
- Craine JM, Elmore AJ, Aidar MP, Bustamante M, Dawson TE, Hobbie EA, Kahmen A, Mack MC, McLauchlan KK, Michelsen A, Nardoto GB, Pardo LH, Penuelas J, Reich PB, Schuur EA, Stock WD, Templer PH, Virginia RA, Welker JM, Wright IJ (2009) Global patterns of foliar nitrogen isotopes and their relationships with climate, mycorrhizal fungi, foliar nutrient concentrations, and nitrogen availability. *New Phytol* 183(4):980–992
- Craine JM, Elmore AJ, Wang L, Augusto L, Baisden WT, Brookshire EN, Cramer MD, Hasselquist NJ, Hobbie EA, Kahmen A, Koba K, Kranabetter JM, Mack MC, Marin-Spiotta E, Mayor JR, McLauchlan KK, Michelsen A, Nardoto GB, Oliveira RS, Perakis SS, Peri PL, Quesada CA, Richter A, Schipper LA, Stevenson BA, Turner BL, Viani RA, Wanek W, Zeller B (2015) Convergence of soil nitrogen isotopes across global climate gradients. *Nature* 5:8280
- Dawes MA, Schleppei P, Hättenschwiler S, Rixen C, Hagedorn F (2017) Soil warming opens the nitrogen cycle at the alpine treeline. *Glob Chang Biol* 23(1):421–434
- Doucet A, Savard MM, Bégin C, Smirnov A (2011) Is wood pre-treatment essential for tree-ring nitrogen concentration and isotope analysis? *Rapid Commun Mass Spectrom* 25(4):469–475
- Elhani S, Lema BF, Zeller B, Bréchet C, Guehl J-M, Dupouey J-L (2003) Inter-annual mobility of nitrogen between beech rings: a labelling experiment. *Ann For Sci* 60(6):503–508
- Elhani S, Guehl JM, Nys C, Picard JF, Dupouey J-L (2005) Impact of fertilization on tree-ring delta N-15 and delta C-13 in beech stands: a retrospective analysis. *Tree Physiol* 25:1437–1446
- Elmore AJ, Craine JM, Nelson DM, Guinn SM (2017) Continental scale variability of foliar nitrogen and carbon isotopes in *Populus balsamifera* and their relationships with climate. *Sci Rep* 7(1):7759
- Evans RD (2001) Physiological mechanisms influencing plant nitrogen isotope composition. *Trends Plant Sci* 6(3):121–126
- Garten CT, Hanson PJ (1990) Foliar retention of  $^{15}\text{N}$ -nitrate and  $^{15}\text{N}$ -ammonium by red maple (*Acer rubrum*) and white oak (*Quercus alba*) leaves from simulated rain. *Environ Exp Bot* 30(3):333–342
- Gebauer G, Taylor AFS (1999)  $^{15}\text{N}$  natural abundance in fruit bodies of different functional groups of fungi in relation to substrate utilization. *New Phytol* 142(1):93–101
- Gerhart LM, McLauchlan KK (2014) Reconstructing terrestrial nutrient cycling using stable nitrogen isotopes in wood. *Biogeochemistry* 120(1–3):1–21
- Hart SC, Classen AT (2003) Potential for assessing long-term dynamics in soil nitrogen availability from variations in  $\delta^{15}\text{N}$  of tree rings. *Isot Environ Health Stud* 39(1):15–28
- Hobbie EA, Höglberg P (2012) Nitrogen isotopes link mycorrhizal fungi and plants to nitrogen dynamics. *New Phytol* 196(2):367–382
- Hobbie EA, Macko SA, Shugart HH (1999) Interpretation of nitrogen isotope signatures using the NIFTE model. *Oecologia* 120(3):405–415
- Höglberg MN, Höglberg P, Myrold DD (2007) Is microbial community composition in boreal forest soils determined by pH, C-to-N ratio, the trees, or all three? *Oecologia* 150(4):590–601
- Höglberg P, Johannisson C, Yarwood S, Callesen I, Nasholm T, Myrold DD, Höglberg MN (2011) Recovery of ectomycorrhiza after ‘nitrogen saturation’ of a conifer forest. *New Phytol* 189(2):515–525
- Houlton BZ, Morford SL, Dahlgren RA (2018) Convergent evidence for widespread rock nitrogen sources in Earth’s surface environment. *Science* 360(6384):58

- Hyodo F, Kusaka S, Wardle DA, Nilsson M-C (2012) Changes in stable nitrogen and carbon isotope ratios of plants and soil across a boreal forest fire chronosequence. *Plant Soil* 364(1–2):315–323
- Islam MA, Macdonald SE (2009) Current uptake of  $^{15}\text{N}$ -labeled ammonium and nitrate in flooded and non-flooded black spruce and tamarack seedlings. *Ann For Sci* 66(1):102–102
- Kjoller R, Nilsson LO, Hansen K, Schmidt IK, Vesterdal L, Gundersen P (2012) Dramatic changes in ectomycorrhizal community composition, root tip abundance and mycelial production along a stand-scale nitrogen deposition gradient. *New Phytol* 194(1):278–286
- Knicker H (2004) Stabilization of N-compounds in soil and organic-matter-rich sediments—what is the difference? *Mar Chem* 92(1–4):167–195
- Kolb KJ, Evans RD (2002) Implications of leaf nitrogen recycling on the nitrogen isotope composition of deciduous plant tissues. *New Phytol* 156(1):57–64
- Kronzucker HJ, Siddiqi MY, Glass ADM (1997) Conifer root discrimination against soil nitrate and the ecology of forest succession. *Nature* 385(6611):59–61
- Krupa SV (2003) Effects of atmospheric ammonia ( $\text{NH}_3$ ) on terrestrial vegetation: a review. *Environ Pollut* 124(2):179–221
- Larry LCM, Chitoshi M, Toshiro Y, Yoshihiro N (2010) Temporal changes in tree-ring nitrogen of *Pinus thunbergii* trees exposed to Black-tailed Gull (*Larus crassirostris*) breeding colonies. *Appl Geochem* 25(11):1699–1702
- Lilleskov E, Hobbie E, Timothy JF (2002) Ectomycorrhizal fungal taxa differing in response to nitrogen deposition also differ in pure culture organic nitrogen use and natural abundance of nitrogen isotopes. *Ecology* 154:219–231
- Lilleskov EA, Kuyper TW, Bidartondo MI, Hobbie EA (2019) Atmospheric nitrogen deposition impacts on the structure and function of forest mycorrhizal communities: a review. *Environ Pollut* 246:148–162
- Mayor JR, Schuur EA, Henkel TW (2009) Elucidating the nutritional dynamics of fungi using stable isotopes. *Ecol Lett* 12(2):171–183
- Mayor JR, Schuur EAG, Mack MC, Hollingsworth TN, Bååth E (2012) Nitrogen isotope patterns in alaskan black spruce reflect organic nitrogen sources and the activity of ectomycorrhizal fungi. *Ecosystems* 15(5):819–831
- McLauchlan KK, Craine JM (2012) Species-specific trajectories of nitrogen isotopes in Indiana hardwood forests, USA. *Biogeosciences* 9(2):867–874
- Millard P, Grelet GA (2010) Nitrogen storage and remobilization by trees: ecophysiological relevance in a changing world. *Tree Physiol* 30(9):1083–1095
- Millard P, Proe MF (1993) Nitrogen uptake, partitioning and internal cycling in *Picea sitchensis* (Bong.) Carr. As influenced by nitrogen supply. *New Phytol* 125:113–119
- Miller BD, Hawkins BJ (2007) Ammonium and nitrate uptake, nitrogen productivity and biomass allocation in interior spruce families with contrasting growth rates and mineral nutrient preconditioning. *Tree Physiol* 27:901–909
- Mizota C (2009) Temporal variations in the concentration and isotopic signature of ammonium- and nitrate-nitrogen in soils under a breeding colony of Black-tailed Gulls (*Larus crassirostris*) on Kabushima Island, northeastern Japan. *Appl Geochem* 24(2):328–332
- Näsholm T, Kielland K, Ganeteg U (2009) Uptake of organic nitrogen by plants. *New Phytol* 182(1):31–48
- Ogaya R, Peñuelas J (2008) Changes in leaf  $\delta^{13}\text{C}$  and  $\delta^{15}\text{N}$  for three Mediterranean tree species in relation to soil water availability. *Acta Oecol* 34(3):331–338
- Ohlund J, Näsholm T (2002) Growth of conifer seedlings on organic and inorganic nitrogen sources. *Tree Physiol* 21:1319–1326
- Pardo LH, Nadelhoffer KJ (2010) Using nitrogen isotope ratios to assess terrestrial ecosystems at regional and global scales. In: West JB, Bowen GJ, Dawson TE, Tu KP (eds) *Isoscapes: understanding movement, pattern, and process on earth through isotope mapping*. Springer, Netherlands, Dordrecht, pp 221–249

- Pardo LH, Hemond HF, Montoya JP, Fahey TJ, Siccama TG (2002) Response of the natural abundance of  $^{15}\text{N}$  in forest soils and foliage to high nitrate loss following clear-cutting. *Can J For Res* 32(7):1126–1136
- Pardo LH, Templer PH, Goodale CL, Duke S, Groffman PM, Adams MB, Boeckx P, Boggs J, Campbell J, Colman B, Compton J, Emmett B, Gundersen P, Kjønaas J, Lovett G, Mack M, Magill A, Mbila M, Mitchell MJ, McGee G, McNulty S, Nadelhoffer K, Ollinger S, Ross D, Rueth H, Rustad L, Schaberg P, Schiff S, Schleppi P, Spoelstra J, Wessel W (2006) Regional assessment of N saturation using foliar and root  $\delta^{15}\text{N}$ . *Biogeochemistry* 80(2):143–171
- Pardo LH, McNulty SG, Boggs JL, Duke S (2007) Regional patterns in foliar  $^{15}\text{N}$  across a gradient of nitrogen deposition in the northeastern US. *Environ Pollut* 149(3):293–302
- Pardo LH, Semaoune P, Schaberg PG, Eagar C, Sebilo M (2013) Patterns in  $\delta^{15}\text{N}$  in roots, stems, and leaves of sugar maple and American beech seedlings, saplings, and mature trees. *Biogeochemistry* 112(1–3):275–291
- Qi H, Coplen TB, Jordan JA (2016) Three whole-wood isotopic reference materials, USGS54, USGS55, and USGS56, for  $\delta^2\text{H}$ ,  $\delta^{18}\text{O}$ ,  $\delta^{13}\text{C}$ , and  $\delta^{15}\text{N}$  measurements. *Chem Geol* 442:47–53
- Rennenberg H, Gessler A (1999) Consequences of N deposition to forest ecosystems—recent results and future research needs. *Water Air Soil Pollut* 116(1):47–64
- Rusch H, Rennenberg H (1998) Black alder (*Alnus Glutinosa* (L.) Gaertn.) trees mediate methane and nitrous oxide emission from the soil to the atmosphere. *Plant Soil* 201:1–7
- Saurer M, Cherubini P, Ammann M, De Cinti B, Siegwolf R (2004) First detection of nitrogen from NOx in tree rings: a  $^{15}\text{N}/^{14}\text{N}$  study near a motorway. *Atmos Environ* 38(18):2779–2787
- Savard MM, Bégin C, Smirnoff A, Marion J, Rioux-Paquette E (2009) Tree-ring nitrogen isotopes reflect anthropogenic NOx emissions and climatic effects. *Environ Sci Technol* 43(3):604–609
- Savard MM, Cole A, Smirnoff A, Vet R (2017)  $\delta^{15}\text{N}$  values of atmospheric N species simultaneously collected using sector-based samplers distant from sources—isotopic inheritance and fractionation. *Atmos Environ* 162:11–22
- Schleppi P, Bucher-Wallin L, Siegwolf R, Saurer M, Muller N, Bucher JB (1999) Simulation of increased nitrogen deposition to a montane forest ecosystem: partitioning of the added  $^{15}\text{N}$ . *Water Air Soil Pollut* 116(1):129–134
- Shi J, Ohte N, Tokuchi N, Imamura N, Nagayama M, Oda T, Suzuki M (2014) Nitrate isotopic composition reveals nitrogen deposition and transformation dynamics along the canopy–soil continuum of a suburban forest in Japan. *Rapid Commun Mass Spectrom* 28(23):2539–2549
- Siegwolf RTW, Matyssek R, Saurer M, Maurer S, Günthardt-Goerg MS, Schmutz P, Bucher JB (2001) Stable isotope analysis reveals differential effects of soil nitrogen and nitrogen dioxide on the water use efficiency in hybrid poplar leaves. *New Phytol* 149(2):233–246
- Takebayashi Y, Koba K, Sasaki Y, Fang Y, Yoh M (2010) The natural abundance of  $^{15}\text{N}$  in plant and soil-available N indicates a shift of main plant N resources to  $\text{NO}_3^-$  from  $\text{NH}_4^+$  along the N leaching gradient. *Rapid Commun Mass Spectrom* 24(7):1001–1008
- Templer P, Dawson TE (2004) Nitrogen uptake by four tree species of the Catskill Mountains, New York: implications for forest N dynamics. *Plant Soil* 262:251–261
- Tomlinson G, Buchmann N, Siegwolf R, Weber P, Thimonier A, Pannatier EG, Schmitt M, Schaub M, Waldner P (2015) Can tree-ring  $\delta^{15}\text{N}$  be used as a proxy for foliar  $\delta^{15}\text{N}$  in European beech and Norway spruce? *Trees* 3(3):627–638
- Trudell SA, Rygielwicz PT, Edmonds RL (2004) Patterns of nitrogen and carbon stable isotope ratios in macrofungi, plants and soils in two old-growth conifer forests. *New Phytol* 164(2):317–335
- Vallano DM, Sparks JP (2007) Foliar  $\delta^{15}\text{N}$  values as indicators of foliar uptake of atmospheric nitrogen pollution. *Terr Ecol* 1:93–109
- Vallano DM, Sparks JP (2013) Foliar  $\delta^{15}\text{N}$  is affected by foliar nitrogen uptake, soil nitrogen, and mycorrhizae along a nitrogen deposition gradient. *Oecologia* 172(1):47–58
- Van der Linde S, Suz LM, Orme CDL, Cox F, Andreae H, Asi E, Atkinson B, Benham S, Carroll C, Cools N, De Vos B, Dietrich H-P, Eichhorn J, Gehrman J, Grebenc T, Gweon HS, Hansen K, Jacob F, Kristöfel F, Lech P, Manninger M, Martin J, Meesenburg H, Merilä P, Nicolas M, Pavlenda P, Rautio P, Schaub M, Schröck H-W, Seidling W, Šrámek V, Thimonier A, Thomsen

- IM, Titeux H, Vanguelova E, Verstraeten A, Vesterdal L, Waldner P, Wijk S, Zhang Y, Žlindra D, Bidartondo MI (2018) Environment and host as large-scale controls of ectomycorrhizal fungi. *Nature* 558(7709):243–248
- Vizoso S, Gerant D, Marc Guehl J, Joffre R, Chalot M, Gross P, Maillard P (2008) Do elevation of CO<sub>2</sub> concentration and nitrogen fertilization alter storage and remobilization of carbon and nitrogen in pedunculate oak saplings? *Tree Physiol* 28:1729–1739
- Warren C, Dreyer E, Adams AM (2003) Photosynthesis-Rubisco relationships in foliage of *Pinus sylvestris* in response to nitrogen supply and the proposed role of Rubisco and amino acids as nitrogen stores. *Trees* 17:359–366
- Welch B, Gauci V, Sayer EJ (2019) Tree stem bases are sources of CH<sub>4</sub> and N<sub>2</sub>O in a tropical forest on upland soil during the dry to wet season transition. *Glob Chang Biol* 25(1):361–372
- Wright IJ, Reich PB, Westoby M, Ackerly DD, Baruch Z, Bongers F, Cavender-Bares J, Chapin T, Cornelissen JHC, Diemer M, Flexas J, Garnier E, Groom PK, Gulias J, Hikosaka K, Lamont BB, Lee T, Lee W, Lusk C, Midgley JJ, Navas M-L, Niinemets Ü, Oleksyn J, Osada N, Poorter H, Poot P, Prior L, Pyankov VI, Roumet C, Thomas SC, Tjoelker MG, Veneklaas EJ, Villar R (2004) The worldwide leaf economics spectrum. *Nature* 428(6985):821–827
- Zhang C, Meng S, Li Y, Su L, Zhao Z (2016) Nitrogen uptake and allocation in *Populus simonii* in different seasons supplied with isotopically labeled ammonium or nitrate. *Trees* 30(6):2011–2018
- Balster NJ, Marshall JD, Clayton M (2009) Coupling tree-ring  $\delta^{13}\text{C}$  and  $\delta^{15}\text{N}$  to test the effect of fertilization on mature Douglas-fir (*Pseudotsuga menziesii* var. *glauca*) stands across the Interior northwest, USA. *Tree Physiol* 29(12):1491–1501
- Bauer GA, Gebauer G, Harrison AF, Högborg P, Högbom L, Schinkel H, Taylor AFS, Novak M, Buzek F, Harkness D, Persson T, Schulze ED (2000) Biotic and abiotic controls over ecosystem cycling of stable natural nitrogen, carbon and sulphur isotopes. In: Schulze E-D (ed) Carbon and nitrogen cycling in European forest ecosystems. Springer, Berlin, Heidelberg, pp 189–214
- Craine JM, Elmore AJ, Wang L, Aranibar J, Bauters M, Boeckx P, Crowley BE, Dawes MA, Delzon S, Fajardo A, Fang Y, Fujiyoshi L, Gray A, Guerrieri R, Gundale MJ, Hawke DJ, Hietz P, Jonard M, Kearsley E, Kenzo T, Makarov M, Maranon-Jimenez S, McGlynn TP, McNeil BE, Mosher SG, Nelson DM, Peri PL, Roggy JC, Sanders-DeMott R, Song M, Szpak P, Templer PH, Van der Colff D, Werner C, Xu X, Yang Y, Yu G, Zmudczynska-Skarbek K (2019) Isotopic evidence for oligotrophication of terrestrial ecosystems. *Nat Ecology Evol* 2(11):1735–1744
- Durán J, Morse J, Groffman P, Campbell J, Christenson L, Driscoll C, J. Fahey T, Fisk M, E. Likens G, Melillo J, Mitchell M, Templer P, Vadeboncoeur M (2016) Climate change decreases nitrogen pools and mineralization rates in northern hardwood forests. *Ecosphere* 7
- Etzold S, Ferretti M, Reinds GJ, Solberg S, Gessler A, Waldner P, Schaub M, Simpson D, Benham S, Hansen K, Ingerslev M, Jonard M, Karlsson PE, Lindroos A-J, Marchetto A, Manninger M, Meessenburg H, Merilä P, Nöjd P, Rautio P, Sanders TGM, Seidling W, Skudnik M, Thimonier A, Verstraeten A, Vesterdal L, Vejputskova M, de Vries W (2020) Nitrogen deposition is the most important environmental driver of growth of pure, even-aged and managed European forests. *For Ecol Manag* 458:117762
- Gebauer G, Schulze DE (1991) Carbon and nitrogen isotope ratios in different compartments of a healthy and a declining *Picea abies* forest in the fichtelgebirge. *NE Bavaria* 87
- Gebauer G, Zeller B, Schmidt G, May C, Buchmann N, Colin-Belgrand M, Dambrine E, Martin F, Schulze E-D, Botner P (2000) The fate of <sup>15</sup>N-labelled nitrogen inputs to coniferous and broadleaf forests. In: Schulze E-D (ed) Carbon and nitrogen cycling in European forest ecosystems. Springer, Berlin, Heidelberg, pp 144–170
- Handley LL, Scrimgeour CM, Raven JA (1998) <sup>15</sup>N natural abundance levels in terrestrial vascular plants: a précis. In: Griffiths H (ed). Bios Scientific Publishers, Oxford, UK
- Härdtle W, Niemeyer T, Assmann T, Baiboks S, Fichtner A, Friedrich U, Lang AC, Neuwirth B, Pfister L, Ries C, Schuldt A, Simon N, von Oheimb G (2013) Long-term trends in tree-ring width and isotope signatures ( $\delta^{13}\text{C}$ ,  $\delta^{15}\text{N}$ ) of *Fagus sylvatica* L. on soils with contrasting water supply. *Ecosystems* 16(8):1413–1428

- Harrison AF, Harkness DD, Rowland AP, Garnett JS, Bacon PJ (2000a) Annual carbon and nitrogen fluxes in soils along the European forest transect, determined using  $^{14}\text{C}$ -bomb. In: Schulze E-D (ed) Carbon and nitrogen cycling in European forest ecosystems. Springer, Berlin, Heidelberg, pp 237–256
- Harrison AF, Schulze ED, Gebauer G, Bruckner G (2000b) Canopy uptake and utilization of atmospheric pollutant nitrogen. In: Schulze E-D (ed) Carbon and nitrogen cycling in European forest ecosystems. Springer, Berlin, Heidelberg, pp 171–188
- Hobbie E, Colpaert J (2002) Nitrogen availability and colonization by mycorrhizal fungi correlate with nitrogen isotope patterns in plants. *New Phytol* 157
- Högberg P (1997) Tansley review no. 95.  $^{15}\text{N}$  natural abundance in soil-plant systems. *New Phytol* 137(2):179–203
- Holdaway RN, Hawke DJ, Hyatt OM, Wood GC (2010) Stable isotopic ( $\delta^{15}\text{N}$ ,  $\delta^{13}\text{C}$ ) analysis of wood in trees growing in past and present colonies of burrow-nesting seabirds in New Zealand. I.  $\delta^{15}\text{N}$  in two species of conifer (*Podocarpaceae*) from a mainland colony of Westland petrels (*Procellaria westlandica*), Punakaiki, South Island. *J R Soc N Z* 37(2):75–84
- Holloway JM, Dahlgren RA (2002) Nitrogen in rock: occurrences and biogeochemical implications. *Glob Biogeochem Cycles* 16(4):65–61–65–17
- Hopkins DW, Wheatley RE, Robinson D (1998) In: Griffiths H (ed) Stable isotope studies of soil nitrogen. Bios Scientific Publishers, Oxford, UK
- Kendall C, Elliott EM, Wankel SD (2007) Tracing anthropogenic inputs of nitrogen to ecosystems. In: Michener RH, Lajtha K (eds) Stable isotopes in ecology and environmental science. Blackwell Publishing, Hoboken
- Kluber LA, Carrino-Kyker SR, Coyle KP, DeForest JL, Hewins CR, Shaw AN, Smemo KA, Burke DJ (2012) Mycorrhizal response to experimental pH and P manipulation in acidic hardwood forests. *PLoS ONE* 7(11):e48946
- Macklon AES, Sheppard LJ, Sim A, Leith ID (1996) Uptake of ammonium and nitrate ions from acid mist applied to Sitka spruce [*Picea sitchensis* (Bong.) Carr.] grafts over the course of one growing season. *Trees* 10(4):261–267
- Mathias JM, Thomas RB (2018) Disentangling the effects of acidic air pollution, atmospheric  $\text{CO}_2$  and climate change on recent growth of red spruce trees in the Central Appalachian Mountains. *Glob Chang Biol* 24(9):3938–3953
- McLauchlan KK, Gerhart LM, Battles JJ, Craine JM, Elmore AJ, Higuera PE, Mack MC, McNeil BE, Nelson DM, Pederson N, Perakis SS (2017) Centennial-scale reductions in nitrogen availability in temperate forests of the United States. *Sci Rep* 7(1)
- Qian XM, Kottke I, Oberwinkler F (1998) Influence of liming and acidification on the activity of the mycorrhizal communities in a *Picea abies* (L.) Karst. stand. *Plant Soil* 199(1):99–109
- Savard MM, Marion J, Bégin C (2020) Nitrogen isotopes of individual tree-ring series—the validity of middle- to long-term trends. *Dendrochronologia* 62:125726
- Scarascia-Mugnozza G, Bauer GA, Persson H, Matteucci G, Masci A (2000) Tree biomass, growth and nutrient pools. In: Caldwell MM, Heldmaier G, Lange OL, Mooney HA, Schulze E-D, Sommer U (eds) Carbon and nitrogen cycling in European forest ecosystems. Springer, Heidelberg, Germany
- Schulze E-D, Högberg P, van Oene H, Persson T, Harrison AF, Read D, Kjelller A, Matteucci G (2000) Interactions between the carbon and nitrogen cycles and the role of biodiversity: a synopsis of a study along a North-South transect through Europe. In: Schulze E-D (ed) Carbon and nitrogen cycling in European forest ecosystems. Springer, Berlin, Heidelberg, pp 468–491
- Sparks JP, Roberts JM, Monson RK (2003) The uptake of gaseous organic nitrogen by leaves: a significant global nitrogen transfer process. *Geophys Res Lett* 30(23)
- Sun F, Kuang Y, Wen D, Xu Z, Li J, Zuo W, Hou E (2010) Long-term tree growth rate, water use efficiency, and tree ring nitrogen isotope composition of *Pinus massoniana* L. in response to global climate change and local nitrogen deposition in Southern China. *J Soils Sediments* 10(8):1453–1465

- Tomlinson G, Siegwolf RT, Buchmann N, Schleppei P, Waldner P, Weber P (2014) The mobility of nitrogen across tree-rings of Norway spruce (*Picea abies* L.) and the effect of extraction method on tree-ring  $\delta^{15}\text{N}$  and  $\delta^{13}\text{C}$  values. *Rapid Commun Mass Spectrom* 28(11):1258–1264
- Wallander H, Arnebrant K, Östrand F, Kårén O (1997) Uptake of  $^{15}\text{N}$ -labelled alanine, ammonium and nitrate in *Pinus sylvestris* L. ectomycorrhiza growing in forest soil treated with nitrogen, sulphur or lime. *Plant Soil* 195(2):329–338
- Yoneyama T, Fujiwara H, Wilson JM (1998) Variations in fractionation of carbon and nitrogen isotopes in higher plants: N metabolism and partitioning of phloem and xylem. In: Griffiths H (ed) *Stable isotopes: integration of biological, ecological and geochemical processes*. BIOS Scientific Publishers, Oxford, UK

**Open Access** This chapter is licensed under the terms of the Creative Commons Attribution 4.0 International License (<http://creativecommons.org/licenses/by/4.0/>), which permits use, sharing, adaptation, distribution and reproduction in any medium or format, as long as you give appropriate credit to the original author(s) and the source, provide a link to the Creative Commons license and indicate if changes were made.

The images or other third party material in this chapter are included in the chapter's Creative Commons license, unless indicated otherwise in a credit line to the material. If material is not included in the chapter's Creative Commons license and your intended use is not permitted by statutory regulation or exceeds the permitted use, you will need to obtain permission directly from the copyright holder.



# Chapter 13

## Postphotosynthetic Fractionation in Leaves, Phloem and Stem



Arthur Gessler and Juan Pedro Ferrio

**Abstract** Stable carbon isotope ratios ( $\delta^{13}\text{C}$ ) in organic matter convey important integrated and (if assessed in the tree ring archive) dateable information on plant physiology and related environmental drivers. While the generation of the  $\delta^{13}\text{C}$  signal in the primary assimilates in the leaves via photosynthetic carbon isotope fractionation is well understood, we still lack detailed knowledge of the processes that determine the isotopic fractionation in downstream processes in the leaves and during the transport in the stem, which in turn affect  $\delta^{13}\text{C}$  in the tree-ring archive. We here provide an update on processes that drive post-carboxylation carbon isotope fractionation in the leaves, on potential changes in  $\delta^{13}\text{C}$  related to phloem loading and transport and we also discuss the role of stem  $\text{CO}_2$  fluxes (bark photosynthesis, stem respiration and  $\text{CO}_2$  fixation by phosphoenol pyruvate carboxylase). Moreover, we address the impact of carbon storage and remobilization on the intra-annual variation of  $\delta^{13}\text{C}$  in tree rings. Finally, we point to the potential importance of the intra-molecular carbon isotope distribution in carbohydrates for tree ring  $\delta^{13}\text{C}$  and its relation to shifts in metabolic pathways.

### 13.1 Introduction

Stable carbon isotope ratios ( $\delta^{13}\text{C}$ ) in tree ring—either determined compound-specific in cellulose or in whole wood consisting of various chemical compounds—are widely assessed to obtain retrospective information on tree gas exchange physiology and the related environmental drivers (e.g., Saurer et al. 1997; Schleser et al. 1999; McCarroll and Loader 2004; Marshall and Monserud 2006; Rinne et al. 2010). The tree-ring archive allows on the one hand accurate dating and on the other hand integrates  $\delta^{13}\text{C}$  of the canopy, so that biophysical processes occurring at the leaf

---

A. Gessler (✉)

Swiss Federal Institute for Forest, Snow and Landscape Research WSL, Birmensdorf, Switzerland  
e-mail: [arthur.gessler@wsl.ch](mailto:arthur.gessler@wsl.ch)

J. P. Ferrio

Centro de Investigación Y Tecnología Agroalimentaria de Aragón (CITA), Unidad de Recursos Forestales, Avda. Montañana 930, 50059 Zaragoza, Spain

© The Author(s) 2022

R. T. W. Siegwolf et al. (eds.), *Stable Isotopes in Tree Rings*, Tree Physiology 8,  
[https://doi.org/10.1007/978-3-030-92698-4\\_13](https://doi.org/10.1007/978-3-030-92698-4_13)

381



scale can be transferred to the whole tree and further to the ecosystem scale. The original signal imprinted in the primary photoassimilates is depending on the  $\delta^{13}\text{C}$  of  $\text{CO}_2$  and the photosynthetic carbon isotope discrimination. The latter is in a first approximation proportional to the ratio of leaf internal and ambient  $\text{CO}_2$  concentration  $c_i/c_a$  or—to be more precise—of chloroplastic  $\text{CO}_2$  concentration ( $c_p$ ) and  $c_a$  (Farquhar et al. 1982). Thus the  $\delta^{13}\text{C}$  of organic matter can be used to characterise environmental effects and their influences on diffusional versus biochemical controls over photosynthesis. The details on photosynthetic carbon isotope discrimination are given in Chap. 9.

While the understanding of stable isotope fractionation during photosynthesis and the environmental factors affecting it is well developed (Cernusak et al. 2013), there is a larger gap of knowledge about the processes leading to alteration of  $\delta^{13}\text{C}$  in downstream metabolic processes in the leaves and in heterotrophic tissues as well as during transport. Such processes lead to the generally observed pattern that non-photosynthetic tissues are enriched in  $^{13}\text{C}$  compared to leaves in  $\text{C}_3$  plants (Badeck et al. 2005; Cernusak et al. 2009). In this chapter we will thus mainly focus on the path of carbon and its carbon isotopic composition from leaf photosynthate production to wood formation, as summarised in Fig. 13.1. We will discuss here the different post-assimilation processes that might be able to alter  $\delta^{13}\text{C}$  and thus cause a (partial) decoupling between the original leaf isotopic signals and the archived signals in tree rings and aim to provide an update of a recent review also tackling this topic (Gessler et al. 2014). As almost all trees are  $\text{C}_3$  plants (but see Pearcy and Troughton 1975; Lüttge 2006) we only refer to processes in  $\text{C}_3$  plants. Tree-ring carbon isotopes are determined on a broad range of temporal scales from very fine scale interannual variations up to millennial time scales (Barbour and Song 2014). Knowledge of the potential alteration of the isotope signal on its way to the tree ring at various time scales allows for a better estimation of the uncertainties when reconstructing the coupling between tree processes and climatic drivers.

## 13.2 Post-Carboxylation Fractionation in the Leaves

Metabolically downstream from the  $\text{CO}_2$  fixation by RubisCO, there is one important reaction imposing post-carboxylation fractionation on the newly-fixed assimilates, which involves the aldolase reaction within the Calvin cycle. Due to its location in the metabolic pathway between triose phosphate and fructose 1,6-bisphosphate, aldolase imposes a diurnally distinct isotope signal on the assimilates available in the leaf cytoplasm. During the light, starch that is derived from fructose-6-phosphate via fructose 1,6-bisphosphate is produced and accumulated in the chloroplasts of leaves. On the other hand, sucrose is produced in the cytoplasm and this synthesis is based on the triose phosphates exported from the chloroplast. The triose-phosphates are  $^{13}\text{C}$  depleted, which is a direct consequence of transitory starch synthesis, which favours  $^{13}\text{C}$  during production of fructose 1,6-bisphosphate by aldolase, leading to

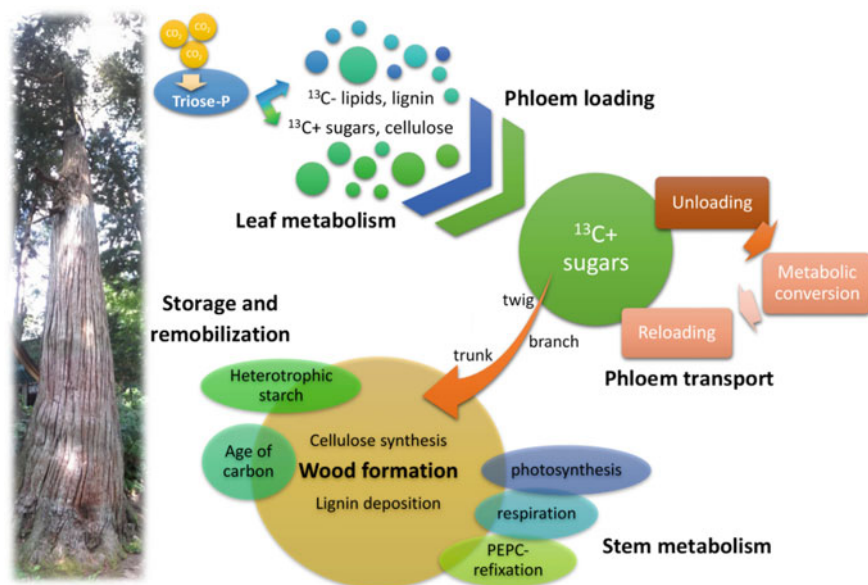


**Fig. 13.1** Conceptual scheme summarizing the main processes in the way from primary assimilates (triose-P) to the wood that may cause fractionation at time scales relevant to tree-ring archives. The first fractionation processes occur already within the leaf, where various isotopic effects during metabolic pathways and phloem loading cause lipids and lignin to be depleted, and sugars and cellulose to be enriched in  $^{13}\text{C}$ . For some species, a basipetal enrichment in phloem sap from twigs to basal stem has been described, potentially associated with the continuous unloading and reloading of sugars during phloem transport. This sugar would be partially exposed to metabolic reactions (e.g. production of lignin) in stem tissues, causing an enrichment of the fraction that is reloaded in the phloem. Wood formation could also be affected by fractionations occurring during stem metabolism. Bark photosynthesis, respiratory fractionation, or PEPC  $\text{CO}_2$  refixation processes are known to produce fractionations, but their direct effect on tree rings is not clear. Finally, the source of carbon used for wood formation could show seasonal and inter-annual variations. In particular, remobilization of stored carbon is crucial for leaf development and early stem growth in deciduous trees but could also play a key role during stress episodes. See text for further details

a relative  $^{13}\text{C}$  enrichment of starch (Rossmann et al. 1991; Gleixner and Schmidt 1997). During the night, the sucrose synthesized in the cytoplasm of leaf mesophyll cells is originating from the  $^{13}\text{C}$ -enriched starch, which is degraded via maltose (Weise et al. 2004). As a consequence of this fractionation step, leaf exported sucrose during the day has been shown to be relatively  $^{13}\text{C}$ -depleted while night sucrose was enriched in  $^{13}\text{C}$  (Gessler et al. 2008). Observations of diel variation in  $\delta^{13}\text{C}$  of leaf sugars exported into the phloem in different tree species (*Pinus sylvestris*; *Eucalyptus delegatensis*) showed day-night differences of up to 1.7‰ (Brandes et al. 2006; Gessler et al. 2007; Kodama et al. 2008). However, there are also indications from other trees species that such diel variations in leaf-exported sugars might not always occur (*Fagus sylvatica*, *Pseudotsuga menziesii*) (Bögelein et al. 2019). Moreover, only recently, Lehmann et al. (2019) showed with starch deficient mutants that

post-carboxylation carbon isotope fractionation was low in three herbaceous species. Thus, there is still some uncertainty regarding which species and under which environmental conditions the aldolase related isotope effects and thus diel variations in  $\delta^{13}\text{C}$  of leaf sugars are expressed. This might also depend on species specific differences in day vs. night phloem loading even though there is some evidence that sugar transport is not changing during the diel cycle (Peuke et al. 2001).

If, however, occurring, diel variations in  $\delta^{13}\text{C}$  of leaf exported and phloem transported sugars may affect the carbon isotope composition of cellulose in tree rings (Tcherkez et al. 2007), as cellulose is mainly constructed from this carbon source. Cell expansion in plants is known to depend on turgor. Steppe et al. (2015) assumed that all stem growth processes, including cell expansion and deposition of cell wall, occurs during the night, when the tree's water status and thus cell turgor is most favourable. This is in line with molecular studies that show highest night-time gene expression for enzymes of the lignin (Rogers et al. 2005) and cellulose (Harmer et al. 2000; Solomon et al. 2010) metabolism. If we now assume that mainly sucrose produced from starch during the night is used for tree ring production,  $\delta^{13}\text{C}$  of this tissue might be more than 2‰ enriched compared to the situation where 50% night and 50% day sucrose would be used (Tcherkez et al. 2007). Since phloem transport velocities vary between *ca.* 0.1 and 1 m h<sup>-1</sup> (Jensen et al. 2012) for different species, with conifers at the lower and broadleaf trees at the higher end, not only species but also tree height might influence the proportion of starch-derived (<sup>13</sup>C enriched) assimilates that are used for wood production at a particular position at the tree trunk. There is, however, indication that even in trees where diel variations in  $\delta^{13}\text{C}$  of leaf-exported sugars occur, the amplitude of variation gets strongly dampened during transport in basipetal direction in the trunk so that aldolase fractionation in the leaves does not likely affect tree ring  $\delta^{13}\text{C}$ . The mechanisms leading to the loss of diel oscillation are discussed below.

Besides temporal variation in  $\delta^{13}\text{C}$  of assimilates, also a relative <sup>13</sup>C enrichment of sugars loaded into the phloem - compared to primary assimilates or bulk leaf material - is observed. A process, leading to an apparent enrichment of the leaf sugar fraction that can be exported to the phloem compared to bulk leaf material is related to the different  $\delta^{13}\text{C}$  among distinct chemical compounds (for a comprehensive list of enzyme reactions that are involved in producing compound-specific isotope differences see Hobbie and Werner 2004). Primary assimilates are used in the leaves to produce <sup>13</sup>C-depleted compounds, such as lignin and lipids. Consequently, the unreacted sugars that can be loaded into the phloem are assumed to be isotopically heavier than the primary assimilates, due to mass balance reasons (see Fig. 13.1). As woody plants have especially high lipid and lignin contents in the leaves, the carbohydrates that can be loaded to and subsequently allocated in the phloem are more strongly <sup>13</sup>C-enriched as compared to non-woody plants (Hobbie and Werner 2004). This assumption of an enrichment of unreacted sugars compared to primary assimilates is in agreement with measurement of Brandes et al. (2006), who showed that this offset amounts to >1.5‰ in Scots pine.

### 13.3 Changes in $\delta^{13}\text{C}$ Related to Phloem Loading and Transport

There are two main alterations of the  $\delta^{13}\text{C}$  directly related to phloem transport: one (a) that acts on the temporal (i.e. diel) scale and one (b) on the spatial scale along the transport pathway. Both changes might, however, be due to one common mechanism.

The dampening of the short-term diel variations (a) in  $\delta^{13}\text{C}$  of sugars along the tree axis in basipetal direction is assumed to be a result of the mixing of different sugar pools with different age and metabolic history during transport between the leaf and the trunk cambium (Brandes et al. 2006; Kodama et al. 2008). Such mixing of pools lead to a reduction of the diel amplitude: while the amplitude amounted to 2.5‰ for sugars transported in the twig phloem, it was reduced to <0.5‰ at the trunk base in *Eucalyptus delegatensis*, where normally tree rings are sampled (Gessler et al. 2007). Thus, this dampening prevents any fractionation related to leaf starch synthesis to be imprinted in tree ring material. Gessler et al. (2014) proposed that the mixing of different sugar pools during basipetal transport might be explained by intrinsic properties of the dynamic Münch mass flow model (see review by Van Bel 2003). The model proposes the sieve tubes to act as a leaky pipe during transport: a proportion of the sucrose from sieve tubes is always released to the surrounding parenchyma, and to compensate for the loss sugars from the surrounding tissues are reloaded back to the sieve tubes (Minchin and Thorpe 1987; see Fig. 13.1). The loss and retrieval of sugars may allow for continuous mixing of different sugar pools along the transport pathway towards the trunk base, and as a consequence dampen the diel variations in  $\delta^{13}\text{C}$ . Further research is, however, needed to clarify if this mixing effect is universal and occurs in all tree species and under all environmental conditions.

This process might, however, also explain (b) the often observed  $^{13}\text{C}$  enrichment of phloem sugars from the twig to the trunk base phloem (Brandes et al. 2006). In a comparable way as for the primary assimilates in the leaves, the sugars leaking out of the phloem will be used as substrates for different metabolic conversions (see Fig. 13.1). Assuming that the produced non-exported compounds (i.e. lignin) are  $^{13}\text{C}$ -depleted compared to the original sugar substrates originating from the phloem, the unreacted sugars, reloaded into the phloem, will be  $^{13}\text{C}$ -enriched. The continuous unloading, metabolic conversion and reloading of unreacted sugars would consequently lead to an enrichment of phloem transported sucrose in basipetal direction. Such an enrichment is not always observed, sometimes occurs only between branch and trunk phloem but not along the trunk (Bögelein et al. 2019), or is detected only during particular periods of the growing season (Gessler et al. 2004). To understand such differences, a complete isotopic mass balance taking into account the  $\delta^{13}\text{C}$  phloem sugars as well as the  $\delta^{13}\text{C}$  of non-exported compounds over the growing season would be extremely useful.

### 13.4 The Hidden Stem Metabolism: Bark Photosynthesis, Stem Respiration, and the Role of Carbon Re-fixation

Tree ring wood or cellulose has been shown to differ in the carbon isotopic composition from the phloem sugars, which are thought to be the source for cellulose formation. In general, an enrichment between 1 and 2‰ has been observed (Gessler et al. 2009a; Wei et al. 2014). Thus, wood formation can be also affected by different fractionations associated to stem metabolism (see Fig. 13.1). Firstly, bark photosynthesis and re-fixation of stem-respired CO<sub>2</sub> have a significant effect on total tree carbon balance (Pfanz et al. 2002). In angiosperm trees, it has been estimated that 30–90% of the CO<sub>2</sub> respired in the stem could be re-fixed (Pfanz et al. 2002; Hilman et al. 2018), and *ca.* 25% of re-fixation has been also reported in the upper stem of Scots pine (Tarvainen et al. 2018). Bark photosynthesis is widely found in young twigs and branches, but in the main stem it seems to be restricted to species with thin (<8 mm) outer bark (Rosell et al. 2015; Tarvainen et al. 2018). During bark photosynthesis, the main source of CO<sub>2</sub> is stem respiration, which is <sup>13</sup>C-depleted as compared to ambient air, and photosynthesis further discriminates against <sup>13</sup>C (Cernusak et al. 2001). CO<sub>2</sub> re-fixation may also occur in non-photosynthetic bark, mainly driven by phosphoenol pyruvate carboxylase (PEPC), thus resulting in <sup>13</sup>C-enriched products (Cernusak et al. 2009), although this could be compensated by the use of a <sup>13</sup>C-depleted substrate (stem-respired CO<sub>2</sub>). An additional source of uncertainty is the role of xylem sap as a CO<sub>2</sub> carrier, potentially allowing the re-fixation of root-respired CO<sub>2</sub> in the trunk (Bloemen et al. 2013). Nevertheless, given the tight association found between bark photosynthesis and both phloem load and xylem refilling (De Baerdemaeker et al. 2017; Konrad et al. 2018; Liu et al. 2019), it is likely that bark photosynthates are mainly used to force changes in osmotic pressure in the xylem and phloem sap, rather than to build new tissues. Therefore, although significant for the whole-plant carbon balance and potentially also for branch growth (Cernusak and Hutley 2011), so far there is no clear evidence that these processes contribute to wood formation in the main stem.

Another metabolic process that may affect the isotope signal in the wood is respiratory isotope fractionation (Ghashghaie et al. 2003). Pyruvate dehydrogenase (PDH) and key enzymes in the Krebs cycle may cause kinetic isotopic effects, but they cannot explain alone the observed respiratory fractionation (Werner et al. 2011). PDH and the Krebs cycle also provide substrates for the shikimate pathway, and thus may affect the isotopic signature of (depleted) lignin precursors (Hobbie and Werner 2004). Depending on the demand of different products, PEPC re-fixation may contribute with malate to the Krebs cycle, in order to restore temporal metabolic imbalances, thus resulting in <sup>13</sup>C-enriched respired CO<sub>2</sub> (Cernusak et al. 2009; Gessler et al. 2009b). These metabolic changes appear as the best explanation for observed diel cycles in the relative enrichment of stem-respired CO<sub>2</sub>, which becomes negatively correlated with respiration rates (Kodama et al. 2008). Although a direct connection with wood δ<sup>13</sup>C is not clear, respiratory fractionation may have an indirect effect on

the remaining substrates for wood formation (Eglin et al. 2010; Rinne et al. 2015; Vincent-Barbaroux et al. 2019).

Stem metabolism may also play a role in the seasonal pattern of  $\delta^{13}\text{C}$ . Only recently, Budzinski et al. (2016) reported large seasonal variation in expressed transcripts, proteins and metabolites in the bark of *Eucalyptus grandis*. For example, they found that during the wet summer the expression of cytosolic 1–6-Fructose biphosphate aldolase and PEPC increased, together with the accumulation of organic acids (malate, fumarate). This suggests a larger relative contribution of PEPC-derived malate to the Krebs cycle, which contributes to the aforementioned  $^{13}\text{C}$  enrichment in respired  $\text{CO}_2$  (Cernusak et al. 2009; Gessler et al. 2009b). Conversely, during the dry winter, both, sugars (sucrose, fructose, glucose) and secondary metabolites (shikimate, taxifolin) tended to accumulate in the bark. Hence, this is likely a period when isotopic signatures of lignin precursors are formed, and these precursors subsequently accumulate at the onset of cambium initiation (Förster et al. 2000). Evidence so far indicates that the environmental signal stored in lignin is comparable to that in cellulose, but in agreement with these metabolic changes, lignin  $\delta^{13}\text{C}$  seems to be more sensitive to early-season temperature (Loader et al. 2003; Ferrio and Voltas 2005; Gori et al. 2013).

### 13.5 Imprint of Storage and Remobilization on the Intra-annual Variation in Tree Rings

As pointed above, starch-derived carbon is  $^{13}\text{C}$ -enriched, as compared to primary assimilates (Rossmann et al. 1991; Gleixner and Schmidt 1997). Therefore, seasonal variations in the contribution of stored carbon to growth may lead to intra-annual  $\delta^{13}\text{C}$  patterns that are not linked to leaf-level processes (Helle and Schleser 2004; Eglin et al. 2010; Offermann et al. 2011). Helle and Schleser (2004) first proposed the existence of three phases in the seasonal evolution of tree-ring  $\delta^{13}\text{C}$ . Phase 1 shows the highest seasonal values for  $\delta^{13}\text{C}$ , indicative of the incorporation of starch-derived carbon into the growing tissue (both leaves and wood). This has been consistently observed in a range of deciduous broadleaves (Fig. 13.2b–d; see also Helle and Schleser 2004; Eglin et al. 2010; Schollaen et al. 2014). During this phase, Eglin et al. (2010) further interpreted the initial increase in  $\delta^{13}\text{C}$  as a transition from stored soluble sugars to stored starch. After this peak, Phase 2 shows a decline in wood  $\delta^{13}\text{C}$ , in many cases opposing the expected positive effect on  $\delta^{13}\text{C}$  of increasing water deficit from spring to summer. This has been interpreted as a transition from (enriched) storage to (more depleted) current assimilates as the main source of carbon in the wood (Helle and Schleser 2004, Eglin et al. 2010), and is supported by an increase in phloem sugar concentration (Offermann et al. 2011). According to Helle and Schleser (2004), during Phase 3 the source strength of leaves is reduced due to leaf senescence, and wood formation again relies more on stored carbon, thus becoming enriched. However, this late-season increase is less consistent across studies, and most likely

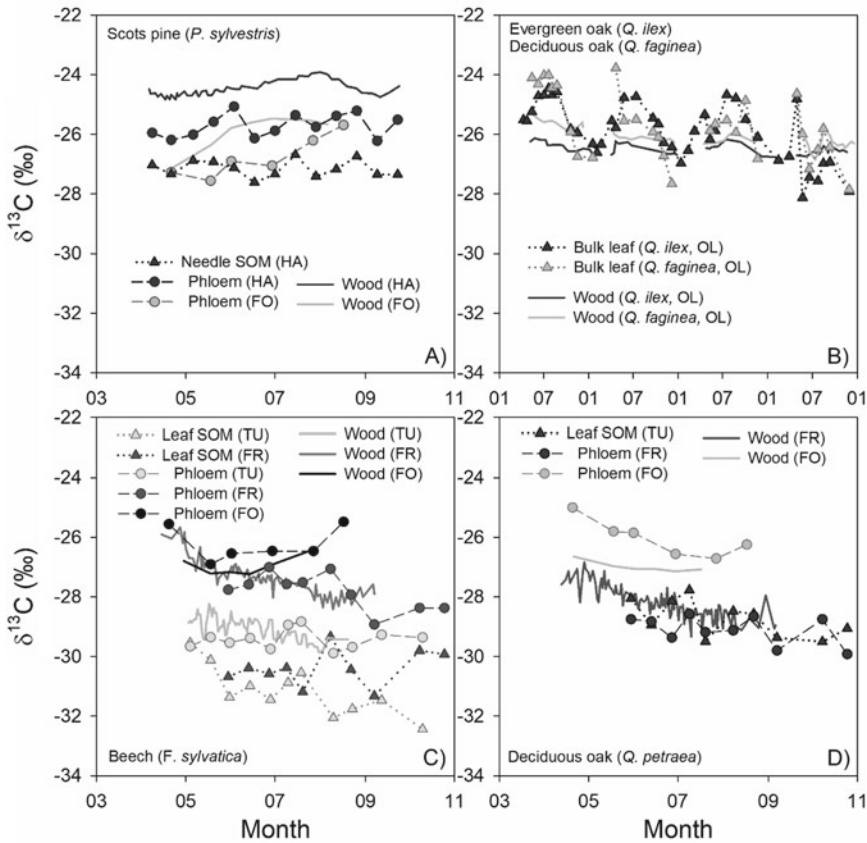


**Fig. 13.2** Seasonal trends and offsets in carbon isotope composition ( $\delta^{13}\text{C}$ ) from leaves (triangles, dotted lines) to stem phloem (circles, dashed lines) and whole wood (solid lines) in different tree species and locations. Note that the scaling of X axis in panel B is different. **a** Scots pine (*Pinus sylvestris* L.) in Hartheim, SW Germany (HA) and Fontainebleau, N France (FO). **b** holm oak (*Quercus ilex* L., Subsp. *ballota*) and the portuguese oak (*Quercus faginea* Lam.) in Oliola, SE Spain (OL). **c** Beech (*Fagus sylvatica* L.) in Freiburg-Zähringen, SW Germany (FR), Tuttlingen, SW Germany (TU) and FO. **d** Sessile oak (*Quercus petraea* (Matt.) Liebl.) in FR and FO. SOM, water soluble organic matter. Sampling years and data source for each site: HA, year 2004, (Brandes et al. 2006; Gessler et al. 2009a); TU, year 2007, (Offermann et al. 2011); FR, year 2007, Ferrio, Offermann, Gessler, unpublished; OL, years 2005–2008 (leaf data: Aguilera et al. 2010; whole wood data: Aguilera, Ferrio, Voltas, unpublished); FO, year 2009, (Michelot 2011)

depends on the interaction between wood and leaf phenology. In some cases, leaf senescence begins well after the end of wood growth, and thus cannot be reflected in the tree rings (e.g. Aguilera et al. 2010; Eglin et al. 2010; Offermann et al. 2011). Under such conditions, Phase 3 would be a period of predominant use of current assimilates, during which wood variations would respond mainly to environmental conditions (Eglin et al. 2010; Offermann et al. 2011). Still seasonal variation in

photosynthetic discrimination might additionally influence such intra-annual patterns in tree rings.

In evergreens, seasonal shifts between storage and current-assimilates are not so evident, neither in conifers (Fig. 13.2a; see also Barbour et al. 2002; Klein et al. 2005; Sarris et al. 2013; Schollaen et al. 2014), nor in the few evergreen angiosperms studied so far (Fig. 13.2b; see also Battipaglia et al. 2010; Schubert and Timmermann 2015; Vincent-Barbaroux et al. 2019). This further supports the interpretation of the early-season  $\delta^{13}\text{C}$  peak in deciduous trees as a starch signature. Whereas deciduous species depend on stored carbon during the initial stages of wood formation (Kagawa et al. 2006; Klein et al. 2016; Andrianantenaina et al. 2019), evergreens would be able to rely more on current assimilates (Ogé et al. 2009; Klein and Hoch 2015). Regarding deciduous conifers (e.g. larch), the few studies performed so far show contradictory results. Kagawa et al. (2006), following an isotope-labelling approach, estimated that about 40% of the carbon used in wood formation was derived from previous-year photoassimilates. Conversely, Rinne et al. (2015) found a good agreement between exported sucrose and tree-rings, concluding that, similar to evergreen conifers, storage dynamics had little effect on the intra-annual patterns.

In summary, intra-annual trends in deciduous broadleaf trees are largely dominated by storage dynamics, whereas evergreen species, and particularly conifers, seem to track the seasonal response of current assimilates. Besides seasonal cycles linked to leaf phenology, the existence of periods of stress (e.g. summer drought) during the growing season might also force a major reliance on stored carbon (Sarris et al. 2013; Klein and Hoch 2015; Hentschel et al. 2016). However, wood growth is also restricted under stress, and therefore severe stress episodes often result in temporal gaps in the wood archive (see e.g. Sarris et al. 2013; Forner et al. 2014). Nevertheless, and regardless of leaf habit, there is increasing evidence of the existence of soluble carbon pools of mixed age within the stem, which could eventually contribute to wood formation (Muhr et al. 2015; Trumbore et al. 2015; Klein et al. 2016).

In the near future, recent technical advances like laser ablation and microdissection are likely to facilitate the construction of high-resolution intra-annual records in tree-rings (Schollaen et al. 2014; Rinne et al. 2015; see also Chap. 7). However, one key limitation in our understanding of the link between leaf and wood seasonal trends remains unsolved, and that is the need of an accurate dating of wood and carbon deposition in the tree ring. Although stem increment can be estimated from dendrometer records, carbon deposition may lag over one month girth growth (Cuny et al. 2015; Andrianantenaina et al. 2019; for further discussion see Chap. 15). So far, repeated sampling of microcores appears as the most reliable way to characterize xylogenesis, but is time-consuming and destructive (Cuny et al. 2015; De Micco et al. 2019). Further research should focus on the characterization of the link between xylogenesis, carbon deposition and stem growth, in order to develop alternative approaches for intra-annual tree dating.



### 13.6 Intra-molecular Isotope Distribution in Wood Tissues

Most of the organic carbon in plants is due to the CO<sub>2</sub> fixation by RubisCo in the leaves (but see PEPC carbon fixation above). The RubisCo mediated reaction adds one single C-atom from CO<sub>2</sub> to the acceptor molecule ribulose-1,5-bisphosphate and due to the cyclic nature of the Calvin cycle the acceptor is regenerated. Since (almost) all organic carbon originates from this process the variations in the fractionation related to this step (i.e. photosynthetic carbon discrimination; see Chap. 9) explain variations in the  $\delta^{13}\text{C}$  of the whole molecules synthesized (i.e., triose-phosphates, sugars) but cannot cause intra-molecular differences in  $\delta^{13}\text{C}$ . Rossmann et al. (1991) showed for the first time evidence of such non-statistical intramolecular <sup>13</sup>C isotope distribution in starch and sugars and Gilbert et al. (2012) provided an extensive review on the potential underlying mechanisms. Only recently, intramolecular patterns were also observed in the glucose units of tree-ring cellulose (Wieloch et al. 2018).

Post-photosynthetic carbon isotope fractionation related to enzyme reactions that occur at individual C positions within metabolites are able to imprint position-specific carbon isotope differences. Rossmann et al. (1991) as well as Hobbie and Werner (2004) assumed this intramolecular <sup>13</sup>C distribution, with a strong enrichment in the C-4 position of glucose, to be due to the aldolase and transketolase reactions in the Calvin cycle. Tcherkez et al. (2004) developed a model that takes into account the isotope effects of C–C bond-breaking reactions (including aldolase and transketolase) of the Calvin cycle, which consequently lead to a mathematical expression for the isotope ratios in hexoses in the steady state. The assumptions made in this model were verified by assessing day-night differences in leaf and phloem sugars (Gessler et al. 2008). Theoretically, changes in metabolite allocation to a metabolic pathway that includes branching point(s) can change the intramolecular <sup>13</sup>C pattern. At such isotope-sensitive metabolic branching point, enzyme-related isotope effects might be more or less expressed depending how much substrate is allocated to the branches of the pathways. Thus, environmental factors that cause shifts in metabolic pathway commitment might affect intramolecular <sup>13</sup>C distributions. Thus, any shift in intramolecular <sup>13</sup>C distributions in sugar moieties laid down in the tree archives is assumed to reflect such shifts in metabolic branching. In fact, Wieloch et al. (2018) found temporal variability in the intramolecular <sup>13</sup>C pattern of glucose units of cellulose across a 34 year-long tree ring series. They could also show that intramolecular <sup>13</sup>C abundances can give a purer signal of photosynthetic isotope discrimination and a better estimate of VPD than the whole molecule. This was mainly attributed to the fact that the molecule averaged signal is strongly influenced by both, variation in photosynthetic and post-photosynthetic fractionation, while mainly the C-1 to C-3 position of glucose captures the photosynthetic signal. Moreover, position-specific <sup>13</sup>C analysis in tree rings might allow for distinguishing environmental effects on photosynthetic gas exchange (via photosynthetic fractionation) from effects on downstream metabolism (via postphotosynthetic fractionation). At the downside,

measurements of intramolecular  $^{13}\text{C}$  abundances are time consuming and limited to small sample sets but the analytical advancements in future might make this approach feasible for higher throughput analysis (see Wieloch et al. 2018).

### 13.7 Can We Actually Assess Water Use Efficiency from Tree-Ring $\delta^{13}\text{C}$ ?

The link between leaf-level processes and wood  $\delta^{13}\text{C}$  is not straightforward, but with some caution we still can retrieve a relevant environmental/physiological signal. In this regard,  $\delta^{13}\text{C}$  in tree rings has been widely used as a proxy for variations in intrinsic water use efficiency (iWUE) across time, space, or genetic populations (e.g. Saurer et al. 2004; Del Castillo et al. 2013; Fardusi et al. 2016) (for further insight into iWUE see Chap. 17). However, the fractionation processes discussed in this chapter may hinder the physiological interpretation of wood or cellulose  $\delta^{13}\text{C}$ , particularly those linked to carbon partition and storage/remobilization patterns. This is particularly relevant for the interpretation of intra-annual variation, but may also have an imprint on a multi-year scale, partly explaining the drought-legacy often reported after extreme dry events (Sarris et al. 2013; Del Castillo et al. 2015; Hentschel et al. 2016). Evidence so far suggests that deciduous species are more affected by storage-remobilization processes than evergreens, and angiosperms more than gymnosperms (Ogée et al. 2009; Eglin et al. 2010; Rinne et al. 2015; Vincent-Barbaroux et al. 2019). This fits well with our knowledge on their use of carbon resources (Hoch et al. 2003) and early empirical observations of a stronger current-year signal in latewood than in earlywood for deciduous trees (Loader et al. 1995). As a consequence, a single-substrate mechanistic model may be enough to explain seasonal and inter-annual trends in evergreen conifers (Ogée et al. 2009), but more complex models are needed to explain isotope variations in deciduous trees (Eglin et al. 2010; Offermann et al. 2011; Rinne et al. 2015). Overall, although the imprint of photosynthetic discrimination is retained in the isotope signature of tree-rings, physiological information tends to be dampened as compared to the leaves (Roden and Farquhar 2012; Gessler et al. 2014; Fardusi et al. 2016). On top of that, fractionation processes can be modelled with reasonable accuracy, but their magnitude seems to be species- and site- specific (see e.g. Fig. 13.2). Therefore, trends in iWUE can be tracked using  $\delta^{13}\text{C}$  in tree rings, but without external validation it is not advisable to compare absolute estimates of intrinsic water use efficiency based on tree rings, e.g. among contrasting species or sites. Current advances in position-specific isotope analysis may offer in the future an alternative to overcome (or at least to better account for) post-photosynthetic fractionation, allowing to retrieve a 'clean' leaf-derived signal (Wieloch et al. 2018).

## References

- Aguilera M, Voltas J, Ferrio JP, Serrano L (2010) Evolución estacional de  $\delta^{13}\text{C}$  en hojas y madera de dos quercíneas mediterráneas concurrentes (*Quercus ilex* subsp. *ballota* L. y *Quercus faginea* Lam.): dinámica. *Ecosistemas* 19:6–13
- Andrianantenaina AN, Rathgeber CBK, Pérez-de-Lis G, Cuny H, Ruelle J (2019) Quantifying intra-annual dynamics of carbon sequestration in the forming wood: a novel histologic approach. *Ann For Sci* 76:1–12
- Badeck FW, Tcherkez G, Nogues S, Piel C, Ghashghaie J (2005) Post-photosynthetic fractionation of stable carbon isotopes between plant organs—a widespread phenomenon. *Rapid Commun Mass Spectrom* 19:1381–1391
- Barbour M, Song X (2014) Do tree-ring stable isotope compositions faithfully record tree carbon/water dynamics? *Tree Physiol* 34:792–795
- Barbour MM, Walcroft AS, Farquhar GD (2002) Seasonal variation in delta C-13 and delta O-18 of cellulose from growth rings of *Pinus radiata*. *Plant Cell Environ* 25:1483–1499
- Battipaglia G, Cherubini P, De Micco V, Aronne G, Brand WA, Linke P, Saurer M (2010) Variations of vessel diameter and  $\delta^{13}\text{C}$  in false rings of *Arbutus unedo* L. reflect different environmental conditions. *New Phytol* 188:1099–1112
- Bloemen J, Mcguire MA, Aubrey DP, Teskey RO, Steppe K (2013) Transport of root-respired  $\text{CO}_2$  via the transpiration stream affects aboveground carbon assimilation and  $\text{CO}_2$  efflux in trees. *New Phytol* 555–565
- Bögelein R, Lehmann MM, Thomas FM (2019) Differences in carbon isotope leaf-to-phloem fractionation and mixing patterns along a vertical gradient in mature European beech and Douglas fir. *New Phytol* 222:1803–1815
- Brandes E, Kodama N, Whittaker K, Weston C, Rennenberg H, Keitel C, Adams MA, Gessler A (2006) Short-term variation in the isotopic composition of organic matter allocated from the leaves to the stem of *Pinus sylvestris*: effects of photosynthetic and postphotosynthetic carbon isotope fractionation. *Glob Chang Biol* 12:1922–1939
- Budzinski IGF, Moon DH, Morosini JS, Lindén P, Bragatto J, Moritz T, Labate CA (2016) Integrated analysis of gene expression from carbon metabolism, proteome and metabolome, reveals altered primary metabolism in *Eucalyptus grandis* bark, in response to seasonal variation. *BMC Plant Biol* 16:1–15
- Cernusak LA, Hutley LB (2011) Stable isotopes reveal the contribution of cortical photosynthesis to growth in branches of *Eucalyptus miniata*. *Plant Physiol* 155:515–523
- Cernusak LA, Marshall JD, Comstock JP, Balster NJ (2001) Carbon isotope discrimination in photosynthetic bark RID A-6859-2011. *Oecologia* 128:24–35
- Cernusak LA, Tcherkez G, Keitel C, Cornwell WK, Santiago LS, Knohl A, Barbour MM, Williams DG, Reich PB, Ellsworth DS, Dawson TE, Griffiths HG, Farquhar GD, Wright IJ (2009) Viewpoint: why are non-photosynthetic tissues generally C-13 enriched compared with leaves in C-3 plants? Review and synthesis of current hypotheses. *Funct Plant Biol* 36:199–213
- Cernusak LA, Ubierna N, Winter K, Holtum JAM, Marshall JD, Farquhar GD (2013) Environmental and physiological determinants of carbon isotope discrimination in terrestrial plants. *New Phytol* 200:950–965
- Cuny HE, Rathgeber CBK, Frank D, Fonti P, Mäkinen H, Prislán P, Rossi S, del Castillo EM, Campelo F, Vavřík H et al (2015) Woody biomass production lags stem-girth increase by over one month in coniferous forests. *Nature Plants* 1:15160
- De Baerdemaeker NJF, Salomón RL, De Roo L, Steppe K (2017) Sugars from woody tissue photosynthesis reduce xylem vulnerability to cavitation. *New Phytol* 216:720–727
- De Micco V, Carrer M, Rathgeber CBK, Julio Camarero J, Voltas J, Cherubini P, Battipaglia G (2019) From xylogenesis to tree rings: wood traits to investigate tree response to environmental changes. *IAWA J* 40:155–182

- Del Castillo J, Aguilera M, Voltas J, Ferrio JP (2013) Isoscapes of tree-ring carbon-13 perform like meteorological networks in predicting regional precipitation patterns. *J Geophys Res Biogeosci* 118:352–360
- Del Castillo J, Voltas J, Ferrio JP (2015) Carbon isotope discrimination, radial growth, and NDVI share spatiotemporal responses to precipitation in Aleppo pine. *Trees Struct Funct* 29:223–233
- Eglin T, Francois C, Michelot A, Delpierre N, Damesin C (2010) Linking intra-seasonal variations in climate and tree-ring  $\delta^{13}\text{C}$ : a functional modelling approach. *Ecol Model* 221:1779–1797
- Fardusi MJ, Ferrio JP, Comas C, Voltas J, Resco de Dios V, Serrano L (2016) Intra-specific association between carbon isotope composition and productivity in woody plants: a meta-analysis. *Plant Sci* 251:110–118
- Farquhar GD, O'Leary MH, Berry JA (1982) On the relationship between carbon isotope discrimination and the inter-cellular carbon-dioxide concentration in leaves. *Aust J Plant Physiol* 9:121–137
- Ferrio JP, Voltas J (2005) Carbon and oxygen isotope ratios in wood constituents of *Pinus halepensis* as indicators of precipitation, temperature and vapour pressure deficit. *Tellus B Chem Phys Meteorol* 57:164–173
- Forner A, Aranda I, Granier A, Valladares F (2014) Differential impact of the most extreme drought event over the last half century on growth and sap flow in two coexisting Mediterranean trees. *Plant Ecol* 215:703–719
- Förster H, Steeves V, Pommer U, Savidge RA (2000) UDPG: coniferyl alcohol glucosyltransferase and coniferin biosynthesis—a regulatory link to seasonal cambial growth in conifers. In: Savidge RA, Barnett JR, Napier R (eds) *Cell and molecular biology of wood formation*. BIOS Scientific Publishers Ltd., Oxford, U.K., pp 189–201
- Gessler A, Rennenberg H, Keitel C (2004) Stable isotope composition of organic compounds transported in the phloem of European beech—evaluation of different methods of phloem sap collection and assessment of gradients in carbon isotope composition during leaf-to-stem transport. *Plant Biol* 6:721–729
- Gessler A, Keitel C, Kodama N, Weston C, Winters AJ, Keith H, Grice K, Leuning R, Farquhar GD (2007)  $\delta^{13}\text{C}$  of organic matter transported from the leaves to the roots in *Eucalyptus delegatensis*: short-term variations and relation to respired  $\text{CO}_2$ . *Funct Plant Biol* 34:692–706
- Gessler A, Tcherkez G, Peuke AD, Ghashghaie J, Farquhar GD (2008) Experimental evidence for diel variations of the carbon isotope composition in leaf, stem and phloem sap organic matter in *Ricinus communis*. *Plant Cell Environ* 31:941–953
- Gessler A, Tcherkez G, Karyanto O, Keitel C, Ferrio JP, Ghashghaie J, Kreuzwieser J, Farquhar GD (2009) On the metabolic origin of the carbon isotope composition of  $\text{CO}_2$  evolved from darkened light-acclimated leaves in *Ricinus communis*. *New Phytol* 181:374–386
- Gessler A, Brandes E, Buchmann N, Helle G, Rennenberg H, Barnard RL (2009) Tracing carbon and oxygen isotope signals from newly assimilated sugars in the leaves to the tree-ring archive. *Plant Cell Environ* 32:780–795
- Gessler A, Ferrio JP, Hommel R, Treydte K, Werner RA, Monson RK (2014) Stable isotopes in tree rings: towards a mechanistic understanding of isotope fractionation and mixing processes from the leaves to the wood. *Tree Physiol* 34:796–818
- Ghashghaie J, Badeck FW, Lanigan G, Nogués S, Tcherkez G, Deléens E, Cornic G, Griffiths H (2003) Carbon isotope fractionation during dark respiration and photorespiration in  $\text{C}_3$  plants. *Phytochem Rev* 2:145–161
- Gilbert A, Silvestre V, Robins RJ, Remaud GS, Tcherkez G (2012) Biochemical and physiological determinants of intramolecular isotope patterns in sucrose from  $\text{C}_3$ ,  $\text{C}_4$  and CAM plants accessed by isotopic  $^{13}\text{C}$  NMR spectrometry: a viewpoint. *Nat Prod Rep* 29:476–486
- Gleixner G, Schmidt HL (1997) Carbon isotope effects on the fructose-1,6-bisphosphate aldolase reaction, origin for non-statistical C-13 distributions in carbohydrates. *J Biol Chem* 272:5382–5387

- Gori Y, Wehrens R, Greule M, Keppler F, Ziller L, La Porta N, Camin F (2013) Carbon, hydrogen and oxygen stable isotope ratios of whole wood, cellulose and lignin methoxyl groups of *Picea abies* as climate proxies. *Rapid Commun Mass Spectrom* 27:265–275
- Harmer SL, Hogenesch JB, Straume M, Chang H-S, Han B, Zhu T, Wang X, Kreps JA, Kay SA (2000) Orchestrated transcription of key pathways in *Arabidopsis* by the circadian clock. *Science* 290:2110–2113
- Helle G, Schleser GH (2004) Beyond CO<sub>2</sub>-fixation by Rubisco—an interpretation of <sup>13</sup>C/<sup>12</sup>C variations in tree rings from novel intra-seasonal studies on broad-leaf trees. *Plant Cell Environ* 27:367–380
- Hentschel R, Hommel R, Poschenrieder W, Grote R, Holst J, Biernath C, Gessler A, Priesack E (2016) Stomatal conductance and intrinsic water use efficiency in the drought year 2003: a case study of European beech. *Trees Struct Funct* 30:153–174
- Hilman B, Muhr J, Trumbore SE, Carbone MS, Yuval P, Wright SJ, Moreno G, Pérez-Priego O, Migliavacca M, Carrara A, et al (2018) Comparison of CO<sub>2</sub> and O<sub>2</sub> fluxes demonstrate retention of respired CO<sub>2</sub> in tree stems from a range of tree species. *Biogeosciences Discuss* 1–30
- Hobbie EA, Werner RA (2004) Intramolecular, compound-specific, and bulk carbon isotope patterns in C-3 and C-4 plants: a review and synthesis. *New Phytol* 161:371–385
- Hoch G, Richter A, Korner C (2003) Non-structural carbon compounds in temperate forest trees. *Plant Cell Environ* 26:1067–1081
- Jensen KH, Liesche J, Bohr T, Schulz A (2012) Universality of phloem transport in seed plants. *Plant Cell Environ* 35:1065–1076
- Kagawa A, Sugimoto A, Maximov TC (2006) Seasonal course of translocation, storage and remobilization of <sup>13</sup>C pulse-labeled photoassimilate in naturally growing *Larix gmelinii* saplings. *New Phytol* 171:793–804
- Klein T, Hoch G (2015) Tree carbon allocation dynamics determined using a carbon mass balance approach. *New Phytol* 205:147–159
- Klein T, Hemming D, Lin T, Grünzweig JM, Maseyk K, Rotenberg E, Yakir D (2005) Association between tree-ring and needle  $\delta^{13}\text{C}$  and leaf gas exchange in *Pinus halepensis* under semi-arid conditions. *Oecologia* 144:45–54
- Klein T, Vitasse Y, Hoch G (2016) Coordination between growth, phenology and carbon storage in three coexisting deciduous tree species in a temperate forest. *Tree Physiol* 36:847–855
- Kodama N, Barnard R, Salmon Y, Weston C, Ferrio JP, Holst J, Werner RA, Saurer M, Rennenberg H, Buchmann N, Gessler A (2008) Temporal dynamics of the carbon isotope composition in a *Pinus sylvestris* stand: from newly assimilated organic carbon to respired carbon dioxide. *Oecologia* 156:737–750
- Konrad W, Katul G, Roth-nebelsick A, Jensen KH (2018) Xylem functioning, dysfunction and repair: a physical perspective and implications for phloem transport. *Tree Physiol* 243–261
- Lehmann MM, Ghiasi S, George GM, Cormier M-A, Gessler A, Saurer M, Werner RA (2019) Influence of starch deficiency on photosynthetic and post-photosynthetic carbon isotope fractionations. *J Exp Bot* 70:1829–1841
- Liu J, Qian Y, Gu L, Wan X, Sun Z (2019) Corticular photosynthesis drives bark water uptake to refill embolized vessels in dehydrated branches of *Salix matsudana*. 1–13
- Loader NJ, Switsur VR, Field EM (1995) High-resolution stable isotope analysis of tree rings: implications of ‘microdendroclimatology’ for palaeoenvironmental research. *Holocene* 5:457–460
- Loader NJ, Robertson I, McCarroll D (2003) Comparison of stable carbon isotope ratios in the whole wood, cellulose and lignin of oak tree-rings. *Palaeogeogr Palaeoclimatol Palaeoecol* 196:395–407
- Lüttge U (2006) Photosynthetic flexibility and ecophysiological plasticity: questions and lessons from *Clusia*, the only CAM tree, in the neotropics. *New Phytol* 171:7–25
- Marshall JD, Monserud RA (2006) Co-occurring species differ in tree-ring  $\delta^{18}\text{O}$  trends. *Tree Physiol* 26:1055–1066
- McCarroll D, Loader NJ (2004) Stable isotopes in tree rings. *Quat Sci Rev* 23:771–801

- Michelot A (2011) Growth and ring  $\delta^{13}\text{C}$  of three temperate forest species (*Fagus sylvatica*, *Quercus petraea* et *Pinus sylvestris*) under climatic variations at interannual and seasonal scales. PhD thesis, Agricultural Sciences, Université Paris Sud—Paris XI. <https://tel.archives-ouvertes.fr/tel-00652599>
- Minchin P, Thorpe M (1987) Measurement of unloading and reloading of photo-assimilate within the stem of bean. *J Exp Bot* 38:211–220
- Muhr J, Messier C, Delagrangé S, Trumbore S, Xu X, Hartmann H (2015) Rapid report how fresh is maple syrup? Sugar maple trees mobilize carbon stored several years previously during early springtime sap-ascend
- Offermann C, Ferrio JP, Holst J, Grote R, Siegwolf R, Kayler Z, Gessler A (2011) The long way down—are carbon and oxygen isotope signals in the tree ring uncoupled from canopy physiological processes? *Tree Physiol* 31:1088–1102
- Ogée J, Barbour MM, Wingate L, Bert D, Bosc A, Stievenard M, Lambrot C, Pierre M, Bariac T, Loustau D et al (2009) A single-substrate model to interpret intra-annual stable isotope signals in tree-ring cellulose. *Plant Cell Environ* 32:1071–1090
- Pearcy RW, Troughton J (1975)  $\text{C}_4$  photosynthesis in tree form *Euphorbia* species from Hawaiian rainforest sites. *Plant Physiol* 55:1054–1056
- Peuke A, Rokitta M, Zimmermann U, Schreiber L, Haase A (2001) Simultaneous measurement of water flow velocity and solute transport in xylem and phloem of adult plants of *Ricinus communis* over a daily time course by nuclear magnetic resonance spectrometry. *Plant Cell Environ* 24:491–504
- Pfanz H, Aschan G, Langenfeld-Heysler R, Wittmann C, Loose M (2002) Ecology and ecophysiology of tree stems: corticular and wood photosynthesis. *Naturwissenschaften* 89:147–162
- Rinne KT, Loader NJ, Switsur VR, Treydte KS, Waterhouse JS (2010) Investigating the influence of sulphur dioxide ( $\text{SO}_2$ ) on the stable isotope ratios ( $\delta^{13}\text{C}$  and  $\delta^{18}\text{O}$ ) of tree rings. *Geochim Cosmochim Acta* 74:2327–2339
- Rinne KT, Saurer M, Kirilyanov AV, Loader NJ, Bryukhanova MV, Werner RA, Siegwolf RTW (2015) The relationship between needle sugar carbon isotope ratios and tree rings of larch in Siberia. *Tree Physiol* 35:1192–1205
- Roden JS, Farquhar GD (2012) A controlled test of the dual-isotope approach for the interpretation of stable carbon and oxygen isotope ratio variation in tree rings. *Tree Physiol* 32:490–503
- Rogers LA, Dubos C, Cullis IF, Surman C, Poole M, Willment J, Mansfield SD, Campbell MM (2005) Light, the circadian clock, and sugar perception in the control of lignin biosynthesis. *J Exp Bot* 56:1651–1663
- Rosell JA, Castorena M, Laws CA, Westoby M (2015) Bark ecology of twigs vs. main stems: functional traits across eighty-five species of angiosperms. *Oecologia* 178:1033–1043
- Rossmann A, Butzenlechner M, Schmidt HL (1991) Evidence for a nonstatistical carbon isotope distribution in natural glucose. *Plant Physiol* 96:609–614
- Sarris D, Siegwolf R, Körner C (2013) Inter- and intra-annual stable carbon and oxygen isotope signals in response to drought in Mediterranean pines. *Agric For Meteorol* 168:59–68
- Saurer M, Aellen K, Siegwolf R (1997) Correlating  $\delta^{13}\text{C}$  and  $\delta^{18}\text{O}$  in cellulose of trees. *Plant Cell Environ* 20:1543–1550
- Saurer M, Siegwolf R, Schweingruber FH (2004) Carbon isotope discrimination indicates improving water-use efficiency of trees in northern Eurasia over the last 100 years. *Glob Chang Biol* 10:2109–2120
- Schleser GH, Helle G, Lucke A, Vos H (1999) Isotope signals as climate proxies: the role of transfer functions in the study of terrestrial archives. *Quat Sci Rev* 18:927–943
- Schollaen K, Heinrich I, Helle G (2014) UV-laser-based microscopic dissection of tree rings—a novel sampling tool for  $\delta^{13}\text{C}$  and  $\delta^{18}\text{O}$  studies. *New Phytol* 201:1045–1055
- Schubert BA, Timmermann A (2015) Reconstruction of seasonal precipitation in Hawai'i using high-resolution carbon isotope measurements across tree rings. *Chem Geol* 417:273–278
- Solomon OL, Berger DK, Myburg AA (2010) Diurnal and circadian patterns of gene expression in the developing xylem of *Eucalyptus* trees. *S Afr J Bot* 76:425–439

- Steppe K, Sterck F, Deslauriers A (2015) Diel growth dynamics in tree stems: linking anatomy and ecophysiology. *Trends Plant Sci* 20:335–343
- Tarvainen L, Wallin G, Lim H, Linder S, Oren R, Löfvenius MO, Råntfors M, Tor-Ngern P, Marshall J (2018) Photosynthetic refixation varies along the stem and reduces CO<sub>2</sub> efflux in mature boreal *Pinus sylvestris* trees. *Tree Physiol* 38:558–569
- Tcherkez G, Farquhar G, Badeck F, Ghashghaie J (2004) Theoretical considerations about carbon isotope distribution in glucose of C-3 plants. *Funct Plant Biol* 31:857–877
- Tcherkez G, Ghashghaie J, Griffiths H (2007) Methods for improving the visualization and deconvolution of isotopic signals. *Plant Cell Environ* 30:887–891
- Trumbore S, Czimeczik CI, Sierra CA, Muhr J, Xu X (2015) Non-structural carbon dynamics and allocation relate to growth rate and leaf habit in California oaks. *Tree Physiol* 35:1206–1222
- Van Bel AJE (2003) The phloem, a miracle of ingenuity. *Plant Cell Environ* 26:125–149
- Vincent-Barbaroux C, Berveiller D, Lelarge-Trouverie C, Maia R, Máguas C, Pereira J, Chaves MM, Damesin C (2019) Carbon use strategies in stem radial growth of two oak species, one temperate deciduous and one Mediterranean evergreen: what can be inferred from seasonal variations in the  $\delta^{13}\text{C}$  of the current year ring? *Tree Physiol* 1–13
- Wei L, Marshall JD, Link TE, Kavanagh KL, Du E, Pangle RE, Gag PJ, Ubierna N (2014) Constraining 3-PG with a new  $\delta^{13}\text{C}$  submodel: a test using the  $\delta^{13}\text{C}$  of tree rings. *Plant Cell Environ* 37:82–100
- Weise SE, Weber APM, Sharkey TD (2004) Maltose is the major form of carbon exported from the chloroplast at night. *Planta* 218:474–482
- Werner RA, Buchmann N, Siegwolf R, Kornexl B, Gessler A (2011) Metabolic fluxes, carbon isotope fractionation and respiration—lessons to be learned from plant biochemistry. *New Phytol* 191:10–15
- Wieloch T, Ehlers I, Yu J, Frank D, Grabner M, Gessler A, Schleucher J (2018) Intramolecular  $^{13}\text{C}$  analysis of tree rings provides multiple plant ecophysiology signals covering decades. *Sci Rep* 8:5048

**Open Access** This chapter is licensed under the terms of the Creative Commons Attribution 4.0 International License (<http://creativecommons.org/licenses/by/4.0/>), which permits use, sharing, adaptation, distribution and reproduction in any medium or format, as long as you give appropriate credit to the original author(s) and the source, provide a link to the Creative Commons license and indicate if changes were made.

The images or other third party material in this chapter are included in the chapter's Creative Commons license, unless indicated otherwise in a credit line to the material. If material is not included in the chapter's Creative Commons license and your intended use is not permitted by statutory regulation or exceeds the permitted use, you will need to obtain permission directly from the copyright holder.



**Part IV**  
**Physiological Interpretations**



# Chapter 14

## Limits and Strengths of Tree-Ring Stable Isotopes



**Laia Andreu-Hayles, Mathieu Lévesque, Rossella Guerrieri,  
Rolf T. W. Siegwolf, and Christian Körner**

**Abstract** This chapter aims at summarizing strengths and caveats on the suitability of stable carbon and oxygen isotopes in tree rings as recorders for fingerprints of environmental influences. First, environmental constraints limiting tree growth and shaping tree species distribution worldwide are discussed. Second, examples are presented for environmental conditions under which tree-ring isotopes record environmental signals particularly well, but also cases where physiological processes can mask climate signals. Third, the link between leaf-level carbon assimilation and the investment of assimilates in the stem during the annual ring formation are discussed in light of the resulting deviations of the isotopic values between leaves and tree rings. Finally, difficulties and pitfalls in the interpretation of stable isotope signals in tree rings are reviewed. These problems often result from a poor understanding of when and how the tree canopy, stems and roots are physiologically interconnected. Current literature suggests that photosynthesis and radial growth are only loosely coupled, if at all, challenging the interpretation of environmental signals recorded in

---

L. Andreu-Hayles (✉)

Lamont-Doherty Earth Observatory of Columbia University, Palisades, NY 10964, USA

e-mail: [lah@ldeo.columbia.edu](mailto:lah@ldeo.columbia.edu)

CREAF, Bellaterra (Cerdanyola del Vallés), Barcelona, Spain

L. Andreu-Hayles · R. Guerrieri

ICREA, Pg. Lluís Companys 23, Barcelona, Spain

M. Lévesque

Forest Ecology, Institute of Terrestrial Ecosystems, Department of Environmental Systems Science, ETH Zurich, 8092 Zurich, Switzerland

R. Guerrieri

Forest Ecology Lab, Department of Agricultural and Food Sciences, University of Bologna, 40127 Bologna, Italy

R. T. W. Siegwolf

Swiss Federal Institute for Forest, Snow and Landscape Research WSL, Birmensdorf, Switzerland

Lab of Atmospheric Chemistry, Paul Scherrer Institute, Villigen, Switzerland

C. Körner

Department of Environmental Sciences, University of Basel, Basel, Switzerland

© The Author(s) 2022

R. T. W. Siegwolf et al. (eds.), *Stable Isotopes in Tree Rings*, Tree Physiology 8,  
[https://doi.org/10.1007/978-3-030-92698-4\\_14](https://doi.org/10.1007/978-3-030-92698-4_14)

tree-ring isotopes. Harsh environmental conditions (e.g. low temperatures, drought) often result in a decoupling of carbon assimilation and growth. The chapter closes by providing possible solutions on how to improve the detection of environmental information from stable isotope signals by integrating scales and different methodological approaches.

## 14.1 Introduction

Climate exerts a major control of tree growth and has shaped the current phytogeographical distribution of tree species and populations within tree species worldwide. Understanding the interactions between environmental factors and physiological responses at leaf and tree level and for tree growth is key for understanding tree species distributions, ecosystem functioning and the role of forests in the carbon and hydrological cycles (Pallardy 2008). Tree rings represent a proxy for radial growth that result from cambial activity (Chap. 3) integrating metabolic processes over time and space. Climate variations influence carbon sink processes such as radial growth (Körner 2003) and can be inferred using tree-ring width records (Fritts 1976), but they also modulate photosynthesis, transpiration and other physiological processes that are recorded in the stable isotopic composition of plant tissues (Dawson and Siegwolf 2007). The use of stable isotopes as an indicator of physiological responses to climate relies on a mechanistic understanding of the isotopic fractionation during metabolic and transport processes (see Chaps. 9 and 10). These isotopic “fingerprints” recorded in the tree’s tissue (such as leaf, wood and roots) represent the tree-environment interactions over a lifetime (McCarroll and Loader 2004; Cernusak et al. 2013). Environmental information reflected in isotopic signatures is fundamental for the reconstruction of past environmental changes and periods of extreme conditions such as flooding, drought, temperature extremes (Chaps. 19–22) or exposition to pollutants (Chap. 24).

Traditional tree-ring studies solely based on temporal variations in tree-ring width have been mostly conducted on trees from locations with limiting or extreme climatic growth conditions (Fritts 1976). This approach provides information on the dominant climate factor limiting tree growth, which is reflected in tree-ring width. Fritts (1976) postulated that under non-limiting environmental conditions for growth, high growth rates and low inter-annual variability (“complacent” tree growth) are observed, while for trees located at the limit of their distribution range, reduced growth rates and high inter-annual variations (“sensitive” tree growth) are found. However, advances in tree-ring analyses have shown a higher complexity in this conceptual framework. For instance, under non-limiting growth conditions, extreme events and environmental stressors can occur in specific moments of the growing seasons leading to differential imprints in tree-ring anatomical features. Nevertheless, samples for dendroclimatic purposes are often taken from trees growing near their ecological distribution limits with inter-annual variations in tree-ring width, which are more likely related to a single limiting environmental factor, e.g. temperature or precipitation. In contrast,

stable isotopic ratios in tree-ring samples usually show a higher sensitivity under non-limiting growth conditions than tree-ring width. For example, numerous studies have reported a stronger sensitivity of stable carbon, C ( $\delta^{13}\text{C}$ ) and oxygen, O ( $\delta^{18}\text{O}$ ) isotopes than ring width to temperature and moisture under temperate moist climates (e.g. Treydte et al. 2007; Hartl-Meier et al. 2015; Young et al. 2015; Levesque et al. 2017), but also in humid tropical regions (e.g. Brienen et al. 2012; van der Sleen et al. 2017 and references therein, see Chap. 22).

## 14.2 Environmental Constraints Impacting Tree Growth and Tree Species Distribution

Numerous biophysical and biogeochemical factors and their interactions limit tree physiology and growth, and thus species distribution and terrestrial vegetation growth. Besides soil nutrient availability (Du et al. 2020), the most important factors influencing distribution, physiology and vegetation growth of plant species (Pallardy 2008), are temperature, water availability, air humidity, sunlight and atmospheric  $\text{CO}_2$  concentrations (Nemani et al. 2003; Running et al. 2004; Seddon et al. 2016). However, biogeochemical models often operate with a stringent hierarchy of the driving variables starting with water availability and temperature as the most important limiting factors for terrestrial net primary productivity, followed by sunlight limitation (Fig. 14.1a), while neglecting the importance of nutrient availability (Churkina and Running 1998). These models are often inaccurate because they frequently ignore the variability of the local site properties together with the available resources and environmental conditions as driving factors. The requirements and strategies in using resources, i.e. moisture, nutrients, and responsiveness to light, temperature and air humidity is species specific and impact their phytogeographical distribution across the globe in a mechanistic way. Stochastic events such as environmental extremes (e.g. frost, drought, fires events) or forest dynamics (e.g. mortality, regeneration, species competition) may also shape tree species distribution.

At high latitude and high elevation sites, temperature exerts the strongest control on plant physiology and growth, while in arid and semi-arid temperate and tropical regions soil moisture and air humidity are the most limiting factors. In regions with high frequency of cloud occurrence and/or cloud immersion light scattering via cloud / fog droplets improves the light distribution within the crown enhancing the irradiation for the shaded leaves in the lower tree crown sections. This often leads to a higher total crown C-acquisition (Berry and Goldsmith 2020), which impacts the isotope ratio in leaves and potentially growth. While water, irradiance and temperature are co-limiting photosynthesis and transpiration (Pallardy 2008) impacting the isotopic composition of plant tissues directly, nutrient availability is key for tree growth, with nitrogen (N) being most limiting in temperate and boreal forests and phosphorus (P) in tropical forests (Reich and Oleksyn 2004; Pallardy 2008). Recent estimates (Fig. 14.1) indicate that for natural terrestrial ecosystems about 18% are limited by

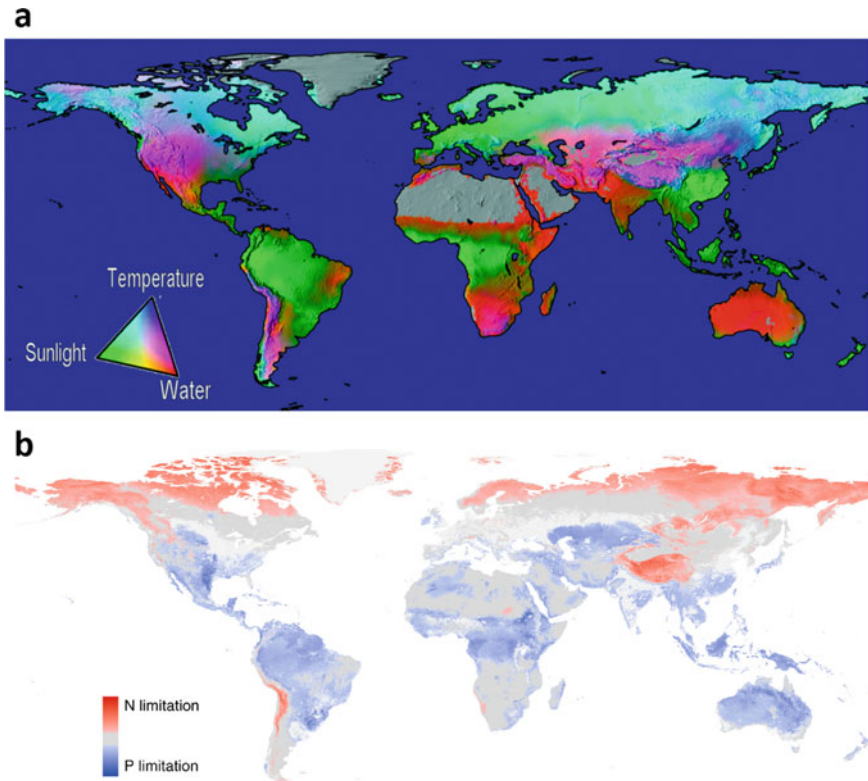


**Fig. 14.1** Relative importance of temperature, water availability and sunlight on global terrestrial vegetation productivity (a), and soil nutrients (b). Figure (a) is reproduced from Churkina and Running 1998; Nemani et al. 2003; Running et al. 2004, and (b) from Du et al. (2020). Figure 14.1b reprinted by permission from Springer Nature: Nature Geoscience, Global patterns of terrestrial nitrogen and phosphorus limitation by Du et al. (2020), license number 4964260783580

N and 43% are limited by P (Du et al. 2020a). Although N deposition could partially alleviate N limitation in certain environments, excessive N or P deposition can have a detrimental effect on tree growth (e.g. Etzold et al. 2020). Therefore, tree growth can also be reduced when N (Norby et al. 2010) or P (Fleischer et al. 2019) availability are not limiting and other nutrients (Mg, Mn, Mo, K etc.) come into play. N-deposition can actually drive ecosystems into P-limitation as occurs in central Europe (Braun et al. 2010). In all these cases, growth rates are not regulated through C supply. Depending on seasonal, annual and decadal changes of these environmental factors and their interactions, tree physiology and growth vary in time and can leave their imprints in tree-ring isotopes.

### 14.3 Climatic Factors Recorded in Tree-Ring Isotopes

The interaction between environmental factors and isotopic fractionations at the leaf level are generally well understood (Chaps. 9 and 10). However, the processes responsible for the isotopic variation in tree rings still need a thorough examination for a correct interpretation of climatic and ecological information represented by tree-ring isotopes. Environmental signals recorded in tree-ring isotope ratios depend essentially on (a) temporal changes in environmental factors, including the intensity and duration of the environmental stressors (see also Chaps. 19–22) and their interactions; (b) their effect on the coupling between leaf gas exchanges ( $\text{CO}_2$  and  $\text{H}_2\text{O}$ ) and secondary growth, and their associated isotope fractionation processes (McCarroll and Loader 2004; Cernusak et al. 2013; Gessler et al. 2014; see also Chaps. 13, 19 and 23). Finally, the isotopic signals in leaves and even more so in tree rings integrate the variation of isotopic fractionation during the entire growth period represented by the sample (i.e. an annual ring). This integrated signal more strongly reflects periods when  $\text{CO}_2$  uptake was greatest by the tree and contributed most strongly to the sampled biomass.

Along with the climate variability during the growing season, the isotopic ratios and growth are fluctuating as well. Therefore, the isotope signals are not uniformly distributed within a given tree ring. Tree-ring formation is a rather complex process where fluctuations in temperature and moisture, as well as in stored carbohydrates, influence the variations in the isotopic signal. The isotopic ratios of whole tree rings predominantly reflect the environmental conditions during which the photoassimilates were produced and allocated to woody tissue. This explains why tree-ring isotope studies, based on samples from trees growing under harsh environmental conditions may not reflect the actual severity of the conditions because no tissue was produced during such periods. In fact, such extremes may not show up in isotopic chronologies, while more moderate stress situations (with slowly ongoing growth and assimilation) do, and thus, produce tree rings with a strong isotope signal (Fig. 14.2) (Rodríguez-Caton et al. 2022). Under most severe drought conditions that prevent tissue production, no  $\delta^{13}\text{C}$  and  $\delta^{18}\text{O}$  signals representing that event will be present in the ring produced during that current growing season (Körner et al. 2005; Cernusak and English 2015). On the other hand, if tree roots are exposed to too much moisture (submerged) an anaerobic condition develops and they gradually lose their functionality, impairing water uptake. Here we observe the paradox, that trees experience an “above ground drought”, while the roots are submerged in water, but non functional due to an anaerobic situation. Some trees are adapted to cope with flooded roots.

In contrast, other tree-ring parameters such as tree-ring width are most sensitive when trees grow in growth-limiting environments (very cold/hot or moist/dry) (Fig. 14.2). Tree-ring maximum latewood density and blue reflectance or intensity, a proxy for wood density (Campbell et al. 2007; Björklund et al. 2019), are also known to be very sensitive proxies in temperature-limited regions such as high-latitudes in North America (Wilson et al. 2017, 2019) or Europe (Björklund et al. 2013, 2019).

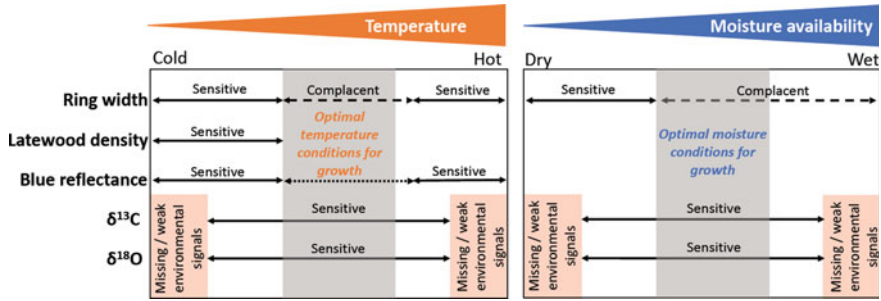


**Fig. 14.2** Schematic representation of the variability and sensitivity of tree-ring variables (ring width, latewood density, blue reflectance and isotopes) to record environmental and climatic signals across a range of temperature and moisture conditions. No arrows indicate that not enough information is available. The orange rectangles indicate extreme climate conditions, where missing or weak environmental signals are recorded by  $\delta^{13}\text{C}$  and  $\delta^{18}\text{O}$  in tree-ring cellulose. Modified from Fritts (1976, p. 301) and Cernusak and English (2015)

Recent studies report that blue intensity measured in earlywood in tropical conifers in Vietnam was sensitive to maximum temperature variations during the monsoon season (Buckley et al. 2018). Therefore, the combination of these other proxies beside stable isotopes can help to disentangle the relative influence of each factor (Levesque et al. 2017).

## 14.4 Climatic Controls of Plant Physiology as Reflected in Isotopic Signals

As the isotopic patterns and signal amplitudes between tree rings and leaves often differ, particularly under harsh climatic conditions, we focus on the influence of extremes such as low/high temperatures and mesic/xeric conditions. Which are the mechanisms responsible for the respective differences and which are the resulting interpretations? While the fractionation principles for C and O isotopes are presented in Chaps. 9, 10, and 13, here we focus our discussion on the processes that are relevant for the tree-ring signals detected under different climatic situations.

### 14.4.1 Meteorological, Microclimatic and Biogeochemical Impacts on the Isotopic Fractionations

Dominant climatic factors that exert control on carbon isotopic discrimination are those that control stomatal conductance and the rate of photosynthesis at the leaf level (Farquhar et al. 1982, 1989; McCarroll and Loader 2004), and thus modify the leaf

$\delta^{13}\text{C}$  values. Vapor pressure deficit (VPD) and soil moisture have the predominant control on stomatal conductance, whereas irradiance,  $\text{CO}_2$  and air/leaf temperature control photosynthetic rates (Von Caemmerer and Farquhar 1981; Larcher 2003; see also Chap. 9). Variation of stomatal conductance at wide stomatal apertures exerts proportional changes in transpiration (at a given VPD), but hardly affects photosynthesis, simply because mesophyll resistance is almost 5 times larger than minimum leaf (stomatal) diffusive resistance, both operating in series (Körner et al. 1979), an insight that also relates to the ‘operating point’ as coined by Farquhar and Sharkey (1982).

Overall, the well-understood fractionation processes during photosynthesis are commonly the basis for interpreting  $\delta^{13}\text{C}$  in tree rings, which per se is correct. This facilitates the decoding for climate reconstruction and tree physiological responses to various environmental impacts. Yet, during transport of fresh assimilates, post photosynthetic processes such as conversion of photoassimilates to structural biomass or storage reserves and remobilization of sugars, etc., modify the original isotope signals formed in leaves, which can result in considerable deviations between leaves and wood for both C and O isotope values. Here we refer to Chap. 13 where this topic is discussed in detail.

Besides post-photosynthetic fractionation and climate, other processes impact the isotopic composition in wood. The fractionation for  $\delta^{18}\text{O}$  occurs at two different scales. At the first (meteorological) scale, fractionations occur before water is incorporated in the plants (Chap. 18), and at the second (microclimatic) scale, fractionations take place in the leaf and the whole plant (Chap. 10). In the first case, air temperature and evaporation are the main controlling factors. During condensation of water vapor the prevalent temperature determines the  $^{18}\text{O}/^{16}\text{O}$  ratio in meteoric water (Dansgaard 1964), thus incoming precipitation varies seasonally. In the canopy and soil surface, some water may evaporate, causing enrichment in  $^{18}\text{O}$  of the remaining water depending on the degree of evaporation. As water infiltrates into the soil, it mixes with residual water (Chap. 18, also Allen et al. 2019). This mixing between rainwater of different seasonal origins occurs mainly in temperate and boreal regions (Szejner et al. 2018), whereas in tropical regions the  $^{18}\text{O}/^{16}\text{O}$  ratio in meteoric water have been related to the wet season (e.g. Brienen et al. 2012; Rodríguez-Catón et al. 2021, 2022). Irrespective of soil depth, plants absorb water where it is easiest accessible. No measurable fractionation occurs during water uptake. Deviations in  $\delta^{18}\text{O}$  between xylem and soil water result from a mixture of water, absorbed along the rooting depth with varying  $\delta^{18}\text{O}$  values of the soil moisture at different depths (Sprengrer et al. 2016; Barbeta et al. 2020). Source water can change in time depending on the water availability and changes in the seasonal amount and precipitation type (Brinkmann et al. 2018; Allen et al. 2019), or shifts in rooting depth and water uptake from different soil water pools (Sarris et al. 2013; Barbeta and Penuelas 2017; Brinkmann et al. 2019).

At the second (microclimatic) scale, fractionations occurring in leaves (described in detail in Chap. 10) are essentially influenced by VPD and temperature (both controlling transpiration and stomatal conductance), as well as  $\delta^{18}\text{O}$  of source water

and  $\delta^{18}\text{O}$  of water vapor. The  $^{18}\text{O}$  enrichment in leaf water is tightly linked to transpiration and stomatal conductance ( $g_s$ ), with the lighter water molecule ( $\text{H}_2^{16}\text{O}$ ) evaporating more easily than the heavier  $\text{H}_2^{18}\text{O}$ , leaving the remaining leaf water enriched in  $\text{H}_2^{18}\text{O}$  (Craig and Gordon 1965; Dongmann et al. 1974). The following three scenarios illustrate the significance on leaf water enrichment of VPD,  $g_s$  and soil water supply, as well as of the source water  $\delta^{18}\text{O}$  and the ambient water vapor  $\delta^{18}\text{O}$ :

1. Low air humidity (high VPD) with sufficient soil water supply, high  $g_s$  and high net transpiration (E): large humidity gradient between the ambient air ( $e_a$ ) and the leaf intercellular spaces ( $e_i$ ) results in high evaporative losses and a moderate to low leaf  $\text{H}_2^{18}\text{O}$  enrichment. To maintain the plant water balance, water loss via E is continuously replenished with non  $^{18}\text{O}$  enriched xylem (source) water. This results in a reduced leaf water  $^{18}\text{O}$  enrichment, described by the Péclet effect (see Chap. 10; Farquhar and Lloyd 1993). The higher E, the less the leaf water enrichment due to less back-diffusion of  $^{18}\text{O}$  enriched water at the evaporative site (in the leaf) with the non  $^{18}\text{O}$  enriched xylem water that is continuously replenishing the leaf water pool. Under these conditions the variation in source water  $\delta^{18}\text{O}$  is the basis for the  $\delta^{18}\text{O}$  variation in the leaf water and organic matter. For example, this is found in temperate forests with abundant water supply.

2. High air humidity (low VPD) with sufficient soil water supply, high  $g_s$  and low E: small humidity gradient between  $e_i$  and  $e_a$  results in a low transpiration rate and minimal leaf  $\text{H}_2^{18}\text{O}$  enrichment. Under such conditions hardly any water flow occurs from the xylem into the leaf as VPD is low and the Péclet effect is minimal to ineffective. But the large exchange of  $^{18}\text{O}$  depleted water molecules from the ambient air (i.e. vapor exchange) into the leaf via stomata results in a reduced to no leaf  $\text{H}_2^{18}\text{O}$  enrichment (Goldsmith et al. 2017; Lehmann et al. 2020). Under these circumstances the ambient water vapor  $\delta^{18}\text{O}$  is reflected in the  $\delta^{18}\text{O}$  of the leaf water and organic material. For example, this is the case in humid tropical forests or regions exposed to high occurrence of fog (e.g. Dawson 1998) or rain events.

3. Low to moderate air humidity (high VPD) with scarce soil water supply, thus low  $g_s$  and E: large humidity gradient between  $e_i$  and  $e_a$  with insufficient water supply results in closed stomata and low transpiration and high leaf  $\text{H}_2^{18}\text{O}$  enrichment. Since E is low the xylem flow into the leaf is low thus allowing back-diffusion of  $^{18}\text{O}$  enriched water from the site of evaporation. Furthermore, the ambient water vapor pressure and  $g_s$  are lower too, resulting in a considerably reduced exchange with  $\text{H}_2^{18}\text{O}$  depleted, ambient vapor. Under these conditions the climate i.e., VPD and temperature are predominantly imprinted in the  $\delta^{18}\text{O}$  of the leaf water and biomass, additionally to the  $\delta^{18}\text{O}$  of the given source water. This is found under xeric, Mediterranean or drought conditions.

In reality there may be gradual transitions between the different scenarios. From scenario 1 to 3, stomatal conductance ( $g_s$ ) is inversely related to leaf  $\text{H}_2^{18}\text{O}$  enrichment (Barbour et al. 2004). However, whether low leaf  $\text{H}_2^{18}\text{O}$  enrichment (i.e., similar values for leaf water  $\delta^{18}\text{O}$  and xylem water  $\delta^{18}\text{O}$ ) in very humid environment



with enough soil water supply is the result of high VPD (scenario 1) or low VPD (scenario 2) cannot be distinguished with tree-ring  $\delta^{18}\text{O}$  alone. Other proxies, i.e.,  $\delta^{13}\text{C}$ , tree-ring width or density could be useful to clarify the mechanism. In any case, a good knowledge of the site conditions is mandatory for a correct interpretation of the isotopic signals in tree rings. Although in scenarios 1 and 2 we find low, to no leaf  $\text{H}_2^{18}\text{O}$  enrichment with little variability, the causes can be different as shown above (i.e., very humid environment or abundant water supply allowing for high E). Scenario 3 is most frequent as the air humidity on average is more variable and generally lower in boreal, temperate and Mediterranean regions than in the tropics or at certain treelines/sites.

Numerous studies assume similar or even identical  $\delta^{18}\text{O}$  values between source water and summer precipitation. Recent studies, however, indicated considerable deviations between  $\delta^{18}\text{O}$  of precipitation and xylem (source) water. Depending on the soil structure (heavy, dense and clay rich versus light, predominantly organic soils), the infiltration of precipitation water can vary considerably, which is reflected in the infiltration time and  $\delta^{18}\text{O}$  gradient from the soil surface to the roots. Brinkmann et al. (2018) and Allen et al. (2019) showed that trees rely only partly on the growing seasons precipitation and use considerable amounts of precipitation from winter and diverse seasonal origins. This can lead to a temporal shift in the seasonal course of the  $\delta^{18}\text{O}$  values of source water. Therefore, Brinkmann et al. (2018) and Allen et al. (2019) refer to this temporal shift in source water  $\delta^{18}\text{O}$  as seasonal origin. These shifts can potentially mask the physiological response signals of trees to variations in temperature and moisture, and thus they can dampen the prevalent climate signals in tree-ring  $\delta^{18}\text{O}$  records (see Chap. 18). Such disparities between precipitation and source water have implications on tree-ring based climate reconstructions and deserve a cautious consideration in the data interpretation.

#### ***14.4.2 Tree-Ring Isotopic Signals Under Non-limiting Climate Conditions for Growth***

In the absence of severe growth constraints, tree response to climate conditions for optimal growth can differ between species and is dependent on ecosystem properties (soil, water and nutrient availability, stand structure, species composition). In general, abundant precipitation, moderate temperatures, non-limiting light and adequate nutrient conditions are a precondition for detecting clear isotopic signals (Cernusak and English 2015; Hartl-Meier et al. 2015). The likelihood that a strong temperature and humidity signal is recorded in source water is given with high precipitation as indicated above and preferably on porous, organic soils where water infiltrates into the soil rapidly. For instance, the strongest precipitation signal recorded in tree-ring  $\delta^{18}\text{O}$  observed in temperate regions is where soil water supply relies mostly on precipitation during the growing season (Treydte et al. 2014). Studies based on

tree-ring isotope networks agree with this theory and reported the strongest correlation between tree-ring  $\delta^{18}\text{O}$  and precipitation in regions with abundant precipitation during summer in Europe and North America (Treydte et al. 2007; Hartl-Meier et al. 2015; Levesque et al. 2019), but also in the Southern Hemisphere in South America (Rodríguez-Catón et al. 2021, 2022).

For a clear interpretation of isotopic signals in tree rings, one needs to know when (season) and where (region) tree rings were produced. This requires a definition of conditions under which tree-ring  $\delta^{13}\text{C}$  and  $\delta^{18}\text{O}$  signals are less influenced by confounding factors and under which conditions the strongest environmental and climatic signals can be obtained. As shown above, trees growing under quasi non-limiting growth conditions provide the most representative isotopic signal of environmental conditions.

In areas where a single limiting factor has the strongest effect on isotopic composition, the interpretation of the physiological and climatic signals is usually straightforward. For example, in regions where temperature is the most limiting factor for tree physiology during the growing season, tree-ring isotopes are expected to respond specifically to temperatures (e.g. Porter et al. 2009; for other examples see Chaps. 20 and 21). However, under natural conditions, it is rarely the case that a single limiting environmental factor is recorded in the isotopic composition of plant materials. Often several environmental variables impact physiological responses at the same time such as temperature and VPD (Grossiord et al. 2020). Such interactions complicate the interpretation of the environmental signals recorded in stable isotopes despite the relatively well understood physiological processes influencing isotopic fractionation at the tree level (Gessler et al. 2014).

### ***14.4.3 Tree-Ring Isotopic Signals Resulting from Extreme Climate Conditions***

The strength of the isotopic signal in tree rings in response to environmental changes may not be proportional to the strength of the environmental stressors. For instance, very low temperatures or severe water limitations during the growing season may halt growth, and thus, there is no woody tissue that the isotopic signal can be related to.

#### **14.4.3.1 Cold Conditions**

At high latitudes and in mountainous environments, low temperatures limit cambial activity, and thus, growth (Körner 2012). Although radial growth is very low when air temperature drops below 5–6 °C (Körner 2016), leaves are still producing photoassimilates (Körner 1991). So, the specific isotopic patterns in the freshly produced assimilates may represent a cold environment, while the amount of wood produced

during this cold phase is negligible. With temperature above 5–6 °C, wood production rate increases following a sigmoidal course. To the extent that temperature *per se* influences isotopic signals of the produced wood biomass in a warmer phase. Thus the isotope values representing higher temperatures is usually much larger than wood produced during the cold phase. This results in a disproportionate relationship between wood masses formed during cold versus warm phases for a given year. This means that the isotope signals from cold periods within the season may be underrepresented relative to the warmer phases due to less amount of wood mass. Therefore, isotopic signals specific to cold periods can be difficult to detect in tree rings. Still, climate signals from cold periods recorded by tree-ring isotopes have been used to reconstruct cold winter anomalies (Szejner et al. 2016, 2018; Voelker et al. 2019). Whatever the reason, such an analysis requires a careful splitting of tree-ring segments with either a microtome or ideally via laser ablation. Having very thin sections, which might consist of only a few cell layers, intra annual climatic variability can be uncovered even from periods with very small parts of the tree-ring material (Monson et al. 2018).

To summarize: During critically cold periods tree-ring increments are very small because cell division is very slow at low temperatures (Rossi et al. 2007; Körner 2015), but cell division increases with rising temperatures until a maximum growth rate is reached. Thus, the amount of wood that carries the isotopic signals for cold periods is very small relative to the whole tree ring. Consequently, the cold signal may be hardly detected in tree-ring isotopes.

#### 14.4.3.2 Dry/Hot Conditions

With increasing temperature, the atmospheric evapo-transpirative demand (i.e. VPD) increases as well (Novick et al. 2016; Grossiord et al. 2020). However, as plants are generally more sensitive to VPD than to high temperature, VPD is predominantly limiting both assimilation and growth before temperature does. What is often indicated as temperature limitation could be in fact a limitation by VPD (Grossiord et al. 2020).

Drought and heat combined have a similar effect with regard to wood production as low temperature conditions (see above). These climatic signals (dry/hot) expressed in isotope ratios of individual tree rings may also be underrepresented. Beyond a species-specific maximum air temperature and VPD threshold, photosynthesis declines, and carbon allocation is shifted towards root expansion, rather than in radial growth (Pallardy 2008; Teskey et al. 2015). While these physiological responses to drought and heat alter the isotopic ratios at the leaf level, they can deviate strongly from the  $\delta$ -values of tree rings. Such drought situations slow down or prevent xylogenesis and can result in a growth cessation leading to an isotopic uncoupling between leaves and tree rings (Pflug et al. 2015). In contrast, during situations with sufficient soil water and reduced VPD (spring/fall, e.g., in the Mediterranean), the wood production rate is much higher (Sarris et al. 2013). Again, this leads to a disproportionate relationship between wood masses formed during dry/hot versus wet/cool

phases. As the wood mass produced during cooler wetter phases is much more abundant, its isotopic signal is proportionally more expressed in the tree ring (similar to the cold but inverse situation, with regard to temperature, see Sect. 14.4.3.1).

To summarize: With increasing temperature, VPD increases as well, and this is often associated with a reduction in soil water availability. Both radial growth and physiological processes at leaf level, namely photosynthesis and stomatal conductance, can be affected. However, photosynthesis is restrained or even ceased, commonly long after cell and tissue growth had been halted. Thus, the isotopic signals in leaves could be decoupled from the isotopic signals in wood (Pflug et al. 2015). No new cell produced means no tree-ring isotopic signals are representing this specific climate situation.

## 14.5 Carbon Storage and Carry-Over Effects on Tree-Ring Isotope Signals

The approach to use stable isotopes in tree rings to reconstruct changes in leaf gas exchanges, over decades to centuries in response to anthropogenic (e.g. rising CO<sub>2</sub>, Voelker et al. 2016, Chap. 24) and climate factors (Leonardi et al. 2012; Saurer et al. 2014; Frank et al. 2015; Levesque et al. 2017; Mathias and Thomas 2018; Guerrieri et al. 2019) is based on the assumption that carbon sources (tree canopies) and sinks (tree stem) are tightly coupled and synchronized in time. This implies that the isotopic signal in the annual rings, which is imprinted in foliage during photosynthesis and transpiration, would be closely related to the environmental impact. As discussed above, this is rarely the case, particularly when trees are not living at their most favorable environmental conditions (in terms of resource availability). Hence, they may allocate the recently assimilated carbon to sinks other than radical growth (C-storage see Sects. 14.5.3.1 and root biomass 14.5.3.2).

Translocation, storage and remobilization of old and new assimilates within a tree affect the isotopic composition of tree rings (see Chap. 13). Understanding how these processes influence  $\delta^{13}\text{C}$  and  $\delta^{18}\text{O}$  in tree rings at the inter- and intra-annual time scale is a prerequisite for improving the use of isotope signals in tree rings to derive climate and environmental conditions retrospectively. This section will take a closer look at the dynamic of the annual ring formation, and at the fate of recently assimilated carbon and its isotopic signals when stored in tree rings.

### 14.5.1 Annual Ring Formation Through Xylogenesis (Tree Carbon Sink)

The production of new cells during the formation of annual tree rings—the xylogenesis occurs through a few steps, separated in space and time, but connected

among them: cell division, cell enlargement, deposition of secondary wall and finally maturation when thickening and lignification are completed. The production of new woody cells results in a tree carbon sink occurring during a given growing season (in temperate and boreal forests) and all year around (in humid tropical forests). Xylogenesis and the cambial activity, depends on the activity of meristem tissues and the rate at which new tissue becomes differentiated and matured (Rossi et al. 2012; see Chap. 3). All this relies on the developmental ‘preparedness’ to grow (hormones), the existence of active sinks (Körner 2015) and the coordination between phloem loading with sugars, the transport from autotrophic to heterotrophic tissues (Hölttä et al. 2014; Ainsworth and Lemonnier 2018), and the downloading capacity in developing xylem tissue. Xylogenesis is affected by developmental (genomic) and environmental factors (with particular reference to temperature, photoperiod and water). Assimilate availability is rarely limited in nature except for plants in deep shade. Temperature and photoperiod define the onset of cambial activity, particularly in temperate and boreal forest. Water availability and sugar concentrations plays a significant role in the cell growth by maintaining the turgor pressure needed for cellular expansion (e.g. Steppe et al. 2015 and references therein). Dynamics of cambial activity vary depending on tree age (Rossi et al. 2008) and environmental conditions. Xylogenesis lasts longer in young compared to mature trees, though this may be the result of tree size rather than simply an age-effect (Rossi et al. 2008; Zeng et al. 2018). Overall, previous findings in literature seem to indicate that xylogenesis is not limited by assimilate availability, but by developmental, thus hormonal and ultimately genetic factors (e.g. Grattapaglia et al. 2009) and direct environmental influences on the tissue forming processes (meristems, Körner 2015, and references therein).

In boreal and high-elevation forests at the treeline, growth occurs continuously following a unimodal curve during a short season when growth is determined by temperature thresholds (Fig. 14.3). In contrast, growth in Mediterranean ecosystems, can last longer, but is often discontinuous, as drought conditions may temporarily stop new cell production, and resume xylogenesis following precipitation. This leads to the formation of the so-called intra-annual density fluctuations (IADFs) (Battipaglia et al. 2016; De Micco et al. 2016). In some tropical trees, tree cambial activity is expected to be constant all year around and without periodicity, though alternation of dry and wet season may pause and resume xylogenesis, and reproductive cycles can induce growth cycles that materialize as growth rings (see Chaps. 3).

### ***14.5.2 Tree Carbon Pools and Their Effect on the Isotopic Ratio in Tree Rings***

Recently produced carbohydrates can move from the canopy down to the tree stem and roots within hours (Keel et al. 2006, 2007; Gessler et al. 2009a) and return back to the atmosphere through respiration from the soil within a few days (Steinmann et al. 2004; Högberg et al. 2008; Mildner et al. 2014) or even become transferred

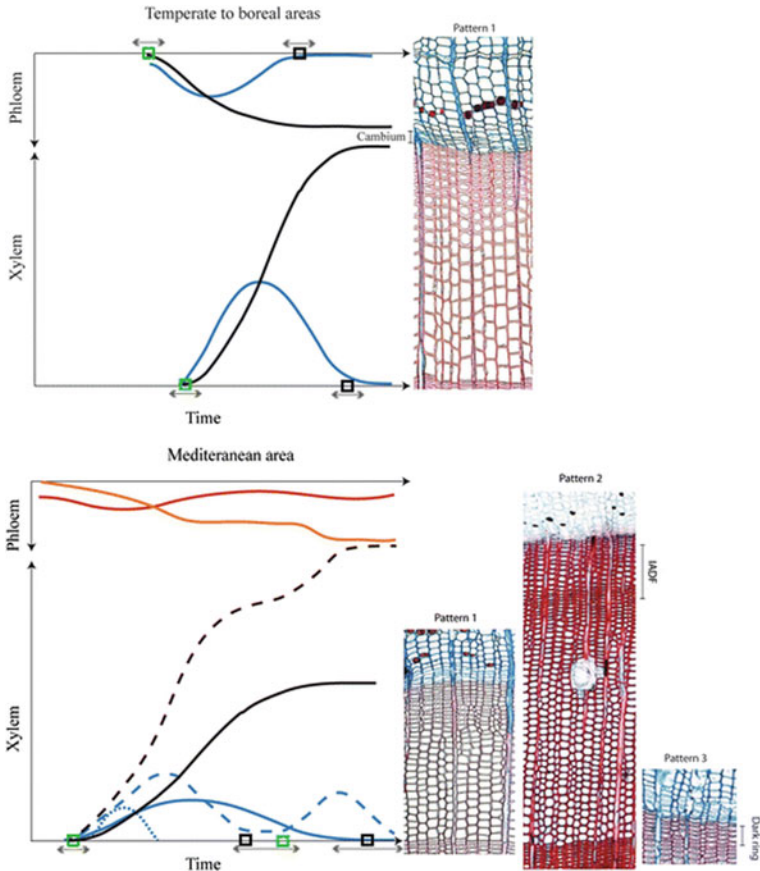


**Fig. 14.3** Variation of growth patterns in two contrasting biomes. Xylem and phloem growth over one growing season resulting from cambium activity in (top) boreal or temperate and (bottom) Mediterranean forests. In each case, the periods of growth are defined by the onset (green squares) and cessation (black squares) while the arrow represents the time variability in the onset and cessation. For both xylem and phloem, the progress of growth over time (black lines) is quantified either as the number of cells or ring width produced within a year. A general rate of growth (blue lines), which indicates how fast the process occurs in terms of the measured quantity per time unit, can be represented as the first derivative of the progress of growth (black lines). Only one pattern of xylem and phloem growth over time was represented for temperate- boreal areas illustrated as the S-shaped (top, pattern 1) growth pattern (black line). The general rate of growth of this pattern is typically bell shaped (top, blue line in pattern 1). For Mediterranean areas, three patterns of growth over time were represented: (bottom, pattern 1) S-shaped growth, such as for temperate-boreal conifers with its bell-shaped rate of growth (solid black and blue lines); (pattern 2) Intra-annual density fluctuation (IADF, dashed black line) with its bimodal rate of growth (dashed blue line); (pattern 3) missing rings or dark rings (illustrated as the rate of growth only, dotted blue line) where few xylem cells are formed (less than five cells), which slowly differentiate and can look like latewood cells. Orange and red lines indicate the progress of phloem growth over time and phloem growth rate, respectively. Phloem growth rate (in red) is hypothetical and has been shown to be bimodal like the xylem of pattern 2. [Source figure and text: (Deslauriers et al. 2017)]. Reprinted by permission from Springer Nature: Springer, *Ecophysiology and Plasticity of Wood and Phloem Formation* by Deslauriers et al. (2017), license number 4971200864679

to the adjacent trees via mycorrhiza (Klein et al. 2016a). However, high rates of transfer does not necessarily indicate a high, direct and lasting incorporation of new assimilates into structural growth, because the mobile carbohydrates can mix, and thus, get diluted by the old carbon pool, with only the mixture becoming invested in new growth (Keel et al. 2007; Mildner et al. 2014).

#### 14.5.2.1 Assimilation at Leaf Level (Tree Carbon Source)

At the canopy level during the photosynthetic assimilate production (Fig. 14.4) the

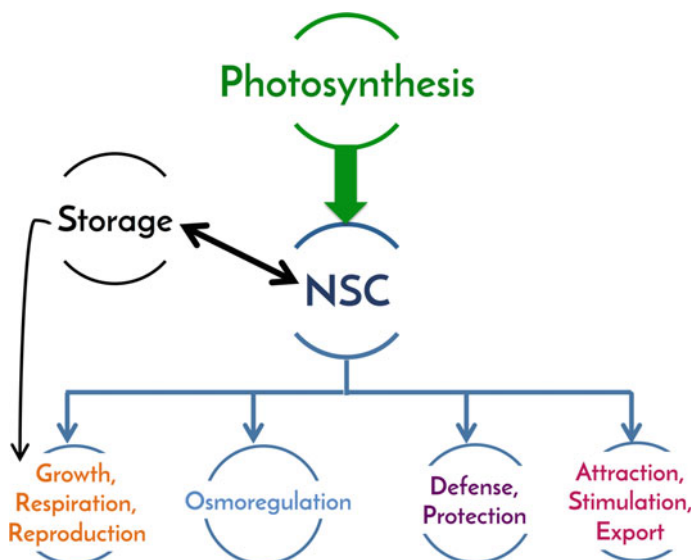


**Fig. 14.4** Scheme showing the fate of non-structural carbohydrate (NSC) in trees. Modified from (Hartmann and Trumbore 2016)

$\delta^{13}\text{C}$  signature of new carbohydrates at leaf level reflects the dominant climate factors controlling stomatal conductance and/or photosynthetic rates (see Chap. 9). The  $\delta^{18}\text{O}$  signature of new carbohydrates is driven by climate variations responsible for the isotopic fractionations before water is incorporated in the plants (Chap. 18) and in leaves controlling transpiration and stomatal conductance (see Chap. 10).

#### 14.5.2.2 Non-structural Carbohydrates

Non-structural carbohydrates (NSC) are photassimilates produced during a given growing season in the leaves and are mostly composed of starch and sugars, but also fructans, sugar-alcohols and other compounds. NSC are not directly invested

in growth but they are used by trees to fulfill different functions (Fig. 14.4) such as storage, reproduction, growth and respiration (maintenance of life sustaining processes). Furthermore, they are used for osmoregulation, defense (synthesis of biogenic volatile organic compounds, BVOCs), protection, attraction, stimulation and export (e.g., root exudates). They also provide a neutral disposal avenue for overabundant photoassimilates, similar to storage lipids (Hartmann and Trumbore 2016; Martinez-Vilalta et al. 2016), or may simply be exuded for no other reason than a C overflow (Prescott et al. 2020).

However, the hierarchy or priority of certain uses of fresh photoassimilates is unclear. Evidence is accumulating that storage has a very high priority. Plants tend to prioritize storage even under C shortage (Weber et al. 2018), indicating that survival has a higher rank than adding structural biomass (growth). When meristematic activity is inhibited or slowed because of critically low temperatures, drought, lack of nutrients, or phenology, photosynthates are simply stored, since photosynthesis is commonly less sensitive to such stressors or limitations than meristem activity (Körner 2003, 2015; Muller et al. 2011). Under such conditions, the concentration of C stores rises and these stores either become mobilized as meristems resume their activity when conditions improve (Würth et al. 2005) or they remain disposed forever in heartwood. The only alternative is down regulation of photosynthetic capacity. Seasonal changes in cambial activity are coupled with a higher sugar concentration in the cambial zone, with highest demand during the cell differentiation and wall-thickening phase (Deslauriers et al. 2009; Perez-de-Lis et al. 2016). The NSC pool also undergoes seasonal variation, and is negatively correlated with the rate of structural growth. Whenever growth slows, NSC content increases, when growth resumes, NSC declines (Körner 2003; Würth et al. 2005; Streit et al. 2013). The alternatives are down regulation of photosynthetic capacity or export of excess carbon as discussed by Prescott et al. (2020).

### 14.5.3 *Coherency Between C-Sources and Sinks*

There is no evidence that mature trees in forest ecosystems with a natural nutrient cycle are carbon limited at current atmospheric CO<sub>2</sub> concentrations (Norby and Zak 2011; Bader et al. 2013; Sigurdsson et al. 2013; Klein et al. 2016b; Ellsworth et al. 2017); for a review see also Palacio et al (2014). The proposed trade-off between C storage and growth (Wiley and Helliker 2012) is not driven by C shortage but rather reflects investment opportunities driven by meristem activity (C sink limitation to growth) as set by environmental cues. In other words, the allocation of new assimilates to storage is an active or passive response by trees, particularly under limiting environmental conditions (Körner and Paulsen 2004; Dietze et al. 2014; Hartmann 2015; Galiano et al. 2017; Piper et al. 2017), and depends on when trees prioritize growth over storage or defense (Huang et al. 2019).

At the beginning of seasonal growth, some stored carbohydrates that were produced in previous years, or during the non-growing season in evergreen species,



are used for the onset of tree growth. Therefore, the isotope signals of stored carbohydrates used for growth in the current growing season are not necessarily representative of the concurrent climate. With the ongoing foliage development, tree growth is progressively supplied with freshly formed assimilates, which carry the isotope signals representing the current climate, stored in the late wood formation (see Sect. 14.6). Thus, in the short term, environmental signals are well represented in fresh photoassimilates, but only to a minor degree in lasting tissue signals such as those captured in bulk stem wood.

### 14.5.3.1 Evidences from Intra-annual Ring Measurements

Recent improvements in dendro-isotopic analysis, such as sampling thin sections of tree rings either by microtome slicing (Sarris et al. 2013) or by laser ablation techniques (Schollaen et al. 2014; Rinne et al. 2015; Soudant et al. 2016; Loader et al. 2017) have greatly enhanced the possibility to simultaneously study xylogenesis and isotopic composition at high-temporal intra-annual resolution (Chap. 7). High-resolution intra-annual analyses of tree-ring isotope ratios (Rinne et al. 2015; Belmecheri et al. 2018) disclosed time lags in the isotope ratios resulting from climatic impacts, remobilization of carbohydrates and tree-ring formation. Intra-annual analyses assessing tree response to the seasonal variation of climatic conditions have mostly separately analyzed the isotopic ratios in early- and latewood sections (Kress et al. 2009; Lévesque et al. 2014). Kimak and Leuenberger (2015) confirmed that  $\delta^{13}\text{C}$  in earlywood material was strongly dependent on previous year reserves (although the usage of stored versus fresh assimilate can vary between species and seasons depending on the prevalent climatic conditions), while latewood material was mostly formed from assimilates of the current growth year. Thus, earlywood and latewood need to be analyzed separately for their isotopic composition, even for trees from cold environments with narrow rings if possible (Kagawa et al. 2006a).

The examination of the xylogenesis dynamics can help to identify temporal lags between cell formation and cell thickening such as lignification (Cuny et al. 2015). The interactions between cambial phenology and seasonal climate result in seasonal lags of the isotope ratios, stressing the importance of properly aligning isotopic measurements with the phenology of the xylogenesis (Belmecheri et al. 2018; Castagneri et al. 2018). The amount of cellulose produced during the development of the primary cell wall (cell enlargement) is smaller than during the cell wall thickening phase (Cuny et al. 2015), with the latter (reflecting the concurrent climate conditions) having a greater weight in the overall tree-ring isotope signal. This implies a bias toward the climatic controls of the main part of cell wall thickening (Cuny et al. 2015; Castagneri et al. 2017; Belmecheri et al. 2018). Finally, lignification, the last stage of cell maturation, can last until the end of the growing season, so it can be also associated with late season climate. By aligning tree-ring isotope series with xylogenesis and climate conditions, the robustness of ecological and paleoclimatic studies will improve considerably (Monson et al. 2018). Consequently, the need

of cellulose extraction prior isotopic analysis should be carefully considered based on the questions being addressed. Removing other wood constituents could prevent the detection of the full dynamics of carbon allocation during tree-ring formation. Indeed, lignification can last up to one month after growth cessation (Cuny et al. 2015), hence potentially losing physiological and environmental signals associated with these compounds (Barbour et al. 2001; Guerrieri et al. 2017). See also Chaps. 3 and 5.

#### 14.5.3.2 Species Specific Dynamics in Xylogenesis and the Use of Stored and New Carbohydrates

The seasonal stages of xylogenesis are also species-specific. These NSC dynamics (i.e., production in the canopy and NSC investment during xylogenesis in the stem) differ among species (Hoch and Körner 2003). In ring-porous species, earlywood formation relies almost exclusively on previous year(s) carbohydrates, exhibiting isotopic carry-over effects (Helle and Schleser 2004). The onset of cambial activity and vessel formation in ring porous tree species occurs prior to budburst and depends on the remobilization of carbohydrates from storage (Gonzalez-Gonzalez et al. 2013; Perez-de-Lis et al. 2017). Yet a large fraction of these C storages is never mobilized, but rather stays in ray tissues, with the climatic signal related to the time when they were assimilated. This lack of synchronicity between photosynthesis and stem growth leads to temporal shifts between C assimilation and investment in secondary tissues, which is reflected in the isotopic values.

In contrast, diffuse-porous species rely mostly on new assimilates to build up new woody biomass (Keel et al. 2006; Palacio et al. 2011; Michelot et al. 2012; Carbone et al. 2013; Vincent-Barbaroux et al. 2019). Conifers use mostly newly formed sugars (see early studies from Glerum 1980; Michelot et al. 2012; Rinne et al. 2015; Deslauriers et al. 2016). These potential lags between C assimilation and xylem formation can also be bimodal if spring and autumn activity are separated by a dry summer such as in the southwestern United States (Belmecheri et al. 2018) or in Mediterranean regions (Sarris et al. 2013; Castagneri et al. 2018). In contrast, when trees were irrigated in precipitation manipulation experiments after a long drought period (e.g. *Pinus sylvestris* in a dry valley in the Alps), the  $\delta^{13}\text{C}$  signals were more depleted in  $^{13}\text{C}$ , for both, earlywood and latewood, evidencing an almost synchronic coupling between new assimilates and xylem formation (Eilmann et al. 2010).

Generally deciduous conifer species (i.e. *Larix* spp.) show a lower use of stored assimilates produced in previous years as indicated by  $\delta^{13}\text{C}$  intra-annual patterns of sucrose and tree-ring samples of *Larix sibirica* (Rinne et al. 2015). Still earlywood formation relies on both carried-over photoassimilates from the previous year(s) and to the degree as current photoassimilates are available, whereas latewood formation depends predominantly on current assimilates, as demonstrated with  $\delta^{13}\text{C}$  pulse-labeling and intra-annual  $\delta^{13}\text{C}$  analysis (Kagawa et al. 2006a, b).

### 14.5.3.3 Coupling and Decoupling Between Carbon Source and Sinks and Their Isotopic Coupling

Under the assumption that source (canopy physiology) and sink (stem growth) are strongly linked and synchronized, tree-ring width and isotope compositions are an ideal proxy to reconstruct changes in leaf physiological responses to environmental limitations retrospectively. However, this agreement is rare (Michelot et al. 2012; Belmecheri et al. 2014; Guerrieri et al. 2016, see also Chap. 9). When trees are exposed to severe environmental limitations, photosynthesis and tree growth are uncoupled to the degree that an isotopic decoupling occurs, i.e., the isotopic signals in tree rings do not correspond with the prevalent environmental conditions. For example, drought can stop radial growth and cold conditions can slow it significantly, even though there are no changes in NSC concentration (Lempereur et al. 2015; Fernandez-de-Una et al. 2017; Dietrich et al. 2019) while photosynthesis is still ongoing (Pflug et al. 2015). As mentioned before, growth is more drought sensitive than photosynthesis (Muller et al. 2011; Piper et al. 2017). Source and sink activities were also found not to be fully coupled in a mesic forest, with growth being more sensitive to atmospheric, soil moisture limitation and low temperature than canopy C uptake in a temperate oak forest (Delpierre et al. 2016). At the world's highest elevation treeline in the South American Altiplano, a coupling and decoupling between physiological processes at leaf level (carbon source) and wood formation (carbon sink) was observed along an aridity gradient likely associated to similar or different climate sensitivity of these carbon source and sink processes (Rodríguez-Catón et al. 2021). The accumulation of soluble NSC under drought conditions in the cambium zone could be a strategy for trees to prioritize maintenance of cell turgor (Deslauriers et al. 2014; Piper et al. 2017) and to keep an efficient vascular system (including phloem and xylem (Sala et al. 2012)). However, the quantities required for osmoregulation are small, with one mole of solutes already creating an osmotic pressure of 2.24 MPa, and cells already operate under 'normal' conditions at an osmotic pressure between 0.5 and 1 MPa. The increase in NSC with increasing elevation (Hoch and Körner 2002, 2012; Fajardo et al. 2013), although not always observed (Simard et al. 2013), was associated with sink rather than source limitation (Körner 2003) and hence, to environmental control on cambial activity (Rossi et al. 2016).

Beside the time lag in the transfer and mixing between recently fixed and old assimilates, other factors may contribute to mask the isotopic tree-ring signal. First, soluble sugars may undergo biochemical transformation (e.g., synthesis of cellulose or lignin) within the canopy and later they are loaded to the phloem (during the export) and used during the annual ring formation, with associated isotope fractionations (Cernusak et al. 2013; Gessler et al. 2014). This can cause an offset between sink and source in both  $\delta^{13}\text{C}$  and  $\delta^{18}\text{O}$ . Its magnitude has shown to be species-specific (Cernusak et al. 2005; Gessler et al. 2009b; Bögelein et al. 2019), and can partially uncouple tree rings from isotopic signals in fresh assimilates in the canopy (see also the post-photosynthetic fractionation in Chap. 13; Cernusak et al. 2013; Gessler et al. 2014).

Another aspect to consider is the confounding effect of changes in atmospheric CO<sub>2</sub> and air pollutants (Ozone, SO<sub>2</sub>, NO<sub>y</sub> and NH<sub>x</sub>) on tree physiological processes. This topic is discussed in detail in Chap. 24.

## 14.6 Concluding Remarks

The dendro-isotope approach is one of the few reliable methods allowing for the assessment of tree carbon and water relations in response to changes in environmental conditions. It facilitates the reconstruction of climate signals (Chap. 1) and environmental changes retrospectively over long temporal and large spatial scales and at high spatial and time resolution (Babst et al. 2017). Yet this approach has also some weak points in particular when trees are exposed to chronic or severe stress episodes: (1) an isotopic decoupling between leaves and tree rings occurs under limiting environmental conditions when growth is restricted e.g., either by low temperatures (<5–6 °C) or drought. (2) A temporal decoupling related to the different carbon pools used for growth, with different isotopic signals. While stored assimilates (starch, sugars) carry a mixture of isotopic signals from past and current growing seasons, they are distinctly different from the isotopic values of freshly synthesized assimilates. (3) Shifts in the oxygen isotope signals can occur due to usage of different water sources that vary in their temporal origin. In temperate sites during the growing season, trees can utilize large proportions of winter water deeper in the soil profile, which can lead to an asynchrony between the  $\delta^{18}\text{O}$  values in tree rings and recent precipitation water carrying the growing season temperature/humidity signal. (4) Post photosynthetic fractionations can dampen the amplitude of the initial signal in the leaves, to a degree, that a poor signal to noise ratio hampers a straightforward data interpretation.

To overcome these difficulties, we suggest an isotopic intra-annual assessment (IAA) of tree rings (using microtomes, laser ablation, etc.) to gain access to isotopic signals, which are formed under boundary conditions, particularly for trees living under extreme environments (cold/hot, dry). Moreover, the interpretation of the intra-annual stable isotope-climate relationships, with particular reference to the seasonal changes in the NSC and water source for  $\delta^{18}\text{O}$ , could be greatly improved when different stages of xylogenesis are accounted for (Szejner et al. 2016; Belmecheri et al. 2018). Furthermore, the IAA facilitates the study of physiological processes at a finer temporal resolution. In a combined effort with controlled experiments and field studies one could be looking at dynamics and isotopic composition of NSC with the help of CSIA (Compound Specific Isotope Analysis) in autotrophic and heterotrophic tissues, which reflect the instantaneous changes in leaf gas exchanges better (e.g. Keitel et al. 2003). Thus it is possible to account for the lag between C assimilation in foliage and investment in the annual ring formation through xylogenesis (Rinne et al. 2015).

The development for fine resolution intra annual tree-ring analysis is highly promising, thanks to the recent instrumental development (Chap. 7). Not only it will help to improve the interpretation of tree-ring isotope values, but it will widen the field

of tree-ring analyses and advance the detection of tree physiological mechanisms we can gain from them.

## References

- Ainsworth EA, Lemonnier P (2018) Phloem function: a key to understanding and manipulating plant responses to rising atmospheric CO<sub>2</sub>? *Curr Opin Plant Biol* 43:50–56
- Allen ST, Kirchner JW, Braun S, Siegwolf RTW, Goldsmith GR (2019) Seasonal origins of soil water used by trees. *Hydrol Earth Syst Sci* 23:1199–1210
- Babst F, Poulter B, Bodesheim P, Mahecha MD, Frank DC (2017) Improved tree-ring archives will support earth-system science. *Nat Ecol Evol* 1, Article number: 0008
- Bader MKF, Leuzinger S, Keel SG, Siegwolf RTW, Hagedorn F, Schleppi P, Körner C (2013) Central European hardwood trees in a high-CO<sub>2</sub> future: synthesis of an 8-year forest canopy CO<sub>2</sub> enrichment project. *J Ecol* 101:1509–1519
- Barbeta A, Penuelas J (2017) Increasing carbon discrimination rates and depth of water uptake favor the growth of Mediterranean evergreen trees in the ecotone with temperate deciduous forests. *Glob Change Biol* 23:5054–5068
- Barbeta A, Burrell R, Martín-Gómez P, Fréjaville B, Devert N, Wingate L, Domec J-C, Ogée J (2020) Evidence for distinct isotopic composition of sap and tissue water in tree stems: consequences for plant water source identification. *bioRxiv* 2020.06.18.160002
- Barbour MM, Andrews TJ, Farquhar GD (2001) Correlations between oxygen isotope ratios of wood constituents of *Quercus* and *Pinus* samples from around the world. *Aust J Plant Physiol* 28
- Barbour MM, Roden JS, Farquhar GD, Ehleringer JR (2004) Expressing leaf water and cellulose oxygen isotope ratios as enrichment above source water reveals evidence of a Pecllet effect. *Oecologia* 138:426–435
- Battipaglia G, Campelo F, Vieira J, Grabner M, De Micco V, Nabais C, Cherubini P, Carrer M, Bräuning A, Čufar K, Di Filippo A, García-González I, Koprowski M, Klisz M, Kirilyanov AV, Zafirov N, de Luis M (2016) Structure and function of intra-annual density fluctuations: mind the gaps. *Front Plant Sci* 7
- Belmecheri S, Wright WE, Szejner P, Morino KA, Monson RK (2018) Carbon and oxygen isotope fractionations in tree rings reveal interactions between cambial phenology and seasonal climate. *Plant Cell Environ* 41:2758–2772
- Belmecheri S, Maxwell RS, Taylor AH, Davis KJ, Freeman KH, Munger WJ (2014) Tree-ring delta C-13 tracks flux tower ecosystem productivity estimates in a NE temperate forest. *Environ Res Lett* 9
- Berry ZC, Goldsmith GR (2020) Diffuse light and wetting differentially affect tropical tree leaf photosynthesis. *New Phytol* 225:143–153
- Björklund J, von Arx G, Nievergelt D, Wilson R, Van den Bulcke J, Gunther B, Loader NJ, Rydval M, Fonti P, Scharnweber T, Andreu-Hayles L, Buntgen U, D'Arrigo R, Davi N, De Mil T, Esper J, Gartner H, Geary J, Gunnarson BE, Hartl C, Hevia A, Song H, Janecka K, Kaczka RJ, Kirilyanov AV, Kochbeck M, Liu Y, Meko M, Mundo I, Nicolussi K, Oelkers R, Pichler T, Sanchez-Salguero R, Schneider L, Schweingruber F, Timonen M, Trouet V, Van Acker J, Verstege A, Villalba R, Wilmking M, Frank D (2019) Scientific merits and analytical challenges of tree-ring densitometry. *Rev Geophys* 41
- Björklund JA, Gunnarson BE, Seftigen K, Esper J, Linderholm HW (2013) Is blue intensity ready to replace maximum latewood density as a strong temperature proxy? A tree-ring case study on Scots pine from northern Sweden. *Clim Past Discuss* 9:5227–5261
- Bjorkman AD, Myers-Smith IH, Elmendorf SC, Normand S, Ruger N, Beck PSA, Blach-Overgaard A, Blok D, Cornelissen JHC, Forbes BC, Georges D, Goetz SJ, Guay KC, Henry GHR, HilleRis-Lambers J, Hollister RD, Karger DN, Kattge J, Manning P, Prevey JS, Rixen C, Schaepman-Strub

- G, Thomas HJD, Vellend M, Wilmking M, Wipf S, Carbognani M, Hermanutz L, Levesque E, Molau U, Petraglia A, Soudzilovskaia NA, Spasojevic MJ, Tomaselli M, Vowles T, Alatalo JM, Alexander HD, Anadon-Rosell A, Angers-Blondin S, te Beest M, Berner L, Bjork RG, Buchwal A, Buras A, Christie K, Cooper EJ, Dullinger S, Elberling B, Eskelinen A, Frei ER, Grau O, Grogan P, Hallinger M, Harper KA, Heijmans M, Hudson J, Hulber K, Iturrate-Garcia M, Iversen CM, Jaroszynska F, Johnstone JF, Jorgensen RH, Kaarlejarvi E, Klady R, Kuleza S, Kulonen A, Lamarque LJ, Lantz T, Little CJ, Speed JDM, Michelsen A, Milbau A, Nabe-Nielsen J, Nielsen SS, Ninot JM, Oberbauer SF, Olofsson J, Onipchenko VG, Rumpf SB, Semenchuk P, Shetti R, Collier LS, Street LE, Suding KN, Tape KD, Trant A, Treier UA, Tremblay JP, Tremblay M, Venn S, Weijers S, Zamin T, Boulanger-Lapointe N, Gould WA, Hik DS, Hofgaard A, Jonsdottir IS, Jorgenson J, Klein J, Magnusson B, Tweedie C, Wookey PA, Bahn M, Blonder B, van Bodegom PM, Bond-Lamberty B, Campetella G, Cerabolini BEL, Chapin FS, Cornwell WK, Craine J, Dainese M, de Vries FT, Diaz S, Enquist BJ, Green W, Milla R, Niinemets U, Onoda Y, Ordóñez JC, Ozinga WA, Penuelas J, Poorter H, Poschold P, Reich PB, Sande B, Schamp B, Sheremetev S, Weiher E (2018) Plant functional trait change across a warming tundra biome. *Nature* 562:57–61
- Bögelein R, Lehmann MM, Thomas FM (2019) Differences in carbon isotope leaf-to-phloem fractionation and mixing patterns along a vertical gradient in mature European beech and Douglas fir. *New Phytol* 222:1803–1815
- Braun S, Thomas VFD, Quiring R, Flückiger W (2010) Does nitrogen deposition increase forest production? The role of phosphorus. *Environ Pollut* 158:2043–2052
- Brienen RJW, Helle G, Pons TL, Guyot J-L, Gloor M (2012) Oxygen isotopes in tree rings are a good proxy for Amazon precipitation and El Niño-Southern Oscillation variability. *Proc Natl Acad Sci* 109:16957–16962
- Brinkmann N, Eugster W, Buchmann N, Kahmen A (2019) Species-specific differences in water uptake depth of mature temperate trees vary with water availability in the soil. *Plant Biol* 21:71–81
- Brinkmann N, Seeger S, Weiler M, Buchmann N, Eugster W, Kahmen A (2018) Employing stable isotopes to determine the residence times of soil water and the temporal origin of water taken up by *Fagus sylvatica* and *Picea abies* in a temperate forest. *New Phytol* 219:1300–1313
- Buckley BM, Hansen KG, Griffin KL, Schmiede S, Oelkers R, D'Arrigo RD, Stahle DK, Davi N, Nguyen TQT, Le CN, Wilson RJS (2018) Blue intensity from a tropical conifer's annual rings for climate reconstruction: an ecophysiological perspective. *Dendrochronologia* 50:10–22
- Campbell R, McCarroll D, Loader NJ, Grudd HK, Robertson I, Jalkanen R (2007) Blue intensity in *Pinus sylvestris* tree-rings: developing a new palaeoclimate proxy. *The Holocene* 17:821–828
- Carbone MS, Czimczik CI, Keenan TF, Murakami PF, Pederson N, Schaberg PG, Xu XM, Richardson AD (2013) Age, allocation and availability of nonstructural carbon in mature red maple trees. *New Phytol* 200:1145–1155
- Castagneri D, Fonti P, von Arx G, Carrer M (2017) How does climate influence xylem morphogenesis over the growing season? Insights from long-term intra-ring anatomy in *Picea abies*. *Ann Bot* 119:1011–1020
- Castagneri D, Battipaglia G, von Arx G, Pacheco A, Carrer M (2018) Tree-ring anatomy and carbon isotope ratio show both direct and legacy effects of climate on bimodal xylem formation in *Pinus pinea*. *Tree Physiol* 38:1098–1109
- Cernusak LA, English NB (2015) Beyond tree-ring widths: stable isotopes sharpen the focus on climate responses of temperate forest trees. *Tree Physiol* 35:1–3
- Cernusak LA, Farquhar GD, Pate JS (2005) Environmental and physiological controls over oxygen and carbon isotope composition of Tasmanian blue gum, *Eucalyptus globulus*. *Tree Physiol* 25:129–146
- Cernusak LA, Ubierna N, Winter K, Holtum JAM, Marshall JD, Farquhar GD (2013) Environmental and physiological determinants of carbon isotope discrimination in terrestrial plants. *New Phytol* 200:950–965
- Churkina G, Running SW (1998) Contrasting climatic controls on the estimated productivity of global terrestrial biomes. *Ecosystems* 1:206–215

- Craig H, Gordon LI (1965) Deuterium and oxygen 18 variations in the ocean and the marine atmosphere. Consiglio nazionale delle ricerche, Laboratorio de geologia nucleare
- Cuny HE, Rathgeber CBK, Frank D, Fonti P, Makinen H, Prislán P, Rossi S, del Castillo EM, Campelo F, Vavrcik H, Camarero JJ, Bryukhanova MV, Jyske T, Gricar J, Gryc V, De Luis M, Vieira J, Cufar K, Kirdyanov AV, Oberhuber W, Trembl V, Huang J-G, Li X, Swidrak I, Deslauriers A, Liang E, Nojd P, Gruber A, Nabais C, Morin H, Krause C, King G, Fournier M (2015) Woody biomass production lags stem-girth increase by over one month in coniferous forests. *Nat Plants* 1
- Dansgaard W (1964) Stable isotopes in precipitation. *Tellus* 16:436–468
- Dawson TE (1998) Fog in the California redwood forest: ecosystem inputs and use by plants. *Oecologia* 117:476–485
- Dawson TE, Siegwolf RTW (2007) Stable isotopes as indicators of ecological change. Elsevier Academic Press Inc., San Diego
- De Micco V, Balzano A, Cufar K, Aronne G, Gricar J, Merela M, Battipaglia G (2016) Timing of false ring formation in *Pinus Halepensis* and *Arbutus unedo* in Southern Italy: outlook from an analysis of xylogenesis and tree-ring chronologies. *Front Plant Sci* 7:14
- Delpierre N, Berveiller D, Granda E, Dufrière E (2016) Wood phenology, not carbon input, controls the interannual variability of wood growth in a temperate oak forest. *New Phytol* 210:459–470
- Deslauriers A, Huang JG, Balducci L, Beaulieu M, Rossi S (2016) The contribution of carbon and water in modulating wood formation in black spruce saplings. *Plant Physiol* 170:2072–2084
- Deslauriers A, Fonti P, Rossi S, Rathgeber CBK, Gricar J (2017) Ecophysiology and plasticity of wood and phloem formation. In: Amoroso MM, Daniels LD, Baker PJ, Camarero JJ (eds) *Dendroecology: tree-ring analyses applied to ecological studies*, pp 13–33
- Deslauriers A, Giovannelli A, Rossi S, Castro G, Fragnelli G, Traversi L (2009) Intra-annual cambial activity and carbon availability in stem of poplar. *Tree Physiol* 29:1223–1235
- Deslauriers A, Beaulieu M, Balducci L, Giovannelli A, Gagnon MJ, Rossi S (2014) Impact of warming and drought on carbon balance related to wood formation in black spruce. *Ann Bot* 114:335–345
- Dietrich L, Delzon S, Hoch G, Kahmen A (2019) No role for xylem embolism or carbohydrate shortage in temperate trees during the severe 2015 drought. *J Ecol* 107:334–349
- Dietze MC, Sala A, Carbone MS, Czimczik CI, Mantoosh JA, Richardson AD, Vargas R (2014) Nonstructural carbon in woody plants. In: Merchant ss (ed) *Annual review of plant biology*, vol 65, pp 667–687
- Dongmann G, Nurnberg HW, Forstel H, Wagener K (1974) Enrichment of  $H_2^{18}O$  in leaves of transpiring plants. *Radiat Environ Biophys* 11:41–52
- Du E, Terrer C, Pellegrini AFA, Ahlstrom A, van Lissa CJ, Zhao X, Xia N, Wu X, Jackson RB (2020) Global patterns of terrestrial nitrogen and phosphorus limitation. *Nat Geosci* 13, 221–+
- Eilmann B, Buchmann N, Siegwolf R, Saurer M, Cherubini P, Rigling A (2010) Fast response of Scots pine to improved water availability reflected in tree-ring width and delta  $^{13}C$ . *Plant Cell Environ* 33:1351–1360
- Ellsworth DS, Anderson IC, Crous KY, Cooke J, Drake JE, Gherlenda AN, Gimeno TE, Macdonald CA, Medlyn BE, Powell JR, Tjoelker MG, Reich PB (2017) Elevated  $CO_2$  does not increase eucalypt forest productivity on a low-phosphorus soil. *Nat Clim Chang* 7:279
- Etzold S, Ferretti M, Reinds GJ, Solberg S, Gessler A, Waldner P, Schaub M, Simpson D, Benham S, Hansen K, Ingerslev M, Jonard M, Karlsson PE, Lindroos AJ, Marchetto A, Manninger M, Meesenburg H, Merila P, Nojd P, Rautio P, Sanders TGM, Seidling W, Skudnik M, Thimonier A, Verstraeten A, Vesterdal L, Vejputskova M, de Vries W (2020) Nitrogen deposition is the most important environmental driver of growth of pure, even-aged and managed European forests. *For Ecol Manage* 458:13
- Fajardo A, Piper FI, Hoch G (2013) Similar variation in carbon storage between deciduous and evergreen treeline species across elevational gradients. *Ann Bot* 112:623–631
- Farquhar GD, Sharkey TD (1982) Stomatal conductance and photosynthesis. *Annu Rev Plant Physiol Plant Mol Biol* 33:317–345

- Farquhar GD, Lloyd J (1993) Carbon and oxygen isotope effects in the exchange of carbon dioxide between terrestrial plants and the atmosphere. *Stable isotopes and plant carbon-water relations*. Academic Press, San Diego, pp 47–70
- Farquhar GD, O'Leary MH, Berry JA (1982) On the Relationship between carbon isotope discrimination and the intercellular carbon dioxide concentration in leaves. *Aust J Plant Physiol* 9:121–137
- Farquhar GD, Ehleringer FR, Hubick KT (1989) Carbon isotope discrimination and photosynthesis. *Ann Rev Plant Physiol Plant Mol Biol* 40:503–537
- Fernandez-de-Una L, Rossi S, Aranda I, Fonti P, Gonzalez-Gonzalez BD, Canellas I, Gea-Izquierdo G (2017) Xylem and leaf functional adjustments to drought in *Pinus sylvestris* and *Quercus pyrenaica* at their elevational boundary. *Front Plant Sci* 8
- Fleischer K, Rammig A, De Kauwe MG, Walker AP, Domingues TF, Fuchslueger L, Garcia S, Goll DS, Grandis A, Jiang M, Haverd V, Hofhansl F, Holm JA, Kruijt B, Leung F, Medlyn BE, Mercado LM, Norby RJ, Pak B, von Randow C, Quesada CA, Schaap KJ, Valverde-Barrantes OJ, Wang Y-P, Yang X, Zaehle S, Zhu Q, Lapola DM (2019) Amazon forest response to CO<sub>2</sub> fertilization dependent on plant phosphorus acquisition. *Nat Geosci* 12:736–741
- Frank DC, Poulter B, Saurer M, Esper J, Huntingford C, Helle G, Treydte K, Zimmermann NE, Schleser GH, Ahlstrom A, Ciais P, Friedlingstein P, Levis S, Lomas M, Sitch S, Viovy N, Andreu-Hayles L, Bednarz Z, Berninger F, Boettger T, D'Alessandro CM, Daux V, Filot M, Grabner M, Gutierrez E, Haupt M, Hilasvuori E, Jungner H, Kalela-Brundin M, Krapiec M, Leuenberger M, Loader NJ, Marah H, Masson-Delmotte V, Pazzur A, Pawelczyk S, Pierre M, Planells O, Pukiene R, Reynolds-Henne CE, Rinne KT, Saracino A, Sonninen E, Stievenard M, Switsur VR, Szczepanek M, Szychowska-Krapiec E, Todaro L, Waterhouse JS, Weigl M (2015) Water-use efficiency and transpiration across European forests during the Anthropocene. *Nature Clim Change* 5:579–583
- Fritts H (1976) *Tree rings and climate*. Academic Press, New York, p 433
- Galiano L, Timofeeva G, Saurer M, Siegwolf R, Martínez-Vilalta J, Hommel R, Gessler A (2017) The fate of recently fixed carbon after drought release: towards unravelling C storage regulation in *Tilia platyphyllos* and *Pinus sylvestris*. *Plant Cell Environ* 40:1711–1724
- Gessler A, Brandes E, Buchmann N, Helle G, Rennenberg H, Barnard RL (2009a) Tracing carbon and oxygen isotope signals from newly assimilated sugars in the leaves to the tree-ring archive. *Plant, Cell Environ* 32:780–795
- Gessler A, Low M, Heerd C, Op de Beeck M, Schumacher J, Grams TEE, Bahnweg G, Ceulemans R, Werner H, Matyssek R, Rennenberg H, Haberer K (2009b) Within-canopy and ozone fumigation effects on delta C-13 and Delta O-18 in adult beech (*Fagus sylvatica*) trees: relation to meteorological and gas exchange parameters. *Tree Physiol* 29:1349–1365
- Gessler A, Pedro Ferrio J, Hommel R, Treydte K, Werner RA, Monson RK (2014) Stable isotopes in tree rings: towards a mechanistic understanding of isotope fractionation and mixing processes from the leaves to the wood. *Tree Physiol* 34:796–818
- Glerum C (1980) Food sinks and food reserves of trees in temperate climates. *NZ J Forest Sci* 10:176–185
- Goldsmith GR, Lehmann MM, Cernusak LA, Arend M, Siegwolf RTW (2017) Inferring foliar water uptake using stable isotopes of water. *Oecologia* 184:763–766. <https://doi.org/10.1007/s00442-017-3917-1>
- Gonzalez-Gonzalez BD, Garcia-Gonzalez I, Vazquez-Ruiz RA (2013) Comparative cambial dynamics and phenology of *Quercus robur* L. and *Q. pyrenaica* Willd. in an Atlantic forest of the Northwestern Iberian Peninsula. *Trees-Struct Funct* 27:1571–1585
- Grattapaglia D, Plomion C, Kirst M, Sederoff RR (2009) Genomics of growth traits in forest trees. *Curr Opin Plant Biol* 12:148–156
- Grossiord C, Buckley TN, Cernusak LA, Novick KA, Poulter B, Siegwolf RTW, Sperry JS, McDowell NG (2020) Plant responses to rising vapor pressure deficit. *New Phytol* 226:1550–1566



- Guerrieri R, Lepine L, Asbjornsen H, Xiao JF, Ollinger SV (2016) Evapotranspiration and water use efficiency in relation to climate and canopy nitrogen in US forests. *J Geophys Res-Biogeosci* 121:2610–2629
- Guerrieri R, Jennings K, Belmecheri S, Asbjornsen H, Ollinger S (2017) Evaluating climate signal recorded in tree-ring delta C-13 and delta O-18 values from bulk wood and alpha-cellulose for six species across four sites in the northeastern US. *Rapid Commun Mass Spectrom* 31:2081–2091
- Guerrieri R, Belmecheri S, Ollinger SV, Asbjornsen H, Jennings K, Xiao J, Stocker BD, Martin M, Hollinger DY, Bracho-Garrillo R, Clark K, Dore S, Kolb T, Munger JW, Novick K, Richardson AD (2019) Disentangling the role of photosynthesis and stomatal conductance on rising forest water-use efficiency. *Proc Natl Acad Sci* 116:16909–16914
- Hartl-Meier C, Zang C, Buentgen U, Esper J, Rothe A, Goettlein A, Dimboeck T, Treydte K (2015) Uniform climate sensitivity in tree-ring stable isotopes across species and sites in a mid-latitude temperate forest. *Tree Physiol* 35:4–15
- Hartmann H (2015) Carbon starvation during drought-induced tree mortality—are we chasing a myth? *J Plant Hydraul* 2
- Hartmann H, Trumbore S (2016) Understanding the roles of nonstructural carbohydrates in forest trees—from what we can measure to what we want to know. *New Phytol* 211:386–403
- Helle G, Schleser G (2004) Interpreting climate proxies from tree-rings. In: Fischer H, Kumke T, Lohmann G, Miller H, Negendank JFW, Von Storch H (eds) *Towards a synthesis of Holocene proxy data and climate models*. Springer, Berlin
- Hoch G, Körner C (2002) Are treeline trees carbon limited? *Ecol Soc Am Ann Meet Abstr* 87:365
- Hoch G, Körner C (2003) The carbon charging of pines at the climatic treeline: a global comparison. *Oecologia* 135:10–21
- Hoch G, Körner C (2012) Global patterns of mobile carbon stores in trees at the high-elevation tree line. *Glob Ecol Biogeogr* 21:861–871
- Högberg P, Högberg MN, Gottlicher SG, Betson NR, Keel SG, Metcalfe DB, Campbell C, Schindlbacher A, Hurry V, Lundmark T, Linder S, Nasholm T (2008) High temporal resolution tracing of photosynthate carbon from the tree canopy to forest soil microorganisms. *New Phytol* 177:220–228
- Hölttä T, Mencuccini M, Nikinmaa E (2014) Ecophysiological aspects of phloem transport in trees. In: Tausz M, Grulke N (eds) *Trees in a changing environment. Plant ecophysiology*, vol 9. Springer, Dordrecht
- Huang JB, Hammerbacher A, Weinhold A, Reichelt M, Gleixner G, Behrendt T, van Dam NM, Sala A, Gershenson J, Trumbore S, Hartmann H (2019) Eyes on the future—evidence for trade-offs between growth, storage and defense in Norway spruce. *New Phytol* 222:144–158
- Kagawa A, Sugimoto A, Maximov TC (2006a) Seasonal course of translocation, storage and remobilization of C-13 pulse-labeled photoassimilate in naturally growing *Larix gmelinii* saplings. *New Phytol* 171:793–804
- Kagawa A, Sugimoto A, Maximov TC (2006b) (CO<sub>2</sub>)-C-13 pulse-labelling of photoassimilates reveals carbon allocation within and between tree rings. *Plant Cell Environ* 29:1571–1584
- Keel SG, Siegwolf RTW, Körner C (2006) Canopy CO<sub>2</sub> enrichment permits tracing the fate of recently assimilated carbon in a mature deciduous forest. *New Phytol* 172:319–329
- Keel SG, Siegwolf RTW, Jaggi M, Körner C (2007) Rapid mixing between old and new C pools in the canopy of mature forest trees. *Plant Cell Environ* 30:963–972
- Keitel C, Adams MA, Holst T, Matzarakis A, Mayer H, Rennenberg H, Gessler A (2003) Carbon and oxygen isotope composition of organic compounds in the phloem sap provides a short-term measure for stomatal conductance of European beech (*Fagus sylvatica* L.). *Plant Cell Environ* 26:1157–1168
- Kimak A, Leuenberger M (2015) Are carbohydrate storage strategies of trees traceable by early-latewood carbon isotope differences? *Trees-Struct Funct* 29:859–870
- Klein T, Siegwolf RTW, Körner C (2016a) Belowground carbon trade among tall trees in a temperate forest. *Science* 352:342–344

- Klein T, Bader MKF, Leuzinger S, Mildner M, Schleppei P, Siegwolf RTW, Körner C (2016b) Growth and carbon relations of mature *Picea abies* trees under 5 years of free-air CO<sub>2</sub> enrichment. *J Ecol* 104:1720–1733
- Körner C (1991) Some often overlooked plant characteristics as determinants of plant growth: a reconsideration. *Funct Ecol* 5:162–173
- Körner C (2003) Carbon limitation in trees. *J Ecol* 91:4–17
- Körner, C. (2012) Alpine treelines: functional ecology of the global high elevation tree limits. Springer Science & Business Media
- Körner C (2015) Paradigm shift in plant growth control. *Curr Opin Plant Biol* 25:107–114
- Körner, C. (2016) Plant adaptation to cold climates. *F1000Research* 5
- Körner C, Paulsen J (2004) A world-wide study of high altitude treeline temperatures. *J Biogeogr* 31:713–732
- Körner C, Scheel JA, Bauer H (1979) Maximum leaf diffusive conductance in vascular plants. *Photosynthetica* 13:45–82
- Körner C, Sarris D, Christodoulakis D (2005) Long-term increase in climatic dryness in the East-Mediterranean as evidenced for the island of Samos. *Reg Environ Change* 5:27–36
- Kress A, Saurer M, Büntgen U, Treyde KS, Bugmann H, Siegwolf RTW (2009) Summer temperature dependency of larch budmoth outbreaks revealed by alpine tree-ring isotope chronologies. *Oecologia* 160, 353–365
- Larcher W (2003) Physiological plant ecology—ecophysiology and stress physiology of functional groups, 4th edn. Springer, Berlin
- Lehmann MM, Goldsmith GR, Mirande-Ney C, Weigt RB, Schönbeck L, Kahmen A, Gessler A, Siegwolf RTW, Saurer M (2020) The <sup>18</sup>O-signal transfer from water vapour to leaf water and assimilates varies among plant species and growth forms. *Plant, Cell Environ* 43(2):510–523
- Lempereur M, Martin-StPaul NK, Damesin C, Joffre R, Ourcival J-M, Rocheteau A, Rambal S (2015) Growth duration is a better predictor of stem increment than carbon supply in a Mediterranean oak forest: implications for assessing forest productivity under climate change. *New Phytol* 207:579–590
- Leonardi S, Gentilella T, Guerrieri R, Ripullone F, Magnani F, Mencuccini M, Noije TV, Borghetti M (2012) Assessing the effects of nitrogen deposition and climate on carbon isotope discrimination and intrinsic water-use efficiency of angiosperm and conifer trees under rising CO<sub>2</sub> conditions. *Glob Change Biol* 18:2925–2944
- Levesque M, Andreu-Hayles L, Pederson N (2017) Water availability drives gas exchange and growth of trees in northeastern US, not elevated CO<sub>2</sub> and reduced acid deposition. *Sci Rep* 7:9
- Levesque M, Andreu-Hayles L, Smith WK, Williams AP, Hobi ML, Allred BW, Pederson N (2019) Tree-ring isotopes capture interannual vegetation productivity dynamics at the biome scale. *Nat Commun* 10:742
- Lévesque M, Rigling A, Bugmann H, Weber P, Brang P (2014) Growth response of five co-occurring conifers to drought across a wide climatic gradient in Central Europe. *Agric for Meteorol* 197:1–12
- Loader NJ, McCarroll D, Barker S, Jalkanen R, Grudd H (2017) Inter-annual carbon isotope analysis of tree-rings by laser ablation. *Chem Geol* 466:323–326
- Martinez-Vilalta J, Sala A, Asensio D, Galiano L, Hoch G, Palacio S, Piper FI, Lloret F (2016) Dynamics of non-structural carbohydrates in terrestrial plants: a global synthesis. *Ecol Monogr* 86:495–516
- Mathias JM, Thomas RB (2018) Disentangling the effects of acidic air pollution, atmospheric CO<sub>2</sub>, and climate change on recent growth of red spruce trees in the Central Appalachian Mountains. *Glob Change Biol* 24:3938–3953
- McCarroll D, Loader NJ (2004) Stable isotopes in tree rings. *Quat Res Rev* 23:771–801
- Michelot A, Simard S, Rathgeber C, Dufrene E, Damesin C (2012) Comparing the intra-annual wood formation of three European species (*Fagus sylvatica*, *Quercus petraea* and *Pinus sylvestris*) as related to leaf phenology and non-structural carbohydrate dynamics. *Tree Physiol* 32:1033–1045

- Mildner M, Bader MKF, Leuzinger S, Siegwolf RTW, Körner C (2014) Long-term C-13 labeling provides evidence for temporal and spatial carbon allocation patterns in mature *Picea abies*. *Oecologia* 175:747–762
- Monson RK, Szejner P, Belmecheri S, Morino KA, Wright WE (2018) Finding the seasons in tree ring stable isotope ratios. *Am J Bot* 105:819–821
- Muller B, Pantin F, Genard M, Turc O, Freixes S, Piques M, Gibon Y (2011) Water deficits uncouple growth from photosynthesis, increase C content, and modify the relationships between C and growth in sink organs. *J Exp Bot* 62:1715–1729
- Nemani RR, Keeling CD, Hashimoto H, Jolly WM, Piper SC, Tucker CJ, Myneni RB, Running SW (2003) Climate-driven increases in global terrestrial net primary production from 1982 to 1999. *Science* 300:1560–1563
- Norby RJ, Zak DR (2011) Ecological lessons from Free-Air CO<sub>2</sub> Enrichment (FACE) experiments. In: Futuyama DJ, Shaffer HB, Simberloff D (eds) *Annual review of ecology, evolution, and systematics*, vol 42, pp 181–203
- Norby RJ, Warren JM, Iversen CM, Medlyn BE, McMurtrie RE (2010) CO<sub>2</sub> enhancement of forest productivity constrained by limited nitrogen availability. *Proc Natl Acad Sci USA* 107:19368–19373
- Novick KA, Ficklin DL, Stoy PC, Williams CA, Bohrer G, Oishi AC, Papuga SA, Blanken PD, Noormets A, Sulman BN, Scott RL, Wang LX, Phillips RP (2016) The increasing importance of atmospheric demand for ecosystem water and carbon fluxes. *Nat Clim Chang* 6:1023–1027
- Palacio S, Paterson E, Sim A, Hester AJ, Millard P (2011) Browsing affects intra-ring carbon allocation in species with contrasting wood anatomy. *Tree Physiol* 31:150–159
- Palacio S, Hoch G, Sala A, Körner C, Millard P (2014) Does carbon storage limit tree growth? *New Phytol* 201:1096–1100
- Pallardy SG (2008) *Physiology of woody plants*, 3rd edn. Academic Press, New York, NY, USA
- Perez-de-Lis G, Garcia-Gonzalez I, Rozas V, Olano JM (2016) Feedbacks between earlywood anatomy and non-structural carbohydrates affect spring phenology and wood production in ring-porous oaks. *Biogeosciences* 13:5499–5510
- Perez-de-Lis G, Olano JM, Rozas V, Rossi S, Vazquez-Ruiz RA, Garcia-Gonzalez I (2017) Environmental conditions and vascular cambium regulate carbon allocation to xylem growth in deciduous oaks. *Funct Ecol* 31:592–603
- Pflug EE, Siegwolf R, Buchmann N, Dobbertin M, Kuster TM, Guenthardt-Goerg MS, Arend M (2015) Growth cessation uncouples isotopic signals in leaves and tree rings of drought-exposed oak trees. *Tree Physiol* 35:1095–1105
- Piper FI, Fajardo A, Hoch G (2017) Single-provenance mature conifers show higher non-structural carbohydrate storage and reduced growth in a drier location. *Tree Physiol* 37:1001–1010
- Porter TJ, Pisaric MFJ, Kokelj SV, Edwards TWD (2009) Climatic signals in  $\delta^{13}\text{C}$  and  $\delta^{18}\text{O}$  of tree-rings from White Spruce in the Mackenzie Delta Region, Northern Canada. *Arct Antarct Alp Res* 41:497–505
- Prescott CE, Grayston SJ, Helmisaari H-S, Kaštovská E, Körner C, Lambers H, Meier IC, Millard P, Ostonen I (2020) Surplus carbon drives allocation and plant–soil interactions. *Trends Ecol Evol* 35:1110–1118
- Reich PB, Oleksyn J (2004) Global patterns of plant leaf N and P in relation to temperature and latitude. *Proc Natl Acad Sci USA* 101:11001–11006
- Rinne KT, Saurer M, Kirilyanov AV, Loader NJ, Bryukhanova MV, Werner RA, Siegwolf RTW (2015) The relationship between needle sugar carbon isotope ratios and tree rings of larch in Siberia. *Tree Physiol* 35:1192–1205
- Rodríguez-Catón M, Andreu-Hayles L, Morales MS, Daux V, Christie DA, Coopman RE, Alvarez C, Palat Rao M, Aliste D, Flores F, Villalba R (2021) Different climate sensitivity for radial growth, but uniform for tree-ring stable isotopes along an aridity gradient in *Polylepis tarapacana*, the world's highest elevation tree species. *Tree Physiology* (in press)

- Rodríguez-Catón M, Andreu-Hayles L, Daux V, Vuille M, Varuolo-Clarke AM, Oelkers R, Christie DA, D'Arrigo R, Morales MS, Palat Rao M, Srur AM, Vimeux F, Villalba, R (2022) Hydroclimate and ENSO variability recorded by oxygen isotopes from tree rings in the South American Altiplano. *Geophys Res Lett* 49: e2021GL095883
- Rossi S, Morin H, Deslauriers A (2012) Causes and correlations in cambium phenology: towards an integrated framework of xylogenesis. *J Exp Bot* 63:2117–2126
- Rossi S, Deslauriers A, Anfodillo T, Carraro V (2007) Evidence of threshold temperatures for xylogenesis in conifers at high altitudes. *Oecologia* 152:1–12
- Rossi S, Deslauriers A, Anfodillo T, Carrer M (2008) Age-dependent xylogenesis in timberline conifers. *New Phytol* 177:199–208
- Rossi S, Anfodillo T, Cufar K, Cuny HE, Deslauriers A, Fonti P, Frank D, Gricar J, Gruber A, Huang JG, Jyske T, Kaspar J, King G, Krause C, Liang EY, Mäkinen H, Morin H, Nojd P, Oberhuber W, Prislán P, Rathgeber CBK, Saracino A, Swidrak I, Trembl V (2016) Pattern of xylem phenology in conifers of cold ecosystems at the Northern Hemisphere. *Glob Change Biol* 22:3804–3813
- Running SW, Nemani RR, Heinsch FA, Zhao MS, Reeves M, Hashimoto H (2004) A continuous satellite-derived measure of global terrestrial primary production. *Bioscience* 54:547–560
- Sala A, Woodruff DR, Meinzer FC (2012) Carbon dynamics in trees: feast or famine? *Tree Physiol* 32:764–775
- Sarris D, Siegwolf R, Körner C (2013) Inter- and intra-annual stable carbon and oxygen isotope signals in response to drought in Mediterranean pines. *Agric for Meteorol* 168:59–68
- Saurer M, Spahni R, Frank DC, Joos F, Leuenberger M, Loader NJ, McCarroll D, Gagen M, Poulter B, Siegwolf RTW, Andreu-Hayles L, Boettger T, Dorado Liñán I, Fairchild IJ, Friedrich M, Gutierrez E, Haupt M, Hiltunen E, Heinrich I, Helle G, Grubb H, Jalkanen R, Levanič T, Linderholm HW, Robertson I, Sonninen E, Treydte K, Waterhouse JS, Woodley EJ, Wynn PM, Young GHF (2014) Spatial variability and temporal trends in water-use efficiency of European forests. *Glob Change Biol* 20:3700–3712
- Schollaen K, Heinrich I, Helle G (2014) UV-laser-based microscopic dissection of tree rings—a novel sampling tool for delta C-13 and delta O-18 studies. *New Phytol* 201:1045–1055
- Seddon AWR, Macias-Fauria M, Long PR, Benz D, Willis KJ (2016) Sensitivity of global terrestrial ecosystems to climate variability. *Nature* 531:229–+
- Sigurdsson BD, Medhurst JL, Wallin G, Eggertsson O, Linder S (2013) Growth of mature boreal Norway spruce was not affected by elevated CO<sub>2</sub> and/or air temperature unless nutrient availability was improved. *Tree Physiol* 33:1192–1205
- Simard S, Giovannelli A, Treydte K, Traversi ML, King GM, Frank D, Fonti P (2013) Intra-annual dynamics of non-structural carbohydrates in the cambium of mature conifer trees reflects radial growth demands. *Tree Physiol* 33:913–923
- Soudant A, Loader NJ, Back J, Levula J, Kljun N (2016) Intra-annual variability of wood formation and delta C-13 in tree-rings at Hyytiälä, Finland. *Agric for Meteorol* 224:17–29
- Sprenger M, Leistert H, Gimbel K, Weiler M (2016) Illuminating hydrological processes at the soil-vegetation-atmosphere interface with water stable isotopes. *Rev Geophys* 54:674–704
- Steinmann KTW, Siegwolf R, Saurer M, Körner C (2004) Carbon fluxes to the soil in a mature temperate forest assessed by C-13 isotope tracing. *Oecologia* 141:489–501
- Steppe K, Sterck F, Deslauriers A (2015) Diel growth dynamics in tree stems: linking anatomy and ecophysiology. *Trends Plant Sci* 20:335–343
- Streit K, Rinne KT, Hagedorn F, Dawes MA, Saurer M, Hoch G, Werner RA, Buchmann N, Siegwolf RTW (2013) Tracing fresh assimilates through *Larix decidua* exposed to elevated CO<sub>2</sub> and soil warming at the alpine treeline using compound-specific stable isotope analysis. *New Phytol* 197:838–849
- Szejner P, Wright WE, Belmecheri S, Meko D, Leavitt SW, Ehleringer JR, Monson RK (2018) Disentangling seasonal and interannual legacies from inferred patterns of forest water and carbon cycling using tree-ring stable isotopes. *Glob Change Biol* 24:5332–5347
- Szejner P, Wright WE, Babst F, Belmecheri S, Trouet V, Leavitt SW, Ehleringer JR, Monson RK (2016) Latitudinal gradients in tree ring stable carbon and oxygen isotopes reveal differential

- climate influences of the North American Monsoon System. *J Geophys Res-Biogeosci* 121:1978–1991
- Teskey R, Wertin T, Bauweraerts I, Ameye M, McGuire MA, Steppe K (2015) Responses of tree species to heat waves and extreme heat events. *Plant Cell Environ* 38:1699–1712
- Treydte K, Boda S, Pannatier EG, Fonti P, Frank D, Ullrich B, Saurer M, Siegwolf R, Battipaglia G, Werner W, Gessler A (2014) Seasonal transfer of oxygen isotopes from precipitation and soil to the tree ring: source water versus needle water enrichment. *New Phytol* 202:772–783
- Treydte K, Frank D, Esper J, Andreu L, Bednarz Z, Berninger F, Boettger T, D'Alessandro CM, Etien N, Filot M, Grabner M, Guillemin MT, Gutierrez E, Haupt M, Helle G, Hilasvuori E, Jungner H, Kalela-Brundin M, Krapiec M, Leuenberger M, Loader NJ, Masson-Delmotte V, Pazdur A, Pawelczyk S, Pierre M, Planells O, Pukiene R, Reynolds-Henne CE, Rinne KT, Saracino A, Saurer M, Sonninen E, Stievenard M, Switsur VR, Szczepanek M, Szychowska-Krapiec E, Todaro L, Waterhouse JS, Weigl M, Schleser GH (2007) Signal strength and climate calibration of a European tree-ring isotope network. *Geophys Res Lett* 34:L24302
- van der Sleen P, Zuidema PA, Pons TL (2017) Stable isotopes in tropical tree rings: theory, methods and applications. *Funct Ecol* 31:1674–1689
- Vincent-Barbaroux C, Berveiller D, Lelarge-Trouverie C, Maia R, Máguas C, Pereira J, Chaves MM, Damesin C (2019) Carbon-use strategies in stem radial growth of two oak species, one Temperate deciduous and one Mediterranean evergreen: what can be inferred from seasonal variations in the  $\delta^{13}\text{C}$  of the current year ring? *Tree Physiol* 39:1329–1341
- Voelker SL, Brooks JR, Meinzer FC, Anderson R, Bader MKF, Battipaglia G, Becklin KM, Beerling D, Bert D, Betancourt JL, Dawson TE, Guyette RP, Korner C, Leavitt SW, Linder S, Marshall JD, Mildner M, Ogee J, Panyushkina I, Plumpton HJ, Pregitzer KS, Saurer M, Smith AR, Siegwolf RTW, Stambaugh MC, Talhelm AF, Tardif JC, Van de Water PK, Ward JK, Wingate L (2016) A dynamic leaf gas-exchange strategy is conserved in woody plants under changing ambient  $\text{CO}_2$ : Evidence from carbon isotope discrimination in paleo and  $\text{CO}_2$  enrichment studies. *Glob Change Biol* 22:889–902. <https://doi.org/10.1111/gcb.13102>
- Voelker SL, Wang SYS, Dawson TE, Roden JS, Still CJ, Longstaffe FJ, Ayalon A (2019) Tree-ring isotopes adjacent to Lake Superior reveal cold winter anomalies for the Great Lakes region of North America. *Sci Rep* 9
- Von Caemmerer S, Farquhar GD (1981) Some relationships between the biochemistry of photosynthesis and the gas-exchange of leaves. *Planta* 153:376–387
- Weber R, Schwendener A, Schmid S, Lambert S, Wiley E, Landhausser SM, Hartmann H, Hoch G (2018) Living on next to nothing: tree seedlings can survive weeks with very low carbohydrate concentrations. *New Phytol* 218:107–118
- Wiley E, Helliker B (2012) A re-evaluation of carbon storage in trees lends greater support for carbon limitation to growth. *New Phytol* 195:285–289
- Wilson R, D'Arrigo R, Andreu-Hayles L, Oelkers R, Wiles G, Anchukaitis K, Davi N (2017) Experiments based on blue intensity for reconstructing North Pacific temperatures along the Gulf of Alaska. *Climate of the past* 13:1007–1022
- Wilson R, Anchukaitis K, Andreu-Hayles L, Cook E, D'Arrigo R, Davi N, Haberbauer L, Krusic P, Luckman B, Morimoto D, Oelkers R, Wiles G, Wood C (2019) Improved dendroclimatic calibration using blue intensity in the southern Yukon. *Holocene* 14
- Wurth MKR, Pelaez-Riedl S, Wright SJ, Körner C (2005) Non-structural carbohydrate pools in a tropical forest. *Oecologia* 143:11–24
- Young GHF, Loader NJ, McCarroll D, Bale RJ, Demmler JC, Miles D, Nayling NT, Rinne KT, Robertson I, Watts C, Whitney M (2015) Oxygen stable isotope ratios from British oak tree-rings provide a strong and consistent record of past changes in summer rainfall. *Clim Dyn* 45:3609–3622
- Zeng Q, Rossi S, Yang B (2018) Effects of age and size on xylem phenology in two conifers of Northwestern China. *Front Plant Sci* 8:9

**Open Access** This chapter is licensed under the terms of the Creative Commons Attribution 4.0 International License (<http://creativecommons.org/licenses/by/4.0/>), which permits use, sharing, adaptation, distribution and reproduction in any medium or format, as long as you give appropriate credit to the original author(s) and the source, provide a link to the Creative Commons license and indicate if changes were made.

The images or other third party material in this chapter are included in the chapter's Creative Commons license, unless indicated otherwise in a credit line to the material. If material is not included in the chapter's Creative Commons license and your intended use is not permitted by statutory regulation or exceeds the permitted use, you will need to obtain permission directly from the copyright holder.



# Chapter 15

## Post-photosynthetic Carbon, Oxygen and Hydrogen Isotope Signal Transfer to Tree Rings—How Timing of Cell Formations and Turnover of Stored Carbohydrates Affect Intra-annual Isotope Variations



Akira Kagawa and Giovanna Battipaglia

**Abstract** In this chapter, we discuss post-photosynthetic processes that affect intra-annual variation in the stable isotopes of tree rings, such as timing of cell formations and turnover of stored carbohydrates, by combining research findings gained by using either natural-abundance or artificially-enriched carbon, oxygen and hydrogen isotopes. We focus on within-ring variation in stable isotope ratios, with an emphasis on aligning observed ratios in whole wood or extracted cellulose to seasonal dynamics in climate and phenology. We also present a discussion of isotopic fractionation that operates within the scope of observed variations across individual rings. We then introduce a model that traces the seasonal partitioning of photosynthate into tree rings via storage pool, which is based on experimental data gained from labeling studies using artificially enriched  $^{13}\text{CO}_2$  gas. Finally, we will describe our current understanding of post-photosynthetic signal transfer processes of oxygen and hydrogen isotopes from leaves to tree rings, such as exchange of oxygen and hydrogen between storage carbohydrates and local cambial water, and possible causes of difference in oxygen and hydrogen isotope fractionations. Finally, we discuss mechanisms behind how oxygen and hydrogen from foliar-absorbed liquid water is then incorporated into wood biomass, by introducing results gained from recent  $\text{H}_2^{18}\text{O}$  and HDO pulse-labeling experiments.

---

A. Kagawa (✉)

Wood Anatomy and Quality Laboratory, Forestry and Forest Products Research Institute, 1 Matsuno-sato, Tsukuba, Ibaraki 300-1244, Japan  
e-mail: [akagawa@ffpri.affrc.go.jp](mailto:akagawa@ffpri.affrc.go.jp)

G. Battipaglia

Department of Environmental, Biological and Pharmaceutical Sciences and Technologies, University of Campania, Via Vivaldi, 43-81100 Caserta, Italy  
e-mail: [giovanna.battipaglia@unicampania.it](mailto:giovanna.battipaglia@unicampania.it)

© The Author(s) 2022

R. T. W. Siegwolf et al. (eds.), *Stable Isotopes in Tree Rings*, Tree Physiology 8,  
[https://doi.org/10.1007/978-3-030-92698-4\\_15](https://doi.org/10.1007/978-3-030-92698-4_15)

429

## 15.1 Introduction

Conventional tree-ring analyses have focused on the annual growth ring with a primary aim of inter-annual-to-inter-decadal translation of growth-climate relations. Partitioning of annual rings into earlywood and latewood, in those species that show such differentiation, has been used in some studies to extract early- and late-season growth trends, though the attribution of those trends to more specific dates during the growing season has been impeded by lack of knowledge about the use of stored carbon and seasonal lags in the phases of xylogenesis. As a result, intra-annual dendrochronological perspectives have been considerably fewer in number than inter-annual perspectives, and when developed, they have been relatively coarse in their alignment to patterns of seasonal climate variation. Compared to ring width and density measurement, tree-ring isotope analysis used to be much more costly and time-consuming in 1990s, and the number of tree-ring isotope research has been limited. However, this situation has changed markedly over the past decade as sample preparation and analytical approaches have improved (see Chap. 7).

In the last decade, the labor required for intra-annual analysis of tree-ring isotope ratio analysis has decreased, while the precision associated with these measures has increased (Kagawa et al. 2015, Chaps. 5 and 6). Analysis of intra-annual variations of tree-ring isotope ratio was first conducted by separating single annual rings into sub-sections by means of a knife or chisel under a microscope (Wilson and Grinstead 1977, Leavitt 1993; Kagawa et al. 2003) and isotope analysis of up to 0.1 mm resolution became possible by manually subdividing  $\alpha$ -cellulose lath under stereomicroscope, which is prepared directly from thin cross-section (Kagawa et al. 2015; Ohashi et al. 2016; Xu et al. 2016; Chap. 4). Higher spatial resolution is achieved by using a sliding microtome to cut serial tangential sections from wood blocks at thicknesses of 10–240  $\mu\text{m}$  (Ogle and McCormac 1994; Walcroft et al. 1997; Helle and Schleser 2004). Robotic micromilling (Dodd et al. 2008) and UV-laser based dissection (Schollaen et al. 2014, Chap. 7) allow serial isolation of tissue from the millimeter-to-micrometer scale. Although its use is currently limited to carbon isotope analysis and on whole wood, laser ablation can achieve an ultimate spatial resolution of 10  $\mu\text{m}$ , enabling observations at the cellular level (Schulze et al. 2004, Moran et al. 2011; Soudant et al. 2016; Loader et al. 2017). Using these more recent techniques, it is now foreseeable to routinely assess patterns in the seasonal variation of multiple elements, including carbon, oxygen and hydrogen isotope ratios. However, for accurate interpretation, researchers must understand the linkage between an intra-annual sample, and the seasonal timing that the sample represents.

In this chapter, we discuss post-photosynthetic processes that affect intra-annual variation in the stable isotopes of carbon, oxygen and hydrogen in tree rings, such as timing of cell formations and turnover of stored carbohydrates. We discuss past findings and the knowledge-gaps that are most likely to constrain efforts to expand our understanding in the future. In Sect. 15.2, we present a general overview of studies to date that have aimed to assess intra-annual variation in tree ring growth as presented



through the anatomical analysis of wood. Scientists have used observable variation in wood density, and cellular differentiation within the wood, to infer seasonal patterns in radial growth rates and general responses to warming and drying as the growing season progresses.

In Sect. 15.3, we focus on within ring variation in carbon and oxygen isotope ratios, with an emphasis on aligning observed ratios in whole wood or extracted cellulose to seasonal dynamics in climate and phenology. We not only present the principal findings from past studies, but also note the likely uncertainties that exist due to a lack of complete knowledge about fractionation processes and seasonal lags in cambial phenology. One of the primary considerations in this topic involves the degree to which stored carbohydrate, which carries isotope signals from antecedent climate conditions is used for xylem maturation, and therefore causes mixing of the isotopic signals recorded during past and present-day climate (Chap. 14). The identification of growth periods when stored carbohydrates are used will be considered in this section, but we will defer to a later section the discussion of experimental studies aimed at revealing the physiology of stored carbohydrates use during xylogenesis.

In Sect. 15.4, we present a discussion of isotopic fractionation that operates within the scope of observed variations across individual rings. We start with consideration of processes at the site of photosynthetic CO<sub>2</sub> assimilation in the chloroplasts of leaves or needles. The processes recorded in leaf-scale sugar isotope ratios vary on the order of fractions of seconds, though by the time the sugars have been transported to intra-leaf storage pools or to the phloem for transport to other parts of the plant, time-averaged isotope fractionation can be well-approximated by the steady-state assumption in observations and models. Following a discussion of leaf-scale photosynthetic dynamics, we progress to 'downstream' influences that have the potential to scramble the association of observed sugar isotope ratios with the short-term physiological and climate controls over leaf physiology, and thus mask efforts to trace tree-ring isotope time series with seasonally-resolved influences.

In Sect. 15.5, we consider xylogenesis itself as a cause in the disruption of the association of observed intra-annual isotope ratios with specific climate and phenological phases during the growing season. The incorporation of photosynthate into cellulose during xylogenesis is affected by seasonal lags in the processes of cell formation and maturation. Thus, the anatomical attributes of variation in the cellular appearance of xylem may not align seasonally with the isotopic attributes of the cellulose that makes up the primary and secondary cell walls of individual xylem elements and tracheids. We discuss new approaches relying on cambial phenology modeling conditioned on high-frequency micro-core sampling to resolve lags in the seasonal phases of xylogenesis.

In Sect. 15.6, we present a discussion of experimental studies that have traced the seasonal partitioning of photosynthate into tree rings. The research developments discussed in this section, when coupled with recent approaches that identify the intra-annual domains of tree rings according to isotope ratios and phases of xylogenesis, hold the greatest promise to provide explanations of intra-annual patterns of isotopic fractionation, especially those fractionations associated with

post-assimilation processes.  $^{13}\text{CO}_2$  pulse-labeling used in combination with high-resolution analysis of tree-ring isotopes is an effective tool to elucidate the processes that transfer fractionation signals from assimilation processes 'in the current moment' versus those from past processes that are stored in carbon reservoirs and subsequently transferred to the archived cellulose isotope record in tree rings. We also discuss future applications of  $\text{H}_2^{18}\text{O}$  and HDO pulse labeling for elucidating the post-photosynthetic processes of oxygen and hydrogen isotope signal transfer from leaves to tree rings, such as exchange of oxygen and hydrogen between carbohydrates and local water.

## 15.2 Intra-annual Variation in Wood Structure

Wood structure variation within a ring is important to understanding variation in intra-annual isotope ratios, because (1) these differences are caused by seasonal changes in the climate and phenology, and are often visual cues to guide sample analysis, and (2) are related to the seasonal course of storage carbon allocation to wood (e.g. ring-porous wood). Therefore, measures of wood density, width of early- and latewood, and/or chemical composition can be highly useful for helping to interpret the isotope ratio variance.

The earlywood-to-latewood variations in wood anatomy across individual rings are aligned with seasonal phases associated with the earliest and latest portions of the growing season (Brown 1912; Pallardy 2008). Earlywood (EW) consists of larger cells with thinner secondary walls, and is overall less dense than latewood (LW). The anatomical differences of EW and LW reflect differences in the seasonal phases of xylogenesis (Butto et al. 2019). Despite general correlations of EW and LW growth with variations in seasonal climate, detailed alignment of these tissue types with specific dates during the growing season is difficult; the time-dependent growth rate of woody tissues within an annual ring does not occur linearly (Camarero et al. 1998; Rossi et al. 2003; Kagawa et al. 2005; Soudant et al. 2016; Belmecheri et al. 2018). Furthermore, there is ample evidence that antecedent (previous-year) climate conditions and stored water and carbon resources can influence the current-year growth of both EW and LW (e.g. Seargent and Singer 2016; Kerhoulas et al. 2017; Szejner et al. 2018). EW and LW designations in trees from Mediterranean or humid tropical ecosystems is often challenging (Cherubini et al. 2003; Sass et al. 1995), due to stochastic occurrence of droughts (resulting in the formation of false rings) or the lack of seasonality (resulting in a lack of ring boundaries).

In the literature, several classifications of false ring, or double rings, or intra annual density fluctuations (IADF) exist. The appearance of an IADF can create errors in dendrochronological dating as it can be mistaken for a true LW band, and therefore cause a false assumption of annual growth truncation; this is the so-called 'false ring' phenomenon. The formation of IADFs has been related to physiological responses

at the leaf scale, including stomatal diffusion restrictions and photosynthetic water-use efficiency (WUE), that are induced by extreme mid-season droughts (Battipaglia et al. 2010, 2013; Balzano et al 2018, 2019; Zalloni et al 2016, 2018a, b, 2019).

The seasonal variations that are evident in the wood structure of annual rings are due to both phenological dynamics in cambial activity and influences from the ambient environment. McCarroll et al. (2003) explored the relationships of ten tree proxies, including several related to wood structure variation, with seasonal climate in *Pinus sylvestris* from three sites in northern Finland. Clear distinctions were noted in the correlations of EW and LW density and width-increment and seasonal climate variables. EW width was best correlated with late-summer temperature from the previous (antecedent) growing season, and it was hypothesized that overwinter stores of carbohydrate were used for EW construction. No clear climate signal could be associated with EW density. Latewood width and density were best correlated with late-summer (July and August) temperature of the current year, though the correlation was only strong at the southernmost site, and density alone was highly correlated with late-summer temperature at all sites. Similarly, using *Quercus robur* in Hungary, Kern et al. (2013) showed no significant correlation between EW width-increment and monthly precipitation or temperature, whereas LW width-increment was significantly correlated with July precipitation, but not with temperature. In ring-porous oak species, traits associated with individual EW xylem vessel size, rather than EW ring-width increment, have been shown to respond to site differences in spring moisture availability (Fonti and Garcia-Gonzalez 2008) and appear to be capable of acclimation to changes in spring temperature and moisture conditions (Gea-Izquierdo et al. 2012; Nabeshima et al. 2015). Thus, correlations between anatomical features of tree rings (width/density) and monthly climatic parameters (temperature, precipitation etc.) are closely related to seasonal dynamics of photosynthetic carbon allocation to tree rings, because, typically, latewood is mainly made from current summer and autumn photosynthate and earlywood is made from the mixture of photosynthate from current spring and the previous summer and autumn as we will discuss in Sect. 15.6 (Fig. 15.5, Kagawa 2006; Kagawa et al. 2006a).

### 15.3 Theoretical Considerations of Intra-annual Variation in Tree-Ring Isotope Fractionation

The theory regarding fractionation processes that lead to observed  $^{13}\text{C}/^{12}\text{C}$ ,  $^{18}\text{O}/^{16}\text{O}$ , and  $^2\text{H}/^1\text{H}$  ratios in the cellulose of tree rings has been covered in other chapters of this book (Chaps. 9–11). In this section, we focus on those processes that underlie intra-annual variation in  $\delta^{13}\text{C}$ ,  $\delta^{18}\text{O}$  and  $\delta^2\text{H}$ . The principle determinant of seasonal variation in the  $\delta^{13}\text{C}$  of the photosynthate used in xylogenesis is due to climate variation in the atmospheric environment—specifically, atmospheric humidity and available precipitation. Soil characteristics affect infiltration and drainage of precipitation into and out from soil, and thus alter the availability of source water, locally;

but, ultimately the amount of rain and snow deposited to the surface will control soil moisture availability, and thus the physiological states of trees. The  $^{13}\text{C}/^{12}\text{C}$  ratio observed at the moment of photosynthetic  $\text{CO}_2$  assimilation depends on the atmospheric (source) ratio, the kinetic fractionations associated with diffusion in the air and cellular cytosol between the outer edge of the leaf boundary layer and the site of carboxylation within the chloroplast, and that associated with the active site of the chloroplastic enzyme, ribulose 1,5-bisphosphate (RuBP) carboxylase. Each isotopic form of  $\text{CO}_2$  can either diffuse to the chloroplast and be assimilated biochemically or it can diffuse back out of the leaf and rejoin the atmospheric source. The relative fates of these molecules can be mathematically predicted by the ratio of stomatal conductance (which controls the diffusive entry and exit from the leaf) to RuBP carboxylation (which controls biochemical removal from the leaf). An equation that has been shown to approximate the interactions of these determining processes is:

$$\Delta_A = a + (b - a) \frac{c_i}{c_a} \quad (15.1)$$

where  $\Delta_A$  is the overall fractionation associated with  $\text{CO}_2$  assimilation,  $a$  is the fractionation of  $^{12}\text{CO}_2$  and  $^{13}\text{CO}_2$  due to diffusion through air,  $b$  is the biochemical fractionation associated with RuBP carboxylase, and  $c_i$  and  $c_a$  are the  $\text{CO}_2$  ( $^{12}\text{CO}_2$  and  $^{13}\text{CO}_2$  combined) concentrations in the intercellular air space and atmosphere, respectively (Farquhar et al. 1989). Equation 15.1 is simplified in that it ignores the liquid-phase diffusion paths within the cell, as well as some additional biochemical processes that can influence the overall fractionation, such as photorespiration. It is important to note that a principal concept underlying the weighting employed in Eq. 15.1 is the requirement for discriminated isotopes to leave (or leak) from a fractionation process. That is, there is no fractionation associated with processes and reactions that are truly closed, and thus capable of producing product from all available reactants. Fractionation requires the 'escape' of discriminated reactants.

Working from Eq. 15.1, seasonal variations in  $\delta^{13}\text{C}$  in the cellulose of tree-rings will depend on seasonal variations in  $c_i/c_a$ , which in turn reflect dynamics in  $g_s$  (stomatal conductance) relative to  $A$  (the biochemical capacity for photosynthetic  $\text{CO}_2$  assimilation). Although the potential exists for seasonal variation in  $A$  through changes in light levels,  $V_{\text{cmax}}$  (carboxylation capacity) or  $J_{\text{max}}$  (electron transport), which are the biochemical determinants of the maximum photosynthetic rate, the primary influences imposed on Eq. 15.1 will be due to seasonal climate attributes that affect  $g_s$ . Thus, precipitation and atmospheric humidity reflect the first-order seasonal climate drivers of intra-annual variation in tree-ring  $\delta^{13}\text{C}$ .

The initial control of the atmospheric environment on cellulose  $\delta^{13}\text{C}$  is often not straightforward because of the temporal offsets between the time of photosynthate production and its eventual use during xylogenesis (Badeck et al. 2005; Kagawa et al. 2005, 2006a). Offsets in the timing of the production and use of photosynthate are the result of non-structural carbohydrates (NSC) storage and remobilization, and the phenological lags that are imposed on xylogenesis as it proceeds through its phased

time course. In both cases, photosynthate that was produced with a unique relation to the atmospheric environment at one point in time, is incorporated into the cellulose of xylem cell walls, where the photosynthetic signals are time-averaged over the period of xylogenesis (as we discuss later in Sect. 15.6.4, Fig. 15.5). For example, the offsets in the timing of the production and use of photosynthate for tree-ring formation can range from 9–42 days in Japanese cedar (Kagawa et al. 2005) to 1–2 years in Dahurian larch (Kagawa et al. 2006a). Efforts to reconstruct the atmospheric environment, using theory such as that presented in Eq. 15.1, must include reconciliation of any time gaps between photosynthate production and utilization.

Theoretical models that aim to couple cellulose oxygen isotope ratios to the surrounding environment begin with consideration of leaf or needle water, which exchanges isotopes with CO<sub>2</sub> during photosynthesis (Chap. 10). The current model assumes leaf surfaces without wetting, as in the case of sunny or cloudy days, and this model does not apply to wet leaf surfaces covered with liquid water, as in the case of rainy days (see Sect. 15.6.5). The isotope composition of leaf water during steady-state transpiration reflects the combined influences of atmospheric vapor pressure deficit (VPD), the kinetic and equilibrium exchanges between the leaf and atmospheric vapor, and the advective mixing of non-fractionated (xylem) and fractionated (mesophyll) water (the Péclet effect) (Dongmann et al. 1974; Farquhar and Lloyd 1993; Farquhar 1998; Barbour et al. 2004). Modeling of this dynamic interaction starts from the Craig-Gordon model (1965):

$$\Delta_e \approx \varepsilon^+ + \varepsilon_k + (\Delta_v - \varepsilon_k) \frac{e_a}{e_i} \quad (15.2)$$

where  $\Delta_e$  is overall evaporative fractionation,  $\varepsilon^+$  and  $\varepsilon_k$  are the equilibrium and kinetic fractionations, respectively,  $\Delta_v$  is the isotope enrichment in atmospheric water vapor relative to source water,  $e_a$  is the ambient mole fraction of water vapor, and  $e_i$  is the mole fraction of water vapor in the leaf. Equation 15.2 has been modified in some studies to account for the serial diffusive fractionations occurring through the stomatal pore (still-air diffusion) versus the leaf boundary layer (still-air diffusion plus turbulent transfer) (Flanagan et al. 1991).

The observed fractionation of evaporating leaf water is seldom as great as that predicted by Eq. 15.2. Recognition of this discrepancy has led to modification of the model in one of two ways: (1) a transport-based kinetic dilution of  $\Delta_e$  through advective mixing of fractionated and non-fractionated water in the leaf (the Péclet effect), and (2) a simpler, linear mixing of two pools of leaf water, one enriched (mesophyll) and one not (xylem):

(Péclet modification)

$$\Delta_{blw} = \Delta_e (1 - e^{-\rho}) / \rho \quad (15.3)$$

(Two-pool modification)

$$\delta_{\text{blw}} = \delta_{\text{c}}(1 - f_{\text{u}}) + \delta_{\text{wx}}f_{\text{u}} \quad (15.4)$$

where  $\Delta_{\text{blw}}$  refers to fractionation of the bulk leaf water and  $\wp$  is a Péclet number, reflecting the ratio between advective and diffusive transport in the leaf (Farquhar and Lloyd 1993). In Eq. 15.4, the notation has switched from fractionation ( $\Delta$ ) to delta-ratio ( $\delta$ ), and includes the isotope ratio of the unfractionated xylem water pool ( $\delta_{\text{wx}}$ ) and the fraction of leaf water in that pool ( $f_{\text{u}}$ ) (Roden et al. 2015). Conifer needles are difficult for predicting Péclet modifications due to uncertainties in transport path length, velocity of water movement and degree of xylem suberization (Song et al. 2013; Roden et al. 2015). A simpler 2-pool model may be more appropriate (Roden et al. 2015).

Photosynthates that reflect the isotope effects of transpiration and needle water mixing is modified further during tree-ring cellulose production and deposition. A post-assimilation fractionation occurs when carbonyl oxygens in phloem-transported sucrose exchange with the oxygens of cambial water during cellulose synthesis (Sternberg et al. 1986). This secondary fractionation of cellulose oxygen ( $\Delta_{\text{c}}$ ), can be defined mathematically as:

$$\Delta_{\text{c}} = \Delta_{\text{blw}}(1 - p_{\text{x}} p_{\text{ex}}) + \varepsilon^+ \quad (15.5)$$

where  $p_{\text{x}}$  is the fraction of cambial cellular water that is not isotopically fractionated ( $p_{\text{x}} \approx 1.0$ ), and  $p_{\text{ex}}$  is the fraction of carbonyl oxygen atoms that exchange with non-fractionated water (Barbour and Farquhar 2000). Fractionation occurs when mobilized hexoses are broken down to the triose sugar (Hill et al. 1995), dihydroxyacetone phosphate (DHAP), and in the process, exposed to an opportunity to exchange oxygen (and hydrogen) atoms with the surrounding water (Reynolds et al. 1971; Knowles and Albery 1977; Sternberg et al. 1986; Kagawa 2020; Chap. 11). The post-assimilation fractionation of cellulose oxygen subjected to exchange with source water ( $p_{\text{ex}}$ ) has been shown to vary across spatial climate gradients and seasonally (Gessler et al. 2009; Offermann et al. 2011; Cheesman and Cernusak 2016). Cheesman and Cernusak (2016) estimated the exchange fraction as 0.21–0.68 for Australian eucalypts, and observed it to be highest in the most arid sites. Belmecheri et al. (2018) provided indirect evidence that  $p_{\text{ex}}$  varies from 0.1–0.4 seasonally in *P. ponderosa*. Using dual-isotope ( $\text{H}_2^{18}\text{O}$  and HDO) labeling method, Kagawa (2020) found that *Cryptomeria japonica* under rainy conditions shows increased exchange ( $p_{\text{ex}} = 0.9$ ). The significance of  $p_{\text{ex}}$  to observed intra-annual variations in cellulose  $\delta^{18}\text{O}$  is a topic that needs more study. As we later discuss in Sect. 15.6.5, incorporation of oxygen and hydrogen originating from foliar-absorbed water (Eller et al. 2013; Goldsmith et al. 2013) into photosynthetic sugars and organic matter (Studer et al. 2015; Lehmann et al. 2018, 2020a) and wood (Kagawa 2020) is interesting phenomenon and might be related to intra-annual oxygen and hydrogen variations in the wood formed during rainy seasons (Nakatsuka et al. 2004; Roden et al. 2009; Managave et al. 2010a; Ohashi et al. 2016; Xu et al. 2016; Nabeshima et al. 2018).

Both in hydrological cycles and inside trees, hydrogen and oxygen isotopes of water behave, more or less, similarly (Dansgaard 1964; Kagawa 2020) and fractionations of hydrogen isotopes in leaf water are explained by the same Eq. (15.2), with specific fractionation factors for hydrogen (Roden et al. 2000). The fraction of carbon-bound hydrogen atoms that exchange with non-fractionated water is also similar to that of oxygen ( $p_{ex}$ ) (Yakir and DeNiro 1990; Roden and Ehleringer 1999; Roden et al. 2000; Kagawa 2020). Oxygen and hydrogen show parallel fractionations through hydrological cycles (i.e. non-biological systems) along the meteoric water line (Dansgaard 1964). However, hydrogen isotopes show larger fractionations than oxygen at the cambium, before and during cellulose synthesis (Yakir and DeNiro 1990) and isotopic deviations of hydrogen from oxygen off the meteoric water line (Yakir et al. 1990; Voelker et al. 2014) seem to be related to metabolic activities (Lehmann et al. 2020b, Nakatsuka et al. 2020). One possible cause for such deviations is respiration, because oxygen is eliminated by both carbon dioxide and water released from trees, and hydrogen would be eliminated only by the water. Such deviations are closely related to the amount of respired  $CO_2$  in humans and animals (Schoeller and Van Santen 1982; Speakman 1997), and similar phenomenon might be happening in plants where respiration is high, in such places as symplastic leaf water pool (Kagawa 2020). In support of this hypothesis, Cormier et al. (2018) reports associations between hydrogen isotope fractionations of plants and carbon and energy metabolism under low light conditions.

## 15.4 Seasonal Isotope Fractionation Recorded in the Cellulose of Tree Rings

Numerous studies have reported on the isotope composition of wood or cellulose (e.g.,  $\delta^{13}C$  and  $\delta^{18}O$ ) as a means of revealing seasonal dynamics in tree-climate relationships (Wilson and Grinstead 1977; Leavitt and Long 1986, 1991; Kitagawa and Wada 1993; Ogle and McCormac 1994; Li et al. 1996; Livingston and Spittlehouse 1996; Sheu et al. 1996; Jordan and Mariotti 1998; Jäggi et al. 2002; Helle and Schleser 2004; Eglin et al. 2010; An et al. 2012; Kimak and Leuenberger 2015). Variation in  $\delta^{13}C$  across individual rings can be as large as 4‰, though 1–2‰ is most common (Barbour et al. 2002; Kagawa et al. 2003; Helle and Schleser 2004; Li et al. 2005; Kimak and Leuenberger 2015; Fu et al. 2017). This amount of variation is most likely due to the physiological response of trees to climate forcings and/or biochemical and physiological fractionation, and is not related to seasonal variation in the isotopic composition of source  $CO_2$  (Jäggi et al. 2002; Helle and Schleser 2004; Li et al. 2005; Voelker et al. 2016; Fu et al. 2017). Variation in  $\delta^{18}O$  across individual rings tends to be greater than that for  $\delta^{13}C$ , ranging as high as 6‰ and often being between 2–4‰ (Wilson and Grinstead 1977; Zeng et al. 2014; Fu et al. 2017; Szejner et al. 2016; Belmecheri et al. 2018). The variation in cellulose  $\delta^{18}O$  reflects an important influence of seasonal variation in the isotopic composition of

source water (Chap. 18). Because of this variation, intra-annual variations of oxygen isotopes show annual cyclicality in tropical areas and are often used for identifying annual rings in tropical trees that lack anatomically distinct annual rings (Poussart et al. 2004, Managave et al. 2010a, b, Pons and Helle 2011, Ohashi et al. 2016).

Numerous past studies have reported differences in chemical composition between earlywood and latewood in a range of softwoods and hardwoods (Ritter and Fleck 1926; Wilson and Wellwood 1965; Khattak and Mahmood 1986; Bergander 2001; Gindl 2001; Bertaud and Holmbom 2004). Generally, all these authors found that earlywood contained more lignin and less cellulose than latewood. The difference was explained in terms of the structure of the cell wall since earlywood consists of a larger proportion of lignin-rich middle lamella, due to larger tracheid diameters, and thinner cell walls, compared to latewood (Fredriksson et al. 2018). The cellulose and lignin that compose tree rings can be distinguished on the basis of stable isotope ratios (Borella et al. 1998, 1999; Barbour et al. 2001; Loader et al. 2003; Verheyden et al. 2005). Observed  $\delta^{13}\text{C}$  values for cellulose are isotopically enriched by approximately 3‰ compared to those for lignin (Loader et al. 2003).  $\delta^{18}\text{O}$  values are significantly lower in lignin ( $22.7 \pm 2.4\text{‰}$ ), compared to whole-wood ( $27.7 \pm 0.5\text{‰}$ ) or cellulose ( $31.4 \pm 1.4\text{‰}$ ) (Ferrio and Voltas, 2005). In this context, it needs to be considered that lignin composition and percentage is variable, not only between EW and LW, but also among different species and even within a single population of the same plant species depending on age (Campbell and Sederoff 1996).

Several past research efforts have shown that seasonal patterns of  $\delta^{13}\text{C}$  differ between EW and LW. Winter deciduous trees must, by phenological constraint, draw on stored carbohydrate (NSC) resources to support their earliest cambial activity. Using this assumption, several studies have interpreted the cellulose  $\delta^{13}\text{C}$  values of EW as reflecting fractionation processes from antecedent growing seasons (Jaggi et al. 2002, Helle and Schleser 2004; Li et al. 2005; Eglin et al. 2010; Hafner et al. 2015; Kimak and Leuenberger 2015; Fu et al. 2017; Zeng et al. 2017). Helle and Schleser (2004) described a tri-phasic seasonal response in the  $\delta^{13}\text{C}$  from thin sections across individual rings in four deciduous species. In the earliest phase,  $\delta^{13}\text{C}$  ratios were at a seasonal high and it was assumed that cellulose deposition was supported by overwintered NSC stores. The enriched  $\delta^{13}\text{C}$  values of stored NSC was attributed to post-photosynthetic fractionation related to carbohydrate conversions between free sugars and polymeric starch (Scott et al. 1999). The earliest phase can potentially be short, as current-season autotrophic capacity and NSC export from developing leaves can occur relatively early in the spring (Keel and Schadel 2010). In the second phase, young leaves expand and become net exporters of photosynthates. During this phase, tree-ring  $\delta^{13}\text{C}$  was observed to decline and this was attributed to current-season coupling between photosynthetic fractionation during a period of cooler temperature and replete soil moisture. In the third and latest seasonal phase at the end of the growing season, an increase in tree-ring  $\delta^{13}\text{C}$  was observed, which is attributed to the late-summer translocation of leaf sugars into storage pools in the stems and bole, and concomitant isotopic enrichment during NSC transformations, as in the start of the growing season. In other studies, the enriched  $\delta^{13}\text{C}$  values observed in the EW of temperate-latitude trees has been linked to the use of stored NSCs, but the cause



of enrichment was attributed to antecedent climate-induced fractionation, not the fractionation of sugar transformations (Kimak and Leuenberger 2015; Hafner et al. 2015). For example, Hafner et al. (2015) observed that  $\delta^{13}\text{C}$  ratios in a 38-year EW chronology of the winter-deciduous species, *Quercus robur*, were best correlated with climate conditions during the previous year's summer; suggesting a minor role, if any, for non-climatic fractionation effects. Given contrasts within the existing literature, there is a need to better resolve the determinants of EW  $\delta^{13}\text{C}$  ratios in deciduous trees.

Evergreen species have opportunities to commence photosynthesis even in winter prior to the growing season where climate is mild, such as temperate European climate, and they may rely less on stored carbon for EW formation (see Zweifel et al. 2006; Kimak and Leuenberger 2015; Soudant et al. 2016). However, the study by Castagneri et al. (2018) showed evidence of significant reliance on stored carbon in the Mediterranean pine, *Pinus pinea*, for construction of both EW and LW. In contrast, Alvarez et al. (2018) observed no difference in the  $\delta^{13}\text{C}$  ratios of LW and whole rings in Canadian black spruce (*Picea mariana*) trees, and concluded that both EW and LW were constructed from current-year photosynthate. Intra-annual  $\delta^{13}\text{C}$  (and  $\delta^{18}\text{O}$ ) variations are closely related to the water status at the time of wood formation (Leavitt and Long 1991; Kagawa et al. 2003; Verheyden et al. 2004; Roden et al. 2009; Li et al. 2011; Sarris et al. 2013; Schubert and Jahren 2015) and Barbour et al. (2002) reported seasonal variation in the  $\delta^{13}\text{C}$  of tree-ring cellulose in *Pinus radiata* that was consistently explained by theory relating intrinsic water-use efficiency (iWUE, Chap. 17) to current-season climatic variation and soil water availability. There was no need to invoke the withdrawal of stored carbohydrate reserves to explain the seasonal variation in  $\delta^{13}\text{C}$ . Similarly, Li et al. (2005) attributed the enriched  $\delta^{13}\text{C}$  in the EW of *Pinus tabulaeformis* in the China Loess Plateau as being explained largely by seasonal climate conditions, rather than the reliance on stored NSCs.

Jäggi et al. (2002) conducted a detailed study of  $\delta^{13}\text{C}$  ratios in the bulk biomass of needles, needle starch, and the cellulose of EW and LW in *Picea abies* in an effort to differentiate the effects of stored NSC use from current-year climate fractionation. There was a significant positive correlation between the  $\delta^{13}\text{C}$  of current-season starch in 1-year old needles and the current-year's EW, suggesting the use of short-term needle stores to support xylogenesis. There was an additional positive correlation between the  $\delta^{13}\text{C}$  of the bulk biomass of current-year needles and the current-year's EW, showing that the ultimate  $\delta^{13}\text{C}$  of the EW was likely the result of mixed NSCs from older and newer needles. In either case, however, the NSCs would have resulted from current-year  $\text{CO}_2$  assimilation, providing the basis for linkage between EW  $\delta^{13}\text{C}$  and current-year spring climate. The starch signals from 1-year old needles and current-year needles did not show correlation with current-year LW  $\delta^{13}\text{C}$ . Rather, the LW  $\delta^{13}\text{C}$  were best explained by climatically-linked fractionation from mid growing-season of the current year. These mechanistic observations tend to support at least the first two phases of the tri-phasic pattern described by Helle and Schleser (2004), though in this case for an evergreen conifer, and with the caveat of utilization of recent NSC stores.

In the case of  $\delta^{18}\text{O}$ , seasonal fluctuations as noted in the cellulose of EW and LW were reflecting variation in source water as well as enrichment fractionation (McCarroll and Loader 2004). The close association of the oxygen isotope ratios with source water variation is exemplified in the study by Miller et al. (2006) in which LW cellulose  $\delta^{18}\text{O}$  values in southeastern U.S. pines were able to predict inter-annual variation in the highly depleted precipitation water of hurricanes, Li et al. (2011) confirmed this finding at higher time-resolution. Presence of intra-annual isotopic variations are also reported in paleo wood samples and suggests the possibility of reconstructing paleo-hydrological climate at higher time resolution (Jahren and Sternberg 2008). Tree-ring hydrogen isotopes show similar intra-annual variations to oxygen isotopes, however,  $\delta^2\text{H}$  was slightly different from  $\delta^{18}\text{O}$  in that  $\delta^2\text{H}$  shows maximum at the beginning of each oak tree ring (Nabeshima et al. 2018). Deviation of hydrogen from oxygen isotope ratios is related to relative humidity (Voelker et al. 2014), and it is also related to plant metabolic activity such as remobilization of storage (Cormier et al. 2018, Chap. 11). The latter might explain observed negative correlation between  $\delta^2\text{H}$  and ring widths (Voelker et al. 2014) and positive and negative juvenile effects observed in long-term tree-ring  $\delta^{18}\text{O}$  and  $\delta^2\text{H}$  from central Japan, respectively (Nakatsuka et al. 2020).

An et al. (2012) were able to partially deconstruct the complex influences of precipitation from two separate monsoon systems, and cyclic variability in sea surface temperature, on EW versus LW cellulose  $\delta^{18}\text{O}$  in a coniferous forest of southwestern China. This knowledge was subsequently used as a basis for concluding that regional coherence exists in the hydrological determinants of EW and LW  $\delta^{18}\text{O}$  values (An et al. 2012; Fu et al. 2017).

Barbour et al. (2002) made observations of  $\delta^{18}\text{O}$  and  $\delta^{13}\text{C}$  in thin slices across two annual rings in *Pinus radiata* growing in three sites with different hydrology regimes. Generally, the two ratios were positively correlated across the growing season, showing that as evaporative enrichment of the isotopic content of leaf water increases, the iWUE of the leaf also increases. Furthermore, both  $\delta^{18}\text{O}$  and  $\delta^{13}\text{C}$  reflected increases in seasonally-averaged values among the three sites according to increased tendency for drought. These relationships are best explained by the correlated, but opposing, effects of increasing atmospheric VPD on stomatal conductance (decreases as VPD increases) and transpiration (increases as VPD increases). Thus, at the scale of selected trees growing across an individual season, ecophysiological responses to climate were a relatively accurate reflection of leaf gas-exchange theory (sensu Farquhar et al. 1982), however, a complete understanding of the tree-ring record of seasonal climate requires knowledge of the phenological gaps that occur in the process of xylogenesis.

## 15.5 Seasonal Lags in Cambial Phenology and Isotope Variation in Tree Rings

As interest in the intra-annual record of stable-isotope fractionation in tree rings has increased, it has become clear that an accurate alignment of that record with seasonal weather events requires knowledge about the timing and progression of xylogenesis (Rathgeber et al. 2016, Chap. 3). The progression of xylogenesis from incipient cell formation by the cambial meristem to eventual maturation (when carbon deposition to cell walls is complete) can take weeks to months (Kagawa et al. 2005), meaning that cell-wall cellulose that is extracted and analyzed for  $\delta^{13}\text{C}$ ,  $\delta^{18}\text{O}$ , and  $\delta^2\text{H}$  reflects fractionation that occurred across a broad seasonal climate gradient. At the onset of seasonal cambial activity, the production of radial files of newly-formed cells occurs, and continues until the cessation of xylogenesis, either due to temperature or water stress prior to the end of the growing season, or to programmed phenology that is determined by day-length and/or temperature at the end of the growing season. Following their respective production, cells will begin the processes of enlargement, secondary wall formation and programmed death, in turn, according to interactions between environmental constraints on metabolic processes and intrinsic controls by plant growth regulators. This creates a continuous intra-annual record of cellular isotope fractionation, but one that is ultimately determined by environment-phenology interactions. The rate of cell division is relatively fast early in the growing season, and the cell enlargement phase is relatively long, creating EW cells. As the season progresses, the rate of cell division will slow and the enlargement phase will shorten, producing the smaller, denser cells that characterize LW. Conventionally, the duration of the wall thickening phase was thought to be the primary cause of thicker cell walls with more stored cellulose in LW tissues, especially in conifers (Skene 1969; Wodzicki 1971; Denne 1972). Cuny et al. (2014) have challenged this view with support from detailed measurements of each phase of xylogenesis in several temperate-latitude species. Their observations showed that it is the duration of cell enlargement, early in the process of xylogenesis, combined with a constant deposition of cellulose to secondary cell wall formation, that ultimately determines cell wall thickness in LW. According to this view, the amount of cellulose per cell, and thus carbon per cell, stored in both EW and LW is roughly equal, but it is spread across the surface area of smaller cells in the case of LW. This provides the visible appearance of thicker cell walls in LW. Recent  $^{13}\text{CO}_2$  pulse-labeling experiment of evergreen conifer (*Chamaecyparis obtusa*) found that early-spring photosynthate appears in the previous late-latewood cells. In fact, late-latewood cells stay alive during winter, because these cells retain nucleus during winter (Ino et al. 2018).

Cuny et al. (2015) reported that the phased nature of xylogenesis sub-processes underlies a phenology gap between the time of cell enlargement, which controls increases in stem diameter, and deposition of cellulose in secondary cell walls, which controls the storage of carbon in temperate-latitude coniferous species. This observation provides a basis for temporal offsets in the seasonal analysis of ring-width

increment and cellulose stable isotope fractionation; with the latter reflecting seasonal climate conditions that exist days to weeks later in the season, compared to the former. These results have great importance for efforts to align intra-annual tree-ring stable isotope records with the climate regime that existed during the time of initial photosynthetic fractionation (Post-assimilation fractionation is a separate, but potentially as important a factor, in determining the relation of observed tree-ring cellulose isotope ratios to the seasonal climate during the time of initial photosynthetic fractionation).

In a follow-up study, Cuny et al. (2019) observed variance in xylogenesis sub-processes across an altitudinal temperature gradient. They found that cooler temperature regimes slow the rates of cell enlargement and cell-wall thickening during xylogenesis, but that the tree compensates through longer duration of the enlargement and thickening phases. Thus, there potentially exists an interaction between extrinsic (environmental) control over metabolic factors, such as the enzyme activities that enable cell differentiation, and intrinsic (hormonal) factors that control the duration of phenological phases. The temperature-dependent compensatory relation of these processes appears to breakdown in the final LW tissues produced, late in the growing season. In Mediterranean environments, studies of xylogenesis have shown that cambium in *Pinus pinea* (Balzano et al. 2018) and *P. halepensis* (De Micco et al 2016) were productive throughout the calendar year, while in *Arbutus unedo*, a double pause in cell production was observed, in summer and winter with the formation on more than one IADF.

## 15.6 The Transport and Utilization of Stored Photosynthate for Xylogenesis

Post-photosynthetic metabolic processes leading to wood formation, such as translocation, storage and remobilization of photoassimilate are closely related to intra-annual variation of stable isotope ratios in tree rings. Although the seasonal course of leaf  $\delta^{13}\text{C}$  is well reflected in intra-annual variation of tree-ring  $\delta^{13}\text{C}$  in some cases (Leavitt and Long 1991; Leavitt 1993), the signal transfer is non-linear, rather than direct. For example, there are seasonally variable time lags between photosynthetic carbon incorporation and its use for wood formation (Schleser et al. 1999; Helle and Schleser 2004), due to phloem transport and storage processes lying between initial assimilation and the eventual use of photosynthate for xylogenesis. Here, we are referring to interannual time lags on the scale of years, not the intra-annual time lags of cambial phenology. Partly because of the time lag, which can last up to 1–2 years, first- and second order interannual auto-correlations are frequently observed in isotope dendroclimatological studies (Monserud and Marshall 2001; Szejner et al. 2018).

A model that takes into account the relative contribution of current photosynthate directly translocated from the leaves (new carbon) and older photosynthate remobilized from the storage pool (old carbon) was developed in 2001 to explain intra-annual variation of tree-ring  $\delta^{13}\text{C}$  (Hemming et al. 2001). This carryover phenomenon has since been verified by the use of an artificially enriched  $^{13}\text{C}$  tracer and it is now clear that the EW is made of the mixture of new and old carbon (Kagawa et al. 2006a; von Felten et al. 2007). Recent labeling studies have revealed a wide range of mixing ratios of new to old carbon among different tree species (Keel et al. 2007; He et al. 2020), and mobile carbon pools of trees have been classified into fast- and slow-turnover pools (Keel et al. 2006). However, such carryover phenomenon was absent, at least for root formation of pulse-labeled trees with  $\text{H}_2^{18}\text{O}$  and HDO (Kagawa 2020) and future investigations are necessary, into the use of carried-over O and H signals in carbohydrate pools, if any, for tree ring formation.

### 15.6.1 *The Experimental Design of Isotope-Labeling Experiments*

During the 1960s and continuing into the 1980s, numerous experiments on tree carbon allocation were conducted with a radioactive  $^{14}\text{CO}_2$  tracer (Hansen et al. 1997), notably in field studies. Due largely to the development of new analytical capabilities with stable carbon isotopes, researchers started and have been using  $^{13}\text{CO}_2$  (>98 atom %) as a substitute for  $^{14}\text{CO}_2$  in tree carbon allocation studies since the late 1990s (Simard et al. 1997a, b; Lacoite et al. 2004; Kagawa et al. 2005; Keel et al. 2007; Talhelm et al. 2007).

In this chapter, we define “pulse-labeling” as a short-term isotope labeling where fumigation of leaves with labeled  $\text{CO}_2$  ( $^{13}\text{CO}_2$  or  $^{14}\text{CO}_2$ ) lasts not more than a few days. The length of such a short input signal can be regarded as a pulse compared to the length of the tree’s growing season. In pulse-labeling experiments, either a whole tree or a branch is enclosed in a sealed chamber into which labeled  $\text{CO}_2$  is injected. Fumigating a tree for one day with  $^{13}\text{CO}_2$  at atmospheric concentration (380 ppm) provides a  $^{13}\text{C}$  signal sufficiently greater than the natural abundance ratio in each tree body part (Kagawa et al. 2005, 2006b). Strong  $^{13}\text{CO}_2$  signal is efficiently incorporated into the tree within a short period and loss of labeled gas to the atmosphere is minimal. Efficient incorporation is especially important when using expensive  $^{13}\text{CO}_2$  gas.

Alternatively, cheaper fossil  $\text{CO}_2$  gas depleted in  $^{13}\text{C}$  ( $\delta^{13}\text{C} = -29.7\text{‰}$  according to Körner et al. 2005) is available in large quantities and can be used for long-term web-FACE labeling experiments (Pepin and Körner 2002) lasting more than one growing season (Helle and Panferov 2004; Körner et al. 2005; Keel et al. 2006). The main advantage of web-face labeling is that artificial changes to the photosynthetic environment caused by the labeling experiment are minimal.

In order to study phloem translocation pathways of Japanese cedar, Kagawa et al. (2005) injected  $^{13}\text{CO}_2$  to a branch on the upper side of the stem in June, during

the earlywood formation period. Since Japanese cedar has straight grain,  $^{13}\text{C}$  was translocated in parallel to the phloem grain, and confined to the specific side of the stem showing little tangential diffusion.  $^{13}\text{CO}_2$  was injected again to the same branch in September, during latewood formation, and detected a stronger  $^{13}\text{C}$  signal at a slightly different location within latewood (Fig. 15.1, Kagawa et al. 2005). At another experiment,  $^{13}\text{CO}_2$  was injected to a branch of Dahurian larch, which has spiral grain, in August during latewood formation, and spiral translocation of  $^{13}\text{C}$  was observed (Fig. 15.1, Kagawa et al. 2006a).

Kagawa et al. (2005, 2006a) drew lines in parallel to the straight and spiral grain of Japanese cedar and Dahurian larch, originating from the base of the pulse-labeled branch (Fig. 15.1), and  $^{13}\text{C}$  was detected along the line in both cases. This means, straight and spiral phloem translocation happens in parallel to the straight and spiral grain of Japanese cedar and Dahurian larch, respectively. These results supported the pipe model theory, where the stem and branches are considered as the assemblage of unit pipes and photosynthetic organs connected to each unit pipe provide carbon to each connected side of the stem (Shinozaki et al. 1964).

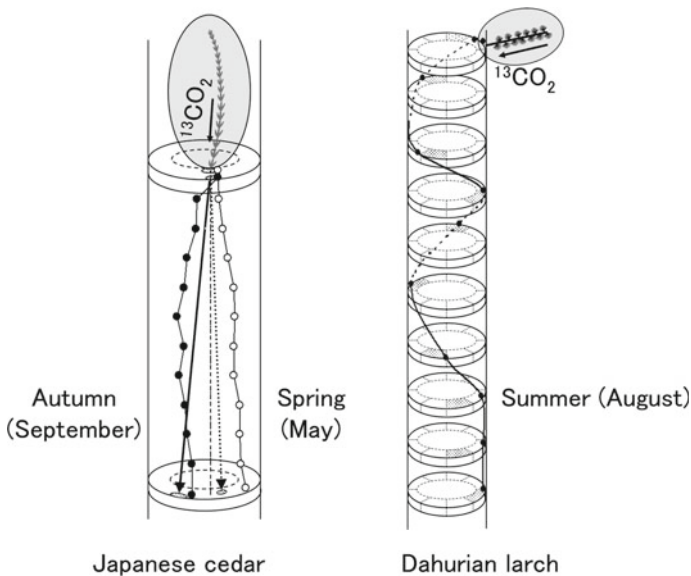


**Fig. 15.1** Phloem translocation pathways for straight-grained wood (Japanese Cedar, *Cryptomeria japonica*) and spiral-grained wood (Dahurian Larch, *Larix gmelinii*). In three different experiments, a piece of branch was enclosed in a transparent bag and  $^{13}\text{CO}_2$  (> 98%) gas was injected over a few sunny days. Shaded areas on the stem disks illustrate the locations where  $^{13}\text{C}$  label was detected in the wood of the stem. After sampling trees, the outer bark on each stems was removed, then slivers were pulled off from the inner bark and outermost tracheids originating from the base of the  $^{13}\text{C}$ -fed branch. Since slivers are pulled off in parallel to the grain direction, a cell alignment line was continuously drawn following the vertical cell direction from the branch base to the disk below. Open circles indicate cell alignment line for Japanese cedar in May, and filled circles for Japanese cedar in September, or Dahurian larch in August

### 15.6.2 Evidence from Isotope-Labeling Studies for the Use of Stored Carbon in Tree-Ring Production

Directions of phloem translocation and the allocation ratio of photosynthetic products to storage versus net production show seasonal changes, and such changes are governed by the source (photosynthetic activity, amount of available storage)-sink (consumption of photosynthetic products and storage for growth and respiration) relationship (Hansen et al. 1997). Cambium-derived sinks (e.g. EW and LW) gain carbon from nearby sources (e.g. storage in xylem and phloem parenchyma cells or transport from phloem sieve-tube members). In spring-time, when EW formation happens, acropetal translocation prevails because newly forming leaves, and shoots becomes a strong sink (Hansen and Beck 1994; Gordon and Larson 1968). On the other hand, part of the photosynthetic products assimilated at the lower part of the crown is translocated and used for tree ring formation at breast height. When shoot elongation slows down in the early summer, basipetal translocation becomes prevailing (Gordon and Larson 1968). There is a time lag between carbon assimilation via photosynthesis and use of the assimilated carbon for tree-ring formation (Figs. 15.1, 15.2 and 15.3). Part of photosynthetic product is instantly used for tree-ring formation (new carbon), and part of the new carbon (sucrose) is converted to storage substance such as starch, before being stored in parenchyma cells of the bole or branches. For evergreen conifers, a significant amount of carbohydrate can be stored also in needles, then used later for tree-ring formation (Jäggi et al 2002).

Kagawa et al. (2006b) enclosed whole saplings of Dahurian larch in transparent bags and conducted pulse-labeling over two sunny days in summer (July), and also in the spring of the following year (June) and tracked allocation of  $^{13}\text{C}$  to the different parts of each tree. In spring, sink strength at the apical parts were strong and spring photosynthetic products were allocated mainly to the apex; a lesser amount went to the below-ground parts of the tree. Spring photosynthetic products were also used for EW formation right after the labeling (Fig. 15.3 left, Kagawa et al. 2006a). When new carbon is directly used for tree-ring formation, the  $^{13}\text{C}$  concentration of wood shows a higher concentration than that of starch (horizontal dotted line in Fig. 15.3 left). On the other hand, if  $^{13}\text{C}$ -labeled photosynthetic products are used for tree-ring formation via the storage pool, the  $^{13}\text{C}$  concentrations of wood become lower than those of starch (Fig. 15.3 right). Photosynthetic products labeled during the previous summer are directed to the storage pool, where  $^{13}\text{C}$  concentrations are diluted with non-labeled carbon, then carried over to the current year. It is further diluted with newly assimilated spring photosynthetic products (new carbon) as shown in the EW of Fig. 15.3 right. Based on these results, we believe that EW is made of the mixture of “new and old carbon”. “New carbon” is newly assimilated spring photosynthate, translocated in phloem from the crown, and “old carbon” is storage carbon that is carried over from previous years and transferred from xylem and phloem parenchyma from above- or belowground (von Felten et al. 2007).

On the other hand, the EW of broad-leaved species that form ring-porous wood, such as oak, should be mostly made of storage, because formation of EW vessels

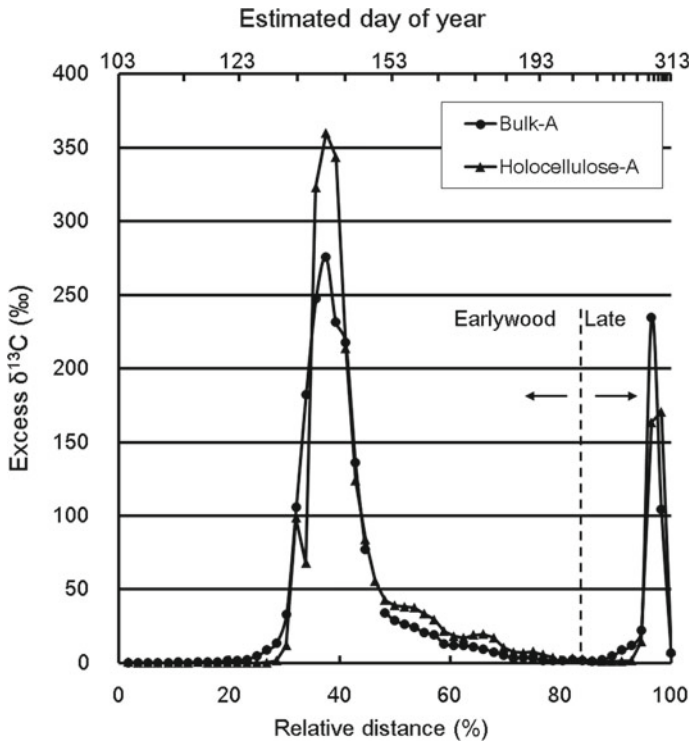


**Fig. 15.2** Timing of cell formation and intra-annual isotopic depositions of pulse-labeled photosynthetic carbon. Use of spring (May 29th) and autumn (September 18th) photosynthetic carbon for tree-ring formation of Japanese cedar in Tsukuba, Japan. In this region, tree-ring formation starts around April 13th and ends around November 9th. A shift from earlywood to latewood formation happens around July 22nd (Kagawa et al. 2005). Solid circles indicate  $^{13}\text{C}$  concentrations in wholewood, and solid triangles indicate that in holocellulose. Horizontal axis at the bottom indicate relative position within the tree ring formed, and the axis at the top indicate estimated date of cell formation

of ring-porous trees precedes the onset of leaf flushing. In ring-porous oak, not only carbon but also oxygen and hydrogen isotope ratios show unusual values in EW (Helle and Schleser 2004; Nabeshima et al. 2018), which cannot be explained by climate at the time of formation. Carbon isotope ratios of storage carbohydrates, such as starch, shows higher carbon isotope ratios than newly assimilated sucrose. Initially, oak EW is made only from storage, then, as photosynthetic production from leaves becomes available, the proportion of newly-assimilated carbon for wood formation is increased. In summer, sink strength at the apical tissues becomes weak, and basipetal translocation of photosynthetic products prevails. In the LW formation of Dahurian larch in eastern Siberia, production is driven by both spring and summer photoassimilates from the same year and it relies less on storage carried over from previous years. However, if there is an unusually strong carbon demand, such as compression wood formation, a larger remobilization of storage resources is observed



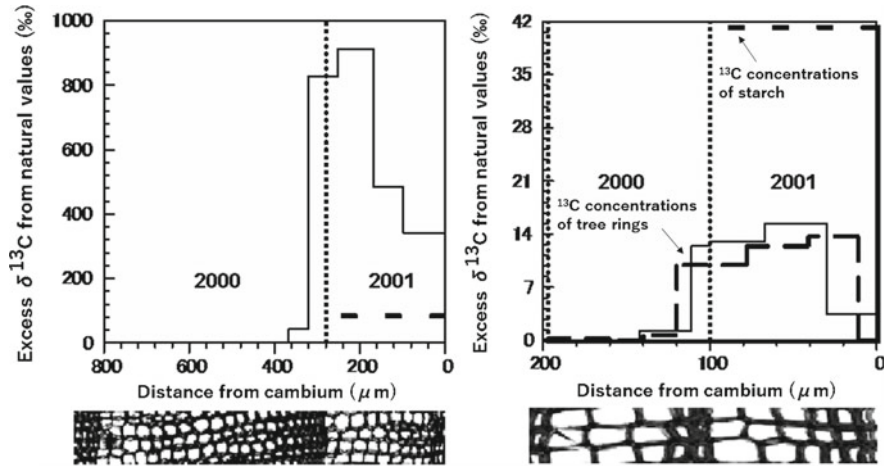


**Fig. 15.3** Deposition of spring and summer photoassimilates into tree rings.  $^{13}\text{CO}_2$  pulse-labeling was conducted in June, 2001 (left) and July, 2000 (right) in eastern Siberia. Horizontal dashed lines with larger spacing show  $^{13}\text{C}$  concentrations of starch. Thin solid line and thick dashed line with smaller spacing in the right subfigure show  $^{13}\text{C}$  concentrations of tree rings from two individual trees (Kagawa et al. 2006a). The vertical dotted line indicates the tree-ring boundary between rings formed within the two years

(Kagawa et al. 2006a), suggesting that storage can be an important source for wood formation, whenever an unusual demand arises.

### 15.6.3 The Time Resolution of Intra-annual Variation in Tree Ring Isotopes

Analogous to the peaks observed in chromatography, a signal output is observed as a broadened  $^{13}\text{C}$  peak in the tree ring after pulse-labeling with  $^{13}\text{CO}_2$  (Fig. 15.4, Kagawa et al. 2005). The pulse signal is transferred as  $^{13}\text{C}$  labeled sugars dissolved in phloem sap. If we make an analogy of a tree's sieve cells to a liquid chromatographic column and tree rings to a chromatogram recorder ( $D$ ), then we can expect to observe a Gaussian peak in the rings as a function of time-since-labeling as expressed in the formula,

$$D(t) = \exp\left(-\left(\frac{t - t_c}{H_{1/2}}\right)^2 \cdot \ln 2\right) \quad (15.6)$$

where  $t_c$  is the time when labeled carbon reaches the cambium for tree ring formation.  $H_{1/2}$ , which is a measure of time resolution, is the half width at half maximum of the

peak observed in the tree ring. Apart from a small tail to the right, this Gaussian peak matches the observed peak shape from a pulse-labeling experiment with fast-growing Japanese cedar (Figs. 15.2 and 15.4d, Kagawa et al. 2005).

The time delay  $t_c$  is the time needed for new carbon to be transported from leaves to the cambium for tree-ring formation. According to estimates based on the natural fluctuation of the  $\delta^{13}\text{C}$  values of soluble organic matter in leaves and in the stem-base phloem, the time of phloem transport of new carbon from leaves to stem base has been estimated to be 1–2 days for adult beech trees of 25–27 m of height (Keitel et al. 2003) and the velocity of phloem transport has been estimated to be ca. 0.2–1.2 m h<sup>-1</sup> (Brandes et al. 2006; Dannoura et al 2011). However, carbon in the starch pool turns over slower than carbon in the soluble organic matter pool in leaves (Brugnoli et al. 1988). Residence time, or time required to replace old carbon pools in leaves with new carbon, is 9 days in deciduous species and 39–63 days in evergreen conifer species (Keel et al. 2007). It thus takes much longer than 1–2 days for non-structural

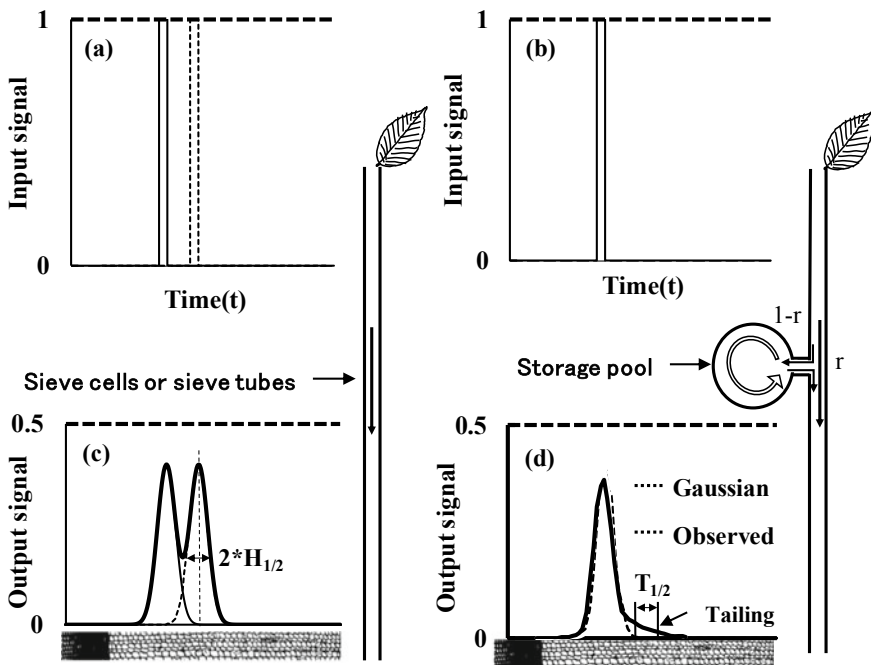


**Fig. 15.4** Time resolution of tree-ring archive and residence time of storage carbon. Time resolutions can be estimated from half-widths at the half height of the peaks ( $H_{1/2}$ ). Storage pool with longer residence time ( $T_{1/2}$ ) can generate peak tail to the right of each peak. **a** two discrete pulses of label given to a tree. Solid vertical lines represent the start and end of the first pulse, and dashed lines for the second pulse. **b**, **c** expected tree-ring output signal from the two pulses in **(a)**. **d** predicted Gaussian peak from Eq. 15.6 (dashed line) and the observed peak shape from a pulse-labeling experiment with fast-growing Japanese cedar (solid line).  $r$  and  $1-r$  are the ratios of the carbon contribution from new and old carbon pools, respectively

carbohydrates in leaves to be exported, and the averaged time lag ( $t_c$ ) for the carbon used for wood formation may be accordingly longer.

If we give two discrete pulses to a tree (Fig. 15.4a), then one would observe two small overlapping peaks instead of one large peak (Fig. 15.4c). Thus, time resolution of a time series can be estimated by a half-width at half height of a peak, as two same-sized peaks separated by an interval of more than twice the half-width ( $2 \cdot H_{1/2}$ ) are discernible as separate peaks (thick line in the Fig. 15.4c, IUPAC 1997). By fitting a Gaussian curve to the observed  $^{13}\text{C}$  peaks, we have estimated the time resolution of tree-ring  $\delta^{13}\text{C}$  proxy to be on a weekly to monthly level for a fast-growing ever-green conifer (*Cryptomeria japonica*) in temperate area (Tsukuba, Japan; Kagawa et al. 2005) and on a seasonal to yearly level for a slow-growing deciduous conifer (*Larix gmelinii*) in boreal area (Yakutsk, Russia; Kagawa et al. 2006a).

However, to explain the  $^{13}\text{C}$  peak shape more precisely, the peak's tail has to be accounted for by an additional correction term. Tails with larger areas and longer durations are observed with boreal *Larix gmelinii*. The size of the tail of such slow-growing species depends primarily on the turnover of  $^{13}\text{C}$  tracer in the storage pool near the site of wood formation, e.g. sugars and starch in parenchyma cells. This is especially the case when a peak's tail extends beyond the ring boundary into the following year's ring ("Summer" and "Autumn" peaks in Fig. 15.5, Kagawa et al. 2006a). In recent pulse-labeling experiments with Japanese cypress (*Chamaecyparis obtusa*), pulse-labeled photoassimilates in early spring was used for formation of late-latewood cells of previous year (Ino et al. 2018). Overwintering cells of late-latewood can stay alive, because when overwintering latewood cells are observed under microscope, the last few latewood cells still keep their nucleus (Keiji Takabe, unpublished). They probably stay alive until early spring to finish the last part of latewood formation, hence carbon deposition of hemicellulose and lignin observed at the late-latewood of previous year. Such phenomenon, less clear though, was also observed in Dahurian larch. Early-spring photoassimilates in June 2001 was actually used for making the last few latewood cells of tree ring formed in 2000 (Fig. 15.3 left), giving another explanation for auto-correlation in addition to carry-over of storage from previous year. To summarize, photoassimilates of a given year can be used for tree ring of previous, current and the following year.

We observed an exponential decrease of  $^{13}\text{C}$  concentrations in the storage pool of Dahurian larch over time (Kagawa et al. 2006b), therefore, the isotope signal transfer model from leaves to tree rings should involve a storage term (S),

$$S(t) = \exp\left(-\left(\frac{t - t_r}{T_{1/2}}\right)^2 \cdot \ln 2\right) \quad (15.7)$$

where  $T_{1/2}$  is residence time, the time needed for half of the old carbon in the storage pool to be replaced with new carbon. In other words, the time required for  $^{13}\text{C}$  concentrations in the storage pool to be reduced by half (Fig. 15.4c, d), and  $t_r$  is the time when the storage pool is remobilized. Residence time can be calculated by

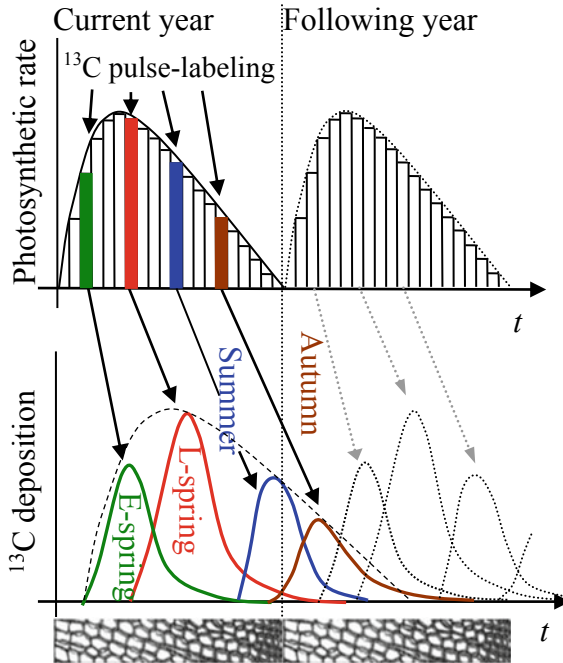


**Fig. 15.5** A model for carbon isotope signal transfer from leaves to tree rings of deciduous conifer. The colored bars in the top panel represent the amount of  $^{13}\text{C}$  label fixed during 4 different labeling events, representing early spring (E-spring, green), late spring (L-spring, red), summer (blue) and autumn (brown), which are distributed through the current year. Dotted lines in the upper panel represent seasonal variation of net photosynthetic rate. In the lower panel, the colored lines represent the proportion carbon from each labeling event to form the tree rings. Shape of the signal transfer function from leaves to tree rings,  $LT(m,t)$ , differs between early-spring, late-spring, summer and autumn. Therefore,  $LT(m,t)$  depends on the month when  $^{13}\text{C}$  is assimilated by leaves (Drawn based on the results of Kagawa et al. 2006a). Dashed black lines in the bottom panel on the right side represent signal transfer function for  $^{13}\text{C}$  assimilated in the following year

fitting an exponential curve to the tail of the  $^{13}\text{C}$  peak. For example, residence time has been calculated in this way to be 10.5 days for storage within a branch of Japanese cedar (Fig. 15.4d, Kagawa et al. 2005). The calculation for the boreal Dahurian larch, revealed a much longer residence time of ca. 1 year (Kagawa et al. 2006a). According to labeling experiments of mature trees with fossil  $\text{CO}_2$ , a residence time ( $T_{1/2}$ ) of NSC pool within wood was estimated to be ca. 50–200 days (Keel et al. 2007).

### 15.6.4 A Preliminary Model for Carbon Isotope Signal Transfer from Leaves to Tree Rings

The concept of a non-linear signal transfer function was introduced to explain the transfer of environmental signals (temperature, VPD) to tree-ring  $\delta^{13}\text{C}$  (Schleser et al. 1999). Here we present another signal transfer function, to explain the carbon isotope signal transfer from leaves to tree rings. In order to explain how the temporal carbon isotopic signal of photosynthetic products assimilated on a given day is transferred to tree rings, we have developed a signal transfer function which is a function of the month ( $m$ ) when photosynthetic fixation of carbon (or  $^{13}\text{C}$  label) takes place at certain month ( $m$ ) and the time thereafter ( $t$ ) when the carbon (or the  $^{13}\text{C}$  label) is used for wood formation (Fig. 15.4). For example, the EW of boreal *Larix gmelinii* is made of a mixture of photoassimilate from the current June–July and the previous July–August (Fig. 15.3, Kagawa et al. 2006a). The total carbon used for tree-ring formation (LT) is therefore expected to be derived from both new (current photosynthate) and old (storage pool) carbon pools (Hemming et al. 2001; Kagawa et al. 2006a; Keel et al. 2007) as follows,

$$\text{LT}(t) = r \cdot \exp\left(-\left(\frac{t-t_c}{H_{1/2}}\right)^2 \cdot \ln 2\right) + (1-r) \cdot \exp\left(-\left(\frac{t-t_r}{T_{1/2}}\right)^2 \cdot \ln 2\right) \quad (15.8)$$

where  $r$  and  $1-r$  are the ratios of the carbon (or  $^{13}\text{C}$ ) contribution from new and old carbon pools, respectively (Fig. 15.4).

If we make an analogy of phloem sieve cells to a liquid chromatographic column, then an input  $^{13}\text{C}$  pulse (solid line peak in Fig. 15.4b) would appear on a tree ring as a Gaussian peak (Fig. 15.4d). If the two input pulses are far apart from each other more than twice the half width at the half height of the peaks ( $2 \cdot H_{1/2}$ ), then summation of the two peaks (thick solid line peaks in Fig. 15.4c) can be recognized as two separate peaks on the tree ring. Thus, half-width at the half height (HWHF or  $H_{1/2}$ ) can be used as an indicator for time resolution of tree-ring isotope archives. The observed  $^{13}\text{C}$  peak has a tail due to retention in the storage pool, and a correction term must be added to adequately model this shape. The  $\delta^{13}\text{C}$  of photosynthate in leaves  $\Delta_A$  is given by Eq. 15.1 (Farquhar et al. 1989), and  $\Delta_A$  varies according to the month of photosynthetic production. Then the carbon isotope ratio of tree-ring cell layer,  $\delta^{13}_{\text{TR}}$ , formed at the time  $t$  can be expressed as,

$$\begin{aligned} \Delta_{\text{TR}}(t) &= \int^t A(m) \cdot \Delta_A(m) \cdot (\text{LT}(m, t) + \delta_{\text{PP}}) \cdot dm \\ &= \int^t A(m) \cdot \Delta_A(m) \cdot \left\{ \begin{array}{l} r(m) \cdot (D(m, t) + \delta_D) \\ + (1-r(m)) \cdot (S(m, t) + \delta_S) \end{array} \right\} \cdot dm \quad (15.9) \end{aligned}$$

where  $A(m)$  is the photosynthetic assimilation rate of all carbon used for tree-ring formation (Fig. 15.5). The term  $r$  is known to change seasonally and is therefore written as  $r(m)$ . For example, the EW of ring-porous species relies less on current photoassimilate and more on storage photosynthate, yielding a small  $r$  value. The ratio  $r$  also varies widely among tree species (Keel et al. 2007) and under different weather conditions (He et al. 2020). We added the terms  $\delta_{pp}$ ,  $\delta_D$ , and  $\delta_S$  to account for the post-photosynthetic fractionation of total, new and old carbon, respectively.

### 15.6.5 Future Prospects

Since our current knowledge of post-photosynthetic carbon isotope signal transfer processes is not yet sufficient to fully explain intra-annual tree-ring  $\delta^{13}\text{C}$ , the preliminary model described here is based on limited experimental data. We could quantify important parameters such as the time resolution of tree-ring  $\delta^{13}\text{C}$  ( $2 * H_{1/2}$ ) (Kagawa et al. 2005) or the residence time of carbon in the storage pool ( $T_{1/2}$ ) (Kagawa et al. 2006b), the model is too simplistic. In order to provide an experimental basis for validation and further refinement of this preliminary model, we need to conduct pulse-labeling experiments with mature, large trees as opposed to the young trees used in many of our own studies. By pulse-labeling trees in different seasons and later analyzing intra-annual  $\delta^{13}\text{C}$  of the tree rings subsequently formed, exact shape of the signal transfer function ( $LT(m,t)$ ) can be determined. We also need to measure seasonal variation of natural carbon isotope ratios of leaf photosynthate ( $\delta^{13}L(m)$ ) and tree rings ( $\delta^{13}TR(t)$ ) at the same site to check if the model can precisely predict intra-annual tree-ring  $\delta^{13}\text{C}$  variation ( $\delta^{13}TR(t)$ ) from  $\delta^{13}L(m)$ . In fact, natural early-wood  $\delta^{13}\text{C}$  of boreal larch is correlated to the temperature of the current June-July and the previous August (Kagawa 2006), reflecting a seasonal lag between photosynthetic carbon assimilation and xylogenesis as we discussed in previous Sects. 15.3–5. The shape of the signal transfer function (Fig. 15.5) is expected to differ between different types of trees, such as coniferous vs. broad-leaved, ring porous vs. diffuse porous, deciduous vs. evergreen, and fat vs. starch tree species. A variety of such representative tree species frequently used for isotope dendroclimatology studies should be chosen for future pulse-labeling experiments.

Although single-substrate model exists to explain intra-annual oxygen isotope variation of tree rings (Ogé et al. 2009), post-photosynthetic oxygen and hydrogen isotope signal transfer processes are much less explored compared to those of carbon isotopes, partly because effective pulse-labeling method with oxygen and hydrogen isotopes has been lacking. However, recent development of pulse-labeling techniques with enriched or depleted  $\text{H}_2^{18}\text{O}$  and HDO (Lehman et al. 2018, 2020a, Kagawa 2020) might contribute to the improvement of such model. For example, new roots formed in the post-labeling period (within six months of heavy-water labeling) did not contain significant oxygen and hydrogen labeling signals, possibly due to post-labeling exchange of oxygen and hydrogen in carbohydrate pool with those of non-labeled water (Kagawa 2020). In a previous study, Kagawa et al. (2006b) successfully

detected signals from photosynthate labeled with  $^{13}\text{CO}_2$  in July in roots formed later that year. Therefore, turnover rates of oxygen and hydrogen in carbohydrate pool may turn out to be much faster than those of carbon. Future analysis of intra-annual oxygen and hydrogen isotope analysis of the pulse-labeled trees in Kagawa (2020) will answer how pulse-labeled  $^{18}\text{O}$  and  $^2\text{H}$  signals in storage carbohydrates, if any, will affect intra-annual oxygen and hydrogen isotope signals of tree rings. Furthermore, pulse-labeling trees with three different isotopes ( $^{13}\text{CO}_2$ ,  $\text{H}_2^{18}\text{O}$ , and HDO) at the same time should highlight similarities and differences of carbon, oxygen and hydrogen in post-fixation and exchange processes in carbohydrate pools.

Another interesting discovery from recent dual labeling experiments with  $\text{H}_2^{18}\text{O}$  and HDO is the use of foliar-absorbed water for wood formation. Recent studies have identified foliar water uptake as a significant net water source for terrestrial plants (Eller et al. 2013; Goldsmith et al. 2013; Dawson and Goldsmith 2018; Berry et al. 2019; Schreel and Steppe 2020) and not only is foliar-absorbed water incorporated into leaf water, it is also assimilated into leaf sugar and organic matter (Studer et al. 2015; Lehman et al. 2018, 2020a) and cellulose of leaves, wood and roots (Kagawa 2020). Surprisingly, approximately half of oxygen and hydrogen in branch wood of Japanese cedar formed during simulated rain event originated from foliar-absorbed water, and the other half from root-absorbed water, which was caused by an increased oxygen and hydrogen exchange between sugars and local cambial water under rainy conditions. These results suggest foliar water uptake as a significant oxygen and hydrogen source of tree rings formed during rainy seasons (Kagawa 2020), and current mechanistic models explaining oxygen and hydrogen isotope ratios of leaf water and tree rings might need to be revised in future to account for contributions of oxygen and hydrogen from foliar-absorbed liquid water.

## 15.7 Conclusions

In this chapter, we discussed state-of-understanding of intra-annual variation in the stable isotopes of tree rings. Isotope signal transfer processes from leaves to tree rings include phloem translocation of photosynthetic products and storage of carbohydrates. There are seasonally variable time lags between photosynthetic carbon incorporation at leaves and its use for wood formation, and the time lags range widely from a week to years (Kagawa et al. 2005, 2006a). Incorporation of photosynthetic carbon into cellulose during xylogenesis is further affected by the processes of cell formation and maturation. There are larger volume of work on intra-annual tree-ring  $\delta^{13}\text{C}$  than for  $\delta^{18}\text{O}$  and  $\delta^2\text{H}$ , both on natural and pulse-labeled trees. Therefore, our current understanding of oxygen and hydrogen isotope signal transfer processes are limited compared to that of carbon. Our understanding is especially limited on oxygen and hydrogen isotopic exchange processes between carbohydrates and local cambial water before xylogenesis. However, recently developed  $\text{H}_2^{18}\text{O}$  and HDO pulse-labeling techniques are beginning to uncover such processes. For example, recent experiments with heavy (or depleted)  $\text{H}_2^{18}\text{O}$ , and HDO water identified foliar

water uptake as a significant water source for trees (Eller et al. 2013; Goldsmith et al. 2013; Lehmann et al. 2018) and hence a significant source of oxygen and hydrogen in sugars, organic matter, and wood cellulose (Studer et al. 2015; Lehmann et al. 2018, 2020a; Kagawa 2020).

## References

- Alvarez C, Begin C, Savard MM, Dinis L, Marion J, Smirnoff A, Begin Y (2018) Relevance of using whole-ring stable isotopes of black spruce trees in the perspective of climate reconstruction. *Dendrochronologia* 50:64–69
- An WL, Liu XH, Leavitt SW, Ren JW, Sun WZ, Wang WZ, Wang Y, Xu GB, Chen T, Qin DH (2012) Specific climatic signals recorded in earlywood and latewood  $\delta^{18}\text{O}$  of tree rings in southwestern China. *Tellus B* 64:18703
- Badeck FW, Tcherkez G, Noges S, Piel C, Ghashghaie J (2005) Post-photosynthetic fractionation of stable carbon isotopes between plant organs—a widespread phenomenon. *Rapid Commun Mass Spectrom* 19:1381–1391
- Balzano A, Eufar K, Battipaglia G, Merela M, Prislán P, Aronne G, De Micco V (2018) Xylogenesis reveals the genesis and ecological signal of IADFs in *Pinus pinea* L. and *Arbutus unedo* L. *Ann Bot* 121:1231–1242. <https://doi.org/10.1093/aob/mcy008>
- Balzano A, Battipaglia G, De Micco V (2019) Wood-trait analysis to understand climatic factors triggering intra-annual density-fluctuations in co-occurring Mediterranean trees. *IAWA J* 40(2):241–258
- Barbour MM, Farquhar GD (2000) Relative humidity and ABA induced variation in carbon and oxygen isotope ratios of cotton leaves. *Plant Cell Environ* 23(5):473–485
- Barbour MM, Andrews TJ, Farquhar GD (2001) Correlations between oxygen isotope ratios of wood constituents of *Quercus* and *Pinus* samples from around the world. *Funct Plant Biol* 28(5):335–348
- Barbour MM, Walcroft AS, Farquhar GD (2002) Seasonal variation in  $\delta^{13}\text{C}$  and  $\delta^{18}\text{O}$  of cellulose from growth rings of *Pinus radiata*. *Plant Cell Environ* 25:1483–1499
- Barbour MM, Roden JS, Farquhar GD, Ehleringer JR (2004) Expressing leaf water and cellulose oxygen isotope ratios as enrichment above source water reveals evidence of a Péclet effect. *Oecologia* 138(3):426–435
- Battipaglia G, De Micco V, Brand WA, Linke P, Aronne G, Saurer M, Cherubini P (2010) Variations of vessel diameter and  $\delta^{13}\text{C}$  in false rings of *Arbutus unedo* L reflect different environmental conditions. *New Phytol* 188:1099–1112
- Battipaglia G, DeMicco V, Brand WA, Saurer M, Aronne G, Linke P, Cherubini P (2013) Drought impact on water-use efficiency and intra-annual density fluctuations in *Erica arborea* on Elba (Italy). *Plant Cell Environ* 37:382–391
- Belmecheri S, Wright WE, Szejner P, Morino K, Monson RK (2018) Carbon and oxygen isotope fractionation in tree rings reveal interactions between cambial phenology and seasonal climate. *Plant Cell Environ* 41:2758–2772
- Berry ZC, Emery NC, Gotsch SG, Goldsmith GR (2019) Foliar water uptake: processes, pathways, and integration into plant water budgets. *Plant Cell Environ* 42(2):410–423
- Bertaud F, Holmbom B (2004) Chemical composition of earlywood and latewood in Norway spruce heartwood, sapwood and transition zone wood. *Wood Sci Technol* 38(4):245–256
- Borella S, Leuenberger M, Saurer M, Siegwolf R (1998) Reducing uncertainties in  $\delta^{13}\text{C}$  analysis of tree rings: Pooling, milling and cellulose extraction. *J Geophys Res D* 16:19516–19526
- Borella S, Leuenberger M, Saurer M (1999) Analysis of  $\delta^{18}\text{O}$  in tree rings: wood-cellulose comparison and method dependent sensitivity. *J Geophys Res Atmos* 104(D16):19267–19273



- Brandes E, Kodama N, Whittaker K, Weston C, Rennenberg H, Keitel C, Adams MA, Gessler A (2006) Short-term variation in the isotopic composition of organic matter allocated from the leaves to the stem of *Pinus sylvestris*: effects of photosynthetic and postphotosynthetic carbon isotope fractionation. *Glob Change Biol* 12:1922–1939
- Brown HP (1912) Growth studies in forest trees. 1 *Pinus Rigida* Mill. *Bot Gaz* 54:386–403
- Bruognoli E, Hubick KT, Caemmerer SV, Wong SC, Farquhar GD (1988) Correlation between the carbon isotope discrimination in leaf starch and sugars of C3 plants and the ratio of intercellular and atmospheric partial pressures of carbon dioxide. *Plant Physiol* 88:1418–1424
- Butto V, Rossi S, Deslauriers A (2019) Is size an issue of time? Relationship between the duration of xylem development and cell traits. *Ann Bot* 123:1257–1265
- Camarero JJ, Guerrero-Campo J, Gutiérrez E (1998) Tree-ring growth and structure of *Pinus uncinata* and *Pinus sylvestris* in the Central Spanish Pyrenees. *Arct Alp Res* 30:1–10
- Campbell MM, Sederoff RR (1996) Variation in lignin and implications for the genetic improvement of plants. *Plant Physiol* 110:3–13
- Castagneri D, Battipaglia G, vonArx G, Pacheco A, Carrer M (2018) Tree-ring anatomy and carbon isotope ratio show both direct and legacy effects of climate on bimodal xylem formation in *Pinus pinea*. *Tree Physiol* 38:1098–1109
- Cheesman AW, Cernusak LA (2016) Infidelity in the outback: Climate signal recorded in  $\Delta^{18}\text{O}$  of leaf but not branch cellulose of eucalypts across an Australian aridity gradient (ed Meinzer F). *Tree Physiol* 37:554–564
- Cherubini P, Gartner BL, Tognetti R, Braker OU, Schoch W, Innes JL (2003) Identification, measurement and interpretation of tree rings in woody species from Mediterranean climates. *Biol Rev* 78:119–148
- Cormier MA, Werner RA, Sauer PE, Gröcke DR, Leuenberger MC, Wieloch T, Schleucher J, Kahmen A (2018)  $^2\text{H}$ -fractionations during the biosynthesis of carbohydrates and lipids imprint a metabolic signal on the  $\delta^2\text{H}$  values of plant organic compounds. *New Phytol* 218(2):479–491
- Cuny HE, Rathgeber CBK, Frank D, Fonti P, Fournier M (2014) Kinetics of tracheid development explain conifer tree-ring structure. *New Phytol* 203:1231–1241
- Cuny HE, Rathgeber CBK, Frank D, Fonti P, Mäkinen H, Prislan P, Fournier M (2015) Woody biomass production lags stem-girth increase by over one month in coniferous forests. *Nat Plants* 1:15160
- Cuny HE, Fonti P, Rathgeber CB, von Arx G, Peters RL, Frank DC (2019) Couplings in cell differentiation kinetics mitigate air temperature influence on conifer wood anatomy. *Plant Cell Environ* 42(4):1222–1232
- Dannoura M, Maillard P, Fresneau C, Plain C, Berveiller D, Gerant D, Chipeaux C, Bosc A, Ngao J, Damesin C, Loustau D, Epron D (2011) In situ assessment of the velocity of carbon transfer by tracing  $^{13}\text{C}$  in trunk  $\text{CO}_2$  efflux after pulse labeling: variations among tree species and seasons. *New Phytol* 190(1):181–192
- Dansgaard W (1964) Stable isotopes in precipitation. *Tellus* 16(4):436–468
- Dawson TE, Goldsmith GR (2018) The value of wet leaves. *New Phytol* 219(4):1156–1169
- De Micco V, Campelo F, de Luis M, Bräuning A, Grabner M, Battipaglia G, Cherubini P (2016) Formation of intra-annual-density-fluctuations in tree rings: how, when, where and why? *IAWA J* 37:232–259. <https://doi.org/10.1163/22941932-20160132>
- Denne MP (1972) A comparison of root- and shoot-wood development in conifer seedlings. *Ann Bot* 36:579–587
- Dodd JP, Patterson WP, Holmden C, Brasseur JM (2008) Robotic micromilling of tree-rings: a new tool for obtaining subseasonal environmental isotope records. *Chem Geol* 252(1–2):21–30
- Dongmann G, Nürnberg HW, Förstel H, Wagener K (1974) On the enrichment of  $\text{H}_2^{18}\text{O}$  in the leaves of transpiring plants. *Radiat Environ Biophys* 11(1):41–52
- Eglin T, Francois C, Michelot A, Delpierre N, Damesin C (2010) Linking intra-seasonal variations in climate and tree-ring  $\delta\text{C-13}$ : A functional modelling approach. *Ecol Model* 221:1779–1797

- Eller CB, Lima AL, Oliveira RS (2013) Foliar uptake of fog water and transport belowground alleviates drought effects in the cloud forest tree species, *Drimys brasiliensis* (Winteraceae). *New Phytol* 199(1):151–162
- Farquhar GD, O'Leary MH, Berry JA (1982) On the relationship between carbon isotope discrimination and the intercellular carbon dioxide concentration in leaves. *Funct Plant Biol* 9(2):121–137
- Farquhar GD, Ehleringer JR, Hubick KT (1989) Carbon isotope discrimination and photosynthesis. *Annu Rev Plant Physiol Plant Mol Biol* 40:503–537
- Flanagan LB, Comstock JP, Ehleringer JR (1991) Comparison of modeled and observed environmental influences on the stable oxygen and hydrogen isotope composition of leaf water in *Phaseolus vulgaris* L. *Plant Physiol* 96:588–596
- Fonti P, Garcia-Gonzalez I (2008) Earlywood vessel size of oak as a potential proxy for spring precipitation in mesic sites. *J Biogeogr* 35:2249–2257
- Fredriksson M, Pedersen NB, Thygesen LG (2018) The cell wall composition of Norway spruce earlywood and latewood revisited. *Int Wood Prod J* 9(2):80–85. <https://doi.org/10.1080/20426445.2018.1479680>
- Fu PL, Griessinger J, Gebrekirstos A, Fan ZX, Brauning A (2017) Earlywood and latewood stable carbon and oxygen isotope variations in two Pine species in Southwestern China during the recent decades. *Front Plant Sci* 7:2050
- Gea-Izquierdo G, Fonti P, Cherubini P, Martin-Benito D, Chaar H, Canellas I (2012) Xylem hydraulic adjustment and growth response of *Quercus canariensis* Willd to climatic variability. *Tree Physiol* 32:401–413
- Gessler A, Brandes E, Buchmann N, Helle G, Rennenberg H, Barnard RL (2009) Tracing carbon and oxygen isotope signals from newly assimilated sugars in the leaves to the tree-ring archive. *Plant Cell Environ* 32:780–795
- Gindl W (2001) The effect of varying latewood proportion on the radial distribution of lignin content in a pine stem. *Holzforschung* 55(5):455–458
- Goldsmith GR, Matzke NJ, Dawson TE (2013) The incidence and implications of clouds for cloud forest plant water relations. *Ecol Lett* 16(3):307–314
- Gordon JC, Larson PR (1968) Seasonal course of photosynthesis, respiration and distribution of  $^{14}\text{C}$  in young *Pinus resinosa* trees as related to wood formation. *Plant Physiol* 43:1617–1624
- He M, Bräuning A, Rossi S, Gebrekirstos A, Grießinger J, Mayr C, Peng C, Yang B (2020) No evidence for carryover effect in tree rings based on a pulse-labeling experiment on *Juniperus communis* in South Germany. *Trees* 152:1–10
- Helle G, Panferov O (2004) Tree rings, isotopes, climate and environment—trice pages. *Newsletter* 12(2):22–23
- Helle G, Schleser GH (2004) Beyond  $\text{CO}_2$ -fixation by Rubisco – an interpretation of  $^{13}\text{C}/^{12}\text{C}$  variations in tree rings from novel intra-seasonal studies on broad-leaf trees. *Plant Cell Environ* 27:367–380
- Hemming DL, Fritts H, Leavitt SW, Wright W, Long A, Shashkin A (2001) Modelling tree-ring  $\delta^{13}\text{C}$ . *Dendrochronologia* 19:23–38
- Hill SA, Waterhouse JS, Field EM, Switsur VR, Aprees T (1995) Rapid recycling of triose phosphates in oak stem tissue. *Plant Cell Environ* 18:931–936
- Jäggi M, Saurer M, Fuhrer J, Siegwolf R (2002) The relationship between the stable carbon isotope composition of needle bulk material, starch, and tree rings in *Picea abies*. *Oecologia* 131:325–332
- Jordan MO, Mariotti A (1998) Can carbon isotopic discrimination in young peach trees be considered as a tool to understand the seasonal dynamic of the stored carbon? *Acta Hort* 465:327–335
- Kagawa A, Sugimoto A, Yamashita K, Abe H (2005) Temporal photosynthetic carbon isotope signatures revealed in a tree ring through  $^{13}\text{CO}_2$  pulse-labeling. *Plant Cell Environ* 28(7):906–915
- Kagawa A, Sano M, Nakatsuka T, Ikeda T, Kubo S (2015) An optimized method for stable isotope analysis of tree rings by extracting cellulose directly from cross-sectional laths. *Chem Geol* 393:16–25

- Keel SG, Schadel C (2010) Expanding leaves of mature deciduous forest trees rapidly become autotrophic. *Tree Physiol* 30:1253–1259
- Keel SG, Siegwolf RTW, Körner C (2006) Canopy CO<sub>2</sub> enrichment permits tracing the fate of recently assimilated carbon in a mature deciduous forest. *New Phytol* 172:319–329
- Keel SG, Siegwolf RTW, Jäggi M, Körner C (2007) Rapid mixing between old and new C pools in the canopy of mature forest trees. *Plant Cell Environ* 30:963–972
- Keitel C, Adams MA, Holst T, Matzarakis A, Mayer H, Rennenberg H, Geßler A (2003) Carbon and oxygen isotope composition of organic compounds in the phloem sap provides a short-term measure for stomatal conductance of European beech (*Fagus sylvatica* L.). *Plant Cell Environ* 26:1157–1168
- Kerhoulas LP, Kolb TE, Koch GW (2017) The influence of monsoon climate on latewood growth of Southwestern Ponderosa pine. *Forests* 8:140
- Kern Z, Patkó M, Kázmér M, Fekete J, Kele S, Pályi Z (2013) Multiple tree-ring proxies (earlywood width, latewood width and  $\delta^{13}\text{C}$ ) from pedunculate oak (*Quercus robur* L.) Hungary. *Q Int* 293:257–267
- Khattak TM, Mahmood A (1986) Estimation of lignin, holocellulose and alphacellulose content of earlywood and latewood among innerwood and outerwood of blue pine (*Pinus walllichiana* A.B. Jacks). *Pak J Bot* 18:235–241
- Kitagawa H, Wada H (1993) Seasonal and secular  $\delta^{13}\text{C}$  variations in annual growth rings of Japanese cedar tree from Mt. Amagi, Izu Peninsula Central Japan. *Geochem J* 27:391–396
- Knowles JR, Albery WJ (1977) Perfection in enzyme catalysis: the energetics of triosephosphate isomerase. *Acc Chem Res* 10:105–111
- Körner C, Asshoff R, Bignucolo O, Hättenschwiler S, Keel SG, Pelaez-Riedl S, Pepin S, Siegwolf RTW, Zotz G (2005) Carbon flux and growth in mature deciduous forest trees exposed to elevated CO<sub>2</sub>. *Science* 309:1360–1362
- Lacointe A, Deleens E, Ameglio T, Saint-joanis B, Lelarge C, Vandame M, Song GC, Daudet FA (2004) Testing the branch autonomy theory: a  $^{13}\text{C}/^{14}\text{C}$  double-labeling experiment on differentially shaded branches. *Plant Cell Environ* 27:1159–1168
- Leavitt SW (1993) Seasonal  $^{13}\text{C}/^{12}\text{C}$  changes in tree rings: species and site coherence, and a possible drought influence. *Can J for Res* 23:210–218
- Leavitt SW, Long A (1986) Stable-carbon isotope variability in tree foliage and wood. *Ecology* 67:1002–1010
- Leavitt SW, Long A (1991) Seasonal stable-carbon isotope variability in tree rings: possible paleoenvironmental signals. *Chem Geol* 87:59–70
- Li ZH, Liu RM, An ZS, Wu XD (1996) Climatic implications of seasonal delta C-13 in tree rings from Huangling of Shaanxi Province. *Chin Sci Bull* 41:326–329
- Li ZH, Leavitt SW, Mora CI, Liu RM (2005) Influence of earlywood–latewood size and isotope differences on long-term tree-ring  $\delta^{13}\text{C}$  trends. *Chem Geol* 216(3–4):191–201
- Li ZH, Labbé N, Driese SG, Grissino-Mayer HD (2011) Micro-scale analysis of tree-ring  $\delta^{18}\text{O}$  and  $\delta^{13}\text{C}$  on  $\alpha$ -cellulose spline reveals high-resolution intra-annual climate variability and tropical cyclone activity. *Chem Geol* 284(1–2):138–147
- Livingston NJ, Spittlehouse DL (1996) Carbon isotope fractionation in tree ring early and late wood in relation to intra-growing season water balance. *Plant Cell Environ* 19:768–774
- Loader NJ, Robertson I, McCarroll D (2003) Comparison of stable carbon isotope ratios in the whole wood, cellulose and lignin of oak tree-rings. *Palaeogeogr Palaeoclimatol Palaeoecol* 196(3–4):395–407
- Loader NJ, McCarroll D, Barker S, Jalkanen R, Grudd H (2017) Inter-annual carbon isotope analysis of tree-rings by laser ablation. *Chem Geol* 466:323–326
- McCarroll D, Loader NJ (2004) Stable isotopes in tree rings. *Q Sci Rev* 23:771–801
- McCarroll D, Jalkanen R, Hicks S, Tuovinen M, Gagen M, Pawellek F, Eckstein D, Schmitt U, Autio J, Heikkinen O (2003) Multiproxy dendroclimatology: a pilot study in northern Finland. *Holocene* 13:829–838

- Miller DL, Mora CI, Grissino-Mayer HD, Mock CJ, Uhle ME, Sharp Z (2006) Tree-ring isotope records of tropical cyclone activity. *Proc Nat Acad Sci* 103:14294–14297
- Monserud RA, Marshall JD (2001) Time-series analysis of  $\delta^{13}\text{C}$  from tree rings. I time trends and autocorrelation. *Tree Physiol* 21:1087–1102
- Moran JJ, Newburn MK, Alexander ML, Sams RL, Kelly JF, Kreuzer HW (2011) Laser ablation isotope ratio mass spectrometry for enhanced sensitivity and spatial resolution in stable isotope analysis. *Rapid Commun Mass Spectrom* 25(9):1282–1290
- Nabeshima E, Nakatsuka T, Kagawa A, Hiura T, Funada R (2018) Seasonal changes of  $\delta\text{D}$  and  $\delta^{18}\text{O}$  in tree-ring cellulose of *Quercus crispula* suggest a change in post-photosynthetic processes during earlywood growth. *Tree Physiol* 38:1829–1840
- Nakatsuka T, Ohnishi K, Hara T, Sumida A, Mitsuishi D, Kurita N, Uemura S (2004) Oxygen and carbon isotopic ratios of tree-ring cellulose in a conifer-hardwood mixed forest in northern Japan. *Geochim J* 38(1):77–88
- Nakatsuka T, Sano M, Li Z, Xu C, Tsushima A, Shigeoka Y, Sho K, Ohnishi K, Skaamoto M, Ozaki H, Higami N, Nakao N, Yokoyama M, Mitsutani T (2020) A 2600-year summer climate reconstruction in central Japan by integrating tree-ring stable oxygen and hydrogen isotopes. *Clim past* 16(6):2153–2172
- Offermann C, Ferrio JP, Holst J, Grote R, Siegwolf R, Kayler Z, Gessler A (2011) The long way down—Are carbon and oxygen isotope signals in the tree ring uncoupled from canopy physiological processes? *Tree Physiol* 31:1088–1102
- Ogé J, Barbour MM, Wingate L, Bert D, Bosc A, Stievenard M, Lambrot C, Pierre M, Bariac T, Lostau D, Dewar RC (2009) A single-substrate model to interpret intra-annual stable isotope signals in tree-ring cellulose. *Plant Cell Environ* 32(8):1071–1090
- Ogle N, McCormac FC (1994) High-resolution  $\delta^{13}\text{C}$  measurements of oak show a previously unobserved spring depletion. *Geophys Res Lett* 21:2373–2375
- Ohashi S, Durgante FM, Kagawa A, Kajimoto T, Trumbore SE, Xu X, Ishizuka M, Higuchi N (2016) Seasonal variations in the stable oxygen isotope ratio of wood cellulose reveal annual rings of trees in a Central Amazon terra firme forest. *Oecologia* 180(3):685–696
- Pallardy SG (2008) *Physiology of woody plants*, 3rd edn. Elsevier Academic Press, New York, NY, USA
- Pepin S, Körner C (2002) Web-FACE: a new canopy free-air  $\text{CO}_2$  enrichment system for tall trees in mature forests. *Oecologia* 133:1–9
- Pons TL, Helle G (2011) Identification of anatomically non-distinct annual rings in tropical trees using stable isotopes. *Trees* 25(1):83–93
- Poussart PF, Evans MN, Schrag DP (2004) Resolving seasonality in tropical trees: multi-decade, high-resolution oxygen and carbon isotope records from Indonesia and Thailand. *Earth Planet Sci Lett* 218(3–4):301–316
- Rathgeber CBK, Cuny HE, Fonti P (2016) Biological basis of tree-ring formation: a crash course. *Front Plant Sci* 7:734
- Reynolds SJ, Yates DW, Pogson CI (1971) Dihydroxyacetone phosphate: its structure and reactivity with  $\alpha$ -glycerophosphate dehydrogenase, aldolase and triose phosphate isomerase and some possible metabolic implications. *Biochem J* 122:285–297
- Ritter GJ, Fleck LC (1926) *Chemistry of wood*. IX. *Springwood and summerwood*. *Ind Eng Chem* 18:608–609
- Roden JS, Ehleringer JR (1999) Observations of hydrogen and oxygen isotopes in leaf water confirm the Craig-Gordon model under wide-ranging environmental conditions. *Plant Physiol* 120(4):1165–1174
- Roden JS, Lin G, Ehleringer JR (2000) A mechanistic model for interpretation of hydrogen and oxygen isotope ratios in tree-ring cellulose. *Geochim Cosmochim Acta* 64(1):21–35
- Roden JS, Johnstone JA, Dawson TE (2009) Intra-annual variation in the stable oxygen and carbon isotope ratios of cellulose in tree rings of coast redwood (*Sequoia sempervirens*). *The Holocene* 19(2):189–197

- Roden J, Kahmen A, Buchmann N, Siegwolf R (2015) The enigma of effective path length for  $^{18}\text{O}$  enrichment in leaf water of conifers. *Plant Cell Environ* 38(12):2551–2565
- Rossi S, Deslauriers A, Morin H (2003) Application of the Gompertz equation for the study of xylem cell development. *Dendrochronologia* 21:33–39
- Sarris D, Siegwolf R, Körner C (2013) Inter- and intra-annual stable carbon and oxygen isotope signals in response to drought in Mediterranean pines. *Agric Meteorol* 168:59–68
- Sass U, Killmann W, Eckstein D (1995) Wood formation in two species of Dipterocarpaceae in peninsular Malaysia. *IAWA J* 16:371–384
- Schleser GH, Helle G, Lücke A, Vos H (1999) Isotope signals as climate proxies: the role of transfer functions in the study of terrestrial archives. *Quatern Sci Rev* 18:927–943
- Schoeller DA, Van Santen E (1982) Measurement of energy expenditure in humans by doubly labeled water method. *J Appl Physiol* 53:955–959
- Schollaen K, Heinrich I, Helle G (2014) UV-laser-based microscopic dissection of tree rings—a novel sampling tool for  $\delta^{13}\text{C}$  and  $\delta^{18}\text{O}$  studies. *New Phytol* 201(3):1045–1055
- Schreel JD, Steppe K (2020) Foliar water uptake in trees: negligible or necessary? *Trends Plant Sci.* <https://doi.org/10.1016/j.tplants.2020.01.003>
- Schubert BA, Jahren AH (2015) Seasonal temperature and precipitation recorded in the intra-annual oxygen isotope pattern of meteoric water and tree-ring cellulose. *Quatern Sci Rev* 125:1–14
- Schulze B, Wirth C, Linke P, Brand WA, Kuhlmann I, Horna V, Schulze ED (2004) Laser ablation-combustion-GC-IRMS – a new method for online analysis of intra-annual variation of  $\delta^{13}\text{C}$  in tree rings. *Tree Physiol* 24:1193–1201
- Scott MP, Jane JL, Soundararajan M (1999) Carbon isotope ratios of amylose, amylopectin and mutant starches. *Phytochemistry* 52:555–559
- Seargent CI, Singer MB (2016) Sub-annual variability in historical water source use by Mediterranean riparian trees. *Ecohydrology* 9:1328–1345
- Sheu DD, Kou P, Chiu CH, Chen MJ (1996) Variability of tree ring  $\delta^{13}\text{C}$  in Taiwan fir: growth effect and response to May–October temperatures. *Geochim Cosmochim Acta* 60:171–177
- Shinozaki K, Yoda K, Hozumi K, Kira T (1964) A quantitative analysis of plant form—the pipe model theory: I basic analyses. *Japan J Ecol* 14(3):97–105
- Skene DS (1969) The period of time taken by cambial derivatives to grow and differentiate into tracheids in *Pinus radiata* D Don. *Ann Botany* 33:253–262
- Song XIN, Barbour MM, Farquhar GD, Vann DR, Helliker BR (2013) Transpiration rate relates to within- and across-species variations in effective path length in a leaf water model of oxygen isotope enrichment. *Plant Cell Environ* 36(7):1338–1351
- Soudant A, Loader NJ, Bäck J, Levula J, Kljun N (2016) Intra-annual variability of wood formation and  $\delta^{13}\text{C}$  in tree-rings at Hyytiälä, Finland. *Agric Meteorol* 224:17–29
- Sternberg LSL, DeNiro MJ, Savidge RA (1986) Oxygen isotope exchange between metabolites and water during biochemical reactions leading to cellulose synthesis. *Plant Physiol* 82:423–427
- Studer MS, Siegwolf RTW, Leuenberger M, Abiven S (2015) Multi-isotope labelling of organic matter by diffusion of  $^2\text{H}/^{18}\text{O}$   $\text{H}_2\text{O}$  vapour and  $^{13}\text{C}$ - $\text{CO}_2$  into the leaves and its distribution within the plant. *Biogeosci* 12:1865–1879
- Szejner P, Wright WE, Belmecheri S, Meko D, Leavitt SW, Ehleringer JR, Monson RK (2018) Disentangling seasonal and interannual legacies from inferred patterns of forest water and carbon cycling using tree-ring stable isotopes. *Glob Change Biol* 24:5332–5347
- Talhelm AF, Qadir SA, Powers MD, Bradley KL, Friend AL, Pregitzer KS (2007)  $^{13}\text{C}$  labeling of plant assimilates using a simple canopy-scale open air system. *Plant Soil* 296:227–234
- Verheyden A, Helle G, Schleser GH, Dehairs F, Beeckman H, Koedam N (2004) Annual cyclicity in high-resolution stable carbon and oxygen isotope ratios in the wood of the mangrove tree *Rhizophora mucronata*. *Plant Cell Environ* 27(12):1525–1536
- Verheyden A, Roggeman M, Bouillon S, Elskens M, Beeckman H, Koedam N (2005) Comparison between  $\delta^{13}\text{C}$  of  $\alpha$ -cellulose and bulk wood in the mangrove tree *Rhizophora mucronata*: implications for dendrochemistry. *Chem Geol* 219(1–4):275–282

- Voelker SL, Brooks R, Meinzer FC, Roden J, Pazdur A, Pawelczyk S, Hartsough P, Snyder K, Plavcova L, Santrucek J (2014) Reconstructing relative humidity from plant  $\delta^{18}\text{O}$  and  $\delta\text{D}$  as deuterium deviations from the global meteoric water line. *Ecol Appl* 24:960–975
- Voelker SL, Brooks JR, Meinzer FC, Anderson R, Bader MKF, Battipaglia G et al (2016) A dynamic leaf gas-exchange strategy is conserved in woody plants under changing ambient  $\text{CO}_2$ : evidence from carbon isotope discrimination in paleo and  $\text{CO}_2$  enrichment studies. *Glob Change Biol* 22:889–902
- von Felten S, Hättenschwiler S, Saurer M, Siegwolf R (2007) Carbon allocation in shoots of alpine treeline conifers in a  $\text{CO}_2$  enriched environment. *Trees* 21(3):283
- Walcroft AS, Silvester WB, Whitehead D, Kelliher FM (1997) Seasonal changes in stable carbon isotope ratios within annual rings of *Pinus radiata* reflect environmental regulation of growth processes. *Funct Plant Biol* 24(1):57–68
- Wilson AT, Grinstead MJ (1977)  $^{12}\text{C}/^{13}\text{C}$  in cellulose and lignin as paleothermometers. *Nature* 265:133–135
- Wodzicki TJ (1971) Mechanism of xylem differentiation in *Pinus sylvestris* L. *J Exp Bot* 22:670–687
- Xu C, Zheng H, Nakatsuka T, Sano M, Li Z, Ge J (2016) Inter- and intra-annual tree-ring cellulose oxygen isotope variability in response to precipitation in Southeast China. *Trees* 30(3):785–794
- Yakir D, DeNiro MJ (1990) Oxygen and hydrogen isotope fractionation during cellulose metabolism in *Lemna gibba* L. *Plant Physiol* 93(1):325–332
- Yakir D, DeNiro MJ, Gat JR (1990) Natural deuterium and oxygen-18 enrichment in leaf water of cotton plants grown under wet and dry conditions: evidence for water compartmentation and its dynamics. *Plant Cell Environ* 13(1):49–56
- Zalloni E, de Luis M, Campelo F, Novak K, De Micco V, di Filippo A, Vieira J, Nabais C, Rozas V, Battipaglia G (2016) Climatic signals from intra-annual density fluctuation frequency in Mediterranean pines at a regional scale. *Front Plant Sci* 7:579. <https://doi.org/10.3389/fpls.2016.00579>
- Zeng XM, Liu XH, Wang WZ, Xu GB, An WL, Wu GJ (2014) No altitude-dependent effects of climatic signals are recorded in Smith fir tree-ring  $^{18}\text{O}$  on the southeastern Tibetan Plateau, despite a shift in tree growth. *Boreas* 43:588–599
- Zeng XM, Liu XH, Treydte K, Evans MN, Wang WZ, An WL, Sun WZ, Xu GB, Wu GJ, Zhang XW (2017) Climate signals in tree-ring  $\delta^{18}\text{O}$  and  $\delta^{13}\text{C}$  from southeastern Tibet: insights from observations and forward modelling of intra- to inter-decadal variability. *New Phytol* 216:1104–1118
- Zweifel R, Zimmermann L, Zeugin F, Newbery DM (2006) Intra-annual radial growth and water relations of trees: implications towards a growth mechanism. *J Exp Bot* 57:1445–1459
- Bergander A (2001) Local variability in chemical and physical properties of spruce wood fibers. Doctoral dissertation, Institutionen för pappers-och massateknologi
- Craig H, Gordon L (1965) Deuterium and oxygen-18 in the ocean and the marine atmosphere. In: Tongiorgi E (eds) *Stable isotopes in oceanographic studies and paleotemperatures*, pp 9–130. Spoleto
- Farquhar GD (1998) Interpretation of oxygen isotope composition of leaf material. In: Griffiths H (eds) *Stable isotopes: the integration of biological, ecological and geochemical processes*. Environmental Plant Biology Series, vol 27–62. Garland Science. <https://doi.org/10.1201/9781003076865-3>
- Farquhar GD, Lloyd J (1993) Carbon and oxygen isotope effects in the exchange of carbon dioxide between terrestrial plants and the atmosphere. In: *Stable isotopes and plant carbon-water relations*, pp 47–70. Academic Press
- Ferrio PJ, Voltas J (2005) Carbon and oxygen isotope ratios in wood constituents of *Pinus halepensis* as indicators of precipitation, temperature and vapor pressure deficit. *Tellus* 57(2), 164–173
- Hafner P, Gricar J, Skudnik M, Levanič T (2015) Variations in environmental signals in tree-ring indices in trees with different growth potential. *PLOS One* 10:e0143918
- Hansen J, Beck E (1994) Seasonal changes in the utilization and turnover of assimilation products in 8-year-old Scots pine (*Pinus sylvestris* L.) trees. *Trees* 8(4):172–182

- Hansen J, Tuerk R, Vogg G, Heim R, Beck E (1997) Conifer carbohydrate physiology: updating classical views. In: Rennenberg H, Eschrich W, Ziegler H (eds) *Trees—contributions to modern tree physiology*, pp 97–108. Back-huys Publishers, Leiden, The Netherlands
- Ino S, Shoji G, Kagawa A, Dannoura M, Kobayashi H, Hirano Y, Saito T, Yasue K (2018) Seasonal variation of photoassimilate allocation in radial growth of *Chamaecyparis obtusa* and *Cryptomeria japonica* using  $^{13}\text{C}$  pulse-labeling. In: Proceedings of 2018 SWST/JWRS international convention, Nagoya, Japan
- IUPAC (1997) Compendium of chemical terminology. Peak Resolution Rs in Chromatography. <https://doi.org/10.1351/goldbook.P04465>
- Jahren AH, Sternberg LS (2008) Annual patterns within tree rings of the Arctic middle Eocene (ca. 45 Ma): isotopic signatures of precipitation, relative humidity, and deciduousness. *Geology* 36(2):99–102
- Kagawa A (2006) Physiological basis for carbon isotope dendroclimatology in Siberia. Ph.D thesis, Hokkaido University
- Kagawa A (2020) Foliar water uptake as a source of hydrogen and oxygen in plant biomass. <https://doi.org/10.1101/2020.08.20.260372>
- Kagawa A, Naito D, Sugimoto A, Maximov TC (2003) Effects of spatial and temporal variability in soil moisture on widths and  $\delta^{13}\text{C}$  values of eastern Siberian tree rings. *J Geophys Res Atmos* 108(D16)
- Kagawa A, Sugimoto A, Maximov TC (2006a)  $^{13}\text{C}$  pulse-labeling of photoassimilates reveals carbon allocation within and between tree rings. *Plant Cell Environ* 29:1571–1584
- Kagawa A, Sugimoto A, Maximov TC (2006b) Seasonal course of translocation, storage, and remobilization of  $^{13}\text{C}$  pulse-labeled photoassimilate in naturally growing *Larix gmelinii* saplings. *New Phytol* 171:793–804
- Kimak A, Leuenberger M (2015) Are carbohydrate storage strategies of trees traceable by early-latewood carbon isotope differences? *Trees Struct Funct* 29:859–870
- Lehmann MM, Goldsmith GR, Schmid L, Gessler A, Saurer M, Siegwolf RT (2018) The effect of  $^{18}\text{O}$ -labeled water vapour on the oxygen isotope ratio of water and assimilates in plants at high humidity. *New Phytol* 217(1):105–116
- Lehmann MM, Goldsmith GR, Mirande-Ney C, Weigt RB, Schönbeck L, Kahmen A, Gessler A, Siegwolf RTW, Saurer M (2020a) The  $^{18}\text{O}$ -signal transfer from water vapour to leaf water and assimilates varies among plant species and growth forms. *Plant Cell Environ* 43(2):510–523
- Lehmann MM, Vitali V, Schuler P, Leuenberger M, Saurer M (2020b) More than climate: hydrogen isotope ratios in tree rings as novel plant physiological indicator for stress conditions. *Dendrochronologia* 65:125788
- Managave SR, Sheshshayee MS, Borgaonkar HP, Ramesh R (2010a) Intra-annual oxygen isotope variations in central Indian teak cellulose: possibility of improved resolution for past monsoon reconstruction. *Curr Sci* 98(7):930–937
- Managave SR, Sheshshayee MS, Borgaonkar HP, Ramesh R (2010b) Past break-monsoon conditions detectable by high resolution intra-annual  $\delta^{18}\text{O}$  analysis of teak rings. *Geophys Res Lett* 37(5)
- Nabeshima E, Kubo T, Yasue K, Hiura T, Funada R (2015) Changes in radial growth of earlywood in *Quercus crispula* between 1970 and 2004 reflect climate change. *Trees Struct Funct* 29:1273–1281
- Simard SW, Durall DM, Jones MD (1997a) Carbon allocation and carbon transfer between *Betula papyrifera* and *Pseudotsuga menziesii* seedlings using a  $^{13}\text{C}$  pulse-labeling method. *Plant Soil* 191:41–55
- Simard SW, Perry DA, Jones MD, Myrold DD, Durall DM, Molina R (1997b) Net transfer of carbon between ectomycorrhizal tree species in the field. *Nature* 388:579–582
- Speakman J (1997) Doubly labeled water: theory and practice. Springer Science & Business Media
- Szejner P, Wright WE, Babst F, Belmecheri S, Trouet V, Leavitt SW, Ehleringer JR, Monson RK (2016) Latitudinal gradients in tree ring stable carbon and oxygen isotopes reveal differential climate influences of the North American Monsoon System. *J Geophys Res Biogeosci* 121:1978–1991

- Wilson JW, Wellwood RW (1965) Intra-increment chemical properties of certain western Canadian coniferous species. Cellular Ultrastructure of Woody Plants. Ed. Côté, WA Syracuse University Press, Syracuse, 551–559
- Zalloni E, Battipaglia G, Cherubini P, De Micco V (2018a) Site conditions influence the climate signal of intra-annual density fluctuations in tree rings of *Q. ilex* L. Ann For Sci 75–68. <https://doi.org/10.1007/s13595-018-0748-0>
- Zalloni E, Battipaglia G, Cherubini P, Saurer M, De Micco V (2018b) Contrasting physiological responses to Mediterranean climate variability are revealed by intra-annual density fluctuations in tree rings of *Quercus ilex* L. and *Pinus pinea* L. Tree Physiol 38:1–12. <https://doi.org/10.1093/treephys/tpy061>
- Zalloni E, Battipaglia G, Cherubini P, Saurer M, De Micco V (2019) Wood growth in pure and mixed *Quercus ilex* L. forests: drought influence depends on site conditions. Front Plant Sci 10:397

**Open Access** This chapter is licensed under the terms of the Creative Commons Attribution 4.0 International License (<http://creativecommons.org/licenses/by/4.0/>), which permits use, sharing, adaptation, distribution and reproduction in any medium or format, as long as you give appropriate credit to the original author(s) and the source, provide a link to the Creative Commons license and indicate if changes were made.

The images or other third party material in this chapter are included in the chapter's Creative Commons license, unless indicated otherwise in a credit line to the material. If material is not included in the chapter's Creative Commons license and your intended use is not permitted by statutory regulation or exceeds the permitted use, you will need to obtain permission directly from the copyright holder.





# Chapter 16

## Probing Tree Physiology Using the Dual-Isotope Approach



John Roden, Matthias Saurer, and Rolf T. W. Siegwolf

**Abstract** The environmental and physiological interpretation of stable isotope variation in organic matter is affected by many different and interacting factors. This is especially true when considering isotope variation in tree rings, which are influenced not only by leaf-level photosynthetic gas exchange processes but also by post-photosynthetic fractionation. It has been proposed that measuring multiple isotopes on the same sample may constrain such interpretations if one isotope provides independent information about important fractionation events that cause variation in another isotope. Here we describe one such “dual-isotope approach” where oxygen isotope variation ( $\delta^{18}\text{O}$ ) is used to probe the effects of stomatal conductance on carbon isotope ( $\delta^{13}\text{C}$ ) variation for the same sample. This chapter describes the development of this conceptual model, constraints on model applicability, particularly with respect to tree rings, and how it has been utilized to explore aspects of tree physiology.

### 16.1 Introduction

The visionary scientist Harmon Craig was one of the first to measure stable isotopes in wood and argued that  $\delta^{13}\text{C}$  in tree rings might be linked to environmental variation (Craig 1954). Others followed and measured different isotopes such as  $\delta^2\text{H}$  and  $\delta^{18}\text{O}$  (Schiegl 1974; Gray and Thompson 1976, see also Chap. 1). However, due to instrument and sample size limitations, most early studies focused on one element at a time. Once it became possible to measure more than one element on a single sample, researchers began to see the benefits of multiple proxy information to reconstruct historical climate and physiological responses to climate variability. With the

---

J. Roden (✉)

Biology Department, Southern Oregon University, 1250 Siskiyou Blvd., Ashland, OR, USA  
e-mail: [rodenj@sou.edu](mailto:rodenj@sou.edu)

M. Saurer · R. T. W. Siegwolf

Swiss Federal Institute for Forest, Snow and Landscape Research WSL, Birmensdorf, Switzerland

R. T. W. Siegwolf

Lab of Atmospheric Chemistry, Paul Scherrer Institute, Villigen-PSI, Switzerland

© The Author(s) 2022

R. T. W. Siegwolf et al. (eds.), *Stable Isotopes in Tree Rings*, Tree Physiology 8,  
[https://doi.org/10.1007/978-3-030-92698-4\\_16](https://doi.org/10.1007/978-3-030-92698-4_16)

463

advent of software that can switch tuning during analysis of a single sample, IRMS instruments commonly provide both  $\delta^{13}\text{C}$  and  $\delta^{15}\text{N}$  values after combustion and separation for the same organic matter sample (Pate et al. 1998; Cernusak et al. 2007). While this approach has many uses in ecological studies (Ohkouchi et al. 2015), wood contains very little nitrogen and so relatively few stable isotope dendrochronologists have applied  $\delta^{15}\text{N}$  as secondary proxy (although see Chap. 12). Although measuring both  $\delta^{13}\text{C}$  and  $\delta^{18}\text{O}$  values for the same sample commonly involves separate IRMS runs (combustion for  $\delta^{13}\text{C}$  and pyrolysis for  $\delta^{18}\text{O}$ ), analysis of the carbon and oxygen isotope ratios from one sample is also possible with newer pyrolysis techniques (Woodley et al. 2012; Weigt et al. 2015). With the advent of new techniques to more easily measure  $\delta^2\text{H}$  in cellulose (to deal with exchangeable H, see methods in Chaps. 7 and 11), some are beginning to look at all three primary stable isotopes in cellulose (Etien et al. 2009; Loader et al. 2016).

Regardless of using a dual-isotope approach as a way to constrain physiological interpretations of one isotope, multiple isotopic information from the same sample provide added information for analysis. Each element has a different pathway for inclusion into organic matter with different fractionation events that potentially capture a unique set of physiological and environmental information. Even oxygen and hydrogen, which are both incorporated into cellulose via source water and thus would seemingly provide identical environmental information, can be used to examine evaporative conditions through measuring deuterium excess (Voelker et al. 2014) and may also act as a proxy for carbon metabolism (Cormier et al. 2019). In addition, it is always useful to add non-isotope components of the annual ring as a third or fourth proxy (see Churakova (Sidorova) et al. 2019). Ring width is related to growth rates and can help to interpret isotope variation that, for example, may be indicating drought or other growth limiting conditions. Though not commonly done, there is good reason to think that combining newer techniques of tree ring analysis (maximum latewood density, Chen et al. 2012 or Blue Intensity, Campbell et al. 2007) with isotopes could clarify climatic relationships (temperature and precipitation). This chapter will focus on the most common dual-isotope approach, the measurement of both  $\delta^{13}\text{C}$  and  $\delta^{18}\text{O}$  from the same sample. We first explain the relevant isotope fractionation processes in plants, then detail the principles of the conceptual model and later discuss the potential and caveats when this concept is applied to plant studies, with a particular focus on tree rings.

## 16.2 Carbon Isotope Fractionation

Briefly (see also Chap. 9), the  $\delta^{13}\text{C}$  variation in photosynthate that could be incorporated into tree rings is primarily the function of internal  $\text{CO}_2$  concentrations ( $c_i$ , Farquhar et al. 1989) for a given  $\delta^{13}\text{C}$  value of atmospheric  $\text{CO}_2$ . Since Rubisco discriminates against  $^{13}\text{C}$ , the amount incorporated into organic matter will be determined by its potential to use  $^{12}\text{C}$  preferentially. At high  $c_i$ , unfixed  $^{13}\text{CO}_2$  can diffuse back out the stomatal pores whereas at low  $c_i$  the enzyme will discriminate less and

capture relatively more  $^{13}\text{C}$  because it is substrate limited. As a consequence, conditions that promote relatively low  $c_i$  during the growing season (e.g. stomatal closure due to water stress) will result in relatively high  $\delta^{13}\text{C}$  in organic matter, and vice versa for high  $c_i$ .  $C_i$  is set by a supply (stomatal conductance) and demand (photosynthetic rate) process (Farquhar and Sharkey 1982; Farquhar et al. 1989; Ehleringer 1993) and thus numerous studies also demonstrate a relationship between  $\delta^{13}\text{C}$  and intrinsic water-use efficiency (the ratio of photosynthetic rate to stomatal conductance, see Chap. 17).

When making use of variations in stable isotopes to interpret and disentangle plant responses to a changing environment, we must keep in mind that numerous environmental factors impact  $\text{CO}_2$  and  $\text{H}_2\text{O}$  gas exchange, (the primary drivers for isotopic fractionation in leaves). In the real world, a whole assemblage of variables impact plant metabolism simultaneously. Therefore because  $\delta^{13}\text{C}$  variation of plant organic matter (also tree-ring cellulose) relates to supply and demand, it reflects a variety of aspect of tree functional biology. Any aspect of tree status that leads to modifications of photosynthetic rates (light interception associated with tree fall gaps, nitrogen fertilization, temperature changes etc., Flanagan et al. 1997; Roden and Farquhar 2012) would modify  $\delta^{13}\text{C}$  values through an altered  $\text{CO}_2$  demand. Factors that modify  $\text{CO}_2$  supply primarily through changes in stomatal conductance (water status, humidity etc., Saurer et al. 1995b; Leavitt et al. 2002), will also influence tree-ring  $\delta^{13}\text{C}$  values. Thus  $\delta^{13}\text{C}$  variation could be associated with either changes in stomatal conductance, net carbon assimilation or a combination of both. And herein lies the impetus for the approach developed by Scheidegger et al. (2000), see also Grams et al. (2007) where they add a second element ( $\delta^{18}\text{O}$ ) as a way to distinguish between stomatal vs assimilatory control over  $\delta^{13}\text{C}$  variation.

## 16.3 Oxygen Isotope Fractionation

It is useful to distinguish the isotope fractionation processes on two different levels: (1) processes which alter the isotope ratio before water is taken up by plants (source effects) and (2), changes which result from fractionation processes in the leaf during transpiration ( $E$ ) and incorporation into plant organic matter (plant effects).

### 16.3.1 Source Effects (see Chap. 18)

Source water  $\delta^{18}\text{O}$  depends on three main components, (1) the geographic origin of clouds that provide meteoric waters and associated  $\delta^{18}\text{O}$  values. Precipitation falling in warmer regions is more enriched in  $^{18}\text{O}$  than colder ones (Dansgaard 1953, 1964). Meteoric water  $\delta^{18}\text{O}$  is also impacted by continental effects causing precipitation to be more depleted in  $^{18}\text{O}$  toward interior regions associated with rain out events (Rozanski et al. 1993) and altitude with colder condensation temperatures

producing more depleted precipitation with increasing elevation (Bortolami et al. 1979). Another source of variation is (2) seasonality which can have annual cycles closely linked to temperature variation such that summer rainfall is more enriched in  $^{18}\text{O}$  than winter precipitation (Dansgaard 1964; Rozanski et al. 1993). As water infiltrates into soils further fractionation can occur particularly during periods of high evaporation demand. As such, (3) soil matrix water  $\delta^{18}\text{O}$  may vary with depth depending on soil structure, season and climate (Darling and Bath 1988; Allison et al. 1984). Since roots can absorb water from a large range of soil depths (Dawson et al. 2002) source water  $\delta^{18}\text{O}$  values (xylem water) can differ from meteoric water inputs, which provides the baseline water that is modified by leaf-level processes (Goldsmith et al. 2019; Allen et al. 2018a, b).

### 16.3.2 *Plant Effects*

Briefly (see also Chap. 10), the  $\delta^{18}\text{O}$  variation in organic matter that could be incorporated into wood cellulose is primarily impacted by source water  $\delta^{18}\text{O}$ , atmospheric vapor  $\delta^{18}\text{O}$  and evaporative conditions influencing fractionation processes in the leaf during transpiration (Roden et al. 2000; Barbour 2007; Cernusak et al. 2016; Lehmann et al. 2018). Further factors influence bulk leaf water such as progressive enrichment where leaf venation patterns lead to previously enriched water re-entering the xylem and moving to more distal regions and becoming further enriched in  $^{18}\text{O}$  (Helliker and Ehleringer 2002) and compartmentation where pools of water are isolated from evaporation leading to a leaf being less enriched than expected based on models (Roden et al. 2015). Péclet effects, where the back diffusion of water from the sites of evaporative enrichment in the leaves as opposed by the flow of less-enriched water from the xylem, also impact bulk leaf water enrichment (Farquhar and Lloyd 1993). The  $\delta^{18}\text{O}$  signals from leaf water are incorporated into carbohydrates and are then modified by proportional exchange during phloem transport as well as at the site of organic matter synthesis (Barbour et al. 2004; Barbour 2007; Sternberg 2009; Gessler et al. 2014).

### 16.3.3 *Combined Effect on Tree Rings*

As a result of these processes, oxygen isotope variation in tree rings can be used to probe a number of environmental impacts on tree physiology. Due to the primary influence of source water  $\delta^{18}\text{O}$  associated with variation in meteoric waters, which in turn can be a function of condensation temperature, tree-ring  $\delta^{18}\text{O}$  time series may be a proxy for temperature variation (Gray and Thompson 1976). While this may appear straight forward, there are a variety of potential fractionation events that can modify that signal (e.g. soil evaporation) even to the extent of ecohydrologic separation leading to soil water available to trees in antiphase to seasonal temperatures

(Brooks et al. 2010; Allen et al. 2019). Many studies have demonstrated that  $\delta^{18}\text{O}$  variation in organic matter track leaf evaporative conditions, especially vapor pressure deficit (VPD, but also relative humidity, Edwards et al. 1985; Lipp et al. 1996; Kahmen et al. 2011). The connection between tree ring  $\delta^{18}\text{O}$  values and stomatal conductance relates to evaporative enrichment through non-steady state conditions (but see Chap. 10). The Craig–Gordon model (Craig and Gordon 1965; Dongmann et al. 1974) was developed for bodies of water and mostly over-predicts evaporative enrichment in leaves. This model assumes a known fractionation for a given VPD and temperature, and when used with leaves, is insensitive to stomatal conductance. However, diurnal variation in leaf water  $\delta^{18}\text{O}$  can be quite dramatic and sensitive to stomatal opening (Cernusak et al. 2002, 2005). Despite the numerous processes impacting the isotopic ratio from source via leaf water to organic matter, controlled experiments have confirmed that tree ring  $\delta^{18}\text{O}$  does indeed record evaporative conditions (Roden and Ehleringer 1999; Grams et al. 2007; Roden and Farquhar 2012) and thus should capture stomatal conductance variation, which is mostly accounted for via the Péclet effect.

Physiologically, photosynthetic rates do not directly influence  $\delta^{18}\text{O}$ , in contrast to transpiration and stomatal conductance and its associated impact on evaporative enrichment. This is the link that Scheidegger et al. (2000) aimed to exploit with their dual-isotope model in that  $\delta^{18}\text{O}$  helps constrain interpretations of  $\delta^{13}\text{C}$  variation in leaves by using  $\delta^{18}\text{O}$  as an indicator of changes in stomatal conductance. While this appears reasonable and promising, we must keep in mind the many additional factors that influence leaf evaporative enrichment described above and others that modify that signal as sucrose is transported to sites of cellulose synthesis in the stem (Gessler et al. 2009; Offermann et al. 2011, see also Chap. 13). These factors contribute to signal complexity and make the use of  $\delta^{18}\text{O}$  variation as a proxy for stomatal conductance in tree rings more challenging, which requires a careful evaluation of the data and its interpretation, as outlined henceforth.

## 16.4 Dual-Isotope Conceptual Model

The seminal paper to propose the dual-isotope approach was Scheidegger et al. (2000). They proposed measuring both  $\delta^{13}\text{C}$  and  $\delta^{18}\text{O}$  on the same sample in order to constrain the interpretation of  $\delta^{13}\text{C}$  variation as primarily a function of carbon assimilation ( $A$ ) or stomatal conductance ( $g_s$ ) or a combination of both. To achieve this goal, Scheidegger et al. (2000) developed a theoretical framework for interpreting all possible changes in both isotopes. The concepts for this approach are strictly based on well-accepted carbon (Farquhar et al. 1982, 1989) and oxygen isotope fractionation models (Dongmann et al. 1974; Farquhar and Lloyd 1993; Cernusak et al. 2016) and  $\text{CO}_2$  and  $\text{H}_2\text{O}$  gas exchange principles (Gaastra 1959; von Caemmerer and Farquhar 1981). If any of these principles are violated, the dual-isotope approach would yield non-plausible results. Carbon isotope ratios ( $\delta^{13}\text{C}$ ) or inverse discrimination ( $-\Delta^{13}\text{C}$ , Grams et al. 2007) is plotted on the Y axis and  $\delta^{18}\text{O}$  or  $\Delta^{18}\text{O}$

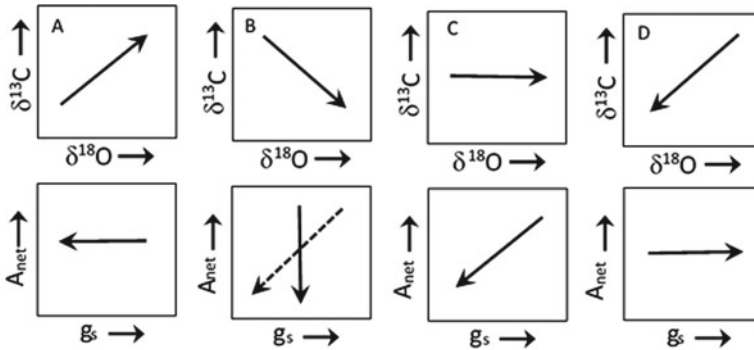


**Fig. 16.1** A subset of potential scenarios on how the dual-isotope conceptual model is used to interpret  $\delta^{13}\text{C}$  variation. Adapted from Scheidegger et al. (2000). The alternate interpretation for scenario B (dashed line) is given by Grams et al. (2007)

on the X with an arrow indicating the change in both isotopes between organisms of different species or treatments or sites, etc. being compared (Fig. 16.1). These plots must not be interpreted as plots of dependent and independent variables as one isotope's variation is not a causal factor for the other. These plots only represent how both isotopes vary in tandem. The slope and direction of the arrow is then used to imply the impact on net photosynthesis ( $A_{\text{net}}$ ) or  $g_s$  and consequently on  $\delta^{13}\text{C}$  variation between comparator organisms (Fig. 16.1).

The basic assumption is that changes in  $\delta^{13}\text{C}$  result from changes in  $A_{\text{net}}$  (the demand) or  $g_s$  (supply function) or both, which are driven by temperature, VPD, light,  $\text{CO}_2$  etc., while  $\delta^{18}\text{O}$  varies independently of carbon isotope fractionation during photosynthesis. Based on Farquhar and Lloyd (1993) and Barbour et al. (2000, 2004),  $\delta^{18}\text{O}$  and  $g_s$  are negatively correlated. Therefore any variable (VPD, soil water content, light,  $\text{CO}_2$  etc.) that reduces  $g_s$  will result in an increase of  $\delta^{18}\text{O}$  or vice versa. With this additional value, we can determine whether a change in  $\delta^{13}\text{C}$  was predominantly influenced by  $A_{\text{net}}$  or  $g_s$ . For example, in scenario A of Fig. 16.1, an increase in both  $\delta^{18}\text{O}$  and  $\delta^{13}\text{C}$  would imply both a reduction in  $g_s$ , (inverse relationship with  $\delta^{18}\text{O}$ ) and  $c_i/c_a$  (leading to reduced discrimination of  $^{13}\text{C}$  by Rubisco), implying that photosynthetic rates remained unchanged. If  $A_{\text{net}}$  also declined with  $g_s$  then  $c_i/c_a$  might remain unchanged and  $\delta^{13}\text{C}$  values should be similar between conditions (scenario C in Fig. 16.1).

Another premise is that these changes are sufficiently large since uncertainty increases with decreasing signal strength. The dual-isotope methodology can be used to study treatment and species differences or changes in the environment over time, provided that the assumptions of similar  $\delta^{18}\text{O}$  of source water and water vapor hold. Some studies try to account for source water  $\delta^{18}\text{O}$  variation between treatments or species etc. by plotting  $\Delta^{18}\text{O}$  (enrichment above source water). In situations with high relative humidity, the  $\delta^{18}\text{O}$  of vapor can contribute to the uncertainty in leaf  $\delta^{18}\text{O}$  because of the bidirectional diffusion of the  $\text{H}_2\text{O}$  molecules (Lehmann et al. 2018, see also Fiorella et al. 2019 for related processes from an atmospheric perspective).

In cases where the  $\delta^{18}\text{O}$  of source water or water vapor cannot be measured, they may be estimated from models though interpretations must be tempered as uncertainties compound when models are nested within models.

## 16.5 Testing the Model

Scheidegger et al. (2000) tested this conceptual model using leaf organic matter from three herbaceous species growing in fields with differences in land management (mowed and fertilized fields or those abandoned from agricultural manipulations for an extended period). The experiment produced two distinct microclimatic scenarios impacting plant physiology, which was reflected in C and O isotope ratios. The predictions from the conceptual model for  $A_{\text{net}}$  and  $g_s$  agreed qualitatively with gas exchange measurements from the same plots. Yet in their paper, Scheidegger et al. (2000) indicated that controlled experiments would be the next step to clarify the viability of the model for other systems and scenarios and to what extent it could be used to interpret C and O isotope variations in terms of physiology with confidence. Since then, more than 330 studies (controlled and field) have applied the dual-isotope approach (see Siegwolf et al. 2022).

Grams et al. (2007) tested this approach on trees, using leaf cellulose from beech and spruce trees from field sites or grown in controlled environments and exposed to treatments that influenced  $A_{\text{MAX}}$  and  $g_s$  (ozone, elevated  $\text{CO}_2$  and light). They too validated model output with gas exchange data and went a step further by comparing simulated C and O isotope values with measured data. They found that leaf cellulose  $\delta^{18}\text{O}$  can be related to stomatal conductance and by using C and O simulations they could improve the correlation between  $g_s$  and  $\delta^{18}\text{O}$  via additional adjustments of fractionation model parameters such as kinetic fractionation, leaf temperature (and  $e_a/e_i$ ) associated with transpirational cooling, and the Péclet correction (associated with transpiration rate,  $E$  and effective pathlength,  $L$ , a scaling factor assumed to be associated with leaf anatomy and hydraulic resistance). They concluded that the dual-isotope approach can help delineate the effects of their treatments on stomatal conductance and carbon assimilation.

## 16.6 Testing the Model Using Tree Rings

The expansion of the dual-isotope approach from leaf cellulose to tree-ring cellulose is a critical issue for those who wish to interpret historical changes in tree physiology (the topic of this volume). While it may seem likely that all organic matter should follow the same general rules for isotope fractionation, tree rings have a number of unique attributes due to their temporal and physical separation from the sites of photosynthetic carbon assimilation (see Chaps. 13 and 15 in this compilation). And

so, the application of the Scheidegger et al. (2000) model to  $\delta^{13}\text{C}$  and  $\delta^{18}\text{O}$  variation using tree-ring cellulose time series requires further validation.

Roden and Farquhar (2012), tested the dual-isotope approach for wood cellulose in a control experiment (growth chambers) on pine and eucalypt seedlings grown under a variety of conditions designed to alter stomatal conductance (VPD, drought, and temperature) and/or photosynthetic rates (light levels and nitrogen nutrition). While humidity treatments (46 versus 65%) produced significant effects on leaf transpiration, leaf water evaporative enrichment in  $^{18}\text{O}$ , and wood cellulose  $\delta^{18}\text{O}$  (from 2 to 3‰), they produced only minor changes in  $g_s$  (Roden and Farquhar 2012). Non-significant differences in stomatal behavior was partly due to highly variable measurements of  $g_s$  and as well as humidity treatments that may not have limited plant function and water status. Within a humidity treatment, the dual-isotope approach accurately predicted A: $g_s$  relationships for some of the other treatments (Fig. 16.2, only the low humidity treatment is shown for clarity as both humidity treatments showed similar patterns, see Roden and Farquhar 2012 and stomata should be most responsive at high VPD, see below). Both the low light and low nitrogen treatments produced reductions in photosynthetic carbon assimilation with little change in stomatal conductance, while both the elevated temperature and drought treatments produced reductions in both A and  $g_s$  (Fig. 16.2). For both species, the dual-isotope approach accurately predicted the response to increased temperature but not the response to reduced nitrogen nutrition (Fig. 16.2a). The dual-isotope approach accurately predicted the response to low light and drought for the eucalypt but not for the pine (Fig. 16.2b). It should be noted that this was a seedling study and impacts related to long-distance transport of assimilates through the bole were not captured. Another difficulty in this technique is choosing which interpretation should be used if the dual-isotope plot produces an arrow between two options (e.g. part way between angled and vertical). This study provides a cautionary note that dual-isotope interpretations of C and O isotope variation in tree-ring cellulose may not be able to clearly delineate all hypothetical variations in the A: $g_s$  relationship as often assumed. The results of this study demonstrated that the dual-isotope model works better for some environmental effects and for some species than for others.

## 16.7 Utilization of the Dual-Isotope Conceptual Model

A number of studies have utilized the dual-isotope approach to probe a variety of questions. Sullivan and Welker (2007) found the approach useful to qualitatively differentiate the contributions of  $g_s$  and A on site differences in  $^{13}\text{C}$  discrimination for willows in Greenland. Keitel et al. (2006) applied the conceptual model to phloem sap and leaf organic matter for European beech along a continental scale transect and argue that organic matter  $\Delta^{18}\text{O}$  reflects canopy level conductance (estimated not measured). Since neither study utilized a common garden experimental design, some assumptions of the dual-isotope model may have been violated, but they claim that with environmental quantification and reasonable assumptions their analysis could



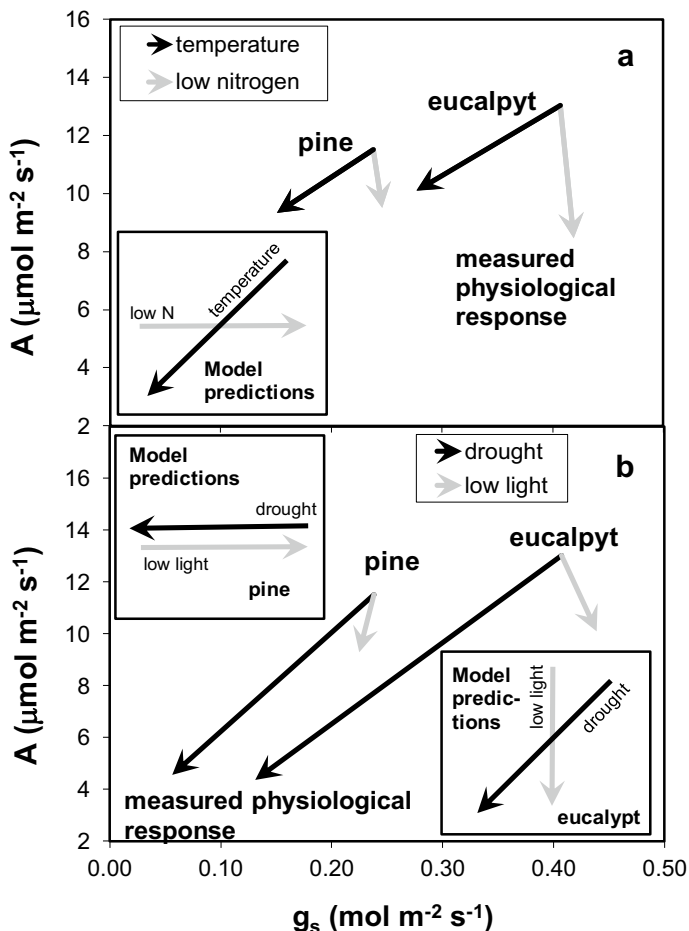


**Fig. 16.2** Measured physiological response (see Roden and Farquhar 2012 for details) of *Eucalyptus globulus* and *Pinus radiata* grown in chambers controlled for temperature (21 °C), humidity (46%), light level ( $1000 \text{ mol photons m}^{-2} \text{ s}^{-1}$ ), source water  $\delta^{18}\text{O}$  ( $-6\text{‰}$ ) and atmospheric vapor  $\delta^{18}\text{O}$  ( $-17\text{‰}$ ). Compared to standard (**control**) conditions, separate treatments were increased **temperature** ( $+3 \text{ °C}$ ), reduced nitrogen nutrition ( $1/2$  the N inputs, **low N**), reduced moisture inputs (**drought**) and reduced light inputs (50% of ambient, **low light**). All arrows extend from the mean physiological measurements of control plants to the mean for plants exposed to each indicated treatment (separated into 2 panels, **a** and **b** to reduce clutter). Inset plots are predicted responses derived from dual-isotope plots (data not shown, but see Roden and Farquhar 2012) for each treatment

produce valid conclusions. Moreno-Gutiérrez et al. (2011) applied the dual-isotope approach to needle organic matter from a pine plantation and assert that the model provided insights into tree physiological changes after forest thinning treatments. For a grassland ecosystem, Flanagan and Farquhar (2014) interpreted their variation in

dual-isotope space as indicating stomatal control as the principle effect on photosynthetic rates and  $^{13}\text{C}$  discrimination during periods of water stress. Prieto et al. (2018) measured leaf  $\delta^{13}\text{C}$ ,  $\delta^{18}\text{O}$ , and morphological traits on 15 herbaceous species in a rangeland common garden to investigate diversity in leaf functional traits including water use efficiency and nutrient economies. They conclude that the dual-isotope approach can be used to probe water use strategies among species and broad-scale studies on ecological adaptations. While more examples could be included, these diverse studies show that the dual-isotope model has gained traction in the plant physiological community as a way to constrain the interpretation of  $\delta^{13}\text{C}$  variation, stomatal conductance and water use strategies in leaf organic matter.

While the dual-isotope model was developed for leaf tissues, numerous studies expanded its use to tree-ring cellulose exploring how environmental changes affect physiological properties over time. Sidorova et al. (2009) noted a change in correlation between C and O isotopes in Siberian larch over time and used the dual-isotope model to infer changes in stomatal conductance and carbon assimilation associated with water stress. Brooks and Mitchell (2011) used  $\delta^{13}\text{C}$  and  $\delta^{18}\text{O}$  variation in Douglas-fir tree-ring cellulose to probe intrinsic water-use efficiency and changes in stomatal conductance from before and after fertilization and thinning treatments. Similarly, Barnard et al. (2012) utilized the dual-isotope approach to infer physiological changes in Douglas-fir trees differing in canopy position. Voltas et al. (2013) studied winter dieback, and hydraulic limitations for Scots pine trees in marginal habitats. In their system, oxygen isotope variation indicated greater stomatal control of water loss in declining trees. Giuggiola et al. (2016) combined the dual-isotope approach with a canopy-level mechanistic model (MuSICA, Ogée et al. 2003) to clarify the effects on stomatal conductance and carbon assimilation on thinning induced growth enhancement in a xeric Scots pine plantation. While the studies highlighted above have provided valuable insights, as the complexity of the system tested increases, the application of the dual-isotope model may become problematic as the number of untested assumptions and unmeasured variables expand (similar source water and atmospheric vapor  $\delta^{18}\text{O}$  inputs, common humidity between treatments in complex canopies, etc.).

## 16.8 Points of Caution

Before tree physiologists and dendro-climatologists consider using the dual-isotope approach in tree rings to interpret historic variation in  $\delta^{13}\text{C}$ , they need to pay special attention to model assumptions and constraints. The most obvious pitfall of this approach is accurate determination of source water and water vapor  $\delta^{18}\text{O}$  values as both can mimic stomatal impacts. The greater the fractionation events that could be attributed to factors other than stomatal conductance, the less useful the model output becomes for constraining the interpretation of carbon isotope variation (see also Chap. 18). In addition, we must consider for the interpretation of tree-ring isotope values that  $\text{CO}_2$  assimilation and growth are different processes, which are

not as tightly linked as usually assumed (Körner 2018). Tree growth can be fueled from carbohydrate reserves as well as directly from fresh leaf assimilates depending on phenological stage and dampening isotope signals. Furthermore, there can be considerable time gaps between the synthesis of carbohydrates and its use for cellulose production in the stem (Gessler et al. 2009, 2014; Offermann et al. 2011). This can be problematic, as the isotopic signal in tree rings is not synchronized with the time of the climatic event. An extreme case of this phenomenon is the complete isotopic decoupling between leaf organic matter production and cambial activity in the stem. Sarris et al. (2013) and Pflug et al. (2015) described this for trees exposed to severe and chronic drought. A similar effect has been observed at low temperatures (5–7 °C) where growth is severely limited, potentially making summer conditions a disproportionately greater influence on whole tree ring isotope signals (Körner 2018, See also Chap. 14). Using specific portions of the tree ring (earlywood, latewood etc.) may be important to connect isotope variation to relevant periods of interest. Studies with air pollutants and isotopes show that some principles for carbon isotope fractionation in  $C_3$  plants were violated (Chap. 24). This was observed for ozone, which caused an increase in  $\delta^{13}C$  due to enhanced PEP carboxylase activity, although  $c_i/c_a$  was elevated in damaged leaves (Saurer et al. 1995a). A similar effect was observed with  $SO_2$ . In such situations the C and O isotope model will yield physiologically non-plausible results.

Roden and Siegwolf (2012) highlighted ten areas of caution for this conceptual model and encouraged research that could reduce model uncertainties. Some issues they discuss have been mentioned above (e.g. common environmental inputs and evaluation of the humidity/ $g_s$  relationship for a species), but they also highlight areas of caution specific to tree-ring studies. For example, tree-ring cellulose has a dampened signal as compared to leaf cellulose due to isotope exchange with medium water in the vascular cambium (unenriched compared to leaf water, Roden et al. 2000, Barbour et al. 2004, but see also Treydte et al. 2014, for complications with relative contributions) and dilution of signal when utilizing stored carbohydrate reserves (Roden and Siegwolf 2012). They also indicate that site ambient humidity may determine if tree ring  $\delta^{18}O$  variation can detect changes in  $g_s$ . At high humidity, mechanistic models that describe  $^{18}O$  fraction in cellulose (Roden et al. 2000; Barbour et al. 2004) predict that  $\delta^{18}O$  variation in organic matter will be insensitive to variation in stomatal conductance. In addition, while the dual-isotope model predicts that changes in  $g_s$  will modify organic matter  $\delta^{18}O$  via differences in kinetic fractionation and transpiration (through the Péclet effect, Farquhar and Lloyd 1993), they rarely consider the influence of  $g_s$  on bidirectional flow of isotopically distinct water vapor (Roden and Siegwolf 2012; Lehmann et al. 2018). Most studies assume  $\delta^{18}O$  of water vapor in the atmosphere is in equilibrium with tree source water, which may rarely be the case (White and Gedzelman 1984; Fiorella et al. 2019). In addition, atmospheric turbulences as they occur throughout the day in most forests disturb steady state conditions and this can impair this assumption as well.

Many researchers (Keitel et al. 2006; Sidorova et al. 2009; Moreno-Gutiérrez et al. 2011; Barnard et al. 2012; Flanagan and Farquhar 2014; Prieto et al. 2018) utilize regression analysis of  $\delta^{18}O$  and  $\delta^{13}C$  data sets to provide some statistical

confidence regarding trends in highly variable data sets and time series rather than directional arrows (as in Fig. 16.1). However, Roden and Siegwolf (2012) argue that regression analysis cannot be used exclusively because non-significant relationships (vertical or horizontal slopes) have meaningful interpretations in the Scheidegger et al. (2000) and Grams et al. (2007) conceptual models. They also argue against the use of  $A_{MAX}$  to interpret changes in assimilation because it is not the photosynthetic capacity (which can be defined in a variety of ways) that sets the demand side of the  $A:g_s$  relationship that sets chloroplast  $CO_2$  concentrations which influences  $^{13}C$  discrimination, but rather integrated or average assimilation ( $A_{net}$ ). There are numerous environmental factors that affect integrated assimilation without altering photosynthetic capacity such as light, water status,  $CO_2$ , and temperature variation.

## 16.9 Alternative Dual-Isotope Approaches

Utilizing information from both C and O isotopes in organic matter can be approached in a number of ways other than that proposed by Scheidegger et al. (2000), making it possible to derive information beyond the influence of  $A$  and  $g_s$  on  $\delta^{13}C$  variation. Recently, another take on the dual-isotope approach was made by Goud et al. (2019) where they introduced a way to quantify the relationship between  $\delta^{13}C$  and  $\Delta^{18}O$  in leaf cellulose they termed integrated metabolic strategy (IMS). Instead of visualizing  $\delta^{13}C$  and  $\delta^{18}O$  together in isotope space (as in Fig. 16.1), they calculate a ratio between the two isotopes that reflect leaf-level metabolic efficiency. Their equation scales both isotopes such that an increasing IMS implies more carbon gain per unit water loss (water-use efficiency) rather than using  $\delta^{13}C$  alone to infer  $c_i/c_a$  and  $iWUE$ . They tested the concept of IMS on 20 milkweed (*Asclepias*) species with different leaf attributes associated with ecological and evolutionary diversity and found that IMS has the potential to provide valuable insights on phylogenetic relationships and phenotypic plasticity regarding tradeoffs between  $CO_2$  uptake and water loss (Goud et al. 2019). In another example, Saurer et al. (1997) utilized combined  $\delta^{13}C$  and  $\delta^{18}O$  information to derive the sensitivity of  $c_i/c_a$  of different tree species to changing humidity. Approaches that combine mechanistic models, like MuSICA (Guiggiola et al. 2016) can improve model predictive power and physiological interpretations. Even if  $\delta^{18}O$  cannot be directly related to changes in stomatal conductance, but say, rooting depths, plots of  $\delta^{18}O$  versus  $\delta^{13}C$  could be useful to see if different species having different source water access have different  $\delta^{13}C$  and thus  $iWUE$ .

### 16.9.1 Conclusions

The theoretical framework of the dual-isotope model introduced by Scheidegger et al. (2000) is valid and can be used to probe the degree of carbon isotope variation in plant organic matter that is determined by the supply side (stomatal conductance)

drivers of internal CO<sub>2</sub> concentrations ( $c_i/c_a$ ). As the model is rather simple at first sight it is tempting to apply it like a “plug and play tool”. However, applying the dual-isotope approach, particularly for stable isotope variation in tree-ring cellulose, and linking it with the principles of gas exchange, requires special attention to keep the physiological mechanistic context in mind and to ensure that the assumptions of the conceptual model are not violated. Nevertheless, considering the myriad of plant responses to the environment in a multi-species ecosystem context, it is very useful to have a tool available that helps guiding the physiological interpretation. Despite issues of applicability, measuring more than one stable isotope on a single sample will generally provide added information and allow for better characterization of environmental variation and physiological attributes.

## References

- Allen S, Kirchner J, Goldsmith G (2018) Predicting spatial patterns in precipitation isotope ( $\delta^2\text{H}$  and  $\delta^{18}\text{O}$ ) seasonality using sinusoidal isoscapes. *Geophys Res Lett* 45:4859–4868
- Allen S, Kirchner J, Braun S, Siegwolf RTW, Goldsmith G (2019) Seasonal origins of soil water used by trees. *Hydrol Earth Syst Sci* 23:1199–1210. <https://doi.org/10.5194/hess-23-1199-2019>
- Allison G, Barnes CJ, Hughes MW, Leaney FWJ (1984) The effect of climate and vegetation on the oxygen-18 and deuterium profiles in soils. In: *Isotope hydrology, IAEA Symposium 270*, Sept 1982, Vienna, pp 105–123
- Barbour MM (2007) Stable oxygen isotope composition of plant tissue: a review. *Funct Plant Biol* 34:83–94. <https://doi.org/10.1071/FP06228>
- Barbour MM, Schurr U, Henry BK, Wong SC, Farquhar GD (2000) Variation in oxygen isotope ratio of phloem sap sucrose from castor bean. Evidence in support of the Péclet effect. *Plant Physiol* 123:671–679
- Barbour MM, Roden JS, Farquhar GD, Ehleringer JR (2004) Expressing leaf water and cellulose oxygen isotope ratios as enrichment above source water reveals evidence of a Péclet effect. *Oecologia* 138:426–435
- Barnard HR, Brooks JR, Bond BA (2012) Applying the dual-isotope conceptual model to interpret physiological trends under uncontrolled conditions. *Tree Physiol* 32:1183–1198. <https://doi.org/10.1093/treephys/tps078>
- Bortolami GC, Ricci B, Susella GF, Zuppi GM (1979) Isotope hydrology of the Val Corsaglia, Maritime Alps Piedmont Italy. In: *Isotope hydrology, vol. 1, IAEA symposium 228*, Neuherberg, Germany, pp 327–350
- Brooks JR, Mitchell AK (2011) Interpreting tree responses to thinning and fertilization using tree-ring stable isotopes. *New Phytol* 190:770–782
- Brooks JR, Barnard HR, Coulombe R, McDonnell JJ (2010) Ecohydrolic separation of water between trees and streams in a Mediterranean climate. *Nat Geosci* 3:100–104. <https://doi.org/10.1038/ngeo722>
- Campbell R, McCarroll D, Loader N, Grudd H, Robertson I, Jalkanen R (2007) Blue intensity in *Pinus sylvestris* tree-rings: developing a new palaeoclimate proxy. *Holocene* 17(6):821–828
- Cernusak LA, Pate JS, Farquhar GD (2002) Diurnal variation in the stable isotope composition of water and dry matter in fruiting *Lupinus angustifolius* under field conditions. *Plant Cell Environ* 25:893–907
- Cernusak LA, Farquhar GD, Pate JS (2005) Environmental and physiological controls over oxygen and carbon isotope composition of Tasmanian blue gum, *Eucalyptus globulus*. *Tree Physiol* 25:129–146

- Cernusak L, Aranda J, Marshall J, Winter K (2007) Large variation in whole-plant water-use efficiency among tropical tree species. *New Phytol* 173(2):294–305
- Cernusak et al., 2016. Cernusak L, Barbour M, Arndt S, Cheesman A, English N, Feild T, Farquhar G (2016) Stable isotopes in leaf water of terrestrial plants. *Plant Cell Environ* 39:1087–1102
- Chen F, Yuan Y, Wei W, Fan Z, Zhang T, Shang H, Zhang R, Yu S, Ji C, Qin L (2012) Climatic response of ring width and maximum latewood density of *Larix sibirica* in the Altay Mountains, reveals recent warming trends. *Ann For Sci* 69(6):723–733
- Churakova et al., 2019. Churakova (Sidorova) OV, Fonti MV, Saurer M, Guillet S, Corona C, Fonti P, Myglan VS, Kirilyanov AV, Naumova OV, Ovchinnikov DV, Shashkin AV, Panyushkina IP, Büntgen U, Hughes MK, Vaganov EA, Siegwolf RW, Stoffel M (2019) Siberian tree-ring and stable isotope proxies as indicators of temperature and moisture changes after major stratospheric volcanic eruptions. *Clim Past* 15:685–700. <https://doi.org/10.5194/cp-15-685-2019>
- Cormier M, Werner R, Leuenberger A, Kahmen M (2019) 2H-enrichment of cellulose and n-alkanes in heterotrophic plants. *Oecologia* 189:365–373
- Craig H (1954) Carbon-13 variation in Sequoia rings and the atmosphere. *Science* 119:141–143
- Craig H, Gordon LI (1965) Deuterium and oxygen-18 variations in the ocean and marine atmosphere. In: Tongiorgi E (ed) *Proceedings of a conference on stable isotopes in oceanographic studies and paleotemperatures*, Spoleto Italy. Lischi and Figli, Pisa Italy, pp 9–130
- Dansgaard W (1953) The abundance of  $^{18}\text{O}$  in atmospheric water and water vapor. *Tellus* 5:461–469
- Dansgaard W (1964) Stable isotopes in precipitation. *Tellus* 16:436–468
- Darling WG, Bath AH (1988) A stable isotope study of recharge processes in the English chalk. *J Hydrol* 101:31–46
- Dawson TE, Mambelli S, Plamboeck AH, Templer PH, Tu KP (2002) Stable isotopes in plant ecology. *Ann Rev Ecol Syst* 33:507–559
- Dongmann G, Nurnberg HW, Forstel H, Wagener K (1974) On the enrichment of  $\text{H}_2^{18}\text{O}$  in the leaves of transpiring plants. *Radiat Environ Biophys* 11:41–52
- Edwards TWD, Aravena RO, Fritz P, Morgan AV (1985) Interpreting paleoclimate from  $^{18}\text{O}$  and  $^2\text{H}$  in plant cellulose: comparison with evidence from fossil insects and relict permafrost in southwestern Ontario. *Can J Earth Sci* 22:1720–1726
- Ehleringer JR (1993) Carbon and water relations in desert plants: an isotopic perspective. In: Ehleringer JR, Hall AE, Farquhar GD (eds) *Stable isotopes and plant carbon–water relations*. Academic Press, Inc., San Diego, pp 155–172
- Etien N, Daux V, Masson-Delmotte V, Mestre O, Stievenard M, Guillemin M, Boettger T, Breda N, Haupt M, Perraud P (2009) Summer maximum temperature in northern France over the past century: instrumental data versus multiple proxies (tree-ring isotopes, grape harvest dates and forest fires). *Clim Chang* 94(3–4):429–456
- Farquhar GD, Lloyd J (1993) Carbon and oxygen isotope effects in the exchange of carbon dioxide between terrestrial plants and the atmosphere. In: Ehleringer JR, Hall AE, Farquhar GD (eds) *Stable isotopes and plant carbon–water relations*. Academic Press, Cambridge, pp 47–70
- Farquhar GD, Sharkey T (1982) Stomatal conductance and photosynthesis. *Annu Rev Plant Physiol* 33:317–345
- Farquhar GD, O’Leary MH, Berry JA (1982) On the relationship between carbon isotope discrimination and the intercellular carbon dioxide concentration in leaves. *Aust J Plant Physiol* 9:121–137
- Farquhar GD, Ehleringer JR, Hubick KT (1989) Carbon isotope discrimination and photosynthesis. *Ann Rev Plant Physiol Plant Mol Biol* 40:503–537
- Fiorella RP, West JB, Bowen GJ (2019) Biased estimates of the isotope ratios of steady-state evaporation from the assumptions of equilibrium between vapour and precipitation. *Hydrol Process* 33:2576–2590. <https://doi.org/10.1002/hyp.13531>
- Flanagan LB, Brooks JR, Ehleringer JR (1997) Photosynthesis and carbon isotope discrimination in boreal forest ecosystems: a comparison of functional characteristics in plants from three mature forest types. *J Geophys Res D* 102:28861–28869

- Flanagan L, Farquhar G (2014) Variation in the carbon and oxygen isotope composition of plant biomass and its relationship to water-use efficiency at the leaf- and ecosystem-scales in a northern Great Plains grassland. *Plant Cell Environ* 37(2):425–438
- Gaastera P (1959) Photosynthesis of crop plants as influenced by light, carbon dioxide, temperature and stomatal diffusion resistance. *Mededelingen van de Landbouwhogeschool te Wageningen Nederland* 59:1–68
- Gessler A, Brandes E, Buchmann N, Helle G, Rennenberg H, Barnard RL (2009) Tracing carbon and oxygen signals from newly assimilated sugars in the leaves to the tree-ring archive. *Plant Cell Environ* 32:780–795
- Gessler A, Ferrio JP, Hommel R, Treydte K, Werner RA, Monson RK (2014) Stable isotopes in tree rings: towards a mechanistic understanding of isotope fractionation and mixing processes from the leaves to the wood. *Tree Physiol* 34:796–818
- Giuggiola A, Ogée J, Rigling A, Gessler A, Bugmann H, Treydte K (2016) Improvement of water and light availability after thinning at a xeric site: which matters more? A dual isotope approach. *New Phytol* 210:108–121
- Goldsmith G, Allen S, Braun S, Engbersen N, González-Quijano C, Kirchner J, Siegwolf R (2019) Spatial variation in throughfall, soil, and plant water isotopes in a temperate forest. *Ecohydrology* 12:e2059. <https://doi.org/10.1002/eco.2059>
- Goud EJP, Sparks MF, Agrawal AA (2019) Integrated metabolic strategy: a mechanistic framework for predicting the evolution of carbon gain and water loss tradeoffs within plant clades. *J Ecol* 107:1633–1644. <https://doi.org/10.1111/1365-2745.13204>
- Grams TEE, Kozovits AR, Häberle K-H, Matyssek R, Dawson TE (2007) Combining  $\delta^{13}\text{C}$  and  $\delta^{18}\text{O}$  analyses to unravel competition,  $\text{CO}_2$  and  $\text{O}_3$  effects on the physiological performance of different-aged trees. *Plant Cell Environ* 30:1023–1034
- Gray J, Thompson P (1976) Climatic information from  $^{18}\text{O}/^{16}\text{O}$  ratios of cellulose in tree rings. *Nature* 262:481–482
- Helliker BR, Ehleringer JR (2002) Grass blades as tree rings: environmentally induced changes in oxygen isotope ratios of cellulose along the length of grass blades. *New Phytol* 155:417–424
- Kahmen A, Sachse D, Arndt SK, Tu KP, Farrington H, Vitousek PM, Dawson TE (2011) Cellulose  $\delta^{18}\text{O}$  is an index of leaf-to-air vapor pressure difference (VPD) in tropical plants. *Proc Natl Acad Sci* 108:1981–1986
- Keitel C, Matzarakis A, Rennenberg H, Gessler A (2006) Carbon isotopic composition and oxygen isotopic enrichment in phloem and total leaf organic matter of European beech (*Fagus sylvatica* L.) along a climate gradient. *Plant Cell Environ* 29:1492–1507
- Körner C (2018) Concepts in empirical plant ecology. *Grubb Review. J Plant Ecol Div* 11(4):405–428. <https://doi.org/10.1080/17550874.2018.1540021>
- Leavitt SW, Wright WE, Long A (2002) Spatial expression of ENSO, drought, and summer monsoon in seasonal  $\delta^{13}\text{C}$  of ponderosa pine tree rings in southern Arizona and New Mexico. *J Geophys Res* 107:4349. <https://doi.org/10.1029/2001JD001312>
- Lehmann MM, Goldsmith GR, Schmid L, Gessler A, Saurer M, Siegwolf RTW (2018) The effect of  $^{18}\text{O}$ -labelled water vapour on the oxygen isotope ratio of water and assimilates in plants at high humidity. *New Phytol* 217:105–116. <https://doi.org/10.1111/nph.14788>
- Lipp J, Trimbom P, Edwards T, Waisel Y, Yakir D (1996) Climatic effects on the  $\delta^{18}\text{O}$  and  $\delta^{13}\text{C}$  of cellulose in the desert tree *Tamarix jordanis*. *Geochim Cosmochim Acta* 60:3305–3309
- Loader N, Street-Perrott F, Mauquoy D, Roland T, Daley T, Davies D, Hughes PDM, Pancotto VO, Young GHF, Amesbury MJ, Charman D, Mallon G, Yu Z (2016) Measurements of hydrogen, oxygen and carbon isotope variability in Sphagnum moss along a micro-topographical gradient in a southern Patagonian peatland. *J Quat Sci* 31:426–435
- Moreno-Gutiérrez C, Barberá GG, Nicolás E, Luis MD, Castillo VM, Martínez-Fernández F, Querejeta JI (2011) Leaf  $\delta^{18}\text{O}$  of remaining tree is affected by thinning intensity in a semiarid pine forest. *Plant Cell Environ* 34:1009–1019

- Offermann C, Ferrio JP, Holst J, Grote R, Siegwolf R, Kayler Z, Gessler A (2011) The long way down—are carbon and oxygen isotope signals in the tree ring uncoupled from canopy physiological processes? *Tree Physiol* 31:1088–1102
- Ogé J, Brunet Y, Loustau D, Berbigier P, Delzon S (2003) MuSICA, a CO<sub>2</sub>, water and energy multilayer, multileaf pine forest model: evaluation from hourly to yearly time scales and sensitivity analysis. *Glob Chang Biol* 9:697–717
- Ohkouchi N, Ogawa N, Chikaraishi O, Tanaka Y, Wada H (2015) Biochemical and physiological bases for the use of carbon and nitrogen isotopes in environmental and ecological studies. *Prog Earth Planet Sci* 2:1–17
- Pate JS, Unkovich MJ, Erskine PD, Stewart GR (1998) Australian mulga ecosystems—<sup>13</sup>C and <sup>15</sup>N natural abundances of biota components and their ecophysiological significance. *Plant Cell Environ* 21:1231–1242
- Pflug EE, Siegwolf R, Buchmann N, Dobbertin M, Kuster TM, Günthardt-Goerg MS, Arend M (2015) Growth cessation uncouples isotopic signals in leaves and tree rings of drought-exposed oak trees. *Tree Physiol* 35:1095–1105. <https://doi.org/10.1093/treephys/tpv079>
- Prieto I, Querejeta J, Segrestin J, Volaire F, Roumet C (2018) Leaf carbon and oxygen isotopes are coordinated with the leaf economics spectrum in Mediterranean rangeland species. *Funct Ecol* 32:612–625
- Roden JS, Ehleringer JR (1999) Hydrogen and oxygen isotope ratios of tree-ring cellulose for riparian trees grown long-term under hydroponic, controlled environments. *Oecologia* 121:467–477
- Roden JS, Farquhar GD (2012) A controlled test of the dual isotope approach for interpretation of stable carbon and oxygen isotope ratio variation in tree-rings. *Tree Physiol* 32:490–503. <https://doi.org/10.1093/treephys/tbs019>
- Roden JS, Siegwolf R (2012) Is the dual isotope conceptual model fully operational? *Tree Physiol* 32:1179–1182. <https://doi.org/10.1093/treephys/tbs099>
- Roden JS, Lin G, Ehleringer JR (2000) A mechanistic model for the interpretation of hydrogen and oxygen isotope ratios in tree-ring cellulose. *Geochim Cosmochim Acta* 64:21–35
- Roden JS, Kahmen A, Buchmann N, Siegwolf R (2015) The enigma of effective pathlength for <sup>18</sup>O enrichment in leaf water of conifers. *Plant Cell Environ* 38:2551–2565. <https://doi.org/10.1111/pce.12568>
- Rozanski K, Araguas-Araguas L, Gionfanti R (1993) Isotopic patterns in modern global precipitation. In: *Continental Isotope Indicators of Climate*. American Geophysical Union Monograph, Washington, DC
- Sarris D, Siegwolf R, Körner C (2013) Inter- and intra-annual stable carbon and oxygen isotope signals in response to drought in 2 Mediterranean pines. *Agric For Meteorol* 168:59–68
- Saurer M, Maurer S, Matyssek R, Landolt W, Günthardt-Goerg MS, Siegenthaler U (1995a) The influence of ozone and nutrition on  $\delta^{13}\text{C}$  in *Betula pendula*. *Oecologia* 103:397–406
- Saurer M, Siegenthaler U, Schweingruber F (1995b) The climate–carbon isotope relationship in tree rings and the significance of site conditions. *Tellus* 47B:320–330
- Saurer M, Aellen K, Siegwolf R (1997) Correlating  $\delta^{13}\text{C}$  and  $\delta^{18}\text{O}$  in cellulose of trees. *Plant Cell Environ* 20:1543–1550
- Scheidegger Y, Saurer M, Bahn M, Siegwolf R (2000) Linking stable oxygen and carbon isotopes with stomatal conductance and photosynthetic capacity: a conceptual model. *Oecologia* 125(3):350–357
- Schiegl WE (1974) Climatic significance of deuterium abundance in growth rings of *Picea*. *Nature* 251:582–584
- Sidorova OV, Siegwolf RTW, Saurer M, Shashkin AV, Knorre AA, Prokushkin AS, Vaganov EA, Kirilyanov AV (2009) Do centennial tree-ring and stable isotope trends of *Larix gmelinii* (Rupr.) Rupr. indicate increasing water shortage in the Siberian north? *Oecologia* 161:825–835
- Siegwolf RTW, Lehmann MM, Goldsmith GG, Churakova (Sidorova) O, Mirande-Ney C, Timofeeva G, Weigt RB, Saurer M (2022) Updating the dual C and O isotope – gas exchange model: A



- concept for understanding plant-environment responses and its implications for tree rings. PCE. In Review
- Sternberg LdSLOR (2009) Oxygen stable isotope ratios of tree-ring cellulose: the next phase of understanding. *New Phytol.* 181:553–562
- Sullivan PF, Welker JM (2007) Variation in leaf physiology of *Salix arctica* within and across ecosystems in the High Arctic: test of a dual isotope ( $\Delta^{13}\text{C}$  and  $\Delta^{18}\text{O}$ ) conceptual model. *Oecologia* 151:372–386
- Treydte K, Boda S, Graf Pannatier E, Fonti P, Frank D, Ullrich B, Saurer M, Siegwolf R, Battipaglia G, Werner W, Gessler A (2014) Seasonal transfer of oxygen isotopes from precipitation and soil to the tree ring: source water versus needle water enrichment. *New Phytol* 202:772–783. <https://doi.org/10.1111/nph.12741>
- Voelker SL, Brooks JR, Meinzer FC, Roden J, Pazdur A, Pawelczyk S, Hartsough P, Snyder K, Plavcova L, Šantrůček J (2014) Reconstructing relative humidity from plant  $\delta^{18}\text{O}$  and  $\delta\text{D}$  as deuterium deviations from the global meteoric water line. *Ecol Appl* 24:960–975
- Voltas J, Camarero J, Carulla D, Aguilera M, Ortiz A, Ferrio J (2013) A retrospective, dual-isotope approach reveals individual predispositions to winter-drought induced tree dieback in the southernmost distribution limit of *S. cots* pine. *Plant Cell Environ* 36:1435–1448
- Von Caemmerer S, Farquhar GD (1981) Some relationships between the biochemistry of photosynthesis and the gas exchange of leaves. *Planta* 153:376–387
- Weigt RB, Bräunlich S, Zimmermann L, Saurer M, Grams TEE, Dietrich H-P, Siegwolf RTW, Nikolova PS (2015) Comparison of  $\delta^{18}\text{O}$  and  $\delta^{13}\text{C}$  between tree-ring whole wood and cellulose in five species growing under two different site conditions. *Rapid Commun Mass Spectrom* 29:2233–2244
- White JWC, Gedzelman SD (1984) The isotopic composition of atmospheric water vapor and the concurrent meteorological conditions. *J Geophys Res* 89:4937–4939
- Woodley EJ, Loader NJ, McCarroll D, Young GHF, Robertson I, Gagen MH, Warham JO (2012) High-temperature pyrolysis/gas chromatography/isotope ratio mass spectrometry: simultaneous measurement of the stable isotopes of oxygen and carbon in cellulose. *Rapid Commun Mass Spectrom* 26:109–114. <https://doi.org/10.1002/rcm.5302>

**Open Access** This chapter is licensed under the terms of the Creative Commons Attribution 4.0 International License (<http://creativecommons.org/licenses/by/4.0/>), which permits use, sharing, adaptation, distribution and reproduction in any medium or format, as long as you give appropriate credit to the original author(s) and the source, provide a link to the Creative Commons license and indicate if changes were made.

The images or other third party material in this chapter are included in the chapter's Creative Commons license, unless indicated otherwise in a credit line to the material. If material is not included in the chapter's Creative Commons license and your intended use is not permitted by statutory regulation or exceeds the permitted use, you will need to obtain permission directly from the copyright holder.



# Chapter 17

## Intrinsic Water-Use Efficiency Derived from Stable Carbon Isotopes of Tree-Rings



Matthias Saurer and Steve Voelker

**Abstract** Stable carbon isotopes in tree-rings are not only useful to derive climatic information of the past. Based on the isotope fractionations during uptake and fixation of CO<sub>2</sub>, physiological information can be retrieved, namely the ratio of assimilation to stomatal conductance, which is termed the intrinsic water-use efficiency (iWUE). This crucial plant physiological trait varies among species and environments and is characteristic of how much water is lost from leaves for a certain carbon gain. iWUE is of great importance at the scale of individual plants because it can determine plant performance and survival. iWUE also contributes how closely canopy- or ecosystem-scale carbon and water fluxes are coupled or divergent, which has implications for understanding biogeochemical cycling. Carbon isotopes in tree-rings can be used to estimate how iWUE of trees has changed in the past, e.g. due to increasing CO<sub>2</sub>, nitrogen or other factors. Accordingly, many applications have explored this tool for various forest ecosystems across the globe, often reporting a strong increase in iWUE over the twentieth century. Explicit comparisons of tree-ring iWUE to growth-data obtained from the same rings can help distinguish among strategies plants employ under various environmental impacts, like increasing CO<sub>2</sub>, light limitation, drought or too much water. In this chapter, we describe the theory behind iWUE, show some limitations of the method, give examples of the combined application of iWUE and tree-ring width, discuss photosynthetic limitations of iWUE and finally show how the method has been applied in large-scale tree-ring networks.

---

M. Saurer (✉)

Swiss Federal Institute for Forest, Snow and Landscape Research WSL, Birmensdorf, Switzerland  
e-mail: [matthias.saurer@wsl.ch](mailto:matthias.saurer@wsl.ch)

S. Voelker

College of Forest Resources and Environmental Science, Michigan Technological University,  
Houghton, MI 49931, USA

© The Author(s) 2022

R. T. W. Siegwolf et al. (eds.), *Stable Isotopes in Tree Rings*, Tree Physiology 8,  
[https://doi.org/10.1007/978-3-030-92698-4\\_17](https://doi.org/10.1007/978-3-030-92698-4_17)

481

## 17.1 Introduction

The development of the Farquhar-model of carbon isotope fractionation during photosynthesis was a milestone in the application of stable isotopes in ecology and many other fields (Farquhar et al. 1982). This model enabled a straightforward interpretation of carbon isotope values of plant organic matter in terms of physiology. One of the primary predictands of the Farquhar model is the internal  $\text{CO}_2$ -concentration inside the leaf ( $c_i$ ). Soon it was realized that this predictand can be directly linked to the so-called intrinsic water-use efficiency (iWUE), the ratio between assimilation (A) and stomatal conductance for water vapour (g) (Ehleringer and Cerling 1995; Farquhar et al. 1989) (see Sect. 17.2 for more details). The regulation of stomatal opening is one of the most intricate and essential functions of terrestrial plants, as water-limited systems demand that stomatal behavior simultaneously constrain water loss while assuring sufficient carbon gain for survival. This makes iWUE such a useful property to know, although the actual water-use efficiency (WUE), defined as the ratio of transpiration to assimilation, may even be more relevant in determining how plants respond to dry conditions. The analysis of carbon isotope values of organic matter is nowadays an efficient method to determine iWUE that integrates minute-to-minute signals in leaves over the days to months it may take to synthesize plant tissues. The isotopic composition can be determined efficiently via on-line coupling of elemental analysers to isotope-ratio mass-spectrometers (see Chap. 7), which has allowed for scientists to produce much larger data sets compared to studies taking place 20 years ago.

Given the advancements in isotopic theory and technical ability, it is not surprising that the Farquhar-model has found increasingly widespread application in tree-ring studies e.g. (Marshall and Monserud 1996; Penuelas et al. 2011; Waterhouse et al. 2004). In turn, many investigators have realized that the doors have been flung open to reveal retrospective insights on how physiological processes have shifted in response to myriad changing environmental conditions. Particularly important avenues of research for projecting carbon-climate-vegetation feedbacks within the biosphere have addressed how forests have responded to ongoing climate change and increasing  $\text{CO}_2$  in the atmosphere (Saurer et al. 2014, Voelker et al. 2016). Although numerous studies of how plants have responded to  $\text{CO}_2$ , temperature, drought and other factors have been carried out in greenhouses or growth chambers, such studies of small plants may not be representative of how adult trees in natural environments may have responded. Where tree longevity and size have made experimentation extraordinarily difficult, the use of tree-ring stable carbon isotopes can provide a more realistic view by studying trees in their natural habitat and over their entire life-cycle. Intriguingly, information on iWUE can be retrieved for times when  $\text{CO}_2$ -concentration was different, for instance on the pre-industrial level of 280 ppm compared to current levels that exceed 400 ppm. We can thus obtain information on the ratio between A and g of trees living at times when scientific inquiry into plant function was in its infancy and when leaf gas-exchange equipment did not even exist. Stable carbon isotopes of tree-ring cellulose can therefore provide accurately

and absolutely dated archives of annual and intra-annual past plant physiological responses to climate, CO<sub>2</sub> and other environmental drivers that are unavailable from experimental methods and other paleoecological data sources.

Despite the power of pairing carbon isotope measurements and theory with tree-rings, some limitations should also be mentioned (Sect. 17.3). As *i*WUE only resolves the ratio of *A* to *g*, it often remains elusive, which of the two changed and to what degree. An increase in *i*WUE, for instance, can theoretically be caused by higher *A* or by lower *g* or a combination of the two. Furthermore, it should always be considered that *i*WUE is a different metric than the actual WUE (see Sect. 17.3 for details). Nevertheless, independent data confirm the usefulness of δ<sup>13</sup>C-derived *i*WUE-estimates from tree rings. Accordingly, *i*WUE-time series from multiple sites across the globe have provided numerous and invaluable insights into tree responses to global climate change. Increases in *i*WUE have been documented by essentially all studies spanning multiple decades of tree-ring isotope data and have occurred within the last ca. 100 years. However, the rate of change of increase in *i*WUE is quite variable and the reason for this range of responses not well understood. To provide additional insights, some studies have combined tree-ring derived *i*WUE with growth data originating from the same tree-rings. This can help the interpretation of growth trajectories by adding a physiological perspective, for instance in studies of drought-related decline (Sect. 17.4). While most studies focused on stomatal limitations of *i*WUE, photosynthetic limitation may be an under-explored topic (Sect. 17.5). Finally, due to the construction of large networks of sites with tree-ring isotope data, it recently became feasible to study spatial patterns of *i*WUE on regional to continental scales (Sect. 17.6). Hence, with these examples, the breadth and success of *i*WUE-reconstructions using tree-ring isotopes is on full display and portends many novel findings in the future.

## 17.2 Model and Scenarios

The potential to derive physiological information from δ<sup>13</sup>C of plant material (δ<sup>13</sup>C<sub>plant</sub>) is strongly based on the Farquhar-model (1982), which in its simplest form is given as:

$$\delta^{13}C_{plant} = \delta^{13}C_{atm} - a - (b - a)\frac{c_i}{c_a}, \quad (17.1)$$

where δ<sup>13</sup>C<sub>atm</sub> is the carbon isotope ratio of atmospheric CO<sub>2</sub>, *a* (4.4‰) is the fractionation associated with the diffusion of CO<sub>2</sub> through the stomata, *b* (27‰) the fractionation resulting from enzymatic C fixation by RubisCO, and *c<sub>i</sub>/c<sub>a</sub>* is the ratio of leaf internal to ambient CO<sub>2</sub>-concentrations. This mechanistic model for C<sub>3</sub>-plants was experimentally verified in many studies (Evans et al. 1986) and predicts

a depletion in the isotope ratio in the plant compared to the isotope ratio in the atmosphere, but to a varying degree depending on  $c_i/c_a$ . Equation (17.1) can be applied directly to tree-rings by using the measured tree-ring isotope value of a specific year as  $\delta^{13}C_{plant}$ , provided the corresponding value for  $\delta^{13}C_{atm}$  for the same year is used. The  $\delta^{13}C_{atm}$ -values have declined over the past 150 years due to fossil CO<sub>2</sub> emissions and are known either from atmospheric measurements or derived from ice-core studies (Leuenberger 2007). A modified equation is sometimes used in biological studies, based on carbon isotope discrimination ( $\Delta$ ), which approximates the difference between  $\delta^{13}C_{atm}$  and  $\delta^{13}C_{plant}$ , thus a positive number:

$$\Delta^{13}C_{plant} = \frac{\delta^{13}C_{atm} - \delta^{13}C_{plant}}{1 + \delta^{13}C_{plant}} = a + (b - a) \frac{c_i}{c_a}. \quad (17.2)$$

These equations can be solved for  $c_i/c_a$ . In the following, we explain how the intrinsic water-use efficiency *iWUE* is derived from this information, which is the ratio of net photosynthesis (*A*) to conductance for water vapor ( $g_{H_2O}$ ) (Ehleringer and Cerling 1995):

$$iWUE = \frac{A}{g_{H_2O}}, \quad (17.3)$$

expressed in units of  $\mu\text{mol mol}^{-1}$ . Using the equation for net photosynthesis

$$A = g_{CO_2}(c_a - c_i), \quad (17.4)$$

with  $g_{CO_2}$  as the conductance for CO<sub>2</sub>, and considering

$$g_{H_2O} = 1.6g_{CO_2}, \quad (17.5)$$

we obtain the following relationship

$$iWUE = \frac{(c_a - c_i)}{1.6}. \quad (17.6)$$

Finally, using  $c_i/c_a$  derived from Eq. (17.1), we find:

$$iWUE = c_a \frac{b - (\delta^{13}C_{atm} - \delta^{13}C_{plant})}{1.6(b - a)}. \quad (17.7)$$

Such derived *iWUE* has been widely employed in tree-ring isotopic studies.

*A* and  $g_{H_2O}$  and thus  $c_i$  depend on various environmental drivers (light, CO<sub>2</sub>, VPD, etc.) and are dependent on species and site conditions. To group different

tree physiological responses, a useful heuristic has classified three primary leaf gas-exchange scenarios (Saurer et al. 2004): In response to changing  $\text{CO}_2$  and other environmental variability over time, there can be trees that (1) tend to keep  $c_i$  constant representing a homeostatic gas-exchange regulation (Marshall and Monserud 1996), (2) trees that keep  $c_i/c_a$  constant like a set-point (Ehleringer and Cerling 1995), or (3) trees that keep  $c_a - c_i$  constant, which is the equivalent of no increase in  $i\text{WUE}$ . Over large gradients in  $c_a$ , however, meta-analysis of empirical data indicates there is a shift between scenarios (Voelker et al. 2016). Equations (17.1 and 17.7) shown here are easily applicable due to their simple form, but additional fractionation effects occur during and after photosynthesis that could in principle also be included. Such effects are, for instance, due to the mesophyll conductance and other diffusive limitations within the leaf as well as photorespiration (discussed in Chap. 9), post-photosynthetic fractionations during biochemical reactions and phloem transport (Chap. 13) as well as effects related to timing of wood formation, use of stored carbohydrates and subsequent mixing of carbon pools of different age (Chap. 15).

### 17.3 Limitations and Verifications

While  $i\text{WUE}$  has proven useful in numerous studies, one needs to be aware of some limitations of this metric. The actual  $\text{WUE}$  is a closely related, but still different concept, which is calculated as the ratios of net photosynthesis ( $A$ ) to transpiration ( $E$ ) (rather than  $A$  to  $g_{\text{H}_2\text{O}}$  only):

$$\text{WUE} = \frac{A}{E}, \quad (17.8)$$

with  $E$  defined as:

$$E = g_{\text{H}_2\text{O}}(e_i - e_a) = g_{\text{H}_2\text{O}}\text{VPD}, \quad (17.9)$$

whereby  $e_i$  and  $e_a$  are the vapor pressures in the leaf cellular air space and ambient air, respectively. Such  $\text{WUE}$  may be ecologically more relevant than  $i\text{WUE}$  because it is based on the water fluxes and depends directly on  $\text{VPD}$ , which has been shown to be important in amplifying recent warming trends (Breshears et al. 2013; Szejner et al. 2019). Furthermore,  $\text{WUE}$  can be calculated over different periods, for instance, as the ratio of carbon uptake to water loss at the plant level over a growing season or plant life, which is also influenced by respiratory losses. It has been shown that different concepts of  $\text{WUE}$ , like intrinsic and actual  $\text{WUE}$ , are sometimes poorly correlated (Seibt et al. 2008).  $\text{WUE}$  can also be considered at a larger scale: at the ecosystem-level, where it is defined as gross primary production ( $\text{GPP}$ ) relative to evapotranspiration ( $\text{ET}$ ). In our opinion, it is of great importance to be aware of the different scales at which  $\text{WUE}$  can be calculated and be cognizant that one is

not compared directly with another without acknowledging how they may differ. It should be quite obvious that plant-level and, for instance, ecosystem level WUE are not the same and therefore should also not be expected to respond similarly to environmental variability. Nonetheless, comparisons of WUE-estimates obtained by different techniques may yield new insights on leaf, plant and ecosystem functioning.

As an example where different techniques resulted in comparable WUE estimates, a study in a *Quercus petraea* forest indicated that seasonal iWUE data obtained via a process-based physiological model matched well with iWUE derived from intra-annual  $\delta^{13}\text{C}$  of tree-rings (Michelot et al. 2011). The authors concluded that latewood may be a good proxy for assessing seasonal variations of the ratio of assimilation to stomatal conductance, despite some delay in organic matter deposition in the ring. In contrast, WUE at the ecosystem level determined as GPP/ET at eddy-covariance-based ecosystem flux tower monitoring sites across North America showed that WUE at the ecosystem scale has been increasing much faster than that recorded by tree-ring isotope-based iWUE (Guerrieri et al. 2019). The authors speculated that reasons for this discrepancy could be different time-scales of the two approaches or fluxes not accounted for, like non-transpirational water fluxes and contribution from understory vegetation. In a study using satellite-based NPP estimates, a relationship between tree-ring  $\delta^{13}\text{C}$  values of an Eastern US network of sites and NPP was found, rather than with WUE (Levesque et al. 2019). Finally, at a site in California, Keen (2019) showed that intra-annual tree-ring derived iWUE responded positively to VPD, whereas ecosystem-level WUE responded negatively to VPD, and this opposing VPD-response drove a negative response between iWUE and WUE during a range of wet to historically severe drought conditions. Together, these studies demonstrate that tree-ring carbon isotopes can contain valuable information on large-scale fluxes, but that more studies are needed to determine under what conditions iWUE is related to ecosystem-scale WUE (Seibt et al. 2008).

A complication of interpreting tree growth patterns and iWUE-estimation that needs careful consideration are the effects of age, tree size or height (Brienen et al. 2017; McDowell et al. 2011). Dendrochronologists have conventionally used empirical detrending methods to remove age-related growth patterns from ring-width data prior to assessing climate-sensitivity of tree growth. In recent decades it has become popular among ecologists and ecophysiologicalists to convert tree-ring data to basal area increment (BAI) or BAI/basal area for a given year, often putatively as a means to avoid the need to detrend ring-width data that decline with tree size and age. However, the often-stated or implied contention that these variables overcome the need for detrending is a misconception. For example, BAI tends to increase with tree size, but trees with initially greater BAI tend to have steeper positive relationships between BAI and tree age (Voelker et al. 2008). Likewise, BAI/basal area has a negative trend with age that is particularly steep when trees are young and BAI/basal area is nearer to one. Hence, it should be obvious that use of BAI or BAI/basal area may include biases in tree growth trends and should not be compared when groups of trees differ in age or size. Overall, BAI or BAI/basal area methods may not be an improvement over conventional detrending methods for comparison to stable isotopes in the

same tree rings, particularly for studies of trees that are young (i.e., <100 years in age).

The carbon isotopes of tree-rings can change as trees grow, and depending somewhat on species and stand density, foliage is displayed at further distances from soil water sources as they get taller and form larger branches (McDowell et al. 2011). This change in stature results in a greater hydrostatic gradient in water potential and higher hydraulic resistance that impacts canopy-level stomatal conductance and thus iWUE. Such long-term trends owing to changes in tree stature can be mistakenly attributed to climate and/or CO<sub>2</sub>, so care should be taken to minimize the potential for this bias by considering it in assessments of carbon isotope responses to long-term environmental change (Brienen et al. 2017). If neglected, this bias could result in an over-estimation of how CO<sub>2</sub> modifies leaf gas exchange. Several studies have, however, highlighted that  $\delta^{13}\text{C}$  mainly has age-related trends in the first few decades, forming a so-called juvenile trend, but not later on (Gagen et al. 2007; McCarroll and Loader 2004). This problem can be avoided by simply not using the juvenile phase or by applying appropriate corrections if known for a specific species or site (Vadeboncoeur et al. 2020). The age-trend can well be tested for trees growing in pre-industrial times where there are no strong variations in CO<sub>2</sub>-concentration by aligning them according their cambial age. This was done in a recent study with coastal redwood trees where indeed the age-trend was strongest in the first few decades of their life, but extended several centuries before finally levelling off (Voelker et al. 2018) (Fig. 17.1). These trees are, however, almost 100 m tall and take exceptionally long to reach this height, showing that there is no universal juvenile phase that is applicable across species and forest types.

Some studies have tried to exclude age-effects by comparing different age cohorts, i.e. comparing iWUE of young trees with mature trees during the same time period (Bert et al. 1997; Brienen et al. 2017; Marshall and Monserud 1996). These studies have not addressed a potential sampling bias, whereby mature trees are the survivors of decades to centuries of mortality processes and also may not reflect the overall stand structure and history (Brienen et al. 2017). Microclimatic conditions are also different for saplings near the ground as compared to larger trees, e.g. regarding light and VPD, which affects the relationship between  $\delta^{13}\text{C}$  and growth (Fardusi et al. 2016). In other studies, stand structure has been shown to affect  $\delta^{13}\text{C}$ -trends of understory beech and spruce trees, emphasizing the effects of competition and light (Klesse et al. 2018) as well as in overstory ponderosa pine and grand fir trees (Voelker et al. 2019a) due to increasing competition for water in the absence of wildfire. Clearly, more research is needed to reliably separate the effects of CO<sub>2</sub>, climate, age and tree height. Nevertheless, the strong increases in iWUE as a result of the atmospheric CO<sub>2</sub>-increase has been found to be widespread and thereby clearly cannot be an artefact (Guerrieri et al. 2019).



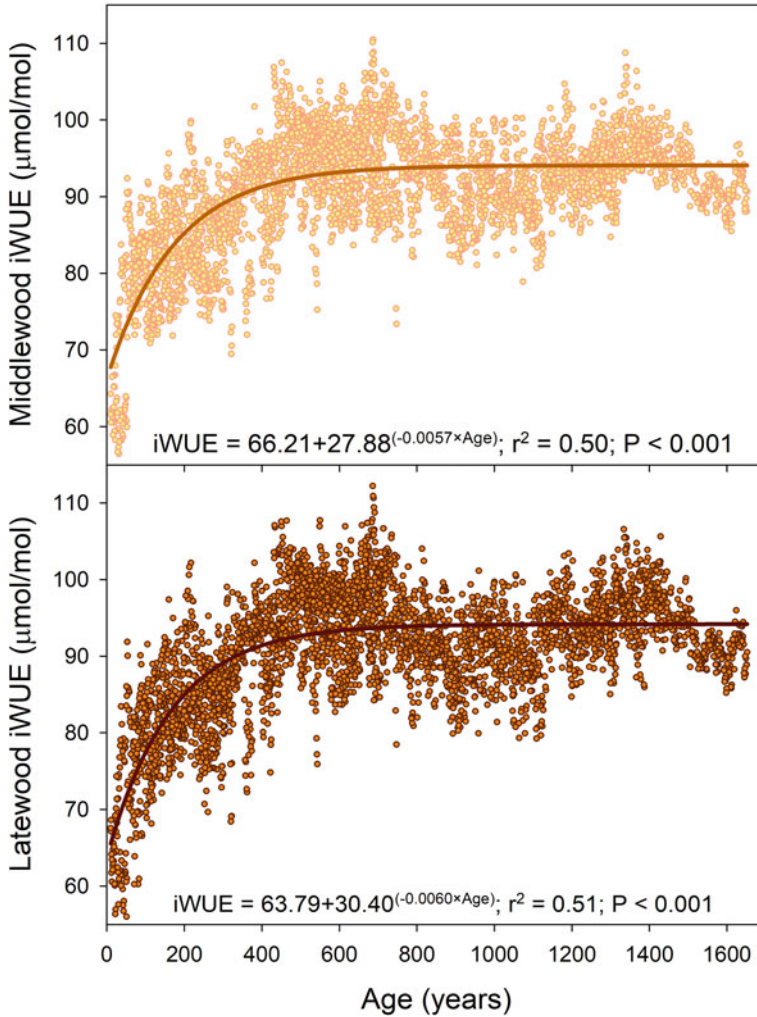


**Fig. 17.1** Examples of inter-annual iWUE, sampled for two intra-annual ring divisions (latewood and middlewood), from seven coastal redwoods (*Sequoia sempervirens*) growing in northern California, USA (after Voelker et al. (2018)). Tree age data were corrected to ground level from tree cross-section sampling height and pith dates were estimated using conventional techniques. To minimize the potential impact of atmospheric CO<sub>2</sub> concentrations or <sup>13</sup>CO<sub>2</sub>, no data from years later than 1880 were used. Finally, tree-level variation was minimized by iteratively fitting negative exponential curves and correcting each data point with the tree-level mean residual. There were no significant changes to the relationship after three iterations. Note that middlewood was defined as the central 60% of each ring while the latewood occupied the last 25% and the first 15% of each ring was discarded

## 17.4 Combination of Growth and iWUE: The Case of Drought

The combination of conventional dendrochronological analyses of growth and stable isotope methods can be very powerful. With a multi-proxy approach, the particular strength of tree rings is taken full advantage of as all the measurable parameters originate from the same absolutely dated rings, but contain different environmental information. Tree ring widths or basal area increments provide cumulative growth information that is related to the complex interplay of environmental conditions and limiting factors to xylogenesis during the growing season, whereas stable isotopes measured in the cellulose of these tree rings are rather recording the physiological conditions at the canopy level. Stable isotopes are also influenced by seasonal timing of wood formation as periods of extreme growth limitation, e.g. drought, may not be reflected in the isotope signal of the tree ring when xylogenesis is halted (Sarris et al. 2013). Furthermore, drought legacy effects may differ between tree-ring width and stable isotopes as the recovery after an extreme event may be different for the two parameters (Szejner et al. 2019). Hence, stable isotopes can help decipher causes of growth variations more clearly in many cases. Tree growth and iWUE may or may not show similar trends and may also display positive or negative correlations. With careful consideration of biological trends due to tree age and size, the combined analysis of tree growth and iWUE or carbon isotope discrimination can help to decipher what relevant environmental mechanisms may be impacting trees by affecting leaf gas exchange, growth, or both factors together (Brienen et al. 2021; Sun et al. 2018; Voelker et al. 2014). This multi-proxy approach may be particularly relevant for better understanding tree responses to climate warming and various aspects of drought (Levesque et al. 2014). Indeed, the area of land classified as very dry has more than doubled globally in the last 50 years and accordingly drought conditions are affecting many forest ecosystems, resulting in reduced growth and increased stress and tree mortality (Allen et al. 2010). For example, in areas such as the Central Mediterranean, Central and Western Europe, California and much of the Western United States and elsewhere, warmer temperatures have amplified droughts (Dai 2013). California and the west US coast in particular has undergone recent extremes (Keen et al. 2022) that are expected to become more severe in the future based on climate model predictions (Wang et al. 2017; Yoon et al. 2015). These projections are further supported by long tree-ring isotope chronologies that demonstrated greater hydroclimate variability during the warmer Medieval Climate Anomaly and the period of recent warming compared to the colder Little Ice Age (Voelker et al. 2018).

Considering projections of increased drought frequency and severity, there is a crucial need to understand mechanisms leading to drought-induced tree mortality, which may be provided by investigating how some trees, species and different forest ecosystems have responded to acute or chronic drought stress (Allen et al. 2010). Although drought-related physiological effects on trees have long been studied, the significance of different mechanisms is still unclear (McDowell et al. 2008). When

pests and pathogens do not act as the primary cause of tree mortality, the most important processes leading to death are hydraulic failure (desiccation) in extreme drought events and a reduction of the trees' carbon storage through gradual depletion of carbohydrates (starvation) induced by protracted drought episodes. The mechanism of carbon starvation is likely related to water-use efficiency, as plants may reduce stomatal conductance strongly to avoid loss of water, and therefore this process may be elucidated using stable carbon isotopes. In such a situation, the plant is no longer capable of producing enough non-structural carbohydrates to maintain essential metabolic functions and stored non-structural carbohydrates are inaccessible due to compartmentalization and lack of enzymatic energy (Sala et al. 2010).

Studies of trees that survived or died during intense periods of drought have been particularly effective at applying tree-ring growth and stable carbon isotopes to highlight physiological factors that ostensibly predisposed trees to mortality. One of the first such investigations to do so used a rather narrow time window for assessment, but nonetheless found that trees that died during a severe drought had similar *i*WUE, but lower tree growth rates, compared to co-occurring trees that survived (McDowell et al. 2010). However, the surviving trees showed a strong climatic sensitivity of gas exchange (i.e.  $\delta^{13}\text{C}$ ) in contrast to dying trees, which was attributed to dead trees having undergone chronic drought stress and carbon starvation prior to death. Other more recent studies have further refined this type of approach. For example, high mortality rates of Scots pine (*Pinus sylvestris* L.) in lower altitudes in inner-Alpine valleys such as the Valais (Switzerland) (Rigling et al. 2013) exemplify a region that was undergoing drought-induced forest decline. At one site, analyses of growth and stable carbon isotope ratios in tree rings over the twentieth century were combined with a 10-year irrigation experiment that doubled annual precipitation (Timofeeva et al. 2017). There was a strong growth increase and concurrent depletion of  $\delta^{13}\text{C}$  values for irrigated trees, indicating reduced *i*WUE. This demonstrated that progressive limitation of leaf gas-exchange by drought-induced stomatal closure was reversible when extra water was supplied. In the same stand, Scots pine trees that had recently died had more than 100 years of lower growth and higher *i*WUE derived from  $\delta^{13}\text{C}$  values compared with surviving trees. This indicates a conservative water-use strategy for trees that had died, which resulted in a lack of carbohydrates, reduction of the needle mass and long-term weakening. In contrast, a study with Norway Spruce (*Picea abies* L. Karst.) indicated a different cause for mortality, as dying trees grew significantly better and had higher *i*WUE in the earlier life phase than surviving trees (Hentschel et al. 2014). Similarly, it was found for Scots pine (Voltas et al. 2013) and for a Mediterranean oak species (Colangelo et al. 2017) that "fast growing" and "less efficient" individuals were more affected, whereas (Heres et al. 2014) observed that declining trees were less sensitive in *i*WUE than non-declining trees. Such differences in tree response strategies to drought could be summarized in a conceptual diagram (Fig. 17.2).

The diagram shows differences between surviving and dead trees, where the surviving trees are considered as the reference. These two tree groups have differed in their past growth patterns and physiology prior to the actual, final decline phase. Trees following a conservative strategy are located in the upper, left-hand sector of

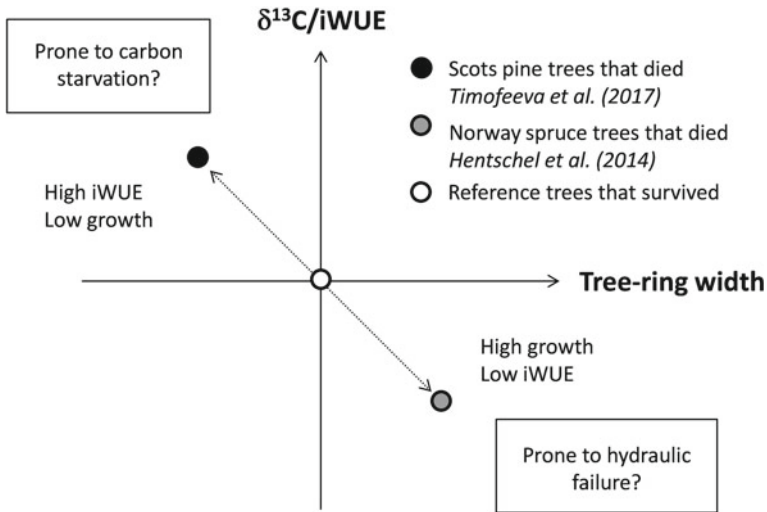


**Fig. 17.2** Conceptual diagram for explaining death or survival of trees from the same stand based on their earlier physiology and growth patterns. The location of the black circle indicates the position of dead trees from the Scots pine site in Switzerland (Timofeeva et al. 2017), while the grey circle refers to Norway spruce trees from southern Norway (Hentschel et al. 2014). Surviving trees indicated as open circle are considered as the reference in both studies

the diagram, as was observed for Scots pine at the Swiss study site (Fig. 17.2). These trees are expected to be prone to carbon starvation rather than to hydraulic failure. It should be considered that carbon starvation may just mean a lack of carbohydrates and energy to maintain vital functions, although not a complete exhaustion of storage pools (Hartmann and Trumbore 2016). In contrast, for Norway spruce (Hentschel et al. 2014), trees that died later had higher growth and were not following a strict water-use strategy. Therefore, these trees were prone to hydraulic failure rather than carbon starvation. This less conservative water-use strategy falls in the lower, right-hand sector of the diagram (Fig. 17.2).

Absolute values of growth and iWUE can provide one continuum on which trees can be ordered that can provide valuable physiological interpretations (Fig. 17.2). Additional insights may be gained by assessing the sensitivity of growth or carbon isotopes to various metrics of meteorological drought or the coupling of growth to carbon isotope variation each provide additional windows on the relative degree of drought stress and how that response may have changed over time (Keen 2019, McDowell et al. 2010, Urrutia-Jalabert et al. 2015, Voelker et al. 2014, Voelker et al. 2019a). Overall, stable isotope analysis in combination with the study of growth patterns is therefore a promising approach for elucidating relevant physiological processes under drought, even more so when including oxygen isotope ratios as their changes are influenced by transpiration rate, but not photosynthesis (Gessler et al. 2018) (Chap. 10). This may ultimately result in improved predictions of forest ecosystem changes in the future.

## 17.5 Photosynthetic Limitations to iWUE

Most investigations of tree-ring carbon isotopes have highlighted how interannual variability in iWUE is driven by stomatal closure during drought and that this pattern is superimposed on how gradually rising CO<sub>2</sub> has driven long-term changes in A. Since so few studies have demonstrated evidence for how A has formed the primary physiological constraint on interannual variability on tree-ring carbon isotopes and iWUE, a few examples warrant specific mention here because they may continue to lead to particularly novel insights. Two forest health studies on species located in the eastern United States have shown that iWUE has been strongly influenced by sulfur emissions and associated acidic deposition that increased during most of the twentieth century and then showed a reversal in trend near 1980 after US federal legislation and enforcement was increasingly implemented from 1963 through 1990 (Mathias and Thomas 2018; Thomas et al. 2013). The authors concluded that increasing A was an important component for explaining recent tree recovery. Other records where inter-annual variability in tree-ring isotopes were controlled by how A was modified by temperature and/or sunshine occurred in cold northerly regions such as Northern Norway and Sweden (Loader et al. 2013; Young et al. 2012). Alternatively, Voelker et al. (2019b) showed that similar constraints on A by temperature could be identified in temperate trees growing adjacent Lake Superior, which modulates near-lake air temperature regimes due to the large heat capacity of the lake reflecting previous winter conditions during spring and early summer. The last study was careful to utilize only “middlewood” formed during the early growing season, which contrasts with many other studies of drought stress that focus on whole rings or latewood. Hence, this emphasizes the need for future studies of tree-ring isotopes to carefully consider which intra-annual sampling scheme may be most appropriate where differences in the primary constraints on leaf carbon uptake may shift on a seasonal basis between photosynthetic rates and stomatal conductance (see also Chap. 15). Finally, Breinen et al. (2021) has shown that during understory phases of tree development, tree growth is often negatively correlated to carbon isotope discrimination but had neutral or weak positive correlations once the same trees were in canopy dominant positions, which implies that both the photosynthetic rates and growth of these trees were limited by irradiance when they were in the understory.

## 17.6 Large-Scale Patterns

Earth System Models and Dynamic Global Vegetation Models (DGVMs) are the workhorses to explore many large-scale terrestrial processes and climate-land biosphere interactions. These models are routinely used to project future changes in climate and Earth System processes under anthropogenic forcing in a detailed spatio-temporal context (Sitch et al. 2003). DGVMs represent the basic physiological processes responsible for plant growth via sets of interconnected equations

such as those for photosynthesis, respiration, and stomatal conductance, and the dependence of these physiological processes on the environmental (e.g., atmospheric CO<sub>2</sub> concentration, temperature, and water availability) conditions. A particular challenge for these models is to correctly capture and project changes at decadal-to-century timescales of utmost relevance for predicting short-term anthropogenic climate perturbations. For example, mechanisms of the contemporary terrestrial carbon sink are poorly understood which leads to large uncertainties in twenty-first century climate projections (Cox et al. 2000). The representation of many physiological mechanisms and plant-atmosphere interactions is still crudely or not at all implemented in these DGVMs, and appears to significantly contribute to uncertainties in predictions. Improving and validating the modeling of key processes with empirical data are thus particularly important.

Based on development of tree-ring isotopic networks over the past two decades (Saurer et al. 2014; Treydte et al. 2007), it has become feasible to link such tree-ring data to DGVMs on a large spatial and temporal scale. While not strictly leading to a validation of either model nor tree-ring data, this comparison can be profitable for both fields of scientific inquiry, as independent assessment of similar variables, like iWUE. Furthermore, DGVMs can also add more interpretation to a tree-ring network, as variables like *g<sub>s</sub>* and *A* can be obtained. In a recent study using a 35-site network across Europe with coniferous and deciduous species, changes in iWUE from 1901–2000 and the spatial distribution of these changes across Europe were investigated (Saurer et al. 2014). On average, iWUE increased in European forests by 28%, with clear spatial differences across the continent. Moreover, comparison of these data with iWUE simulations by a dynamic vegetation model (LPX-Bern 1.0) showed good agreement with spatial patterns and overall twentieth century trends in tree ring derived iWUE. Across the 27 conifer sites, tree-ring derived iWUE showed strong differences between sites grouped in three latitudinal bands, i.e. <45°N, 45–60°N, and >60°N (Fig. 17.3). The northernmost sites showed the lowest iWUE and also the lowest increase over the twentieth century (60.3–70.3 μmol/mol from the first to last decade of twentieth century, i.e. an increase by 16.6%). They also showed a rather homogenous signal as reflected in relatively low variability among sites. In comparison, the most southern sites, from Mediterranean climate, showed the highest overall values, an increase of 23% over the twentieth century, and also were characterized by relatively high variability among sites, showing that different ecosystems react rather differently to increasing CO<sub>2</sub> depending on local site factors. Sites from temperate climates, i.e. intermediate latitudes, showed intermediate overall iWUE, the strongest increase over the twentieth century by 31%, and further a notable increase in the variability over time. This patterns of iWUE-increase might reflect a generally strong, but variable sensitivity to increasing CO<sub>2</sub>, compared to where temperature (i.e. northern latitude sites) or precipitation (i.e. low latitude mediterranean sites) have historically been strongly limiting to leaf gas-exchange and growth.

These analyses clearly demonstrate the usefulness of such networks of tree-ring data for better understanding physiological tree responses to climate and CO<sub>2</sub> across

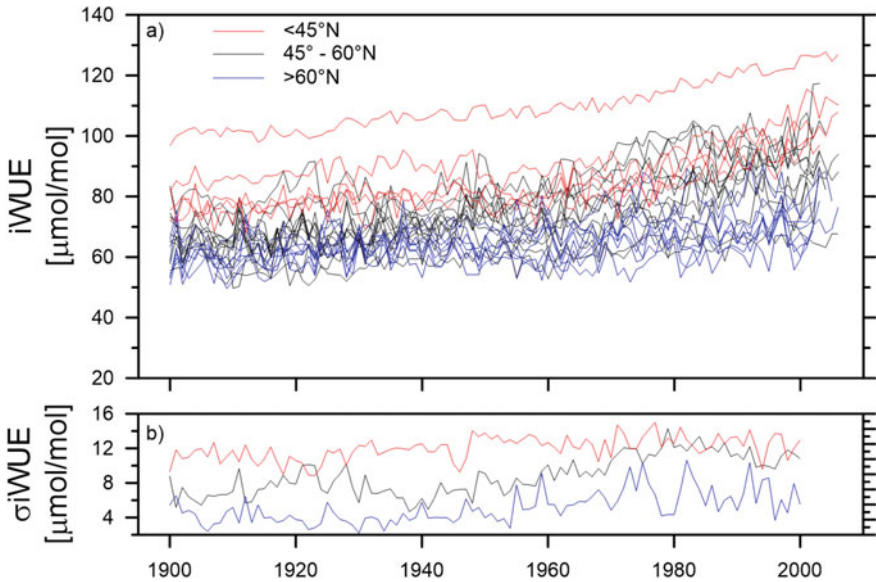


**Fig. 17.3** Reconstructed  $iWUE$  from 27 conifer sites across Europe grouped into different latitudinal bands (a). Variability of  $iWUE$  between sites (standard deviation) for these latitudinal bands (b)

different ecosystems. It might be further interesting to consider that net photosynthesis tends to play a larger role in determining growth and  $\delta^{13}C$  in more energy-limited environments, such as boreal forests, than in drought-prone environments. Under scenarios of increasing drought, this may imply that changes in the relative weight of energy and water limitations could be assessed through the combined use of  $\delta^{13}C$  and tree-rings. Nevertheless, the interpretation of  $iWUE$ -trends is not straightforward and can be enhanced by DGVM-results as shown in another recent study (Frank et al. 2015). Here, increases in European forest transpiration were calculated over the twentieth century, although a general decrease in stomatal conductance was also inferred, which seems at first view to be contradictory. The increased model transpiration results were due to longer growing seasons, enhanced evaporative demand in a warmer climate, and increased leaf area, which in total were outweighing the effect of reduced conductance. These results suggest caution may need to be applied when interpreting  $iWUE$ -results physiologically from  $\delta^{13}C$  of tree-rings without additional information on seasonality of tree-ring growth, but also shows the enormous potential of combining tree-ring isotopes and DGVM- or other large-scale model outputs for yielding new insights on carbon and water cycling.

**Acknowledgements** Steve Voelker was supported by US-NSF Award #1903721.

## References

- Allen CD, Macalady AK, Chenchouni H, Bachelet D, McDowell N, Vennetier M, Kitzberger T, Rigling A, Breshears DD, Hogg EH, Gonzalez P, Fensham R, Zhang Z, Castro J, Demidova N, Lim JH, Allard G, Running SW, Semerci A, Cobb N (2010) A global overview of drought and heat-induced tree mortality reveals emerging climate change risks for forests. *For Ecol Manag* 259:660–684
- Bert D, Leavitt SW, Dupouey JL (1997) Variations of wood  $\delta^{13}\text{C}$  and water-use efficiency of *Abies alba* during the last century. *Ecology* 78:1588–1596
- Breshears DD, Adams HD, Eamus D, McDowell NG, Law DJ, Will RE, Williams AP, Zou CB (2013) The critical amplifying role of increasing atmospheric moisture demand on tree mortality and associated regional die-off. *Front Plant Sci* 4
- Brienen RJW, Gloor E, Clerici S, Newton R, Arppe L, Boom A, Bottrell S, Callaghan M, Heaton T, Helama S, Helle G, Leng MJ, Mielikainen K, Oinonen M, Timonen M (2017) Tree height strongly affects estimates of water-use efficiency responses to climate and  $\text{CO}_2$  using isotopes. *Nat Commun* 8
- Brienen R, Helle G, Pons T, Boom A, Gloor M, Groenendijk P, Clerici S, Leng M, Jones C (2021) Paired analysis of tree ring width and carbon isotopes indicates when controls on tropical tree growth change from light to water limitations. *Tree Physiol* tpab142. <https://doi.org/10.1093/treephys/tpab142>
- Colangelo M, Camarero JJ, Battipaglia G, Borghetti M, De Micco V, Gentilesca T, Ripullone F (2017) A multi-proxy assessment of dieback causes in a Mediterranean oak species. *Tree Physiol* 37:617–631
- Cox PM, Betts RA, Jones CD, Spall SA, Totterdell IJ (2000) Acceleration of global warming due to carbon-cycle feedbacks in a coupled climate model. *Nature* 408:184–187
- Dai A (2013) Increasing drought under global warming in observations and models. *Nat Clim Chang* 3:52–58
- Ehleringer JR, Cerling TE (1995) Atmospheric  $\text{CO}_2$  and the ratio of intercellular to ambient  $\text{CO}_2$  concentrations in plants. *Tree Physiol* 15:105–111
- Evans JR, Sharkey TD, Berry JA, Farquhar GD (1986) Carbon isotope discrimination measured concurrently with gas-exchange to investigate  $\text{CO}_2$  diffusion in leaves of higher plants. *Aust J Plant Physiol* 13:281–292
- Fardusi MJ, Ferrio JP, Comas C, Voltas J, de Dios VR, Serrano L (2016) Intra-specific association between carbon isotope composition and productivity in woody plants: a meta-analysis. *Plant Sci* 251:110–118
- Farquhar GD, O’Leary MH, Berry JA (1982) On the relationship between carbon isotope discrimination and the intercellular carbon dioxide concentration in leaves. *Aust J Plant Physiol* 9:121–137
- Farquhar GD, Ehleringer JR, Hubick KT (1989) Carbon isotope discrimination and photosynthesis. *Annu Rev Plant Physiol Plant Mol Biol* 40:503–537
- Frank DC, Poulter B, Saurer M, Esper J, Helle G, Treydte KS, Zimmermann NE, Andreu L, Bednarz Z, Berninger F, Böttger T, D’Alessandro CD, Daux V, Filot M, Grabner M, Gutierrez E, Haupt M, Hilasvuori E, Jungner H, Kalela-Brundin M, Krapiec M, Leuenberger M, Loader NJ, Marah H, Masson-Delmotte V, Pazdur A, Pawelczyk S, Pierre M, Planells O, Pukiene R, Reynolds-Henne CE, Rinne KT, Saracino A, Sonninen E, Stievenard M, Switsur VR, Szczepanek M, Szychowska-Krapiec E, Todaro L, Waterhouse JS, Weigl M, Schleser GH (2015) Water use efficiency and transpiration across European forests during the Anthropocene. *Nat Clim Chang* 5:579
- Gagen M, McCarroll D, Loader NJ, Robertson L, Jalkanen R, Anchukaitis KJ (2007) Exorcising the ‘segment length curse’: summer temperature reconstruction since AD 1640 using non-detrended stable carbon isotope ratios from pine trees in northern Finland. *Holocene* 17:435–446
- Gessler A, Caillieret M, Joseph J, Schonbeck L, Schaub M, Lehmann M, Treydte K, Rigling A, Timofeeva G, Saurer M (2018) Drought induced tree mortality—a tree-ring isotope based conceptual model to assess mechanisms and predispositions. *New Phytol* 219:485–490



- Guerrieri R, Belmecheri S, Ollinger SV, Asbjornsen H, Jennings K, Xiao J, Stocker BD, Martin M, Hollinger DY, Bracho-Garrillo R, Clark K, Dore S, Kolb T, Munger JW, Novick K, Richardson AD (2019) Disentangling the role of photosynthesis and stomatal conductance on rising forest water-use efficiency. *Proc Natl Acad Sci USA* 116:16909–16914
- Hartmann H, Trumbore S (2016) Understanding the roles of nonstructural carbohydrates in forest trees—from what we can measure to what we want to know. *New Phytol* 211:386–403
- Hentschel R, Rosner S, Kayler ZE, Andreassen K, Borja I, Solberg S, Tveito OE, Priesack E, Gessler A (2014) Norway spruce physiological and anatomical predisposition to dieback. *For Ecol Manag* 322:27–36
- Heres AM, Voltas J, Lopez BC, Martinez-Vilalta J (2014) Drought-induced mortality selectively affects Scots pine trees that show limited intrinsic water-use efficiency responsiveness to raising atmospheric CO<sub>2</sub>. *Funct Plant Biol* 41:244–256
- Keen RM (2019) Using tree-ring growth and stable isotopes to explore ponderosa pine ecophysiological responses to climate variability and the 2012–2015 California drought. Master's thesis, Utah State University
- Keen RM, Voelker SL, Wang S-YS, Bentz BJ, Goulden ML, Dangerfield CR, Reed CC, Hood SM, Csank AZ, Dawson TE, Merschel AG, Still CJ (2022) Changes in tree drought sensitivity provided early warning signal to the California drought and forest mortality event. *Global Change Biol* 28: 1119–1132
- Klesse S, Weigt R, Treydte K, Saurer M, Schmid L, Siegwolf RTW, Frank DC (2018) Oxygen isotopes in tree rings are less sensitive to changes in tree size and relative canopy position than carbon isotopes. *Plant Cell Environ* 41:2899–2914
- Leuenberger M (2007) To what extent can ice core data contribute to the understanding of plant ecological developments of the past? In: Dawson TE, Siegwolf RTW (eds) *Stable isotopes as indicators of ecological change*. Elsevier Academic Press, London, pp 211–233
- Levesque M, Siegwolf R, Saurer M, Eilmann B, Rigling A (2014) Increased water-use efficiency does not lead to enhanced tree growth under xeric and mesic conditions. *New Phytol* 203:94–109
- Levesque M, Andreu-Hayles L, Smith WK, Williams AP, Hobi ML, Allred BW, Pederson N (2019) Tree-ring isotopes capture interannual vegetation productivity dynamics at the biome scale. *Nat Commun* 10
- Loader NJ, Young GHF, Grudd H, McCarroll D (2013) Stable carbon isotopes from Torne-trask, northern Sweden provide a millennial length reconstruction of summer sunshine and its relationship to Arctic circulation. *Quat Sci Rev* 62:97–113
- Marshall JD, Monserud RA (1996) Homeostatic gas-exchange parameters inferred from <sup>13</sup>C/<sup>12</sup>C in tree rings of conifers. *Oecologia* 105:13–21
- Mathias JM, Thomas RB (2018) Disentangling the effects of acidic air pollution, atmospheric CO<sub>2</sub>, and climate change on recent growth of red spruce trees in the Central Appalachian Mountains. *Glob Chang Biol* 24:3938–3953
- McCarroll D, Loader NJ (2004) Stable isotopes in tree rings. *Quat Sci Rev* 23:771–801
- McDowell NG, Pockman WT, Allen CD, Breshears DD, Cobb N, Kolb T, Plaut J, Sperry J, West A, Williams DG, Yezzer EA (2008) Mechanisms of plant survival and mortality during drought: why do some plants survive while others succumb to drought? *New Phytol* 178:719–739
- McDowell NG, Allen CD, Marshall L (2010) Growth, carbon-isotope discrimination, and drought-associated mortality across a *Pinus ponderosa* elevational transect. *Glob Chang Biol* 16:399–415
- McDowell NG, Bond BJ, Dickman LT, Ryan MG, Whitehead D (2011) Relationships between tree height and carbon isotope discrimination. In: Meinzer FC, Lachenbruch B, Dawson TE (eds) *Size- and age-related changes in tree structure and function*, pp 255–286
- Michelot A, Eglin T, Dufrene E, Lelarge-Trouverie C, Damesin C (2011) Comparison of seasonal variations in water-use efficiency calculated from the carbon isotope composition of tree rings and flux data in a temperate forest. *Plant Cell Environ* 34:230–244
- Penuelas J, Canadell JG, Ogaya R (2011) Increased water-use efficiency during the 20th century did not translate into enhanced tree growth. *Glob Ecol Biogeogr* 20:597–608

- Rigling A, Bigler C, Eilmann B, Feldmeyer-Christe E, Gimmi U, Ginzler C, Graf U, Mayer P, Vacchiano G, Weber P, Wohlgemuth T, Zweifel R, Dobbertin M (2013) Driving factors of a vegetation shift from Scots pine to pubescent oak in dry Alpine forests. *Glob Chang Biol* 19:229–240
- Sala A, Piper F, Hoch G (2010) Physiological mechanisms of drought-induced tree mortality are far from being resolved. *New Phytol* 186:274–281
- Sarris D, Siegwolf R, Körner C (2013) Inter- and intra-annual stable carbon and oxygen isotope signals in response to drought in Mediterranean pines. *Agric For Meteorol* 168:59–68
- Saurer M, Siegwolf RTW, Schweingruber FH (2004) Carbon isotope discrimination indicates improving water-use efficiency of trees in northern Eurasia over the last 100 years. *Glob Chang Biol* 10:2109–2120
- Saurer M, Spahni R, Frank DC, Joos F, Leuenberger M, Loader NJ, McCarroll D, Gagen M, Poulter B, Siegwolf RTW, Andreu-Hayles L, Boettger T, Linan ID, Fairchild IJ, Friedrich M, Gutierrez E, Haupt M, Hilasvuori E, Heinrich I, Helle G, Grudd H, Jalkanen R, Levanić T, Linderholm HW, Robertson I, Sonninen E, Treydte K, Waterhouse JS, Woodley EJ, Wynn PM, Young GHF (2014) Spatial variability and temporal trends in water-use efficiency of European forests. *Glob Chang Biol* 20:3700–3712
- Seibt U, Rajabi A, Griffiths H, Berry JA (2008) Carbon isotopes and water use efficiency: sense and sensitivity. *Oecologia* 155:441–454
- Sitch S, Smith B, Prentice IC, Arneñ A, Bondeau A, Cramer W, Kaplan JO, Levis S, Lucht W, Sykes MT, Thonicke K, Venevsky S (2003) Evaluation of ecosystem dynamics, plant geography and terrestrial carbon cycling in the LPJ dynamic global vegetation model. *Glob Chang Biol* 9:161–185
- Sun SJ, Qiu LF, He CX, Li CY, Zhang JS, Meng P (2018) Drought-affected *Populus simonii* Carr. show lower growth and long-term increases in intrinsic water-use efficiency prior to tree mortality. *Forests* 9
- Szejner P, Belmecheri S, Ehleringer JR, Monson RK (2019) Recent increases in drought frequency cause observed multi-year drought legacies in the tree rings of semi-arid forests. *Oecologia*. <https://doi.org/10.1007/s00442-00019-04550-00446>
- Thomas RB, Spal SE, Smith KR, Nippert JB (2013) Evidence of recovery of *Juniperus virginiana* trees from sulfur pollution after the clean air act. *Proc Natl Acad Sci USA* 110:15319–15324
- Timofeeva G, Treydte K, Bugmann H, Rigling A, Schaub M, Siegwolf R, Saurer M (2017) Long-term effects of drought on tree-ring growth and carbon isotope variability in Scots pine in a dry environment. *Tree Physiol* 37:1028–1041
- Treydte K, Frank D, Esper J, Andreu L, Bednarz Z, Berninger F, Böttger T, D'Allessandro CD, Etien N, Filot M, Grabner M, Guillemin MT, Gutierrez E, Haupt M, Helle G, Hilasvuori E, Jungner H, Kalela-Brundin M, Krapiec M, Leuenberger M, Loader NJ, Masson-Delmotte V, Pazdur A, Pawelczyk S, Pierre M, Planells O, Pukiene R, Reynolds-Henne CE, Rinne KT, Saracino A, Saurer M, Sonninen E, Stievenard M, Switsur VR, Szczepanek M, Szychowska-Krapiec E, Todaro L, Waterhouse JS, Weigl M, Schleser GH (2007) Signal strength and climate calibration of a European tree ring isotope network. *Geophys Res Lett* 34. <https://doi.org/10.1029/2007GL031106>
- Urrutia-Jalabert R, Malhi Y, Barichivich J, Lara A, Delgado-Huertas A, Rodriguez CG, Cuq E (2015) Increased water use efficiency but contrasting tree growth patterns in *Fitzroya cupressoides* forests of southern Chile during recent decades. *J Geophys Res Biogeosciences* 120:2505–2524
- Vadeboncoeur MA, Jennings KA, Ouimette AP, Asbjornsen H (2020) Correcting tree-ring  $\delta^{13}\text{C}$  time series for tree-size effects in eight temperate tree species. *Tree Physiol*. <https://doi.org/10.1093/treephys/tpz1138>
- Voelker SL, Muzika RM, Guyette RP (2008) Individual tree and stand level influences on the growth, vigor, and decline of red oaks in the Ozarks. *For Sci* 54:8–20
- Voelker SL, Meinzer FC, Lachenbruch B, Brooks JR, Guyette RP (2014) Drivers of radial growth and carbon isotope discrimination of bur oak (*Quercus macrocarpa* Michx.) across continental gradients in precipitation, vapour pressure deficit and irradiance. *Plant Cell Environ* 37:766–779

- Voelker SL, Roden JS, Dawson TE (2018) Millennial-scale tree-ring isotope chronologies from coast redwoods provide insights on controls over California hydroclimate variability. *Oecologia* 187:897–909
- Voelker SL, Merschel AG, Meinzer FC, Ulrich DEM, Spies TA, Still CJ (2019) Fire deficits have increased drought sensitivity in dry conifer forests: Fire frequency and tree-ring carbon isotope evidence from Central Oregon. *Glob Chang Biol* 25:1247–1262
- Voelker SL, Brooks JR, Meinzer FC, Anderson R, Bader MKF, Battipaglia G, Becklin KM, Beerling D, Bert D, Betancourt JL, Dawson TE, Domec JC, Guyette RP, Korner C, Leavitt SW, Linder S, Marshall JD, Mildner M, Ogee J, Panyushkina I, Plumpton HJ, Pregitzer KS, Saurer M, Smith AR, Siegwolf RTW, Stambaugh MC, Talhelm AF, Tardif JC, Van de Water PK, Ward JK, Wingate L (2016) A dynamic leaf gas-exchange strategy is conserved in woody plants under changing ambient CO<sub>2</sub>: evidence from carbon isotope discrimination in paleo and CO<sub>2</sub> enrichment studies. *Glob Chang Biol* 22:889–902
- Voelker SL, Wang SYS, Dawson TE, Roden JS, Still CJ, Longstaffe FJ, Ayalon A (2019b) Tree-ring isotopes adjacent to Lake Superior reveal cold winter anomalies for the Great Lakes region of North America. *Sci Rep* 9
- Voltas J, Camarero JJ, Carulla D, Aguilera M, Ortiz A, Ferrio JP (2013) A retrospective, dual-isotope approach reveals individual predispositions to winter-drought induced tree dieback in the southernmost distribution limit of Scots pine. *Plant Cell Environ* 36:1435–1448
- Wang SYS, Yoon JH, Becker E, Gillies R (2017) California from drought to deluge. *Nat Clim Chang* 7:465–468
- Waterhouse JS, Switsur VR, Barker AC, Carter AHC, Hemming DL, Loader NJ, Robertson I (2004) Northern European trees show a progressively diminishing response to increasing atmospheric carbon dioxide concentrations. *Quat Sci Rev* 23:803–810
- Yoon JH, Wang SYS, Gillies RR, Kravitz B, Hipps L, Rasch PJ (2015) Increasing water cycle extremes in California and in relation to ENSO cycle under global warming. *Nat Commun* 6
- Young GHF, McCarroll D, Loader NJ, Gagen MH, Kirchhefer AJ, Demmler JC (2012) Changes in atmospheric circulation and the Arctic Oscillation preserved within a millennial length reconstruction of summer cloud cover from northern Fennoscandia. *Clim Dyn* 39:495–507

**Open Access** This chapter is licensed under the terms of the Creative Commons Attribution 4.0 International License (<http://creativecommons.org/licenses/by/4.0/>), which permits use, sharing, adaptation, distribution and reproduction in any medium or format, as long as you give appropriate credit to the original author(s) and the source, provide a link to the Creative Commons license and indicate if changes were made.

The images or other third party material in this chapter are included in the chapter's Creative Commons license, unless indicated otherwise in a credit line to the material. If material is not included in the chapter's Creative Commons license and your intended use is not permitted by statutory regulation or exceeds the permitted use, you will need to obtain permission directly from the copyright holder.



**Part V**  
**Environmental Factors Impacting**  
**the Isotopic Fractionation**

# Chapter 18

## Spatial and Temporal Variations in Plant Source Water: O and H Isotope Ratios from Precipitation to Xylem Water



Scott T. Allen, Matthias Sprenger, Gabriel J. Bowen, and J. Renée Brooks

**Abstract** The water present within trees when sugars and cellulose are formed is the source of hydrogen and oxygen atoms that are incorporated into tree-ring cellulose (see Chaps. 10 and 11). However, the isotope composition of relevant water pools is often unknown when trying to interpret  $\delta^{18}\text{O}$  and  $\delta^2\text{H}$  isotopic records in tree rings. This chapter focuses on the factors that can influence the O and H isotope ratios of source waters for trees. Trees generally use water that originated as precipitation, but this does not mean that the isotope ratios of water used by trees—predominantly taken up by roots from soils—and incorporated in cellulose exactly matches precipitation isotope ratios. Precipitation isotope ratios vary in space and time, and only a fraction of all precipitation infiltrates soils, reaches roots, and is ultimately taken up by trees. Considering species, soils, and climates may allow for predicting which fraction of water resides in the root-zone during the growing seasons, and how its isotope ratios deviate from that of average precipitation. Here we provide an overview of the terrestrial water cycle and the associated transport and fractionation processes that influence the stable isotope ratios of water used by trees. We highlight obstacles and opportunities to be considered, towards more accurately interpreting the records of O and H isotope ratios in tree cellulose.

---

S. T. Allen (✉)

Department of Natural Resources and Environmental Science, University of Nevada, Reno, Reno, NV, USA

e-mail: [Scottallen@unr.edu](mailto:Scottallen@unr.edu)

M. Sprenger

College of Natural Resources, North Carolina State University, Raleigh, NC, USA

Institute of Environmental Assessment and Water Research (IDAEA-CSIC), Barcelona, Spain

G. J. Bowen

Geology and Geophysics, University of Utah, Salt Lake City, UT, USA

J. R. Brooks

Pacific Ecological Systems Division, U.S. Environmental Protection Agency, Center for Public Health and Environmental Assessment, Corvallis, OR, USA

© The Author(s) 2022

R. T. W. Siegwolf et al. (eds.), *Stable Isotopes in Tree Rings*, Tree Physiology 8, [https://doi.org/10.1007/978-3-030-92698-4\\_18](https://doi.org/10.1007/978-3-030-92698-4_18)

501

## 18.1 Introduction

Understanding the isotopic composition of the water that supplies trees ( $\delta_{\text{Source}}$ ) and is incorporated into sugars and cellulose is central to interpreting tree-ring  $\delta^{18}\text{O}$  and  $\delta^2\text{H}$ . When using stable isotope ratios in tree rings,  $\delta_{\text{Source}}$  is often subtracted from the isotopic values in cellulose ( $\delta_{\text{cellulose}}$ ) to isolate the fractionation effects that reflect physiological and climatic controls over leaf gas exchange (Chap. 10, 11, 16); however, especially when using  $\delta_{\text{cellulose}}$  as a proxy for past conditions, measurements of  $\delta_{\text{Source}}$  are rarely available. Thus, predictions and assumptions are often necessary for interpreting tree-ring  $\delta^{18}\text{O}$  and  $\delta^2\text{H}$ . Analytical approaches have relied on predicting  $\delta_{\text{Source}}$  by averaging across some compilation of isotopic values of local precipitation (e.g., Anderson et al. 1998), sometimes implicitly assuming static values (e.g., Helliker and Richter 2008). However,  $\delta_{\text{Source}}$  varies throughout years, among years, among trees, and among sites, yielding measurement and prediction challenges.

The value of  $\delta_{\text{Source}}$  that is recorded in an annual tree ring (after accounting for fractionation) should equal the mean isotopic ratio of xylem water ( $\delta_{\text{xylem}}$ ), weighted by the photosynthetic rate and integrated over the time when that tree grows radially. However, not only are  $\delta_{\text{xylem}}$  measurements generally unavailable for long tree-ring records, using them would involve uncertainties (e.g., regarding the timing of sugars forming cellulose; see Chap. 13). Instead,  $\delta_{\text{Source}}$  is commonly assumed to be constant and equal to the isotopic value of long-term-mean precipitation, but such assumptions have known limitations (e.g., as discussed in Chap. 16 and Roden and Siegwolf 2012). To better account for variations in  $\delta_{\text{Source}}$  and more precisely interpret tree-ring cellulose isotope ratios, several factors should be considered if  $\delta_{\text{Source}}$  estimates are needed (see Fig. 18.1).

The objective of this chapter is to provide an overview of how precipitation, soil, and tree water-uptake processes manifest in variations in  $\delta_{\text{Source}}$ , and how our understanding of those processes informs the interpretation of tree-ring isotope ratios. The numerous biochemical synthesis and translocation processes that further alter  $\delta_{\text{cellulose}}$  in trees, convolving the relationship between  $\delta_{\text{Source}}$  and  $\delta_{\text{cellulose}}$  are discussed in Chaps. 10, 11, and 13, and not covered here. Understanding the processes that control  $\delta_{\text{Source}}$  found in the xylem can lead to practical assumptions and new ways of using tree-ring  $\delta^{18}\text{O}$  and  $\delta^2\text{H}$ , despite the uncertainties in  $\delta_{\text{Source}}$ .

## 18.2 Precipitation Inputs and Their Spatially and Temporally Varying Isotope Ratios

Isotope ratios of precipitation ( $\delta_{\text{precip}}$ ) have been measured and monitored since the 1950s (Dansgaard 1953, 1954), producing a rich body of data and theory describing controls on meteoric-water isotope-ratio variation in space and time. Even these earliest studies recognized that isotope ratios of rainfall were related to meteorology,

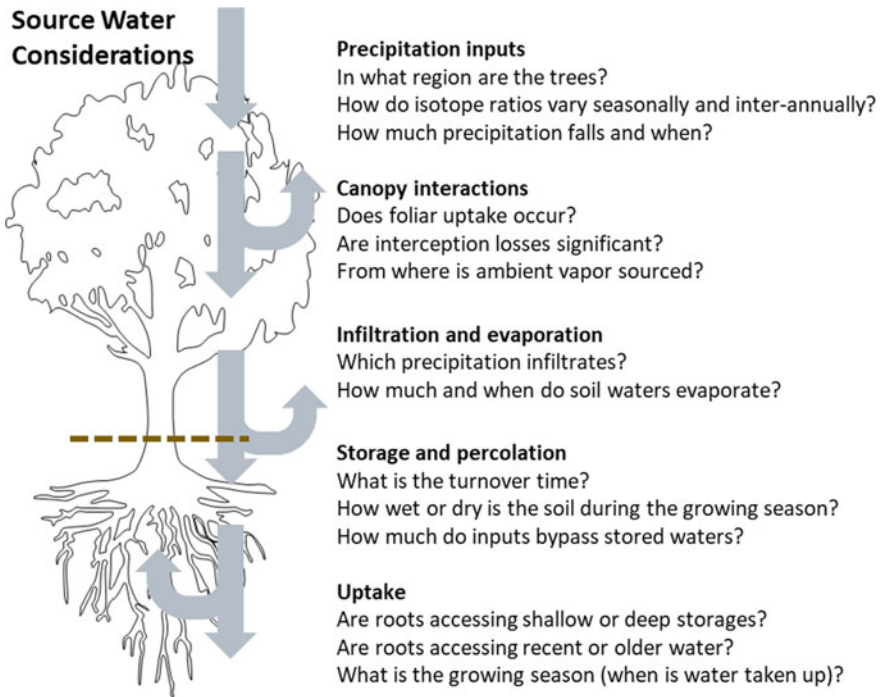


**Fig. 18.1** To estimate the isotopic composition of  $\delta$  source waters to trees, we need to not only consider the average isotopic composition of precipitation at a site. We must also consider which water reaches the soil layers from which roots take up water during the time when plants are transpiring, and how the isotope ratio of that water was influenced by mixing and fractionation processes before reaching roots. While these steps can rarely be quantitatively addressed, asking these questions can help in evaluating which factors should be considered to improve the accuracy of  $\delta_{\text{Source}}$  estimates when interpreting tree-ring isotope ratios

and that different storm systems and different climatic regimes produced rain and snow with contrasting isotope ratios (Dansgaard 1954; Craig 1961). By the mid-1960s, many of the underlying principles had been established, including equilibrium and kinetic fractionation effects that lead to isotopic differences between liquid (isotopically heavier) and vapor-phase (isotopically lighter) water (Fig. 18.2; Dansgaard 1964; Craig and Gordon 1965). These fractionation factors also lead to the progressive depletion of heavy isotopes from the atmosphere as air masses cool and lose water as liquid- or solid-phase condensate (following a so-called Rayleigh distillation process; Kendall and Caldwell 1998). Together these processes explain most of the isotopic variation in meteoric waters, though progress building on this early work has improved understanding of how dynamics and transport within the atmospheric water cycle are expressed in  $\delta_{\text{Precip}}$  across different systems and timescales. The fundamental theory of isotope fractionation in the water cycle was reviewed by

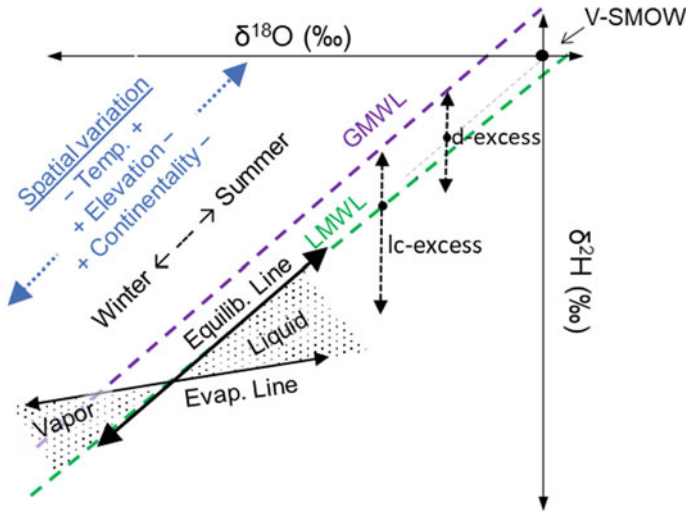


**Fig. 18.2** Water isotope variations in dual-isotope space and the effects of climate variations on environmental water isotope ratios. Incoming precipitation generally falls along a meteoric water line (MWL) which can be described by either the global meteoric water line (GMWL,  $\delta^2\text{H} = 8\delta^{18}\text{O} + 10$ ), or a local meteoric water lines (LMWL) if available for a specific site. The range of precipitation isotope ratio in a given location is strongly related to its temperature, elevation, continentality. The slope of 8, reflecting the relative equilibrium fractionation factors between  $\delta^2\text{H}$  and  $\delta^{18}\text{O}$ , defines the GMWL but it is also common that LMWLs have similar slopes. Variation in precipitation isotope ratios along those MWLs is strongly affected by season. Phase changes result in fractionation, with lighter isotopologues favoring the vapor phase. Thus, fractionation from evaporation causes the remaining liquid water to become isotopically enriched in the heavy isotopes because the departing vapor contains more light isotopes. Fractionation caused by evaporation also results in water isotopes deviating from the MWL, following an evaporation line with a lower slope than that of the MWL. This evaporation line slope relates to the relative humidity, where evaporation lines associated with higher humidity are more similar to the equilibrium fractionation line; at very low humidity, the slope is controlled by the relative diffusivity ratios of  $^1\text{H}^2\text{H}^{16}\text{O}$  to  $^1\text{H}_2^{16}\text{O}$  versus  $^1\text{H}_2^{18}\text{O}$  to  $^1\text{H}_2^{16}\text{O}$ . Deviations from the MWL can be measured as d-excess—the deviation in  $\delta^2\text{H}$  units from the line passing through the origin (defined by the standard V-SMOW) along the equilibrium fractionation slope (equal to 8); thus,  $\text{d-excess} = \delta^2\text{H} - 8\delta^{18}\text{O}$  and the GMWL has a d-excess of 10. To account for LMWLs not always matching the GMWL, lc-excess—the deviation in  $\delta^2\text{H}$  units from the LMWL, where LMWL lc-excess = 0—better quantifies the effects of evaporative fractionation on pools supplied by local precipitation

Gat (1996), and Bowen et al. (2019) provide an update focusing on the integrated expression of these processes in large-scale climatic and hydrological systems.

An assumption in many tree-ring studies has been that water used by trees reflects the isotopic composition of annually- or seasonally-averaged local precipitation (e.g., Anderson et al. 2002; Danis et al. 2006; Evans 2007; Zeng et al. 2016; Lin et al. 2019), which are well-known for the modern climate across much of the Earth through a combination of monitoring and statistical modeling (Aggarwal et al. 2010; Bowen 2010). This assumption implies that the processes delivering water to trees naturally integrate across precipitation inputs at a given site. However, systematic variation in



$\delta_{\text{Precip}}$  exists at many spatial and temporal scales relevant to ecohydrology, and the processes routing meteoric water to plants are selective so the validity of this assumption is often compromised. Here we introduce relevant sources of  $\delta_{\text{Precip}}$  variability, working from large to small spatiotemporal scales, and we discuss the question of routing and selectivity of water uptake in subsequent sections.

Long-term, annual-average  $\delta_{\text{Precip}}$  exhibits substantial (i.e.  $>1 \text{‰ } \delta^{18}\text{O}$ ) variation at spatial scales of tens to thousands of kilometers (Fig. 18.3a). In non-mountainous regions, local isotopic variation (at scales less than 100 km) is more limited (e.g., Price et al. 2008; Liu et al. 2010). In contrast, areas of high topographic relief form

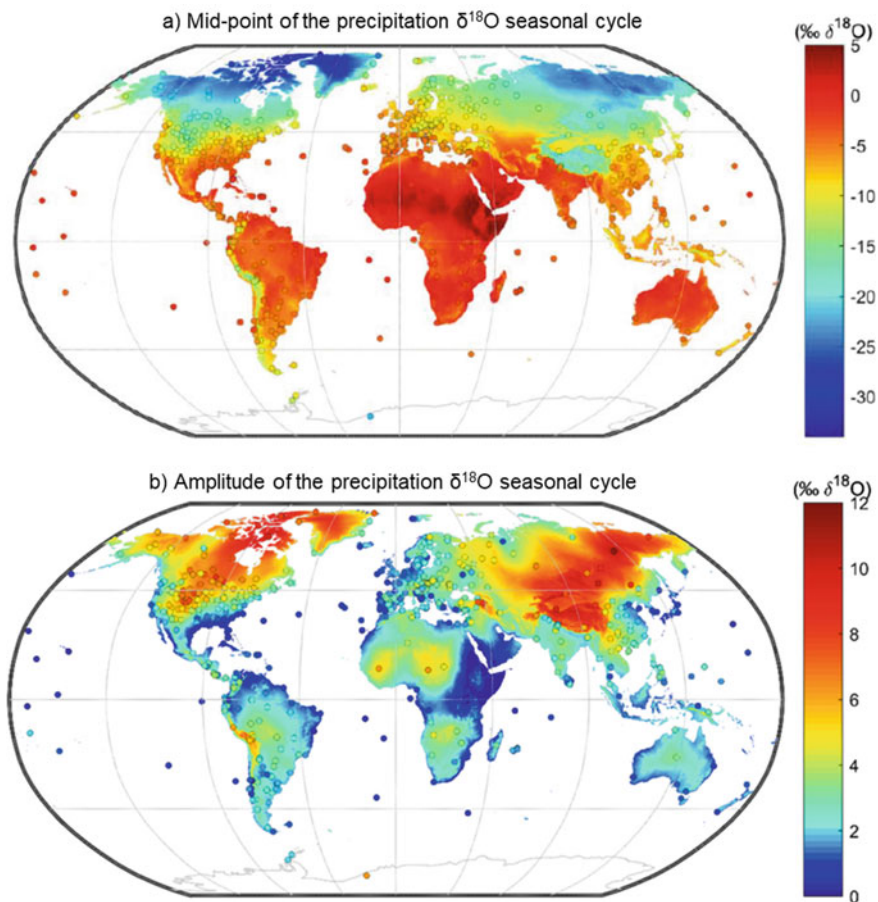


**Fig. 18.3** Maps of global variations in **a** typical average precipitation  $\delta^{18}\text{O}$  and **b** seasonal amplitude (i.e., absolute differences between mean values and either typical mid-summer or typical mid-winter values) of precipitation  $\delta^{18}\text{O}$  (adapted from Allen et al. 2019a). Circles reflect the locations of precipitation isotope monitoring sites, and their fitted average values and seasonal anomalies from those average values. In extra-tropical regions, the highest values occur in summer; elsewhere, the timing of seasonal cycles varies with the migration of the Inter Tropical Convergence Zone

precipitation due to orographic lifting and produce strong and systematic decreases in  $\delta_{\text{Precip}}$  with increasing elevation (Dansgaard 1964; Poage and Chamberlain 2001). The average decrease in  $\delta^{18}\text{O}$  with elevation is approximately  $-0.28\text{‰}$  per 100 m (Poage and Chamberlain 2001) and approximately  $-2.2\text{‰}$   $\delta^2\text{H}$  per 100 m. Consequently, downslope routing of groundwater, streamwater, or other surface waters that generated in higher elevations can result in water available to trees that is isotopically lighter than local precipitation; in such systems the resulting isotopic contrast among locally-available water sources has been used to identify sources of plant water uptake (Dawson and Ehleringer 1991; Chimner and Cooper 2004).

Old groundwater (which could be a tree-water source in areas where that groundwater exfiltrates) can be isotopically distinct from modern precipitation. Evidence from paleo-waters, climate proxy records, and models also clearly suggest large shifts in average  $\delta_{\text{Precip}}$  as Earth's climate system has changed. For example, estimated  $\delta_{\text{Precip}}$  across the northeastern USA during the last glacial period ( $\sim 20,000$  years ago) were likely lighter in  $^{18}\text{O}$  by  $8\text{‰}$  or more relative to modern precipitation (Jouzel et al. 1994). Paleo-waters are relatively common in the subsurface (Jasechko et al. 2017), and although these old waters mostly exist at depths that prohibit their use by plants, they represent an isotopically distinctive source of water that may, in rare cases, be accessed.

Potentially more common are ecosystems in which plants sample unevenly from the seasonal precipitation cycle, and thus the seasonality of  $\delta_{\text{Precip}}$  is an important determinant of source water composition (Fig. 18.3b). Isotopic seasonality is a common feature in the atmospheric water cycle, and is typical of most regions that exhibit climatic seasonality (Bowen 2008). In the extratropics, the lowest isotope ratios are nearly ubiquitously associated with the cold season, whereas isotopic seasonality at lower latitudes is largely associated with seasonal migration of the intertropical convergence zone and associated wet/dry climate cycles (Feng et al. 2009). The largest range of seasonal variation is found in the mid- to high-latitude continental interiors of the Northern Hemisphere, where inter-seasonal  $\delta^{18}\text{O}$  ranges can exceed  $20\text{‰}$  (Bowen 2008). Allen et al. (2019a, b) illustrated how seasonality of  $\delta_{\text{Precip}}$  influences  $\delta_{\text{Xylem}}$ , and that co-occurring species do not necessarily use the same precipitation (more below), so seasonal bias needs to be considered in  $\delta_{\text{Source}}$  estimation.

Understanding inter-annual variations in  $\delta_{\text{Precip}}$  is especially important for tree-ring isotope studies. Inter-annual variability in annual-mean  $\delta_{\text{Precip}}$  can result from not only annual or seasonal  $\delta_{\text{Precip}}$  deviating from its normal pattern, but also from anomalous amounts of summer (higher  $\delta_{\text{Precip}}$ ) or winter (lower  $\delta_{\text{Precip}}$ ) precipitation in given years. Inter-annual variations in annual mean  $\delta_{\text{Precip}}$  often exceed  $1.0\text{‰}$   $\delta^{18}\text{O}$  (Fig. 18.4). Among precipitation monitoring stations with at least five full years of data, standard deviations describing inter-annual variability in amount-weighted annual mean precipitation  $\delta^{18}\text{O}$  ranged from  $0.2$  to  $1.6\text{‰}$  (with a mean of  $0.7\text{‰}$  across 27 sites; Fig. 18.4). In general, inter-annual variability is highest—with maximum ranges among annual means exceeding  $4\text{‰}$   $\delta^{18}\text{O}$ —in regions with larger seasonal  $\delta^{18}\text{O}$  amplitudes ( $r = 0.62$ ), which also tended to have the lowest average  $\delta_{\text{Precip}}$  values.

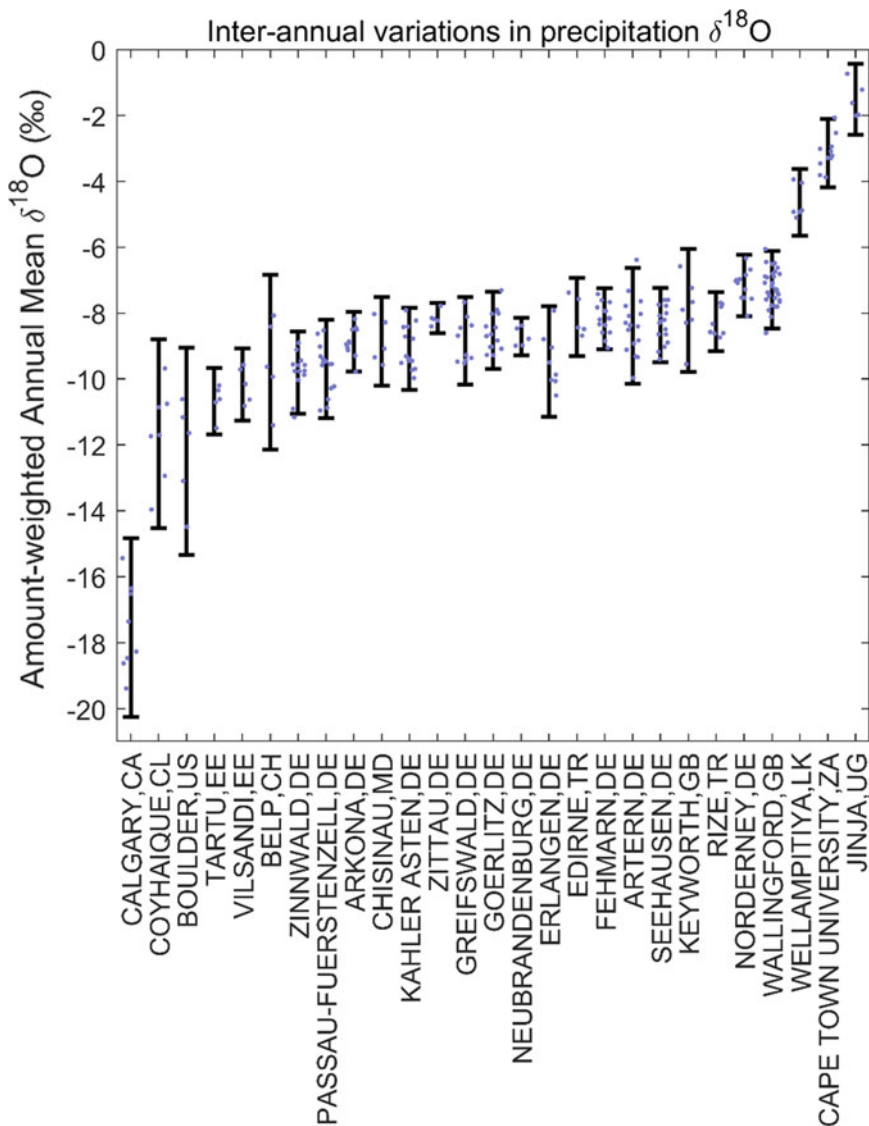


**Fig. 18.4** Amount weighted annual precipitation  $\delta^{18}\text{O}$  means for individual years at GNIP sites. Dots represent individual years and the bars represent  $\pm 2$  standard deviations, describing inter-annual variations. These data are from GNIP sites (IAEA/WMO 2020) that have at least five full years of both monthly  $\delta^{18}\text{O}$  and monthly precipitation amounts; note that there is a several-fold larger set of sites if these criteria are loosened, allowing for gaps in records. Nonetheless, these sites (city and country code indicated on the horizontal axis) span a range of climates and latitudes (e.g., ranging from tropical sites in Uganda and Sri Lanka to northern latitudes in Canada). The monitoring sites are ranked by mean  $\delta^{18}\text{O}$ , demonstrating that the lower values are also associated with higher inter-annual variability in  $\delta^{18}\text{O}$ .

The literature also includes a growing number of examples of  $\delta_{\text{Precip}}$  variation among events or over the course of individual storm events (e.g., Munksgaard et al. 2012; Coplen et al. 2015; Fischer et al. 2017). This evidence extends back to the work of Dansgaard (1953), who measured sub-daily changes in rainfall isotope ratios in Denmark associated with the passage of weather systems. In particular, this work showed a substantial increase in  $^{18}\text{O}/^{16}\text{O}$  as condensation altitude lowered throughout a warm frontal storm, and this general pattern has been subsequently documented and modeled for several other well-organized synoptic-scale events (Gedzelman and Lawrence 1990; Coplen et al. 2008; Pfahl et al. 2012; Aemisegger et al. 2015). While inter-event variations may be mostly damped out in soils and thus not detectable in tree rings, such patterns can be strongly accentuated in large-scale systems such as tropical and extratropical cyclones; in those storms,  $\delta_{\text{Precip}}$  changes of 8–10 ‰ ( $\delta^{18}\text{O}$ ; 60 to 80 ‰ for  $\delta^2\text{H}$ ) have been observed over timescales of hours and/or spatial scales of  $\sim 100$  km (Gedzelman et al. 2003; Coplen et al. 2008; Good et al. 2014a, b). These storms can produce heavy rains with unusually low isotope ratios, in particular (Lawrence and Gedzelman 1996), and evidence suggests that these isotopic anomalies can be passed along to trees and tree rings if the events are especially large or anomalous events (Weiguo et al. 2004; Miller et al. 2006; Berkelhammer and Stott 2008). The evolution of precipitating storms can be complex and spatially heterogeneous, particularly for less organized and/or convective systems. Routine prediction of isotopic variations throughout individual events has not been demonstrated, and many examples of seemingly chaotic fluctuations (Kennedy et al. 2012) suggest that within-storm variation is the norm. However, predicting these patterns remains a research frontier, and thus we do not really know their potential to bias soil water isotope ratios, relative to average  $\delta_{\text{Precip}}$ , if different-sized events infiltrate the soil differently. With that stated, small-scale variations are often less relevant to tree rings because they integrate water signals across longer timescales.

In forests, canopy interception and interception loss can alter the isotopic composition of precipitation reaching soils. During events, slight evaporation occurs from waters stored in canopies that may evaporatively enrich the water that is eventually transmitted downward (i.e., throughfall). Perhaps more importantly (Gat and Tzur 1968), interception also involves the selective transmission of throughfall during events and the omission of the water stored at the end of events that evaporates completely. Given that  $\delta_{\text{Precip}}$  can trend upward or downward throughout events, this selective transmission can result in erratic differences between event-mean throughfall and open-precipitation  $\delta_{\text{Precip}}$ . A synthesis of interception studies (Allen et al. 2017) shows that, on average, the net-precipitation below forest canopies was mostly between 0.2 ‰ lighter to 0.6 ‰ heavier in  $\delta^{18}\text{O}$  than open precipitation (the mean long-term enrichment was 0.19 ‰  $\delta^{18}\text{O}$ ); while individual-event differences can be much larger than these mean values, those short-term variations are erratic. Accordingly, because individual events are small compared to the storage in soils, event-level effects due to interception are likely inconsequential to variations in  $\delta_{\text{Source}}$  and the coarse-resolution signals inferred from tree rings. Nonetheless, enrichment is observed on average over long time scales and thus would represent a small systematic bias if ignored.

Resources to aid in predicting  $\delta_{\text{Precip}}$  inputs to a location are widely available, although subsequent infiltration and uptake processes need to be considered to predict  $\delta_{\text{Source}}$ . Databases of  $\delta_{\text{Precip}}$  and volumes are available for thousands of locations with monthly or better resolution through the IAEA's Global Network of Isotopes in Precipitation (GNIP; Aggarwal et al. 2011), and the Water Isotope Database (waterisotopes.org; Putman and Bowen 2019). Additionally, the National Ecological Observatory Network (NEON) provides a rapidly growing public dataset containing time-series of biweekly  $\delta_{\text{Precip}}$  for sites spanning the United States; however, none are yet long time series, which are especially useful (see Sect. 18.5 and Fig. 18.4). Country-specific precipitation-isotope monitoring networks also exist for Switzerland, Austria, Germany, and elsewhere. Global interpolated data products are also available; for example, see those generated from the Water Isotope Database, which can be queried online (see IsoMap <http://isomap.org> and the Online Isotopes in Precipitation Calculator, <http://wateriso.utah.edu/waterisotopes/>) or downloaded as maps (Bowen et al. 2014). Another option is to develop predictive isoscape maps for the specific study domain (Bowen 2010). In addition to the raw isotope values provided by GNIP and elsewhere, Allen et al. (2019a) provides fitted sine coefficients that describe  $\delta_{\text{Precip}}$  seasonality at > 600 sites globally, along with various site-characteristic covariates. Another promising source of  $\delta_{\text{Precip}}$  estimates, especially for interpreting isotope paleo-proxy records, is isotope-enabled circulation models that output global spatiotemporal variations in  $\delta_{\text{Precip}}$  over past centuries as estimated from sea surface temperatures (Dee et al. 2015; Konecky et al. 2019). Any of these data products can be useful for constraining  $\delta_{\text{Source}}$  estimates in areas where  $\delta_{\text{Precip}}$  data are not available.

### 18.3 From precipitation to Soils and Other Subsurface Storages

Nearly all water used by plants originates from precipitation, whether it be from fog, rain or snow. This precipitation is available to plants from different pools within ecosystems. Two predominant pools are water held under tension in soils (the vadose zone), and water held under pressure in groundwater (the saturated zone). Each can be complex water storages that vary spatially and temporally in isotopic values. Water enters these pools by infiltrating locally or flowing in from upslope areas. In most cases, the local infiltration of rainfall and snowmelt provides water to plants. In other cases, shallow groundwater can directly supply trees. These isotopically diverse subsurface waters largely determine the  $\delta^2\text{H}$  and  $\delta^{18}\text{O}$  in tree rings; therefore, considering how water resides, mixes, percolates, and evaporates in the subsurface is critical to relating precipitation patterns to plant-tissue isotope ratios.

Two aspects mainly affect the isotope ratios of the water in the vadose zone: (1) the transport, mixing and storage of precipitation with varying isotopic composition

within the vadose zone; and (2) the changes of water isotope ratios caused by fractionation during evaporation from soil. Here, we introduce the processes that result in variability in subsurface pore-water isotope ratios. Understanding such processes (e.g., soil–water turnover times or typical depths of evaporative fractionation) can aid in understanding which precipitation may be stored in a soil during the growing season and to what degree soil waters might be evaporatively enriched in heavy isotopes.

### 18.3.1 Water Transport and Mixing

Given that precipitation and  $\delta_{\text{precip}}$  are highly variable, understanding how precipitation travels through the subsurface is key to knowing which precipitation (and associated isotope ratios) will be accessible to plants. Water transport in the unsaturated zone occurs by various mechanisms, with characteristics that can be abstractly characterized as well-mixed flow, uniform translatory (piston) flow (Hewlett and Hibbert 1967) or non-uniform preferential flow (Beven and Germann 1982); in reality, aspects of all of these flow behaviors are relevant.

Subsurface waters are rarely well mixed (Penna and Meerveld 2019), even though well-mixed assumptions are often implicit to common representations of soil and groundwater systems (e.g., Lawrence, et al. 2011). In hypothetical well-mixed systems, a single isotope ratio could be assumed for an entire storage pool, representing the mixture of new inputs and prior storages; in that scenario, the fraction of water extracted by plants, as well as that draining downward from soils, are both unbiased representations of the stored precipitation. This means that more recent precipitation will dominate the storage, and the ‘age’ of the water in storage will match the turnover time (storage/flux). This transport scenario will yield spatially uniform soil–water isotope ratios that vary in time, mimicking a damped and lagged seasonal precipitation isotope cycle. Such assumptions may not apply for soil or shallow groundwater (Penna and Meerveld 2019), but may better apply for large groundwater aquifers that store a mixture of many years or decades of past precipitation; in those conditions, values are relatively spatially and temporally uniform (Vogel and Van Urk 1975), supporting accurate estimates of  $\delta_{\text{Source}}$  waters if it is known that trees are using groundwater.

An older conceptual model of soil–water infiltration is that of uniform translatory flow (also known as plug flow or piston flow), where newly infiltrating precipitation pushes down the previous precipitation stored in soil pores; however, this model has decreased in popularity since the majority of soil isotopic data does not fit this model (Fig. 18.5). This uniform-flow mechanism leads to depth-stratified soil waters, with the shallowest soils containing the most recent inputs (e.g., Fig. 18.5a) and increasingly older precipitation with depth. If newly infiltrated water entirely replaces previously stored water (“piston flow”), (a) no water in the profile will be older than the turnover time and (b) the temporal variations in  $\delta_{\text{precip}}$  would be preserved by depth in soil water isotope profiles (Fig. 18.5a), and (c) tree water isotope ratios would

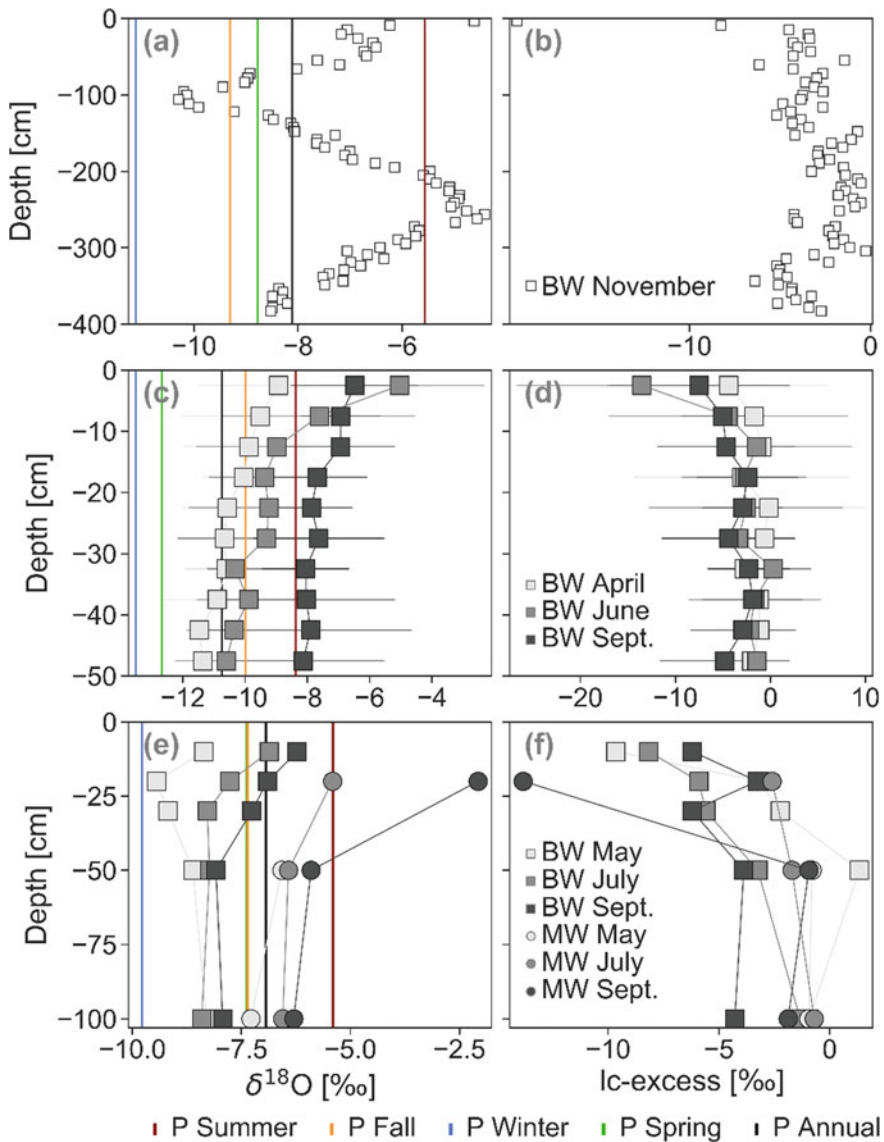


**Fig. 18.5** Example profiles of soil–water  $\delta^{18}\text{O}$  (left) and lc-excess (right) for (a and b) a vineyard near Freiburg, Germany, (c and d) a humid, cold, continental pine forest in southeastern Canada, and (e and f) a Mediterranean pine forest in the Pyrenees, Spain. For c–f, the error bars represent  $\pm 2$  SD and the data show beginning, the middle and end of the growing season. All vertical colored and black lines represent weighted seasonal or annual averages of the  $\delta^{18}\text{O}$  for the sites. For e and f, both the so-called “mobile” (circles) and “bulk” (squares) water values are shown. For further details, see (Sprenger et al. 2016a, 2018b, 2019)

look similar to that of long-term mean precipitation if soils are deep enough to hold years of precipitation and roots take up soil water uniformly across the rooting profile (Sect. 18.4). Alternatively, if trees predominantly use shallow soil water,  $\delta_{\text{Source}}$  would approximate rainfall that fell recently (i.e., usually during the growing season). The rate that this oscillating signal propagates downward (e.g., Fig. 18.5a) depends on how much precipitation falls and how much the soils store. In reality, because flow is never entirely uniform, variation in soil water isotope ratios typically decrease substantially with depth due to mixing (dispersion) during percolation (e.g., Thomas et al. 2013; Barbecot et al. 2018; also see Fig. 18.5).

With non-uniform preferential flow, infiltrating precipitation follows the route of least resistance; new inputs differentially bypass storages to yield an isotopically heterogeneous subsurface (Brooks et al. 2010; Sprenger et al. 2018a, 2019). The more that infiltrating water bypasses storages, the more likely it is that soil matrix water will reflect older precipitation that resides across seasons and disproportionately supplies plants (often referred to ecohydrologic separation; Brooks et al. 2010). How much water flows in preferential flow paths versus trickling through the matrix can depend on soil texture, structure, wetness (Weiler and Naef 2003), biological activity (Schaik et al. 2014), and input amount or intensity (Nimmo 2011). With preferential flow, the refilling of soil water stores may occur periodically, resulting in, for example, the under-representation of precipitation that fell at higher intensities (Jasechko and Taylor 2015; Allen et al. 2019b) or when soils are wet (Brooks et al. 2010; Sprenger et al. 2019). These preferential flows have been observed through showing that (a) waters quickly passing through soils are more similar to recent precipitation than is the entirety of water in soils (including finer pores), and (b) the waters stored in the soil matrix are older than they would be if well-mixed or uniform-flow conditions dominated (Fig. 18.5c; see Berghuijs and Allen 2019). Conventional wisdom in hydrology is increasingly gravitating towards assuming that soil–water transport is highly preferential, especially in forest soils (Flury et al. 1994; Nimmo 2011), and thus  $\delta_{\text{Source}}$  can be potentially biased towards reflecting precipitation from specific times or events when recharge occurs.

To estimate  $\delta_{\text{Source}}$ , researchers should not only consider these soil–water transport concepts but also the general empirical patterns seen in soil–water isotope studies. Real-world soil water transport does not solely reflect any one of these processes, even if we should expect evidence of preferential flows in shallower soils and mixing in deeper soils. These dynamic subsurface flow processes affect the pattern of subsurface isotope ratios in ways that are difficult to predict; this is an active area of research in ecohydrology, with recent progress in generalizing patterns across climates (Sprenger et al. 2016b; Allen et al. 2019b) and across inter-annual climatic variations (Berkelhammer et al. 2020). In general, the isotope ratios of soil water change over the growing season from lower isotope ratios in spring to higher in summer and fall (Fig. 18.5b, c). That is to say, early growing season soil waters are typically lighter than average  $\delta_{\text{Precip}}$ , because they reflect storage of cold-season precipitation, and (at least in shallow soils) later growing season soil waters are typically heavier than average  $\delta_{\text{Precip}}$  (Figs. 18.5). Late growing-season shallow soil water is not only isotopically heavier because of the heavier isotopic



composition of summer rainfall (e.g., compare the red and blue vertical lines in Fig. 18.5), it also results from progressive evaporative fractionation (described in the next section). Deeper soils tend to reflect a more wintry signature, even in regions with summer precipitation (Ehleringer et al. 1991; Williams and Ehleringer 2000; Martin et al. 2018; Allen et al. 2019b). Woody plant xylem frequently expresses this lighter isotope ratio associated with deeper or older precipitation.

### 18.3.2 Evaporation Fractionation of Soil Water

Just as in leaves (Chaps. 10 and 11), evaporation from soils results in the enrichment of heavy isotopes in the residual soil water because light isotopes are preferentially evaporated (Gat and Gonfiantini 1981); however, unlike in leaves, a constant resupply of water rarely exists to move up and replace the evaporated fraction. Evaporation results in heavy isotopes accumulating in the residual soil water until new precipitation mixes with or displaces the enriched pool. Thus, soil water will often be more enriched in heavy isotopes relative to the original precipitation water (Fig. 18.2). These effects are very prominent in shallow soil–water samples (Fig. 18.6), although, the most evaporatively enriched soil–water pools are generally of small volume and not necessarily a major contributor to plants (discussed further in Sect. 18.4). Nonetheless, studies inferring uptake depths or precipitation sources should consider potential alterations in  $\delta_{\text{Source}}$  attributable to evaporation (Tang and Feng 2001).

Kinetic fractionation of stable isotopes of water leads to sources deviating from the meteoric water line (Fig. 18.2) because of differences in the relative diffusivities between  $^2\text{H}^1\text{HO}$  and  $^1\text{H}_2\text{O}$  compared to  $^1\text{H}_2^{18}\text{O}$  and  $^1\text{H}_2^{16}\text{O}$  (Horita et al. 2008). Until recently, deviations from meteoric water lines were mostly quantified using d-excess ( $\delta^2\text{H} - 8 \times \delta^{18}\text{O}$ ), where 8 is the ratio of equilibrium fractionation factors of O and H, defining the slope of the global meteoric water line (Dansgaard 1964); however, local meteoric water lines (LMWLs) often deviate from a slope of 8 (Putman et al. 2019). Thus, variation in d-excess does not imply evaporation because precipitation inputs along a LMWL with slopes different from eight will also vary in d-excess, regardless of any subsequent evaporation. Accordingly, the line-conditioned excess (lc-excess), defined relative to LMWLs ( $\text{lc-excess} = \delta^2\text{H} - \text{slope}_{\text{LMWL}} \times \delta^{18}\text{O} - \text{intercept}_{\text{LMWL}}$ ) is more appropriate for inferring terrestrial evaporation (Landwehr and Coplen 2006). Shallow soil lc-excess values can be well below zero, even in humid climates (Sprenger et al. 2016). Low lc-excess values are especially common following extended warm periods without rain (Sprenger et al. 2018b), e.g., in summer and early autumn (Fig. 18.5d). Although few tree ring isotopic studies have used both  $\delta^2\text{H}$  and  $\delta^{18}\text{O}$  from plant tissue in conjunction (but see Voelker et al. 2014), this area of research is advancing because this dual-isotope approach can provide new insights into past evaporative conditions (see Chaps. 10 and 11). Alternatively, evaporation effects in dual isotope space can also be ‘compensated’ by assuming theoretical evaporation lines (which can be notably different than

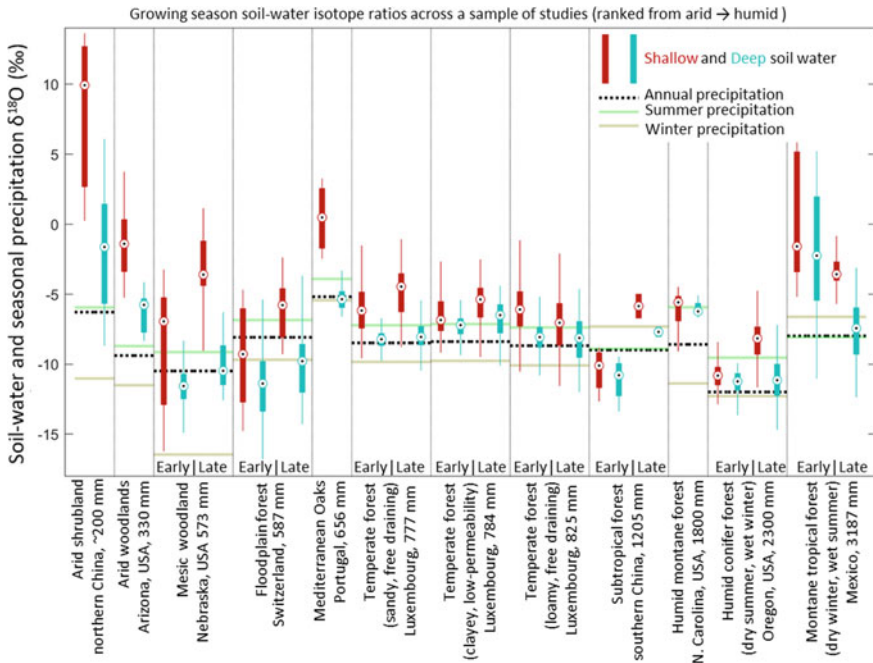


**Fig. 18.6** Soil–water isotope values compared to the estimated seasonal precipitation inputs at those sites. All soil–water values are from the growing season, when possible separated as early (April–June) versus late (July–September) growing season values. Summer and winter precipitation are defined relative to the solar cycle (thus, for the tropical sites, winter is not necessarily colder). “Shallow” includes depths from 5–30 cm; “Deep” includes depths from 30–100 cm (and to 300 cm for the Nebraska and Luxembourg sites). The studies are as follows: Arid shrubland in China (Zhou et al. 2011), Arid woodlands in Arizona (Snyder and Williams 2000), mesic woodland in Nebraska (Eggemeyer et al. 2009), Floodplain forest in Switzerland (Bertrand et al. 2014), Mediterranean oaks in Portugal (Kurz-Besson et al. 2006), sites in Luxembourg (Sprenger et al. 2016c), Subtropical forest in southern China (Rong et al. 2011), humid montane forest in North Carolina (Berry et al. 2014), a Humid conifer forest (Brooks et al. 2010), and a montane tropical rainforest (Goldsmith et al. 2012). Precipitation data are calculated using the online isotope in precipitation calculator: <http://wateriso.utah.edu/waterisotopes/>. Note that precipitation estimates can be imprecise; for example, in the Goldsmith et al. study, positive  $\delta^{18}\text{O}$  values for summer rainfall are common. Also, note that the most evaporative enriched soil waters are unlikely to be a substantial source to plants because there is usually minimal water content in these locations

empirical ‘evaporation’ lines) and relating soil and plant waters to their precipitation sources (Benettin et al. 2018; Bowen et al. 2018), for insights into how soil–water is recharged by precipitation.

### 18.3.3 Predicting Soil Water Isotope Ratios from $\delta_{\text{Precip}}$

Methods for predicting the complex interplay between newly infiltrating precipitation and previously stored water (that is often evaporatively fractionated) could support more accurate uses of tree-ring isotope ratios. Hydrologists use both mechanistic simulation models and statistical, “lumped” models to represent soil water processes. Parameterizing those models is data intensive, requiring measurements of soil water or outflow isotope ratios (e.g., Braud et al. 2005; Haverd and Cuntz 2010; Stump et al. 2012; Mueller et al. 2014; Sprenger et al. 2015) to capture the dominant mixing processes (Sect. 3.1), towards generating simulated rooting-zone water isotope time series. While such models can be effective, requiring data-driven parametrizations undermines their usefulness with long tree-ring isotopic records. Given that soil water is an ensemble of fractions of previous precipitation events, soil–water can be estimated as a distribution of those past events (Groh et al. 2018; Benettin et al. 2019); thus transfer functions capturing a statistical relationship between inputs and outputs may be more practical than mechanistic models and outperform estimates implying that soils contain an even mixture of annual precipitation. Otherwise, syntheses of growing season soil–water isotopes measurements show some generalities that aid in constraining expectations.

Soil water  $\delta^{18}\text{O}$  generally deviates from local  $\delta_{\text{Precip}}$  across a wide range of sites (as shown here; Fig. 18.6). Shallow soil–water is isotopically heavier than the typical seasonal precipitation inputs, especially in arid regions, demonstrating strong evaporative enrichment. This pattern diminishes from arid to humid (left to right), with exceptions occurring in sites with extended dry seasons (e.g., during the dry summer in Portugal and following the dry winter in Mexico; Fig. 18.6). In regions where the growing season involves more continuous evaporation, soil water  $\delta^{18}\text{O}$  in the late growing season is usually higher than early growing season  $\delta^{18}\text{O}$  (Fig. 18.6); thus, changes in soil water  $\delta^{18}\text{O}$  throughout a season can be confounded with changes in depth of uptake. Importantly, these highly enriched shallow soil waters should be scarce and under high tension after undergoing significant evaporation, and thus they are not likely to be the primary water source to trees; furthermore, most tree radial growth occurs near the beginning of the growing season (Zweifel et al. 2006; Swidrak et al. 2013), often prior to the development of strong evaporation signatures in soil water isotope ratios. Hence, tree source waters recorded in tree ring  $\delta_{\text{cellulose}}$  are unlikely to have  $\delta_{\text{Source}}$  values that are as high as late-season shallow soil water values (Fig. 18.6).

In wetter regions, evaporation effects are less prominent and thus isotope ratios in soils tend to be bounded by seasonal  $\delta_{\text{Precip}}$ ; however, conditions need to be considered on a case-by-case basis. For example, the Swiss floodplain forest (Fig. 18.6) is likely influenced by a riparian aquifer, explaining its lack of evaporative signal; in general, groundwater tends to be dominated by winter precipitation (Jasechko 2019), and in this case, groundwater is likely sourced from higher elevation precipitation (Bertrand et al. 2014). Another prominent feature across these sites is that deeper soil waters are typically isotopically lighter, because they generally experience less

evaporation and water with this evaporated signal only partially trickles downward (i.e., preferential flow), and less variable because of mixing with stored preferential flow; furthermore, the conventional wisdom is that winter precipitation tends to percolate deeper because surface soils are drying less during summer. The deeper soil waters are mostly enveloped by the typical summer and winter  $\delta_{\text{Precip}}$ ; notable exceptions are the driest site, where deeper soil waters may still show strong evaporative enrichment, and the tropical rainforest in Mexico, where the original study (Goldsmith et al. 2012) reports higher precipitation  $\delta^{18}\text{O}$  than those predicted by the Online Isotopes in Precipitation Calculator (waterisotopes.org). While using these precipitation predictions provides consistency across studies,  $\delta_{\text{Precip}}$  predictions can be uncertain across topographically complex regions, especially when predicting  $\delta_{\text{Precip}}$  in individual years (Sect. 18.2).

These patterns shown (Fig. 18.5) are explainable, albeit not necessarily a-priori predictable. Nonetheless, our first-order theoretical expectation should be that with larger fluxes (i.e., precipitation inputs) or shallower rooting zones (smaller storages), soil–water turnover times are higher and thus they should more reflect in-phase precipitation isotope values (i.e., growing season). This general pattern is shown in xylem water collected in a snapshot sample across >100 sites in Switzerland, defining steep climate and elevation gradients (Fig. 18.7a). While estimated  $\delta_{\text{Precip}}$  decreases near monotonically with elevation, xylem water  $\delta^{18}\text{O}$  does not; these measurements highlight the influence of climate gradients on  $\delta_{\text{Source}}$ . Deviations of xylem water (and thus soil–water available to those plants) from mean annual  $\delta_{\text{Precip}}$  increase with elevation and precipitation amount (Fig. 18.7b), which mostly co-vary in Switzerland; thus, the drier region trees used out-of-season precipitation whereas the wetter region trees use growing-season precipitation, demonstrating the higher turnover in wetter regions. This one example demonstrates how considering the relationship between more precipitation and higher turnover times can guide evaluations of  $\delta_{\text{Source}}$  variations across sites.

## 18.4 Roots and Uptake Patterns

Patterns in root water uptake add another layer of uncertainty to assumptions about how  $\delta_{\text{xylem}}$  relates to annual  $\delta_{\text{Precip}}$ . Earlier, we discussed how soils do not behave like sponges that store and perfectly reflect the isotopic composition of annual rainfall. Similarly, the water that roots take up does not perfectly reflect the isotopic composition of the average soil water. In this section, we highlight how roots take up water, and how those processes influence  $\delta_{\text{Source}}$ .

Water flows from soils into plants along a passive water potential gradient known as the soil–plant atmosphere continuum (SPAC). Water enters trees primarily through their non-suberized fine roots along an apoplastic route, and minimally through a symplastic route where water is actively transported across cell membranes. Water traveling along the SPAC apoplastically does not isotopically fractionate (Dawson and Ehleringer 1991, 1993), albeit analytical errors can occur and soil and plant

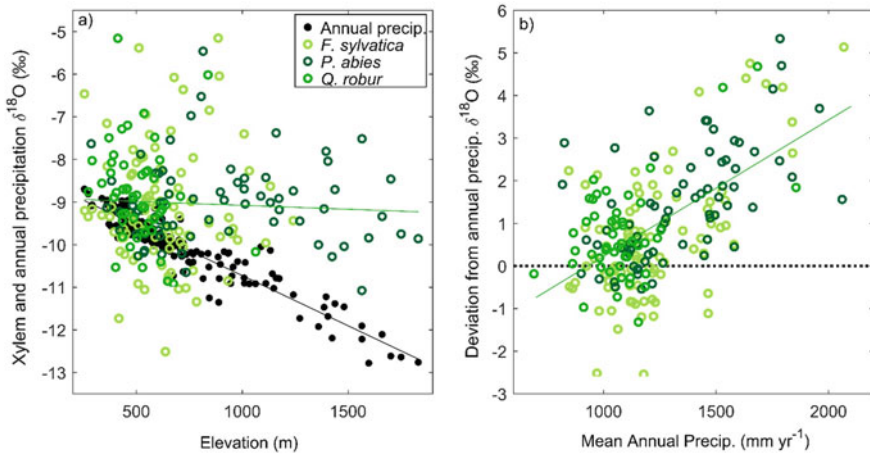


**Fig. 18.7** **a** Annual precipitation and xylem water  $\delta^{18}\text{O}$  versus elevation and **b** xylem water  $\delta^{18}\text{O}$  differences from precipitation  $\delta^{18}\text{O}$  versus mean-annual precipitation amount in Switzerland; elevation and annual precipitation are largely collinear here. Panel a shows decreasing  $\delta^{18}\text{O}$  of precipitation with increasing elevation, which is true for most locations on Earth. However, xylem-water (mid-summer values)  $\delta^{18}\text{O}$  did not decrease with elevation. This probably relates to the greater precipitation amounts in higher elevations driving shorter soil–water turnover times, such that the water stored in soils is more in-phase with current precipitation (i.e., wetter climate soils store more summer precipitation in summer). Panel b shows the relationship between xylem-water  $\delta^{18}\text{O}$  at the same sites, but as deviations from annual precipitation  $\delta^{18}\text{O}$  which range from  $-3$  to  $5\%$   $\delta^{18}\text{O}$ ; in wetter areas, this  $\delta^{18}\text{O}$  deviation increases ( $r = 0.59$  and Spearman's  $\rho = 0.47$ ,  $p < 0.001$ ), consistent with the greater soil–water turnover. Considering these relationships allows for avoiding the systematic biases that can result from assuming that xylem water equals annual precipitation across climatologically distinct sites

water are not always identical in a given instance in time (Vargas et al. 2017; Penna et al. 2018; Barbeta et al. 2020). However, plants that do use symplastic transport for water uptake, such as salt tolerant plants that exclude salts from uptake pathways, have shown isotopic fractionation of  $^2\text{H}$  during water uptake (Lin and Sternberg 1993; Ellsworth and Williams 2007). Many salt-excluding species have a highly developed Casparian strip which impedes apoplastic water movement into the endodermis, forcing water through symplastic routes crossing cell membranes. The symplastic route of water movement allows for exclusion of unwanted molecules such as salts, but costs energy for active transport. The energy required for disassociating hydrogen bonding of individual water molecules is greatest for water molecules containing  $^2\text{H}$ , compared to other isotopologues of water (Clark and Fritz 1997). As a result, water within stems of salt tolerant species has lower  $\delta^2\text{H}$  values relative to the source water, without having measurable differences in  $\delta^{18}\text{O}$  (Lin and Sternberg 1993; Ellsworth and Williams 2007).

For the majority of tree species with apoplastic water uptake, water within the xylem approximates a spatially integrated mixture of soil water from a plant's population of fine unsuberized roots, proportional to their uptake rates. Therefore, the origin

of water within the xylem will depend on a plant's root distribution and water uptake rates. Roots decline in density asymptotically with soil depth, with the majority of plant roots occurring within the upper 30 cm of the soil profile (Gale and Grigal 1987; Jackson et al. 1996; Warren et al. 2005). For tree species, the percentage of roots in the upper 30 cm varies from a high of 83% in boreal forests, to a low of 52% in temperate coniferous forests (Jackson et al. 1996). However, variation between sites was highly dependent on soil texture, water availability, and depth to water table, permafrost, or rock. In general, roots are deeper in seasonally dry regions and shallower in regions where soils remain wet (Fan et al. 2017). Thus, in humid regions, not only do soils hold waters sourced from recent, growing-season precipitation (Sect. 18.3), trees are more shallowly rooted and likely use shallower water which should generally be composed of more recent precipitation (Figs. 18.7 and 18.8). In contrast, drier regions likely contain a long-duration mixture of past precipitation and trees are more deeply rooted and thus likely use deeper waters that have dampened and lagged expressions of  $\delta_{\text{Precip}}$ . Xylem water from deeply rooted trees should rarely express the highly evaporated waters observed in shallow soils in the same sites (Figs. 18.7 and 18.8). Some roots can extend down far below the soil bedrock interface allowing them to access deep water reserves (Canadell et al. 1996). Thus while the majority of roots are located in the top of the soil profile,

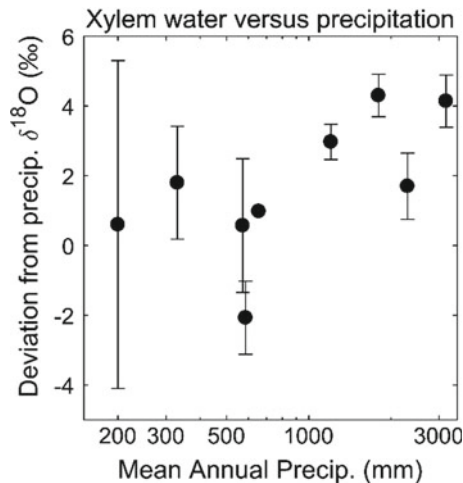


**Fig. 18.8** Mean growing season xylem-water isotope values as a deviation from annual precipitation  $\delta^{18}\text{O}$ , plotted against site mean annual precipitation amount; these are data from the same sites as those in Fig. 18.6, minus the Luxembourg sites because they lacked xylem water measurements. Note that xylem water does not reflect evaporative enrichment above  $\delta_{\text{Precip}}$  as strongly as does soil water (Fig. 18.6) because trees often use deeper waters, although the high variability in the driest site likely results from evaporation effects. Xylem water in wetter sites is generally more enriched compared mean precipitation ( $r = 0.67$ ,  $p < 0.05$ ), in contrast with the expected effects of evaporative enrichment being greater in drier sites; this presumably reflects the presence of shallower roots and more in-growing-season precipitation in soils of wetter regions

rooting depths can extend below 50 m allowing trees access to many isotopically different water pools.

In some cases, a subset of roots can account for the majority of water uptake, which can explain dissimilarities between physical root distributions and isotope-inferred uptake depths. If all roots were equally taking up water, then the proportion of water acquired from different depths would match the distribution of fine roots; however, root water uptake rates vary with depth depending on root hydraulic properties, soil moisture content and soil water potential. When soils are at field capacity and both soil water content and plant water potential are high, small gradients in water potential are associated with relatively large fluxes of water. The majority of root water uptake during these periods is from the upper soil layer where rooting density is high. As soils dry, equivalent drops in soil water potential yield smaller and smaller volumes of water since soil moisture release curves relating water potential to water content are non-linear (Selker et al. 1999). Root water uptake shifts to deeper layers as the soil moisture content in the upper soils decreases (Warren et al. 2005; Brooks et al. 2006). The ability of roots to extract water also varies by species and with depth in the soil. Meinzer et al. (2007) found that relative uptake per root area increased with rooting depth for both Douglas-fir and western hemlock. Plants with roots extending far beyond the soil can access rock water and deep water aquifers which can sometimes make up a substantial portion of xylem water even though only a small proportion of roots extend to those depths (Schwinning 2010; Oshun et al. 2016), regardless of shallow root abundances. Phreatophytes—plants using groundwater—often have deep taproots reaching water tables which can account for a large portion of their water uptake, even though the taproot is a small portion of their rooting system (Burgess et al. 2000; Hultine et al. 2003a, b). Thus, roots at deeper depths are not only likely to be rooted in soils or substrates that maintain moisture for longer, these deep roots can transport more water, compensating for the relatively fewer roots at deeper depths in soil profiles. Ultimately, the isotopic composition of xylem water of an individual tree will reflect the integrated isotopic composition of soil water accessed by that tree's roots, weighted by those root's water uptake rates.

Isotopic approaches have been used extensively to understand the dynamics of root water uptake, and niche partitioning of soil water resources by plants within a community (e.g., Ehleringer et al. 1991; Meinzer et al. 2007; Goldsmith et al. 2012; Guo et al. 2018). Inferring uptake depth using isotopes requires known isotopic variation within the soil either spatially, temporally or both (see Sect. 18.3). Generally, spatial variation in soil water isotopic composition is measured along a depth profile, but spatial variation within a soil layer is also likely (e.g., Goldsmith et al. 2019), and the isotopic composition of water being extracted by roots may not match the bulk isotopic composition of soil water within a layer. Where exactly root tips are located within a layer (e.g., within or around soil pedons) will influence water potential and content they experience, and which water pool they can take up. Spatial variation in all of these factors is complicated even when soils are relatively uniform (McCully 1999; Carminati et al. 2010). While water flows passively along a water potential gradient, roots are alive and the rhizosphere around roots are filled with living organisms that can excrete compounds that can change water potentials (McCully 1999).

Additionally, mycorrhiza have been shown to transport water that is taken up by plants (Warren et al. 2008). Understanding these living interactions and how they influence water traveling along the SPAC has implications for the isotopic composition of xylem water; this is an active area of research.

Another complicating factor in determining the source of water uptake within the soil is hydraulic redistribution. Hydraulic redistribution is the passive movement of soil water from one region of the soil to another via roots along a water potential gradient (Caldwell and Richards 1989; Caldwell et al. 1998; Neumann and Cardon 2012). When plants are transpiring, the water potential gradient within the plant drives water flow to the leaves and the atmosphere. However, if transpiration stops, e.g., during the night, then water can flow along potential gradients within the soil. Generally, water will flow from moist soils at depth to the dryer surface soils, and this process was originally described as hydraulic lift. However, water can flow downward via roots after rains (Ryel 2004), as well as laterally (Brooks et al. 2002, 2006), prompting the more generalized term of hydraulic redistribution. Hydraulic redistribution would act to mute isotopic variation within the soil profile, but the volumes of water that are released to the soil are small compared to the volume of water within the soil (Neumann and Cardon 2012). For example, at 5% soil water content, 10 cm of soil would hold 5 mm of water, but rates of hydraulic redistribution are around 0.02 mm within 10 cm of soil per night, several orders of magnitude smaller than the water content (Warren et al. 2007). In addition, the water excreted from the root during the night is the first water to be taken up as transpiration begins again, so isotopic differences between redistributed water and the soil water would not accumulate over time. Thus, the resulting isotopic shifts in soil water are unlikely to be detectable unless a strong isotopic label is used (Brooks et al. 2002, 2006), implying that they are unlikely to strongly influence tree-ring isotope applications.

Roots extract and integrate water from different pores and depths, and thus  $\delta_{\text{Source}}$  variations are dampened compared to those of individual soil samples. Nonetheless, temporal variation in soils and xylem water sources can manifest in  $\delta_{\text{Source}}$  varying spatially and temporally, introducing challenges to tree-ring  $\delta^2\text{H}$  and  $\delta^{18}\text{O}$  interpretations. Furthermore, xylem water concurrently sampled from individual trees or branches in the same site can vary by 1–2 ‰  $\delta^{18}\text{O}$  (Goldsmith et al. 2019). Thus, uncertainties and variations in source waters (and thus  $\delta_{\text{Source}}$ ) should always be assumed. Nonetheless, plant-rooting characteristics are a tertiary control over  $\delta_{\text{Source}}$ , because roots can only extract water from that which is input to the system as precipitation and held in the subsurface rooting zone (i.e., the primary and secondary controls). Therefore, discussion of how rooting depth relates to  $\delta_{\text{Source}}$  depends on some understanding of  $\delta_{\text{Precip}}$ , its variations, and how it resides in soils.

Foliar uptake is an alternative uptake pathway that bypasses root and soil processes. The uptake of water on leaf surfaces, typically occurring under foggy, humid conditions (Simonin et al. 2009; Gerlein-Safdi et al. 2018) when plants have lower water potentials (Goldsmith et al. 2013), represents a potentially different isotopic signature. These are generally small supplements of water (Gotsch et al. 2014), and identifying their magnitude is difficult because the isotopic effects of foliar uptake are also not always distinguishable from the back diffusion into stomata



that occurs with transpiration (Goldsmith et al. 2017; Lehmann et al. 2017; also see Chaps. 10 and 11). Foliar uptake effects on tree-ring isotope ratios are not well described, but if boundary layer vapor isotope ratios are roughly in equilibrium with precipitation (see Fiorella et al. 2019), foliar uptake may not have a substantial effect on  $\delta_{\text{Source}}$ ; this is because the fluxes are small and the effects match those of the back diffusion already accounted for in leaf-atmosphere fractionation representations (Chap. 10).

## 18.5 Applications and Practical Considerations

### 18.5.1 Assuming $\delta_{\text{Source}}$ Values to Study Leaf-Climatic Interactions

Knowing the value of  $\delta_{\text{Source}}$  is critical for many applications using tree-ring  $\delta^{18}\text{O}$  (and  $\delta^2\text{H}$ ) because much of the theory is based on isotopic shifts relative to  $\delta_{\text{Source}}$  and is calculated as  $\Delta_{\text{cellulose}} \approx \delta_{\text{cellulose}} - \delta_{\text{Source}}$  (Barbour 2007). Often  $\Delta_{\text{cellulose}}$  is used to infer leaf-atmosphere interactions, because transpiration and vapor exchange with the atmosphere alter the isotopic ratio of leaf water in systematic ways (Chaps. 10 and 11). As a result,  $\Delta_{\text{cellulose}}$  is used as a proxy for climate and leaf physiology, after accounting for the many mixing and fractionation processes that occur during the incorporation of leaf water into cellulose (see Chaps. 10, 13, and 16). Thus, accurate knowledge or predictions of  $\delta_{\text{Source}}$  through time are key to accurate  $\Delta_{\text{cellulose}}$  estimates and interpretations.

A common assumption for estimating  $\delta_{\text{Source}}$  to calculate  $\Delta_{\text{cellulose}}$  of an annual increment is that  $\delta_{\text{Source}}$  is equal to long-term mean  $\delta_{\text{Precip}}$  at a given location. Indeed, trees integrate soil water both temporally and spatially so that the annual value of  $\delta_{\text{Source}}$  is often bounded by the annual range of  $\delta_{\text{Precip}}$  inputs to a site (unless the trees use shallow soil waters that are especially fractionated by evaporation). Soils could possibly be an unbiased mixture of a year's precipitation, but in most scenarios (especially in more humid regions), the rooting-zone in soils can only hold a small fraction of a year's precipitation: e.g., consider that most roots are within the upper 30 cm of soil (Gale and Grigal 1987), which could hold a maximum of 90 mm of precipitation if the field capacity is 30%. In contrasting settings with deep roots, water may only occasionally percolate to the deeper depths that disproportionately supply trees. Thus, where evaporation ratios or seasonal variation in  $\delta_{\text{Precip}}$  is large,  $\delta_{\text{Source}}$  could deviate (systematically) from long-term mean  $\delta_{\text{Precip}}$  by several ‰  $\delta^{18}\text{O}$  or tens of ‰  $\delta^2\text{H}$ .

Assuming  $\delta_{\text{Source}}$  is always equal to long-term mean  $\delta_{\text{Precip}}$ , and thereby also assuming that  $\delta_{\text{Precip}}$  is constant over time (Fig. 18.4) can confound interpretations of *inter-annual variations* in  $\Delta_{\text{cellulose}}$ . To mitigate temporal uncertainties, where possible, one can:

- Select sites where soil or xylem water isotope ratios have been measured over years of contrasting meteorological conditions to test how dry or wet years affect the soil–water or xylem–water isotope ratios, e.g., to rule out their influence on signals that are assumed to be due to  $\Delta_{\text{cellulose}}$ . For measuring soil water, bulk samples (e.g., taken with an auger) should be used because suction lysimeters sample water that is more likely to drain quickly and not contribute to transpiration. For xylem water, twigs or cores should be collected. Both soils and xylem material should be sampled a few times throughout the growing season and extracted water by cryogenic vacuum distillation (see the discussion on sampling in Penna et al. 2018).
- Select sites where inter-annual variations in  $\delta_{\text{Source}}$  are small, e.g., because  $\delta_{\text{Precip}}$  variations are small, or trees use streamwater or groundwater with a less dynamic stable isotope signature (e.g. Ulrich et al. 2019). Interestingly, these site conditions for stable  $\delta_{\text{Source}}$  contrast with the droughty edaphic sites where tree-ring widths are more responsive to temperature, precipitation, or humidity, and thus droughty sites are often preferred for dendroclimatological applications.
- Select sites where long records of  $\delta_{\text{Precip}}$  exist, or where magnitudes of inter-annual variations in mean  $\delta_{\text{Precip}}$  can be constrained using publicly available  $\delta_{\text{Precip}}$  datasets, which should provide a basis for estimations of uncertainties in assuming constant  $\delta_{\text{Source}}$ .
- If there are no means of estimating  $\delta_{\text{Precip}}$  and  $\delta_{\text{Source}}$  variability, then uncertainties in  $\delta_{\text{Source}}$  should be assumed and interpreted accordingly. While values of assumed uncertainty cannot be universally prescribed, Figs. 18.4 and 18.8 show potential ranges of inter-annual  $\delta_{\text{Precip}}$  variability and  $\delta_{\text{Source}} - \delta_{\text{Precip}}$  differences that can occur.

Assuming  $\delta_{\text{Source}}$  is always equal to long-term mean  $\delta_{\text{Precip}}$  can confound interpretations of *spatial variations* in  $\Delta_{\text{cellulose}}$  across climate gradients. For example, deviations of  $\delta_{\text{Source}}$  from mean annual  $\delta_{\text{Precip}}$  can depend on climate (Fig. 18.7). To mitigate spatial uncertainties associated with  $\delta_{\text{Source}}$ , where possible, one can:

- Select sites where trees have predictable sources with relatively stable isotope ratios (e.g., obligate phreatophytes), and measure their xylem water isotopic values.
- Select sites where precipitation, xylem and/or soil water isotopic data are available or can be measured to estimate how  $\delta_{\text{Source}}$  relates to  $\delta_{\text{Precip}}$ .
- Select sites with similar climates, soils, and species to where past studies have estimated the relationship of  $\delta_{\text{Source}}$  to mean  $\delta_{\text{Precip}}$ .
- Search online isotopic databases for  $\delta_{\text{Precip}}$  data and streamwater isotope time series (i.e. IAEA Global Network of Isotopes in Rivers, GNIR, Water Isotope Database wiDB, waterisotopes.org, etc.). These data can be used to estimate the mean isotope ratio of evapotranspired waters (see Eq. 21 in Kirchner and Allen, 2020).
- If there is no way to estimate or constrain how  $\delta_{\text{Source}}$  differs from mean annual  $\delta_{\text{Precip}}$ , then  $\delta_{\text{Source}}$  can be assumed to have uncertainties of magnitudes reflecting the seasonal amplitude in  $\delta_{\text{Precip}}$  (Fig. 18.3).

Assuming  $\delta_{\text{Source}}$  is always equal to long-term mean  $\delta_{\text{Precip}}$  can confound interpretations of *species or individual-tree differences* in  $\Delta_{\text{cellulose}}$ , even at the same site. Many species and individuals use different water pools in the subsurface (e.g., due to differences in rooting depths). To mitigate inter species uncertainties, where possible, one can:

- Select sites where all species use groundwater or soil waters  $\delta^{18}\text{O}$  is relatively homogenous (which should involve measuring xylem water  $\delta^{18}\text{O}$  to document the similarity between species).
- Measure xylem water  $\delta^{18}\text{O}$  over a growing season to benchmark expected differences between  $\delta_{\text{Source}}$  and  $\delta_{\text{Precip}}$  for each species. This assumes that measurements of  $\delta_{\text{Precip}}$  are available or are also measured.
- Select sites where rooting depth information is available for the species of interest. Insights into the relative rooting depths can be used to understand how  $\delta_{\text{Source}}$  may differ in time for different trees at the same site (e.g., a tree that uses shallow water exclusively may experience more inter-annual variation in  $\delta_{\text{Source}}$  than does one that uses deeper soil water with less variation in  $\delta^{18}\text{O}$ ).
- Assume that trees within a single site vary substantially, and the variation is not always attributable to species. The mean within-plot range was 1.8 ‰ for the xylem-water samples in Fig. 18.7. Without some information on  $\delta_{\text{Source}}$  or rooting depth, it may be impossible to interpret species or individual differences in  $\Delta_{\text{cellulose}}$ .

### 18.5.2 *Inferring the Source of Water from Tree Rings Isotope Ratios*

Another application of tree-ring  $\delta^{18}\text{O}$  ratios is identifying the water sources used by trees. Often questions pertain to inferring changes in sources of water to trees (e.g., by depth, or between soil water, stream water and groundwater), across species, climates, landscapes, or time (e.g., (Sargeant et al. 2020; Miller et al. 2006; Sarris et al. 2013; Saurer et al. 2016; Sargeant and Singer 2016)). All of these questions require first accounting for the fractionation undergone from source-water to cellulose, a sequence known to vary with meteorological conditions, species, and canopy position (this is the subject of Chaps. 10, 11 and 13); it should also be noted that constraining the leaf-atmosphere exchange fractionation sequence described in Chaps. 10, 11, and 13 also assumes knowledge of the isotopic ratio of ambient atmospheric water vapor, which can be out of equilibrium with local water sources (Fiorella et al. 2019).

After accounting for leaf-level fractionation effects, this application assumes that residual **variations in cellulose  $\delta^{18}\text{O}$  reflect variations in  $\delta_{\text{Source}}$** . Indeed  $\delta_{\text{source}}$  can be substantially different between pools: shallow soil waters are often isotopically heavier (than deeper soil water, river water, or groundwater), because they are influenced more by evaporative fractionation, and they are also more likely to be sourced from recent growing season precipitation that is isotopically heavier than

winter precipitation in most extra-tropical regions; Fig. 18.3). Alternatively, deeper soils, groundwater, and streamwater tend to be isotopically lighter than shallow soil water because they recharge more in colder seasons or often from higher elevations (Sect. 18.3). However, interpretations of source waters from cellulose need to consider the following possible confounding factors.

First, it needs to be recognized that predicting source water isotope ratios from cellulose requires estimating leaf-water evaporative enrichment and fractionation processes that occur with sugar assimilation. These processes can be uncertain and their effect size can be similar or greater in magnitude than the effects of  $\delta_{\text{Source}}$  variation (Song et al. 2014). As a starting point to constrain those processes, inter-annual variations in temperature and relative humidity are key data, which can be applied in models to constrain expected inter-annual variability attributable to leaf fractionation processes (Sargeant et al. 2020; Cernusak et al. 2016). These processes (described in Chap. 11–13) must be constrained prior to estimating source waters from cellulose.

Second, *inter-annual variations* within a water source can confound the ability to separate between the use of different water sources over time. For example, source differentiation will be confounded if (a) the range of isotope ratios in those sources vary among years (e.g., shallow soils are isotopically lighter in years with less summer precipitation because they are not diluted by summer rain's higher  $\delta_{\text{Precip}}$ ), (b) values of  $\delta_{\text{Precip}}$  are anomalously high or low in a given year, (c) the growing seasons and thus water uptake seasons differed among years such that the rings reflect larger proportions of uptake during either spring (light, less evaporated) or late summer (heavy, more evaporated). To mitigate uncertainties in interpreting source water signals, where possible, one can:

- Select sites where seasonal and inter-annual isotope variations are smaller, such as lower elevation or more coastal regions, but where the potential sources have large isotopic differences. If the goal is to identify inter-annual differences in use of groundwater relative to soil water, select sites where groundwater is sourced by rain from much higher elevations so that its influence can be clearly distinguished (e.g., Oerter et al. 2019).
- To account for inter-annual cellulose isotopic variations attributable to inter-annual variations in  $\delta_{\text{Precip}}$ , select regions where inter-annual  $\delta_{\text{Precip}}$  was measured, or estimate likely ranges of inter-annual  $\delta_{\text{Precip}}$  to see whether they could explain tree-ring variations.
- To rule out the possibility that inter-annual isotope signatures change because the mixtures of seasonal precipitation in soils, groundwater, or streams are changing, examine inter-seasonal precipitation amount variations (and  $\delta_{\text{Precip}}$  seasonal amplitude) to see whether their effects on weighted-mean annual  $\delta_{\text{Precip}}$  are large enough to explain inter-annual variations in ring isotope ratios (e.g., during the calibration period when data are available). These data are more widely available than records of inter-annual variation in  $\delta_{\text{Precip}}$ .
- To rule out the influence of variations in the radial growth season, use dendrometer records of radial growth phenology to indicate how growing season varies; this

issue may not matter if intra-annual (e.g., early-wood versus late-wood) isotope variations are small anyway.

Third, confounding factors in inferring *site-and-species differences* in source can arise, for example, when (a) comparing across soils or landscapes where water turnover times differ due to storage capacity or climate (e.g., a soil in a very wet region might hold recent precipitation whereas one in a dry site may contain several previous years of precipitation) (b) comparing across soils where infiltration processes differ and include substantial bypass flow (e.g., allowing more recent precipitation to show up lower in soil profiles or in stream or groundwater sources), or (c) species differ in growth and water-uptake seasons such that isotopic differences might reflect trees taking up water from the same pools but at different times. To mitigate uncertainties, where possible, one can:

- Select trees that co-occupy sites (or at least occupying sites with similar climates and soils) to rule out the effects of soils differences in species comparisons.
- Use multi-seasonal xylem water measurements to show that potential sources across sites similarly respond to precipitation inputs and seasonal climate variations, to rule out the possibility that tree-ring isotope variations are due to soil and  $\delta_{\text{precip}}$  dynamics, rather than changes in sources used by trees.

And last, confounding factors in inferring *intra-annual variations* (i.e., from sub-annual slices of cellulose) in sources can arise, for example when (a) water that was enriched due to evaporation from stems over winter (Treydte et al. 2014) is incorporated in early radial growth, (b) sources change isotopically throughout the growing season, confounding estimates of the relative use of each source, (e.g., rain dilutes evaporatively enriched soils resulting in profiles that are inverse to the more typical ones seen in growing seasons; Figs. 18.5 and 18.6). To mitigate uncertainties, where possible, one can:

- Interpret the earliest early-wood isotope values cautiously to avoid misinterpreting the effects of evaporative enrichment throughout the dormant seasons or of stored carbohydrates that contain source information from previous years.
- Unless the potential end-members are consistently very distinct, use a calibrated physical model to account for the source-water dynamics and interactions; these finer scale dynamics should be considered when making finer-resolution inferences from sub-annual isotopic variations.

## 18.6 Conclusions

Geographic, vertical, and temporal variations in the isotopic composition of potential water sources to plants should be considered when interpreting tree-ring  $\delta^{18}\text{O}$  or  $\delta^2\text{H}$ . While tree rings provide opportunity for studying these variations, there are many potential confounding factors. When interpreting tree-ring isotope ratios, the relative influences of source water variations versus climate and physiology effects

on leaf-water enrichment (Chaps. 10 and 11) should both be considered; there are only few circumstances where spatiotemporal variability in source water isotopic composition can be ignored. There are many reasons why one ring, one tree, or one site may have more enriched  $\delta^{18}\text{O}$  or  $\delta^2\text{H}$  than another, and these could result in confounded interpretations; Table 18.1 demonstrates this challenge by offering a list of hypothetical explanations for heavier-than-normal  $\delta^{18}\text{O}$  in a ring. Nonetheless, by recognizing the full suite of controlling processes (Sects. 18.2, 18.3, and 18.4), many potential confounding factors can be eliminated when interpreting data (Sect. 18.5). Accounting for source-water isotope variations involves first examining the average and seasonal precipitation inputs to a site (Figs. 18.3 and 18.4), then considering how fast soil–water pools may turnover and how evaporation may affect their isotope ratios (Figs. 18.5, 18.6, 18.7), and last, considering which soil-waters will be taken up by trees (Figs. 18.7 and 18.8). Fortunately, soil–water-transport and plant-uptake

**Table 18.1** There are many causes for high or low  $\delta^{18}\text{O}$  in tree rings. Here are many examples of diverse, potentially contrasting ecohydrological explanations for heavier-than-average  $\delta^{18}\text{O}$  in a single ring—commonly assumed to result from greater leaf water enrichment in drier years (Chap. 10)—demonstrating how the interaction among climate, soil, and tree processes can complicate interpreting tree-ring  $\delta^{18}\text{O}$ . With knowledge of the system and conditions, many of these alternative hypothetical explanations can be dismissed

Scenario	Hypothetical interpretation: high $\delta^{18}\text{O}$ reflects...	Explanation: high $\delta^{18}\text{O}$ results from...
1	<i>dry summers</i>	– strong evaporative enrichment of leaf water (i.e., independent of source water)
2	<i>wet summers</i>	– more summer precipitation (which has heavier $\delta^{18}\text{O}$ ) falling and thus it composes a larger fraction of rhizosphere storage
3	<i>dry summers</i>	– evaporative enrichment of soil water
4	<i>wet summers</i>	– trees growing radially later into summer when soil waters have higher $\delta^{18}\text{O}$ , as opposed to just during spring (when soil water has lower $\delta^{18}\text{O}$ )
5	<i>dry summers</i>	– trees growing and incorporating xylem water only in early spring, when waters stored in plants can be enriched in $\delta^{18}\text{O}$ because of evaporation from stems throughout winter (more common in deciduous trees)
6	<i>wet summers</i>	– trees being able to rely on just shallow waters, which are more evaporatively enriched in heavy isotopes
7	<i>dry winters</i>	– a lack of winter (lower $\delta^{18}\text{O}$ ) precipitation in soil storage
8	<i>any conditions</i>	– from precipitation having higher $\delta^{18}\text{O}$ values than in normal years

dynamics both tend to correspond with climate, allowing source water to be partially predictable and interpretable. Understanding these processes and moving beyond assuming that source-waters isotopic compositions are constant or equal to that of long-term mean precipitation is an important step towards improved interpretation of tree-ring isotope ratios.

**Acknowledgements** We thank Holly Barnard, Elizabeth Olson, Margaret Barbour, and Paul Mayer for their thoughtful and detailed reviews of this chapter. This chapter has been subjected to Agency review and has been approved for publication. The views expressed in this paper are those of the author(s) and do not necessarily reflect the views or policies of the U.S. Environmental Protection Agency. Mention of trade names or commercial products does not constitute endorsement or recommendation for use.

## References

- Aemisegger F, Spiegel J, Pfahl S et al (2015) Isotope meteorology of cold front passages: a case study combining observations and modeling. *Geophys Res Lett* 42:5652–5660
- Aggarwal PK, Araguas-Araguas L, Groening M et al (2010) Global hydrological isotope data and data networks. In: West JB, Bowen GJ, Dawson TE, Tu KP (eds) *Isoscapes: understanding movement, pattern, and process on earth through isotope mapping*, pp 33–50
- Aggarwal PK, Froehlich K, Gonfiantini R (2011) Contributions of the International Atomic Energy Agency to the development and practice of isotope hydrology. *Hydrogeol J* 19:5–8. <https://doi.org/10.1007/s10040-010-0648-3>
- Allen ST, Jasechko S, Berghuijs WR, et al (2019a) Global sinusoidal seasonality in precipitation isotopes. *Hydrol Earth Syst Sci Discuss*, 1–23. <https://doi.org/10.5194/hess-2019-61>
- Allen ST, Kirchner JW, Braun S et al (2019b) Seasonal origins of soil water used by trees. *Hydrol Earth Syst Sci* 23:1199–1210. <https://doi.org/10.5194/hess-23-1199-2019>
- Allen ST, Keim RF, Barnard HR et al (2017) The role of stable isotopes in understanding rainfall interception processes: a review. *WIREs Water* 4:n/a-n/a. <https://doi.org/10.1002/wat2.1187>
- Anderson WT, Bernasconi SM, McKenzie JA et al (2002) Model evaluation for reconstructing the oxygen isotopic composition in precipitation from tree ring cellulose over the last century. *Chem Geol* 182:121–137. [https://doi.org/10.1016/S0009-2541\(01\)00285-6](https://doi.org/10.1016/S0009-2541(01)00285-6)
- Anderson WT, Bernasconi SM, McKenzie JA, Saurer M (1998) Oxygen and carbon isotopic record of climatic variability in tree ring cellulose (*Picea abies*): an example from central Switzerland (1913–1995). *J Geophys Res Atmos* 103:31625–31636. <https://doi.org/10.1029/1998JD200040>
- Barbecot F, Guillon S, Pili E, et al (2018) Using water stable isotopes in the unsaturated zone to quantify recharge in two contrasted infiltration regimes. *Vadose Zone J* 17:170170. <https://doi.org/10.2136/vzj2017.09.0170>
- Barbeta A, Gimeno TE, Clavé L et al (2020) An explanation for the isotopic offset between soil and stem water in a temperate tree species. *New Phytol*. <https://doi.org/10.1111/nph.16564>
- Benettin P, Queloz P, Bensimon M et al (2019) Velocities, residence times, tracer breakthroughs in a vegetated Lysimeter: a multitracer experiment. *Water Resour Res* 55:21–33. <https://doi.org/10.1029/2018WR023894>
- Benettin P, Volkmann THM, von Freyberg J et al (2018) Effects of climatic seasonality on the isotopic composition of evaporating soil waters. *Hydrol Earth Syst Sci* 22:2881–2890. <https://doi.org/10.5194/hess-22-2881-2018>
- Berghuijs WR, Allen ST (2019) Waters flowing out of systems are younger than the waters stored in those same systems. *Hydrol Process*. <https://doi.org/10.1002/hyp.13569>

- Berkelhammer M, Still CJ, Ritter F et al (2020) Persistence and plasticity in conifer water-use strategies. *J Geophys Res Biogeosci* 125:e2018JG004845. <https://doi.org/10.1029/2018JG004845>
- Berkelhammer MB, Stott LD (2008) Recent and dramatic changes in Pacific storm trajectories recorded in  $\delta^{18}\text{O}$  from Bristlecone Pine tree ring cellulose. *Geochem Geophys Geosyst* 9. <https://doi.org/10.1029/2007GC001803>
- Berry ZC, Hughes NM, Smith WK (2014) Cloud immersion: an important water source for spruce and fir saplings in the southern Appalachian Mountains. *Oecologia* 174:319–326. <https://doi.org/10.1007/s00442-013-2770-0>
- Bertrand G, Masini J, Goldscheider N et al (2014) Determination of spatiotemporal variability of tree water uptake using stable isotopes ( $\delta^{18}\text{O}$ ,  $\delta^2\text{H}$ ) in an alluvial system supplied by a high-altitude watershed, Pfyn forest, Switzerland. *Ecohydrology* 7:319–333. <https://doi.org/10.1002/eco.1347>
- Beven K, Germann P (1982) Macropores and water flow in soils. *Water Resour Res* 18:1311–1325. <https://doi.org/10.1029/WR018i005p01311>
- Bowen GJ (2010) Statistical and geostatistical mapping of precipitation water isotope ratios. *Isoscapes*. Springer, Dordrecht, pp 139–160
- Bowen GJ (2008) Spatial analysis of the intra-annual variation of precipitation isotope ratios and its climatological corollaries. *J Geophys Res* 113:D05113. <https://doi.org/10.1029/2007JD009295>
- Bowen GJ, Cai Z, Fiorella RP, Putman AL (2019) Isotopes in the water cycle: regional- to global-scale patterns and applications. *Annu Rev Earth Planet Sci* 47:453–479
- Bowen GJ, Liu Z, Vander Zanden HB et al (2014) Geographic assignment with stable isotopes in IsoMAP. *Methods Ecol Evol* 5:201–206. <https://doi.org/10.1111/2041-210X.12147>
- Bowen GJ, Putman A, Brooks JR et al (2018) Inferring the source of evaporated waters using stable H and O isotopes. *Oecologia*, 1–15. <https://doi.org/10.1007/s00442-018-4192-5>
- Braud I, Bariac T, Gaudet JP, Vauclin M (2005) SiSPAT-Isotope, a coupled heat, water and stable isotope (HDO and H<sub>2</sub>18O) transport model for bare soil. Part I. Model description and first verifications. *J Hydrol* 309:277–300. <https://doi.org/10.1016/j.jhydrol.2004.12.013>
- Brooks JR, Barnard HR, Coulombe R, McDonnell JJ (2010) Ecohydrologic separation of water between trees and streams in a Mediterranean climate. *Nat Geosci* 3:100–104. <https://doi.org/10.1038/ngeo722>
- Brooks JR, Meinzer FC, Coulombe R, Gregg J (2002) Hydraulic redistribution of soil water during summer drought in two contrasting Pacific Northwest coniferous forests. *Tree Physiol* 22:1107–1117. <https://doi.org/10.1093/treephys/22.15-16.1107>
- Brooks JR, Meinzer FC, Warren JM et al (2006) Hydraulic redistribution in a Douglas-fir forest: lessons from system manipulations. *Plant, Cell Environ* 29:138–150. <https://doi.org/10.1111/j.1365-3040.2005.01409.x>
- Burgess SSO, Pate JS, Adams MA, Dawson TE (2000) Seasonal water acquisition and redistribution in the Australian Woody Phreatophyte, *Banksia prionotes*. *Ann Bot* 85:215–224. <https://doi.org/10.1006/anbo.1999.1019>
- Caldwell MM, Dawson TE, Richards JH (1998) Hydraulic lift: consequences of water efflux from the roots of plants. *Oecologia* 113:151–161. <https://doi.org/10.1007/s004420050363>
- Caldwell MM, Richards JH (1989) Hydraulic lift: water efflux from upper roots improves effectiveness of water uptake by deep roots. *Oecologia* 79:1–5. <https://doi.org/10.1007/BF00378231>
- Canadell J, Jackson RB, Ehleringer JB et al (1996) Maximum rooting depth of vegetation types at the global scale. *Oecologia* 108:583–595. <https://doi.org/10.1007/BF00329030>
- Carminati A, Moradi AB, Vetterlein D et al (2010) Dynamics of soil water content in the rhizosphere. *Plant Soil* 332:163–176. <https://doi.org/10.1007/s11104-010-0283-8>
- Cernusak LA, Barbour MM, Arndt SK et al (2016) Stable isotopes in leaf water of terrestrial plants. *Plant Cell Environ* 39:1087–1102. <https://doi.org/10.1111/pce.12703>
- Chimner RA, Cooper DJ (2004) Using stable oxygen isotopes to quantify the water source used for transpiration by native shrubs in the San Luis Valley, Colorado U.S.A. *Plant Soil* 260:225–236



- Clark ID, Fritz P (1997) Environmental isotopes in hydrogeology. CRC Press, Boca Raton
- Coplen TB, Neiman PJ, White AB et al (2008) Extreme changes in stable hydrogen isotopes and precipitation characteristics in a landfalling Pacific storm. *Geophys Res Lett* 35:L21808. <https://doi.org/10.1029/2008GL035481>
- Coplen TB, Neiman PJ, White AB, Ralph FM (2015) Categorisation of northern California rainfall for periods with and without a radar brightband using stable isotopes and a novel automated precipitation collector. *Tellus B Chem Phys Meteorol* 67:28574. <https://doi.org/10.3402/tellusb.v67.28574>
- Craig H (1961) Isotopic Variations in meteoric waters. *Science* 133:1702–1703. <https://doi.org/10.1126/science.133.3465.1702>
- Craig H, Gordon LI (1965) Deuterium and oxygen-18 variations in the ocean and the marine atmosphere. In: Tongiorgi E (ed) Proceedings of a conference on stable isotopes in oceanographic studies and paleotemperatures, Spoleto, Italy
- Danis PA, Masson-Delmotte V, Stievenard M et al (2006) Reconstruction of past precipitation  $\delta^{18}\text{O}$  using tree-ring cellulose  $\delta^{18}\text{O}$  and  $\delta^{13}\text{C}$ : A calibration study near Lac d'Annecy, France. *Earth Planet Sci Lett* 243:439–448. <https://doi.org/10.1016/j.epsl.2006.01.023>
- Dansgaard W (1953) The abundance of O18 in atmospheric water and water vapour. *Tellus* 5:461–469
- Dansgaard W (1954) The O18-abundance in fresh water. *Geochim Cosmochim Acta* 6:241–260
- Dansgaard W (1964) Stable isotopes in precipitation. *Tellus* 16:436–468. <https://doi.org/10.1111/j.2153-3490.1964.tb00181.x>
- Dawson TE, Ehleringer JR (1991) Streamside trees that do not use stream water. *Nature* 350:335–337
- Dawson TE, Ehleringer JR (1993) Isotopic enrichment of water in the “woody” tissues of plants: Implications for plant water source, water uptake, and other studies which use the stable isotopic composition of cellulose. *Geochim Cosmochim Acta* 57:3487–3492. [https://doi.org/10.1016/0016-7037\(93\)90554-A](https://doi.org/10.1016/0016-7037(93)90554-A)
- Dee S, Noone D, Buening N et al (2015) SPEEDY-IER: A fast atmospheric GCM with water isotope physics. *J Geophys Res Atmos* 120:73–91. <https://doi.org/10.1002/2014JD022194>
- Eggemeyer KD, Awada T, Harvey FE et al (2009) Seasonal changes in depth of water uptake for encroaching trees *Juniperus virginiana* and *Pinus ponderosa* and two dominant C4 grasses in a semiarid grassland. *Tree Physiol* 29:157–169. <https://doi.org/10.1093/treephys/tpn019>
- Ehleringer JR, Phillips SL, Schuster WSF, Sandquist DR (1991) Differential utilization of summer rains by desert plants. *Oecologia* 88:430–434. <https://doi.org/10.1007/BF00317589>
- Ellsworth PZ, Williams DG (2007) Hydrogen isotope fractionation during water uptake by woody xerophytes. *Plant Soil* 291:93–107. <https://doi.org/10.1007/s11104-006-9177-1>
- Evans MN (2007) Toward forward modeling for paleoclimatic proxy signal calibration: a case study with oxygen isotopic composition of tropical woods. *Geochem Geophys Geosyst*, 8. <https://doi.org/10.1029/2006GC001406>
- Fan Y, Miguez-Macho G, Jobbágy EG et al (2017) Hydrologic regulation of plant rooting depth. *PNAS* 114:10572–10577. <https://doi.org/10.1073/pnas.1712381114>
- Feng X, Faiia AM, Posmentier ES (2009) Seasonality of isotopes in precipitation: a global perspective. *J Geophys Res Atmos* 114. <https://doi.org/10.1029/2008JD011279>
- Fiorella RP, West JB, Bowen GJ (2019) Biased estimates of the isotope ratios of steady-state evaporation from the assumption of equilibrium between vapour and precipitation. *Hydrol Process* 33:2576–2590. <https://doi.org/10.1002/hyp.13531>
- Fischer BMC, van Meerveld HJ (Ilja), Seibert J (2017) Spatial variability in the isotopic composition of rainfall in a small headwater catchment and its effect on hydrograph separation. *J Hydrol* 547:755–769. <https://doi.org/10.1016/j.jhydrol.2017.01.045>
- Flury M, Flühler H, Jury WA, Leuenberger J (1994) Susceptibility of soils to preferential flow of water: a field study. *Water Resour Res* 30:1945–1954. <https://doi.org/10.1029/94WR00871>
- Gale MR, Grigal DF (1987) Vertical root distributions of northern tree species in relation to successional status. *Can J for Res* 17:829–834. <https://doi.org/10.1139/x87-131>

- Gat JR (1996) Oxygen and hydrogen isotopes in the hydrologic cycle. *Annu Rev Earth Planet Sci* 24:225–262. <https://doi.org/10.1146/annurev.earth.24.1.225>
- Gat JR, Gonfiantini R (1981) Stable isotope hydrology. Deuterium and oxygen-18 in the water cycle
- Gat JR, Tzur Y (1968) Modification of the isotopic composition of rainwater by processes which occur before groundwater recharge. In: *Isotope hydrology, proceedings of symposium on Vienna 1966*. International Atomic Energy Agency, pp 49–60
- Gedzelman SD, Lawrence J (1990) The isotopic composition of precipitation from two extratropical cyclones. *Mon Weather Rev* 118:495–509
- Gedzelman SD, Lawrence J, Gamache J et al (2003) Probing hurricanes with stable isotopes of rain and water vapor. *Mon Weather Rev* 131:1112–1127
- Gerlein-Safdi C, Gauthier PPG, Caylor KK (2018) Dew-induced transpiration suppression impacts the water and isotope balances of *Colocasia* leaves. *Oecologia* 187:1041–1051. <https://doi.org/10.1007/s00442-018-4199-y>
- Goldsmith GR, Allen ST, Braun S et al (2019) Spatial variation in throughfall, soil, and plant water isotopes in a temperate forest. *Ecohydrology* 12:e2059. <https://doi.org/10.1002/eco.2059>
- Goldsmith GR, Lehmann MM, Cernusak LA et al (2017) Inferring foliar water uptake using stable isotopes of water. *Oecologia* 184:763–766. <https://doi.org/10.1007/s00442-017-3917-1>
- Goldsmith GR, Matzke NJ, Dawson TE (2013) The incidence and implications of clouds for cloud forest plant water relations. *Ecol Lett* 16:307–314. <https://doi.org/10.1111/ele.12039>
- Goldsmith GR, Muñoz-Villers LE, Holwerda F et al (2012) Stable isotopes reveal linkages among ecohydrological processes in a seasonally dry tropical montane cloud forest. *Ecohydrology* 5:779–790. <https://doi.org/10.1002/eco.268>
- Good SP, Mallia DV, Denis EH et al (2014a) High frequency trends in the isotopic composition of Superstorm Sandy. In: Bennington JB, Farmer EC (eds) *Learning from the impacts of Superstorm Sandy*. Academic Press, pp 41–55
- Good SP, Mallia DV, Lin JC, Bowen GJ (2014b) Stable isotope analysis of precipitation samples obtained via crowdsourcing reveals the spatiotemporal evolution of Superstorm Sandy. *PLOS ONE* 9:e91117. <https://doi.org/10.1371/journal.pone.0091117>
- Gotsch SG, Asbjornsen H, Holwerda F et al (2014) Foggy days and dry nights determine crown-level water balance in a seasonal tropical montane cloud forest. *Plant Cell Environ* 37:261–272. <https://doi.org/10.1111/pce.12151>
- Groh J, Stumpp C, Lücke A et al (2018) Inverse estimation of soil hydraulic and transport parameters of layered soils from water stable isotope and lysimeter data. *Vadose Zone J* 17. <https://doi.org/10.2136/vzj2017.09.0168>
- Guo JS, Hungate BA, Kolb TE, Koch GW (2018) Water source niche overlap increases with site moisture availability in woody perennials. *Plant Ecol* 219:719–735. <https://doi.org/10.1007/s11258-018-0829-z>
- Haverd V, Cuntz M (2010) Soil–Litter–Iso: a one-dimensional model for coupled transport of heat, water and stable isotopes in soil with a litter layer and root extraction. *J Hydrol* 388:438–455. <https://doi.org/10.1016/j.jhydrol.2010.05.029>
- Helliker BR, Richter SL (2008) Subtropical to boreal convergence of tree-leaf temperatures. *Nature* 454:511–514. <https://doi.org/10.1038/nature07031>
- Hewlett JD, Hibbert AR (1967) Factors affecting the response of small watersheds to precipitation in humid areas. In: Sopper W, Lull HW (eds) *Forest hydrology*. Pergamon Press, New York, NY, USA, pp 275–290
- Horita J, Rozanski K, Cohen S (2008) Isotope effects in the evaporation of water: a status report of the Craig-Gordon model. *Isot Environ Health Stud* 44:23–49. <https://doi.org/10.1080/10256010801887174>
- Hultine KR, Cable WL, Burgess SSO, Williams DG (2003a) Hydraulic redistribution by deep roots of a Chihuahuan Desert phreatophyte. *Tree Physiol* 23:353–360. <https://doi.org/10.1093/treephys/23.5.353>

- Hultine KR, Williams DG, Burgess SSO, Keefer TO (2003b) Contrasting patterns of hydraulic redistribution in three desert phreatophytes. *Oecologia* 135:167–175. <https://doi.org/10.1007/s00442-002-1165-4>
- IAEA/WMO (2020) Global network of isotopes in precipitation. The GNIP Database. <http://www.iaea.org/water>. Vienna, Austria
- Jackson RB, Canadell J, Ehleringer JR et al (1996) A global analysis of root distributions for terrestrial biomes. *Oecologia* 108:389–411. <https://doi.org/10.1007/BF00333714>
- Jasechko S (2019) Global isotope hydrogeology—review. *Rev Geophys*. <https://doi.org/10.1029/2018RG000627>
- Jasechko S, Perrone D, Befus KM et al (2017) Global aquifers dominated by fossil groundwaters but wells vulnerable to modern contamination. *Nat Geosci* 10:425
- Jasechko S, Taylor RG (2015) Intensive rainfall recharges tropical groundwaters. *Environ Res Lett* 10:124015. <https://doi.org/10.1088/1748-9326/10/12/124015>
- Jouzel J, Koster RD, Suozzo RJ, Russell GL (1994) Stable water isotope behavior during the last glacial maximum: a general circulation model analysis. *J Geophys Res* 99:25791–25801
- Kendall C, Caldwell E (1998) Fundamentals of isotope geochemistry. In: *Isotope tracers in catchment hydrology (Developments in water science)*. Elsevier Science, pp 51–86
- Kennedy CD, Bataille CP, Liu Z et al (2012) Dynamics of nitrate and chloride during storm events in agricultural catchments with different subsurface drainage intensity (Indiana, USA). *J Hydrol* 466–467:1–10. <https://doi.org/10.1016/j.hydrol.2012.05.002>
- Kirchner JW, Allen ST (2020) Seasonal partitioning of precipitation between streamflow and evapotranspiration, inferred from end-member splitting analysis. *Hydrol Earth Syst Sci* 24:17–39. <https://doi.org/10.5194/hess-24-17-2020>
- Konecky B, Dee SG, Noone DC (2019) WaxPSM: a forward model of leaf wax hydrogen isotope ratios to bridge proxy and model estimates of past climate. *J Geophys Res Biogeosci* 124:2107–2125. <https://doi.org/10.1029/2018JG004708>
- Kurz-Besson C, Otiño D, Lobo do Vale R, et al (2006) Hydraulic lift in cork oak trees in a savannah-type Mediterranean ecosystem and its contribution to the local water balance. *Plant Soil* 282:361–378. <https://doi.org/10.1007/s11104-006-0005-4>
- Landwehr JM, Coplen TB (2006) Line-conditioned excess: a new method for characterizing stable hydrogen and oxygen isotope ratios in hydrologic systems
- Lawrence, DM, Oleson KW, Flanner MG et al (2011) Parameterization improvements and functional and structural advances in Version 4 of the Community Land Model. *J Adv Model Earth Syst* 3. <https://doi.org/10.1029/2011MS00045>
- Lawrence J, Gedzelman SD (1996) Low stable isotope ratios of tropical cyclone rains. *Geophys Res Lett* 23:527–530
- Lehmann M, Goldsmith G, Schmid L et al (2017) The effect of  $^{18}\text{O}$ -labelled water vapour on the oxygen isotope ratio of water and assimilates in plants at high humidity. *New Phytol* 217:105–116. <https://doi.org/10.1111/nph.14788>
- Lin G, Sternberg L (1993)  $\delta^2\text{H}$ —hydrogen isotopic fractionation by plant roots during water uptake in coastal wetland plants. In: Ehleringer JR, Hall AE, Farquhar GD (eds) *Stable isotopes and plant carbon-water relations*. Academic Press, San Diego, pp 497–510
- Lin W, Domec J-C, Ward EJ et al (2019) Using  $\delta^{13}\text{C}$  and  $\delta^{18}\text{O}$  to analyze loblolly pine (*Pinus taeda* L.) response to experimental drought and fertilization. *Tree Physiol* 39:1984–1994. <https://doi.org/10.1093/treephys/tpz096>
- Liu Z, Bowen GJ, Welker JM (2010) Atmospheric circulation is reflected in precipitation isotope gradients over the conterminous United States. *J Geophys Res* 115:D22120. <https://doi.org/10.1029/2010JD014175>
- Martin J, Looker N, Hoylman Z et al (2018) Differential use of winter precipitation by upper and lower elevation Douglas fir in the Northern Rockies. *Glob Change Biol* 24:5607–5621. <https://doi.org/10.1111/gcb.14435>

- McCully ME (1999) Root xylem embolisms and refilling. relation to water potentials of soil, roots, and leaves, and osmotic potentials of root xylem sap. *Plant Physiol* 119:1001–1008. <https://doi.org/10.1104/pp.119.3.1001>
- Meinzer FC, Warren JM, Brooks JR (2007) Species-specific partitioning of soil water resources in an old-growth Douglas-fir–western hemlock forest. *Tree Physiol* 27:871–880. <https://doi.org/10.1093/treephys/27.6.871>
- Miller DL, Mora CI, Grissino-Mayer HD et al (2006) Tree-ring isotope records of tropical cyclone activity. *PNAS* 103:14294–14297. <https://doi.org/10.1073/pnas.0606549103>
- Mueller MH, Alaoui A, Kuells C et al (2014) Tracking water pathways in steep hillslopes by  $\delta^{18}\text{O}$  depth profiles of soil water. *J Hydrol* 519:340–352. <https://doi.org/10.1016/j.jhydrol.2014.07.031>
- Munksgaard NC, Wurster CM, Bass A, Bird MI (2012) Extreme short-term stable isotope variability revealed by continuous rainwater analysis. *Hydrol Process* 26:3630–3634. <https://doi.org/10.1002/hyp.9505>
- Neumann RB, Cardon ZG (2012) The magnitude of hydraulic redistribution by plant roots: a review and synthesis of empirical and modeling studies. *New Phytol* 194:337–352. <https://doi.org/10.1111/j.1469-8137.2012.04088.x>
- Nimmo JR (2011) Preferential flow occurs in unsaturated conditions. *Hydrol Process* 26:786–789. <https://doi.org/10.1002/hyp.8380>
- Oerter EJ, Siebert G, Bowling DR, Bowen G (2019) Soil water vapour isotopes identify missing water source for streamside trees. *Ecohydrology* 12:e2083. <https://doi.org/10.1002/eco.2083>
- Oshun J, Dietrich WE, Dawson TE, Fung I (2016) Dynamic, structured heterogeneity of water isotopes inside hillslopes. *Water Resour Res* 52:164–189. <https://doi.org/10.1002/2015WR017485>
- Penna D, Hopp L, Scandellari F et al (2018) Tracing ecosystem water fluxes using hydrogen and oxygen stable isotopes: challenges and opportunities from an interdisciplinary perspective. *Biogeosciences* 15:6399–6415. <https://doi.org/10.5194/bg-2018-286>
- Penna D, Meerveld HJ (Ilja) van (2019) Spatial variability in the isotopic composition of water in small catchments and its effect on hydrograph separation. *Wiley Interdiscip Rev Water* 6:e1367. <https://doi.org/10.1002/wat2.1367>
- Pfahl S, Wernli H, Yoshimura K (2012) The isotopic composition of precipitation from a winter storm—a case study with the limited-area model COSMOiso. *Atmos Chem Phys* 12:1629–1648
- Poage MA, Chamberlain CP (2001) Empirical relationships between elevation and the stable isotope composition of precipitation and surface waters: considerations for studies of paleoelevation change. *Am J Sci* 301:1–15
- Price RM, Swart PK, Willoughby HE (2008) Seasonal and spatial variation in the stable isotopic composition ( $\delta^{18}\text{O}$  and  $\delta\text{D}$ ) of precipitation in south Florida. *J Hydrol* 358:193–205. <https://doi.org/10.1016/j.jhydrol.2008.06.003>
- Putman AL, Bowen GJ (2019) Technical note: a global database of the stable isotopic ratios of meteoric and terrestrial waters. *Hydrol Earth Syst Sci* 23:4389–4396. <https://doi.org/10.5194/hess-23-4389-2019>
- Putman AL, Fiorella RP, Bowen GJ, Cai Z (2019) A global perspective on local meteoric water lines: meta-analytic insight into fundamental controls and practical constraints. *Water Resour Res* 55:6896–6910. <https://doi.org/10.1029/2019WR025181>
- Roden J, Siegwolf R (2012) Is the dual-isotope conceptual model fully operational? *Tree Physiol* 32:1179–1182. <https://doi.org/10.1093/treephys/tps099>
- Rong L, Chen X, Chen X et al (2011) Isotopic analysis of water sources of mountainous plant uptake in a karst plateau of southwest China. *Hydrol Process* 25:3666–3675. <https://doi.org/10.1002/hyp.8093>
- Ryel RJ (2004) Hydraulic redistribution. In: Esser K, Lüttge U, Beyschlag W, Murata J (eds) *Progress in botany: genetics physiology systematics ecology*. Springer, Berlin, Heidelberg, pp 413–435
- Sargeant CI, Singer MB (2016) Sub-annual variability in historical water source use by Mediterranean riparian trees. *Ecohydrology* 9:1328–1345. <https://doi.org/10.1002/eco.1730>

- Sargeant CI, Singer MB, Vallet-Coulomb C (2020) Identification of source-water oxygen isotopes in trees toolkit (ISO-Tool) for deciphering historical water use by forest trees. *Water Resour Res* n/a. <https://doi.org/10.1029/2018WR024519>
- Sarris D, Siegwolf R, Körner C (2013) Inter- and intra-annual stable carbon and oxygen isotope signals in response to drought in Mediterranean pines. *Agric for Meteorol* 168:59–68. <https://doi.org/10.1016/j.agrformet.2012.08.007>
- Saurer M, Kirdeyanov AV, Prokushkin AS et al (2016) The impact of an inverse climate–isotope relationship in soil water on the oxygen-isotope composition of *Larix gmelinii* in Siberia. *New Phytol* 209:955–964. <https://doi.org/10.1111/nph.13759>
- Schwinnig S (2010) The ecohydrology of roots in rocks. *Ecohydrology* 3:238–245. <https://doi.org/10.1002/eco.134>
- Selker JS, McCord JT, Keller CK (1999) *Vadose zone processes*. CRC Press, Boca Raton
- Simonin KA, Santiago LS, Dawson TE (2009) Fog interception by *Sequoia sempervirens* (D. Don) crowns decouples physiology from soil water deficit. *Plant Cell Environ* 32:882–892. <https://doi.org/10.1111/j.1365-3040.2009.01967.x>
- Snyder KA, Williams DG (2000) Water sources used by riparian trees varies among stream types on the San Pedro River, Arizona. *Agric for Meteorol* 105:227–240. [https://doi.org/10.1016/S0168-1923\(00\)00193-3](https://doi.org/10.1016/S0168-1923(00)00193-3)
- Song X, Farquhar GD, Gessler A, Barbour MM (2014) Turnover time of the non-structural carbohydrate pool influences  $\delta^{18}\text{O}$  of leaf cellulose. *Plant Cell Environ* 37:2500–2507. <https://doi.org/10.1111/pce.12309>
- Sprenger M, Erhardt M, Riedel M, Weiler M (2016a) Historical tracking of nitrate in contrasting vineyards using water isotopes and nitrate depth profiles. *Agr Ecosyst Environ* 222:185–192. <https://doi.org/10.1016/j.agee.2016.02.014>
- Sprenger M, Leistert H, Gimbel K, Weiler M (2016b) Illuminating hydrological processes at the soil-vegetation-atmosphere interface with water stable isotopes. *Rev Geophys* 54:2015RG000515. <https://doi.org/10.1002/2015RG000515>
- Sprenger M, Seeger S, Blume T, Weiler M (2016c) Travel times in the vadose zone: variability in space and time. *Water Resour Res* 52:5727–5754. <https://doi.org/10.1002/2015WR018077>
- Sprenger M, Llorens P, Cayuela C et al (2019) Mechanisms of consistently disjunct soil water pools over (pore) space and time. *Hydrol Earth Syst Sci* 23:2751–2762. <https://doi.org/10.5194/hess-23-2751-2019>
- Sprenger M, Tetzlaff D, Buttle J et al (2018a) Measuring and modeling stable isotopes of mobile and bulk soil water. *Vadose Zone J* 17. <https://doi.org/10.2136/vzj2017.08.0149>
- Sprenger M, Tetzlaff D, Buttle J et al (2018b) Storage, mixing, and fluxes of water in the critical zone across northern environments inferred by stable isotopes of soil water. *Hydrol Process* 32:1720–1737. <https://doi.org/10.1002/hyp.13135>
- Sprenger M, Volkmann THM, Blume T, Weiler M (2015) Estimating flow and transport parameters in the unsaturated zone with pore water stable isotopes. *Hydrol Earth Syst Sci* 19:2617–2635. <https://doi.org/10.5194/hess-19-2617-2015>
- Stump C, Stichler W, Kandolf M, Šimůnek J (2012) Effects of land cover and fertilization method on water flow and solute transport in five lysimeters: a long-term study using stable water isotopes. *Vadose Zone J* 11:0–0. <https://doi.org/10.2136/vzj2011.0075>
- Swidrak I, Schuster R, Oberhuber W (2013) Comparing growth phenology of co-occurring deciduous and evergreen conifers exposed to drought. *Flora Morphol Distrib Funct Ecol Plants* 208:609–617. <https://doi.org/10.1016/j.flora.2013.09.004>
- Tang K, Feng X (2001) The effect of soil hydrology on the oxygen and hydrogen isotopic compositions of plants' source water. *Earth Planet Sci Lett* 185:355–367. [https://doi.org/10.1016/S0012-821X\(00\)00385-X](https://doi.org/10.1016/S0012-821X(00)00385-X)
- Thomas EM, Lin H, Duffy CJ et al (2013) Spatiotemporal patterns of water stable isotope compositions at the shale hills critical zone observatory: linkages to subsurface hydrologic processes. *Vadose Zone J* 12. <https://doi.org/10.2136/vzj2013.01.0029>

- Treydte K, Boda S, Graf Pannatier E et al (2014) Seasonal transfer of oxygen isotopes from precipitation and soil to the tree ring: source water versus needle water enrichment. *New Phytol* 202:772–783. <https://doi.org/10.1111/nph.12741>
- Ulrich DEM, Still C, Brooks JR et al (2019) Investigating old-growth ponderosa pine physiology using tree-rings,  $\delta^{13}\text{C}$ ,  $\delta^{18}\text{O}$ , and a process-based model. *Ecology* 100:e02656. <https://doi.org/10.1002/ecy.2656>
- van Schaik L, Palm J, Klaus J et al (2014) Linking spatial earthworm distribution to macropore numbers and hydrological effectiveness. *Ecohydrology* 7:401–408. <https://doi.org/10.1002/eco.1358>
- Vargas AI, Schaffer B, Yuhong L, Sternberg LDSL (2017) Testing plant use of mobile vs immobile soil water sources using stable isotope experiments. *New Phytol* 215:582–594. <https://doi.org/10.1111/nph.14616>
- Voelker SL, Brooks JR, Meinzer FC et al (2014) Reconstructing relative humidity from plant delta 18O and delta D as deuterium deviations from the global meteoric water line. *Ecol Appl* 24:960–975
- Vogel JC, Van Urk H (1975) Isotopic composition of groundwater in semi-arid regions of southern Africa. *J Hydrol* 25:23–36. [https://doi.org/10.1016/0022-1694\(75\)90036-0](https://doi.org/10.1016/0022-1694(75)90036-0)
- Warren JM, Brooks JR, Meinzer FC, Eberhart JL (2008) Hydraulic redistribution of water from *Pinus ponderosa* trees to seedlings: evidence for an ectomycorrhizal pathway. *New Phytol* 178:382–394. <https://doi.org/10.1111/j.1469-8137.2008.02377.x>
- Warren JM, Meinzer FC, Brooks JR et al (2007) Hydraulic redistribution of soil water in two old-growth coniferous forests: quantifying patterns and controls. *New Phytol* 173:753–765. <https://doi.org/10.1111/j.1469-8137.2006.01963.x>
- Warren JM, Meinzer FC, Brooks JR, Domec JC (2005) Vertical stratification of soil water storage and release dynamics in Pacific Northwest coniferous forests. *Agric For Meteorol* 130:39–58
- Weiguo L, Xiahong F, Yu L et al (2004)  $\delta^{18}\text{O}$  values of tree rings as a proxy of monsoon precipitation in arid Northwest China. *Chem Geol* 206:73–80. <https://doi.org/10.1016/j.chemgeo.2004.01.010>
- Weiler M, Naef F (2003) An experimental tracer study of the role of macropores in infiltration in grassland soils. *Hydrol Process* 17:477–493. <https://doi.org/10.1002/hyp.1136>
- Williams DG, Ehleringer JR (2000) Intra- and interspecific variation for summer precipitation use in pinyon–juniper woodlands. *Ecol Monogr* 70:517–537. [https://doi.org/10.1890/0012-9615\(2000\)070\[0517:IAIVFS\]2.0.CO;2](https://doi.org/10.1890/0012-9615(2000)070[0517:IAIVFS]2.0.CO;2)
- Zeng X, Liu X, Evans MN et al (2016) Seasonal incursion of Indian Monsoon humidity and precipitation into the southeastern Qinghai-Tibetan Plateau inferred from tree ring  $\delta^{18}\text{O}$  values with intra-seasonal resolution. *Earth Planet Sci Lett* 443:9–19. <https://doi.org/10.1016/j.epsl.2016.03.011>
- Zhou Y, Chen S, Song W et al (2011) Water-use strategies of two desert plants along a precipitation gradient in northwestern China. *Chin J Plant Ecol* 35:789–800
- Zweifel R, Zimmermann L, Zeugin F, Newbery DM (2006) Intra-annual radial growth and water relations of trees: implications towards a growth mechanism. *J Exp Bot* 57:1445–1459. <https://doi.org/10.1093/jxb/erj125>

**Open Access** This chapter is licensed under the terms of the Creative Commons Attribution 4.0 International License (<http://creativecommons.org/licenses/by/4.0/>), which permits use, sharing, adaptation, distribution and reproduction in any medium or format, as long as you give appropriate credit to the original author(s) and the source, provide a link to the Creative Commons license and indicate if changes were made.

The images or other third party material in this chapter are included in the chapter's Creative Commons license, unless indicated otherwise in a credit line to the material. If material is not included in the chapter's Creative Commons license and your intended use is not permitted by statutory regulation or exceeds the permitted use, you will need to obtain permission directly from the copyright holder.



# Chapter 19

## Climate Signals in Stable Isotope Tree-Ring Records



**Mary Gagen, Giovanna Battipaglia, Valerie Daux, Josie Duffy, Isabel Dorado-Liñán, Laia Andreu Hayles, Elisabet Martínez-Sancho, Danny McCarroll, Tatiana A. Shestakova, and Kerstin Treydte**

**Abstract** In this chapter we introduce the climate signal in stable isotope tree-ring records, with the emphasis on temperate forests. The development of the subdiscipline is recapped followed by an exploration of isotope dendroclimatic records by geography and, broadly, by isotopic species. Whilst there are still questions to be answered around signal strength and age-related effects in different environments and in different species, the proxy is now contributing to palaeoclimatology in a far greater way than in the days of the first hints of ‘isotope tree thermometers’. We include two summary tables. Table 19.1 exemplifies the range of climate information available from stable carbon isotope time series and Table 19.2 explores oxygen isotope proxy signals. Due to the greater complexity seen in stable carbon isotope interpretations we explore response groupings with example references given

---

M. Gagen (✉) · J. Duffy · D. McCarroll

Department of Geography, Swansea University, Singleton Park, Swansea SA2 8PP, UK  
e-mail: [m.h.gagen@swansea.ac.uk](mailto:m.h.gagen@swansea.ac.uk)

G. Battipaglia

Department of Environmental, Biological and Pharmaceutical Sciences and Technologies, University of Campania “L. Vanvitelli”, Via Vivaldi 43, 81100 Caserta, Italy

V. Daux

Laboratoire des Sciences du Climat et de l’Environnement, Université Paris-Saclay, CNRS, CEA, UVSQ, Gif-sur-Yvette, France

I. Dorado-Liñán

Forest Genetics and Ecophysiology Research Group, E.T.S. Forestry Engineering, Universidad Politécnica de Madrid, Madrid, Spain

L. A. Hayles

Lamont-Doherty Earth Observatory of Columbia University, Palisades, NY 10964, USA

ICREA, Barcelona, Spain

CREAF, Cerdanyola del Vallés, Barcelona, Spain

E. Martínez-Sancho · K. Treydte

Swiss Federal Institute for Forest, Snow and Landscape Research, WSL Research Unit Forest Dynamics, Birmensdorf, Switzerland

T. A. Shestakova

Woodwell Climate Research Center, 149 Woods Hole Rd, Falmouth, MA 02540, USA

© The Author(s) 2022

R. T. W. Siegwolf et al. (eds.), *Stable Isotopes in Tree Rings*, Tree Physiology 8,  
[https://doi.org/10.1007/978-3-030-92698-4\\_19](https://doi.org/10.1007/978-3-030-92698-4_19)



for each category of proxy response. Finally, we summarize the state of the art in isotope dendroclimatology and discuss possible future directions.

## 19.1 Introduction

Our understanding of the climate variability of the last two thousand years has been significantly aided by large, network tree-ring reconstructions, the dendroclimatic contribution to which is based almost exclusively on ring width and density data (e.g. PAGES 2k Consortium 2013, 2017; Neukom et al. 2019; Esper et al. 2014; Luterbacher et al. 2016). However, the increase in proxy data availability, for example of temperature reconstructions (Wilson et al. 2016; Mann et al. 1999; Helama et al. 2002; McCarroll et al. 2013; Linderholm et al. 2014; Dorado-Liñán et al. 2012, 2015; Klippel et al. 2019) has been accompanied by an understanding of the vital need for more information, at greater spatial resolutions, for more regions and including more variables than warm season temperatures (Smerdon and Pollack 2016; Gouirand et al. 2008; Frank et al. 2010). There is a particular need for additional tree-ring data from areas spatially underrepresented in climate proxy databases, in order to capture the regional signature of past climate variability (Smerdon and Pollack 2016). A key drive is an emerging picture of significant differences in the magnitude and dynamics of forced and internal climate variability which requires stronger regional detail through high-resolution regional reconstructions of multiple climate variables (e.g. Gagen et al. 2016; Smerdon and pollack 2016; Young et al. 2019).

Tree-ring width and density-based dendroclimatology has, in the last ten years, coalesced around four key efforts. To: (a) improve reconstructions of large scale changes to explore the hemispheric temperature signature of climate change, (b) to expand the geographic reach of regional temperature reconstructions to explore the dynamics of forced and internal variability, (c) to increase the breadth and depth of our understanding of the temporal variations in proxy records and the statistical fingerprints of different reconstruction methods and, (d) to expand the non-temperature (e.g. hydroclimate) potential of the tree-ring archive. Stable isotope measurements from tree rings, both annual and non-annual, contain valuable climatic, physiological and environmental information that can contribute to these research drives (McCarroll and Loader 2004). Here we review the research frontier in stable isotope dendroclimatology and explore the subject's contribution to palaeoclimate science.

### 19.1.1 *The Development of Stable Isotope Measurements from Tree Rings*

A cluster of studies carried out in the 1970s (Libby and Pandolfi 1974; Epstein and Yapp 1976; Libby et al. 1976; Yapp and Epstein 1977), began the process of exploring

what environmental information could be accessed by measuring isotopic variations in tree rings (see also Chap. 1). These early studies explored a range of isotope species and, whilst the methods were evolving, the earliest and most critical studies were of relevance to the exploration of both the water and carbon isotopes. Early tree-ring isotope time series were based largely on samples from a single tree, which required a huge time and monetary cost to produce and used a variety of measurement methodologies, analyzing pools of years together and often not extracting samples to cellulose before measurement. However, without the quantitative knowledge of how plant functions fractionate isotopes as they moved through the metabolic pathways of photosynthesis, and physically around the plant, and how sensitive these fractionations are to temperature changes, the tantalizing evidence for a new climate proxy was effectively stalled until the underlying fractionation theoretical frameworks were in place. When this happened in the 1980s and 1990s (e.g. Farquhar et al. 1982, 1989b; Francey and Farquhar 1982; Marshall and Monserud 1996) we were able to state unequivocally that stable isotope ratios measured from tree rings provided a usable environmental archive for the first time (see Chaps. 9, 10 and 13).

Early isotopic investigations on blocks of whole wood showed relatively little similarity in common isotopic signal (see Craig 1954; Farmer and Baxter 1974; Pearman et al. 1976; Libby and Pandolfi 1974). Whole wood contains varying amounts of resins and waxes, as well as lignin and cellulose (see Chap. 5). Without extracting and separating such components prior to analysis, it is difficult to obtain a common environmental signal not masked by noise from the isotopically heterogeneous resins, waxes and lignin. This problem was worked through by Epstein and Yapp (1977) and Wilson and Grinsted (1977). From this point onwards, it gradually became the working norm to extract tree-ring samples from wood to cellulose (or cellulose nitrate for  $\delta D$  in order to ensure that only non-exchangeable hydrogen is analyzed (Epstein and Krishnamurthy 1990) and Chap. 11), prior to the analysis of stable isotope ratios (Bradley 1985). Wilson and Grinsted (1977) established the methodology for cellulose extraction, based on the works of Green (1963), the so called 'Jayme-Wise' method. It is this method, or the alternative Brendel method (Brendel et al. 2000) that are generally used to extract whole wood tree-ring samples to cellulose still, often in fast batch processing systems to reduce lab time (Loader et al. 1997). Andreu-Hayles et al. (2019) summarizes the state of the art in isotope dendroclimatology preparation options (see also Chap. 5).

There is evidence that, with non-resinous species in particular, using whole wood can increase the efficiency of sample processing and still retain common signal coherence (Loader et al. 2003). The use of whole wood in isotopic tree-ring studies was encouraged by the revelation that there is a high degree of coherence between  $\delta^{13}C$  derived from cellulose and that from (resin-extracted) whole wood, with an offset between 1.5 and 3‰ (e.g. Loader et al. 2003) with variability between tree taxa. As the majority of climate reconstructions derived from stable isotope time series do not use absolute isotopic values, such an offset does not have consequences for reconstruction accuracy, and analyzing resin-extracted whole wood can heavily reduce lab time. A suite of studies has now developed climate reconstructions from

stable carbon isotope series based on whole wood measurements (e.g. Verheyden et al. 2005; Harlow et al. 2006).

Multiyear and multi-tree pooling methodologies have once again become popular, following increased knowledge about the between-tree levels of isotopic variability for commonly samples tree species (see Chaps. 4 and 6). These methods considerably increase time efficiency and reduce costs while providing comparable results to single tree studies, if certain conditions are met (Dorado-Liñán et al. 2011; Woodley et al. 2012).

For several decades after the palaeoclimatic potential of the stable isotope tree-ring proxies was first explored following the establishment of the models describing isotopic fractionation in C3 plants (e.g. Burk and Stuiver 1981; Farquhar et al. 1982), the literature remained dominated by single site studies with results from a few tree cores, with relatively low sample replication (Ramesh et al. 1986; Buhay and Edwards 1995; Anderson et al. 1998; Gagen et al. 2004, 2006; McCarroll and Pawellek 1998, 2001). Such studies offered exciting evidence of a strong, new climate proxy (McCarroll and Loader 2004) but its exploitation was limited by the time and costs associated with mass spectrometric analysis. The 2000s were thus marked by methodology developments that could be explored with low sample numbers, rather than large replication climate reconstructions from stable isotope dendroclimatology. There were hints of relatively simple age-related trends in carbon isotope time series (Gagen et al. 2007, 2008) and, eventually, in oxygen (Duffy et al. 2017, 2019; Büntgen et al. 2020) as compared to ring width proxies. Aspects remain to be explored, however, because there are mixed results from different species and sites (Treydte et al. 2006; Esper et al. 2010; Brienen et al. 2017). Non-climatic trends in multi-tree stable carbon isotope time series also revealed information on changing plant carbon water relationships (Gagen et al. 2011a; Andreu-Hayles et al. 2011) useful to future climate projections where an accurate estimate of physiological forcing from the biosphere is needed. Methods for pre-reconstruction corrections for the effects of the changing stable isotopic composition of atmospheric CO<sub>2</sub> (McCarroll and Loader 2004) and for the bulk rise in atmospheric CO<sub>2</sub> amount (McCarroll et al. 2009) were developed (see Chaps. 17 and 25).

Advances in analysis increased the sample replication that could be achieved in a reasonably equipped stable isotope dendroclimatology lab, by an order of magnitude (see Chap. 7) (Loader et al. 1997, 2017; Brendel et al. 2000; Gagen et al. 2012). By the 2010s isotope dendroclimatic reconstructions often had sample replications equivalent to studies using ring width or density data (Gagen et al. 2011b; Young et al. 2012a, b, c; Loader et al. 2013). However, the time and cost of producing these climate reconstructions, using stable isotope mass spectrometry, was astronomical in comparison to equivalent growth proxy times series based on ring width measurements. Moreover, the general dependence on a laboratory process that involves physically cutting each ring to be analyzed has limited the exploitation of the stable isotope tree-ring proxies at a time when they have much to contribute.

Whilst the first tree-ring network analyses using stable isotope data from multiple sites are emerging (e.g. Szejner et al. 2016; Young et al. 2019), exploitation of the full potential of the proxy is still held back by the maximum speed of mass spectrometry,

as the primary measurement method. At present a high-end stable isotope dendroclimatology lab uses some version of the following standard methodologies (see McCarroll and Loader 2004) to prepare samples for, and measure, stable isotopes of carbon, oxygen and hydrogen.

1. Dating via standard methods generally (see Loader et al. 2019 for an exception).
2. Physically isolating each ring, or a portion of each ring (e.g. latewood), by cutting.
3. Performing a variety of chemical extractions on individual samples, ranging from simple resin removal to full extraction to alpha-cellulose.
4. Drain, freeze dry, weigh out and individually ‘wrap’ samples.
5. Perform mass spectrometric analysis.

There is a pressing need to increase the speed, and reduce the cost, at which we can produce stable isotope tree-ring time series in order to reach the sample replication necessary for statistically high-quality networks of climate reconstructions.


The analysis method noted above typically achieves measurement precisions around 0.15‰ for  $\delta^{13}\text{C}$  and 0.3‰ for  $\delta^{18}\text{O}$  ( $\sigma_{n-1}$   $n = 10$ ) (Loader et al. 2016). In terms of increasing sampling speeds, at the very best step 1 is carried out by an ablating laser (Loader et al. 2017) and step 2 skipped in the analysis of non-resinous tree species. However, a more typical analysis time, from start to finish, is in the region of one week per 100 samples. Whilst the laborious nature of measuring stable isotopes by mass spectrometry is a limiting factor, there are other limitations to the reliance on this technique. Mass spectrometry typically requires a sample of the ring equivalent to approximately 2–300  $\mu\text{g}$  dry weight of alpha cellulose (Rinne et al. 2005). This can require a whole wood cut of several cubic mm of wood from each ring.

Stable isotope measurements are routinely reported using the delta notation (‰). This notation gives the ratio of the heavier to the lighter stable isotope relative to an isotope standard, in parts per mille. V-*SMOW* (Vienna Standard Mean Oceanic Water) is used as a standard for stable hydrogen and stable oxygen isotope measurements in tree-rings ( $\delta^2\text{H}$  and  $\delta^{18}\text{O}$ ) and V-*PDB* (Vienna Pee Dee Belemnite) as the standard for  $\delta^{13}\text{C}$  analyses (see Chap. 8 for a full discussion of the relevant isotopic notations and standards).

## 19.2 Dendroclimatic Information from Stable Carbon isotope Time Series

The use of  $\delta^{13}\text{C}$  as a tree-ring proxy is based on a mechanistic framework for the leaf-level fractionations of  $^{13}\text{C}/^{12}\text{C}$ , which allows us to understand the relationships between climate and variations in the stable carbon isotope ratio of photosynthate. In Table 19.1 we give an overview of the range of climate information, which can be derived from stable carbon isotope time series. In plants, discrimination against the heavier carbon isotope at the point that ambient  $\text{CO}_2$  enters the leaf, and again

**Table 19.1** Common climate signals in stable carbon isotope measurements from the rings of trees. Work on carbon isotope dendroclimatology is wider ranging than that on the water isotopes. A summary of the common signals and their associated environments is given in this table

	Site and isotope	Context	Common signals
<p>Less moisture stress—carbon isotope signal dominated by photon flux control over photosynthetic assimilation rate</p>  <p>More moisture stressed—carbon isotope signal dominated by hydroclimatic control of rate of stomatal conductance to CO<sub>2</sub></p>	Stable carbon isotopes (generally of latewood in conifers)	Stable carbon isotopes at high latitude, moist sites, generally in Boreal forest conifers	A photosynthetic proxy, not a growth proxy, variability is sensitive to (in addition to warm season temperature) cloud related hydroclimate e.g. summer % cloud cover (e.g. see Young et al. 2019) Summer temperature (often where sunshine data unavailable), in Russian Altai (Sidorova et al. 2013), Canadian Boreal forests (Gennaretti et al. 2017), Canada (Bégin et al. 2015). growing season relative humidity (Edwards et al. 2008)
	Stable carbon isotopes in tropical wood	Moist tropical environments	Moist tropics, relationship between stable carbon isotope variability and light availability remains (Brienen et al. 2016; van der sleen et al. 2014)
	Stable carbon isotopes in temperate regions, high elevation forest	Where moisture is available throughout the growing season	Summer sunshine and solar radiation (Hafner et al. 2014; Dorado-Liñan et al. 2016), summer temperatures in Europe (Lipp et al. 1991; Esper et al. 2015), Asia (Liu et al. 2014; Treydte et al. 2009) and South America (Lavergne et al. 2018)
	Stable carbon isotopes in lower latitude drier environments	High elevation ‘Mediterranean’ type forest or American latitudinal equivalents. Moisture stress restricts stomatal conductance to CO <sub>2</sub> in the summer	Cool season temperature (Heinrich et al. 2013) Summer precipitation and drought (Leavitt and Long 1989a, b, Bale et al. 2011; Kress et al. 2010). Also spring relative humidity in Asia (Liu et al. 2018). Extreme precipitation events in spring and summer in Iberia (Andreu-Hayles et al. 2017)

(continued)

**Table 19.1** (continued)

	Site and isotope	Context	Common signals
		Seasonally dry tropics	Seasonal drought signal (Gebrekirstos et al. 2009; Brienen et al. 2016) Use of dendrochemical and stable isotope methods to try and identify the annual ring boundary (with varying degrees of success), (Leavitt and Long 1991; Poussart and Schrag 2005; Ohashi et al. 2009; Evans and Schrag 2004; Anchukaitis et al. 2008; Pons and Helle 2011)

upon assimilation by the plant, depends on the internal leaf concentration of CO<sub>2</sub> ( $ci$ ) and on atmospheric CO<sub>2</sub> concentration ( $ca$ ) expressed as the ratio  $ci/ca$  (Farquhar et al. 1982, 1989b). Chapter 9 gives a full discussion of these fractionation and discrimination processes. In trees growing in climates which are not water limited,  $ci$  is regulated primarily by photosynthetic rate, controlled by variations in temperature and sunlight. In climates that are water limited,  $ci$  is more often regulated by stomatal conductance to CO<sub>2</sub>, controlled by antecedent precipitation and relative humidity (Gebrekirstos et al. 2009; Brienen et al. 2016). Thus, at sites where the fundamental laws of dendroclimatology apply (Fritts 1976) stable carbon isotope measurements in tree rings, have successfully been used to reconstruct summer sunshine (e.g. Young et al. 2019) temperature (e.g. Payomrat et al. 2018) as well as hydroclimate proxies (e.g. Liu et al. 2004; Roden and Ehleringer 2007).

Dendroclimatic reconstructions based on stable carbon isotopes still represent a small fraction compared to those based on more readily measured variables such as tree-ring width and maximum latewood density. Although they have a higher production cost, stable carbon isotope measurements from tree rings also offer a record of changes in plant carbon–water relationships via Intrinsic Water Use Efficiency (iWUE) as it responds to changes in atmospheric CO<sub>2</sub> (i.e., Leavitt and Long 1986, 1988; Granda et al. 2017). We can summarize the proxy potential of stable isotope dendroclimatology:

- Stable carbon isotope tree-ring time series record the interaction between photosynthetic rate and stomatal conductance. As such they are not a growth proxy, their variability is sensitive to parameters including warm season temperature and sunlight as well as hydroclimate e.g. summer cloud cover at moist, high latitude sites.
- Age related trends in stable carbon isotope tree-ring time series are less complicated than in growth proxy series, and their impacts on signal strength are easier to mitigate via simple mathematical standardizations and juvenile cut-off points.

- The capture of additional information in stable carbon isotope series related to changes in plant carbon–water relationships through time (e.g. Intrinsic Water Use Efficiency, discussed below and in Chap. 17), which add to the range of paleoenvironmental information available from tree-ring records.

Carbon isotopes in tree rings have some advantages of interpretation, in comparison to growth proxies, because the fractionation mechanisms controlling carbon isotope variability are known (Farquhar et al. 1982, 1989), the signal-to-noise ratio between trees is high (McCarroll and Pawellek 1998), they can preserve high-to-low frequency common climate signals and the number of samples required to build a statistically robust chronology is often lower than for other tree-ring proxies (Leavitt and Long 1986; McCarroll and Loader 2004). The proxy is an integration of (1) the stable isotope composition of atmospheric carbon dioxide, (2) the relevant regulation rates within trees (photosynthetic and stomatal conductance rates), and (3) the environmental variables, which influence those rates, including temperature, sunlight, relative humidity and precipitation (McCarroll and Loader 2004). All climate reconstructions based on carbon isotope measurements from tree rings are built upon the theory of how carbon dioxide is fractionated at the entrance to the stomatal pores and in the C3 photosynthetic pathway (Farquhar et al. 1982, 1989b). A suite of environmental variables influences these fractionation set points by exerting control over two rates – stomatal conductance to CO<sub>2</sub> (generally noted as *g<sub>s</sub>*) and photosynthetic assimilation rate (generally noted as *A<sub>N</sub>*). Sites at which stomatal conductance to CO<sub>2</sub> dominates the stable carbon isotope signal are usually restricted to dry, or moisture stressed, forests. In non-moisture-limited settings carbon isotope discrimination is generally controlled by photosynthetic rate, driven by temperature and/or sunlight (Farquhar et al. 1989a; McCarroll and Loader 2004). Unlike ring-width and density tree-ring proxies, carbon isotope series contain simpler age-related trends and, at some sites, do not require detrending, allowing low-frequency variability to be fully preserved in the final reconstruction (McCarroll and Loader 2004; Gagen et al. 2007). Comparisons between paleoclimate reconstructions based on ring width and carbon isotopes in some cases reveal similar (Esper et al. 2015; Bale et al. 2011) or even larger (e.g., Lavergne et al. 2018) variability in the carbon isotope series and increased signal capture at variable frequencies. However, this is not the case for all species and all sites (Esper et al. 2010, 2015; Helama et al. 2015; Brienen et al. 2017).

At sites where significant age-related trends do exist in stable carbon isotopes, tree-ring density series, or their digital equivalent (McCarroll et al. 2002; Campbell et al. 2011; Wilson et al. 2014) are more suited to the reconstruction of past temperature variations because of their lower analysis costs. However, stable carbon isotopes offer additional advantages due to their increased frequency capture and as they appear be less prone to the ‘divergence problem’ (i.e., the loss of climate sensitivity in growth proxies, during recent decades, Jacoby and D’Arrigo 1995; Savard and Daux 2020).

### ***19.2.1 Dendroclimatic Information from Stable Carbon Isotope Time Series in Temperate Regions***

In temperate regions and high latitude forests, where adequate moisture is usually available throughout the growing season, stable carbon isotopes from tree rings have been successfully used to reconstruct past changes in summer sunshine and solar radiation (Hafner et al. 2014; Dorado-Liñan et al. 2016) and summer temperatures, further south into Europe (Lipp et al. 1991; Esper et al. 2015), Asia (Liu et al. 2014; Treydte et al. 2009) and South America (Lavergne et al. 2018). Temperature reconstructions at high latitude sites have traditionally been assessed based on tree-ring width and maximum density (Wilson et al. 2016, St. George and Esper 2019 and references therein). Heinrich et al. (2013) expanded the focus of European carbon isotope-based reconstructions of temperature to Turkey with an 850-year reconstructions of cool season (winter-to-spring) temperature, consistent with the atmospheric circulation patterns governing the cool season climatology of the region.

At higher latitude, moist, sites, stable carbon isotopes have proven a strong and reliable proxy for cloudiness and parameters related to summer sunshine hours (e.g., Gagen et al. 2011b; Loader et al. 2013; Young et al. 2010). However, the extension of successful reconstructions of sunshine from stable carbon isotopes into drier regions, below the high latitudes, also reflects the strength of the relationship between the variable and sunshine. Reconstructions include sunshine hours in the Alps (Hafner et al. 2014) and surface solar radiation in mountainous area of Spain (Dorado-Liñan et al. 2016). The strength of the carbon isotope ‘palaeocloud’ proxy is unsurprising given that the action of rubisco is far more strongly controlled by photon flux (sunlight) than temperature (Farquhar et al. 1982). At more mesic sites related climatic variables share influence over the carbon isotope signal and temperature can be reconstructed via its co variation with summer sunshine, solar radiation or vapor pressure deficit (McCarroll and Loader 2004; Treydte et al. 2009; Dorado-Liñan et al. 2016). Care must be taken not to extend this assumption to areas where summer sunshine and temperatures do not co vary, particularly at lower frequencies (e.g. Young et al. 2019). Emerging reconstructions of past cloudiness and summer sunshine are of crucial importance in current climate research since it may allow for an integrated assessment of the cloud-climate feedback, an important cause of the large spread in climate sensitivity between climate models (Dessler 2010; Flato et al. 2013).

At sites where summer moisture stress restricts stomatal conductance to CO<sub>2</sub>, or where moisture stress is involved in the covariation of multiple climate variables (precipitation, temperature, cloudiness etc.) carbon isotope variability can be used to reconstruct summer precipitation and drought, in the USA (Leavitt and Long 1989a, b; Bale et al. 2011), and in central Europe (Kress et al. 2010) as well as spring relative humidity in Asia (Liu et al. 2018). Andreu-Hayles et al. (2017) used carbon isotopes to explore and corroborate extreme precipitation events in spring and summer in the Iberian Peninsula. This study also explored non stationarity in carbon isotopes, in this case shifts through time in the dominant climatic limiting factor (from control of carbon variability by spring precipitation to summer precipitation). Beyond the



reconstruction of specific climate parameters, carbon isotope variability in trees has also been used to reconstruct global modes of atmospheric circulation such as ENSO (Bale et al. 2011; Liu et al. 2014; Lavergne et al. 2018).

The carbon isotope proxy, in the temperate latitudes where tree rings excel in climate reconstructions, has clear potential to develop the continental scale network reconstructions that now dominate efforts with growth proxy time series (D'Arrigo et al. 2006a; Schneider et al. 2015; Stoffel et al. 2015; Wilson et al. 2016). Leavitt and Long (1989b) represent one such attempt, to reconstruct regional July drought variability across the north American southwest using a stable carbon isotope tree-ring network. To date, however, the regional networks of carbon isotopes chronologies, spanning several centuries, that do exist across North America and Europe, have predominantly been used to track changes in plant physiological responses such as Intrinsic Water Use Efficiency (i.e., Saurer et al. 2014; Frank et al. 2015; Shestakova et al. 2019).

As the palaeoclimate potential of well-replicated carbon isotope series was fully explored for the first time in the high latitudes (e.g. McCarroll and Pawellek 1998, 2001) the discipline has tended to focus on the conifer species, which dominate the northern forest zones. Whilst there are many species used to explore stable carbon isotope proxies in temperate forest, there are some taxa that have contributed most significantly to palaeoclimate products. These are *Fagus*, *Picea*, *Quercus*, *Abies*, *Larix* and *Pinus* (e.g. Saurer et al. 1997; Skomarkova et al. 2006; McCarroll and Loader 2004; Gagen et al. 2007; Churakova et al. 2019; Esper et al. 2015; Ferrio and Voltas 2005; Hafner et al. 2014; Helama et al. 2015; Holzkämper et al. 2012; Kirilyanov et al. 2008).

Stable carbon isotopes in tree rings from temperate regions offer an incomparable source of information to reconstruct climate variables that are unlikely to be accessible using other proxy records, such as summer cloudiness and non-age detrended temperature reconstructions, as well as having the potential to enhance our picture of climate variability in the southern hemisphere. The dominance of conifers in our understanding of carbon isotope variability should be useful as the discipline starts to focus on the underrepresented southern hemisphere, where preliminary results in conifers have shown the potential of carbon isotopes (Gebrekirstos et al. 2009).

### ***19.2.2 Dendroclimatic Information from Stable Carbon Isotope Time Series in Northern and Boreal Regions***

The limitation of photosynthetic assimilation rate by temperature and/or sunlight is common across northern latitudinal and boreal forests (see also Chap. 20). In those regions, moisture limitation is not as common as in lower latitudes and carbon isotope variability in trees is found to be driven primarily by the limitation of photosynthetic rate by photon flux. The capacity of stable carbon isotopes in Fennoscandian conifer

tree rings to track historical changes in sunlight and, where it covaries with cloudiness, summer temperatures too, has been consistently demonstrated (e.g. Gagen et al. 2011a; Loader et al. 2013; Young et al. 2010, 2019). Those reconstructions have not only described past changes in sunlight, but also revealed changes in atmospheric circulation patterns (Young et al. 2012b, 2019; Loader et al. 2013) providing the first attempt to better understand the largest source of uncertainty in modelling future changes in climate: the cloud-climate feedback (Dessler 2010; Flato et al. 2013; Boucher et al. 2013). Whilst the relationship between summer cloud and temperature was revealed, across the Fennoscandian boreal zone, as negative at interannual time scales, analysis of millennial length temperature and summer cloud cover reconstructions revealed the relationship to be positive at decadal time scales (Young et al. 2012b, 2019). Thus, warmer periods in the past were associated with increases in cloud cover at decadal time-scales, linked to the position of the polar vortex and the variability of the Arctic Oscillation (Young et al. 2012b, 2019; Loader et al. 2013). At these sites, cloudiness is likely modulating local summertime temperature at inter-annual time scales, but at longer timescales, cloud cover may respond to large-scale multidecadal temperature changes (Dessler 2010). Thus, assessments of the relationship between cloud cover and temperature at both hemispherical and millennial time-scales are needed to provide a more complete picture, spatially and temporally, of the cloud-climate feedback. In this context, carbon isotope records derived from subfossil wood (e.g. Helama et al. 2018) offer a promising opportunity for extending the Fennoscandia summer cloud reconstructions back in time to tease apart the high latitude cloud-temperature feedback further. This endeavor becomes more pressing the more we learn about how significantly clouds are involved in moderating or enhancing greenhouse gas induced warming in the past (Zhu et al. 2019).

Stable carbon isotopes in combination with other tree-ring variables have also been used to estimate July–August mean temperature in the Russian Altai for the last 200 years (Sidorova et al. 2013) and Canadian Boreal forests for the last millennium (Gennaretti et al. 2017). Bégin et al. (2015) reconstructed 200 years of June–August maximum temperature in northeast Canada by combining stable carbon and oxygen time series. Edwards et al. (2008) reconstructed growing season relative humidity for the last thousand years based on carbon isotopes from living and subfossil conifer species in boreal western Canada. In the highest Arctic environments methods have also been pioneered to explore carbon isotope variability in the annual stem growth increments of Arctic Bell Heather *Cassiope tetragona* (Rayback and Henry 2006) and *Salix* species (Schifman et al. 2012), with correlations to growing season precipitation in these strongly climate limited shrub species.

In addition to complexity of decoding the prime driver of isotopic fractionation in different climatic settings, carbon isotope records also experience common tree-ring proxy pitfalls such as non-linearities (Schleser et al. 1999) and changes in climate sensitivity through time (Daux et al. 2011; Andreu-Hayles et al. 2017). Non-linear responses to climate, and shifts or loss, of climate sensitivity are well-known issues in tree-ring growth, particularly at low latitude and high-altitude sites (Esper and Frank 2009; St. George and Esper 2019). Isotopic fractionation is an active mechanism that involves active physiological adjustments by the tree to changing environmental

conditions. Non-linear responses due to shifts in the acclimation strategy to new conditions have been described in old boreal trees (Giguère-Croteau et al. 2019) as water use efficiency changes in response to rising CO<sub>2</sub> (see Chap. 17).

The regularity with which carbon isotope series from moist high latitude sites are interpreted as temperature proxies may be partly related to the scarcity of reliable instrumental records of sunlight and cloud cover. These parameters are sometimes not even considered as potential drivers of isotopic fractionation (e.g., Kirilyanov et al. 2008; Naulier et al. 2014). Where cloud data is available, the often-limited length of those records can prevent testing of the co variance of summer cloudiness with temperature on all time scales or the stability of the climate signal through time leading to assumptions about the linearity of the climate-carbon isotope relationship through time (e.g., Helama et al. 2018; Churakova et al. 2019). As a result, carbon isotopes have been interpreted as palaeotemperature records where temperature is in fact not the primary driver of carbon fractionation at the site (e.g. Gagen et al. 2007). Where temperature and cloud cover co vary in the summer, which should be explored in the instrumental record wherever possible before regression-based reconstruction of either parameter from carbon isotope records is attempted (see Young et al. 2019 for an example), the reconstruction of one variable from the other is not necessarily problematic. Where cloud cover and temperature do not co vary in a region a divergence between the temperature reconstruction from carbon and independent temperature reconstructions will appear back in time (e.g. Gagen et al. 2007). The identification of periods in which temperature and sunshine or cloud cover may have diverged might be the key to unequivocally identify the primary driver of carbon fractionation at such sites, or its non-stationarity through time. In this context, the atmospheric alteration caused by large volcanic eruptions may cause a large-scale cooling, which is detectable in temperature sensitive tree-ring records (D'Arrigo et al. 2013; Stoffel et al. 2015) but may not affect the photosynthetic capacity of the tree, which translates in non-significant changes in carbon isotopes (Gu et al. 2003; Battipaglia et al. 2007; Dorado-Liñán et al. 2016).

Tree-ring stable carbon isotopes in boreal forests offer perhaps the best opportunity to accurately constrain one of the main sources of uncertainty in the simulation of climate models: the cloud-climate feedback. By focusing on unequivocally identifying the main limiting factor of carbon fractionation and ensuring the stability of the climate signal, it should be possible to assess hemispheric relationships and feedbacks between cloud cover and temperature and vapor pressure deficit (VPD) providing critical information for the climate modelling community.

### ***19.2.3 Dendroclimatic Information from Stable Carbon Isotope Time Series in the Tropics***

Tropical forests hold about half of the planet's total terrestrial carbon biomass (Pan et al. 2011; Hunter et al. 2013). They home ecosystems spanning from humid to sub

humid to dry (Fig. 19.1). They are considered one of the major environments under threat from habitat loss and climate change (Holm et al. 2017) and the drive to find ways to develop tree-based climate proxies for the tropical forest regions of the world has a long history (Worbes 2002; Stahle 1999). Carbon isotope studies in tropical trees have much to contribute to tropical environmental science because of debates around the future behavior of the tropical forest carbon sink (Körner 2009; Lloyd and Farquhar 2008), and because proxy climate records for the tropics are still profoundly limited (see also Chap. 22). The scarcity of long instrumental climate records for the tropics, and the importance of the tropics in global climate dynamics (Chiang 2009), drives the motivation to expand the field of tropical isotope dendroclimatology. Settling questions around carbon dynamics in tropical trees requires a more detailed understanding of tropical plant carbon water dynamics (e.g. Loader et al. 2011) as well as detailed analyses of physiological and environmental drivers of tropical wood formation at daily, seasonal and multi-annual timescales (Steppe et al. 2015, Chap. 22). Whilst studies on tropical wood remain scarce, compared to temperate

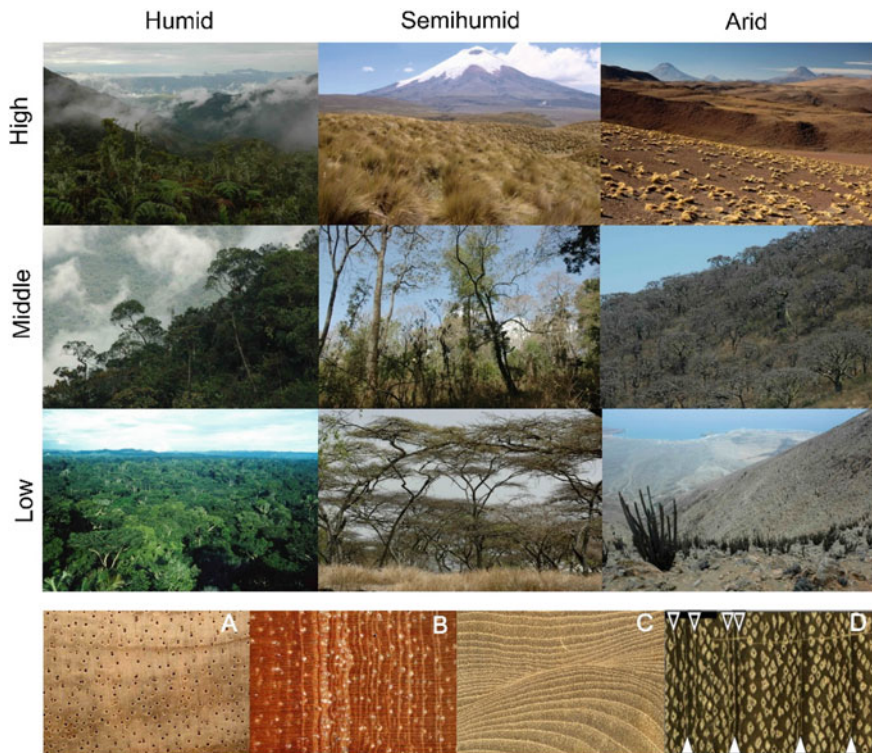


**Fig. 19.1** Ecosystems included in the tropical area and pictures of wood with **A**) poorly visible rings , **B**) suppressed rings , **C**) wedging rings : **D**) false (empty triangle) and real rings. Examples are given for lowland, mid (forested) and upper (tree line) elevations. Modified from Brienen and Gebrekirstos (adapted from TRACE 2019, San Leucio Caserta)

and high-latitude regions, there is a common agreement about the need to integrate methodologies to explore tropical isotope dendroclimatology (Sass-Klaassen et al. 2016; Van der Sleen et al. 2017).

Tropical dendrochronology is a relatively new discipline in and of itself, because of the difficulties of cross dating tropical wood, caused by the lack of simple warm-cool seasonality in the tropics. Cross dating tree rings visually is, at best, challenging and in 'ever wet' areas of the humid tropics impossible due to the lack of the climate seasonality needed to form an annual growth cycle in trees. Early studies focused on seasonally dry regions where the climate was capable of forcing a ring boundary. Coster (1927) and Berlage (1931) described annual growth rings in teak trees from tropical Indonesia, because the dry season provoked the cambial dormancy necessary for annual ring formation. This has been found to be the case across the seasonally dry tropics, including Australia (e.g. Buckley et al. 2010; D'Arrigo et al. 2006b; Heinrich et al. 2008; Pumijumnong and Eckstein 2011), tropical Africa (e.g. Therrell et al. 2006; Trouet et al. 2010) and the American tropics (e.g. Biondi 2001; Worbes 1999). Elsewhere ring boundaries have also been found to be caused by cambial activity cessation in flood periods within seasonally flooded Amazonian forests (e.g. Schöngart et al. 2002, 2004) or during salinity fluctuations in mangrove forests (e.g. Robert et al. 2011; Verheyden et al. 2004b). Whilst a number of tropical trees do grow annual rings, which can be cross dated (see Worbes 2002), there are many other problems facing the tropical dendrochronologists once they have found a species that at least grows annual rings. Indistinct ring boundaries are common, and many of the above studies mention low correlations with climate when calibration is attempted (generally with the short instrumental climate data typical for much of the global south). Tropical isotope dendroclimatology (Evans and Schrag 2004) emerged as a drive to resolve seasonality in tropical trees that lack visible tree-ring-boundaries by using seasonal stable isotope variability (e.g. Poussart and Schrag 2005).

An early endeavor was to utilize stable isotope variability to define the ring boundary in tropical trees (Leavitt and Long 1991). In Thailand Poussart and Schrag (2005) and later Ohashi et al. (2009) applied a version of this method seeking to use seasonal peaks and troughs in dendrochemical variables to identify non-visible tree ring boundaries isotopically. However, Poussart and Schrag (2005) seminal study achieving dendro isotope dating in the tropics has not been widely replicated. Tropical oxygen isotope dendroclimatology, or the combination of both isotopes (carbon and oxygen), has also been used to facilitate boundary identification in Costa Rica (Evans and Schrag 2004; Anchukaitis et al. 2008), Kenya (Verheyden et al. 2004a), Central Guyana (Pons and Helle 2011) and Brazil (Ohashi et al. 2015). These methods take advantage of the fact that in tropical areas where temperature and photoperiod are more or less constant through the year (Fromm 2013) a driver for periodic wood formation can be identified through changes in precipitation seasonality (Worbes and Junk 1999) or seasonal shifts in isotopic source water signal (Anchukaitis et al. 2008).

Several studies also reveal strong correlations between stable carbon isotopes and climate in seasonal tropical trees. In tropical regions with a pronounced dry season, the limitation of stomatal conductance by moisture stress gives rise to robust climate

variability in tree-rings that is effectively a seasonal drought signal (Gebrekirstos et al. 2009; Brienen et al. 2016), providing the growth rings can be dated by traditional means. The signal is generally thought to be linked to water availability and precipitation amount provoking stomatal limitation of the internal partial pressure of carbon dioxide (Leavitt and Long 1991; Schubert and Timmermann 2015; Li et al. 2011). However, in moist environments the relationship between stable carbon isotope variability and parameters related to sunlight availability seems to hold true in the tropics as it does elsewhere (Brienen et al. 2016; van der Sleen et al. 2014).

In a recent review by van der Sleen et al. (2017) the theory, methods and results of tropical isotope dendroclimatology are reviewed and summarized (see also Chap. 22). Their review of 50 studies revealed a dominance of controls over stable carbon isotope variability by water availability, light and nutrient supply in tropical studies. Whilst oxygen isotope variability was dominated by source water signals with the potential for additional variables influencing fractionation, such as rooting depth and evaporative enrichment at the leaf (van der Sleen et al. 2017). The review also mentions the emerging importance of nitrogen isotope investigations, which can be used to explore the nitrogen cycle in complex tropical ecosystems.

#### ***19.2.4 Carbon Isotope Climate Sensitivity in Response to Increasing CO<sub>2</sub>***

Intrinsic Water Use Efficiency (iWUE) is a useful variable for studying spatial and temporal changes in plant carbon–water relations and provides information on climate–vegetation feedbacks at broad geographical scales (Dekker et al. 2016; Lavergne et al. 2019). In the context of stable isotope tree-ring science, iWUE can be derived from  $\delta^{13}\text{C}$ . A detailed description and explanation of iWUE is given in Chap. 17.

Assessing changes in iWUE inferred from the stable carbon isotopes across tree-ring networks reports an average global increase in tree iWUE of 0.1–0.3% per year over the last century (Peñuelas et al. 2011; Battipaglia et al. 2013; Saurer et al. 2014; Frank et al. 2015). Increases in iWUE are detected regardless of biome (Andreu-Hayles et al. 2011; Silva and Anand 2013), tree species (Martínez-Sancho et al. 2018; Lévesque et al. 2014) or tree status (Hereş et al. 2014; Voltas et al. 2013). Rises in iWUE seem generally to be more rapid during the second half of the twentieth century (up to >0.5% per year) (see Gagen et al. 2011b) at some sites. However, the rate of change is strongly site and species specific (e.g. Saurer et al. 2004). iWUE time series have been observed where increases are halted by active stomatal control in response to rising atmospheric CO<sub>2</sub> (Waterhouse et al. 2004; Gagen et al. 2011b; Bert et al. 1997; Saurer et al. 2004) and time series where ‘spikes’ of very large changes in iWUE occur against a background of a broadly passive response to rising CO<sub>2</sub> (Belmecheri et al. 2014). Increases in iWUE are still observed when solely accounting for the effect of increasing atmospheric CO<sub>2</sub> concentrations after

removing the climatic signal from stable carbon isotope series (Frank et al. 2015). This suggests that trees may have adapted allowing the CO<sub>2</sub> partial pressure within the stomatal cavities to rise in balance with atmospheric CO<sub>2</sub> concentration.

The species' and geographical variability in iWUE increases is unsurprising for two reasons, first, because of the range of carbon water economics that have evolved in trees, such that for some species it is beneficial to increase iWUE and for others less so (Lin et al. 2015). Second, CO<sub>2</sub>-induced increases in iWUE can be a response to more than one change within the tree (Franks et al. 2013). Elevated CO<sub>2</sub> does stimulate photosynthesis (Lloyd and Farquhar 2008), reduce stomatal conductance to a minor degree (Ehleringer et al. 1993; Farquhar et al. 1989) and allow trees to absorb the same amount of carbon with less water loss. However, FACE (Free Air CO<sub>2</sub> Enrichment) experiments have found little stomatal response to increasing CO<sub>2</sub> in mature trees (see Chap. 21 and 24). Reductions in stomatal conductance can also, however, be linked to increases in the costs of respiration (Clark et al. 2013; Wright et al. 2009), heat stress (Corlett 2011) and drought stress due to increasing transpiration as our climate dries out (Wright et al. 2009). Climatic drying is considered to be causal at several sites where an increase in iWUE does not translate in enhanced tree growth (Peñuelas et al. 2011).

Spatial variability in iWUE also assists with interpreting temporal changes in  $\delta^{13}\text{C}$  derived iWUE time series. Large changes in iWUE are found across regional aridity gradients, in particular in isohydric species (gymnosperms), which respond to water stress by strongly regulating transpiration to maintain near constant leaf water potentials when soil moisture drops (Brodribb et al. 2014). In such species, at arid sites, negative correlations are found between iWUE and metrics of water availability such as annual precipitation (*Pinus halepensis*, Ferrio and Voltas 2005), groundwater access (*Pinus sylvestris*, Song et al. 2016), or rooting depth (*Pinus sylvestris*, Santini et al. 2018). Differences in iWUE (from pooled analyses) may exceed 30% between aridity extremes (Santini et al. 2018). Strong latitudinal gradients, linked to hydro-climatic conditions, have been reported for iWUE across Europe, with increasing values southwards (Saurer et al. 2014). However, factors such as nutrient supply and interactions with climate influence the regional variability in iWUE, which may confound water availability effects across spatial scales (Silva et al. 2015).

A better understanding of how plant carbon water relationships change across environmental gradients is needed to improve predictions of how water and carbon balance within forest ecosystems are changing with climate (Saurer et al. 2014; Frank et al. 2015). The extent to which variation in iWUE translates into carbon-water changes at the ecosystem scale remains unclear. The complexities of changes in leaf area index and canopy structure under climate change, along with atmospheric boundary-layer feedbacks, challenge upscaling leaf-level information from tree rings to the whole ecosystem scale (Medlyn et al. 2017; Lavergne et al. 2019).

Outside the temperate regions, Rahman et al. (2019) summarize evidence for trends in tree growth and iWUE triggered by elevated CO<sub>2</sub> against the background of climate change. The authors report that almost all studies show a consistent decrease of carbon discrimination over time, resulting in an increase in iWUE. Van der Sleen et al. (2014) estimate an increase of iWUE of 30–35% across the tropics in response

to elevated CO<sub>2</sub> but expect no similar increase in radial growth due to the impact of other factors in the nutrient-limited tropics. In a study of iWUE changes in non-annual ring forming trees in Borneo, Loader et al. (2011) found postindustrial increase in iWUE of similar magnitude as described by Van der Sleen et al. (2014). Rahman et al. (2019), reviewing iWUE histories in 81 species at 115 tropical sites, found increases in iWUE but no stimulated radial growth, as the negative effects of climate change overrode the fertilization potential of rising CO<sub>2</sub>.

Disentangling the iWUE/fertilization response in the tropics will take multi proxy ecophysiological studies of tropical wood formation, combining stable isotope, radio-carbon, wood anatomy and X-ray densitometry (De Mil et al. 2017). The climatic responses in these multiple proxies could then be combined to provide more robust long-term estimates of the response of tropical trees to past climate and improve model simulations of the impact of future climate change on tropical trees (De Micco et al. 2019).

## 19.3 Dendroclimatic Information from Stable Oxygen Isotope Time Series

### 19.3.1 *Early Literature and Progress in Interpretations of $\delta^{18}\text{O}$ Values in Tree-Rings*

In the mid-1970s, trees were postulated to contain an ‘isotopic thermometer’ in the  $\delta^{18}\text{O}$  of tree-ring wood or extracted cellulose (Libby 1972; Libby and Pandolfi 1974). These early investigations were conducted on oak, cedar or spruce from temperate areas (Libby 1972; Libby and Pandolfi 1974; Libby et al. 1976; Gray and Thompson 1977). Following technical improvements in mass spectrometry, stable oxygen isotope tree-ring chronologies from sub-tropical to sub-arctic sites also began to be explored, revealing correlations with hydroclimate variables (including air humidity) and the isotopic signature of source water, whilst progress was also made in the mechanistic modeling of isotopes in soil and plant cellulose (Burk and Stuiver 1981; Edwards and Fritz 1986; Ramesh et al. 1986). In 2006 Treydte et al. published the first millennial length, annually resolved, well replicated stable oxygen isotope chronology, with results from seven *Juniperus turcestanica* from Northern Pakistan. This study also led the way in applying the standard statistical practices of traditional dendroclimatology - calibration/verification techniques—to a long, well replicated oxygen isotope tree-ring time series (Masson-Delmotte et al. 2005; Treydte et al. 2006).

Table 19.2 summarizes the range of climatic and environmental information, which can be derived from stable oxygen isotopes in tree rings. The climate signal in tree-ring stable oxygen isotopes arises from the influence of (a) meteorological processes before the water is incorporated into the tree (Chap. 18) and (b) the interaction between the atmosphere and the leaf (Chap. 10, see also Sects. 14.4.1 and 16.3).



**Table 19.2** Examples of oxygen isotope dendroclimatology studies across the boreal zone and high latitude areas of the northern hemisphere, the mid latitude temperate forest zone in northern and southern hemisphere and tropical forests. The examples are not exhaustive but provide an overview of available records and climate signals recorded in tree-ring oxygen stable isotopes in different biomes

Biome	Climate signal	Examples
Arctic tundra (high latitude)	Summer temperatures and North Atlantic Oscillation (NAO)	<i>Betula pubescens</i> January–August (1950–1999, Xu et al.2021)
		<i>Cassiope tetragona</i> (Welker et al.2005)
Boreal forests (high latitude)	Summer season temperatures	<i>Picea mariana</i> warm season (1936–2004, Holzkämper et al. 2012) and summer (1000–2000, Naulier et al. 2015; 997–2006, Gennaretti et al. 2017); combined with $\delta^{13}\text{C}$ (1800–2003, Bégin et al. 2015)
		<i>Picea glauca</i> (1780–2003, Porter et al. 2013)
		<i>Pinus sylvestris</i> (1736–2006, Seftigen et al. 2011)
	Spring and summer precipitation	<i>Pinus sylvestris</i> July (1600–2002, and summer (1736–2006, Seftigen et al. 2011); <i>Picea mariana</i> May (1936–2004, Holzkämper et al. 2012)
Temperate forests (mid latitude) Northern Hemisphere	Summer temperatures	<i>Pinus sibirica</i> 1901–2000, Loader et al. 2010), <i>Quercus</i> sp (1596–2000, Etien et al. 2008a); <i>Larix decidua</i> (1980–2010, Leonelli et al. 2017); with low cloud fog <i>Sequoia sempervirens</i> (1952–2003, Johnstone et al. 2013)
	Precipitation (different seasons)	Summer: <i>Larix sibirica</i> (2 centuries, Sidorova et al. 2013); <i>Quercus</i> sp. (1600–2000, Labuhn et al. 2014); <i>Quercus robur</i> (1613–2003, Rinne et al. 2013); <i>Pinus ponderosa</i> (1967–2002, Roden and Ehleringer 2007), <i>Abies alba</i> (1840–1997, Saurer et al. 2000) Spring/Summer: <i>Pinus sylvestris</i> (1600–2002, Andreu-Hayles et al. 2017)

(continued)

**Table 19.2** (continued)

Biome	Climate signal	Examples
		October–September: <i>Pinus sylvestris</i> (1950–2009, Giuggiola et al. 2016) Winter: <i>Quercus robur</i> (Robertson et al. 2001)
	Summer season precipitation and temperature	<i>Picea abies</i> (1913–1995, Anderson et al.1998); <i>Pinus sylvestris</i> and <i>Quercus petraea</i> (1660–2002, Reynolds-Henne et al.2007); various? (1800–2000, Saurer et al. 2008); <i>Quercus</i> sp (1850–2012, Young et al. 2015)
	Summer drought, summer temperature, relative humidity (RH) and/or vapor pressure deficit (VPD)	<i>Pinus sylvestris</i> (1935–2005, Esper et al. 2018); <i>Quercus petraea</i> , <i>Fagus sylvatica</i> and <i>Pinus sylvestris</i> (1960–2007, Daux et al. 2018); <i>Quercus petraea</i> (1900–2000, Etien et al. 2008a); <i>Picea abies</i> , <i>Fagus sylvatica</i> and <i>Larix decidua</i> (1970–2010, Hartl-Meier et al. 2015); <i>Quercus</i> sp (1600–2000, Labuhn et al.2014; 1326–2000, Labuhn et al. 2016); <i>Quercus</i> sp (1600–2000, Masson-Delmotte et al.2005); <i>Quercus</i> sp (1885–1996, Raffalli-Delerce et al.2004); <i>Quercus robur</i> (1895–1994, Robertson et al. 2001); <i>Quercus</i> sp., <i>Pinus sylvestris</i> and <i>Cedrus deodora</i> (1900–2004, Treydte et al. 2007)
	Various warm season climate variables	<i>Liriodendron tulipifera</i> and <i>Quercus rubra</i> (1950–2014/2015 and 1980–2015, Levesque et al. 2019); <i>Quercus</i> sp (1200–2000, Loader et al. 2019)
Temperate forests (mid latitude) Southern Hemisphere	Summer temperature	<i>Austrocedrus chilensis</i> Sep–March (1890–1998, Roig et al. 2006) <i>Nothofagus pumilio</i> Dec–May (1952–2011, Lavergne et al. 2016)

(continued)

**Table 19.2** (continued)

Biome	Climate signal	Examples
		<i>Nothofagus pumilio</i> Oct–Jan (1809–2013, Griebinger et al. 2018)
	Summer precipitation	<i>Nothofagus pumilio</i> Oct–Jan (1809–2013, Griebinger et al. 2018)
	Supper relative Humidity	<i>Nothofagus betuloides</i> Oct–Feb (1861–2015, Meier et al. 2020) <i>Agathis australis</i> May–Dec (1985–2002, Lorrey et al. 2016)
	Summer Vapour pressure (VP)	<i>Agathis australis</i> Oct–Dec (1985–2002, Lorrey et al. 2016)
Tropical forests (low latitude)	Precipitation, temperature, relative humidity or/and ENSO	<i>Metrosideros polymorpha</i> (Kahmen et al. 2011), <i>Cedrela odorata</i> (Brienen and Helle 2012), various (Zuidema et al. 2012, 2013), <i>Polylepis tarapacana</i> (Rodríguez-Catón et al. 2021), <i>Hyeronima alcornceides</i> (Evans et al. 2006), <i>Pouteria</i> sp. (Anchukaitis and Evans 2010), <i>Cedrela montana</i> (Volland et al. 2016)

At the meteorological scale, origin of the water vapor, temperature, evaporation and condensation processes are the dominant controlling factors. During condensation of water vapor the ambient air temperature determines the  $^{18}\text{O}/^{16}\text{O}$  ratio in meteoric water (Dansgaard 1964), resulting in a seasonal variation of the  $\delta^{18}\text{O}$  in precipitation water (Rozanski et al. 1993). During rain events some water evaporates at the plant and soil surfaces, leaving the remaining water enriched in  $\text{H}_2$  and  $^{18}\text{O}$  relative to the precipitation water. Water, infiltrating into the soil mixes with the residual soil water (Chap. 18). This mixing between infiltrated rain and residual soil water of different temporal origins (Allen et al. 2019) is reflected in tree rings mainly in temperate regions (Szejner et al. 2016), whereas in the tropics the  $\delta^{18}\text{O}$  values of tree rings corresponds to the wet season variables (Brienen and Helle 2012). During plant water uptake no measurable fractionation occurs. Differences in  $\delta^{18}\text{O}$  between xylem (source) water and soil water are due to a mixture of water absorbed from different soil depths with varying  $\delta^{18}\text{O}$  values (Sprenger et al., 2016). In Chap. 18 this topic is discussed in depth.

A detailed discussion about the variation in  $\delta^{18}\text{O}$  at leaf level is given in Chap. 10. Here, we present a summarizing overview. The  $^{18}\text{O}$  fractionation in the leaf is tightly linked to transpiration (E) and stomatal conductance (gs), both mainly controlled by air humidity with its  $\delta^{18}\text{O}$  value and leaf temperature. During transpiration the O isotope fractionation occurs as a result of the phase transition from liquid water to

the gaseous phase. As the lighter  $\text{H}_2^{16}\text{O}$  molecules evaporate more readily than the heavier ones the remaining leaf water pool becomes enriched in  $\text{H}_2^{18}\text{O}$  relative to the source water (Dongmann et al. 1974; Craig and Gordon 1965). The  $^{18}\text{O}$  enrichment is increased, with decreasing air humidity. To maintain the leaf water balance the transpired water is replenished with unenriched source water, leading to a reduction in the leaf water  $^{18}\text{O}$  enrichment, which is inverse proportional to the transpiration rate and  $g_s$ . This inverse proportional relationship between  $E$  and  $g_s$  is described as the Pecllet effect (Farquhar and Lloyd 1993; Barbour 2007).

During photosynthetic assimilate production the  $\delta^{18}\text{O}$  signal of the leaf water is transferred to the assimilates. During the assimilate transport in the phloem, the  $\delta^{18}\text{O}$  of the assimilates is modified by a proportional oxygen exchange with the xylem water and at the sites of organic matter synthesis (Barbour 2007; Sternberg 2009; Gessler et al. (2014).

### ***19.3.2 Dendroclimatic Information from Stable Oxygen Isotope Time Series in Temperate Regions***

Traditional tree-ring parameters, such as tree-ring width or maximum latewood density have proved most useful where species ranges are strongly limited by a single climatic variable, such as summer rainfall or temperature, and it is these locations which dominate growth proxy climate reconstruction networks. In the past, stable-isotope studies have followed the same sampling strategy, starting at latitudinal or altitudinal limits to maximize the changes of accessing a strong common climate signal (Breshears et al. 2009; Loader et al. 2013). There is, however, increasing evidence, that stable oxygen isotope ratios in tree rings from temperate regions, where trees grow in favorable and moist climates, also carry strong climatic signals (Loader et al. 2019).

The strong source water signal in moist parts of the globe has steered the development of oxygen isotope dendroclimatology. Young et al. (2015) discuss such an example in UK oak that went on to reveal such strong climate signals in stable oxygen isotope variations that it led to the establishment of oxygen isotope dating of archaeological timbers, in sites where tree-ring growth was too complacent to allow for dendro dating via ring width variations (Loader et al. 2019). Similarly,  $\delta^{18}\text{O}$  measurements from subfossil wood (e.g. late glacial pines) is being explored as a method by which to reduce dating uncertainties in tree-ring width time series and radiocarbon dating (Pauly et al. 2018, 2020).

In the UK anticyclonic summers are dry and what precipitation does fall is enriched by short-lived, locally derived convective rain bearing clouds. This enriched source water signal is then further enhanced, in warm anticyclonic summers, by evaporative enrichment at the leaf, and thus high tree-ring stable oxygen isotope values in the wood. The opposite occurs in wet, cool cyclonic British summers where longer-lived Atlantic air masses, where many rainout events have depleted the source water, arrive

on UK shores and ultimately lead to the synthesis of photosynthate with low tree-ring oxygen isotope values (Young et al. 2015; Loader et al. 2019).

In the early decades of stable isotope dendroclimatology many studies focused on exploring the different signal strengths in the isotope and growth proxies (e.g. McCarroll and Pawellek 1998). Now multi parameter studies, bolstered by improved understanding of the mechanistic models of the isotope-climate system, allow for the reconstruction of more climate variables. Hartl-Meier et al. (2015) systematically assessed the climate response of tree-ring width,  $\delta^{13}\text{C}$  and  $\delta^{18}\text{O}$  from a temperate mountain forest in the Austrian pre-Alps. Variations in stem growth and isotopic composition of Norway spruce, common beech and European larch from dry, medium and moist sites were compared with records of sunshine, temperature, hydroclimate, and cloud cover. Results indicated uniform year-to-year variations in  $\delta^{13}\text{C}$  and  $\delta^{18}\text{O}$  across sites and species, but distinct differences in ring width according to habitat and species. Whilst the climate sensitivity of ring widths was generally weak, the  $\delta^{13}\text{C}$  and  $\delta^{18}\text{O}$  chronologies contained strong common signals. This pattern is often found in areas where stand dynamics impact growth proxies but isotopic variables are more simply related to climate. It is in such 'mesic' growth environments where the isotopes proxies may have most to contribute. As discussed, stable oxygen isotopes have revealed particularly high common signal strength and climate reconstruction potential throughout the geographical ranges of temperate tree species, rather than just on the periphery of their distributions (Cernusak and English 2015). These findings are also in line with studies from temperate sites across Switzerland (Saurer et al. 2008), in China (Liu et al. 2012; Xu et al. 2020), in the Tibetan Plateau (Qin et al. 2015; Bräuning 2006; Wernicke et al. 2015; Holmes et al. 2007; Griebinger et al. 2011), and in India (Ramesh et al. 1986).

In Europe a tree-ring isotope network study, ISONET, explored  $\delta^{18}\text{O}$  variability across 35 sites from Northern Fennoscandia to the Mediterranean. The ISONET time series revealed that the strongest twentieth century climatic signals were contained in tree-ring  $\delta^{18}\text{O}$  from sites across the Northwest (UK, France) and Central (Germany, Austria, Switzerland) European sites (Treydte et al. 2007). The close association of tree-ring  $\delta^{18}\text{O}$  with precipitation and temperature variables was postulated to be due to isotopic fractionation being a function of air mass sourcing (temperature of condensation) and air mass trajectory (Treydte et al. 2007; Rozanski et al. 1993).

Studies on individual sites within the ISONET network made use of the strong dependency of  $\delta^{18}\text{O}$  variation on moisture conditions and created robust multi-century precipitation and drought reconstructions for both the UK and France. Similarly, Rinne et al. (2013) developed a 400-year May–August precipitation reconstruction for Southern England from tree-ring  $\delta^{18}\text{O}$  of pedunculate oak. The analysis demonstrated a statistically robust signal back to 1697, and was robust over a larger area of the UK, later confirmed to cover the entire UK (Loader et al. 2019; Young et al. 2015), such is the strength of the source water signal in the UK's temperate oak. Critically UK oak stable oxygen isotope ratios retain both low- and high frequency precipitation variability (Rinne et al. 2013; Young et al. 2015). In northwestern Iberia, extremes in a centennial stable oxygen isotopic record tracked distinct seasonal hydroclimate conditions: wetter June–July periods were associated

with extremely low  $\delta^{18}\text{O}$  values, while extreme high  $\delta^{18}\text{O}$  values were associated with warm and dry conditions in the spring (Andreu-Hayles et al. 2017).

Lowland sites in France have also revealed strong hydroclimate reconstruction potential. Labuhn et al. (2016) developed a long, continuous cellulose  $\delta^{18}\text{O}$  chronology for France, using living oak trees and timber from historic buildings. They provide a regional reconstruction of summer drought covering more than six centuries, coherent with other proxies of summer climate from the region. Again, the trees show very strong inter-annual variability, and highly significant correlations with temperature, precipitation and drought during the twentieth century. The changes in coherence between two sites within their chronology, during earlier centuries, indicated that the response of the proxy to climate might be non-linear, or that the spatial patterns of climate in France have changed (Labuhn et al. 2016). Such findings are supported by other studies revealing the sensitivity of tree-ring  $\delta^{18}\text{O}$  to the combined effects of temperature and humidity, and therefore of drought (Raffalli-Delercq et al. 2004; Masson-Delmotte et al. 2005; Etien et al. 2008b; Labuhn et al. 2014, see also further discussions in Chap. 14). Temperate stable oxygen isotope time series from tree rings, particularly in oak species, are now strongly evidenced to retain a strong hydroclimate signal (Levesque et al. 2019; Roden and Ehleringer 2007; Szejner et al. 2016; Roden et al. 2011).

In Argentina, the  $\delta^{18}\text{O}$  tree-ring of *Nothofagus pumilio* and *Fitzroya cupressoides*, at relatively humid sites, was shown to be comparable and related to temperature (December through May) (Lavergne et al. 2016). The temperature signal encompassed a large area in southern South America geographically under the influence of the Southern Annular Mode (SAM). In light of the significant correlation between the oxygen and carbon isotope records at the site the correlation between  $\delta^{18}\text{O}$  and temperature was ascribed to the effect of temperature on isotopic enrichment of leaf water, more than to its effect on precipitation  $\delta^{18}\text{O}$  (Lavergne et al. 2017a). A modeling experiment later confirmed this interpretation (Lavergne et al. 2017b). Further South, at Perito Moreno glacier (Santa Cruz Province, Argentina), also a moist site, the  $\delta^{18}\text{O}$  of *Nothofagus pumilio* was found to be sensitive both to temperature and hydroclimate (Grießinger et al. 2018; Meier et al. 2020). Though changes in moisture source origin may have been involved via the SAM.

In a pioneering Antipodean study, Wilson and Grinsted (1978) were early to hypothesize that  $\delta^{18}\text{O}$  in wood could be used to reconstruct past temperature and the  $\delta^{18}\text{O}$  of source water. Whilst regional dendrochronology challenges, due to the variations in ring width coherence, may have slowed progress in creating long-term isotope series, a larger number of prominent New Zealand and Australia ecophysiological investigations explore  $\delta^{18}\text{O}$  (e.g. Barbour et al. 2002; Cernusak et al. 2005; Ellsworth et al. 2013). Brookman (2014) demonstrated that tree-ring  $\delta^{18}\text{O}$  in New Zealand conifers was a promising tool for regional hydroclimate reconstruction via a comparison of the  $\delta^{18}\text{O}$  records from *Agathis australis* and *Libocedrus bidwillii* from sites on South Island. Again, a hydroclimate signal dominated (air humidity, soil moisture deficit and rainfall amount) from previous autumn through the concurrent growth season. Isotope climate correlations were strong in several different species. In the North Island, Lorrey et al. (2016) also explored the palaeoclimate potential

of long-lived *Agathis australis* via  $\delta^{18}\text{O}$  in earlywood and evidenced statistically significant correlations with hydroclimate (October–December vapor pressure and May–December air humidity). The relationships were shown to be consistent with mechanistic  $\delta^{18}\text{O}$  simulations. These results suggested that *Agathis australis*  $\delta^{18}\text{O}$  has the potential to provide quantitative climate information to explore past ENSO activity in the region with sub-fossil chronologies having the potential to provide insights back into the late Quaternary.

### ***19.3.3 Dendroclimatic Information from Stable Oxygen Isotope Time Series at High Latitudes and in the Boreal Forest***

At high latitudes in the Northern Hemisphere annually resolved  $\delta^{18}\text{O}$  chronologies have been developed across the Boreal zone. Buhay and Edwards (1995) carried out an early exploration of hydroclimate in Canada based on tree-ring water isotopes. They used an isotope model to account for the impact of fractionation on source water signal in different moisture environments allowing for a reconstruction resolved by hydroclimatic environment, over 275 years prior to the instrumental period. Birks and Edwards (2009) described changes in atmospheric circulation patterns for the North Pacific from water isotopes, showing the strongest relationship with temperature variations and a precipitation amount effect. Temperature variability for the last millennia has also been reconstructed using  $\delta^{18}\text{O}$  tree-ring records in Canada from Boreal-lake subfossil trees, revealing the speed of recent climatic warming at that latitude as well as a connection between the coldest periods of the nineteenth century and the volcanic eruptions and low solar activity associated with the late Little Ice Age (Naulier et al. 2015). Gennaretti et al. (2017) combined  $\delta^{18}\text{O}$ ,  $\delta^{13}\text{C}$  and ring-width chronologies to develop an improved multi-proxy temperature reconstruction (using a Bayesian framework) for the same region. Annual temperature and  $\delta^{18}\text{O}$  meteoric water records have also been estimated using  $\delta^{18}\text{O}$  tree-ring reconstructions from Pleistocene subfossil wood in Nunavut (Csank et al. 2013). Further studies in the Northwestern Territories showed positive correlations between a tree-ring  $\delta^{18}\text{O}$  record and summer temperatures and negative relationships with summer humidity, also involving an oxygen isotope evaporative enrichment signal in warmer summers (Porter et al. 2009). Using longer  $\delta^{18}\text{O}$  records for the same site, a ~200-year spring–summer temperature reconstruction was generated (Porter et al. 2013). Further Canadian examples show the strength of Boreal  $\delta^{18}\text{O}$  for reconstructing source water dominated precipitation and temperature histories, where the two climate parameters co-vary (Holzkämper et al. 2012; Bégin et al. 2015). Even further north, in High Arctic environments, a significant correlation between the  $\delta^{18}\text{O}$  of birch trees growing in Southwestern Greenland and NAO was evidenced (Xu et al. 2021). Similarly, tree-ring cellulose of the shrub *Cassiope tetragona* in Ellesmere Island in Canada at 79 °N recorded Arctic and NAO variability (Welker

et al. 2005). Rayback and Henry (2006) reconstructed 100 years of summer temperatures using cellulose material from tree rings of the shrub *Cassiope tetragona* in Ellesmere Island.

Moving to consider the European context,  $\delta^{18}\text{O}$  records of *Pinus sylvestris* in Finland and Sweden also reveal hydroclimate sensitivity (Seftigen et al. 2011; Esper et al. 2018). In the Russian Altai, at the limit of the Boreal forest, summer temperature and precipitation signals were both preserved in  $\delta^{18}\text{O}$  chronologies of *Larix decidua* (Sidorova et al. 2013). High latitude Boreal forest has also formed the backdrop for ring width and densitometry-based dendroclimatology to develop networks reconstructions (e.g. Anchukaitis et al. 2017; Wilson et al. 2016) and so were a natural starting place for isotope dendroclimatology (e.g. McCarroll and Pawellek 1998, Robertson et al. 1997).

Trees are long lived in the Boreal and high-latitude forests and abundant subfossil material is available and well-preserved due to the cold environment. With the underlying isotope fractionation models described above and in Chaps. 10 and 18 suggesting that water isotopes in tree rings should sensitively record a source water signal in these moist, cool forests it is not surprising that tree-ring  $\delta^{18}\text{O}$  has proven to be a reliable hydroclimate proxy far into the northern forests. See also Chap. 20 for a discussion of relevant reconstructions.

### ***19.3.4 Dendroclimatic Information from Stable Oxygen Isotope Time Series in the Tropics***

A major research gap exists in the network of high-resolution proxy reconstructions for palaeoclimatology, in the terrestrial tropics (Evans and Schrag 2004). As discussed, this is in part due to the challenges of using traditional dendroclimatology in these regions (Worbes 2002). However, over the last two decades several authors have tried to address this research gap by exploring the source water signal and evaporative enrichment signal in cellulose  $\delta^{18}\text{O}$  from tropical trees to resolve both dating and climate signal (see Brienen et al. 2016; Rozendaal and Zuidema 2011; van der Sleen et al. 2017 for a review). In Chap. 22 we summarize major findings regarding the climatic information recorded in tree-ring  $\delta^{18}\text{O}$  from trees growing in tropical regions.

Away from the ‘ever wet’ regions, most parts of the tropics do experience precipitation seasonality, even with annually stable temperatures. Wet seasons are typified by  $\delta^{18}\text{O}$  depleted source water (Araguás-Araguás et al. 2000) with dryer periods seeing enriched source water. Moreover, even in regions with very little rainfall amount variability through the year, there is geographical source water variability, as the monsoon seasons shift through the year (Loader et al. 2011). Several studies have attempted to detect seasonality via source water variability as both a dating method in non-annual ring forming tropical trees, and a climate signal (Evans and Schrag 2004).



Kahmen et al. (2011) explored the mechanistic explanations for sensitivity of  $\delta^{18}\text{O}$  to climate in tropical tree rings. Using the mechanistic Péclet-modified Craig-Gordon model (PMGG) they reported that both air temperature and air humidity influenced tree  $\delta^{18}\text{O}$ , integrated via VPD, along an aridity gradient of *Metrosideros polymorpha* in Hawaii. Xylem water  $\delta^{18}\text{O}$  decreased along the gradient whilst leaf and stem  $\delta^{18}\text{O}$  increased, suggesting that evaporative enrichment dominated the source water signal in Hawaii's coastal island environment.

In tropical rainforest environments of Central Guyana, Pons and Helle (2011) found  $\delta^{18}\text{O}$  cellulose patterns mimicked the source water annual isotope cycle well, with minima in both rainfall and cellulose at the start of the area's primary wet season. They tested their hypothesis with dual isotope measurements, which revealed that cellulose  $\delta^{13}\text{C}$  also showed low moisture stress at the same time as the minima in cellulose  $\delta^{18}\text{O}$ . Moreover, these revealing studies were successfully carried out in tropical trees with anatomically indistinct tree rings (Pons and Helle 2011).

In South America, in the western Amazon basin, Brienen and Helle (2012) reported a lower influence of temperature and vapor pressure variations on tree-ring  $\delta^{18}\text{O}$  records from *Cedrela odorata*. Tree-ring  $\delta^{18}\text{O}$  correlated well with  $\delta^{18}\text{O}$  in precipitation, regional precipitation variability during the wet season and streamflow from Amazonian rivers. Non time stable relationships with ENSO parameters were also observed, as well as an increase in  $\delta^{18}\text{O}$  values over the twentieth century, shared with ice core records. Baker et al. (2015) reinforced the dominance of a source water signal in the Brienen and Helle (2012)  $\delta^{18}\text{O}$  *Cedrela* record via correlations with other  $\delta^{18}\text{O}$  tree-ring records from low altitude rainforest tree species, and with high altitude *Polylepis tarapacana* in the Bolivian Altiplano. The  $\delta^{18}\text{O}$  signature of *Polylepis tarapacana* chronologies along the South American Altiplano revealed a strong signal of December to March precipitation associated to the South American Summer Monsoon (Rodríguez-Catón et al. 2021). In Southern Ecuador, ENSO variability has also been shown to be recorded in  $\delta^{18}\text{O}$  tree-ring records of *Cedrela montana* (Volland et al. 2016). Good agreement with wet season precipitation was found in high-resolution  $\delta^{18}\text{O}$  records of *Tachigali myrmecophila* in Manaus, Brazil, in *Cedrela odorata* at 12 °S in the Amazonian and a 150-year *Polylepis tarapacana* tree-ring  $\delta^{18}\text{O}$  record from the Bolivian Altiplano at 22 °S (Ballantyne et al. 2011).

In Costa Rica variations in the tree-ring  $\delta^{18}\text{O}$  records from 16-year old *Hyeronima alcorneides* were found to be sensitive to tropical precipitation amount, especially during ENSO events (Evans et al. 2006). The  $\delta^{18}\text{O}$  cycles measured in two *Pouteria* trees, which did not have visible tree rings, and were assigned a calendar year via a radiocarbon age-depth model, showed enriched  $\delta^{18}\text{O}$  during warm ENSO wet seasons (Anchukaitis and Evans 2010). Annual cyclicity in  $\delta^{18}\text{O}$  has also been revealed in ring-less mangrove *Rhizophora mucronata* which also recorded sensitivity to the ENSO event in 1997 (Verheyden et al. 2004a).

In Central Java in Indonesia, Schollaen et al. (2013) reported that  $\delta^{18}\text{O}$  chronologies from rainforest teak (*Tectona grandis*) recorded precipitation signals during the dry and the rainy season. The  $\delta^{18}\text{O}$  teak tree-ring record also showed strong sensitivity to ENSO events driven by warmer sea surface temperatures over the central Pacific (Schollaen et al. 2015). In Indonesia and Thailand, high-resolution  $\delta^{18}\text{O}$  records from

cross dated tree rings of *Tectona grandis*, and ring-less *Samanea saman* grown at the same locality, show high correlations with instrumental data, reflecting the seasonal cycles of rainfall and air humidity (Poussart et al. 2004).

Tropical oxygen isotope dendroclimatology, to date, has revealed coherent correlations between various hydroclimate and source water signals and  $\delta^{18}\text{O}$  in tree-rings, often in trees with indistinct growth rings (e.g. Sano et al. 2009). These examples highlight opportunities to extend our understanding of past climate from trees to many parts of the tropics, from remote to highly populated areas where climate change may have direct and serious implications. Despite these promising single site studies, the environmental and physiological mechanisms controlling tropical isotopic signals between the atmosphere and soil, through the stem and canopy to the wood and into the cellulose of the tree-ring are highly complex, and more so in the tropics. The interplay between isotopic signals carried in the source water and those produced at the leaf level and during downstream enrichment and photosynthetic processes are still not well understood (Gessler et al. 2014). The mechanistic interpretation of  $\delta^{18}\text{O}$  in tropical trees remains therefore often problematic. Additional relevant discussions can also be found in Chaps. 13 and 22.

## 19.4 Conclusions

The contributions of stable isotope dendroclimatology have increased tenfold, over recent decades, thanks to better analytical systems allowing greater sample throughput and replication, improved understandings of the mechanistic controls over the isotope signal and increased geographical and species coverage in example studies. Contributions to our understanding of the carbon–water–climate relationship in trees are now available from long, well replicated stable isotope tree-ring series across the old world, with pockets of emerging studies in previously under-represented geographical areas. As global average temperatures continue to rise and we move into a ‘1.5-degree world’ with increasing climate extremes, the additional glimpses into our pre anthropogenic climate that we obtain from tree-ring isotope records becomes ever more important. Coupled with the ability to explore how trees and woodland respond to changing climate and  $\text{CO}_2$  levels in the atmosphere, the isotope dendro proxies are now a vital part of the palaeoenvironmental toolbox.

## References

- Allen ST, Kirchner JW, Braun S, Siegwolf RTW, Goldsmith GR (2019) Seasonal origins of soil water used by trees. *Hydrol Earth Syst Sci* 23:1199–1210
- Anchukaitis KJ et al (2008) Stable isotope chronology and climate signal calibration in neotropical montane cloud forest trees. *J Geophys Res American Geophysical Union (AGU)* 113(G3). <https://doi.org/10.1029/2007jg000613>

- Anchukaitis KJ, Evans MN (2010) Tropical cloud forest climate variability and the demise of the Monteverde golden toad. *Proc Natl Acad Sci* 107(11):5036–5040. <https://doi.org/10.1073/pnas.0908572107>
- Anchukaitis KJ, Wilson R, Briffa KR, Buntgen U, Cook ER, D'Arrigo R, Davi N, Esper J, Frank D, Gunnarson BE, Hegerl G, Helama S, Klesse S, Krusic PJ, Linderholm HW, Myglan V, Osborn TJ, Zhang P, Rydval M, Schneider L, Schurer A, Wiles G, Zorita E (2017) Last millennium Northern Hemisphere summer temperatures from tree rings: Part II, spatially resolved reconstructions. *Quat Sci Rev* 163:1–22
- Anderson WT et al (1998) Oxygen and carbon isotopic record of climatic variability in treering cellulose (*Picea abies*): an example from central Switzerland (1913–1995). *J Geophys Res Atmos* (Blackwell Publishing Ltd) 103(D24):31625–31636. <https://doi.org/10.1029/1998JD200040>
- Andreu-Hayles L et al (2011) Long treering chronologies reveal 20th century increases in water-use efficiency but no enhancement of tree growth at five Iberian pine forests. *Glob Change Biol* 17(6):2095–2112. <https://doi.org/10.1111/j.1365-2486.2010.02373.x>
- Andreu-Hayles L et al (2017) 400 Years of summer hydroclimate from stable isotopes in Iberian trees. *Clim Dyn* (Springer Verlag) 49(1–2):143–161. <https://doi.org/10.1007/s00382-016-3332-z>
- Andreu-Hayles L et al (2019) A high yield cellulose extraction system for small whole wood samples and dual measurement of carbon and oxygen stable isotopes. *Chem Geol* (Elsevier) 504(November 2017):53–65. <https://doi.org/10.1016/j.chemgeo.2018.09.007>
- Araguás-Araguás L, Froehlich K, Rozanski K (2000) Deuterium and oxygen-18 isotope composition of precipitation and atmospheric moisture. *Hydrol Process* 14(8):1341–1355. [https://doi.org/10.1002/1099-1085\(20000615\)14:8%3c1341::AID-HYP983%3e3.0.CO;2-Z](https://doi.org/10.1002/1099-1085(20000615)14:8%3c1341::AID-HYP983%3e3.0.CO;2-Z)
- Baker JCA et al (2015) Oxygen isotopes in treerings show good coherence between species and sites in Bolivia. *Glob Planet Change* (Elsevier (BV)) 133:298–308. <https://doi.org/10.1016/j.gloplacha.2015.09.008>
- Bale RJ et al (2011) An annually resolved bristlecone pine carbon isotope chronology for the last millennium. *Quat Res* 76(1):22–29. <https://doi.org/10.1016/j.yqres.2011.05.004>
- Ballantyne AP et al (2011) Regional differences in South American monsoon precipitation inferred from the growth and isotopic composition of tropical trees, earth interactions. *Earth Interact Am Meteorol Soc* 15(5):1–35. <https://doi.org/10.1175/2010ei277.1>
- Barbour M, Walcroft AS, Farquhar GD (2002) Seasonal variation in  $\delta^{13}\text{C}$  and  $\delta^{18}\text{O}$  of cellulose from growth rings of *Pinus radiata*. *Plant Cell Environ* 25:1483–1499
- Barbour MM (2007) Stable oxygen isotope composition of plant tissue: a review. *Funct Plant Biol* 34:83–94
- Battipaglia G, Cherubini P, Saurer M, Siegwolf RTW, Strumia S, Cotrufo MF (2007) Volcanic explosive eruptions of the Vesuvio decrease tree-ring growth but not photosynthetic rates in the surrounding forests. *Glob Change Biol* 13(6):1122–1137. <https://doi.org/10.1111/j.1365-2486.2007.01350.x>
- Battipaglia G et al (2013) Special issue: WSE symposium: wood growth under environmental changes: the need for a multidisciplinary approach. *Tree Physiol* (Oxford University Press (OUP)) 34(8):787–791. <https://doi.org/10.1093/treephys/tpu076>
- Bégin C et al (2015) Assessing treering carbon and oxygen stable isotopes for climate reconstruction in the Canadian northeastern boreal forest. *Palaeogeogr Palaeoclimatol Palaeoecol* 423:91–101. <https://doi.org/10.1016/j.palaeo.2015.01.021>
- Belmecheri S, Maxwell RS, Taylor AH, Davis KJ, Freeman KH, Munger WJ (2014) Treering  $\delta^{13}\text{C}$  tracks flux tower ecosystem productivity estimates in a NE temperate forest. *Environ Res Lett* (IOP Publishing) 9(7):074011. <https://doi.org/10.1088/1748-9326/9/7/074011>
- Berlage HP (1931) On the relationship between thickness of treerings of Djati (teak) trees and rainfall on Java. *Tectona* 24:939–953
- Bert D, Leavitt SW, Dupouey J-L (1997) Variations of wood  $\Delta^{13}\text{C}$  and water-use efficiency of *Abies alba* during the last century. *Ecology* 78(5):1588–1596. [https://doi.org/10.1890/0012-9658\(1997\)078\[1588:VOWCAW\]2.0.CO;2](https://doi.org/10.1890/0012-9658(1997)078[1588:VOWCAW]2.0.CO;2)

- Biondi F (2001) A 400-year tree-ring chronology from the tropical treeline of North America. *AMBIO J Humn Environ* *Am Bryol Lichenol Soc* 30(3):162. [https://doi.org/10.1639/0044-7447\(2001\)030\[0162:aytrcf\]2.0.co;2](https://doi.org/10.1639/0044-7447(2001)030[0162:aytrcf]2.0.co;2)
- Birks SJ, Edwards TWD (2009) Atmospheric circulation controls on precipitation isotope-climate relations in western Canada. *Tellus B Chem Phys Meteorol (informa UK, Limited)* 61(3):566–576. <https://doi.org/10.1111/j.1600-0889.2009.00423.x>
- Boucher O, Randall D, Artaxo P, Bretherton C, Feingold G, Forster P, Kerminen V-M, Kondo Y, Liao H, Lohmann U et al (2013) Clouds and aerosols. In: Stocker TF, Qin D, Plattner G-K, Tignor M, Allen SK, Boschung J, Nauels A, Xia Y, Bex V, Midgley PM (eds) *Climate change 2013: the physical science basis. Contribution of working group I to the fifth assessment report of the intergovernmental panel on climate change*. Cambridge University Press, Cambridge and New York, NY, pp 571–657
- Bradley RS (1985) *Quaternary paleoclimatology: methods of paleoclimatic reconstruction*. Allen & Unwin, Boston
- Bräuning A (2006) Tree-ring evidence of ‘Little Ice Age’ glacier advances in Southern Tibet. *The Holocene* 16:369–380
- Brendel O, Iannetta PPM, Stewart D (2000) A rapid and simple method to isolate pure alpha-cellulose. *Phytochem Anal* 11(1):7–10. [https://doi.org/10.1002/\(SICI\)1099-1565\(200001/02\)11:1%3c7::AID-PCA488%3e3.0.CO;2-U](https://doi.org/10.1002/(SICI)1099-1565(200001/02)11:1%3c7::AID-PCA488%3e3.0.CO;2-U)
- Breshears DD, Myers OB et al (2009) Tree die-off in response to global change-type drought: mortality insights from a decade of plant water potential measurements. *Front Ecol Environ* 7:185–189. <https://doi.org/10.1890/080016>
- Brienen R, Helle G (2012) Oxygen isotopes in tree rings are a good proxy for Amazon precipitation and El Niño-Southern oscillation variability. *PNAS* 1–6. <https://doi.org/10.1073/pnas.1205977109>
- Brienen RJW et al (2017) Tree height strongly affects estimates of water-use efficiency responses to climate and CO<sub>2</sub> using isotopes. *Nature Commun (Springer, US)* 8(1):288. <https://doi.org/10.1038/s41467-017-00225-z>
- Brienen RJW, Schöngart J, Zuidema PA (2016) Treerings in the tropics: insights into the ecology and climate sensitivity of tropical trees, pp 439–461. [https://doi.org/10.1007/978-3-319-27422-5\\_20](https://doi.org/10.1007/978-3-319-27422-5_20)
- Brodribb TJ, McAdam SAM, Jordan GJ, Martins SCV (2014) Conifer species adapt to low-rainfall climates by following one of two divergent pathways. *Proc Natl Acad Sci* 111(40):14489–14493. <https://doi.org/10.1073/pnas.1407930111>
- Brookman TH (2014) *Stable isotope dendroclimatology of New Zealand kauri (Agathis australis (D. Don) Lindl.) and cedar (Libocedrus bidwillii Hook. F.)*, University of Canterbury, Christchurch, New Zealand
- Buckley BM et al (2010) Climate as a contributing factor in the demise of Angkor, Cambodia. *Proc Natl Acad Sci* 107(15):6748–6752. <https://doi.org/10.1073/pnas.0910827107>
- Buhay WM, Edwards TWD (1995) Climate in southwestern Ontario, Canada, between AD 1610 and 1885 inferred from oxygen and hydrogen isotopic measurements of wood cellulose from trees in different hydrologic settings. *Quat Res* 44(3):438–446. <https://doi.org/10.1006/qres.1995.1089>
- Büntgen U, Kolář T, Rybníček M, Koňasová E, Trnka M, Ač A, Krusic PJ, Esper J, Treydte K, Reinig F, Kirilyanov A, Herzig F, Urban O (2020) No evidence of age trends in oak stable isotopes. *Paleoceanogr Paleoclimatol*. <https://doi.org/10.1029/2019PA003831>
- Burk R, Stuiver M (1981) Oxygen isotope ratios in trees reflect mean annual temperature and humidity. *Science* 211(4489):1417–1419. <https://doi.org/10.1126/science.211.4489.1417>
- Campbell R et al (2011) Blue intensity in *Pinus sylvestris* tree-rings: a manual for a new palaeoclimate proxy. *Tree-Ring Res* 127–134
- Cernusak LA, Farquhar GD, Pate JS (2005) Environmental and physiological controls over oxygen and carbon isotope composition of Tasmanian blue gum, *Eucalyptus globulus*. *Tree Physiol*. Oxford University Press (OUP) 25(2):129–146. <https://doi.org/10.1093/treephys/25.2.129>

- Cernusak LA, English NB (2015) Beyond tree-ring widths: stable isotopes sharpen the focus on climate responses of temperate forest trees. *Tree Physiol* 35:1–3. <https://doi.org/10.1093/treephys/tpu115>
- Chiang JCH (2009) The tropics in paleoclimate, annual review of earth and planetary sciences. *Ann Rev* 37(1):263–297. <https://doi.org/10.1146/annurev.earth.031208.100217>
- Churakova OV et al (2019) Siberian tree-ring and stable isotope proxies as indicators of temperature and moisture changes after major stratospheric volcanic eruptions. *Clim past*. Copernicus GmbH 15(2):685–700. <https://doi.org/10.5194/cp-15-685-2019>
- Clark DA, Clark DB, Oberbauer SF (2013) Field-quantified responses of tropical rainforest above-ground productivity to increasing CO<sub>2</sub> and climatic stress, 1997–2009. *J Geophys Res Biogeosci* (American Geophysical Union (AGU)) 118(2):783–794. <https://doi.org/10.1002/jgrg.20067>
- Corlett RT (2011) Impacts of warming on tropical lowland rainforests. *Trends Ecol Evolut* (Elsevier (BV)) 26(11):606–613. <https://doi.org/10.1016/j.tree.2011.06.015>
- Coster C (1927) Zur Anatomie und Physiologie der Zuwachszonen- und Jahresringbildung in den Tropen. *Ann Jard Bot* 37:49–160. <https://scholar.google.com/scholar?oi=gsb40&q=Coster%2CC.%2C.Zur+Anatomie+und+Physiologie+der+Zuwachszonen-+und+Jahresringbildung+in+den+Tropen.+Ann+Jard+Bot+Buitenzong+37%2C+49-160&lookup=0&hl=en>. Accessed 31 Oct 2019
- Craig H (1954) Carbon-13 variations in sequoia rings and the atmosphere. *Science* 119(3083)
- Craig H, Gordon LI (1965) Deuterium and oxygen-18 variations in the ocean and the marine atmosphere. In: Tongiorgi E (ed) Proceedings of a conference on stable isotopes in oceanographic studies and paleotemperatures. Lischi and Figli, Pisa, Italy, pp 9–130
- Csank AZ, Fortier D, Leavitt SW (2013) Annually resolved temperature reconstructions from a late Pliocene-early Pleistocene polar forest on Bylot Island, Canada. *Palaeogeogr Palaeoclimatol Palaeoecol* (Elsevier (BV)) 369:313–322. <https://doi.org/10.1016/j.palaeo.2012.10.040>
- Dansgaard W (1964) Stable isotopes in precipitation. *Tellus* 16:436–468
- D'Arrigo R, Wilson R, Anchukaitis KJ (2013) Volcanic cooling signal in tree-ring temperature records for the past millennium. *J Geophys Res Atmos* (Blackwell Publishing Ltd.) 118(16):9000–9010. <https://doi.org/10.1002/jgrd.50692>
- D'Arrigo R et al (2006a) The reconstructed Indonesian warm pool sea surface temperatures from tree-rings and corals: linkages to Asian monsoon drought and El Niño-Southern Oscillation. *Paleoceanography* (American Geophysical Union (AGU)) 21(3). <https://doi.org/10.1029/2005pa001256>
- D'Arrigo R, Wilson R, Jacoby G (2006b) On the long-term context for late twentieth century warming. *J Geophys Res Atmos* (Blackwell Publishing Ltd.) 111(3). <https://doi.org/10.1029/2005JD006352>
- Daux V et al (2011) Can climate variations be inferred from tree-ring parameters and stable isotopes from *Larix decidua*? Juvenile effects, budmoth outbreaks, and divergence issue. *Earth Planet Sci Lett* (Elsevier (BV)) 309(3–4):221–233. <https://doi.org/10.1016/j.epsl.2011.07.003>
- Daux V, Michelot-Antalik A, Lavergne A, Pierre M, Stievenard M, Bréda N, Damesin C (2018) Comparisons of the performance of  $\delta^{13}\text{C}$  and  $\delta^{18}\text{O}$  of *Fagus sylvatica*, *Pinus sylvestris*, and *Quercus petraea* in the record of past climate variations. *J Geophys Res Biogeosci* 123:1145–1160. <https://doi.org/10.1002/2017JG004203>
- Dekker SC et al (2016) Spatial and temporal variations in plant water-use efficiency inferred from tree-ring, eddy covariance and atmospheric observations. *Earth Syst Dyn* (Copernicus (GmbH)) 7(2):525–533. <https://doi.org/10.5194/esd-7-525-2016>
- Dessler AE (2010) A determination of the cloud feedback from climate variations over the past decade. *Science* 330(6010):1523–1527. <https://doi.org/10.1126/science.1192546>
- Dongmann G, Nurnberg HW, Forstel H, Wagener K (1974) Enrichment of H<sub>2</sub><sup>18</sup>O in leaves of transpiring plants. *Radiat Environ Biophys* 11:41–52
- Dorado-Liñán I, Büntgen U, González-Rouco F, Zorita E, Montávez JP, Gómez-Navarro JJ, Brunet M, Heinrich I, Helle G, Gutiérrez E (2012) Estimating 750 years of temperature variations and its uncertainties in the Pyrenees by tree-ring reconstructions and climate simulations. *Clim past* 8:919–933

- Dorado-Liñán I, Zorita E, González-Rouco JF, Heinrich I, Campello F, Andreu-Hayles L, Muntán E, Gutiérrez E (2015) Eight-hundred years of summer temperature variations in the southeast of the Iberian Peninsula reconstructed from tree rings. *Clim Dyn* 44(1–2):75–93
- Dorado-Liñán I et al (2011) Pooled versus separate measurements of treering stable isotopes. *Sci Total Environ* (Elsevier (BV)) 409(11):2244–2251. <https://doi.org/10.1016/j.scitotenv.2011.02.010>
- Dorado-Liñán I et al (2016) Changes in surface solar radiation in Northeastern Spain over the past six centuries recorded by treering  $\delta^{13}\text{C}$ . *Clim Dyn* (Springer Verlag) 47(3–4):937–950. <https://doi.org/10.1007/s00382-015-2881-x>
- Duffy JE et al (2017) Short-lived juvenile effects observed in stable carbon and oxygen isotopes of UK oak trees and historic building timbers. *Chem Geol* 472(September):1–7. <https://doi.org/10.1016/j.chemgeo.2017.09.007>
- Duffy JE et al (2019) Absence of age-related trends in stable oxygen isotope ratios from Oak treerings. *Glob Biogeochem Cycles* (American Geophysical Union (AGU)). <https://doi.org/10.1029/2019gb006195>
- Edwards TWD, Fritz P (1986) Assessing meteoric water composition and relative humidity from  $^{18}\text{O}$  and  $^2\text{H}$  in wood cellulose: paleoclimatic implications for southern Ontario, Canada. *Appl Geochem* 1:715–723
- Edwards TWD et al (2008) Climatic and hydrologic variability during the past millennium in the eastern Rocky Mountains and northern Great Plains of western Canada. *Quat Res* 70(2):188–197. <https://doi.org/10.1016/j.yqres.2008.04.013>
- Ehleringer JR, Hall AE, Farquhar GD (1993) Preface. In: *Stable isotopes and plant carbon-water relations*. Elsevier, p xix. <https://doi.org/10.1016/b978-0-08-091801-3.50005-2>
- Ellsworth PV, Anderson WT, Sonninen E, Barbour MM, Sternberg LSL (2013) Reconstruction of source water using the  $\text{d}^{18}\text{O}$  of treering phenylglucosazone: a potential tool in paleoclimate studies. *Dendrochronologia* 31:153–158. <https://doi.org/10.1016/j.dendro.2012.10.004>
- Epstein S, Krishnamurthy RV (1990) Environmental information in the isotopic record in trees. *Philos Trans R Soc A Math Phys Eng Sci* (The Royal Society 330(1615):427–439. <https://doi.org/10.1098/rsta.1990.0023>
- Epstein S, Yapp C (1977) Isotope tree thermometers. *Nature* 266:477–478. <https://doi.org/10.1038/266477a0>
- Epstein S, Yapp C (1976) Climatic implications of the D/H ratio of hydrogen in CH groups in tree cellulose. *Earth Planet Sci Lett* 30:255–261. <http://www.sciencedirect.com/science/article/pii/0012821X76902521>. Accessed on 26 November 2015
- Esper J et al (2010) Low-frequency noise in  $\delta^{13}\text{C}$  and  $\delta^{18}\text{O}$  treering data: a case study of *Pinus uncinata* in the Spanish Pyrenees. *Global Biogeochem Cycles* 24(2):1–11. <https://doi.org/10.1029/2010GB003772>
- Esper J et al (2014) Northern European summer temperature variations over the common era from integrated treering density records. *J Quat Sci* 29(5):487–494. <https://doi.org/10.1002/jqs.2726>
- Esper J et al (2015) Long-term summer temperature variations in the Pyrenees from detrended stable carbon isotopes. *Geochronometria* (Walter De Gruyter GmbH) 42(1):53–59. <https://doi.org/10.1515/geochr-2015-0006>
- Esper J, Frank D (2009) Divergence pitfalls in treering research. *Clim Change* 94:261–266. <https://doi.org/10.1007/s10584-009-9594-2>
- Esper J, Holzkamper S, Büntgen U, Schone B, Keppler F, Hartl C, St. George S, Riechelmann DFC, Treydte K (2018) Site-specific climatic signals in stable isotope records from Swedish pine forests. *Trees-Struct Funct* 32:855–869
- Etien N, Daux V et al (2008a) Summer maximum temperature in northern France over the past century: instrumental data versus multiple proxies (tree-ring isotopes, grape harvest dates and forest fires). *Clim Change* 94:429–456
- Etien N, Daux V, Masson-Delmotte V, Stievenard M, Bernard V, Durost S, Guillemin MT, Mestre O, Pierre M (2008b) A bi-proxy reconstruction of Fontainebleau (France) growing season temperature from A.D. 1596 to 2000. *Clim Past* 4:91–106

- Evans MN et al (2006) A forward modeling approach to paleoclimatic interpretation of tree-ring data. *J Geophys Res* (American Geophysical Union (AGU)) 111(G3). <https://doi.org/10.1029/2006jg000166>
- Evans MN, Schrag DP (2004) A stable isotope-based approach to tropical dendroclimatology. *Geochim Cosmochim Acta* (Elsevier (BV)) 68(16):3295–3305. <https://doi.org/10.1016/j.gca.2004.01.006>
- Farmer JG, Baxter MS (1974) Atmospheric carbon dioxide levels as indicated by the stable isotope record in wood. *Nature* 247(5439):273. <https://www.nature.com/articles/247273a0>. Accessed on 28 October 2019
- Farquhar GD et al (1989a) Carbon isotope fractionation and plant water-use efficiency. In: *Stable isotopes in ecological research*. Springer, New York, pp 21–40. [https://doi.org/10.1007/978-1-4612-3498-2\\_2](https://doi.org/10.1007/978-1-4612-3498-2_2)
- Farquhar GD, Lloyd J (1993) Carbon and oxygen isotope effects in the exchange of carbon dioxide between terrestrial plants and the atmosphere. *Stable isotopes and plant carbon-water relations*. Academic Press, San Diego, pp 47–70
- Farquhar GD, Ehleringer JR, Hubick KT (1989b) Carbon isotope discrimination and photosynthesis. *Annu Rev Plant Physiol Plant Mol Biol* 40:503–537. <https://doi.org/10.1146/annurev.pp.40.060189.002443>
- Farquhar GD, O'Leary MH, Berry JA (1982) On the relationship between carbon isotope discrimination and the intercellular carbon dioxide concentration in leaves. *Aust J Plant Physiol* 9:121–137
- Ferrio JP, Voltas J (2005) Carbon and oxygen isotope ratios in wood constituents of *Pinus halepensis* as indicators of precipitation, temperature and vapour pressure deficit. *Tellus B Chem Phys Meteorol* (informa UK Limited) 57(2):164–173. <https://doi.org/10.3402/tellusb.v57i2.16780>
- Flato G, Marotzke J, Abiodun B, Braconnot P, Chou SC, Collins W, Cox P, Driouech F, Emori S, Eyring V, Forest C, Gleckler P, Guilyardi E, Jakob C, Kattsov V, Reason C, Rummukainen M (2013) Evaluation of climate models. In: Stocker TF, Qin D, Plattner G-K, Tignor M, Allen SK, Doschung J, Nauels A, Xia Y, Bex V, Midgley PM (eds) *Climate change 2013: the physical science basis. Contribution of working Group I to the fifth assessment report of the intergovernmental panel on climate change*. Cambridge University Press, pp 741–882. <https://doi.org/10.1017/CBO9781107415324.020>
- Francey RJ, Farquhar GD (1982) An explanation of  $^{13}\text{C}/^{12}\text{C}$  variations in tree-rings. *Nature* 297(5861):28–31. <https://doi.org/10.1038/297028a0>
- Frank D et al (2010) A noodle, hockey stick, and spaghetti plate: a perspective on high-resolution paleoclimatology. *Wiley Interdiscip Rev Clim Change* (Wiley-Blackwell) 1(4):507–516. <https://doi.org/10.1002/wcc.53>
- Frank DC et al (2015) Water-use efficiency and transpiration across European forests during the anthropocene. *Nat Clim Chang* 5(6):579–583. <https://doi.org/10.1038/nclimate2614>
- Franks PJ et al (2013) Sensitivity of plants to changing atmospheric  $\text{CO}_2$  concentration: from the geological past to the next century. *New Phytologist* (Wiley) 197(4):1077–1094. <https://doi.org/10.1111/nph.12104>
- Fritts HC (1976) *Tree rings and climate*. Academic Press, London, New York and San Francisco, p 567
- Fromm J (2013) Cellular aspects of wood formation. *Plant Cell Monographs*. <https://doi.org/10.1007/978-3-642-36491-4>
- Gagen M et al (2007) Exorcising the 'segment length curse': summer temperature reconstruction since AD 1640 using non-detrended stable carbon isotope ratios from pine trees in northern Finland. *The Holocene* 17(4):435–446
- Gagen M et al (2008) Do tree-ring  $\delta^{13}\text{C}$  series from *Pinus sylvestris* in northern Fennoscandia contain long-term non-climatic trends? *Chem Geol* 252:42–51. <https://doi.org/10.1016/j.chemgeo.2008.01.013>
- Gagen M, Zorita E et al (2011a) Cloud response to summer temperatures in Fennoscandia over the last thousand years. *Geophys Res Lett* 38:1–5. <https://doi.org/10.1029/2010GL046216>

- Gagen M, Finsinger W et al (2011b) Evidence of changing intrinsic water-use efficiency under rising atmospheric CO<sub>2</sub> concentrations in Boreal Fennoscandia from subfossil leaves and treering  $\delta^{13}\text{C}$  ratios. *Global Change Biol* (Blackwell Publishing Ltd) 17(2):1064–1072. <https://doi.org/10.1111/j.1365-2486.2010.02273.x>
- Gagen M et al (2012) A rapid method for the production of robust millennial length stable isotope treering series for climate reconstruction. *Global Planet Change* 82–83:96–103. <https://doi.org/10.1016/j.gloplacha.2011.11.006>
- Gagen MH et al (2016) North Atlantic summer storm tracks over Europe dominated by internal variability over the past millennium. *Nat Geosci* (Nature Publishing Group) 9(8):630–635. <https://doi.org/10.1038/ngeo2752>
- Gagen M, McCarroll D, Edouard J-L (2004) The effect of site conditions on pine treering width, density and  $\delta^{13}\text{C}$  series. *Arct Antarct Alp Res* 36(2):166–171
- Gagen M, McCarroll D, Edouard JL (2006) Combining ring width, density and stable carbon isotope proxies to enhance the climate signal in treerings: an example from the southern French Alps. *Clim Change* 78:363–379. <https://doi.org/10.1007/s10584-006-9097-3>
- Gebrekirostos A et al (2009) Stable carbon isotope ratios in treerings of co-occurring species from semi-arid tropics in Africa: patterns and climatic signals. *Global Planet Change* 66(3–4):253–260. <https://doi.org/10.1016/j.gloplacha.2009.01.002>
- Gennaretti F et al (2017) Bayesian multiproxy temperature reconstruction with black spruce ring widths and stable isotopes from the northern Quebec taiga. *Clim Dyn* (Springer Verlag) 49(11–12):4107–4119. <https://doi.org/10.1007/s00382-017-3565-5>
- St. George S, Esper J (2019) ‘Concord and discord among Northern Hemisphere paleotemperature reconstructions from treerings. *Quat Rev* (Elsevier Ltd) 203:278–281. <https://doi.org/10.1016/j.quascirev.2018.11.013>
- Gessler A et al (2014) Stable isotopes in treerings: towards a mechanistic understanding of isotope fractionation and mixing processes from the leaves to the wood. *Tree Physiol* 00:1–23. <https://doi.org/10.1093/treephys/tpu040>
- Giguère-Croteau C et al. (2019) North America’s oldest boreal trees are more efficient water users due to increased [CO<sub>2</sub>], but do not grow faster. *Proc Natl Acad Sci U S A* (National Academy of Sciences) 116(7):2749–2754. <https://doi.org/10.1073/pnas.1816686116>
- Giuggiola A, Ogee J, Gessler A, Rigling A, Bugmann H, Treydte K (2016) Improvement of water and light availability after thinning at a xeric site: which matters more? A dual isotope approach. *New Phytol* 210:108–121
- Gouirand I et al (2008) On the spatiotemporal characteristics of Fennoscandian treeringbased summer temperature reconstructions. *Theor Appl Climatol* (Springer Wien) 91(1–4):1–25. <https://doi.org/10.1007/s00704-007-0311-7>
- Granda E et al (2017) Aged but withstanding: maintenance of growth rates in old pines is not related to enhanced water-use efficiency. *Agric Forest Meteorol* (Elsevier (BV)) 243:43–54. <https://doi.org/10.1016/j.agrformet.2017.05.005>
- Gray J, Thompson P (1977) Climatic information from  $^{18}\text{O}/^{16}\text{O}$  ratios of cellulose in tree rings. *Nature* 262:481–482
- Green JW (1963) *Methods of carbohydrate chemistry*, Whistler RL (ed), 3rd edn. Academic Press, New York, NY
- Grießinger J, Bräuning A, Helle G, Thomas A, Schleser G (2011) Late Holocene Asian summer monsoon variability reflected by  $\delta^{18}\text{O}$  in tree-rings from Tibetan junipers. *Geophys Res Lett* 38. <https://doi.org/10.1029/2010GL045988>
- Grießinger J et al (2018) Imprints of climate signals in a 204 year  $\delta^{18}\text{O}$  treering record of *Nothofagus pumilio* from Perito Moreno Glacier, Southern Patagonia (50°S). *Front Earth Sci* (Frontiers Media (SA)) 6. <https://doi.org/10.3389/feart.2018.00027>
- Gu L et al (2003) Response of a deciduous forest to the Mount Pinatubo eruption: enhanced photosynthesis. *Science* 299(5615):2035–2038. <https://doi.org/10.1126/science.1078366>



- Hafner P et al (2014) A 520 year record of summer sunshine for the eastern European Alps based on stable carbon isotopes in larch treerings. *Clim Dyn* (Springer Verlag) 43(3–4):971–980. <https://doi.org/10.1007/s00382-013-1864-z>
- Harlow BA, Marshall JD, Robinson AP (2006) A multi-species comparison of  $\delta^{13}\text{C}$  from whole wood, extractive-free wood and holocellulose. *Tree Physiol* (Oxford University Press) 26(6):767–774. <https://doi.org/10.1093/treephys/26.6.767>
- Hartl-Meier C, Zang C, Büntgen U, Esper J, Rothe A, Göttele A, Dirnböck T, Treydte K (2015) Uniform climate sensitivity in tree-ring stable isotopes across species and sites in a mid-latitude temperate forest. *Tree Physiol* 35(1):4–15. <https://doi.org/10.1093/treephys/tpu096> Epub 2014 Dec 2 PMID: 25466725
- Heinrich I et al (2008) Hydroclimatic variation in Far North Queensland since 1860 inferred from treerings. *Palaeogeogr Palaeoclimatol Palaeoecol* (Elsevier (BV)) 270(1–2):116–127. <https://doi.org/10.1016/j.palaeo.2008.09.002>
- Heinrich I et al (2013) Winter-to-spring temperature dynamics in Turkey derived from treerings since AD 1125. *Clim Dyn* 41(7–8):1685–1701. <https://doi.org/10.1007/s00382-013-1702-3>
- Helama S et al (2002) The supra-long Scots pine treering record for Finnish Lapland: Part 2, interannual to centennial variability in summer temperatures for 7500 years. *Holocene* 12(6):681–687. <https://doi.org/10.1191/0959683602h1581rp>
- Helama S et al (2015) Age-related trends in subfossil treering  $\delta^{13}\text{C}$  data. *Chem Geol* (Elsevier (BV)) 416:28–35. <https://doi.org/10.1016/j.chemgeo.2015.10.019>
- Helama S, Arppe L, Timonen M, Mielikäinen K, Oinonen M (2018) A 7.5 chronology of stable carbon isotopes from tree rings with implications for their use in palaeo-cloud reconstruction. *Global Planet Change* 170:20–33
- Hereş AM et al (2014) Drought-induced mortality selectively affects Scots pine trees that show limited intrinsic water-use efficiency responsiveness to raising atmospheric  $\text{CO}_2$ . *Funct Plant Biol* (CSIRO Publishing) 41(3):244. <https://doi.org/10.1071/fp13067>
- Holm JA, Kueppers LM, Chambers JQ (2017) Novel tropical forests: response to global change. *New Phytologist* (Wiley) 213(3):988–992. <https://doi.org/10.1111/nph.14407>
- Holmes JA, Zhang J, Chen F, Qiang M, (2007) Paleoclimatic implications of an 850-year oxygen-isotope record from the northern Tibetan Plateau. *Geophys Res Lett* 24. <https://doi.org/10.1029/2007GL032228>
- Holzkämper S et al (2012) Comparison of stable carbon and oxygen isotopes in *Picea glauca* treerings and *Sphagnum fuscum* moss remains from subarctic Canada. *Quat Res* (Cambridge University Press (CUP)) 78(2):295–302. <https://doi.org/10.1016/j.yqres.2012.05.014>
- Hunter MO et al (2013) Tree height and tropical forest biomass estimation. *Biogeosciences* (Copernicus (GmbH)) 10(12):8385–8399. <https://doi.org/10.5194/bg-10-8385-2013>
- Jacoby GC, D'Arrigo RD (1995) Treering width and density evidence of climatic and potential forest change in Alaska. *Glob Biogeochem Cycles* 9(2):227–234
- Johnstone JA, Roden JS, Dawson TE (2013) Oxygen and carbon stable isotopes in coast redwood tree rings respond to spring and summer climate signals. *JGR Biogeosci* 118:1438–1450
- Kahmen A et al (2011) Cellulose  $\delta^{18}\text{O}$  is an index of leaf-to-air vapor pressure difference (VPD) in tropical plants. *Proc Natl Acad Sci* 108(5):1981–1986. <https://doi.org/10.1073/pnas.1018906108>
- Klippel L, Krusic PJ, Konter O, St. George S, Trouet V, Esper J (2019) A 1200+ year reconstruction of temperature extremes for the northeastern Mediterranean region. *Int J Climatol* 39:2336–2350
- Kirilyanov AV et al (2008) Climate signals in treering width, density and  $\delta^{13}\text{C}$  from larches in Eastern Siberia (Russia). *Chem Geol* 252(1–2):31–41. <https://doi.org/10.1016/j.chemgeo.2008.01.023>
- Körner C (2009) Responses of humid tropical trees to rising  $\text{CO}_2$ . *Ann Rev Ecol Evol Syst* (Ann Rev) 40(1):61–79. <https://doi.org/10.1146/annurev.ecolsys.110308.120217>
- Kress A et al (2010) A 350 year drought reconstruction from Alpine treering stable isotopes. *Global Biogeochem Cycles* 24(2):1–16. <https://doi.org/10.1029/2009GB003613>

- Labuhn I et al (2014) Tree age, site and climate controls on treering cellulose  $\delta^{18}\text{O}$ : a case study on oak trees from south-western France. *Dendrochronologia* (Elsevier (GmbH)) 32(1):78–89. <https://doi.org/10.1016/j.dendro.2013.11.001>
- Labuhn I, Daux V, Girardclos O, Stievenard M, Pierre M, Masson-Delmotte V (2016) French summer droughts since 1326AD: a reconstruction based on treering cellulose  $\delta^{18}\text{O}$ . *Clim past Discuss* 12:1101–1117. <https://doi.org/10.5194/cpd-11-5113-2015>
- Lavergne A et al (2016) Are the oxygen isotopic compositions of *Fitzroya cupressoides* and *Nothofagus pumilio* cellulose promising proxies for climate reconstructions in northern Patagonia? *J Geophys Res Biogeosci* (American Geophysical Union (AGU)) 121(3):767–776. <https://doi.org/10.1002/2015Jg003260>
- Lavergne A, Daux V, Villalba R, Pierre M, Stievenard M, Srur AM (2017a) Improvement of isotope-based climate reconstructions in Patagonia through a better understanding of climate influences on isotopic fractionation in tree rings. *Earth Planet Sci Lett* 459:372–380
- Lavergne A, Gennaretti F, Risi C, Daux V, Boucher E, Savard MM, Naulier M, Villalba R, Bégin C, Guiot J (2017b) Modelling tree-ring cellulose  $\delta^{18}\text{O}$  variations of two temperature-sensitive tree species from North and South America. *Clim Past Discuss* 13:1515–1526. <https://www.clim-past-discuss.net/cp-2017-93/>
- Lavergne A et al (2018) Past summer temperatures inferred from dendrochronological records of *fitzroya cupressoides* on the eastern slope of the northern Patagonian andes. *J Geophys Res* (Blackwell Publishing Ltd) 123(1):32–45. <https://doi.org/10.1002/2017JG003989>
- Lavergne A et al (2019) Observed and modelled historical trends in the water-use efficiency of plants and ecosystems. *Glob Change Biol* (Wiley). <https://doi.org/10.1111/gcb.14634>
- Leavitt SW, Long A (1991) Seasonal stable-carbon isotope variability in treerings: possible paleoenvironmental signals. *Chem Geol Isotope Geosci Sect* (Elsevier (BV)) 87(1):59–70. [https://doi.org/10.1016/0168-9622\(91\)90033-s](https://doi.org/10.1016/0168-9622(91)90033-s)
- Leavitt SW, Long A (1986) Stable-carbon isotope variability in tree foliage and wood. *Ecology* 67(4):1002–1010
- Leavitt SW, Long A (1988) Stable carbon isotope chronologies from trees in the southwestern United States. *Global Biogeochem Cycles* 2(3):189–198. <https://doi.org/10.1029/GB002i003p00189>
- Leavitt SW, Long A (1989a) Drought indicated in carbon-13/carbon-12 ratios of southwestern treerings. *JAWRA J Am Water Resour Assoc* 25(2):341–347. <https://doi.org/10.1111/j.1752-1688.1989.tb03070.x>
- Leavitt SW, Long A (1989b) The atmospheric  $\delta^{13}\text{C}$  record as derived from 56 pinyon trees at 14 sites in the Southwestern United States. *Radiocarbon* (Cambridge University Press (CUP)) 31(03):469–474. <https://doi.org/10.1017/s0033822200012054>
- Leonelli G, Battipaglia G, Cherubini P, Saurer M, Siegwolf RTW, Maugeri M, Stenni B, Fusco S, Maggi V, Pelfin M (2017) *Larix decidua*  $\delta^{18}\text{O}$  tree-ring cellulose mainly reflects the isotopic signature of winter snow in a high-altitude glacial valley of the European Alps. *Sci Total Environ* 579:230–237
- Lévesque M et al (2014) Increased water-use efficiency does not lead to enhanced tree growth under xeric and mesic conditions. *New Phytologist* 203(1):94–109. <https://doi.org/10.1111/nph.12772>
- Levesque M, Andreu-Hayles L, Smith WK, Williams AP, Hobi ML, Allred BW, Pederson N (2019) Tree-ring isotopes capture interannual vegetation productivity dynamics at the biome scale. *Nat Commun* 10:1–10. <https://doi.org/10.1038/s41467-019-08634-y>
- Li Z-H et al (2011) Micro-scale analysis of treering  $\delta^{18}\text{O}$  and  $\delta^{13}\text{C}$  on  $\alpha$ -cellulose spline reveals high-resolution intra-annual climate variability and tropical cyclone activity. *Chem Geol* (Elsevier (BV)) 284(1–2):138–147. <https://doi.org/10.1016/j.chemgeo.2011.02.015>
- Libby LM et al (1976) Isotopic tree thermometers. *Nature* 261(5558):284–288. <https://doi.org/10.1038/261284a0>
- Libby LM (1972) Multiple thermometry in paleo climate and historic climate. *Tech Rep*
- Libby LM, Pandolfi LJ (1974) Temperature dependence of isotope ratios in treerings. *Proc Natl Acad Sci U S A* 71(6):2482–2486. <http://www.pubmedcentral.nih.gov/articlerender.fcgi?artid=388483&tool=pmcentrez&rendertype=abstract>

- Lin YS et al (2015) Optimal stomatal behaviour around the world. *Nat Clim Change* (Nature Publishing Group) 5(5):459–464. <https://doi.org/10.1038/nclimate2550>
- Linderholm HW et al (2014) Fennoscandia revisited: a spatially improved tree-ring reconstruction of summer temperatures for the last 900 years. *Clim Dyn*. <https://doi.org/10.1007/s00382-014-2328-9>
- Lipp J et al (1991) Stable isotopes in tree-ring cellulose and climatic change. *Tellus* 322–330. <https://doi.org/10.1034/j.1600-0889.1991.t01-2-00005.x>
- Liu Y et al (2004) A preliminary seasonal precipitation reconstruction from tree-ring stable carbon isotopes at Mt. Helan, China, since AD 1804. *Glob Planet Change* 229–239. <https://doi.org/10.1016/j.gloplacha.2004.01.009>
- Liu Y, Wang R, Leavitt SW, Song H, Linderholm HW, Li Q, An Z (2012) Individual and pooled tree-ring stable-carbon isotope series in Chinese pine from the Nan Wutai region, China: common signal and climate relationships. *Chem Geol* 330–331:17–26. <https://doi.org/10.1016/j.chemgeo.2012.08.008>
- Liu Y et al (2014) Tree-ring stable carbon isotope-based May–July temperature reconstruction over Nanwutai, China, for the past century and its record of 20th century warming. *Quat Sci Rev* (Elsevier Ltd) 93(July):67–76. <https://doi.org/10.1016/j.quascirev.2014.03.023>
- Liu Y et al (2018) Tree-ring stable carbon isotope-based April–June relative humidity reconstruction since AD 1648 in Mt. Tianmu, China. *Clim Dyn* (Springer Verlag) 50(5–6):1733–1745. <https://doi.org/10.1007/s00382-017-3718-6>
- Lloyd J, Farquhar GD (2008) Effects of rising temperatures and [CO<sub>2</sub>] on the physiology of tropical forest trees. *Philos Trans R Soc B Biol Sci* (The Royal Society) 363(1498):1811–1817. <https://doi.org/10.1098/rstb.2007.0032>
- Loader N et al (1997) An improved technique for the batch processing of small wholewood samples to  $\alpha$ -cellulose. *Chem Geol* 136:313–317
- Loader NJ, Heller G, Los SO, Lehmkuhl F, Schleser GH (2010) Twentieth-century summer temperature variability in the southern Altai Mountains: carbon and oxygen isotope study of tree-rings. *The Holocene* 20:1149–1156
- Loader NJ et al (2011) Recent trends in the intrinsic water-use efficiency of ringless rainforest trees in Borneo. *Philos Trans R Soc B: Biol Sci* 366:3330–3339. <https://doi.org/10.1098/rstb.2011.0037>
- Loader NJ et al (2013) Stable carbon isotopes from Torneträsk, northern Sweden provide a millennial length reconstruction of summer sunshine and its relationship to Arctic circulation. *Quat Sci Rev* 62:97–113. <https://doi.org/10.1016/j.quascirev.2012.11.014>
- Loader NJ et al (2016) Measurements of hydrogen, oxygen and carbon isotope variability in Sphagnum moss along a micro-topographical gradient in a southern Patagonian peatland. *J Quat Sci* 31(4):426–435. <https://doi.org/10.1002/jqs.2871>
- Loader NJ et al (2017) Inter-annual carbon isotope analysis of tree-rings by laser ablation. *Chem Geol* (Elsevier (BV)) (2016). <https://doi.org/10.1016/j.chemgeo.2017.06.021>
- Loader NJ et al (2019) Tree-ring dating using oxygen isotopes: a master chronology for central England. *J Quat Sci* (Wiley) 34(6):475–490. <https://doi.org/10.1002/jqs.3115>
- Loader NJ, Robertson I, McCarroll D (2003) Comparison of stable carbon isotope ratios in the whole wood, cellulose and lignin of Oak tree-rings. *Palaeogeogr Palaeoclimatol Palaeoecol* 196:395–407
- Lorrey AM et al (2016) Stable oxygen isotope signatures of early season wood in New Zealand kauri (*Agathis australis*) tree-rings: prospects for palaeoclimate reconstruction. *Dendrochronologia* (Elsevier (BV)) 40:50–63. <https://doi.org/10.1016/j.dendro.2016.03.012>
- Luterbacher J et al (2016) European summer temperatures since Roman times. *Environ Res Lett* (IOP Publishing) 11(2):024001. <https://doi.org/10.1088/1748-9326/11/2/024001>
- Mann ME, Bradley RS, Hughes MK (1999) Northern hemisphere temperatures during the past millennium: inferences, uncertainties, and limitations. *Geophys Res Lett* 26(6):759–762. <https://doi.org/10.1029/1999GL900070>

- Marshall JD, Monserud RA (1996) Homeostatic gas-exchange parameters inferred from  $^{13}\text{C}/^{12}\text{C}$  in treerings of conifers. *Oecologia* (Springer Verlag) 105(1):13–21. <https://doi.org/10.1007/BF00328786>
- Martínez-Sancho E et al (2018) Increased water-use efficiency translates into contrasting growth patterns of Scots pine and sessile oak at their southern distribution limits. *Glob Change Biol* (Wiley) 24(3):1012–1028. <https://doi.org/10.1111/gcb.13937>
- Masson-Delmotte V et al (2005) Changes in European precipitation seasonality and in drought frequencies revealed by a four-century-long treeringisotopic record from Brittany, western France. *Clim Dyn* (Springer Science and Business Media (LLC)) 24(1):57–69. <https://doi.org/10.1007/s00382-004-0458-1>
- McCarroll D et al (2002) Blue reflectance provides a surrogate for latewood density of high-latitude pine treerings. *Arct Antarct Alp Res* 34(4):450–453. <https://doi.org/10.1080/15230430.2002.12003516>
- McCarroll D et al (2009) Correction of treering stable carbon isotope chronologies for changes in the carbon dioxide content of the atmosphere. *Geochim Cosmochim Acta* 73(6):1539–1547. <https://doi.org/10.1016/j.gca.2008.11.041>
- McCarroll D et al (2013) A 1200-year multiproxy record of tree growth and summer temperature at the northern pine forest limit of Europe. *The Holocene* 23:471–484. <https://doi.org/10.1177/0959683612467483>
- McCarroll D, Loader NJ (2004) Stable isotopes in treerings. *Quat Sci Rev* 23:771–801. <https://doi.org/10.1016/j.quascirev.2003.06.017>
- McCarroll D, Pawellek F (1998) Stable carbon isotope ratios of latewood cellulose in *Pinus sylvestris* from northern Finland: variability and signal-strength. *The Holocene* 8:675–684. <https://doi.org/10.1191/095968398675987498>
- McCarroll D, Pawellek F (2001) Stable carbon isotope ratios of *Pinus sylvestris* from northern Finland and the potential for extracting a climate signal from long Fennoscandian chronologies. *The Holocene* 11(5):517–526
- Medlyn BE et al (2017) How do leaf and ecosystem measures of water-use efficiency compare? *New Phytologist* (Wiley) 216(3):758–770. <https://doi.org/10.1111/nph.14626>
- Meier WJH, Aravena JC, Jaña R, Braun MH, Hochreuther P, Soto-Rogel P, Griebinger J (2020) A tree-ring  $\delta^{18}\text{O}$  series from southernmost Fuego-Patagonia is recording flavors of the Antarctic oscillation. *Glob Planet Change* 195:103302
- De Micco V et al (2019) From xylogenesis to treerings: wood traits to investigate tree response to environmental changes. *IAWA J* (Brill) 40(2):155–182. <https://doi.org/10.1163/22941932-40190246>
- De Mil T et al (2017) Cambial activity in the understory of the Mayombe forest, DR Congo. *Trees Struct Funct* (Springer Verlag) 31(1):49–61. <https://doi.org/10.1007/s00468-016-1454-x>
- Naulier M et al (2014) Carbon and oxygen isotopes of lakeshore black spruce trees in northeastern Canada as proxies for climatic reconstruction. *Chem Geol* 374–375(May 2014):37–43. <https://doi.org/10.1016/j.chemgeo.2014.02.031>
- Naulier M et al (2015) A millennial summer temperature reconstruction for northeastern Canada using oxygen isotopes in subfossil trees. *Clim Past* (Copernicus (GmbH)) 11(9):1153–1164. <https://doi.org/10.5194/cp-11-1153-2015>
- Neukom R et al (2019) No evidence for globally coherent warm and cold periods over the preindustrial common era. *Nature* 571(7766):550–554. <https://doi.org/10.1038/s41586-019-1401-2>
- Ohashi S et al (2009) Detecting invisible growth rings of trees in seasonally dry forests in Thailand: isotopic and wood anatomical approaches. *Trees* (Springer Science and Business Media (LLC)) 23(4):813–822. <https://doi.org/10.1007/s00468-009-0322-3>
- Ohashi S et al (2015) Seasonal variations in the stable oxygen isotope ratio of wood cellulose reveal annual rings of trees in a Central Amazon terra firme forest. *Oecologia* (Springer Science and Business Media (LLC)) 180(3):685–696. <https://doi.org/10.1007/s00442-015-3509-x>

- PAGES 2k Consortium (2013) Continental-scale temperature variability during the past two millennia. *Nat Geosci* 6(5). <https://doi.org/10.1038/ngeo1797>
- PAGES 2k Consortium (2017) A global multiproxy database for temperature reconstructions of the common era. *Scientific Data*. The Author(s), 4:170088. <https://doi.org/10.1038/sdata.2017.88>
- Pan Y et al (2011) A large and persistent carbon sink in the world's forests. *Science* (American Association for the Advancement of Science (AAAS)) 333(6045):988–993. <https://doi.org/10.1126/science.1201609>
- Pauly M, Helle G, Miramont C, Büntgen U, Treydte K, Reinig F, Guibal F, Sivan O, Heinrich I, Riedel F, Kromer B (2018) Subfossil trees suggest enhanced Mediterranean hydroclimate variability at the onset of the Younger Dryas. *Sci Rep* 8(1):1–8
- Pauly M, Helle G, Büntgen U, Wacker L, Treydte K, Reinig F, Turney C, Nievergelt D, Kromer B, Friedrich M, Sookdeo A, Heinrich I, Riedel F, Brauer A (2020) An annual-resolution stable isotope record from Swiss subfossil pine trees growing in the late Glacial. *Quat Sci Rev*. <https://doi.org/10.1016/j.quascirev.2020.106550>
- Payomrat P et al (2018) Treeringstable carbon isotope-based June–September maximum temperature reconstruction since AD 1788, north-west Thailand. *Tellus Ser B Chem Phys Meteorol* (Taylor and Francis Ltd.) 70(1). <https://doi.org/10.1080/16000889.2018.1443655>
- Pearman GI, Francey RJ, Fraser PJB (1976) Climatic implications of stable carbon isotopes in tree rings. *Nature* 260:771–772
- Peñuelas J, Canadell JG, Ogaya R (2011) Increased water-use efficiency during the 20th century did not translate into enhanced tree growth. *Glob Ecol Biogeogr* (Wiley) 20(4):597–608. <https://doi.org/10.1111/j.1466-8238.2010.00608.x>
- Pons TL, Helle G (2011) Identification of anatomically non-distinct annual rings in tropical trees using stable isotopes. *Trees* (Springer Science and Business Media (LLC)) 25(1):83–93. <https://doi.org/10.1007/s00468-010-0527-5>
- Porter TJ et al (2009) Climatic signals in  $\delta^{13}\text{C}$  and  $\delta^{18}\text{O}$  of treerings from White Spruce in the Mackenzie Delta Region, Northern Canada. *Arct Antarct Alp Res* (Informa (UK) Limited) 41(4):497–505. <https://doi.org/10.1657/1938-4246-41.4.497>
- Porter TJ et al (2013) Spring-summer temperatures since {AD} 1780 reconstructed from stable oxygen isotope ratios in white spruce treerings from the Mackenzie Delta, northwestern Canada. *Clim Dyn* (Springer Science and Business Media (LLC)) 42(3–4):771–785. <https://doi.org/10.1007/s00382-013-1674-3>
- Poussart PF, Evans MN, Schrag DP (2004) Resolving seasonality in tropical trees: multi-decade, high-resolution oxygen and carbon isotope records from Indonesia and Thailand. *Earth Planet Sci Lett* (Elsevier (BV)) 218(3–4):301–316. [https://doi.org/10.1016/s0012-821x\(03\)00638-1](https://doi.org/10.1016/s0012-821x(03)00638-1)
- Poussart PF, Schrag DP (2005) Seasonally resolved stable isotope chronologies from northern Thailand deciduous trees. *Earth Planet Sci Lett* (Elsevier (BV)) 235(3–4):752–765. <https://doi.org/10.1016/j.epsl.2005.05.012>
- Pumijumnong N, Eckstein D (2011) Reconstruction of pre-monsoon weather conditions in north-western Thailand from the treeringwidths of *Pinus merkusii* and *Pinus kesiya*. *Trees* (Springer Science and Business Media (LLC)) 25(1):125–132. <https://doi.org/10.1007/s00468-010-0528-4>
- Qin C, Yang B, Bräuning A, Griebinger J, Wernicke J (2015) Drought signals in tree-ring stable oxygen isotope series of Qilian juniper from the arid northeastern Tibetan Plateau. *Glob Planet Change* 125:48–59
- Raffalli-Delerc G, Masson-Delmotte V, Dupouey JL, Stievenard M, Breda N, Moisselin JM (2004) Reconstruction of summer droughts using tree-ring cellulose isotopes: a calibration study with living oaks from Brittany (Western France). *Tellus B Chem Phys Meteorol* 56:160–174. <https://doi.org/10.1111/j.1600-0889.2004.00086.x>
- Rahman M et al (2019) Trends in tree growth and intrinsic water-use efficiency in the tropics under elevated  $\text{CO}_2$  and climate change. *Trees* (Springer Science and Business Media (LLC)) 33(3):623–640. <https://doi.org/10.1007/s00468-019-01836-3>

- Ramesh R, Bhattacharya SK, Gopalan K (1986) Climatic correlations in the stable isotope records of silver fir (*Abies pindrow*) trees from Kashmir, India. *Earth Planet Sci Lett* 79(1–2):66–74. [https://doi.org/10.1016/0012-821X\(86\)90041-5](https://doi.org/10.1016/0012-821X(86)90041-5)
- Rayback SA, Henry GHR (2006) Reconstruction of summer temperature for a Canadian high arctic site from retrospective analysis of the dwarf shrub, *Cassiope tetragona*. *Arct Antarct Alp Res* 38(2):228–238. [https://doi.org/10.1657/1523-0430\(2006\)38\[228:ROSTFA\]2.0.CO;2](https://doi.org/10.1657/1523-0430(2006)38[228:ROSTFA]2.0.CO;2)
- Reynolds-Henne CE, Siegwolf RTW, Henne S, Treydte KS, Esper J, Saurer M (2007) Temporal stability of climate-isotope relationships in tree rings of oak and pine (Ticino, Switzerland). *Glob Biogeochem Cycles* 21(GB4009):2007. <https://doi.org/10.1029/2007GB002945>
- Rinne KT et al (2005) On the purification of  $\alpha$ -cellulose from resinous wood for stable isotope (H, C and O) analysis. *Chem Geol* 222:75–82
- Rinne KTK, Loader NJN, Switsur VR, Waterhouse JS (2013) 400-year May–August precipitation reconstruction for Southern England using oxygen isotopes in tree rings. *Quat Sci Rev* 60:13–25. <https://doi.org/10.1016/j.quascirev.2012.10.048>
- Robert EMR et al (2011) Mangrove growth rings: fact or fiction? *Trees* (Springer Science and Business Media (LLC)) 25(1):49–58. <https://doi.org/10.1007/s00468-010-0487-9>
- Robertson I, Waterhouse JS, Barker AC, Carter AHC, Switsur VR (2001) Oxygen isotope ratios of oak in east England: implications for reconstructing the isotopic composition of precipitation. *Earth Planet Sci Lett* 191:21–31
- Robertson I, Rolfe J et al (1997) Signal strength and climate relationships in  $^{13}\text{C}/^{12}\text{C}$  ratios of tree-ring cellulose from oak in southwest Finland. *Geophys Res Lett* (American Geophysical Union) 24(12):1487–1490. <https://doi.org/10.1029/97GL01293>
- Roden JS, Ehleringer JR (2007) Summer precipitation influences the stable oxygen and carbon isotopic composition of tree-ring cellulose in *Pinus ponderosa*. *Tree Physiol* 27(4):491–501. <https://doi.org/10.1093/treephys/27.4.491>
- Roden JS, Johnstone JA, Dawson TE (2011) Regional and watershed-scale coherence in the stable-oxygen and carbon isotope ratio time series in tree rings of coast redwood (*Sequoia sempervirens*). *Tree-Ring Res* 67:71–86. <https://doi.org/10.3959/2010-4.1>
- Rodríguez-Catón, M., Andreu-Hayles, L., Morales, M.S., Daux, V., Christie, D.A., Coopman, R.E., Alvarez, C., Rao, M.P., Aliste, D., Flores, F. & Villalba, R. (2021) Different climate sensitivity for radial growth, but uniform for tree-ring stable isotopes along an aridity gradient in *Polylepis tarapacana*, the world's highest elevation tree species. *Tree Physiology*, 41, 1353–1371
- Roig FA, Siegwolf R, Boninsegna JA (2006) Stable oxygen isotopes ( $\delta^{18}\text{O}$ ) in *Austrocedrus chilensis* tree-rings reflect climate variability in northwestern Patagonia, Argentina. *Int J Biometeorol* (Springer Science and Business Media (LLC)) 51(2):97–105. <https://doi.org/10.1007/s00484-006-0049-4>
- Rozanski K, Araguas-Araguas GL (1993) Isotopic patterns in modern global precipitation. *Geophys Monogr Ser*. <https://doi.org/10.1029/GM078p0001>
- Rozendaal DMA, Zuidema PA (2011) Dendroecology in the tropics: a review. *Trees Struct Funct* 3–16. <https://doi.org/10.1007/s00468-010-0480-3>
- Sano M, Buckley BM, Sweda T (2009) Tree-ring based hydroclimate reconstruction over northern Vietnam from *Fokienia hodginsii*: eighteenth century mega-drought and tropical Pacific influence. *Clim Dyn* (Springer Science and Business Media (LLC)) 33(2–3):331–340. <https://doi.org/10.1007/s00382-008-0454-y>
- Santini F et al (2018) Scarce population genetic differentiation but substantial spatiotemporal phenotypic variation of water-use efficiency in *Pinus sylvestris* at its western distribution range. *Eur J Forest Res* (Springer Science and Business Media (LLC)) 137(6):863–878. <https://doi.org/10.1007/s10342-018-1145-9>
- Sass-Klaassen U et al (2016) A tree-centered approach to assess impacts of extreme climatic events on forests. *Front Plant Sci* (Frontiers Media (SA)) 7. <https://doi.org/10.3389/fpls.2016.01069>
- Saurer M, Cherubini P, Siegwolf R (2000) Oxygen isotopes in tree rings of *Abies alba*: the climatic significance of interdecadal variations. *J Geophys Res* 105:12461–12470

- Saurer M, Cherubini P, Reynolds-Henna CE, Treydte KS, Anderson WT, Siegwolf RTW (2008) An investigation of the common signal in tree-ring stable isotope chronologies at temperate sites. *J Geophys Res* 113:1–11. <https://doi.org/10.1029/2008jg000689>
- Saurer M, Borella S, Schweingruber F et al (1997) Stable carbon isotopes in tree rings of beech: climatic versus site-related influences. *Trees* 11:291–297. <https://doi.org/10.1007/s004680050087>
- Saurer M et al (2014) Spatial variability and temporal trends in water-use efficiency of European forests. *Glob Change Biol* 20(12). <https://doi.org/10.1111/gcb.12717>
- Saurer M, Siegwolf RTW, Schweingruber FH (2004) Carbon isotope discrimination indicates improving water-use efficiency of trees in northern Eurasia over the last 100 years. *Glob Change Biol* (Wiley) 10(12):2109–2120. <https://doi.org/10.1111/j.1365-2486.2004.00869.x>
- Savard MM, Daux V (2020) An overview on isotopic divergences—causes for instability of tree-ring isotopes and climate correlations. *Clim past* 16:1223–1243. <https://doi.org/10.5194/cp-16-1223-2020>
- Schifman LA et al (2012) Carbon isotope variation in shrub willow (*Salix* spp.) ring-wood as an indicator of long-term water status, growth and survival. *Biomass Bioenerg* 36:316–326. <https://doi.org/10.1016/j.biombioe.2011.10.042>
- Schleser GH et al (1999) Isotope signals as climate proxies: the role of transfer functions in the study of terrestrial archives. *Quat Sci Rev* (Elsevier Ltd) 18(7):927–943. [https://doi.org/10.1016/S0277-3791\(99\)00006-2](https://doi.org/10.1016/S0277-3791(99)00006-2)
- Schneider L et al (2015) Revising midlatitude summer temperatures back to A.D. 600 based on a wood density network. *Geophys Res Lett* (Wiley) 42(11):4556–4562. [https://doi.org/10.1002/2015GL063956@10.1002/\(ISSN\)1944-8007.2015EDHIGHLIGHTS](https://doi.org/10.1002/2015GL063956@10.1002/(ISSN)1944-8007.2015EDHIGHLIGHTS)
- Schollaen K et al (2013) {ENSO} flavors in a tree-ring  $\delta^{18}\text{O}$  record of *Tectona grandis* from Indonesia. *Clim Past* (Copernicus (GmbH)) 11(10):1325–1333. <https://doi.org/10.5194/cp-11-1325-2015>
- Schollaen K, Karamperidou C, Krusic P, Cook E, Helle G (2015) ENSO flavors in a tree-ring delta O-18 record of *Tectona grandis* from Indonesia. *Clim past* 11:1325–1333
- Schongart J et al (2004) Teleconnection between tree growth in the Amazonian floodplains and the El Niño-Southern Oscillation effect. *Glob Change Biol* (Wiley) 10(5):683–692. <https://doi.org/10.1111/j.1529-8817.2003.00754.x>
- Schöngart J et al (2002) Phenology and stem-growth periodicity of tree species in Amazonian floodplain forests. *J Trop Ecol* (Cambridge University Press (CUP)) 18(4):581–597. <https://doi.org/10.1017/s0266467402002389>
- Schubert BA, Timmermann A (2015) Reconstruction of seasonal precipitation in Hawai'i using high-resolution carbon isotope measurements across treerings. *Chem Geol* (Elsevier (BV)) 417:273–278. <https://doi.org/10.1016/j.chemgeo.2015.10.013>
- Seftigen K, Linderholm HW, Loader NJ, Liu Y, Young GHF (2011) The influence of climate on  $^{13}\text{C}/^{12}\text{C}$  and  $^{18}\text{O}/^{16}\text{O}$  ratios in tree ring cellulose of *Pinus sylvestris* L. growing in the central Scandinavian Mountains. *Chem Geol* 286:84–93
- Shestakova TA et al (2019) Spatio-temporal patterns of tree growth as related to carbon isotope fractionation in European forests under changing climate. *Glob Ecol Biogeogr* (Blackwell Publishing Ltd). <https://doi.org/10.1111/geb.12933>
- Sidorova OV et al (2013) The application of tree-rings and stable isotopes for reconstructions of climate conditions in the Russian Altai. *Clim Change* 120:153–167. <https://doi.org/10.1007/s10584-013-0805-5>
- Silva LCR et al (2015) Isotopic and nutritional evidence for species- and site-specific responses to N deposition and elevated  $\text{CO}_2$  in temperate forests. *J Geophys Res Biogeosci* (American Geophysical Union (AGU)) 120(6):1110–1123. <https://doi.org/10.1002/2014jg002865>
- Silva LCR, Anand M (2013) Probing for the influence of atmospheric  $\text{CO}_2$  and climate change on forest ecosystems across biomes. *Glob Ecol Biogeogr* Edited by b. Shipley (Wiley) 22(1):83–92. <https://doi.org/10.1111/j.1466-8238.2012.00783.x>

- Skomarkova MV, Vaganova EA, Mund M, Knohl A, Linke P, Boerner A, Schulze ED (2006) Inter-annual and seasonal variability of radial growth, wood density and carbon isotope ratios in tree rings of beech (*Fagus sylvatica*) growing in Germany and Italy. *Trees* 20(5):571–586
- van der Sleen P et al (2014) Understanding causes of tree growth response to gap formation:  $\Delta^{13}\text{C}$ -values in treerings reveal a predominant effect of light. *Trees* (Springer Science and Business Media (LLC)) 28(2):439–448. <https://doi.org/10.1007/s00468-013-0961-2>
- van der Sleen P, Zuidema PA, Pons TL (2017) Stable isotopes in tropical treerings: theory, methods and applications. *Funct Ecol* Edited by r. Oliveira (Wiley) 31(9):1674–1689. <https://doi.org/10.1111/1365-2435.12889>
- Smerdon JE, Pollack HN (2016) Reconstructing earth's surface temperature over the past 2000 years: the science behind the headlines. *Wiley Interdiscip Rev Clim Change* (Wiley-Blackwell) 746–771. <https://doi.org/10.1002/wcc.418>
- Song L et al (2016) Water use patterns of *Pinus sylvestris* var. *mongolica* trees of different ages in a semiarid sandy lands of Northeast China. *Environ Exp Bot* (Elsevier (BV)) 129:94–107. <https://doi.org/10.1016/j.envexpbot.2016.02.006>
- Sprenger M, Seeger S, Blume T, Weiler M (2016) Travel times in the vadose zone: variability in space and time. *Water Resour Res* 52:5727–5754. <https://doi.org/10.1002/2015WR018077>
- Stahle DW (1999) Useful strategies for the development of tropical tree-ring chronologies. *IAWA J* (Brill) 20(3):249–253. <https://doi.org/10.1163/22941932-90000688>
- Steppe K, Sterck F, Deslauriers A (2015) Diel growth dynamics in tree stems: linking anatomy and ecophysiology. *Trends Plant Sci* (Elsevier (BV)) 20(6):335–343. <https://doi.org/10.1016/j.tplants.2015.03.015>
- Sternberg LDSL O'Reilly (2009) Oxygen stable isotope ratios of tree-ring cellulose: the next phase of understanding. *New Phytologist* 181:553–562. <https://doi.org/10.1111/j.1469-8137.2008.02661.x>
- Stoffel M et al (2015) Estimates of volcanic-induced cooling in the Northern Hemisphere over the past 1,500 years. *Nat Geosci* (Nature Publishing Group) 8(10):784–788. <https://doi.org/10.1038/ngeo2526>
- Szejner P et al (2016) Latitudinal gradients in tree-ring stable carbon and oxygen isotopes reveal differential climate influences of the North American Monsoon system. *J Geophys Res Biogeosci* (Blackwell Publishing Ltd) 121(7):1978–1991. <https://doi.org/10.1002/2016JG003460>
- Therrell MD et al (2006) Tree-ring-reconstructed rainfall variability in Zimbabwe. *Clim Dyn* (Springer Science and Business Media (LLC)) 26(7–8):677–685. <https://doi.org/10.1007/s00382-005-0108-2>
- Treydte KS et al (2006) The twentieth century was the wettest period in northern Pakistan over the past millennium. *Nature* 440(April):1179–1182. <https://doi.org/10.1038/nature04743>
- Treydte K, Frank D et al (2007) Signal strength and climate calibration of a European tree-ring isotope network. *Geophys Res Lett* 34:L24302. <https://doi.org/10.1029/2007GL031106>
- Treydte KS et al (2009) Impact of climate and CO<sub>2</sub> on a millennium-long tree-ring carbon isotope record. *Geochim Cosmochim Acta* (Elsevier Ltd) 73(16):4635–4647. <https://doi.org/10.1016/j.gca.2009.05.057>
- Trouet V, Esper J, Beekman H (2010) Climate/growth relationships of *Brachystegia spiciformis* from the miombo woodland in south central Africa. *Dendrochronologia* (Elsevier (BV)) 28(3):161–171. <https://doi.org/10.1016/j.dendro.2009.10.002>
- Verheyden A et al (2004a) Annual cyclicity in high-resolution stable carbon and oxygen isotope ratios in the wood of the mangrove tree *Rhizophora mucronata*. *Plant Cell Environ* (Wiley) 27(12):1525–1536. <https://doi.org/10.1111/j.1365-3040.2004.01258.x>
- Verheyden A et al (2004b) Growth rings, growth ring formation and age determination in the mangrove *Rhizophora mucronata*. *Ann Bot* 94(1):59–66. <https://doi.org/10.1093/aob/mch115>
- Verheyden A et al (2005) Comparison between  $\delta^{13}\text{C}$  of  $\alpha$ -cellulose and bulk wood in the mangrove tree *Rhizophora mucronata*: implications for dendrochemistry. *Chem Geol* 219(1–4):275–282. <https://doi.org/10.1016/j.chemgeo.2005.02.015>



- Volland F, Pucha D, Bräuning A (2016) Hydro-climatic variability in southern Ecuador reflected by tree-ring oxygen isotopes. *Erdkunde* 70(1):69–82. <https://doi.org/10.3112/erdkunde.2016.01.05>
- Voltas J et al (2013) A retrospective, dual-isotope approach reveals individual predispositions to winter-drought induced tree dieback in the southernmost distribution limit of Scots pine. *Plant Cell Environ* 36(8):1435–1448. <https://doi.org/10.1111/pce.12072>
- Waterhouse JS et al (2004) Northern European trees show a progressively diminishing response to increasing atmospheric carbon dioxide concentrations. *Quat Sci Rev* 23(7–8):803–810. <https://doi.org/10.1016/j.quascirev.2003.06.011>
- Welker JM, Rayback S, Henry GHR (2005) Arctic and North Atlantic Oscillation phase changes are recorded in the isotopes ( $\delta^{18}\text{O}$  and  $\delta^{13}\text{C}$ ) of *Cassiope tetragona* plants. *Glob Change Biol* 11:997–1002
- Wernicke J, Grieflinger J, Hochreuther P, Bräuning A (2015) Variability of summer humidity during the past 800 years on the eastern Tibetan Plateau inferred from  $\delta^{18}\text{O}$  of tree-ring cellulose. *Clim past* 11:327–337
- Wilson AT, Grinsted MJ (1977)  $^{12}\text{C}/^{13}\text{C}$  in cellulose and lignin as palaeothermometers. *Nature* 265(5590):133. <https://www.nature.com/articles/265133a0>. Accessed on:28 October 2019
- Wilson AT, Grinsted MJ (1978) The possibilities of deriving past climate information from stable isotope studies on tree-rings. *N Z Dep Sci Ind Res Bull* 220:61–66. [https://inis.iaea.org/search/search.aspx?orig\\_q=RN:9394183](https://inis.iaea.org/search/search.aspx?orig_q=RN:9394183). Accessed on 1 November 2019
- Wilson R et al (2014) Blue Intensity for dendroclimatology: the BC blues: a case study from British Columbia, Canada. *Holocene* (SAGE Publications Ltd) 24(11):1428–1438. <https://doi.org/10.1177/0959683614544051>
- Wilson R et al (2016) Last millennium northern hemisphere summer temperatures from tree-rings: Part I: The long term context. *Quat Sci Rev*. <https://doi.org/10.1016/j.quascirev.2015.12.005>
- Woodley EJ et al (2012) Estimating uncertainty in pooled stable isotope time-series from tree-rings. *Chem Geol* 294–295:243–248. <https://doi.org/10.1016/j.chemgeo.2011.12.008>
- Worbes M (1999) Annual growth rings, rainfall-dependent growth and long-term growth patterns of tropical trees from the Caparo forest reserve in Venezuela. *J Ecol* (Wiley) 87(3):391–403. <https://doi.org/10.1046/j.1365-2745.1999.00361.x>
- Worbes M (2002) One hundred years of tree-ring research in the tropics - a brief history and an outlook to future challenges. *Dendrochronologia* (Elsevier (GmbH)) 20(1–2):217–231. <https://doi.org/10.1078/1125-7865-00018>
- Worbes M, Junk WJ (1999) How old are tropical trees? The persistence of a Myth. *IAWA J* (Brill) 20(3):255–260. <https://doi.org/10.1163/22941932-90000689>
- Wright SJ, Muller-Landau HC, Schipper JAN (2009) The future of tropical species on a warmer planet. *Conserv Biol* (Wiley) 23(6):1418–1426. <https://doi.org/10.1111/j.1523-1739.2009.01337.x>
- Xu C, Buckley BM, Wang S-YS, An W, Li Z, Nakatsuka T, Guo Z (2021) Oxygen isotopes in tree rings from Greenland: a new proxy of NAO. *Atmosphere* 12:39
- Xu G, Liu X, Sun W, Szejner P, Zeng X, Yoshimura K, Trouet V (2020) Seasonal divergence between soil water availability and atmospheric moisture recorded in intra-annual tree-ring  $\delta^{18}\text{O}$  extremes. *Environ Res Lett* 15:094036
- Yapp CJ, Epstein S (1977) Climatic implications of D/H ratios of meteoric water over North America (9500–22,000 B.P.) as inferred from ancient wood cellulose CH hydrogen. *Earth Planet Sci Lett* 34(3):333–350. [https://doi.org/10.1016/0012-821X\(77\)90043-7](https://doi.org/10.1016/0012-821X(77)90043-7)
- Young GHF et al (2010) A 500-year record of summer near-ground solar radiation from tree-ring stable carbon isotopes. *The Holocene* 20(3):315–324
- Young GHF et al (2012a) Central England temperature since AD 1850: the potential of stable carbon isotopes in British oak trees to reconstruct past summer temperatures. *J Quat Sci* 27(6):606–614
- Young GHF et al (2012b) Changes in atmospheric circulation and the Arctic Oscillation preserved within a millennial length reconstruction of summer cloud cover from northern Fennoscandia. *Clim Dyn* 39(1–2):495–507. <https://doi.org/10.1007/s00382-011-1246-3>

- Young GHF, Bale RJ, Loader NJ, Mccarroll D, Nayling N, Vousden N (2012c) Central England temperature since AD 1850: the potential of stable carbon isotopes in British oak trees to reconstruct past summer temperatures. *J Quat Sci* 27:606–614
- Young GHF et al (2015) Oxygen stable isotope ratios from British oak treerings provide a strong and consistent record of past changes in summer rainfall. *Clim Dyn*. <https://doi.org/10.1007/s00382-015-2559-4>
- Young GHF et al (2019) Cloud cover feedback moderates fennoscandian summer temperature changes over the past 1,000 years. *Geophys Res Lett* (Blackwell Publishing Ltd) 46(5):2811–2819. <https://doi.org/10.1029/2018GL081046>
- Zhu J, Poulsen CJ, Tierney JE (2019) Simulation of Eocene extreme warmth and high climate sensitivity through cloud feedbacks. *Sci Adv* (American Association for the Advancement of Science (AAAS)) 5(9):eaax1874. <https://doi.org/10.1126/sciadv.aax1874>
- Zuidema PA et al (2013) Tropical forests and global change: filling knowledge gaps. *Trends Plant Sci* (Elsevier (BV)) 18(8):413–419. <https://doi.org/10.1016/j.tplants.2013.05.006>
- Zuidema PA, Brienen RJW, Schöngart J (2012) Tropical forest warming: looking backwards for more insights. *Trends Ecol Evol* (Elsevier (BV)) 27(4):193–194. <https://doi.org/10.1016/j.tree.2011.12.007>

**Open Access** This chapter is licensed under the terms of the Creative Commons Attribution 4.0 International License (<http://creativecommons.org/licenses/by/4.0/>), which permits use, sharing, adaptation, distribution and reproduction in any medium or format, as long as you give appropriate credit to the original author(s) and the source, provide a link to the Creative Commons license and indicate if changes were made.

The images or other third party material in this chapter are included in the chapter's Creative Commons license, unless indicated otherwise in a credit line to the material. If material is not included in the chapter's Creative Commons license and your intended use is not permitted by statutory regulation or exceeds the permitted use, you will need to obtain permission directly from the copyright holder.



# Chapter 20

## Stable Isotopes in Tree Rings of Boreal Forests



Olga V. Churakova, Trevor J. Porter, Alexander V. Kirdyanov, Vladimir S. Myglan, Marina V. Fonti, and Eugene A. Vaganov

**Abstract** The boreal forests are widely expanded from subarctic forest to tundra, and from taiga to forest-steppe zone (from 50 °N to 70 °N). We reviewed available stable isotope chronologies in tree-ring cellulose ( $\delta^{13}\text{C}$ ,  $\delta^{18}\text{O}$  and  $\delta^2\text{H}$ ) from 16 sites located in the Russian Federation; 4 research sites from Fennoscandia (Finland, Sweden and Norway); 5 sites from Canada, and 1 site from Alaska (USA) to evaluate impact of climatic changes from seasonal to annual scale across boreal forest ecosystems. Results of our review of carbon isotope data showed that drought conditions (mainly high vapour pressure deficit) are prevalent for western and central regions of Eurasia, Alaska and Canada, while northeastern and eastern sites of Eurasian subarctic are showing water shortage developments resulting from decreasing precipitation. Oxygen isotope chronologies show increasing trends towards the end of the twentieth century mainly for all chronologies, except for the Siberian northern and southern sites. The application of the multiple stable isotope proxies ( $\delta^{13}\text{C}$ ,  $\delta^{18}\text{O}$ ,  $\delta^2\text{H}$ )

---

**Supplementary Information** The online version contains supplementary material available at [https://doi.org/10.1007/978-3-030-92698-4\\_20](https://doi.org/10.1007/978-3-030-92698-4_20).

---

O. V. Churakova (✉) · A. V. Kirdyanov · M. V. Fonti · E. A. Vaganov  
Institute of Ecology and Geography, Siberian Federal University, Svobodny pr. 79, Krasnoyarsk 660041, Russian Federation  
e-mail: [ochurakova@sfu-kras.ru](mailto:ochurakova@sfu-kras.ru)

O. V. Churakova · M. V. Fonti  
Forest Dynamics, Swiss Federal Institute for Forest, Snow and Landscape Research WSL, Birmensdorf, Switzerland

T. J. Porter  
Department of Geography, Geomatics and Environment, University of Toronto Mississauga, 3359 Mississauga Road, L5L 1C6 Mississauga, Canada

A. V. Kirdyanov · E. A. Vaganov  
V. N. Sukachev Institute of Forest SB RAS, Federal Research Center “Krasnoyarsk Science Center SB RAS”, Akademgorodok 50/28, Krasnoyarsk 660036, Russian Federation

V. S. Myglan  
Siberian Dendrochronological Laboratory, Siberian Federal University, Svobodny pr. 82, Krasnoyarsk 660041, Russian Federation

is beneficial to study responses of boreal forests to climate change in temperature-limited environments. However, a deeper knowledge of hydrogen isotope fractionation processes at the tree-ring cellulose level is needed for a sound interpretation and application of  $\delta^2\text{H}$  for climate reconstructions, especially for the boreal forest zone where forest ecosystems are more sensitive to climatic and environmental changes.

## 20.1 Introduction

The boreal forest, including areas classically known as taiga, is the largest biome on earth (Apps et al. 2006), representing 17% of the earth's terrestrial ecosystems. It holds an estimated ~30% of terrestrial carbon stocks (Pan et al. 2011), making it a significant variable in the global carbon cycle. The boreal forest encompasses a zonal band roughly defined by 50–70 °N and occupies 1.2 billion hectares of land area (Soja et al. 2007), with the Siberian taiga accounting for 70% of this area (Kasischke 2000). The typical boreal climate is subarctic (e.g., Köppen zones Dfc and Dwc). In contrast to tundra areas to the north, the relatively low albedo of the boreal forest plays an important role in regulating the surface energy balance and climate of the subarctic latitudes (Bonan 2008).

Large areas of Fennoscandia, central and eastern Siberia (Russian Federation), northern Canada and Alaska represent the most extensive remaining areas of natural forests on the planet. The boreal forests are globally important for their economic and environmental values. Extensive areas of the boreal forests of Finland, Sweden, and parts of Canada are intensively managed for timber production and contribute 10–30% of the export income of these nations (ACIA 2004).

The study of boreal forest ecosystems is important because of their high sensitivity to regional and global climate changes, and potential to influence ground temperatures and the stability of vast pools of carbon currently locked in permafrost in the subarctic regions (Fig. 20.1a). Permafrost plays an important role in stabilizing the climatic system and climate-albedo feedbacks that are unique to the northern range of the boreal forest (Bonan 2008). Due to climate warming, both vapor-pressure deficit (VPD) and evapotranspiration are expected to increase in the boreal region, which has implications for tree's water relations (Sugimoto et al. 2002; ACIA 2004; Churakova (Sidorova) et al. 2016, 2020).

Many impacts of climate change are already apparent in the boreal forest including:

(i) spatially complex patterns of reduced and increased rates of tree growth (Briffa et al. 1998; Briffa 2000; Lloyd and Bunn 2007); (ii) larger and more extensive fires and insect outbreaks (Soja et al. 2007); and (iii) a range of effects due to permafrost degradation, including new wetland development and subsidence of the ground surface (Turetsky et al. 2019), with the associated loss of trees and ecological succession toward wetland plant communities.

In boreal regions, the traditional tree-ring parameters like tree-ring width and maximum latewood density are typically positively correlated with June-July and

June–August temperatures, and therefore, have been successfully used to reconstruct summer temperatures over the past millennium (Briffa 2000; Sidorova and Naurzbaev 2002; Naurzbaev et al. 2002; Hantemirov et al. 2011; Grudd 2008; Kononov et al. 2009; D’Arrigo et al. 2008; Myglan et al. 2008; Schneider et al. 2015; Büntgen et al. 2021). However, in some areas of Alaska and northwestern Canada where the rate of recent climate warming has been most rapid, the generally reliable association between ring width and summer climate has been demonstrated to break down, potentially linked to warming-induced drought stress (Briffa 2000; Wilmking et al. 2004; D’Arrigo et al. 2008; Porter and Pisaric 2011; Porter et al. 2013). This phenomenon is referred to the “Divergence Problem” (DP) in the dendrochronology literature (D’Arrigo et al. 2008; Camarero et al. 2021). The emergence of the DP has stimulated the search for a more reliable tree-ring climate proxy in affected regions, including tree-ring  $\delta^{13}\text{C}$  and  $\delta^{18}\text{O}$  (Barber et al. 2000; Sidorova et al. 2009, 2010; Porter et al. 2009; Zharkov et al. 2021).

## 20.2 Characteristic of Boreal Zone

### 20.2.1 Study Sites and Tree Species

Trees in the boreal zone have showed great potential for stable isotope studies due to long-term tree longevity (Sidorova et al. 2008, 2010) and good subfossil wood preservation due to severe climate conditions and permafrost availability (Sidorova et al. 2013a, b; Helama et al. 2018; Churakova (Sidorova) et al. 2019) (Fig. 20.1).

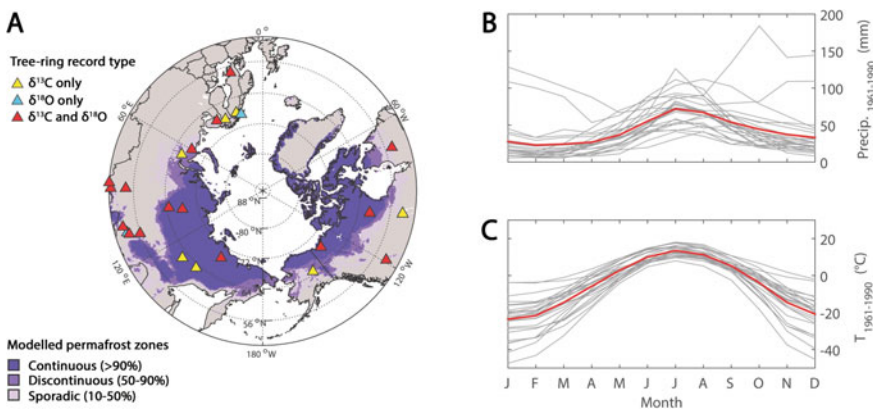


**Fig. 20.1** Location of the study sites (Table S20.1) with  $\delta^{13}\text{C}$  (yellow triangles),  $\delta^{18}\text{O}$  (light blue triangles) and both  $\delta^{13}\text{C}$  and  $\delta^{18}\text{O}$  (red triangles) isotope tree-ring cellulose chronologies (a). Monthly precipitation (b) and mean air temperature (c) climatologies for the common period (1961–1990) for all published sites, calculated from the  $10'$ -spatial resolution dataset by New et al. (2002). Permafrost distribution from continuous to sporadic is available in Obu et al. (2019)

Dominant tree species are white spruce (*Picea glauca*) and black spruce (*Picea mariana* Mill.) in Canada and the USA (Alaska), Scots pine (*Pinus sylvestris* L.) in Fennoscandia, and a variety of larch tree species (*Larix sibirica* Ledeb., *Larix gmelinii* Rupr., *Larix cajanderi* Mayr.) in central, eastern and northeastern Siberia. Previous tree-ring isotope studies in the boreal region have focused mainly on developing stable carbon ( $\delta^{13}\text{C}$ ) and oxygen ( $\delta^{18}\text{O}$ ) isotope chronologies from cellulose (Fig. 20.1, Table 20.1 and Supplementary Table 20.1). To date there have been only a few studies in the boreal region focusing on hydrogen ( $\delta^2\text{H}$ ) in tree-ring cellulose (e.g., in Finland, see Hiltunen et al. 2011). Based on the available literature and knowledge, our review focusses primarily on stable carbon and oxygen isotope studies in tree rings from the boreal zone.

### 20.2.2 Permafrost

About 80% of the world's boreal forests are located in the circumpolar permafrost zone (Helbig et al. 2016) which makes permafrost a particularly important component of the boreal forest. Boreal forests respond to both the timing and magnitude of changes in soil moisture and soil temperature, nutrient availability, as well as permafrost distribution and dynamics, which themselves are directly affected by snow and vegetation cover, soil texture and geothermal heat flux (ACIA 2004; Cable et al. 2013; Boike et al. 2013). Water released from thawing ice-rich permafrost can be an important moisture source for trees growing in regions with severe temperature limitations and low amount of precipitation (Sidorova et al. 2010; Churakova (Sidorova) et al. 2016; Zhang et al. 2000; Sugimoto et al. 2002; Saurer et al. 2016). Due to low temperatures in the subarctic belt, water loss is not yet as large as observed in European forest ecosystems (Saurer et al. 2014). However, with a continued increase in temperature (Sidorova et al. 2010), drought stress may increase accordingly (Sidorova et al. 2009; Knorre et al. 2010; Bryukhanova et al. 2015; Saurer et al. 2016; Ohta et al. 2019) in the boreal forest regions.

Under the projected climate warming, permafrost is expected to degrade and initially wetland areas (thermokarst lakes) will increase in extent (IPCC 2014), which has the potential to shift the regional carbon balance from a net carbon sink (under productive boreal vegetation) to a carbon source (microbial emission of  $\text{CO}_2$  and  $\text{CH}_4$  driven by access to thawed permafrost carbon). Lake drainage, hydroclimatic change and ecological succession also have the potential to moderate thermokarst-carbon balance impacts. A number of studies have reported a pronounced increase in the seasonal thaw depth in Western Siberia (Melnikov et al. 2004; Pavlov et al. 2004; Fyodorov-Davydov et al. 2009). Fyodorov-Davydov et al. (2009) investigated the spatial and temporal trends in the active soil layer (ASL) depth in northern Yakutia, Russia (Table S20.1). The ASL is the top layer of soil with high activity of microbial processes and which thaws during summer and freezes back again in autumn.

Seasonal dynamics of the cryosphere also have implications for the phenology of tree growth, on carbon and oxygen isotope ratios in plants due to the influence

**Table 20.1** Summary of available stable isotope chronologies in tree rings from the boreal forest

Proxy	Outcome	Tree species	References
$\delta^{13}\text{C}$			
Spring temperature	April–May temperature increases towards recent century	<i>L. sibirica</i> Ledeb <i>P. glauca</i>	Tartakovsky et al. (2012), Porter et al. (2014)
Summer temperature	June–August temperature increases	<i>L. cajanderi</i> Mayr <i>L. gmelinii</i> Rupr <i>P. sylvestris</i> L. <i>L. sibirica</i> Ledeb <i>P. glauca</i>	Porter et al. (2009), Loader et al. (2010, 2013), Sidorova et al. (2008), Sidorova et al. (2013a, b), Churakova (Sidorova) et al. (2016, 2019), Kononov et al. (2009), personal communication, Tartakovsky et al. (2012), Holzkämper et al. (2008), Gennaretti et al. (2017)
Winter temperature	Annual and decadal temporal resolution Winter (February) temperature trend	<i>L. gmelinii</i> Rupr <i>P. sylvestris</i> L.	Sidorova et al. (2010), Edwards et al. (2017)
Sunshine duration	Impact of June–August sunshine duration on $\delta^{13}\text{C}$ isotope chronologies	<i>P. sylvestris</i> L.	Loader et al. (2013)
Cloud cover	July–August percentage of cloud cover suggest strong negative relationship between cloud cover and temperature. High percentage of summer cloud cover during the 14-fifteenth and nineteenth centuries and famines due to crop failures caused by very wet (rather than cold) summer conditions	<i>P. sylvestris</i> L.	Young et al. (2012), Loader et al. (2013)
Arctic Oscillation	Recent period becomes cloudier compared to the past millennia	<i>P. sylvestris</i> L.	Young et al. (2012)

(continued)

**Table 20.1** (continued)

Proxy	Outcome	Tree species	References
Water-use efficiency	Increasing WUE towards the recent decades, Increasing water shortage	<i>L. gmelinii</i> Rupr <i>L. cajanderi</i> Mayr <i>L. sibirica</i> Ledeb	Saurer et al. (2002, 2004, 2014), Churakova (Sidorova) (2018), Siegwolf et al. (2022) Keller et al. (2017)
Vapor pressure deficit	Increasing June-July VPD towards twentieth century over past millennia	<i>L. cajanderi</i> Mayr <i>L. gmelinii</i> Rupr	Sidorova et al. (2009), Churakova (Sidorova) et al. (2019, 2020) in preparation
Drought reconstruction	Physiological adaptations to drought and correspondence to the drought intervals of the 1790, 1840, 1890, 1930, and 1960–1970	<i>T. occidentalis</i>	Au and Tardif (2012)
River flow	Potential for river flow reconstruction	<i>P. sylvestris</i>	Waterhouse et al. (2000)
Summer precipitation	June moisture reconstructions Moisture summers during the early millennium and dry summers during the late millennium, twentieth century warm and moist	<i>P. sylvestris</i> L.	Edwards et al. (2017)
$\delta^{18}\text{O}$			
Summer temperature	Increasing Siberian thaw permafrost depth Link with summer temperature	<i>L. sibirica</i> Ledeb, <i>P. sylvestris</i> L.	Sidorova et al. (2012), Churakova (Sidorova) et al. (2016, 2019, 2020), Naulier et al. (2015), Porter et al. (2014), Hiltunen et al. (2009)
Sunshine duration	Recent period becomes sunnier compared to the past century	<i>L. cajanderi</i> Mayr;	Churakova (Sidorova) et al. (2019)
Arctic Oscillation	Teleconnection via winter-spring and summer precipitation. Reduction of summer precipitation, triggered by a positive phase of the Arctic Oscillation in May	<i>L. gmelinii</i> Rupr	Sidorova et al. (2010), Churakova (Sidorova) et al. (2019, 2021b)

(continued)



**Table 20.1** (continued)

Proxy	Outcome	Tree species	References
$\delta^{13}\text{C}$ and $\delta^{18}\text{O}$			
Mixed signal in spring, summer temperature and precipitation, vapor pressure deficit	Increasing spring and summer temperatures, decreasing July precipitation Increasing drought, limited access to nutrients suggest $\text{CO}_2$ saturation of Siberian larch trees Vegetation period becomes drier in the second half of the twentieth century and the beginning of the twenty-first century due to decreased precipitation. Vegetation period shifted to an earlier date in the course of the last century	<i>L. gmelinii</i> Rupr; <i>P. glauca</i> <i>L. sibirica</i> Ledeb	Sidorova et al. (2009), Knorre et al. (2010), Bryukhanova et al. (2015), Tartakovsky et al. (2012), Holzkämper et al. (2008)
Arctic Oscillation	Teleconnection via precipitation patterns	<i>L. cajanderi</i> Mayr; <i>L. gmelinii</i> Rupr; <i>P. sylvestris</i> L.	Sidorova et al. (2010), Young et al. (2012), Churakova (Sidorova) et al. (2021a)
Relative air humidity, winter temperature and precipitation	Reconstructed relative air humidity reflected the predominating influence of stomatal conductance on carbon-isotope discrimination, while reconstructed winter temperature reflected separation of the $\Delta^{18}\text{O}$ record into $\Delta\text{T}$ -and $\Delta\text{RH}$ -dependent signals of similar magnitude. High growth season humidity persisted from AD 1900 compared to the Little Ice Age	<i>P. engelmannii</i> <i>P. albicaulus</i> <i>L. gmelinii</i> Rupr	Edwards et al. (2008)

(continued)

**Table 20.1** (continued)

Proxy	Outcome	Tree species	References
$\delta^2\text{H}$ and $\delta^{18}\text{O}$			
Cloud cover, temperature, precipitation, relative humidity	The strongest relationship ( $r = 0.70$ , $P < 0.001$ ) was observed between $\delta^{18}\text{O}$ and cloud cover, yet, $r$ values for $\delta^{18}\text{O}$ , $\delta^2\text{H}$ and temperature, $\delta^{18}\text{O}$ , $\delta^2\text{H}$ and precipitation, all exceeded 0.5 and were statistically highly significant for the oak tree-ring chronologies from southern Finland Reconstructing relative humidity from plant $\delta^{18}\text{O}$ and $\delta^2\text{H}$ as deuterium deviations from the global meteoric water line	<i>Quercus robur</i> L. <i>P. sylvestris</i> L. <i>Quercus macrocarpa</i> <i>Q. robur</i> <i>Pseudotsuga menziesii</i>	Hilasvuori (2011), Voelker et al. (2014)

of active layer thaw on soil water availability and plant gas exchange, and on the isotope composition of soil water. The freezing process itself induces a soil water fractionation during the autumn freeze-back period (Lacelle 2011). In a closed system with converging freezing fronts extending downward from the surface and upward from the permafrost table, soil water fractionation is expected to obey Rayleigh distillation principles, with the most enriched ice forming first (i.e., near the surface and at the permafrost table) and progressively more  $^{18}\text{O}$ -depleted ice as the two freezing fronts converge roughly at the mid-point of the active layer (Lacelle 2011). This process, therefore, can lead to isotopic stratification of soil water with depth, which has potential implications for the mean isotopic composition of soil water used by trees in the early growing season.

The oxygen isotopic signal in tree-rings of trees growing on permafrost is also masked by the supply of isotopically depleted water from melted frozen soil leading to 'inverse' climate to tree-ring isotope relationship, as dry and warm summer conditions result in lower soil, root and wood in  $\delta^{18}\text{O}$  values (Sugimoto et al. 2002; Saurer et al. 2002, 2016).

A further complication of the isotope composition in tree-rings within the permafrost zone is caused by the impact of forest fires. Wildfires lead to significant changes in active soil layer depth and seasonal dynamics, with potentially long-term consequences for carbon, nutrient and water balance of the ecosystem (Sidorova et al. 2009; Kirilyanov et al. 2020). As both water and nutrient supply for plants predominantly depend on the freeze-thaw processes in the active soil layer (Zhang et al. 2000; Prokushkin et al. 2018), the wildfire-induced changes in isotopic

composition of the source water and water availability for trees as well as changes in photosynthesis rate are recorded in tree-ring carbon and oxygen isotopes.

### 20.2.3 *Climate*

The major advantage in studying northern forests is their distance to populated regions, allowing the study of tree responses to environmental changes without anthropogenic disturbances. A major disadvantage is the difficult accessibility, especially in northeastern Siberia, and the scarcity of weather stations. Yet, seasonal continuous measurements of climatic parameters are needed for future eco-physiological studies. Gridded large-scale climate data (CRU TS 4.02,  $0.5^\circ \times 0.5^\circ$ ) (New et al. 2002; Harris et al. 2014) can help filling the gaps in the climate data. Gridded temperature and precipitation data are an important source of information to quantify climate reconstructions during the last decade and further back in time (first half of twentieth century). Several studies on stable isotope tree-ring cellulose chronologies for the boreal zone showed good correspondence with temperature signals from both, local weather stations and gridded data (<http://climexp.knmi.nl>) back in time (>100 years) (Sidorova et al. 2010; Churakova (Sidorova) et al. 2019). However, precipitation signals are better recorded by the local weather stations at the local scale compared to the gridded averaged data at the regional scale.

Sunshine duration and cloud cover are distributed heterogeneously across boreal regions. In summer, light duration lasts longer at high-latitudes than at the southern taiga and forest steppe zone (Young et al. 2012; Gagen et al. 2016; Churakova (Sidorova) et al. 2019).

Depending on the site location and impact of environmental parameters, conifer trees in the boreal zone can adapt to extremely low annual temperatures ( $-19.2^\circ\text{C}$  in northeastern Yakutia, data from the local Chokurdach weather station for the period from 1961 to 1990). The climate data obtained from the local weather stations (direct measurements) represent a wide range of minimum and maximum temperature extremes (e.g.,  $-60^\circ\text{C}$  in Yakutia to  $+45^\circ\text{C}$  in Khakassia, Russian Federation). The amount of annual precipitation varies from 236 to 310 mm in northeastern Siberia and Northern America, respectively (Fig. 20.1b) to 502 mm towards Baikalskii ridge (Russian Federation), and further double increases to 1353 mm towards Norway's northeastern coastline.

## 20.3 Stable Carbon ( $\delta^{13}\text{C}$ ) Isotopes

### 20.3.1 Isotope Ecophysiology

Application of stable carbon isotopes in tree-ring studies for the boreal zone has increased over the past decades because these proxies record information not only about temperature (Knorre et al. 2010; Sidorova et al. 2008, 2009, 2013a, b), but also about moisture changes (Kirilyanov et al. 2008; Sidorova et al. 2010; Tartakovsky et al. 2012; Churakova (Sidorova) et al. 2019, 2020, 2021b), as well as changes in sunshine duration/cloudiness (Young et al. 2012; Loader et al. 2013; Helama et al. 2018) (Table 20.1). Moreover, carbon isotope chronologies in tree-rings also captured signals of atmospheric circulation patterns (Saurer et al. 2004; Sidorova et al. 2010; Gagen et al. 2016) and facilitated the reconstruction of the river flow in Siberia (Waterhouse et al. 2000).

Climatic parameters like temperature, water availability, air humidity and vapor pressure deficit, and the impact of changes in ambient  $\text{CO}_2$  concentration on photosynthetic  $\text{CO}_2$  assimilation and water balance are reflected in the  $\delta^{13}\text{C}$  values of plant organic matter and provide an isotopic fingerprint in the wood of tree rings (see Chap. 9). The analysis of tree physiological properties using carbon isotope ratios is particularly useful when combined with a photosynthesis model. This facilitates the functional attribution of meteorological impacts to plant responses, such as stomatal and substomatal conductance vs. ambient  $\text{CO}_2$  concentrations ( $c_i/c_a$  ratio) (Farquhar and Lloyd 1989). Detailed insight into physiology (see Chap. 9) and resource distribution during tree-ring formation (see Chaps. 3, 13 and 15) may also be obtained through  $^{13}\text{C}$ -labeling experiments (Kagawa et al. 2006a, b; Masyagina et al. 2016).

### 20.3.2 Seasonal Variability

Short growing season (up to 90 days in far North) and harsh climatic conditions of the boreal zone result in low tree stem increment (Vaganov et al. 2006). Compared to temperate trees with wider rings (Leavitt 1993), boreal trees might show a slower carbon turnover rate (Kagawa et al. 2006b). The highly resolved intra-annual measurements of  $\delta^{13}\text{C}$  within tree rings (earlywood/latewood or laser ablation with the step of 80–200  $\mu\text{m}$ , see Chap. 7) helped to link changes in physiological and metabolic processes and, as a result, tree-ring growth and xylem anatomical structure associated to seasonal climatic variability.

Deciduous and evergreen angiosperms and gymnosperms depend on stored carbohydrates during their first stages of leaves/wood development (Ericsson 1979).

Boreal deciduous (*Betula pubescens* Ehrh., *Populus tremula* L.), conifer deciduous (*Larix gmelinii* (Rupr.) Rupr.) and conifer evergreen species (*Pinus sylvestris* L., *Picea obovata* Ledeb., *Picea abies* (L.) H. Karst.) were used to identify the

physiological principle of climate responses related to the phenology and structural–functional features of wood. Intra-annual  $\delta^{13}\text{C}$  tree-ring analysis of gymnosperm and angiosperm species in Scandinavia (Vaganov et al. 2009), central and eastern Siberia (Kagawa et al. 2006b; Bryukhanova et al. 2011; Rinne et al. 2015; Fonti et al. 2018) and southern Siberia (Voronin et al. 2012) have shown that not only the temperature, but also soil moisture and rainfall might affect the dynamics of  $\delta^{13}\text{C}$  in tree rings. In particular,  $\delta^{13}\text{C}$  in latewood of *L. gmelinii* in Yakutia was reported to show better correlations with the growing season precipitation and soil water conditions than  $\delta^{13}\text{C}$  in earlywood (Kagawa et al. 2003). Variability of tree-ring width and  $\delta^{13}\text{C}$  under climatic conditions of extreme years in central Siberia indicated that an increased spring temperature initially led to an increase of tree growth. However, due to an increased use of water through transpiration, tree growth could be progressively reduced from temperature to moisture limitation.

To determine the extent to which trees rely on stored carbohydrates from previous years for tree-ring formation and how strongly the current photosynthates were used, the intra-annual  $\delta^{13}\text{C}$  variability was measured. Samples from *Larix gmelinii* (Rupr.) from two Siberian sites with a different hydro-thermal regime of permafrost soils were analyzed using (a)  $\delta^{13}\text{C}$ -labeling (Kagawa et al. 2006b) and (b) laser ablation coupled to the Compound-Specific Isotope Analysis (CSIA) (Rinne et al. 2015). Kagawa et al. (2006b) showed that latewood in *Larix gmelinii* Rupr. was mainly formed from current-year photoassimilates with minimal carry-over effect of carbohydrates from the previous year, while the early wood is produced from a mixture of current-year photoassimilates and previous-year carbohydrates. In *P. sylvestris* from the same site,  $\delta^{13}\text{C}$  values of early wood were significantly correlated with the previous year late wood ( $r = 0.42$ ;  $P < 0.01$ ) in a 100-year  $\delta^{13}\text{C}$  chronology, which is evidence of a carry-over effect. In contrast, Rinne et al. (2015) provided the evidence of a minimal carry-over effect of photosynthates formed during the previous year(s). The combination of different methods, such as CSIA and intra-annual tree-ring isotope analyses will enhance a further mechanistic understanding of the carbon–water relationships within ecosystems, in particular, for the interpretation of retrospective tree-ring analyses (Rinne et al. 2015).

### 20.3.3 Annual and Decadal Carbon Isotope Variability Over Past 100 Years

The mean  $\delta^{13}\text{C}$  value in tree-ring cellulose chronologies from Fennoscandia, Yakutia, the high-elevated mountain range in Khibini (Kola Peninsula) and the Altai Mountain range, analysed for the period from 1900 to 1998, showed mean values of  $-24\text{‰}$ . These earlier published chronologies indicated wetter conditions for these sites in the boreal zone compared to the drier northeastern and central sites of Eurasia and Alaska. Based on the available  $\delta^{13}\text{C}$  tree-ring cellulose chronologies from the southern part

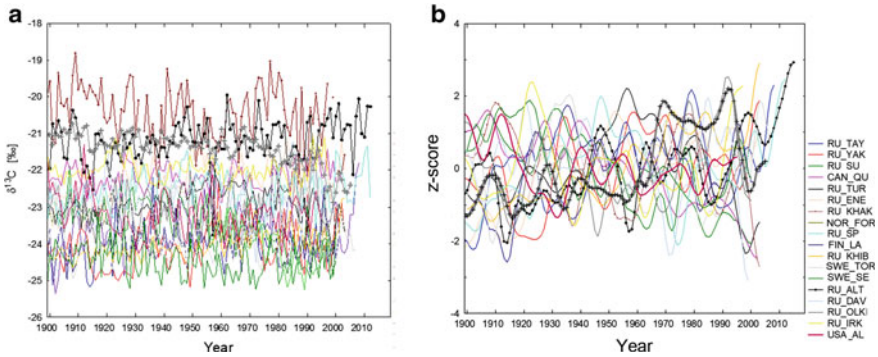


**Fig. 20.2** Annual (a) and smoothed by a 11-year Hamming window (b)  $\delta^{13}\text{C}$  tree-ring cellulose chronologies obtained from conifer tree species from the boreal zone (for details see supplementary Table S20.1)

(Khakasia, Russian Federation) of the boreal zone, reduced soil moisture availability is reflected by mean  $\delta^{13}\text{C}$  values of  $-20.4\text{‰}$  (Fig. 20.2a).

The  $\delta^{13}\text{C}$  in tree-ring cellulose chronologies (standardised to z-score) smoothed by a 11-year Hamming window show a general significant increasing trend over the recent decades for all, except for a few sites in northern Eurasia: Davan Pass (Tartakovsky et al. 2012), Khakasia forest steppe (Knorre et al. 2010), Tura (Sidorova et al. 2009) as well as Alaska (Barber et al. 2000), Canada (Porter et al. 2009) and Sweden, Torneträsk (Loader et al. 2013) (Fig. 20.2b).

These decreasing  $\delta^{13}\text{C}$  trends in tree-ring cellulose chronologies towards recent century from permafrost sites over the past decades were explained as an earlier beginning of the vegetation period in spring and increased use of residual soil carried over from autumn of the previous year (Sidorova et al. 2009; Knorre et al. 2010). Another reason, e.g., physiological effect of increasing atmospheric  $\text{CO}_2$ , is also responsible for lower  $\delta^{13}\text{C}$  values. Thus, an earlier start of the vegetation period could lead to tree-ring formation during a period with higher water availability, resulting in stronger isotopic fractionation and  $^{13}\text{C}$  depletion (Knorre et al. 2010).

## 20.4 Stable Oxygen ( $\delta^{18}\text{O}$ ) Isotopes

### 20.4.1 Isotope Ecophysiology

Oxygen isotopes in organic matter are modified by variation in the isotopic composition of source water, which is closely related to that of precipitation and soil water (though modified by evaporation at the soil surface). The  $\delta^{18}\text{O}$  of meteoric water is directly related to cloud/atmosphere air temperatures (Dansgaard 1964) as well as evaporation and condensation processes in the global water cycle. This is especially

true in northern high-latitudes, as has been demonstrated at broad spatial scales across the North American arctic and subarctic based on precipitation isotope data from the Global Network of Isotopes in Precipitation (Porter et al. 2016). An earlier study by Saurer et al. (2002) also showed that average isotope values of 130 trees of a widely distributed genus (*Larix*, *Picea*, *Pinus*) within the Eurasian subarctic from Norway to Siberia are highly correlated with the modeled isotope distribution of precipitation showing a large east-to-west gradient (see Chap. 18). Input waters are modified (enrichment in  $^{18}\text{O}$ ) in the leaf during transpiration, which is imprinted on photosynthates and cellulose through biochemical fractionation and exchange processes. In Siberia, the inter-annual variability of winter precipitation  $\delta^{18}\text{O}$  is closely related to temperature variability and the North Atlantic Oscillation, while the variability of summer  $\delta^{18}\text{O}$  appears to be dominated by regional processes involving evaporation and convection (Butzin et al. 2014). Therefore,  $\delta^{18}\text{O}$  values of tree rings reflect, as a first approximation, average ambient temperatures and humidity. Progress has been made in understanding the fractionation processes, where  $\text{H}_2^{18}\text{O}$ -molecule goes from soil water to tree-ring cellulose (Craig and Gordon 1965; Dongmann et al. 1974; Farquhar and Lloyd 1989; Roden et al. 2000). These models have been validated with experimental data from deciduous and coniferous tree species. A detailed description of the leaf water enrichment processes is given in Chap. 10.

### 20.4.2 Seasonal Variability

The highly complex hydrological regime of boreal forests is given by a strong sinusoidal seasonal course of  $\delta^{18}\text{O}$  imprinted in precipitation water, reflecting the cloud condensation temperatures. Winter precipitation uptake is only possible in the warming spring and summer months after snow melt and active layer thaw. This explains the often good correlation between tree-ring  $\delta^{18}\text{O}$  values and winter temperature, when this fraction of the annual precipitation becomes available for trees (Sidorova et al. 2010). Oxygen isotopes are then incorporated and become visible in the tree rings. As described in part Sect. 20.2.1 of this chapter the hydrology of forests growing under permafrost conditions, only a shallow layer of soil thaws in summer, each soil layer with its own  $\delta^{18}\text{O}$  of soil water. This variation of seasonal  $\delta^{18}\text{O}$  from permafrost water must be taken into account for the evaluation of tree-ring chronologies. It is therefore not surprising that only few studies about the seasonal  $\delta^{18}\text{O}$  fluctuations in wood are available for the boreal zone, i.e. southern Siberia (Voronin et al. 2012) and central Siberia (Saurer et al. 2016).

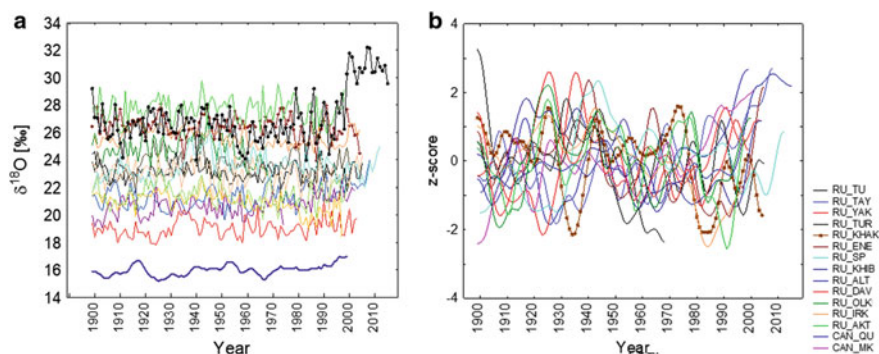


**Fig. 20.3** Annual (a) and smoothed by a 11-year Hamming window (b)  $\delta^{18}\text{O}$  tree-ring cellulose chronologies obtained from conifer tree species from the boreal zone

### 20.4.3 Annual and Decadal Oxygen Isotope Variability Over Past 100 Years

Annual  $\delta^{18}\text{O}$  values in tree-ring cellulose chronologies (Fig. 20.3) showed clear isotopic differences from the coldest sites in northeastern Yakutia (19.0‰) (Sidorova et al. 2008) and Canada (19.1‰) (Porter et al. 2009) towards warmest sites in Russian Altai (up to 27.7‰) (Loader et al. 2010; Sidorova et al. 2012, 2013a, b) and Khakassia (26.4‰) (Knorre et al. 2010). A 5-year block  $\delta^{18}\text{O}$  tree-ring cellulose chronology of black spruce trees (*Picea mariana* [Mill] B.S.P) from the Québec–Labrador peninsula, northeastern Canada (Naulier et al. 2015) showed the lowest isotopic value (16‰) compared to all other reviewed sites (Fig. 20.3a).

A decreasing  $\delta^{18}\text{O}$  trend was detected in the early 1900's between 11-year smoothed  $\delta^{18}\text{O}$  tree-ring cellulose isotope chronologies from Tura site (TUR) (Sidorova et al. 2009) and Canadian site Mackenzie Delta (Porter et al. 2009, 2014). This discrepancy can be explained by cold conditions in Canada compared to warmer periods at Siberian Tura site. Almost all  $\delta^{18}\text{O}$  values in tree-ring cellulose chronologies showed increasing temperature trends towards the end of the twentieth century, except for the Siberian sites in Yakutsk (Spasskaya Pyad) (Tei et al. 2013) and Khakassia (Knorre et al. 2010) (Fig. 20.3). Decreasing  $\delta^{18}\text{O}$  values in tree-ring cellulose chronologies can be explained by  $^{18}\text{O}$  depleted water from autumn precipitation of the previous year absorbed by the tree rings (Sidorova et al. 2009; Knorre et al. 2010).

The combination of tree-ring and stable isotope parameters (e.g., tree-ring width, cell wall thickness, maximum late wood density, Sidorova et al. 2010, 2012; Churakova (Sidorova) et al. 2019) enhances the strength of our interpretations and need to be pursued where possible.



## 20.5 Stable Hydrogen ( $\delta^2\text{H}$ ) Isotopes

As the oxygen and hydrogen isotopic composition of precipitation was already recognized to be related to temperature (Dansgaard 1964), early work on oxygen and hydrogen in plant material was conducted with the aim of using tree rings as an isotopic thermometer. Although the fractionation mechanisms in leaf water are the same for  $\delta^2\text{H}$  as for  $\delta^{18}\text{O}$ , the incorporation of hydrogen follows a different metabolic pathway. Therefore, correlation analyses with tree-ring hydrogen isotope time series and annual temperature records have been less successful (Epstein et al. 1976; Waterhouse et al. 2002; Augusti et al. 2006). Most recent studies by Voelker et al. (2014) showed potential for reconstruction of relative humidity from plant  $\delta^2\text{H}$  and  $\delta^{18}\text{O}$  as deuterium deviations from the global meteoric water line (GMWL).

The analysis of  $\delta^2\text{H}$  in tree-rings is still in an explorative stage (Kimak and Leuenberger 2015; Cormier et al. 2019; Lehman et al. 2021; Churakova (Sidorova) et al. 2021a; Schuler et al. 2022), but the application of the dual stable isotope approach ( $\delta^{18}\text{O}$  and  $\delta^2\text{H}$ ) in tree-ring analyses is promising and will strengthen our future isotope interpretation. Chapter 11 discusses the principles of  $\delta^2\text{H}$  in tree rings in detail.

## 20.6 Conclusion and Outlook

Carbon isotopes proved to be a reliable proxy for spring and summer temperature, vapor pressure deficit, sunshine duration/cloud cover and soil moisture changes. Oxygen isotopes were not only a temperature proxy but also an indicator for air humidity and water origin, showing also teleconnection with Arctic Oscillation via precipitation patterns. A mixed temperature and precipitation signal is mainly recorded for subarctic regions, covered by permafrost (Chap. 18).

The dual carbon and oxygen isotope approach is highly recommended for the interpretation of stable isotope chronologies from the boreal forest due to often mixed signals recorded in tree rings and the complex hydrology, which can be analyzed best by using dual or even triple isotopes ( $\delta^{13}\text{C}$ ,  $\delta^{18}\text{O}$ ,  $\delta^2\text{H}$ ).

Based on the available stable carbon and oxygen isotope data sets across the boreal forest zone, we conclude that trees from western and central regions of Eurasia, Alaska and Canada are exposed to drought conditions, while no strong evidence for drought is observed at the northeastern and eastern sites of the Eurasian subarctic.

There are only few nitrogen isotope measurements in tree tissues, mainly in needles of conifer trees (Mack et al. 2004; Prokushkin et al. 2018) and in soil samples, e.g., northern Sweden (Högberg et al. 2006). So far, no data is available for  $\delta^{15}\text{N}$  in tree-ring chronologies from the boreal zone, because no strong  $\delta^{15}\text{N}$  signal in tree rings was found.

Trees growing at the circumpolar zone are a valuable archive and monitoring system for information not only about temperature but also about currently ongoing

hydrological changes. A multi-proxy approach as a combination of stable isotopes and tree-ring parameters, new approaches (intra annual tree-ring analyses,  $\delta^2\text{H}$  and CSIA), and eco-physiological modelling ( $\delta^{13}\text{C}$ ,  $\delta^{18}\text{O}$ ,  $\delta^2\text{H}$ ) will strengthen our interpretations and improve the quality of available climate reconstructions with annual time resolution.

**Acknowledgements** This work was supported by the *Russian Science Foundation (RSF)* (project 21-17-00006) granted to O.C. (S.) and (project 19-14-00028) granted to V.M.

## References

- ACIA (2004) Impacts of a warming arctic. In: Arctic climate impact assessment. ACIA overview report. Cambridge University Press, pp 140
- Apps MJ, Shvidenko AZ, Vaganov EA (2006) Boreal forests and the environment: a foreword. *Mitig Adapt Strat Glob Change* 11(1):1–4. <https://doi.org/10.1007/s11027-006-0985-7>
- Au R, Tardif JC (2012) Drought signals inferred from ring-width and stable carbon isotope chronologies from *Thuja occidentalis* trees growing at their northwestern distribution limit, central Canada. *Canadian J For Res* 42:517–531. <https://doi.org/10.1139/x2012-012>
- Augusti A, Betson TR, Schleucher J (2006) Hydrogen exchange during cellulose synthesis distinguishes climatic and biochemical isotope fractionations in tree rings. *New Phytol* 172:490–499. <https://doi.org/10.1111/j.1469-8137.2006.01843.x>
- Barber VA, Juday GP, Finney BP (2000) Reduced growth of Alaskan white spruce in the twentieth century from temperature-induced drought stress. *Nature* 405:668–673. <https://doi.org/10.1038/35015049>
- Boike J, Kattenstroth B, Abramova K et al (2013) Baseline characteristics of climate, permafrost and land cover from a new permafrost observatory in the Lena River Delta, Siberia (1998–2011). *Biogeosciences* 10:2105–2128. <https://doi.org/10.5194/bg-10-2105-2013>
- Bonan B (2008) Forests and climate change: forcings, feedbacks, and the climate benefits of forests. *Science* 1444–1449. <https://doi.org/10.1126/science.1155121>
- Briffa KR, Schweingruber FH, Jones PD, Osborn TJ, Shiyatov SG, Vaganov EA (1998) Reduced sensitivity of recent tree-growth to temperature at Northern high latitudes. *Nature* 391(6668):678–682. <https://doi.org/10.1038/35596>
- Briffa KR (2000) Annual climate variability in the Holocene: interpreting the message of ancient trees. *Quat Sci Rev* 19:87–105
- Bryukhanova MV, Fonti P, Kirilyanov AV, Siegwolf RTW, Saurer M, Pochebyt NP, Churakova (Sidorova) OV, Prokushkin AS (2015) The response of  $\delta^{13}\text{C}$ ,  $\delta^{18}\text{O}$  and cell anatomy of *Larix gmelinii* tree rings to differing soil active layer depths. *Dendrochronologia* 34:51–59. <https://doi.org/10.1016/j.dendro.2015.05.002>
- Bryukhanova MV, Vaganov EA, Wirth C (2011) Variability of radial growth and  $\delta^{13}\text{C}$  in tree rings of deciduous and coniferous species in relation to climate and the use of reserve assimilates. *Contemp Probl Ecol* 4(2):126–132
- Büntgen U, Allen K, Anchukaitis K, Arseneault D, Boucher É, Bräuning A, Chatterjee S, Cherubini P, Churakova (Sidorova) OV, Corona C, Gennaretti F, Gießinger J, Guillet S, Guiot J, Gunnarson B, Helama S, Hochreuther P, Hughes MK, Huybers P, Kirilyanov AV, Krusic PJ, Ludescher J, Meier W.J.-H, Myglan VS, Nicolussi K, Oppenheimer C, Reinig F, Salzer MW, Seftigen K, Stine AR, Stoffel M, George SS, Tejedor E, Trevino A, Trouet V, Wang J, Wilson R, Yang B, Xu G, Esper J (2021) The influence of decision-making in tree ring-based climate reconstructions. *Nat Commun* 12:3411. <https://doi.org/10.1038/s41467-021-23627-6>

- Butzin M, Werner M, Masson-Delmotte V, Risi C, Frankenberg C, Gribanov K, Jouzel J, Zakharov VI (2014) Variations of oxygen-18 in West Siberian precipitation during the last 50 years. *Atmos Chem Phys* 14:5853–5869. <https://doi.org/10.5194/acp-14-5853-2014>
- Cable JM, Ogle K, Bolton RW et al (2013) Permafrost thaw affects boreal deciduous plant transpiration through increased soil water, deeper thaw and warmer soil. *Ecohydrology*. <https://doi.org/10.1002/eco.1423>
- Camarero JJ, Gazol A, Sánchez-Salguero R, Fajardo A, McIntire EJB, Gutiérrez E, Batllori E, Boudreau S, Carrer M, Diez J, Dufour-Tremblay G, Gaire NP, Hofgaard A, Jomelli V, Kirilyanov AV, Lévêque E, Liang E, Linares JC, Mathisen IE, Moiseev PA, Sangüesa-Barreda G, Shrestha KB, Toivonen JM, Tutubalina OV, Wilmking M (2021) Global fading of the temperature-growth coupling at alpine and polar treelines. *Glob Change Biol* 27(9):1879–1889. <https://doi.org/10.1111/gcb.15530>
- Churakova (Sidorova) OV (2018) Climatic changes at the high-latitude and -altitude regions in Eurasia based on the stable carbon and oxygen isotope analyses in conifer tree rings. *Habil. Thesis in biology (ecology)*, Krasnoyarsk, Siberian Federal University, 279 pp
- Churakova (Sidorova) OV, Fonti MV, Saurer M, Guillet S, Corona S, Fonti P, Mygland VS, Kirilyanov AV, Naumova OV, Ovchinnikov DV, Shashkin AV, Panyushkina IP, Büntgen U, Hughes MK, Vaganov EA; Siegwolf RTW, Stoffel M (2019) Siberian tree-ring and stable isotope proxies as indicators of temperature and moisture changes after major stratospheric volcanic eruptions. *Clim Past*. <https://doi.org/10.5194/cp-2018-70>
- Churakova (Sidorova) OV, Corona C, Fonti MV, Guillet S, Saurer M, Siegwolf RTW, Stoffel M, Vaganov EA (2020) Recent atmospheric drying in Siberia is not unprecedented over the last 1500 years. *Sci Rep*. <https://www.nature.com/articles/s41598-020-71656-w>
- Churakova (Sidorova) OV, Shashkin AV, Siegwolf R, Spahni R, Launois T, Saurer M, Bryukhanova MV, Benkova AV, Kupzova AV, Vaganov EA, Peylin P, Masson-Delmotte V, Roden J (2016) Application of eco-physiological models to the climatic interpretation of  $\delta^{13}\text{C}$  and  $\delta^{18}\text{O}$  measured in Siberian larch tree-rings. *Dendrochronologia*. <https://doi.org/10.1016/j.dendro.2015.12.008>
- Churakova (Sidorova) OV, Fonti MV, Trushkina TV, Zharkov MS, Taynik AV, Barinov VV, Porter TJ, Saurer M (2021a) Hydrogen isotopes in boreal conifers as indicator of extreme hydrological changes AGU Fall meeting 2021, p 796127
- Churakova (Sidorova) OV, Siegwolf RTW, Fonti MV, Vaganov EA, Saurer M (2021b) Spring Arctic Oscillation as a trigger of summer drought in Siberian subarctic over the past 1494 years. *Sci Rep* 11:19010. <https://doi.org/10.1038/s41598-021-97911-2>
- Cormier M, Werner RA, Leuenberger MC, Kahmen A (2019)  $^2\text{H}$ -enrichment of cellulose and n-alkanes in heterotrophic plants. *Oecologia* 189(2):365–373. <https://doi.org/10.1007/s00442-019-04338-8>
- Craig H, Gordon LI (1965) Deuterium and oxygen - 18 variations in the ocean and marine atmosphere. In: Tongiogi E, Lishi V (eds) *Proceedings of the stable isotopes in oceanographic studies and paleotemperatures*, Spoleto, Italy. Pisa, pp 9–130
- Dansgaard W (1964) Stable isotopes in precipitation. *Tellus* 16:436–468
- D'Arrigo RD, Wilson R, Liepert B, Cherubini P (2008) On the 'Divergence Problem' in Northern forests: a review of the tree-ring evidence and possible causes. *Glob Planet Change* 60:289–305
- Dongmann G, Nürnberg HW, Förstel H, Wagener K (1974) On the enrichment of  $\text{H}_2^{18}\text{O}$  in the leaves of transpiring plants. *Radiat Environ Biophys* 11:41–52. <https://doi.org/10.1007/BF01323099>
- Edwards T, Hammarlund D, Newton BW, Sjolte J, Linderson H, Sturm C, St. Amour NA, Bailey JNL, Nilsson AL (2017) Seasonal variability in Northern Hemisphere atmospheric circulation during the medieval climate anomaly and the little ice age. *Quat Sci Rev* 165:102e110. <https://doi.org/10.1016/j.quascirev.2017.04.018>
- Edwards TWD, Birks SJ, Luckman BH, MacDonald GM (2008) Climatic and hydrologic variability during the past millennium in the eastern Rocky Mountains and northern Great Plains of western Canada. *Quat Res* 70:188–197. <https://doi.org/10.1016/j.yqres.2008.04.013>

- Epstein S, Yapp CJ, Hall JH (1976) The determination of the D/H ratio of non-exchangeable hydrogen in cellulose extracted from aquatic and land plants Earth planet. Sci Lett 30:241. [https://doi.org/10.1016/0012-821X\(76\)90251-X](https://doi.org/10.1016/0012-821X(76)90251-X)
- Ericsson A (1979) Effects of fertilization and irrigation on the seasonal changes of carbohydrate reserves in different age-classes of needle on 20-year-old Scots pine trees (*Pinus silvestris*). Physiol Plant 45:270–280. <https://doi.org/10.1111/j.1399-3054.1979.tb01700.x>
- Farquhar G, Lloyd J (1989) Carbon and oxygen isotope effects in the exchange of carbon dioxide between terrestrial plants and the atmosphere. In: Ehleringer JR, Hall AE, Farquhar GD (eds) Stable isotope and plant carbon/water relations. Academic Press, San Diego, pp 47–70
- Fonti MV, Vaganov EA, Wirth C, Shashkin AV, Astrakhantseva NV, Schulze E-D (2018) Age-effect on intra-annual  $\delta^{13}\text{C}$ -variability within Scots pine tree-rings from Central Siberia 9(6):1–14. <https://doi.org/10.3390/f9060364>
- Fyodorov-Davydov DG, Kholodov VE, Kraev GN, Sorokovikov VA, Davydov SP, Merekalova AA (2009) Seasonal thaw of soils in the North Yakutian ecosystems. In: International conference on cryopedology diversity of forest affected soils and their role in ecosystems, At Ulan-Ude, Buryatia, Russia, September 14–20
- Gagen M, Zorita E, McCarroll D, Zahn M, Young G, Robertson I (2016) North Atlantic summer storm tracks over Europe dominated by internal variability over the past millennium. Nat Geosci 9(8):630–635. <https://doi.org/10.1038/ngeo2752>
- Gennaretti F, Huard D, Naulier M, Savard M, Bégin C, Arseneault D, Guiot J (2017) Bayesian multiproxy temperature reconstruction with black spruce ring widths and stable isotopes from the northern Quebec taiga. Clim Dyn. <https://doi.org/10.1007/s00382-017-3565-5>
- Grudd H (2008) Torneträsk tree-ring width and density AD 500–2004: a test of climatic sensitivity and a new 1500-year reconstruction of north Fennoscandian summers. Clim Dyn 31:843–857. <https://doi.org/10.1007/s00382-007-0358-2>
- Hantemirov R, Gorlanova LA; Surkov AYu, Shiyativ SG (2011) Extreme climate events on Yamal for the last 4100 years according to dendrochronological data. Ivestiya RAN Ser Geogr 2:89–102
- Harris I, Jones PD, Osborn TJ, Lister DH (2014) Updated high-resolution grids of monthly climatic observations – the CRU TS3.10 Dataset. Int J Climatol 34:623–642. <https://doi.org/10.1002/joc.3711>
- Helama S, Arppe L, Uusitalo J, Holopainen J, Mäkelä HM, Mäkinen H, Mielikäinen K, Nöjd P, Sutinen R, Taavitsainen J-P, Timonen M, Oinonen M (2018) Volcanic dust veils from sixth century tree-ring isotopes linked to reduced irradiance, primary production and human health. Nat Sci Rep 8:1339. <https://doi.org/10.1038/s41598-018-19760-w>
- Helbig M, Pappas C, Sonnetag O (2016) Permafrost thaw and wildfire: equally important drivers of boreal tree cover changes in the Taiga Plains, Canada. Geophys Res Lett 43:1598–1606. <https://doi.org/10.1002/2015GL067193>
- Hilasvuori E (2011) Environmental and climatic dependences of stable isotopes in tree rings on different temporal scales. Department of Environmental Sciences, Faculty of Biological and Environmental Sciences, University of Helsinki, 2011, 41 pp
- Hilasvuori E, Berninger F, Sonninen E, Tuomenvirta H, Jungner H (2009) Stability of climate signal in carbon and oxygen isotope records and ring width from Scots pine (*Pinus sylvestris* L.) in Finland. J Quat Sci 24(5):469–480. <https://doi.org/10.1002/jqs.1260>
- Högberg P, Fan H, Quist M, Binkley D, Tamm CO (2006) Tree growth and soil acidification in response to 30 years of experimental N loading. Glob Change Biol 12:489–499. <https://doi.org/10.1111/j.1365-2486.2006.01102.x>
- Holzkämper S, Kuhry P, Kultti S, Gunnarson B, Sonninen E (2008) Stable isotopes in tree rings as proxies for winter precipitation changes in the Russian Arctic over the past 150 years. Geochronometria 32:37–46. <https://doi.org/10.2478/v10003-008-0025-6>
- IPCC (2014) Climate change 2014: synthesis report contribution of working Groups I, II and III to the fifth assessment report of the intergovernmental panel on climate change. In: Pachauri RK, Meyer LA (eds) IPCC, Geneva, Switzerland, 151 pp

- Kasischke EC (2000) Boreal ecosystems in the global carbon cycle. In: Fire, climate change, and carbon cycling in the boreal forest. Springer. Nature Switzerland AG, pp 19–30. [https://doi.org/10.1007/978-0-387-21629-4\\_2](https://doi.org/10.1007/978-0-387-21629-4_2)
- Kagawa A, Naito D, Sugimoto A, Maximov TC (2003) Effects of spatial and temporal variability in soil moisture on widths and  $\delta^{13}\text{C}$  values of eastern Siberian tree rings. *J Geophys Res* 108(D16):4500. <https://doi.org/10.1029/2002JD003019>
- Kagawa A, Sugimoto A, Maximov TC (2006a) Seasonal course of translocation, storage and remobilization of  $^{13}\text{C}$  pulse-labeled photoassimilate in naturally growing *Larix gmelinii* saplings. *New Phytol* 171(4):793–804. <https://doi.org/10.1111/j.1469-8137.2006.01780.x>
- Kagawa A, Sugimoto A, Maximov TC (2006b)  $^{13}\text{CO}_2$  pulse-labelling of photoassimilates reveals carbon allocation within and between tree rings. *Plant Cell Environ* 29:1571–1584. <https://doi.org/10.1111/j.1365-3040.2006.01533.x>
- Keller KM, Lienert S, Bozbiyik A, Stocker TF, Churakova (Sidorova) OV, Frank DC, Klesse S, Koven CD, Leuenberger M, Riley WJ, Saurer M, Siegwolf RTW, Weigt RB, Joos F (2017) 20th-century changes in carbon isotopes and water-use efficiency: tree-ring based evaluation of the CLM4.5 and LPX-Bern models. *Biogeosciences* 14:2641–2673. <https://doi.org/10.5194/bg-14-2641-2017>
- Kimak A, Leuenberger M (2015) Are carbohydrate storage strategies of trees traceable by early-latewood carbon isotope differences? *Trees* 29:859–870. <https://doi.org/10.1007/s00468-015-1167-6>
- Kirilyanov AV, Saurer M, Siegwolf R, Knorre A, Prokushkin A, Churakova (Sidorova) OV, Fonti M, Büntgen U (2020) Long-term ecological consequences of forest fires in the permafrost zone of Siberia. *Environ Res Lett* 15:034061. <https://doi.org/10.1088/1748-9326/ab7469>
- Kirilyanov AV, Treydte KS, Nikolaev A, Helle G, Schleser GH (2008) Climate signals in tree-ring width, density and  $\delta^{13}\text{C}$  from larches in Eastern Siberia (Russia). *Chem Geol* 252:31–41. <https://doi.org/10.1016/j.chemgeo.2008.01.023>
- Knorre AA, Siegwolf R, Saurer M, Sidorova OV, Vaganov EA, Kirilyanov AV (2010) Twentieth century trends in tree rings stable isotopes ( $\delta^{13}\text{C}$  and  $\delta^{18}\text{O}$ ) of *Larix sibirica* under dry conditions in the forest steppe in Siberia. *Geophys Res Biogeosci* 115:G03002. <https://doi.org/10.1029/2009JG000930>,1-12
- Kononov Y, Friedrich M, Boettger T (2009) Regional summer temperature reconstruction in the Khibiny low mountains (Kola Peninsula, NW Russia) by means of tree-ring width during the last four centuries. *Arct Antarct Alp Res* 4(4):460–468. <https://doi.org/10.1657/1938-4246-41.4.460>
- Lacelle D (2011) On the  $\delta^{18}\text{O}$ ,  $\delta\text{D}$  and  $\text{d}$ -excess relations in meteoric precipitation and during equilibrium freezing: theoretical approach and field examples. *Permafrost Periglacial Process* 22:13–25. <https://doi.org/10.1002/ppp.712>
- Leavitt SW (1993) Seasonal  $^{13}\text{C}/^{12}\text{C}$  changes in tree rings: species and site coherence, and a possible drought influence. *Can J Res* 23:210–218. <https://doi.org/10.1139/x93-028>
- Lehmann MM, Vitali V, Schuler P, Leuenberger M, Saurer M (2021) More than climate: Hydrogen isotope ratios in tree rings as novel plant physiological indicator for stress conditions. *Dendrochronologia* 65:125788. <https://doi.org/10.1016/j.dendro.2020.125788>
- Lloyd AH, Bunn AG (2007) Responses of the circumpolar boreal forest to 20th century climate variability. *Environ Res Lett* 2. <https://doi.org/10.1088/1748-9326/2/4/045013>
- Loader NJ, Helle G, Los SO, Lehmkuhl F, Schleser GH (2010) Twentieth-century summer temperature variability in the southern Altai Mountains: a carbon and oxygen isotope study of tree-rings. *The Holocene*. <https://doi.org/10.1177/0959683610369507>
- Loader NJ, Young GHF, Grudd H, McCarroll D (2013) Stable carbon isotopes from Torneträsk, northern Sweden provide a millennial length reconstruction of summer sunshine and its relationship to Arctic circulation. *Quat Sci Rev* 62:97–113. <https://doi.org/10.1016/j.quascirev.2012.11.014>
- Mack MC, Schuur EA, Bret-Harte MS, Shaver GR, Chapin FS (2004) Ecosystem carbon storage in arctic tundra reduced by long-term nutrient fertilization. *Nature* 23:431(7007):440–443. <https://doi.org/10.1038/nature02887>

- Masyagina O, Prokushkin A, Kirilyanov A, Artyukhov A, Udalova T, Senchenkov S, Rublev A (2016) Intra-seasonal carbon sequestration and allocation in larch trees growing on permafrost in Siberia after  $^{13}\text{C}$  labeling (two seasons of 2013–2014 observation). *Photosynth Res* 130:267–274. <https://doi.org/10.1007/s11120-016-0250-1>
- Melnikov ES, Leibman MO, Moskalenko NG, Vasiliev AA (2004) Active-layer monitoring in the cryolithozone of West Siberia. *Polar Geogr* 28(4):267–285. <https://doi.org/10.1080/789610206>
- Mygland VS, Oidupaa OCh, Kirilyanov AV, Vaganov EA (2008) 1929-year tree-ring chronology for Altai-Sayan region (Western Tuva). *J Archeol Ethnogr Anthropol Eurasia* 4(36):25–31
- Naulier M, Savard MM, Bégin C, Gennaretti F, Arseneault D, Marion J, Nicault A, Bégin Y (2015) A millennial summer temperature reconstruction for northeastern Canada using oxygen isotopes in subfossil trees. *Clim Past* 11:1153–1164. <https://doi.org/10.5194/cp-11-1153-2015>
- Naurzbaev MM, Vaganov EA, Sidorova OV, Schweingruber FH (2002) Summer temperatures in eastern Taimyr inferred from a 2427-year late-Holocene tree-ring chronology and earlier floating series. *The Holocene* 12(6):727–736. <https://doi.org/10.1191/0959683602hl586rp>
- New M, Lister D, Hulme M, Makin I (2002) A high-resolution data set of surface climate over global land areas. *Clim Res* 21. <https://doi.org/10.3354/cr021001>
- Obu J, Westermann S, Bartsch A, Berdnikov N, Christiansen AD, Delaloye R, Elberling B, Etzelmüller B, Kholodov A, Khomutov A, Kääb A, Leibman MO, Lewkowicz AG, Panda SK, Romanovsky V, Way RG, Westergaard-Nielsen A, Wu T, Yamkhin J, Zou D (2019) Northern Hemisphere permafrost map based on TTOP modelling for 2000–2016 at 1 km<sup>2</sup> scale. *Earth/sci Rev* 193:299–316. <https://doi.org/10.1016/j.earscirev.2019.04.023>
- Ohta T, Hiyama T, Iijima Y, Kotani A, Maximov TC (2019) Water-carbon dynamics in eastern Siberia. *Springer Nature, Singapore*, 309 pp. <https://doi.org/10.1007/978-981-13-6317-7>
- Pan Y, Birdsey RA, Fang J, Houghton R, Kauppi PE, Kurz WA, Phillips OL, Shvidenko A, Lewis SL, Canadell JG, Ciais P, Jackson RB, Pacala SW, McGuire AD, Piao S, Rautiainen A, Sitch S, Hayes D (2011) A large and persistent carbon sink in the world's forests. *Sci* 333:988–993. <https://doi.org/10.1126/science.1201609>
- Pavlov AV, Skachkov YuB, Kakunov NB (2004) An interaction between the active layer depth changing and meteorological factors. *Earth Cryosphere*, VIII 4:3–11 (in Russian)
- Porter TJ, Froese DG, Feakins SJ, Bindeman I, Mahony ME, Pautler BG, Reichart G-J, Sanborn PT, Simpson MJ, Weijers JWH (2016) Multiple water isotope proxy reconstruction of extremely low last glacial temperatures in Eastern Beringia (Western Arctic). *Quat Sci Rev* 137:113–125. <https://doi.org/10.1016/j.quascirev.2016.02.006>
- Porter TJ, Pisaric MFJ (2011) Temperature–growth divergence in white spruce forests of Old Crow Flats, Yukon Territory, and adjacent regions of northwestern North America. *Glob Change Biol* 17:3418–3430. <https://doi.org/10.1111/j.1365-2486.2011.02507.x>
- Porter TJ, Pisaric MFJ, Field R, Kokel SV, Edwards TWD, deMontigny P, Healy R, LeGrande A (2014) Spring–summer temperatures since AD 1780 reconstructed from stable oxygen isotope ratios in white spruce tree-rings from the Mackenzie Delta, northwestern Canada. *Clim Dyn* 42:771–785. <https://doi.org/10.1657/1938-4246-41.4.497>
- Porter TJ, Pisaric MFJ, Kokelj SV, deMontigny P (2013) A ring-width-based reconstruction of June–July minimum temperatures since AD 1245 from white spruce stands in the Mackenzie Delta region, northwestern Canada. *Quat Res* 80:167–179. <https://doi.org/10.1016/j.yqres.2013.05.004>
- Porter TJ, Pisaric MFJ, Kokelj SV, Edwards TWD (2009) Climate signals in  $\delta^{13}\text{C}$  and  $\delta^{18}\text{O}$  of tree-rings from white spruce in the Mackenzie Delta region, northern Canada. *Arct Antarct Alp Res* 41:497–505. <https://doi.org/10.1657/1938-4246-41.4.497>
- Prokushkin AS, Hagedorn F, Pokrovsky OS, Viers J, Kirilyanov AV, Masyagina OV, Prokushkina MP, McDowell WH (2018) Permafrost regime affects the nutritional status and productivity of larches in Central Siberia. *Forests* 9:314. <https://doi.org/10.3390/f9060314>
- Rinne KT, Saurer M, Kirilyanov AV, Loader N, Bryukhanova MV, Werner R, Siegwolf RTW (2015) The relationship between needle sugar carbon isotope ratios and tree rings of larch in Siberia. *Tree Physiol* 35(11):1192–1205. <https://doi.org/10.1093/treephys/tpv096>

- Roden JS, Lin G, Ehleringer JR (2000) A mechanistic model for interpretation of hydrogen and oxygen isotopic ratios in tree-ring cellulose. *Geochim Cosmochim Acta* 64:21–35
- Saurer M, Kirilyanov AV, Prokushkin AS, Rinne KT, Siegwolf RTW (2016) The impact of an inverse climate-isotope relationship in soil water on the oxygen-isotope composition of *Larix gmelinii* in Siberia. *New Phytol* 209:955–964
- Saurer M, Schweingruber F, Vaganov EA, Shiyatov SG, Siegwolf R (2002) Spatial and temporal oxygen isotope trends at the northern tree-line in Eurasia. *Geophys Res Lett* 29. <https://doi.org/10.1029/2001GL013739>
- Saurer M, Siegwolf R, Schweingruber FH (2004) Carbon isotope discrimination indicates improving water-use efficiency of trees in northern Eurasia over the last 100 years. *Glob Change Biol* 10:2109–2121. <https://doi.org/10.1111/j.1365-2486.2004.00869.x>
- Saurer M, Spahni R, Frank DC, Joos F, Leuenberger M, Loader NJ, McCarroll D, Gagen M, Poulter B, Siegwolf RT, Andreu-Hayles L, Boettger T, Dorado LI, Fairchild IJ, Friedrich M, Gutierrez E, Haupt M, Hiltunen E, Heinrich I, Helle G, Grudd H, Jalkanen R, Levanić T, Linderholm HW, Robertson I, Sonninen E, Treydte K, Waterhouse JS, Woodley EJ, Wynn PM, Young GH (2014) Spatial variability and temporal trends in water-use efficiency of European forests. *Glob Change Biol* 20:3700–3712
- Schneider L, Smerdon JE, Büntgen U, Wilson RJS, Myglan VS, Kirilyanov AV, Esper J (2015) Revising mid-latitude summer temperatures back to A.D. 600 based on a wood density network. *Geophys Res Lett* 42(11):4556–4562. <https://doi.org/10.1002/2015GL063956>
- Schuler P, Cormier M-A, Werner RA, Buchmann N, Gessler A, Vitali V, Saurer M, Lehmann MM (2022) A high-temperature water vapor equilibration method to determine non-exchangeable hydrogen isotope ratios of sugar starch and cellulose. *Plant Cell Environ* 45(1):12–22. <https://doi.org/10.1111/pce.14193>
- Sidorova OV, Naurzbaev M (2002) Response of *Larix cajanderi* to climatic changes at the upper timberline and flood-plain terrace from Indigirka River valley. *Russian for Manag* 2:73–75
- Sidorova OV, Saurer M, Myglan VS, Eichler A, Schwikowski M, Kirilyanov AV, Bryukhanova MV, Gerasimova OV, Kalugin I, Daryin A, Siegwolf R (2012) A multi-proxy approach for revealing recent climatic changes in the Russian Altai. *Clim Dyn* 38(1–2):175–188
- Sidorova OV, Siegwolf R, Myglan VS, Loader NJ, Helle G, Saurer M (2013a) The application of tree-rings and stable isotopes for reconstructions of climate conditions in the Altai-Sayan Mountain region. *Clim Changes*. <https://doi.org/10.1007/s10584-013-0805>
- Sidorova OV, Saurer M, Andreev A, Fritzsche D, Opel T, Naurzbaev M, Siegwolf R (2013b) Is the 20th century warming unprecedented in the Siberian north? *Quat Sci Rev* 73:93–102. <https://doi.org/10.1016/j.quascirev.2013.05.015>
- Sidorova OV, Siegwolf R, Saurer M, Naurzbaev M, Shashkin AV, Vaganov EA (2010) Spatial patterns of climatic changes in the Eurasian north reflected in Siberian larch tree-ring parameters and stable isotopes. *Glob Change Biol* 16:1003–1018. <https://doi.org/10.1111/j.1365-2486.2009.02008.x>
- Sidorova OV, Siegwolf R, Saurer M, Naurzbaev MM, Vaganov EA (2008) Isotopic composition ( $\delta^{13}\text{C}$ ,  $\delta^{18}\text{O}$ ) in Siberian tree-ring chronology. *Geophys Res Biogeosci* 113:G02019. <https://doi.org/10.1029/2007JG000473>
- Sidorova OV, Siegwolf R, Saurer M, Shashkin AV, Knorre AA, Prokushkin AS, Vaganov EA, Kirilyanov AV (2009) Do centennial tree-ring and stable isotope trends of *Larix gmelinii* (Rupr.) indicate increasing water shortage in the Siberian north? *Oecologia* 161(4):825–835. <https://doi.org/10.1007/s00442-009-1411-0>
- Siegwolf RTW, Lehmann MM, Goldsmith G, Churakova (Sidorova) O, Mirande-Ney C, Timoveeva G, Weigt R, Saurer M (2022) Updating the dual C and O isotope – gas exchange model: A concept for understanding plant-environment responses and its implications for tree rings. *PCE*. In review
- Soja AJ, Tchepakova NM, French NHF, Flannigan MD, Shugart HH, Stocks BJ, Sukhinin AI, Parfenova EI, Chapin FS, Stackhouse PW (2007) Climate induced boreal forest change: predictions versus current observations. *Glob Planet Change* 56:274–296

- Sugimoto A, Yanagisawa N, Naito D, Fujita N, Maximov TC (2002) Importance of permafrost as a source of water for plants in East Siberian taiga. *Ecol Res* 17(4):493–503. <https://doi.org/10.1046/j.1440-1703.2002.00506.x>
- Tartakovsky VA, Voronin VI, Markelova AN (2012) External forcing factor reflected in the common signals of  $\delta^{18}\text{O}$ -tree-ring series of *Larix sibirica* Ledeb. in the Lake Baikal region. *Dendrochronologia* 30:199–208. <https://doi.org/10.1016/j.dendro.2011.08.004>
- Tei S, Sugimoto A, Yonenobu H, Yamazaki T, Maximov MC (2013) Reconstruction of soil moisture for the past 100 years in eastern Siberia by using  $\delta^{13}\text{C}$  of larch tree rings. *J Geophys Res Biogeosci* 118:1256–1265. <https://doi.org/10.1002/jgrg.20110>
- Turetsky MR, Abbott BW, Jones MC, Walter AK, Olefeldt D, Schuur EAG, Koven C, McGuire AD, Grosse G, Kuhnz P, Hugelius G, Lawrence DM, Gibson C, Sannel ABK (2019) Permafrost collapse is accelerating carbon release. *Nature*. <https://doi.org/10.1038/d41586-019-01313-4>
- Vaganov EA, Hughes MK, Shashkin AV (2006) Growth dynamics of conifer tree rings: images of past and future environments. Springer, 372 pp
- Vaganov EA, Schulze E.-D., Skomarkova MV, Knohl A, Brand W, Roscher C (2009) Intra-annual variability of anatomical structure and  $\delta^{13}\text{C}$  values within tree rings of spruce and pine in alpine, temperate and boreal Europe. *Oecologia* 161:729–745. <https://doi.org/10.1007/s00442-009-1421-y>
- Voelker SL, Brooks JR, Meinzer FC, Roden J, Pazdur A, Pawelczyk S, Hartsough P, Snyder K, Plavcova L, Šantrůček J (2014) Reconstructing relative humidity from plant  $\delta^{18}\text{O}$  and  $\delta\text{D}$  as deuterium deviations from the global meteoric water line. *Ecol Appl* 24:960–975. <https://doi.org/10.1890/13-0988.1>
- Voronin V, Ivlev AV, Oskolkov V, Boettger T (2012) Intra-seasonal dynamics in metabolic processes of  $^{13}\text{C}/^{12}\text{C}$  and  $^{18}\text{O}/^{16}\text{O}$  in components of Scots pine twigs from southern Siberia interpreted with a conceptual framework based on the carbon metabolism oscillatory model. *BMC Plant Biol* 12:76. <https://doi.org/10.1186/1471-2229-12-76>
- Waterhouse JS, Barker AC, Carter AHC, Agafonov LI, Loader NJ (2000) Stable carbon isotopes in Scots pine tree rings preserve a record of flow of the river Ob. *Geophys Res Lett* 27(21):3529–3532. <https://doi.org/10.1029/2000GL006106>
- Waterhouse JS, Switsur VR, Barker AC, Carter AHC, Robertson I (2002) Oxygen and hydrogen isotope ratios in tree rings: how well do models predict observed values? *Earth Planet Sci Lett* 201:421–430. [https://doi.org/10.1016/S0012-821X\(02\)00724-0](https://doi.org/10.1016/S0012-821X(02)00724-0)
- Wilmking M, Juday GP, Barber VA, Zald HSJ (2004) Recent climate warming forces contrasting growth responses of white spruce at treeline in Alaska through temperature thresholds. *Glob Change Biol* 10:1724–1736. <https://doi.org/10.1111/j.1365-2486.2004.00826.x>
- Young GHF, McCarroll D, Loader NJ, Gagen MH, Kirchhefer AJ, Demmler JC (2012) Changes in atmospheric circulation and the Arctic Oscillation preserved within a millennial length reconstruction of summer cloud cover from northern Fennoscandia. *Clim Dyn* 39:495–507. <https://doi.org/10.1007/s00382-011-1246-3>
- Zhang T, Heginbottom JA, Barry RG, Brown J (2000) Further statistics on the distribution of permafrost and ground ice in the Northern Hemisphere. *Polar Geogr* 24(2):126–131. <https://doi.org/10.1080/10889370009377692>
- Zharkov MV, Fonti MV, Trushkina TV, Barinov VV, Taynik AV, Porter T, Saurer M, Churakova (Sidorova) OV (2021) Mixed temperature-moisture signal in  $\text{d}18\text{O}$  records of boreal conifers from the permafrost zone. *MDPI Atmos* 12(11):1416. <https://doi.org/10.3390/atmos12111416>



**Open Access** This chapter is licensed under the terms of the Creative Commons Attribution 4.0 International License (<http://creativecommons.org/licenses/by/4.0/>), which permits use, sharing, adaptation, distribution and reproduction in any medium or format, as long as you give appropriate credit to the original author(s) and the source, provide a link to the Creative Commons license and indicate if changes were made.

The images or other third party material in this chapter are included in the chapter's Creative Commons license, unless indicated otherwise in a credit line to the material. If material is not included in the chapter's Creative Commons license and your intended use is not permitted by statutory regulation or exceeds the permitted use, you will need to obtain permission directly from the copyright holder.



# Chapter 21

## Stable Isotopes in Tree Rings of Mediterranean Forests



Giovanna Battipaglia and Paolo Cherubini

### 21.1 Introduction

Tree-ring studies in the Mediterranean Basin and in regions characterized by Mediterranean climates are scarce because of a lack of old trees and difficulties related to the clear identification of individual rings. Old trees are lacking because most regions with a Mediterranean climate have long histories of human activity; logging, grazing, and human-induced fires have occurred over millennia. Annual rings are difficult to identify in some woody plant species because highly variable climatic conditions can lead to the formation of intra-annual density fluctuations, which hamper the cross-dating of tree-ring series (Cherubini et al. 2013). Stable isotopes may help in identifying intra-annual density fluctuations (De Micco et al. 2007) and in understanding the physiological processes behind tree-ring formation, carbon uptake, and water use (Battipaglia et al. 2010a, 2014a).

Most of the tree-ring stable isotope studies carried out on Mediterranean tree and shrub species include the use of both carbon and oxygen stable isotopes (Table 21.1), which help to reconstruct past climate and retrospectively assess tree responses to the environment (McCarroll and Loader 2004). The values of the isotopic ratios reflect the extent to which the heavier isotope is discriminated compared to the lighter one during the physical and chemical processes involved in the synthesis of plant organic matter (Farquhar et al. 1989).

---

G. Battipaglia (✉)

Department of Environmental, Biological and Pharmaceutical Sciences and Technologies,  
University of Campania «L. Vanvitelli», via Vivaldi 43, 81100 Caserta, Italy  
e-mail: [giovanna.battipaglia@unicampania.it](mailto:giovanna.battipaglia@unicampania.it)

P. Cherubini

Swiss Federal Institute for Forest, Snow and Landscape Research WSL, Birmensdorf, Switzerland  
Department of Forest and Conservation Sciences, The University of British Columbia, Main Mall,  
Vancouver, BC 3041-2424, Canada

© The Author(s) 2022

R. T. W. Siegwolf et al. (eds.), *Stable Isotopes in Tree Rings*, Tree Physiology 8,  
[https://doi.org/10.1007/978-3-030-92698-4\\_21](https://doi.org/10.1007/978-3-030-92698-4_21)

605

**Table 21.1** Summary of the main aim and outcomes of studies measuring stable isotopes in Mediterranean tree rings. References given in chronological order

Stable isotope	Main usage	Main outcome	Number of species	References
<sup>13</sup> C	Unravelling isotope-climate relations	Negative correlation with precipitation; water availability triggers tree growth and stomatal conductance	15	Shestakova et al. (2019), Castagneri et al. (2018), Fernández-de-Uña et al. (2017), Shestakova et al. (2017), Voelker et al. (2014), Bogino and Bravo (2014), Granda et al. (2014), del Castillo et al. (2013), De Micco et al. (2012), Battipaglia et al. (2010a; b), De Micco et al. (2007), Ferrio et al. (2003), Liñán et al. (2012)
	Proxy for iWUE	Generally, an increase in iWUE shows that the potential <i>fertilization effect</i> of increasing atmospheric CO <sub>2</sub> does not <i>compensate</i> for the negative <i>effects</i> of stress factors such as drought	41	Camarero et al. (2018), Martínez-Sancho et al. (2018), Paris et al. (2018), Brito et al. (2016), Fernández-de-Uña et al. (2016), González-Muñoz et al. (2015), Lucas et al. (2013), Peñuelas et al. (2011), Linares et al. (2011), Di Matteo et al. (2010), Linares et al. (2009)
	Reconstruction of past climate	Good prospect for temperature and past precipitation regimes	3	Heinrich et al. (2013), Szymczak et al. (2012a; b), Aguilera et al. (2009)
<sup>18</sup> O	Reconstruction of water resources	Trees show contrasting patterns of water use	4	Sargeant et al. (2016), Singer et al. (2013)
<sup>13</sup> C & <sup>18</sup> O	Drought effect on trees	Dying trees showed reduced productivity and lower intrinsic water-use efficiency compared with healthy trees due to enhanced water loss through transpiration	7	Barbeta & Peñuelas (2017), Colangelo et al. (2017), Sarris et al. (2013), Brooks & Coulombe (2009), Battipaglia et al. (2009), Voltas et al. (2013)

(continued)

**Table 21.1** (continued)

Stable isotope	Main usage	Main outcome	Number of species	References
	Proxy for species iWUE	Variations in stable carbon and oxygen isotope compositions of co-occurring plant species reflect their different water-use strategies	10	Battipaglia et al. (2016a, 2017; b), Altieri et al. (2015), Moreno-Gutierrez et al. (2015), Shestakova et al. (2014), Maseyk et al. (2011)
	Effects of fire on tree physiology	Fire increases tree iWUE, decreases tree growth and relative conductivity. Prescribed fire reduces stress competition for water and nutrients	3	Niccoli et al. (2019), Valor et al. (2018), Battipaglia et al. (2014a, 2016a; b, c, b), Beghin et al. 2011)
	IADF characterization	IADFs formation is mainly species and site specific, related to high temperature, precipitation patterns, and/or soil water availability, which differ at the selected study sites	3	Zalloni et al. (2018), Battipaglia et al. (2014a, b, c)
	Effect of natural CO <sub>2</sub> spring	Downward adjustment of photosynthesis under elevated CO <sub>2</sub> in a dry, nutrient-poor environment	1	Saurer et al. (2003)
	Solar flare effects on trees	No clear effects on ecophysiology	2	Bartolomei et al. (1995)
	Reconstruction of past climate	Summer climate influences trees performance	5	Konter et al. (2014), Hafner et al. (2011), Aguilera et al. (2011)
	Methodological approach	Necessity of cellulose extraction depends on species and research questions	1	Szymczak et al. (2011, 2014), Battipaglia et al. (2008)

(continued)

**Table 21.1** (continued)

Stable isotope	Main usage	Main outcome	Number of species	References
<sup>15</sup> N	Climate change effect on carbon and nitrogen cycles	Decreasing trend in $\delta^{15}\text{N}$ in both herbarium material and tree rings, indicating that ecosystems might cope with higher plant N demand by decreasing N losses and increasing N fixation and mineralization	4	Peñuelas & Estiarte (1996)
	Effect of fire and drought on trees	The post-fire growth responses and changes in wood C and N isotope composition depend on site water availability and fire severity	1	Alfaro-Sanchez et al. (2016)
	Pollution effects on trees	N deposition influences iWUE and photosynthetic activity	4	Guerrieri et al. (2009, 2010, 2011), Battipaglia et al. (2010a, b)

In this chapter, we highlight the importance of stable isotope research in Mediterranean ecosystems and explain the link between the morphological and functional characteristics of Mediterranean species and the climatic and environmental adaptations that have occurred over millennia.

## 21.2 Mediterranean Climates

Mediterranean climates occur around the world: in California, central Chile, western and southwestern Australia, southwestern South Africa, and in the Mediterranean Basin. As most tree-ring studies have been carried out in the Mediterranean, we focus on this region in this chapter. In a typical Mediterranean climate, winters are wet and rather mild, although frost and cold stress can occur (Larcher 2000; Mitrakos 1980; Terradas and Save 1992). Rainfall starts in September and continues until April, with a total precipitation amount of 400–1200 mm (Pignatti 2008). Summers are hot and dry; rainfall events are rare, and the season is often characterized by an extremely dry period, the so-called *summer drought*. These general features can vary

in different coastal areas of the Mediterranean Basin depending on their elevation and local geomorphological and soil features, but the summer drought is always present (see Fig. 21.1). The main factors leading to the formation of Mediterranean-type climates are air circulation, latitude, topography, and the surface temperature of the surrounding water.

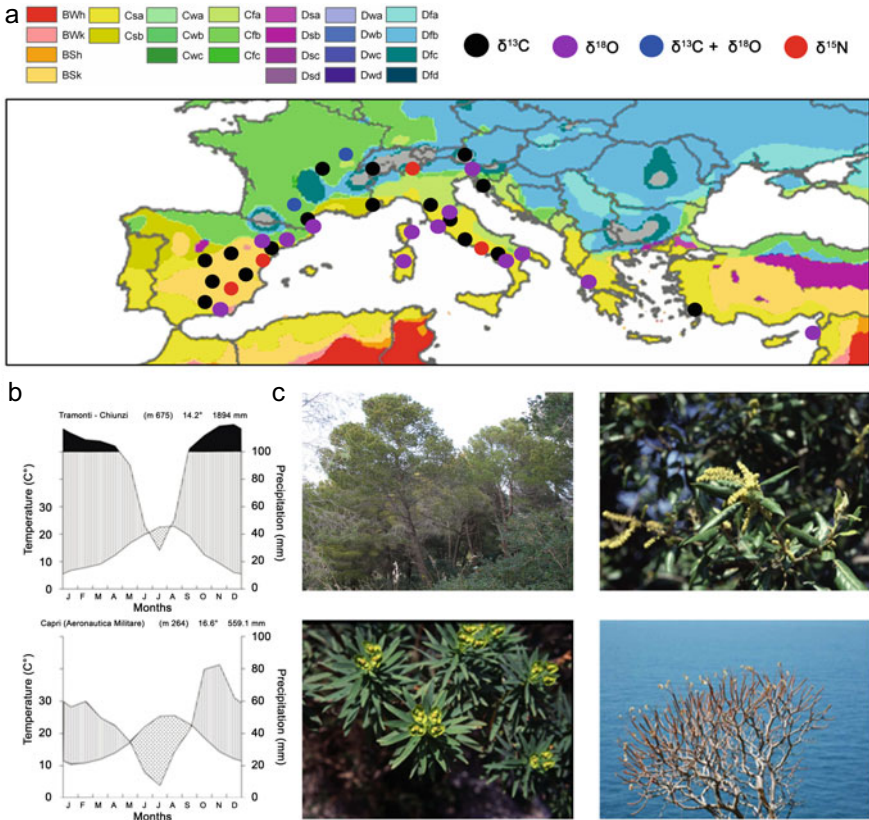


**Fig. 21.1** **a** Map of the Mediterranean Basin showing locations of stable isotope tree-ring studies. The main findings of these studies are summarized in Table 21.1. Background map showing Mediterranean climates according to Köppen classification. **b** Two Walter and Lieth climate diagrams depicting the climate of two typical Mediterranean areas. Lower diagram: Capri (an island in the Tyrrhenic sea); upper diagram: Tramonti, at a higher altitude (period 1960–2010). **c** A few examples of Mediterranean species. Clockwise from top left: *Pinus halepensis* Mill of southern Spain; *Quercus ilex* L from southern Italy; *Euphorbia dendroides* L.: winter habitus and summer habitus

### 21.2.1 *Mediterranean Climate and Vegetation*

Mediterranean plants are adapted to this climate and cope with summer drought through several changes at the phenological, morphological, physiological,

or biochemical levels (Pignatti 2008). These adaptations influence all relevant ecophysiological processes, i.e., transpiration and carbon assimilation, as well as the isotopic signal imprinted in plant organic matter. Hence, the isotopic composition of the wood material of Mediterranean trees reflects their functionality and adaptation strategies. To cope with drought stress, two main strategies are observed in Mediterranean plants: avoidance and tolerance (Pignatti 2008).

Many species survive summer drought by avoiding it through summer dormancy. This strategy is adopted by annual and perennial herbs and by woody species. Annual herbs have a very short life cycle that starts in late winter so that fruits are mature at the beginning of summer. Seeds then remain dormant until conditions are optimal for successful growth. Perennial herbaceous species often have a geophyte life-form, in which the above-ground parts of the plants (leaves, stems) are shed at the beginning of summer and the individual remains dormant by means of a perennating below-ground organ (bulb, tuber, rhizome). Some woody species also have summer dormancy, shedding all their leaves (e.g. *Euphorbia dendroides* L.) at the end of spring or summer. Several species, such as *Cistus*, change their leaves according to the season and are characterised by the alternation of a winter and a summer *leaf habitus*.

Plants without summer dormancy present tolerance attributes, which help them to face summer drought. Many species have a low leaf surface area, e.g., the needle-like leaves of *Rosmarinus officinalis* L. or *Juniperus phoenicea* L. subsp. *phoenicea*, whose juvenile needle-like leaves turn into scale-like leaves that are densely arranged around the stem in older branches. Other species have sclerophyllous leaves, with very dense mesophyll and thick cuticles to constrain water loss. Regulation of stomatal activity is a good strategy to cope with summer drought: stomatal closure can reduce transpiration rate and water loss. Several *species* count on *stomata*, which are *sunken* into the leaf surface and protected by dense, short trichomes, to reduce water loss. The lower leaf blades of *R. officinalis*, *Quercus ilex* L., and *Olea europaea* L. are examples of this feature. Other plants without summer dormancy tolerate high solar radiation by means of a reflecting cuticle (e.g., *Myrtus communis* L. subsp. *communis*) or long (often white) hairs on the upper leaf blade (e.g., *Centaurea cineraria* L. subsp. *cineraria*) that protect inner tissues from excessive radiation.

The adaptation mechanisms of Mediterranean plants are often linked with human activity, since their long association with humans has left its mark across much of the landscape. Human activities have influenced not only the type of community and forest composition, but also their main characteristics.

Four major types of vegetation can be recognized in the Mediterranean-European region according to the bioclimate type and the elevation (Quézel and Médail 2003; Rivas-Martínez et al. 2007; Médail 2008). First, a thermo-Mediterranean vegetation rises from sea level to ~200–500/800 m a.s.l. and is dominated by sclerophyllous communities (e.g., *Olea europaea*, *Ceratonia siliqua*, *Chamaerops humilis*,

*Pistacia lentiscus*, *Pinus halepensis*, *Pinus brutia*, etc.). A meso-Mediterranean vegetation takes over between ~100–500/1000 m a.s.l. and is dominated by sclerophyllous forests (*Quercus ilex*, *Quercus suber*, and *Q. coccifera*) or *Pinus halepensis*/*P. brutia* forests in drought-prone forest systems. This then transitions to a supra-Mediterranean vegetation between ~500–1500/1800 m a.s.l., with deciduous oaks forests (e.g. *Acer*, *Carpinus*, *Ostrya*, *Quercus*, and *Sorbus*) in the more humid areas. Finally, a mountain-Mediterranean vegetation belt between ~1500–2000 m a.s.l. includes *Fagus* and deciduous and semi-deciduous *Quercus* forests, as well as several coniferous forests with *Pinus nigra*, *Pinus sylvestris*, firs (*Abies alba* and most of the Mediterranean *Abies* spp.), and even cedar (*Cedrus libani* s.l.) on Cyprus (Médail et al. 2019).

### 21.3 Mediterranean Wood Formation in Mediterranean Tree Species

The Mediterranean basin has an extension of more than 2 million square kilometers, and it is the largest of the world's five mediterranean-climate regions, as well as the world's second largest biodiversity hotspot (Myers et al. 2000).

The Mediterranean region is considered to be one of the climate-change hotspots, being a transition zone between temperate and arid and tropical regions (Diffenbaugh and Giorgi 2012). It has experienced an increase in drought frequency in the past three decades, and forecasts predict increased irregularity of the intra-annual precipitation pattern, and increasing temperature in the next decades (IPCC 2017). Water availability is considered the key factor driving ecophysiological processes in Mediterranean vegetation. It influences cambial activity, photosynthetic rates, dry matter production, phenology, allocation of carbon to roots and leaves, and overall growth activity of woody plants (Margaris and Papadogianni 1977; Lo Gullo and Salleo 1988; Orshan 1989; Gratani 1995; Salleo et al. 1997; Davis et al. 1999).

In Mediterranean ecosystems, tree species are adapted to cope with the so-called “double stress” of summer drought and winter low temperatures (Mitrakos 1980; Cherubini et al. 2003). These stressors trigger the formation of Intra Annual Density Fluctuations (IADFs) (Campelo et al. 2007; Battipaglia et al. 2016a; De Micco et al. 2016), which are caused by the interruption of the normal course of growth during the growing season. When favorable growth conditions resume, growth resumes, resulting in a change in wood density (Tingley 1937; Schulman 1938). In Mediterranean regions, this happens irregularly in space (at different sites at the same time), time (in different years at the same site), and among species (as well as individual trees). This ability to stop and restart growth within a growth season is indicative of the high plasticity of Mediterranean species, whose wood functional traits enable them to preserve hydraulic conductivity throughout the different seasons, achieving a trade-off between hydraulic efficiency and safety (see Beeckman 2016).



IADFs make it difficult to clearly identify individual annual rings; as a result, the tree rings of Mediterranean species are used less often for dendroecological purposes less than those of plants growing in temperate environments. However, a variety of recent research techniques have provided valuable information about the short-term growth variability of Mediterranean trees and shrubs. These include the intensive monitoring of stem radial variation using dendrometers (Sánchez-Costa et al. 2015), the assessment of cambial phenology (Camarero et al. 2010; Vieira et al. 2017), the measurement of xylem anatomical traits (De Micco et al. 2019; Carvalho et al. 2015; Pacheco et al. 2016), stable isotopes within tree rings (on tree-ring sub-sections, Klein et al. 2005; in continuum by laser ablation, Battipaglia et al. 2010a, b; 2014a) and a combination of methodologies (Zalloni et al. 2018, 2019; Balzano et al. 2018; Castagneri et al. 2018).

## 21.4 Carbon and Oxygen Stable Isotopes in Tree Rings of Mediterranean Species

### 21.4.1 Carbon Isotopes

Mediterranean species, which grow in climates characterized by summer drought and wet periods during the growing season, show wood structure adjustments that are mostly related to the need to maintain high conductivity when water is available, and to prevent xylem embolism when dry conditions occur (Cherubini et al. 2003; De Micco and Aronne 2012; Meinzer et al. 2010; Sperry et al. 2008). Tree-ring formation is therefore directly influenced by these adjustment processes and carbon stable isotopes can investigate the link between xylem hydraulic properties and the related physiological mechanisms.

Water shortage negatively influences carboxylation rates by reducing the  $\text{CO}_2$  concentration in the gaseous spaces within the plant ( $C_i$ ) due to stomata closure, causing a decrease in carbon isotope discrimination (Farquhar et al. 1989; Scheidegger et al. 2000). Many studies conducted in Mediterranean climates have shown that plants growing under water stress (stress induced by low soil water content and high evaporative atmospheric demand) produce tree-rings with higher  $\delta^{13}\text{C}$  (Ferrio et al. 2003; Battipaglia et al. 2010a; Maseyk et al. 2011). However, leaf water availability ultimately influences tree-ring  $\delta^{13}\text{C}$ . This availability is a consequence not only of soil water content, but also of the physical structure and hydraulic resistance along the plant xylem and the way the plant transports and uses water (e.g. leaf phenology) (Masle and Farquhar 1988; Warren and Adams 2000). Further, tree  $\delta^{13}\text{C}$  is influenced by the leaf-to-air vapour pressure deficit (VPD), which is the driving force for transpiration. Studies on isotope-climate relationships have shown that mean annual precipitation controls carbon discrimination ( $\Delta^{13}\text{C}$ ) in several forest ecosystem types (Schulze et al. 1998; Diefendorf et al. 2010; Kohn 2010), as well as in tree rings of a large range of Mediterranean species (Shestakova et al. 2019;

del Castillo et al. 2013). These studies generally suggest a stronger influence of precipitation on  $\Delta^{13}\text{C}$  in drier environments (Warren et al. 2001).

### ***21.4.2 Carbon Isotope Discrimination as a Proxy for iWUE***

Carbon isotope composition has been used to calculate intrinsic water-use efficiency (iWUE) (see Chap. 17) in Mediterranean species (Ehleringer et al. 1993; Altieri et al. 2015; Battipaglia et al. 2016b; Dawson and Ehleringer 1993; Moreno-Gutiérrez et al. 2012). iWUE is key to the survival of Mediterranean species under drought conditions (Farquar et al. 1989); according to Medrano et al. (2009), a high iWUE can be considered an adaptive trait of Mediterranean species. Inter- and intra-species interactions influence iWUE, and iWUE can vary with inter- and intra-annual climate variability, stand density, and tree size (Forrester 2015). Within and across tree species, variations in iWUE reveal a continuous ecophysiological gradient of plant water-use strategies ranging from “profligate/opportunistic” (low iWUE) to “conservative” (high iWUE) (Moreno-Gutiérrez et al. 2012). Several factors can affect iWUE at individual and stand levels, such as tree age and height (Francey and Farquhar 1982; Farquhar et al. 1982, Bert et al. 1997; McDowell et al. 2011a, b; Brienen et al. 2017), site density and characteristics (Battipaglia et al. 2010a; Zalloni et al. 2018), forest management, climate, and increasing atmospheric  $\text{CO}_2$  (Silva and Horward 2013, De Micco et al. 2019).

Both network studies and case studies have highlighted a general increase in iWUE in Mediterranean species (Linares et al. 2009; Di Matteo et al. 2010; Linares et al. 2011; Peñuelas et al. 2011; González-Muñoz et al. 2015; Brito et al. 2016; Fernández-de-Uña et al. 2016; Paris et al. 2018; Shestakova et al. 2019). All studies agree that the increase in iWUE does not translate into growth enhancement in response to increasing atmospheric  $\text{CO}_2$ . However, it is not yet clear why this occurs because it is extremely difficult to disentangle the influence of single factors on iWUE variation and to quantify the extent to which drought overrides a positive  $\text{CO}_2$  fertilization effect (see Peñuelas et al. 2011). Moreover, iWUE can vary due to both photosynthetic and stomatal conductance rates, since both affect the ratio between  $\text{CO}_2$  partial pressure in leaf intercellular space and in the atmosphere. To better understand the role of assimilation on iWUE, several authors have coupled tree-ring  $\delta^{13}\text{C}$  values with wood  $\delta^{18}\text{O}$  values (the dual isotope approach; Chap. 16, paragraph 5).

### ***21.4.3 Oxygen Isotopes as a Proxy for Source Water***

Oxygen isotopes can provide valuable information about changes in source water, which is typically either precipitation or groundwater (Dansgaard, 1964). No fractionation occurs when water is taken up by the roots (Wershaw et al. 1966), so the

$\delta^{18}\text{O}$  of xylem water can be used to investigate plant water source use in a range of environmental conditions (Sternberg and Swart 1987; Ehleringer and Dawson 1992; Dawson et al. 1998a, b). Very few studies, however, have focused on Mediterranean environments (Sargeant and Singer 2016; Singer et al. 2013), where water sources are quite complex and subject to strong seasonal fluctuations. The interface between the influx of marine water and the freshwater table depends strongly on climatic factors and on the exploitation of groundwater for urban or rural purposes, both of which influence the quality of water available for plant communities.

The isotopic composition of rainfall is typically subject to seasonal patterns that are influenced by geographic and climatic factors. Generally, autumn–winter precipitation has a more negative isotopic signature (ranging between  $\sim -7.8$  and  $-6.0$  ‰) than spring–summer precipitation (ranging between  $\sim -4.0$  and  $+0.8$  ‰) (Alessio et al. 2004). Consequently, the freshwater table is labelled by meteoric water, and primarily by the abundant autumn–winter and spring precipitation events (Wu et al. 1996). In contrast, soil water in the shallow layers depends on spring–summer precipitation. Further, water occurring 10–50 cm below the dry soil surface is subject to evaporative enrichment and therefore attains less negative or even positive  $\delta^{18}\text{O}$  values (Craig and Gordon 1965; Allison and Leaney 1982; Yakir et al. 2000). A further source of water is the marine water table, which is typically characterized by enriched values of  $\delta^{18}\text{O}$  ( $\sim 0$  ‰).

Thus, the  $\delta^{18}\text{O}$  composition of tree rings will reflect the isotopic signature of the tree's water source: rings will have a depleted  $\delta^{18}\text{O}$  signature if trees take up water from the groundwater table (Dawson and Ehleringer 1998), and an enriched  $\delta^{18}\text{O}$  signature if trees take up water from the vadose zone. Indeed, water in the vadose zone is generally linked to recent precipitation and is subject to high evaporative enrichment of  $\delta^{18}\text{O}$  (Dawson and Ehleringer 1998). These source-water signatures will be different for individual rings within a given species depending on the annual position of the water table and the degree of mixing between precipitation, surface flow, and groundwater during periods of xylem uptake (McCarroll and Loader 2004). It should also be noted that considerable fractionation occurs at the leaf/needle level, where lighter isotopes are preferentially lost via transpiration, leading to an enrichment in plant tissue  $\delta^{18}\text{O}$  of up to 20‰ compared to soil water (Craig and Gordon 1965; Saurer et al. 1998; McCarroll and Loader 2004; Barbour 2007; Cernusak et al. 2016). Indeed, it has been demonstrated that the source water signal can be modified by large changes in evaporative enrichment in drought-adapted Mediterranean species. These species tightly regulate transpiration through their stomata (Ferrio and Voltas, 2005), an ability that is thought to be a functional adaptation to drought (Pallary et al. 1995; Battipaglia et al. 2009).

Singer et al. (2013) and Sargeant and Singer (2016) used annual tree-ring  $\delta^{18}\text{O}$  analyses to interpret plant water use at various temporal and spatial scales as a function of regional hydrology and climate. Both studies underlined the great plasticity of plants as evinced by their ability to take up different sources of water and to modulate their root depth to take up water from different compartments in order to avoid competition. This promising approach needs to be exploited further, as it

could provide important information regarding the ability of plants to survive drought events cooperatively (Altieri et al. 2015).

## 21.5 Application of Carbon and Oxygen Isotopes in Tree-Rings of Mediterranean Species

The carbon and oxygen composition of tree-rings has been used for elucidating whether plant functional responses are related to stomata control of water losses ( $g_s$ ) or to varying assimilation rates ( $A$ ), since  $\delta^{18}\text{O}$  shared a dependence on  $g_s$  with  $\delta^{13}\text{C}$ , but is thought to be independent of variation in  $A$  (Scheidegger et al. 2000; Grams et al. 2007; Roden and Farquhar 2012).

Indeed, even if the interpretation of the double model  $\delta^{13}\text{C}$ — $\delta^{18}\text{O}$  is not straightforward (Roden and Siegwolf 2012), and may sometimes be hampered by changes in the source water isotopes (Gessler et al. 2014), it can still provide important information when applied in strongly water-limited ecosystems, such as the Mediterranean (Ripullone et al. 2009; Moreno-Gutiérrez et al. 2012; Voltas et al. 2013; Gessler et al. 2014; Altieri et al. 2015; Battipaglia et al. 2016a). In the next paragraphs, we will illustrate specific examples of a double  $\delta^{13}\text{C}$ — $\delta^{18}\text{O}$  model that is relevant for the Mediterranean region.

### 21.5.1 Carbon and Oxygen Isotopes and Forest Dieback in the Mediterranean Basin

Forest vulnerability is reported to be increasing worldwide; forest dieback episodes have been recorded for different species in all biomes (Allen et al. 2015; Adams et al. 2017; Hartmann et al. 2018) and particularly for tree and shrub species in Mediterranean ecosystems. Manifested by a loss in tree vigour (leaf shedding, canopy and shoot dieback) and growth declines, these dieback cases reveal the high vulnerability of forest ecosystems. Increased tree mortality seems to be a response to the rapid rise in temperature and associated drying trends (Camarero et al. 2015; Colangelo et al. 2017). In the Mediterranean, trends of increasing temperature and altered precipitation patterns lead to higher probabilities of extreme events, such as heat waves and fires (IPPC 2014). Species-, age- and microsite-specific plant responses to changing climatic conditions are responsible for the degree of adaptation and survival under limiting conditions. These factors also determine interspecific competition, and thus vegetation dynamics.

The main mechanisms triggering tree decline and mortality have been identified as carbon starvation and hydraulic failure, but the relative importance of the two processes and their link are not clear yet (McDowell et al. 2008, Sala 2009, Sala et al. 2010, Gruber et al. 2010, Sevanto et al. 2014, Gaylord et al. 2015, Hartmann

2015, Rowland et al. 2015, Salmon et al. 2015; Adams et al. 2017). Plants experience hydraulic failure when more water is lost by transpiration than a plant can take up through its root. This creates high xylem water tension and results in progressive cavitation and conductivity loss of the xylem (Sperry et al. 1998; McDowell et al. 2008; Sevanto et al. 2014; Salmon et al. 2015). This process may be most relevant during very severe, short-term droughts (McDowell et al. 2008). On the other hand, carbon starvation occurs when plants close their stomata to prevent desiccation under drought conditions (McDowell et al. 2008). Low water supply leads to a reduction of photosynthetic activity, which, when coupled with the depletion of non-structural carbohydrates (NSC), can induce a negative carbon balance, leading to so-called starvation (McDowell et al. 2008; McDowell and Sevanto 2010; Hartmann 2015; Salmon et al. 2015).

Gessler et al. (2018) developed a conceptual model, based on the Scheidegger model (Scheidegger et al. 2000, see Chap. 16), to assess the mechanisms of drought-induced tree mortality. Using a synchronic approach, they investigated the tree-ring  $\delta^{13}\text{C}$  and  $\delta^{18}\text{O}$  data for different species and found that an increase in  $\delta^{13}\text{C}$  and  $\delta^{18}\text{O}$  in dying trees as compared to surviving ones indicates low photosynthetic activity and stomatal conductance. These conditions can lead to a slow or continuous decline in growth, possibly followed by carbon starvation-induced death. On the other hand, the long-term reduction of  $i\text{WUE}$  in dying trees seems to be associated with increased growth and higher stomatal conductance, inducing possible hydraulic failure in dying trees. However, those findings show a huge variability among species and sites. This variability is linked to the complex processes regulating growth and, in particular, the fractionation processes that take place during the mobilization of photosynthetic assimilates from the leaf to the wood (Gessler et al. 2014). Indeed, it has been demonstrated that trees may use remobilized carbohydrates (primarily starch) for the formation of tree rings. These stored carbohydrates may have been produced months or even years earlier (Gessler et al. 2014). This is especially possible in Mediterranean biomes, where the growing season is very long (Castagneri et al. 2018) and where xylogenesis can be interrupted more than once during the year (Balzano et al. 2019, 2018). In this case, a multidisciplinary approach is required to disentangle the different processes underpinning changes in growth and  $i\text{WUE}$ , and to better understand the causes of tree diebacks (Cailleret et al. 2017; Colangelo et al. 2017; Camarero et al. 2015, 2019).

### ***21.5.2 Carbon and Oxygen Isotopes and IADF***

Intra-annual density fluctuations (IADFs) are abrupt changes in density within a tree ring, and are frequently found in Mediterranean species as a response to seasonal climate fluctuations between dry and wet periods (Bräuning 1999; Campelo et al. 2007; Cherubini et al. 2003; Rigling et al. 2001; Schulman 1938; Tingley 1937; De Micco et al. 2016). Although IADF frequency is related to tree age, size, and tree-ring width, as well as to genetic and site conditions, it mainly depends on drought. IADF

frequency is the result of wood functional trait adjustments to preserve hydraulic conductivity under Mediterranean “double stress” conditions (De Micco et al. 2016). The ability to adapt to highly seasonal Mediterranean conditions may depend on a species’ capacity to adjust cambial activity in order to cope with the prevailing environmental conditions. Trees that are not able to quickly adjust their wood traits to respond to climate are more vulnerable to drought (Martinez-Meier et al. 2008). Nevertheless, the question of whether these adaptations result from a hydraulic structure adjustment to avoid stressful conditions or to take advantage of favorable ones is still open (Battipaglia et al. 2016a).

Carbon and oxygen stable isotopes have been used both separately and together to study IADF formation in *Pinus pinaster* (De Micco et al. 2007), *Arbutus unedo* (Battipaglia et al. 2010a; b), *Erica arborea* (Battipaglia et al. 2014a), *Quercus ilex*, and *Pinus pinea* (Zalloni et al. 2018, 2019), and to infer information about IADF functionality. In particular, the position of IADF within the rings is linked with several microclimatic factors and varies within the same species according to the soil water availability, reflects different  $\delta^{13}\text{C}$  signals (Battipaglia et al. 2010a). An increase in  $\delta^{13}\text{C}$  is almost always found in the first half of the ring (in the so-called E-IADF band of latewood-like cells in the earlywood; see De Micco et al. 2016) as a consequence of stomatal closure under drought stress, when the tree reduces its vulnerability to cavitation, with a low hydraulic conductivity (De Micco et al. 2007, Battipaglia et al. 2010a, 2014a). A decrease in  $\delta^{13}\text{C}$  is typically found in the second half of the ring in the so-called L-IADF (earlywood-like cells in the latewood) and corresponds with a reactivation of the cambium and of photosynthetic activity due to late-summer or early-autumn water availability following summer dormancy (Battipaglia et al. 2014a). The importance of the position of IADFs and their link to a common ecophysiological process was analysed using a network approach to examine  $\delta^{13}\text{C}$  and  $\delta^{18}\text{O}$  in several species (*P. pinea* from Italy, *Pinus halepensis* from Spain and Slovenia; *P. pinaster* from Portugal, *Larix decidua* from Poland, and *L. decidua xkaempferi* from Austria). For all the different sites and species, the types of IADF and their positions had the same isotopic signals in terms of carbon and oxygen. E-IADFs presented  $\delta^{13}\text{C}$  and  $\delta^{18}\text{O}$  in the range of  $-23 \pm 0.6\text{‰}$  and  $32 \pm 1\text{‰}$ , respectively; L-IADFs had  $\delta^{13}\text{C}$  and  $\delta^{18}\text{O}$  values of  $-27 \pm 0.7\text{‰}$  and  $29 \pm 0.5\text{‰}$ , respectively (Battipaglia et al. 2016a). These results should be extended to a larger database in order to assess how the isotopic composition of IADFs could help with dating problematic samples and support the interpretation of phenomena that trigger the formation of IADFs in the Mediterranean environment.

### 21.5.3 Carbon and Oxygen Isotopes and Fire

Fire has been a frequent and important disturbance in Mediterranean forest ecosystems throughout the Holocene (Heinselman 1981; FAO, State of Mediterranean Forest 2018), shaping landscapes and determining vegetation distribution and dynamics. Tree rings have been used to reconstruct fire history and to determine

the effects of fire on forest productivity. In recent years, carbon and oxygen isotopes measured in tree rings have proved to be a useful tool for understanding the complex ecophysiological processes that occur in Mediterranean tree species following a wildfire or prescribed burning (Beghin et al. 2011; Battipaglia et al. 2014b, c, 2016b, 2019; De Micco et al. 2014; Valor et al. 2018; Niccoli et al. 2019). Because conifers are widespread in the Mediterranean Basin and highly prone to fire damage, many studies have focused on conifer species, including *Pinus sylvestris* (Beghin et al., 2011), *Pinus halepensis* (Battipaglia et al. 2014b; c; Valor et al. 2018), *Pinus pinea* (Battipaglia et al. 2016b), and *Pinus pinaster* (Niccoli et al. 2019). Stable isotopes studies indicate that tree response and their potential to recover over the short- and long-term depends on fire severity. Strong wildfires produce a simultaneous increase in tree-ring  $\delta^{13}\text{C}$  and  $\delta^{18}\text{O}$ , suggesting a strong reduction in stomatal conductance and assimilation rate, which are often linked to crown damage (Battipaglia et al. 2014b; Niccoli et al. 2019). When fire severity is low to moderate, the effect on trees is less pronounced; often, the tree rings only report a small variation in  $\delta^{13}\text{C}$ , with no change of  $\delta^{18}\text{O}$ . In these cases, a reduction in tree growth is largely due to the reduced photosynthetic capacity of the burned trees (Battipaglia et al. 2016b). Following prescribed burning s, however, trees show a decrease in both  $\delta^{13}\text{C}$  and  $\delta^{18}\text{O}$ , indicating a possible favorable effect of reduced competition between the surviving plants. In addition to reducing competition, prescribed burning seems to lead to a release of nutrients, which can also stimulate the growth of surviving trees (Battipaglia et al. 2014c, 2016b; Valor et al. 2018; Niccoli et al. 2019).

## 21.6 Nitrogen Stable Isotopes

Nitrogen availability is an important factor limiting productivity in Mediterranean ecosystems (Noy-Meir 1973; Gutierrez and Withford 1987; Lloret et al. 1999) and therefore influencing wood formation. Tree-ring  $\delta^{15}\text{N}$  is mainly influenced by the isotopic ratio of the available nitrogen sources (Nadelhoffer and Fry 1994; Peñuelas and Estiarte 1997; Evans 2001, Stewart et al. 2001). Thus, tree-ring  $\delta^{15}\text{N}$  allows for the reconstruction of the nitrogen source and the relative activity of the different biogeochemical processes that affect the  $\delta^{15}\text{N}$  of nitrogen compounds taken up by trees in the surrounding ecosystem (i.e., mineralization, nitrification, denitrification and,  $\text{NO}_3$  leaching; see Chap. 12). However, other fractionation events that occur in plants during assimilation processes can also influence tree-ring  $\delta^{15}\text{N}$  and complicate interpretation of the nitrogen sources (Evans 2001). Indeed, tree-ring  $\delta^{15}\text{N}$  may also depend on nitrogen reabsorption or re-translocation (Kolb and Evans 2002) or fractionation by different mycorrhizal associations (Michelsen et al. 1998; Craine et al. 2009). The incorporated tree-ring  $\delta^{15}\text{N}$  signature thus results from an integration of nitrogen sources and internal transformations. These complications may explain why only a limited number of studies have been carried out in Mediterranean ecosystems, most of which have focused on understanding the effects of climate change on carbon and nitrogen cycles (Peñuelas et al. 1996; Alfaro-Sanchez et al. 2016).

Tree-ring  $\delta^{15}\text{N}$  has also been used to assess changes in nitrogen availability due to (i) variations in atmospheric nitrogen deposition and (ii) their influence on ecosystem nitrogen dynamics, since the nitrogen isotope ratio in compounds produced as a result of anthropogenic activities may be significantly different from the natural background  $\delta^{15}\text{N}$  in the soil (Freyer 1991). Guerrieri et al. (2009, 2011) and Battipaglia et al. (2010b) showed that increases in nitrogen deposition from the atmosphere or from fertilization are reflected in tree-ring  $\delta^{15}\text{N}$  signals as a result of source  $\delta^{15}\text{N}$  (e.g.,  $\text{NO}_x$ ,  $\text{NH}_x$  forms, or  $\text{NH}_4^+$  vs  $\text{NO}_3^-$ ) and the processes occurring during different phases of soil biogeochemical processes (i.e., losses caused by  $\text{NO}_3^-$  leaching, denitrification, and  $\text{NH}_3$  volatilization; see also Chap. 12). Changes in  $\delta^{15}\text{N}$  in annual tree-rings reflect the causes of variation in the tree's iWUE due to climatic or anthropogenic impacts, suggesting that an increase in nitrogen input from the atmosphere (Guerrieri et al. 2011) or from consociation from nitrogen-fixing species could lead to an increase of trees iWUE under a scenario of reduction in precipitation, such as in Mediterranean area (Guerrieri et al. 2011; Battipaglia et al. 2017). Measurement of  $\delta^{15}\text{N}$  of the different possible sources, and a better understanding of the fractionation processes in the different species, is needed for a proper interpretation of tree-ring  $\delta^{15}\text{N}$  data.

## 21.7 Conclusions and Outlook

Tree-ring isotope studies in the Mediterranean Basin have increased in the last years for two main reasons. First, there is general agreement regarding the importance of reliable information about how Mediterranean trees are responding to a changing climate. Such information informs assessments of the future state of such vulnerable forests, as well as their role in carbon sequestration and ecosystem services. Second, stable isotopes help to identify the ecological behavior and vulnerability of Mediterranean tree and shrub species, information that can improve management options. Further research is needed to improve our knowledge about the xylem plasticity of the different Mediterranean species. This will help pinpoint how cambial activity affects the functional processes of trees and their responses to climate change. The combination of multiple approaches, including stable isotopes, xylogenesis, wood anatomy, and long-term growth and isotope-based gas exchange data, may provide more insight on how plants optimize growth and minimize costs.

**Acknowledgements** The authors thank Francesco Niccoli for helping with Figure 21.1 and Erin Gleeson for English editing.



## References

- Adams HD, Zeppel MJB, Anderegg WRL, Hartmann H, Landhäusser SM, Tissue DT, Huxman TE, Hudson PJ, Franz TE, Allen CD, Anderegg LD, Allen CD (2017) A multi-species synthesis of physiological mechanisms in drought-induced tree mortality. *Nature Ecol Evol* 1(9):1285–1291. <https://doi.org/10.1038/s41559-017-0248-x>
- Aguilera M, Espinar C, Ferrio JP, Pérez G, Voltas J (2009) A map of autumn precipitation for the third millennium BP in the eastern Iberian Peninsula from charcoal carbon isotopes. *J Geochem Explor* 102(3):157–165. <https://doi.org/10.1016/j.gexplo.2008.11.019>
- Aguilera M, Ferrio JP, Araus JL, Tarrús J, Voltas J (2011) Climate at the onset of western Mediterranean agriculture expansion: evidence from stable isotopes of sub-fossil oak tree rings in Spain. *Palaeogeogr, Palaeoclimatol, Palaeoecol* 299(3–4):541–551. <https://doi.org/10.1016/j.palaeo.2010.11.026>
- Alfaro-Sánchez R, Camarero JJ, Sánchez-Salguero R, Sangüesa-Barreda G, De Las HJ (2016) Post-fire Aleppo pine growth, C and N isotope composition depend on site dryness. *Trees—Struct Funct* 30(3):581–595. <https://doi.org/10.1007/s00468-015-1342-9>
- Allen CD, Breshears DD, McDowell NG (2015) On underestimation of global vulnerability to tree mortality and forest die-off from hotter drought in the Anthropocene. *Ecosphere* 6(8). <https://doi.org/10.1890/ES15-00203.1>
- Alessio GA, de Lillis M, Brugnoli E, Lauteri M (2004) Water sources and water-use efficiency in Mediterranean coastal dune vegetation. *Plant Boil* 6:350–357. <https://doi.org/10.1055/s-2004-820882>
- Allison GB, Leaney FW (1982) Estimation of isotopic exchange parameters, using constant-feed pans. *J Hydrol* 55:151–161
- Altieri S, Mereu S, Cherubini P, Castaldi S, Sirignano C, Battipaglia LC, G, (2015) Tree-ring carbon and oxygen isotopes indicate different water use strategies in three Mediterranean shrubs at Capo Caccia (Sardinia, Italy). *Trees—Struct Funct* 29(5):1593–1603. <https://doi.org/10.1007/s00468-015-1242-z>
- Balzano A, Cufar K, Battipaglia G, Merela M, Prislán P, Aronne G, De Micco V (2018) Xylogenesis reveals the genesis and ecological signal of IADFs in *Pinus pinea* L. and *Arbutus unedo* L. and. *Ann Botany* 121(6):1231–1242. <https://doi.org/10.1093/aob/mcy008>
- Balzano A, Battipaglia G, De Micco V (2019) Wood-trait analysis to understand climatic factors triggering intra-annual density-fluctuations in co-occurring Mediterranean trees. *IAWA J* 40(2):241–258. <https://doi.org/10.1163/22941932-40190220>
- Barbeta A, Peñuelas J (2017) Increasing carbon discrimination rates and depth of water uptake favor the growth of Mediterranean evergreen trees in the ecotone with temperate deciduous forests. *Glob Change Biol* 23(12):5054–5068. <https://doi.org/10.1111/gcb.13770>
- Barbour MM (2007) Stable oxygen isotope composition of plant tissue: a review. *Funct Plant Biol* 34(2):83. <https://doi.org/10.1071/fp06228>
- Bartolomei P (1995) Solar flare particle effects and seasonal radiocarbon variations in tree rings of the Northern and Southern Hemispheres. *Radiocarbon* 37(2):593–598. <https://doi.org/10.1017/S003822200031088>
- Battipaglia G, Jäggi M, Saurer M, Siegwolf RTW, Cotrufo MF (2008) Climatic sensitivity of  $\delta^{18}\text{O}$  in the wood and cellulose of tree rings: results from a mixed stand of *Acer pseudoplatanus* L. and *Fagus sylvatica* L. *Palaeogeogr Palaeoclimatol Palaeoecol* 261(1–2):193–202. <https://doi.org/10.1016/j.palaeo.2008.01.020>
- Battipaglia G, Saurer M, Cherubini P, Siegwolf RTW, Cotrufo MF (2009) Tree rings indicate different drought resistance of a native (*Abies alba* mill.) and a nonnative (*Picea abies* (L.) karst.) species co-occurring at a dry site in southern Italy. *Forest Ecol Manage* 257(3):820–828. <https://doi.org/10.1016/j.foreco.2008.10.015>
- Battipaglia G, De Micco V, Brand WA, Linke P, Aronne G, Saurer M, Cherubini P (2010a) Variations of vessel diameter and  $\delta^{13}\text{C}$  in false rings of *Arbutus unedo* L. reflect different environmental conditions. *New Phytol* 188(4):1099–1112. <https://doi.org/10.1111/j.1469-8137.2010.03443.x>

- Battipaglia G, Marzaioli F, Lubritto C, Altieri S, Strumia S, Cherubini P, Cotrufo MF (2010b) Traffic pollution affects tree-ring width and isotopic composition of *Pinus pinea*. *Sci Total Environ* 408(3):586–593. <https://doi.org/10.1016/j.scitotenv.2009.09.036>
- Battipaglia G, De Micco V, Brand WA, Saurer M, Aronne G, Linke P, Cherubini P (2014a) Drought impact on water use efficiency and intra-annual density fluctuations in *Erica arborea* on Elba (Italy). *Plant, Cell Environ* 37(2):382–391. <https://doi.org/10.1111/pce.12160>
- Battipaglia G, De Micco V, Fournier T, Aronne G, Carcaillet C (2014b) Isotopic and anatomical signals for interpreting fire-related responses in *Pinus halepensis*. *Trees—Struct Funct* 28(4):1095–1104. <https://doi.org/10.1007/s00468-014-1020-3>
- Battipaglia G, Strumia S, Esposito A, Giuditta E, Sirignano C, Altieri S, Rutigliano FA (2014c) The effects of prescribed burning on *Pinus halepensis* mill. as revealed by dendrochronological and isotopic analyses. *Forest Ecol Manage* 334:201–208. <https://doi.org/10.1016/j.foreco.2014.09.010>
- Battipaglia G, Campelo F, Vieira J, Grabner M, De Micco V, Nabais C, de Luis M et al (2016a) Structure and function of intra-annual density fluctuations: mind the gaps. *Front Plant Sci* 7:1–8. <https://doi.org/10.3389/fpls.2016.00595>
- Battipaglia G, Savi T, Ascoli D, Castagneri D, Esposito A, Mayr S, Nardini A (2016b) Effects of prescribed burning on ecophysiological, anatomical and stem hydraulic properties in *Pinus pinea* L. *Tree Physiol* 36(8):1–13. <https://doi.org/10.1093/treephys/tpw034>
- Battipaglia G, Pelleri F, Lombardi F, Altieri S, Vitone A, Conte E, Tognetti R (2017) Effects of associating *Quercus robur* L. and *Alnus cordata* loisel. on plantation productivity and water use efficiency. *Forest Ecol Manage* 391:106–114. <https://doi.org/10.1016/j.foreco.2017.02.019>
- Beeckman H (2016) Wood anatomy and trait-based ecology. *IAWA J* 37:127–151
- Beghin R, Cherubini P, Battipaglia G, Siegwolf R, Saurer M, Bovio G (2011) Tree-ring growth and stable isotopes ( $^{13}\text{C}$  and  $^{15}\text{N}$ ) detect effects of wildfires on tree physiological processes in *Pinus sylvestris* L. *Trees Struct Funct* 25:627–636. <https://doi.org/10.1007/s00468-011-0539-9>
- Bogino SM, Bravo F (2014) Carbon stable isotope-climate association in tree rings of *Pinus pinaster* and *Pinus sylvestris* in Mediterranean environments. [Asociación entre el clima y los isótopos estables de carbono en los anillos de crecimiento de *Pinus pinaster* y *Pinus sylvestris* en ambientes Mediterráneos]. *Bosque* 35(2):175–184. <https://doi.org/10.4067/S0717-92002014000200005>
- Bräuning A (1999) Dendroclimatological potential of drought-sensitive tree stands in Southern Tibet for the reconstruction of monsoonal activity. *IAWA J* 20(3):325–338
- Brienen RJW, Gloor E, Clerici S, Newton R, Arppe L, Boom A, Timonen M et al (2017) Tree height strongly affects estimates of water-use efficiency responses to climate and  $\text{CO}_2$  using isotopes. *Nat Commun* 8(1). <https://doi.org/10.1038/s41467-017-00225-z>
- Brito P, Grams TEE, Matyssek R, Jimenez MS, Gonzalez-Rodríguez AM, Oberhuber W, Wieser G (2016) Increased water use efficiency does not prevent growth decline of *Pinus canariensis* in a semi-arid treeline ecotone in tenerife, canary islands (Spain). *Ann Forest Sci* 73(3):741–749. <https://doi.org/10.1007/s13595-016-0562-5>
- Brooks JR, Coulombe R (2009) Physiological responses to fertilization recorded in tree rings: isotopic lessons from a long-term fertilization trial. *Ecol Appl* 19(4):1044–1060. <https://doi.org/10.1890/08-0310.1>
- Bert D, Leavitt SW, Dupouey JL (1997) Variations of wood  $\delta^{13}\text{C}$  and water-use efficiency of *Abies alba* during the last century. *Ecology* 78(1997):1588–1596. [https://doi.org/10.1890/0012-9658\(1997\)078\[1588:vowcaw\]2.0.co](https://doi.org/10.1890/0012-9658(1997)078[1588:vowcaw]2.0.co)
- Caillieret M, Jansen S, Robert EMR, deSoto L, Martinez-Vilalta J et al (2017) A synthesis of radial growth patterns preceding tree mortality. *Glob Chang Biol* 23:1675–1690
- Camarero JJ, Olano JM, Perras A (2010) Plastic bimodal xylogenesis in conifers from continental Mediterranean climates. *New Phytol* 185:471–480
- Camarero JJ, Gazol A, Sangüesa-Barreda G, Oliva J, Vicente-Serrano SM (2015) To die or not to die: early-warning signals of dieback in response to a severe drought. *J Ecol* 103:44–57

- Camarero JJ, Sangüesa-Barreda G, Pérez-Díaz S, Montiel-Molina C, Seijo F, López-Sáez JA (2019) Abrupt regime shifts in post-fire resilience of Mediterranean mountain pinewoods are fuelled by land use. *Int J Wildland Fire*. <https://doi.org/10.1071/wf18160>
- Campelo F, Nabais C, Freitas H, Gutiérrez E (2007) Climatic significance of tree-ring width and intra-annual density fluctuations in *Pinus pinea* from a dry Mediterranean area in Portugal. *Ann for Sci* 64:229–238
- Carvalho A, Nabais C, Vieira J, Rossi S, & Campelo F (2015) Plastic response of tracheids in *Pinus pinaster* in a water-limited environment: adjusting lumen size instead of wall thickness. *PLoS ONE* 10:e0136305. <https://doi.org/10.1371/journal.pone.0136305>
- Castagneri D, Battipaglia G, Von Arx G, Pacheco A, Carrer M (2018) Tree-ring anatomy and carbon isotope ratio show both direct and legacy effects of climate on bimodal xylem formation in *Pinus pinea*. *Tree Physiol* 38(8):1098–1109. <https://doi.org/10.1093/treephys/tpy036>
- Cernusak LA, Barbour MM, Arndt SK et al (2016) Stable isotopes in leaf water of terrestrial plants. *Plant Cell Environ* 39:1087–1102
- Cherubini P, Gartner BL, Tognetti R, Brañker OU, Schoch W, Innes JL. (2003) Identification, measurement and interpretation of tree rings in woody species from Mediterranean climates. *Biol Rev Cambridge Philos Soc* 78:119–148
- Cherubini P, Humbel T, Beeckman H, Gartner H, Mannes D, Pearson C, Schoch W, Tognetti R, Levyadun S (2013) Olive tree-ring problematic dating: a comparative analysis on Santorini (Greece). *PLoS ONE* 8(1):1–5, e54730
- Colangelo M, Camarero JJ, Battipaglia G, Borghetti M, De Micco V, Gentilesca T, Ripullone F (2017) A multi-proxy assessment of dieback causes in a mediterranean oak species. *Tree Physiol* 37(5):617–631. <https://doi.org/10.1093/treephys/tpx002>
- Craig H, Gordon LI (1965) Deuterium and oxygen 18 variations in the ocean and the marine atmosphere. In: Tongiorgi E (ed) Stable isotopes in oceanographic studies and paleotemperatures. Laboratorio di Geologia Nucleare, Pisa, pp 9–130
- Craine JM, Elmore AJ, Aidiar MPM, Bustamante M, Dawson TE, Hobbie EA, Kahmen A, Mack MC, McLaughlan KK, Michelsen A et al (2009) Global patterns of foliar nitrogen isotopes and their relationships with climate, mycorrhizal fungi, foliar nutrient concentrations, and nitrogen availability. *New Phytol* 183:980–992
- Dansgaard W (1964) Stable isotopes in precipitation. *Tellus* 16:436–468
- Davis MA, Wrage KJ, Reich PB, Tjoelker MG, Schaeffer T, Muermann C (1999) Survival, growth, and photosynthesis of tree seedlings competing with herbaceous vegetation along a water-light-nitrogen gradient. *Plant Ecol* 145:341–350
- Dawson TE (1998) Fog in the California redwood forest: ecosystem inputs and use by plants. *Oecologia* 117(4):476–485. <https://doi.org/10.1007/s004420050683>
- Dawson TE, Ehleringer JR (1993) Isotopic enrichment of water in the “woody” tissues of plants: implications for plant water source, water uptake, and other studies which use stable isotopic composition of cellulose. *Geochim Cosmochim Acta* 57:3487–3492
- Dawson TE, Ehleringer JR (1998) The role of plants in catchment-level hydraulic processes: insights from stable isotope studies. In: Kendall C, McDonnell JJ (eds) Isotope tracers in catchment hydrology. Elsevier; Amsterdam, pp 165–202
- Del Castillo J, Aguilera M, Voltas J, Ferrio JP (2013) Isoscapes of tree-ring carbon-13 perform like meteorological networks in predicting regional precipitation patterns. *J Geophys Res: Biogeosci* 118(1):352–360. <https://doi.org/10.1002/jgrg.20036>
- De Micco V, Aronne G (2012) Occurrence of morphological and anatomical adaptive traits in young and adult plants of the rare Mediterranean cliff species *Primula palinuri* Petagna. *The Sci World J*. <https://doi.org/10.1100/2012/471814>
- De Micco V, Saurer M, Aronne G, Tognetti R, Cherubini P (2007) Variations of wood anatomy and  $\delta^{13}\text{C}$  within-tree rings of coastal *Pinus pinaster* showing intra-annual density fluctuations. *IAWA J* 28(1):61–74
- De Micco V, Battipaglia G, Brand WA, Linke P, Saurer M, Aronne G, Cherubini P (2012) Discrete versus continuous analysis of anatomical and  $\delta^{13}\text{C}$  variability in tree rings with intra-annual

- density fluctuations. *Trees—Struct Funct* 26(2):513–524. <https://doi.org/10.1007/s00468-011-0612-4>
- De Micco V, Battipaglia G, Cherubini P, Aronne G (2014) Comparing methods to analyse anatomical features of tree rings with and without intra-annual-density-fluctuations (IADFs). *Dendrochronologia* 32:1–6. <https://doi.org/10.1016/j.dendro.2013.06.001>
- De Micco V, Campelo F, De Luis M, Bräuning A, Grabner M, Battipaglia G, Cherubini P (2016) Intra-annual density fluctuations in tree rings: how, when, where, and why? *IAWA J* 37(2):232–259. <https://doi.org/10.1163/22941932-20160132>
- De Micco V, Carrer M, Rathgeber CBK, Julio Camarero J, Voltas J, Cherubini P, Battipaglia G (2019) From xylogenesis to tree rings: wood traits to investigate tree response to environmental changes. *IAWA J* 40(2):155–182. <https://doi.org/10.1163/22941932-40190246>
- Diefendorf AF, Mueller KE, Wing SL, Koch PL, Freeman KH (2010) Global patterns in leaf  $^{13}\text{C}$  discrimination and implications for studies of past and future climate. *Proc Natl Acad Sci* 107(13):5738–5743. <https://doi.org/10.1073/pnas.0910513107>
- Diffenbaugh NS, Giorgi F (2012) Climate change hotspots in the CMIP5 global climate model ensemble. *Clim Change* 114(3–4):813–822. <https://doi.org/10.1007/s10584-012-0570-x>
- Di Matteo G, De Angelis P, Brugnoli E, Cherubini P, & Scarascia-Mugnozza G (2010) Tree-ring  $\Delta^{13}\text{C}$  reveals the impact of past forest management on water-use efficiency in a mediterranean oak coppice in Tuscany (Italy). *Ann Forest Sci* 67(5). <https://doi.org/10.1051/forest/2010012>
- Ehleringer JR, Dawson TE (1992) Water uptake by plants: perspectives from stable isotope composition. *Plant, Cell Environ* 15(9):1073–1082. <https://doi.org/10.1111/j.1365-3040.1992.tb01657.x>
- Ehleringer JR, Hall AE, Farquhar GD (1993) Introduction: water use in relation to productivity. In: Ehleringer JR, Hall AE, Farquhar GD (eds) *Stable isotopes and plant carbon–water relations*. Academic Press, New York, pp 3–8
- Evans R (2001) Physiological mechanisms influencing plant nitrogen isotope composition. *Trends Plant Sci* 6:121–126
- Farquhar GD, Leary MHO, Berry JA (1982) On the relationship between carbon isotope discrimination and the intercellular carbon dioxide concentration in leaves. *Aust J Plant Physiol* 9:121–137
- Farquhar GD, Ehleringer JR, Hubick KT (1989) Carbon isotope discrimination and photosynthesis. *Ann Rev Plant Physiol Plant Mol Biol* 40:503–537
- Fernández-de-Uña L, McDowell NG, Cañellas I, Gea-Izquierdo G (2016) Disentangling the effect of competition,  $\text{CO}_2$  and climate on intrinsic water-use efficiency and tree growth. *J Ecol* 104(3):678–690. <https://doi.org/10.1111/1365-2745.12544>
- Fernández-De-Uña L, Rossi S, Aranda I, Fonti P, González-González BD, Cañellas I, Gea-Izquierdo G (2017) Xylem and leaf functional adjustments to drought in *Pinus sylvestris* and *Quercus pyrenaica* at their elevational boundary. *Front Plant Sci* 8. <https://doi.org/10.3389/fpls.2017.01200>
- Ferrio JP, Florit A, Vega A, Serrano L, Voltas J (2003)  $\text{D}^{13}\text{C}$  and tree-ring width reflect different drought responses in *Quercus ilex* and *Pinus halepensis*. *Oecologia* 137(4):512–518. <https://doi.org/10.1007/s00442-003-1372-7>
- Ferrio JP, Voltas J (2005) Carbon and oxygen isotope ratios in wood constituents of *Pinus halepensis* as indicators of precipitation, temperature and vapour pressure deficit. *Tellus* 57B:164–173
- Forrester DI (2015) Transpiration and water-use efficiency in mixed-species forests versus monocultures: effects of tree size, stand density and season. *Tree Physiol* 35(3):289–304. <https://doi.org/10.1093/treephys/tpv011>
- Francey RJ, Farquhar GD (1982) An explanation of  $^{13}\text{C}/^{12}\text{C}$  variations in tree rings. *Nature* 297:28–31
- Freyer HD (1991) Seasonal variation of  $^{15}\text{N}/^{14}\text{N}$  ratios in atmospheric nitrate species. *Tellus B* 43(1):30–44. <https://doi.org/10.1034/j.1600-0889.1991.00003.x>
- Gaylord ML, Kolb TE, McDowell NG (2015) Mechanisms of piñon pine mortality after severe drought: a retrospective study of mature trees. *Tree Physiol* 35:806–816

- Gessler A, Ferrio JP, Hommel R, Treydte K, Werner RA, Monson RK (2014) Stable isotopes in tree rings: towards a mechanistic understanding of isotope fractionation and mixing processes from the leaves to the wood. *Tree Physiol* 34(8):796–818. <https://doi.org/10.1093/treephys/tpu040>
- Gessler A, Caillieret M, Joseph J, Schönbeck L, Schaub M, Lehmann M, Treydte K, Rigling A, Timofeeva G, Saurer M (2018) Drought induced tree mortality—a tree-ring isotope based conceptual model to assess mechanisms and predispositions. *New Phytol* 219(2):485–490. <https://doi.org/10.1111/nph.15154>
- González-Muñoz N, Linares JC, Castro-Díez P, Sass-Klaassen U (2015) Contrasting secondary growth and water-use efficiency patterns in native and exotic trees co-occurring in inner Spain riparian forests. *Forest Syst* 24(1). <https://doi.org/10.5424/fs/2015241-06586>
- Grams TE, Kozovits AR, Haberle KH, Matyssek R, Dawson TE (2007) Combining  $\delta^{13}\text{C}$  and  $\delta^{18}\text{O}$  analyses to unravel competition,  $\text{CO}_2$  and  $\text{O}_3$  effects on the physiological performance of different-aged trees. *Plant, Cell Environ* 30:1023–1034
- Granda E, Rossatto DR, Camarero JJ, Voltas J, Valladares F (2014) Growth and carbon isotopes of Mediterranean trees reveal contrasting responses to increased carbon dioxide and drought. *Oecologia* 174(1):307–317. <https://doi.org/10.1007/s00442-013-2742-4>
- Gratani L (1995) Structural and ecophysiological plasticity of some evergreen species of the Mediterranean maquis in response to climate. *Photosynthetica* 31:335–343
- Gutierrez JR, Whitford WG (1987) Chihuahuan desert annuals: importance of water and nitrogen. *Ecology* 68:2032–2045
- Guerrieri MR, Siegwolf RTW, Saurer M, Jäggi M, Cherubini P, Ripullone F, Borghetti M (2009) Impact of different nitrogen emission sources on tree physiology as assessed by a triple stable isotope approach. *Atmos Environ* 43(2):410–418. <https://doi.org/10.1016/j.atmosenv.2008.08.042>
- Guerrieri R, Siegwolf R, Saurer M, Ripullone F, Mencuccini M, Borghetti M (2010) Anthropogenic  $\text{NO}_x$  emissions alter the intrinsic water-use efficiency (WUEi) for quercus cerris stands under Mediterranean climate conditions. *Environ Pollut* 158(9):2841–2847. <https://doi.org/10.1016/j.envpol.2010.06.017>
- Guerrieri R, Mencuccini M, Sheppard LJ, Saurer M, Perks MP, Levy P, Sutton MA, Borghetti M, Grace J (2011) The legacy of enhanced N and S deposition as revealed by the combined analysis of  $\delta^{13}\text{C}$ ,  $\delta^{18}\text{O}$  and  $\delta^{15}\text{N}$  in tree rings. *Glob Change Biol* 17(5):1946–1962. <https://doi.org/10.1111/j.1365-2486.2010.02362.x>
- Gruber A, Strobl S, Veit B, Oberhuber W (2010) Impact of drought on temporal dynamics of wood formation in *Pinus sylvestris*. *Tree Physiol* 30:490–501
- Hartmann H (2015) Carbon starvation during drought-induced tree mortality—are we chasing a myth? *J Plant Physiol* 2(e005):1–5
- Hartmann H, Moura CF, Anderegg WRL, Ruehr NK, Salmon Y, Allen CD, O'Brien M et al (2018) Research frontiers for improving our understanding of drought-induced tree and forest mortality. *New Phytol* 218(1):15–28. <https://doi.org/10.1111/nph.15048>
- Heinselman ML (1981) Fire and succession in the conifer forest of northern North America. In: West DC, Shugart HH, Botkin DB (eds) *Forest succession: concepts and application*. Springer, New York, pp 374–405
- IPCC (2014) *Climate Change 2014: Synthesis Report*. Contribution of Working Groups I, II and III to the Fifth Assessment Report of the Intergovernmental Panel on Climate Change. IPCC, Geneva
- IPCC (2017) *IPCC Fifth Assessment Report (AR5) Observed Climate Change Impacts Database*, Version 2.01. Palisades, NY: NASA Socioeconomic Data and Applications Center (SEDAC). <https://doi.org/10.7927/H4FT8J0X>
- Klein T, Hemming D, Lin T, Grünzweig JM, Maseyk K, Rotenberg E, Yakir D (2005) Association between tree-ring and needle  $\delta^{13}\text{C}$  and leaf gas exchange in *Pinus halepensis* under semi-arid conditions. *Oecologia* 144(1):45–54. <https://doi.org/10.1007/s00442-005-0002-y>

- Konter O, Holzkämper S, Helle G, Büntgen U, Saurer M, Esper J (2014) Climate sensitivity and parameter coherency in annually resolved  $\delta^{13}\text{C}$  and  $\delta^{18}\text{O}$  from *pinus uncinata* tree-ring data in the Spanish Pyrenees. *Chem Geol* 377:12–19. <https://doi.org/10.1016/j.chemgeo.2014.03.021>
- Kohn MJ (2010) Carbon isotope compositions of terrestrial C3 plants as indicators of (paleo)ecology and (paleo)climate. *Proc Natl Acad Sci* 107(46):19691–19695. <https://doi.org/10.1073/pnas.1004933107>
- Kolb KJ, Evans RD (2002) Implications of leaf nitrogen recycling on the nitrogen isotope composition of deciduous plant tissues. *New Phytol* 156:57–64
- Larcher W (2000) Temperature stress and survival ability of Mediterranean sclerophyllous plants. *Plant Biosyst* 134:279–295
- Liñán ID, Gutiérrez E, Andreu-Hayles L, Heinrich I, Helle G (2012) Potential to explain climate from tree rings in the south of the Iberian Peninsula. *Climate Res* 55(2):119–134. <https://doi.org/10.3354/cr01126>
- Linares JC, Delgado-Huertas A, Camarero JJ, Merino J, Carreira JA (2009) Competition and drought limit the response of water-use efficiency to rising atmospheric carbon dioxide in the Mediterranean fir *Abies pinsapo*. *Oecologia* 161(3):611–624. <https://doi.org/10.1007/s00442-009-1409-7>
- Linares JC, Delgado-Huertas A, Carreira JA (2011) Climatic trends and different drought adaptive capacity and vulnerability in a mixed *Abies pinsapo*-*Pinus halepensis* forest. *Clim Change* 105(1):67–90. <https://doi.org/10.1007/s10584-010-9878-6>
- Lloret F, Casanovas C, Peñuelas J (1999) Seedling survival of Mediterranean shrubland species in relation to root: shoot ratio, seed size and water and nitrogen use. *Funct Ecol* 13:210–216
- Lo Gullo MA, Salleo S (1988) Different strategies of drought resistance in three Mediterranean sclerophyllous trees growing in the same environmental conditions. *New Phytol* (Cambridge, Great Britain) 108:267–276
- Margaris NS, Papadogianni P (1977) Cambial activity in some plants dominating phryganean formations in Greece. *Phyton* (Greece) 36:1–5
- Martínez-Meier A, Sánchez L, Pastorino M, Gallo L, Rozenberg P (2008) What is hot in tree rings? The wood density of surviving Douglas-firs to the 2003 drought and heat wave. *For Ecol Manage* 256(4):837–884
- Martínez-Sancho E, Dorado-Liñán I, Gutiérrez Merino E, Matiu M, Helle G, Heinrich I, Menzel A (2018) Increased water-use efficiency translates into contrasting growth patterns of Scots pine and sessile oak at their southern distribution limits. *Glob Change Biol* 24(3):1012–1028. <https://doi.org/10.1111/gcb.13937>
- Masle J, Farquhar GD (1988) Effects of soil strength on the relation of water-use efficiency and growth to carbon isotope discrimination in wheat seedlings. *Plant Physiol* 86:32–38
- Maseyk K, Hemming D, Angert A, Leavitt SW, Yakir D (2011) Increase in water-use efficiency and underlying processes in pine forests across a precipitation gradient in the dry Mediterranean region over the past 30 years. *Oecologia* 167(2):573–585
- McCarroll D, Loader NJ (2004) Stable isotope in tree rings. *Quatern Sci Rev* 23:771–801
- McDowell NG, Sevanto S (2010) The mechanisms of carbon starvation: how, when, or does it even occur at all? *New Phytol* 186:264–266
- McDowell NG, Beerling D, Breshears D, Fisher R, Raffa K, Stitt M (2011) Interdependence of mechanisms underlying climate-driven vegetation mortality. *Trends Ecol Evol* 26:523–532
- McDowell N, Pockman WT, Allen CD, Breshears DD, Cobb N, Kolb T, Sperry J, West A, Williams D, Yepez EA (2008) Mechanisms of plant survival and mortality during drought: why do some plants survive while others succumb to drought? Tansley review. *New Phytol* 178:719–739
- McDowell NG, Bond BJ, Dickman LT, Ryan MG, Whitehead D (2011) Relationships between tree height and carbon isotope discrimination. In: Meinzer FC et al (eds) *Size- and age-related changes in tree structure and function*. Springer, New York, NY, USA, pp 255–285
- Meinzer FC, McCulloh KA, Lachenbruch B, Woodruff DR, Johnson DM (2010) The blind men and the elephant: the impact of context and scale in evaluating conflicts between plant hydraulic safety and efficiency. *Oecologia* 164:287–296

- Médail F (2008) Ecosystems: Mediterranean. In: Jørgensen SE, Fath B (eds) *Encyclopedia of ecology*, vols 3, 5. Elsevier, Oxford, pp 2296–2308
- Médail F, Monnet AC, Pavon D, Nikolic T, Dimopoulos P, Bacchetta G, Arroyo J, Barina Z, Albassatneh MC, Domina G, Fady B, Matevski V, Mifsud S, Leriche A (2019) What is a tree in the Mediterranean basin hotspot? A critical analysis. *For Ecosyst* 6 (2019):17. <https://doi.org/10.1186/s40663-019-0170-6>
- Medrano H, Flexas J, Galmés J (2009) Variability in water use efficiency at the leaf level among Mediterranean plants with different growth forms. *Plant Soil* 317(1–2):17–29. <https://doi.org/10.1007/s11104-008-9785-z>
- Michelsen AC, Quarmby C, Sleep D, Jonasson S (1998) Vascular plant  $^{15}\text{N}$  abundance in heath and forest tundra ecosystems is closely correlated with presence and type of mycorrhizal fungi in roots. *Oecologia* 115:406–418
- Mitrakos KA (1980) A theory for Mediterranean plant life. *Acta Oecol* 1:245–252
- Moreno-Gutiérrez C, Battipaglia G, Cherubini P, Saurer M, Nicolás E, Contreras S, Querejeta JJ (2012a) Stand structure modulates the long-term vulnerability of *pinus halepensis* to climatic drought in a semiarid mediterranean ecosystem. *Plant, Cell Environ* 35(6):1026–1039. <https://doi.org/10.1111/j.1365-3040.2011.02469.x>
- Moreno-Gutiérrez C, Dawson TE, Nicolás E, & Querejeta JJ (2012b) Isotopes reveal contrasting water use strategies among coexisting plant species in a Mediterranean ecosystem. *New Phytol* 196:489–496
- Moreno-Gutiérrez C, Battipaglia G, Cherubini P, Delgado Huertas A, Querejeta JJ (2015) Pine afforestation decreases the long-term performance of understorey shrubs in a semi-arid mediterranean ecosystem: a stable isotope approach. *Funct Ecol* 29(1):15–25. <https://doi.org/10.1111/1365-2435.12311>
- Myers N, Mittermeier RA, Mittermeier CG, da Fonseca GAB, Kent J (2000) Biodiversity hotspots for conservation priorities. *Nature* 403:853–858
- Nadelhoffer KJ, Fry B (1994) Nitrogen isotope studies in forest ecosystems. In: Lajtha K, Michener RH (eds) *Stable isotopes in ecology and environmental science*. Blackwell, Oxford, pp 22–44
- Niccoli F, Esposito A, Altieri S, Battipaglia G (2019) Fire severity influences ecophysiological responses of *Pinus pinaster* ait. *Front Plant Sci* 10:539. <https://doi.org/10.3389/fpls.2019.00539>
- Noy-Meir I (1973) Desert ecosystems: environments and producers. *Annu Rev Ecol Syst* 4:25–51
- Pacheco A, Camarero JJ, Carrer M (2016) Linking wood anatomy and xylogenesis allows pinpointing of climate and drought influences on growth of coexisting conifers in continental Mediterranean climate. *Tree Physiol* 36:502–512. <https://doi.org/10.1093/treephys/tpv125>
- Pallardy SG, Čermák J, Ewers FW, Kaufmann MR, Parker WC, Sperry JS (1995) Water transport dynamics in trees and stands. In: Smith TM, Hinckley TM (eds) *Resource physiology of conifers*. Academic Press, San Diego, p 301
- Paris P, Di Matteo G, Tarchi M, Tosi L, Spaccino L, Lauteri M (2018) Precision subsurface drip irrigation increases yield while sustaining water-use efficiency in mediterranean poplar bioenergy plantations. *Forest Ecol Manage* 409:749–756. <https://doi.org/10.1016/j.foreco.2017.12.013>
- Peñuelas J, Estiarte M (1996) Trends in plant carbon concentration and plant demand for N throughout this century. *Oecologia* 109(1):69–73. <https://doi.org/10.1007/s004420050059>
- Peñuelas J, Canadell JG, Ogaya R (2011) Increased water-use efficiency during the 20th century did not translate into enhanced tree growth. *Glob Ecol Biogeogr* 20(4):597–608. <https://doi.org/10.1111/j.1466-8238.2010.00608.x>
- Quézel P, Médail F (2003) *Ecologie et biogéographie des forêts du bassin méditerranéen*. Elsevier, Paris
- Rigling A, Waldner PO, Forster T, Bräker OU, Pouttu A (2001) Ecological interpretation of tree-ring width and intraannual density fluctuations in *pinus sylvestris* on dry sites in the central alps and Siberia. *Can J Forest Res* 31(1):18–31. <https://doi.org/10.1139/x00-126>
- Ripullone F, Guerrieri MR, Saurer M, Siegwolf RTW, Jäggi M, Guarini R, Magnani F (2009) Testing a dual isotope model to track carbon and water gas exchanges in a Mediterranean forest. *iForest* 2:59–66

- Rivas-Martínez S, Asensi A, Garretas B, Valle F, Cano E, Costa M, Luisa López M, Díaz T, Fernández Prieto JA, Llorens L, Del Arco AM, Osorio VE, Pérez L, de Paz P, Wildpret W, Reyes-Betancort J, García Gallo A, Rodríguez O, Acebes J, Gaisberg M, Soriano P (2007) Mapa de series, geoserias y geo-permaseries de vegetación de España. *Itinera Geobot* 17:5–436
- Roden JS, Siegwolf R (2012) Is the dual isotope conceptual model fully operational? *Tree Physiol* 32:1179–1182
- Roden JS, Farquhar GD (2012) A controlled test of the dual-isotope approach for the interpretation of stable carbon and oxygen isotope ratio variation in tree rings. *Tree Physiol* 32:490–503
- Rowland L, da Costa ACL, Galbraith DR, Oliveira RS, Binks OJ, Oliveira AAR, Pullen AM, Doughty CE, Metcalfe DB, Vasconcelos SS, Ferreira LV, Meir P (2015) Death from drought in tropical forests is triggered by hydraulics not carbon starvation. *Nature*. <https://doi.org/10.1038/nature15539>
- Sala A (2009) Lack of direct evidence for the carbon-starvation hypothesis to explain drought-induced mortality in trees. *Proc Natl Acad Sci United States of Am* 106(26). <https://doi.org/10.1073/pnas.0904580106>
- Sala A, Piper F, Hoch G (2010) Physiological mechanisms of drought-induced tree mortality are far from being resolved. *New Phytol* 186(2):274–281. <https://doi.org/10.1111/j.1469-8137.2009.03167.x>
- Salleo S, Nardini A, Lo Gullo MA (1997) Is sclerophylly of Mediterranean evergreens an adaptation to drought? *New Phytol* 135:603–612
- Salmon Y, Torres-Ruiz JM, Poyatos R, Martínez-Vilalta J, Meir P, Cochard H, Mencuccini M (2015) Balancing the risks of hydraulic failure and carbon starvation: a twig scale analysis in declining Scots pine. *Plant, Cell Environ* 38:2575–2588
- Sánchez-Costa E, Poyatos R, Sabaté S, (2015) Contrasting growth and water use strategies in four co-occurring Mediterranean tree species revealed by concurrent measurements of sap flow and stem diameter variations. *Agric for Meteorol* 207:24–37. <https://doi.org/10.1016/j.agrformet.2015.03.012>
- Sargeant CI, Singer MB (2016) Sub-annual variability in historical water source use by mediterranean riparian trees. *Ecohydrology* 9(7):1328–1345. <https://doi.org/10.1002/eco.1730>
- Sarris D, Siegwolf R, Körner C (2013) Inter- and intra-annual stable carbon and oxygen isotope signals in response to drought in Mediterranean pines. *Agric Forest Meteorol* 168:59–68. <https://doi.org/10.1016/j.agrformet.2012.08.007>
- Saurer M, Robertson I, Siegwolf R, Leuenberger M (1998) Oxygen isotope analysis of cellulose: an interlaboratory comparison. *Anal Chem* 70(10):2074–2080. <https://doi.org/10.1021/ac971022f>
- Scheidegger Y, Saurer M, Bahn M, Siegwolf R (2000) Linking stable oxygen and carbon isotopes with stomatal conductance and photosynthetic capacity: a conceptual model. *Oecologia* 125:350–357. <https://doi.org/10.1007/s004420000466>
- Schulman E (1938) Classification of false annual rings in Monterey pine. *Tree-Ring Bull* 4:4–7
- Sevanto S, McDowell NG, Dickman LT, Pangle R, Pockman WT (2014) How do trees die? A test of the hydraulic failure and carbon starvation hypotheses. *Plant Cell Environ* 37:153–151
- Shestakova TA, Aguilera M, Ferrio JP, Gutiérrez E, Voltas J (2014) Unravelling spatiotemporal tree-ring signals in mediterranean oaks: a variance-covariance modelling approach of carbon and oxygen isotope ratios. *Tree Physiol* 34(8):819–838. <https://doi.org/10.1093/treephys/tpu037>
- Shestakova TA, Camarero JJ, Ferrio JP, Knorre AA, Gutiérrez E, Voltas J (2017) Increasing drought effects on five european pines modulate  $\Delta^{13}\text{C}$ -growth coupling along a Mediterranean altitudinal gradient. *Funct Ecol* 31(7):1359–1370. <https://doi.org/10.1111/1365-2435.12857>
- Shestakova TA, Voltas J, Saurer M, Berninger F, Esper J, Andreu-Hayles L, Gutiérrez E et al (2019) Spatio-temporal patterns of tree growth as related to carbon isotope fractionation in european forests under changing climate. *Glob Ecol Biogeogr*. <https://doi.org/10.1111/geb.12933>
- Silva LCR, Horwath WR (2013) Explaining global increases in water use efficiency: why have we overestimated responses to rising atmospheric  $\text{CO}_2$  in natural forest ecosystems? *PLoS ONE* 8(1). <https://doi.org/10.1371/journal.pone.0053089>



- Singer MB, Stella JC, Dufour S, Piégay H, Wilson RJS, Johnstone L (2013) Contrasting water-uptake and growth responses to drought in co-occurring riparian tree species. *Ecohydrology* 6(3):402–412. <https://doi.org/10.1002/eco.1283>
- Sperry JS, Adler FR, Campbell GS, Comstock JP (1998) Limitation of plant water use by rhizosphere and xylem conductance: results from model. *Plant, Cell Environ* 21:347–359
- Sperry JS, Meinzer FC, McCulloh KA (2008) Safety and efficiency conflicts in hydraulic architecture: scaling from tissues to trees. *Plant Cell Environ* 31:632–645
- Stemberg L, Swart PK (1987) Utilization of fresh- water and ocean water by coastal plants of southern Florida. *Ecology* 68:1898–1905
- Stewart D, Barnes J, Cote J, Cudeck R, Malthouse E (2001) Factor analysis. *J Consum Psychol* 10(1–2):75–82. [https://doi.org/10.1207/s15327663jep1001&2\\_07](https://doi.org/10.1207/s15327663jep1001&2_07)
- Szymczak S, Joachimski MM, Bräuning A, Hetzer T, Kuhlemann J (2011) Comparison of whole wood and cellulose carbon and oxygen isotope series from *Pinus nigra* ssp. *laricio* (Corsica/France). *Dendrochronologia* 29(4):219–226. <https://doi.org/10.1016/j.dendro.2011.04.001>
- Szymczak S, Joachimski MM, Bräuning A, Hetzer T, Kuhlemann J (2012a) A 560 yr summer temperature reconstruction for the western mediterranean basin based on stable carbon isotopes from *pinus nigra* ssp. *laricio* (Corsica/France). *Climate of the Past* 8(5):1737–1749. <https://doi.org/10.5194/cp-8-1737-2012>
- Szymczak S, Joachimski MM, Bräuning A, Hetzer T, Kuhlemann J (2012b) Are pooled tree ring  $\delta^{13}\text{C}$  and  $\delta^{18}\text{O}$  series reliable climate archives?—a case study of *Pinus nigra* ssp. *laricio* (Corsica/France). *Chem Geol* 308–309:40–49. <https://doi.org/10.1016/j.chemgeo.2012.03.013>
- Szymczak S, Hetzer T, Bräuning A, Joachimski MM, Leuschner H, Kuhlemann J (2014) Combining wood anatomy and stable isotope variations in a 600-year multi-parameter climate reconstruction from Corsican black pine. *Quatern Sci Rev* 101:146–158. <https://doi.org/10.1016/j.quascirev.2014.07.010>
- Terradas J, Save R (1992) The influence of summer and winter stress and water relationships on the distribution of *Quercus ilex* L. *Vegetatio* 99(100):137–145
- Tingley MA (1937) Double growth rings in Red Astrachan. *Proc Am Soc Horticultural Sci* 34:61
- Valor T, Casals P, Altieri S, González-Olabarria JR, Piqué M, Battipaglia G (2018) Disentangling the effects of crown scorch and competition release on the physiological and growth response of *Pinus halepensis* Mill. using  $\delta^{13}\text{C}$  and  $\delta^{18}\text{O}$  isotopes. *For Ecol Manag* 424:276–287. <https://doi.org/10.1016/j.foreco.2018.04.056>
- Vieira J, Nabais C, Rossi S, Carvalho A, Freitas H, Campelo F (2017) Rain exclusion affects cambial activity in adult maritime pines. *Agric for Meteorol* 237:303–310. <https://doi.org/10.1016/j.agrfor.2017.02.024>
- Voelker SL, Meinzer FC, Lachenbruch B, Brooks JR, Guyette RP (2014) Drivers of radial growth and carbon isotope discrimination of bur oak (*Quercus macrocarpa* michx.) across continental gradients in precipitation, vapour pressure deficit and irradiance. *Plant, Cell Environment* 37(3):766–779. <https://doi.org/10.1111/pce.12196>
- Voltas J, Camarero JJ, Carulla D, Aguilera M, Oriz A, Ferrio JP (2013) A retrospective, dual-isotope approach reveals individual predispositions to winter-drought induced tree dieback in the southernmost distribution limit of Scots pine. *Plant, Cell Environ* 36:1435–1448
- Warren CR, Adams MA (2000) Water availability and branch length determine  $\delta^{13}\text{C}$  in foliage of *Pinus pinaster* *Tree Physiol* 10:637–644
- Wershaw RL, Friedman I, Heller SJ, Frank PA (1966) Hydrogen isotope fractionation of water passing through trees. In: Hobson GD (ed) *Advances in organic geochemistry*. Pergamon Press, New York, pp 55–67
- Wu J, Zhang R, Yang J (1996) Analysis of rainfall-recharge relationships. *J Hydrol* 177:143–160
- Yakir D, da Sternberg L, S. L. (2000) The use of stable isotopes to study ecosystem gas exchange. *Oecologia* 123(3):297–311. <https://doi.org/10.1007/s004420051016>
- Zalloni E, Battipaglia G, Cherubini P, Saurer M, & De Micco V (2018) Contrasting physiological responses to mediterranean climate variability are revealed by intra-annual density fluctuations

in tree rings of *Quercus ilex* L. and *Pinus pinea* L. and. *Tree Physiol* 38(8):1213–1224. <https://doi.org/10.1093/treephys/tpy061>

Zalloni E, Battipaglia G, Cherubini P, Saurer M, De Micco V (2019) Wood growth in pure and mixed *Quercus ilex* l. forests: drought influence depends on site conditions. *Front Plant Sci* 10. <https://doi.org/10.3389/fpls.2019.00397>

**Open Access** This chapter is licensed under the terms of the Creative Commons Attribution 4.0 International License (<http://creativecommons.org/licenses/by/4.0/>), which permits use, sharing, adaptation, distribution and reproduction in any medium or format, as long as you give appropriate credit to the original author(s) and the source, provide a link to the Creative Commons license and indicate if changes were made.

The images or other third party material in this chapter are included in the chapter's Creative Commons license, unless indicated otherwise in a credit line to the material. If material is not included in the chapter's Creative Commons license and your intended use is not permitted by statutory regulation or exceeds the permitted use, you will need to obtain permission directly from the copyright holder.



# Chapter 22

## Stable Isotopes in Tree Rings of Tropical Forests



Peter van der Sleen, Pieter A. Zuidema, and Thijs L. Pons

### 22.1 Introduction

The analysis of growth rings in the stems of trees is a relatively new tool in tropical forests, as the existence of annual rings in tropical trees was not commonly recognized until recently. For a long time, the tropical environment was associated with year-round favorable growth conditions that were thought to prevent the formation of distinct annual growth rings. However, most tropical environments are seasonal to a various extent (Fig. 22.1), and the formation of annual tree rings in deciduous species growing in tropical climates with a pronounced dry season has been known for a long time (Coster 1927). Although ring boundaries of trees in the humid tropics are generally less clear than those in temperate trees, the formation of distinct annual growth rings has been shown for a large number of tropical tree species (Worbes 2002; Rozendaal and Zuidema 2011; Zuidema et al. 2012; Brienen et al. 2016; Schöngart et al. 2017). In addition to drought, other seasonally changing environmental factors, such as flooding and soil salinity, are known to induce the formation of annual ring boundaries (Schöngart et al. 2002; Chowdhury et al. 2008).

---

**Supplementary Information** The online version contains supplementary material available at ([https://doi.org/10.1007/978-3-030-92698-4\\_22](https://doi.org/10.1007/978-3-030-92698-4_22)).

---

P. van der Sleen (✉) · P. A. Zuidema  
Forest Ecology and Forest Management Group, Wageningen University and Research,  
Droevendaalsesteeg 3, 6708 PB Wageningen, The Netherlands  
e-mail: [peter.vandersleen@wur.nl](mailto:peter.vandersleen@wur.nl)

P. van der Sleen  
Wildlife Ecology and Conservation Group, Wageningen University and Research,  
Droevendaalsesteeg 3, 6708 PB Wageningen, The Netherlands

T. L. Pons  
Plant Ecophysiology, Institute of Environmental Biology, Utrecht University, Padualaan 8, 3584  
CH Utrecht, The Netherlands

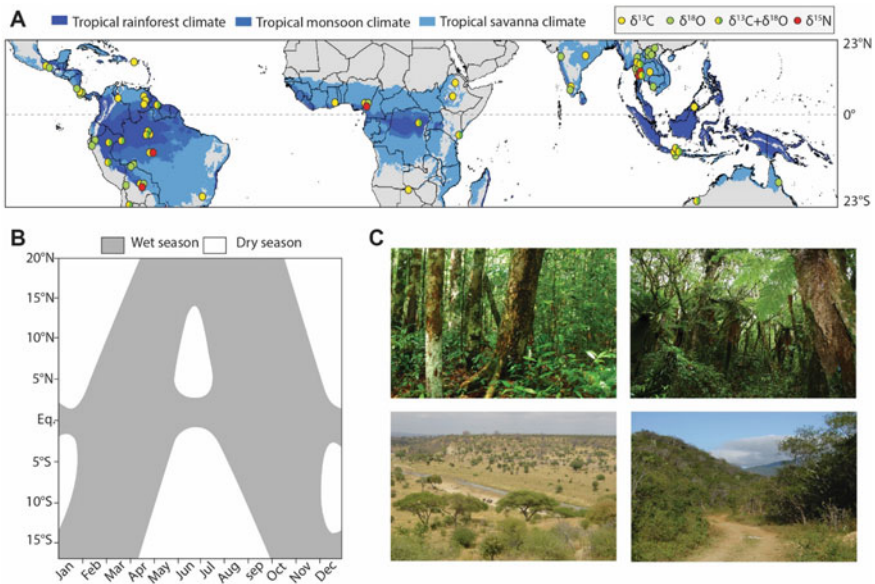


**Fig. 22.1** **a** Map of the tropics showing locations of studies on stable isotopes in tropical tree-rings. Main findings of these studies summarized in Table 22.1. Background map showing tropical climates according to Köppen classification (map from Beck et al. 2018), with grey continental areas belonging to arid (mostly treeless) climate types. **b** Diagram showing general rainfall seasonality in the tropics, with a dry month defined as a month with <100 mm average precipitation. Figure adapted from Kricher (2011). **c** A few examples of tropical (woody) ecosystems. Clockwise from top left: evergreen rainforest close to the equator (no dry season) in Brazil, mountain cloud forest in Bolivia (moderate dry season; but moist year round), deciduous dry forest in Mexico (long dry season), and savanna vegetation in Tanzania (long dry season)

The “re-discovery” of annual growth-ring formation in tropical trees, and developments in stable isotope analyses has triggered studies on the variation of the natural abundance of isotopes in tropical trees, with the number of publications on stable isotopes in tropical tree rings increasing rapidly in recent years (Fig. 22.1). In this chapter, we provide an overview of research on stable isotopes in tropical tree rings, and the insights gained on the functioning of tropical forests and the impacts of global change. This chapter is a condensed and updated version of our earlier review (van der Sleen et al. 2017), with a main focus on lowland forests in the wet tropics between 23.5°N/S (Fig. 22.1).

## 22.2 Tropical climate

The tropics are generally warm (mean annual temperature of  $>24\text{ }^{\circ}\text{C}$ ) and wet (except for dry grasslands and deserts). Most tropical ecosystems are seasonal to some extent, but in contrast to temperate regions, seasonal weather patterns are primarily driven by variation in precipitation amount and not temperature fluctuations. Across the tropics, rainfall seasonality is a result of large-scale atmospheric circulation patterns. At the equator, heat builds up, causing warm and moisture-laden air to rise. The ascending air diverges at the top of the troposphere and flows to more northern and southern latitudes. As the air cools, it loses its moisture as precipitation, becomes more dense, and ultimately descends as dry air in the subtropics, from where it returns equatorward near the surface, giving rise to the trade winds. These circulation patterns, on both the northern and southern hemisphere, are called the Hadley cells. The great equatorial convection zone, where the trade winds meet is known as the Intertropical Convergence Zone (ITCZ), and characterized by violent thunderstorms and high quantities of precipitation. The ITCZ moves north during the Northern hemisphere summer, and south during the austral summer, as a consequence of the Earth's tilt. This seasonal movement induces wet and dry seasons in most tropical regions (Fig. 22.1). At locations lacking a true dry season, forests will remain evergreen throughout the year. At locations with a longer or drier dry season, the number of deciduous species increases. Further away from the Equator, forests give way to savanna, shrubland or grassland (Fig. 22.1). Although climate is an important factor determining forest type, it is also affected by other factors, such as soil characteristics and fire regime.

Another important climatic feature in tropical regions is the El Niño–Southern Oscillation (ENSO), which are irregular periodic variations in winds and sea surface temperatures over the tropical eastern Pacific Ocean. Although the factors responsible for the occurrence of ENSO events remain incompletely understood, the phenomenon occurs when the ITCZ migrates more southwards than normal. This raises sea surface temperature and disrupts the normal upwelling pattern along the west coast of South America. Eventually, this reduces the transport of warm surface water across the Pacific Ocean toward Asia, and as a result affects weather systems throughout the tropics and subtropics, causing heavy downpours and flooding in some regions and severe droughts in others. El Niño occurs every two to seven years and tends to alternate with another climatic phenomenon with opposite effects. This is called La Niña, and happens when trade winds gain abnormal strengths, increasing upwelling along the west Coast of South America and strengthening the flow of warm surface water westwards across the Pacific.

Local climate conditions, and its variability (including ENSO-driven anomalies), affect tree physiology and thus tree-ring isotope values. In addition, large-scale circulation patterns affect the  $\delta^{18}\text{O}$  signature of precipitation, which can be recorded in tree rings (Table 22.1).

**Table 22.1** Summary of the main usage and outcomes of studies measuring stable isotopes in tropical tree rings. References given in chronological order (detailed version of the table is available, see Supplementary Table S1)

Stable isotope	Main usage	Main outcome	Number of species*	References
<sup>13</sup> C	Proxy for iWUE	iWUE generally increased over time	21(3)	Hietz et al. (2005), Brienen et al. (2011), Loader et al. (2011), Locosselli et al. (2013), van der Sleen et al. (2015a), Rahman et al. (2020)
	Identification of annual rings in ring-less wood	Moderate potential to identify annual rings through intra-annual sampling	12(8)	Leavitt and Long (1991), Ohashi et al. (2009), Krepkowski et al. (2013), Schubert and Timmermann (2015)
	Unravelling isotope-climate relationships	Negative correlation with rainfall	16(0)	Gebrekirstos et al. (2009), Fichtler et al. (2010), Brienen et al. (2011), Gebrekirstos et al. (2011), van der Sleen et al. (2014), Schubert and Timmermann (2015), Boakye et al. (2019)
	Reconstruction of past climate	Some prospect for rainfall reconstruction	1(0)	Wils et al. (2010), Mokria et al. (2018)
<sup>18</sup> O	Unravelling isotope-climate relationships	Correlations with rainfall, humidity and ENSO in shallow rooting trees	11(0)	Anchukaitis et al. (2008), Anchukaitis and Evans (2010), Managave et al. (2011b), Managave et al. (2011a), Xu et al. (2011), Brienen et al. (2012), Zhu et al. (2012a), Zhu et al. (2012b), Sano et al. (2012), Brienen et al. (2013), Xu et al. (2013), Boysen et al. (2014), van der Sleen et al. (2015b), Schollaen et al. (2015), Xu et al. (2015), Volland et al. (2016), Cintra et al. (2019)

(continued)

**Table 22.1** (continued)

Stable isotope	Main usage	Main outcome	Number of species*	References
	Reconstruction of past climate	Good prospect for rainfall reconstruction	14(0)	Managave et al. (2011b), Managave et al. (2011a), Brienen et al. (2012), Zhu et al. (2012a), Zhu et al. (2012b), Sano et al. (2012), Xu et al. (2013), van der Sleen et al. (2015b), Baker et al. (2015), Xu et al. (2015), Pumijumnong et al. (2020)
	Identification of annual rings in ring-less wood	Good potential to identify annual rings through intra-annual sampling	6(6)	Evans and Schrag (2004), Evans (2007), Anchukaitis et al. (2008), Managave et al. (2010), Xu et al. (2014)
	Identification of annual rings in ring-less wood	Good potential to identify annual rings through intra-annual sampling	20(17)	Verheyden et al. (2004), Poussart et al. (2004), Poussart and Schrag (2005), Pons and Helle (2011), Ohashi et al. (2016), Managave et al. (2017), Cintra et al. (2019)
<sup>13</sup> C and <sup>18</sup> O	Unravelling isotope-climate relationships	Correlations with rainfall and ENSO	6(0)	Cullen and Grierson (2007), Ballantyne et al. (2011), Schollaen et al. (2013), Colombaroli et al. (2016), Managave et al. (2017)
	Identification of drivers of changes in iWUE (stomatal conductance vs. photosynthesis)	Some evidence that iWUE increased through decreased <i>g<sub>s</sub></i>	4(0)	Cullen et al. (2008), Nock et al. (2011)
<sup>15</sup> N	Effects of increased N deposition on N cycling	Potential to record aspects of nitrogen cycle	9(0)	Hietz et al. (2010), Hietz et al. (2011), van der Sleen et al. (2015c)

ENSO, el Niño Southern Oscillation; iWUE, intrinsic water-use efficiency; *g<sub>s</sub>* stomatal conductance

\* Total number of species and those with non-distinct growth rings between brackets. Some species were involved in multiple studies, notable *Tectona grandis*, *Cedrela odorata*, and *Fokienia hodginsii*

## 22.3 Carbon Stable Isotopes

### 22.3.1 Carbon Isotope Ecophysiology in the Tropics

The stable carbon isotopic signature in the wood of tropical trees is influenced by a variety of factors related to rainfall, temperature, light conditions and species' responses to drought (for the basics of the  $^{13}\text{C}/^{12}\text{C}$  isotope fractionation in plants see Chap. 9). The combined effects of these factors determine  $\delta^{13}\text{C}$  values measured in tropical tree rings. In some cases, contributions of individual environmental factors are hard to disentangle, as they can covary and exert similar effects on tree-ring  $\delta^{13}\text{C}$ .

Ontogenetic trends in tree-ring  $\delta^{13}\text{C}$  series can be substantial for tropical trees, as was illustrated for *Cedrela odorata* from Bolivia (Brienen et al. 2017). Juvenile trees growing under a forest canopy are exposed to reduced irradiance that is associated with a high ratio of intercellular over atmospheric  $\text{CO}_2$  concentration ( $c_i/c_a$ ), and young trees possibly also absorb  $^{13}\text{C}$ -depleted  $\text{CO}_2$  near the forest floor (Medina and Minchin 1980; Medina et al. 1991; Buchmann et al. 1997). Both factors contribute to low  $\delta^{13}\text{C}$  values in the stem wood of small trees. Sub-canopy trees are exposed to higher light levels and slightly  $^{13}\text{C}$ -enriched  $\text{CO}_2$  due to high photosynthetic activity in the canopy, leading to higher  $\delta^{13}\text{C}$  values in their wood. Canopy and emergent trees are exposed to high light levels and  $\text{CO}_2$  with an atmospheric  $\delta^{13}\text{C}$  signature (Buchmann et al. 1997). In addition, ontogenetic trends in tree-ring  $\delta^{13}\text{C}$  may be driven by increased vapor pressure deficit (VPD) from understory to canopy and increases in hydraulic resistance with tree height. Therefore, changes in  $\delta^{13}\text{C}$  with tree size can provide valuable information in an ecological context (e.g. on light conditions; van der Sleen et al. 2014), but are an important confounding factor in a dendroclimatological context.

Decreasing water availability, or increasing VPD, results in stomatal closure, and therefore lowers the  $C_i/C_a$  ratio (e.g. Gebrekirstos et al. 2011). As a result, drought increases tree-ring  $\delta^{13}\text{C}$  values and intrinsic water-use efficiency (iWUE; the ratio of photosynthetic rate over stomatal conductance;  $A/g_s$ ) (e.g. Lambers et al. 2008; Cernusak et al. 2009; Craven et al. 2013). The available evidence suggests that the relationship between water availability and tree-ring  $\delta^{13}\text{C}$  also holds in regions with humid climatic conditions:  $\delta^{13}\text{C}$  of leaves collected in the rainy season was lower than in leaves collected in the dry season (French Guyana, Buchmann et al. 1997), and wood  $\delta^{13}\text{C}$  of trees growing near a creek was lower than that of trees growing on a comparatively drier ridge (Guyana, Pons et al. 2005).

Changes in light and nutrient conditions can also affect tree-ring  $\delta^{13}\text{C}$  values when photosynthetic activity increases ( $A$ ) more than stomatal opening ( $g_s$ ) (e.g. Cernusak et al. 2009; van der Sleen et al. 2014). Interestingly, average tree-ring  $\delta^{13}\text{C}$  values and the impact of environmental conditions on  $\delta^{13}\text{C}$  ratios is species specific. Co-occurring tree species of similar DBH can exhibit large variations in  $\delta^{13}\text{C}$  values, which has been related to differences in successional status (Bonal et al. 2007), shade tolerance (Guehl et al. 1998; Bonal et al. 2000), leaf phenology patterns (Bonal et al. 2000), and drought tolerance (Craven et al. 2013).



### 22.3.2 *Seasonal Variation in Tree-Ring $\delta^{13}\text{C}$*

Early studies on  $\delta^{13}\text{C}$  in tropical wood showed the presence of intra-annual variation, similar to what was found for other climatic regions (Leavitt and Long 1991). Subsequent studies confirmed this seasonality (e.g. Poussart et al. 2004; Verheyden et al. 2004; Ohashi et al. 2009), suggesting seasonal variation in water availability as underlying cause. Variation in  $\delta^{13}\text{C}$  within a single growth ring can however, not be unequivocally understood from current photosynthesis on the basis of the Farquhar et al. (1989) model. Other processes may interfere with patterns driven by climate seasonality, such as utilization of stored reserves early in the growing season, potential fractionation downstream from the carbon fixation in the leaves, and a varying fraction of C allocated to other processes than diameter increment in the growing season (Helle and Schleser 2004; Kagawa et al. 2006; Krepkowski et al. 2013; Fu et al. 2017). Although attempts have been made to identify annual rings in tropical trees that lack visible increment ring boundaries based on intra-annual  $\delta^{13}\text{C}$  patterns,  $\delta^{18}\text{O}$  proved to be more useful for that purpose.

### 22.3.3 *Annual and Decadal Variation in Tree-Ring $\delta^{13}\text{C}$*

Several studies have investigated the inter-annual variation of  $\delta^{13}\text{C}$  and its correlation with precipitation amount (Table C). Strong negative correlations between tree-ring  $\delta^{13}\text{C}$  and annual precipitation were found for species from various sites in tropical America, Asia and Africa, whose growing conditions differed widely in annual precipitation (e.g. Fichtler et al. 2010; Rahman et al. 2020). Such climate sensitivity was further linked to ENSO variability in some studies (e.g. Brienen et al. 2011). In semi-arid Ethiopia, Gebrekirstos et al. (2009) also found a strong correlation of  $\delta^{13}\text{C}$  with precipitation for three *Acacia* species, but less so in *Balanites aegyptiaca*. Such differences may relate to water-use strategies, with drought-tolerant species showing a lower sensitivity to inter-annual variability in precipitation amount (Gebrekirstos et al. 2011; Craven et al. 2013).

Other studies combined  $\delta^{13}\text{C}$  sequences with measurements of  $\delta^{18}\text{O}$ . In some of these,  $\delta^{13}\text{C}$  showed correlation with other precipitation variables than those found for  $\delta^{18}\text{O}$  (Cullen and Grierson 2007; Schollaen et al. 2013). Nevertheless,  $\delta^{18}\text{O}$  series generally yielded stronger correlations with precipitation variables than  $\delta^{13}\text{C}$  series (Poussart and Schrag 2005; Ballantyne et al. 2011: and see discussion in the next section).

Studies using longer tree-ring sequences have consistently shown a declining  $\delta^{13}\text{C}$  trend over the last century in tropical trees (Hietz et al. 2005; Brienen et al. 2011; Loader et al. 2011), also when explicitly correcting for potential ontogenetic effects (Nock et al. 2011; van der Sleen et al. 2015a). After correcting for decreasing atmospheric  $\delta^{13}\text{C}$  over that period (the Suess effect), a rather constant  $^{13}\text{C}$  discrimination ( $\Delta^{13}\text{C}$ ) generally remains. This leads to the conclusion that  $C_i/C_a$  remained constant

over time and that, as a result of the increasing atmospheric CO<sub>2</sub> concentration, iWUE has increased consistently over time (Silva and Anand 2013, see Chap. 17). A sustained increase of photosynthesis and/or a higher water-use efficiency under elevated CO<sub>2</sub> are expected to stimulate tree growth if carbon and/or water are limiting factors (Körner 2009). A few studies also quantified temporal trends in tree growth using the same tree-ring sequences as used to determine  $\delta^{13}\text{C}$  trends (Nock et al. 2011; van der Sleen et al. 2015a). Interestingly, these studies found no indications for a growth stimulation over the past century. Stem diameter growth is not necessarily linearly linked to photosynthetic activity, because other aspects of the carbon balance of trees may have changed as well, such as phenology, leaf turnover, respiration and biomass allocation. However, if it is reasonable to assume that diameter growth can reflect changes in the total carbon balance of a tree, in particular on longer time scales, than the available tree-ring studies suggest that photosynthesis did not increase as a result of rising atmospheric CO<sub>2</sub> concentration. This scenario could arise if tree growth is ultimately limited by nutrient availability in most tropical regions, or if a CO<sub>2</sub>-induced stimulation of photosynthesis has been compensated by an external climate-related stressor, such as increased temperature or decreased precipitation.

## 22.4 Oxygen Stable Isotopes

### 22.4.1 Oxygen Stable Isotope Ecophysiology in the Tropics

Water taken up by trees becomes enriched in  $^{18}\text{O}$  in leaves as a result of transpiration. The strength of this enrichment is mediated by environmental conditions (Barbour 2007; Chap. 10). CO<sub>2</sub> taken up by the leaves exchanges its oxygen atoms with that of leaf water, causing a transfer of the isotopic signature of leaf water to sucrose. In addition, when cellulose is synthesized from sucrose in the stem, about 42% of the oxygen atoms are again exchanged with xylem water. This exchange causes the effect of enriched leaf water to be partly reverted, and results in a strong imprinting of the isotope signature of source water in the wood of trees. Unfortunately, the  $\delta^{18}\text{O}$  signature of absorbed source water is commonly unknown, especially over longer time scales. In addition, it is often unknown from what depth the root systems of tropical trees take up water, which further complicates the determination of the  $\delta^{18}\text{O}$  of source water, and thus the interpretation of intra- and inter-annual variation in  $\delta^{18}\text{O}$  in wood. Shallow-rooting trees, growing in dense canopies where isotopic enrichment at the soil surface is minimal, likely absorb water that consists mainly of recent precipitation, and hence tree-rings are imprinted with an  $^{18}\text{O}$  signal that is rather similar to that of rainwater. As rainwater resides only shortly at the soil surface before percolating down to the groundwater, the  $\delta^{18}\text{O}$  signature of groundwater likely integrates variation in  $\delta^{18}\text{O}$  in precipitation over several years (Chap. 18). The depth of water uptake has been estimated by measuring natural abundance of  $^{18}\text{O}$  in the soil

profile and in xylem water (Jackson et al. 1995; Hasselquist et al. 2010; Ellsworth and Sternberg 2015) or by labelling soil water (Stahl et al. 2013). These studies show that deciduous trees tend to take up water from shallower depths than evergreen trees and that the depth of water uptake generally increases with tree age and size.

### 22.4.2 *Seasonal Variation in Tree-Ring $\delta^{18}\text{O}$*

The first  $\delta^{18}\text{O}$  studies on tropical trees quantified radial variation of  $\delta^{18}\text{O}$  in tree stems to reconstruct annual ring boundaries of tree species without anatomically distinct rings or to confirm the annual nature of ring formation (Evans and Schrag 2004; Poussart et al. 2004; Verheyden et al. 2004; Poussart and Schrag 2005; Evans 2007). In some of these studies,  $\delta^{13}\text{C}$  was also measured, but  $\delta^{18}\text{O}$  was found to be generally superior for this purpose. The suitability of  $\delta^{18}\text{O}$  for the identification of annual rings is based on its seasonal change in precipitation: rainwater  $\delta^{18}\text{O}$  is low during the rainy season and with heavy precipitation events (Dansgaard 1964; Villacis et al. 2008; Kurita et al. 2009). High  $\delta^{18}\text{O}$  values of precipitation during the dry season can be further amplified in both soil and leaves due to higher evaporation at low humidity (Jackson et al. 1995; Cintra et al. 2019). This seasonality in  $\delta^{18}\text{O}$  was confirmed in tropical trees with distinct annual rings (Poussart et al. 2004; Managave et al. 2010; Ballantyne et al. 2011; Managave et al. 2011a; Schollaen et al. 2013). The identification of annual rings in homogeneous (ring-less) wood is most successfully done when intra-annual variation in source  $\delta^{18}\text{O}$  is large. This is the case in the western parts of the Amazon basin, where  $\delta^{18}\text{O}$  in precipitation is low in the rainy season due to rain-out of the heavy isotopes as water vapor travels from the Atlantic ocean across the basin (Sturm et al. 2007). Evidence for this effect is provided by the lower intra-annual variation in  $\delta^{18}\text{O}$  in evergreen trees from Guyana (1–4‰; Pons and Helle 2011) compared to trees sampled near Manaus, Brazil (3–6‰; Ohashi et al. 2016). A special case are trees in montane forests where the uptake of water during the rainy season is from precipitation, whereas moisture can also be directly absorbed from clouds in the dry season. These two water sources differ in  $\delta^{18}\text{O}$  values, which can result in large seasonal variation of tree-ring  $\delta^{18}\text{O}$  (Anchukaitis et al. 2008; Anchukaitis and Evans 2010). As the strength of intra-annual variation in  $\delta^{18}\text{O}$  varies across species (Poussart and Schrag 2005; Anchukaitis et al. 2008) and climatic conditions, selection of species and sites will determine the ability to identify annual rings in homogeneous wood.

### 22.4.3 *Annual and Decadal Variation in Tree-Ring $\delta^{18}\text{O}$*

Because some trees incorporate the  $\delta^{18}\text{O}$  signature of rainwater in stem wood, time series of tree-ring  $\delta^{18}\text{O}$  can be used to quantify past variability in precipitation. Tree-ring  $\delta^{18}\text{O}$  has been correlated with basin-wide precipitation in the Amazon

(Ballantyne et al. 2011; Brienen et al. 2012; Baker et al. 2015, 2016), and regional precipitation in Thailand (Poussart and Schrag 2005; Pumijumong et al. 2020), Costa Rica (Anchukaitis and Evans 2010), India (Managave et al. 2011b), Indonesia (Schollaen et al. 2013, 2015), Laos and Vietnam (Xu et al. 2011), West Africa (van der Sleen et al. 2015b), and central Africa (Colombo et al. 2016). Particularly El Niño Southern Oscillation (ENSO) variability is often evident in  $\delta^{18}\text{O}$  sequences either from positive anomalies (Verheyden et al. 2004; Anchukaitis and Evans 2010; Zhu et al. 2012a) or negative ones (Evans and Schrag 2004; Brienen et al. 2012). The analysis of tropical tree-ring  $\delta^{18}\text{O}$  is developing into a powerful tool for reconstructing the variability of precipitation on regional scales.

Good synchronization of  $\delta^{18}\text{O}$  patterns among individual trees was found for several species (e.g. Poussart and Schrag 2005; Managave et al. 2011b; Brienen et al. 2012; van der Sleen et al. 2015b), sometimes over large spatial distances (Baker et al. 2015; Schwendenmann et al. 2015; Volland et al. 2016). Synchronous variability in  $\delta^{18}\text{O}$  can be higher than for ring-width, thus providing an alternative tool for cross dating (Baker et al. 2015; van der Sleen et al. 2015b; Volland et al. 2016) and identification of false and missing rings (Boysen et al. 2014). However,  $\delta^{18}\text{O}$  synchronization between individuals may be low for certain species or sites (e.g. Poussart and Schrag 2005; Baker et al. 2015). For  $\delta^{18}\text{O}$  in *Toona ciliata* from Thailand, low  $\delta^{18}\text{O}$  synchronization occurred (van der Sleen 2014), in spite of the ring-width series showing strong synchronization (Vlam et al. 2014). It is likely that trees that lack a common signal in tree-ring  $\delta^{18}\text{O}$  values exploit other water sources than recent precipitation (e.g. ground water). These results suggest that shallow rooting tree species on well-drained soils have the highest probability to record the  $\delta^{18}\text{O}$  variability of precipitation and thus have the highest potential as tools for climate reconstructions.

In several studies the two stable isotopes  $^{18}\text{O}$  and  $^{13}\text{C}$  were combined using a mechanistic interpretation, the so-called dual isotope approach (see Chap. 16), where  $A/g_s$  obtained from  $\Delta^{13}\text{C}$  and  $g_s$  derived from  $\Delta^{18}\text{O}$  could potentially provide an estimate of  $A$  (Scheidegger et al. 2000). This approach was used by Nock et al. (2011), who interpreted an increase of  $\Delta^{18}\text{O}$  over time as an indication of a decreasing  $g_s$  in trees from Thailand. The observed decrease of  $\Delta^{13}\text{C}$ , and thus increasing  $A/g_s$ , would then be the result of this decreasing  $g_s$  and not an increasing  $A$ . However, the underlying assumptions in this approach are that the  $\delta^{18}\text{O}$  signature of source water is known and that the leaf to air vapor pressure difference (LAVPD) has remained constant over the period studied. In many tropical regions, this LAVPD may have increased as a result of global warming and/or decreased precipitation, leading to increased transpiration and  $\delta^{18}\text{O}$  over time. Even though  $g_s$  is also partly controlled by LAVPD, this makes it nonetheless difficult to separate the  $g_s$  effect from the LAVPD effect on transpiration.

A long-term increase of  $\delta^{18}\text{O}$  values has been encountered in several studies conducted on tropical tree species (Poussart and Schrag 2005; Xu et al. 2011; Brienen et al. 2012; van der Sleen 2014; van der Sleen et al. 2015b; Volland et al. 2016). Some of these trends could be caused by ontogenetic changes, but a consistent small trend over the past century was also found in studies that did correct for ontogenetic trends (van der Sleen 2014; van der Sleen et al. 2015b; Volland et al. 2016). For

the Amazon region, these results are consistent with similar increases of  $\delta^{18}\text{O}$  in Andean ice cores (Thompson et al. 2006) and Andean lake sediments (Bird et al. 2011). Thus, the increasing trend in  $\delta^{18}\text{O}$  in tree rings likely reflects a pan-tropical phenomenon. The cause of this increase is yet unknown, and it is unclear whether it relates to climate change.

## 22.5 Nitrogen Stable Isotopes

### 22.5.1 Nitrogen Stable Isotope Ecophysiology

The value of plant  $\delta^{15}\text{N}$  depends on the  $\delta^{15}\text{N}$  of the N taken up and N losses in leaves, fruits, etc. Uptake can be in the form of nitrate, ammonium, organic N compounds or  $\text{N}_2$  in the case of nitrogen fixation. The  $\delta^{15}\text{N}$  of these sources varies in a complex manner (except for  $\text{N}_2$ , which is used as standard and is thus 0‰ by definition; Chap. 12).

Higher soil and foliage  $\delta^{15}\text{N}$  are generally reported for tropical lowland forests, compared to temperate and boreal forests (Martinelli et al. 1999; Amundson et al. 2003), and tropical montane forest (Brearley 2013). This pattern is considered as evidence of more N losses and thus a more open N cycle in tropical lowland forests, because nitrate lost through leaching and/or denitrification is  $^{15}\text{N}$ -depleted. Temperate forests are generally more N-limited, whereas tropical forests tend to be more P-limited (Vitousek and Howarth 1991), which is consistent with their higher  $\delta^{15}\text{N}$ . Leguminous trees are abundant in tropical forests, although not all can form an effective symbiosis with Rhizobia. Yet, facultative leguminous  $\text{N}_2$ -fixers can still be abundant (Menge and Chazdon 2016) and contribute to N-accumulation also in late successional stages of tropical forests (Roggy et al. 1999; Pons et al. 2007). This could be the reason for an alleviation of N-limitation, whereas  $\text{N}_2$ -fixing trees are virtually lacking in temperate forest (except for early successional stages; Menge et al. 2009).

### 22.5.2 Annual and Decadal Variability in Tree-Ring $\delta^{15}\text{N}$

So far, only three studies on temporal variation or trends  $\delta^{15}\text{N}$  in tree rings have been carried out in tropical forests (Hietz et al. 2010, 2011; van der Sleen et al. 2015c). Hietz et al. (2010) using two species in a Brazilian forest, found a gradual increase of tree-ring  $\delta^{15}\text{N}$  over time after statistical correction for tree age. The authors suggested that this result could be caused by an increase in tree turnover and thus gap formation that generates  $\text{NO}_3^-$  losses and thereby increasing  $\delta^{15}\text{N}$  of the remaining soil N pool. In a subsequent study, Hietz et al. (2011) reported also an increase in  $\delta^{15}\text{N}$  in three species from a monsoon forest in Thailand. They

also found a similar increase when comparing 40-year-old herbarium leaves with recent leaves from the same species and sample location in a Panamanian forest (BCI). The two forests are intensively monitored and there are no indications that the level of disturbance has increased over the past century. Such a consistent trend in  $\delta^{15}\text{N}$  in three widely separated tropical forests may therefore indicate an effect of increased anthropogenic N-deposition, which causes higher  $\text{NO}_3^-$  losses (and thus  $\delta^{15}\text{N}$  enrichment of remaining soil nitrogen). However, in the most recent study, van der Sleen et al. (2015c) sampled annual rings in six species from three sites at different continents. They corrected for possible tree size effects by comparing wood sampled at a fixed diameter (20 cm) from different sized trees. Ten-year pooled samples were also collected between 1955 and 2005 from single trees, which showed increasing trends of  $\delta^{15}\text{N}$  in Bolivia and Cameroon. Surprisingly, the trends were absent in the fixed diameter sampling, showing evidence of potential ontogenetic effects. The discrepancy between the results of Hietz et al. (2011) and van der Sleen et al. (2015c) may also have been caused by a lower statistical power in the latter. Unfortunately, the interpretation of temporal changes in  $\delta^{15}\text{N}$  in the few available tropical tree-ring studies remain strongly hampered by a limited understanding of the factors that influence soil- and tree  $\delta^{15}\text{N}$  values.

## 22.6 Conclusion and Perspective

Tropical forests harbor an incredible biodiversity and provide ecosystem services on which millions of people depend. They are a major component of the global carbon cycle, storing some 25% of the total terrestrial carbon and accounting for a third of net primary production (Bonan 2008). Understanding the functioning of these forests and their responses to global change is therefore an urgent need for ecology, climate science and conservation. The study of stable isotopes in tropical tree rings offers unique opportunities to quantify how these trees respond to their environment, and can fill an important void in many tropical areas where the availability of climate data is limited or of short duration. In fact, stable isotopes in tree rings are essentially the only tools available to obtain cost-effective, high-resolution, long-term retrospective data on tree physiology and the environmental conditions affecting it.

Currently, stable isotopes research in the tropics has mainly focused on (i) quantifying the effects of rising atmospheric  $\text{CO}_2$  and climate change on tree physiology, (ii) identifying the drivers of growth variability and reconstruction of past climate, and (iii) the identification of annual rings in wood lacking anatomically distinct growth boundaries. The main findings of the available studies are shortly summarized for each isotope in Table 22.1. The application of stable isotopes continues to expand. New applications are numerous, and include the potential use of stable isotopes for timber tracing and to identify illegally logged wood (e.g. Vlam et al. 2018), to benchmark the predictions of dynamic global vegetation models (e.g. Zuidema et al. 2018), and for reconstructions of atmospheric  $\text{CO}_2$  and  $\delta^{13}\text{C}$  values (using trees with a C4 photosynthetic pathway; Ben et al. 2017).

Although tropical isotope research has centered on three stable isotopes (C, O, and to a lesser degree N), advances in analytical techniques and reductions in associated costs continue to broaden these analyses. This not only includes the analyses of other stable isotopes, but also the analyses of the intramolecular distribution of isotopes. For example, the position of  $^{18}\text{O}$  in the glucose moiety in cellulose can be used to separate source water from leaf water enrichment effects (Sternberg 2009; Waterhouse et al. 2013), and the position of  $^2\text{H}$  was related to the oxygenation/carboxylation ratio that depends on  $C_i$  (Ehlers et al. 2015). These techniques can be used to infer more details about environmental effects on tropical trees than is possible with bulk isotopic ratios as done so far. Even though stable isotope research in the tropics still faces methodological and interpretation issues, we anticipate that it will continue to play a crucial role for our understanding of the functioning of tropical forests and their resilience to global change.

## References

- Amundson R, Austin AT, Schuur EAG, Yoo K, Matzek V, Kendall C, Uebersax A, Brenner D, Baisden WT (2003) Global patterns of the isotopic composition of soil and plant nitrogen. *Glob Biogeochem Cycles* 17:31–31
- Anchukaitis KJ, Evans MN, Wheelwright NT, Schrag DP (2008) Stable isotope chronology and climate signal calibration in neotropical montane cloud forest trees. *J Geophys Res G Biogeosciences* 113
- Anchukaitis KJ, Evans MN (2010) Tropical cloud forest climate variability and the demise of the Monteverde golden toad. *Proc Natl Acad Sci USA* 107:5036–5040
- Baker JC, Hunt SF, Clerici SJ, Newton RJ, Bottrell SH, Leng MJ, Heaton TH, Helle G, Argollo J, Gloor M, Brienen RJ (2015) Oxygen isotopes in tree rings show good coherence between species and sites in Bolivia. *Glob Planet Chang* 133:298–308
- Baker JCA, Gloor M, Spracklen DV, Arnold SR, Tindall JC, Clerici SJ, Leng MJ, Brienen RJW (2016) What drives interannual variation in tree ring oxygen isotopes in the Amazon? *Geophys Res Lett* 43:11831–11840
- Ballantyne AP, Baker PA, Chambers JQ, Villalba R, Argollo J (2011) Regional differences in South American monsoon precipitation inferred from the growth and isotopic composition of tropical trees. *Earth Interact* 15:1–35
- Barbour MM (2007) Stable oxygen isotope composition of plant tissue: a review. *Funct Plant Biol* 34:83–94
- Beck HE, Zimmermann NE, McVicar TR, Vergopolan N, Berg A, Wood EF (2018) Present and future Koppen-Geiger climate classification maps at 1-km resolution. *Sci Data* 5
- Ben T, Hart PJ, Helle G (2017) Towards establishing a new environmental archive—annual growth periodicity, stable carbon isotope variability and reconstruction potential of 'akoko (*Euphorbia olowaluana*), a native Hawaiian tree with C-4 photosynthetic pathway. *Erdkunde* 71:77–92
- Bird BW, Abbott MB, Vuille M, Rodbell DT, Stansell ND, Rosenmeier MF (2011) A 2,300-year-long annually resolved record of the South American summer monsoon from the Peruvian Andes. *Proc Natl Acad Sci USA* 108:8583–8588
- Boakye EA, Gebrekirstos A, Hyppolite DN, Barnes VR, Porembski S, Brauning A (2019) Carbon isotopes of riparian forests trees in the savannas of the Volta sub-basin of Ghana reveal contrasting responses to climatic and environmental variations. *Forests* 10:251

- Bonal D, Atger C, Barigah TS, Ferhi A, Guehl JM, Ferry B (2000) Water acquisition patterns of two wet tropical canopy tree species of French Guiana as inferred from (H<sub>2</sub>O)-O-18 extraction profiles. *Ann For Sci* 57:717–724
- Bonal D, Born C, Brechet C, Coste S, Marcon E, Roggy JC, Guehl JM (2007) The successional status of tropical rainforest tree species is associated with differences in leaf carbon isotope discrimination and functional traits. *Ann For Sci* 64:169–176
- Bonan GB (2008) Forests and climate change: forcings, feedbacks, and the climate benefits of forests. *Science* 320:1444–1449
- Boysen, BMM, Evans MN, Baker PJ (2014)  $\delta^{18}\text{O}$  in the tropical conifer *Agathis robusta* records ENSO-related precipitation variations. *PLoS One* 9:e102336
- Brearley FQ (2013) Nitrogen stable isotopes indicate differences in nitrogen cycling between two contrasting Jamaican montane forests. *Plant Soil* 367:465–476
- Brienen RJW, Wanek W, Hietz P (2011) Stable carbon isotopes in tree rings indicate improved water use efficiency and drought responses of a tropical dry forest tree species. *Trees Struct Funct* 25:103–113
- Brienen GH, Pons TL, Guyot JL, Gloor M (2012) Oxygen isotopes in tree rings are a good proxy for Amazon precipitation and El Niño-Southern oscillation variability. *Proc Natl Acad Sci USA* 109:16957–16962
- Brienen RJW, Hietz P, Wanek W, Gloor M (2013) Oxygen isotopes in tree rings record variation in precipitation  $\delta^{18}\text{O}$  and amount effects in the south of Mexico. *J Geophys Res Biogeosci* 118:1604–1615
- Brienen RJW, Schöngart J, Zuidema PA (2016) Tree rings in the tropics: insights into the ecology and climate sensitivity of tropical trees. In: Goldstein G, Santiago LS (eds) *Tropical tree physiology*. Springer, Switzerland, pp 439–461
- Brienen RJW, Gloor E, Clerici S, Newton R, Arppe L, Boom A, Bottrell S, Callaghan M, Heaton T, Helama S, Helle G, Leng MJ, Mielikäinen K, Oinonen M, Timonen M (2017) Tree height strongly affects estimates of water-use efficiency responses to climate and CO<sub>2</sub> using isotopes. *Nat Commun* 8:288
- Buchmann N, Guehl JM, Barigah TS, Ehleringer JR (1997) Interseasonal comparison of CO<sub>2</sub> concentrations, isotopic composition, and carbon dynamics in an Amazonian rain forest (French Guiana). *Oecologia* 110:120–131
- Cernusak LA, Winter K, Turner BL (2009) Physiological and isotopic ( $\delta^{13}\text{C}$  and  $\delta^{18}\text{O}$ ) responses of three tropical tree species to water and nutrient availability. *Plant Cell Environ* 32:1441–1455
- Chowdhury M, Schmitz N, Verheyden A, Sass-Klaassen U, Koedam N, Beeckman H (2008) Nature and periodicity of growth rings in two Bangladeshi mangrove species. *IAWA J* 29:265–276
- Cintra BBL, Gloor M, Boom A, Schongart J, Locosselli GM, Brienen R (2019) Contrasting controls on tree ring isotope variation for Amazon floodplain and terra firme trees. *Tree Physiol* 39:845–860
- Colombaroli D, Cherubini P, De Ridder M, Saurer M, Toirambe B, Zweifel N, Beeckman H (2016) Stable carbon and oxygen isotopes in tree rings show physiological responses of *Pericopsis elata* to precipitation in the Congo Basin. *J Trop Ecol* 32:213–225
- Coster C (1927) Zur Anatomie und Physiologie der Zuwachszonen und Jahresbildung in den Tropen. *Annales des Jardin Botanique de Buitenzorg* 37:49–160
- Craven D, Hal JS, Ashton MS, Berlyn GP (2013) Water-use efficiency and whole-plant performance of nine tropical tree species at two sites with contrasting water availability in Panama. *Trees* 27:639–653
- Cullen LE, Grierson PF (2007) A stable oxygen, but not carbon, isotope chronology of *Callitris columellaris* reflects recent climate change in north-western Australia. *Clim Chang* 85:213–229
- Cullen LE, Adams MA, Anderson MJ, Grierson PF (2008) Analyses of  $\delta^{13}\text{C}$  and  $\delta^{18}\text{O}$  in tree rings of *Callitris columellaris* provide evidence of a change in stomatal control of photosynthesis in response to regional changes in climate. *Tree Physiol* 28:1525–1533
- Dansgaard W (1964) Stable isotopes in precipitation. *Tellus* 16:436–468



- Ehlers I, Augusti A, Betson TR, Nilsson MB, Marshall JD, Schleucher J (2015) Detecting long-term metabolic shifts using isotopomers: CO<sub>2</sub>-driven suppression of photorespiration in C3 plants over the 20th century. *Proc Natl Acad Sci USA* 112:15585–15590
- Ellsworth PZ, Sternberg LSL (2015) Seasonal water use by deciduous and evergreen woody species in a scrub community is based on water availability and root distribution. *Ecohydrology* 8:538–551
- Evans MN, Schrag DP (2004) A stable isotope-based approach to tropical dendroclimatology. *Geochim Cosmochim Acta* 68:3295–3305
- Evans MN (2007) Toward forward modeling for paleoclimatic proxy signal calibration: a case study with oxygen isotopic composition of tropical woods. *Geochem Geophys Geosystems* 8
- Farquhar GD, Ehleringer JR, Hubick KT (1989) Carbon isotope discrimination and photosynthesis. *Annu Rev Plant Physiol Plant Mol Biol* 40:503–537
- Fichtler E, Helle G, Worbes M (2010) Stable-carbon isotope time series from tropical tree rings indicate a precipitation signal. *Tree Ring Res* 66:35–49
- Fu PL, Griessinger J, Gebrekirstos A, Fan ZX, Brauning A (2017) Earlywood and latewood stable carbon and oxygen isotope variations in two pine species in southwestern China during the recent decades. *Front Plant Sci* 7
- Gebrekirstos A, Worbes M, Teketay D, Fetene M, Mitlöhner R (2009) Stable carbon isotope ratios in tree rings of co-occurring species from semi-arid tropics in Africa: patterns and climatic signals. *Glob Planet Chang* 66:253–260
- Gebrekirstos A, van Noordwijk M, Neufeldt H, Mitlöhner R (2011) Relationships of stable carbon isotopes, plant water potential and growth: an approach to assess water use efficiency and growth strategies of dry land agroforestry species. *Trees Struct Funct* 25:95–102
- Guehl JM, Domenach AM, Bereau M, Barigah TS, Casabianca H, Ferhi A, Garbaye J (1998) Functional diversity in an Amazonian rainforest of French Guyana: a dual isotope approach ( $\delta^{15}\text{N}$  and  $\delta^{13}\text{C}$ ). *Oecologia* 116:316–330
- Hasselquist NJ, Allen MF, Santiago LS (2010) Water relations of evergreen and drought-deciduous trees along a seasonally dry tropical forest chronosequence. *Oecologia* 164:881–890
- Helle G, Schleser GH (2004) Beyond CO<sub>2</sub>-fixation by Rubisco—an interpretation of  $^{13}\text{C}/^{12}\text{C}$  variations in tree rings from novel intra-seasonal studies on broad-leaf trees. *Plant Cell Environ* 27:367–380
- Hietz P, Wanek W, Dünisch O (2005) Long-term trends in cellulose  $\delta^{13}\text{C}$  and water-use efficiency of tropical *Cedrela* and *Swietenia* from Brazil. *Tree Physiol* 25:745–752
- Hietz P, Dünisch O, Wanek W (2010) Long-term trends in nitrogen isotope composition and nitrogen concentration in Brazilian rainforest trees suggest changes in nitrogen cycle. *Environ Sci Technol* 44:1191–1196
- Hietz P, Turner BL, Wanek W, Richter A, Nock CA, Wright SJ (2011) Long-term change in the nitrogen cycle of tropical forests. *Science* 334:664–666
- Jackson PC, Cavelier J, Goldstein G, Meinzer FC, Holbrook NM (1995) Partitioning of water-resources among plants of a lowland tropical forest. *Oecologia* 101:197–203
- Kagawa A, Sugimoto A, Maximov TC (2006)  $^{13}\text{C}$  CO<sub>2</sub> pulse-labelling of photoassimilates reveals carbon allocation within and between tree rings. *Plant Cell Environ* 29:1571–1584
- Körner C (2009) Responses of humid tropical trees to rising CO<sub>2</sub>. *Annu Rev Ecol Evol Syst* 40:61–79
- Krepkowski J, Gebrekirstos A, Shibistova O, Brauning A (2013) Stable carbon isotope labeling reveals different carry-over effects between functional types of tropical trees in an Ethiopian mountain forest. *New Phytol* 199:431–440
- Kricher J (2011) *Tropical ecology*. Princeton University Press, Princeton and Oxford
- Kurita N, Ichiyanaagi K, Matsumoto J, Yamanaka MD, Ohata T (2009) The relationship between the isotopic content of precipitation and the precipitation amount in tropical regions. *J Geochem Explor* 102:113–122
- Lambers H, Chapin FS III, Pons TL (2008) *Plant physiological ecology*. Springer, New York
- Leavitt SW, Long A (1991) Seasonal stable isotope variability in tree rings—possible paleoenvironmental signals. *Chem Geol* 87:59–70

- Loader NJ, Walsh RPD, Robertson I, Bidin K, Ong RC, Reynolds G, McCarroll D, Gagen M, Young GHF (2011) Recent trends in the intrinsic water-use efficiency of ringless rainforest trees in Borneo. *Philos Trans R Soc B Biol Sci* 366:3330–3339
- Locosselli GM, Buckeridge MS, Moreira MZ, Ceccantini G (2013) A multi-proxy dendroecological analysis of two tropical species (*Hymenaea* spp., Leguminosae) growing in a vegetation mosaic. *Trees Struct Funct* 27:25–36
- Managave S, Sheshshayee M, Borgaonkar H, Ramesh R (2010) Past break-monsoon conditions detectable by high resolution intra-annual  $\delta^{18}\text{O}$  analysis of teak rings. *Geophys Res Lett* 37:L05702
- Managave SR, Sheshshayee MS, Ramesh R, Borgaonkar HP, Shah SK, Bhattacharyya A (2011) Response of cellulose oxygen isotope values of teak trees in differing monsoon environments to monsoon rainfall. *Dendrochronologia* 29:89–97
- Managave S, Sheshshayee M, Bhattacharyya A, Ramesh R (2011) Intra-annual variations of teak cellulose  $\delta^{18}\text{O}$  in Kerala, India: implications to the reconstruction of past summer and winter monsoon rains. *Clim Dyn* 37:555–567
- Managave SR, Shimla P, Borgaonkar HP, Bhattacharyya A, Ramesh R (2017) Regional differences in the carbon isotopic compositions of teak from two monsoonal regimes of India. *Dendrochronologia* 44:203–210
- Martinelli LA, Piccolo MC, Townsend AR, Vitousek PM, Cuevas E, McDowell W, Robertson GP, Santos OC, Treseder K (1999) Nitrogen stable isotopic composition of leaves and soil: tropical versus temperate forests. *Biogeochemistry* 46:45–65
- Medina E, Minchin P (1980) Stratification of  $\delta^{13}\text{C}$  values of leaves in Amazonian rainforests. *Oecologia* 45:377–378
- Medina E, Sternberg L, Cuevas E (1991) Vertical stratification of  $^{13}\text{C}$  values in closed natural and plantation forests in the Luquillo mountains, Puerto Rico. *Oecologia* 87:369–372
- Menge DNL, Chazdon RL (2016) Higher survival drives the success of nitrogen-fixing trees through succession in Costa Rican rainforests. *New Phytol* 209:965–977
- Menge DNL, Levin SA, Hedin LO (2009) Facultative versus obligate nitrogen fixation strategies and their ecosystem consequences. *Am Nat* 174:465–477
- Mokria M, Gebrekirstos A, Abiyu A, Brauning A (2018) Upper Nile River flow reconstructed to AD 1784 from tree-rings for a long-term perspective on hydrologic-extremes and effective water resource management. *Quat Sci Rev* 199:126–143
- Nock CA, Baker PJ, Wanek W, Leis A, Grabner M, Bunyavejchewin S, Hietz P (2011) Long-term increases in intrinsic water-use efficiency do not lead to increased stem growth in a tropical monsoon forest in western Thailand. *Glob Chang Biol* 17:1049–1063
- Ohashi S, Durgante FM, Kagawa A, Kajimoto T, Trumbore SE, Xu X, Ishizuka M, Higuchi N (2016) Seasonal variations in the stable oxygen isotope ratio of wood cellulose reveal annual rings of trees in a Central Amazon terra firme forest. *Oecologia* 180:685–696
- Ohashi S, Okada N, Nobuchi T, Siripatanadilok S, Veenin T (2009) Detecting invisible growth rings of trees in seasonally dry forests in Thailand: isotopic and wood anatomical approaches. *Trees Struct Funct* 23:813–822
- Pons TL, Helle G (2011) Identification of anatomically non-distinct annual rings in tropical trees using stable isotopes. *Trees Struct Funct* 25:83–93
- Pons TL, Alexander EE, Houter NC, Rose SA, Rijkers T (2005) Ecophysiological patterns in Guianan forest plants. In: Hammond DS (ed) *Tropical forests of the Guiana shield; Ancient forests in a Modern World*. CABI Publishing, Wallingford, UK, pp 195–231
- Pons TL, Perreijn K, Van Kessel C, Werger MJA (2007) Symbiotic nitrogen fixation in a tropical rainforest:  $^{15}\text{N}$  natural abundance measurements supported by experimental isotopic enrichment. *New Phytol* 173:154–167
- Poussart PF, Schrag DP (2005) Seasonally resolved stable isotope chronologies from northern Thailand deciduous trees. *Earth Planet Sci Lett* 235:752–765

- Poussart PF, Evans MN, Schrag DP (2004) Resolving seasonality in tropical trees: multi-decade, high-resolution oxygen and carbon isotope records from Indonesia and Thailand. *Earth Planet Sci Lett* 218:301–316
- Pumijumnong N, Brauning A, Sano M, Nakatsuka T, Muangsong C, Buajan S (2020) A 338-year tree-ring oxygen isotope record from Thai teak captures the variations in the Asian summer monsoon system. *Sci Rep* 10
- Rahman M, Islam M, Gebrekirstos A, Bräuning A (2020) Disentangling the effects of atmospheric CO<sub>2</sub> and climate on intrinsic water-use efficiency variability in South Asian tropical moist forest trees. *Tree Physiol* 40:904–916
- Roggy JC, Prévost MF, Gourbiere F, Casabianca H, Garbaye J, Domenach AM (1999) Leaf natural <sup>15</sup>N abundance and total N concentration as potential indicators of plant N nutrition in legumes and pioneer species in a rain forest of French Guiana. *Oecologia* 120:171–182
- Rozendaal DMA, Zuidema PA (2011) Dendroecology in the tropics: a review. *Trees Struct Funct* 25:3–16
- Sano M, Xu CX, Nakatsuka T (2012) A 300-year Vietnam hydroclimate and ENSO variability record reconstructed from tree ring δ<sup>18</sup>O. *J Geophys Res Atmos* 117
- Scheidegger Y, Saurer M, Bahn M, Siegwolf R (2000) Linking stable oxygen and carbon isotopes with stomatal conductance and photosynthetic capacity: a conceptual model. *Oecologia* 125:350–357
- Schollaen K, Heinrich I, Neuwirth B, Krusic PJ, D'Arrigo RD, Karyanto O, Helle G (2013) Multiple tree-ring chronologies (ring width, δ<sup>13</sup>C and δ<sup>18</sup>O) reveal dry and rainy season signals of rainfall in Indonesia. *Quat Sci Rev* 73:170–181
- Schollaen K, Karamperidou C, Krusic P, Cook E, Helle G (2015) ENSO flavors in a tree-ring δ<sup>18</sup>O record of *Tectona grandis* from Indonesia. *Clim Past* 11:1325–1333
- Schöngart J, Piedade MTF, Ludwigshausen S, Horna V, Worbes M (2002) Phenology and stem-growth periodicity of tree species in Amazonian floodplain forests. *J Trop Ecol* 18:581–597
- Schöngart J, Bräuning A, Maioli Campos Barbosa AC, Lisi CS, Moraes de Oliveira J (2017) Dendroecological studies in the neotropics: history, status and future challenges. In: Amoroso MM, Daniels LD, Baker PJ, Camarero JJ (eds) *Dendroecology—tree-ring analyses applied to ecological studies*. Springer International Publishing, Switzerland
- Schubert BA, Timmermann A (2015) Reconstruction of seasonal precipitation in Hawai'i using high-resolution carbon isotope measurements across tree rings. *Chem Geol* 417:273–278
- Schwendenmann L, Pendall E, Sanchez-Bragado R, Kunert N, Hoelscher D (2015) Tree water uptake in a tropical plantation varying in tree diversity: interspecific differences, seasonal shifts and complementarity. *Ecohydrology* 8:1–12
- Silva LCR, Anand M (2013) Probing for the influence of atmospheric CO<sub>2</sub> and climate change on forest ecosystems across biomes. *Glob Ecol Biogeogr* 22:83–92
- Stahl C, Herault B, Rossi V, Burban B, Brechet C, Bonal D (2013) Depth of soil water uptake by tropical rainforest trees during dry periods: does tree dimension matter? *Oecologia* 173:1191–1201
- Sternberg LSLO (2009) Oxygen stable isotope ratios in tree-ring cellulose: the next phase of understanding. *New Phytol* 181:553–562
- Sturm C, Hoffmann G, Langmann B (2007) Simulation of the stable water isotopes in precipitation over South America: comparing regional to global circulation models. *J Clim* 20:3730–3750
- Thompson LG, Mosley-Thompson E, Brecher H, Davis M, León B, Les D, Lin PN, Mashiotta T, Mountain K (2006) Abrupt tropical climate change: past and present. *Proc Natl Acad Sci USA* 103:10536–10543
- van der Sleen P, Soliz-Gamboa CC, Helle G, Pons TL, Anten NPR, Zuidema PA (2014) Understanding causes of tree growth response to gap formation: Δ<sup>13</sup>C-values in tree rings reveal a predominant effect of light. *Trees Struct Funct* 28:439–448
- van der Sleen P, Vlam M, Groenendijk P, Anten NPR, Bongers F, Bunyavejchewin S, Hietz P, Pons TL, Zuidema PA (2015) <sup>15</sup>N in tree rings as a bio-indicator of changing nitrogen cycling in tropical forests: an evaluation at three sites using two sampling methods. *Front Plant Sci* 6:229

- van der Sleen P, Groenendijk P, Zuidema PA (2015) Tree-ring  $\delta^{18}\text{O}$  in African mahogany (*Entandrophragma utile*) records regional precipitation and can be used for climate reconstructions. *Glob Planet Chang* 127:58–66
- van der Sleen P, Groenendijk P, Vlam M, Anten NPR, Boom A, Bongers F, Pons TL, Terburg G, Zuidema PA (2015) No growth stimulation of tropical trees by 150 years of  $\text{CO}_2$  fertilization but water-use efficiency increased. *Nat Geosci* 8:24–28
- van der Sleen P, Zuidema PA, Pons TL (2017) Stable isotopes in tropical tree rings: theory, methods and applications. *Funct Ecol* 31:1674–1689
- van der Sleen P (2014) Environmental and physiological drivers of tree growth. Wageningen University, the Netherlands
- Verheyden A, Helle G, Schleser GH, Dehairs F, Beeckman H, Koedam N (2004) Annual cyclicity in high-resolution stable carbon and oxygen isotope ratios in the wood of the mangrove tree *Rhizophora mucronata*. *Plant Cell Environ* 27:1525–1536
- Villacis M, Vimeux F, Taupin JD (2008) Analysis of the climate controls on the isotopic composition of precipitation ( $\delta^{18}\text{O}$ ) at Nuevo Rocafuerte, 74.5°W, 0.9°S, 250 m Ecuador. *Comptes Rendus Geosci* 340:1–9
- Vitousek PM, Howarth RW (1991) Nitrogen limitation on land and in the sea: how can it occur? *Biogeochemistry* 13:87–115
- Vlam M, Baker PJ, Bunyavejchewin S, Zuidema PA (2014) Temperature and rainfall strongly drive temporal growth variation in Asian tropical forest trees. *Oecologia* 174:1449–1461
- Vlam M, de Groot GA, Boom A, Copinid P, Larosb I, Veldhuijzena K, Zakamdie D, Zuidema PA (2018) Developing forensic tools for an African timber: regional origin is revealed by genetic characteristics, but not by isotopic signature. *Biol Cons* 220:262–271
- Volland F, Pucha D, Bräuning A (2016) Hydro-climatic variability in southern Ecuador reflected by tree-ring oxygen isotopes. *Erdkunde* 70:69–82
- Waterhouse JS, Cheng SY, Juchelka D, Loader NJ, McCarroll D, Switsur VR, Gautam L (2013) Position-specific measurement of oxygen isotope ratios in cellulose: isotopic exchange during heterotrophic cellulose synthesis. *Geochim Cosmochim Acta* 112:178–191
- Wils THG, Robertson I, Eshetu Z, Koprowski M, Sass-Klaassen UGW, Touchan R, Loader NJ (2010) Towards a reconstruction of Blue Nile baseflow from Ethiopian tree rings. *Holocene* 20:837–848
- Worbes M (2002) One hundred years of tree-ring research in the tropics—a brief history and an outlook to future challenges. *Dendrochronologia* 20:217–231
- Xu C, Sano M, Nakatsuka T (2011) Tree ring cellulose  $\delta^{18}\text{O}$  of *Fokienia hodginsii* in northern Laos: a promising proxy to reconstruct ENSO? *J Geophys Res D Atmos* 116:D24109
- Xu CX, Sano M, Yoshimura K, Nakatsuka T (2014) Oxygen isotopes as a valuable tool for measuring annual growth in tropical trees that lack distinct annual rings. *Geochem J* 48:371–378
- Xu CX, Pumijumong N, Nakatsuka T, Sano M, Li Z (2015) A tree-ring cellulose  $\delta^{18}\text{O}$ -based July–October precipitation reconstruction since AD 1828, northwest Thailand. *J Hydrol* 529:433–441
- Xu C, Sano M, Nakatsuka T (2013) A 400-year record of hydroclimate variability and local ENSO history in northern Southeast Asia inferred from tree-ring  $\delta^{18}\text{O}$ . *Palaeogeogr Palaeoclim Palaeoecol* 386:588–598
- Zhu M, Stott L, Buckley B, Yoshimura K (2012) 20th century seasonal moisture balance in Southeast Asian montane forests from tree cellulose  $\delta^{18}\text{O}$ . *Clim Chang* 115:505–517
- Zhu MF, Stott L, Buckley B, Yoshimura K, Ra K (2012b) Indo-Pacific Warm Pool convection and ENSO since 1867 derived from Cambodian pine tree cellulose oxygen isotopes. *J Geophys Res Atmos* 117
- Zuidema PA, Brienens RJW, Schöngart J (2012) Tropical forest warming: looking backwards for more insights. *Trends Ecol Evol* 27:193–194
- Zuidema PA, Poulter B, Frank DC (2018) A wood biology agenda to support global vegetation modelling. *Trends Plant Sci* 23:1006–1015

**Open Access** This chapter is licensed under the terms of the Creative Commons Attribution 4.0 International License (<http://creativecommons.org/licenses/by/4.0/>), which permits use, sharing, adaptation, distribution and reproduction in any medium or format, as long as you give appropriate credit to the original author(s) and the source, provide a link to the Creative Commons license and indicate if changes were made.

The images or other third party material in this chapter are included in the chapter's Creative Commons license, unless indicated otherwise in a credit line to the material. If material is not included in the chapter's Creative Commons license and your intended use is not permitted by statutory regulation or exceeds the permitted use, you will need to obtain permission directly from the copyright holder.



# Chapter 23

## Forest Management and Tree-Ring Isotopes



John D. Marshall, J. Renée Brooks, and Alan F. Talhelm

**Abstract** Forest management can be improved by the mechanistic understanding that tree-ring stable isotopes provide. Key management tools include genetic selection, competing vegetation control, thinning, and fertilization. These tools frequently change environmental conditions and physiological processes, such as photosynthesis, stomatal conductance, water uptake, and nitrogen cycling, which may leave isotopic signatures in tree-rings, providing detailed responses to management over decadal time periods. While data sets remain small, some trends have emerged from previous forest management studies using stable isotopes. Genotype selection sometimes shows isotopic evidence of maladaptation, especially in the presence of climate change. Competition control and thinning have different isotopic reactions depending on the dryness of the site; they generally obtain different responses depending on whether competition is primarily for aboveground (light) or belowground (water and nutrient) resources. Fertilization responses recorded in tree rings appear to be driven by initial increases in photosynthesis, and later by increases in leaf area index. Tree-ring isotopic applications can provide key insights to a much broader range of silvicultural objectives than included here, and we encourage their application in large-scale silvicultural experiments to reduce uncertainties and explain mechanisms of response. In future work, we suggest that management studies wishing to utilize tree-ring stable isotopic analysis include key ancillary measurements, especially leaf nitrogen concentrations, leaf-area index, xylem water sources, and canopy temperature, to help support interpretation of the isotopic data.

---

J. D. Marshall (✉)

Department of Forest Ecology and Management, Swedish University of Agricultural Sciences, 90183 Umeå, Sweden

e-mail: [john.marshall@slu.se](mailto:john.marshall@slu.se)

J. R. Brooks

Pacific Ecological Systems Division, Center for Public Health and Environmental Assessment, Office of Research and Development, U. S. Environmental Protection Agency, 200 SW 35th St. Corvallis, Corvallis, OR 97333, USA

A. F. Talhelm

Department of Forest, Rangeland, and Fire Sciences, University of Idaho, Moscow, ID 83844, USA

© The Author(s) 2022

R. T. W. Siegwolf et al. (eds.), *Stable Isotopes in Tree Rings*, Tree Physiology 8, [https://doi.org/10.1007/978-3-030-92698-4\\_23](https://doi.org/10.1007/978-3-030-92698-4_23)

## 23.1 Introduction

Forest management activities are designed to alter stand and tree growth, composition, structure, and/or other ecosystem properties (Smith et al. 1997). Management activities such as thinning, prescribed burning, herbicide application, or fertilization change resource availability within forests, altering tree growth (Fox et al. 2007; Johnson and Curtis 2001; Jurgensen et al. 1997; Neary et al. 1999). However, because these activities often change the availability of multiple resources—including moisture, nutrients, and light (e.g. Jurgensen et al. 1997; Neary et al. 1999)—the physiological or ecological mechanisms responsible for changes in tree growth can be unclear. The forestry research community has long been interested in understanding how management activities affect both resource availability and tree physiology. Their wish has been for more mechanistic prescriptions to meet objectives including the optimization of forest productivity (e.g., Campoe et al. 2013; Forrester et al. 2013; Gauthier and Jacobs 2009; Gspaltl et al. 2013), adaptation to climate change (e.g. Chmura et al. 2011; Lindner et al. 2014; Martin-Benito et al. 2011), and the production and maintenance of ecosystem services (Deal et al. 2012; Ford et al. 2011; Luysaert et al. 2018).

Stable isotopes are an important tool to understand the response to trees, stands and ecosystems to management because they integrate and trace physical and physiological processes over time and space (Dawson et al. 2002; West et al. 2006; Sulzman 2008; Werner et al. 2012). Forestry researchers were early adopters of some stable isotope techniques (e.g., Heilman et al. 1982; Högberg et al. 1993; Nambiar and Bowen 1986). The use of these techniques has expanded rapidly in the last decade to encompass a variety of management practices in ecosystems from the African savanna to giant sequoia forests in California (e.g., Cramer et al. 2010; York et al. 2010). However, although stable isotopes can be powerful analytical tools, the application and interpretation of stable isotope methods can be complex because numerous abiotic and biotic processes alter the relative abundance of individual isotopes (Dawson et al. 2002; Sulzman 2008; Werner et al. 2012; West et al. 2006).

In this chapter, we describe isotopic consequences of management effects and discuss their mechanistic interpretation. We first present, in chronological order, several of the traditional management tools used in even-aged stands from planting to harvest, largely because much of the isotopic literature examining forest management occurred in such stands. This organization is intended to clarify, not to suggest that forest managers are limited to these tools and applications. In fact, these management tools can be used to foster a broad range of ecosystem services, which isotopic data can help inform. We provide both illustrative examples and, in the cases of nutrient additions (fertilization) and thinning, meta-analyses. We present the results of a new meta-analysis here, but we also summarize an earlier meta-analysis (Sohn et al. 2016) of thinning effects on drought responses of tree growth.

We focus here on carbon isotope discrimination ( $\Delta^{13}\text{C}$ , Chap. 9) and oxygen isotopic ratios ( $\delta^{18}\text{O}$ , Chap. 10), with brief mention of nitrogen isotope ratios ( $\delta^{15}\text{N}$ ,

Chap. 12). We neglect hydrogen isotope ratios ( $\delta^2\text{H}$ ) because they are often so correlated with  $\delta^{18}\text{O}$  and because hydrogen exchanges so readily with atmospheric water vapor that the samples must undergo complex preparation (Chap. 11). The method is therefore not prevalent in forest management applications. Intense work is going on with  $\delta^2\text{H}$  preparation techniques and it seems likely that they will become more feasible in the near future.

## 23.2 Choice of Species and Genotype

One of the most powerful tools of forest management is the ability to select the species and genotypes comprising the stand. Foresters can plant favored trees, cull unwanted species or phenotypes, or create conditions that are favorable for particular trees. Tree species differ substantially in  $\Delta^{13}\text{C}$ , which is correlated with intrinsic water-use efficiency (iWUE, Chap. 17) defined as the ratio of net photosynthetic rate to stomatal conductance ( $A/g_s$ ). Numerous studies have evaluated interspecific differences in  $\Delta^{13}\text{C}$  in order to evaluate traits such as drought tolerance and water-use efficiency (e.g., Bonhomme et al. 2008; Jansen et al. 2013; Voltas et al. 2006). Broadly, in interspecific studies, deciduous trees show more positive  $\Delta^{13}\text{C}$  and lower iWUE (intrinsic water-use efficiency) than co-occurring needle-leaved evergreens, which themselves have more positive  $\Delta^{13}\text{C}$  and lower iWUE than scale-leaved evergreens (Marshall and Zhang 1994). Long-lived leaves tend to have greater leaf mass per area ( $\text{g/m}^2$ ) (Wright et al. 2004), which is associated with lower mesophyll conductance (Flexas et al. 2014; Niinemets et al. 2009). This relationship is thought (Hultine and Marshall 2000) to be the primary reason why a negative correlation between leaf  $\Delta^{13}\text{C}$  and leaf mass per area has been frequently observed (Araus et al. 1997; Hanba et al. 1999; Hultine and Marshall 2000; Körner et al. 1991; Takahashi and Miyajima 2008; Talhelm et al. 2011). In any case, if a forest is likely to deplete the soil water supply during the growing season, then efficient use of that water generally enhances forest growth (Zhang et al. 1995; Zhang and Marshall 1995) and possibly survival (Timofeeva et al. 2017).

Species differences in water access have also been detected in  $\delta^{18}\text{O}$  of xylem water or wood. These differences in water source may be caused by differences in vertical root distribution, where water deeper in the soil tends to be more depleted in heavy isotopes ( $^{18}\text{O}$ ,  $^2\text{H}$ ) than water found near the soil surface (Hartl-Meier et al. 2015; see Chap. 18). This isotopic difference within the soil profile has been used to understand how species partition water resources (Flanagan et al. 1992) and how water-use patterns change seasonally (Dawson 1998; Meinzer et al. 1999). When species are mixed, the root systems may be deployed at different depths, leading to differences in vertical water-uptake. The resulting niche partitioning may give rise to overcompensation, the tendency of a species mixture to be more productive than monospecific stands of either species alone (Pretzsch et al. 2013). However, species mixtures may also lead to growth reductions and mortality for some of the species (Granda et al. 2014). For example, shallow-rooted spruce trees were more



negatively influenced by drought than more deeply rooted beech trees in a mixed stand (Brinkmann et al. 2018). Alternatively, differences in tissue or leaf water  $\delta^{18}\text{O}$  may also reflect differences in transpiration timing or rate (Chap. 10). In either case,  $\delta^{18}\text{O}$  differences provide an index of water sources and water use (Marshall and Monsrud 2006). When combined with  $\delta^{13}\text{C}$ ,  $\delta^{18}\text{O}$  in cellulose may allow one to distinguish whether water-use efficiency has been modified by changes in photosynthesis or transpiration (Scheidegger et al. 2000; see Chap. 16). However, using  $\delta^{18}\text{O}$  to draw insight into leaf gas exchange requires knowledge or assumptions about the  $\delta^{18}\text{O}$  of xylem water (Gessler et al. 2018; Roden and Siegwolf 2012; Chap. 18).

Seedling planting also offers the opportunity to control genetic composition (e.g., species, genotype, and clone) and initial stand structure. In intensive forestry, “tree improvement” is almost always focused on increased timber yield through rapid growth, wood quality, or increased pest resistance. Careless matching of genotype to environment can be deleterious, causing frost damage when coastal Douglas-fir (*Pseudotsuga menziesii*) was moved inland (Rehfeldt 1977), or suboptimal growth when cold-tolerant lodgepole pine (*Pinus contorta*; McLane et al. 2011) or Douglas-fir (Leites et al. 2012) were moved to warmer climates. Planting can also be used to assist the migration of warm climate genotypes toward areas that were once too cold for them, but are no longer (Savolainen et al. 2004). Isotopic data have been used as a screening criterion to describe the populations within a species, often from young trees planted in common gardens (Gornall and Guy 2007; Guerra et al. 2016; Monclus et al. 2006). This approach has also identified provenance differences in rooting depth using  $\delta^{18}\text{O}$  (Voltas et al. 2015). Although these studies have mostly focused on ecological questions related to species adaptations to a particular climate, the observed correlation of  $\Delta^{13}\text{C}$  with height growth or biomass production has also been used to justify genotype selections (Marguerit et al. 2014; Zhang et al. 1995; Zhang and Marshall 1994, 1995). In addition, quantitative trait loci have been applied in native populations to determine whether WUE can be increased without decreasing productivity (Brendel et al. 2002, 2008; Marguerit et al. 2014). In a recent paper, Isaac-Renton et al. (2014) provided a compelling assessment of the climate-change consequences of climate maladaptation in lodgepole pine (Fig. 23.1). The northern populations were defined as “leading edge” because the species is presumably moving northward. These northern populations lacked some of the drought adaptations found in the southern “trailing edge” populations, which may reduce their ability to deal with future droughts. Lodgepole pine has been well studied in this respect, but these same questions can and should be asked about other species as well.

### 23.3 Control of Competing Vegetation

Managers often prepare sites for planting or improve growing conditions for young trees by removing competing vegetation with herbicides or mechanical treatments. These treatments increase the availability of light, water, and nutrients and improve

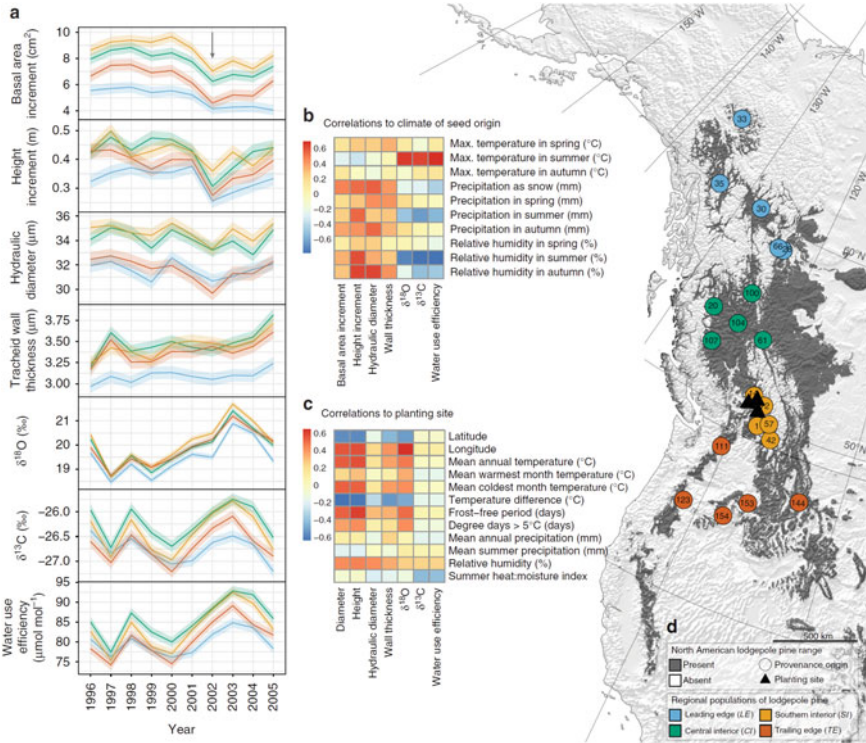


**Fig. 23.1** Variations in growth and physiology of lodgepole pine (*Pinus contorta*) in relation to climate and provenance. **a** serial changes in several growth and tree-ring traits, including stable carbon isotope ratios emphasizing the excursion from the long-term mean in the drought year, 2002. **b** correlations among traits. **c** map of the seed sources and the planting sites. From Isaac-Renton et al. (2014)

tree growth. Because competition control increases the availability of several important resources simultaneously, stable isotopes can be useful for identifying the primary mechanism creating the growth response, particularly when complemented by supporting observations.

Competition control often increases  $\Delta^{13}\text{C}$  by releasing water to the trees, which would increase stomatal conductance. For instance, Ares and colleagues (2007) observed that five years of herbicide treatments reduced canopy cover of competing vegetation from 95 to 7% among newly established Douglas-fir saplings on the western slope of the Coast Range in the northwestern United States. For the Douglas-fir, competition control increased tree growth, foliar N concentrations, and soil moisture availability. In analysis of tree ring  $\Delta^{13}\text{C}$  of the Douglas-fir trees, earlywood  $\Delta^{13}\text{C}$  was unaffected by the herbicide treatments, but the latewood was higher in  $\Delta^{13}\text{C}$ , which led Ares et al. (2008) to conclude that increased soil moisture availability in the late summer was the primary driver of increased tree growth. Likewise, in young ponderosa pine seedlings, reduced competition reduced water stress and

increased  $\Delta^{13}\text{C}$  (Pinto et al. 2011, 2012). Similarly, removal of understory shrubs from stands of *Pinus densiflora* in western Japan increased foliar  $\Delta^{13}\text{C}$  and both stomatal conductance and foliar N. Increased foliar  $\Delta^{13}\text{C}$  suggests that the observed increases in growth were caused primarily by increased water availability (Kume et al. 2003).

In contrast, competition control sometimes improves light or nutrient status, which increases photosynthesis, decreasing  $\Delta^{13}\text{C}$ . For instance, mechanical and herbicide treatments to control grass growing beneath 10-year old white spruce (*Picea glauca*) trees in boreal Canada also increased tree growth, foliar N, and soil moisture, but reduced foliar  $\Delta^{13}\text{C}$  (Matsushima et al. 2012). This reduction in foliar  $\Delta^{13}\text{C}$ , which was correlated with foliar N concentration and coupled with a concomitant increase in foliar  $\delta^{15}\text{N}$ , led the authors to conclude that the increase in N availability was the primary mechanism by which competition control increased growth in their study. Similarly, competition control decreased red pine (*Pinus resinosa*) tree ring  $\Delta^{13}\text{C}$  in the north-central United States (Powers et al. 2010). Clearly, the physiological effects of competition control depend on which resources are released and the ability of trees to utilize these resources to acquire C.

## 23.4 Thinning

Managers thin forests primarily to increase growth of the remaining trees or to create stands that are more resilient to climate stress, insects, disease, and wildfire. Like the removal of competing vegetation, decreasing tree density within a stand reduces competition for resources that limit tree productivity. Thinning can increase the availability of water, nutrients, and light; trees respond physiologically to an increase in each of those resources with changes in the isotopic signatures recorded in tree rings.

We assessed the  $\Delta^{13}\text{C}$  response across all years and all studies in a meta-analysis (Fig. 23.2) and found that the direction of the discrimination change depended on the mean annual precipitation at the site. While we note that this analysis contains data from only a relative handful of studies, we presume that this reflects differences in physiological responses to thinning. At low precipitation sites, discrimination increases due to the water released to the remaining trees when the thinned trees are removed. The released water increases conductance more than it does photosynthesis, increasing  $\Delta^{13}\text{C}$  relative to the control. In contrast, at sites with high precipitation,  $\Delta^{13}\text{C}$  decreases after thinning, presumably due to improvements in the light or nitrogen status of the remaining trees, either of which would tend to increase rates of net photosynthesis. The water released by thinning sites must have less influence on  $\Delta^{13}\text{C}$  than the light and nutrient increases on these high-precipitation sites. These responses are unlikely to be species-specific responses as nearly all species respond to water stress by decreasing  $\Delta^{13}\text{C}$  (Granda et al. 2014; Grossiord et al. 2014).

Under dry conditions, thinning can mitigate drought stress and tree ring stable isotopes have helped illuminate the physiological mechanisms of drought resistance

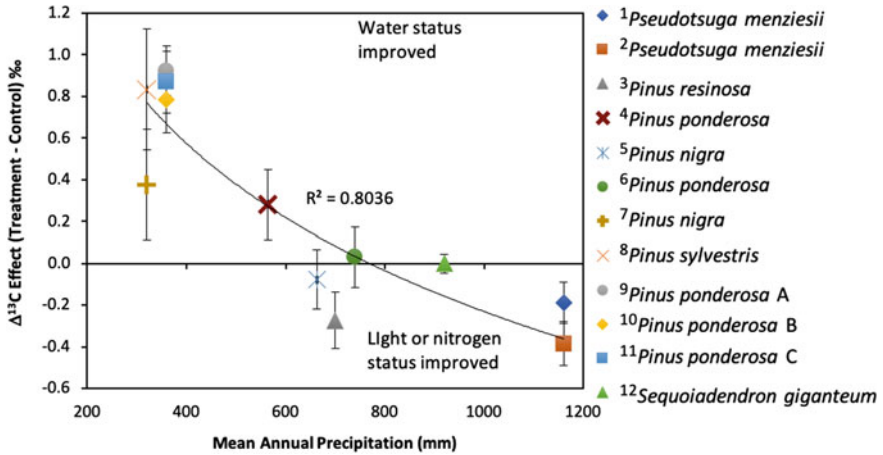


**Fig. 23.2** Normalized change in discrimination  $\pm$  SE Versus mean annual precipitation at the study site.  $\Delta^{13}\text{C}$  values are mean responses from each study from the period up to 10 years following the thinning treatment. 1. Brooks and Mitchell (2011) (Thin); 2. Brooks and Mitchell (2011) (Thin x Fertilization); 3. Powers et al. (2010); 4. Sohn et al. (2014); 5. Martin-Benito et al. (2011); 6. Leavitt and Long (1986); 7. Navarro-Cerrillo et al. (2019) (*Pinus nigra*); 8. Navarro-Cerrillo et al. (2019) (*Pinus sylvestris*); 9. McDowell et al. (2003) Stand A; 10. McDowell et al. (2003) Stand B; 11. McDowell et al. (2003) Stand C; 12. York et al. (2010)

(Sohn et al. 2012, 2014, 2016). In an earlier meta-analysis of thinning effects on drought response, tree ring isotopic data revealed that in conifers, heavy thinning influenced  $\Delta^{13}\text{C}$  in a drought year more strongly than in the other years (Sohn et al. 2016). The heavy thinning treatments also changed  $\delta^{18}\text{O}$  more strongly in the drought year. However, thinning influenced the isotopic data both before and after the drought year as well. An analysis of ring-width data in the same paper showed clearer patterns, in part because it included broadleaf species. For the broadleaves, thinning appeared to increase soil moisture available to the trees during drought, allowing them to resist changes in growth during the drought year. Voelker et al. (2019) also found that stand basal area influenced drought sensitivity; stands at lower basal areas demonstrated decreasing trends in  $A/g_s$ , and greater resilience to droughts. However, they found stands with high basal area had increasing trends in  $A/g_s$  over the same period of time, which they attributed to greater water limitations and lower drought resilience. Kruse et al. (2012) also noted that stand density influenced the degree of stomatal control over  $A/g_s$ .

In more mesic environments, thinning can increase exposure of the remaining canopy to both greater light and higher vapor pressure deficits, as well as increase nutrient availability (Fig. 23.2). For example, *Pinus pinaster*, *Pinus radiata* and *Pinus resinosa* all decreased  $\Delta^{13}\text{C}$  after thinning, presumably from an increase in  $A$  relative to  $g_s$  from greater light exposure and/or greater leaf nitrogen content (Warren et al. 2001; Powers et al. 2010). However, for *Pinus nigra*, *Pinus halepensis*, and *Pseudotsuga menziesii* growing in mesic environments, tree ring  $\Delta^{13}\text{C}$  did not

change significantly with thinning while growth increased, implying that both  $A$  and  $g_s$  increased in response to increased canopy light exposure and water resources.

Responses of trees to thinning are not always intuitive. Ruzicka et al. (2017) used  $\Delta^{13}C$  and ring widths to examine stand responses to thinning in three Douglas-fir sites that varied along a moisture gradient. Similar to what was reported above for mesic sites, trees in the thinned stands grew more at the wet and intermediate sites, but had no significant change in  $iWUE$  relative to the unthinned control trees. However, at the driest site, trees in the thinned stand did not produce larger growth increments, and increased in  $iWUE$ , which implies that water was not the main limiting factor. Instead, they speculated that  $g_s$  decreased from greater exposure to the surrounding atmosphere and increased evaporative demand.

Forest thinning is usually applied at long intervals, with a decade or more to recover between operations. Therefore, the physiological responses to thinning should exhibit a regular temporal pattern in the subsequent years. As noted above, when water resources are limiting growth, density reduction should result in greater water availability to the remaining trees. An initial increase in water resources should increase stomatal conductance if leaf area, sapwood area and root area do not immediately adjust. As a result,  $iWUE$  would be expected to decrease and discrimination would be expected to increase in water-limited site. As shown by the red and pink points in Fig. 23.3, the expected increase did occur, but only on the driest sites and only in the first and second years after thinning. This may be due to increases in water availability leading to increased growth (McDowell et al. 2003, 2006; Giuggiola

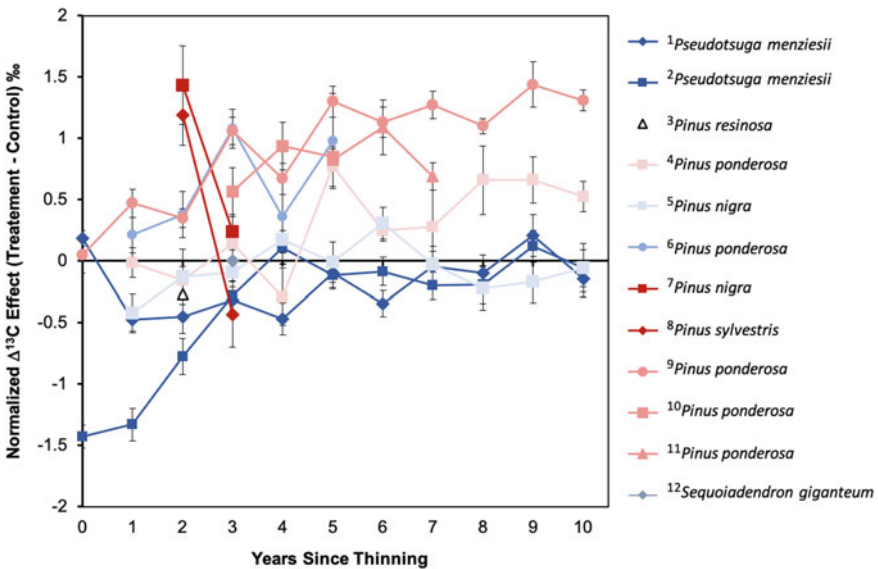
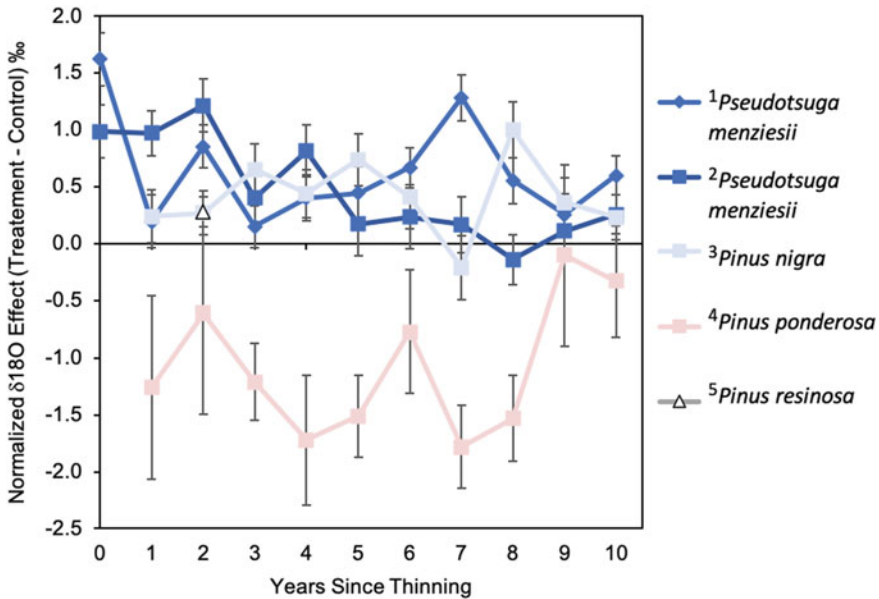


Fig. 23.3 Carbon isotope discrimination ( $\pm$  variance) by year after thinning, where year 0 is the year the thinning treatment was applied. Data series displayed in rank order of wet (dark blue) to dry (dark red) based on mean annual precipitation. See Fig. 23.2 for precipitation values and citations

et al. 2016; Di Matteo et al. 2010). However, these stands varied in the duration of the response (Fig. 23.3). For example in eastern Oregon, McDowell et al. (2003) examined the change in cellulose  $\delta^{13}\text{C}$  in a stand of 250-year old ponderosa pine trees (*Pinus ponderosa*) where thinning selectively left the largest trees with wide spacing, removing 60–80% of the basal area.  $\Delta^{13}\text{C}$  increased a year after the thinning treatment and remained higher for at least 12 years when they collected cores, whereas growth differences were not noted until 4 years after the treatment. Predawn water potentials of the foliage were significantly less negative in the thinned trees compared to neighboring control stands, indicating that soil water availability was still higher in the thinned stands 12 years after the treatment. In another ponderosa pine stand located in Arizona, McDowell et al. (2006) noted that after a four-year lag,  $\Delta^{13}\text{C}$  values increased for approximately 12 years of a density reduction experiment (shown in Fig. 23.3 as Sohn et al. 2014, who re-analyzed the McDowell et al. 2006 data). In this study, the basal area increment (BAI) produced in a given year was related to this change in  $\Delta^{13}\text{C}$ , with higher levels of thinning producing a greater increase in  $\Delta^{13}\text{C}$  and greater increases in BAI. However, after 12 years,  $\Delta^{13}\text{C}$  returned to pretreatment levels even though stand densities of the treatments were maintained. They found that the whole tree leaf area to sapwood area had adjusted such that trees in the low basal area stands had significantly more leaf area per unit sapwood area, and suspected that increases in tree leaf area returned to a homeostatic balance of  $A/g_s$  at pretreatment levels. Giuggiola et al. (2016) found similar results in a xeric Scots pine (*Pinus sylvestris*) thinning experiment they followed for over 40 years. At least in xeric locations, thinning does appear to increase water to the remaining trees initially, increasing stomatal conductance of the existing foliage. However, after a decade or so, the trees at xeric sites adjusted their leaf area and root area and returned to homeostasis in  $A/g_s$ .

Our meta-analysis of  $\delta^{18}\text{O}$  responses to thinning was based on few studies, but we again found different responses depending on the precipitation amount at the site (Fig. 23.4). The change was positive on the wetter sites and negative on the one drier site. Increases in cellulose  $\delta^{18}\text{O}$  indicate that the environment around the trees changed in some way, perhaps with decreased relative humidity, increased leaf temperatures, and/or shallower root water uptake for the thinned trees (Brooks and Mitchell 2011; Martin-Benito et al. 2011; Moreno-Gutiérrez et al. 2011). These studies with increased  $\delta^{18}\text{O}$  assumed that source water between control and thinned plots did not change, so speculated that the increases in  $\delta^{18}\text{O}$  from thinning were from increased leaf temperatures from increased solar irradiance, and decreased relative humidity around the foliage from increased boundary layer conductance in the open stands (Jarvis and McNaughton 1986). Canopy coupling to the ambient air is generally high for conifers (Jarvis and McNaughton 1986), which would minimize the change in boundary layer with thinning, but thinning in Brooks and Mitchell (2011) removed 2/3 of the basal area, changing the remaining trees from being in dense closed canopies to having completely exposed canopies (Martin et al. 1999). This dramatic shift in canopy density could be enough change in leaf temperature and relative humidity to cause the modest change in  $\delta^{18}\text{O}$ . However, the assumption of constant water sources between treatments may not be accurate as water uptake may



**Fig. 23.4** Difference in  $\delta^{18}\text{O}$  of tree rings between thinned and control stands as a function of time since thinning. Positive values indicate higher  $\delta^{18}\text{O}$  in the thinned stands. Colors designate mean annual precipitation as in Fig. 23.2. 1. Brooks and Mitchell (2011) (Thin); 2. Brooks and Mitchell (2011) (Thin x Fertilization); 3. Martin-Benito et al. (2011); 4. Sohn et al. (2014); 5. Powers et al. (2010)

shift within the soil profile. An upward shift in root water uptake in thinned stands might favor more enriched source water (Brinkmann et al. 2018). The downward shift after thinning on the drier site is difficult to explain, but the authors speculated a decrease in the isotopic value of source water in the thinned stands (Sohn et al. 2014). Higher transpiration rates in the thinned stands would lead to use of deeper, isotopically more depleted water sources (Chap. 18). This shift in water uptake might be consistent with the hypothesis presented earlier for these same stands, that the root:shoot balance is modified such that the roots can reach deeper depleted water. In future studies, measurements of xylem source water and leaf temperature between treatments would greatly assist in the process of choosing among these potential explanations.

One additional complication to interpreting tree ring stable isotopes in trees is that stress may increase their reliance on stored carbohydrates (Helle and Schleser 2004). As a result, slow-growing stressed trees appear to have less isotopic variance over time compared to neighboring trees in stands that have been thinned (McDowell et al. 2006; Sohn et al. 2014). Both  $\delta^{13}\text{C}$  and  $\delta^{18}\text{O}$  showed much lower variance between years in control stands and in pretreatment values as compared to after

the density reduction (McDowell et al. 2006; Sohn et al. 2014). This difference in isotopic variance for both  $\delta^{13}\text{C}$  and  $\delta^{18}\text{O}$  could be caused by a greater reliance on stored carbohydrates in the slow-growing control trees, which would mute the isotopic response to perturbation in any particular year.

### 23.5 Fertilization and Nutrition

Nutrient fertilization is typically applied to forest stands after a pre-commercial or commercial thinning or after stand differentiation has occurred in order to accelerate tree growth and shorten the rotation (Miller 1981). As with thinning, the date of fertilization provides an obvious reference point for analysis of its effects, and tree ring studies can compare pre- and post-treatment responses. As noted above, the response of  $\Delta^{13}\text{C}$  to fertilization depends on the mechanism of response. If fertilization increases the nitrogen concentration within foliage, photosynthesis would be expected to increase (Brix 1971, 1981). Since water resources are not directly altered by fertilization, stomatal conductance could be expected to remain similar to pre-fertilization rates. Thus, increases in foliar N concentration are expected to decrease  $\Delta^{13}\text{C}$  and increase iWUE.

In the meta-analysis of  $\Delta^{13}\text{C}$ , we found a short-term response that generally supported this scenario (Fig. 23.5). Discrimination decreased in years 1 and 2, however the significant effect disappeared thereafter. However, the responses among

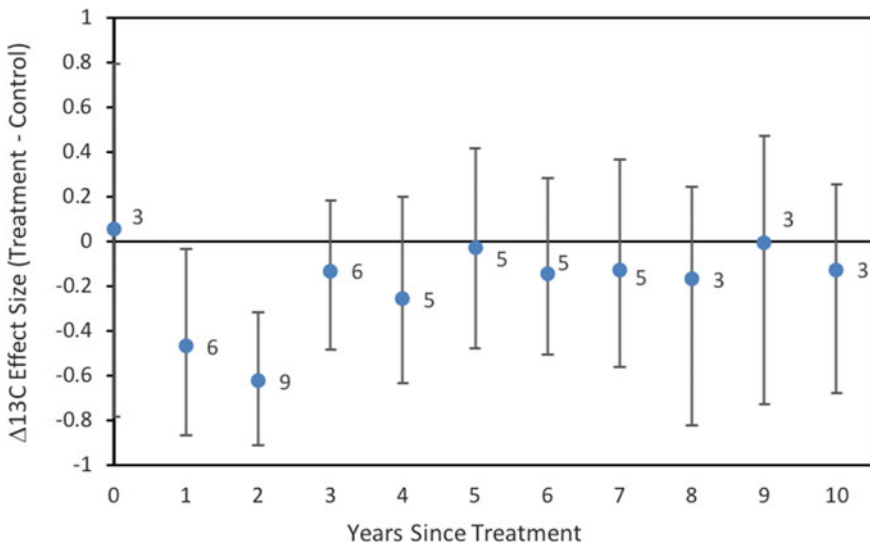


**Fig. 23.5** Mean  $\Delta^{13}\text{C}$  effect by time since fertilization from meta-analysis. Numbers near means represent the sample size of values (contrasts) included in the analysis for each year



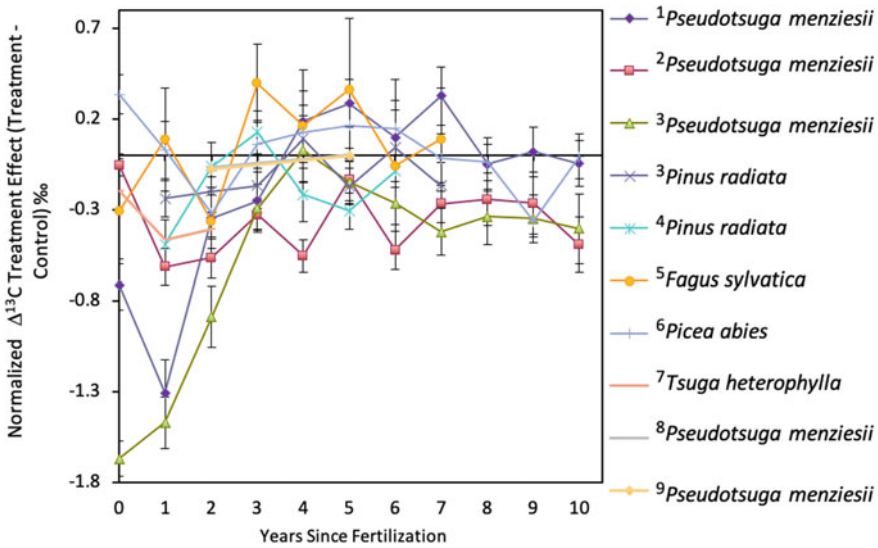


**Fig. 23.6** Differences in carbon isotope discrimination between fertilized and control stands. Negative values indicate lower discrimination and higher iWUE on the fertilized plots. 1. Brooks and Coulombe (2009); 2. Brooks and Mitchell (2011) (Fertilization); 3. Brooks and Mitchell (2011) (Thin xFertilization); 4. Kruse et al. (2012) (Daylesford); 5. Kruse et al. (2012) (Lyons); 6. Elhani et al. (2005); 7. Krause et al. (2012); 8. Walia et al. (2010); 9. Balster et al. (2009) (First Fertilization); 10. Balster et al. (2009) (Second Fertilization)

individual studies were rather different (Fig. 23.6). For example, Brooks and Mitchell (2011) found reduced discrimination, yielding the negative values in Fig. 23.6, for at least four years after fertilization in a nutrient-limited coastal Douglas-fir stand. These decreases in discrimination were correlated with increases in measured leaf nitrogen levels (Mitchell et al. 1996). Similarly, Brooks and Coulombe (2009) found a decrease in  $\Delta^{13}\text{C}$  for four years after fertilization in another nutrient-limited Douglas-fir stand in the Cascade Mountains, and speculated a similar increase in foliage nitrogen. Increasing foliar nitrogen is a common short-term response in these fertilization studies and as with studies of competition control and thinning, the increase in foliar N can help support interpretation of  $\Delta^{13}\text{C}$  and  $\delta^{18}\text{O}$  observations. For this reason, we suggest that measurement of foliar N should be incorporated in future stable isotope studies of leaf gas exchange.

In the longer term, fertilization can also cause increases in foliage leaf area, which may dilute the foliar nitrogen (Balster and Marshall 2000; Binkley and Reid 1985). If leaf area increases without an increase in foliar N levels, then foliar gas-exchange rates and  $\Delta^{13}\text{C}$  may not change. Photosynthetic rates may even decrease due to canopy shading, in which case  $\Delta^{13}\text{C}$  might increase. Note that this would offset the decrease that follows the fertilization immediately after the application. In the Brooks and Mitchell (2011) study, the decrease in  $\Delta^{13}\text{C}$  was observed even in the 10th and 11th years after fertilization. Likewise, the growth increase lasted many

more years and both stands were documented to have increased in leaf area. It is plausible that longer-term decreases in  $\Delta^{13}\text{C}$  in response to fertilization could be a consequence of increased leaf area or height growth, either of which might lead to stomatal closure (McDowell et al. 2002, 2011). In contrast to Brooks and Mitchell (2011), Balster et al. (2009) found no significant shifts in  $\Delta^{13}\text{C}$  from fertilization in Douglas-fir at 24 sites located in the interior northwest USA, although growth responses lasted for 8 years after treatment. However, leaf area index was increased (Balster and Marshall, 2000), providing a likely increase in canopy photosynthesis without a change in the gas-exchange setpoint reflected in  $\Delta^{13}\text{C}$ .

Antecedent site fertility influences the longevity of the  $\Delta^{13}\text{C}$  response to fertilization. Cornejo-Oviedo et al. (2017) found an increase in iWUE in both late and earlywood one year after fertilization in a productive coastal stand, in contrast to the 3–4 year increase in more nutrient limited stands mentioned above. Site moisture availability also has an influence. Liles et al. (2019) found no changes in iWUE in their most productive, wettest ponderosa pine site, but found increases in iWUE from fertilization at their drier sites.

Changes in  $\delta^{18}\text{O}$  in response to fertilization might be expected if fertilization influenced transpiration, the canopy microclimate (mostly relative humidity) or the source water accessed by the trees (Chaps. 10, 16, and 18). Some fertilization studies have reported strong changes to  $\delta^{18}\text{O}$ , while others have reported no significant changes. Brooks and Coulombe (2009) found a 2% increase in latewood  $\delta^{18}\text{O}$  with fertilization that lasted nearly a decade with the highest level of fertilization, but no change relative to controls for earlywood. They speculated that the  $\delta^{18}\text{O}$  increase in latewood was caused by the combination of high leaf-area index and late-summer drought in the dry Mediterranean summers of the Pacific Northwestern USA.

Although  $\delta^{18}\text{O}$  data showed significant treatment effects to the fertilization in a range of studies (Fig. 23.7), the effects were in different directions and they occurred at different times. Interpretation is limited by the small number of studies and the many possible sources of variation (Roden and Siegwolf 2012). Especially important are understanding which  $\delta^{18}\text{O}$  differences are caused by changes in canopy conditions and exposure following thinning and fertilization, as well as source-water variation (Sarris et al. 2013). Source water could be tested by measuring the isotopic composition of xylem water (Marshall et al. 2020; Volkman et al. 2016; White et al. 1985). We strongly recommend these measurements to minimize the uncertainties in these studies.

Nitrogen fertilization can also influence the  $\delta^{15}\text{N}$  of tree rings (Elhani et al. 2005; Peñuelas and Estiarte 1996; Poulson et al. 1995), particularly when the applied nitrogen has a different isotopic composition than native nitrogen in the soil, or when the fertilizer material tends to volatilize, leading to strong kinetic fractionation and a  $\delta^{15}\text{N}$  increase in the remaining nitrogen. This occurred in a study in which urea was applied to Douglas-fir forests in the northwestern US (Balster et al. 2009). In this study, the urea was converted to  $\text{NH}_4^+$ , which is quickly transformed to  $\text{NH}_3$  and released to the atmosphere. Although the fertilizer could not be detected through increases in wood N concentrations, the  $\delta^{15}\text{N}$  was significantly enriched in fertilized trees. Tree ring  $\delta^{15}\text{N}$  analyses are difficult because the nitrogen concentrations in

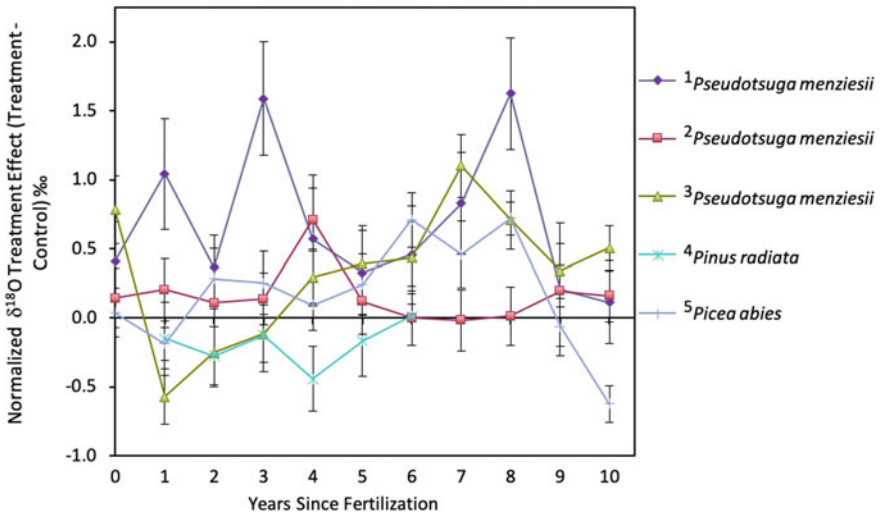


**Fig. 23.7** The change in  $\delta^{18}\text{O}$  of tree rings induced by a fertilization event at year zero. Positive values indicate that the  $\delta^{18}\text{O}$  of the fertilized plots were higher than those of the controls. 1. Brooks and Coulombe (2009); 2. Brooks and Mitchell (2011) (Fertilization); 3. Brooks and Mitchell (2011) (Thin x Fertilization); 4. Kruse et al. (2012) (Lyons); 5. Krause et al. (2012)

wood are so low compared to leaves or roots (Chap. 12). Further, interpretation of tree ring  $\delta^{15}\text{N}$  data should recognize that the labeled nitrogen can be translocated across the rings over time (Balster et al. 2009; Hart and Classen 2003; Sheppard and Thompson 2000), unlike the isotopic labels embedded in the C, H, and O in cell walls.

Experimental long-term annual fertilization is sometimes applied in forests. In such cases, changes in  $\delta^{15}\text{N}$  of plant tissues can be stark (Högberg and Johannisson 1993; Marshall and Linder 2013). Although they do not simulate standard management practice, these studies provide clear insights into mechanism of response. These clear differences are attributed to a combination of decreased N retention by mycorrhizal fungi and increased leaching of depleted nitrate, both of which tend to enrich  $^{15}\text{N}$  in leaves and tree rings (Högberg et al. 2014).

## 23.6 Modeling of Management Effects

Although stable isotopes are often used for assessment of treatment responses, the milieu of environmental, ecological, and physiological changes can be complex and difficult to interpret. These complexities can be addressed via models of tree ecophysiology and forest growth (see Chap. 26). This is especially important because forest management decisions are often driven by expectations about future growth. Wei et al. (2014) used  $\Delta^{13}\text{C}$  data to parameterize a physiological growth model in an

attempt to explain how large increases in tree growth were obtained from replicated fertilization and herbicide treatments. The model, 3-PG, includes an empirical parameter that describes the influence of nutrition on photosynthate allocation. Wei et al. (2014) set that parameter to its maximum in the treatments that combined fertilizer and herbicide, then empirically fitted the parameter to the other treatments. This was possible because all of the major fluxes of carbon and water were measured, as was the  $\Delta^{13}\text{C}$  of photosynthate. With so many parameters constrained by measurements, the allocation parameter could be fitted with more confidence.

The 3-PG model has also recently been modified to predict tree-ring  $\delta^{18}\text{O}$  (Ulrich et al. 2019). The model was applied to ponderosa pine trees growing over 107 years in a riparian and an upslope area. Key parameters in the  $\delta^{18}\text{O}$  model remained difficult to measure or verify, in particular the Péclet effect, which describes the back-diffusion of enriched water against the xylem flow into the leaf (Chap. 10). However, the model provided a validated estimate of the gas-exchange predictions based on their isotopic consequences. Such constraints would increase the confidence of model predictions as it is used, for example, to predict responses to changed climates, genotypes, or novel management regimes.

These models might be usefully combined with the meta-analyses presented above. In particular, it would be worthwhile to vary precipitation amount or soil depth to create differences in water availability and then thin or fertilize the modeled stand. If such an exercise could recreate the pattern observed in Fig. 23.2, it would increase our confidence in interpreting it as an effect of water availability. Likewise, if the site-specificity of the fertilization response in Fig. 23.6 could be recreated by site-specific parameterization of the models, this would help to explain the differences in direction and timing of the fertilization response.

## 23.7 Conclusions

Stable isotope analysis of tree rings is a powerful tool for exploring the long-term and complex physiological responses to forest management. The thinning response differs between wet and dry sites, where the trees reduce their water-use efficiency on dry sites and increase it on wet. These patterns are consistent with the release of water limitations on dry sites and of light and nutrient limitations on wet sites. Carbon isotope discrimination data revealed that fertilization has two dominant effects: a short-term increase in foliar nitrogen, and a longer-term increase in leaf area. We have noted the timing and site-specificity of the isotopic changes after thinning and fertilization, which indicate that physiological responses to these management actions can last for decades, but the responses vary in direction and timing among studies. We encourage the development and parameterization of models to test the mechanisms proposed here and to improve predictions about management responses at a given site. Stable isotope tree-ring studies on management actions could reduce uncertainties and explain mechanisms of response, especially with increased auxiliary measurements of leaf nitrogen, leaf area, and xylem and soil water isotopes.

**Acknowledgements** This chapter has been subjected to U.S. Environmental Protection Agency review and has been approved for publication. The views expressed in this paper are those of the author(s) and do not necessarily reflect the views or policies of the U.S. Environmental Protection Agency. Mention of trade names or commercial products does not constitute endorsement or recommendation for use. JDM was supported by the K.A. Wallenberg Foundation (#2015.0047).

## References

- Araus JL, Amaro T, Zuhair Y, Nachit MM (1997) Effect of leaf structure and water status on carbon isotope discrimination in field-grown durum wheat. *Plant, Cell Environ* 20(12):1484–1494. <https://doi.org/10.1046/j.1365-3040.1997.d01-43.x>
- Ares A, Harrington CA, Terry TA, Kraft JM (2008) Vegetation control effects on untreated wood, crude cellulose and holocellulose  $\delta^{13}\text{C}$  of early and latewood in 3 to 5-year-old rings of Douglas-fir. *Trees* 22(5):603–609. <https://doi.org/10.1007/s00468-008-0227-6>
- Ares A, Terry T, Harrington C, Devine W, Peter D, Bailey J (2007) Biomass removal, soil compaction, and vegetation control effects on five-year growth of Douglas-fir in coastal Washington. *For Sci* 53(5):600–610. <https://doi.org/10.1093/forestscience/53.5.600>
- Balster NJ, Marshall JD (2000) Decreased needle longevity of fertilized Douglas-fir and grand fir in the northern Rockies. *Tree Physiol* 20(17):1191–1197
- Balster NJ, Marshall JD, Clayton M (2009) Coupling tree-ring  $\delta^{13}\text{C}$  and  $\delta^{15}\text{N}$  to test the effect of fertilization on mature Douglas-fir (*Pseudotsuga menziesii* var. *Glauca*) stands across the Interior northwest, USA. *Tree Phys* 29(12):1491–1501
- Binkley D, Reid P (1985) Long-term increase of nitrogen availability from fertilization of Douglas-fir. *Can J For Res* 15(4):723–724. <https://doi.org/10.1139/x85-117>
- Bonhomme L, Barbaroux C, Monclus R, Morabito D, Berthelot A, Villar M, Dreyer E, Brignolas F (2008) Genetic variation in productivity, leaf traits and carbon isotope discrimination in hybrid poplars cultivated on contrasting sites. *Ann For Sci* 65(5):503–503. <https://doi.org/10.1051/forest:2008024>
- Brendel O, Pot D, Plomion C, Rozenberg P, Guehl J-M (2002) Genetic parameters and QTL analysis of  $\delta^{13}\text{C}$  and ring width in maritime pine. *Plant, Cell Environ* 25(8):945–953. <https://doi.org/10.1046/j.1365-3040.2002.00872.x>
- Brendel O, Le Thiec D, Scotti-Saintagne C, Bodénès C, Kremer A, Guehl J-M (2008) Quantitative trait loci controlling water use efficiency and related traits in *Quercus robur* L. *Tree Genet Genomes* 4(2):263–278. <https://doi.org/10.1007/s11295-007-0107-z>
- Brinkmann N, Seeger S, Weiler M, Buchmann N, Eugster W, Kahmen A (2018) Employing stable isotopes to determine the residence times of soil water and the temporal origin of water taken up by *Fagus sylvatica* and *Picea abies* in a temperate forest. *New Phytol* 219(4):1300–1313. <https://doi.org/10.1111/nph.15255>
- Brix H (1971) Effects of nitrogen fertilization on photosynthesis and respiration in Douglas-Fir. *For Sci* 17(4):407–414. <https://doi.org/10.1093/forestscience/17.4.407>
- Brix H (1981) Effects of nitrogen fertilizer source and application rates on foliar nitrogen concentration, photosynthesis, and growth of Douglas-fir. *Can J For Res* 11(4):775–780. <https://doi.org/10.1139/x81-111>
- Brooks JR, Coulombe R (2009) Physiological responses to fertilization recorded in tree rings: isotopic lessons from a long-term fertilization trial. *Ecol Appl* 19(4):1044–1060. <https://doi.org/10.1890/08-0310.1>
- Brooks JR, Mitchell AK (2011) Interpreting tree responses to thinning and fertilization using tree-ring stable isotopes. *New Phytol* 190(3):770–782. <https://doi.org/10.1111/j.1469-8137.2010.03627.x>

- Campoe OC, Stape JL, Albaugh TJ, Lee Allen H, Fox TR, Rubilar R, Binkley D (2013) Fertilization and irrigation effects on tree level aboveground net primary production, light interception and light use efficiency in a loblolly pine plantation. For Ecol Manage 288:43–48. <https://doi.org/10.1016/j.foreco.2012.05.026>
- Chmura DJ, Anderson PD, Howe GT, Harrington CA, Halofsky JE, Peterson DL, Shaw DC, Brad St. Clair J (2011) Forest responses to climate change in the northwestern United States: ecophysiological foundations for adaptive management. For Ecol Manage 261(7):1121–1142. <https://doi.org/10.1016/j.foreco.2010.12.040>
- Cornejo-Oviedo EH, Voelker SL, Mainwaring DB, Maguire DA, Meinzer FC, Brooks JR (2017) Basal area growth, carbon isotope discrimination, and intrinsic water use efficiency after fertilization of Douglas-fir in the Oregon coast range. For Ecol Manage 389:285–295. <https://doi.org/10.1016/j.foreco.2017.01.005>
- Cramer MD, Cauter AV, Bond WJ (2010) Growth of N<sub>2</sub>-fixing African savanna Acacia species is constrained by below-ground competition with grass. J Ecol 98(1):156–167. <https://doi.org/10.1111/j.1365-2745.2009.01594.x>
- Dawson TE (1998) Fog in the California redwood forest: ecosystem inputs and use by plants. Oecologia 117(4):476–485. <https://doi.org/10.1007/s004420050683>
- Dawson TE, Mambelli S, Plamboeck AH, Templer PH, Tu KP (2002) Stable isotopes in plant ecology. Annu Rev Ecol Syst 33(1):507–559. <https://doi.org/10.1146/annurev.ecolsys.33.020602.095451>
- Deal RL, Cochran B, LaRocco G (2012) Bundling of ecosystem services to increase forestland value and enhance sustainable forest management. For Policy Econ 17:69–76. <https://doi.org/10.1016/j.forpol.2011.12.007>
- Elhani S, Guehl J-M, Nys C, Picard J-F, Dupouey J-L (2005) Impact of fertilization on tree-ring <sup>15</sup>N and <sup>13</sup>C in beech stands: a retrospective analysis. Tree Physiol 25(11):1437–1446. <https://doi.org/10.1093/treephys/25.11.1437>
- Flanagan LB, Ehleringer JR, Marshall JD (1992) Differential uptake of summer precipitation among co-occurring trees and shrubs in a pinyon-juniper woodland. Plant, Cell Environ 15(7):831–836
- Flexas J, Carriqui M, Coopman RE, Gago J, Galmés J, Martorell S, Morales F, Diaz-Espejo A (2014) Stomatal and mesophyll conductances to CO<sub>2</sub> in different plant groups: underrated factors for predicting leaf photosynthesis responses to climate change? Plant Sci 226:41–48. <https://doi.org/10.1016/j.plantsci.2014.06.011>
- Ford CR, Laseter SH, Swank WT, Vose JM (2011) Can forest management be used to sustain water-based ecosystem services in the face of climate change? Ecol Appl 21(6):2049–2067. <https://doi.org/10.1890/10-2246.1>
- Forrester DI, Collopy JJ, Beadle CL, Baker TG (2013) Effect of thinning, pruning and nitrogen fertiliser application on light interception and light-use efficiency in a young Eucalyptus nitens plantation. For Ecol Manage 288:21–30. <https://doi.org/10.1016/j.foreco.2011.11.024>
- Fox TR, Jokela EJ, Allen HL (2007) The development of pine plantation silviculture in the southern United States. J For 105(7):337–347. <https://doi.org/10.1093/jof/105.7.337>
- Gauthier M-M, Jacobs DF (2009) Short-term physiological responses of black Walnut (*Juglans nigra* L.) to plantation thinning. For Sci 55(3):221–229. <https://doi.org/10.1093/forestscience/55.3.221>
- Gessler A, Cailleret M, Joseph J, Schönbeck L, Schaub M, Lehmann M, Treydte K, Rigling A, Timofeeva G, Saurer M (2018) Drought induced tree mortality—a tree-ring isotope based conceptual model to assess mechanisms and predispositions. New Phytol 219(2):485–490. <https://doi.org/10.1111/nph.15154>
- Giuggiola A, Ogée J, Rigling A, Gessler A, Bugmann H, Treydte K (2016) Improvement of water and light availability after thinning at a xeric site: which matters more? A dual isotope approach. New Phytol 210(1):108–121. <https://doi.org/10.1111/nph.13748>
- Gornall JL, Guy RD (2007) Geographic variation in ecophysiological traits of black cottonwood (*Populus trichocarpa*). This article is one of a selection of papers published in the special issue on poplar research in Canada. Can J Bot 85(12):1202–1213. <https://doi.org/10.1139/B07-079>

- Granda E, Rossatto DR, Camarero JJ, Voltas J, Valladares F (2014) Growth and carbon isotopes of Mediterranean trees reveal contrasting responses to increased carbon dioxide and drought. *Oecologia* 174(1):307–317. <https://doi.org/10.1007/s00442-013-2742-4>
- Grossiord C, Granier A, Ratcliffe S, Bouriaud O, Bruehlheide H, Chečko E, Forrester DI, Dawud SM, Finér L, Pollastrini M, Scherer-Lorenzen M, Valladares F, Bonal D, Gessler A (2014) Tree diversity does not always improve resistance of forest ecosystems to drought. *Proc Natl Acad Sci USA* 111(41):14812–14815. <https://doi.org/10.1073/pnas.1411970111>
- Gspaltl M, Bauerle W, Binkley D, Sterba H (2013) Leaf area and light use efficiency patterns of Norway spruce under different thinning regimes and age classes. *For Ecol Manage* 288:49–59. <https://doi.org/10.1016/j.foreco.2011.11.044>
- Guerra FP, Richards JH, Fiehn O, Famula R, Stanton BJ, Shuren R, Sykes R, Davis MF, Neale DB (2016) Analysis of the genetic variation in growth, ecophysiology, and chemical and metabolomic composition of wood of *Populus trichocarpa* provenances. *Tree Genet Genomes* 12(1):6. <https://doi.org/10.1007/s11295-015-0965-8>
- Hanba YT, Miyazawa S-I, Terashima I (1999) The influence of leaf thickness on the CO<sub>2</sub> transfer conductance and leaf stable carbon isotope ratio for some evergreen tree species in Japanese warm-temperate forests. *Funct Ecol* 13(5):632–639. <https://doi.org/10.1046/j.1365-2435.1999.00364.x>
- Hart SC, Classen AT (2003) Potential for assessing long-term dynamics in soil nitrogen availability from variations in  $\delta^{15}\text{N}$  of tree rings. *Isot Environ Health Stud* 39(1):15–28. <https://doi.org/10.1080/1025601031000102206>
- Hartl-Meier C, Zang C, Büntgen U, Esper J, Rothe A, Göttelein A, Dirnböck T, Treyde K (2015) Uniform climate sensitivity in tree-ring stable isotopes across species and sites in a mid-latitude temperate forest. *Tree Physiol* 35(1):4–15. <https://doi.org/10.1093/treephys/tpu096>
- Heilman PE, Dao TH, Cheng HH, Webster SR, Christensen L (1982) Comparison of fall and spring applications of <sup>15</sup>N-labeled urea to Douglas-Fir: II. Fertilizer nitrogen recovery in trees and soil after 2 years. *Soil Sci Soc Am J* 46(6):1300–1304. <https://doi.org/10.2136/sssaj1982.03615995004600060035x>
- Helle G, Schleser GH (2004) Beyond CO<sub>2</sub>-fixation by Rubisco—an interpretation of <sup>13</sup>C/<sup>12</sup>C variations in tree rings from novel intra-seasonal studies on broad-leaf trees. *Plant, Cell Environ* 27(3):367–380. <https://doi.org/10.1111/j.0016-8025.2003.01159.x>
- Högberg P, Johansson C (1993) <sup>15</sup>N Abundance of forests is correlated with losses of nitrogen. *Plant Soil* 157(1):147–150. <https://doi.org/10.1007/BF00038758>
- Högberg P, Johansson C, Hällgren J-E (1993) Studies of <sup>13</sup>C in the foliage reveal interactions between nutrients and water in forest fertilization experiments. *Plant Soil* 152(2):207–214. <https://doi.org/10.1007/BF00029090>
- Högberg P, Johansson C, Högberg MN (2014) Is the high <sup>15</sup>N natural abundance of trees in N-loaded forests caused by an internal ecosystem N isotope redistribution or a change in the ecosystem N isotope mass balance? *Biogeochem* 117(2):351–358. <https://doi.org/10.1007/s10533-013-9873-x>
- Hultine KR, Marshall JD (2000) Altitude trends in conifer leaf morphology and stable carbon isotope composition. *Oecologia* 123(1):32–40
- Isaac-Renton MG, Roberts DR, Hamann A, Spiecker H (2014) Douglas-fir plantations in Europe: a retrospective test of assisted migration to address climate change. *Glob Change Biol* 20(8):2607–2617. <https://doi.org/10.1111/gcb.12604>
- Jansen K, Sohr J, Kohnle U, Ensminger I, Gessler A (2013) Tree ring isotopic composition, radial increment and height growth reveal provenance-specific reactions of Douglas-fir towards environmental parameters. *Trees* 27(1):37–52. <https://doi.org/10.1007/s00468-012-0765-9>
- Jarvis PG, McNaughton KG (1986) Stomatal control of transpiration: scaling up from leaf to region. In: MacFadyen A, Ford ED (eds) *Advances in ecological research*, vol 15. Academic Press, pp 1–49 [https://doi.org/10.1016/S0065-2504\(08\)60119-1](https://doi.org/10.1016/S0065-2504(08)60119-1)
- Johnson DW, Curtis PS (2001) Effects of forest management on soil C and N storage: meta analysis. *For Ecol Manage* 140(2):227–238. [https://doi.org/10.1016/S0378-1127\(00\)00282-6](https://doi.org/10.1016/S0378-1127(00)00282-6)

- Jurgensen MF, Harvey AE, Graham RT, Page-Dumroese DS, Tonn JR, Larsen MJ, Jain TB (1997) Impacts of timber harvesting on soil organic matter, nitrogen, productivity, and health of inland Northwest forests. For Sci 43(2):234–251. <https://doi.org/10.1093/forestscience/43.2.234>
- Körner Ch, Farquhar GD, Wong SC (1991) Carbon isotope discrimination by plants follows latitudinal and altitudinal trends. Oecologia 88(1):30–40. <https://doi.org/10.1007/BF00328400>
- Krause K, Cherubini P, Bugmann H, Schleppei P (2012) Growth enhancement of *Picea abies* trees under long-term, low-dose N addition is due to morphological more than to physiological changes. Tree Physiol 32(12):1471–1481. <https://doi.org/10.1093/treephys/tps109>
- Kruse J, Hopmans P, Rennenberg H, Adams M (2012) Modern tools to tackle traditional concerns: evaluation of site productivity and *Pinus radiata* management via  $\delta^{13}\text{C}$ - and  $\delta^{18}\text{O}$ -analysis of tree-rings. For Ecol Manage 285:227–238. <https://doi.org/10.1016/j.foreco.2012.08.011>
- Kume A, Satomura T, Tsuboi N, Chiwa M, Hanba YT, Nakane K, Horikoshi T, Sakugawa H (2003) Effects of understory vegetation on the ecophysiological characteristics of an overstory pine, *Pinus densiflora*. For Ecol Manage 176(1):195–203. [https://doi.org/10.1016/S0378-1127\(02\)00282-7](https://doi.org/10.1016/S0378-1127(02)00282-7)
- Leavitt SW, Long A (1986) Stable-carbon isotope variability in tree foliage and wood. Ecol 67(4):1002–1010. <https://doi.org/10.2307/1939823>
- Leites LP, Robinson AP, Rehfeldt GE, Marshall JD, Crookston NL (2012) Height-growth response to climatic changes differs among populations of Douglas-fir: a novel analysis of historic data. Ecol Appl 22(1):154–165
- Liles GC, Maxwell TM, Silva LCR, Zhang J, Horwath WR (2019) Two decades of experimental manipulation reveal potential for enhanced biomass accumulation and water use efficiency in ponderosa pine plantations across climate gradients. J Geophys Res Biogeosci 124:2321–2334, 9(1982), 121. <https://doi.org/10.1029/2019JG005183>
- Lindner M, Fitzgerald JB, Zimmermann NE, Reyer C, Delzon S, van der Maaten E, Schelhaas M-J, Lasch P, Eggers J, van der Maaten-Theunissen M, Suckow F, Psomas A, Poulter B, Hanewinkel M (2014) Climate change and European forests: what do we know, what are the uncertainties, and what are the implications for forest management? J Environ Manage 146:69–83. <https://doi.org/10.1016/j.jenvman.2014.07.030>
- Luyssaert S, Marie G, Valade A, Chen Y-Y, Njakou Djomo S, Ryder J, Otto J, Naudts K, Lansø AS, Ghattas J, McGrath MJ (2018) Trade-offs in using European forests to meet climate objectives. Nature 562(7726):259–262. <https://doi.org/10.1038/s41586-018-0577-1>
- Marguerit E, Bouffier L, Chanceler E, Costa P, Lagane F, Guehl J-M, Plomion C, Brendel O (2014) The genetics of water-use efficiency and its relation to growth in maritime pine. J Exp Bot 65(17):4757–4768. <https://doi.org/10.1093/jxb/eru226>
- Marshall JD, Cuntz M, Beyer M, Dubbert M, Kuehnhammer K (2020) Borehole equilibration: testing a new method to monitor the isotopic composition of tree xylem water in situ. Front Plant Sci 11. <https://doi.org/10.3389/fpls.2020.00358>
- Marshall JD, Linder S (2013) Mineral nutrition and elevated  $[\text{CO}_2]$  interact to modify  $\delta^{13}\text{C}$ , an index of gas exchange, in Norway spruce. Tree Phys 33(11):1132–1144
- Marshall JD, Monserud RA (2006) Co-occurring species differ in tree-ring  $\delta^{18}\text{O}$  trends. Tree Physiol 26(8):1055–1066
- Marshall JD, Zhang J (1994) Carbon isotope discrimination and water-use efficiency in native plants of the north-central Rockies. Ecol 75(7):1887–1895. <https://doi.org/10.2307/1941593>
- Martin TA, Hinckley TM, Meinzer FC, Sprugel DG (1999) Boundary layer conductance, leaf temperature and transpiration of *Abies amabilis* branches. Tree Physiol 19(7):435–443. <https://doi.org/10.1093/treephys/19.7.435>
- Martin-Benito D, Kint V, del Río M, Muys B, Cañellas I (2011) Growth responses of West-Mediterranean *Pinus nigra* to climate change are modulated by competition and productivity: past trends and future perspectives. For Ecol Manage 262(6):1030–1040. <https://doi.org/10.1016/j.foreco.2011.05.038>



- Matsushima M, Choi W-J, Chang SX (2012) White spruce foliar  $\delta^{13}\text{C}$  and  $\delta^{15}\text{N}$  indicate changed soil N availability by understory removal and N fertilization in a 13-year-old boreal plantation. *Plant Soil* 361(1):375–384. <https://doi.org/10.1007/s11104-012-1254-z>
- Matteo G, Angelis P, Brugnoli E, Cherubini P, Scarascia-Mugnozza G (2010) Tree-ring  $\Delta^{13}\text{C}$  reveals the impact of past forest management on water-use efficiency in a Mediterranean oak coppice in Tuscany (Italy). *Ann For Sci* 67(5):510–510. <https://doi.org/10.1051/forest/2010012>
- McDowell N, Barnard H, Bond B, Hinckley T, Hubbard R, Ishii H, Köstner B, Magnani F, Marshall J, Meinzer F (2002) The relationship between tree height and leaf area: sapwood area ratio. *Oecologia* 132(1):12–20
- McDowell N, Brooks JR, Fitzgerald SA, Bond BJ (2003) Carbon isotope discrimination and growth response of old *Pinus ponderosa* trees to stand density reductions. *Plant, Cell Environ* 26(4):631–644
- McDowell NG, Adams HD, Bailey JD, Hess M, Kolb TE (2006) Homeostatic maintenance of *ponderosa* pine gas exchange in response to stand density changes. *Ecol Appl* 16(3):1164–1182. [https://doi.org/10.1890/1051-0761\(2006\)016\[1164:HMOPPG\]2.0.CO;2](https://doi.org/10.1890/1051-0761(2006)016[1164:HMOPPG]2.0.CO;2)
- McDowell NG, Bond BJ, Dickman LT, Ryan MG, Whitehead D (2011) Relationships between tree height and carbon isotope discrimination. In: Frederick C Meinzer, B Lachenbruch, TE Dawson (eds) *Size- and age-related changes in tree structure and function*. Springer Netherlands, pp 255–286 [https://doi.org/10.1007/978-94-007-1242-3\\_10](https://doi.org/10.1007/978-94-007-1242-3_10)
- McLane SC, LeMay VM, Aitken SN (2011) Modeling lodgepole pine radial growth relative to climate and genetics using universal growth-trend response functions. *Ecol Appl* 21(3):776–788. JSTOR
- Meinzer FC, Andrade JL, Goldstein G, Holbrook NM, Cavelier J, Wright SJ (1999) Partitioning of soil water among canopy trees in a seasonally dry tropical forest. *Oecologia* 121(3):293–301. <https://doi.org/10.1007/s004420050931>
- Miller HG (1981) Forest fertilization: some guiding concepts. *For* 54(2):157–167. <https://doi.org/10.1093/forestry/54.2.157>
- Mitchell AK, Barclay HJ, Brix H, Pollard DFW, Benton R, deJong R (1996) Biomass and nutrient element dynamics in Douglas-fir: effects of thinning and nitrogen fertilization over 18 years. *Can J For Res* 26(3):376–388. <https://doi.org/10.1139/x26-042>
- Monclus R, Dreyer E, Villar M, Delmotte FM, Delay D, Petit J-M, Barbaroux C, Thiec DL, Bréchet C, Brignolas F (2006) Impact of drought on productivity and water use efficiency in 29 genotypes of *Populus deltoides* × *Populus nigra*. *New Phytol* 169(4):765–777. <https://doi.org/10.1111/j.1469-8137.2005.01630.x>
- Moreno-Gutiérrez C, Barberá GG, Nicolás E, Luis MD, Castillo VM, Martínez-Fernández F, Querejeta JI (2011) Leaf  $\delta^{18}\text{O}$  of remaining trees is affected by thinning intensity in a semiarid pine forest. *Plant, Cell Environ* 34(6):1009–1019. <https://doi.org/10.1111/j.1365-3040.2011.02300.x>
- Nambiar EK, Bowen GD (1986) Uptake, distribution and retranslocation of nitrogen by *Pinus radiata* from  $^{15}\text{N}$ -labelled fertilizer applied to podzolized sandy soil. *For Ecol Manage* 15(4):269–284. [https://doi.org/10.1016/0378-1127\(86\)90164-7](https://doi.org/10.1016/0378-1127(86)90164-7)
- Navarro-Cerrillo RM, Sánchez-Salguero R, Rodríguez C, Duque Lazo J, Moreno-Rojas JM, Palacios-Rodríguez G, Camarero JJ (2019) Is thinning an alternative when trees could die in response to drought? The case of planted *Pinus nigra* and *P. Sylvestris* stands in southern Spain. *For Ecol Manage* 433:313–324. <https://doi.org/10.1016/j.foreco.2018.11.006>
- Neary DG, Klopatek CC, DeBano LF, Ffolliott PF (1999) Fire effects on belowground sustainability: a review and synthesis. *For Ecol Manage* 122(1):51–71. [https://doi.org/10.1016/S0378-1127\(99\)00032-8](https://doi.org/10.1016/S0378-1127(99)00032-8)
- Niinemets Ü, Díaz-Espejo A, Flexas J, Galmés J, Warren CR (2009) Role of mesophyll diffusion conductance in constraining potential photosynthetic productivity in the field. *J Exp Bot* 60(8):2249–2270. <https://doi.org/10.1093/jxb/erp036>
- Peñuelas J, Estiarte M (1996) Trends in plant carbon concentration and plant demand for N throughout this century. *Oecologia* 109(1):69–73. <https://doi.org/10.1007/s004420050059>

- Pinto JR, Marshall JD, Dumroese RK, Davis AS, Cobos DR (2011) Establishment and growth of container seedlings for reforestation: a function of stocktype and edaphic conditions. *For Ecol Manage* 261(11):1876–1884
- Pinto JR, Marshall JD, Dumroese RK, Davis AS, Cobos DR (2012) Photosynthetic response, carbon isotopic composition, survival, and growth of three stock types under water stress enhanced by vegetative competition. *Can J For Res* 42(2):333–344
- Poulson SR, Chamberlain CP, Friedland AJ (1995) Nitrogen isotope variation of tree rings as a potential indicator of environmental change. *Chem Geol* 125(3):307–315. [https://doi.org/10.1016/0009-2541\(95\)00097-6](https://doi.org/10.1016/0009-2541(95)00097-6)
- Powers MD, Pregitzer KS, Palik BJ, Webster CR (2010) Wood  $\delta^{13}\text{C}$ ,  $\delta^{18}\text{O}$  and radial growth responses of residual red pine to variable retention harvesting. *Tree Physiol* 30(3):326–334. <https://doi.org/10.1093/treephys/tp119>
- Pretzsch H, Schütze G, Uhl E (2013) Resistance of European tree species to drought stress in mixed versus pure forests: evidence of stress release by inter-specific facilitation. *Plant Biol* 15(3):483–495. <https://doi.org/10.1111/j.1438-8677.2012.00670.x>
- Rehfeldt GE (1977) Growth and cold hardiness of intervarietal hybrids of douglas-fir. *Theor Appl Genet* 50(1):3–15. <https://doi.org/10.1007/BF00273790>
- Roden J, Siegwolf R (2012) Is the dual-isotope conceptual model fully operational? *Tree Physiol* 32(10):1179–1182
- Ruzicka KJ, Puettmann KJ, Brooks JR (2017) Cross-scale interactions affect tree growth and intrinsic water use efficiency and highlight the importance of spatial context in managing forests under global change. *J Ecol* 105(5):1425–1436. <https://doi.org/10.1111/1365-2745.12749>
- Sarris D, Siegwolf R, Körner C (2013) Inter- and intra-annual stable carbon and oxygen isotope signals in response to drought in Mediterranean pines. *Agric For Meteorol* 168:59–68. <https://doi.org/10.1016/j.agrformet.2012.08.007>
- Savolainen O, Bokma F, García-Gil R, Komulainen P, Repo T (2004) Genetic variation in cessation of growth and frost hardiness and consequences for adaptation of *Pinus sylvestris* to climatic changes. *For Ecol Manag* 197(1):79–89. <https://doi.org/10.1016/j.foreco.2004.05.006>
- Scheidegger Y, Saurer M, Bahn M, Siegwolf R (2000) Linking stable oxygen and carbon isotopes with stomatal conductance and photosynthetic capacity: a conceptual model. *Oecologia* 125(3):350–357. <https://doi.org/10.2307/4222781>
- Sheppard P, Thompson TL (2000) Effect of extraction pretreatment on radial variation of nitrogen concentration in tree rings. *J Environ Qual* 29(6):2037–2042
- Smith DM, Larson BC, Kely MJ, Ashton PMS (1997) *The practice of silviculture: applied forest ecology*. 9th edn. <https://www.cabdirect.org/cabdirect/abstract/19980608088>
- Sohn JA, Brooks JR, Bauhus J, Kohler M, Kolb TE, McDowell NG (2014) Unthinned slow-growing ponderosa pine (*Pinus ponderosa*) trees contain muted isotopic signals in tree rings as compared to thinned trees. *Trees* 28(4):1035–1051. <https://doi.org/10.1007/s00468-014-1016-z>
- Sohn JA, Kohler M, Gessler A, Bauhus J (2012) Interactions of thinning and stem height on the drought response of radial stem growth and isotopic composition of Norway spruce (*Picea abies*). *Tree Physiol* 32(10):1199–1213. <https://doi.org/10.1093/treephys/tps077>
- Sohn JA, Saha S, Bauhus J (2016) Potential of forest thinning to mitigate drought stress: a meta-analysis. *For Ecol Manage* 380:261–273. <https://doi.org/10.1016/j.foreco.2016.07.046>
- Sulzman EW (2008) Stable isotope chemistry and measurement: a primer. In *stable isotopes in ecology and environmental science*. John Wiley & Sons, Ltd., pp 1–21 <https://doi.org/10.1002/9780470691854.ch1>
- Takahashi K, Miyajima Y (2008) Relationships between leaf life span, leaf mass per area, and leaf nitrogen cause different altitudinal changes in leaf  $\delta^{13}\text{C}$  between deciduous and evergreen species. *Bot* 86(11):1233–1241. <https://doi.org/10.1139/B08-093>
- Talhelm AF, Pregitzer KS, Burton AJ (2011) No evidence that chronic nitrogen additions increase photosynthesis in mature sugar maple forests. *Ecol Appl* 21(7):2413–2424. <https://doi.org/10.1890/10-2076.1>

- Timofeeva G, Treydte K, Bugmann H, Rigling A, Schaub M, Siegwolf R, Saurer M (2017) Long-term effects of drought on tree-ring growth and carbon isotope variability in Scots pine in a dry environment. *Tree Physiol* 37(8):1028–1041. <https://doi.org/10.1093/treephys/tpx041>
- Ulrich DEM, Still C, Brooks JR, Kim Y, Meinzer FC (2019) Investigating old-growth ponderosa pine physiology using tree-rings,  $\delta^{13}\text{C}$ ,  $\delta^{18}\text{O}$ , and a process-based model. *Ecol* 100(6):e02656. <https://doi.org/10.1002/ecy.2656>
- Voelker SL, Merschel AG, Meinzer FC, Ulrich DEM, Spies TA, Still CJ (2019) Fire deficits have increased drought sensitivity in dry conifer forests: fire frequency and tree-ring carbon isotope evidence from central Oregon. *Glob Change Biol* 25(4):1247–1262. <https://doi.org/10.1111/gcb.14543>
- Volkman THM, Kühnhammer K, Herbstritt B, Gessler A, Weiler M (2016) A method for in situ monitoring of the isotope composition of tree xylem water using laser spectroscopy. *Plant, Cell Environ* 39(9):2055–2063. <https://doi.org/10.1111/pce.12725>
- Voltas J, Lucabaugh D, Chambel MR, Ferrio JP (2015) Intraspecific variation in the use of water sources by the circum-Mediterranean conifer *Pinus halepensis*. *New Phytol* 208(4):1031–1041. <https://doi.org/10.1111/nph.13569>
- Voltas J, Serrano L, Hernández M, Pemán J (2006) Carbon isotope discrimination, gas exchange and stem growth of four Euramerican hybrid poplars under different watering regimes. *New for* 31(3):435–451. <https://doi.org/10.1007/s11056-005-0879-7>
- Walia A, Guy RD, White B (2010) Carbon isotope discrimination in western hemlock and its relationship to mineral nutrition and growth. *Tree Physiol* 30(6):728–740. <https://doi.org/10.1093/treephys/tpq020>
- Warren CR, McGrath JF, Adams MA (2001) Water availability and carbon isotope discrimination in conifers. *Oecologia* 127(4):476–486. <https://doi.org/10.1007/s004420000609>
- Wei L, Marshall JD, Zhang J, Zhou H, Powers RF (2014) 3-PG simulations of young ponderosa pine plantations under varied management intensity: why do they grow so differently? *For Ecol Manage* 313:69–82. <https://doi.org/10.1016/j.foreco.2013.10.035>
- Werner C, Schnyder H, Cuntz M, Keitel C, Zeeman MJ, Dawson TE, Badeck F-W, Brugnoli E, Ghashghaie J, Grams TEE, Kayler ZE, Lakatos M, Lee X, Máguas C, Ogée J, Rascher KG, Siegwolf RTW, Unger S, Welker J, Gessler A (2012) Progress and challenges in using stable isotopes to trace plant carbon and water relations across scales. *Biogeosciences* 9(8):3083–3111. <https://doi.org/10.5194/bg-9-3083-2012>
- West JB, Bowen GJ, Cerling TE, Ehleringer JR (2006) Stable isotopes as one of nature's ecological recorders. *Trends Ecol Evol* 21(7):408–414. <https://doi.org/10.1016/j.tree.2006.04.002>
- White JWC, Cook ER, Lawrence JR, and Wallace SB (1985) The  $\text{DH}$  ratios of sap in trees: implications for water sources and tree ring  $\text{DH}$  ratios. *Geochimica et Cosmochimica Acta* 49(1), 237–246. [https://doi.org/10.1016/0016-7037\(85\)90207-8](https://doi.org/10.1016/0016-7037(85)90207-8)
- Wright IJ, Reich PB, Westoby M, Ackerly DD, Baruch Z, Bongers F, Cavender-Bares J, Chapin T, Cornelissen JHC, Diemer M, Flexas J, Garnier E, Groom PK, Gulias J, Hikosaka K, Lamont BB, Lee T, Lee W, Lusk C, Villar R (2004) The worldwide leaf economics spectrum. *Nature* 428(6985):821–827. <https://doi.org/10.1038/nature02403>
- York RA, Fuchs D, Battles JJ, Stephens SL (2010) Radial growth responses to gap creation in large, old *Sequoiadendron giganteum*. *Appl Veg Sci* 13(4):498–509. <https://doi.org/10.1111/j.1654-109X.2010.01089.x>
- Zhang J, Marshall JD (1994) Population differences in water-use efficiency of well-watered and water-stressed western larch seedlings. *Can J For Res* 24(1):92–99
- Zhang J, Marshall JD, Jaquish BC (1995) Genetic differentiation in carbon isotope discrimination and gas exchange in *Pseudotsuga menziesii*. A common-garden experiment. *Oecologia* 101(1):132
- Zhang JW, Marshall, JD (1995) Variation in carbon isotope discrimination and photosynthetic gas exchange among populations of *Pseudotsuga menziesii* and *Pinus ponderosa* in different environments. *Funct Ecol* 402–412

**Open Access** This chapter is licensed under the terms of the Creative Commons Attribution 4.0 International License (<http://creativecommons.org/licenses/by/4.0/>), which permits use, sharing, adaptation, distribution and reproduction in any medium or format, as long as you give appropriate credit to the original author(s) and the source, provide a link to the Creative Commons license and indicate if changes were made.

The images or other third party material in this chapter are included in the chapter's Creative Commons license, unless indicated otherwise in a credit line to the material. If material is not included in the chapter's Creative Commons license and your intended use is not permitted by statutory regulation or exceeds the permitted use, you will need to obtain permission directly from the copyright holder.



# Chapter 24

## Impact of Increasing CO<sub>2</sub>, and Air Pollutants (NO<sub>x</sub>, SO<sub>2</sub>, O<sub>3</sub>) on the Stable Isotope Ratios in Tree Rings



Rolf T. W. Siegwolf, Martine M. Savard, Thorsten E. E. Grams,  
and Steve Voelker

**Abstract** Anthropogenic activities such as industrialization, land use change and intensification of agriculture strongly contribute to changes in the concentrations of atmospheric trace gases. Carbon dioxide (CO<sub>2</sub>), oxidized N compounds (NO<sub>x</sub>), sulfur dioxide (SO<sub>2</sub>) and ozone (O<sub>3</sub>) have particularly significant impacts on plant physiology. CO<sub>2</sub>, the substrate for plant photosynthesis, is in the focus of interest as the ambiguous effect of its increasing concentration is controversially discussed. Is its increase beneficial for plants or are plants non-responsive? NO<sub>x</sub>, a product of combustion and lightning, can have either fertilizing or toxic effects depending on the concentration and form. This is also the case for reduced forms of nitrogen (NH<sub>y</sub>), which are mostly emitted from agricultural and industrial activities. In combination CO<sub>2</sub> and N compounds can have a fertilizing effect. SO<sub>2</sub> and ground-level O<sub>3</sub> are mostly phytotoxic, depending on their concentrations, daily and seasonal exposure dynamics, and tree health condition. Elevated concentrations of both substances arise from industrial combustion processes and car emissions. All of the above-mentioned gaseous compounds affect plant metabolism in their specific ways and to different degrees. This impacts the isotope fractionation leaving specific fingerprints in the C, O, (H) and N isotope ratios of organic matter. In this chapter we will show how the impact of increasing CO<sub>2</sub> and air pollutants are reflected in the isotopic ratios of tree rings. Increasing CO<sub>2</sub> shows a considerable variation in responses of δ<sup>13</sup>C

---

R. T. W. Siegwolf (✉)

Swiss Federal Institute for Forest, Snow and Landscape Research WSL, Birmensdorf, Switzerland  
e-mail: [rolf.siegwolf@wsl.ch](mailto:rolf.siegwolf@wsl.ch)

Lab of Atmospheric Chemistry, Paul Scherrer Institute (PSI), Villigen, Switzerland

M. M. Savard

Geological Survey of Canada (Natural Resources Canada), 490 de la Couronne, Québec, QC G1K 99, Canada

T. E. E. Grams

Ecophysiology of Plants, Technical University of Munich, Hans-Carl-von-Carlowitz-Platz 2, 85354 Freising, Germany

S. Voelker

College of Forest Resources and Environmental Science, Michigan Technological University, Houghton, USA MI, 49931

© The Author(s) 2022

R. T. W. Siegwolf et al. (eds.), *Stable Isotopes in Tree Rings*, Tree Physiology 8,  
[https://doi.org/10.1007/978-3-030-92698-4\\_24](https://doi.org/10.1007/978-3-030-92698-4_24)

675

and to a minor degree in  $\delta^{18}\text{O}$ . Ozone and  $\text{SO}_2$  exposure cause an overall increase of the  $\delta^{13}\text{C}$  values in tree rings and a slight decrease in  $\delta^{18}\text{O}$ , mimicking an increase in net photosynthesis ( $A_N$ ) and to a minor degree in stomatal conductance ( $g_s$ ). However, directly measured  $A_N$  and  $g_s$  values show the opposite, which does not always correspond with the isotope derived gas exchange data.  $\text{NO}_2$  concentration as it is found near highly frequented freeways or industrial plants causes an increase of  $\delta^{13}\text{C}$  while  $\delta^{18}\text{O}$  decreases. This indicates an increase in both  $A_N$  and  $g_s$ , which corresponds well with directly measured gas exchange data. Thus the air quality situation must be taken in consideration for the interpretation of isotope values in tree rings.

## 24.1 Introduction

Stable C and O isotope ratios are indicative for changes at the leaf level  $\text{CO}_2$  and  $\text{H}_2\text{O}$  exchange (Chap. 9; Farquhar et al. 1989; Chap. 10; Farquhar and Lloyd 1993). Via assimilates, the specific isotope signals are stored in tree rings making them an ideal recorder for information on past environmental changes. The goal of this chapter is to highlight the impact of changes in atmospheric  $\text{CO}_2$  and air pollutants on stable isotope ratios in tree rings. Herein, we describe the pathways by which gaseous compounds are incorporated into plants with an emphasis on uptake via leaves through stomata. Impacts on tree physiology and potential phytotoxicity are discussed with respect to effects on isotopic fractionation that can lead to detectable isotopic variation in tree-rings. Overall, this chapter provides a broad review of the literature that demonstrates the effect of  $\text{CO}_2$  and pollutants on tree-ring isotopes and how these influences need to be considered for the interpretation of stable isotopes in tree rings.

### 24.1.1 *Reactive Pollutants and Trees*

Reactive gaseous compounds, such as  $\text{O}_3$ ,  $\text{SO}_2$  and  $\text{NO}_x$ , which are mainly products of high temperature combustion processes (e.g., ore smelters, oil refineries, chemical industrial plants, coal-fired power plants, and combustion driven mobility) were identified early on as the most relevant phytotoxic air pollutants (Ashmore 2005; Wellburn 1990; Martin and Sutherland 1990; Frank et al. 1979, Choi and Lee 2012). Over recent decades,  $\text{SO}_2$  emissions have been substantially reduced through air quality regulations in most Western countries. Such a decrease for airborne N compounds is observed since the mid 1980s, with the introduction of catalyzers for car exhausts (Geng et al. 2014; Etzold et al. 2020). While a fraction of the N- and S-compounds are deposited on the soil surface and absorbed by microorganisms and roots (their ambiguous effects are described below), the gaseous forms are taken up via stomata through diffusional processes and directly metabolized. Before stomatal

uptake, a portion of the reactive pollutant species are deposited on branch, leaf and soil surfaces (Fig. 24.1), which makes the quantification of leaf uptake rather difficult. Where possible, isotopic tracer studies (<sup>15</sup>N, <sup>34</sup>S) in the field (Ammann et al. 1999, Saurer et al. 2004) and in the laboratory (Chaparro-Suarez et al. 2011; Vallano and Sparks 2013) can lead to more realistic flux estimates including eddy covariance measurements. A broad overview about the impact of air pollutants on physiological responses as reflected in stable isotopes is given in Savard (2010).

In the 1970's and later, increasing concentrations of air pollutants were causing significant losses in agricultural crop yields and were regionally identified as causing significant forest decline (McLaughlin 1985; Heck et al. 1988; Slovik et al. 1996; Bytnerowicz and Fenn 1996; Muzika et al. (2004); Ashmore 2005; Matyssek et al. 2010, 2012). Climatic variation in combination with air pollutants can exacerbate the impact of stress modulating canopy-integrated leaf gas exchange, and thus tree growth. Indeed, one of the most toxic pollutants besides SO<sub>2</sub> (Darral 1989; Lee et al. 2017) is O<sub>3</sub> (Cailleret et al. 2018; Jolivet et al. 2016). Whereas SO<sub>2</sub> pollution is not as globally distributed as tropospheric O<sub>3</sub>, and is mainly a regional problem near the vicinity of smelters and coal driven energy production, ozone has greater areal coverage as well as more spatial and temporal variation (Lefohn et al. 2018; Mills et al. 2018; Tarasick et al. 2019). In particular, photochemical reactions producing O<sub>3</sub> are enhanced during warm and sunny days when nitrogen oxides and volatile organic compounds are present (Royal Society 2008). Weather situations favoring ozone formation are often associated with dry and warm conditions that lead to low stomatal conductance ( $g_s$ ) or stomatal closure, which reduces uptake and hence toxic dose effects. Thus, less injury will occur when stomata are closed even if O<sub>3</sub> or SO<sub>2</sub> concentrations are high. In contrast, conditions characterized by high air pollution concentrations and high  $g_s$  occur when the air is humid leading to higher uptake, which will exacerbate the effects of these pollutants (Jolivet et al. 2016). These include sluggish stomata and lower  $g_s$ . Sluggish stomata become unresponsive to sudden changes in environmental cues that affect stomatal aperture, such as light or humidity or even pollution levels. Generally, plants respond to the exposure of air pollutants and CO<sub>2</sub> with changes in  $g_s$ , net photosynthesis ( $A_N$ ), and biochemical processes (e.g., Savard et al. 2020a), which reflect how O<sub>3</sub> and SO<sub>2</sub> can directly damage cells via oxidation of lipids in the plasma membrane (Jolivet et al. 2016; Duan et al. 2019) and impairment of other plant biochemical processes (decrease in Rubisco and potential increase in PEP carboxylase. Ainsworth et al. 2012).

While O<sub>3</sub> and SO<sub>2</sub> are predominantly phytotoxic, N compounds can be either beneficial or detrimental (Etzold et al. 2020), depending on their concentration and form. The ultimate impact of N can be dependent on its availability in the ecosystem. In N-limited forests, N deposition modifies the soil biogeochemical dynamics and can increase tree growth (Högberg 2007; Thomas et al. 2015), whereas in high N-systems, additional N-deposition can lead to soil acidification, and excessive foliar and root N, which can foster tree mortality (Aber et al. 1989; Vitousek et al. 1997; Galloway et al. 2004). The combined increase in CO<sub>2</sub> and N-deposition can often enhance C uptake and can result in an enhanced tree and forest growth (Norby 1998; Gruber and Galloway 2008; Etzold et al. 2020). However, where stem growth was

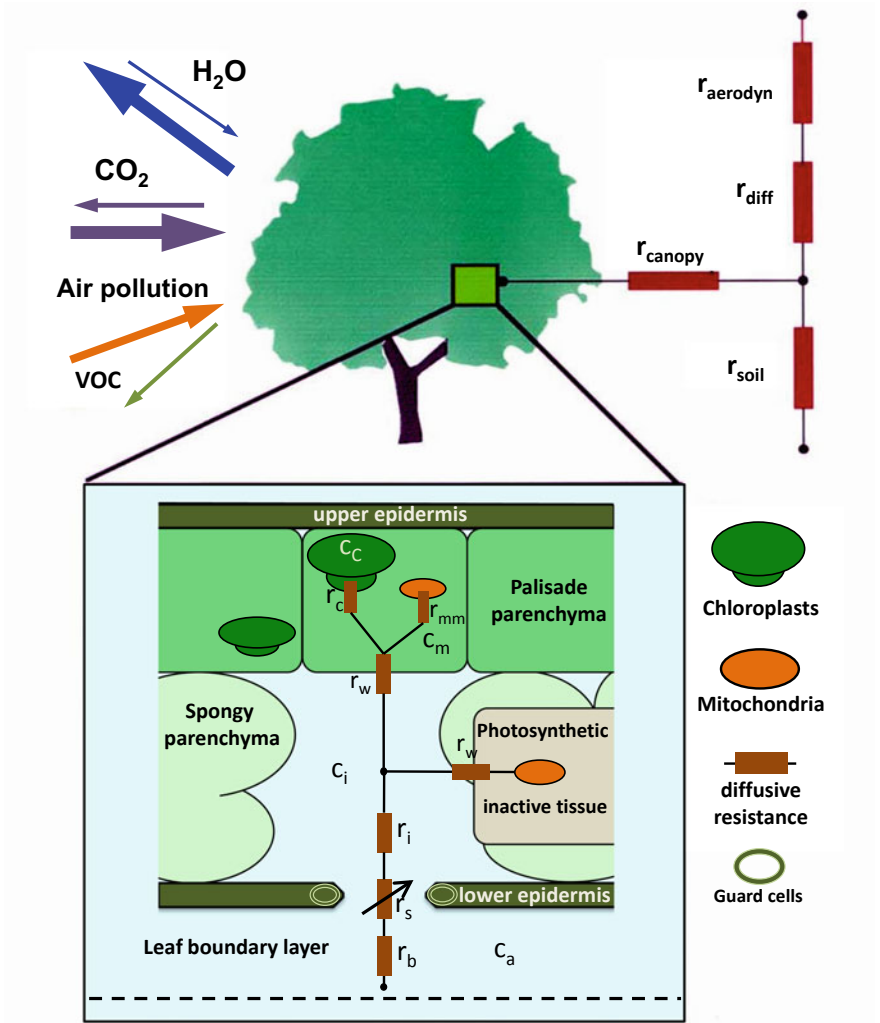


**Fig. 24.1** Pathways for the gaseous exchange between atmosphere and plant canopies and leaves (After Larcher, 2003). The arrows indicate the fluxes of the respective gas species. Diffusive resistances are shown as brown rectangles:  $r_{aerodyn}$  → Aerodynamic resistance;  $r_{diff}$  → diffusive resistance;  $r_{canopy}$  → diffusive resistances as the molecules diffuse through the canopy;  $r_{soil}$  → diffusive resistance as the molecules diffuse into or out of the soil;  $r_b$  → boundary layer resistance;  $r_s$  → physiologically controllable stomatal resistance;  $r_i$  → resistances in the intercellular system;  $r_w$  → cell wall resistance to  $CO_2$  includes the transition of  $CO_2$  in the liquid phase;  $r_{mm}$  → mitochondrial membrane resistance.  $r_c$  → chloroplast resistance to  $CO_2$ , includes the resistance of the chloroplast envelope and stroma. Mesophyll resistance is defined as  $r_m = r_w + r_c$ ;  $CO_2$  concentrations are shown for the ambient air ( $c_a$ ), inside the leaf intercellular spaces ( $c_i$ ), in the mesophyll cytosol ( $c_m$ ) and in the chloroplast ( $c_c$ )



either reduced or unchanged, access to nutrients was found to be restricted or the air contained other pollutants that were potentially phytotoxic (Giguère-Croteau et al. 2019; Savard et al. 2020a).

Air pollutants generally cause direct damages on the cell wall structure and impair biochemical processes (Jolivet et al. 2016), while CO<sub>2</sub> and N-compounds can be beneficial through various pathways, from the roots to the mesophyll (Fowler et al. 1998; 2001) (Fig. 24.1).

### **24.1.2 General Effects of Changes in the Atmosphere on Stable C, O and N Isotope Ratios**

As shown in Chapters 9, 10 and 19 any environmental impact that alters the source isotopic signals or the foliar gas exchange of CO<sub>2</sub> and H<sub>2</sub>O will result in specific changes of the stable C and O isotope ratios ( $\delta^{13}\text{C}$  and  $\delta^{18}\text{O}$  values) in plant organic matter. An increase in CO<sub>2</sub> concentration enhances photosynthesis and can cause a reduction in  $g_s$ . However, exposure to pollutants such as O<sub>3</sub> and SO<sub>2</sub> also induces stomatal closure, but in contrast is often accompanied by a concomitant decrease in net photosynthesis ( $A_N$ ) (Matyssek et al. 1997; Linzon 1972; Ziegler 1972; Parry and Gutteridge 1984; Martin et al. 1988; Wedler et al. 1995). Exposure to NOx sometimes leads to an increase in both  $A_N$  and  $g_s$  (Gessler et al. 2000; Siegwolf et al. 2001). Changes in  $A_N$  and  $g_s$  alter the ratio of internal (leaf intercellular) [CO<sub>2</sub>] ( $c_i$ ) to external [CO<sub>2</sub>] ( $c_a$ ), i.e.,  $c_i/c_a$ . When  $A_N$  increases without a change in  $g_s$ ,  $c_i/c_a$  decreases. Since <sup>12</sup>CO<sub>2</sub> is preferably assimilated relative to <sup>13</sup>CO<sub>2</sub> the partial pressure of <sup>12</sup>CO<sub>2</sub> decreases to a larger proportion than <sup>13</sup>CO<sub>2</sub> augmenting the ratio of <sup>13</sup>CO<sub>2</sub> / <sup>12</sup>CO<sub>2</sub> in the favor of <sup>13</sup>C. As a consequence the uptake of <sup>13</sup>CO<sub>2</sub> rises, resulting in an increase of the  $\delta^{13}\text{C}$  values. Under conditions where there is an increase in  $g_s$  at a constant  $A_N$ , or a decrease in  $A_N$  at a constant  $g_s$ , the  $c_i/c_a$  will increase, leading to a decrease in  $\delta^{13}\text{C}$  values (Farquhar et al. 1989; Chap. 9). Chapter 10 describes the formation of  $\delta^{18}\text{O}$  values in plant organic matter, which is given by the  $\delta^{18}\text{O}$  ratio of source water (water before it enters the leaves, see Chaps. 10 and 18) and subsequently by the  $\delta^{18}\text{O}$  of leaf water, which is modified by the variability of  $g_s$  and water vapor in the air. The role of  $g_s$  is reflected in an inverse proportional relationship to  $\delta^{18}\text{O}$  values (an increase in  $g_s$  results in a decrease in  $\delta^{18}\text{O}$  and vice versa, Barbour et al. 2004; see also Chap. 10). As the <sup>18</sup>O/<sup>16</sup>O ratio is independent of  $A_N$ , the combination of  $\delta^{13}\text{C}$  and  $\delta^{18}\text{O}$  from the same sample allows for the distinction of whether  $\delta^{13}\text{C}$  changes are a result of changes in  $A_N$  or  $g_s$  (Scheidegger et al. 2000). Here the application of the C and O dual isotope approach can be very useful for data interpretation (Chap. 16) and facilitates a more detailed analysis of the physiological plant responses to variable impacts of air pollutants, assuming that only intrinsic reactions (i.e., non-responsive to air pollutants) control the foliar isotopic signals. The specific isotopic ratio, formed in the leaves and imprinted on assimilates,

are then transferred to stems (tree rings) and roots forming organic material (see Chap. 13).

Next we discuss the specific impact of gaseous N compounds taken up via stomata. Chapter 12 ( $\delta^{15}\text{N}$  values) and 23 (fertilization effects) provide a general discussion about N-absorption via roots and leaves. Various quantities for stomatal uptake of N compounds are provided in literature, i.e. values up to 30% of the total plant N uptake (Amman et al. 1999). In most cases, the N isotopic ( $\delta^{15}\text{N}$ ) signature of the gaseous forms is reflected in the foliar organic matter (amino acids) and the N isotopic fractionation is low. However, the  $\delta^{15}\text{N}$  values of soil N compounds can depart largely from what is assimilated by the roots (see Chap. 12). An overview on the various N-fractionations during N incorporation in leaves is given in Tcherkez (2011) and Craine et al. (2015).

As the nitrogen content in tree rings is low and varies (on average 0.04–0.12%), the isotopic analysis of  $\delta^{15}\text{N}$  values in wood is quite challenging (Savard et al. 2020b). Where possible, the analysis should be done on single rings. In cases with very little material, samples can be pooled. Another challenge is the mobility of N compounds across several rings (Tomlinson et al. 2014). Yet numerous studies have made use of the  $\delta^{15}\text{N}$  values in tree rings and of the atmospheric sources to calculate the N incorporation of specific anthropogenic sources that have an isotopic signature distinct from natural  $\delta^{15}\text{N}$  values (Elhani et al. 2003; Amman et al. 1999; Saurer et al. 2004, Guerrieri et al. 2009, see below).

## 24.2 Sampling, Sample Preparation, Isotope Analysis and Flux Determination of Gaseous Pollutants

### 24.2.1 Sample Processing

In the following, we refer to Chaps. 4, 5 and 12 with regard to sampling and sample preparation. For the analysis of  $\delta^{15}\text{N}$  values in tree rings, whole wood is collected and milled the same way as for the  $^{13}\text{C}$  and  $^{18}\text{O}$  analyses. However, procedures for sample preparation to determine the  $^{15}\text{N}/^{14}\text{N}$  ratio in wood are still under debate, in particular, the question of whether the mobile fraction of N compounds in tree rings should be removed. While some authors recommend removal to prevent false trends, other studies have shown no effect on the N concentration and  $\delta^{15}\text{N}$  values (Doucet et al. 2011; Tomlinson et al. 2014; Guerrieri et al. 2017; Chap. 12 for more details). Once the samples are ready for analysis, they are combusted in an elemental analyzer (analogous to the determination of  $\delta^{13}\text{C}$ ), which is linked via an open split interface with a sector isotope ratio mass spectrometer to determine the C or N isotope ratios. A recent evaluation of the methodology for preparing spruce tree-ring  $\delta^{15}\text{N}$  series for the purpose of conducting environmental research used a total of 16 trees from two sites exposed to different types and levels of anthropogenic N emissions (Savard et al. 2020b). This study suggested that short-term  $\delta^{15}\text{N}$  changes (<7 years) are difficult

to relate to long term environmental impacts, but that middle to long-term trends do. The authors also suggest that pooling tree rings of several trees from a site can provide reliable results provided that the sub-samples are of equal weight, but that the ideal method is to calculate the arithmetic mean of  $\delta^{15}\text{N}$  series from a minimum of three individual trees.

For  $\delta^{18}\text{O}$  determination samples are thermally decomposed in a helium stream under exclusion of oxygen (pyrolysis). The resulting CO is analyzed in the mass spectrometer (Farquhar et al. 1997; Woodley et al. 2012, Weigt et al. 2015).

### 24.2.2 *Foliar Flux Quantification of Pollutants*

Flux quantification of gaseous pollutants from the atmosphere into the leaf intercellular spaces follows the same principle as for CO<sub>2</sub> and H<sub>2</sub>O gas exchange (Gessler et al. 2000; Siegwolf et al. 2001, Teklemariam and Sparks 2004). The pollutant fluxes are calculated by multiplying  $g_s$  with the gaseous pollutant concentration difference between the ambient ( $[\text{O}_{3a}]$ ) and intercellular ( $[\text{O}_{3i}]$ ) for the respective gas molecule. The latter is mostly assumed to be zero (Gessler et al. 2000, 2002; Laisk et al. 1989) or where available, values from the literature are used (Yamulki et al. 1996; Thoene et al. 1996; Rennenberg and Geßler 1999). The stomatal conductance is either determined using gas exchange systems or derived from sap flux measurements (Köstner et al. 1996; Zweifel et al. 2007) or meteorological approaches (eddy covariance or energy balance, Wehr et al. 2017). A direct approach to determine gaseous pollutant uptake uses gas exchange chambers, where the pollutant concentration before and after the chamber is measured and the difference is multiplied with the gas flux through the chamber system (Neubert et al. 1993; Teklemariam and Sparks 2004; Grulke et al. 2005, 2007; Chaparro-Suarez et al. 2011). This approach is mostly applied in laboratory experiments or when leaves or twigs can be enclosed in cuvettes. In addition, the use of enriched labeled gases, e.g.,  $^{15}\text{NH}_3$ ,  $^{15}\text{NO}_2$  or  $^{34}\text{SO}_2$  is an elegant and reliable method as the assimilated substance can be traced and quantified within the plants (Nussbaum et al. 1993; Segschneider et al. 1995; Vallano and Sparks 2007). In close vicinity of emission sources, the isotopic values of the pollutants are often different from the natural background values, e.g., heavily frequented roads (Amman et al. 1999; Saurer et al. 2004; Guerrieri et al. 2009) or industry plants (Guerrieri et al. 2009; Savard 2010; Savard et al. 2017) vs. clean air regions.

All these methods have their pros and cons. The most prominent disadvantage is that the accurate quantification of the pollutant fluxes is very challenging, since O<sub>3</sub> or NO<sub>x</sub> as well as NH<sub>y</sub> react with the surfaces of the leaf environment (i.e., the canopy, adjacent branches and leaf surfaces) and the instrument itself (walls of the tubing and measuring equipment resulting in a gas phase destruction), which can lead to an over-estimation of the real fluxes into the leaves.

## 24.3 Specific Impacts of Gaseous Compounds on Isotopic Ratios in Tree Rings

### 24.3.1 Increasing Atmospheric CO<sub>2</sub> Concentration

As atmospheric CO<sub>2</sub> is the primary C-source for terrestrial plants, its variations in concentration and  $\delta^{13}\text{C}$  values impact the isotopic ratios in organic matter via CO<sub>2</sub> and H<sub>2</sub>O gas exchange. Since the initial stages of industrialization around 1850 the CO<sub>2</sub> concentration has increased from  $\sim 270 \mu\text{mol/mol}$  to  $415 \mu\text{mol/mol}$  by 2020 (Belmecheri and Lavergne 2020). This  $145 \mu\text{mol/mol}$  increase in  $c_a$  can have strong impacts on various aspects of plant physiology and lead to higher  $c_i$  as CO<sub>2</sub> diffuses through stomata and into leaves. During much of the last 20,000 years, long time periods have corresponded to increasing CO<sub>2</sub> ( $c_a$ ). For plant carbon uptake, these increases in  $c_a$  caused increases in the difference of  $c_a - c_i$  as a consequence of an enhanced CO<sub>2</sub> fixation into sugars within the leaf by photosynthesis, but this also caused  $c_i$  to increase in absolute concentrations. Following Fick's Law, the increasing difference of  $c_a - c_i$  is directly proportional to the stimulation of  $A_N$ , assuming  $g_s$  stays constant (Farquhar et al. 1989):

$$A_N = g_s (c_a - c_i). \quad (24.1)$$

The same relationship can be re-written as:

$$A_N = g_s (1 - (c_i/c_a)). \quad (24.2)$$

The term  $c_i/c_a$  in Eq. (24.2) is particularly important to understanding how CO<sub>2</sub> may affect tree-ring carbon isotope signatures because Farquhar et al. (1989) further showed that carbon isotope discrimination ( $\Delta^{13}\text{C}$ , see Chaps. 9 and 17 for details) can be described by:

$$\Delta^{13}\text{C} = a - (b - a) (c_i/c_a), \quad (24.3)$$

where  $a$  is the fractionation from diffusion through the stomata (4.4‰) and  $b$  is the fractionation by carboxylation by Rubisco ( $\sim 27\%$ ).

Equations 24.1–24.3 summarize the simplest version of a much more complex relationship provided by Farquhar et al. (1989) and these have been employed a large number of studies of terrestrial, marine and atmospheric carbon isotope signatures. However, reconsiderations of this approach have increasingly advocated modifying Eq. 24.3 as:

$$\Delta^{13}\text{C} = a - (b - a) (c_i/c_a) - f(\Gamma^*/c_a) \quad (24.4)$$

where  $f$  is the fractionation factor during photorespiration (‰) and  $\Gamma^*$  is the CO<sub>2</sub> compensation point in the absence of CO<sub>2</sub> (Seibt et al. 2008; Keeling et al. 2017; Schubert and Jahren 2018; Laverne et al. 2019).

The goal of this section is not to delve too deeply into the plant physiology and isotopic theory, and applications to Earth systems modeling, which many other papers have addressed within the past 10 years. Moreover, variation in mesophyll conductance is known to have a substantial effect on  $\Delta^{13}\text{C}$  values, but it will not be discussed in this chapter due to the great variation among species and a lack of consensus on the magnitude with which changing atmospheric CO<sub>2</sub> can affect this aspect of leaf gas exchange. Rather, this section serves to set the stage for understanding what CO<sub>2</sub>-induced trends we should expect to observe in tree-ring  $\Delta^{13}\text{C}$  signatures, which is a function of  $c_i/c_a$  and  $f$  and  $\Gamma^*$ , which in turn are directly related to intrinsic water-use efficiency (iWUE; see Chap. 17). Whether CO<sub>2</sub> may affect  $\Delta^{13}\text{C}$  values is a long-running and important question to dendrochronologists, plant physiologists, paleoecologists, and a broad array of scientists that use atmospheric  $\delta^{13}\text{C}$  or  $\Delta^{13}\text{C}$  as a tracer of past global-scale changes to climate and vegetation patterns. Therefore, relevant information for interpreting tree-ring isotope patterns has arisen in diverse fields of scientific inquiry that we will briefly summarize here.

The least intrusive and most realistic way to expose vegetation to elevated CO<sub>2</sub> (eCO<sub>2</sub>) is to use chamberless exposure systems, also known as FACE systems (Free Air CO<sub>2</sub> Exposure). FACE studies undertaken in forests are logistically difficult and operationally expensive, so only a handful of these experiments have been undertaken or are still operating (Bader et al. 2013; Norby et al. 2016). Overall, these and other eCO<sub>2</sub> experiments have generally confirmed an expected fertilizing effect on A<sub>N</sub>; whereas the expected reductions in g<sub>s</sub> have often been absent or smaller than expected on mature trees (Körner et al. 2005; Bader et al. 2013; Keel et al. 2007, Streit et al. 2014; Klein et al. 2016; Gimeno et al. 2020; Jiang et al. 2020; Walker et al. 2020). In forest settings, g<sub>s</sub> responses to eCO<sub>2</sub> tend to be a function of various other biological, physical and ecological factors mediating tree- or canopy-level whereas potted plants in the lab or in controlled environments show a strong responsiveness to changes in CO<sub>2</sub> (Jarvis and McNaughton 1986; Buckley et al. 2017; Sperry et al. 2019). Hence, if trees growing in natural environments respond similarly to what has been documented experimentally, with historical increases in A<sub>N</sub> and little to no change in g<sub>s</sub> (sensu Wieser et al. 2018), then we should expect that trees and forests should become more water-use efficient. Indeed, most tree-ring carbon isotope studies that focus on this issue have documented this shift in water-use efficiency. Most of these hundreds of studies have been recently digitized and summarized by Adams et al. (2020), confirming in a massive meta-analysis what has been demonstrated by a previous and somewhat smaller meta-analysis (Leonardi et al. 2012). Such increases in WUE can, but do not stringently demand, changes in  $\Delta^{13}\text{C}$  or  $c_i/c_a$ . Saurer et al. (2004) first noted how tree-ring carbon isotope records spanning 1861–1990 documented no change or moderate decreases in  $\Delta^{13}\text{C}$  or  $c_i/c_a$  despite substantial gains in iWUE. Since then, research interests have focused on whether CO<sub>2</sub> modifies  $\Delta^{13}\text{C}$  or  $c_i/c_a$ , because such knowledge could provide for more accurate determination of the magnitude

with which  $\Delta^{13}\text{C}$  has responded to climate or other environmental variability from isotope signals in tree-rings and other plant and paleoecological or geological records.

As  $\text{CO}_2$  increases it is often assumed that  $\Delta^{13}\text{C}$  or the  $c_i/c_a$  ratio remains constant. However, numerous studies show considerable variations in the isotopic responses (Fig. 24.2), which is either species specific or due to habitat properties or changes in the environment. Variations in isotopic response patterns as described by Saurer et al (2004) can even occur within the same tree during its life span (Wieser et al. 2018). To assess the potential impact of  $c_a$  on leaf gas exchange, a review of theory and modeling combined with estimates of past  $c_a$  and stomatal measurements over geological times concluded that plants maintain a constant  $c_i/c_a$  (Franks et al. 2013).

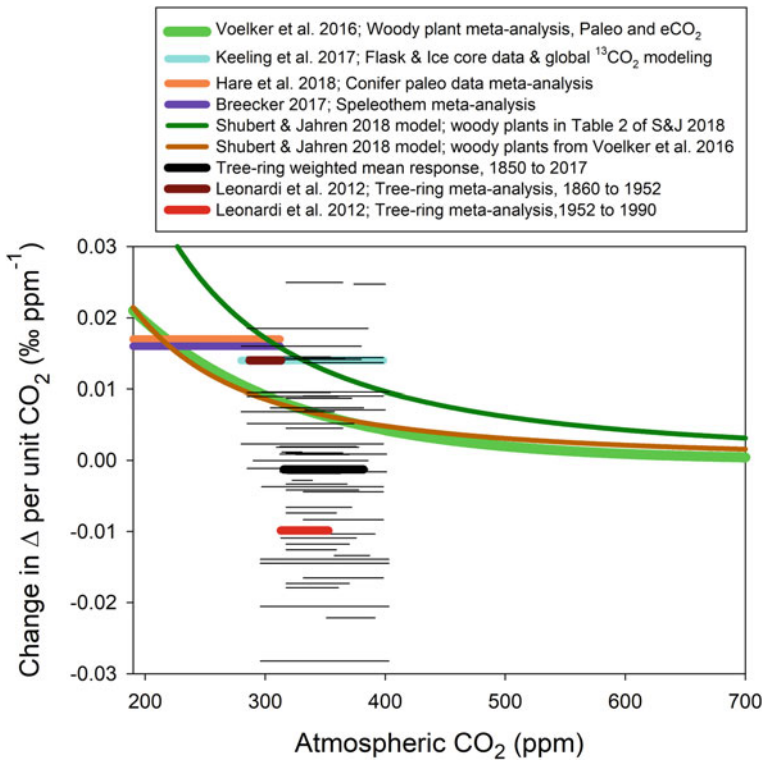


**Fig. 24.2** Responses of  $\Delta^{13}\text{C}/\text{ppm CO}_2$  exemplifying the variation among selected individual tree-ring  $\Delta^{13}\text{C}$  studies that span at least 25 years and up to 1850 to 2017 (narrow black lines) as well as large-scale meta-analyses and modeling results (thick lines). The thin lines were calculated as the slope of a linear regression of  $\Delta^{13}\text{C}$  vs. atmospheric  $\text{CO}_2$  concentration, and demonstrate the large potential range in variation that can be encountered for any given tree species and site combination, and thereby the danger in extrapolating a  $\Delta^{13}\text{C}/\text{ppm CO}_2$  response from one or only a few such studies. The thick black line gives the mean value of these individual studies, weighted by the inverse of the range of  $\text{CO}_2$  concentrations spanned by each study. In this figure,  $\Gamma^*$  was assumed constant for all studies and was only formally incorporated into the calculation of  $\Delta^{13}\text{C}$  by Keeling et al. (2017) and Schubert and Jahren (2018)

Yet, tree-ring  $\Delta^{13}\text{C}$  records tended to indicate that  $\Delta^{13}\text{C}$  changed in response to increasing  $c_a$ , suggesting a correction to  $c_i/c_a$  or some other combination of factors not explicitly considered by previous tree-ring isotopes studies (i.e.,  $f$ ,  $\Gamma^*$ , or mesophyll conductance) may be needed to accurately separate this effect from that of climate variability on tree-ring  $\Delta^{13}\text{C}$  values. However, before a set of mechanisms can be identified, it is first important to identify the magnitude of change. Based on tree-ring  $\Delta^{13}\text{C}$  data from four trees, Feng and Epstein (1995) first proposed a correction to  $\Delta^{13}\text{C}$  of 0.02‰/ppm CO<sub>2</sub>. Soon after Kurschner (1996) proposed a rate of 0.0073‰/ppm CO<sub>2</sub> from a single eCO<sub>2</sub> experiment. Using an 1171-year record from a single species and region, Treydte et al. (2009) concluded that a shift of 0.012‰/ppm CO<sub>2</sub> best fit their data. An over two-fold range of responses among these individual studies clearly demonstrated that a synthesis effort was necessary to determine an overall response, and whether or not a large empirical assessment to determine whether  $c_i/c_a$  responds to  $c_a$  as indicated by tree-ring  $\Delta^{13}\text{C}$  or with the contention of Franks et al. (2013) that  $c_i/c_a$  does not respond to  $c_a$ . To do so,  $\Delta^{13}\text{C}$  responses to CO<sub>2</sub> from many paleo and eCO<sub>2</sub> studies and including all FACE studies that had been conducted in forests up to that time (Voelker et al. 2016; hereafter V16). The three earlier individual studies reporting changes in  $\Delta^{13}\text{C}$ /ppm CO<sub>2</sub> describe linear rates of change whereas the V16 data set and analyses predicted that  $c_i/c_a$  should increase with  $c_a$  but at a non-linear or diminishing rate as:

$$c_i/c_a = -0.3974 + 0.5163(1 - e^{-0.0076c_a}). \quad (24.5)$$

In turn, Eq. (24.5), can be translated to a non-linear change in  $\Delta^{13}\text{C}$  per unit CO<sub>2</sub> as:

$$\text{‰/ppm} = 0.089 e^{-0.0076c_a}. \quad (24.6)$$

The negative exponential relationship given in Eq. (24.6) is plotted in Fig. 24.2 and clearly expands  $c_a$  values far lower and higher than all tree-ring studies. This relationship likely represented the most robust empirical assessment at that time. However, the intervening five years have provided a number of other relevant studies that can shed additional light on whether Eq. (24.6) is supported or refuted by independent analyses, and how trends in tree-ring  $\Delta^{13}\text{C}$  studies should be viewed in light of this body of work. As an example, Lavergne et al. (2019) analyzed > 100 tree-ring  $\Delta^{13}\text{C}$  studies constrained to the period 1950–2014. They found little detectable effect of  $c_a$ , converted pressure units on  $\Delta^{13}\text{C}$  after accounting for immense changes in climate and elevation among studies sites and over time. Ostensibly, this agrees qualitatively with the theory reviewed by Franks et al. (2013). However, the data set investigated by Lavergne et al. (2019) co-varied with a period of recent rapid climate change at many sites and spanned a relatively small gradient in  $c_a$  compared to some other studies, which would make it less likely to detect a response of  $\Delta^{13}\text{C}$  to  $c_a$ .

The  $\Delta^{13}\text{C}$  / ppm CO<sub>2</sub> response rate of the two paleo studies of conifer leaves or wood (Hare et al. 2018) and speleothems (Breeker 2017) both overlapped with that predicted by Eq. (24.6), which provided evidence of a consistent  $\Delta^{13}\text{C}$  / ppm

CO<sub>2</sub> response rate prior to industrialization despite different data types and analytical approaches. Thereafter, Schubert and Jahren (2018) assessed  $\Delta^{13}\text{C} / \text{ppm CO}_2$  across  $c_a$  of ca. 100 to 3000 ppm for *Arabidopsis thaliana*, grown in chambers. The model of change in  $\Delta^{13}\text{C}$  per ppm CO<sub>2</sub> resulting from this meta-analysis was given as:

$$\%_{\text{o}} / \text{ppm} = (f)(\Gamma^*) / (c_a^2), \quad (24.7)$$

where  $\Gamma^*$  was set to 40 ppm (Schubert and Jahren 2018).

When we re-applied this model to the sparse data compilation of woody plant responses to CO<sub>2</sub> provided in Schubert and Jahren (2018) (i.e., excluding the data of herbaceous plants grown in growth chambers), the response was nearly parallel to Eq. (24.5) but shifted substantially higher (Fig. 24.2, dark green line). Notably, the model described about 11% of the variation in  $\Delta^{13}\text{C} / \text{ppm CO}_2$  whereas an empirical fit to the same data explained 11% of the variation and had a muted response at lower CO<sub>2</sub> concentrations. The value of  $f = 38.6\%$  was found to maximize explained variation between the model and data. The value of 38.6 % is substantially higher than the range of 9.1 to 22.0 % that has been reported previously (Schubert and Jahren 2018). These results suggest that their woody plant data set was not large enough for robust parameter estimation. To remedy this problem, we plotted Eq. (24.7) fitted to the much larger V16 data set (Fig. 24.2, thin brown line), which yielded a value of  $f = 19.4\%$ , which is at the high end of the previously reported range, but much more reasonable compared to  $f = 38.6\%$ . Overall, this analysis provides powerful independent confirmation of the shape and magnitude of the  $\Delta^{13}\text{C}$  response to CO<sub>2</sub> despite two very different analytical approaches. More specifically, V16 attributed CO<sub>2</sub>-induced changes to  $\Delta^{13}\text{C}$  entirely to shifts in  $c_i/c_a$ , whereas Schubert and Jahren (2018) attributed the same changes entirely to fractionation associated with photorespiration. It is certainly possible that some combination of these two primary mechanisms, other morphological and biochemical contributing factors, as well as ecological and evolutionary feedbacks operating on long timescales, determine the overall  $\Delta^{13}\text{C}$  response to CO<sub>2</sub> over long time periods.

The measured record of <sup>13</sup>CO<sub>2</sub> in the atmosphere provides yet another means for understanding how terrestrial  $\Delta^{13}\text{C}$  of the vegetation has been influenced by rising CO<sub>2</sub>. When global models of ocean and terrestrial productivity and carbon cycling are constrained to match <sup>13</sup>CO<sub>2</sub> records, the results required that  $\Delta^{13}\text{C}$  increase over the industrial period (Keeling et al. 2017). Although the positive value of this response rate of  $\Delta^{13}\text{C} / \text{ppm CO}_2$  obtained by Keeling et al. (2017) is in broad agreement with many other studies (as noted in Fig. 24.2), it was substantially higher compared to most tree-ring  $\Delta^{13}\text{C}$  responses and meta-analyses for that same range in atmospheric CO<sub>2</sub>. The apparent difference in the  $\Delta^{13}\text{C} / \text{ppm CO}_2$  response rate between the ones reported by Keeling et al. (2017) and that plotted by using Eqs. (24.6) or (24.7) as applied to the V16 data set has most likely multiple, non-exclusive causes as detailed below. The difference may reflect (1) the difference between using woody plant  $\Delta^{13}\text{C}$  responses largely from temperate species as compared to global vegetation responses where C<sub>4</sub> grasses and other vegetation types play a significant



role (2) the lack of a temperature response of  $\Gamma^*$  being incorporated in the analyses of Eqs. (24.6) and (24.7) applied to the V16 data set, and (3) deficiencies in the global modeling approach of Keeling et al. (2017). With respect to point (1), reconciliation of the difference would require that C<sub>4</sub> plants and tropical forests, the vegetation types most conspicuously lacking from paleo and tree-ring  $\Delta^{13}\text{C}$  data sets, be characterized by stronger responses of  $\Delta^{13}\text{C}$  to rising CO<sub>2</sub> concentrations. The  $\Delta$  values of C<sub>4</sub> plants are lower and far less sensitive to changes in CO<sub>2</sub> compared to C<sub>3</sub> plants, so the source of increased  $\Delta^{13}\text{C}$  responses to CO<sub>2</sub> would need an origin in tropical forests. This makes intuitive sense since C<sub>3</sub> net photosynthesis includes more dynamic responses to CO<sub>2</sub> at higher average temperatures characterizing tropical forests. Tropical rainforests would also have fewer and less severe moisture constraints, allowing greater sensitivity to CO<sub>2</sub> compared to many temperate forests. With respect to point (2), the incorporation of a temperature response of  $\Gamma^*$  was not attempted because surface air temperatures are poorly constrained for paleo data collections spanning the Holocene and Last Glacial period. V16 did attempt to provide modern locations with similar climate conditions compared to the paleo data collections. The implicit assumption therein is that differences in temperature and  $\Gamma^*$  would add noise to the data set but be unbiased. That analysis also eliminated the  $\Delta^{13}\text{C}$  difference between paleo and CO<sub>2</sub>-enrichment studies at the approximate breakpoint between the two types of data sets at *ca.* 350 ppm that could have owed to differences in species composition, climates and the temperature dependence of  $\Gamma^*$ . With respect to point (3), the findings of the simulation modeling by Keeling et al. (2017) spanned the years 1765–2014 and concluded that  $\Delta^{13}\text{C}$  of terrestrial vegetation must have changed significantly, and attributed this change to a steady increase in  $\Delta^{13}\text{C}$  of 0.014‰ / ppm CO<sub>2</sub>. Although this change was attributed to the effects of atmospheric CO<sub>2</sub>, this period encompassed increasingly widespread disturbance to forests at a global scale, which certainly decreased vegetation height and competition for soil water, which would have contributed to progressive reductions in globally integrated terrestrial  $\Delta^{13}\text{C}$  over this time period. Hence, other potential sources of bias outside of direct CO<sub>2</sub>-effects on leaf gas exchange influenced <sup>13</sup>CO<sub>2</sub> records and could have been mistakenly been attributed to impacts of rising atmospheric CO<sub>2</sub> on vegetation  $\Delta^{13}\text{C}$  by Keeling et al. (2017). Overall, the reconciliation of results provided here indicates that the  $\Delta^{13}\text{C}$  response to CO<sub>2</sub> in woody plants will generally be expected to follow either Eqs. (24.5) or (24.6) when parameterized with values of  $\Gamma^* = 40$  ppm and  $f = 19.4\%$ , but that the overall  $\Delta^{13}\text{C}$  response to CO<sub>2</sub> of global vegetation may be somewhat greater in magnitude according to the findings of Keeling et al. (2017), unless this attribution to CO<sub>2</sub> was biased by not including the effects of progressively greater disturbance on forest leaf gas exchange.

A number of readers of this text may be wondering what, in practice, should be done about *expected* increases in  $\Delta^{13}\text{C}$  in response to increasing atmospheric CO<sub>2</sub> concentrations. This topic is difficult to address because there is no one correct answer. An important aspect in assessing apparent  $\Delta^{13}\text{C}$  / ppm CO<sub>2</sub> trends at any given site or across sites is that there can be tremendous variation among individual tree-ring studies, as represented by the numerous narrow black lines displayed in Fig. 24.2. This site-to-site variability results from many interacting factors such as

climate change, climate oscillations, tree development (i.e., increased tree height or stature), competition, pollution and other stressors that are superimposed on top of the relatively small effects of CO<sub>2</sub>. Indeed, Leonardi et al. (2012) summarized a large number of tree-ring  $\Delta^{13}\text{C}$  studies and found a huge shift in responses between the periods 1860 and 1990 that included negative overall responses of  $\Delta^{13}\text{C} / \text{ppm CO}_2$  during the 1952–1990 period (Fig. 24.2). Such a negative  $\Delta^{13}\text{C}$  response to CO<sub>2</sub> is probably not realistic based on first principles. At sites with low productivity there may be little to no response of  $\Delta^{13}\text{C}$  to CO<sub>2</sub> (Marchand et al. 2020) whereas in other regions, negative  $\Delta^{13}\text{C}$  trends have been associated with increased stomatal closure associated with warming- or competition-induced drought stress (Peñuelas et al. 2011; Saurer et al. 2014; Lévesque et al. 2014; Frank et al. 2015; Voelker et al. 2019). Indeed, some studies have utilized approaches that have determined differences from the expected trend in  $\Delta^{13}\text{C} / \text{ppm CO}_2$  across a range of sites (Liu et al. 2018; Szejner et al. 2018; Voelker et al. 2019). The approach of these three papers was to remove the expected CO<sub>2</sub> responses with an aim of better isolating the impacts of changing climate or competition on ecophysiology. This approach may prove particularly useful for isolating spatio-temporal impacts of climate and climate change and other factors such as pollution that affect tree-ring carbon isotope signatures if future efforts adjust for the temperature dependence of  $\Gamma^*$  and the partial pressures of CO<sub>2</sub> that differ with elevation (sensu Lavergne et al. 2019).

$\delta^{18}\text{O}$ : In experiments with potted young trees, increases in CO<sub>2</sub> resulted in a distinct reduction of  $g_s$ . However, in some FACE experiments in temperate mixed forest little (Keel et al. 2007) or no stomatal response to changes in CO<sub>2</sub> was found (Bader et al. 2010, 2013; Klein et al. 2016). Even after 9 years of FACE treatment trees growing at the timberline at 2180 m above sea level (Stillberg, Davos, Switzerland) showed no stomatal response to increased CO<sub>2</sub> for either species, *Larix decidua* and *Pinus mugo*. Accordingly, the effect of eCO<sub>2</sub> was not reflected in  $\delta^{18}\text{O}$  values of organic matter, although  $g_s$  of the same plants was highly responsive to changes in VPD, which was clearly reflected in  $\delta^{18}\text{O}$  (Streit et al. 2014). As noted above, site-specific biological, physical and ecological factors cause tree- or canopy-level effects to be diminished compared to leaf-level responses to CO<sub>2</sub>. So far,  $\delta^{18}\text{O}$  data of trees and tree rings from FACE experiments are rare. Before we derive CO<sub>2</sub> responses via stomata reflected in  $\delta^{18}\text{O}$  values from tree rings we must keep in mind that the oxygen isotope composition is modulated by a number of other factors, such as origin of precipitation water (Dansgaard 1953, 1964, Chap. 18), seasonality (Daansgard 1964; Rozanski et al. 1993) air humidity and  $\delta^{18}\text{O}$  of water vapor (Dongmann et al. 1974; Roden et al. 2005; Lehmann et al. 2018) soil properties and soil depth (Sprenger et al. 2018; Brooks et al. 2010). Voelker and Meinzer (2017) summarize further that post photosynthetic fractionation processes alter the  $\delta^{18}\text{O}$  values in wood during the transfer of assimilates in the phloem: an oxygen exchange occurs with <sup>18</sup>O-depleted xylem water, modifying the  $\delta^{18}\text{O}$  of the assimilates (Roden and Ehleringer 1999; Barbour et al. 2004) especially during the synthesis of cellulose (Sternberg 2009, Gessler et al. 2014, Chap. 10). The variability of these processes can add signal noise, masking stomatal signals imprinted on the  $\delta^{18}\text{O}$  of tree rings to a degree that the stomatal signal is no longer detectable. This is especially the case if the

modification of the oxygen isotope ratio by  $g_s$  is small (e.g. at high air humidity; Roden et al. 2005), resulting in an unfavorable signal to “noise” ratio. Nevertheless, we cannot conclude that changes in CO<sub>2</sub> have no effect on  $\delta^{18}\text{O}$ , as other studies for other species have found different responses (Battipaglia et al. 2013).

Albeit the reduced responsiveness of  $g_s$  to CO<sub>2</sub> in the field, using both, C and O isotope values widens the scope of interpretation; even more so if the  $\delta^{18}\text{O}$  of the source water and water vapor are known. The latter can also be estimated with specific models (Barbour et al. 2001). The application of various statistical tools or the dual isotope approach as described in Chap. 16 is valuable to evaluate the impact of long-term CO<sub>2</sub> dynamics on plant physiology, especially for the evaluation of the long-term intrinsic water-use efficiency (iWUE, see Chap. 17). Including tree-ring width and anatomical parameters (cell wall thickness, wood density, etc. see Sidorova et al. 2019) will help to identify, which factors impact tree growth and to what degree besides increasing [CO<sub>2</sub>]. Such an enhanced data set is instrumental to correctly evaluate the carbon gain water loss relationship (see Chaps. 16 and 17).

To summarize: the wide variety in isotopic patterns in response to CO<sub>2</sub> changes reflects the dynamic variability of species-specific responses to elevated CO<sub>2</sub>. This includes (a) stimulation of  $A_N$  under high CO<sub>2</sub> levels (e.g., Herrick and Thomas 2001; Bader et al. 2010; Klein et al. 2016), (b) down regulation of photosynthesis (Sage et al. 1989; Grams et al. 2007), (c) reduction in stomatal conductance (Gunderson et al. 2002), or (d) little (Keel et al. 2007; Bader et al. 2010) to no stomatal response to changes in CO<sub>2</sub> (Bader et al. 2013; Streit et al. 2014; Klein et al. 2016). These short-term responses on the leaf level leave their isotopic fingerprints in the assimilates, which are cumulated and integrated over the growth period and recorded in the biomass of tree ring (Chap. 14).

### 24.3.2 Ozone (O<sub>3</sub>)

Ozone in the troposphere is considered to be one of the most phytotoxic air pollutants, impacting plant and ecosystem functions (Ashmore 2005; Ainsworth et al. 2012). A good description of its formation, propagation and fate is given in the report of the Royal Society (2008). The main process of O<sub>3</sub> removal from the troposphere is the dry deposition on land surfaces, with an important role for vegetation such as forest ecosystems by O<sub>3</sub> uptake through stomata (Cieslik 2004). Non-stomatal removal of O<sub>3</sub> occurs at soil and plant surfaces (e.g. cuticle deposition) and degradation reactions with soil or plant emitted NO<sub>x</sub> or biogenic VOCs (Lenhart et al. 2019; Fowler et al. 1998, 2001). These removal mechanisms complicate the quantification of the O<sub>3</sub> uptake via stomata; nevertheless, significant estimates of non-stomatal O<sub>3</sub> fluxes were reported (20–80%, Cieslik 2009; 26–44%, Rannik et al. 2012), depending on the type of vegetation cover and its surface characteristics. Albeit these uncertainties, flux estimates based on the combination of stomatal conductance and ozone concentration still yield important results (Karlsson et al. 2004, 2007; Grünhage et al. 2004) for the ozone dose effective on plant physiology. More sophisticated models aim at linking

stomatal O<sub>3</sub> uptake to growth decline for a more mechanistic ozone risk assessment to forests (Matyssek et al. 2008, Anav et al. 2016, Feng et al. 2018, for crop plants, Hu et al. 2015, Xu et al. 2018).

#### 24.3.2.1 Damages Caused by Ozone

Once O<sub>3</sub> has been taken up by the plants via the stomata it may cause numerous visible leaf injuries such as chlorosis and necroses, accelerated senescence and pre-mature leaf shedding (Günthardt-Goerg and Vollenweider 2007). Even before these symptoms become visible, a number of responses at the cellular and molecular level have already occurred. Upon uptake, O<sub>3</sub> rapidly reacts with wet surfaces in the intercellular cavity, producing a suite of reactive oxygen species (ROS) that challenge a plant's detoxification mechanisms. Quite similar to defense reactions against pathogens and programmed cell death (for details see Kangasjarvi et al. 2005, Sandermann et al. 1998), the plant amplifies internal ROS production that cause the above-mentioned leaf symptoms in what is known as the hypersensitive response reaction. In the long run and often before visible symptoms develop, or even without them, stomatal functioning and Rubisco activity are affected by chronic O<sub>3</sub> stress. The stomatal response is not the same among species and O<sub>3</sub> concentrations. While short-term exposure to high concentrations typically result in a direct closing response of stomata, long-term exposure to moderately enhanced O<sub>3</sub> levels is also reported to reduce g<sub>s</sub> (Hoshika et al. 2014, 2015; Wittig et al. 2007), and related to declining rates of CO<sub>2</sub> fixation by lower Rubisco protein amount and activity (Karnosky et al. 2005; Wittig et al. 2009; Dizengremel 2001). Other reports, however, describe impaired stomatal functioning by elevated O<sub>3</sub>, causing delayed responses of stomata to environmental changes. This so called "stomatal sluggishness" increases response times of opening and closing movements, which can lead to increased water loss by transpiration under high VPD, respectively (Paoletti and Grulke 2010; Paoletti et al. (2020)). At the whole tree level, elevated O<sub>3</sub> affects allocation processes of photoassimilates. In mature trees, long-term exposure to twice ambient O<sub>3</sub> concentrations significantly reduced allocation to stems (Ritter et al. 2011), which is well in line with the often-found reduction of stem growth in natural environments with high O<sub>3</sub> exposure (Karnosky et al. 2005). Below ground, O<sub>3</sub> impaired source-sink relations are believed to reduce belowground C allocation (reviewed by Andersen 2003, Andersen et al. 2010), typically resulting in lower root/shoot biomass ratios. However, a larger number of studies report on unchanged root/shoot biomass ratios (Agathokleous et al. 2016) and few experiments on field grown trees under long-term O<sub>3</sub> exposure even found fine root growth to be stimulated (Nikolova et al 2010; Pregitzer et al. 2008).

### 24.3.2.2 Consequences for Isotopic Fractionations

Since O<sub>3</sub> impairs stomatal regulation, photosynthesis and its biochemical processes, these impacts will be seen in the carbon and oxygen isotopic fractionations and thus in the variation of the <sup>13</sup>C/<sup>12</sup>C and <sup>18</sup>O/<sup>16</sup>O isotope ratios of different plant compartments. Species respond differently to elevated O<sub>3</sub> depending on O<sub>3</sub> uptake, mesophyll exposure, detoxification capacity, and plant age (Fuhrer and Booker 2003; Matussek and Sandermann 2003).

In a 2-year phytotron study on juvenile *Fagus sylvatica* trees exposed to elevated O<sub>3</sub>, a parallel increase of δ<sup>13</sup>C and δ<sup>18</sup>O was observed (Grams et al. 2007; Grams and Matussek 2010), indicating a concurrent reduction of c<sub>i</sub> as a response to stomatal closure. Likewise for mature trees of the same species, O<sub>3</sub> caused reductions in g<sub>s</sub> and related increases in δ<sup>18</sup>O (Kitao et al. 2009; Gessler et al. 2009) as well as for different herbaceous plants (Jäggi and Fuhrer 2007). In accordance with reductions of g<sub>s</sub>, the phytotron study found A<sub>N</sub> to be reduced as often observed under elevated O<sub>3</sub> (Ainsworth et al. 2012) and not increased as one might have expected from higher δ<sup>13</sup>C values. Moreover, the increase in δ<sup>13</sup>C under O<sub>3</sub> compared to control trees was stronger than expected from measured c<sub>i</sub> and corresponding calculations using the Farquhar model (Kozovits et al. 2005; Grams et al. 2007). This apparent mismatch between gas-exchange measurements and carbon isotope discrimination was also reported by Saurer et al. (1991) for grain (*Triticum aestivum*), Patterson and Rundel (1993) for *Pinus jeffreyi* and by Elsik et al. (1993) for two *Pinus* species. Later studies found PEPC (Phosphoenolpyruvate carboxylase) to be increased in amount and activity under O<sub>3</sub> exposure, resulting in increased δ<sup>13</sup>C values for both leaves and stems (Saurer et al. 1995; Doubnerová and Ryslavá 2011). Regardless of the higher PEPC activity, A<sub>N</sub> was reduced and g<sub>s</sub> showed little response compared to control plants. The increased δ<sup>13</sup>C values were explained by the fact that C-fixation through PEPC does not discriminate as much against <sup>13</sup>C compared to <sup>12</sup>C resulting in an <sup>13</sup>C enrichment in the assimilates (Vogel 1993). Various detoxification mechanisms further the <sup>13</sup>C enrichment along with an enhanced PEPC activity that are generally stimulated under stress (Doubnerová and Ryslavá 2011). An increase in δ<sup>13</sup>C under O<sub>3</sub> exposure, which would suggest an enhanced or constant A<sub>N</sub> at reduced g<sub>s</sub> is not in line with our understanding of <sup>13</sup>C fractionation coherence according to the fractionation model for C<sub>3</sub> plants of Farquhar et al. (1989; 1982). Based on direct CO<sub>2</sub> and H<sub>2</sub>O gas-exchange measurements, we expect more negative δ<sup>13</sup>C values as A<sub>N</sub> is reduced while g<sub>s</sub> stays constant or is reduced to a minor degree (Grams et al. 2007). This example demonstrates once the assumptions of the well-accepted fractionation model are violated, the conclusions drawn from isotope measurements can lead to physiologically implausible results. As the ratio of Rubisco to PEPC activity decreases significantly under elevated O<sub>3</sub> (up to 20-fold, Dizengremel et al. 2009), the fractionation model must be adjusted, e.g., by increasing the parameter “b” representing the fractionation of all carboxylation processes as suggested by Saurer et al. (1995). Therefore, the consultation of the history of human impact in the past for the respective forests is of great value for the data interpretation.

### 24.3.3 Sulphur Dioxide ( $SO_2$ )

Ambient  $SO_2$  concentrations increased considerably since the advent of industrialization and became an increasing problem across Asia, Europe and North America, particularly before the mid-1980s. This pollutant may have had a stronger impact on the isotope ratios in plants and tree rings than previously recognized. Sakata and Suzuki (2000) described a significant  $\delta^{13}C$  increase in Japanese fir trees that underwent diseases and insect pests when being weakened by  $SO_2$ . Savard et al. (2004) reported an unprecedented  $\delta^{13}C$  positive shift by up to 4‰ for spruce tree rings induced by  $SO_2$  emissions from a large smelter in Canada. Wagner and Wagner (2006) and Boettger et al. (2014) described major increases in the long-term trend in pine and fir tree-ring  $\delta^{13}C$  series between 1945 and 1990 and a subsequent decrease after 1990 reflecting the trends of  $SO_2$  concentration in German sites. In their study of English oak trees exposed to  $SO_2$ , Rinne et al. (2010) document a 2.5‰  $\delta^{13}C$  rise with insignificant changes in the  $\delta^{18}O$  series. Many other examples of  $SO_2$  effects in natural settings around the world could be cited, with the singular common impacts of rising tree-ring  $\delta^{13}C$  values during the time of exposure.

A possible explanation for this general  $\delta^{13}C$  increase is a secondary fractionation resulting from  $SO_2$  phytotoxicity, which causes a decline in various physiological activities. Closure of stomata is generally induced by foliar  $SO_2$  uptake, and acidification of solution often invoked to explain this closure. Recently, molecular biological research suggests instead that guard cell mortality cause stomatal closure (Ooi et al. 2019). However, plant response mechanisms are intricate as they depend on the  $SO_2$  concentration (and presence of other co-pollutants), duration of exposure and the availability of water (e.g., Maier-Maercker and Koch 1995; Lee et al. 2017). Under acute controlled exposures ( $25 \text{ mg } SO_2/m^3$ ), the foliar system of trees becomes photo inhibited and exhibits decreasing  $A$ ,  $g_s$  and  $c_i$  (Duan et al. 2019). Overall, authors from diverse research fields ascribe the related tree-ring  $\delta^{13}C$  increase and growth reactions to various combinations of changes in  $g_s$ ,  $A_N$ , starch production and priority of C allocation (e.g., Darral 1989; Meng et al. 1995; Kolb and Matyssek 2001; Grams et al. 2007).

In the Canadian example cited above, a reduction of  $g_s$  was not the only response caused by exposure because a concomitant  $\delta^2H$  decrease in tree-ring nitrated cellulose was significant, and stem growth did not notably change (Savard et al. 2005). Considering intrinsic factors only, decreases in  $\delta^2H$  and  $\delta^{18}O$  generally reflect stomatal opening (Dongmann et al. 1974; Farquhar and Lloyd 1993; Sensula and Wilczynski 2017). When considering extrinsic factors, this case of severe exposure of trees to emissions may have acidified the upper soil layers, damaging fine surface roots and shifting water uptake to large, deeper roots, where source water  $\delta^2H$  ( $\delta^{18}O$ ) values are lower (Chap. 18). In the German examples, the combined physiological responses to high  $SO_2$  pollution are expressed by the long-term positive  $\delta^{13}C$  series with no significant to moderate  $\delta^{18}O$  changes (Wagner and Wagner 2006; Boettger et al. 2014), and no effects on  $\delta^2H$  values (Boettger et al. 2014). This case reflects increased respiration rates that expel higher proportions of  $^{12}C$  and generate tissues with higher

$\delta^{13}\text{C}$  signals, without modifying the  $\delta^{18}\text{O}$  values. Otherwise, foliar gas-exchange responses inferred from increasing  $\delta^{13}\text{C}$  with moderately decreasing  $\delta^{18}\text{O}$  trends a priori should reflect increases in  $A_N$  and  $g_s$ . However, this scenario is in contrast with directly measured CO<sub>2</sub> and H<sub>2</sub>O gas-exchange values under controlled SO<sub>2</sub> exposure, as Atkinson and Winner (1987), Kropff et al. (1990), Wedler et al. (1995) and Randewig et al. (2012) report a reduction in  $A_N$  and  $g_s$ , which should result in an overall decrease in  $\delta^{13}\text{C}$  values. The observed reduction of  $A_N$  better fits with the general observation that ring growth does not increase with the isotopic changes. Hence, aside from the possible extrinsic factors proposed above, the SO<sub>2</sub> induced enzymatic detoxification and reduced carboxylation rate represent other mechanisms that could explain strong increases in  $^{13}\text{C}$  uptake (Randewig et al. 2012), in some cases outweighing the prediction of the widely accepted C-isotope fractionation model by Farquhar et al. (1989, 1982).

As shown for ozone exposure, the impact of SO<sub>2</sub> detoxification and its effect on  $\delta^{13}\text{C}$  values are not considered by the C-isotope fractionation model for C<sub>3</sub> plants. Moreover, foliar response models do not take into account the extrinsic effects on tree-ring  $\delta^{18}\text{O}$  ( $\delta^2\text{H}$ ) changes. Thus, the common data interpretation assuming that a  $\delta^{13}\text{C}$  increase with none to moderate  $\delta^{18}\text{O}$  ( $\delta^2\text{H}$ ) changes would be caused by an increased  $A_N$  is not correct and does not correspond to real physiological responses to SO<sub>2</sub>. Accordingly, paleoclimate reconstruction, the evaluation of the water-use efficiency (Chap. 17), or the use of the dual C and O isotope gas-exchange model (Chap. 16) could all be erroneous if based on tree-ring series impacted by airborne acidifying emissions. Therefore, the effects of these emissions must be considered for the evaluation of tree ring isotope chronologies originating from regions and periods with large SO<sub>2</sub> emissions.

#### 24.3.4 Gaseous Reactive Nitrogen ( $N_r$ ) Compounds: NO, NO<sub>2</sub>, NH<sub>x</sub>

As observed for ozone and SO<sub>2</sub>, the emissions of biologically reactive N compounds ( $N_r$ ) have greatly increased (NO<sub>x</sub> from combustion and NH<sub>y</sub> from agricultural fertilization) since the beginning of the industrialization. The distribution of  $N_r$  occurs via large-scale atmospheric transport and is deposited into terrestrial ecosystems. Although N deposition is identified as the most important growth driver in managed European forests (Etzold et al. 2020), the current often excessive N input can reduce forest growth (Waldner et al. 2014).

Vegetation demand for N is mostly met by root uptake of nitrate (NO<sub>3</sub>), ammonium (NH<sub>4</sub><sup>+</sup>) and dissolved organic N-compounds from the pedosphere (Chap. 12). However, the direct uptake of gaseous  $N_r$  (NO, NO<sub>2</sub>, NH<sub>y</sub>) via stomata can be substantial and several studies report quantities obtained in this manner total between 10 and 37% of plant-N demand (Amman et al. 1999; Harrison et al. 2000; Millard and Grelet 2010; Vallano and Sparks 2013; Chap. 12).

#### 24.3.4.1 Factors Impacting $N_r$ -uptake by Leaves

The main factors influencing the assimilation of N by the foliar system are: (i) the species of trees, (ii) the proximity to anthropogenic emissions, (iii) the plant and canopy structure, and (iv) the type of  $N_r$ . (i) Chaparro-Suarez et al. (2011) reported a species dependent variability for  $NO_2$  uptake, which is directly correlated with  $g_s$  confirming the regulation of stomatal uptake. Accordingly, they report *Betula pendula* had the highest  $g_s$  and highest  $NO_2$  uptake, in contrast to *Pinus sylvestris*, where both values were the lowest. In all cases, they found no  $NO_2$  compensation point (meaning that plants do not produce  $NO_2$ ), or cuticular N transfer, which agrees with other studies (Teklemariam and Sparks (2004); Gessler et al. (2000)). (ii) Savard et al. (2009) and Guerrieri et al. (2010) studied trees exposed to emissions in the vicinity of industrial complexes and reported tree-ring series carrying  $\delta^{15}N$  values apparently reflecting airborne industrial  $NO_2$ . For trees growing in the vicinity of highways, similar  $\delta^{15}N$  values were found in the tree rings as in the atmosphere (Amman et al. 1999; Saurer et al. 2004; Doucet et al. 2012). These authors found an increase in the  $\delta^{15}N$  values of the  $NO_2$  by 5‰ to 8‰ relative to the  $\delta^{15}N$  of the background values. It is assumed that the exhaust treatment by car catalyzers results in an enrichment of the  $^{15}NO_2$  due to the stronger bonding of the heavier  $^{15}N$ . Thus, the lighter  $^{14}NO_2$  reacts more readily on the catalyzer resulting in  $N_2$  and  $O_2$ . (iii) Stand and canopy structure impact N-deposition considerably (Bettinger et al. 2017) as the N-compounds react with the surfaces of leaves, branches and stems, reducing their concentrations in air. Baldocchi and Wilson (2001) indicate a decreasing importance of surface deposition with decreasing foliage density, as indicated by reduced deposition velocities. (iv) For each of the different biological  $N_r$  molecules, different flux rates are found due to the different solubility of the respective molecules in an aqueous milieu.  $NH_3$  shows a much higher water solubility than  $NO_2$  and  $NO$  (Felix et al. 2017; Castro et al. 2005), and  $NO$  is less soluble than  $NO_2$  by an order of magnitude (Neubert et al. 1993). Accordingly, this solubility hierarchy is reflected in the flux rates for all three molecules (Teklemariam and Sparks 2004, Gessler et al. 2000). Likewise, mesophyll resistance ( $r_m$ ) is another critical parameter in the chain of incorporation for gaseous compounds, and is considerably higher for  $NO$  than for  $NO_2$  (Van der Eerden et al. 1998), and higher for  $NO_2$  than for  $NH_3$  (Teklemariam and Sparks 2004; Castro et al. 2005; Gessler et al. 2000). In contrast to  $NO_2$  and  $NH_3$ , most authors found stomatal  $NO$  fluxes negligibly small with little or no impact on plant physiology and in plant organic matter (Neubert et al. 1993). As  $NH_3$  is highly water soluble and rapidly converted to  $NH_4^+$  in the aqueous milieu of the mesophyll cells,  $r_m$  for this gas is low and it is assimilated via the glutamine synthetase / glutamate synthase cycle (Sparks 2009; Castro et al. 2005; Pearson and Soares 1998). In contrast, the assimilation of  $NO_2$  is somewhat more complex. Once this gas enters the intercellular cavity it is rapidly dissolved in the aqueous phase of the apoplast via disproportionation to nitrite and nitrate.  $NO_2$  scavenging by ascorbate represents an alternative parallel pathway. The resulting nitrite and nitrate from both pathways are metabolized via nitrite and nitrate reductase for the ferredoxin dependent reduction of  $NO_2^-$  to  $NH_4^+$  and the glutamine synthetase driven



production of amino acids (Ramage et al. 1993). A good overview is given by Sparks (2009).

#### 24.3.4.2 Physiological Effects Caused by Gaseous N-compounds

The atmospheric  $\delta^{15}\text{N}$  values of  $\text{N}_r$  in the vicinity of emission sources are often distinctly different than those from regions without  $\text{N}_r$ -pollution (background values, either enriched or depleted in  $^{15}\text{N}$ ). This allows the quantification of the direct uptake of  $\text{N}_r$ -gases via stomata and their incorporation into organic matter, as these products are transferred via phloem to branches, stems (tree rings) and roots. Since the  $\delta^{15}\text{N}$  variations are detectable in tree rings (although N is at lower concentrations than in leaves), the historical development of anthropogenic N emissions can be inferred retrospectively (Amman et al. 1999; Saurer et al. 2004; Choi et al. 2005; Guerrieri et al. 2009; Savard et al. 2009; Savard 2010; Sun et al. 2010; Mathias and Thomas 2018).

Assimilation and incorporation of  $\text{N}_r$  impact numerous metabolic processes (see above) reflected in  $A_N$  and  $g_s$  (e.g., Gessler et al. 2000; Siegwolf et al. 2001). However, few studies have investigated the impact of assimilating anthropogenic N on the C and O isotope fractionation in plant organic matter. In 1988, Martin et al. reported increasing  $\delta^{13}\text{C}$  values in leaves and wood of young trees, which were exposed to increased  $\text{SO}_2 + \text{O}_3$  and  $\text{SO}_2 + \text{O}_3 + \text{NO}_2$  concentrations for a four-week period. They argued that the  $\delta^{13}\text{C}$  increase was a result of stomatal limitation. But they did not examine the plant responses for each pollutant separately, thus it was not possible to clearly assign the impact of each pollutant on specific plant mechanisms due to the combined application of all three pollutants. As shown by Saurer et al. (1995), the increase in  $\delta^{13}\text{C}$  values for  $\text{O}_3$  exposed plants was primarily caused by an increased PEPC activity.

In a comprehensive case study, Siegwolf et al. (2001) analyzed the impact of chronic  $\text{NO}_2$  exposure on the C and O isotope ratios and  $\text{CO}_2$  and  $\text{H}_2\text{O}$  gas exchange. *Populus euramericana* vars Dorskamp cuttings were grown in climate-controlled growth chambers under limiting and surplus soil-N regimes. One chamber was supplied with filtered air and in the other an average  $\text{NO}_2$  concentration of 100 nmol/mol was maintained for 12 h per day for three months (details in Siegwolf et al. 2001). Irrespective of the soil-N regime,  $\text{NO}_2$  exposure caused  $\delta^{13}\text{C}$  to increase in leaf organic matter relative to plants grown in clean air as reported in other studies, (Bukata and Kyser 2007, Vallano and Sparks 2013) whereas the  $\delta^{18}\text{O}$  values were reduced (Siegwolf et al. 2001; Fig. 24.3). Leaf uptake of  $\text{N}_r$  compounds allows for a direct and rapid N availability in plant metabolism and has a fertilizing effect. Since  $\text{N}_r$  uptake via leaves stimulates  $A_N$  and leads to higher  $g_s$ , this affects the C and O isotope fractionation (see Chaps. 9, 10 and 19). For both, limiting and surplus soil-N regimes,  $\text{NO}_2$  exposure caused an increase in  $\delta^{13}\text{C}$  and reduction in  $\delta^{18}\text{O}$  values indicating higher  $A_N$  and  $g_s$  values, respectively, which is confirmed by  $\text{CO}_2$  and  $\text{H}_2\text{O}$  gas-exchange measurements. In the absence of  $\text{NO}_2$ , the effect of soil-N surplus relative to soil-N limitation results in a decrease of  $\delta^{13}\text{C}$  and  $\delta^{18}\text{O}$

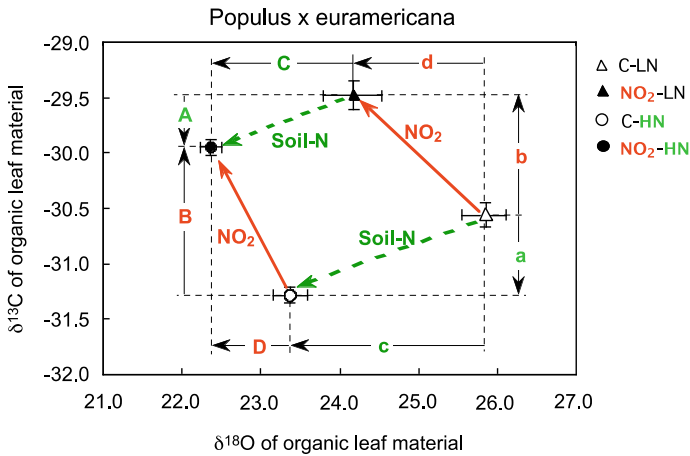


**Fig. 24.3**  $\delta^{13}\text{C}$  plotted against  $\delta^{18}\text{O}$  values from all four treatments (C stands for filtered air, C-low nitrogen (LN), C-high nitrogen (HN),  $\text{NO}_2$ -LN and  $\text{NO}_2$ -HN) in *Populus \times euramericana* (adapted from Siegwolf et al. 2001). The solid orange arrows between data points indicate the  $\delta^{13}\text{C}$  and  $^{18}\text{O}$  shifts caused by  $\text{NO}_2$  exposure, and the dashed green lines indicate the changes resulting from increased soil N addition. The fine lines with capital and small letters, respectively, represent the shifts caused by the N-treatments. The letters ‘b’ and ‘d’ indicate the shifts in  $\delta^{13}\text{C}$  (positive) and  $^{18}\text{O}$  (negative) for the low soil-N supplied plants, when exposed to  $\text{NO}_2$ . The capital letters ‘B’ and ‘D’ stand for the shifts of the high soil-N supplied plants, caused by  $\text{NO}_2$  exposure. The letters ‘a’ and ‘c’ quantify both the  $\delta^{13}\text{C}$  and  $^{18}\text{O}$  negative shifts caused by a high soil-N supply in  $\text{NO}_2$  free air. ‘A’ and ‘C’ represent the shift of the  $\text{NO}_2$  exposed plants, caused by high soil-N supply. The standard error is indicated by the horizontal and vertical bars in each data point ( $n = 6$ )

values, suggesting that  $A_N$  might be reduced or constant whereas  $g_s$  is considerably increased. Yet, an increase of the soil-N supply results in an increase of  $A_N$  and  $g_s$ , while  $g_s$  rises over-proportionally relative to  $A_N$  (Sage and Pearcy 1987; Dinh et al. 2017). The  $\text{CO}_2$  and  $\text{H}_2\text{O}$  gas exchange measurements confirm an increase in  $g_s$ , while  $A_N$  is increased as well but not to the degree that  $\delta^{13}\text{C}$  would increase. However, care must be taken when generalizing this response to changes in soil N-supply. Chapter 23 describes different responses, mostly for coniferous species (see Figs. 23.5 and 23.6). A meta-analysis showed an opposite trend in response to soil-N fertilization (decrease in  $\Delta^{13}\text{C}$ , increase in  $\delta^{13}\text{C}$ ) after the first few years. The impact of N-deposition can cause divergent isotopic response patterns, depending on the nutrient status, water supply, canopy traits and structure, species composition etc., which needs to be considered for the data interpretation.

It is noteworthy how the isotopic response patterns in deciduous trees differ between the cases of “soil N-changes only”, “ $\text{NO}_2$  exposure only”, or “soil N change and  $\text{NO}_2$  exposure” (Fig. 24.3). These isotopic patterns (Fig. 24.3) as a result of  $\text{NO}_2$  exposure were also found in air pollution studies using tree-ring samples. Saurer and Siegwolf (2007) and Guerrieri et al. (2009) analyzed tree rings from *Picea abies* growing along a highly frequented freeway in Switzerland and found  $\delta^{13}\text{C}$  and  $\delta^{18}\text{O}$  patterns invoked by  $\text{NO}_2$  exposure. However this pattern as shown in Fig. 24.3 might

change with the occurrence of other more dominant impacts such as drought. In the same study of Guerrieri et al. (2009), the impact of NO<sub>2</sub> emissions from an oil refinery in Southern Italy were analyzed for changes in  $\delta^{15}\text{N}$  (as an indicator),  $\delta^{13}\text{C}$  and  $\delta^{18}\text{O}$  values from tree rings. Drought events at this Mediterranean site occur frequently, in contrast to the sites along the Swiss freeway where water supply is not limiting. Thus the trees near the oil refinery responded primarily to drought stress by reducing  $g_s$  to minimize water loss. Consequently, the protection against drought is more relevant for plant survival therefore the drought response outweighs the influence of NO<sub>2</sub>, which was also reflected in the increased iWUE (Guerrieri et al. 2010). For trees, which are not subject to other dominant stressors (drought, high concentrations of pollutants, flooding or abrupt changes in the vegetation), this isotopic pattern as shown in Fig. 24.3 was seen in most NO<sub>2</sub>-controlled studies, and its application can serve for diagnostic or monitoring purposes.

Regarding NH<sub>3</sub> or NO we have not found any literature that described the impact of NH<sub>3</sub> or NO on the isotopic fractionation in trees, which does not mean that we can exclude any isotopic effect. Based on gas-exchange data we assume the following isotopic response as a result of NH<sub>3</sub> exposure: Fangmeier et al. (1994) and Krupa (2003) report an increase in  $A_N$  and  $g_s$  with increasing NH<sub>3</sub> concentration. They hypothesized that  $g_s$  was indirectly impacted because an increase in NH<sub>3</sub> enhanced the carbon demand for building skeleton C compounds. This in turn generated an increase of  $A_N$ , reducing  $c_i$ , leading to an increase in  $g_s$ . Based on this mechanistic chain, we premise that  $\partial E/\partial A$  (E is transpiration and A assimilation) is a constant (Cowan and Farquhar 1977). Therefore, we assume a decrease in  $\delta^{18}\text{O}$  (increase of  $g_s$ , Chap. 10), while  $\delta^{13}\text{C}$  stays constant, as a consequence of the proportional increase in  $A_N$ . However, this hypothesis must be verified experimentally. With regard to the small NO flux and its low aqueous solubility, we assume that its physiological impact is negligible at ambient concentrations.

#### 24.3.4.3 Impact of Anthropogenic N<sub>r</sub> on Root N Assimilation and Tree-Ring $\delta^{15}\text{N}$ Series

The reader interested in the airborne N<sub>r</sub> transformations in soils can find a relevant discussion in Chap. 12. A final point regarding the assimilation of anthropogenic N compounds as depicted by tree-ring series grown under natural conditions is that soil biogeochemical conditions can play a key role in the way coniferous trees respond to anthropogenic N deposition, especially in forests where soil is N limited. Indeed, depending on the N status of the forest and on soil conditions (pH, action exchange capacity, base cation saturation ratio, etc.), direct or ectomycorrhizal (EcM) root uptake may take place. The direct assimilation may not fractionate N isotopes prior to biological reactions within trees, but it is well known that EcM fungi generally are enriched in <sup>15</sup>N in the process of fungal metabolism, and release the relatively light N that is transferred to the roots and stems of trees, with different degrees of fractionation depending on the abundance and diversity of the various community components (e.g., Hobbie and Högberg 2012). The proportions of direct and EcM

N uptake modulate the final  $\delta^{15}\text{N}$  values recorded in tree-ring series. There might be a tipping point at which the bacterial and fungi communities in close association with the root system are modified so that trees exposed to similar enhancement of bioavailable N but growing on different physicochemical soil conditions will record opposite long-term  $\delta^{15}\text{N}$  trends (Savard et al. 2019). All things considered, it is no surprise that soil dynamics will impact the tree-ring series as the dominant part of N in coniferous stems originates from soil N compounds. It is clear however that research is needed on the ultimate modulation of tree-ring  $\delta^{15}\text{N}$  series by long-term changes of microbial dynamics in soils.

## 24.4 Concluding Remarks

Airborne pollutants may alter both the leaf and root assimilation paths for carbon and nutrients in trees. It is often difficult to uncover and identify the coherences between the impact of a single air pollutant or other environmental vectors and specific plant responses with their stable isotopic composition. In the real world, plants are often exposed to many pollutants, that together modify the atmospheric and soil environments. Therefore, the knowledge on how each pollutant specifically affects plant metabolism is instrumental for a better understanding of the combined impact under consideration of a given environmental situation. Furthermore, it facilitates the planning of combined experimental assessments and for modeling ecosystem responses to pollution exposure. The consideration of the vegetation and management history facilitates an accurate interpretation of the isotope values from long-term chronologies and the inclusion of other parameters (tree ring width, wood density etc.; Sidorova et al. 2019) strengthens the interpretations of tree-ring isotopic data.

## References

- Adams MA, Buckley TN, Turnbull TL (2020) Diminishing  $\text{CO}_2$ -driven gains in water-use efficiency of global forests. *Nat Clim Chang* 10:466–471
- Aber JD, Nadelhoffer KN, Steudler P, Melillo JM (1989) Nitrogen saturation in Northern forest ecosystems: excess nitrogen from fossil fuel combustion may stress the biosphere. *Bioscience* 39(6):378–386. <https://doi.org/10.2307/1311067>
- Ainsworth EA, Yendrek CR, Sitch S, Collins WJ, Emberson LD (2012) The effects of tropospheric ozone on net primary productivity and implications for climate change. *Annu Rev Plant Biol* 63:637–661. <https://doi.org/10.1146/annurev-arplant-042110-103829>
- Ammann M, Siegwolf RTW, Pichlmayer F, Suter M, Saurer M, Brunold C (1999) Estimating the uptake of traffic derived  $\text{NO}_2$  from  $^{15}\text{N}$  abundance Norway spruce needles. *Oecologia* 118:124–131
- Andersen CP (2003) Source–sink balance and carbon allocation below ground in plants exposed to ozone. *New Phytologist* 157: 213–228

- Anav A, De Marco A, Proietti C, Alessandri A, Dell'Aquila A, Cionni I, Vitale M (2016) Comparing concentration-based (AOT40) and stomatal uptake (PODY) metrics for ozone risk assessment to European forests. *Glob Change Biol* 22, 1608–1627. <https://doi.org/10.1111/gcb.13138>
- Andersen CP, Ritter W, Gregg J, Matyssek R, Grams TEE (2010) Below-ground carbon allocation in mature beech and spruce trees following long-term, experimentally enhanced O<sub>3</sub> exposure in Southern Germany. *Environ Pollut* 158:2604–2609
- Ashmore MR (2005) Assessing the future global impacts of ozone on vegetation. *Plant Cell Environ* 28:949–964. <https://doi.org/10.1111/j.1365-3040.2005.01341.x>
- Atkinson CJ, Winner WE (1987) Gas exchange characteristics of heteromeles arbutifolia during fumigation with sulphur dioxide. *New Phytol* 106:423–436
- Bader M, Siegwolf RTW, Körner Ch (2010) Sustained enhancement of photosynthesis in mature deciduous forest trees after 8 years of free air CO<sub>2</sub> enrichment (FACE). *Planta* 232(5):1115
- Bader MKF, Leuzinger S, Keel SG, Siegwolf RTW, Hagedorn F, Schleppl P, Ch, Körner (2013) Central European hardwood trees in a high-CO<sub>2</sub> future: synthesis of an 8-year forest canopy CO<sub>2</sub> enrichment project. *J Ecol* 101:1509–1519. <https://doi.org/10.1111/1365-2745.12149>
- Baldocchi DD, Wilson K (2001) Forest canopies as sources and sinks of atmospheric trace gases: scaling up to ecosystem level. In: Gasche R, Papen H, Rennenberg H (eds) Trace gas exchange in forest ecosystems. Kluwer, Boston, pp 229–242
- Barbour MM, Roden JS, Farquhar GD, Ehleringer JR (2004) Expressing leaf water and cellulose oxygen isotope ratios as enrichment above source water reveals evidence of a Péclet effect. *Oecologia* 138:426–435
- Barbour MM, Andrews TJ, Farquhar GD (2001) Correlations between oxygen isotope ratios of wood constituents of *Quercus* and *Pinus* samples from around the world. *Aust J Plant Physiol* 28:335–348
- Battipaglia G et al (2013) Elevated CO<sub>2</sub> increases tree-level intrinsic water use efficiency: insights from carbon and oxygen isotope analyses in tree rings across three forest FACE sites. *New Phytol* 197:544–554. <https://doi.org/10.1111/nph.12044>
- Belmecheri S, Lavergne A (2020) Compiled records of atmospheric CO<sub>2</sub> concentrations and stable carbon isotopes to reconstruct climate and derive plant ecophysiological indices from tree rings. *Dendrochronologia*. <https://doi.org/10.1016/j.dendro.2020.125748>
- Bettinger P, Boston K, Siry JP, Grebner DL (2017) Optimization of tree- and stand-level objectives. In: Forest management and planning. Academic Press, 362p
- Boettger T, Haupt M, Friedrich M, Waterhouse JS (2014) Reduced climate sensitivity of carbon, oxygen and hydrogen stable isotope ratios in tree-ring cellulose of silver fir (*Abies alba* Mill.) influenced by background SO<sub>2</sub> in Franconia (Germany, Central Europe). *Environ Pollut* 185:281–294. <https://doi.org/10.1016/j.envpol.2013.10.030>
- Breeker DO (2017) Atmospheric pCO<sub>2</sub> control on speleothem stable carbon isotope compositions. *Earth Planet Sci Lett* 458:58–68
- Brooks J, Barnard HR, Coulombe R, McDonnell JJ (2010) Ecohydrologic separation of water between trees and streams in a Mediterranean climate. *Nat Geosci* 3:100–104. <https://doi.org/10.1038/ngeo722>
- Buckley TN, Sack L, Farquhar GD (2017) Optimal plant water economy. *Plant Cell Environ* 40:881–896
- Bukata AR, Kyser TK (2007) Carbon and nitrogen isotope variations in tree-rings as records of perturbations in regional carbon and nitrogen cycles. *Environ Sci Technol* 41:1331–1338
- Bytnerowicz A, Fenn ME (1996) Nitrogen deposition in California forests: a review. *Environ Pollut* 92:127–146
- Cailleret M, Ferretti M, Gessler A, Rigling A, Schaub M (2018) Ozone effects on European forest growth-Towards an integrative approach. *J Ecol* 106:1377–1389
- Castro A, Stulen I, De Kok LJ (2005) Impact of NH<sub>3</sub> deposition on plant growth and functioning: a case study with *Brassica oleracea*. In: Omasa K, Nouchi I, De Kok LJ (eds) Plant response to air pollution and global change. Springer, Tokyo

- Chaparro-Suarez IG, Meixner FX, Kesselmeier J (2011) Nitrogen dioxide (NO<sub>2</sub>) uptake by vegetation controlled by atmospheric concentrations and plant stomatal aperture. *Atmos Environ* 45:5742–5750
- Choi WJ, Lee KH (2012) A short overview on linking annual tree ring carbon isotopes to historical changes in atmospheric environment. *For Sci Technol* 8(2):61–66
- Choi WJ, Lee SM, Chang SX, Ro HM (2005) Variations of  $\delta^{13}\text{C}$  and  $\delta^{15}\text{N}$  in *Pinus densiflora* tree-rings and their relationship to environmental changes in Eastern Korea. *Water Air Soil Pollut* 164:173–187
- Cieslik S (2009) Ozone fluxes over various plant ecosystems in Italy: a review. *Environ Pollut* 157:1487–1496. <https://doi.org/10.1016/j.envpol.2008.09.050>
- Cieslik SA (2004) Ozone uptake by various surface types: a comparison between dose and exposure. *Atmos Environ* 38:2409–2420
- Cowan IR, Farquhar GD (1977) Stomatal function in relation to leaf metabolism and environment. In: Jennings DH (ed) *Integration of activity in the higher plant*. Univ. Press Cambridge, pp 471–505
- Craine JM, Brookshire EHJ, Cramer MD, Hasselquist NJ, Koba K, Marin-Spiotta E, Wang L (2015) Ecological interpretations of nitrogen isotope ratios of terrestrial plants and soils. *Plant Soil* 396:1–26
- Dansgaard W (1954) The O18-abundance in fresh water. *Geochim Cosmochim Acta* 6:241–260
- Dansgaard W (1964) Stable isotopes in precipitation. *Tellus* 16:436–468
- Darral NM (1989) The effect of air pollutants on physiological processes in plants. *Plant Cell Environ* 12:1–30
- Doubnerová V, Ryslavá H (2011) What can enzymes of C4 photosynthesis do for C3 plants under stress? *Plant Sci* 180:575–583
- Dinh TH, Watanabe K, Takaragawa H, Nakabaru M, Kawamitsu Y (2017) Photosynthetic response and nitrogen use efficiency of sugarcane under drought stress conditions with different nitrogen application levels. *Plant Production Sci* 20(4):412–422. <https://doi.org/10.1080/1343943X.2017.1371570>
- Dizengremel P (2001) Effects of ozone on the carbon metabolism of forest trees. *Plant Physiol Biochem* 39:729–742
- Dizengremel P, Le Thiec D, Hasenfratz-Sauder MP, Vaultier MN, Bagard M, Jolivet Y (2009) Metabolic-dependent changes in plant cell redox power after ozone exposure. *Plant Biol* 11:35–42
- Dongmann G, Nürnberg HW, Förstel H, Wagener K (1974) On the enrichment of H<sub>2</sub><sup>18</sup>O in the leaves of transpiring plants. *Radiat Environ Biophys* 11:41–52
- Doucet A, Savard MM, Bégin C, Smirnoff A (2012) Tree-ring  $\delta^{15}\text{N}$  values to infer air quality changes at regional scale. *Chem Geol* 320(321):9–16
- Doucet A, Savard MM, Bégin C, Smirnoff A (2011) Is wood pre-treatment essential for tree-ring nitrogen concentration and isotope analysis? *Rapid Commun Mass Spectrom* 25:469–475
- Duan J, Fu B, Kang H, Song Z, Jia M, Cao D, Wei A (2019) Response of gas-exchange characteristics and chlorophyll fluorescence to acute sulfur dioxide exposure in landscape plants. *Ecotoxicol Environ Saf* 171:122–129. <https://doi.org/10.1016/j.ecoenv.2018.12.064>
- Elhani S, Lema BF, Zeller B, Brechet C, Guehl JM, Dupouey JL (2003) Inter-annual mobility of nitrogen between beech rings: a labelling experiment. *Ann For Sci* 60(6):503–508
- Elsik CG, Flagler RB, Boutton TW (1993) Carbon isotope composition and gas exchange of loblolly and shortleaf pine as affected by ozone and water stress. In: Ehleringer JR, Hall AE, Farquhar GD (eds) *Stable isotopes and plant carbon-water relations*. Academic Press, San Diego, pp 227–244
- Etzold S, Ferretti M, Reinds GJ, Solberg S, Gessler A, Waldner P, Schaub M, Simpson D, Benham S, Hansen K, Ingerslev M, Jonard M, Karlsson PE, Lindroos AJ, Marchetto A, Manninger M, Meessenburg H, Merilä P, Nöjd P, Rautio P, Sanders TGM, Seidling W, Skudnik M, Thimonier A, Verstraeten A, Vesterdal L, Vejpustkova M, de Vries W (2020) Nitrogen deposition is the most important environmental driver of growth of pure, even-aged and managed European forests. *For Ecol Manage* 458:117762. <https://doi.org/10.1016/j.foreco.2019.117762>

- Fangmeier A, Hadwiger-Fangmeier A, Van der Eerden LJM, Jäger HJ (1994) Effects of atmospheric ammonia on vegetation – a review. *Environ Pollut* 86:43–82
- Farquhar GD, Ehleringer JR, Hubick KT (1989) Carbon isotope discrimination and photosynthesis. *Annu Rev Plant Physiol Plant Mol Biol* 40:503–537. <https://doi.org/10.1146/annurev.arplant.40.1.503>
- Farquhar GD, O’Leary MH, Berry JA (1982) On the relationship between carbon isotope discrimination and the intercellular carbon dioxide concentration in leaves. *Aust J Plant Physiol* 9:121–137
- Farquhar GD, Lloyd J (1993) Carbon and Oxygen Isotope Effects in the Exchange of Carbon Dioxide between Terrestrial Plants and the Atmosphere. *Stable Isotopes and Plant Carbon-water Relations*. Academic Press, San Diego, pp 47–70
- Farquhar GD, Henry BK, Styles JM (1997) A rapid on-line technique for determination of oxygen isotope composition of nitrogen-containing organic matter and water. *Rapid Commun Mass Spectrom* 11:1554–1560
- Feng Z, Calatayud V, Zhu J, Kobayashi K (2018) Ozone exposure- and flux-based response relationships with photosynthesis of winter wheat under fully open air condition. *Sci Total Environ* 619–62:1538–1544
- Feng X, Epstein S (1994) Carbon isotopes of trees from arid environments and implications for reconstructing atmospheric CO<sub>2</sub> concentration. *Geochimica et Cosmochimica Acta*, 59(12):2599-2608
- Felix JD, Elliott EM, Gay DA (2017) Spatial and temporal patterns of nitrogen isotopic composition of ammonia at U.S. ammonia monitoring network sites. *Atmos Environ* 150:434–442
- Fowler D, Flechard C, Skiba U, Coyle M, Cape JN (1998) The atmospheric budget of oxidized nitrogen and its role in ozone formation and deposition. *New Phytol* 139:11–23
- Fowler D, Flechard C, Cape JN, Storeton-West RL, Coyle M (2001) Measurements of Ozone deposition to vegetation, quantifying the Flux, stomatal and non-stomatal components. *Water Air Soil Poll* 130:63–74
- Frank DC et al (2015) Water-use efficiency and transpiration across European forests during the Anthropocene. *Nat Clim Change* 5:579–584
- Freyer HD et al (1979) On the <sup>13</sup>C record in tree rings. Part 2. Registration of microenvironmental CO<sub>2</sub> and anomalous pollution effect. *Tellus* 31:124–137
- Franks PJ, Adams MA, Amthor JS, Barbour MM, Berry JA, Ellsworth DS, Farquhar GD, Ghannoum O, Lloyd J, McDowell N, Norby RJ, Tissue DT, von Caemmerer S (2013) Sensitivity of plants to changing atmospheric CO<sub>2</sub> concentration: from the geological past to the next century. *New Phytol* 197:1077–1094
- Fuhrer J, Booker F (2003) Ecological issues related to ozone: agricultural issues. *Environ Int* 29:141–154. [https://doi.org/10.1016/s0160-4120\(02\)00157-5](https://doi.org/10.1016/s0160-4120(02)00157-5)
- Galloway JN, Dentener FJ, Capone DG, Boyer EW, Howarth RW et al (2004) Nitrogen cycles: past, present, and future. *Biogeo-Chem* 70:153–226
- Geng L, Becky A, Jihong Cole-Dai, Steig EJ, Savarinod J, Sofena ED, Schauer AJ (2014) Nitrogen isotopes in ice core nitrate linked to anthropogenic atmospheric acidity change. *Proc Nat Acad Sci*. <https://doi.org/10.1073/pnas.1319441111>
- Gessler A et al (2009) Within-canopy and ozone fumigation effects on delta C-13 and Delta O-18 in adult beech (*Fagus sylvatica*) trees: relation to meteorological and gas exchange parameters. *Tree Physiol* 29:1349–1365. <https://doi.org/10.1093/treephys/tpp066>
- Gessler A, Pedro Ferrio J, Hommel R, Treydte K, Werner RA, Monson RK (2014) Stable isotopes in tree rings: towards a mechanistic understanding of isotope fractionation and mixing processes from the leaves to the wood. *Tree Physiol* 34:796–818. <https://doi.org/10.1093/treephys/tpu040>
- Gessler A, Rienks M, Rennenberg H (2000) NH<sub>3</sub> and NO<sub>2</sub> fluxes between beech trees and the atmosphere—correlation with climatic and physiological parameters. *New Phytol* 147:539–560
- Gessler A, Rienks M, Rennenberg H (2002) Stomatal uptake and cuticular adsorption contribute to dry deposition of NH<sub>3</sub> and NO<sub>2</sub> to needles of adult spruce (*Picea abies*) trees. *New Phytol* 156:179–194

- Giguère-Croteau B, Bergeron Y, Girardin MP, Drobyshv I, Silva LCR, Hélie JF, Garneau M (2019) North America's oldest boreal trees are more efficient water users due to increased [CO<sub>2</sub>], but do not grow faster. *PNAS*. <https://doi.org/10.1073/pnas.1816686116>
- Gimeno TE, McVicar TR, O'Grady AP, Tissue DT, Ellsworth DS (2020) Elevated CO<sub>2</sub> did not affect the hydrological balance of a mature native Eucalyptus woodland. *Glob Change Biol* 24:3010–3024
- Grams TEE, Matussek R (2010) Stable isotope signatures reflect competitiveness between trees under changed CO<sub>2</sub>/O<sub>3</sub> regimes. *Environ Pollut* 158:1036–1042. <https://doi.org/10.1016/j.envpol.2009.08.037>
- Grams TEE, Kozovits AR, Häberle KH, Matussek R, Dawson TE (2007) Combining δ<sup>13</sup>C and δ<sup>18</sup>O analyses to unravel competition, CO<sub>2</sub> and O<sub>3</sub> effects on the physiological performance of different-aged trees. *Plant, Cell Environ* 30:1023–1034. <https://doi.org/10.1111/j.1365-3040.2007.01696.x>
- Gruber N, Galloway JN (2008) An earth-system perspective of the global nitrogen cycle. *Nature* 451:293e296
- Grukke N, Paoletti E (2005) A field system to deliver desired O<sub>3</sub> concentrations in leaf-level gas exchange measurements: results for Holm Oak near a CO<sub>2</sub> spring (Engl.). *Phyton-Horn* 45(1):21
- Grukke N, Paoletti E, Heath RL (2007) Comparison of calculated and measured foliar O<sub>3</sub> flux in crop and forest species. *Environ Pollut* 146(3):640–647
- Grünhage L, Krupa SV, Legge AH, Jäger HJ (2004) Ambient flux-based critical values of ozone for protecting vegetation: differing spatial scales and uncertainties in risk assessment. *Atmos Environ* 38:2433–2437. <https://doi.org/10.1016/j.atmosenv.2003.12.039>
- Guerrieri MR, Siegwolf RTW, Saurer M, Jäggi M, Cherubini P, Ripullone F, Borghetti M (2009) Impact of different nitrogen emission sources on tree physiology: a triple stable isotope approach. *Atmos Environ* 43(2009):410–418
- Guerrieri MR, Jennings K, Belmecheri S, Asbjornsen H, Ollinger S (2017) Evaluating climate signal recorded in tree ring δ<sup>13</sup>C and δ<sup>18</sup>O from bulk wood and -cellulose for six species across the northeastern US. *Rapid Commun Mass Spectrom* 31(24):2081–2091
- Guerrieri MR, Siegwolf RTW, Saurer M, Ripullone F, Mencuccini M, Borghetti M (2010) Anthropogenic NO<sub>x</sub> emissions alter the intrinsic water-use efficiency (WUEi) for *Quercus cerris* stands under Mediterranean climate conditions. *Environ Pollut* 158:2841–2847
- Gunderson CA, Sholtis JD, Wullschlegel SD, Tissue DT, Hanson PJ, Norby RJ (2002) Environmental and stomatal control of photosynthetic enhancement in the canopy of a sweetgum (*Liquidambar styraciflua* L.) plantation during 3 years of CO<sub>2</sub> enrichment. *Plant Cell Environ* 25:379–393
- Günthardt-Goerg MS, Vollenweider P (2007) Linking stress with macroscopic and microscopic leaf response in trees: new diagnostic perspectives. *Environ Pollut* 147:467–488
- Hare VJ, Loftus E, Jeffrey A, Ramsey CB (2018) Atmospheric CO<sub>2</sub> effect on stable carbon isotope composition of terrestrial fossil archives. *Nat Commun* 9:252
- Harrison AF, Schulze ED, Gebauer G, Bruckner G (2000) Canopy uptake and utilization of atmospheric pollutant nitrogen. In Schulze ED (ed), *Carbon and nitrogen cycling in European forest ecosystems*, pp 171–188. Springer, Berlin, Heidelberg
- Heck WW, Taylor OC, Tingey DT (1988) Assessment of crop loss from air pollutants. Springer, Dordrecht. <https://doi.org/10.1007/978-94-009-1367-7>
- Herrick JD, Thomas RB (2001) No photosynthetic down-regulation in sweetgum trees (*Liquidambar styraciflua* L.) after three years of CO<sub>2</sub> enrichment at the Duke Forest FACE experiment. *Plant Cell Environ* 24:53–64
- Hobbie EA, Höglberg P (2012) Nitrogen isotopes link mycorrhizal fungi and plants to nitrogen dynamics. *New Phytol* 196(2):367–382
- Höglberg P (2007) Nitrogen impacts on forest carbon. *Nature* 447, 781e782
- Hoshika Y, Carriero G, Feng Z, Zhang Y, Paoletti E (2014) Determinants of stomatal sluggishness in ozone exposed deciduous tree species. *Sci Total Environ* 481:453–458. <https://doi.org/10.1016/j.scitotenv.2014.02.080>



- Hoshika Y, Watanabe M, Kitao M, Häberle KH, Grams TEE, Koike T, Matyssek R (2015) Ozone induces stomatal narrowing in European and Siebold's beeches: a comparison between two experiments of free-air ozone exposure. *Environ Pollut* 196:527–533
- Hu EZ, Gao F, Xin Y, Jia HX, Li KH, Hu JJ, Feng ZZ (2015) Concentration- and flux-based ozone dose-response relationships for five poplar clones grown in North China. *Environ Pollut* 207:21–30
- Jäggi M, Fuhrer J (2007) Oxygen and carbon isotopic signatures reveal a long-term effect of free-air ozone enrichment on leaf conductance in semi-natural grassland. *Atmos Environ* 41:8811–8881
- Jarvis pg, McNaughton kg (1986) Stomatal Control of Transpiration: Scaling Up from Leaf to Region. *Advances in Ecological Research* 15:1–49
- Jiang M et al (2020) The fate of carbon in a mature forest under carbon dioxide enrichment. *Nature* 580:227–231
- Jolivet Y, Bagard M, Cabané M, Vaultier MN, Gandin A, Afif D, Dizengremel P, Le Thiec D (2016) Deciphering the ozone-induced changes in cellular processes: A prerequisite for ozone risk assessment at the tree and forest levels. *Annals For Sci* 73:923–943. <https://doi.org/10.1007/s13595-016-0580-3>
- Kangasjarvi J, Jaspers P, Kollist H (2005) Signalling and cell death in ozone-exposed plants. *Plant Cell Environ* 28:1021–1036
- Karlsson P, Braun S, Broadmeadow M, Elvira S, Emberson L, Gimeno BS, Le Thiec D, Novak K, Oksanen E, Schaub M, Uddling J, Wilkinson M (2007) Risk assessments for forest trees: The performance of the ozone flux versus the AOT concepts. *Environ Pollut* 146:608–616
- Karlsson PE, Uddling J, Braun S, Broadmeadow M, Elvira S, Gimeno BS, Le Thiec D, Oksanen E, Vandermeiren K, Wilkinson M, Emberson L (2004) New critical levels for ozone effects on young trees based on AOT40 and simulated cumulative leaf uptake of ozone. *Atmos Environ* 38:2283–2294. <https://doi.org/10.1016/j.atmosenv.2004.01.027>
- Karnosky DF, Pregitzer KS, Zak DR, Kubiske ME, Hendrey GR, Weinstein D, Nosal M, Percy KE (2005) Scaling ozone responses of forest trees to the ecosystem level in a changing climate. *Plant Cell Environ* 28:965–998
- Keel S, Pepin S, Leuzinger S, Körner Ch (2007) Stomatal conductance in mature deciduous forest trees exposed to elevated CO<sub>2</sub>. *Trees* 21:151–159. <https://doi.org/10.1007/s00468-006-0106-y>
- Keeling RF, Graven HD, Welp LR, Resplandy L, Bi J, Piper SC, Sun Y, Bollenbacher A, Meijer HAJ (2017) Atmospheric evidence for a global secular increase in carbon isotopic discrimination of land photosynthesis. *Proc Nat Acad Sci USA* 114:10361–10366
- Kitao M, Löw M, Heerd C, Grams TEE, Häberle K-H, Matyssek R (2009) Effects of chronic ozone exposure on gas exchange responses of adult beech trees (*Fagus sylvatica*) as related to the within-canopy light gradient. *Environ Pollut* 157:537–544
- Klein T, Bader MKF, Leuzinger S, Mildner M, Schleppi P, Siegwolf RTW, Körner Ch (2016) Growth and carbon relations of mature *Picea abies* trees under 5 years of free-air CO<sub>2</sub> enrichment. *J Ecol* 104:1720–1733
- Kolb TE, Matyssek R (2001) Limitations and perspectives about scaling ozone impacts in trees. *Environ Pollut* 115:373–393. [https://doi.org/10.1016/S0269-7491\(01\)00228-7](https://doi.org/10.1016/S0269-7491(01)00228-7)
- Körner C et al (2005) Carbon flux and growth in mature deciduous forest trees exposed to elevated CO<sub>2</sub>. *Science* 309:1360–1362. <https://doi.org/10.1126/science.1113977>
- Köstner B, Brion P, Siegwolf RTW, Granier A (1996) Estimates of water Vaopr Flux and Canopy Conductance of Scots Pine at three Level Utilizing Different Xylem Sap Flow Methods. *Theor Appl Climatol* 53:105–113
- Kozovits AR, Matyssek R, Blaschke H, Göttlein A, Grams TEE (2005) Competition increasingly dominates the responsiveness of juvenile beech and spruce to elevated CO<sub>2</sub> and/or O<sub>3</sub> concentrations throughout two subsequent growing seasons. *Glob Change Biol* 11:1387–1401
- Kropff MJ, Smeets WLM, Meijer EMJ, van der Zalm AJA, Bakx EJ (1990) Effects of sulphur dioxide on leaf photosynthesis: the role of temperature and humidity. *Physiol Plant* 80:655–661
- Krupa SV (2003) Effects of atmospheric ammonia (NH<sub>3</sub>) on terrestrial vegetation: a review. *Environ Pollut* 124:179–221

- Kurschner K (1996) Leaf stomata as biosensors of paleoatmospheric CO<sub>2</sub> levels. LPP contributions Series 5, Utrecht
- Laisk A, Kull O, Moldau H (1989) Ozone concentration in leaf intercellular air spaces is close to zero. *Plant Physiol* 90:1163–1167
- Lavergne A, Voelker SL, Csank AM, Graven H, de Boer HJ, Daux V, Robertson I, Dorado-Liñán I, Martínez-Sancho E, Battipaglia G, Bloomfield KJ, Meinzer FC, Camarero JJ, Clisby R, Fang Y, Menzel A, Still CJ, Keen RM, Roden JS, Dawson TE, Prentice IC (2019) Historical trends in the stomatal limitation of photosynthesis: empirical support for an optimality principle. *New Phytol* 225:2484–2495
- Lefohn AS et al (2018) Tropospheric ozone assessment report: Global ozone metrics for climate change, human health, and crop/ecosystem research. *Elem Sci Anth* 6(1):28. <https://doi.org/10.1525/elementa.279>
- Lee et al (2017) The relationship between SO<sub>2</sub> exposure and plant physiology: A mini review. <https://doi.org/10.1007/s13580-017-0053-0>
- Lehmann MM, Goldsmith GR, Schmid L, Gessler A, Saurer M, Siegwolf RTW (2018) The effect of 18O-labelled water vapor on the oxygen isotope ratio of water and assimilates in plants at high humidity. *New Phytol* 217:105–116. <https://doi.org/10.1111/nph.14788>
- Lenhart K, Behrendt T, Greiner S, Steinkamp J, Well R, Giesemann A, Keppler F (2019) Nitrous oxide effluxes from plants as a potentially important source to the atmosphere. *New Phytol* 221:1398–1408
- Leonardi S, Gentilesca T, Guerrieri R, Rippullone F, Magnani F, Mencuccini M, Noije TV, Borghetti M (2012) Assessing the effects of nitrogen deposition and climate on carbon isotope discrimination and intrinsic water-use efficiency of angiosperm and conifer trees under rising CO<sub>2</sub> conditions. *Glob Change Biol* 18:2925–2944
- Lévesque MR, Siegwolf RTW, Saurer M, Eilmann B, Rigling A (2014) Increased water-use efficiency does not lead to enhanced tree growth under xeric and mesic conditions. *New Phytol* 203:94–109 <https://doi.org/10.1111/nph.12772>
- Linzon SN (1972) Effects of sulphur oxides on vegetation. *For Chronicle* 48:182–186
- Liu X, Zhao L, Voelker SL, Xu G, Zeng X, Zhang X, Zhang L, Sun W, Zhang Q, Wu G, Li X (2018) Warming and CO<sub>2</sub> enrichment modified the ecophysiological responses of Dahurian larch and Mongolia pine during the past century in the permafrost region of northeastern China. *Tree Physiol* 39:88–103
- Maier-Maercker U, Koch W (1995) Poor stomatal control of water-balance and the abscission of green needles from a declining stand of spruce trees (*Picea abies* [L.] Karst.) from the northern Alps. *Trees Struct Funct* 10:63–73
- Marchand W, Girardin MP, Hartmann H, Depardieu C, Isabel N, Gauthier S, Boucher E, Bergeron Y (2020) Strong overestimation of water-use efficiency responses to rising CO<sub>2</sub> in tree-ring studies. *Glob Change Biol* 26:4538–4558
- Martin B, Bytnerowicz A, Thorstenson YR (1988) Effects of air-pollutants on the composition of stable carbon isotopes, <sup>13</sup>C, of leaves and wood, and on leaf injury. *Plant Physiol* 88:218–223
- Martin B, Sutherland EK (1990) Air pollution in the past recorded in width and composition of stable carbon isotopes of annual growth rings of Douglas-fir. *Plant Cell Environ* 13:839–844
- Mathias JM, Thomas RB (2018) Disentangling the effects of acidic air pollution, atmospheric CO<sub>2</sub>, and climate change on recent growth of red spruce trees in the Central Appalachian Mountains. *Global Change Biology*: 3938–3953
- Matyssek R, Maurer S, Gunthardt-Goerg MS, Landolt W, Saurer M, Polle A (1997) Nutrition determines the ‘strategy’ of *Betula pendula* for coping with ozone stress. *Phyton-Ann Rei Bot A* 37:157–167
- Matyssek R, Sandermann H (2003) Impact of ozone on trees: an ecophysiological perspective. *Progr Bot* 64(64):349–404
- Matyssek R, Sandermann H, Wieser G, Booker F, Cieslik S, Musselman R, Ernst D (2008) The challenge of making ozone risk assessment for forest trees more mechanistic. *Environ Pollut* 156:567–582

- Matyssek R, Wieser G, Calfapietra C, de Vries W, Dizengremel P, Ernst D, Jolivet Y, Mikkelsen TN, Mohren GMJ, Le Thiec D, Tuovinen JP, Weatherall A, Paoletti E (2012) Forests under climate change and air pollution: gaps in understanding and future directions for research. *Environ Pollut* 160:57–65. <https://doi.org/10.1016/j.envpol.2011.07.007>
- Matyssek R, Wieser G, Ceulemans R, Rennenberg H, Pretzsch H, Haberer K, Low M, Nunn AJ, Werner H, Wipfler P, Osswaldg W, Nikolova P, Hanke DE, Kraigher H, Tausz M, Bahnweg G, Kitao M, Dieler J, Sandermann H, Herbinger K, Grebenc T, Blumenrother M, Deckmyn G, Grams TEE, Heerd C, Leuchner M, Fabian P, Haberle KH (2010) Enhanced ozone strongly reduces carbon sink strength of adult beech (*Fagus sylvatica*)—resume from the free-air fumigation study at Kranzberg Forest. *Environ Pollut* 158:2527–2532. <https://doi.org/10.1016/J.Envpol.2010.05.009>
- McLaughlin SB (1985) Effects of air-pollution on forests - a critical-review. *J Air Pollut Control Assoc* 35:512–534
- Meng FR, Bourque CPA, Belczewski RF, Whitney NJ, Arp PA (1995) Foliage responses of spruce trees to long-term low-grade sulfur dioxide deposition. *Environ Pollut* 90:143–152. [https://doi.org/10.1016/0269-7491\(94\)00101-I](https://doi.org/10.1016/0269-7491(94)00101-I)
- Mills G, Pleijel H, Malley CS, Sinha B, Cooper OR, Schultz MG, Neufeld HS, Simpson D, Sharps K, Feng Z, Gerosa G, Harmens H, Kobayashi K, Saxena P, Paoletti E, Sinha V, Xu X (2018) Tropospheric Ozone Assessment Report: Present-day tropospheric ozone distribution and trends relevant to vegetation. *Elem Sci Anth* 6(1):47. <https://doi.org/10.1525/elementa.302>
- Millard P, Grelet G (2010) Nitrogen storage and remobilization by trees: ecophysiological relevance in a changing world. *Tree Physiology*, 30(9):1083–1095. <https://doi.org/10.1093/treephys/tpq042>
- Muzika RM, Guyette RP, Zielonka T, Liebhold AM (2004) The influence of O<sub>3</sub>, NO<sub>2</sub>, and SO<sub>2</sub> on growth of *Picea abies* and *Fagus sylvatica* in the Carpathian Mountains. *Environmental Pollution* 130: 65–71
- Neubert A, Kley D, Wildt J, Segschneider HJ, Förstel H (1993) Uptake of NO, NO<sub>2</sub> and O<sub>3</sub> by sunflower (*Helianthus annuus* L.) and tobacco plants (*Nicotiana tabacum* L.): dependence on stomatal conductivity. *Atmospheric Environ-Ment* 27A:2137–2145
- Nikolova PS, Andersen CP, Blaschke H, Matyssek R, Haeberle K-H (2010) Belowground effects of enhanced tropospheric ozone and drought in a beech/spruce forest (*Fagus sylvatica* L./*Picea abies* [L.] Karst). *Environ Pollut* 158:1071–1078
- Norby RJ, De Kauwe MG, Domingues TF, Duursma RA, Ellsworth DS, Goll DS, Lapola DM, Luus KA, Mackenzie AR, Medlyn BE, Pavlick R, Rammig A, Smith B, Thomas R, Thonicke K, Walker AP, Yang X, Zaehle S (2016) Model-data synthesis for the next generation of forest free-air CO<sub>2</sub> enrichment (FACE) experiments. *New Phytol* 209:17–28
- Norby RJ (1998) Nitrogen deposition: a component of global change analyses. *New Phytol* 139:189–200
- Nussbaum SV, Ballmoos P, Gfeller H, Schlunegger UP, Fuhrer J, Rhodes D, Brunold C (1993) Incorporation of atmospheric 15NO<sub>2</sub>-nitrogen into free amino acids by Norway spruce *Picea abies* (L.) Karst. *Oecologia* 94:408–414
- Ooi L, Matsuura T, Munemasa S, Murata Y, Katsuhara M, Hirayama T, Mori IC (2019) The mechanism of SO<sub>2</sub>-induced stomatal closure differs from O<sub>3</sub> and CO<sub>2</sub> responses and is mediated by nonapoptotic cell death in guard cells. *Plant Cell Environ* 42:437–447. <https://doi.org/10.1111/pce.13406>
- Paoletti E, Grulke NE (2010) Ozone exposure and stomatal sluggishness in different plant physiognomic classes. *Environ Pollut* 158:2664–2671
- Paoletti E, Grulke NE, Matyssek R (2020) Ozone amplifies water loss from mature trees in the short term but decreases it in the long term. *Forests* 11(1), 46; <https://doi.org/10.3390/f11010046>
- Parry MAJ, Gutteridge S (1984) The effect of SO<sub>3</sub><sup>2-</sup> and SO<sub>4</sub><sup>2-</sup> ions on the reactions of ribulose biphosphate carboxylase. *J Exp Bot* 35:157–168
- Patterson MJ, Rundel PW (1993) Carbon Isotope discrimination and gas exchange in Ozone sensitive and resistant Populations of Jeffery Pine. In: Ehleringer JR, Hall AE, Farquhar GD (eds) Stable isotopes and plant carbon-water relations. Academic Press, San Diego, pp 227–244

- Pearson J, Soares S (1998) Physiological response of plant leaves to atmospheric ammonia and ammonium. *Atm. Environ* 32:533–538
- Peñuelas J, Canadell JG, Ogaya R (2011) Increased water-use efficiency during the 20th century did not translate into enhanced tree growth. *Glob Ecol Biogeogr* 20:597–608
- Pregitzer KS, Burton AJ, King JS, Zak DR (2008) Soil respiration, root biomass, and root turnover following long-term exposure of northern forests to elevated atmospheric CO<sub>2</sub> and tropospheric O<sub>3</sub>. *New Phytol* 180:153–161
- Ränge P, Badeck FW, Plöchl M, Kohlmaier GH (1993) Apoplastic antioxidants as decisive elimination factors within the uptake of nitrogen dioxide into leaf tissue. *New Phytol* 125:771–785
- Randewig D, Hamisch D, Herschbach C, Eiblmeier M, Gehl C, Jurgeleit J, Skerra J, Rr M, Rennenberg H, Hänsch R (2012) Sulfite oxidase controls sulfur metabolism under SO<sub>2</sub> exposure in *Arabidopsis thaliana*. *Plant Cell Environ* 35:100–115. <https://doi.org/10.1111/j.1365-3040.2011.02420.x>
- Rannik U, Altimir N, Mammarella I, Back J, Rinne J, Ruuskanen TM, Hari P, Vesala T, Kulmala M (2012) Ozone deposition into a boreal forest over a decade of observations: evaluating deposition partitioning and driving variables. *Atmos Chem Phys* 12:12165–12182. <https://doi.org/10.5194/acp-12-12165-2012>
- Rennenberg H, Geßler A (1999) Consequences of N deposition to forest ecosystems – recent results and future research needs. *Water Air Soil Pollut* 116:47–64
- Rinne KT, Loader NJ, Switsur VR, Treydte KS, Waterhouse JS (2010) Investigating the influence of sulphur dioxide (SO<sub>2</sub>) on the stable isotope ratios ( $\delta^{13}\text{C}$  and  $\delta^{18}\text{O}$ ) of tree rings. *Geochim Cosmochim Acta* 74:2327–2339. <https://doi.org/10.1016/j.gca.2010.01.021>
- Ritter W, Andersen CP, Matyssek R, Grams TEE (2011) Carbon flux to woody tissues in a beech/spruce forest during summer and in response to chronic O<sub>3</sub> exposure. *Biogeosciences* 8:3127–3138
- Roden JS, Ehleringer JR (1999) Observations of hydrogen and oxygen isotopes in leaf water confirm the Craig-Gordon model under wide-ranging environmental conditions. *Plant Physiol* 120:1165–1173
- Roden JS, Bowling DR, McDowell NG, Bond BJ, Ehleringer JR (2005) Carbon and oxygen isotope ratios of tree ring cel- lulose along a precipitation transect in Oregon United States. *J Geophys Res* 110:G02003. <https://doi.org/10.1029/2005JG000033>
- Royal Society (2008) Ground-level ozone in the 21st century: future trends, impacts and policy implications. 132 pp. Science Policy report 15/08. Royal Society, London
- Rozanski K, Araguas-Araguas L, Gonfiantini (1993) Isotopic patterns in modern global precipitation: Cont Isot Indic Clim, American Geophysical Union Monograph
- Sage RF, Sharkey TD, Seemann JR (1989) Acclimation of Photosynthesis to Elevated CO<sub>2</sub> in Five C<sub>3</sub> Species. *Plant Physiol* 89:590–596
- Sage RF, Pearcy RW (1987) The nitrogen use efficiency of C<sub>3</sub> and C<sub>4</sub> plants. II. Leaf nitrogen effects on the gas exchange characteristics of *Chenopodium album* (L.) and *Amaranthus retroroflexus* (L.). *Plant Physiol* 84:959–963
- Sakata M, Suzuki K (2000) Evaluating possible causes for the decline of Japanese fir (*Abies firma*) forests based on  $\delta^{13}\text{C}$  records of annual growth rings. *Environ Sci Technol* 34:373e376
- Sandermann H, Ernst D, Heller W, Langebartels C (1998) Ozone: an abiotic elicitor of plant defence reactions. *Trends Plant Sci* 3:47–50
- Saurer M, Fuhrer J, Siegenthaler U (1991) Influence of ozone on the stable carbon isotope composition,  $\delta^{13}\text{C}$ , of leaves and grain of spring wheat (*Triticum aestivum* L.). *Plant Physiol* 97:313–316
- Saurer M, Maurer S, Matyssek R, Landolt W, Günthardt-Goerg MS, Siegenthaler U (1995) The influence of ozone and nutrition on  $^{13}\text{C}$  in *Betula pendula*. *Oecologia* 103:397–406. <https://doi.org/10.1007/bf00328677>
- Saurer M, Siegwolf RTW (2007) human impacts on tree-ring growth reconstructed from stable isotopes. In: Dawson T, Siegwolf R (eds) Stable isotopes as indicators of ecological change. Elsevier Academic Press, San Diego, CA, pp 49–62

- Saurer M, Cherubini P, Ammann M, De Cinti B, Siegwolf RTW (2004) First detection of nitrogen from NO<sub>x</sub> in tree rings: a 15N/14N study near a motorway. *Atmos Environ* 38:2779–2787
- Saurer M, Spahni R, Frank DC, Joos F, Leuenberger M, Loader NJ, McCarroll D, Gagen M, Poulter B, Siegwolf RTW, Andreu-Hayles L, Boettger T, Liñán ID, Fairchild IJ, Friedrich M, Gutierrez E, Haupt M, Hiltunen E, Heinrich I, Helle G, Grudd H, Jalkanen R, Levanič T, Linderholm HW, Robertson I, Sonninen E, Treydte K, Waterhouse JS, Woodley EJ, Wynn PM, Young GHF (2014) Spatial variability and temporal trends in water-use efficiency of European forests. *Glob Change Biol* 20:3700–3712
- Savard MM, Bégin C, Parent M, Smirnov A, Marion J (2004) Effects of smelter sulfur dioxide emissions: A spatiotemporal perspective using carbon isotopes in tree rings. *J Environ Qual* 33:13–26. <https://doi.org/10.2134/jeq2004.0013>
- Savard MM, Bégin C, Smirnov A, Marion J, Sharp Z, Parent M (2005) Fractionation change of hydrogen isotopes in trees due to atmospheric pollutants. *Geochim Cosmochim Acta* 69:3723–3731. <https://doi.org/10.1016/j.gca.2005.03.046>
- Savard MM, Bégin C, Marion J (2020a) Response strategies of boreal spruce trees to anthropogenic changes in air quality and rising pCO<sub>2</sub>. *Environm Poll* 261. <https://doi.org/10.1016/j.envpol.2020.114209>
- Savard MM, Marion J, Bégin C (2020b) Nitrogen isotopes of individual tree-ring series—The validity of middle- to long-term trends. *Dendrochronologia*. <https://doi.org/10.1016/j.dendro.2020.125726>
- Savard MM, Bégin C, Laganière J, Martineau C, Marion J, Stefani, FOP, Séguin A, Smirnov A, Bergeron J, Morency MJ, Paré D (2019) Anthropogenic N – a global issue examined at regional scale from soils, to fungi, roots and tree rings. *E3S Web Conf*. 98
- Savard MM, Bégin C, Smirnov A (2009) Marion J (2009) Tree-ring nitrogen isotopes reflect anthropogenic NO<sub>x</sub> emissions and climatic effects. *Environ Sci Technol* 43:604–609
- Savard MM, Cole A, Smirnov A, Vet R (2017) δ<sup>15</sup>N values of atmospheric N species simultaneously collected using sector-based samplers distant from sources – isotopic inheritance and fractionation. *Atmos Environ* 162:11–22
- Savard MM (2010) Tree-ring stable isotopes and historical perspectives on pollution—An overview. *Environ Pollut* 158(6):2007–2013
- Scheidegger Y, Saurer M, Bahn M, Siegwolf R (2000) Linking stable oxygen and carbon isotopes with stomatal conductance and photosynthetic capacity: a conceptual model. *Oecologia* 125:350–357
- Schubert BA, Jahren AH (2018) Incorporating the effects of photorespiration into terrestrial paleoclimate reconstruction. *Earth Sci Rev* 177:637–642
- Segsneider HJ, Wildt J, Förstel H (1995) Uptake of <sup>15</sup>NO<sub>2</sub> by sunflower (*Helianthus annuus*) during exposures in light and darkness: quantities, relationship to stomatal aperture and incorporation into different nitrogen pools within the plant. *New Phytol* 131:109–119
- Sensula B, Wilczynski S (2017) Climatic signals in tree-ring width and stable isotopes composition of *Pinus sylvestris* L. growing in the industrialized area nearby Kedzierzyn-Kozle. *Geochronometria* 44:240–255. <https://doi.org/10.1515/geochr-2015-0070>
- Sidorova OV, Fonti MV, Saurer M, Guillet S, Ch, Corona, Fonti P, Myglan VS, Kiryanov AV, Naumova OV, Ovchinnikov DV, Shashkin AV, Panyushkina P, Buntgen U, Hughes MK, Vaganov EA, Siegwolf RTW, Stoffel M (2019) Siberian tree-ring and stable isotope proxies as indicators of temperature and moisture changes after major stratospheric volcanic eruptions. *Clim Past* 15(2):685–700
- Siegwolf RTW, Matyssek R, Saurer M, Maurer S, Gunthardt-Goerg MS, Schmutz P, Bucher JB (2001) Stable isotope analysis reveals differential effects of soil nitrogen and nitrogen dioxide on the water use efficiency in hybrid poplar leaves. *New Phytol* 149:233–246
- Slovik S, Siegmund A, Fuhrer HW, Heber U (1996) Stomatal uptake of SO<sub>2</sub>, NO<sub>x</sub> and O<sub>3</sub> by spruce crowns (*Picea abies*) and canopy damage in Central Europe. *New Phytol* 132:661–676
- Sparks JP (2009) Ecological ramifications of the direct foliar uptake of nitrogen. *Oecologia* 159:1–13

- Sperry JS, Venturas MD, Todd HN, Trugman AT, Anderegg WRL, Wang Y, Tai X (2019) The impact of rising CO<sub>2</sub> and acclimation on the response of US forests to global warming. *Proc Nat Acad Sci USA* 116:25734–25744
- Sprenger M, Tetzlaff D, Buttle J et al (2018) Storage, mixing, and fluxes of water in the critical zone across northern environments inferred by stable isotopes of soil water. *Hydrol Process* 32:1720–1737. <https://doi.org/10.1002/hyp.13135>
- Sternberg L (2009) Oxygen stable isotope ratios of tree-ring cellulose: the next phase of understanding. *New Phytol* 181:553–562. <https://doi.org/10.1111/j.1469-8137.2008.02661.x>
- Streit K, Siegwolf RTW, Hagedorn F, Schaub M, Buchmann N (2014) Lack of photosynthetic or stomatal regulation after 9 years of elevated CO<sub>2</sub> and 4 years of soil warming in two conifer species at the alpine treeline. *Plant Cell Environ* 37:315–326. <https://doi.org/10.1111/pce.12197>
- Sun F, Kuang Y, Wen D, Xu Z, Li J, Zuo W, Hou E (2010) Long-term tree growth rate, water use efficiency, and tree ring nitrogen isotope composition of *Pinus massoniana* L. in response to global climate change and local nitrogen deposition in Southern China. *J Soils Sediments* 10:1453–1465
- Szejner P, Wright WE, Belmecheri S, Meko D, Leavitt SW, Ehleringer JR, Monson RK (2018) Disentangling season and interannual legacies from inferred patterns of water and carbon cycling using tree-ring stable isotopes. *Glob Change Biol* 24:5332–5347
- Tarasick D et al (2019) Tropospheric Ozone Assessment Report: Tropospheric ozone from 1877 to 2016, observed levels, trends and uncertainties. *Elem Sci Anth* 7(1):39. <https://doi.org/10.1525/elementa.376>
- Tcherkez G (2011) Natural <sup>15</sup>N/<sup>14</sup>N isotope composition in C3 leaves: are enzymatic isotope effects informative for predicting the <sup>15</sup>N-abundance in key metabolites? *Funct Plant Biol* 38:1–12
- Teklemariam TA, Sparks JP (2006) Leaf fluxes of NO and NO<sub>2</sub> in four herbaceous plant species: The role of ascorbic acid. *Atmospheric Environment* 40:2235–2244
- Thoene B, Rennenberg H, Weber P (1996) Absorption of atmospheric NO<sub>2</sub> by spruce (*Picea abies*) trees. II. Parameterization of NO<sub>2</sub> fluxes by controlled dynamic chamber experiments. *New Phytol* 134:257–266
- Thomas RQ, Brookshire ENJ, Gerber S (2015) Nitrogen limitation on land: how can it occur in Earth system models? *Glob Change Biol* 21:1777–1793. <https://doi.org/10.1111/gcb.12813>
- Tomlinson G, Siegwolf RTW, Buchmann N, Schleppei P, Waldner P, Weber P (2014) The mobility of nitrogen across tree-rings of Norway spruce (*Picea abies* L.) and the effect of extraction method on tree-ring <sup>15</sup>N and <sup>13</sup>C values. *Rapid Commun Mass Spectrom* 28(11):1258–1264
- Treydte KS, Frank DC, Saurer M, Helle G, Schleser GH, Esper J (2009) Impact of climate and CO<sub>2</sub> on a millennium-long tree-ring carbon isotope record. *Geochim Cosmochim Acta* 73:4635–4647. <https://doi.org/10.1016/j.gca.2009.05.057>
- Seibt U, Rajabi A, Griffiths H, Berry JA (2008) Carbon isotopes and water use efficiency: sense and sensitivity. *Oecologia* 155(3):441–454. <https://doi.org/10.1007/s00442-007-0932-7>
- Vallano D, Sparks JP (2007) Foliar δ<sup>15</sup>N values as indicators of foliar uptake of atmospheric nitrogen pollution. In: Dawson T, Siegwolf R (eds) *Stable isotopes as indicators of ecological change*. Elsevier Academic Press, San Diego, CA, pp 93–109
- Vallano D, Sparks JP (2013) Foliar δ<sup>15</sup>N is affected by foliar nitrogen uptake, soil nitrogen, and mycorrhizae along a nitrogen deposition gradient. *Oecologia* 172:47–58. <https://doi.org/10.1007/s00442-012-2489-3>
- Van der Eerden LJ, De Visser P, Perez-Soba M (1998) Urban and agricultural nitrogen deposition: are there differences in impact? In: De Kok LJ, Stulen I (eds) *Responses of plant metabolism to air pollution and global change*. Backhuys, Leiden, The Netherlands, pp 469–471
- Vitousek PM, Aber JD, Howarth RW et al (1997) Human alteration of global nitrogen cycle: sources and consequences. *Ecol Appl* 7:737–750
- Voelker SL, Meinzer FC (2017) Where and when does stem cellulose δ<sup>18</sup>O reflect a leaf water enrichment signal? *Tree Physiol* 37:551–553. <https://doi.org/10.1093/treephys/tpx029>

- Voelker SL, Merschel AG, Meinzer FC, Still CJ, Ulrich DE, Spies TA (2019) Fire deficits have increased drought-sensitivity in dry conifer forests; fire frequency and tree-ring carbon isotope evidence from Central Oregon. *Glob Change Biol* 25:1247–1262
- Voelker SL et al (2016) A dynamic leaf gas-exchange strategy is conserved in woody plants under changing ambient CO<sub>2</sub>: evidence from carbon isotope discrimination in paleo and CO<sub>2</sub> enrichment studies. *Glob Change Biol* 22(2):889–902. <https://doi.org/10.1111/gcb.13102>
- Vogel JC (1993) Variability of Carbon Isotope Fractionation during Photosynthesis. Stable Isotopes and Plant Carbon-water Relations. Academic Press, San Diego, pp 29–46
- Wagner R, Wagner E (2006) Influence of air pollution and site conditions on trends of carbon and oxygen isotope ratios in tree ring cellulose. *Isot Environ Health Stud* 42:351–365. <https://doi.org/10.1080/10256010600991078>
- Waldner P et al (2014) Detection of temporal trends in atmospheric deposition of inorganic nitrogen and sulphate to forests in Europe. *Atmos Environ* 95:363–374
- Walker AP et al (2020) Tansley Review: Integrating evidence for a terrestrial carbon sink caused by increasing atmospheric CO<sub>2</sub>. *New Phytol*. <https://doi.org/10.1111/nph.16866>
- Wedler M, Weikert RM, Lippert M (1995) Photosynthetic performance, chloroplast pigments and mineral content of Norway spruce (*Picea abies* (L.) Karst.) exposed to SO<sub>2</sub> and O<sub>3</sub> in an open-air fumigation experiment. *Plant Cell Environ* 18:263–276
- Wehr R, Commann R, Munger JW, McManus JB, Nelson DD, Zahniser MS, Saleska SR, Wofsy SC (2017) Dynamics of canopy stomatal conductance, transpiration, and evaporation in a temperate deciduous forest, validated by carbonyl sulfide uptake. *Biogeosciences* 14:389–401
- Weigt RB, Bräunlich S, Zimmermann L, Saurer M, Grams TEE, Dietrich HP, Siegwolf RTW, Nikolova PS (2015) Comparison of δ<sup>18</sup>O and δ<sup>13</sup>C between tree-ring whole wood and cellulose in five species growing under two different site conditions. *Rapid Commun Mass Spectrom* 29:2233–2244
- Wellburn AR (1990) Why are atmospheric oxides of nitrogen usually phytotoxic and not alternative fertilizers. *New Phytol* 115:395–429. <https://doi.org/10.1111/j.1469-8137.1990.tb00467.x>
- Wieser G, Oberhuber W, Waldboth B, Gruber A, Matyssek R, Siegwolf RTW, Grams TEE (2018) Long-term trends in leaf level gas exchange mirror tree-ring derived intrinsic water-use efficiency of *Pinus cembra* at tree line during the last century. *Agric Meteorol* 248:251–258
- Wittig VE, Ainsworth EA, Long SP (2007) To what extent do current and projected increases in surface ozone affect photosynthesis and stomatal conductance of trees? A meta-analytic review of the last 3 decades of experiments. *Plant Cell Environ* 30:1150–1162
- Wittig VE, Ainsworth EA, Naidu SL, Karnosky DF, Long SP (2009) Quantifying the impact of current and future tropospheric ozone on tree biomass, growth, physiology and biochemistry: a quantitative meta-analysis. *Glob Change Biol* 15:396–424
- Woodley EJ, Loader NJ, McCarroll D, Young GHF, Robertson I, Gagen MH, Warham MH (2012) High-temperature pyrolysis/gas chromatography/isotope ratio mass spectrometry: simultaneous measurement of the stable isotopes of oxygen and carbon in cellulose. *Rapid Commun Mass Spectrometry* 26:109–114. <https://doi.org/10.1002/rcm.5302>
- Xu YS, Shang B, Yuan XY, Feng ZZ, Calatayud V (2018) Relationships of CO<sub>2</sub> assimilation rates with exposure- and flux-based O<sub>3</sub> metrics in three urban tree species. *Sci Total Environ* 613:233–239
- Yamulki S, Harrison RM, Goulding KWT (1996) Ammonia surface exchange above an agricultural field in southeast England. *Atmos Environ* 30:109–118
- Ziegler I (1972) The effect of SO<sub>3</sub><sup>2-</sup> on the activity of RuBP carboxylase in isolated spinach chloroplasts. *Planta* 103:155–163
- Zweifel R, Stepe K, Sterck FJ (2007) Stomatal regulation by microclimate and tree water relations: interpreting ecophysiological field data with a hydraulic plant model. *J Exp Bot* 58(8):2113–2131. <https://doi.org/10.1093/jxb/erm050>

**Open Access** This chapter is licensed under the terms of the Creative Commons Attribution 4.0 International License (<http://creativecommons.org/licenses/by/4.0/>), which permits use, sharing, adaptation, distribution and reproduction in any medium or format, as long as you give appropriate credit to the original author(s) and the source, provide a link to the Creative Commons license and indicate if changes were made.

The images or other third party material in this chapter are included in the chapter's Creative Commons license, unless indicated otherwise in a credit line to the material. If material is not included in the chapter's Creative Commons license and your intended use is not permitted by statutory regulation or exceeds the permitted use, you will need to obtain permission directly from the copyright holder.





# Chapter 25

## Insect and Pathogen Influences on Tree-Ring Stable Isotopes



Danielle E. M. Ulrich, Steve Voelker, J. Renée Brooks,  
and Frederick C. Meinzer

**Abstract** Understanding long-term insect and pathogen effects on host tree physiology can help forest managers respond to insect and pathogen outbreaks, and understand when insect and pathogen effects on tree physiology will be exacerbated by climate change. Leaf-level physiological processes modify the carbon (C) and oxygen (O) stable isotopic composition of elements taken up from the environment, and these modifications are recorded in tree-rings (see Chaps. 9, 10, 16 and 17). Therefore, tree-ring stable isotopes are affected by both the tree's environment and the tree's physiological responses to the environment, including insects and pathogens. Tree-ring stable isotopes provide unique insights into the long-term effects of insects and pathogens on host tree physiology. However, insect and pathogen impacts on tree-ring stable isotopes are often overlooked, yet can substantially alter interpretations of tree-ring stable isotopes for reconstructions of climate and physiology. In this chapter, we discuss (1) the effects of insects (defoliators, wood-boring, leaf-feeding), pests (parasitic plants), and pathogens (root and foliar fungi) on host physiology (growth, hormonal regulation, gas exchange, water relations, and carbon and nutrient use) as they relate to signals possibly recorded by C and O stable isotopes in tree-rings, (2) how tree-ring stable isotopes reveal insect and pathogen impacts and the interacting effects of pathogens and climate on host physiology, and (3) the importance of considering insect and pathogen impacts for interpreting tree-ring stable isotopes to reconstruct past climate or physiology.

---

D. E. M. Ulrich (✉)

Department of Ecology, Montana State University, Bozeman, MT 59717-3460, USA

e-mail: [danielle.ulrich@montana.edu](mailto:danielle.ulrich@montana.edu)

S. Voelker

College of Forest Resources and Environmental Science, Michigan Technological University,  
Houghton, MI 49931, USA

J. R. Brooks

Pacific Ecological Systems Division, US EPA/CPHEA, Corvallis, OR 97331, USA

F. C. Meinzer

USDA Forest Service, Pacific Northwest Research Station, Corvallis, OR 97331, USA

© The Author(s) 2022

R. T. W. Siegwolf et al. (eds.), *Stable Isotopes in Tree Rings*, Tree Physiology 8,  
[https://doi.org/10.1007/978-3-030-92698-4\\_25](https://doi.org/10.1007/978-3-030-92698-4_25)

711

## 25.1 Introduction

Harmful insects, pathogenic fungi, and parasitic plants can alter host tree physiology, reduce tree health, and contribute to tree mortality. Native and introduced insects and pathogens influence forest structure, composition, biodiversity, and carbon dynamics (Castello et al. 1995; Clark et al. 2010). Environmental stress can increase biological challenges to tree health and create a greater likelihood of host tree mortality by either insect pests (Waring and Pitman 1985; Fettig et al. 2007; Anderegg et al. 2015) or pathogens (Manion 1991; Marçais and Bréda 2006; Voelker et al. 2008). Forest-pathogen interactions with amplified climate variability have been cited as the primary cause of the widespread forest mortality observed in recent decades (Allen et al. 2010; Hubbart et al. 2016; Hartmann et al. 2018). Mitigating and predicting future mortality events requires understanding the physiological mechanisms underlying interactions among insects and pathogens and trees, and the influence of climate variability on forests (Hartmann et al. 2018). However, the interacting effects of insects and pathogens, and climate on tree physiology are poorly understood, partly due to the long timescales over which all of these impact tree function. Furthermore, separating the effects of insects and pathogens, and climate on tree function is challenging. Therefore, combining annually resolved tree-ring stable isotopes and ring width chronologies that record information over decades to centuries are ideal tools to reconstruct insect and pathogen, and climate impacts on host physiology and to help predict future effects of insects and pathogens on forests.

Tree-rings record both the tree's environmental conditions, and the tree's physiological responses to the environment. Insects and pathogens can alter host physiology (i.e. growth, hormonal regulation, gas exchange, water relations, carbon and nutrient relations), and therefore pathogen effects can be recorded in the tree-ring record. Many studies have used tree-ring widths and growth to reconstruct climate and tree vigor (Fritts 1971; Fritts and Swetnam 1989). However, ring widths have limited use for reconstructing key aspects of tree physiology. In contrast, tree-ring stable isotopes can be used to more precisely infer certain physiological and ecological processes because they can provide more specific and additional information about trees' responses to their environment compared to tree-ring widths alone (Cernusak and English 2015; see Chaps. 16, 17). The carbon (C) from carbon dioxide (CO<sub>2</sub>) in the atmosphere and oxygen (O) from water taken up by the tree reflect climatic conditions, and are then altered by physiological processes before eventually being incorporated into each tree-ring (see Chaps. 9, 10). The stable isotopic composition of the cellulose of each tree-ring can be analyzed over the lifespan of a tree to reveal temporal shifts in physiological responses. Because forest insects and pathogens can affect host physiology, tree-ring stable isotopes combined with ring widths are well-suited to investigate past and long-term impacts of insects and pathogens on host tree physiology.

Here, we synthesize and review how tree-ring stable isotopes record the impacts of insects and pathogens on host physiology over seasonal to multi-decadal timescales and the interacting effects of climate and pathogens on host physiology. First, we

discuss the effects of insects and pathogens on host physiology (focusing primarily on insects and pathogens that have been investigated with tree-ring stable isotopes), and briefly relate that to the isotope theory presented in Chaps. 9, 10, 16, and 17. Second, we discuss how tree-ring stable isotopes can be used to reveal the aforementioned insect and pathogen impacts and to help separate the interacting effects of insects and pathogens, and climate on host physiology. Finally, we conclude by discussing the importance of considering insect and pathogen impacts when interpreting tree-ring stable isotopes to reconstruct past climate or physiology.

## 25.2 Effects of Pathogens on Host Physiology

Forest insects and pathogens have diverse effects on host tree physiology, including alterations in growth, hormonal regulation, gas exchange, water relations, and carbon and nutrient use, many of which can alter the isotopic composition of cellulose in tree-rings. The detrimental effects of forest insects and pathogens on host tree functions often contribute to host tree mortality. Here, we focus on the physiological impacts of insects and pathogens that have also been investigated using tree-ring stable isotope approaches.

Many forest insects and pathogens reduce growth and biomass via partial defoliation and branch dieback. Leaf-feeding, defoliating insects, such as spruce budworm (*Choristoneura*), jack pine budworm (*Choristoneura pinus*), web-spinning sawfly (*Cephalcia*), larch budmoth (*Zeiraphera diniana* Gn), aspen leaf miner (*Phyllocnistis populiella*), and pandora moth (*Coloradia pandora* Blake) cause changes in leaf area (per tree and/or per leaf), photosynthetic capacity, water relations, and photosynthate allocation, often resulting in reduced radial growth (Kozłowski 1969). Artificial defoliation studies have also demonstrated defoliation-induced reductions in phloem sieve tube diameter, reducing C transport capability (Hillabrand et al. 2019), and defoliation-induced increases in C allocation to storage over growth (Wiley et al. 2013; Puri et al. 2015). The reduction in photosynthetic tissue can result in very narrow or one or more locally absent growth rings. This means that a physiological process or climate signal detectable by tree-ring stable isotopes may not be available because cell division is inhibited, phloem transport is disrupted, or recent photosynthetic C uptake is not sufficient to supply sugars to produce tree rings. In some such situations, narrow rings can form if stored C reserves are mobilized for growth (Kozłowski et al. 1991; Helle and Schleser 2004; Kagawa et al. 2006). Utilization of stored starch can alter the tree-ring stable isotope composition of newly synthesized plant compounds because the C stable isotope composition of photosynthetic products stored as starch is relatively enriched compared to that of triose-phosphates (Brugnoli et al. 1988; Cernusak et al. 2009; McKellar et al. 2011). Additionally, the isotopic composition of stored compounds is a mixture from previous photosynthetic activity and will not reflect the current physiological processes within the plant (Sohn et al. 2014). Consequently, plant structural compounds, such as cellulose in tree-rings could potentially be enriched and the intra- or inter-annual variance muted if those

tissues were derived in part from stored starch. Enriched C isotope signals have been observed in early-forming parts of growth rings of some hardwood species (Helle and Schleser 2004). However, to our knowledge, changes in inter-annual C isotope variability due to stress modifying the proportion of C derived from storage has not yet been demonstrated (Sohn et al. 2014). Leaf lifespan also can influence how defoliation events are recorded in the tree-ring record with deciduous species responding more quickly than evergreen species. For example, the larch web-spinning sawfly (*Cephalcia lariciphila* (Wachtl)) reduced radial growth of European larch (*Larix decidua* Mill.) by 67% during the same year as defoliation (Vejpustková and Holuša 2006). In contrast, in evergreen species, substantial radial growth reductions were often observed during the second consecutive year of heavy defoliation. Spruce web-spinning sawfly (*Cephalcia arvensis* Panzer) reduced growth only in the second year of defoliation of Norway spruce (*Picea abies* (L.) Karst.) (Gori et al. 2014a) and similar results were also found for defoliation of white pine (*Pinus strobus* (L.)) by pine false webworm (*Acantholyda erythrocephala* (L.)) (Mayfield et al. 2005). The slower response of evergreen species compared to deciduous species is consistent with a strong legacy effect due to cohorts of evergreen leaves remaining functional for multiple years, as opposed to only months for deciduous species (Zweifel and Sterck 2018). However, sometimes the timing of radial growth reduction in response to defoliation is more variable, such as in *L. decidua* that exhibited radial growth reductions for four years after defoliation by larch budmoth (*Z. diniana*) (Peters et al. 2017). Similarly, growth reductions in balsam fir (*Abies balsamea* (L.) Mill.) and white spruce (*Picea glauca* (Moench) Voss.) were observed 1–4 years after defoliation by spruce budworm (*Choristoneura fumiferana* (Clem.)) (Blais 1958; Krause 1997). Furthermore, leaf lifespan can influence foliage quality for insects, and thus can affect the severity of the insect's impact on tree physiology, how defoliation may be recorded in tree-rings (but not always, see below Sect. 25.2 and also Kress et al. 2009), and consequently the magnitude and/or duration of isotopic departures signaling variations in insect outbreak cycles. For example, in the European Alps during spring, larch budmoth (LBM) has defoliated European larch on a cyclic pattern every 8–10 years (Baltensweiler et al. 2008). After defoliation events, larch will re-foliate in early August if the leaf mass loss exceeds 50% (Baltensweiler et al. 2008). This second flush of short needles is often killed in early frosts in October, preventing defoliated larch trees from accumulating assimilates and nutrients, so resource-deprived trees again produce short needles the following spring. In addition to short needles, resource-deprived trees also produce needles with low nitrogen (N) content and high raw fiber. These alterations in LBM food quality trigger the collapse of the LBM population and create the remarkably regular 8–10 year periodicity of LBM outbreaks that had been observed for 1200 years. Switzerland's forest service had documented regular LBM outbreaks since 1864 (Baltensweiler 1993; Baltensweiler et al. 2008). However, since the 1980s, no alpine-wide synchronized LBM outbreak event has occurred. As a result, tree-ring stable isotopes have been used to reveal that an increase in summer temperatures may explain why no LBM outbreak has occurred since the 1980s (Kress et al. 2009; and for more details, see below Sect. 25.2).

Growth perturbations also have been attributed to insect- and pathogen-induced alterations in host tree hormonal regulation, as is the case with the parasitic plant, dwarf mistletoe (*Arceuthobium* spp.). Dwarf mistletoe, a relative of Christmas mistletoe (*Phoradendron*, *Loranthus*, *Viscum* spp.), is a vascular, obligate, hemiparasitic plant that relies primarily on the host tree for water and nutrients. Dwarf mistletoes, native to and found throughout North America, include 42 species that infect species of *Abies*, *Picea*, *Tsuga*, *Larix*, *Pseudotsuga*, *Keteleeria*, and *Juniperus*, and 95% of the species in *Pinus* (Hawksworth and Wiens 1998; Nickrent et al. 2004). Dwarf mistletoes divert host tree water and nutrients by developing an endophytic system within the host xylem and phloem (Geils and Hawksworth 2002; Mathiasen et al. 2008; Glatzel and Geils 2009). In contrast to Christmas mistletoes, dwarf mistletoe eventually kills its host and instead of leafy shoots, has small diminutive aerial shoots that are essentially leafless. Needles on host branches infected with dwarf mistletoe possessed lower abscisic acid and greater total cytokinin contents than needles on uninfected branches (Logan et al. 2013). Cytokinins are known to delay senescence, promote resource mobilization, and increase the frequency of branching (Mok 1994; Davies 2010). This is likely the cause of a classic symptom of the infection known as a witches' broom, a dense disorganized mass of host tree branches. The self-shaded witches' brooms reduce host light capture and photosynthetic C gain (Logan et al. 2013). The dwarf mistletoe-induced alterations in cytokinins may explain why resources are continuously allocated to self-shaded witches' brooms. The alterations in hormone levels and witches' broom formations also may underlie significantly greater leaf area:sapwood area ratios in infected trees compared to uninfected trees (Sala et al. 2001). These hormonal influences and morphological effects would be expected to alter  $\delta^{13}\text{C}$  and  $\delta^{18}\text{O}$  of infected plant tissues.

Forest insects and pathogens induce alterations in gas exchange, either directly or indirectly. Swiss needle cast is caused by a fungus (*Phaeocryptopus gaeumannii* (T. Rohde) Petr.) that blocks stomata by either the fungal fruiting bodies (pseudothecia) or hyphae. This physical blockage of stomata restricts leaf gas exchange, reducing the  $\text{CO}_2$  assimilation rate ( $A$ ) and stomatal conductance ( $g_s$ ) by 50% and 37%, respectively (Manter et al. 2000). Some insects and pathogens can also restrict leaf gas exchange by interrupting water transport in stems (Parke et al. 2007). Alternatively, forest insects and pathogens can alter gas exchange indirectly. For example, defoliating insects such as spruce budworm induce needle loss which has been shown to have a compensatory effect on the remaining needles where  $A$  of remaining needles increases, possibly due to increased allocation of mineral nutrients to remaining foliage (Reich et al. 1993; Lavigne et al. 2001; Little et al. 2003). In western hemlock trees infected with dwarf mistletoe, photosynthetic capacity was significantly reduced due to sequestration of host N by dwarf mistletoe (Meinzer et al. 2004). White spruce infected with dwarf mistletoe exhibited greater transpiration ( $E$ ) rates than uninfected trees, due to the dwarf mistletoe-induced perturbations in hormonal regulation where needles on infected likely branches possessed lower abscisic acid and greater total cytokinin contents than needles on uninfected branches (Logan et al. 2013). Because abscisic acid promotes stomatal closure (Mittelheuser and Van Steveninck 1969),

whereas cytokinins promote stomatal opening and decrease sensitivity of stomata to abscisic acid (Acharya and Assmann 2009), these combined alterations in hormone levels likely underlie the increase in host  $E$  (Logan et al. 2013). The dwarf mistletoe infection also reduces stomatal limitations on gas exchange, as shown by significant reductions in intrinsic water use efficiency in infected trees compared to uninfected trees (Meinzer et al. 2004; Logan et al. 2013).

Forest insects and pathogens influence host tree water relations. For example, *Heterobasidion parvidporum* (white rot fungus) and *Phytophthora quercina* are fungal root pathogens of conifers and oaks, respectively. These fungal infections result in root mortality and consequently reduced water and nutrient uptake, hydraulic failure, and increased susceptibility to windthrow, wood decay, and mortality (Filip 1999). Host trees of mistletoes and dwarf mistletoes adjust their hydraulic system and water relations to accommodate these parasitic plants that sequester host water, C, and nutrients (Geils and Hawksworth 2002; Mathiasen et al. 2008; Glatzel and Geils 2009). Some mistletoes have leafy shoots that provide a greater surface area for transpiration ( $E$ ), which can result in significant additional water loss from the host tree (Flanagan et al. 1993; Cernusak et al. 2004). Mistletoes can transpire up to 9 times more per unit leaf area and maintain 72% greater rates of  $g_s$  than their hosts (Ullmann et al. 1985; Marshall et al. 1994). This results in significant additional water loss, lowers host tree water potentials, and increases risk for hydraulic failure. To compensate, host trees close their stomata, significantly reducing C assimilation and resulting in a negative host tree C balance (Zweifel et al. 2012). The mistletoe-induced 'leak' in the hydraulic system is intensified under drought conditions (Zweifel et al. 2012). In contrast to leafy mistletoes, dwarf mistletoes have reduced aerial shoots with less leaf area from which water can be lost. Needles of host trees infected with dwarf mistletoe have exhibited greater rates of  $g_s$  and  $E$ , reduced water use efficiency, and consequently more negative  $\delta^{13}\text{C}_{\text{leaf}}$  (Sala et al. 2001; Meinzer et al. 2004; Logan et al. 2013). The vascular occlusions caused by dwarf mistletoe's sinkers tapping into host xylem lead to branch swellings and restrictions in water flow that can either reduce needle size (Logan et al. 2002; Reblin et al. 2006) or cause needle loss (Meinzer et al. 2004). Infected trees exhibited significantly reduced sapwood-area specific hydraulic conductivity ( $K_s$ ) compared to uninfected trees, yet leaf-specific hydraulic conductivity ( $K_L$ ) did not significantly differ between infected and uninfected trees (Meinzer et al. 2004; Logan et al. 2013). The maintenance of  $K_L$  but not  $K_s$  of infected branches was the result of two different infection symptoms: reduced needle size (Logan et al. 2002; Reblin et al. 2006) and needle loss (Meinzer et al. 2004). Due to these differences, Logan et al. (2013) observed significantly greater  $E$  in infected branches while Meinzer et al. (2004) observed no significant differences in  $g_s$  between infected and uninfected trees. Due to significant needle loss and reductions in photosynthetic capacity, infected trees exhibited significantly lower water use and inferred significantly lower C use on the whole tree level compared to controls (Meinzer et al. 2004).

Forest insects and pathogens also disrupt host tree C and nutrient relations. By establishing an endophytic system within the host phloem and xylem, dwarf mistletoes and mistletoes sequester photosynthates and nutrients. As stated above, trees

infected with dwarf mistletoe and mistletoe exhibited significantly reduced leaf N content compared to non-infected trees, presumably due to the sequestration of N by the parasite (Meinzer et al. 2004; Galiano et al. 2011). This contributes to the significantly reduced photosynthetic capacity of infected tree needles compared to uninfected tree needles (Meinzer et al. 2004). Insects such as bark beetles (Coleoptera: Curculionidae, Scolytinae) and the red oak borer (*Enaphalodes rufulus* (Haldeman); Coleoptera: Polyphaga, Cerambycidae) nest in and feed on phloem, impeding photosynthate transport. Bark beetles such as the mountain pine beetle (*Dendroctonus ponderosae* Hopk.) are native forest disturbance agents that infest and kill *Pinus* species. Although tree-ring width records show that bark beetles have been associated with western North American forests for hundreds of years, current outbreaks have increased in duration, intensity, and geographic area affected due to rising temperatures and decreasing precipitation throughout western North America (Samman and Logan 2000; Bentz et al. 2009, 2010). Bark beetles overwinter as larvae and attack trees in the summer (July–August). Females bore through the bark to the phloem and construct egg galleries. Trees can defend themselves by releasing resin, a defense mechanism to “pitch out” and resist beetle attack (Amman et al. 1985). This requires that a tree be healthy enough to allocate current photosynthates and/or stored non-structural carbon to create this resin and healthy enough to transport photosynthate and resin to sites of attack. The first beetles to attack a tree release aggregating pheromones to attract additional beetles to overcome the tree’s defense. In addition to phloem, bark beetles can also injure the xylem because bark beetles vector various fungi that can disrupt xylem functionality (Dysthe et al. 2015), and inhibit water transport and also resin production. The bark beetle-induced, and fungal-enhanced, combination of phloem and xylem dysfunction kills the tree. With longer summers and shorter winters, some bark beetle species like *D. ponderosae* are not killed off by cold temperatures as they generally have been in the past, and can produce more than one generation per year, increasing the duration, intensity, and geographic area of outbreaks (Bentz et al. 2010). However, other species like *D. ruffipennis* are more cold-adapted, and rarely experience winter kill events (Miller and Werner 1987). In addition, warming and drought has stressed trees and weakened their capacity to fend off insects like bark beetles (Raffa et al. 2008; Anderegg et al. 2015).

Red oak borer is another native wood-boring insect that has recently experienced outbreaks of unprecedented magnitude that contribute to oak mortality observed in the Ozark Mountains of Arkansas and Missouri, USA (Crook et al. 2004). Episodic oak mortality in this region and elsewhere have been attributed to “oak decline,” which is often incited by drought, late frosts, or insect defoliation, but is also influenced by a combination of predisposing factors such as tree age, competition, soil quality, and a number of insect pests and pathogens that are effective at contributing to the death of weakened trees, including red oak borer (Manion 1991; Thomas et al. 2002; Crook et al. 2004; Voelker et al. 2008; Gagen et al. 2019). The red oak borer has a two-year cycle with adults emerging in only odd numbered years. Larvae chew through bark into the phloem, sapwood, and heartwood where they build a gallery, feed, and overwinter twice. At low numbers, trees tolerate red oak borer but at extremely high infestation levels, mortality occurs. These physiological effects of

insects and pathogens can all impact the stable C and O isotopic composition within host trees, but because of the diversity of influences described above, each insect- and pathogen-host isotopic pattern can vary substantially (Cernusak et al. 2004).

### **25.3 Tree-Ring Stable Isotopes Record Physiological Impacts of Insects and Pathogens**

Although numerous dendrochronological studies have examined outbreak cycles of pathogens and insects (Lynch 2012), fewer have used tree-ring stable isotopes to investigate host physiological impacts and interactions with climate. Any factors that affect leaf gas exchange ( $A$ ,  $g_s$ ) can influence the tree-ring stable isotope record (see Chaps. 16, 17). The enhanced insight into physiological impacts of insects and pathogens has led to research using tree-ring stable isotopes combined with ring widths to identify physiological outbreak signatures, outbreak cycles, and infestation dynamics. Correlations between the C and O stable isotopic composition of tree-rings and climate variables reveal the bidirectional interactions between climate, and the severity and susceptibility of insect and pathogen infection: how climate affects host susceptibility to insect and pathogen infestation, and how insect and pathogen infestation influences sensitivity to climate. Tree-ring stable isotope records can improve efforts by forest managers to combat insect and pathogen outbreaks by providing early detection of insect or pathogen infection and improving predictions of outbreaks and mortality events under future climate regimes as a result of synergistic insect and pathogen and climate influences. Tree-ring stable isotopes have helped elucidate this interaction between pathogen and climate. Below, we describe how tree-ring stable isotopes have been used to investigate (1) the impacts of insects and pathogens on host tree physiology (growth, hormonal regulation, gas exchange, water relations, and carbon and nutrient use), (2) the effects of climate on insect and pathogen infestation severity levels and host tree susceptibility to infestation, and (3) the effects of insect and pathogen infestation on host tree sensitivity to climate.

#### **25.3.1 *Tree-Ring Stable Isotopes Reveal Insect and Pathogen Impacts on Host Physiology***

Given the potential for greater insights into host tree physiological impacts of insects and pathogens, tree-ring stable isotopes have been used to more precisely identify physiological impacts to reveal infection ‘signatures’ and onset of infection. For example, Marias et al. (2014) used tree-ring growth and  $\delta^{13}\text{C}$  over 100 years and also tree-ring  $\delta^{18}\text{O}$  during 20 years of severe infection to investigate the impacts of hemlock dwarf mistletoe (*Arceuthobium tsugense* (Rosendahl) G.N. Jones ssp. *tsugense*) on the physiology of host western hemlock (*Tsuga heterophylla* (raf.)



Sarg.). Radial growth of infected trees was initially greater than that of uninfected trees in 1886–90 but then declined more rapidly and became significantly lower than uninfected trees in 2006–10 as the infection became severe, suggesting that infected trees were growing faster than uninfected trees prior to becoming infected. During the advanced stage of the infection, infected trees exhibited significantly lower tree-ring  $\delta^{13}\text{C}$  and  $\delta^{18}\text{O}$  than uninfected trees regardless of annual precipitation (drier versus wetter years). The lower  $\delta^{13}\text{C}$  of infected trees supports previous work that the dwarf mistletoe infection reduces host photosynthetic capacity, due to the parasite's sequestration of N from the host tree (Meinzer et al. 2004). Because the impacts on radial growth and  $\delta^{13}\text{C}$  were evident only when the infection became severe, the authors concluded that tree-ring growth and stable isotopes could not be used to identify precisely when trees became infected. However, this information suggests that western hemlock can live for decades with the dwarf mistletoe infection. The lower  $\delta^{18}\text{O}$  of infected trees was unexpected because  $g_s$  and environmental variables, expected to influence  $\delta^{18}\text{O}$  (see Chap. 10), were similar for both infected and uninfected groups of trees. However, estimates of lower mesophyll conductance ( $g_m$ ) in leaves of infected trees from  $A-C_i$  curves led the authors to conclude that effective path length ( $L$ ) estimated from the Peclet effect model (Barbour 2007) was higher in leaves of infected trees, leading to their lower tree-ring  $\delta^{18}\text{O}$ . Although the anatomical causes of the Peclet effect have been debated (Roden et al. 2015), these unexpected findings pointed to limitations in the dual isotope approach (Scheidegger et al. 2000; Roden and Siegwolf 2012) often used to interpret tree-ring  $\delta^{13}\text{C}$  and  $\delta^{18}\text{O}$  because it does not account for changes in traits related to leaf anatomical characteristics such as  $g_m$  and  $L$  that alter gas exchange and may underlie the observed  $\delta^{18}\text{O}$  patterns.

Tree-ring stable isotopes have been used to investigate the long-term impacts of insect-induced defoliation and leaf herbivory on host physiology and tree growth-climate relationships (Leavitt and Long 1986; Simard et al. 2008, 2012; Kress et al. 2009; Gori et al. 2014a). Defoliation and herbivory can be recorded in tree-ring cellulose because they directly influence gas exchange by damaging stomata and photosynthetic machinery (Weidner et al. 2010) and indirectly by increasing  $A$  in remaining leaves (Simard et al. 2008) and reducing stand-level  $E$  and associated competition for water during dry periods. Simard et al. (2008) investigated the effects of western spruce budworm (SBW) (*Choristoneura fumiferana* Clem.) by comparing the C and O tree-ring stable isotope records of SBW's primary host balsam fir (*Abies balsamea*), secondary host black spruce (*Pinus mariana*), and a non-host tree species *Pinus banksiana* (Lamb.). Severe infestations of the leaf-feeding SBW are recorded in the tree-ring record as reduced radial growth lasting 5 years or more (Swetnam et al. 1985). Light to moderate infestation effects on radial growth are less pronounced. SBW-induced defoliation appeared to cause a compensatory increase in  $A$  of the remaining needles with a relatively smaller concurrent increase in  $g_s$ , exhibited by increased tree-ring  $\delta^{13}\text{C}$  (i.e. decreased tree-ring  $\Delta^{13}\text{C}$ ) and reduced radial growth not observed in the non-host species and concurrent with documented SBW outbreaks in the area. The compensatory increase in  $A$  may have resulted from an increase in allocation of mineral nutrients to remaining leaves (Lavigne et al. 2001). In contrast,

the tree-ring  $\delta^{18}\text{O}$  trajectories were synchronous among host and non-host species, supporting that the  $\delta^{13}\text{C}$  signal is most likely due to a compensatory increase in  $A$  (rather than shifts in  $g_s$ ) in remaining needles and suggesting that the tree-ring  $\delta^{18}\text{O}$  signal is driven primarily by climate, rather than SBW.

Compensatory increases in  $A$  in response to defoliation by the web-spinning sawfly also have been recorded in tree-ring stable isotopes of host Norway spruce. Gori et al. (2014a) compared tree-ring growth,  $\delta^{13}\text{C}$ , and  $\delta^{18}\text{O}$  in healthy and defoliated Norway spruce in the southern Alps of Italy. Defoliated trees exhibited significantly greater tree-ring  $\delta^{13}\text{C}$  and lower  $\delta^{18}\text{O}$  values than control trees, suggesting that defoliated trees may have increased the photosynthetic capacity of remaining foliage according to the dual isotope model (Scheidegger et al. 2000). Interestingly, the  $\delta^{13}\text{C}$  and  $\delta^{18}\text{O}$  isotope patterns of defoliated trees began 2 years and 1 year, respectively before defoliation. Using the Scheidegger et al. (2000) model, the authors hypothesized that the isotope patterns observed before defoliation were due to reduced  $g_s$ , suggesting defoliated trees may have been responding to drought stress, which likely contributed to the outbreak. The drought-stressed trees may have mobilized stored starch into tree-ring cellulose, known to have greater  $\delta^{13}\text{C}$  values (Brugnoli et al. 1988; Helle and Schleser 2004; Cernusak et al. 2009).

In contrast to the findings of Gori et al. (2014a) and Simard et al. (2008), other studies have not found evidence for compensatory increases in  $A$  as a result of defoliating insects and pathogens. Leavitt and Long (1986) did not observe a tree-ring  $\delta^{13}\text{C}$  signal of SBW outbreak in infested stands of host species white fir (*Abies concolor*) and Douglas-fir (*Pseudotsuga menziesii*) and non-host ponderosa pine (*Pinus ponderosa*). Furthermore, Ellsworth et al. (1994) observed a decline in instantaneous measures of  $A$  and no change in leaf  $\delta^{13}\text{C}$  of sugar maple (*Acer saccharum* Marsh.) heavily defoliated by pear thrips (*Taeniothrips inconsequens* Uzel), a piercing-sucking insect. Artificially defoliated balsam fir (*Abies balsamea* Mill.) saplings exhibited an increase in tree-ring  $\delta^{13}\text{C}$  but the lack of significant correlations among gas exchange parameters ( $A$ ,  $g_s$ ,  $c_i/c_a$ ) and tree-ring  $\delta^{13}\text{C}$  did not support a compensatory increase in  $A$  (Simard et al. 2012). Instead, the authors attributed the increase in tree-ring  $\delta^{13}\text{C}$  to mobilization of stored carbohydrates enriched in  $^{13}\text{C}$  (Brugnoli et al. 1988; Helle and Schleser 2004; Cernusak et al. 2009).

### ***25.3.2 Tree-Ring Stable Isotopes Inform Effects of Climate on Insect and Pathogen Infestation Severity Levels and Host Tree Susceptibility to Infestation***

Climate-induced alterations in host physiology have been shown to both decrease and increase the severity of and susceptibility to insect and pathogen infections. As mentioned earlier, larch budmoth (LBM) defoliates larch in the European Alps, and had occurred with a regular 8–10-year periodicity for at least 1200 years until

the 1980s after which no regular outbreaks have been observed (Baltensweiler et al. 2008). Tree-ring stable isotopes have been used to determine if climate variables may explain why no LBM outbreak has occurred since the 1980s. Because LBM infestation results in needle loss or damaged, dysfunctional needles, no tree-ring cellulose is formed during an outbreak, and the C isotope signature of outbreak years reflects the cellulose formed either before or after defoliation occurs when normally functioning needles have replaced damaged needles in the second half of the growing season (Baltensweiler et al. 2008). Indeed, the tree-ring  $\delta^{13}\text{C}$  in outbreak years appeared to be dominated by latewood formation due to the second flush of needles because  $\delta^{13}\text{C}$  correlated strongly with summer (July–August) temperatures (Kress et al. 2009; Weidner et al. 2010). Cooler summer temperatures were positively related with severe LBM outbreaks, suggesting that the 1980s halt in infestation may have been due to increasing summer temperatures (Kress et al. 2009). This is likely because winters of sufficient duration (120 days below  $2^\circ\text{C}$ ) are required to successfully induce diapause and protect overwintering insects from low temperatures. However, warmer spring and summer temperatures may lead to an early diapause with fewer frost days, leading to egg mortality (Baltensweiler et al. 1977). Additionally, above-average summer temperatures could influence maturation of needles, the main food source for LBM and result in poor food quality, leading to larval and pupal mortality. Both tree-ring  $\delta^{13}\text{C}$  and  $\delta^{18}\text{O}$  were unaffected by LBM but  $\delta^{18}\text{O}$  was strongly correlated with the  $\delta^{18}\text{O}$  of previous winter (December–March) precipitation, consistent with a winter recharge of the soil (Daux et al. 2011). Because of LBM, the potential for larch, a long-lived (850 + years) economically valuable species, to be used to reconstruct climate was questioned. However, strong correlations between climate and the tree-ring stable isotope record and not LBM suggest that the tree-ring stable isotope record of LBM-infected larch can be used for climate reconstructions (Kress et al. 2009; Weidner et al. 2010; Daux et al. 2011). In contrast, tree-ring widths can be used to track LBM outbreaks but potentially not climate, making radial growth unsuitable for climate reconstructions (Kress et al. 2009; Weidner et al. 2010), unless corrections are made and/or comparison with a non-host species is included (e.g. King et al. 2013; Konter et al. 2015; see Sect. 25.3). Comparison of these LBM studies with other studies on defoliating insects highlights that leaf lifespan and phenology may govern whether insect-induced defoliation is recorded in tree-ring stable isotopes (Simard et al. 2008; Gori et al. 2014a) or not (Kress et al. 2009; Weidner et al. 2010). Because deciduous larch refoliates after defoliation, the tree-ring stable isotope record reflects the physiology of the second flush of foliage. In contrast, evergreen species that are defoliated for multiple years may remobilize stored C reserves to maintain function (e.g. Simard et al. 2012) or exhibit a compensatory increase in A (Simard et al. 2008; Gori et al. 2014a), both of which influence tree-ring  $\delta^{13}\text{C}$ .

Tree-ring stable isotopes have also revealed how climate variables such as relative humidity increase the severity of fungal pathogens such as Swiss Needle Cast (SNC). The fruiting bodies (pseudothecia) of the fungus *Phaeocryptopus gaeumannii* (T. Rohde) Petr.) that causes SNC physically occlude stomata, restricting gas exchange and resulting in premature needle loss in host Douglas-fir (*Pseudotsuga menziesii*) (Manter et al. 2000). In spring, spores land on foliage and colonize needles to the

extent that environmental conditions promote germination and hyphal growth into stomata. Warm winter and spring temperatures and spring/summer leaf wetness may facilitate fungal growth and reproduction (Manter et al. 2005; Stone et al. 2008). Saffell et al. (2014) compared tree-ring growth,  $\Delta^{13}\text{C}$ , and  $\delta^{18}\text{O}$  in SNC-infected Douglas-fir treated and not treated with a fungicide to remove SNC to examine whether  $\Delta^{13}\text{C}$  and  $\delta^{18}\text{O}$  can serve as a tool for detecting past SNC infection and the influence of climate on SNC disease severity. Given the pseudothecia-induced restrictions in gas exchange, SNC reduced  $\Delta^{13}\text{C}$  as expected, suggesting that  $\Delta^{13}\text{C}$  can be used to detect past SNC infection. In contrast, tree-ring  $\delta^{18}\text{O}$  did not differ between treated and untreated trees likely because high humidity masked any effect of SNC on O isotope fractionation (see Chapter 10). High humidity can mask O isotope fractionation because high humidity reduces evaporative enrichment of leaf water and vapor exchange with leaf water is high, reducing physiological  $\delta^{18}\text{O}$  signals within the leaf (Barbour and Farquhar 2000). In diseased trees, a significant negative correlation between  $\Delta^{13}\text{C}$  and relative humidity during the spring sporulation period of antecedent years suggested that high humidity, conditions that promoted fungal growth and reproduction, increased SNC disease severity (Saffell et al. 2014). Other favorable climate conditions for the fungus, including warmer winter temperatures at coastal (relatively cool, wet) sites, and increased summer precipitation at inland (relatively warm, dry) sites, are likely to increase SNC disease severity (Lee et al. 2013, 2017).

Tree-ring  $\delta^{13}\text{C}$  and  $\delta^{18}\text{O}$  have revealed in what situations climate-induced stress may have increased susceptibility to insect-induced mortality. Recent increases in temperature and decreases in precipitation in western North America have promoted unprecedented outbreaks of bark beetles (Samman and Logan 2000; Bentz et al. 2009, 2010). Bark beetle outbreaks have affected tens of millions of hectares in western North America since 1990 (Raffa et al. 2008) and have led to widespread forest mortality and economic timber loss (Corbett et al. 2016). Tree-ring growth has been used to identify bark beetle outbreaks because surviving trees experience prolonged periods of release visible in the tree-ring record (e.g. Alfaro et al. 2004). However, tree-ring stable isotopes provide the physiological information needed to determine if drought may predispose host trees to bark beetle-induced mortality (Gaylord et al. 2013). In south central Alaska, Csank et al. (2016) used tree-ring  $\delta^{13}\text{C}$  and  $\delta^{18}\text{O}$  from live and dead trees to examine whether white spruce (*Picea glauca*) killed by spruce bark beetle (*Dendroctonus rufipennis* Kirby) showed greater evidence of drought stress prior to mortality compared to trees that survived the beetle outbreak. Compared to live trees, dead trees exhibited significantly greater correlation coefficients describing relationships between  $\delta^{13}\text{C}$  and spring/summer temperature; however, the isotopic record in dead trees had no correlation with precipitation, whereas in live trees,  $\delta^{18}\text{O}$  was highly correlated with spring precipitation. As a result, the authors inferred that trees that succumbed to beetle attack were more drought-stressed than those that survived. However, the authors could not determine how drought stress contributes to the development of epidemic outbreaks because they could not determine the stable isotope sensitivity to these climate variables among live versus dead. To more robustly test whether drought stress has a role in

allowing incipient spruce bark beetle populations to build toward epidemic outbreak conditions, mixed-effect modeling of tree-ring stable isotopes is useful (Pettit et al. in prep.; Pettit 2018). Pettit et al. (in prep) sampled tree-ring  $\Delta^{13}\text{C}$  from Engelmann spruce (*P. engelmannii*) trees from six stands in montane forests of southern Utah that died either early or late during an outbreak that killed >95% of overstory spruce trees across the region. As expected, tree-ring  $\Delta^{13}\text{C}$  was consistently lower during progressively more severe droughts across stands, but mixed-effect modeling of  $\Delta^{13}\text{C}$  response to summer drought detected no significant differences between early- and late-dying trees. The lack of a difference in  $\Delta^{13}\text{C}$  sensitivity to drought between early- and late-dying trees indicates that incipient spruce beetle populations did not build into an epidemic outbreak by selecting hosts that were more sensitive to drought stress, but rather that warmer growing season temperatures during this time were the most important direct driver of the spruce beetle outbreak.

Another recent study conducted in California, used tree-ring  $\Delta^{13}\text{C}$  and  $\delta^{18}\text{O}$  to investigate whether paired surviving versus dead ponderosa pines (*Pinus ponderosa* Dougl. ex Laws.) killed by western pine beetle (*Dendroctonus brevicomis*) differed in drought sensitivity prior to the outbreak (Keen 2019). The authors found that although drought sensitivity of growth and  $\Delta^{13}\text{C}$  had increased dramatically since 1900, there were no significant differences between surviving and dead trees in climate sensitivity of  $\Delta^{13}\text{C}$  or  $\delta^{18}\text{O}$  in response to temperature, precipitation, and various drought metrics. Surviving trees grew faster than the paired dead trees and much faster than randomly sampled ponderosa pines from the same region, and were located in stands with more conspecific stem basal area. In this case, tree-ring stable isotopes indicated that drought sensitivity had increased about five-fold between 1900 and the initiation of the bark beetle outbreak, but that tree drought sensitivity did not determine local-scale selection of hosts by bark beetles at sites where at least one overstory tree survived. Overall, increases in drought sensitivity preceded the western pine beetle outbreak that killed >95% of overstory ponderosa pines across the region, and surviving overstory ponderosa pines tended to be the fastest growing and more isolated from conspecifics.

The aforementioned studies using tree-ring stable isotopes to investigate the effect of drought on host susceptibility to insect attack highlight an underexplored line of research: determining the relative contributions of drought-induced stomatal closure versus stress-induced shifts in C allocation to the tree-ring  $\delta^{13}\text{C}$  signal. During drought, stomatal closure restricts gas exchange and is reflected by increased tree-ring  $\delta^{13}\text{C}$ . During insect attack, stressed trees may allocate more current year photosynthate to defense and less to growth, and/or allocate more stored photosynthate to tree-ring growth (Kozłowski et al. 1991; Helle and Schleser 2004; Kagawa et al. 2006; Sohn et al. 2014). This can increase tree-ring  $\delta^{13}\text{C}$  due to more stored C, enriched during remobilization from starch, being allocated to tree-ring growth and/or less current year C being allocated to tree-ring growth. More broadly, drought-induced negative water potentials more strictly constrain cell division and expansive growth of plants compared to leaf gas exchange (Hsiao 1973; Muller et al. 2011). This concept was recently demonstrated for stem radial growth and stomatal conductance in isohydric and anisohydric conifer species adapted to an arid region of Utah,

USA (Voelker et al. 2018). The predictable ordering of these processes governing key aspects of C fixation and allocation to growth make it likely that tree-ring isotope signals will be somewhat lagged and muted during droughts that cause trees to cease growth but maintain low but significant levels of photosynthesis. Overall, it can often remain unclear to what extent the tree-ring  $\delta^{13}\text{C}$  signal is driven by drought-induced growth inhibition, drought-induced stomatal closure, defense-induced shifts in C allocation, or a combination of these effects.

### 25.3.3 *Tree-Ring Stable Isotopes Inform Effects of Insect and Pathogen Infestation on Host Tree Sensitivity to Climate*

Insect- and pathogen-induced alterations in host physiology have been shown to both increase and decrease host tree sensitivity to climate variables. Fungal pathogens such as Armillaria root disease (*Armillaria*) and *Heterobasidion parviporum* cause root and butt rot, needle loss, reduced uptake of water and nutrients, and predisposition of trees to drought-induced decline and mortality (Marçais and Bréda 2006; Colangelo et al. 2018). The tree-ring growth,  $\delta^{13}\text{C}$ , and  $\delta^{18}\text{O}$  of *H. parviporum*-infected and uninfected Norway spruce were compared across three different elevation sites (850, 1300, 1900 m) in the eastern Alps of Italy (Gori et al. 2013, 2014b). Infected trees exhibited the greatest reductions in radial growth,  $\delta^{13}\text{C}$ , and  $\delta^{18}\text{O}$  relative to control trees at the low elevation site compared to the higher elevation sites. This suggests that the infection was most severe at low elevation, likely because conditions were less favorable for the fungus at higher elevations (Gori et al. 2013, 2014b). At higher elevation, the growing season is shorter, and temperatures and water availability are also lower, which makes the fungus less aggressive. Other observational and modeling studies have found similar elevational gradients in insect outbreak intensity (Johnson et al. 2010; Peters et al. 2017). The tree-ring stable isotope data suggested that infection induced an increase in  $g_s$  according to the Scheidegger et al. (2000) model (see Chap. 16). Increased  $g_s$  may compensate for reduced foliage observed in infected trees. Radial growth of low elevation infected trees was the most sensitive to drought stress, as shown by a significant correlation between the Palmer Drought Severity Index (PDSI) and infected tree radial growth that was not observed in low elevation control trees nor in infected or control trees at higher elevation sites.

Just as relative humidity was shown to influence SNC severity (Saffell et al. 2014), SNC severity has also been shown to influence Douglas-fir sensitivity to climate in western Oregon (Lee et al. in review). Consistent with Saffell et al. (2014), Lee et al. (in review) found that the coastal site with greater relative humidity exhibited greater SNC severity compared to the inland sites with lower relative humidity. At the inland sites where SNC severity was low,  $\Delta^{13}\text{C}$  and  $\delta^{18}\text{O}$  in Douglas-fir tree-rings were more sensitive to climate variation than to SNC severity. Growth reductions of trees at the inland sites were primarily attributed to stomatal response to high VPD, consistent

with (Barnard et al. 2012). In contrast, at the coastal site where SNC severity was high,  $\Delta^{13}\text{C}$  and  $\delta^{18}\text{O}$  were less variable over time, showing muted and lagged responses to past climate and suggesting a greater reliance on stored carbohydrates. Growth reductions of trees at the coastal site were primarily attributed to a reduction in  $A$  through an SNC-induced loss of foliage. Growth response to high summer VPD was greater in years with high SNC severity than in years with low disease severity (Lee et al. 2017).

Defoliating insects such as pandora moth (*Coloradia pandora* Blake) can modify co-occurring host and non-host tree sensitivity to PDSI for up to two decades after defoliation events. This has been observed in a dry mixed-conifer landscape in central Oregon where old-growth ponderosa pines were defoliated four times by pandora moth for at least 2–6 years per event at local scales, between the 1850s and the 1990s (Voelker et al. 2019). More comprehensive regional information on defoliations extends back over 600 years (Speer et al. 2001). At this site, historic suppression of wildfire has led to increased sensitivity of leaf gas exchange to drought, which has likely made trees more susceptible to insects and pathogens (Keen et al. in prep, Voelker et al. 2019). Compared to the period prior to defoliation, tree-ring  $\Delta^{13}\text{C}$  during and after defoliation was less sensitive to PDSI (Fig. 25.1). This defoliation-induced reduction in drought sensitivity lasted for 15–20 years, with a

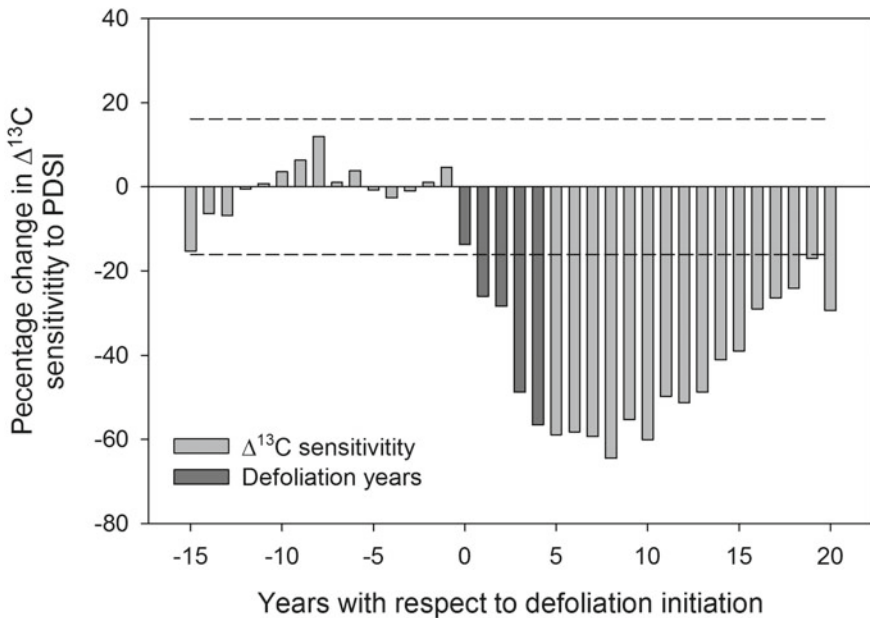


**Fig. 25.1** Percentage change in ponderosa pine tree-ring  $\Delta^{13}\text{C}$  sensitivity to Palmer Drought Severity Index (PDSI) before and after defoliation by pandora moth (*C. pandora*). Dashed lines indicate the percentage change in drought sensitivity that would be considered significantly different than 0 at  $P < 0.01$  ( $\pm 16.16\%$ )

broad peak extending from near the end of the defoliation to about six years thereafter. In Fig. 25.1, both host and non-host trees were included. It is notable that non-host trees were reduced in drought sensitivity to an equal or greater magnitude compared to the host trees (data not shown), suggesting that the greatest effect of defoliation in these dry conifer forests was a reduction in competition for water at the stand-level due to a loss of leaf area and associated  $E$ . This application of tree-ring  $\Delta^{13}\text{C}$  demonstrates that (1) defoliation can affect climate sensitivity of trees for up to two decades, and (2) although no significant changes in absolute  $\Delta^{13}\text{C}$  were detected in host or non-host trees associated with defoliation, if used in a drought reconstruction, tree-ring  $\Delta^{13}\text{C}$  of host or non-host trees would tend to underestimate drought severity for up to twenty years after a defoliation event.

Other tree-ring stable isotope records also have revealed loss of sensitivity to climate variables with increased severity of pathogen infection or insect herbivory. The aspen leaf miner (*Phyllocnistis populiella* Cham.) is responsible for widespread herbivory of trembling aspen since its first recorded outbreak in the early 2000s (Boyd et al. 2019). The aspen leaf miner feeds on leaf epidermal cells during summer months, decreases  $A$ ,  $g_s$ , and growth, and has resulted in increased leaf  $\delta^{13}\text{C}$  due to damaged stomata (Wagner et al. 2008). In contrast to leaf-level measurements of gas exchange and leaf  $\delta^{13}\text{C}$ , under low soil moisture conditions, tree-ring wood  $\delta^{13}\text{C}$  decreased with increasing intensity of leaf mining (Boyd et al. 2019). When leaf mining intensity was low, trees responded as expected to low soil moisture, exhibiting increased tree-ring  $\delta^{13}\text{C}$  and suggesting reduced  $g_s$ . In contrast, when leaf mining was severe, trees did not respond as expected to low soil moisture, exhibiting reduced tree-ring  $\delta^{13}\text{C}$  and suggesting increased  $g_s$  and/or decreased  $A$  relative to any shifts in  $g_s$ . This leaf mining-induced de-coupling of tree-ring  $\delta^{13}\text{C}$ -climate sensitivity may reflect a compensatory response of increased  $g_s$  in remaining leaves due to premature leaf-mining-induced leaf area reductions. Hence, severe leaf mining may override the influence of climate on tree-ring stable isotopes in trembling aspen (Boyd et al. 2019).

An insect-induced reduction in host tree climate sensitivity has also been observed in northern red oak (*Quercus rubra* L. (Fagaceae)) infested with red oak borer, a wood boring insect. "Oak decline" is a widespread phenomenon that is believed to be triggered by a combination of factors including tree age, drought, and soil quality (Manion 1991; Thomas et al. 2002; Crook et al. 2004; Voelker et al. 2008; Gagen et al. 2019). The oak decline episode of the early 2000s in the Ozark forests of central USA was unique because it coincided with drought and red oak borer activity (Muzika and Guyette 2004; Voelker et al. 2008; Haavik et al. 2008). From ~1950–2000, infested trees reduced radial growth more rapidly compared to control trees as red oak borer infestation became severe. However, the tree-ring  $\delta^{13}\text{C}$  signal of infected and healthy trees only diverged during the most advanced stage of infestation when reductions in radial growth were greatest (Haavik et al. 2008; Billings et al. 2016). In both studies, tree-ring  $\delta^{13}\text{C}$  was sensitive to drought early in the study period but not when infestation became severe (Haavik et al. 2008; Billings et al. 2016). This is consistent with the observation that before infestation, trees that



eventually became severely infested exhibited a 20% lower radial growth immediately following a severe drought compared to trees that only became lightly infested. Similar to western hemlock infected with dwarf mistletoe (Marias et al. 2014), it appears that oak can support high levels of wood boring insects for ~17 years without measurable impacts on the tree-ring  $\delta^{13}\text{C}$  record (Haaavik et al. 2008). Oaks stricken by drought-induced dieback have reduced C resources available for defense (sensu Voelker et al. 2008) but increased tissue N concentrations (Billings et al. 2016) after remobilization—both of which would presumably benefit red oak borer fitness. In oaks suffering dieback, live tree crowns (i.e. leaf area) are smaller and made up of more epicormic branches (Voelker et al. 2008). If these tree-level N resources are concentrated in fewer leaves and result in greater leaf-level A, higher tree-ring  $\delta^{13}\text{C}$  would be expected in dying trees. Unexpectedly however, Billings et al. (2016) found that dying trees exhibited lower tree-ring  $\delta^{13}\text{C}$  than healthy trees, which contrasted with the dying trees' greater N concentration than healthy trees. Although dying trees were characterized by greater N concentration, the difference in tree-ring  $\delta^{13}\text{C}$  during later stages of oak decline were apparently more influenced by proportionally greater increases in stomatal conductance as a product of an unbalanced hydraulic system—whereby extensive branch dieback caused large decreases in leaf area and preserved much of the pre-dieback xylem functionality of stems and roots supplying the leaves water. In summary, tree-ring stable isotopes have revealed that infestation by insects and pathogens with diverse impacts on host physiology can increase or decrease the sensitivity of host trees to climate.

## 25.4 Considering Insect and Pathogen Influences on Tree-Ring Stable Isotopes in Future Work

Because tree-ring stable isotopes reflect both the environment and tree physiological responses to the environment, they provide invaluable insights about past climate and physiology, yet can be complicated to interpret (Barbour and Song 2014). The fact that the effect of insects and pathogens on host physiology can be recorded in tree-rings and potentially mask climate signals (e.g. Simard et al. 2008; Marias et al. 2014; Saffell et al. 2014) and also that climate signals can potentially mask insect and pathogen impacts, needs to be considered when using the tree-ring record to reconstruct past climate, climate-growth relationships, and physiological responses to the environment. Moreover, the potential for pests or pathogens to affect both hosts or non-hosts may not be detectable in absolute isotopic values but only in isotopic sensitivity to climate (Fig. 25.1). Insect/pathogen impacts are not always reflected in tree-ring stable isotopes (Kress et al. 2009) and, with proper consideration, tree-ring stable isotopes can often still be useful for reconstruction of climate and physiology. Here, we highlight the importance of considering the limitations to interpreting tree-ring stable isotope signals and ways to address these limitations in future research studies.

The effect of an insect or pathogen can be significant enough to shift tree-ring isotope signals and can confound interpretations of tree-rings to reconstruct climate if it is unknown whether the tree was infected or not. Paleoclimate studies that use dated tree-rings from dead or sub-fossil logs or buildings may in some cases include trees infected with a pathogen or insect (Krause 1997). For example, if the tree-ring  $\Delta^{13}\text{C}$  record of Pandora moth-defoliated Douglas-fir were to have been used to reconstruct climate, one could gain the erroneous inference that climate variability was relatively quiescent for one to two decades after each defoliation event (e.g., Fig. 25.1). To address this issue, corrections can be made to the tree-ring record to properly reconstruct climate if insect or pathogen presence is known. For example, growth rings during LBM events have been removed and replaced with variance-adjusted values obtained from unaffected rings (Esper et al. 2006; Büntgen et al. 2006). Experimental study design can also be used to reduce the confounding effects of climate and insects/pathogens on tree-ring stable isotopes. Studies can be designed where uninfected and infected sets of trees are exposed to the same environmental conditions by sampling trees in a relatively small area (e.g. Marias et al. 2014). Another approach to separate the effect of climate and insects/pathogens is to also sample and compare the tree-ring record of a non-host species that grows in the same area or region to identify climate shifts not associated with insect/pathogen physiological impacts (e.g. Simard et al. 2008; King et al. 2013; Saffell et al. 2014; Konter et al. 2015).

Insect and pathogen influences also challenge traditional isotope theory. For example, Marias et al. (2014) found that the differences in tree-ring  $\delta^{18}\text{O}$  between uninfected and infected trees could not be explained by climate or  $g_s$  alone—the traditional interpretations using the dual isotope approach (Scheidegger et al. 2000). The dual isotope approach does not necessarily incorporate parameters related to leaf anatomy such as  $g_m$  and  $L$ , which appeared to have significantly affected tree-ring  $\delta^{18}\text{O}$  in the study of Marias et al. (2014). Therefore, future research using the dual isotope approach must properly account for its assumptions and consider its limitations, especially in potential insect- and pathogen-infected systems (Roden and Siegwolf 2012).

Research on insect and pathogen effects on tree-ring stable isotopes also sheds light on variation in isotope signals. The competing influences of climate and plant physiological responses to environment or insects and pathogens on tree-ring cellulose may be responsible for discrepancies among studies in how and if insect and pathogen influences are recorded in tree-ring cellulose. For example, defoliation by SBW has been recorded in tree-ring stable isotopes in some studies (Simard et al. 2012), but not in others (Leavitt and Long 1986). This variability in how and if insect/pathogen impacts are recorded in the tree-ring stable isotope record in different systems makes it critical to consider the potential effect of insects and pathogens on host physiology and the tree-ring stable isotope record when using tree-rings to reconstruct past climate and physiology. Insect- and pathogen-induced reductions in radial growth also contribute to discrepancies among studies because many pathogens result in narrow or missing rings, inhibiting the development of cellulose in which C and O stable isotopes can be recorded. In addition, insects and

pathogens, and other stressors can increase the reliance on stored C reserves which would dampen or mute the tree-ring record to the actual climate or physiological responses during any particular year (Kozłowski et al. 1991; Helle and Schleser 2004; Kagawa et al. 2006; Sohn et al. 2014). Other factors that contribute to the variability in results across insect- and pathogen-infested systems include the intensity, frequency, and distribution of the infestation or disturbance, and whether the history of infestation is known or unknown, which varies by type of insect/pathogen. It is clear that when designing experiments and when interpreting tree-ring stable isotope chronologies to reconstruct past climate or physiology, consideration of insect and pathogen impacts is as essential as considering the more well-studied effects of tree age and size on tree-ring  $\delta^{13}\text{C}$  and  $\delta^{18}\text{O}$  (McDowell et al. 2011; Klesse et al. 2018).

Despite challenges to interpreting tree-ring stable isotope signatures, their application to examine the physiological impacts of insects and pathogens can provide valuable information to forest managers on tree responses to insects and pathogens in light of intensifying outbreaks due to climate change. Tree-ring stable isotopes enable examination of spatial and temporal variation in host-insect/pathogen dynamics to inform management plans for the future and in diverse systems. For example, findings that insect/pathogen effects are more severe and result in increased drought stress at low elevation compared to higher elevations highlights that the insect or pathogen could become more aggressive at currently colder high elevation sites as climates become warmer (e.g. Gori et al. 2014b).

## 25.5 Conclusion

Tree-ring stable isotope analyses are a powerful tool because they reveal long-term physiological effects of insects and pathogens on the host tree that would not otherwise be observable in ring widths alone. More detailed information on the impacts of insects and pathogens on host physiology and the bidirectional interacting effects of insects/pathogens and climate on host physiology should increasingly be leveraged to improve predictions of future outbreaks and forest mortality events that can guide forest management. However, interpretation of tree-ring stable isotope ratios may not be straightforward given that they record both climate and physiological responses to abiotic and biotic environmental factors. Therefore, the potential for insect/pathogen impacts on host physiology should be critically evaluated when designing experiments or research that employs tree-ring stable isotopes to reconstruct past plant physiological responses or climate variability.

## References

- Acharya BR, Assmann SM (2009) Hormone interactions in stomatal function. *Plant Mol Biol* 69:451–462
- Alfaro RI, Campbell RA, Vera P, Hawkes BC, Shore TL (2004) Dendroecological reconstruction of mountain pine beetle outbreaks in the Chilcotin Plateau of British Columbia. <https://cfs.nrcan.gc.ca/publications?id=25053>. Accessed 23 Jan 2019
- Allen CD, Macalady AK, Chenchouni H, Bachelet D, McDowell N, Vennetier M, Kitzberger T, Rigling A, Breshears DD, Hogg ET (2010) A global overview of drought and heat-induced tree mortality reveals emerging climate change risks for forests. *For Ecol Manag* 259:660–684
- Amman GD, McGregor MD, Dolph Jr. RE (1985) Mountain Pine Beetle FIDL 2. <https://www.barbketles.org/mountain/fidl2.htm>. Accessed 7 June 2019
- Anderegg WRL, Hicke JA, Fisher RA, Allen CD, Aukema J, Bentz B, Hood S, Lichstein JW, Macalady AK, McDowell N, Pan Y, Raffa K, Sala A, Shaw JD, Stephenson NL, Tague C, Zeppel M (2015) Tree mortality from drought, insects, and their interactions in a changing climate. *New Phytol* 208:674–683
- Baltensweiler W (1993) Why the larch bud-moth cycle collapsed in the subalpine larch-cembra pine forests in the year 1990 for the first time since 1850. *Oecologia* 94:62–66
- Baltensweiler W, Benz G, Bovey P, Delucchi V (1977) Dynamics of larch bud moth populations. *Annu Rev Entomol* 22:79–100
- Baltensweiler W, Weber UM, Cherubini P (2008) Tracing the influence of larch-bud-moth insect outbreaks and weather conditions on larch tree-ring growth in Engadine (Switzerland). *Oikos* 117:161–172
- Barbour MM (2007) Stable oxygen isotope composition of plant tissue: a review. *Funct Plant Biol* 34:83–94
- Barbour MM, Farquhar GD (2000) Relative humidity- and ABA-induced variation in carbon and oxygen isotope ratios of cotton leaves. *Plant Cell Environ* 23:473–485
- Barbour MM, Song X (2014) Do tree-ring stable isotope compositions faithfully record tree carbon/water dynamics? *Tree Physiol* 34:792–795
- Barnard HR, Brooks JR, Bond BJ (2012) Applying the dual-isotope conceptual model to interpret physiological trends under uncontrolled conditions. *Tree Physiol* 32:1183–1198
- Bentz B, Logan J, MacMahon J, Allen CD, Ayres M, Berg E, Carroll A, Hansen M, Hicke J, Joyce L (2009) Bark beetle outbreaks in western North America: causes and consequences
- Bentz BJ, Regniere J, Fettig CJ, Hansen EM, Hayes JL, Hicke JA, Kelsey RG, Negron JF, Seybold SJ (2010) Climate change and bark beetles of the western United States and Canada: direct and indirect effects. *Biosci* 60:602–613
- Billings SA, Boone AS, Stephen FM (2016) Tree-ring  $\delta^{13}\text{C}$  and  $\delta^{18}\text{O}$ , leaf  $\delta^{13}\text{C}$  and wood and leaf N status demonstrate tree growth strategies and predict susceptibility to disturbance. *Tree Physiol* 36:576–588
- Blais J (1958) Effects of defoliation by spruce budworm (*Choristoneura fumiferana* Clem.) on radial growth at breast height of balsam fir (*Abies balsamea* (L.) Mill.) and white spruce (*Picea glauca* (Moench) Voss.). *For Chron* 34:39–47
- Boyd MA, Berner LT, Doak P, Goetz S, Rogers B, Wagner D, Walker X, Mack MC (2019) Impacts of climate and insect herbivory on productivity and physiology of trembling aspen (*Populus tremuloides*) in Alaskan boreal forests. *Environ Res Lett*. <https://doi.org/10.1088/1748-9326/ab215f>. Accessed 20 May 2019
- Brugnoli E, Hubick KT, von Caemmerer S, Wong SC, Farquhar GD (1988) Correlation between the carbon isotope discrimination in leaf starch and sugars of C3 plants and the ratio of intercellular and atmospheric partial pressures of carbon dioxide. *Plant Physiol* 88:1418–1424
- Büntgen U, Frank DC, Nievergelt D, Esper J (2006) Summer temperature variations in the European Alps, AD 755–2004. *J Clim* 19:5606–5623
- Castello JD, Leopold DJ, Smallidge PJ (1995) Pathogens, patterns, and processes in forest ecosystems. *Bioscience* 45:16–24

- Cernusak LA, English NB (2015) Beyond tree-ring widths: stable isotopes sharpen the focus on climate responses of temperate forest trees. *Tree Physiol* 35:1–3
- Cernusak LA, Pate J, Farquhar GD (2004) Oxygen and carbon isotope composition of parasitic plants and their hosts in southwestern Australia. *Oecologia* 139:199–213
- Cernusak LA, Tcherkez G, Keitel C, Cornwell WK, Santiago LS, Knohl A, Barbour MM, Williams DG, Reich PB, Ellsworth DS, Dawson TE, Griffiths HG, Farquhar GD, Wright IJ (2009) Why are non-photosynthetic tissues generally  $^{13}\text{C}$  enriched compared with leaves in  $\text{C}_3$  plants? Review and synthesis of current hypotheses. *Funct Plant Biol* 36:199–213
- Clark KL, Skowronski N, Hom J (2010) Invasive insects impact forest carbon dynamics. *Glob Change Biol* 16:88–101
- Colangelo M, Camarero JJ, Borghetti M, Gentilesca T, Oliva J, Redondo M-A, Ripullone F (2018) Drought and phytophthora are associated with the decline of Oak species in Southern Italy. *Front Plant Sci*. <https://doi.org/10.3389/fpls.2018.01595/full#h4>. Accessed 7 Jan 2019
- Corbett LJ, Withey P, Lantz VA, Ochuodho TO (2016) The economic impact of the mountain pine beetle infestation in British Columbia: provincial estimates from a CGE analysis. *For Int J For Res* 89:100–105
- Crook D, Stephen F, Fierke M, Kinney D, Silisbury V (2004) Biology and Sampling of Red Oak Borer Populations in the Ozark Mountains of Arkansas. Gen Tech Rep SRS-73 Asheville NC US Department of agriculture, forest service, southern research station, pp 223–228 <https://www.fs.usda.gov/treesearch/pubs/6549>. Accessed 7 June 2019
- Csank AZ, Miller AE, Sherriff RL, Berg EE, Welker JM (2016) Tree-ring isotopes reveal drought sensitivity in trees killed by spruce beetle outbreaks in south-central Alaska. *Ecol Appl* 26:2001–2020
- Daux V, Edouard JL, Masson-Delmotte V, Stievenard M, Hoffmann G, Pierre M, Mestre O, Danis PA, Guibal F (2011) Can climate variations be inferred from tree-ring parameters and stable isotopes from *Larix decidua*? Juvenile effects, budmoth outbreaks, and divergence issue. *Earth Planet Sci Lett* 309:221–233
- Davies PJ (2010) The plant hormones: their nature, occurrence, and functions. In: Davies PJ (ed) *Plant hormones: biosynthesis, signal transduction, action!* Springer Netherlands, Dordrecht, pp 1–15. [https://doi.org/10.1007/978-1-4020-2686-7\\_1](https://doi.org/10.1007/978-1-4020-2686-7_1). Accessed 4 June 2019
- Dysthe JC, Bracewell R, Six DL (2015) Temperature effects on growth of fungal symbionts of the western pine beetle, *Dendroctonus brevicomis*. *Fungal Ecol* 17:62–68
- Ellsworth D, Tyree M, Parker B, Skinner M (1994) Photosynthesis and water-use efficiency of sugar maple (*Acer saccharum*) in relation to pear thrips defoliation. *Tree Physiol* 14:619–632
- Esper J, Büntgen U, Frank DC, Nievergelt D, Liebholt A (2006) 1200 years of regular outbreaks in alpine insects. *Proc R Soc B Biol Sci* 274:671–679
- Fettig CJ, Klepzig KD, Billings RF, Munson AS, Nebeker TE, Negrón JF, Nowak JT (2007) The effectiveness of vegetation management practices for prevention and control of bark beetle infestations in coniferous forests of the western and southern United States. *For Ecol Manag* 238:24–53
- Filip GM (1999) Ecology, identification, and management of forest root diseases in Oregon
- Flanagan LB, Marshall JD, Ehleringer JR (1993) Photosynthetic gas exchange and the stable isotope composition of leaf water: comparison of a xylem-tapping mistletoe and its host. *Plant Cell Environ* 16:623–631
- Fritts HC (1971) Dendroclimatology and dendroecology. *Quat Res* 1:419–449
- Fritts HC, Swetnam TW (1989) Dendroecology: a tool for evaluating variations in past and present forest environments. In: Begon M, Fitter AH, Ford ED, MacFadyen A (eds) *Advances in ecological research*. Academic Press, pp 111–188. <http://www.sciencedirect.com/science/article/pii/S0065250408601580>. Accessed 7 Oct 2019
- Gagen M, Matthews N, Denman S, Bridge M, Peace A, Pike R, Young G (2019) The tree ring growth histories of UK native oaks as a tool for investigating chronic oak decline: an example from the forest of dean. *Dendrochronologia* 55:50–59

- Galiano L, Martínez-Vilalta J, Lloret F (2011) Carbon reserves and canopy defoliation determine the recovery of Scots pine 4 yr after a drought episode. *New Phytol* 190:750–759
- Gaylord ML, Kolb TE, Pockman WT, Plaut JA, Yezzer EA, Macalady AK, Pangle RE, McDowell NG (2013) Drought predisposes piñon–juniper woodlands to insect attacks and mortality. *New Phytol* 198:567–578
- Geils B, Hawksworth F (2002) Damage, effects, and importance of dwarf mistletoes. Geils Brian W Cibrián Tovar Jose Moody Benjamin Tech Coords Mistletoes North Am Conifers Gen Tech Rep RMRS-GTR-98 Ogden UT US Department of agriculture, forest service rocky mountain research station, pp 57–65 98
- Glatzel G, Geils BW (2009) Mistletoe ecophysiology: host-parasite interactions. *Bot* 87:10–15
- Gori Y, Camin F, Porta NL, Carrer M, Battisti A (2014) Tree rings and stable isotopes reveal the tree-history prior to insect defoliation on Norway spruce (*Picea abies* (L.) Karst.). *For Ecol Manag* 319:99–106
- Gori Y, Cherubini P, Camin F, La Porta N (2013) Fungal root pathogen (*Heterobasidion parviporum*) increases drought stress in Norway spruce stand at low elevation in the Alps. *Eur J For Res* 132:607–619
- Gori Y, Porta NL, Camin F (2014) Tree-ring isotope analysis of Norway spruce suffering from long-term infection by the pathogenic white-rot fungus *Heterobasidion parviporum*. *For Pathol* 44:160–162
- Haavik LJ, Stephen FM, Fierke MK, Salisbury VB, Leavitt SW, Billings SA (2008) Dendrochronological parameters of northern red oak (*Quercus rubra* L. (Fagaceae)) infested with red oak borer (*Enaphalodes rufulus* (Haldeman) (Coleoptera: Cerambycidae)). *For Ecol Manag* 255:1501–1509
- Hartmann H, Moura CF, Anderegg WRL, Ruehr NK, Salmon Y, Allen CD, Arndt SK, Breshears DD, Davi H, Galbraith D, Ruthrof KX, Wunder J, Adams HD, Bloemen J, Cailleret M, Cobb R, Gessler A, Grams TEE, Jansen S, Kautz M, Lloret F, O'Brien M (2018) Research frontiers for improving our understanding of drought-induced tree and forest mortality. *New Phytol* 218:15–28
- Hawksworth FG, Wiens D (1998) Dwarf mistletoes: biology, pathology, and systematics. Diane Publishing
- Helle G, Schleser GH (2004) Beyond CO<sub>2</sub>-fixation by Rubisco—an interpretation of <sup>13</sup>C/<sup>12</sup>C variations in tree rings from novel intra-seasonal studies on broad-leaf trees. *Plant Cell Environ* 27:367–380
- Hillbrand RM, Hacke UG, Lieffers VJ (2019) Defoliation constrains xylem and phloem functionality. *Tree Physiol* 39:1099–1108
- Hsiao TC (1973) Plant responses to water stress. *Annu Rev Plant Physiol* 24:519–570
- Hubbart JA, Guyette R, Muzika R-M (2016) More than drought: precipitation variance, excessive wetness, pathogens and the future of the western edge of the eastern deciduous forest. *Sci Total Environ* 566–567:463–467
- Johnson DM, Büntgen U, Frank DC, Kausrud K, Haynes KJ, Liebhold AM, Esper J, Stenseth NC (2010) Climatic warming disrupts recurrent Alpine insect outbreaks. *Proc Natl Acad Sci* 107:20576–20581
- Kagawa A, Sugimoto A, Maximov TC (2006) Seasonal course of translocation, storage and remobilization of <sup>13</sup>C pulse-labeled photoassimilate in naturally growing *Larix gmelinii* saplings. *New Phytol* 171:793–804
- Keen R (2019) Using tree-ring growth and stable isotopes to explore ponderosa pine ecophysiological responses to climate variability and the 2012–2015 California drought. *Grad Theses Diss.* <https://digitalcommons.usu.edu/etd/7511>
- Keen R, Voelker S, Wang S, Bentz B, Goulden M, Stil C, Dawson T, Dangerfield C, Ehleringer J (in prep.) Increasing drought sensitivity as a precursor to widespread tree mortality during the 2012–2015 California drought
- King GM, Gugerli F, Fonti P, Frank DC (2013) Tree growth response along an elevational gradient: climate or genetics? *Oecologia* 173:1587–1600

- Klesse S, Weigt R, Treydte K, Saurer M, Schmid L, Siegwolf RTW, Frank DC (2018) Oxygen isotopes in tree rings are less sensitive to changes in tree size and relative canopy position than carbon isotopes. *Plant Cell Environ* 41:2899–2914
- Konter O, Esper J, Liebhold A, Kyncl T, Schneider L, Dühthorn E, Buntgen U (2015) Tree-ring evidence for the historical absence of cyclic larch budmoth outbreaks in the Tatra Mountains. *Trees* 293 809–814
- Kozłowski TT (1969) Tree physiology and forest pests. *J For* 67:118–123
- Kozłowski TT, Kramer PJ, Pallardy SG (1991) The physiological ecology of woody plants. *Tree Physiol* 8:213–213
- Krause C (1997) The use of dendrochronological material from buildings to get information about past spruce budworm outbreaks. *Can J For Res* 27:69–75
- Kress A, Saurer M, Büntgen U, Treydte KS, Bugmann H, Siegwolf RTW (2009) Summer temperature dependency of larch budmoth outbreaks revealed by Alpine tree-ring isotope chronologies. *Oecologia* 160:353–365
- Lavigne M, Little C, Major J (2001) Increasing the sink: source balance enhances photosynthetic rate of 1-year-old balsam fir foliage by increasing allocation of mineral nutrients. *Tree Physiol* 21:417–426
- Leavitt S, Long A (1986) Influence of site disturbance on  $\delta^{13}\text{C}$  isotopic time series from tree rings. In: *Proceedings of the international symposium of ecological aspects of tree-ring analysis*, Tarrytown, New York, pp 119–129
- Lee EH, Beedlow PA, Brooks JR, Tingey DT, Wickham C, Rugh W (in review) Carbon and oxygen isotopes in Douglas-fir tree-rings respond to climate and forest disturbances in western Oregon, USA
- Lee EH, Beedlow PA, Waschmann RS, Burdick CA, Shaw DC (2013) Tree-ring analysis of the fungal disease Swiss needle cast in western Oregon coastal forests. *Can J For Res* 43:677–690
- Lee EH, Beedlow PA, Waschmann RS, Tingey DT, Cline S, Bollman M, Wickham C, Carlile C (2017) Regional patterns of increasing Swiss needle cast impacts on Douglas-fir growth with warming temperatures. *Ecol Evol* 7:11167–11196
- Little C, Lavigne M, Ostaff D (2003) Impact of old foliage removal, simulating defoliation by the balsam fir sawfly, on balsam fir tree growth and photosynthesis of current-year shoots. *For Ecol Manag* 186:261–269
- Logan BA, Huhn ER, Tissue DT (2002) Photosynthetic characteristics of Eastern dwarf mistletoe (*Arceuthobium pusillum* Peck) and its effects on the needles of host white spruce (*Picea glauca* [Moench] Voss). *Plant Biol* 4:740–745
- Logan BA, Reblin JS, Zonana DM, Dunlavey RF, Hricko CR, Hall AW, Schmiege SC, Butschek RA, Duran KL, Emery RJN, Kurepin LV, Lewis JD, Pharis RP, Phillips NG, Tissue DT (2013) Impact of eastern dwarf mistletoe (*Arceuthobium pusillum*) on host white spruce (*Picea glauca*) development, growth and performance across multiple scales. *Physiol Plant* 147:502–513
- Lynch AM (2012) What tree-ring reconstruction tells us about conifer defoliator outbreaks. In: Barbosa Pedro, Letourneau, Deborah K, Agrawal Anurag (eds) *Insect outbreaks revisit Hoboken* NJ Blackwell Publ Ltd., pp 126–154
- Manion PD (1991) *Tree disease concepts*. Prentice-Hall
- Manter DK, Bond BJ, Kavanagh KL, Rosso PH, Filip GM (2000) Pseudothecia of Swiss needle cast fungus, *Phaeocryptopus gaemannii*, physically block stomata of Douglas fir, reducing  $\text{CO}_2$  assimilation. *New Phytol* 148:481–491
- Manter DK, Reeser PW, Stone JK (2005) A climate-based model for predicting geographic variation in Swiss needle cast severity in the Oregon coast range. *Phytopathol* 95:1256–1265
- Marçais B, Bréda N (2006) Role of an opportunistic pathogen in the decline of stressed oak trees. *J Ecol* 94:1214–1223
- Marias DE, Meinzer FC, Woodruff DR, Shaw DC, Voelker SL, Brooks JR, Lachenbruch B, Falk K, McKay J (2014) Impacts of dwarf mistletoe on the physiology of host *Tsuga heterophylla* trees as recorded in tree-ring C and O stable isotopes. *Tree Physiol* 34:595–607

- Marshall JD, Dawson TE, Ehleringer JR (1994) Integrated nitrogen, carbon, and water relations of a xylem-tapping mistletoe following nitrogen fertilization of the host. *Oecologia* 100:430–438
- Mathiasen RL, Nickrent DL, Shaw DC, Watson DM (2008) Mistletoes: pathology, systematics, ecology, and management. *Plant Dis* 92:988–1006
- Mayfield Iii AE, Allen DC, Briggs RD (2005) Radial growth impact of pine false webworm defoliation on eastern white pine. *Can J Forest Res* 35(5):1071–1086 <https://doi.org/10.1139/x05-040>
- McDowell NG, Bond BJ, Dickman LT, Ryan MG, Whitehead D (2011) Relationships between tree height and carbon isotope discrimination. In: Size-and age-related changes in tree structure and function. Springer, pp 255–286
- McKellar RC, Wolfe AP, Karlis M, Ralf T, Engel MS, Tao C, Arturo S-A (2011) Insect outbreaks produce distinctive carbon isotope signatures in defensive resins and fossiliferous ambers. *Proc R Soc B Biol Sci* 278:3219–3224
- Meinzer F, Woodruff D, Shaw D (2004) Integrated responses of hydraulic architecture, water and carbon relations of western hemlock to dwarf mistletoe infection. *Plant Cell Environ* 27:937–946
- Miller LK, Werner RA (1987) Cold-hardiness of adult and larval spruce beetles *Dendroctonus rufipennis* (Kirby) in interior Alaska. *Can J Zool* 65:2927–2930
- Mittelheuser CJ, Van Steveninck R (1969) Stomatal closure and inhibition of transpiration induced by (RS)-abscisic acid. *Nature* 221:281
- Mok MC (1994) Cytokinins and plant development. In: Cytokinins chemistry activity and function. CRC Press Boca Raton, pp 155–166
- Muller B, Pantin F, Génard M, Turc O, Freixes S, Piques M, Gibon Y (2011) Water deficits uncouple growth from photosynthesis, increase C content, and modify the relationships between C and growth in sink organs. *J Exp Bot* 62:1715–1729
- Muzika R-M, Guyette RP (2004) A dendrochronological analysis of red oak borer abundance. Gen Tech Rep SRS-73 Asheville NC US department agriculture forest service southern research station, pp 102–105 <https://www.fs.usda.gov/treearch/pubs/6505>. Accessed 2 July 2019
- Nickrent DL, García MA, Martín MP, Mathiasen RL (2004) A phylogeny of all species of *Arceuthobium* (Viscaceae) using nuclear and chloroplast DNA sequences. *Am J Bot* 91:125–138
- Parke JL, Oh E, Voelker S, Hansen EM, Buckles G, Lachenbruch B (2007) *Phytophthora ramorum* colonizes tanoak xylem and is associated with reduced stem water transport. *Phytopathol* 97:1558–1567
- Peters RL, Klesse S, Fonti P, Frank DC (2017) Contribution of climate vs. larch budmoth outbreaks in regulating biomass accumulation in high-elevation forests. *For Ecol Manag* 401:147–158
- Pettit J (2018) Engelmann spruce survival and regeneration after an epidemic spruce beetle outbreak on the Markagunt plateau in southern Utah. Grad Theses Diss. <https://digitalcommons.usu.edu/etd/7199>
- Pettit J, Voelker S, DeRose R, Burton J (in prep.) Tree-ring isodemography reveals epidemic spruce beetle outbreak is not driven by drought stress.
- Puri E, Hoch G, Körner C (2015) Defoliation reduces growth but not carbon reserves in Mediterranean *Pinus pinaster* trees. *Trees* 29:1187–1196
- Raffa KF, Aukema BH, Bentz BJ, Carroll AL, Hicke JA, Turner MG, Romme WH (2008) Cross-scale drivers of natural disturbances prone to anthropogenic amplification: the dynamics of bark beetle eruptions. *Bioscience* 58:501–517
- Reblin JS, Logan BA, Tissue DT (2006) Impact of eastern dwarf mistletoe (*Arceuthobium pusillum*) infection on the needles of red spruce (*Picea rubens*) and white spruce (*Picea glauca*): oxygen exchange, morphology and composition. *Tree Physiol* 26:1325–1332
- Reich PB, Walters MB, Krause SC, Vanderklein DW, Raffa KF, Tabone T (1993) Growth, nutrition and gas exchange of *Pinus resinosa* following artificial defoliation. *Trees* 7:67–77
- Roden J, Kahmen A, Buchmann N, Siegwolf R (2015) The enigma of effective path length for  $^{18}\text{O}$  enrichment in leaf water of conifers. *Plant Cell Environ* 38:2551–2565
- Roden J, Siegwolf R (2012) Is the dual-isotope conceptual model fully operational? *Tree Physiol* 32:1179–1182



- Saffell BJ, Meinzer FC, Voelker SL, Shaw DC, Brooks JR, Lachenbruch B, McKay J (2014) Tree-ring stable isotopes record the impact of a foliar fungal pathogen on CO<sub>2</sub> assimilation and growth in Douglas-fir. *Plant Cell Environ* 37:1536–1547
- Sala A, Carey EV, Callaway RM (2001) Dwarf mistletoe affects whole-tree water relations of Douglas fir and western larch primarily through changes in leaf to sapwood ratios. *Oecologia* 126:42–52
- Samman S, Logan J (2000) Assessment and response to bark beetle outbreaks in the Rocky Mountain area. Gen Tech Rep RMRS-GTR-62 Ogden UT US Department agriculture forest service Rocky mountain research station, pp 46 <https://www.fs.usda.gov/treearch/pubs/4570> Accessed 7 June 2019
- Scheidegger Y, Saurer M, Bahn M, Siegwolf R (2000) Linking stable oxygen and carbon isotopes with stomatal conductance and photosynthetic capacity: a conceptual model. *Oecologia* 125:350–357
- Simard S, Elhani S, Morin H, Krause C, Cherubini P (2008) Carbon and oxygen stable isotopes from tree-rings to identify spruce budworm outbreaks in the boreal forest of Québec. *Chem Geol* 252:80–87
- Simard S, Morin H, Krause C, Buhay WM, Treydte K (2012) Tree-ring widths and isotopes of artificially defoliated balsam firs: a simulation of spruce budworm outbreaks in Eastern Canada. *Environ Exp Bot* 81:44–54
- Sohn JA, Brooks JR, Bauhus J, Kohler M, Kolb TE, McDowell NG (2014) Unthinned slow-growing ponderosa pine (*Pinus ponderosa*) trees contain muted isotopic signals in tree rings as compared to thinned trees. *Trees* 28:1035–1051
- Speer JH, Swetnam TW, Wickman BE, Youngblood A (2001) Changes in Pandora moth outbreak dynamics during the past 622 years. *Ecol* 82:679–697
- Stone JK, Capitano BR, Kerrigan JL (2008) The histopathology of *Phaeocryptopus gaeumannii* on Douglas-fir needles. *Mycologia* 100:431–444
- Swetnam TW, Thompson MA, Sutherland EK (1985) Using dendrochronology to measure radial growth of defoliated trees. US Department of agriculture, forest service, cooperative state research service.
- Thomas FM, Blank R, Hartmann G (2002) Abiotic and biotic factors and their interactions as causes of oak decline in Central Europe. *For Pathol* 32:277–307
- Ullmann I, Lange OL, Ziegler H, Ehleringer J, Schulze E-D, Cowan IR (1985) Diurnal courses of leaf conductance and transpiration of mistletoes and their hosts in Central Australia. *Oecologia* 67:577–587
- Vejpustková M, Holuša J (2006) Impact of defoliation caused by the sawfly *Cephalcia lariciphila* (Hymenoptera: Pamphilidae) on radial growth of larch (*Larix decidua* Mill.). *Eur J For Res* 125:391–396
- Voelker SL, DeRose RJ, Bekker MF, Sriladda C, Leksungnoen N, Kjelgren RK (2018) Anisohydric water use behavior links growing season evaporative demand to ring-width increment in conifers from summer-dry environments. *Trees* 32:735–749
- Voelker SL, Merschel AG, Meinzer FC, Ulrich DEM, Spies TA, Still CJ (2019) Fire deficits have increased drought sensitivity in dry conifer forests: fire frequency and tree-ring carbon isotope evidence from Central Oregon. *Glob Change Biol* 25:1247–1262
- Voelker SL, Muzika R-M, Guyette RP (2008) Individual tree and stand level influences on the growth, vigor, and decline of red oaks in the Ozarks. *For Sci* 54:8–20
- Wagner D, DeFoliart L, Doak P, Schneiderheinze J (2008) Impact of epidermal leaf mining by the aspen leaf miner (*Phyllocnistis populiella*) on the growth, physiology, and leaf longevity of quaking aspen. *Oecologia* 157:259–267
- Waring RH, Pitman GB (1985) Modifying lodgepole pine stands to change susceptibility to mountain pine beetle attack. *Ecol* 66:889–897
- Weidner K, Heinrich I, Helle G, Löffler J, Neuwirth B, Schleser GH, Vos H (2010) Consequences of larch budmoth outbreaks on the climatic significance of ring width and stable isotopes of larch. *Trees* 24:399–409

- Wiley E, Huepenbecker S, Casper BB, Helliker BR (2013) The effects of defoliation on carbon allocation: can carbon limitation reduce growth in favour of storage? *Tree Physiol* 33:1216–1228
- Zweifel R, Bangerter S, Rigling A, Sterck FJ (2012) Pine and mistletoes: how to live with a leak in the water flow and storage system? *J Exp Bot* 63:2565–2578
- Zweifel R, Sterck F (2018) A conceptual tree model explaining legacy effects on stem growth. *Front For Glob Change* 1. <https://doi.org/10.3389/ffgc.2018.00009/full> Accessed 17 Oct 2019

**Open Access** This chapter is licensed under the terms of the Creative Commons Attribution 4.0 International License (<http://creativecommons.org/licenses/by/4.0/>), which permits use, sharing, adaptation, distribution and reproduction in any medium or format, as long as you give appropriate credit to the original author(s) and the source, provide a link to the Creative Commons license and indicate if changes were made.

The images or other third party material in this chapter are included in the chapter's Creative Commons license, unless indicated otherwise in a credit line to the material. If material is not included in the chapter's Creative Commons license and your intended use is not permitted by statutory regulation or exceeds the permitted use, you will need to obtain permission directly from the copyright holder.



# Chapter 26

## Process-Based Ecophysiological Models of Tree-Ring Stable Isotopes



Liang Wei, John D. Marshall, and J. Renée Brooks

**Abstract** Tree-ring stable isotopes can be used to parameterize process-based models by providing long-term data on tree physiological processes on annual or finer time steps. They can also be used to test process-based ecophysiological models for the assumptions, hypotheses, and simplifications embedded within them. However, numerous physiological and biophysical processes influence the stable carbon ( $\delta^{13}\text{C}$ ) and oxygen ( $\delta^{18}\text{O}$ ) isotopes in tree rings, so the models must simplify how they represent some of these processes to be useful. Which simplifications are appropriate depends on the application to which the model is applied. Fortunately, water and carbon fluxes represented in process-based models often have strong isotopic effects that are recorded in tree-ring signals. In this chapter, we review the status of several tree-ring  $\delta^{13}\text{C}$  and  $\delta^{18}\text{O}$  models simulating processes for trees, stands, catchments, and ecosystems. This review is intended to highlight the structural differences among models with varied objectives and to provide examples of the valuable insights that can come from combining process modeling with tree-ring stable isotope data. We urge that simple stable isotope algorithms be added to any forest model with a process representation of photosynthesis and transpiration as a strict test of model structure and an effective means to constrain the models.

---

L. Wei (✉)

MOE Key Laboratory of Western China's Environmental System, College of Earth and Environmental Sciences, Lanzhou University, Lanzhou 730000, Gansu, China  
e-mail: [liangwei@lzu.edu.cn](mailto:liangwei@lzu.edu.cn)

J. D. Marshall

Department of Forest Ecology and Management, Swedish Agricultural University, Skogmarksgränd, 90736 Umeå, Sweden

J. R. Brooks

Pacific Ecological Systems Division, Center for Environmental and Public Health Assessment, Office of Research and Development, U. S. Environmental Protection Agency, 200 SW 35th St., Corvallis, OR 97333, USA

© The Author(s) 2022

R. T. W. Siegwolf et al. (eds.), *Stable Isotopes in Tree Rings*, Tree Physiology 8,  
[https://doi.org/10.1007/978-3-030-92698-4\\_26](https://doi.org/10.1007/978-3-030-92698-4_26)

737

## 26.1 Introduction

Models are abstract and simplified representations of reality; we use models when they are easier to work on than a real system (Smith and Smith 2009). Models are widely used in studying plant stable isotopes by including processes important to tree physiology and environmental biophysics. Model complexity spans from the conceptual to detailed mathematical representations of system fluxes. Conceptual or diagrammatic models in this book use diagrams or word descriptions instead of equations, such as conceptual models that describe the links between  $\delta^{13}\text{C}$  and  $\delta^{18}\text{O}$  in plants (Grams et al. 2007; Scheidegger et al. 2000; Chap. 16). Classic mathematic models for plant stable isotopes represent the processes in stable isotope fractionations, such as the widely used model for  $\delta^{13}\text{C}$  developed by Farquhar and colleagues (Farquhar et al. 1982, 1989; Chap. 9) and the Craig-Gordon model for  $\delta^{18}\text{O}$  of liquid water pools undergoing evaporation (Craig and Gordon 1965; Farquhar et al. 2007; Chap. 10). Moreover, many other equations in this book explicitly describe processes in stable isotopic fractionation driven by physiology, and/or environmental biophysics. These equations are mechanistic mathematical models; each equation describes a unique aspect underlying the variations of tree-ring stable isotopes.

Because many isotopic models for specific processes are explicitly described in previous chapters, we will not repeat that work in this chapter. Instead, we focus on larger and more complex models that integrate these equations and our knowledge to simulate tree-ring stable isotopes based on processes of water uptake, gas exchange, and tree-ring formation. These models simulate the interactions between environment and plant, and integrate major processes in tree physiology, including photosynthesis, respiration, transpiration, carbon allocation, tree-ring formation, and the corresponding fractionations of stable isotopes in different tissues. One might think that an ideal process-based model would include all the processes to fully represent the variation in tree-ring stable isotopes; however, such a model would be impossible to parameterize (i.e. to determine appropriate values for an accurate quantitative description of a process). Therefore, all models must simplify process representation; the simplification strategies should match the objectives and constraints of the modeling exercise. We cover a range of tree-ring stable isotope models optimized for different objectives from those optimized for gas-exchange fluxes to those for carbon allocation addressing issues of carbon storage and timing of ring formation.

## 26.2 How Tree-Ring Stable Isotopes Help Modeling of Ecosystem Processes

Process-based forest modeling requires significant amounts of data including meteorological and environmental information to drive models, and physiological and mensurational data to parameterize and validate the models. Data shortage—the lack of and need for detailed and long-term data—is a common problem in many

forest modeling applications. Tree-ring stable isotopes can alleviate this need because they can serve as a proxy for some key data requirements, especially long-term physiological information (van der Sleen et al. 2017). Tree rings store decadal- to millennial-scale information about how plants responded physiologically to climatic and environmental changes as well as ontogenetic and size changes. Additionally, the time step of tree-ring records is limited only by our extraction capabilities as detailed intra- and inter-annual information is stored within tree rings (Gessler et al. 2014; McCarroll and Loader 2004; Chaps. 7 and 15). In contrast, observational meteorological records began only ~200 years ago, and studies of plant physiology began only in the last several decades. Moreover, tree-ring stable isotopes are relatively easy to obtain, and sample preparation and measurement procedures have been well developed (Chaps. 4–7). Published stable isotope chronologies are also readily available for modelers (e.g. compiled lists in Keller et al. 2017; McCarroll and Loader 2004).

Tree-ring stable isotopic data are ideal for testing model structure and parameterizing complex models. Models of ecosystem processes (e.g., photosynthesis and transpiration) simulate key physical and biochemical processes within the system and often lead to conclusions that are not intuitive. However, as models have become more comprehensive, they are not only more difficult to parameterize, but also more difficult to test. When models become too complex, we begin to rely on empirical calibrations of simplified models to parameterize the complex model. However, with limited available data used to calibrate and test the model, parameters are often tuned without reference to mechanistic constraints. This practice is dangerous when many parameters need to be tuned, but few observations are available. Tuning can “successfully” fit simulations to observations in a way that does not faithfully represent nature; thus, we get the “right” answer for the wrong reasons. As addressed by Aber (1997): “Perhaps one of the worst characteristics of a calibrated model is that it cannot fail...When models cannot fail, we cannot learn from them”. Even worse, an incorrectly parameterized model would likely yield erroneous answers. Therefore, modelers must (1) test the mechanistic basis of models and (2) calibrate the models within mechanistic constraints. Tree-ring stable isotopes may help to solve this dilemma as they can be related to underlying mechanisms (Fig. 26.1). A prerequisite for successful modeling remains the sound knowledge of the physiological processes and their responses to environmental drivers.

Accurate simulations of  $\delta^{13}\text{C}$  and  $\delta^{18}\text{O}$  require appropriate parameterization of key equations that describe both the fluxes and the isotopic values (Fig. 26.1). Small changes in parameters can result in similar flux values but may create large discrepancies between measured and modeled stable isotopes (Wei et al. 2014a), thus the stable isotopes provide a test for the calibration process. For example, Fig. 26.2 illustrates how a stable isotope component could test alternative model formulations. The simulations were based on a ~80 year-old natural stand of grand fir (*Abies grandis*) in the Mediterranean climate of northern Idaho, where low summer precipitation limits gas exchange (Wei et al. 2014a). Three scenarios in the example represent alternative means to parameterize the model: (1) using default gas exchange parameters; (2) calibrating the model with all available sap flow observations from a nearby site with

shallower soil; and (3) calibrating the model with part of the sap flow observations until the soil dried out. Scenario 1 did not reasonably simulate transpiration and the response of canopy conductance to vapor pressure deficit (VPD), but Scenarios 2 and 3 did (Fig. 26.2a, b). Although the differences were small between Scenarios 2 and 3 in both the calibrated parameter values and simulated transpiration, simulated tree-ring  $\delta^{13}\text{C}$  were clearly separated ( $\sim 2\text{‰}$ ) between Scenarios 2 and 3, and only Scenario 3 matched the  $\delta^{13}\text{C}$  observations (Fig. 26.2c). With  $\delta^{13}\text{C}$  as a constraint, small parameterization errors in gas exchange can be detected, increasing our confidence in the simulations under Scenario 3. Note that the isotopic data were used here

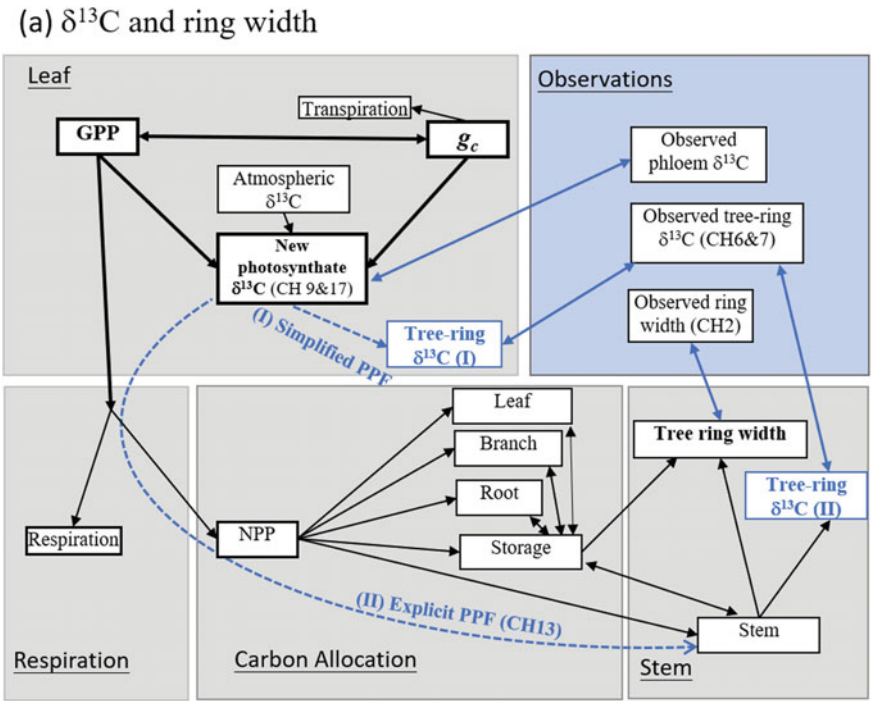


**Fig. 26.1** Simplified schemes of simulating tree-ring stable C ( $\delta^{13}\text{C}$ ) **a** and O isotopes ( $\delta^{18}\text{O}$ ) **b**, and using them as tests for modeling. Major components in process-based physiological models are included in gray boxes. The blue box indicates where stable isotopes can be used for model testing, either providing information for modeling calibration or validating the model. Post-photosynthetic fractionation (PPF) and storage are modeled less comprehensively than other physiological processes. Explicit PPF (I) may include fractionations in respiration, transportation, allocation, and organic matter synthesis. Mixing of stored and new carbohydrates further complicates the simulations of stable isotopes. Therefore, some models apply a simplified PPF scheme (II), such as a fixed offset between stable isotopes in new photosynthate and tree rings. Blue solid lines indicate comparison and testing, and blue dotted lines indicated post-photosynthetic processes. Chapter (CH) numbers are marked in boxes to indicate locations of corresponding contents in this book

(b)  $\delta^{18}\text{O}$

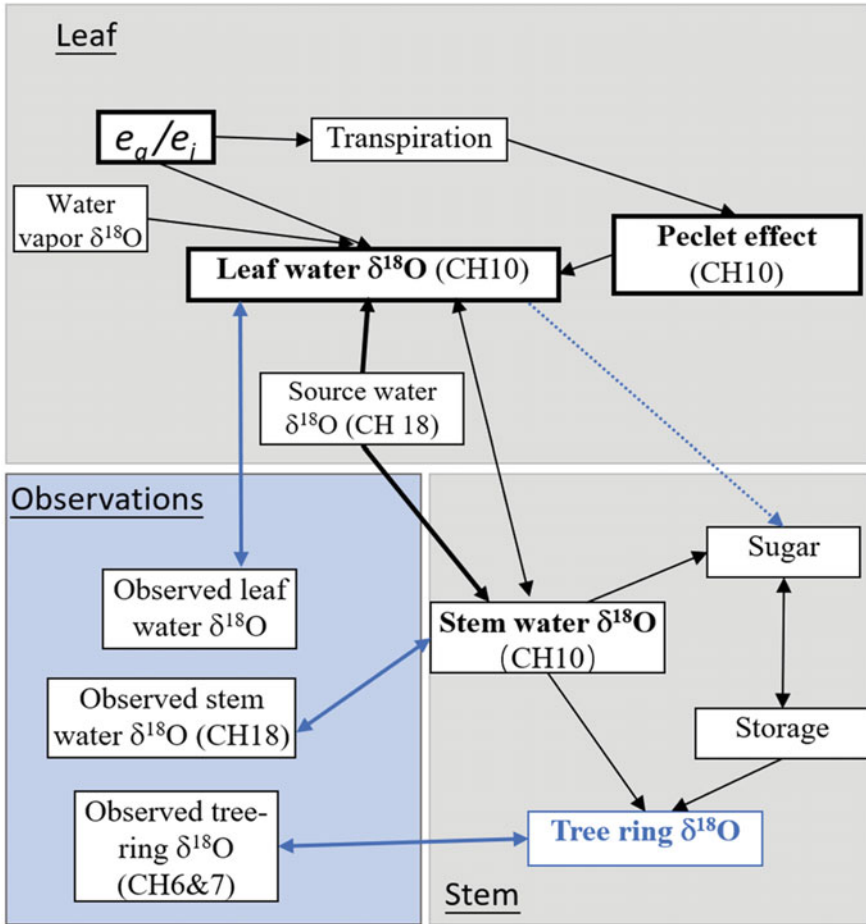
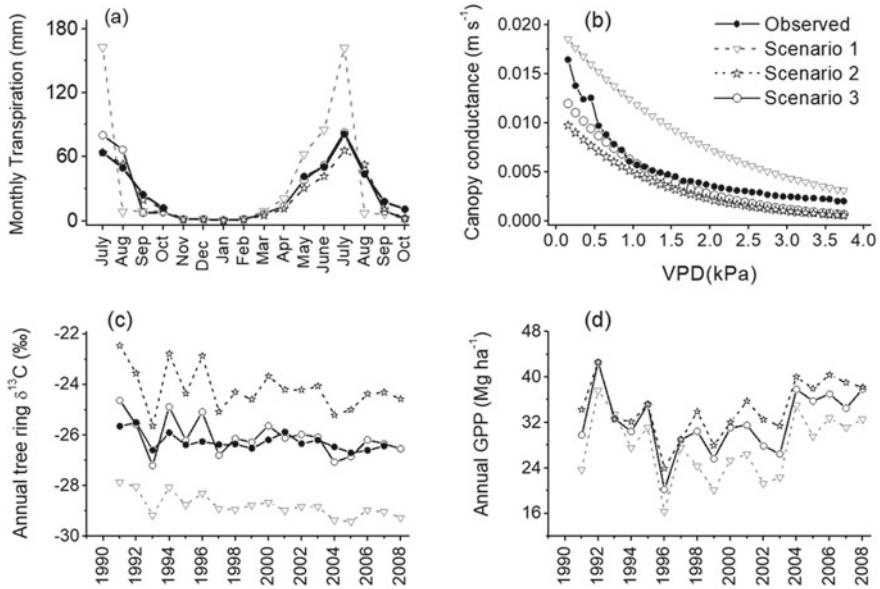


Fig. 26.1 (continued)

not as parameterizations themselves, but as a test of other means of parameterization. As this example illustrates, stable isotopes can serve as a powerful means to test alternative parameterization strategies (Aranibar et al. 2006; Duarte et al. 2017; Ulrich et al. 2019; Walcroft et al. 1997; Wei et al. 2014a).



**Fig. 26.2** Example of using tree-ring  $\delta^{13}\text{C}$  to validate a process-based forest model (3-PG; Wei et al. (2014a) for more details). Three scenarios demonstrate possible means to calibrate a model, where three parameters differed among scenarios, including maximum canopy conductance ( $g_{cmax}$ ,  $\text{m s}^{-1}$ ) the slope of canopy conductance to vapor pressure deficit (VPD;  $k_g$ ,  $\text{mbar}^{-1}$ ) and quantum yield ( $\alpha_{cx}$ ,  $\text{mol C mol}^{-1}$  photon). Scenario 1 used the default parameter set for simulations ( $g_{cmax} = 0.020$ ,  $k_g = 0.05$ ,  $\alpha_{cx} = 0.055$ ). Scenario 2 calibrated these parameters with all available sap flow observations at a nearby site with similar forest type but where the soil dried earlier than at the modeling site ( $g_{cmax} = 0.011$ ,  $k_g = 0.08$ ,  $\alpha_{cx} = 0.0615$ ). Scenario 3 calibrated the model using only part of the sap flow observations at this nearby site before the soils dried, which should be the most reasonable approach ( $g_{cmax} = 0.014$ ,  $k_g = 0.08$ ,  $\alpha_{cx} = 0.0615$ ). Although Scenario 2 and 3 had very similar simulations of transpiration **a** and similar VPD response curve (**b** “observed” shows the 99% percentile of all sap flux-based measurements), only Scenario 3 reasonably simulated tree-ring  $\delta^{13}\text{C}$  **c**. Because reliable  $\delta^{13}\text{C}$  simulations require accurate simulations of photosynthesis and stomatal conductance (Eq. (26.2)), simulations of gas exchanges of Scenario 3 are hence more reliable. We can then accept the simulated GPP of Scenario 3 as a better simulation than the other two scenarios **d**. This figure is redrawn from Wei et al. (2014a), with permission

### 26.3 Components for Modeling Tree-Ring $\delta^{13}\text{C}$ and $\delta^{18}\text{O}$

Our knowledge about causes of variation in tree-ring  $\delta^{13}\text{C}$  and  $\delta^{18}\text{O}$  has continuously improved (Chaps. 9, 10, 16 and 17). The key processes which have been commonly included in process-based modeling of tree-ring  $\delta^{13}\text{C}$  and  $\delta^{18}\text{O}$  can be broken into various components such as fractionation during carbon fixation within leaves, during carbon allocation, or during cellulose formation within the stem (Fig. 26.1). Models tend to focus on one or two of these boxes depending on the model objectives, but the level of process detail varies greatly between models. As mentioned earlier, more complex modeling requires more detailed data for parameterizing and testing the



models. Model predictions are generally validated with data either after simulating leaf-level fractionation or after cellulose formation within the stem. At the leaf level, simulated  $\delta^{13}\text{C}$  can be tested with phloem  $\delta^{13}\text{C}$ , and simulated water  $\delta^{18}\text{O}$  in tissues can be assessed with leaf or stem water observations (Fig. 26.1). However, these observations are normally short-term and non-continuous. Tree-ring stable isotopes provide long-term and continuous data that can be used to validate models over years of simulation.

Leaf-level photosynthetic fractionation for  $\delta^{13}\text{C}\text{-CO}_2$  is relatively well understood. Models for photosynthetic fractionations of  $\delta^{13}\text{C}\text{-CO}_2$  vary in complexity from “simplified” to “comprehensive” and modelers should pick the model that serves their purpose (Ubierna and Farquhar 2014). The comprehensive model includes fractionations related to Rubisco, stomatal conductance, mesophyll conductance, respiration, photorespiration, and ternary effects (Farquhar et al. 1982; Farquhar and Cernusak 2012; Ubierna and Farquhar 2014). The comprehensive model requires many parameters, some of which (e.g. mesophyll conductance) are difficult to estimate. Therefore, few process-based models for tree-ring  $\delta^{13}\text{C}$  have applied the comprehensive model (e.g. Eglin et al. 2010; Rogers et al. 2017). A simplified model is more widely used in studies that simulate tree-ring  $\delta^{13}\text{C}$ ; it highlights the control of intercellular  $\text{CO}_2$  concentration ( $c_i$ ) on fractionation and lumps the impact of other factors into a single parameter that is mostly determined by Rubisco carboxylation ( $b$ , 27‰) (Farquhar et al. 1982).  $\delta^{13}\text{C}$  of new photosynthate can then be approximated as:

$$\delta^{13}\text{C} \approx \delta^{13}\text{C}_a - a - (b - a)(c_i/c_a) \quad (26.1)$$

where  $\delta^{13}\text{C}_a$  is the  $\delta^{13}\text{C}$  of atmospheric  $\text{CO}_2$ ,  $a$  is the fractionation from diffusion through air (4.4‰), and  $c_a$  is the atmospheric  $\text{CO}_2$  concentration. Most components in Eq. (26.1) can either be treated as constants ( $a$ ,  $b$ ) or are easily obtained from observations ( $C_a$  and  $\delta^{13}\text{C}_a$ ). In process-based models,  $c_i$  is driven by the photosynthetic rate ( $A$ ) and the stomatal conductance to  $\text{CO}_2$  ( $g_s$ ) (Farquhar and Sharkey 1982) as follows:

$$A/g_s = (c_a - c_i) \quad (26.2)$$

Therefore, process-based models can be conveniently enabled to simulate  $\delta^{13}\text{C}$  of photosynthate.

Another key source of variation for simulating  $\delta^{13}\text{C}$  is atmospheric  $\text{CO}_2$ ; both  $c_a$  and  $\delta^{13}\text{C}_a$  in Eq. (26.1) are changing due to human activities.  $c_a$  has increased and  $\delta^{13}\text{C}_a$  decreased due primarily to the burning of fossil fuels (Francey et al. 1999, see also Chap. 9). Additionally,  $c_a$  and  $\delta^{13}\text{C}_a$  vary seasonally, mainly due to seasonal changes in global photosynthesis (Keeling et al. 2017). Tree-ring stable isotopes records have been used extensively to understand both the secular change in  $\text{CO}_2$  and plant physiological responses to this change (Chap. 24). However, the concurrent ontogenetic changes in tree age and size are difficult to separate from  $\text{CO}_2$  changes

over time (Monserud and Marshall 2001). Models have the potential to separate these temporal concurrent influences on tree-ring isotopic records (see Sect. 26.5).

Less well understood are fractionations in other tissues (i.e., post-photosynthetic fractionations) (Badeck et al. 2005; Gessler et al. 2014; Offermann et al. 2011; Chap. 13). These include fractionations upon phloem loading (Busch et al. 2020) and unloading, composition changes in phloem contents (Bögelein et al. 2019), leakage and refilling during transport (Gessler et al. 2014; Offermann et al. 2011), and biosynthetic processes during wood formation (Bowling et al. 2008). We do not assess these in detail here as they were already presented in Chap. 13. However, models can assess likely consequences of these fractionations in the tree-ring data (Danis et al. 2012; Eglin et al. 2010).

Stored carbohydrates from previous years are sometimes used to build wood of the current year (Barbour and Song 2014; Chap. 14); this phenomenon is called the carry-over effect, legacy effect, or time-lag effect (Fritts 1966; Zweifel and Sterck 2018). Modeling the carry-over effect requires simulations of the dynamics of carbon storage and their impacts on tree-ring stable isotopes over time. Such components have been included in some process-based models (e.g. Danis et al. 2012; Eglin et al. 2010; Hemming et al. 2001) (see Sect. 26.4). The results of simulating the carry-over effect have varied among studies. For example, storage did not play a significant role in simulating tree-ring  $\delta^{13}\text{C}$  for *Pinus halepensis* (Klein et al. 2005), while it was important in some other studies that simulated tree-ring  $\delta^{13}\text{C}$  with *Pinus arizonica* and *Fagus sylvatica* (Hemming et al. 2001; Skomarkova et al. 2006).

Simulations of tree-ring  $\delta^{18}\text{O}$  are mostly extensions of the Craig-Gordon model, which describes evaporative enrichment at the evaporation site in the leaf and exchange with atmospheric water vapor (Fig. 26.1b, Chap. 10). These predictions are often corrected for the Péclet effect, which describes the diffusion of enriched water into the unenriched xylem water (Farquhar and Lloyd 1993; Barbour 2007; Barbour et al. 2004; Cernusak et al. 2016). This back-diffusion of water from the evaporation site isotopically enriches bulk leaf water where carbohydrates are formed. The Péclet effect is directly influenced by transpiration, whereas the Craig-Gordon model is mainly influenced by relative humidity. These models may also include isotopic variation due to phloem transport (Gessler et al. 2014; Chap. 10) and the impact of  $\delta^{18}\text{O}$  in water vapor on  $\delta^{18}\text{O}$  in plant water and organic compounds (Lehmann et al. 2018, 2020). Models of  $\delta^{18}\text{O}$  vary in the detail of the  $\delta^{18}\text{O}$  evaporative enrichment process in leaf water, and one should choose a model that is most suitable to specific objectives (Cernusak et al. 2016). The influence of the Péclet effect should be damped in simulating flows downstream from leaf water pools, so it may not be necessary to include it in simulating tree-ring  $\delta^{18}\text{O}$  (Cernusak et al. 2016; Ogée et al. 2009). However, including the Péclet effect did improve simulations of tree-ring  $\delta^{18}\text{O}$  in at least one study (Ulrich et al. 2019). All models of  $\delta^{18}\text{O}$  require information on the  $\delta^{18}\text{O}$  of water taken up by the trees (see Chap. 18).

Accurate modeling of tree-ring stable isotopes may require allocating the correct amount of new biomass in the tree stem at the right time to integrate seasonal influences into isotopic values measured within the rings (Chap. 14). Therefore, these models should reasonably simulate tree radial growth across the growing season

(tree-ring width, the increment of basal area, or tree diameter). Simulating radial growth requires not only reasonable simulations of the carbon supply, but also reasonable descriptions of allocating new and stored carbohydrates to tree-rings, and the phenology of ring production. Process-based models with reasonable simulations for  $\delta^{13}\text{C}$  and  $\delta^{18}\text{O}$  have been used to validate simulations of productivity (see Sect. 26.2), which benefited the simulations of radial growth. Several examples (Danis et al. 2012; Ogée et al. 2009; Ulrich et al. 2019) have reasonably simulated both radial growth and stable isotope composition of the ring (see in Sect. 26.4.3).

Scenario and sensitivity analysis of tree-ring isotope models can also provide important insights into potential causes of variation, both during research planning and in post hoc analyses of tree-ring data. For example, Wei et al. (2018) used alternative modeling scenarios to conclude that elevation differences in temperature had little direct effect on productivity in a montane watershed. Lin et al. (2019) analyzed drought effects on  $\delta^{18}\text{O}$  in tree rings, using a sensitivity analysis to conclude that a change in source water was the most probable explanation for the observed  $\delta^{18}\text{O}$  response. Given the many sources of variation in  $\delta^{18}\text{O}$ , this kind of formal analysis may be especially valuable.

Perhaps even more valuable is the notion of using models in research planning. For example, had the Lin et al. (2019) analysis been done before the measurements were conducted, perhaps measurements of xylem water  $\delta^{18}\text{O}$  would have been prioritized. This idea of close collaboration between modelers and experimentalists, from research planning to publication, is common in other disciplines and has begun to take hold in ecology (Medlyn et al. 2015, 2016). Perhaps the tree-ring isotope community has room to grow in this direction.

## 26.4 Models that Simulate Tree-Ring Stable Isotopes

Several process-based models have been used to predict stable isotopic composition at varying levels of complexity. At a small spatial scale, simple leaf- or stand-level models can simulate forest physiology and growth with simple stand structures; at the other end, more complex models can simulate forests with different species, tree sizes, and canopy structures at watershed, regional, and global scales. Here we describe several representative models that have advanced our abilities in modeling tree-ring  $\delta^{13}\text{C}$  and  $\delta^{18}\text{O}$ . All these models have been used to simulate tree-ring stable isotopes for more than one year and have been tested with observed isotopic data. Most models here could simulate time series of tree-ring stable isotopes, but we also include models that simulate  $\delta^{13}\text{C}$  in new photosynthate and/or  $\delta^{18}\text{O}$  in foliage water as they have the potential to also predict tree-ring isotope time series after simple upgrades or modifications.

### 26.4.1 Models for Predicting $\delta^{13}\text{C}$ of Foliage and Tree-Rings

#### Panek and Waring 1997

Panek and Waring (1997) simulated foliage and tree-ring  $\delta^{13}\text{C}$  in a semi-mechanistic way. A process-based model (FOREST-BGC, Running and Coughlan 1988) was used to capture climate constraints on  $g_s$ .  $\delta^{13}\text{C}$  was modeled empirically based on multiple linear regressions between  $\delta^{13}\text{C}$  and climatic constraints on stomata. The study tested how much variance in tree-ring  $\delta^{13}\text{C}$  can be explained by climate controls on  $g_s$ , neglecting all other sources of variation discussed above. The model explained 34% ( $r = 0.58$ ) of the annual variation in tree-ring  $\delta^{13}\text{C}$  across 22 years for Douglas-fir in Oregon, USA.

#### Walcroft 1997

Walcroft et al. (1997) combined process-based modeling with tree-ring  $\delta^{13}\text{C}$  to expand our knowledge in the connections between long-term climate and tree-ring stable isotopes. This study also indicated the possibility of using tree-ring  $\delta^{13}\text{C}$  to validate models. Driven by daily meteorology data, a leaf-level model simulated stomatal conductance, leaf photosynthesis, and stand water balance for *Pinus radiata* over two growing seasons at two sites in New Zealand. The authors used the gas-exchange data to simulate seasonal variations in leaf-level  $c_i$ . They compared this to seasonal canopy-level  $c_i$  estimated from  $\delta^{13}\text{C}$  of intra-annual tree-ring slices using the simplified equation from Farquhar et al. (1982) (Chap. 9). The two sets of  $c_i$  had similar seasonal variations except that simulated  $c_i$  varied over a larger amplitude. This indicated the importance of post-photosynthetic processes, including mixing of stored carbohydrates  $s$ , in damping the signals of gas exchange in tree-rings.

#### SICA

Trees may adjust their stomatal regulation of  $c_i$  in response to rising atmospheric  $\text{CO}_2$  (Voelker et al. 2016), which would change water-use efficiency and tree-ring  $\delta^{13}\text{C}$ . In one of the early attempts to describe these phenomena, Berninger et al. (2000) modeled annual variations of tree-ring carbon isotope values for a long period (1877–1995) using a modified version of the Simple CANopy model (SICA) model (Berninger 1997). Two kinds of stomatal responses to elevated  $\text{CO}_2$  were used: a sensitive scheme that reduced  $g_s$  with increasing  $\text{CO}_2$  and an insensitive scheme that did not. It turned out that the insensitive scheme better predicted tree-ring carbon isotope values with a correlation coefficient ( $r$ ) between simulations and observations as high as 0.74. In contrast,  $r$  reached only 0.58 with the sensitive scheme. This indicated that  $g_s$  had not decreased with increasing  $\text{CO}_2$  and  $\Delta^{13}\text{C}$  increased since the 1950s. The SICA model did not consider ontogenetic effects or post-photosynthetic fractionations; therefore, there was a 4.6% offset between simulated photosynthetic  $\Delta^{13}\text{C}$  and observed  $\Delta^{13}\text{C}$  in tree-ring cellulose.

## TREERING

The TREERING model (Fritts et al. 1999; Hemming et al. 2001) was among the first to incorporate post-photosynthetic discriminations in simulations of tree-ring  $\delta^{13}\text{C}$ . It included the impact of daily cambium activity and carbon storage on the simulations of tree-ring  $\delta^{13}\text{C}$ . The dynamics of two carbohydrate pools were simulated: sucrose as new photosynthate and starch as storage. Sucrose is first spent each day on respiration and growth. If there were remaining sucrose, a fixed percentage of remaining new photosynthate was allocated to starch storage in each day. The results indicated that the stored carbon had a greater impact on tree-ring  $\delta^{13}\text{C}$  than new photosynthate in 16 years of *Pinus arizonica* in Arizona USA (Hemming et al. 2001).

## ISOCASTANEA

ISOCASTANEA (Eglin et al. 2010) is one of the most comprehensive models to simulate tree-ring  $\delta^{13}\text{C}$ . It captures how short-term  $\delta^{13}\text{C}$  signals at the leaf-level are integrated into tree rings. It incorporates two procedures that are currently rare in simulating plant stable isotopes and results in better estimates of post-photosynthetic fractionation with explicit carbon dynamics. First, the model simulates post-photosynthetic translocation and allocation of carbohydrates based on the physiological processes in the phloem. These processes included the phloem loading in canopy and unloading in stem and roots, and mass flow in sieve tubes which include volume and conductance of phloem elements. This model also simulates the dynamics of storage, respiration, and structural biomass formation, which make its post-photosynthetic carbon dynamics more explicit than many other similar models. Second, tree rings are not formed instantaneously in the ISOCASTANEA model. Tree-ring formation is separated into three main stages in nature: cambial cell division, cell expansion, and cell-wall thickening (Eglin et al. 2010; Samuels et al. 2006). The model simulates tree-ring growth by dividing tree rings into growth layers formed continuously in the cambial division stage. After formation, carbohydrate allocation to the growth layer decreases exponentially over time. The later phases of growth represented lignification and cell wall thickening.

### 26.4.2 Models for Predicting $\delta^{18}\text{O}$ of Leaf Water and Tree Rings

#### Roden–Lin–Ehleringer 2000

The Roden–Lin–Ehleringer model (Roden et al. 2000) simulates  $\delta^{18}\text{O}$  and hydrogen isotope ratios ( $\delta^2\text{H}$ ) in tree-ring cellulose. Two major components of the model predict the evaporative enrichment and vapor exchange in leaf water using the Craig-Gordon model, and isotopic exchange during cellulose synthesis. Stable isotope ratios simulated by the Roden–Lin–Ehleringer model were compared to observed values from either hydroponically grown trees in the lab (Roden and Ehleringer 1999a) or trees

grown along stream banks at field sites (Roden and Ehleringer 1999b). The lab trees were grown in altered water vapor  $\delta^{18}\text{O}$  and hydroponic solution  $\delta^{18}\text{O}$ . Simulated  $\delta^{18}\text{O}$  had a good 1:1 relationship with observed  $\delta^{18}\text{O}$  from tree-ring cellulose across experiments. This model is so simple that it might be included as an algorithm inside many existing models of more complexity.

### **Péclet Effect**

The introduction of the Péclet effect into modeling leaf and tree-ring  $\delta^{18}\text{O}$  directly included transpiration effects into leaf water enrichment models (Farquhar and Lloyd 1993). However, the Péclet effect also introduced an effective path length variable ( $L$ ), which describes the distance water moves inside the leaf lamina and is not directly measurable. Using the same data used to develop the Roden-Lin-Ehleringer model above, Barbour et al. (2004) simulated  $\delta^{18}\text{O}$  in leaf water and tree-rings respectively with and without a Péclet effect; simulations with the Péclet effect had better predictive power than without it. Modeled differences in leaf water across 17 *Eucalyptus* species was largely explained by varied  $L$  across species; however,  $L$  was highly unconstrained (Kahmen et al. 2008). Process modeling that predicts transpiration can facilitate estimating  $L$  values (e.g. Loucos et al. 2015; Song et al. 2013; Ulrich et al. 2019). However, Kahmen et al. (2011) found that most variance in leaf and tree-ring  $\delta^{18}\text{O}$  was related to vapor pressure deficit, regardless of the model complexity used to predict it. The debate about including the Péclet effect in tree-ring  $\delta^{18}\text{O}$  models continues, and largely depends on modeling objectives. Like the Roden-Lin-Ehleringer model above, the Péclet effect is simple enough to be included in a model with a few lines of code. More details can be found in Chap. 10.

## **26.4.3 Models for Predicting Both $\delta^{13}\text{C}$ and $\delta^{18}\text{O}$ of Tree Rings**

### **Single-Substrate Model**

Ogée et al. (2009) simulated tree-ring formation from a single well-mixed water-soluble sugar pool that varied in size and  $\delta^{13}\text{C}$  and  $\delta^{18}\text{O}$  signatures. This pool was assumed to be large enough to fulfill the metabolic demand in the growing season, and was filled with new photosynthate and drained by respiration and biomass formation. The dynamics of the carbon pool accompanied the changes in  $\delta^{13}\text{C}$  and  $\delta^{18}\text{O}$  in this pool, which was controlled by the isotopic fractionation of photosynthesis, respiration, and biomass synthesis (Ogée et al. 2009). In a 2 year study with two *Pinus pinaster* trees in France, the single substrate model relied upon model simulations of photosynthesis and respiration from the well-calibrated MuSICA model (multilayer simulator of the interactions between a coniferous stand and the atmosphere) to predict stable isotopes in tree-ring cellulose (Ogée et al. 2003a). MuSICA is a process-based multilayer gas exchange model, which simulates the fluxes of energy,

water, and CO<sub>2</sub> through soil, vegetation, and atmosphere (Ogée et al. 2003a, b). The single substrate model achieved reasonable simulations for seasonal variation in  $\delta^{13}\text{C}$  and  $\delta^{18}\text{O}$  when compared with measured values from 100- $\mu\text{m}$  thick samples within tree rings.

### 3-PG with Isotopic Modules

A widely used forest model, 3-PG (Physiological Principles Predicting Growth) (Landsberg and Waring 1997), has been modified to simulate tree-ring  $\delta^{13}\text{C}$  and  $\delta^{18}\text{O}$ . 3-PG is a big-leaf model describing physiological principles applied to the whole canopy. The model estimates gross primary production (GPP) and a VPD-dependent canopy conductance. The modification by Wei et al. (2014a) used these parameters to calculate  $\delta^{13}\text{C}$  via the simplified (Farquhar et al. 1989) model. The difference between  $\delta^{13}\text{C}$  in new photosynthate and the tree-ring was assumed as a constant offset to bypass the simulations of post-photosynthetic fractionation and keep the model simple (Wei et al. 2014a). The model has also been modified to estimate tree-ring  $\delta^{18}\text{O}$  (Ulrich et al. 2019). Here the modification included  $\delta^{18}\text{O}$  enrichment at the site of evaporation, the Péclet effect, and exchange and fractionation during cellulose formation. The fidelity of modeled GPP and canopy conductance can then be tested by comparing simulated tree-ring  $\delta^{13}\text{C}$  and  $\delta^{18}\text{O}$  with observations; this approach greatly constrained the parameter space and avoided artifacts in simulations of gas exchange, which improved the reliability of this model (Ulrich et al. 2019; Wei et al. 2014a). The modified 3-PG model has also been used to estimate variations of tree-ring  $\delta^{13}\text{C}$  across an elevational gradient in a watershed (Wei et al. 2018) and to estimate responses to forest management practices on tree-ring  $\delta^{13}\text{C}$  (Wei et al. 2014b) (also see Chap. 23).

### MAIDENiso

MAIDENiso (Danis et al. 2012) was designed specifically for modeling tree-ring width and stable isotopes. This upgraded version of the MAIDEN model (Misson 2004) captures ecophysiological processes to simulate carbon allocation to the stem as well as  $\delta^{13}\text{C}$  and  $\delta^{18}\text{O}$  of tree-ring cellulose. Storage of carbon was explicitly modeled with carbon reservoirs in leaf, bole, and root (Boucher et al. 2013; Misson 2004); this enabled carbon storage impacts to be included on stem growth,  $\delta^{13}\text{C}$ , and  $\delta^{18}\text{O}$  simulations. MAIDENiso was able to simulate tree-ring cellulose  $\delta^{13}\text{C}$  and  $\delta^{18}\text{O}$  with  $r$  above 0.5 between simulations and observations for both  $\delta^{13}\text{C}$  and  $\delta^{18}\text{O}$  in an oak species in France (Danis et al. 2012), and 0.52 and 0.62 for  $\delta^{18}\text{O}$  in *Picea mariana* in northeastern Canada and *Nothofagus pumilio* in western Argentina (Lavergne et al. 2017).

A notable use of MAIDENiso applied an inverse modeling approach to change the meteorological data and see if the changes would provide a better fit of simulated tree-ring width,  $\delta^{13}\text{C}$ , and  $\delta^{18}\text{O}$  to their respective observations (Boucher et al. 2013). This approach was designed to find the best combination of the climatic inputs as a robust paleoclimatic reconstruction. This model also enabled the separation of climatic impact and CO<sub>2</sub> influences on plant growth, which is useful for paleoclimatic reconstructions (Boucher et al. 2013; Guiot et al. 2014).

## 26.5 Future Directions

Better modeling of tree-ring stable isotopes relies on the improvement and incorporation of physiological mechanisms that influence plant isotopic values. A particular challenge that modeling could address relates to including ontogenetic changes in CO<sub>2</sub> responses. Ontogenetic change is often attributed to age in the tree-ring community, perhaps because age is easiest to measure from tree-ring chronologies. However, no evidence of an age effect exists per se in trees (e.g. Mencuccini et al. 2005), except as caused by increasing tree height. Tall trees generally face a challenge in lifting water to the canopy, which causes an increase in  $\delta^{13}\text{C}$  with height (Brienen et al. 2017; Marshall and Monserud 1996; McDowell et al. 2011; Voelker et al. 2016). These issues are particularly important when tree-ring  $\delta^{13}\text{C}$  is used to infer responses to CO<sub>2</sub> because the CO<sub>2</sub> effect and the height effect are often confounded. Future work will need to remove the height signal from tree-ring data to draw solid inferences regarding the CO<sub>2</sub> effect (Brienen et al. 2017; Marshall and Monserud 1996). Similarly, the proportion of oxygen atoms exchanged with xylem water upon cellulose formation may be variable (Cheesman and Cernusak 2016) and may need to be accounted for in the traditional model of  $\delta^{18}\text{O}$  in tree rings (Roden and Ehleringer 1999b). As mesophyll conductance becomes easier to determine, there may be value in modeling how it differs among species and growing conditions; this critical parameter influences the relationship between intrinsic water-use efficiency (iWUE) and  $\delta^{13}\text{C}$ . It describes the drawdown in concentration between the intercellular spaces, where iWUE is controlled, to the chloroplasts, where  $\delta^{13}\text{C}$  is set by photosynthesis (Stangl et al. 2019). Finally, the continuing debate about the many forms of post-photosynthetic fractionation will certainly continue to modify our tree-ring isotope models (Gessler et al. 2014; Chap. 13).

Another way to promote tree-ring stable isotope modeling is creating comprehensive databases for tree-ring stable isotopes chronologies. Although sources exist for such chronologies (e.g. compiled lists in Keller et al. 2017; McCarroll and Loader 2004), these data have not been well archived into a single database. The International Tree-Ring Data Bank (ITRDB) (Grissino-Mayer and Fritts 1997) had stable isotope measurements from only 24 sites in 2017 (Babst et al. 2017). The global TRY database had only 59 observations of wood  $\delta^{13}\text{C}$  and none of wood  $\delta^{18}\text{O}$  data in 2020 (Kattge et al. 2020). In comparison, the TRY database includes ~15,000 observations from 468 species for leaf  $\delta^{13}\text{C}$  and 533 observations from 96 species for leaf  $\delta^{18}\text{O}$  in 2020. Moreover, data from 4200 sites are available for tree-ring width (Babst et al. 2017), which made tree-ring width chronologies more readily available to facilitate testing models than stable isotopes. Therefore, we suggest archiving of stable tree-ring stable isotope chronologies whenever possible.

Tree-ring stable isotopes can also provide benchmarks for dynamic global vegetation models (DGVMs) in the future. DGVMs attempt to represent the dynamics of the global biosphere (Schulze et al. 2019). They integrate our understanding of physical, chemical, and biological processes of terrestrial ecosystems at varied scales from sites (represented as grids) to the globe. Several of these models have been upgraded to



simulate plant stable isotopes, including SiB2 (Suits et al. 2005), ISOLSM (Aranibar et al. 2006; Riley et al. 2002, 2003; Still et al. 2009), LPJ-DGVM (Scholze et al. 2003), JULES (Bodin et al. 2013), ORCHIDEE (Churakova et al. 2016; Risi et al. 2016), LPX-Bern (Keel et al. 2016; Keller et al. 2017; Saurer et al. 2014), and CLM (Duarte et al. 2017; Keller et al. 2017; Raczka et al. 2016). Although these DGVMs simulate  $\delta^{13}\text{C}$  in new photosynthate or leaves, and/or  $\delta^{18}\text{O}$  in leaf water, most of them (except LPX-Bern) do not simulate tree-ring stable isotopes at this point and therefore tree-ring stable isotopes have not been used for testing DGVMs. However, because of the modular structure of DGVMs, they can be conveniently upgraded to simulate tree-rings stable isotopes by adding new modules or modifying current ones.

Inverse modeling for paleoclimate is a new frontier of using tree-ring stable isotopes (Boucher et al. 2013; Guiot et al. 2014). This approach rejuvenated the use of tree-ring information for paleoclimate reconstruction. The reconstruction traditionally relies on empirical relationships between tree-ring chronologies (width and stable isotopes), which means only the most limiting climatic factors would have left clear signals in the tree-ring chronologies. Additionally, these traditional reconstructions have obtained the clearest climate signals from trees growing in an extreme environment. Inverse modeling revolutionized the reconstruction by applying process-based approaches. Many climatic factors can be tested at the same time by mathematically estimating their collective impact on forests and statistically testing and improving the climatic variables that are provided as a priori.

Modeling is an important tool to study ecosystem processes because it can integrate physiological and growth processes. Tree-ring isotopic records likewise integrate these processes so the two approaches are certain to continue to develop in tandem, each tested against the other. Moreover, as demonstrated above, stable isotopes are convenient testing for models, and including a stable isotope component in models is relatively simple. Models can add value to completed isotopic datasets by post hoc analyses of the likely controls over isotopic composition. We urge that more process-based forest models include a stable isotope component to help parametrize and validate the models and improve model credibility.

**Acknowledgements** Liang Wei was supported while preparing this manuscript by the National Science Foundation of China (No. 31971492 and 41991254). John Marshall was supported by the Knut and Alice Wallenberg Foundation (#2015.0047). We thank Chris Still and Fabio Gennaretti for thoughtful comments on an earlier draft of this chapter. This manuscript has been subjected to U.S. Environmental Protection Agency review and has been approved for publication. The views expressed in this paper are those of the author(s) and do not necessarily reflect the views or policies of the U.S. Environmental Protection Agency. Mention of trade names or commercial products does not constitute endorsement or recommendation for use.

## References

- Aber JD (1997) Why don't we believe the models? *Bull Ecol Soc Am* 78(3):232–233
- Aranibar JN et al (2006) Combining meteorology, eddy fluxes, isotope measurements, and modeling to understand environmental controls of carbon isotope discrimination at the canopy scale. *Glob Change Biol* 12(4):710–730
- Babst F, Poulter B, Bodesheim P, Mahecha MD, Frank DC (2017) Improved tree-ring archives will support earth-system science. *Nat Ecol Evol* 1:0008
- Badeck F-W, Tcherkez G, Nogués S, Piel C, Ghashghaie J (2005) Post-photosynthetic fractionation of stable carbon isotopes between plant organs—a widespread phenomenon. *Rapid Commun Mass Spectrom* 19(11):1381–1391
- Barbour MM (2007) Stable oxygen isotope composition of plant tissue: a review. *Funct Plant Biol* 34(2):83–94
- Barbour MM, Song X (2014) Do tree-ring stable isotope compositions faithfully record tree carbon/water dynamics? *Tree Physiol* 34(8):792–795
- Barbour MM, Roden JS, Farquhar GD, Ehleringer JR (2004) Expressing leaf water and cellulose oxygen isotope ratios as enrichment above source water reveals evidence of a Péclet effect. *Oecologia* 138(3):426–435
- Berninger F (1997) Effects of drought and phenology on GPP in *Pinus sylvestris*: a simulation study along a geographical gradient. *Funct Ecol* 11(1):33–42
- Berninger F, Sonninen E, Aalto T, Lloyd J (2000) Modeling  $^{13}\text{C}$  discrimination in tree rings. *Glob Biogeochem Cycles* 14(1):213–223
- Bodin PE et al (2013) Comparing the performance of different stomatal conductance models using modelled and measured plant carbon isotope ratios ( $\delta^{13}\text{C}$ ): implications for assessing physiological forcing. *Glob Change Biol* 19(6):1709–1719
- Bögelein R, Lehmann MM, Thomas FM (2019) Differences in carbon isotope leaf-to-phloem fractionation and mixing patterns along a vertical gradient in mature European beech and Douglas fir. *New Phytol* 222(4):1803–1815
- Boucher É et al (2013) An inverse modeling approach for tree-ring-based climate reconstructions under changing atmospheric  $\text{CO}_2$  concentrations. *Biogeosciences Discuss* 10(11):18479–18514
- Bowling DR, Pataki DE, Randerson JT (2008) Carbon isotopes in terrestrial ecosystem pools and  $\text{CO}_2$  fluxes. *New Phytol* 178(1):24–40
- Brienen RJW et al (2017) Tree height strongly affects estimates of water-use efficiency responses to climate and  $\text{CO}_2$  using isotopes. *Nat Commun* 8(1):288
- Busch FA, Holloway-Phillips M, Stuart-Williams H, Farquhar GD (2020) Revisiting carbon isotope discrimination in  $\text{C}_3$  plants shows respiration rules when photosynthesis is low. *Nat Plants* 6(3):245–258
- Cernusak LA et al (2016) Stable isotopes in leaf water of terrestrial plants. *Plant Cell Environ* 39(5):1087–1102
- Cheesman AW, Cernusak LA (2016) Infidelity in the outback: climate signal recorded in  $\Delta^{18}\text{O}$  of leaf but not branch cellulose of eucalypts across an Australian aridity gradient. *Tree Physiol* 37(5):554–564
- Churakova OV et al (2016) Application of eco-physiological models to the climatic interpretation of  $\delta^{13}\text{C}$  and  $\delta^{18}\text{O}$  measured in Siberian larch tree-rings. *Dendrochronologia* 39:51–59
- Craig H, Gordon LI (1965) Deuterium and oxygen-18 variations in the ocean and the marine atmosphere. In: Tongiorgi E (ed) *Proceedings of a conference on stable isotopes in oceanographic studies and paleotemperatures*. Lischi and Figli, Pisa, Italy, pp 9–130
- Danis PA, Hatté C, Misson L, Guiot J (2012) MAIDENiso: a multiproxy biophysical model of tree-ring width and oxygen and carbon isotopes. *Can J For Res* 42(9):1697–1713
- Duarte HF, et al (2017) Evaluating the Community Land Model (CLM4.5) at a coniferous forest site in northwestern United States using flux and carbon-isotope measurements. *Biogeosciences* 14(18):4315–4340

- Eglin T, Francois C, Michelot A, Delpierre N, Damesin C (2010) Linking intra-seasonal variations in climate and tree-ring  $\delta^{13}\text{C}$ : a functional modelling approach. *Ecol Model* 221(15):1779–1797
- Farquhar GD, Cernusak LA (2012) Ternary effects on the gas exchange of isotopologues of carbon dioxide. *Plant Cell Environ* 35(7):1221–1231
- Farquhar GD, Lloyd J (1993) Carbon and oxygen isotope effects in the exchange of carbondioxide between terrestrial plants and the atmosphere. In: Ehleringer JR, Hall AE, Farquhar GD (eds) *Stable isotopes and plant carbon/water relations*. Academic Press, New York, USA, pp 47–79
- Farquhar GD, Sharkey TD (1982) Stomatal conductance and photosynthesis. *Annu Rev Plant Physiol* 33:317–345
- Farquhar G, O'Leary M, Berry J (1982) On the relationship between carbon isotope discrimination and the intercellular carbon dioxide concentration in leaves. *Funct Plant Biol* 9(2):121–137
- Farquhar GD, Ehleringer JR, Hubick KT (1989) Carbon isotope discrimination and photosynthesis. *Annu Rev Plant Biol* 40(1):503–537
- Farquhar G, Cernusak L, Barnes B (2007) Heavy water fractionation during transpiration. *Plant Physiol* 143:11–18
- Francey RJ et al (1999) A 1000-year high precision record of  $\delta^{13}\text{C}$  in atmospheric  $\text{CO}_2$ . *Tellus B* 51(2):170–193
- Fritts HC (1966) Growth-rings of trees: their correlation with climate. *Science* 154(3752):973–979
- Fritts H, Shashkin A, Downes G (1999) A simulation model of conifer ring growth and cell structure. In: *Tree-ring analysis: biological, methodological and environmental aspects*. CABI Publishing, Wallingford, UK, pp 3–32
- Gessler A et al (2014) Stable isotopes in tree rings: towards a mechanistic understanding of isotope fractionation and mixing processes from the leaves to the wood. *Tree Physiol* 34(8):796–818
- Grams TE, Kozovits AR, Häberle KH, Matyssek R, Dawson TE (2007) Combining  $\delta^{13}\text{C}$  and  $\delta^{18}\text{O}$  analyses to unravel competition,  $\text{CO}_2$  and  $\text{O}_3$  effects on the physiological performance of different-aged trees. *Plant Cell Environ* 30(8):1023–1034
- Grissino-Mayer HD, Fritts HC (1997) The International Tree-Ring Data Bank: an enhanced global database serving the global scientific community. *Holocene* 7(2):235–238
- Guiot J, Boucher E, Gea-Izquierdo G (2014) Process models and model-data fusion in dendroecology. *Front Ecol Evol* 2(52)
- Hemming D et al (2001) Modelling tree-ring  $\delta^{13}\text{C}$ . *Dendrochronologia* 19:23–38
- Kahmen A et al (2008) Effects of environmental parameters, leaf physiological properties and leaf water relations on leaf water  $\delta^{18}\text{O}$  enrichment in different Eucalyptus species. *Plant Cell Environ* 31(6):738–751
- Kahmen A et al (2011) Cellulose ( $\delta^{18}\text{O}$ ) is an index of leaf-to-air vapor pressure difference (VPD) in tropical plants. *Proc Natl Acad Sci USA* 108(5):1981–1986
- Kattge J et al (2020) TRY plant trait database—enhanced coverage and open access. *Glob Chang Biol* 26(1):119–188
- Keel SG et al (2016) Simulating oxygen isotope ratios in tree ring cellulose using a dynamic global vegetation model. *Biogeosciences* 13(13):3869–3886
- Keeling RF et al (2017) Atmospheric evidence for a global secular increase in carbon isotopic discrimination of land photosynthesis. *Proc Natl Acad Sci USA* 114(39):10361–10366
- Keller KM, et al (2017) 20th century changes in carbon isotopes and water-use efficiency: tree-ring-based evaluation of the CLM4.5 and LPX-Bern models. *Biogeosciences* 14(10):2641–2673
- Klein T et al (2005) Association between tree-ring and needle  $\delta^{13}\text{C}$  and leaf gas exchange in *Pinus halepensis* under semi-arid conditions. *Oecologia* 144(1):45–54
- Landsberg JJ, Waring RH (1997) A generalised model of forest productivity using simplified concepts of radiation-use efficiency, carbon balance and partitioning. *For Ecol Manag* 95(3):209–228
- Lavergne A et al (2017) Modelling tree ring cellulose  $\delta^{18}\text{O}$  variations in two temperature-sensitive tree species from North and South America. *Clim Past* 13(11):1515–1526
- Lehmann MM et al (2018) The effect of  $^{18}\text{O}$ -labelled water vapour on the oxygen isotope ratio of water and assimilates in plants at high humidity. *New Phytol* 217(1):105–116

- Lehmann MM et al (2020) The  $^{18}\text{O}$ -signal transfer from water vapour to leaf water and assimilates varies among plant species and growth forms. *Plant Cell Environ* 43(2):510–523
- Lin W, et al (2019) Using  $\delta^{13}\text{C}$  and  $\delta^{18}\text{O}$  to analyze loblolly pine (*Pinus taeda L.*) response to experimental drought and fertilization. *Tree Physiol* 39(12):1984–1994
- Loucos K, Simonin K, Song X, Barbour M (2015) Observed relationships between leaf  $\text{H}_2^{18}\text{O}$  Peclet effective length and leaf hydraulic conductance reflect assumptions in Craig-Gordon model calculations. *Tree Physiol* 35:16–26
- Marshall J, Monserud R (1996) Homeostatic gas-exchange parameters inferred from  $^{13}\text{C}/^{12}\text{C}$  in tree rings of conifers. *Oecologia* 105(1):13–21
- McCarroll D, Loader NJ (2004) Stable isotopes in tree rings. *Quat Sci Rev* 23(7–8):771–801
- McDowell NG, Bond BJ, Dickman LT, Ryan MG, Whitehead D (2011) Relationships between tree height and carbon isotope discrimination. In: Meinzer FC, Lachenbruch B, Dawson TE (eds) Size- and age-related changes in tree structure and function. Springer, Netherlands, Dordrecht, pp 255–286
- Medlyn BE et al (2015) Using ecosystem experiments to improve vegetation models. *Nat Clim Chang* 5(6):528–534
- Medlyn BE et al (2016) Using models to guide field experiments: a priori predictions for the  $\text{CO}_2$  response of a nutrient- and water-limited native Eucalypt woodland. *Glob Chang Biol* 22(8):2834–2851
- Mencuccini M et al (2005) Size-mediated ageing reduces vigour in trees. *Ecol Lett* 8(11):1183–1190
- Misson L (2004) MAIDEN: a model for analyzing ecosystem processes in dendroecology. *Can J For Res* 34(4):874–887
- Monserud RA, Marshall JD (2001) Time-series analysis of  $\delta^{13}\text{C}$  from tree rings. I. Time trends and autocorrelation. *Tree Physiol* 21(15):1087–1102
- Offermann C et al (2011) The long way down—are carbon and oxygen isotope signals in the tree ring uncoupled from canopy physiological processes? *Tree Physiol* 31(10):1088–1102
- Ogée J, Brunet Y, Loustau D, Berbigier P, Delzon S (2003) MuSICA, a  $\text{CO}_2$ , water and energy multilayer, multileaf pine forest model: evaluation from hourly to yearly time scales and sensitivity analysis. *Glob Chang Biol* 9(5):697–717
- Ogée J et al (2003) Partitioning net ecosystem carbon exchange into net assimilation and respiration using  $^{13}\text{CO}_2$  measurements: a cost-effective sampling strategy. *Glob Biogeochem Cycles* 17(2):1070
- Ogée J et al (2009) A single-substrate model to interpret intra-annual stable isotope signals in tree-ring cellulose. *Plant Cell Environ* 32(8):1071–1090
- Panek JA, Waring RH (1997) Stable carbon isotopes as indicators of limitations to forest growth imposed by climate stress. *Ecol Appl* 7(3):854–863
- Raczka B, et al (2016) An observational constraint on stomatal function in forests: evaluating coupled carbon and water vapor exchange with carbon isotopes in the Community Land Model (CLM4.5). *Biogeosciences* 13(18):5183–5204
- Riley WJ, Still CJ, Torn MS, Berry JA (2002) A mechanistic model of  $\text{H}_2^{18}\text{O}$  and  $\text{C}^{18}\text{O}$  fluxes between ecosystems and the atmosphere: model description and sensitivity analyses. *Glob Biogeochem Cycles* 16(4):1095
- Riley WJ, Still CJ, Helliker BR, Ribas-Carbo M, Berry JA (2003)  $^{18}\text{O}$  composition of  $\text{CO}_2$  and  $\text{H}_2\text{O}$  ecosystem pools and fluxes in a tallgrass prairie: simulations and comparisons to measurements. *Glob Chang Biol* 9(11):1567–1581
- Risi C et al (2016) Hydrology current research the water isotopic version of the land-surface model ORCHIDEE: implementation, evaluation, sensitivity to hydrological parameters. *Hydrol Curr Res* 7:1–24
- Roden JS, Ehleringer JR (1999) Hydrogen and oxygen isotope ratios of tree-ring cellulose for riparian trees grown long-term under hydroponically controlled environments. *Oecologia* 121(4):467–477

- Roden JS, Ehleringer JR (1999) Observations of hydrogen and oxygen isotopes in leaf water confirm the Craig-Gordon model under wide-ranging environmental conditions. *Plant Physiol* 120(4):1165–1174
- Roden JS, Lin G, Ehleringer JR (2000) A mechanistic model for interpretation of hydrogen and oxygen isotope ratios in tree-ring cellulose. *Geochim Cosmochim Acta* 64(1):21–35
- Rogers A et al (2017) A roadmap for improving the representation of photosynthesis in Earth system models. *New Phytol* 213(1):22–42
- Running SW, Coughlan JC (1988) A general model of forest ecosystem processes for regional applications I. Hydrologic balance, canopy gas exchange and primary production processes. *Ecol Model* 42(2):125–154
- Samuels AL, Kaneda M, Rensing KH (2006) The cell biology of wood formation: from cambial divisions to mature secondary xylem This review is one of a selection of papers published in the Special Issue on Plant Cell Biology. *Can J Bot* 84(4):631–639
- Saurer M et al (2014) Spatial variability and temporal trends in water-use efficiency of European forests. *Glob Chang Biol* 20(12):3700–3712
- Scheidegger Y, Saurer M, Bahn M, Siegwolf R (2000) Linking stable oxygen and carbon isotopes with stomatal conductance and photosynthetic capacity: a conceptual model. *Oecologia* 125(3):350–357
- Scholze M, Kaplan JO, Knorr W, Heimann M (2003) Climate and interannual variability of the atmosphere-biosphere  $^{13}\text{CO}_2$  flux. *Geophys Res Lett* 30(2):1097
- Schulze E-D et al (2019) Dynamic global vegetation models. In: Schulze E-D et al (eds) *Plant ecology*. Springer, Berlin, Heidelberg, pp 843–863
- Skomarkova MV et al (2006) Inter-annual and seasonal variability of radial growth, wood density and carbon isotope ratios in tree rings of beech (*Fagus sylvatica*) growing in Germany and Italy. *Trees* 20(5):571–586
- Smith TM, Smith RL (2009) *Elements of ecology*, 7th edn. Benjamin Cummings, Pearson
- Song X, Barbour MM, Farquhar GD, Vann DR, Helliker BR (2013) Transpiration rate relates to within- and across-species variations in effective path length in a leaf water model of oxygen isotope enrichment. *Plant Cell Environ* 36(7):1338–1351
- Stangl ZR et al (2019) Diurnal variation in mesophyll conductance and its influence on modelled water-use efficiency in a mature boreal *Pinus sylvestris* stand. *Photosynth Res* 141(1):53–63
- Still CJ et al (2009) Influence of clouds and diffuse radiation on ecosystem-atmosphere  $\text{CO}_2$  and  $\text{CO}^{18}\text{O}$  exchanges. *J Geophys Res* 114:G01018
- Suits NS, et al (2005) Simulation of carbon isotope discrimination of the terrestrial biosphere. *Glob Biogeochem Cycles* 19(1):GB1017
- Ubierna N, Farquhar GD (2014) Advances in measurements and models of photosynthetic carbon isotope discrimination in  $\text{C}_3$  plants. *Plant Cell Environ* 37(7):1494–1498
- Ulrich DEM, Still C, Brooks JR, Kim Y, Meinzer FC (2019) Investigating old-growth ponderosa pine physiology using tree-rings,  $\delta^{13}\text{C}$ ,  $\delta^{18}\text{O}$ , and a process-based model. *Ecology* 100(6):e02656
- van der Sleen P, Zuidema P, Pons T (2017) Stable isotopes in tropical tree rings: theory, methods and applications. *Funct Ecol*
- Voelker SL et al (2016) A dynamic leaf gas-exchange strategy is conserved in woody plants under changing ambient  $\text{CO}_2$ : evidence from carbon isotope discrimination in paleo and  $\text{CO}_2$  enrichment studies. *Glob Chang Biol* 22(2):889–902
- Walcroft AS, Silvester WB, Whitehead D, Kelliher FM (1997) Seasonal changes in stable carbon isotope ratios within annual rings of *Pinus radiata* reflect environmental regulation of growth processes. *Funct Plant Biol* 24(1):57–68
- Wei L, Marshall JD, Zhang J, Zhou H, Powers RF (2014) 3-PG simulations of young ponderosa pine plantations under varied management intensity: why do they grow so differently? *For Ecol Manag* 313(2014):69–82
- Wei L et al (2014) Constraining 3-PG with a new  $\delta^{13}\text{C}$  submodel: a test using the  $\delta^{13}\text{C}$  of tree rings. *Plant Cell Environ* 37(1):82–100

- Wei L et al (2018) Forest productivity varies with soil moisture more than temperature in a small montane watershed. *Agric for Meteorol* 259:211–221
- Zweifel R, Sterck F (2018) A conceptual tree model explaining legacy effects on stem growth. *Front For Glob Chang* 1(9)

**Open Access** This chapter is licensed under the terms of the Creative Commons Attribution 4.0 International License (<http://creativecommons.org/licenses/by/4.0/>), which permits use, sharing, adaptation, distribution and reproduction in any medium or format, as long as you give appropriate credit to the original author(s) and the source, provide a link to the Creative Commons license and indicate if changes were made.

The images or other third party material in this chapter are included in the chapter's Creative Commons license, unless indicated otherwise in a credit line to the material. If material is not included in the chapter's Creative Commons license and your intended use is not permitted by statutory regulation or exceeds the permitted use, you will need to obtain permission directly from the copyright holder.



# Index

## Symbols

$\Delta^{13}\text{C}$ , 276–279, 283, 298, 300–301, 434, 484, 682

$\delta^{13}\text{C}$ , 208, 261–263, 275–278, 292–305

$\delta^{15}\text{N}$ , 11, 201, 210, 361–363, 365–374, 464, 595, 608, 618, 619, 641, 642, 652, 656, 663, 664, 680, 681, 694, 695, 697, 698

$\Delta^{18}\text{O}$ , 317, 318, 320, 435–436

$\delta^{18}\text{O}$ , 311–313

$\delta^2\text{H}$ , 335–337, 341, 342

(R)-position, 258

(S)-position, 258

$^{13}\text{C}$  NMR, 176, 234

$^{14}\text{C}$ , 23, 28, 31, 255, 293

$^{17}\text{O}$ , 205, 207, 239, 256, 257, 260

$^{18}\text{O}$ , 205, 208, 224, 233, 239

$^1\text{H}$ , 205, 208, 259, 266, 267, 269, 275

$^2\text{H}$ , 205

3-PG model, 665, 749

$^3\text{H}$ , 267

## A

*Abies*, 22, 77, 87, 140, 170, 353, 546, 554, 611, 714, 715, 719, 720, 739

Abiotic, 312, 313, 332, 354, 652, 729

Accuracy, 28, 117, 191–197, 199–202, 204, 205, 207, 210, 211, 226, 232, 313, 342, 363, 391, 503, 539

Acetyl-CoA, 233, 281, 282

Acidification, 372, 677, 692

Activation energy, 267–270, 272, 273

Active Soil Layer (ASL), 584, 588

Adaptation, 174, 224, 315, 472, 586, 608, 610, 614, 615, 617, 652, 654

Advection, 320

Aerodynamic, 678

Age-related-effect, 106

Age/size trend, 33–36, 39, 40

Airborne, 676, 693, 694, 697, 698

Air quality, 676

Air temperature, 80, 82, 104, 167, 312, 313, 319, 405, 408, 409, 492, 556, 562, 583, 592, 687

Albedo, 582

Aldehyde, 281

Aldolase, 233, 336, 382, 384, 387, 390

Aleppo pine (*Pinus halepensis*), 552, 609, 611, 618, 657, 744

Allocation, C-allocation, below-, above-ground allocation, 690, 713

$\alpha$ -cellulose, 105, 106, 110, 111, 117–120, 122, 123, 126, 136, 137, 163

Amino acids, 233, 363, 364, 366, 369, 680, 695

Ammonia, 363

Ammonification, 366, 370

Analytical error, 191, 193, 277, 516

Angiosperm, 21, 22, 25, 27, 32, 63, 65, 67–69, 75, 80, 81, 85, 86, 90, 113, 139, 169, 227, 386, 389, 391, 590, 591

Anthropogenic, 7, 28, 34, 39, 46, 361, 365, 366, 371–373, 410, 493, 563, 589, 619, 642, 675, 680, 694, 695, 697

Anthropogenic forcing, 492

Apparent fractionation, 324

Archival systems, 361, 373

Arctic Bell Heather, 547

Arctic oscillation, 547, 595

Arginine, 369

ARSTAN, 37, 42, 47

Asparagine, 369

Aspen leaf miner, 713, 726

Assimilates, 61, 81, 89, 222, 224, 334, 335, 349, 351, 354, 361, 363, 367, 368, 372, 381–385, 387–389, 399, 405, 408, 410, 411, 413–418, 470, 473, 557, 591, 616, 676, 679, 688, 689, 691, 714

Assimilation, 10, 224, 291, 292, 362, 363, 365, 367–370, 372, 373, 382, 403, 409, 413, 416, 418, 431, 432, 434, 436, 439, 442, 452, 472, 474, 481, 482, 486, 524, 542–544, 546, 590, 613, 615, 618, 694, 695, 697, 698, 715, 716

Atlantic, 557, 639

Atmospheric CO<sub>2</sub>, 6–8, 10, 104, 107, 108, 137, 236, 237, 291–301, 304, 305, 372, 401, 414, 418, 464, 483, 487, 488, 493, 540, 543, 551, 552, 592, 606, 613, 636, 638, 642, 676, 682–684, 686, 687, 743, 746

Atom fraction, 260, 261, 263

Atomic weight, 208, 255, 256

Autotrophic, 279, 337, 347, 351, 411, 418, 438

Auxins, 69, 72, 73, 83

**B**

Back-diffusion, 320, 406, 665, 744

Backward reaction, 270, 279, 281, 283, 284

Bark, 32, 64, 69, 164, 170, 182, 369, 386, 387, 444, 717, 722, 723

Bark photosynthesis, 323, 381, 383, 386

Basal Area Increment (BAI), 486, 489, 659

Betula pendula, 694

Bicarbonate, 271, 280

Binding enthalpy, 266, 269–271

Bond dissociation, 266

Brendel-method, 160, 172, 174

Biodiversity hotspot, 611

Biosphere, 108, 237, 292, 482, 492, 540, 750

Biosynthesis, 69, 72, 139, 233, 259, 279, 281, 282, 332, 335–337, 351

Biotic, 312, 332, 354, 652, 729

Blue intensity, 404, 464

Boiling point, 174, 264

Bond enthalpy, 269, 270

Bond formation, 266, 269

Bond length, 268, 269

Bond stiffness, 271

Boreal, Boreal forests, 78, 401, 411, 494, 518, 542, 546–548, 554, 581, 582, 584, 593, 641

Boundary layer conductance, 659

Brazil, 550, 562, 632, 639

Broad leaf, 141, 224, 346, 384, 389, 657

Budburst, 78–81, 123, 416

Bulk leaf water, 312, 319, 436, 466, 744

Bulk sugar<sup>13</sup>C, 221

Bulk wood, 67, 89, 90, 136, 139–141, 163–167, 169, 170

**C**

C3, 230, 235, 236, 294, 300, 301, 304, 382, 540, 544

C4, 241, 642, 686

Calibration, 26, 28, 121, 191–196, 200–207, 209–211, 292, 342, 354, 524, 550, 553, 739, 740

Cambial activity, 74–76, 78, 81–83, 123, 400, 408, 411, 414, 416, 417, 433, 438, 441, 473, 550, 611, 617, 619

Cambial cell, 29, 67–69, 72, 73, 76, 78, 87, 747

Cambium, 12, 62–64, 68, 69, 72, 73, 75, 76, 78, 81–83, 89, 225, 385, 387, 412, 417, 437, 442, 445, 447, 448, 617, 747

Canada, 90, 374, 507, 511, 542, 547, 560, 581–584, 592, 594, 595, 656, 692, 749

Canopy coupling, 659

Canopy dominant trees, 34, 105–109, 492

Canopy interception, 508

Canopy position, 34, 107, 472, 523

Canopy temperature, 651

Carbohydrates, 42, 72, 89, 113, 114, 137, 140, 216–219, 221–225, 231, 232, 292, 296, 324, 332, 334, 336–338, 341, 344, 348, 353, 381, 384, 411, 413, 415, 416, 429, 432, 433, 438, 443, 445, 446, 452, 453, 466, 473, 490, 491, 591, 616, 740, 744, 747

Carbon allocation, 86, 302, 409, 416, 432, 433, 443, 738, 742, 749

Carbon assimilation, 89, 105, 399, 400, 445, 452, 465, 467, 469, 470, 472, 610

Carbon cycle, 7, 108, 582, 642

Carbon dioxide, 275, 280, 437, 544, 551, 675, 712

Carbonic anhydrase, 274



- Carbon isotope, 6, 7, 10, 41, 67, 104, 110, 141, 163, 195, 196, 228, 255, 261–263, 266, 271, 280, 292, 381, 382, 384, 388, 390, 430, 443, 446, 450–452, 463, 467, 472, 474, 481–484, 486, 487, 489–492, 537, 539–552, 559, 581, 590, 591, 595, 612, 613, 636, 652, 655, 658, 662, 665, 682, 683, 688, 691, 746
- Carbon isotope discrimination ( $\Delta^{13}\text{C}$ ), 303
- Carbon isotope fractionation, 10, 12, 274, 275, 381, 384, 390, 464, 468, 473, 482
- Carbon isotopic ratio, 104
- Carbon sink, 400, 410, 411, 417, 493, 549
- Carbon sources, 384, 410, 413, 417
- Carbon starvation, 490, 491, 615, 616
- Carbon storage/reserves, 42, 62, 63, 78–81, 89, 113, 114, 140, 219–221, 232, 349, 351, 353, 354, 365, 369, 381, 405, 415, 473, 490, 518, 637, 713, 721, 729, 738, 744, 747, 749
- Carbon use, 383, 389, 449, 451, 452
- Carbonyl bonds, 105
- Carbonyl exchange, 105, 241, 322, 323, 436
- Carbonyl group, 138, 312, 322
- Carboxylation, -decarboxylation, 237, 291, 300, 301, 381, 434, 612, 643, 682, 691, 693, 743
- Carryover effects, 443
- Cedrela odorata*, 174, 562, 635, 636
- Cell differentiation, 62, 63, 66, 68, 69, 71, 77, 78, 84, 88, 414, 442
- Cell division, 66, 68, 69, 72, 73, 76, 78, 87, 90, 409, 411, 441, 713, 723, 747
- Cell enlargement, 27, 69, 72, 73, 76, 78, 85–88, 113, 115, 411, 415, 441, 442
- Cell maturation, 66, 68, 415
- Cell turgor, 384, 417
- Cellulose, 110
- Cellulose deposition, 438
- Cellulose extraction, 72, 105, 115, 118, 119, 135, 136, 163, 169, 170, 172–174, 176, 177, 180–182, 192, 194, 195, 197, 199, 207, 210, 217, 225–227, 230, 416, 539, 607
- Cellulose (holocellulose,  $\alpha$ -cellulose), 105, 136, 163, 174
- Cell Wall Thickness (CWT), 24, 26, 85, 86, 441, 594, 689
- Centrifugation, 174, 222, 264, 339
- Cessation, 69–71, 76, 78, 79, 82, 83, 124, 409, 412, 416, 441, 550
- Chemical bleaching, 176, 182
- Chemical bond, 233, 257, 260, 265–273, 280, 281
- Chemical composition, 168, 183, 210, 432, 438
- Chemical equilibrium, 270, 273, 274, 279, 280
- Chemical extraction, 103, 110, 116–120, 168, 169, 176, 182, 541
- Chemical pretreatment, 7, 173, 369, 659, 660
- Chiral, 258
- Chloroplast, 282, 291, 300–302, 336, 382, 431, 434, 474, 678, 750
- Chromatographic separation, 217
- Chronical, 372
- Chronology, chronologies, 12, 21, 42, 47, 112, 113, 116, 182, 217, 221, 332, 335, 342, 347, 348, 351, 354, 403, 489, 546, 553, 558, 560–562, 581, 583–585, 588–595, 712, 729, 739, 750, 751
- Circumpolar zone, 595
- Climate change, 120, 121, 482, 483, 538, 549, 552, 553, 563, 582, 608, 618, 619, 641, 642, 651, 652, 685, 688, 711, 729
- Climate maladaptation, 654
- Climate model, 489, 545, 548
- Climate proxy, 166, 254, 341, 506, 538–540, 549, 583
- Climate reconstruction, 27, 33, 170, 222, 341, 354, 405, 407, 539–541, 544, 546, 557, 558, 582, 589, 596, 640, 721
- Climate signals, 34, 39, 47, 106, 114, 116, 164, 166, 167, 169, 220, 399, 407, 409, 418, 433, 537, 542, 544, 548, 553–557, 561, 713, 727, 751
- Climate warming, 489, 582–584
- Climatology (paleoclimate, paleoclimatology), 6, 48, 106, 537, 545, 561
- Cloud condensation temperature, 593
- Clumped isotopes, 260
- CO<sub>2</sub>, 201, 217, 218, 229, 235–237, 271
- Commission on Isotopic Abundances and Atomic Weights (CIAAW), 205, 208, 209, 256
- Competition, 105, 106, 108, 183, 236, 401, 487, 607, 614, 615, 618, 651, 655, 656, 662, 687, 688, 717, 719, 726

- Compound Specific Isotope Analysis (CSIA), 216–221, 225, 418, 591, 596
- Comprehensive model, 743, 747
- Conceptual model, 463, 464, 467–470, 473–475, 510, 616, 738
- Condensation, 9, 123, 265, 274, 313, 332, 333, 405, 465, 466, 508, 556, 558, 592
- Conductivity, 607, 611, 612, 616, 617, 716
- Conservative strategy, 490
- Constitutional isotopomer, 257–259
- Constrain physiological interpretations, 464
- Continental, 313, 314, 319, 334, 344, 350, 372, 465, 470, 483, 506, 511, 546, 632
- Continuum, 316, 374, 491, 612
- Conversion, 72, 79, 182, 200, 201, 207, 222, 223, 231, 240, 241, 281, 282, 292, 322, 323, 385, 405, 438
- Correlation coefficient, 30, 43, 165, 167, 237, 314, 722, 746
- Costa Rica, 550, 562, 640
- CO<sub>2</sub>- assimilation, -concentrations, -fixation, -compensation point, 10, 107, 217, 236, 291–299, 301, 303, 305, 351, 381, 382, 390, 401, 414, 431, 434, 439, 464, 472, 474, 475, 482, 483, 487, 488, 493, 543, 551, 552, 590, 636, 638, 678, 679, 682–684, 686, 687, 690, 715, 743
- Craig-Gordon model, 316, 317, 319, 320, 335, 435, 467, 738
- Cross date (Cross dating), 347, 550, 563
- Cross sections, 70, 172, 227
- Cryoprotection, 221
- Cuticle, 610, 689
- Cyclitols, 215, 217–219, 221–225
- Cytokinin, 69, 73, 715, 716
- Cytosol, 434, 678
- D**
- Dalton, 256
- Decarboxylation, 267, 282
- Deciduous, 75, 78–81, 113, 323, 349, 351, 352, 363, 365, 368–370, 372, 383, 387, 389, 391, 416, 438, 439, 448–450, 452, 493, 526, 590, 593, 611, 631–633, 639, 653, 696, 714, 721
- Decode, Decoding, 405, 547
- Decouple, 83
- Defoliate (Defoliation, Defoliators), 714, 720, 721, 725
- Degradation, 105, 170, 171, 175, 176, 254, 260, 332, 339, 341, 370, 689
- Dehydration, 279, 283, 322
- Dendroarchaeology, 31, 48
- Dendrochronology, 3, 4, 7, 8, 13, 21–23, 25, 28, 29, 31, 33–35, 40–42, 47, 48, 107, 550, 559, 583
- Dendroclimatology, 26, 31, 88, 107, 137, 169, 174, 354, 452, 538–543, 549–551, 553, 554, 557, 558, 561, 563
- Dendroecology, 31, 48
- Dendrometers, 27, 63, 231, 389, 524, 612
- Denitrification, 366, 370, 618, 619, 641
- Density, tree density, 656
- Depth profile, 519
- Detoxification, 690, 691, 693
- Detrending, 21, 30, 34, 35, 37–42, 107, 486, 544
- Deuterium, 233, 234, 255, 332, 341, 464, 588, 595
- Deuterium excess (d-excess), 504, 513
- Diatomic, 269
- Diffuse-porous, diffuse-porous wood, 65, 75, 78, 80, 81, 86, 416
- Diffusion, 125, 237, 264, 265, 274, 300, 301, 320, 335, 406, 433–435, 444, 466, 468, 483, 520, 521, 665, 682, 743, 744
- Diglyme-HCL, 172, 174, 182
- Discrimination, 37, 41, 107, 221, 291–293, 297, 298, 300, 301, 382, 389–391, 404, 467, 468, 470, 472, 474, 484, 489, 541, 543, 544, 552, 587, 612, 613, 637, 652, 656–658, 661, 662, 665, 682, 691, 747
- Dissection, 11, 136, 172, 181, 226–228, 231, 430
- Distillation, 223, 264, 313, 503, 522, 588
- Divergence Problem (DP), 544, 583
- Diversity, 13, 48, 322, 372, 472, 474, 697, 718
- Dormancy, 74, 75, 79, 314, 550, 610, 617
- Double stress, 611, 617
- Douglas-fir (*Pseudotsuga menziesii*), 110, 472, 519, 654, 655, 658, 662, 663, 720–722, 724, 728, 746
- Drought, 9, 10, 25, 29, 35, 65, 73, 79, 83, 88, 104, 105, 141, 182, 221, 224, 225, 370, 389, 391, 400, 401, 403, 406, 409, 411, 414, 416–418, 432,

- 433, 440, 464, 470, 471, 473,  
481–483, 486, 489–492, 494, 542,  
543, 545, 546, 551, 555, 558, 559,  
581, 586, 587, 595, 606, 608–617,  
631, 633, 636, 637, 654–657, 663,  
697, 716, 717, 720, 722–727, 745
- Drought-related decline, 724
- Drought resilience, 657
- Drought response, 652, 657, 697
- Drought stress, 27, 224, 489–492, 552, 583,  
584, 610, 617, 656, 688, 697, 720,  
722–724, 729
- Drought tolerance, 636, 653
- Dual-isotope, 11, 436, 463, 464, 465,  
467–475, 504, 513
- Dual-isotope approach, 224, 463, 464, 467,  
469–472, 474, 475, 513, 613, 640,  
679, 689, 719, 728
- Duplicates (duplication), 191–193,  
197–199, 202, 204, 210, 211
- Dynamic Global Vegetation Model  
(DGVMS), 12, 492–494, 642, 750,  
751
- E**
- Earlywood (EW), 11, 21, 24–26, 64, 65, 73,  
80, 81, 86, 88, 89, 110, 111,  
113–116, 121, 122, 140, 163, 199,  
349, 350, 391, 404, 415, 416, 430,  
432, 433, 438–441, 443–446, 451,  
452, 473, 560, 590, 591, 617, 655,  
663
- Earlywood/latewood, 11, 21, 24, 25, 81, 82,  
103, 105, 113, 117, 121, 122, 415,  
432, 590, 591, 617, 655, 663, 721
- Ecohydrology, 346, 505, 512
- Ecophysiology, 4, 10, 40, 103, 106, 108,  
126, 312, 332, 333, 346, 347, 354,  
412, 590, 592, 607, 636, 638, 641,  
664, 688
- Ecosystem-level WUE, 486
- Ecosystem services, 619, 642, 652
- Ectomycorrhiza (ecm), 364, 367, 368, 370,  
372, 373, 697
- Eddy-covariance, 108, 486, 677, 681
- Electrolysis, 264
- Electron shell, 254, 255, 265
- Elemental analyzer, 9, 200, 277, 680
- El Niño Southern Oscillation (ENSO), 9,  
546, 556, 560, 562, 633–635, 637,  
640
- Elution, 218
- Embolism, 65, 612
- Emissions, 293, 361, 365, 366, 371, 372,  
484, 492, 675, 676, 680, 681,  
692–695, 697
- Enantiomer, Enantiomeric, Enantiotropic,  
258
- Endogenous disturbance, 34
- Endothermic, 272, 280
- Energy balance, 582, 681
- Environmental fingerprints, 23, 399
- Environmental stressors, 400, 403, 408
- Enzymatic activity, 219, 283
- Enzyme, -enzymatic, 8, 69, 83, 137, 139,  
171, 233, 235, 259, 273, 274, 281,  
282, 300, 368, 384, 386, 390, 434,  
442
- Epiphyte, 317
- Epoch, 314
- $\epsilon^{13}\text{C}$ , 277
- Equilibrium constant, 266, 270, 275, 279,  
280, 283
- Equilibrium fractionation, 313, 317, 504,  
513
- Equilibrium Isotope Effect (EIE), 138, 233,  
253, 266, 267, 270, 271, 273, 274,  
276, 279, 280, 283, 344
- Error, 30, 31, 34–36, 45, 46, 116, 165, 191,  
192, 199–207, 210, 211, 241, 261,  
432, 511, 696, 740
- Ethanol (etoh), 173, 174, 230, 231, 258
- European black pine (*Pinus nigra*), 148,  
156, 236, 611, 657
- Evaporation (evaporation fractionation,  
evapo-concentration), 8–10, 67, 265,  
274, 317, 332–335, 344, 405–406,  
466, 504, 508, 510, 513–517, 521,  
525–526, 556, 592–593, 639, 738,  
744, 749
- Evaporative enrichment, 104, 114, 123,  
124, 316, 440, 466, 467, 470, 515,  
516, 518, 524–526, 551, 557,  
560–562, 614, 722, 744, 747
- Evaporative site, 317, 319, 320, 406
- Evapotranspiration (ET), 241, 315, 485,  
582
- Evergreen, 74, 75, 79–81, 83, 323, 349,  
351, 352, 389, 391, 414, 439, 441,  
445, 448, 452, 590, 632, 633, 639,  
653, 714, 721
- Exogenous disturbance, 34, 36
- Exothermic, 272
- Expressed Population Signal (EPS), 44–46,  
109
- Extraction, 34, 119, 135–138, 169, 172,  
174–177, 180, 182, 194, 195, 200,  
202, 219, 223, 230, 338, 541, 739

Extractives, 71, 72, 135–137, 140, 141,  
163–170, 173, 174, 182  
Exudation, 219

## F

Fagus, 114, 546, 611  
*Fagus grandifolia*, 362, 368, 370, 371  
*Fagus sylvatica*, 80, 371, 383, 388, 555,  
691, 744  
False Latewood Bands (FLBs), 121,  
123–125  
Fatty acids, 137, 140, 182, 282  
Fennoscandia (Fennoscandian), 546, 547,  
558, 581, 582, 584, 591  
Fertilization (Fertilizing), 38, 363, 368,  
369, 465, 472, 553, 606, 613, 619,  
651, 652, 657, 660–665, 675, 680,  
683, 693, 695, 696  
Fibers, 23, 115, 119, 120, 714  
Fire scars, 29, 33  
Fischer projection, 258  
Flooding, 400, 631, 633, 697  
Fog, 114, 125, 401, 406, 509, 554  
Foliar uptake, 363–365, 520, 521  
Foliar water uptake, 453, 454  
Forams, 7  
Force constant, 268, 270, 271  
Forest dynamics, 401  
Forest health, 492  
Forest Management (management), 39,  
320, 613, 651–653, 664, 665, 729,  
749  
Forest productivity, 12, 25, 108, 618, 652  
Forest-steppe zone, 581, 589  
Forest vulnerability, 615  
Forward reaction, 274, 279, 281  
Fossil, 6, 7, 170, 181, 291, 293, 349, 443,  
450, 484, 560, 728, 743  
Fossil fuel emissions, 293, 296  
Fossil wood, 6, 116, 135, 164, 170, 351  
Fourier-Transformation-Infra-Red  
spectrometry (FTIR), 174, 176, 230  
Fractionation processes, 9, 216, 312, 334,  
354, 383, 391, 403, 405, 431, 433,  
434, 438, 464–466, 501, 503, 521,  
524, 593, 616, 619, 688  
Frederick Soddy, 255  
Free Air Carbon Dioxide Enrichment  
(FACE), 174, 443, 552, 610, 643,  
683, 685, 688, 750  
Free energy, 267, 270, 281  
Frost-rings, 29, 31

Fructose, 70, 218, 220–222, 322, 337, 382,  
387  
Fungal pathogen, 721, 724  
Fungi, 140, 170, 171, 366, 367, 664, 697,  
698, 711, 712, 715–717, 721, 722,  
724

## G

Gas exchange, -measurement, 108, 303,  
469, 696  
GC-C/TC-IRMS, 137, 171  
GC/Pyrolysis-IRMS, 216  
Genetic Selection, 651  
Genotype, 73, 651, 653, 654, 665  
Geographic scale, 314, 319  
Gibberellins, 69, 73, 82  
Gibbs energy, 270  
Glacial, 7, 314, 347, 557  
Glacial period, 506, 687  
Global map, 333, 343, 352  
Global Meteoric Water Line (GMWL), 345,  
346, 504, 513, 588  
Global Network of Isotopes in Precipitation  
(GNIP), 507, 509, 593  
Grinding, 118, 168, 181, 182, 197, 202  
Gross primary production, 485, 749  
Groundwater, 123, 333, 334, 506, 509, 510,  
515, 519, 522–525, 552, 613, 614,  
638  
Growth period, 403, 431, 689  
Growth rates, 26, 37, 39, 80, 105, 199, 227,  
232, 349, 350, 363, 400, 402, 409,  
412, 432, 464, 490  
Guyana, 550, 562, 636, 639  
Gymnosperms, 21, 22, 25, 32, 63, 64, 67,  
69, 80, 113, 139, 169, 391, 552, 590,  
591

## H

Heartwood, 26, 68, 71, 72, 138, 140, 163,  
164, 167, 170, 182, 362, 414, 717  
Heavy atom isotope effect, 267, 282  
Hemicellulose, 65–67, 70, 72, 105, 136,  
137, 139, 175, 176, 222, 449  
Herbaceous, 351, 384, 469, 472, 610, 686,  
691  
Herbicide, 652, 654–656, 665  
Heterogeneity, 72, 366  
Heterotrophic, 239, 279, 337, 347, 351,  
352, 382, 411, 418  
Heterotrophic cellulose synthesis, 241, 242

- Hexoses, 218, 221–225, 322, 323, 336, 390, 436
- High Performance Liquid Chromatography (HPLC), 216–218, 220
- Holocellulose, 172, 175, 446
- Holocene, 347, 617, 687
- Homeostasis, 659
- Homogeneity (Homogenization), 39, 116–118, 126, 136
- Hormonal regulation, 711–713, 715, 718
- Hormones, 69, 72, 73, 75, 411, 715, 716
- Host, 34, 351, 367, 711–713, 715, 716, 718–729
- Humidity, 8, 9, 11, 124, 204, 223, 316, 332, 334, 350, 401, 406, 407, 418, 433, 434, 465, 470–474, 504, 522, 553, 556, 557, 559, 560, 562, 563, 587, 590, 593, 595, 634, 639, 677, 688, 689, 722
- Hydration, 270, 279, 281, 283, 322
- Hydraulic efficiency, 611
- Hydraulic failure, 490, 491, 615, 616, 716
- Hydraulic redistribution, 520
- Hydraulic resistance, 107, 469, 487, 612, 636
- Hydrogen isotope fractionation, 277, 336, 429, 437, 582
- Hydrogen isotope ratio (Hydrogen Isotopes), 165, 171, 181, 195, 208, 209, 217, 239, 255, 262, 264, 269, 270, 272, 275, 331, 332, 334, 335, 337, 344, 347, 429, 430, 432, 437, 440, 446, 452, 453, 595, 653, 747
- Hydrological regime, 593
- Hydrolysis, 68, 138, 239, 241, 242, 267, 366
- Hydrophilic, 222
- Hydrophobic, 71, 222
- Hydroxyl, 195, 201, 222, 258, 338, 339
- I**
- Iberia, 542, 558
- Ice core, 7, 293–295, 298, 299, 304, 373, 562, 641
- Identical Treatment Principle (IT Principle), 194, 195, 204, 209, 210
- Immobilization, 366
- Incremental growth, 316
- Increment borer, 32, 105, 110–112
- India, 558, 640
- Indonesia, 550, 562, 640
- Industrial revolution (Industrialization), 293, 304, 675, 682, 686, 692, 693
- Infection, 170, 715, 716, 718–720, 722, 724, 726
- Infestation, 34, 717–721, 724, 726, 727, 729
- Infiltration, 315, 407, 433, 509, 510, 525
- Infrared spectrometry, 176, 317
- Inhomogeneity, 47, 241, 342
- Injury, 29, 677, 690
- Insect, 4, 10, 25, 33–35, 140, 582, 656, 692, 711–729
- Instrument drift, 203
- Integrated metabolic strategy, 474
- Intercellular CO<sub>2</sub> concentration, 743
- Interglacial, 7, 314
- International Atomic Energy Agency (IAEA), 205, 207–210, 230, 342, 507, 522
- International scale (d scale), 193, 200, 204, 205, 208, 263
- International System of Units (SI), 206, 208, 260, 261
- International Union of Pure and Applied Chemistry (IUPAC), 208, 254–256, 259, 260, 262, 276, 449
- Internuclear distance, 269
- Inter-series correlations, 109
- Inter-tree differences, 109
- Inter-tree variability, 109
- Intra-Annual Density Fluctuation (IADF), 88, 113, 121, 123, 124, 411, 412, 432, 442, 607, 611, 612, 616, 617
- Intra molecular, 11, 215, 216, 233–235, 237, 239, 259, 266, 267, 341, 381, 390, 391, 643
- Intra-molecular isotope distribution, 390
- Intramolecular, 259, 266–267, 390–391, 643
- Intra-tree differences (intra-tree variability), 109, 122
- Intrinsic Water Use Efficiency (iWUE), 11, 104, 107, 108, 293, 300, 391, 439, 440, 474, 481–494, 543, 544, 546, 551–553, 606–608, 613, 616, 619, 634–636, 638, 653, 658, 661–663, 683, 689, 697, 716, 750
- Inverse isotope effect, 266
- Inverse modeling, 749, 751
- Invertase enzymes, 221
- Irradiance, 401, 405, 636, 659
- Irreversible reaction, 271, 276, 281
- IR spectra, 266
- Isobar, 255
- ISOCASTANEA, 747

Isomerization, 218  
 Isotope exchange, 223, 254, 270, 274, 275, 279–281, 322, 323, 339, 473  
 Isotope fractionation, 6, 8, 12, 205, 210, 217, 221–223, 233, 234, 253, 254, 264, 267, 270, 273–280, 282–284, 332, 335, 339–341, 345, 382, 386, 403, 417, 431, 433, 437, 441, 442, 464, 465, 469, 481, 503, 556, 561, 636, 675, 693, 695, 722, 738  
 Isotope fractionation factor, 271, 275, 276, 280, 342  
 Isotope phi, 262, 263  
 Isotope Ratio Mass Spectrometers (IRMS), 6, 191–204, 206, 207, 209, 210, 216, 218–220, 222, 223, 225–232, 234, 239, 241, 261, 265, 267, 277, 339–341, 362, 464, 680  
 Isoscaples, 4, 12, 313  
 Isotope scale, 254, 262, 263  
 Isotope signature, 139, 140, 163, 167, 168, 170, 182, 317, 318, 391, 522, 524, 553, 638, 682, 688, 721, 729  
 Isotopically labelled, 254  
 Isotopically substituted, 254, 257  
 Isotopic decoupling, 417, 418, 473  
 Isotopic enrichment factor, 276  
 Isotopic equilibrium, 270, 274, 279, 280, 283, 317  
 Isotopic exchange, 105, 201, 241, 254, 270, 322, 323, 453, 747  
 Isotopic fractionation, 104, 114, 115, 216, 221, 239, 241, 254, 279, 312, 313, 337, 367, 368, 381, 400, 403, 404, 408, 413, 429, 431, 465, 517, 540, 547, 548, 558, 584, 592, 676, 680, 691, 697, 738, 748  
 Isotopic fractionation factor, 275  
 Isotopic integrity, 361  
 Isotopic mass, 239, 241, 254, 258, 269, 385  
 Isotopic noise, 242  
 Isotopic offset, 164  
 Isotopic separation, 254, 273  
 Isotopic substitution, 254, 266, 267, 269  
 Isotopic tracer, 254, 677  
 Isotopocule, 257, 260, 264–266, 270, 281  
 Isotopologue, 257, 264, 265, 268, 272, 273, 333, 335, 504, 517  
 Isotopomers, 11, 234–238, 257–259, 267  
 Isotope exchange, 280  
 IUPAC Gold Book, 266

## J

*Japanese red pine (Pinus densiflora)*, 656  
 Jayme-Wise method, 172, 174, 175  
 Juvenile effect, 440  
 Juvenile phase, 487

## K

Kenya, 550  
 Ketone, 281  
 Kinetic energy, 265  
 Kinetic fractionation, 317, 434, 435, 469, 473, 503, 513, 663  
 Kinetic Isotope Effect (KIE), 216, 221, 233, 253, 260, 266, 267, 272–274, 281–284  
 Kinetics, 62, 63, 84–86, 88, 115, 125, 137, 253, 254, 260, 265, 267, 269, 273–276, 283, 332, 335, 386, 435

## L

Lamina, 319, 320, 748  
 Larch budmoth, 713, 714, 720  
 Large-scale fluxes, 486  
*Larix*, 85, 219, 229, 416, 444, 449, 451, 546, 554, 584, 590, 591, 593, 715  
*Larix cajanderi* Mayr., 584  
*Larix decidua*, 219, 221, 351, 352, 554, 555, 561, 617, 688, 714  
*Larix gmselinii* Rupr. Rupr., 219, 230, 591  
*Larix sibirica* Ledeb., 584–587  
 Laser ablation (LA-IRMS), 11, 118, 119, 136, 225, 228–231, 389, 409, 415, 418, 430, 590, 591, 612  
 Laser Microscopic Dissection (LMD), 225–227, 229, 231, 232  
 Latewood (LW), 11, 21, 24, 25, 29, 31, 64, 65, 73, 81, 82, 85, 86, 88, 89, 110, 111, 113–116, 121, 122, 140, 349, 391, 404, 412, 415, 416, 430, 432, 433, 438–442, 444–446, 449, 473, 486, 488, 492, 541, 542  
 Leaching, 366, 370, 372, 619, 641, 664  
 Leaf area, 349, 494, 662, 663, 665, 713, 715, 716, 726, 727  
 Leaf Area Index (LAI), 291, 297, 552, 651, 663  
 Leaf-feeding, 711, 713, 719  
 Leaf gas exchange, 300, 302, 403, 410, 418, 487, 489, 502, 654, 662, 677, 683, 684, 687, 715, 718, 723, 725  
 Leaf nitrogen concentrations (foliar N), 651, 657, 662, 665

- Leaf organic matter, 469, 470, 472, 473, 695
- Leaf temperature, 312, 317–319, 405, 469, 556, 659, 660
- Leaf water, 62, 67, 104, 123–125, 138, 223–225, 239, 241, 274, 279, 311, 312, 316, 318, 319, 321–323, 334–337, 344, 349, 354, 406, 435–437, 440, 453, 466, 467, 470, 473, 521, 526, 552, 557, 559, 595, 612, 638, 654, 679, 722, 744, 747, 748, 751
- Leaf water enrichment, 123, 274, 316, 319, 320, 335, 406, 466, 526, 593, 643, 748
- Le Chatelier principle, 283
- Legacy effects, 489, 714, 744
- Lewis structure, 259
- Light compensation points, 107
- Lignification, 29, 67, 68, 70–73, 76, 78, 231, 370, 411, 415, 416, 747
- Lignin, 65–67, 70–73, 89, 105, 135–141, 163, 164, 167, 168, 170, 171, 174, 176, 182, 183, 195, 259, 260, 338, 341, 383–387, 417, 438, 449, 539
- Lignin impregnation, 67
- Linear Aggregate Model, 33, 35, 36, 40, 42
- Line-conditioned excess (lc-excess), 511, 513
- Lipids, 140, 282, 332, 383, 384, 414, 677
- Local meteoric water line (LMWL), 504, 513
- Lodgepole pine (Pinus contorta)*, 654, 655
- Logging, 12, 605
- M**
- Magnetic field, 265
- Maideniso, 749
- Malate, 386, 387
- Mangroves, 550, 562
- Maritime pine (Pinus pinaster)*, 617, 618, 657, 748
- Mass balance, 139, 141, 163, 167, 235, 262, 342, 384
- Mass-dependent isotope effect, 264
- Mass proportion, 136
- Maturation, 68, 74, 75, 78, 81, 82, 90, 120, 124, 125, 348, 349, 411, 431, 441, 453, 721
- Maximum Latewood Density (MXD), 24–26, 30, 33, 37, 46, 88, 403, 464, 543, 557, 582
- Mean Annual Precipitation (MAP), 343, 344, 351–353, 370, 509, 518, 609, 612, 632, 655, 657, 658, 660
- Measurement noise, 193
- Mechanistic model, 9, 312, 313, 337, 391, 453, 472–474, 483, 515, 558
- Mediterranean, 75, 82, 86, 88, 121, 166, 169, 406, 407, 409, 411, 412, 416, 432, 439, 442, 489, 490, 493, 511, 514, 542, 558, 605, 606, 608–619, 663, 697, 739
- Melting point, 174, 264
- Meristem, 75, 411, 414, 441
- Meristematic cells, 64
- Mesophyll, 221, 301, 383, 405, 435, 485, 610, 653, 678, 679, 683, 685, 691, 694
- Mesophyll conductance, -resistance, -membrane, 301, 405, 485, 653, 678, 683, 685, 694, 719, 743, 750
- Meta-analysis, 200, 206, 485, 652, 656, 657, 659, 661, 683, 686, 696
- Metabolic, 12, 64, 71, 137, 171, 217, 223, 233, 235, 237, 322, 323, 333, 350, 351, 383, 385–387, 437, 440, 442, 474, 490, 595, 748
- Metabolic branching, 12, 137, 139, 390
- Metabolic pathway, 67, 137, 235, 237, 332, 347, 381–383, 390, 539
- Metabolic processes, 216, 237, 382, 386, 400, 441, 442, 590, 695
- Metabolism, 63, 114, 137, 163, 279, 281, 292, 353, 383, 384, 386, 387, 390, 400, 437, 464, 465, 675, 695, 697, 698
- Metabolite, 65, 71, 137, 141, 182, 233–235, 387, 390
- Meteoric water, 8, 314, 344, 405, 437, 465, 466, 503–505, 513, 556, 560, 592, 614
- Methoxy group, 259, 260
- Methylation derivatization, 222
- Methylene group, 258
- Microbial activity, 370
- Microclimatic conditions, 487
- Microdissection, 225, 226, 228, 389
- Microtome, 31, 110, 115, 118, 119, 123, 226, 228, 230, 232, 362, 409, 415, 418, 430
- Middle lamella, 66, 67, 70, 72, 438
- Mills (milling), 118, 168, 181
- Mineralization, 366, 608, 618
- Mistletoe, 715–719, 727

- Mitochondria, 282, 302  
 Mobile water, 316  
 Mobility, 136, 230, 362, 369, 676, 680  
 Model assumptions, 472  
 Model constraints, 463  
 Model uncertainties, 473  
 Modulate (Modulating), 547, 677  
 Moisture, 7–10, 12, 23, 25, 34, 104, 182, 401, 403, 404, 407, 433, 471, 519, 542, 544–546, 550, 558–560, 562, 586, 590, 591, 633, 639, 652, 658, 663, 687  
 Molar volume, 264  
 Monomer, 140  
 Monomeric unit, 259  
 Monterey Pine (*Pinus radiata*), 349, 439, 471, 746  
 Morse potential, 268, 269  
 Mortality, 10, 29, 32, 74, 79, 401, 487, 490, 615, 653, 692, 712, 716–718, 721, 722, 724, 729  
 Multiple isotopes, 11, 463  
 Multiple stable isotope proxies, 581  
 MUr (Milli Urey), 208, 262, 263, 276–278, 280, 282  
 Mycorrhiza, 413, 520
- N**
- NADH, 281, 282  
 NaOH, 174–176  
 National Ecological Observatory Network (NEON), 509  
 National Institute of Standards and Technology (NIST), 196  
 Natural Abundance, 219, 239, 256, 260, 261, 365, 443, 632, 638  
 Natural abundance, 255  
 N compounds, 72, 368, 369, 371, 641, 675–677, 680, 693, 697, 698  
 Necroses, 690  
 Net primary productivity, 401  
 Neutron, 254, 255, 332  
 New Zealand, 6, 242, 314, 559, 746  
 NH<sub>4</sub><sup>+</sup>, 363, 364, 366, 368, 369, 371, 372, 619, 663, 693, 694  
 NH<sub>3</sub>, 675, 681, 693  
 Nitrate (NO<sub>3</sub> leaching, NO<sub>3</sub>-), 8, 62, 339, 342, 363, 364, 366, 368, 369, 372, 539, 618, 619, 641, 642, 664, 693, 694  
 Nitrate reductase, 368, 694  
 Nitration, 7, 331, 338, 339, 343
- Nitrification, 366, 370, 372, 618  
 Nitrogen deposition, 619  
 Nitrogen isotope ratios, 619, 652  
 Nitrous oxide, 257, 260  
 NO, 363, 693, 694, 697  
 N<sub>2</sub>O, 257, 362, 373  
 Non-isotope components, 464  
 Non-mass-dependent isotope effect, 264  
 Non-Structural Carbohydrate (NSC), 80, 113, 216, 349, 353, 413, 414, 416–418, 434, 438, 439, 449, 450, 490, 616  
 Normalization, 37, 195, 206, 207  
 North America, 403, 408, 486, 546, 692, 715, 717, 722  
 North Atlantic Oscillation (NAO), 554, 560, 593  
 NO<sub>x</sub>, 11, 619, 675, 676, 679, 681, 689, 693  
 Nuclear Magnetic Resonance (NMR), NMR spectrum, 234, 235  
 Nuclear mass, 264, 266, 270  
 Nuclear volume, 266  
 Nucleon, 254, 256  
 Nucleus, 239, 254, 255, 441, 449  
 Nuclide, 255, 256  
 Nutrient availability, 401, 407, 584, 638, 657  
 Nutrients, 63, 66, 73, 80, 361, 367, 372, 401, 402, 407, 414, 472, 551–553, 587, 588, 607, 618, 636, 651, 652, 654, 656, 661–663, 665, 679, 696, 698, 712, 714–716, 719, 724  
 Nutrient use, 711, 713, 718
- O**
- O<sub>3</sub>, 675–677, 679, 681, 689, 690  
 Oak, 78, 79, 164, 169, 170, 181, 220, 223, 224, 265, 348–350, 365, 369, 388, 417, 433, 440, 445, 446, 490, 514, 553, 557–559, 588, 611, 692, 716, 717, 726, 727, 749  
 Offset error, 203–205  
 Online Isotopes in Precipitation Calculator, 516  
 Organic acid, 217, 271, 387  
 Organic matter, 7, 221, 224, 321, 322, 331, 342, 366, 370, 381, 382, 388, 406, 448, 463–467, 469–471, 473, 474, 482, 486, 557, 590, 592, 605, 610, 675, 679, 680, 682, 688, 694, 695, 740  
 Organoleptic, 264



- Orographic lift, 506  
 Osmoregulation, 414, 417  
 Osmotic pressure, 69, 70, 73, 386, 417  
 Oxidation, 677  
 Oxygenation, 237, 643  
 Oxygen exchange, 241, 322–324, 688  
 Oxygen isotope fractionation, 222–224, 465, 467  
 Oxygen isotope ratios, 222, 238–240, 311, 313, 431, 435, 440, 464, 491, 557, 558, 689  
 Oxygen Isotopes, 12, 33, 40, 67, 89, 103, 104, 110, 138, 222, 223, 238, 241, 257, 260, 274, 280, 281, 312, 316, 320, 322–324, 332, 347, 399, 418, 437, 438, 440, 491, 537, 541, 550, 551, 553, 554, 557–561, 563, 581, 584, 589, 592–595, 607, 613, 615–618, 688  
 Oxygen isotope variation, 233, 452, 463, 466, 472, 557  
 Ozone, 11, 264, 418, 469, 473, 675–677, 689, 690, 693
- P**  
 Pakistan, 553  
 Palaeoclimate,-climatic, 171, 222, 332, 538, 546, 559  
 Paleophysiology, 126  
 Paleo, 344–347, 352, 353, 440, 506, 685, 687  
 Parameterize/parameterization, 316, 664, 665, 737–741  
 Parenchyma cells, 63–65, 68, 71, 72, 445, 449  
 Partial pressure, 335, 551, 552, 613, 679, 688  
 Particle size (particle size reduction, wood sample reduction), 117–120  
 Pathogen, 72, 490, 690, 711–713, 715–718, 720, 724–729  
 Péclet number, - effect, 436  
 Pedosphere, 361, 693  
 PEP carboxylase, 473, 677  
 Percolation, 512  
 Permafrost degradation, 582  
 Permafrost thaw, 584  
 Peroxyacetyl nitrate (PAN), 363, 548, 641  
 Perturbation, 373, 493, 661, 715  
 Pest, 490, 654, 692, 711, 712, 717, 727  
 Phenolic compounds, 219  
 Phenology, 73–75, 78–83, 126, 388, 389, 414, 415, 429, 431, 432, 441, 442, 524, 584, 591, 611, 612, 636, 638, 721, 745  
 Phenophase, 76, 79, 80, 231  
 Phloem, 62, 64, 69, 71, 74, 77, 78, 80, 81, 216, 219, 221, 225, 312, 321, 323, 324, 349, 381, 383–388, 390, 411, 412, 417, 431, 436, 442–445, 447, 448, 451, 453, 466, 470, 485, 557, 688, 695, 713, 715–717, 743, 744, 747  
 Phloem based single leaf method, 321  
 Phospho enol pyruvate (PEP), 473, 677  
 Phospho enol pyruvate carboxylase (PEPC), 219, 383, 386, 387, 390, 691, 695  
 Phosphorus, 401, 402  
 Photoassimilates, 113, 120, 123–125, 353, 382, 389, 403, 405, 408, 414–416, 442, 446, 447, 449, 451, 452, 591, 690  
 Photochemical, 677  
 Photoperiod, 68, 75, 78, 79, 82, 83, 86, 411, 550  
 Photorespiration, 235, 237, 258, 301, 434, 683, 686, 743  
 Photosynthesis (A), 484, 485  
 Photosynthetic gas exchange, 390, 463  
 Photosynthetic rate, 217, 405, 413, 434, 450, 465, 467, 468, 470, 472, 492, 502, 543, 544, 546, 611, 636, 653, 662, 743  
 Phreatophytes, 519, 522  
 Physicochemical, 4, 12, 253, 267, 698  
 Physiological responses, 107, 225, 292, 332, 351, 400, 405, 408, 409, 417, 432, 463, 483, 485, 546, 656, 665, 677, 692, 693, 711, 712, 727–729, 743  
 Physiology, 3, 4, 10, 11, 104, 106, 137, 312, 320, 349, 353, 381, 401, 402, 404, 408, 417, 431, 463, 466, 469, 482, 490, 491, 521, 525, 590, 607, 633, 642, 652, 655, 675, 676, 682, 683, 689, 694, 711–714, 718–721, 724, 727–729, 738, 739, 745  
 Phytogeographical distribution, 400, 401  
 Phytotoxic, 675–677, 679, 689  
*Picea*, 439, 546, 554, 590, 593, 594, 715, 749  
*Picea abies*, 87, 368, 439, 490, 555, 590, 696, 714  
*Picea glauca*, 371, 554, 714  
*Picea mariana* Mill., 584

- Picea rubens*, 362, 372  
 Pinitol, 218, 220, 221, 224  
*Pinus*, 314, 546, 593, 691, 715, 717, 748  
*Pinus cembra*, 351, 352  
*Pinus densiflora*, 656  
*Pinus halepensis*, 552, 609, 611, 617, 618, 657, 744  
*Pinus massioniana*, 371  
*Pinus mugo*, 221, 688  
*Pinus nigra*, 237, 611, 657  
*Pinus ponderosa* (Ponderosa Pine), 36, 111, 112, 122, 362, 487, 554, 655, 663, 665, 720, 723, 725  
*Pinus radiata*, 349, 370, 371, 439, 440, 471, 657, 746  
*Pinus sp.*, 169  
*Pinus strobus*, 371, 714  
*Pinus sylvestris* L., 388, 490, 584, 590  
 Pith, 32, 36, 37, 39, 43, 64, 106, 115, 164, 170, 182, 488  
 Plant available water, 506  
 Plasma membrane, 66, 71, 677  
 Pollutants, pollution, 10, 676, 679, 681, 689, 692, 695, 697, 698  
 Polymeric, 234, 438  
 Polymerization-depolymerization, 72  
 Pooling (sample pooling, pooling rings, pooling material, split-pool protocol, multiple-year pooling, pool), 103, 112, 116, 117, 681  
*Populus euramericana* var. *Dorskamp*, 695  
 Position-specific, 12, 215, 216, 233, 238, 239, 242, 258, 259, 267, 323, 331, 341, 390, 391  
 Position specific isotope analysis, 12, 216, 233, 238, 391  
 Post-photosynthetic fractionation, 89, 217, 302, 390, 405, 417, 438, 452, 740, 749  
 Post-photosynthetic processes, 9, 114, 429, 430, 432, 740, 746  
 Potential energy curve, 268, 269, 272  
 Potential wall, 271  
 Precipitation isotope ratios ( $\delta$ precip), 501, 504  
 Precision, 28, 109, 117, 191–202, 204, 206, 207, 210, 211, 226, 228, 230, 261, 342, 363, 430, 541  
 Preferential flow, 510, 512, 516  
 Pre-industrial, 293, 482, 487  
 Preservation, 42, 141, 171, 232, 583  
 Primary cell wall, 66, 69, 70, 415  
 Primary metabolism, 137, 139, 163  
 Primary production, 642  
 Process-based model, 114, 126, 312, 737, 738, 743, 745, 746  
 Prochiral, 258  
 Productivity, 10, 108, 237, 293, 349, 366, 402, 606, 618, 654, 656, 686, 688, 745  
 Profligate/opportunistic, 613  
 Programmed cell death, 67, 68, 71, 78, 690  
 Proportional exchange, 466  
 Pro-R-H-atom, 258  
 Proteins, 65, 66, 75, 332, 363, 366, 368, 369, 387, 690  
 Protium, 255, 332  
 Proton, 254, 255, 332  
 Provenance, 25, 654, 655  
*Pseudotsuga menziesii* (Douglas-fir), 24, 110, 221, 383, 588, 654, 720, 721  
 Pulse-labeling, 429, 432, 441, 443–450, 452, 453  
 Purification, 9, 208, 219, 223  
 Pyrolysis, 7, 209, 222, 226, 227, 234, 339, 341, 464, 681  
 Pyruvate, 281, 282, 381, 386  
 Pyruvate dehydrogenase (PDH), 281, 282, 386  
  
**Q**  
 Quality Assurance (QA), 191–193, 199, 201, 202, 207, 210, 211  
 Quality Control (QC), 21, 191–202, 205–207, 209–211  
 Quantitative wood anatomy, 26–28  
 Quantum harmonic oscillator, 268, 269  
 Quercus, 22, 36, 113, 314, 349, 353, 368, 388, 546, 554, 555, 609–611, 617, 726  
*Quercus macrocarpa*, 349, 350, 588  
*Quercus petraea*, 80, 388, 486, 555  
*Quercus robur*, 220, 348, 433, 439, 554, 555, 588  
*Quercus sp.*, 164, 554, 555  
  
**R**  
 Radial growth, 23, 25, 30, 63, 78, 80, 115, 399, 400, 408–410, 417, 431, 515, 524, 525, 553, 713, 714, 719, 721, 723, 724, 726–728, 744, 745  
 Radioactive isotope, 255, 256  
 Rainforests, 296, 297, 514, 516, 562, 632, 687  
 Rayleigh distillation, 313, 503, 588

- Raman spectra, 266
- Random error, 195, 196, 200–202, 204
- Rate constant, 266, 281
- Ratio of leaf internal to ambient CO<sub>2</sub> concentrations (*ci/ca*), 217
- Ray tissues, 416
- Rbar, 165
- Reaction coordinate, 271, 272
- Reaction rate, 260, 272, 281
- Reactivation, 78, 81, 617
- Reactive Oxygen Species (ROS), 690
- Reconstruction, 3, 4, 21, 25, 28, 33, 34, 106, 109, 114, 116, 125, 126, 242, 335, 337, 347, 400, 418, 483, 538–540, 543–548, 558–561, 586, 590, 595, 606, 607, 618, 634, 635, 642, 693, 711, 726, 727, 749, 751
- Red pine (*Pinus resinosa*), 656, 657
- Reference material, 196, 206–209, 230, 262, 263, 339
- Regional curve standardization, 37, 107
- Regulation,- down regulation, 414, 689
- Relative humidity, 9, 104, 223, 225, 239, 312, 314, 317, 319, 324, 335, 337, 347, 352, 440, 467, 468, 504, 524, 542–545, 547, 555, 556, 588, 595, 659, 663, 721, 722, 724, 744
- Remobilization, 79, 89, 221, 363, 365, 369, 371, 373, 381, 383, 387, 391, 405, 410, 415, 416, 434, 440, 442, 446, 723, 727
- Repeatability, 103, 117, 197, 206
- Replenish, -ment, 406, 557
- Replicates (replication), 12, 112, 116, 193, 197–199, 202, 540, 563
- Reproducibility, 197, 206, 361
- Research planning, 745
- Resin, 31, 64, 71, 136, 137, 140, 141, 176, 227, 230, 362, 539, 541, 717
- Resin free wood, 160
- Resistance, 79, 300, 301, 405, 512, 654, 656, 678, 694
- Resource availability, 75, 410, 652
- Respiration, 7, 75, 217, 281, 291, 293, 296, 301, 305, 386, 411, 414, 437, 445, 493, 552, 638, 692, 738, 740, 743, 747, 748
- Respiratory losses, 485
- Retrospective, 104, 381, 482, 591, 642
- Reversible reaction, 270, 271, 273, 279
- Ring-porous wood (Ring porous), 22, 416, 452
- Ring-width, 24, 26, 31, 433, 441, 486, 544, 560, 640, 657
- River flow, 586, 590
- Root distribution, 518, 519, 653
- Rooting depth, 333, 349, 405, 474, 519, 520, 523, 551, 552, 654
- Root-zone (rooting zone), 516, 520
- Rubisco, 219, 235, 237, 300, 301, 363, 382, 390, 464, 468, 483, 545, 677, 682, 690, 691, 743
- Russia, 449, 584
- Russian Federation, 581, 582, 589, 592
- S**
- Safety, 611
- Sample collection, 30, 106, 172, 200, 226, 228
- Sample extraction methods, 193
- Sample preparation (sample processing), 106, 107, 112, 116, 126, 135–137, 171, 181, 191, 192, 197, 210, 217, 219, 223, 230, 231, 234, 239, 333, 343, 362, 430, 539, 680, 739
- Sample replication, 22, 28, 41, 42, 46, 47, 108, 116, 540, 541
- Sample resolution, 103, 106, 120, 121, 124, 125, 219, 229, 324
- Sample size (sample mass), 34, 43–47, 104, 109, 110, 117, 118, 199, 201, 202, 208, 218, 463, 661
- Sample tracking, 202, 207
- Sampling, Sampling strategies, sampling design, field sampling, 31, 103, 104, 106, 108, 228, 431, 557
- Sapwood, 26, 68, 71–73, 138, 140, 141, 163, 164, 167, 168, 170, 182, 362, 716, 717
- Sapwood area, 27, 715
- Saturated zone, 509
- Scale factor error, 203
- Scattering, 401
- Sclerophyllous, 610, 611
- Seasonality, 23, 40, 79, 114, 166, 183, 432, 466, 494, 506, 509, 550, 561, 632, 633, 637, 639, 688
- Season, -ally, 72, 166, 293, 294, 316, 366, 405, 431, 436, 440, 442, 452, 453, 504, 543, 550, 631, 653, 743
- Secondary cell wall, 66, 67, 71, 72, 120, 124, 125, 431, 441
- Secondary plant metabolism, 137, 139, 140
- Secondary proxy, 464

- Sectioning method, 105
- Senescence, 79, 80, 83, 387, 388, 690, 715
- Sequoia sempervirens* (Coastal Redwood), 125, 487, 488, 554
- Shade-tolerant species, 108
- Siberia, 12, 219, 446, 447, 582, 584, 589–591, 593
- SICA, 746
- Signal complexity, 467
- Silviculture, 32, 651
- Simplified model, 291, 303, 305, 739, 743
- Single-substrate model, 114, 452, 748
- Sink limitation, 414
- Site microenvironment (micro-environment effects), 106
- Site preference, 257
- Site selection, 21, 31, 33, 104, 106
- Site specific, 607
- SI units, 206, 208
- Size-stratified approach, 107
- Snowmelt, 509
- SO<sub>2</sub>, 10, 418, 473, 675–677, 679, 681, 692, 693, 695
- Sodium chlorite, 175
- Sodium hydroxide, 174, 175
- Soil moisture, 34, 115, 123, 220, 238, 316, 349, 401, 405, 417, 434, 438, 519, 552, 559, 584, 591, 595, 655–657, 726
- Soil-Plant Atmosphere Continuum (SPAC), 516, 520
- Soil temperature, 83, 370, 371, 584
- Soil water, 63, 104, 238, 239, 315, 316, 318, 333, 349, 370, 405–407, 409, 410, 439, 466, 468, 487, 508, 510, 512–524, 526, 556, 588, 591–593, 607, 612, 614, 617, 639, 653, 665, 687
- Soil water (soil-water pools), 513, 526
- Solar radiation, 75, 542, 545, 610
- Solvent isotope effect*, 267
- Source effects, 465
- Source-sink relation, 690
- Source water, 8, 9, 11, 67, 104, 114, 124, 125, 235, 238, 241, 242, 311–314, 316–318, 331–333, 335, 337, 349, 350, 354, 405–407, 433, 435, 436, 438, 440, 464–466, 468, 469, 471–474, 501, 503, 506, 515, 517, 520, 524–527, 550, 551, 553, 557–563, 589, 592, 613–615, 638, 640, 643, 659, 660, 663, 679, 689, 692, 745
- Source water isotopic value ( $\delta_{\text{source}}$ ), 502, 503, 506, 508–510, 512, 513, 515, 516, 520–524
- Southern Annular Mode, 559
- Soxhlet apparatus, 173, 174, 177, 230
- Spatial patterns, 77, 483, 493, 559
- Species, Species-specific, 79, 80, 323, 372, 409, 416, 417, 656, 689
- Splines, 35, 122, 180, 294, 295, 298, 299
- Spruce budworm, 713–715, 719
- Standardization, 21, 35, 40, 41, 262, 543
- Standard Operating Procedures (SOPs), 192, 193, 207
- Standard Reference Materials (SRM), 200, 204–211
- Standards (study standards, laboratory standards, certified international standards, calibration standards, scale-defining international standards), 193, 194, 202–207, 210
- Stand characteristics, 103–105
- Stand density, 107, 108, 487, 613, 657
- Stand status, 109
- Starch, 72, 79, 89, 137, 140, 182, 217, 302, 334, 337, 338, 341, 352, 382–385, 387, 389, 390, 413, 418, 438, 439, 445–449, 452, 616, 692, 713, 714, 720, 723, 747
- Starvation, 490, 616
- Stem, -respiration, 381, 386
- Stereo-isotopomer, 258
- Stimulation, 414, 638, 682, 689
- Stochastic, 35, 41, 260, 401, 432
- Stomata, 125, 224, 274, 291, 316, 317, 335, 364, 406, 470, 483, 520, 610, 612, 614–616, 676, 677, 680, 682, 688–690, 692, 693, 695, 715, 716, 719, 721, 722, 726, 746
- Stomatal, -closure, -conductance (gs), 10, 11, 107, 224, 292, 301, 317, 404–406, 413, 434, 465, 467, 469, 470, 472, 474, 486, 490, 494, 542, 543, 545, 550
- Stored carbohydrate reserves, 439, 473
- Stored carbohydrates, 114, 350, 403, 414, 415, 429–431, 438, 485, 525, 590, 591, 616, 660, 661, 720, 725, 744–746
- Stress, stressor, 25, 354, 414, 611, 638, 688, 697, 729
- Subannual sampling, 105
- Subarctic, 581, 582, 584, 593, 595
- Subdominant (subcanopy) trees, 105–109

- Subfossil, 170, 352, 547, 557, 560, 561, 583  
 Subsample Signal Strength (SSS), 44–46  
 Sub-seasonal sampling, 103  
 Substrate, 3, 80, 89, 114, 115, 267, 292,  
   301, 366, 385–387, 390, 391, 452,  
   465, 519, 675, 748, 749  
 Subsurface water, 509, 510  
 Sucrose, 70, 217–225, 312, 322, 323,  
   382–385, 387, 389, 416, 436, 445,  
   446, 467, 638, 747  
 Sudden oak decline, 717, 726, 727  
 Suess effect, 293, 637  
 Sugar alcohol, 224  
 Sugar sample preparation, 223  
 Suitability, 399, 639  
 Sulfur dioxide, 675  
 Summer dormancy., 610  
 Sunshine duration, 585, 589, 590, 595  
 Surface water, 166, 334, 506, 633  
*Swietenia macrophylla*, 174  
 Swiss needle cast, 715, 721  
 Switzerland, 181, 242, 284, 349, 490, 491,  
   509, 514, 516, 517, 558, 688, 696,  
   714  
 Synchronicity, 416  
 Systematic bias (see Systematic error).,  
   195, 508  
 Systematic error, 200, 202, 203
- T**  
 Taiga, 581, 582, 589  
*Tectona grandis*, 140, 562, 563, 635  
 Temperature-limited environment, 104,  
   494, 582  
 Temporal resolution, 105, 114, 120, 126,  
   343, 418, 585  
 Tertiary, 164, 520  
 Thailand, 550, 562, 640, 641  
 Thermodynamic isotope effect, 266, 270,  
   273  
 Thermodynamic stability, 260  
*Thuja occidentalis*, 586  
 Thinning, 70, 471, 472, 651, 652, 656–663,  
   665  
 Throughfall, 508  
 Tibet, 10  
 Time lag, 86, 321, 415, 417, 442, 445, 449,  
   453  
 Time resolution, 115, 362, 418, 440,  
   447–449, 451, 452, 596  
 Tissue water, 312  
 Tolerance, 610, 636  
 Toxicity, 209, 675, 677  
 Traceability, 202, 206, 207  
 Tracheid, 22, 24, 63–65, 68, 71, 83–86, 88,  
   112, 113, 231, 431, 438, 444  
 Transition state, 267, 271–273  
 Transition zone, 170, 611  
 Translocation, 10, 29, 225, 323, 351, 362,  
   369, 371, 410, 438, 442–446, 453,  
   502, 618, 747  
 Transpiration, 62, 79, 105, 123, 124, 293,  
   301, 312, 316, 320, 334, 335, 400,  
   401, 405, 406, 410, 413, 435, 436,  
   440, 465–467, 469, 470, 473, 482,  
   485, 491, 494, 520–522, 552, 556,  
   557, 591, 593, 606, 610, 612, 614,  
   616, 638, 640, 654, 660, 663, 690,  
   697, 715, 716, 737–740, 742, 744,  
   748  
 Transpiration trichomes, 610  
 Traumatic resin ducts, 29  
 Tree density, 656  
 Tree growth, 12, 23–25, 27, 31–33, 42, 105,  
   107, 108, 232, 312, 332, 399–402,  
   415, 417, 473, 486, 489, 490, 552,  
   582, 584, 591, 606, 607, 618, 638,  
   652, 655, 656, 661, 665, 677, 689,  
   719  
 Tree health, 221, 675, 712  
 Tree height effect (height effect, tree  
   height), 107, 108, 384, 487, 636,  
   688, 750  
 Tree longevity, 482, 583  
 Tree mortality, 25, 489, 490, 615, 616, 677,  
   712, 713  
 Tree-ring cellulose, 7, 121, 137, 167, 169,  
   209, 225, 232, 234, 235, 238, 311,  
   315, 319, 321, 331, 333, 334,  
   343–347, 349, 350, 352, 353, 390,  
   404, 436, 582, 583, 592, 594, 719,  
   720, 728, 747, 749  
 Tree-ring chronology, 35, 37, 39–41, 43,  
   46, 47  
 Tree-ring density, 25, 84, 85, 544  
 Tree-ring growth, 12, 314, 349, 354, 490,  
   494, 547, 557, 590, 718–720,  
   722–724, 747  
 Tree-ring indices, 35, 37–39  
 TREERING model, The, 12, 747  
 Tree-ring parameters, 21, 23, 25, 33, 34, 45,  
   48, 403, 557, 582, 596  
 Tree-ring structure, 22, 61, 67, 75, 84, 85,  
   88, 90, 181, 227, 231  
 Tree-Ring Width (TRW), 351

Tree selection, 106, 107  
 Tree size, 32, 411, 486, 613, 636, 642, 745  
 Triose phosphate, 238, 322, 336, 382  
*Triticum aestivum*, 691  
 Tritium, 255  
 Tropical climate, 631–633  
 Tropical forest, 108, 114, 401, 406, 411, 548, 549, 554, 556, 631, 632, 641–643, 687  
 Tropospheric, 296, 677  
 Tundra, 554, 581, 582  
 Turgor, 27, 69, 70, 107, 113, 384, 411  
 Turnover, 220, 224, 273, 277, 322–23, 429–430, 443, 449, 453, 510, 516–517, 525–526, 590, 638, 641  
 Two-water world, 316  
 Tyloses, 71–73

## U

Ultrasonic device, 168, 181  
 Ultrasonic, filter fiber bag, 177  
 Ultrasonic probe, 117, 119, 120  
 Uncertainty (uncertainties), 8, 21, 39, 109, 116, 117, 126, 169, 191, 192, 194–197, 199, 200, 202, 204, 206–211, 241, 242, 319, 320, 324, 344, 382, 384, 386, 431, 436, 468, 469, 493, 502, 516, 520–525, 547, 548, 557, 651, 663, 665, 689  
 Unidirectional reaction, 273, 281  
 Unified atomic mass unit, 256  
 Unresponsive, 677  
 Urea, 663  
 UV-dissection, 227  
 UV-laser, 136, 181, 215, 216, 225–229, 232, 430

## V

Vadose zone, 509, 510, 614  
 Vapor, 274, 333, 335, 339, 340, 349, 406, 435, 466, 468, 471, 472, 503, 504, 521, 722, 747  
 Vapor pressure, 264, 335, 406, 485, 560, 562, 640  
 Vapor Pressure Deficit (VPD), 9, 34, 105, 107, 122–124, 321, 335, 349, 390, 405–410, 435, 440, 451, 467, 468, 470, 484–487, 545, 548, 555, 562, 581, 582, 586, 590, 595, 612, 636, 657, 688, 690, 724, 725, 740, 742, 748, 749  
 Vascular, 70, 83, 417, 715, 716

Vascular cambium, 64, 473  
 Vessels, 23, 27, 63–65, 68, 71–73, 78, 81, 84, 85, 88, 112, 113, 137, 174, 181, 228, 350, 416, 433, 445  
 Vibration frequency, 268, 269  
 Vienna Pee Dee Belemnite (VPDB), 205, 208, 262, 263, 292, 541  
 Vienna Standard Mean Ocean Water (VSMOW), 204, 205, 208, 333, 342, 343, 345, 346, 348, 350, 352, 353  
 Volatilization, 366, 619

## W

Wall thickening, 27, 68, 76, 78, 84, 85, 87, 90, 115, 415, 441, 442, 747  
 Water availability, 73, 75, 113, 123, 353, 401, 402, 405, 410, 411, 439, 493, 518, 551, 552, 588–590, 592, 606–608, 611, 612, 617, 636, 637, 656, 665, 724  
 Water cycle, 12, 501, 503, 506, 592  
 Water mixing (mixing processes), 436  
 Water potential gradient, 316, 516, 519, 520  
 Water relations, 349, 418, 551, 582, 711–713, 716, 718  
 Water resources, 519, 606, 653, 658, 661  
 Water shortage, 581, 586, 612  
 Water sources, 125, 340, 347, 349, 418, 453, 454, 487, 506, 515, 520, 523–525, 614, 639, 640, 651, 653, 654, 659, 660  
 Water stress, 73, 79, 82, 124, 125, 441, 465, 472, 552, 612, 655, 656  
 Water supply, 316, 406, 407, 616, 653, 696, 697  
 Water transport, 66, 510, 512, 715, 717  
 Water uptake (uptake depth, root uptake, foliar uptake, plant uptake), 505, 506, 516–520, 524, 556, 638, 639, 651, 659, 660, 692, 738  
 Water use efficiency, intrinsic water use efficiency, (iWUE), 107  
 Water vapor, 125, 195, 229, 317, 333–335, 340, 342, 405, 406, 435, 468, 469, 472, 473, 484, 523, 556, 639, 653, 679, 688, 689, 744, 748  
 Wetland, 364, 373, 582  
 White spruce (*Picea glauca*), 584, 656, 714, 715, 722  
 Whole ring, 103, 110–115, 121, 122, 439, 492

Whole wood, 8, 72, 105, 106, 117, 126,  
137, 166, 230, 304, 363, 381, 388,  
429–431, 539–541, 680  
Wildfires, 487, 588, 618, 656, 725  
Witches' broom, 715  
Wood anatomy, 27, 40, 41, 48, 83, 126,  
432, 553, 619  
Wood biomass, 409, 429  
Wood-boring, 711, 717, 726, 727  
Wood constituents, 8, 135–139, 141, 163,  
164, 166–168, 170, 182, 416  
Wood density, 3, 23–25, 27, 31, 85, 86,  
110–112, 117, 232, 403, 431, 432,  
594, 611, 689, 698

**X**

X-ray densitometry, 26, 553

Xylem, 22, 61–71, 73–78, 80, 81, 84–90,  
123, 217, 313–315, 322, 334, 344,  
386, 405–407, 411, 412, 416, 417,  
431, 433, 435, 436, 445, 466, 502,  
513, 516–520, 522, 523, 525, 526,  
556, 557, 562, 590, 612, 614, 616,  
619, 638, 639, 651, 653, 654, 660,  
663, 665, 688, 715–717, 727, 744,  
745, 750

Xylem water isotopic ratio ( $\delta$ xylem), 522

Xylogenesis, 27, 62, 63, 67, 82–85, 113,  
115, 126, 231, 389, 409–411, 415,  
416, 418, 430–435, 439–442, 452,  
453, 489, 616, 619

**Z**

Zero-Point Energy (ZPE), 268–270, 272,  
273